

AD 624814

AD

USAAVLABS TECHNICAL REPORT 64-68H

HEAVY-LIFT TIP TURBOJET ROTOR SYSTEM

VOLUME VIII

WIND-TUNNEL STUDIES

October 1965

CLEARINGHOUSE FOR FEDERAL SCIENTIFIC AND TECHNICAL INFORMATION			
Hardcopy	Microfiche		
\$8.40	\$2.25	540	AD
ARCHIVE COPY			

code 7

U. S. ARMY AVIATION MATERIEL LABORATORIES

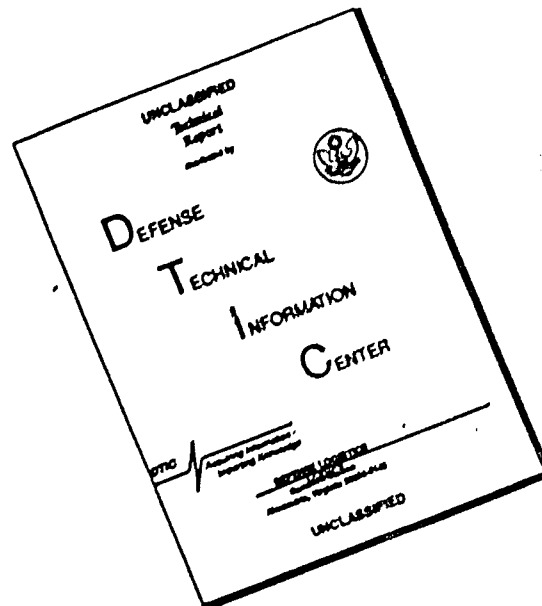
FORT EUSTIS, VIRGINIA

CONTRACT DA 44-177-AMC-25(T)

HILLER AIRCRAFT COMPANY, INC.



DISCLAIMER NOTICE



THIS DOCUMENT IS BEST QUALITY AVAILABLE. THE COPY FURNISHED TO DTIC CONTAINED A SIGNIFICANT NUMBER OF PAGES WHICH DO NOT REPRODUCE LEGIBLY.

DDC Availability Notices

Qualified requesters may obtain copies of this report from DDC.

This report has been furnished to the Department of Commerce for sale to the public.

Disclaimers

The findings in this report are not to be construed as an official Department of the Army position, unless so designated by other authorized documents.

When Government drawings, specifications, or other data are used for any purpose other than in connection with a definitely related Government procurement operation, the United States Government thereby incurs no responsibility nor any obligation whatsoever; and the fact that the Government may have formulated, furnished, or in any way supplied the said drawings, specifications, or other data is not to be regarded by implication or otherwise as in any manner licensing the holder or any other person or corporation, or conveying any rights or permission, to manufacture, use, or sell any patented invention that may in any way be related thereto.

Disposition Instructions

Destroy this report when it is no longer needed. Do not return it to the originator.

**Task 1M121401D14412
Contract DA 44-177-AMC-25(T)
USAAVLABS Technical Report 64-68H
October 1965**

HEAVY-LIFT TIP TURBOJET ROTOR SYSTEM

VOLUME VIII

WIND-TUNNEL STUDIES

Hiller Engineering Report No. 64-48

Prepared by

**Hiller Aircraft Company, Inc.
Subsidiary of Fairchild Hiller Corporation
Palo Alto, California**

For

**U. S. ARMY AVIATION MATERIEL LABORATORIES
FORT EUSTIS, VIRGINIA**

(U. S. Army Transportation Research Command when report prepared)

CONTENTS

	<u>Page</u>
LIST OF ILLUSTRATIONS	iv
LIST OF TABLES	x
LIST OF SYMBOLS	xi
1.0 SUMMARY	1
2.0 CONCLUSIONS	3
3.0 DISCUSSION	4
3.1 Introduction	4
3.2 Test Equipment	4
3.2.1 Wind-Tunnel Facility	4
3.2.2 Model Description	4
3.2.3 Pressure Tap Locations	7
3.2.4 Strain Gage Balances	7
3.2.5 Recording Equipment	12
3.3 Operating Procedures	12
3.4 Data Reduction	13
3.4.1 Definition of Final Reduced Coefficients	13
3.4.2 Stability Axis Reference System	13
3.4.3 Force and Moment Transfer from Model Axes to Stability Axes	14
3.4.4 Effect of Model Weight and Strain Gage No-Load Tares	15
3.4.5 Wind-Tunnel Wall Corrections	16
3.4.6 Position Indication	17
3.4.7 Measurement of Tunnel Dynamic Pressure	17
3.4.8 Repeatability	17
3.5 Summary of Test Runs	17
3.6 Internal Drag	21
4.0 LIST OF REFERENCES	87
5.0 DATA	
5.1 Test Run Schedule	88
5.2 Tuft Photos	96
5.3 Data Plots	118
6.0 APPENDIX	488
6.1 Strain-Gage Balance Reduction Method	488
6.2 Nacelle Airloads at Typical Forward Flight Condition	501
DISTRIBUTION	525

ILLUSTRATIONS

<u>Figure</u>		<u>Page</u>
1	Nacelle Forebody Identification	5
2	Relationship of Model and Stability Axis Forces	15
3	Nacelle Internal Geometry Schematic	23
4	Model Positioned in Test Section	24
5	Model Support Structure	24
6	Model Assembly Dwg., Twin Side-by-Side Configuration . .	25
7	Single Nacelle Comparisons	26
8	Single Nacelle Comparisons	27
9	Nacelle Forebody Contours	28
10	Nacelle Forebody Pressure Tap Locations	29
11	Nacelle Afterbody Contour and Pressure Locations	30
12	Details for Centerbodies and Inlet Pressure Rake	31
13	Twin Over-Under Nacelle Pressure Locations	32
14	Twin Side-by-Side Nacelle Pressure Locations	33
15	Comparison of Fillets for Blade-Nacelle Juncture	34
16	Twin Over-Under Nacelle With and Without Trailing Edge Wake Fairing	35
17	Single Nacelle Model Assembled in Test Section	36
18	Twin Over-Under Nacelle Assembled in Test Section	37
19	Twin Side-by-Side Nacelle Assembled in Test Section . . .	38
20	Blade Alone. Test Runs 1 Through 5	39
21	Single 1-40-100 Nacelle and Blade. Runs 6 Through 62 . .	40
22	Comparison of 1-40-XXX Forebodies. Runs 63 Through 92 .	41
23	Single 1-50-100 Nacelle with Parabolic Centerbody and Blade. Runs 93 Through 117	42
24	Single 1-50-100 Nacelle with Conical Centerbody and Blade. Runs 118 Through 132	43
25	Twin 1-40-100 Over-Under Nacelle and Blade. Runs 133 Through 157	44
26	Twin 1-40-100 Side-by-Side Nacelle and Blade. Runs 158 Through 187	45
27	Internal Support Structure - Side-by-Side Configuration .	46

ILLUSTRATIONS (CONTINUED)

<u>Figure</u>		<u>Page</u>
28	Compressor Face Inlet Pressure Tap Locations - All Single Engine Configurations	47
29	Compressor Face Inlet Pressure Tap Locations - Over-Under Configuration	48
30	Compressor Face Inlet Pressure Tap Locations - Side-by-Side Engine Configuration	49
31	Dymec Multiple Channel Data Logging System	50
32	Force and Moment Reference System, Plan and Section View .	51
33	Force and Moment Reference System, Perspective View . . .	52
34	Internal Airloads, Perspective View	53
35	Exit Flow Contraction Ratio	54
36	Internal Lift and Drag Coefficients - 1-40-100 Nacelle Internal Geometry - 1.0 Exit Plate	55
37	Internal Side Load Coefficient - 1-40-100 Nacelle Internal Geometry - 1.0 Exit Plate	56
38	Internal Lift and Drag Coefficients - 1-40-100 Nacelle Internal Geometry - .95 Exit Plate	57
39	Internal Side Load Coefficient - 1-40-100 Nacelle Internal Geometry - .95 Exit Plate	58
40	Internal Lift and Drag Coefficients - 1-40-100 Nacelle Internal Geometry - .90 Exit Plate	59
41	Internal Side Load Coefficient - 1-40-100 Nacelle Internal Geometry - .90 Exit Plate	60
42	Internal Lift and Drag Coefficients - 1-40-100 Nacelle Internal Geometry - .78 Exit Plate	61
43	Internal Side Load Coefficient - 1-40-100 Nacelle Internal Geometry - .78 Exit Plate	62
44	Internal Lift and Drag Coefficients - 1-40-115 Nacelle Internal Geometry - 1.0 Exit Plate	63
45	Internal Side Load Coefficient - 1-40-115 Nacelle Internal Geometry - 1.0 Exit Plate	64
46	Internal Lift and Drag Coefficients - 1-40-115 Nacelle Internal Geometry - .95 Exit Plate	65
47	Internal Side Load Coefficient - 1-40-115 Nacelle Internal Geometry - .95 Exit Plate	66

ILLUSTRATIONS (CONTINUED)

<u>Figure</u>		<u>Page</u>
48	Internal Lift and Drag Coefficients - 1-40-115 Nacelle Internal Geometry - .90 Exit Plate	67
49	Internal Side Load Coefficient - 1-40-115 Nacelle Internal Geometry - .90 Exit Plate	68
50	Internal Lift and Drag Coefficients - 1-40-115 Nacelle Internal Geometry - .78 Exit Plate	69
51	Internal Side Load Coefficient - 1-40-115 Nacelle Internal Geometry - .78 Exit Plate	70
52	Internal Lift and Drag Coefficients - 1-40-130 Nacelle Internal Geometry - 1.0 Exit Plate	71
53	Internal Side Load Coefficient - 1-40-130 Nacelle Internal Geometry - 1.0 Exit Plate	72
54	Internal Lift and Drag Coefficients - 1-40-130 Nacelle Internal Geometry - .95 Exit Plate	73
55	Internal Side Load Coefficient - 1-40-130 Nacelle Internal Geometry - .95 Exit Plate	74
56	Internal Lift and Drag Coefficients - 1-40-130 Nacelle Internal Geometry - .90 Exit Plate	75
57	Internal Side Load Coefficient - 1-40-130 Nacelle Internal Geometry - .90 Exit Plate	76
58	Internal Lift and Drag Coefficients - 1-40-130 Nacelle Internal Geometry - .78 Exit Plate	77
59	Internal Side Load Coefficient - 1-40-130 Nacelle Internal Geometry - .78 Exit Plate	78
60	Internal Lift and Drag Coefficients - 1-50-100 Nacelle w/Spinner Internal Geometry - 1.0 Exit Plate	79
61	Internal Side Load Coefficient - 1-50-100 Nacelle w/Spinner Internal Geometry - 1.0 Exit Plate	80
62	Internal Lift and Drag Coefficients - 1-50-100 Nacelle w/Spinner Internal Geometry - .95 Exit Plate	81
63	Internal Side Load Coefficient - 1-50-100 Nacelle w/Spinner Internal Geometry - .95 Exit Plate	82
64	Internal Lift and Drag Coefficients - 1-50-100 Nacelle w/Spinner Internal Geometry - .90 Exit Plate	83
65	Internal Side Load Coefficient - 1-50-100 Nacelle w/Spinner Internal Geometry - .90 Exit Plate	84

ILLUSTRATIONS (CONTINUED)

<u>Figure</u>		<u>Page</u>
66	Internal Lift and Drag Coefficients - 1-50-100 Nacelle w/Spinner Internal Geometry - .78 Exit Plate	85
67	Internal Side Load Coefficient - 1-50-100 Nacelle w/Spinner Internal Geometry - .78 Exit Plate	86
	Tuft Photos:	
68a	Run 188, $\alpha = 0$	
68b	" " " "	97
69a	Run 188, $\alpha = 6$	
69b	" " " "	98
70a	Run 188, $\alpha = 12$	
70b	" " " "	99
71a	Run 189, $\alpha = 0$	100
71b	" " $\alpha = 6$	100
71c	" " $\alpha = 12$	101
72a	Run 190, $\alpha = 0$	102
72b	" " $\alpha = 6$	102
72c	" " $\alpha = 12$	103
73a	Run 191, $\alpha = 0$	104
73b	" " $\alpha = 6$	104
73c	" " $\alpha = 12$	105
74a	Run 192, $\alpha = 0$	106
74b	" " $\alpha = 6$	106
74c	" " $\alpha = 12$	107
75a	Run 193, $\alpha = 0$	108
75b	" " $\alpha = 6$	108
75c	" " $\alpha = 12$	109
76a	Run 194, $\alpha = 0$	110
76b	" " $\alpha = 6$	110
76c	" " $\alpha = 12$	111
77a	Run 195, $\alpha = 0$	112
77b	" " $\alpha = 6$	112
77c	" " $\alpha = 12$	113
78a	Run 196, $\alpha = 0$	114
78b	" " $\alpha = 6$	114
78c	" " $\alpha = 12$	115
79a	Run 197, $\alpha = 0$	116
79b	" " $\alpha = 6$	116
79c	" " $\alpha = 12$	117

ILLUSTRATIONS (CONTINUED)

<u>Figure</u>		<u>Page</u>
80 through 441	Lift, Drag, and Pitching Moment Coefficients for Nacelle Alone and Combined Nacelle and Blade, Runs 13 through 187 (Refer to Run Schedule, pages 88 through 95)	118 through 479
442	Comparison of Coefficients for Nacelle Alone, Runs 135 and 235	480
443	Comparison of Coefficients for Combined Nacelle and Blade, Runs 135 and 235	481
444	Side Force Coefficients for Single 1-40-100 Nacelle, Exit Plate = 0	482
445	Side Force Coefficients for Single 1-40-100 Nacelle, Exit Plate = 1.00	483
446	Side Force Coefficients for Twin Vertical Nacelle, Exit Plate = 1.00	484
447	Side Force Coefficients for Twin Vertical Nacelle, Exit Plate = 0	485
448	Side Force Coefficients for Twin Horizontal Nacelle, Exit Plate = 1.00	486
449	Side Force Coefficients for Twin Horizontal Nacelle, Exit Plate = 0	487
450	Typical Balance Calibration Setup and Designations . . .	488
451	Nacelle Balance	495
452	Blade Quarter-Chord Balance	500
453	Plan View of Rotor Disk in Forward Flight	502
454	Nacelle Drag and Side Force Coefficients for $\mu_1 = 0.176$ and $\mu_2 = 0.364$	507
455	Nacelle Surface Static Pressure - $P-P_o/q_o$ Versus Percent Nacelle Chord (1-50-100 Nacelle) - $\mu = .364$, $\psi = 0^\circ, 90^\circ$	508
456	Nacelle Surface Static Pressure - $P-P_o/q_o$ Versus Percent Nacelle Chord (1-50-100 Nacelle) - $\mu = .364$, $\psi = 180^\circ, 220^\circ$	509
457	Nacelle Surface Static Pressure - $P-P_o/q_o$ Versus Percent Nacelle Chord (1-50-100 Nacelle) - $\mu = .176$, $\psi = 0^\circ, 180^\circ$	510

ILLUSTRATIONS (CONTINUED)

<u>Figure</u>		<u>Page</u>
458	Nacelle Surface Static Pressure - $P - P_o/q_o$ Versus Percent Nacelle Chord (1-40-100 Nacelle) - $\mu = .176$, $\psi = 0^\circ, 90^\circ$	511
459	Nacelle Surface Static Pressure - $P - P_o/q_o$ Versus Percent Nacelle Chord (1-40-100 Nacelle) - $\mu = .176$, $\psi = 180^\circ, 220^\circ$	512
460	Internal Pressure Rake Configuration	513
461	Pressure Recovery at Compressor Face for Inlet 1-40-100 .	514
462	Pressure Recovery at Compressor Face for Inlet 1-50-100 with Conical Center	515
463	Pressure Recovery at Compressor Face for Side-by-Side 1-40-100 Inlets	516
464	Pressure Recovery at Compressor Face for Twin Over-Under 1-40-100 Inlets	517
465	Drag Coefficient Versus Angle of Attack - 1-40-100 and 1-50-100 Single Nacelles	520
466	Drag Coefficient Versus Angle of Attack - 1-40-100 Twin Over-Under Nacelle	521
467	Drag Coefficient Versus Angle of Attack - 1-40-100 Twin Side-by-Side Nacelle	522
468	Drag Coefficient Versus Length/Diameter Ratio	523
469	Drag Coefficient Versus Reynolds Number	524

TABLES

<u>Table</u>		<u>Page</u>
1	Pressure Tap Locations for All Single Nacelles	8
2	Pressure Tap Locations for Twin Nacelles	9
3	Pressure Tap Locations Located on Centerline of Pairing Between Twin Nacelles	10
4	Blade Pressure Tap Locations	11
5	Run Summary, Data Runs	19
6	Run Summary, Tuft Photos (No Data Recorded)	20
7	Internal Geometry Constants	23
8	Nacelle Balance Calibration	491
9	Blade Balance Constants	492
10	Nacelle Lift, Drag and Side-Force Coefficients	505

SYMBOLS

A_e	Nacelle exit area, ft^2
A_F	Nacelle frontal area, ft^2
A_I	Engine compressor inlet area, ft^2
A_R	Reference area, based on the blade planform area exposed in the test section, ft^2
c	Blade chord, ft.
C_D	Drag coefficient = $\frac{D_s}{q_o A_R}$
C_L	Lift coefficient = $\frac{L_s}{q_o A_R}$
C_{L_T}	Blade lift coefficient
C_M	Pitching moment coefficient = $\frac{M_s}{q_o A_R (c/4)}$
C_Y	Side force coefficient = $\frac{Y_s}{q_o A_R}$
D	Drag, lb., positive aft
K	Internal total pressure loss coefficient = $\frac{P_{T1} - P_{T2}}{q_o \cos^2 \beta \cos^2 \alpha}$
L	Lift, lb., positive up
M	Pitching moment, ft-lb., positive tending to raise the leading edge up
P	Static pressure, p.s.f.
P_T	Total pressure, p.s.f.
$\frac{\Delta P}{q_o}$	$\frac{P - P_o}{q_o}$, where P = pressure at the point of interest
q_o	Remote or freestream dynamic pressure, p.s.f., = $1/2 \rho V_o^2$
q_T	Dynamic pressure at the rotor blade tip, p.s.f., = $1/2 \rho V_T^2$
R	Rotor blade radius, ft.

SYMBOLS (CONTINUED)

V	Forward flight speed, f.p.s.
V_e	Nacelle exit velocity, f.p.s.
V_o	Freestream velocity, f.p.s.
V_T	Rotor blade tip speed, f.p.s.
$x-x$	Longitudinal axis
$y-y$	Lateral axis
Y	Side force, lb., positive to the right when viewing the model from the rear
$z-z$	Vertical axis
α	Angle of attack of model, positive with wind directed from below
α_i	Angle of incidence between nacelle and blade, positive for nacelle inlet up with respect to blade
β	Sideslip angle, positive with wind directed from the right
δ_{oI}	Nacelle coefficient of drag at $\alpha = 0$, referenced to A_I
δ_{2I}	Nacelle coefficient of drag for use with C_{LrO}^2
δ'_{2I}	Nacelle coefficient of drag for use with engine compressor inlet area and ϕ^2
μ	Advance ratio = V/V_T
ρ	Air mass density, slugs/ft ³
ψ	Rotor blade azimuth position
Ω	Rotor rotational speed, rad/sec.

SYMBOLS (CONTINUED)

Subscripts:

- m Refers to model axis system. This is an orthogonal body axis system, aligned with the model planes of symmetry, and rotating and translating with the model.
- o Refers to remote or freestream condition.
- s Refers to stability axis system. This is an orthogonal set of axes which rotate with the model in yaw, but do not rotate in pitch.

Superscripts:

- []' Refers to nacelle internal forces and coefficients. See Section 3.6.
- []" Refers to nacelle external force coefficients, based on compressor inlet area and dynamic pressure at the rotor tip. See Section 6.2.

Specialized symbols for Section 6.1, "Strain-Gage Balance Reduction Method":

- a_1 Distance between the electrical centers of the forward and aft pitch bridges, in.
- a_3 Distance between the electrical centers of the forward and aft yaw bridges, in.
- D Balance axial (drag) force, lb.
- F Applied force, lb.
- K Conversion constant, mv/unit load
- L Moment arm for the balance normal force, in.
- M Balance pitching moment, in-lb.
- N Balance yawing moment, in-lb.
- R Strain-gage electrical center or reaction outputs, volts. Also used for balance rolling moment, in-lb.

SYMBOLS (CONTINUED)

- x Distance from bridge electrical center to applied force "F"
(see Figure 2), in.
- Y Balance side load, lb.
- δ Interaction coefficient

Subscripts or Superscripts:

- C Corrected for interactions
- 1 Forward pitch bridge
- 2 Aft pitch bridge
- 3 Forward yaw bridge
- 4 Aft yaw bridge
- 5 Roll bridge
- 6 Axial bridge

1.0 SUMMARY

1.1 General

Wind-tunnel tests were conducted to provide nacelle design information which would assist in the design of the tip turbojet installation. The model was constructed to provide for single, over-under, and side-by-side engine arrangements. The nacelle loads were measured with a six-component strain-gage balance.

Tests were conducted at nacelle Reynolds Numbers from 450,000 to 1,830,000 with most of the data taken at the higher value. The model pitch angle was varied from -3 degrees to +12 degrees and the yaw angle was varied from -20 degrees to +20 degrees. Nacelle inlet to freestream velocity ratios were varied from 0 to .7625, the maximum obtainable with freestream total pressure supplying the energy necessary to overcome internal losses.

1.2 Nacelle Drag

Drag coefficients obtained from the tunnel tests indicate that the nacelle drag is two to three times the anticipated value. The source of the high drag is flow separation originating from the blade nacelle junction where the dual expansion on the aft portions of the blade and nacelle proved to be excessive.

The nacelle aerodynamic forces are appreciably altered because the normal pressure distribution is modified over a large percentage of the nacelle surface which is covered by the blade. One result of this modified pressure distribution is the nacelle side load at 0 degrees angle to the flow ($\alpha = 0^\circ$, $\beta = 0^\circ$). The expected symmetrical drag versus sideslip angle was significantly altered as shown in Figures 465, 466, and 467 of the Appendix (Section 6.0).

1.3 Nacelle Inlet Flow

All the nacelle configurations showed acceptable inlet flow conditions at nominal angles (less than 6°). For higher angles of attack or sideslip, the inlet total pressure recovery decreased and the velocity profile deteriorated. Addition of a protruding centerbody effectively prevented internal lip separation and maintained good velocity profiles throughout the range of test variables, with little or no effect of centerbody geometry.

Dual engine inlets produce a mutual interference which is manifested when one inlet is upstream of the other. The downstream engine has poor pressure recovery and at the extreme angles has unsteady flow.

1.4 Nacelle Airloads at Typical Forward Flight Condition

A discussion is presented in the Appendix (Section 6.0) to illustrate the method used to determine nacelle airloads as they vary with blade azimuth position during forward flight. The configuration used for this example is a single-engine nacelle with a conical spinner and no nacelle exit restriction. Lift, drag, and side force coefficients, based on compressor inlet area are calculated and presented vectorially for two advance ratios, $\mu = 0.176$ and $\mu = 0.364$. Schematic diagrams of external and internal pressure distributions are presented for the same two advance ratios and blade azimuth positions of 0° , 90° , 180° , and 270° .

1.5 Comparison of Wind-Tunnel Nacelle Drag to Parametric Study Values

Nacelle drag coefficients, based on frontal area, are compared (in the Appendix) with values used in the parametric design study (Reference 4) as well as published literature so that (a) the applicability of the assumptions in the parametric study can be evaluated, and (b) improvements of nacelle designs from those used in the wind-tunnel tests can be made. The influence of nacelle fineness ratio and Reynolds Number on drag coefficients are shown.

2.0 CONCLUSIONS

2.1 Nacelle Aerodynamic Forces

The aerodynamic flow and the net forces are appreciably altered by the large percentage of the nacelle which is covered by the blade tip. The nacelle produces a side load for a sideslip angle of 0 degrees, indicating an altered pressure distribution. In addition, the presence of the blade on the nacelle causes an unsymmetrical variation of drag with sideslip angle; i.e., the drag increases with increasing sideslip angle and decreases with decreasing sideslip angle, as shown in the Appendix, Figures 462, 463, and 464.

2.2 Nacelle Drag

The drag coefficients obtained are unusually high and result from separation at the blade-nacelle junction. Improved design of the blade-nacelle area should result in drag coefficients equal to or less than the values used in the parametric study. Additional wind-tunnel testing of revised junction contours would be necessary to confirm improvements.

2.3 Nacelle Inlet

All the nacelle inlet configurations had acceptable inlet flow conditions at nominal angles of attack (less than 6°). At higher angles, total pressure recovery and velocity profiles were acceptable only for the inlets with centerbodies. The centerbody effectively prevented internal lip separation and the inlets maintained good velocity profiles throughout the range of angles tested.

2.4 Nacelle Configuration

The single engine nacelle provides the minimum drag and net integrated side force of any configuration when based on an equivalent installed power.

For dual nacelles the side-by-side configuration has the lowest drag and side loads, and the inlet losses are minimum, for advance ratios less than .2125. For greater advance ratios, the sideslip angle exceeds the maximum pitch angle which results in the over-under configuration having lower inlet losses.

3.0 DISCUSSION

3.1 Introduction

These tests were conducted to obtain data for comparison with similar configurations tested by other agencies and to define potential problem areas. The basic nacelle shapes were designed using NACA developed inlet and afterbody contours. These basic contours were incorporated into nacelle designs which would allow changes in engine arrangements (single, twin over-under, and twin side-by-side), and nacelle inlet configurations. The basic NACA contours were modified to provide this flexibility, with a minimum increase in cost. The tunnel data is therefore considered as a first approximation to the final configuration.

An engine nacelle, mounted on a rotor blade tip, will experience cyclic variations in angle of attack, angle of yaw, dynamic pressure, Mach number, and inlet mass flow. While the actual aerodynamic conditions are transient, this test program was conducted under steady-state conditions.

3.2 Test Equipment

3.2.1 Wind-Tunnel Facility

The test program was conducted in the U. S. Naval Postgraduate School, Monterey, California. This is a closed return type wind-tunnel with a 32- by 45-inch test section. Tunnel drive is by a constant speed electric motor with dynamic pressure controlled by blade pitch setting. Several ranges of dynamic pressure are available through a four-speed automotive transmission. The test section is vented to atmospheric pressure.

The majority of the testing was conducted at a nominal dynamic pressure of 48 p.s.f., with a corresponding Reynolds Number of 1,280,000 per foot. A short series of runs were made at dynamic pressures from 3 to 48 p.s.f to establish the effect of Reynolds Number.

3.2.2 Model Description

General:

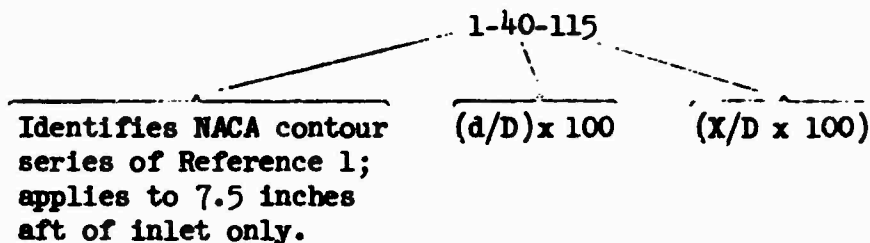
The 1/4-scale nacelle models were mounted on the tip of a segment of rotor blade span. The rotor blade extended through the side of the test section, and was of sufficient length to position the model near the center of the test section. Figure 4 shows a model positioned in the test section at a small angle of attack and yaw. A photograph of the pitch and yaw mechanism, mounted outside of the test section, is shown in Figure 5. The support system is variable in pitch about the blade quarter chord line, and in yaw about a vertical axis located just outside of the viewing window. The loads are transmitted from the nacelles and blade through strain-gage balances to the supporting structure. The location and description of these balances are described in Section 6.1.

Blade Segment:

The blade contour corresponds to an NACA 0015 airfoil section. Figure 6 shows the planform, section characteristics, and pressure tap locations for the blade segment. This figure also shows the complete assembly of the blade, including the twin side-by-side nacelle and support structure.

Single Nacelles:

Four single-nacelle configurations were tested. They are identified as 1-40-100, 1-40-115, 1-40-130, and 1-50-100. Figures 7 and 8 show cross sections of these nacelles, illustrating their relative size and common dimensions. The nacelle code numbers, such as 1-40-115, identify the forebody contour. This code is a modification of the designation used in Reference 1 (NACA Report 920). The following example illustrates the meaning of each term.



where: d = inlet diameter
 D = maximum outside diameter
 X = total forebody length, minus .5 in.

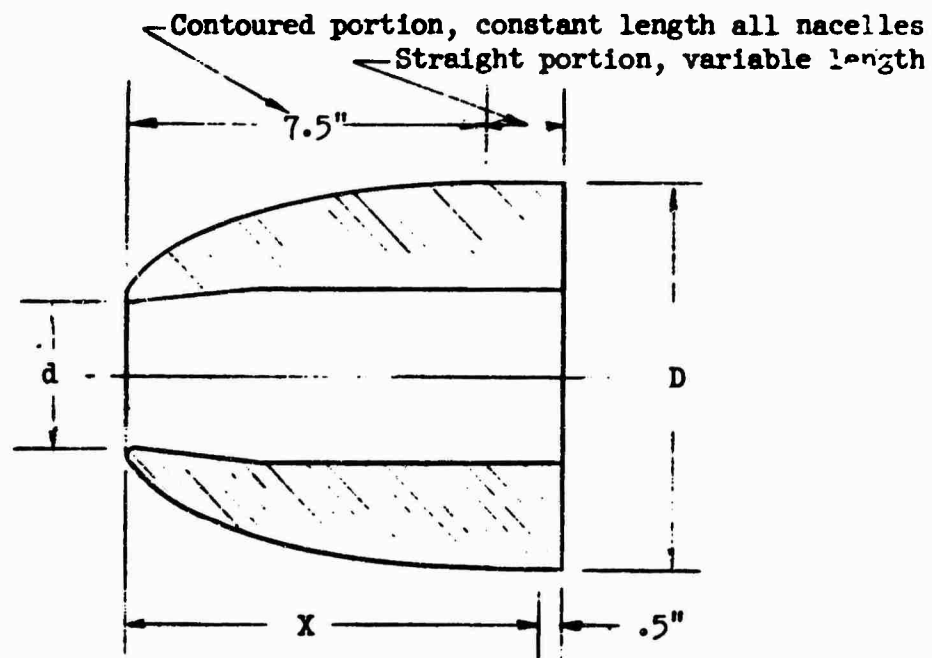


Figure 1. Nacelle Forebody Identification.

Detailed drawings of the forebody contours, including tables of ordinates, are given in Figure 9.

The afterbody contours (aft of the maximum diameter) are identical for all nacelles. A modified NACA 111 body from Reference 2 (NACA TR 1038) was used as the basic shape for the afterbody contour. A detailed drawing of the afterbody, including the table of ordinates, is given in Figure 11.

The internal dimensions of the nacelles consist of a diverging or converging inlet, followed by a straight section and nozzle. The inlets are detailed on the forebody drawings of Figure 9. The straight section and exit nozzle are identical for all nacelles and are detailed on Figure 6.

The centerbody shapes were tested with nacelle 1-50-100 only. Two centerbody shapes were investigated, one a conical shape and the other an NACA 1-30-40 series spinner. The centerbody profiles and table of ordinates are given in Figure 12.

The single 1-40-100 nacelle was mounted at incidence angles (α_i) of 0, 3, and 6 degrees with respect to the plane of symmetry of the blade segment. All other nacelles were tested with their axes in line with the blade plane of symmetry.

Twin Nacelles:

The twin nacelles consisted of two 1-40-100 nacelles with a smooth contour faired between them. Two twin configurations were tested; one with the engines mounted over-under with their axes in a plane perpendicular to the rotor blade plane of symmetry, and the other with the engine axes mounted side-by-side and parallel to the rotor blade plane of symmetry. Three-view drawings of these twin nacelles are given in Figures 13 and 14.

Fairings:

Fillet fairings were made for the nacelle-blade juncture of all nacelles. They consisted of plastic reinforced with glass cloth and were trimmed to allow about 1/16-inch clearance between fairing and nacelle. It should be emphasized that the fairings tested were corner fillets only and are simply a first step in a fairing design program to evaluate the magnitude of the nacelle-blade interference drag. The single 1-40-100 nacelle was run both with and without fairings. The other single nacelles were tested without fairings only. The twin side-by-side nacelle was run both with and without fairings. The twin over-under nacelle was tested with the fairing only. Photographs of the fillet fairings are shown in Figure 15.

A trailing edge wake fairing was tested on the twin over-under nacelle, in addition to the fillet fairings. The nacelle is shown with and without this fairing on Figure 16.

Exit Orifices:

To meter the internal flow, engine exit orifices of several sizes were provided as shown in Figure 11. These exit orifices provided five free-stream-to-inlet-velocity ratios of .765, .675, .590, .416, and 0.0, for the 1-40-100 engine geometry and somewhat less depending on the internal losses for the other configurations.

Complete Model:

Three-view drawings of the assembled model are provided in Figures 17, 18, and 19. These figures show the 1-40-100 single nacelle, the twin over-under nacelle, and the twin side-by-side nacelle, respectively. The nacelles are mounted on the blade segment and shown relative to the wind-tunnel walls for zero angle of attack and yaw.

Photographs of the assembled models are provided in Figures 20 through 27. These photographs show the complete configuration, grouped in their order of testing, except for the following pictures of special interest. In the single 1-40-XXX nacelle series, only the 1-40-100 nacelle is shown completely, Figure 21. The 1-40-XXX series forebodies and inlets are compared in Figure 22. Figure 27 shows the internal structure of the model, with locations of the internal pressure rake and both internal strain-gage balances.

3.2.3 Pressure Tap Locations

The external pressure distribution was obtained by a series of pressure taps installed on the outer surfaces of the nacelles and blade segment. The locations of these pressure taps are identified on Tables 1 through 4.

Inlet performance was monitored by a survey of total and static pressures at the engine compressor face station. A detailed drawing of the internal rake is given in Figure 12, and a photograph of the rake installed in the model is shown in Figure 27. The inlet pressure tap locations are identified on Figures 28, 29, and 30.

3.2.4 Strain-Gage Balances

Two internal strain-gage balances were used for measurement of forces and moments. One, a five-component balance of Hiller Aircraft Company design, determined lift, drag, and pitching moment of the complete model. The second balance (Chance-Vought Aircraft Corp.), a six-component instrument, was used for determination of lift, drag, side force, and pitching moment of the nacelle only.

A description of both balances, including the calibration constants, interactions, and resulting force and moment equations, is provided in the Appendix, Section 6.1.

TABLE 1 PRESSURE TAP LOCATIONS FOR ALL SINGLE NACELLES			
x From Leading Edge (See Fig. 10.)	Top Tube No.	Outboard Tube No.	Bottom Tube No.
.12	111	121	131
.42	112	122	132
.86	113	123	
1.28	114	124	133
1.70	115	125	
2.13	116	126	134
2.56	117	127	
3.31	118	128	135
5.12	119	129	136
6.82	120	130	137
x Aft Of Maximum Dia. (See Fig. 11.)			
.58	99	103	
2.28	98	102	
5.71	97	101	
8.57	96	100	

TABLE 2 PRESSURE TAP LOCATIONS FOR TWIN NACELLES					
	Over / Under		Side-by-Side		
	Upper Nacelle Inboard	Upper Nacelle Top	Inboard Nacelle Top	Outboard Nacelle Outboard	
x From Leading Edge (See Figs. 13 & 14)					
.12	111	118	111	128	
.42	112	119	112	129	
1.28	113	120	113	130	
2.13	114	121	114	131	
3.41	115	122	115	132	
5.13	116	123	116	133	
6.82	117	124	117	134	

TABLE 3
PRESSURE TAP LOCATIONS LOCATED ON
CENTERLINE OF PAIRING BETWEEN TWIN NACELLES

x From Leading Edge (See Figs. 13 & 14.)	Over-Under Outboard Configuration	Side-by-Side Upper Surface Configuration
.10	125	118
.50	126	119
1.00	127	120
1.50	128	121
2.00	129	122
2.50	130	123
3.00	131	124
4.00	132	125
6.00	133	126
8.00	134	127
 x Aft of Maximum Dia. (See Fig. 13.)		
1.28	99	99
2.28	98	98
7.28	97	97
10.68	96	96

TABLE 4 BLADE PRESSURE TAP LOCATIONS		
Pressure Tap Percent x/c (See Fig. 6.)	Outboard Station Tube No.	Inboard Station Tube No.
.5	6	27
2.5	7	28
5.0	8	29
7.5	9	30
10.0	10	31
12.5	11	32
15.0	12	33
20.0	13	34
30.0	14	35
40.0	15	36
50.0	16	37
60.0	17	38
80.0	18	39
97.0	19	40
80.0	20	41
60.0	21	42
40.0	22	43
20.0	23	44
12.5	24	45
7.5	25	46
2.5	26	47

Upper Surface

Lower Surface

3.2.5 Recording Equipment

Force, Moment, and Position Data:

All the data recording was handled by a Hewlett-Packard Dymec Multiple-Channel Data-Logging System (DY-5942B), Figure 31. In addition to supplying power to the strain gage bridges, this system recorded the eleven strain gage outputs, the angle of attack and angle of yaw potentiometer outputs, the wind-tunnel dynamic pressure, and the identifying run number.

Data recording was in two forms: typed tabulation and punched "Flexo-writer" paper tape. Upon signal from the operator, data were read and recorded one component at a time in a predetermined automatic sequence. Time required to read and record 15 components of data at a single test point was about one minute.

Vibratory transients in the strain gages were damped within Dymec by averaging each gage output over a one-second interval and recording this average reading.

Pressure Data:

All of the pressure data were measured on a multiple manometer board. The data were recorded by photographing the board with a 35-mm camera.

3.3 Operating Procedures

A standard operating procedure was followed throughout the testing.

- a. At the start of each day, the recording equipment and strain-gage balances were turned on and allowed to come to operating temperature.
- b. At the start of each day, or at the beginning of each configuration series, the model was pitched through the desired angle of attack range with the wind off. The strain-gage outputs were recorded at the maximum, minimum, and an intermediate angle of attack to obtain the model weight and balance tares.
- c. The tunnel was started and brought to the desired dynamic pressure.
- d. The model was positioned to the desired angle of attack and sideslip.
- e. Data was recorded.
- f. Steps d and e were repeated until the desired angle series was completed.
- g. The tunnel was shut down.

3.4 Data Reduction

3.4.1 Definition of Final Reduced Coefficients

The final reduced coefficients are presented in terms of stability axis forces and moments, as defined below.

$$C_D = \text{Drag coefficient} = \frac{D_s}{q_o A_R} \quad (1)$$

$$C_L = \text{Lift coefficient} = \frac{L_s}{q_o A_R} \quad (2)$$

$$C_M = \text{Pitching moment coefficient} = \frac{M_s}{q_o A_R (c/4)} \quad (3)$$

$$C_Y = \text{Side force coefficient} = \frac{Y_s}{q_o A_R} \quad (4)$$

3.4.2 Stability Axis Reference System

The forces and moment used to obtain the above coefficients have been resolved in a stability axis reference system. This is an orthogonal set of axes which rotate with the model in yaw, but do not rotate in pitch. The forces and moments are illustrated in Figures 32 and 33 and are discussed below.

D_s = Drag, lb., positive aft.

This component of model force is perpendicular to the blade quarter chord axis and lies in a plane which is parallel to the tunnel floor.

L_s = Lift, lb., positive up.

This component of model force is always perpendicular to the tunnel floor, for all pitch or sideslip angles of the model.

M_s = Pitching moment, ft-lb., positive leading edge up.

This is the pitching moment about the blade quarter chord axis. (Note that the pitching moment coefficients for the nacelle-only are plotted negative, so they would not be superimposed on the nacelle drag and lift coefficients.)

Y_s = Side force, lb., positive to the right when viewing the model from the rear.

This component of model force is parallel to the blade quarter chord axis.

The forces and moments were nondimensionalized by the following terms:

$$\begin{aligned} q_o &= \text{tunnel freestream dynamic pressure, p.s.f.} \\ A_R &= \text{blade planform area exposed in the test section, ft}^2 \\ &= 2.939 + \frac{.4695}{\cos \beta} (1.875 \sin \beta - 1) \end{aligned} \quad (5)$$

This equation accounts for the variation in blade area with β , due to the blade being rotated about a point on the quarter chord axis outside of the test section.

c = blade chord, ft.

The same q_o , A_R , and c were used to calculate the nacelle coefficients as were used to calculate the complete model coefficients. Since the reference area is a function of sideslip angle, plotted nacelle coefficients may be directly compared only at the same value of sideslip angle. If it is desired to compare nacelle coefficients at different sideslip angles, the plotted data must be multiplied by the reference area associated with each value of sideslip angle, and then the resultant values must be divided by some constant reference area. Reference areas, calculated from Equation (5), are tabulated below for convenience:

β , deg.	A_R , ft ²
20	2.760
10	2.617
0	2.470
-10	2.307
-20	2.119

3.4.3 Force and Moment Transfer from Model Axes to Stability Axes

The aerodynamic forces and moments were obtained from the electrical outputs of the strain-gage balances by the equations presented in the Appendix, Section 6.1. These equations provide the aerodynamic forces and moments referenced to the model axes. The model axis system is an orthogonal body axis system, aligned with the model planes of symmetry, and rotating and translating with the model.

Figures 32 and 33 show the model and stability axis systems to have identical y-y axes. The z-z and x-x axes are contained in a plane perpendicular to the blade quarter-chord axis for both systems, and differ only in the angle α . We may therefore write the transfer equations by looking at the z-z - x-x plane only. Figure 2 relates the model and stability axis forces and moments.

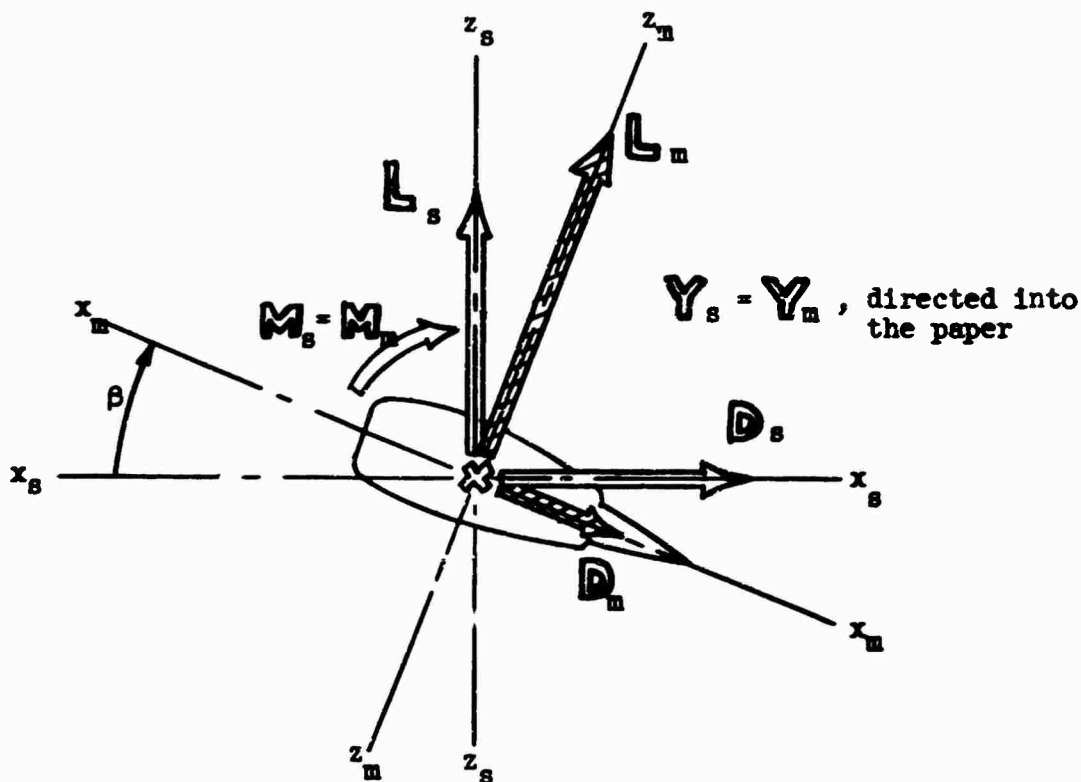


Figure 2. Relationship of Model and Stability Axis Forces.

The transfer equations may be written directly from the above figure.

$$D_s = D_m \cos \alpha + L_m \sin \alpha \quad (6)$$

$$L_s = -D_m \sin \alpha + L_m \cos \alpha \quad (7)$$

$$M_s = M_m \quad (8)$$

$$Y_s = Y_m \quad (9)$$

Equations (6) through (9) apply to the nacelle-only forces as well as the complete model forces. In the case of the nacelle-only, the angle of attack, α , will have to be increased by the angle of incidence between the nacelle and the blade.

3.4.4 Effect of Model Weight and Strain-Gage No-Load Tares

Prior to starting the tunnel, for each configuration series or break in continuous testing sequence, the model was pitched through the angle of attack range. The strain-gage outputs were then recorded at the maximum, minimum, and an intermediate angle of attack. This established a curve

of wind-off strain-gage outputs as a function of angle of attack. These wind-off outputs were subtracted from the wind-on readings, to provide the strain-gage outputs due to airloads only.

3.4.5 Wind-Tunnel Wall Corrections

Corrections for the effect of the wind-tunnel walls were applied to the angle of attack and dynamic pressure. Corrections to the forces and moments were found to be insignificant, and were not included.

The corrections were calculated by the methods outlined in Section 6:30 of Reference 3.

Correction to Angle of Attack:

From Equation (6:67) of Reference 3 we have:

$$\alpha = \alpha_u + \delta \left(\frac{S}{C} \right) C_L (57.3) (1 + \tau_2)$$

where: α = corrected angle of attack, degrees
 α_u = uncorrected angle of attack, degrees
 δ = boundary correction factor
 S = wing area, feet²
 C = test section area, feet²
 C_L = lift coefficient
 τ_2 = streamline curvature effect

Substituting in the above equation, and replacing C_L with the product of the uncorrected lift curve slope and uncorrected angle of attack, we have:

$\alpha = 1.152\alpha_u$ for the single and twin over-under nacelle configuration

$\alpha = 1.285\alpha_u$ for the twin side-by-side nacelle configuration

Correction to Dynamic Pressure:

From Equation (6:64) of Reference 3 we have:

$$q_o = q_u [1 + 2(\epsilon_{sbW} + \epsilon_{sbB} + \epsilon_{wb})]$$

where: q_o = corrected dynamic pressure, psf
 q_u = uncorrected dynamic pressure, psf
 ϵ_{sbW} = solid blocking effect for a wing
 ϵ_{sbB} = solid blocking effect for a body
 ϵ_{wb} = wake blocking effect

Substituting in the above equation, we have:

$$\begin{aligned}q_o &= 1.036 q_u \quad \text{for the blade stub alone} \\q_o &= 1.0614 q_u \quad \text{for the single nacelle configuration} \\q_o &= 1.0842 q_u \quad \text{for both twin nacelle configurations}\end{aligned}$$

3.4.6 Position Indication

The model pitch and yaw angles were measured by potentiometers attached to the model support mechanism. The potentiometers provided a linear output proportional to the length of jack screws which positioned the model attitude. The outputs were calibrated in terms of model angle of attack and sideslip. The pitch and yaw jack screws and one of the potentiometers are visible in Figure 5.

3.4.7 Measurement of Tunnel Dynamic Pressure

The test section dynamic pressure was measured by two separate means. The primary method was to record the difference between total pressure in the settling chamber and test section static pressure. The test section static was obtained from four pressure taps located in the tunnel walls, at the upstream edge of the test section. This pressure difference was related to a calibration of test section dynamic pressure, made with no model in the test section. This value of dynamic pressure was recorded by the Dymec Data System, corrected for tunnel wall effects (Section 3.4.5), and used in the reduction of force and moment data to coefficient form.

The additional means of measuring dynamic pressure was by a pitot-static tube located at the upstream station of the test section. This pressure measurement was recorded on the manometer board.

3.4.8 Repeatability

A pitch run, at near zero yaw angle, was repeated one week apart for the twin over-under nacelle configuration. The test variables were the same for both runs (runs 135 and 235), except for approximately .5 degree difference in sideslip angle. The data from both runs is plotted on Figures 442 and 443 for comparison. The difference in data between the two runs may be somewhat attributed to the yaw angle change.

3.5 Summary of Test Runs

Tables 5 and 6 present a summary of the complete run schedule given in Section 5.1. These tables show the test program summarized in groups of major configuration changes. Photographs of the model are referenced for each configuration.

Table 5 lists the runs where force, moment, and pressure data were recorded. The force and pressure testing was followed by a brief program of flow visualization summarized in Table 6. This program employed rows of tufts taped to the model to indicate local flow direction, relative turbulence, and flow separation. Photographs of the tufts were taken at selected values of pitch and yaw angles, and are presented in Section 5.2.

TABLE 5
RUN SUMMARY, DATA RUNS

Run No.	Test Series	q_0	Configuration				Pairing	Model Photo (Fig.No.)
			Identification	Center-body	Mounting	α_1	Exit Plate	
1-5	P. Y. [1]	48	Blade stub only	-	-	-	-	20
6-12	Reynolds No. Effect, $\alpha = \psi = 0$	3 48	Single, 1-40-100	None	-	0	1.0	21
13-37	P. & Y. [1]	48	Single, 1-40-100	None	-	0	0, .78, .9, .95, 1.0	Without
38-47	P. & Y. [1]	48	Single, 1-40-100	None	-	3	0, 1.0	Without
48-57	P. & Y. [1]	48	Single, 1-40-100	None	-	6	0, 1.0	Without
58-62	P. & Y. [1]	48	Single, 1-40-100	None	-	0	1.0	With
63-77	P. & Y. [1]	48	Single, 1-40-115	None	-	0	0, .9, 1.0	Without
78-92	P. & Y. [1]	48	Single, 1-40-130	None	-	0	0, .9, 1.0	Without
93-117	P. & Y. [1]	48	Single, 1-50-100	Parabolic	-	0	0, .78, .9, .95, 1.0	Without
118-132	P. & Y. [1]	48	Single, 1-50-100	Conical	-	0	0, .9, 1.0	Without
133-157	P. & Y. [1]	48	Twin, 1-40-100	None	Over-Under	0	0, .78, .9, .95, 1.0	With
158-162	P. & Y. [1]	48	Twin, 1-40-100	None	Side-by-Side	0	1.0	Without
163-187	P. & Y. [1]	48	Twin, 1-40-100	None	Side-by-Side	0	0, .78, .9, .95, 1.0	With
235	(Repeat of Run No.135)							

No data taken, runs 1-4, due to balance difficulties.
Runs 133, 135, 137, 153, 155, 157 run with and without trailing edge fairing.
P. & Y. [1]: Pitch and yaw series; $\alpha = -3, 0, 3, 6, 9, 12$ at $\psi = 9, \pm 10, \pm 20$.

TABLE 6 RUN SUMMARY, TUFT PHOTOS (NO DATA RECORDED)										
Run No.	Test Series	q ₀	Configuration					Exit Plate	Pairing	Model Photo (Fig. No.)
			Identification	Center-body	Mounting	α ₁				
188-190	P. & Y. [2]	48	Twin, 1-40-100	None	Side-by-Side	0	1.0	With	26	
191	P. [3]	48	Twin, 1-40-100	None	Side-by-Side	0	1.0	Without	26	
192-194	P. & Y. [2]	48	Twin, 1-40-100	None	Over-Under	0	1.0	With	25	
195-200	P. & Y. [2]	48	Single, 1-40-100	None	-	0	0, 1.0	With	21	
201	P. [3]	48	Single, 1-40-100	None	-	0	1.0	Without	21	
202-204	P. & Y. [2]	48	Single, 1-50-100	Parabolic	-	0	1.0	Without	23	
P. & Y. [2]: Pitch and yaw series; α = 0, 6, 12 at ψ = 0, ±20. P. [3]: Pitch series; α = 0, 6, 12 at ψ = 0.										

3.6 Internal Drag

The tip turbojet model was constructed so that inlet flow conditions could be simulated by controlling mass flow with the exit plates. In providing for and controlling the internal flow, forces are created which must be removed before engine net thrust and nacelle drag can be combined for total blade tip force. Due to the relative clean internal lines on the model nacelle, the internal drag is small compared to the total nacelle drag. The internal forces produce lift and side loads in addition to the drag.

The internal force coefficients are plotted (Figure 36 to 67) for each internal configuration. To obtain the internal force coefficients for either dual engine configuration the 1-40-100 coefficients are doubled. This is possible because the internal geometry is identical to two single 1-40-100 nacelles.

To determine the internal forces that are to be subtracted from the measured nacelle airloads, an analysis of the internal flow is required. The force, velocity, and momentum terms are vector quantities. The inlet momentum vector (\overline{mV}_O) is in the Y-D plane with components $mV_O \cos \beta$ in the drag direction and $mV_O \sin \beta$ in the -Y direction. (See Figure 34). The exit momentum is in the L-D plane with components $mV_e \cos \alpha$ and $mV_e \sin \alpha$ in the drag and lift directions, respectively. The equations for the forces are:

$$D' = mV_O \cos \beta - mV_e \cos \alpha \quad (10)$$

$$L' = mV_e \sin \alpha \quad (11)$$

$$Y' = -mV_O \sin \beta \quad (12)$$

$$\text{Let } V_e/V_O = \lambda$$

$$mV_O = \rho A_e V_e V_O = q_O A_R^2 \left(\frac{A_e}{A_R} \right) \frac{V_e}{V_O} = q_O A_R^2 \left(\frac{A_e}{A_R} \right) \lambda$$

$$mV_e = \rho A_e V_e^2 = q_O A_R^2 \left(\frac{A_e}{A_R} \right) \lambda^2$$

Define the force coefficients as:

$$C_F' = \frac{F'}{q_O A_R}$$

$$\therefore C_D' = \frac{D'}{q_O A_R} = 2(A_e/A_R) \lambda (\cos \beta - \lambda \cos \alpha) \quad (13)$$

$$C_L' = \frac{L'}{q_O A_R} = 2(A_e/A_R) \lambda^2 \sin \alpha \quad (14)$$

$$C_Y' = \frac{Y'}{q_0 A_R} = -2(A_e/A_R) \lambda \sin \beta \quad (15)$$

The velocity ratio (λ) is dependent upon the total pressure ratio across the engine, which supplies the energy to overcome the internal total pressure loss. The total axial pressure at the engine inlet (station ①) is:

$$P_{T1} = P_0 + q_0 \cos^2 \beta \cos^2 \alpha$$

Define the internal total pressure loss coefficient as K.

$$K = \frac{P_{T1} - P_{Te}}{q_0 \cos^2 \beta \cos^2 \alpha}$$

$$K q_0 \cos^2 \beta \cos^2 \alpha = P_0 + q_0 \cos^2 \beta \cos^2 \alpha - P_e - q_e$$

But:

$$P_e = P_0$$

$$K q_0 \cos^2 \beta \cos^2 \alpha = q_0 \cos^2 \beta \cos^2 \alpha - q_e$$

$$K = 1 - \frac{q_e}{q_0 \cos^2 \beta \cos^2 \alpha}$$

$$q_e/q_0 = \lambda^2 = (1 - K) \cos^2 \beta \cos^2 \alpha$$

$$\lambda = \cos \beta \cos \alpha (1 - K)^{\frac{1}{2}} \quad (16)$$

The contraction ratio behind the exit plate can be determined from Figure 35 and the geometric model parameters listed in Table 7. The blade area within the tunnel is used as the reference area (A_R). This area varied with β , as the yaw pivot point was outside of the wind-tunnel boundary.

$$A_R = 2.939 + \frac{.4695}{\cos \beta} (1.875 \sin \beta - 1) \quad (17)$$

The internal total pressure loss coefficient K was determined from test data. The maximum loss will be associated with the largest exit area and maximum P_{T1} , thus providing the maximum internal velocity. The nacelle and balance were mounted in the normal way (single-engine configuration). A blower and tubing were arranged so as to force air through the nacelle. A small gap was maintained between the engine inlet and the blower tube so that forces could not be transmitted through the structure. The leakage flow, from the gap, emitted at right angles to the engine centerline so that the measured drag force contained no external drag and was entirely due to the internal drag.

Equations (13) and (16) are combined to express internal drag in terms of the internal total pressure loss coefficient.

$$C_D' = 2(A_e/A_R) \cos^2 \beta \cos \alpha (1-K)^{\frac{1}{2}} - 2(A_e/A_R) \cos^2 \beta \cos^3 \alpha (1-K)$$

$$\frac{C_D'}{2(A_e/A_R)} = \cos^2 \beta \cos \alpha (1-K)^{\frac{1}{2}} - \cos^2 \beta \cos^3 \alpha (1-K)$$

For $\beta = \alpha = 0^\circ$

$$\frac{C_D'}{2(A_e/A_R)} = (1-K)^{\frac{1}{2}} - (1-K) = \frac{D'}{q_o A_R 2(A_e/A_R)}$$

$$(1-K) - (1-K)^{\frac{1}{2}} + \frac{D'}{2q_o A_e} = 0$$

$$(1-K)^{\frac{1}{2}} = \frac{1}{2} \pm \sqrt{\frac{1}{4} - \frac{D'}{2q_o A_e}} \quad (18)$$

Substitution of the measured drag (from the blower tests) and q_o into Equation (18) provides the internal total pressure loss coefficient K and, therefore, the data necessary to complete the calculations of the force coefficients. Table 7 contains the factor $(1-K)^{\frac{1}{2}}$ for each configuration.

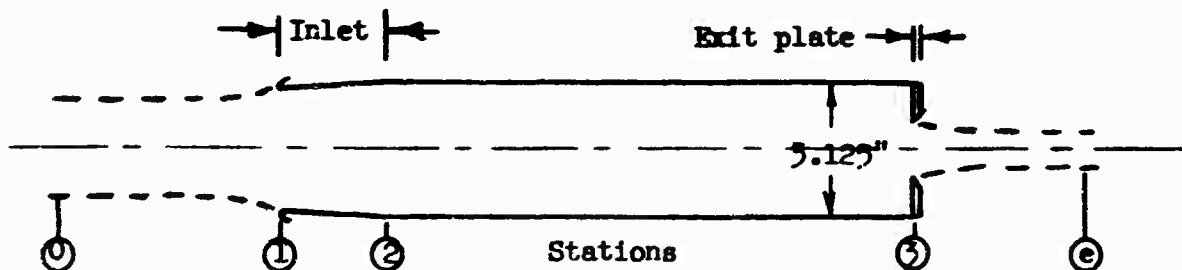


Figure 3. Nacelle Internal Geometry Schematic.

TABLE 7 INTERNAL GEOMETRY CONSTANTS					
INLET	D_1	A_1	A_2/A_1	$(1-K)^{\frac{1}{2}}$	
1-40-100	2.97 in.	.0482	1.288	.9318	
1-40-115	2.97 in.	.0482	1.288	.9232	
1-40-130	2.97 in.	.0482	1.288	.9120	
1-50-100	3.710 - 2.250	.0475	1.308	.8700	
EXIT PLATE	D_3	A_3	A_3/A_2	A_e/A_3	A_e
1.00	3.125 in.	.0532	.860	.741	.0394
.95	2.970 in.	.0482	.776	.725	.0349
.90	2.810 in.	.0431	.695	.707	.0305
.78	2.440 in.	.0325	.523	.661	.0215
0.00	0.000	.0000	.000	.000	.0000

$D_2 = 3.375$ in., $A_2 = .0620$ ft², (engine compressor inlet area)



Figure 4. Model Positioned in Test Section.

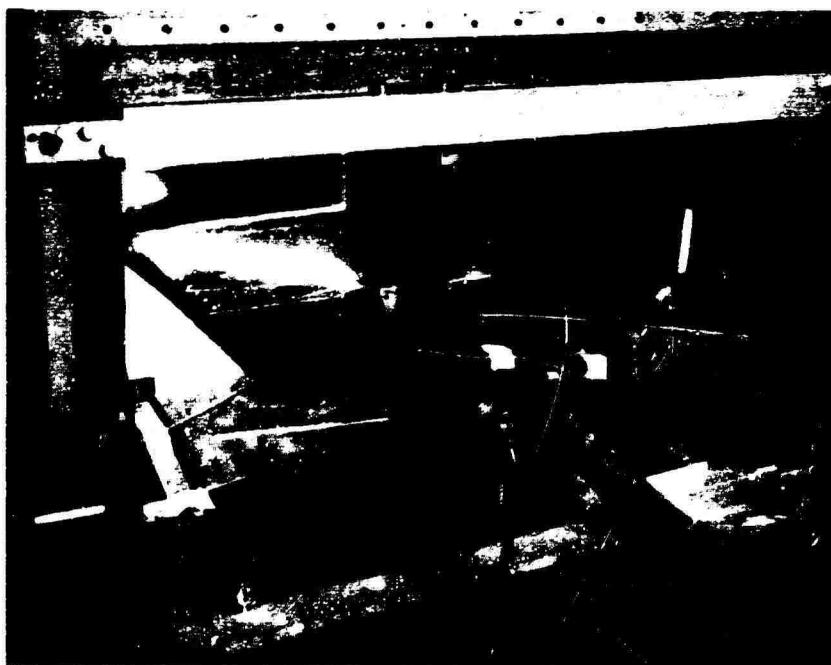


Figure 5. Model Support Structure.

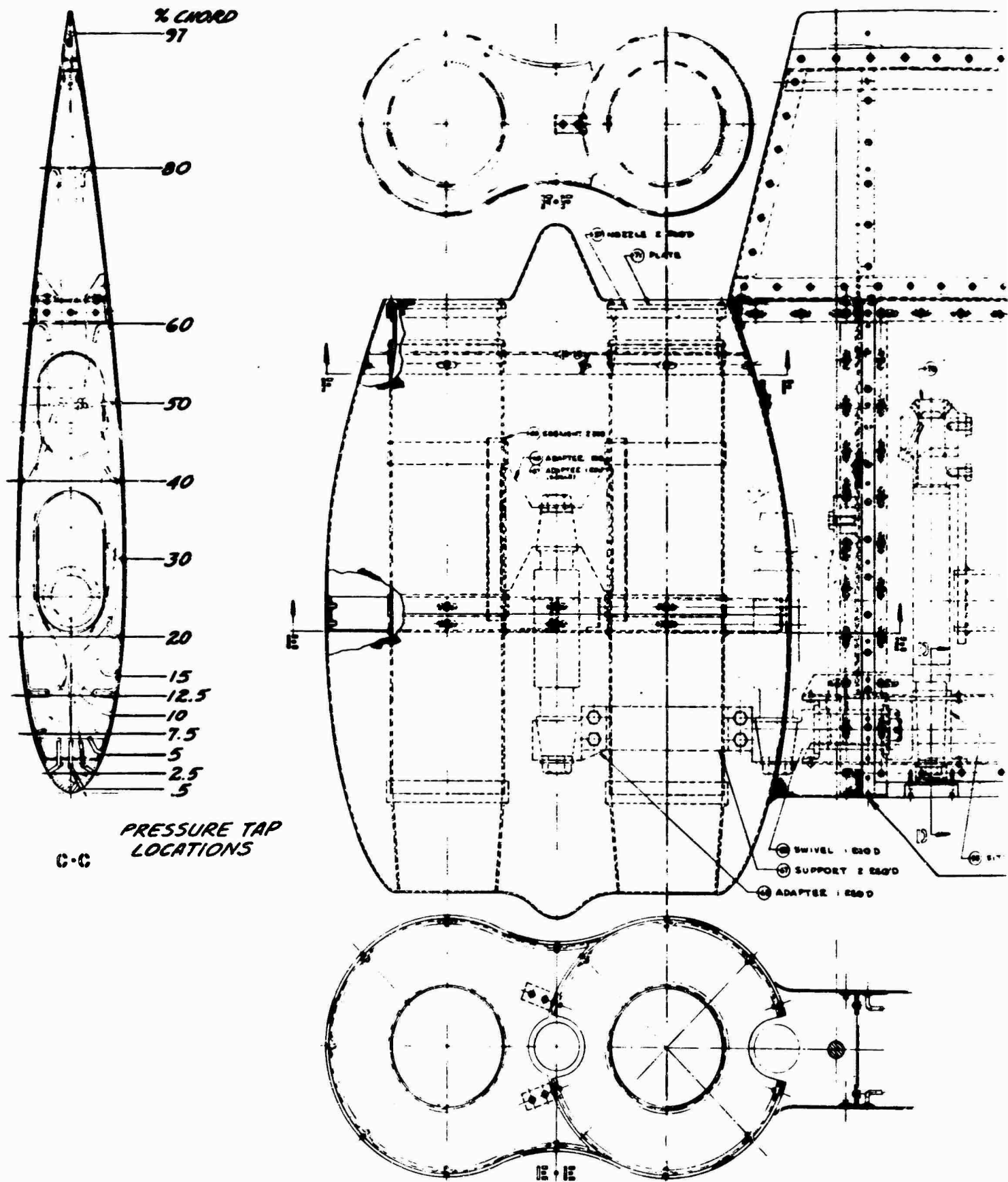
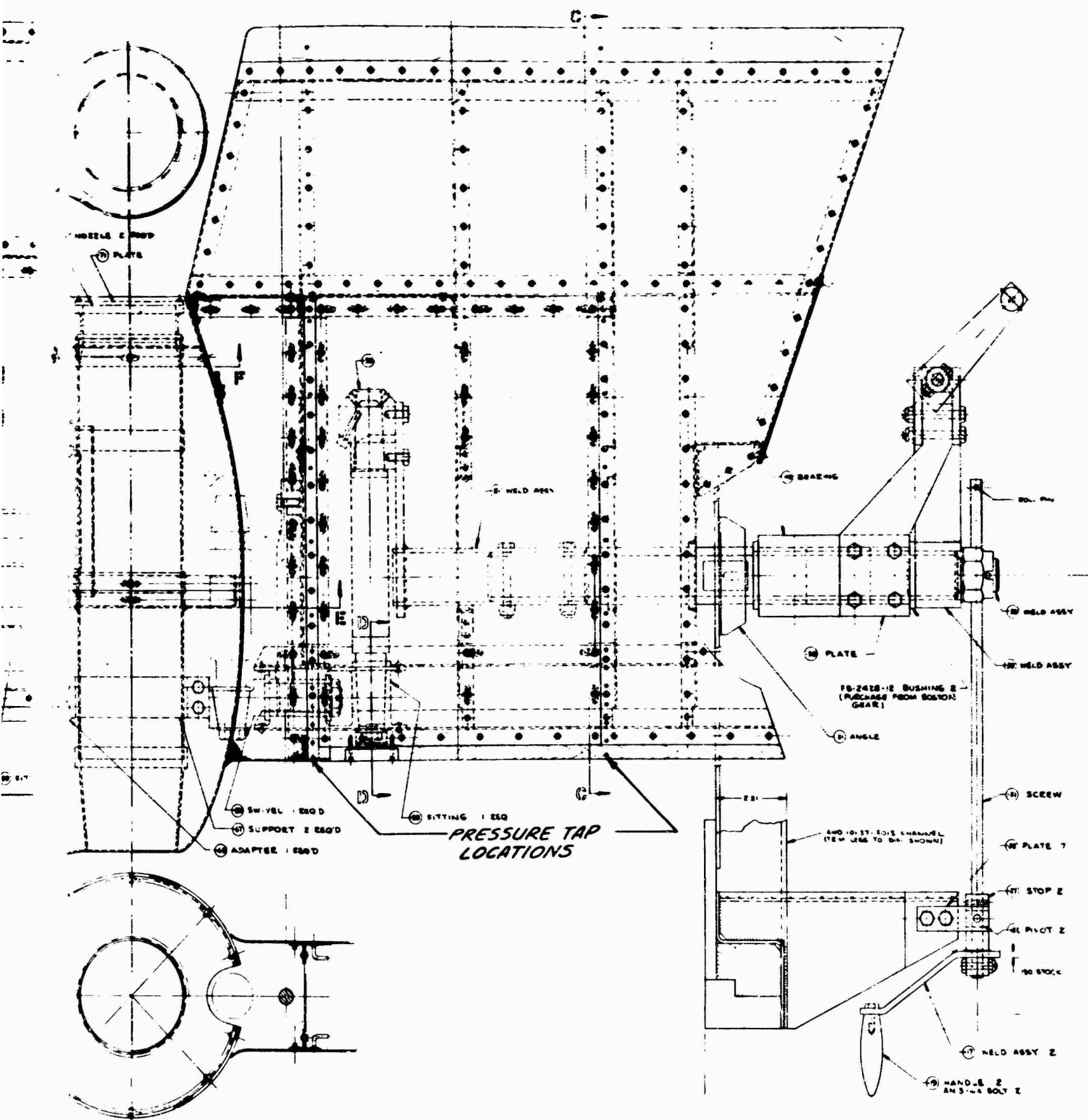
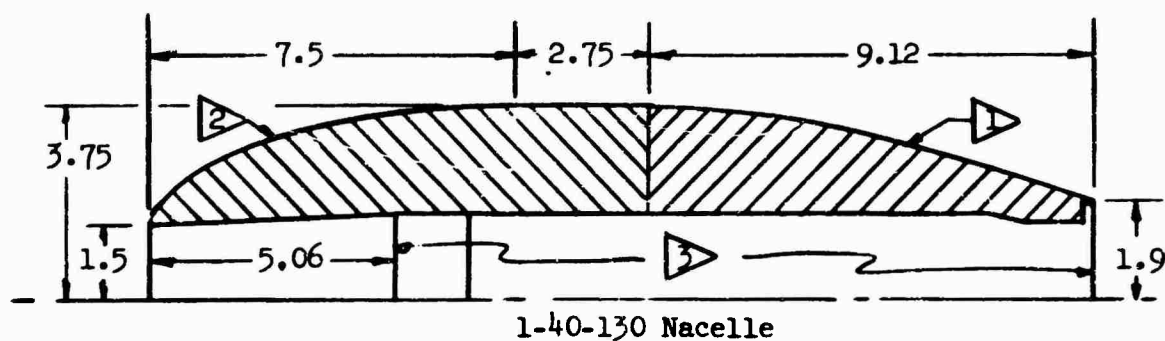
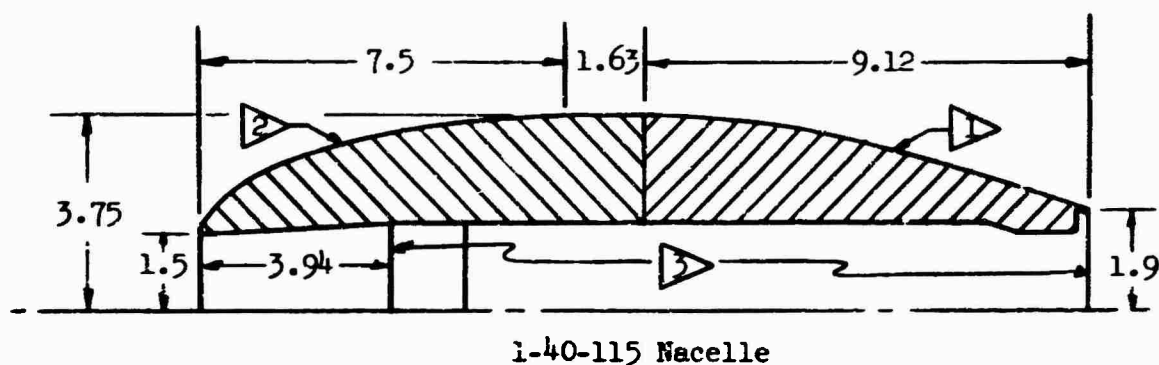
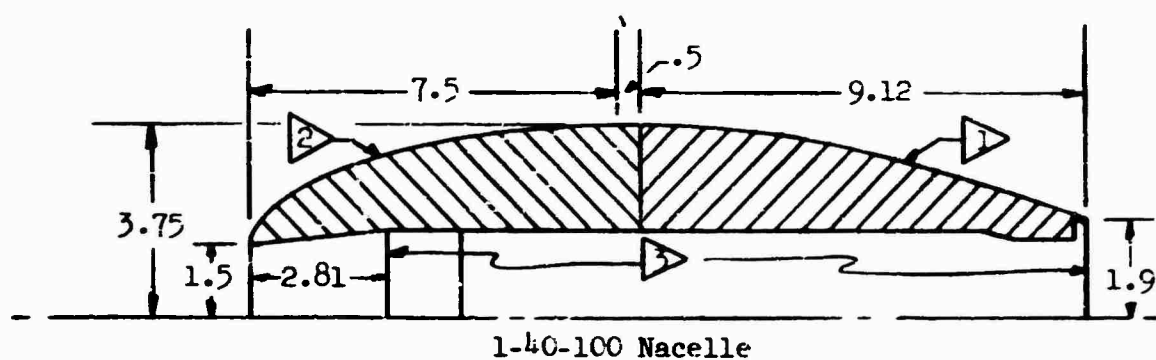


Figure 6. Model Assembly Drawing, Twin Side-



Model Assembly Drawing, Twin Side-By-Side Configuration.

B



Notes:




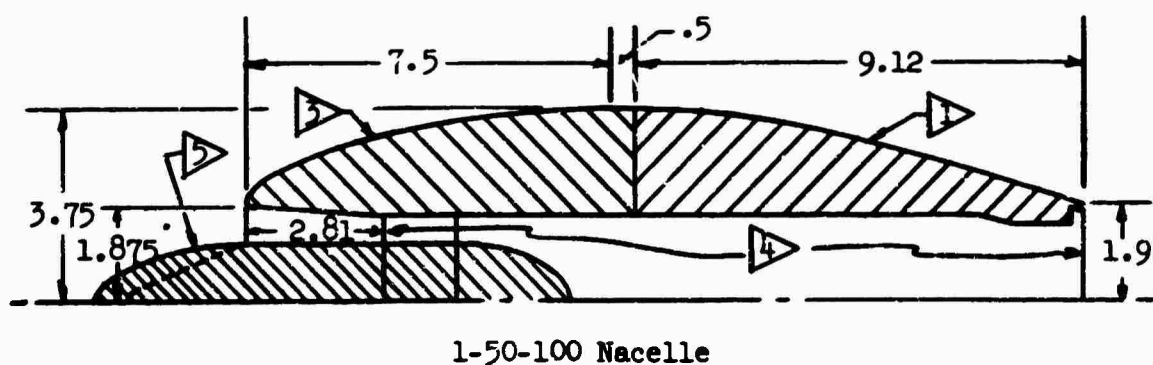
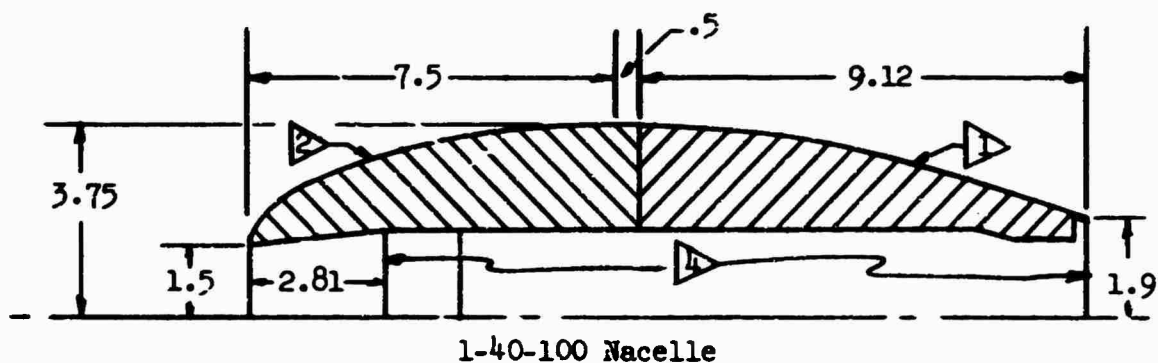
-  Afterbody contour identical all nacelles. See Fig. 11.
-  1-40 forebody contour. See Figure 9.
-  Internal dimensions identical all nacelles. See Fig. 6.

Figure 7. Single Nacelle Comparisons.



Notes:

- 1 Afterbody contour identical all nacelles. See Figure 11.
- 2 1-40 } forebody contour. See Figure 9.
- 3 1-50 }
- 4 Internal dimensions identical all nacelles. See Figure 6.
- 5 Centerbody profiles detailed on Figure 12.

Figure 8. Single Nacelle Comparisons.

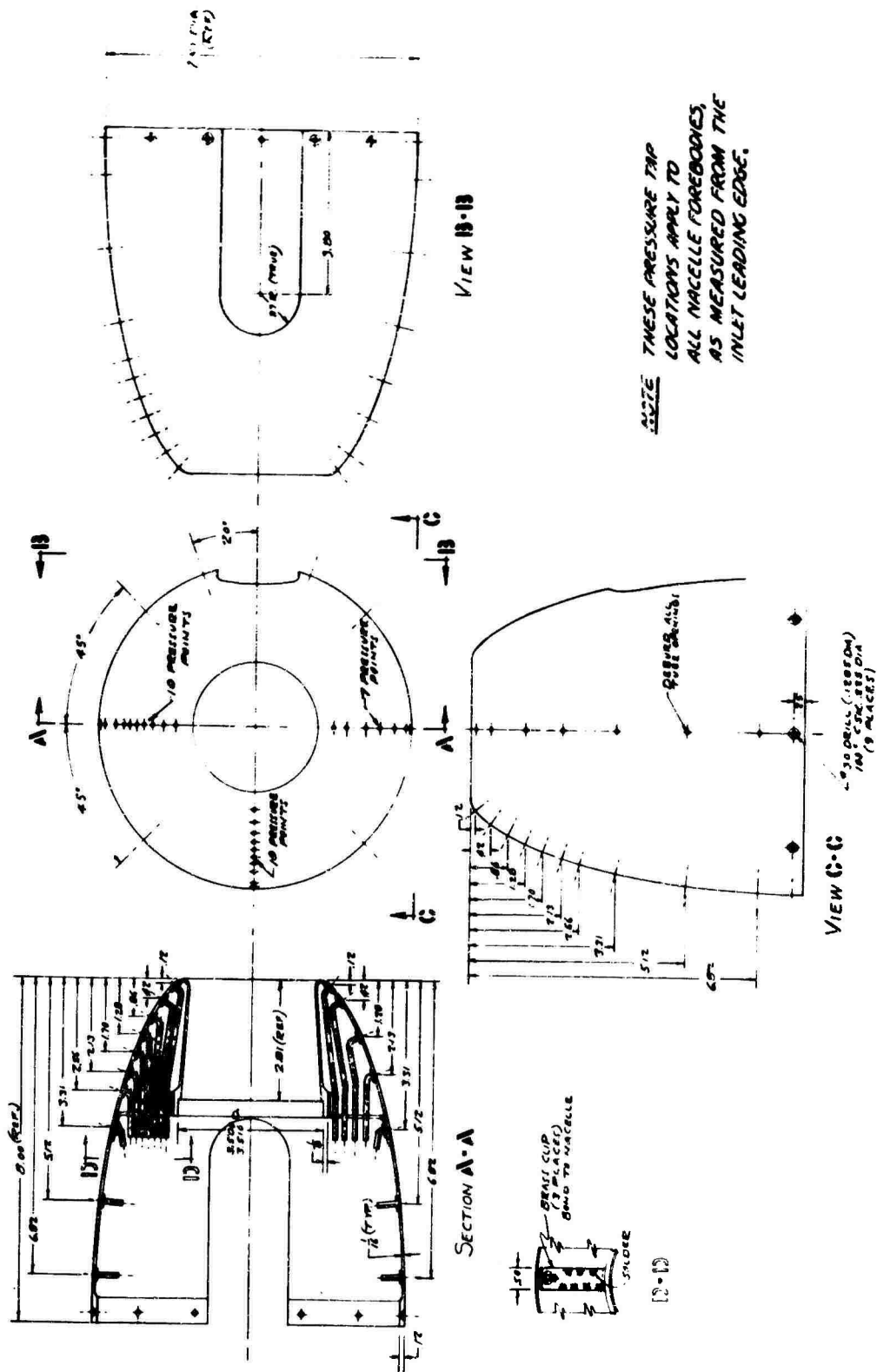
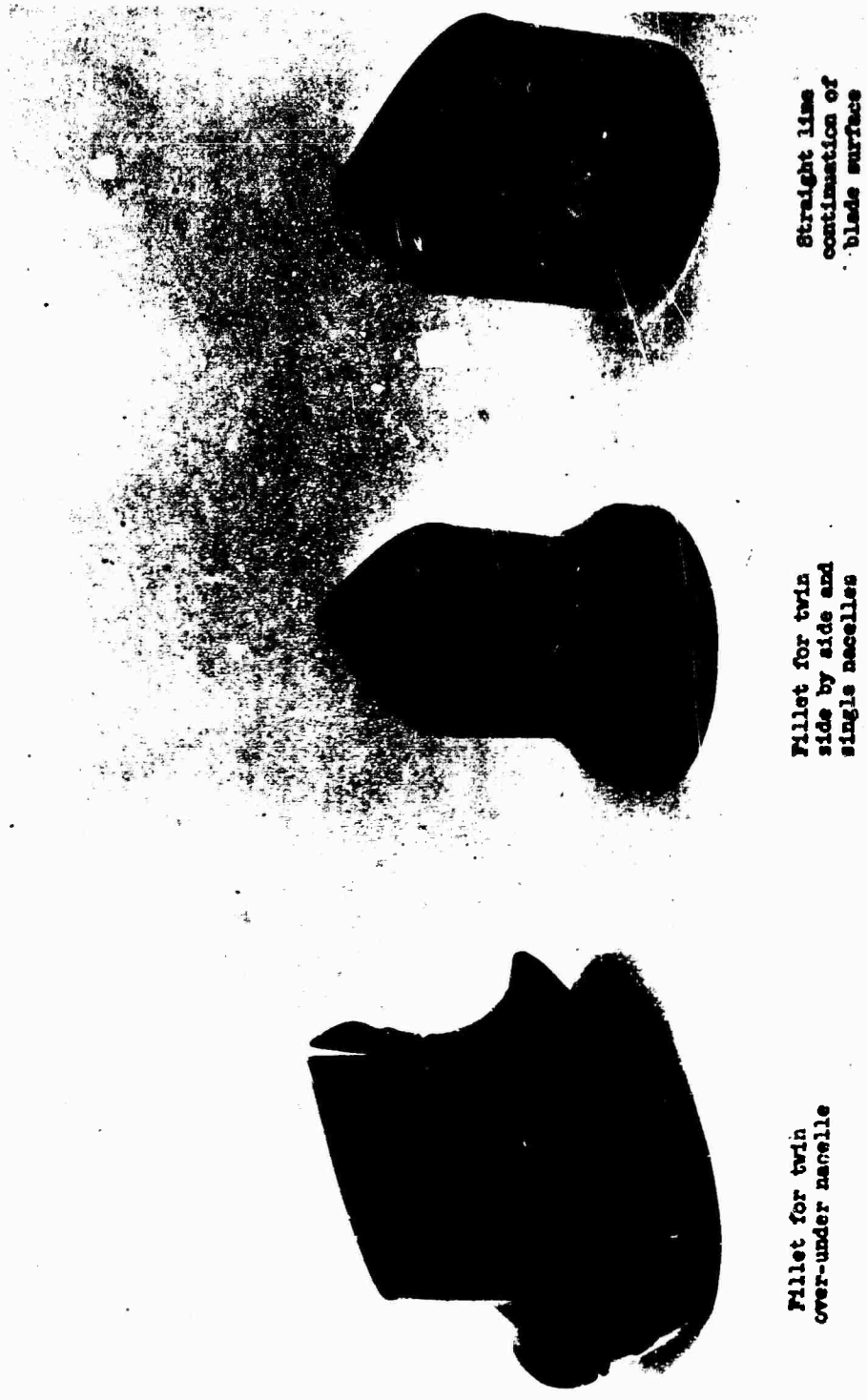


Figure 10. Nacelle Forebody Pressure Tap Locations.

[illegible]

Figure 11. Nacelle Afterbody Contour and Pressure Locations.





Fillet for twin
over-under nacelle

Fillet for twin
side by side and
single nacelles

Straight line
continuation of
blade surface

Figure 15. Comparison of Fillets for Blade-Nacelle Junction.

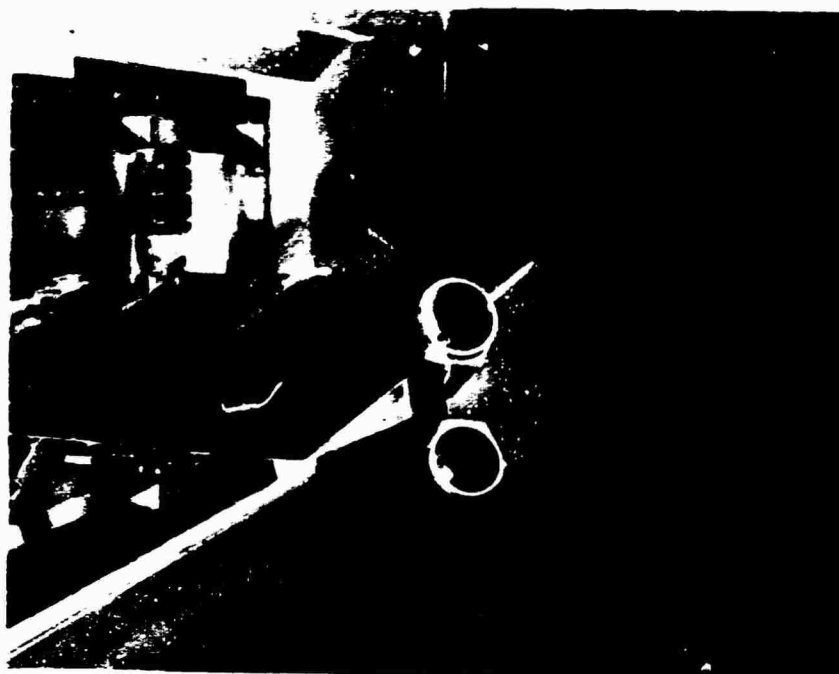


Figure 16. Twin Over-Under Nacelle With and Without Trailing Edge Wake Fairing.

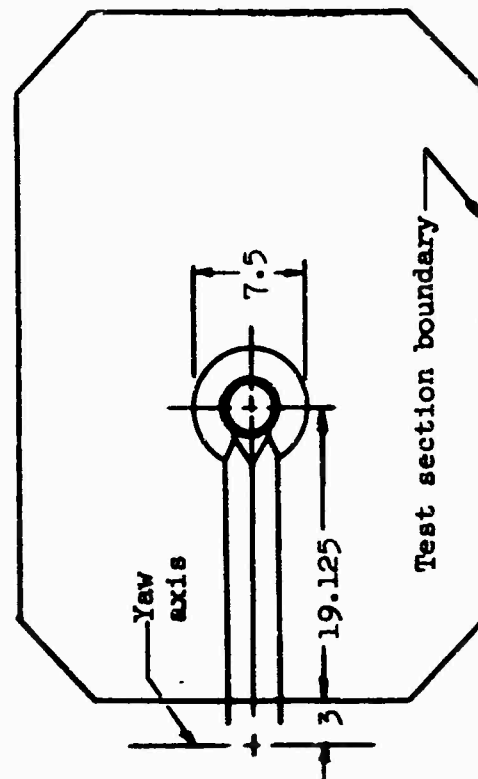
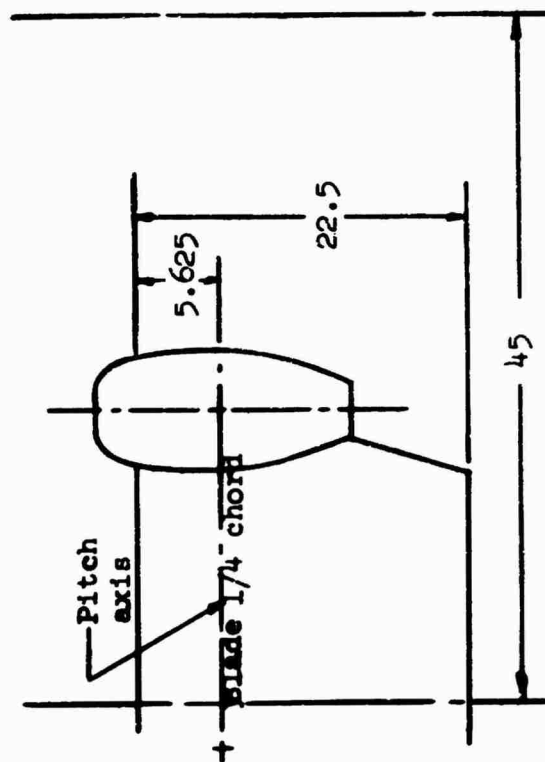


Figure 17. Single Nacelle Model Assembled in Test Section.

l	Nacelle
17.12	1-40-100
18.25	1-40-115
19.37	1-40-130
17.12	1-50-100

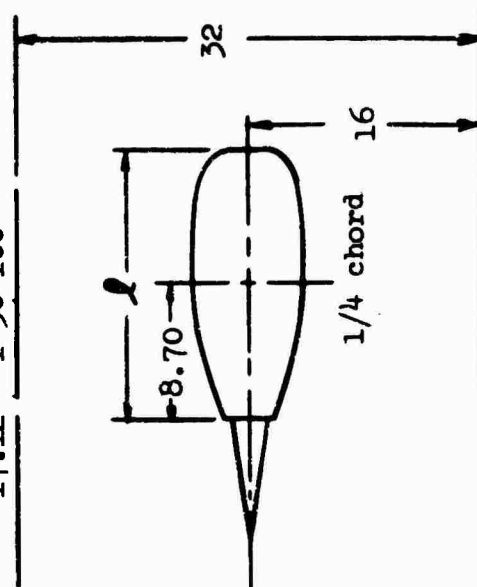


Figure 18. Twin Over-Under Nacelle Assembled in Test Section.

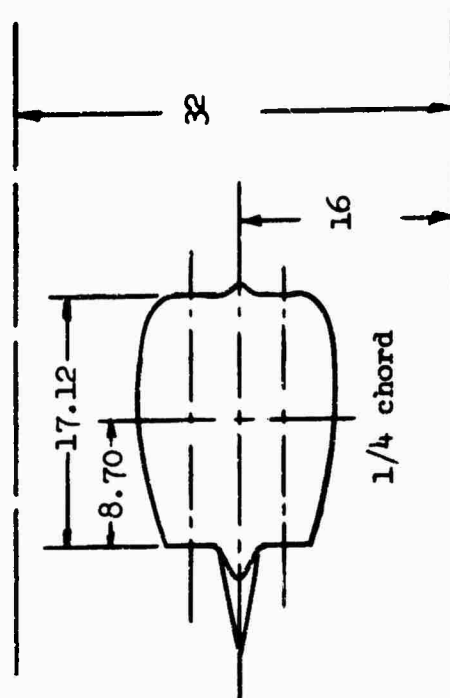
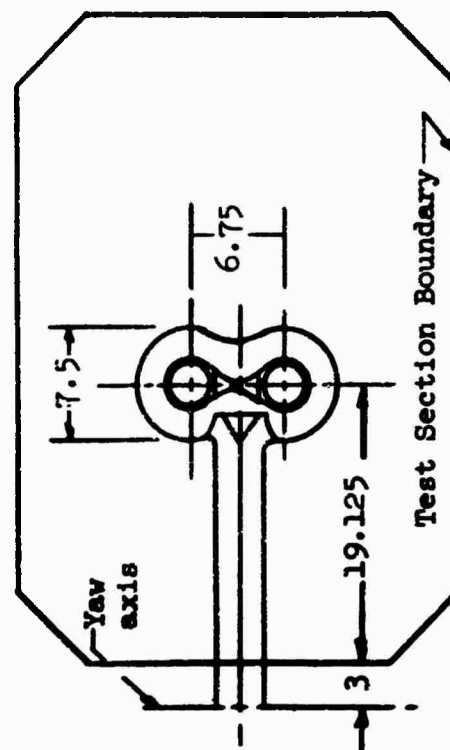
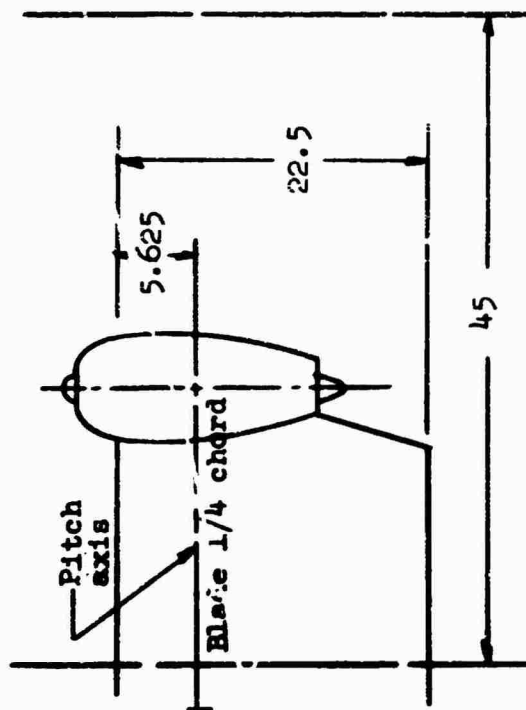


Figure 19. Twin Side-by-Side Nacelle
Assembled in Test Section.

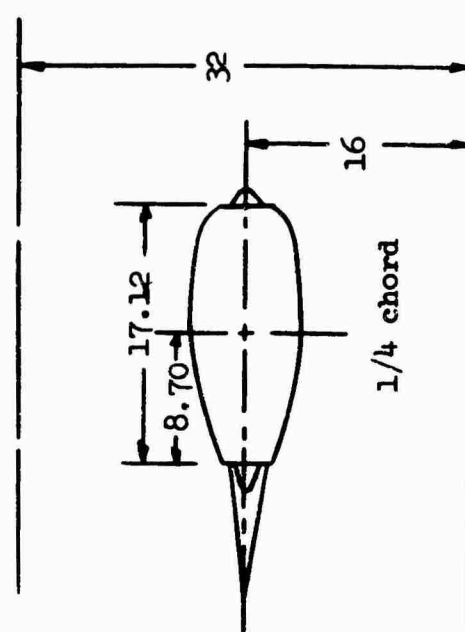
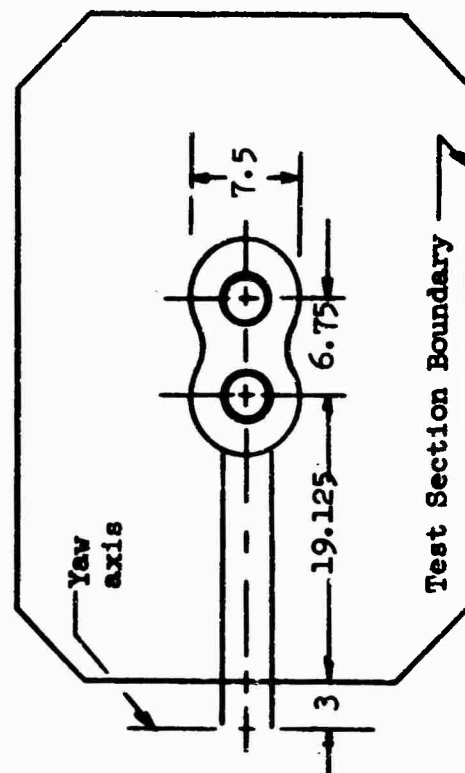
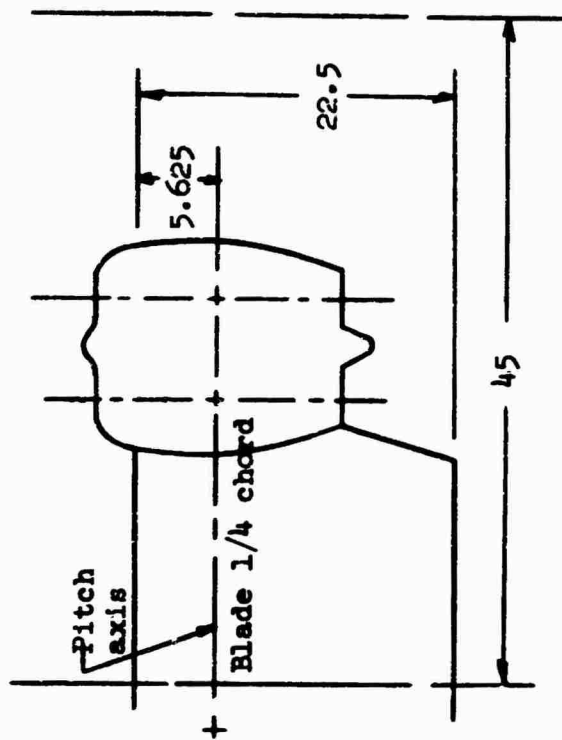




Figure 20. Blade Alone. Test Runs 1 Through 5.



Figure 21. Single 1-40-100 Nacelle and Blade. Runs 6 Through 62.

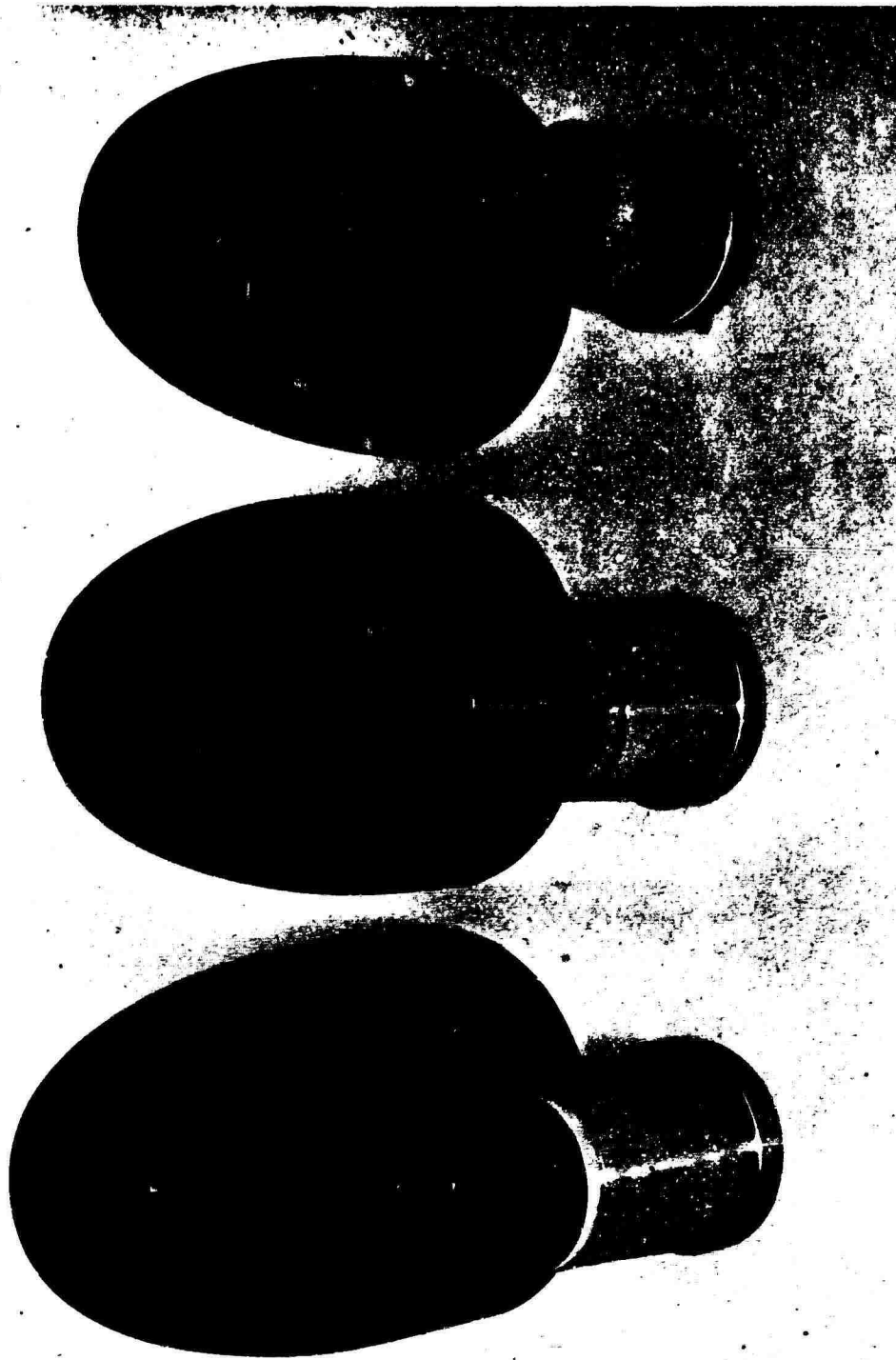


Figure 22. Comparison of 1-40-XXX Forebodies. Runs 63 Through 92.

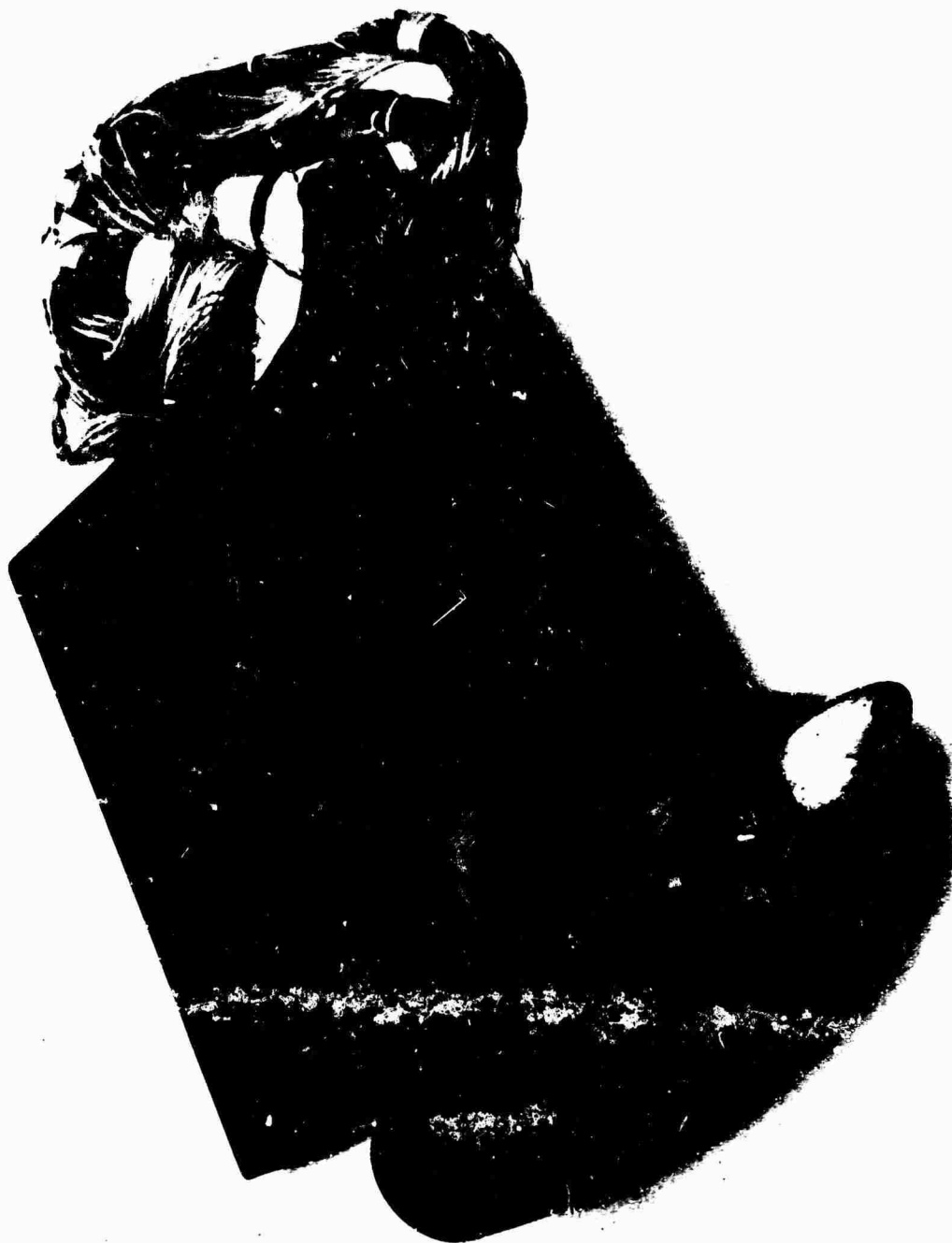


Figure 23. Single 1-50-100 Nacelle With Parabolic Centerbody and Blade.
Runs 93 Through 117.



Figure 24. Single 1-50-100 Nacelle With Conical Centerbody and Blade.
Runs 118 Through 132.



Figure 25. Twin 1-40-100 Over Under Nacelle and Blade. Runs 133 Through 157.



Figure 26. Twin 1-40-100 Side-by-Side Nacelle and Blade. Runs 158 Through 187.

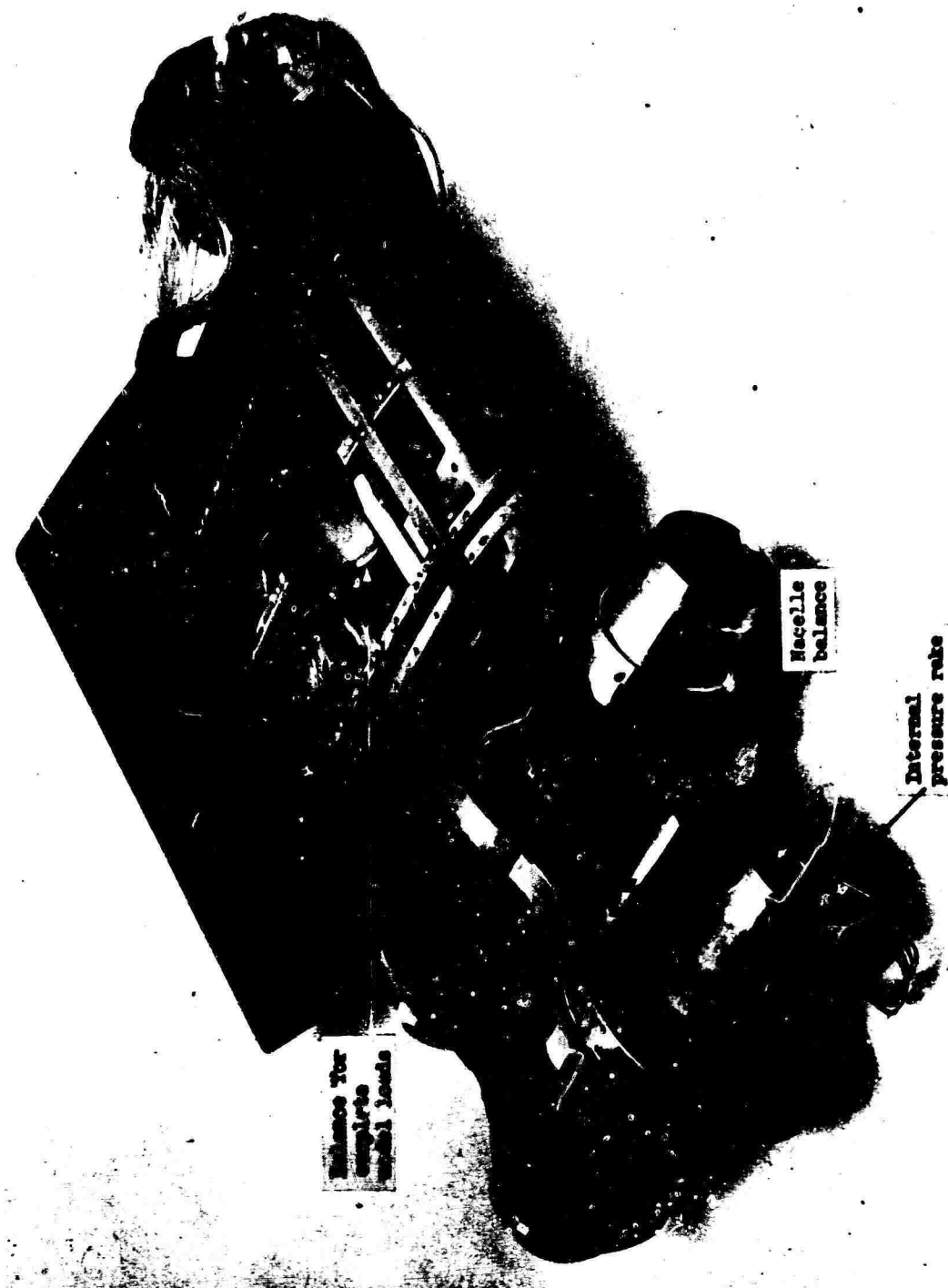
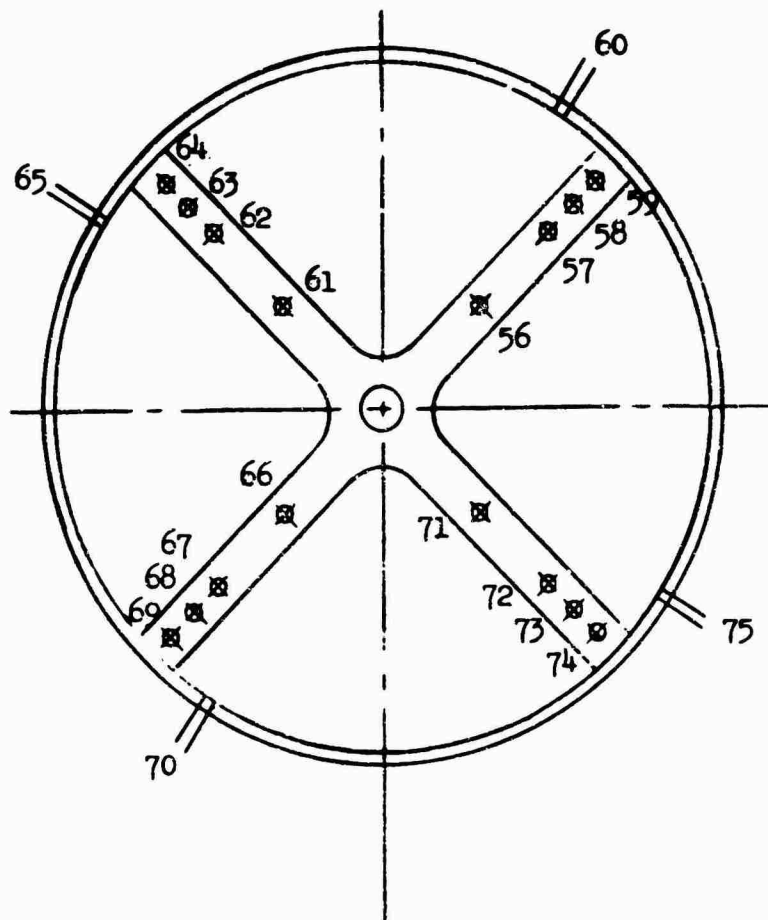


Figure 27. Internal Support Structure - Side-by-Side Configuration.



Front View

Figure 28. Compressor Face Inlet Pressure Tap Locations - All Single Engine Configurations.

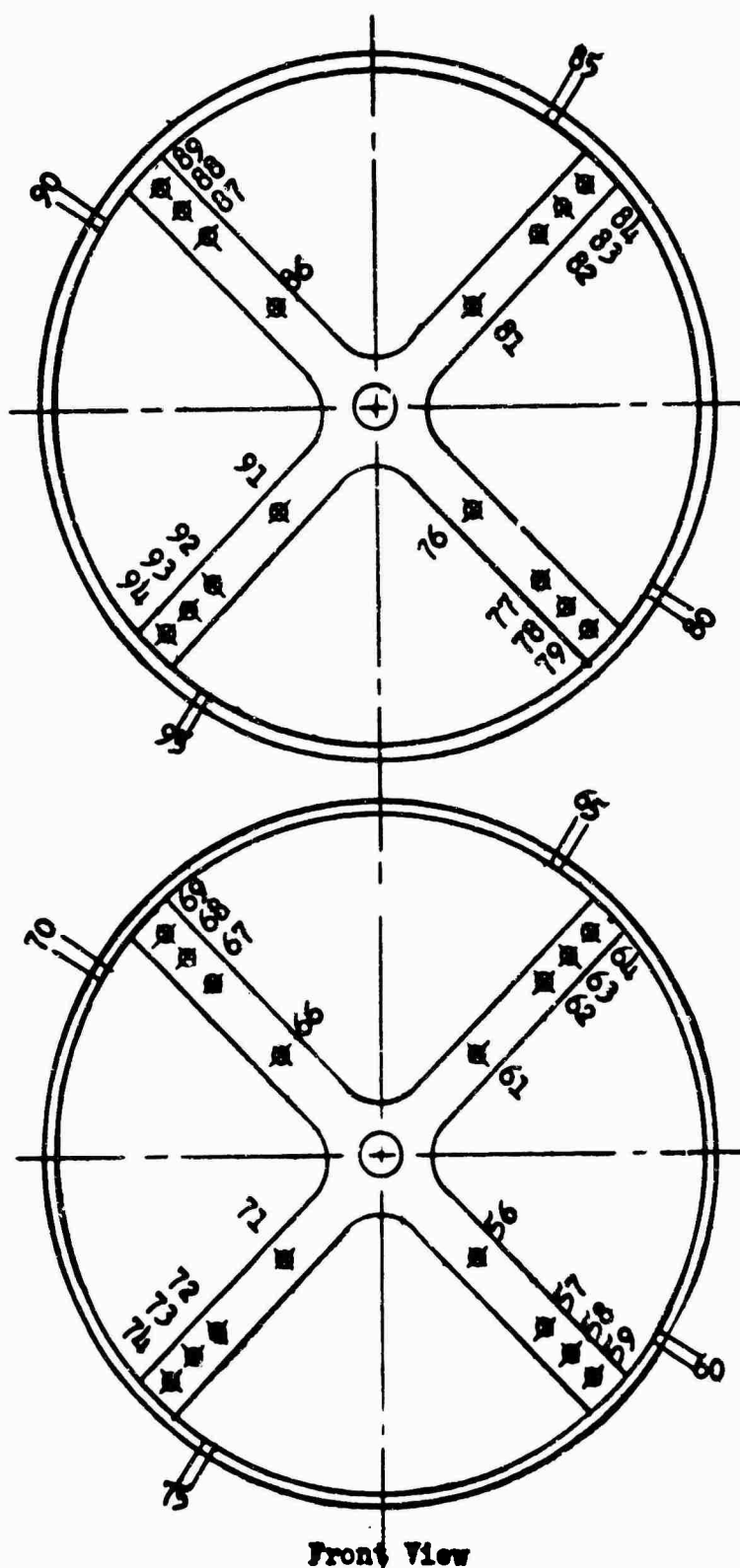
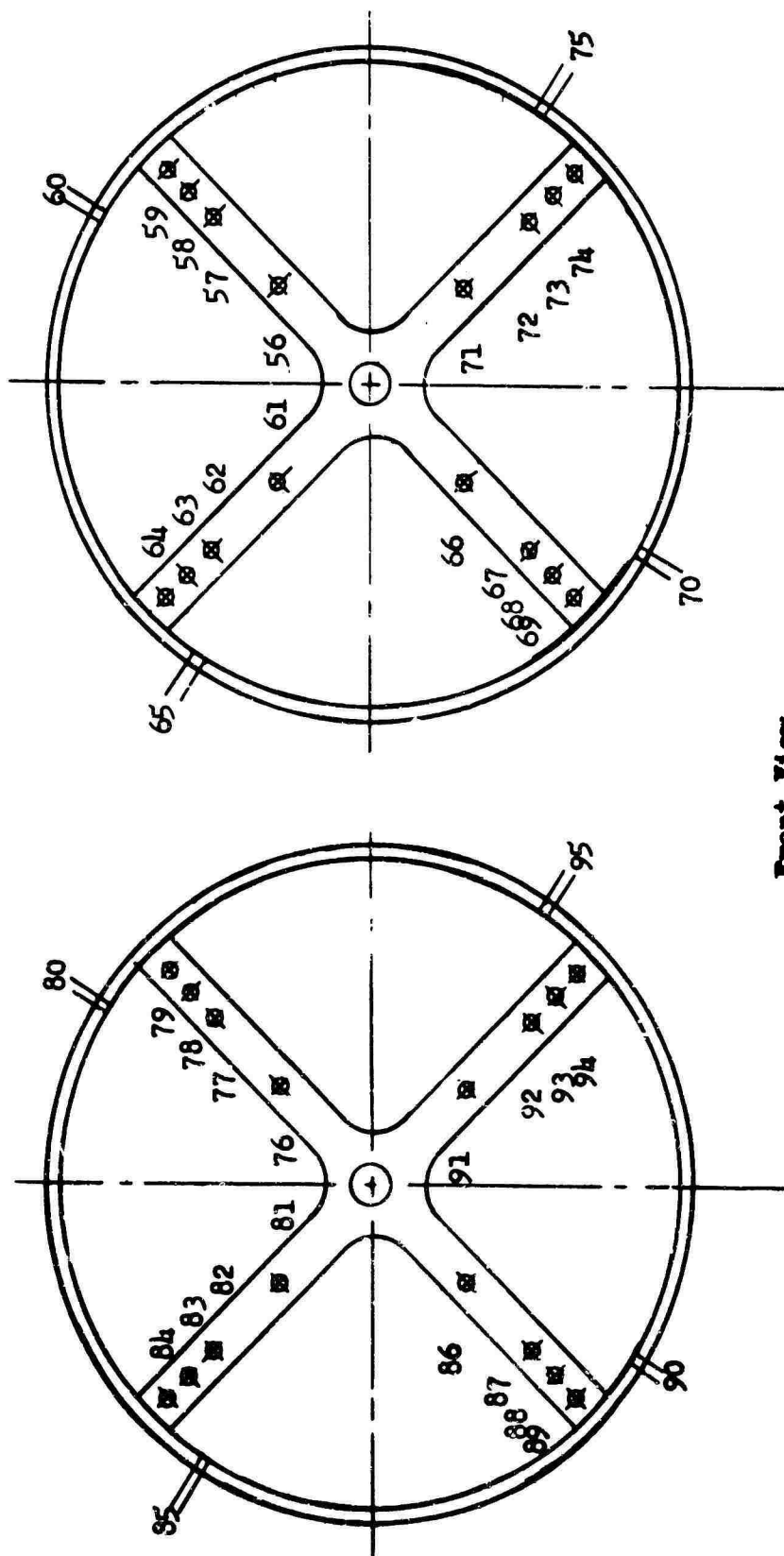


Figure 29. Compressor Face Inlet Pressure Tap Locations - Over-Under Configuration.



Front View

Figure 30. Compressor Face Inlet Pressure Tap Locations - Side-by-Side Engine Configuration.

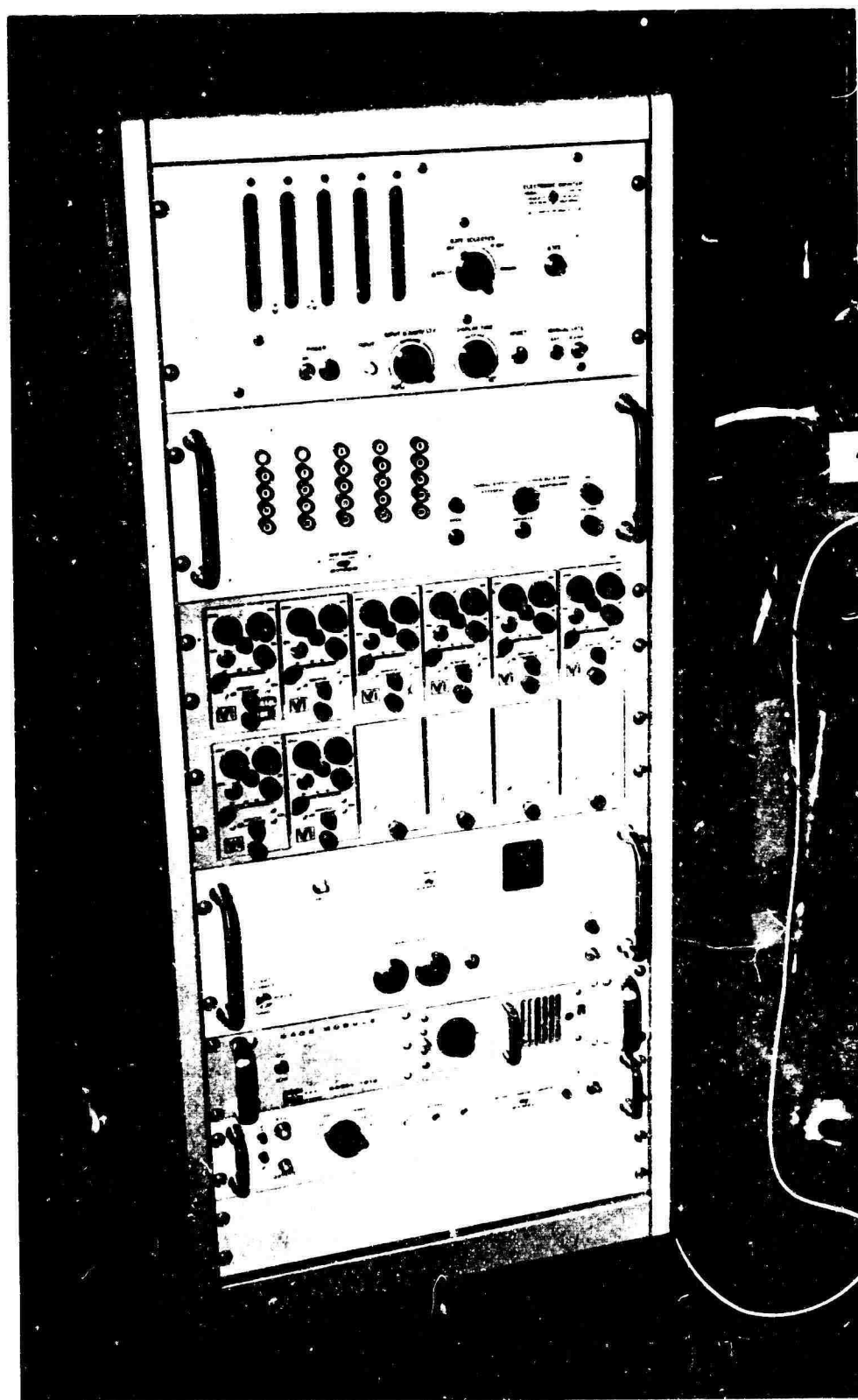


Figure 31. Dymec Multiple Channel Data Logging System.

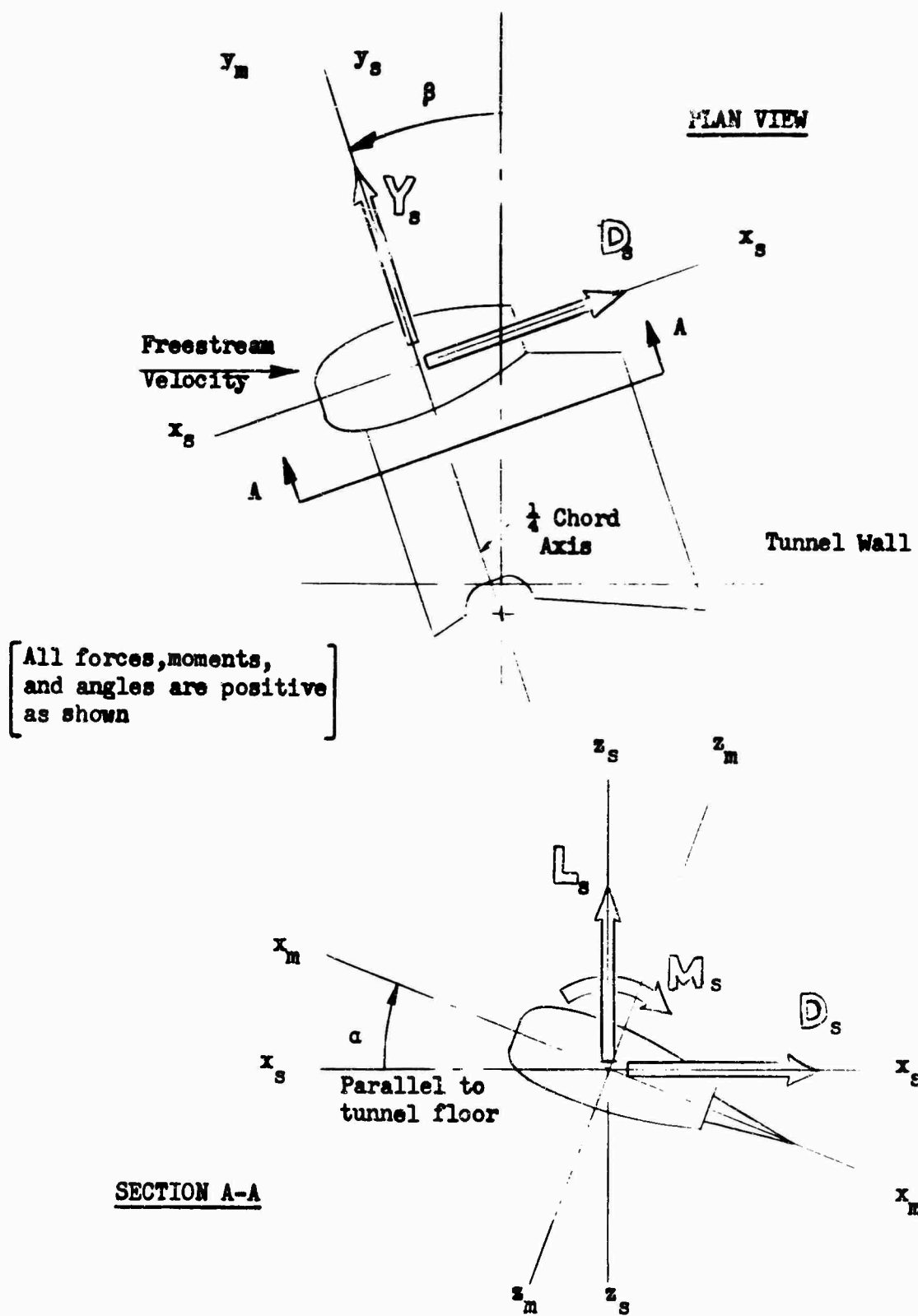


Figure 32. Force and Moment Reference System, Plan and Section View .

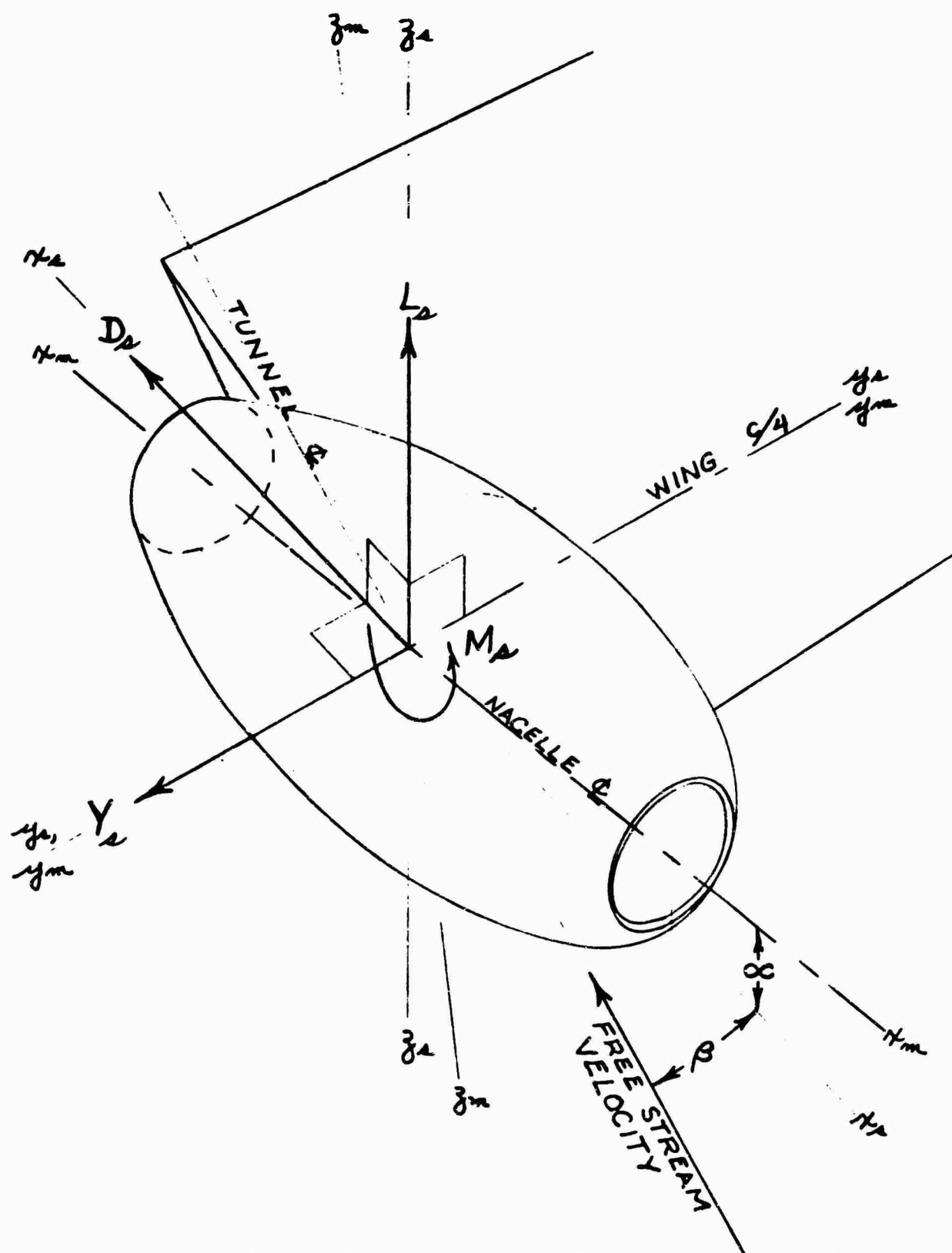


Figure 33. Force and Moment Reference System, Perspective View.

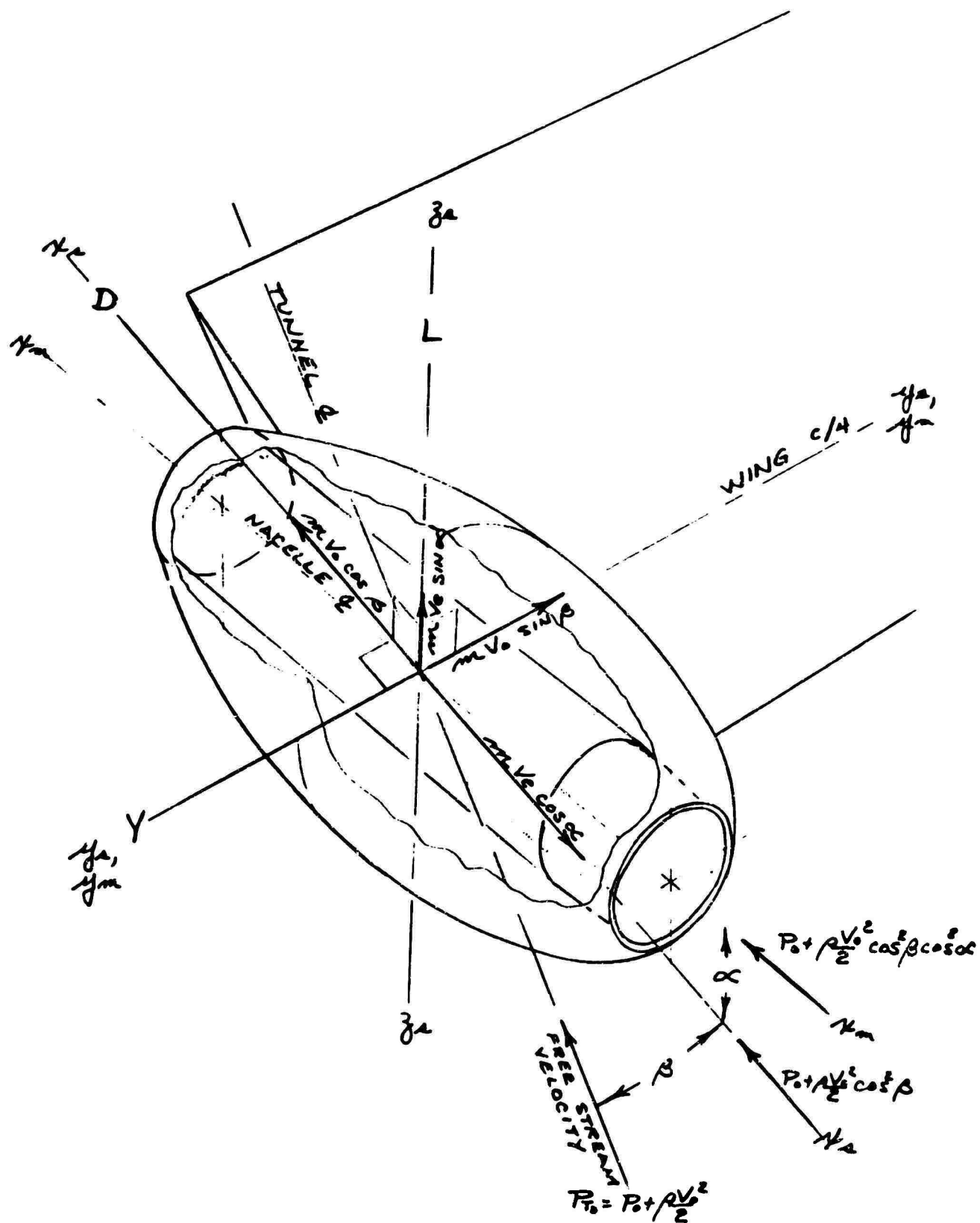


Figure 34. Internal Airloads, Perspective View.

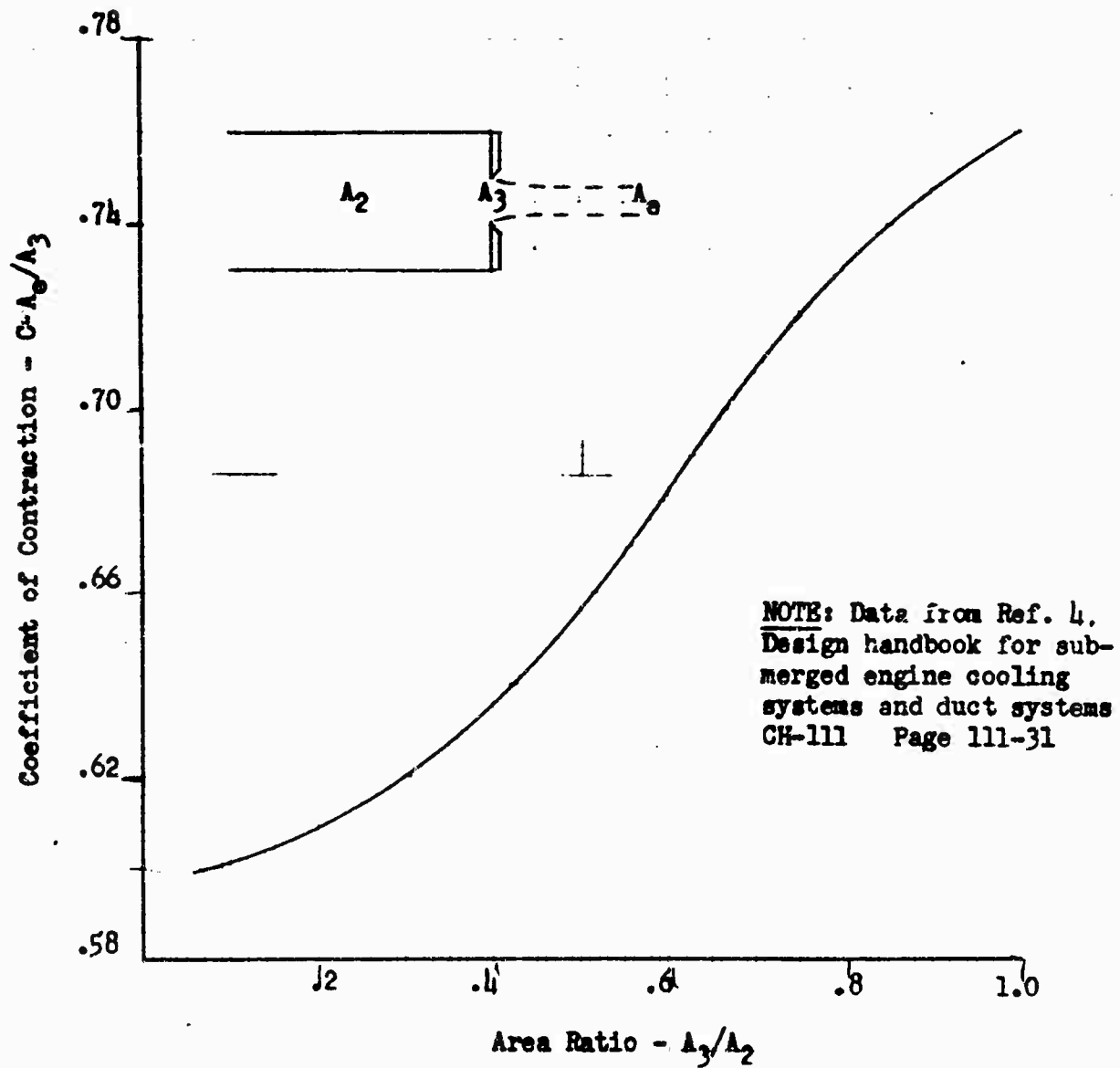
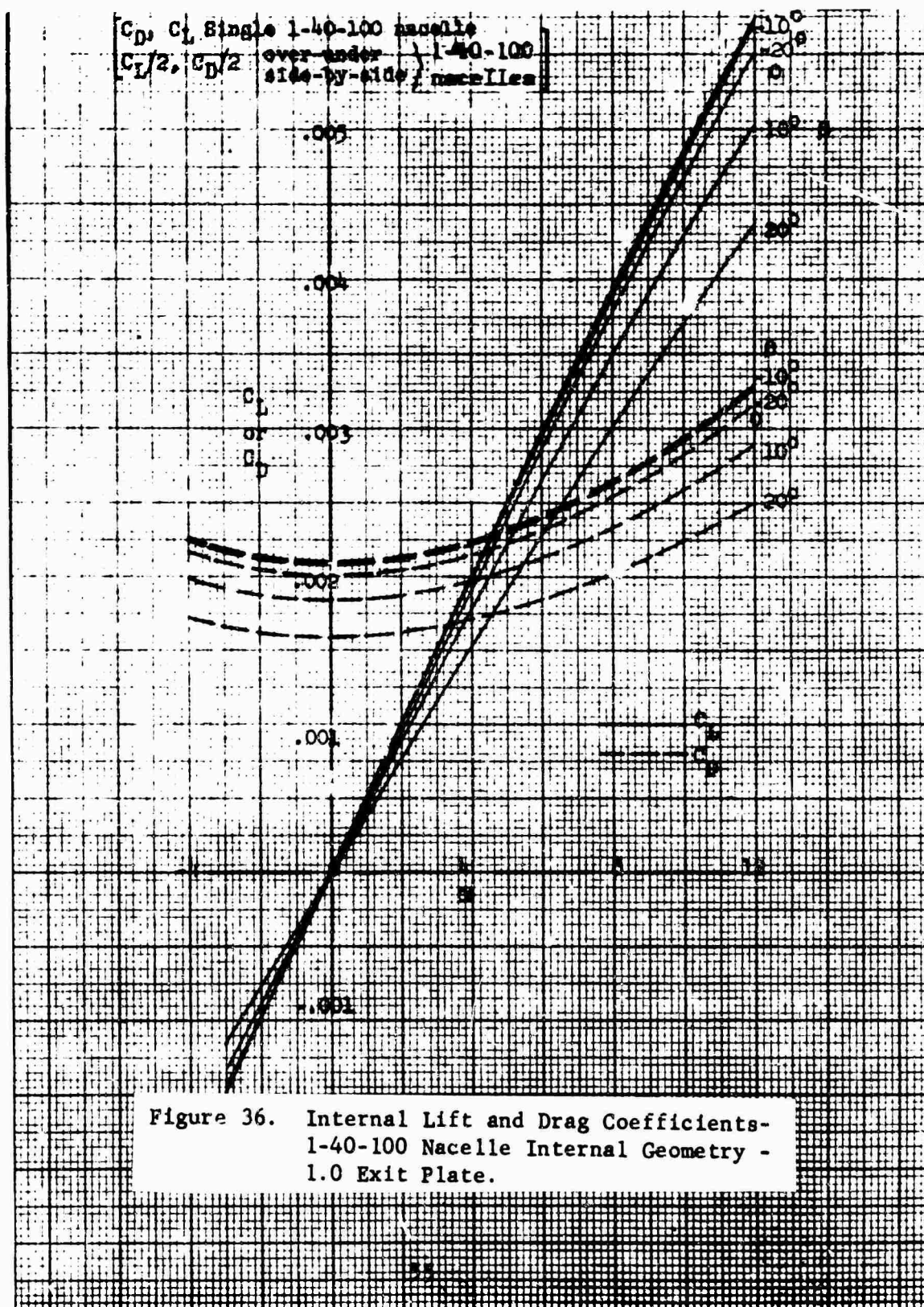


Figure 35. Exit Flow Contraction Ratio.



C_y for single 1-40-100 nacelle

$C_y/2$ for over-center or side-by-side nacelles

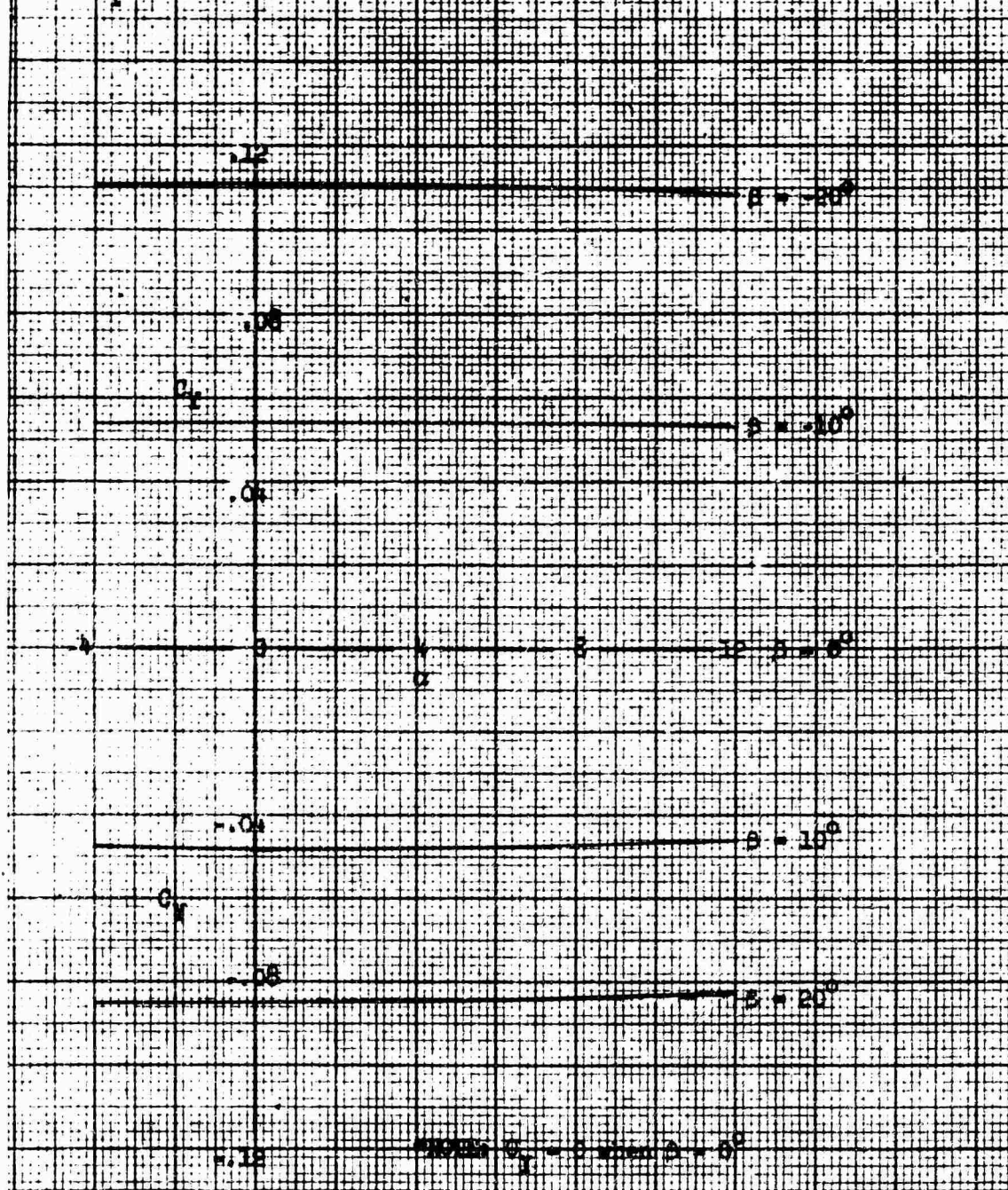
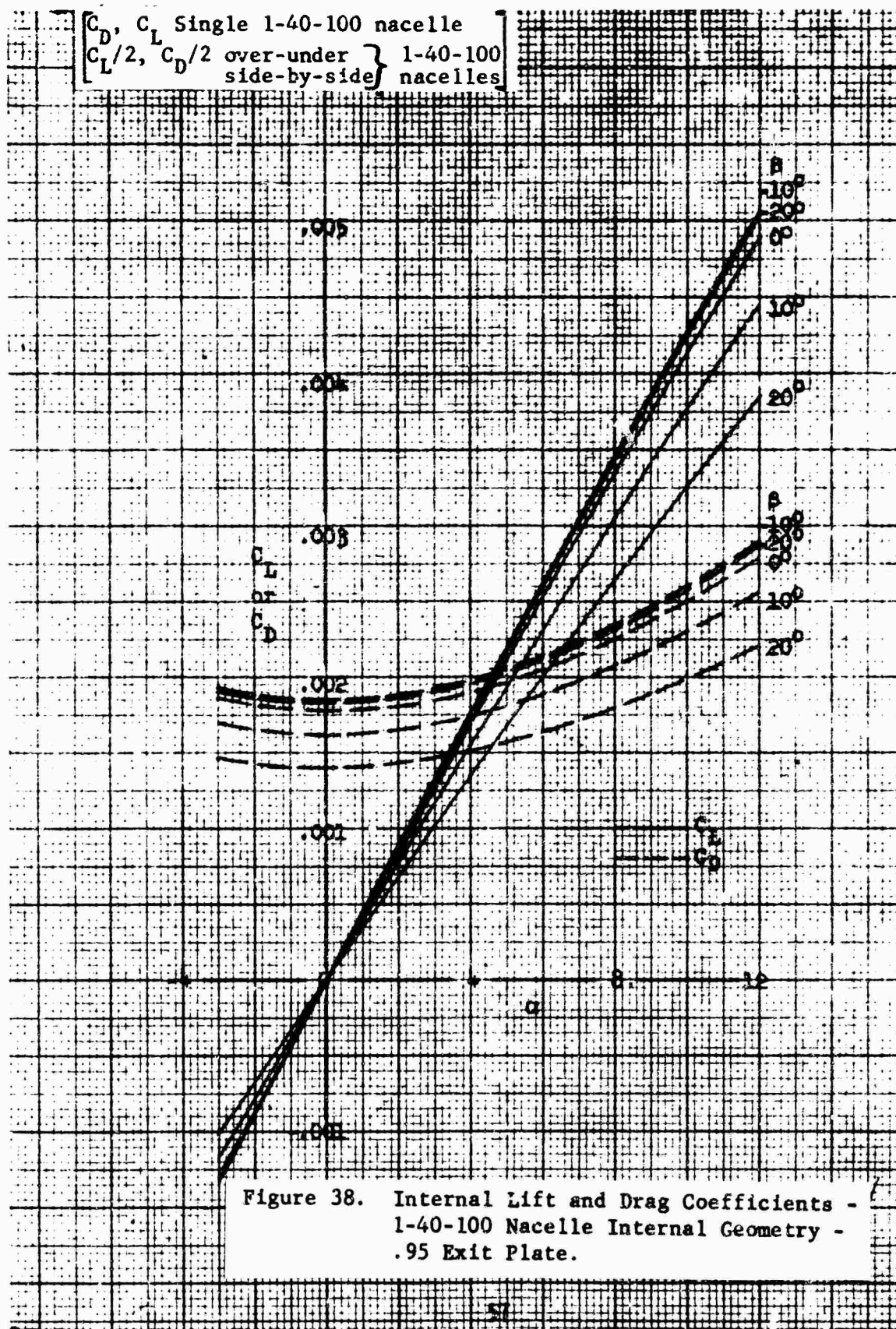


Figure 37. Internal Side Load Coefficient -
1-40-100 Nacelle Internal Geometry -
1.0 Exit Plate.



C_Y for single 1-40-100 nacelle

$C_Y/2$ for over-under or side-by-side nacelles

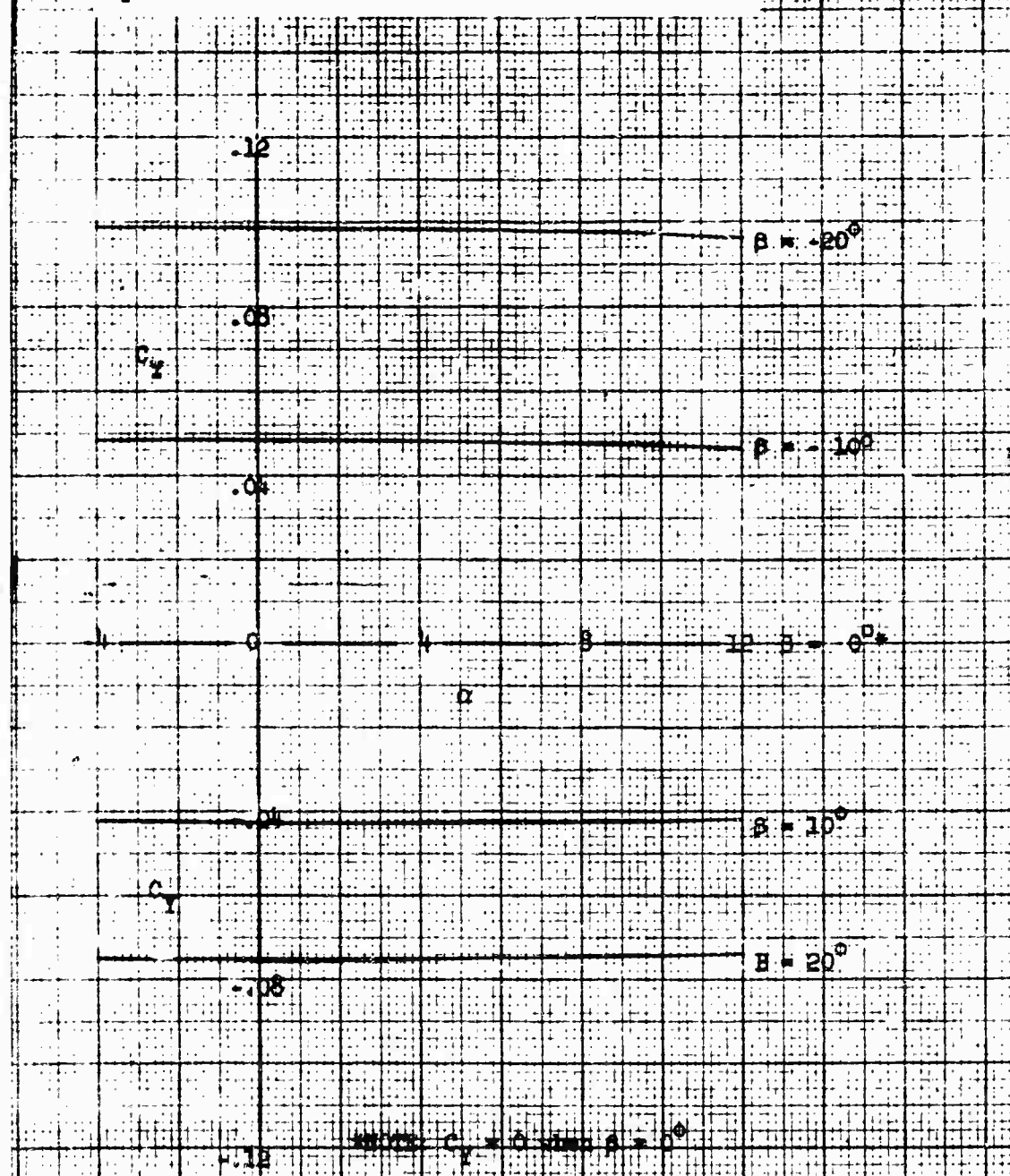
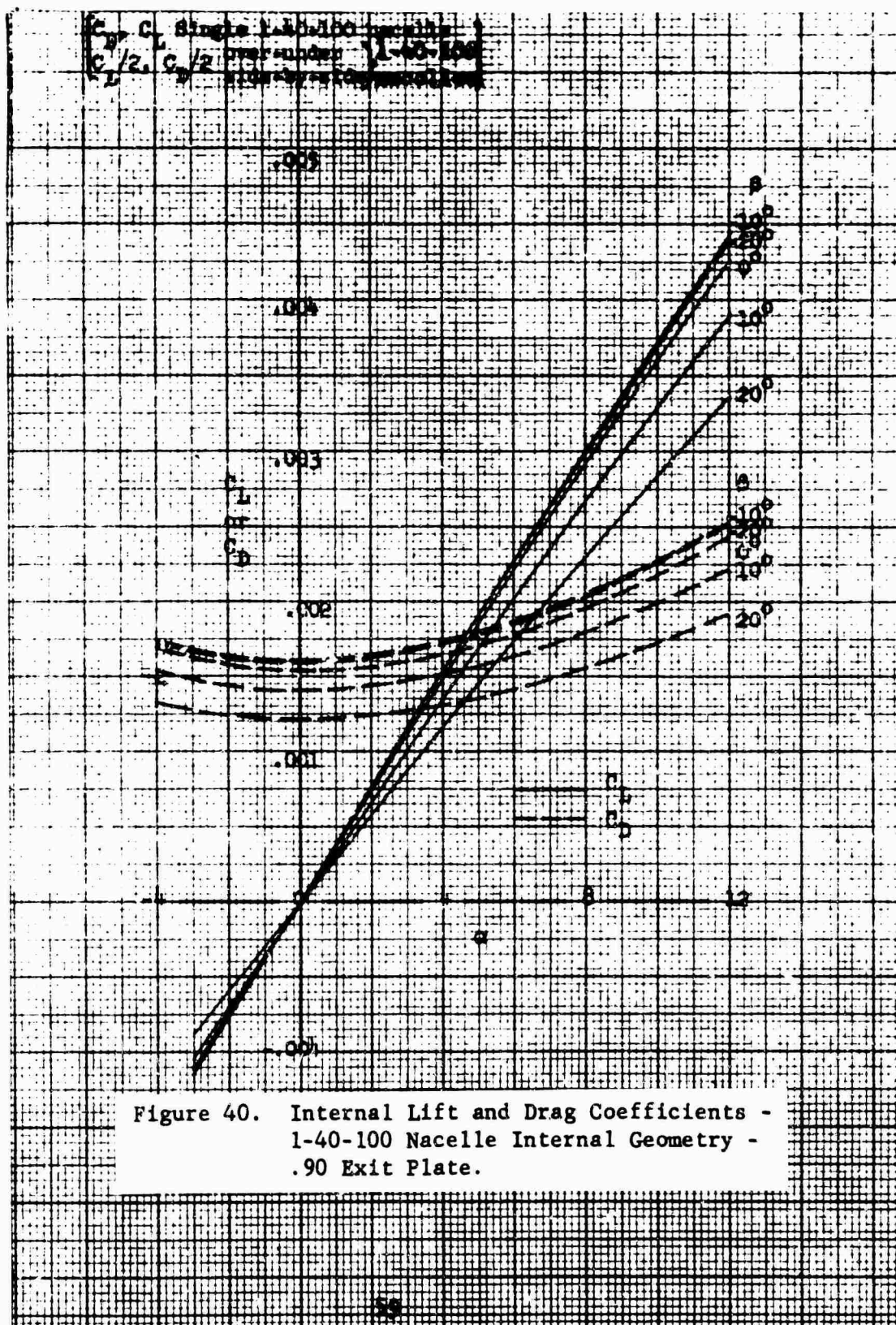
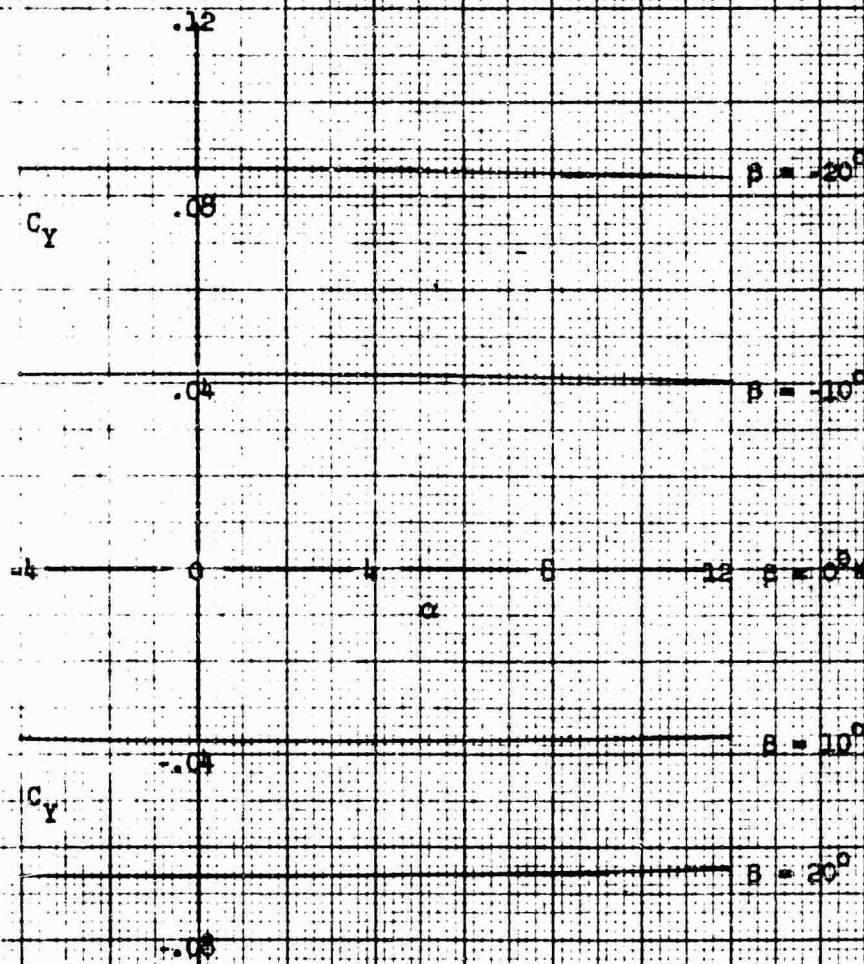


Figure 39. Internal Side Load Coefficient -
1-40-100 Nacelle Internal Geometry -
.95 Exit Plate.



C_Y for single 1-40-100 nacelle

$C_Y/2$ for over-under or side-by-side nacelles



*NOTE: $C_Y = 0$ when $\beta = 0^\circ$

Figure 41. Internal Side Load Coefficient -
1-40-100 Nacelle Internal Geometry -
90 Exit Plane.

C_D, C_L Single 1-40-100 parabolic
 $C_D/2, C_L/2$ over-under (1-40-100)
 side-by-side parabolic

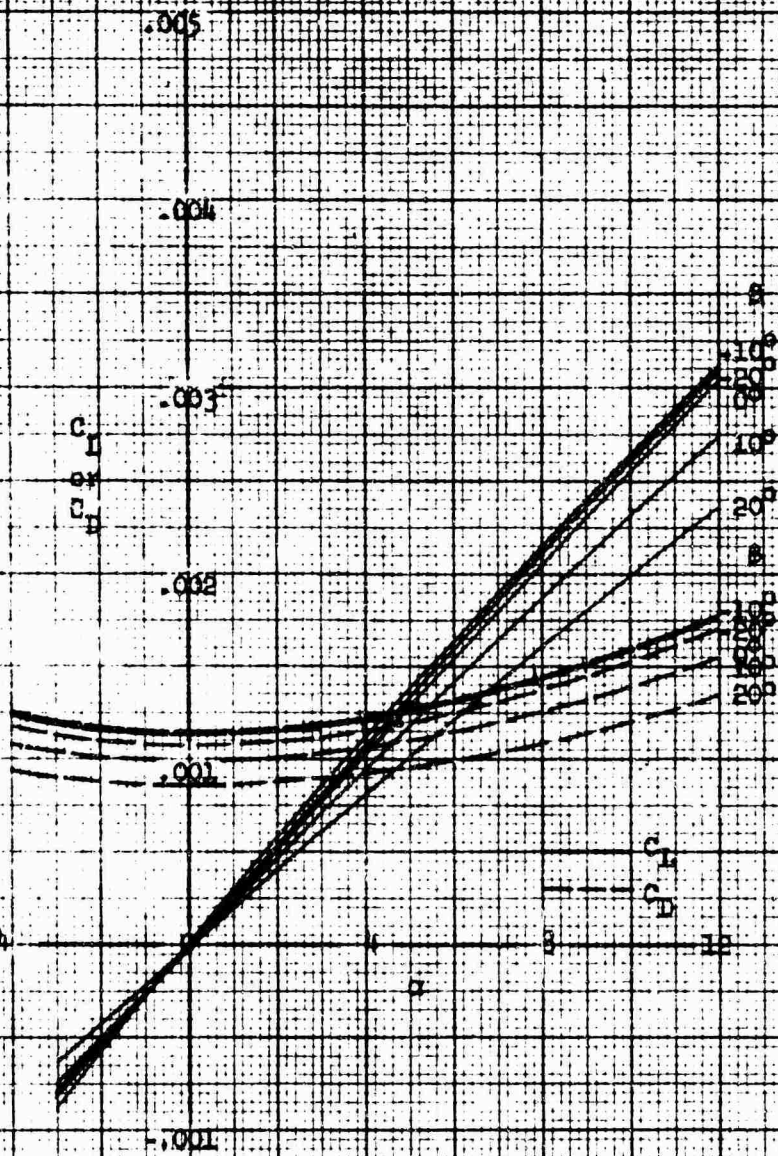


Figure 42. Internal Lift and Drag Coefficients -
 1-40-100 parabolic internal velocity
 75 ft. flat

C_y for single 1-40-100 parallel

$C_y/2$ for over-under or side-by-side assemblies

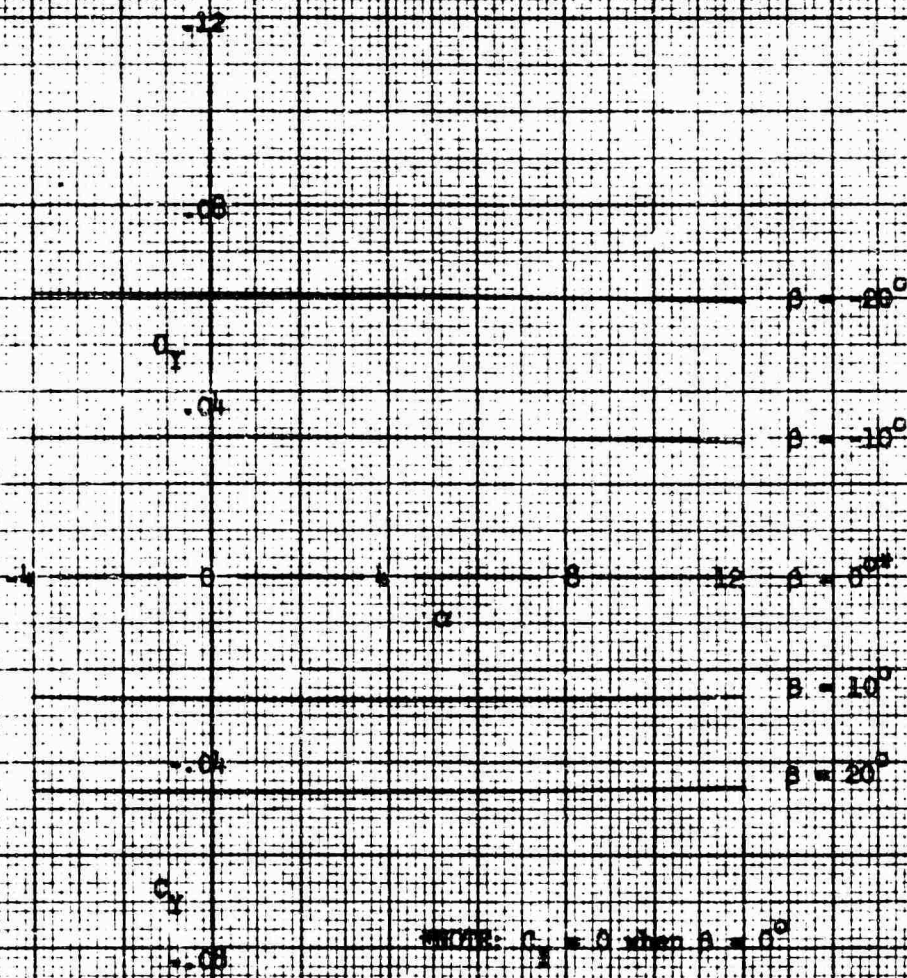
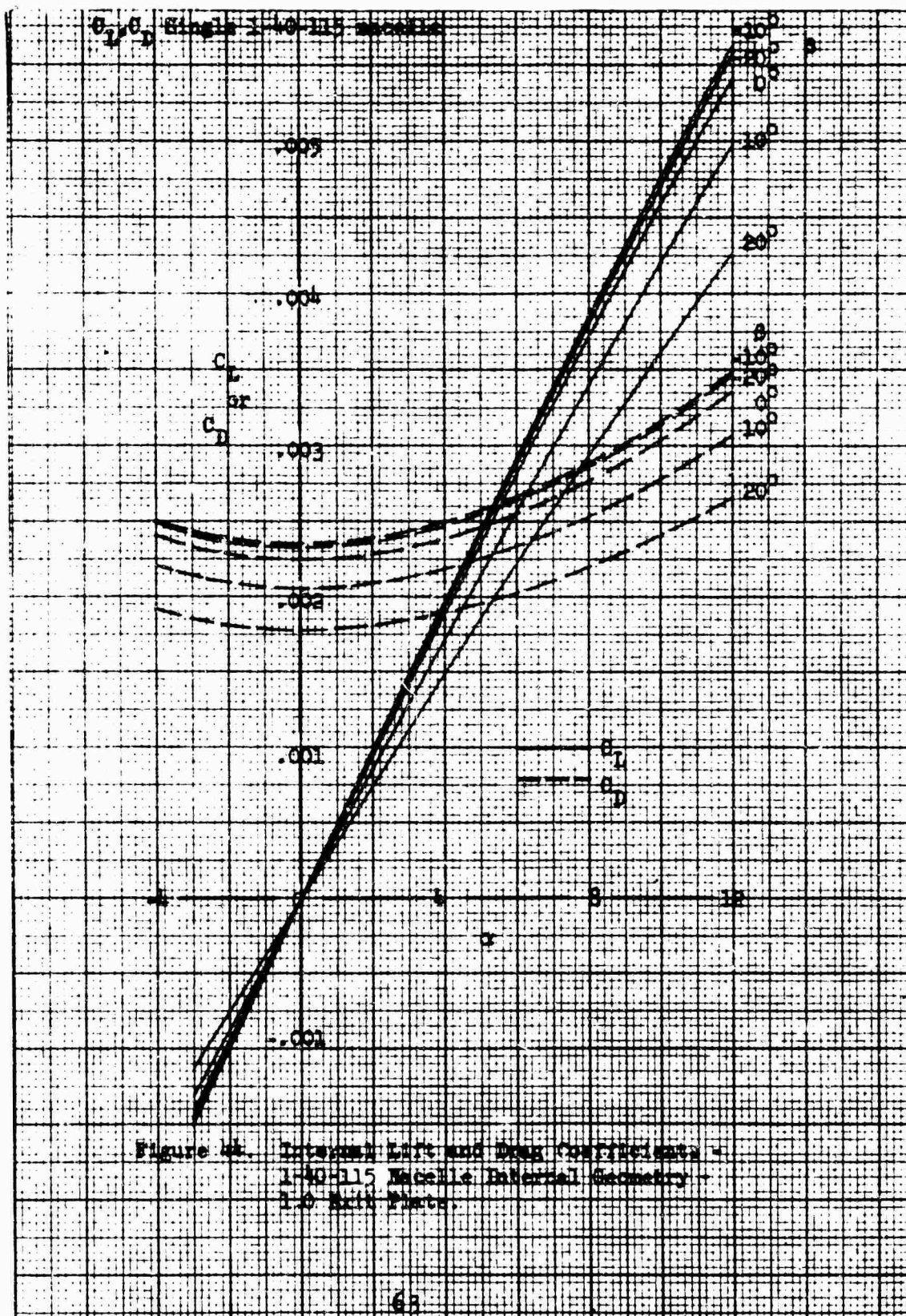
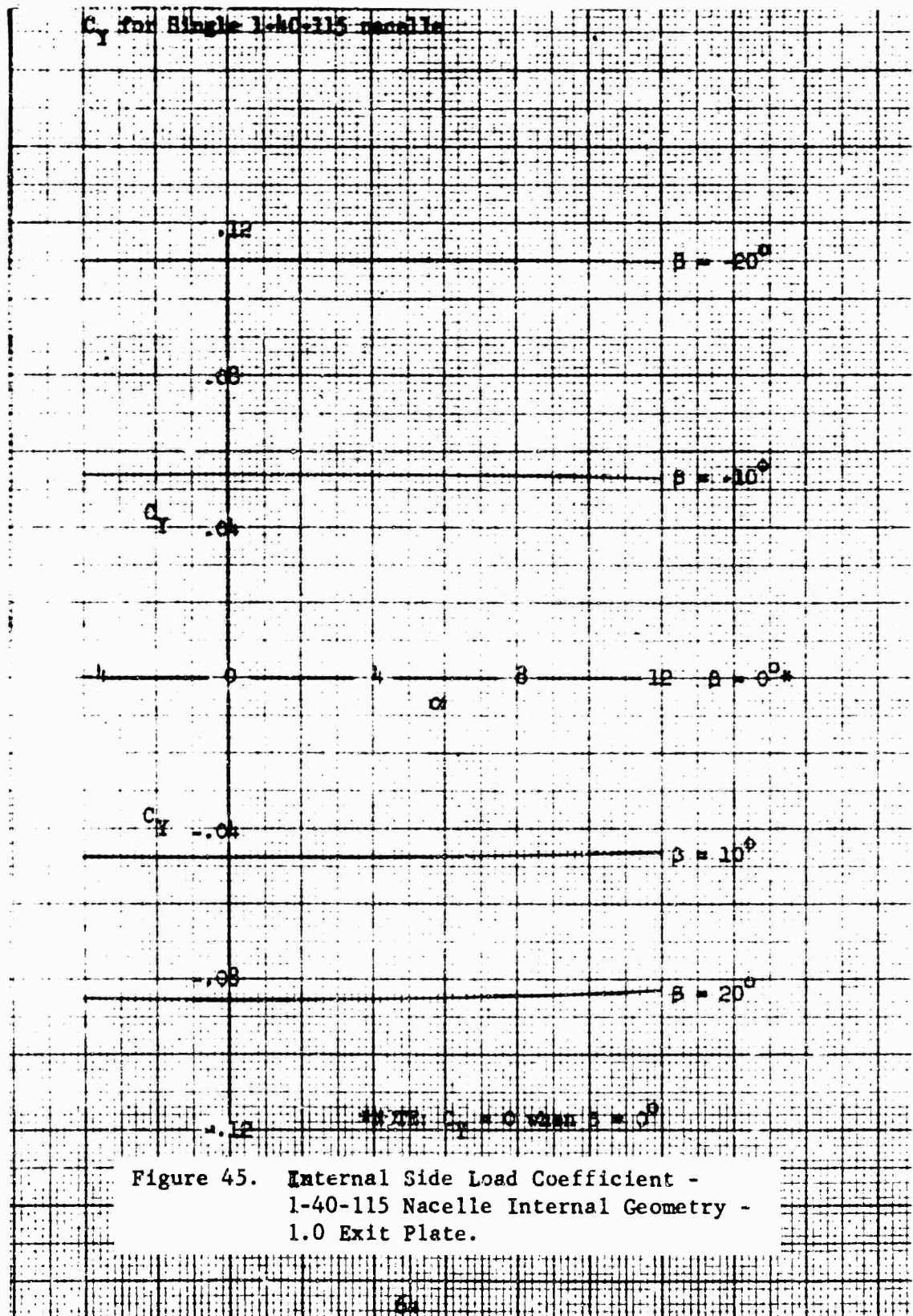


Figure 43. Internal Side Load Coefficient -
1-40-100 Parallel Internal Geometry -
18 Axis Plate





C_L, C_D Single 1-40-115 nacelle

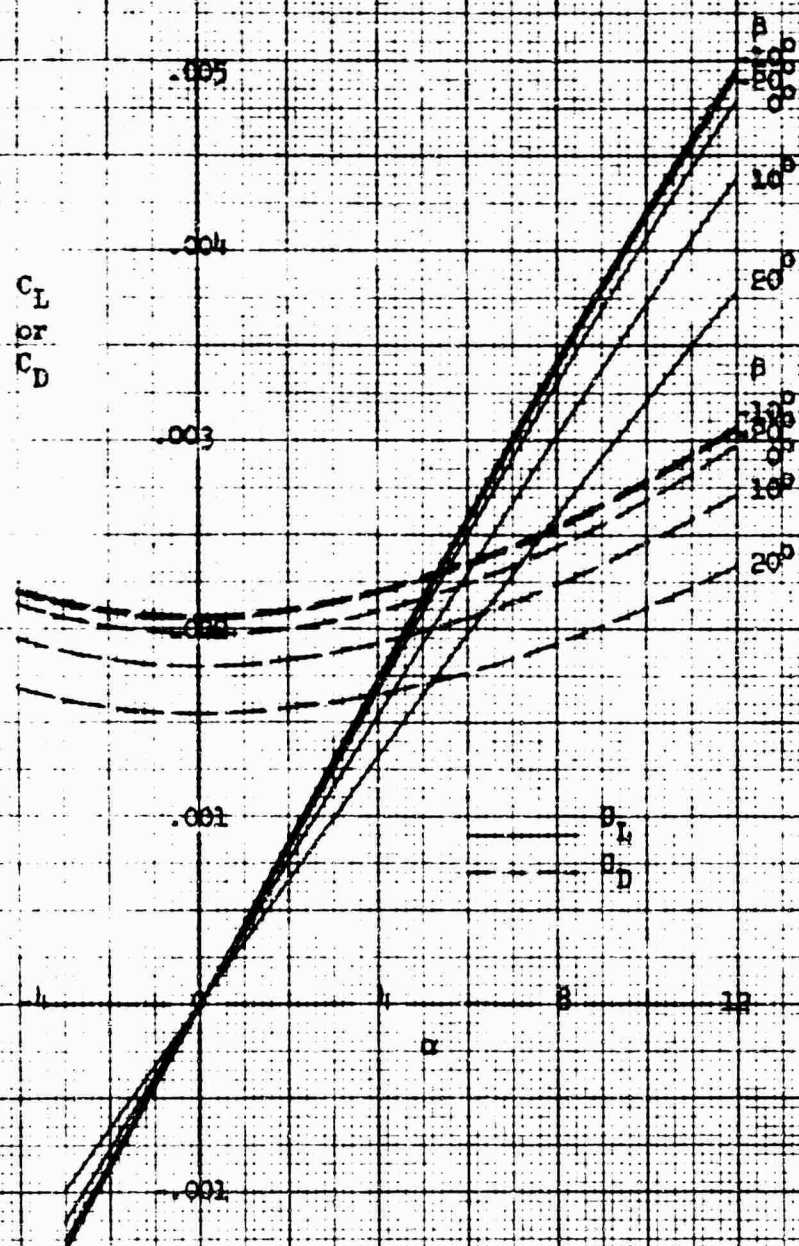
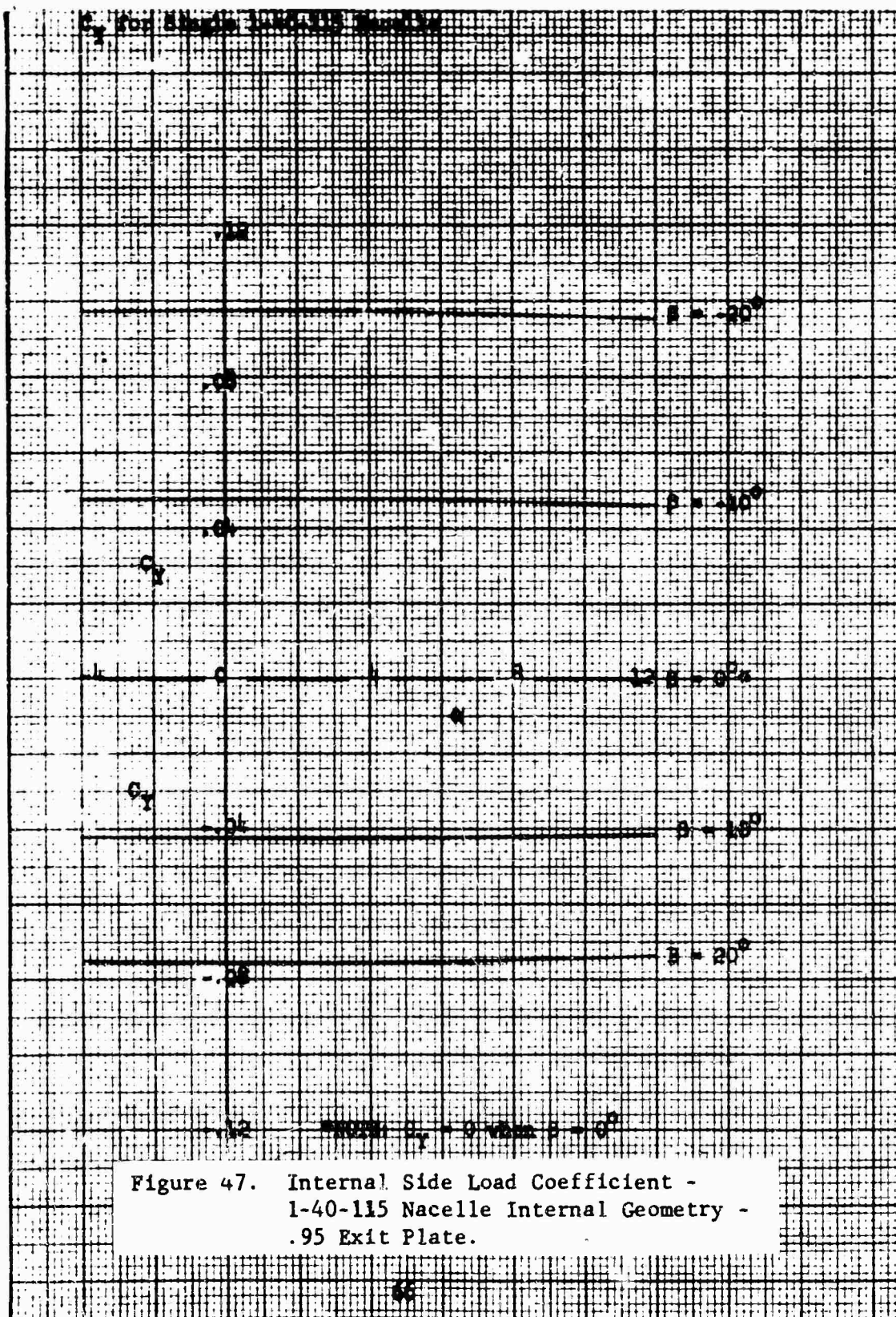
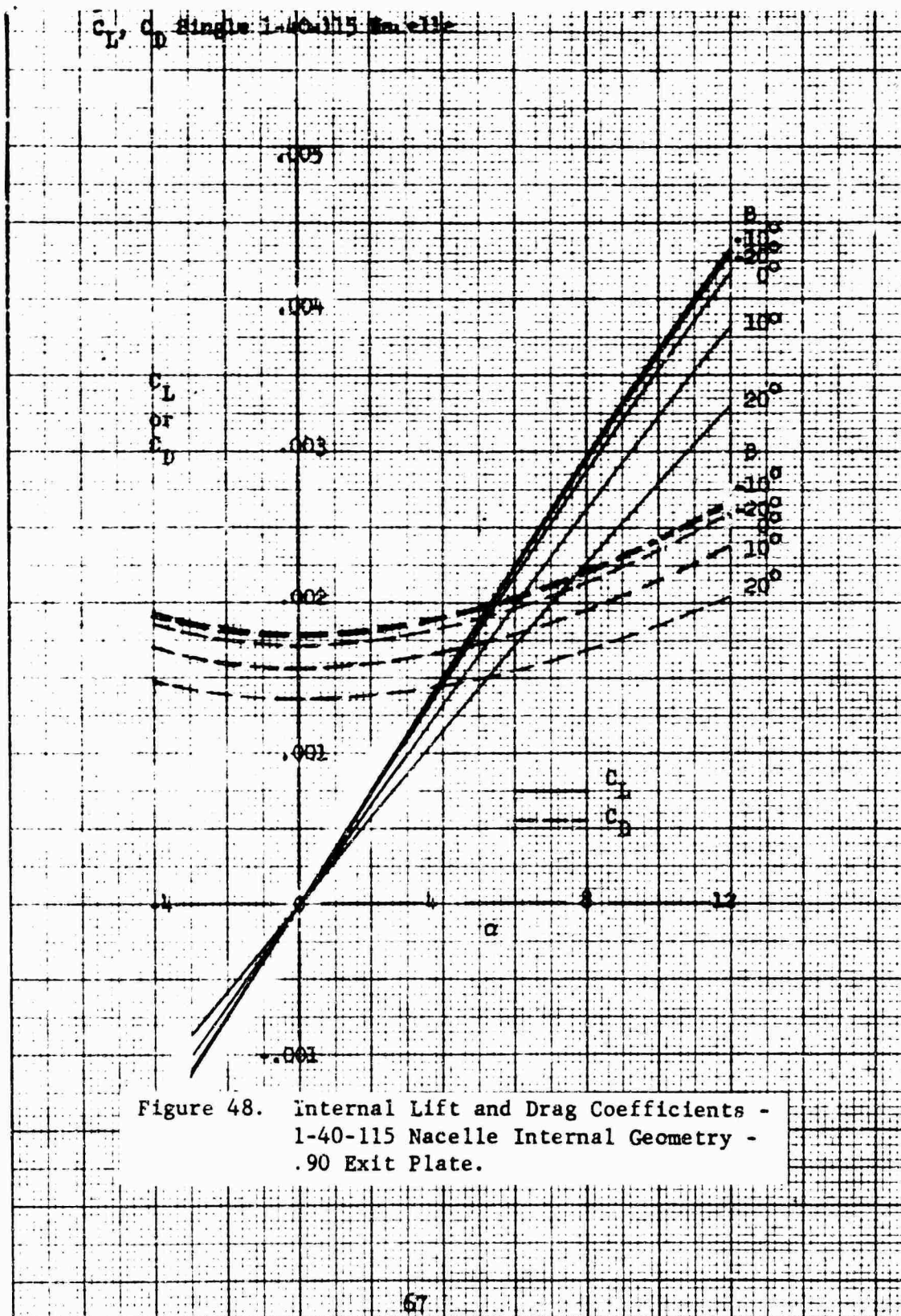
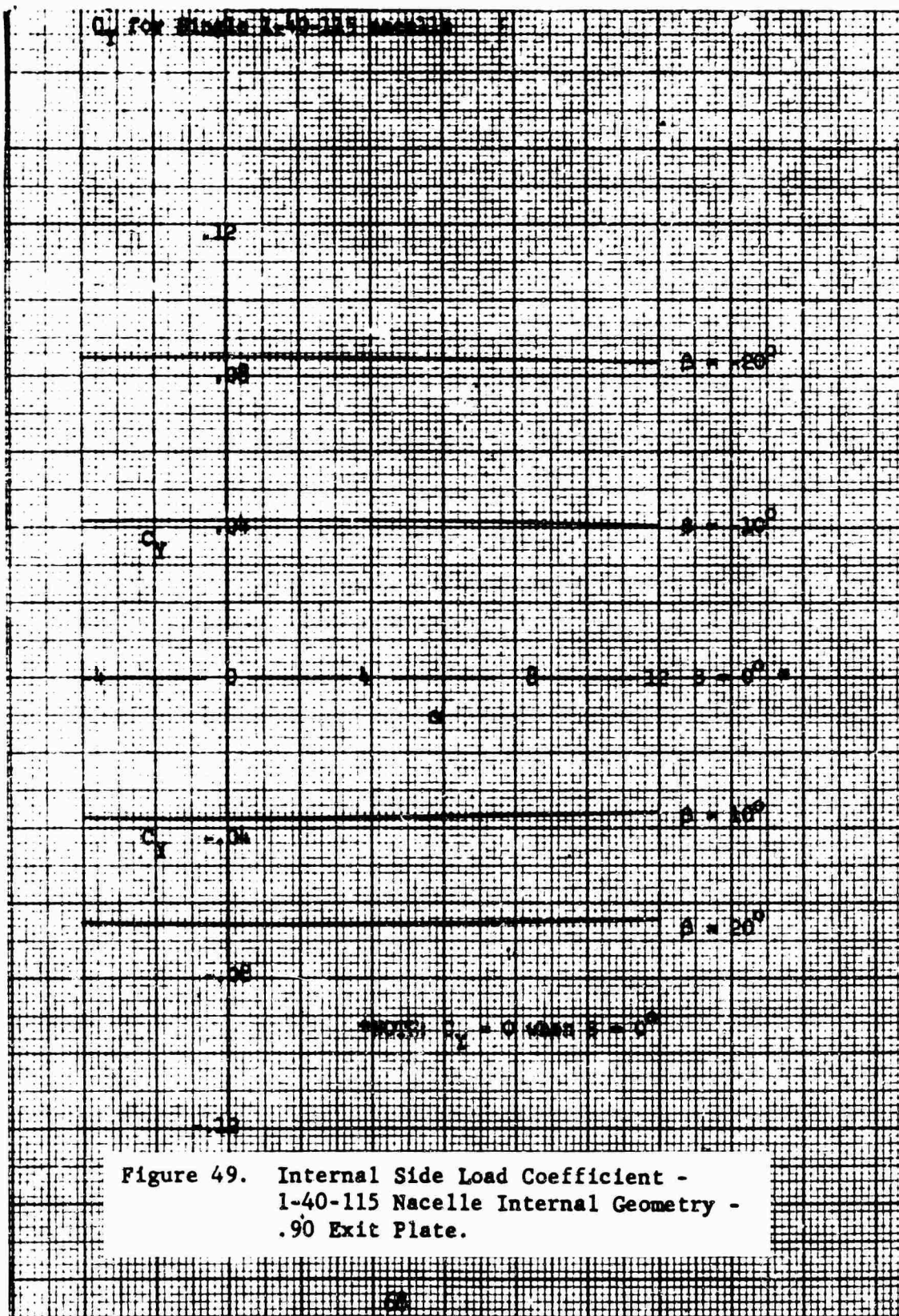


Figure 16. Internal Lift and Drag Coefficients -
1-40-115 Nacelle Internal Geometry -
.95 Exit Plate.







C_L, C_D Single 1-40-115 Nozzle

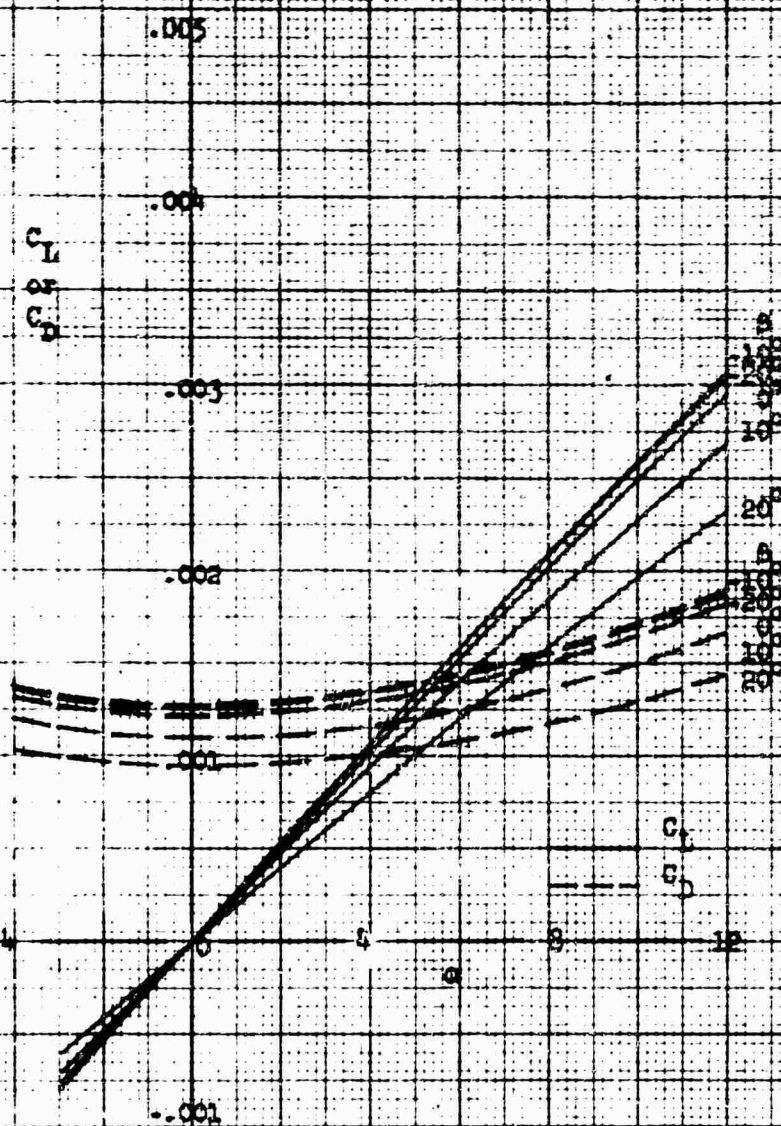


Figure 90. Internal Lift and Drag Coefficients -
1-40-115 Nozzle Internal Geometry -
78 Exit Plane.

C_Y for Single 1-40-115 Nacelle

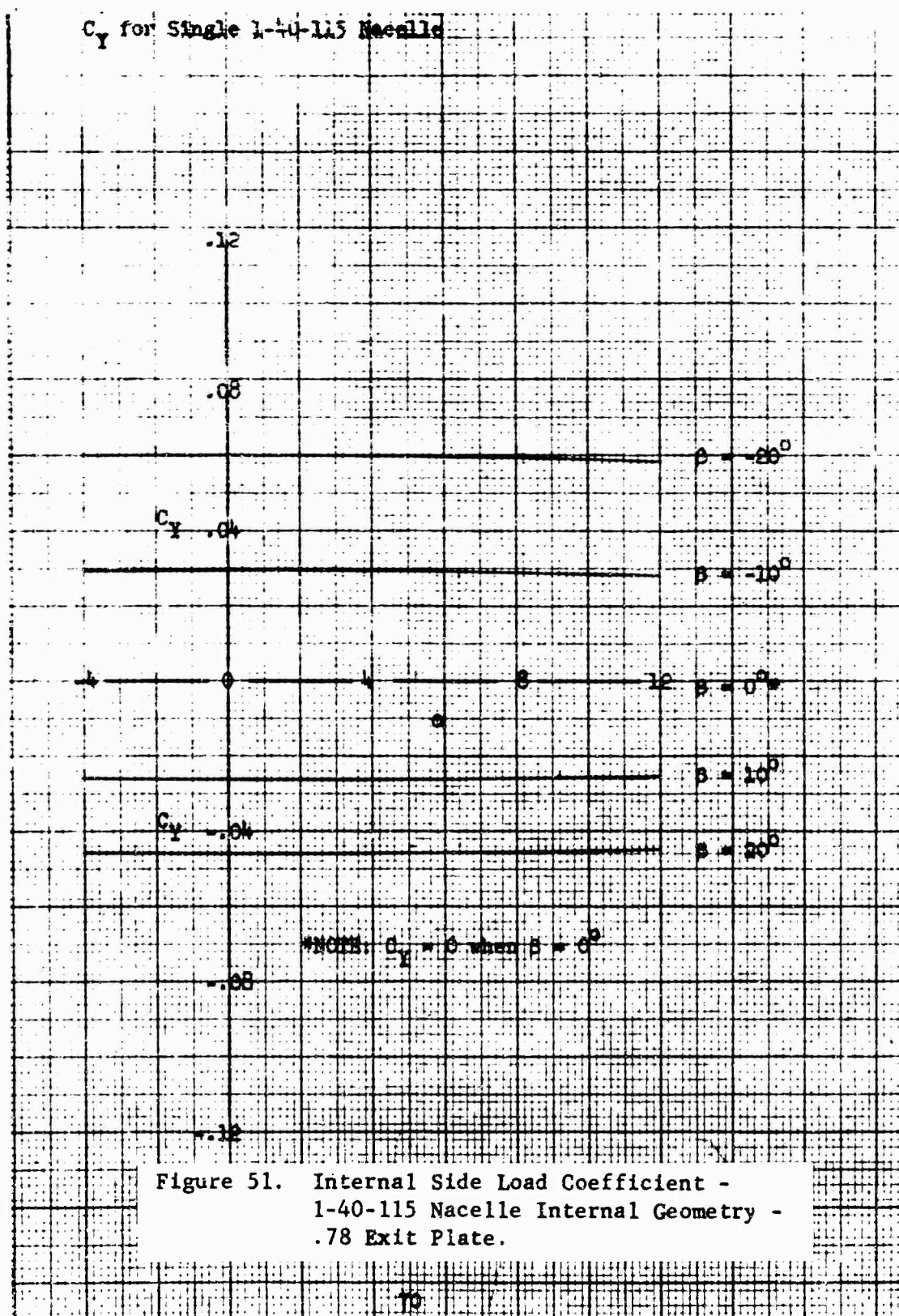
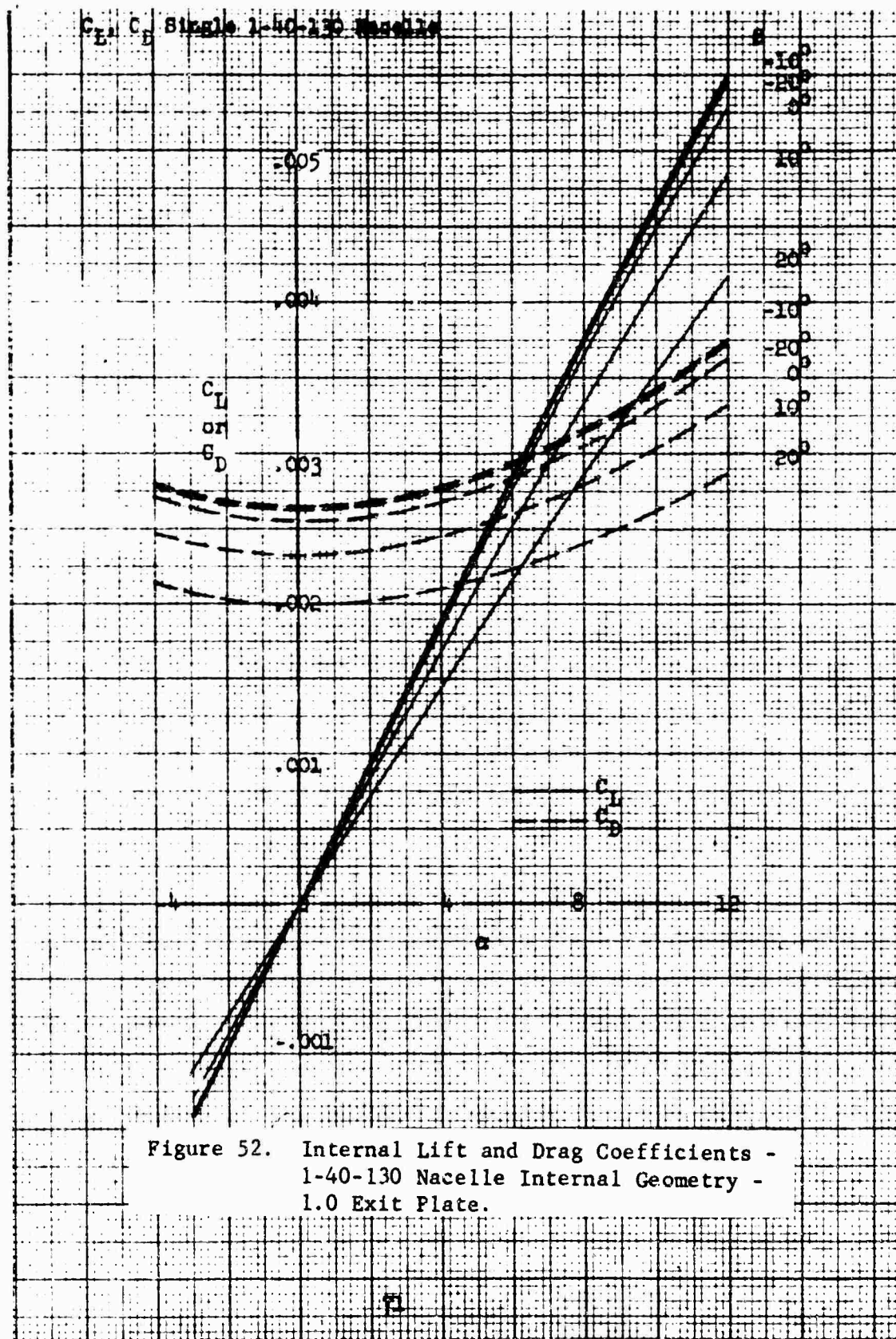
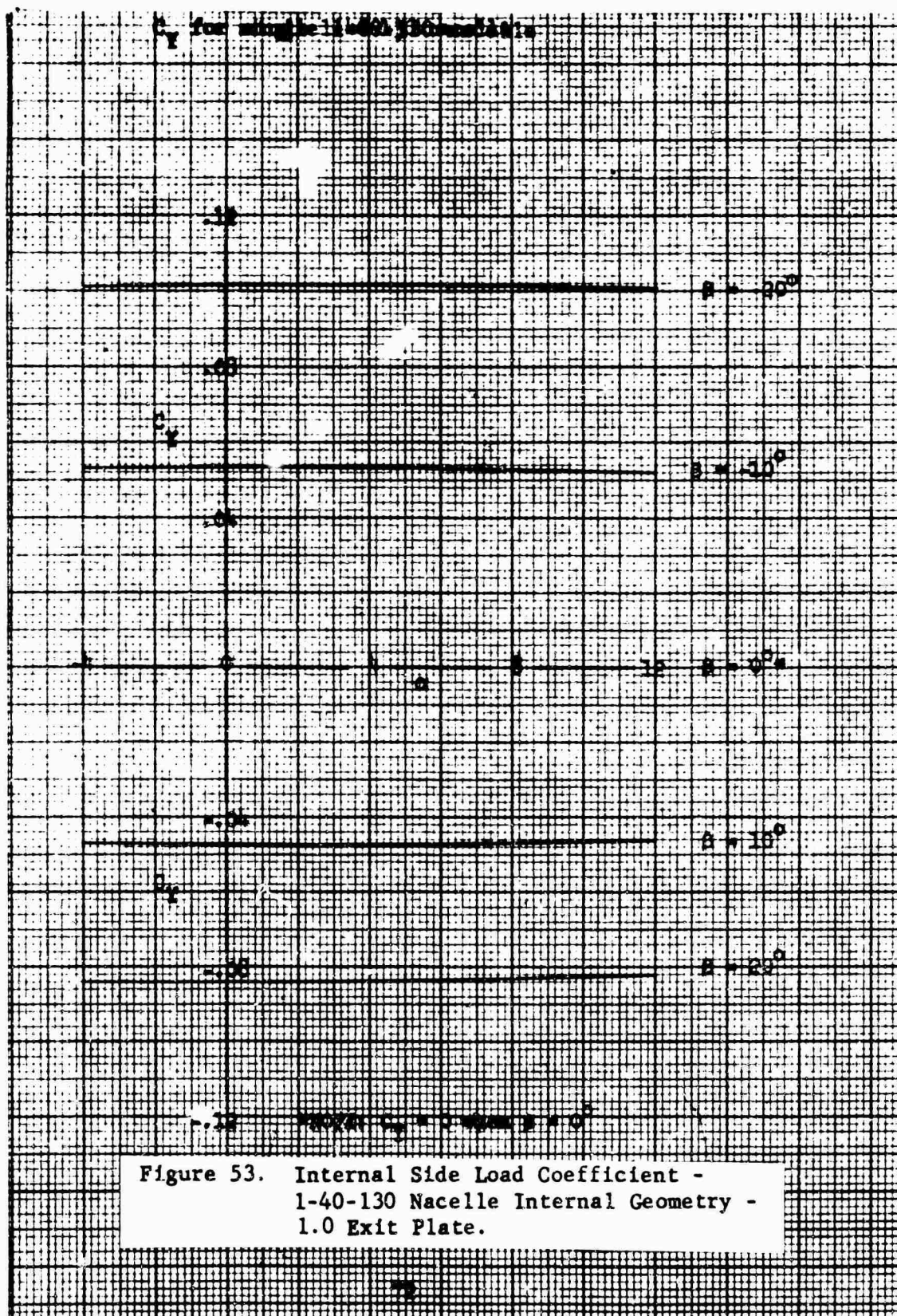


Figure 51. Internal Side Load Coefficient -
1-40-115 Nacelle Internal Geometry -
.78 Exit Plate.





C_L, C_D Single 1-40-130 Nacelle

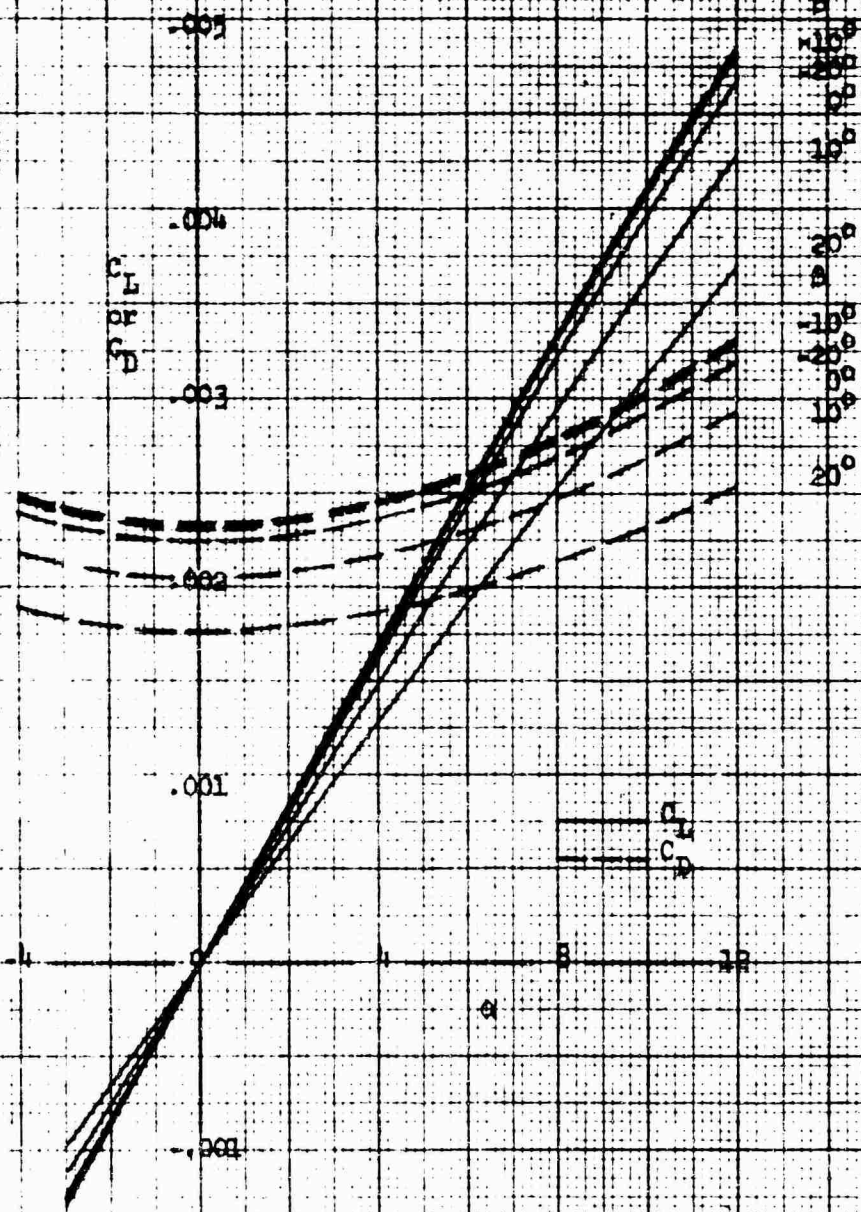


Figure 54. Internal Lift and Drag Coefficients -
1-40-130 Nacelle Internal Geometry -
.95 Exit Plate.

C. for single 1-40-130 Nacelle

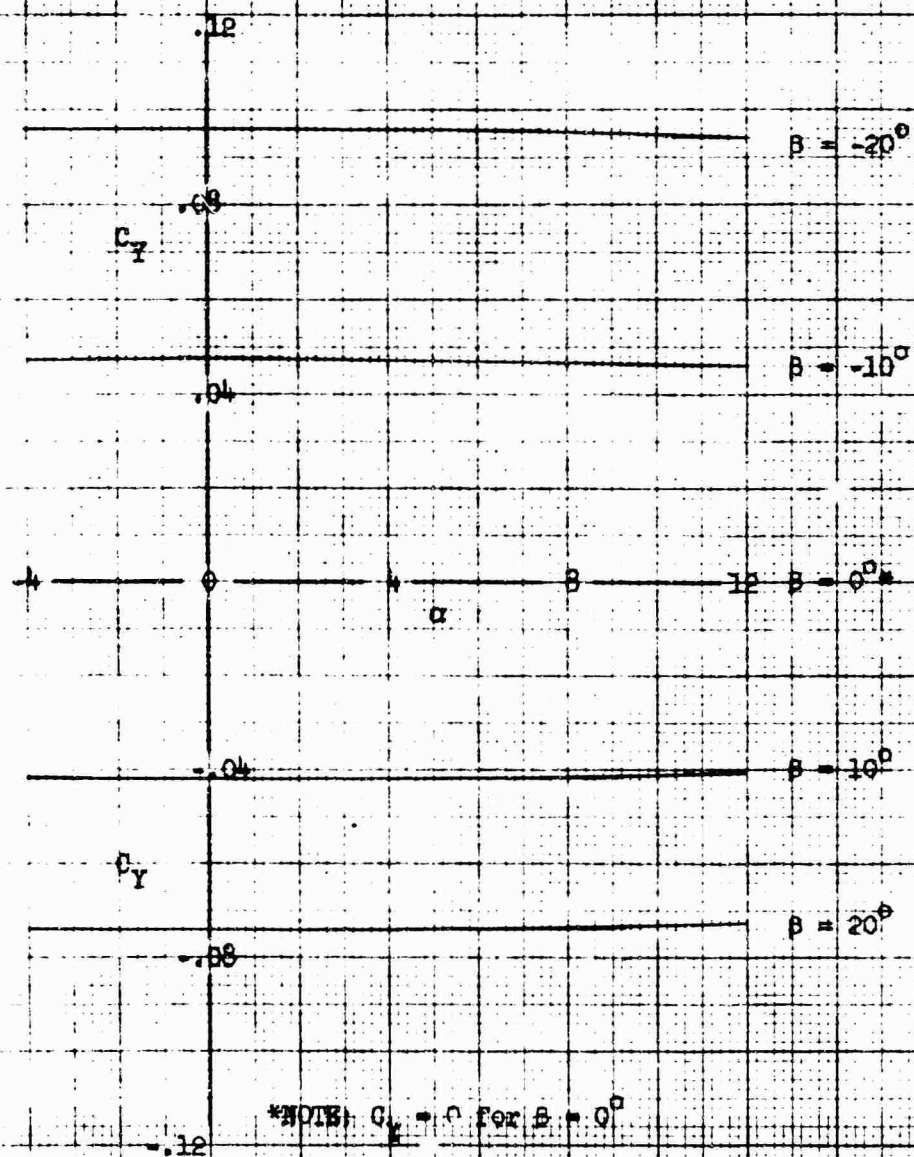


Figure 55. Internal Side Load Coefficient --
1-40-130 Nacelle Internal Geometry --
.95 Exit Plate.

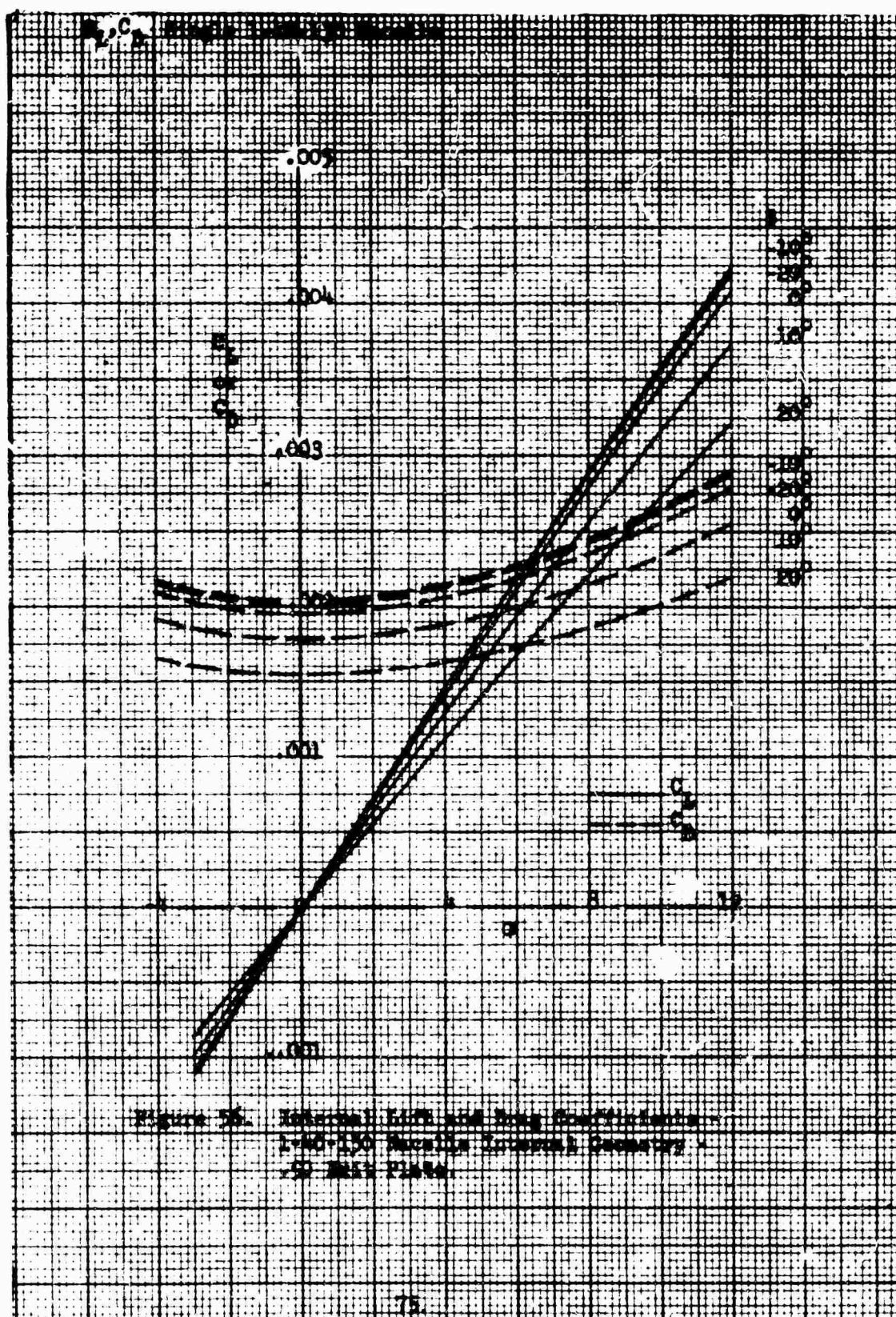
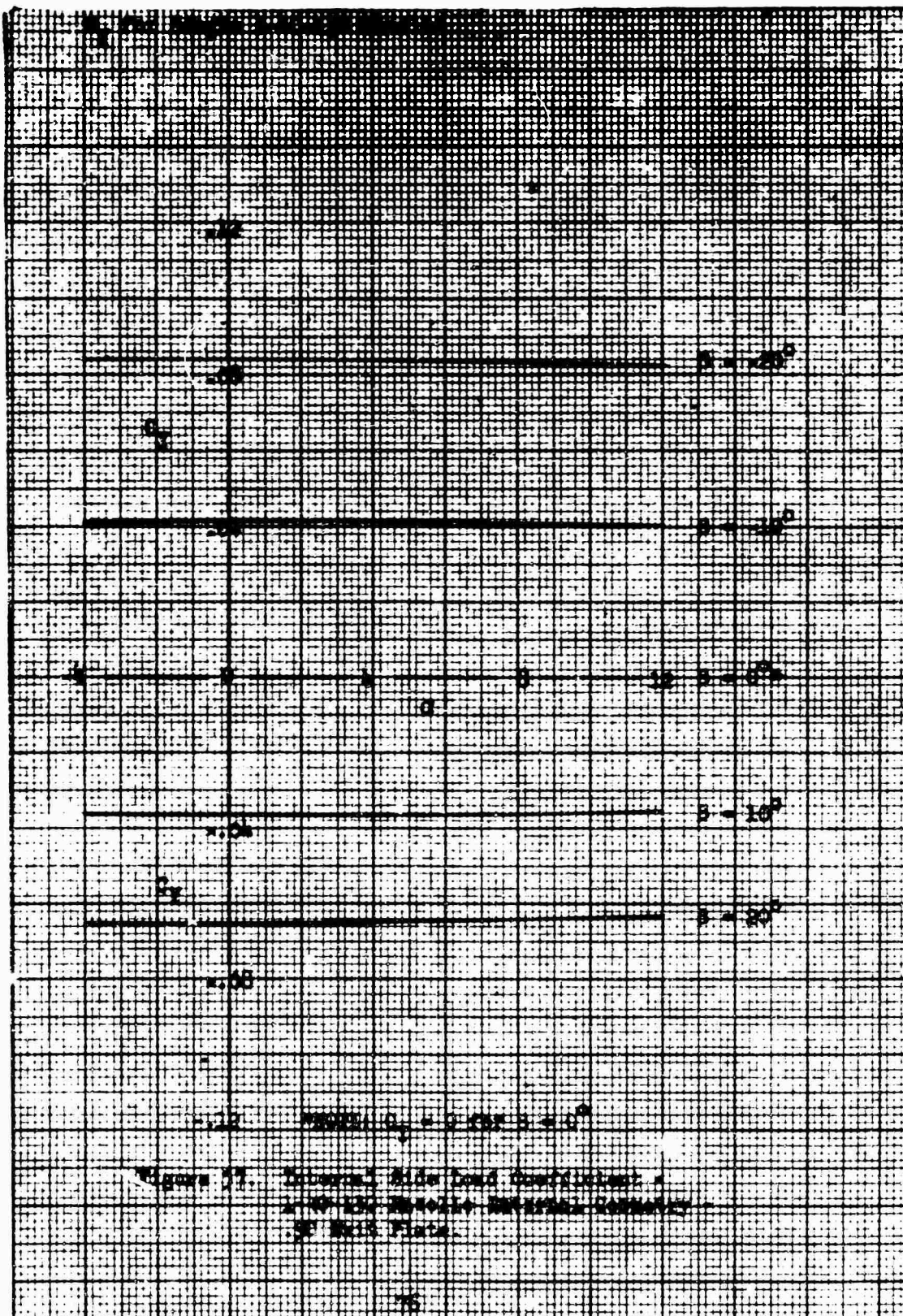
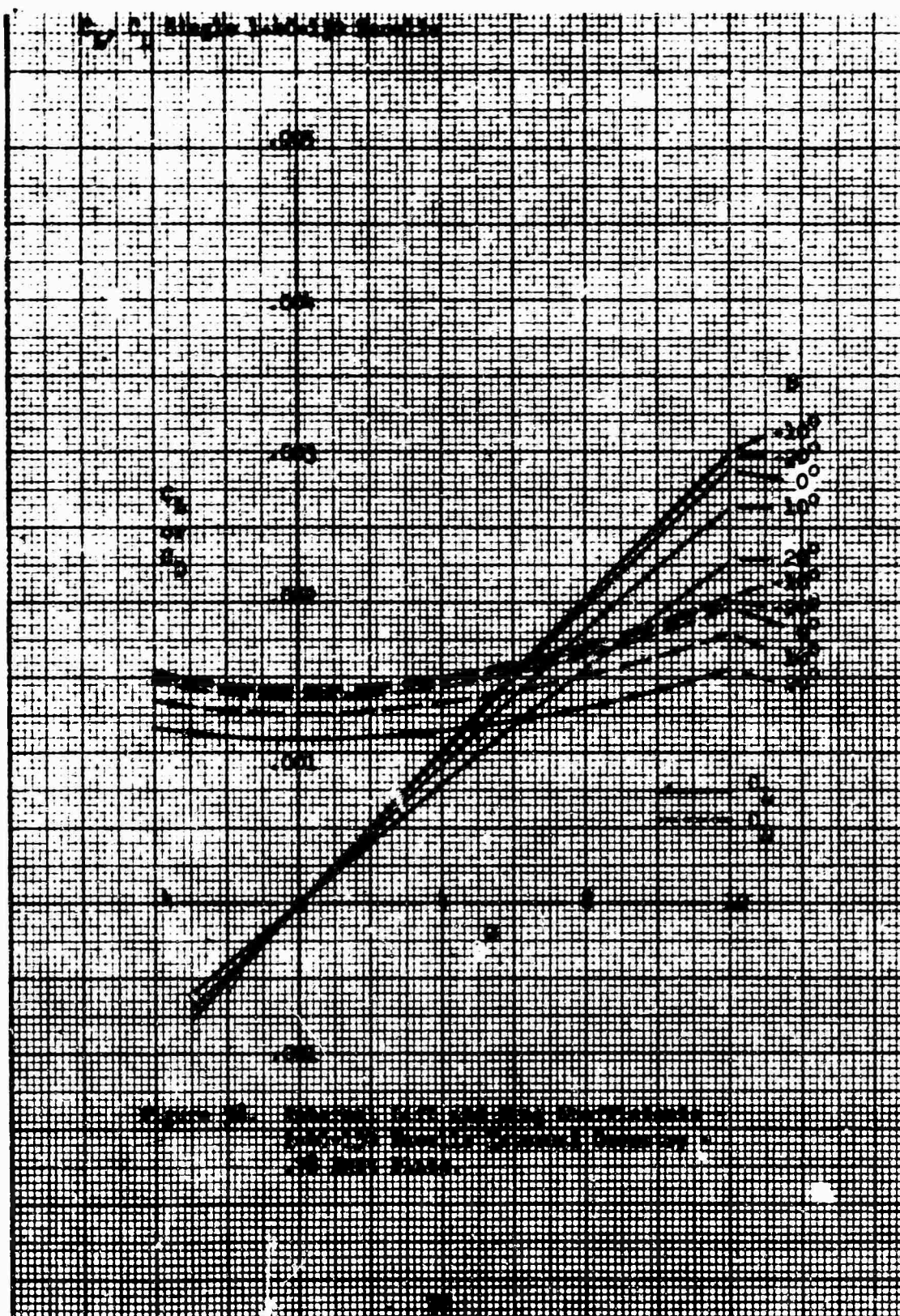
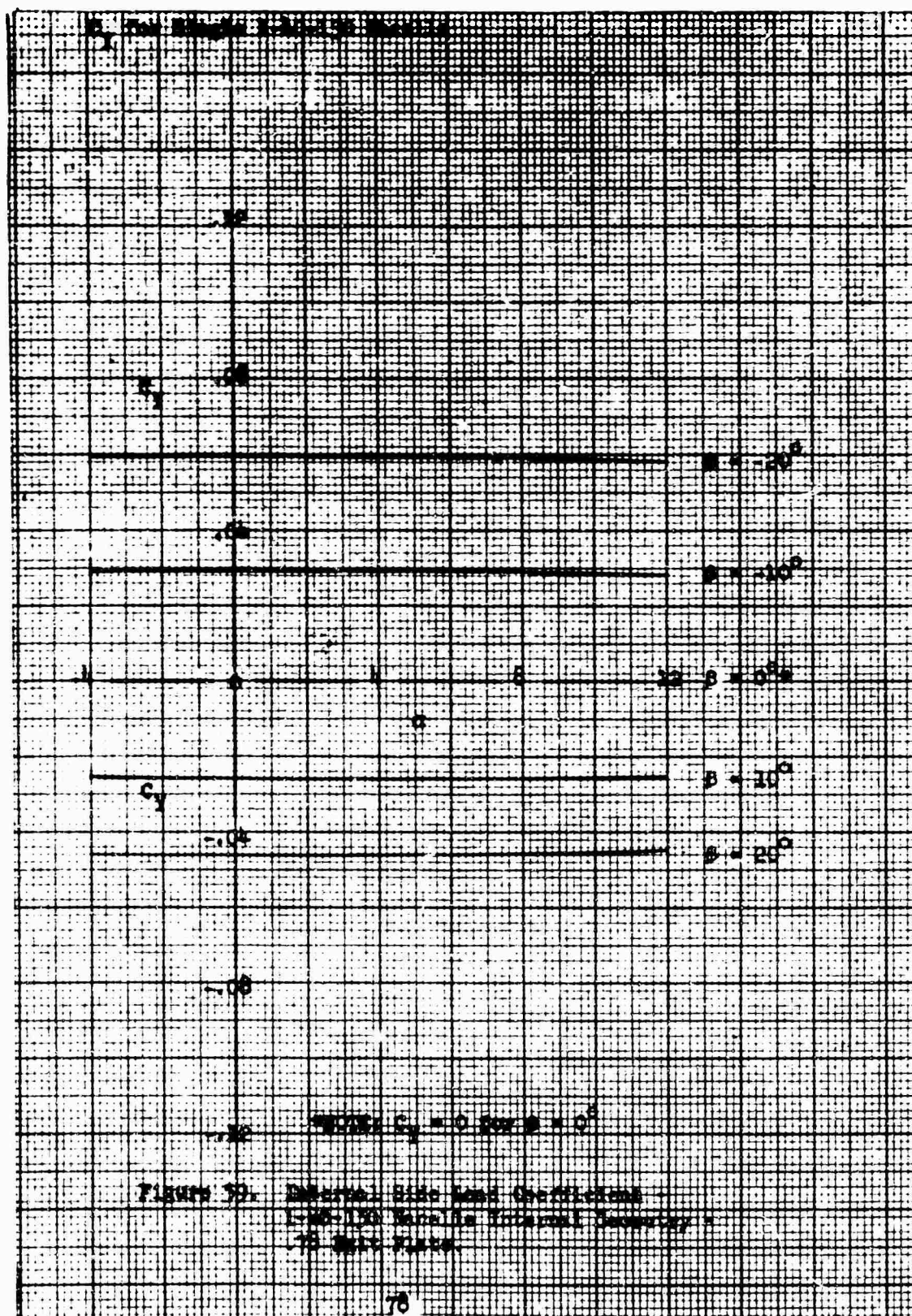


Figure 58. Internal Lift and Drag Coefficients
 1-150 Nozzle External Geometry
 20-250 Nozzle







C_L , C_D for 1-50-100 Macalle w/Spinner Internal
conical or parabolic spinner

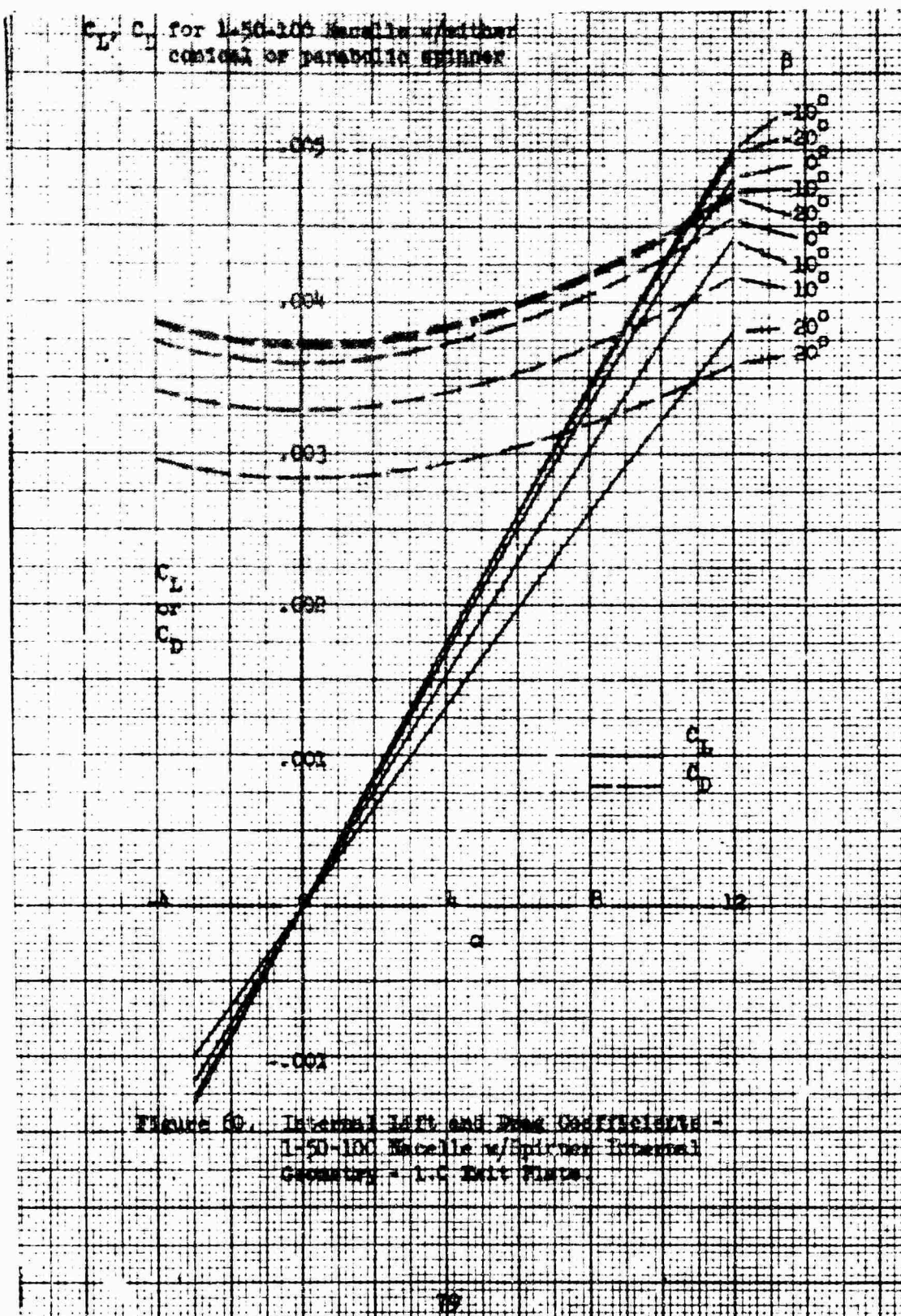
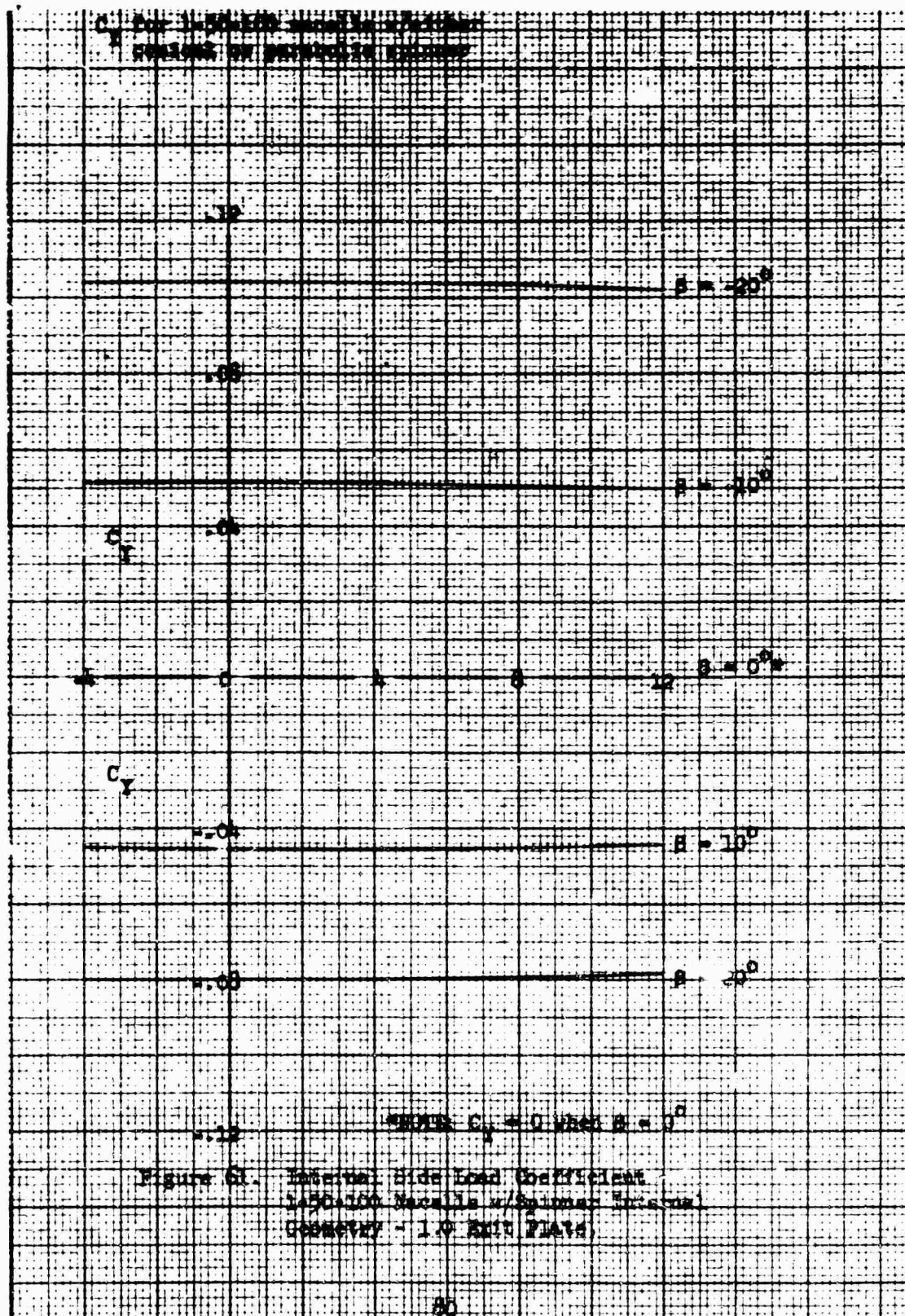


FIGURE 60. INTERNAL LIFT AND DRAG COEFFICIENTS -
1-50-100 Macalle w/Spinner Internal
Geometry - 1-C Belt Flare.



C_L vs δ for 1-50-100 needles w/ either
nominal or maximum thickness

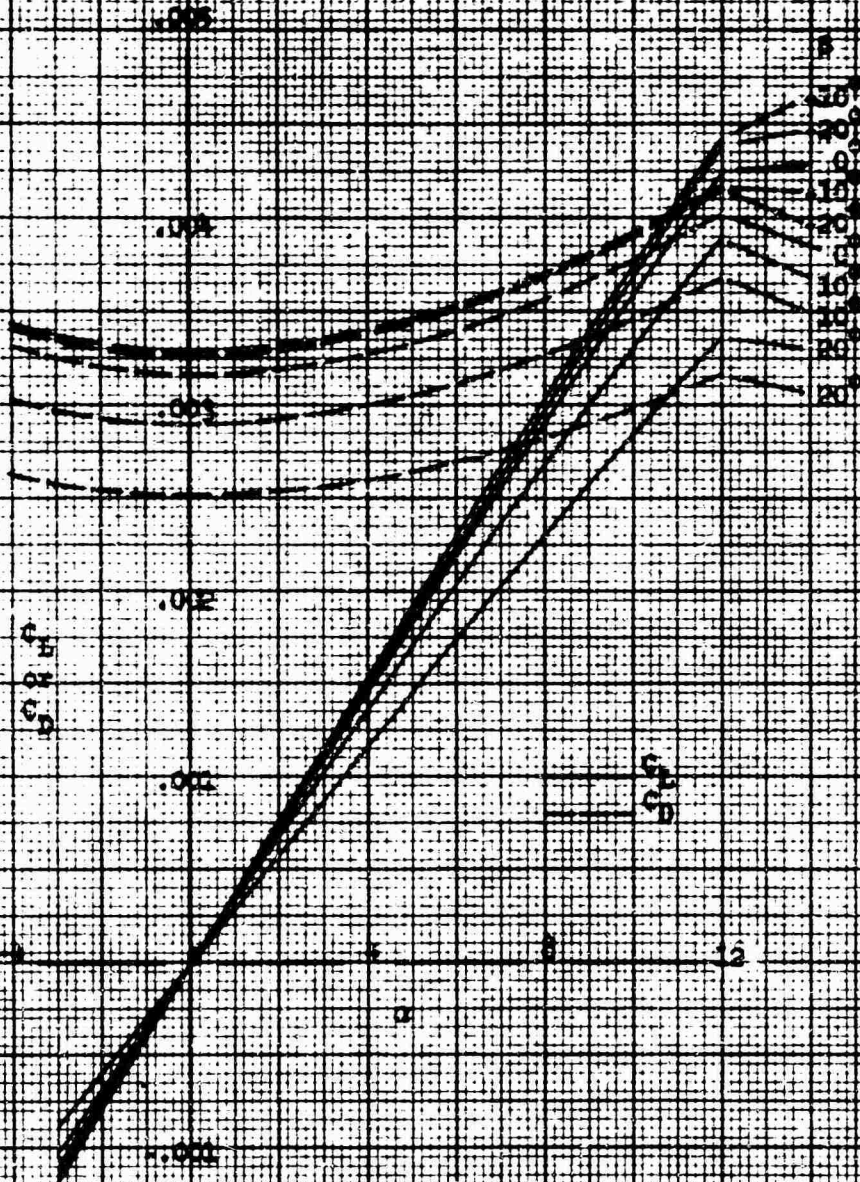


Figure 12 - Internal Lift and Drag Coefficients -
1-50-100 Needles w/ either Nominal
Thickness - 90 deg. Plate

For 1-50-100 model with internal
control or feedback system

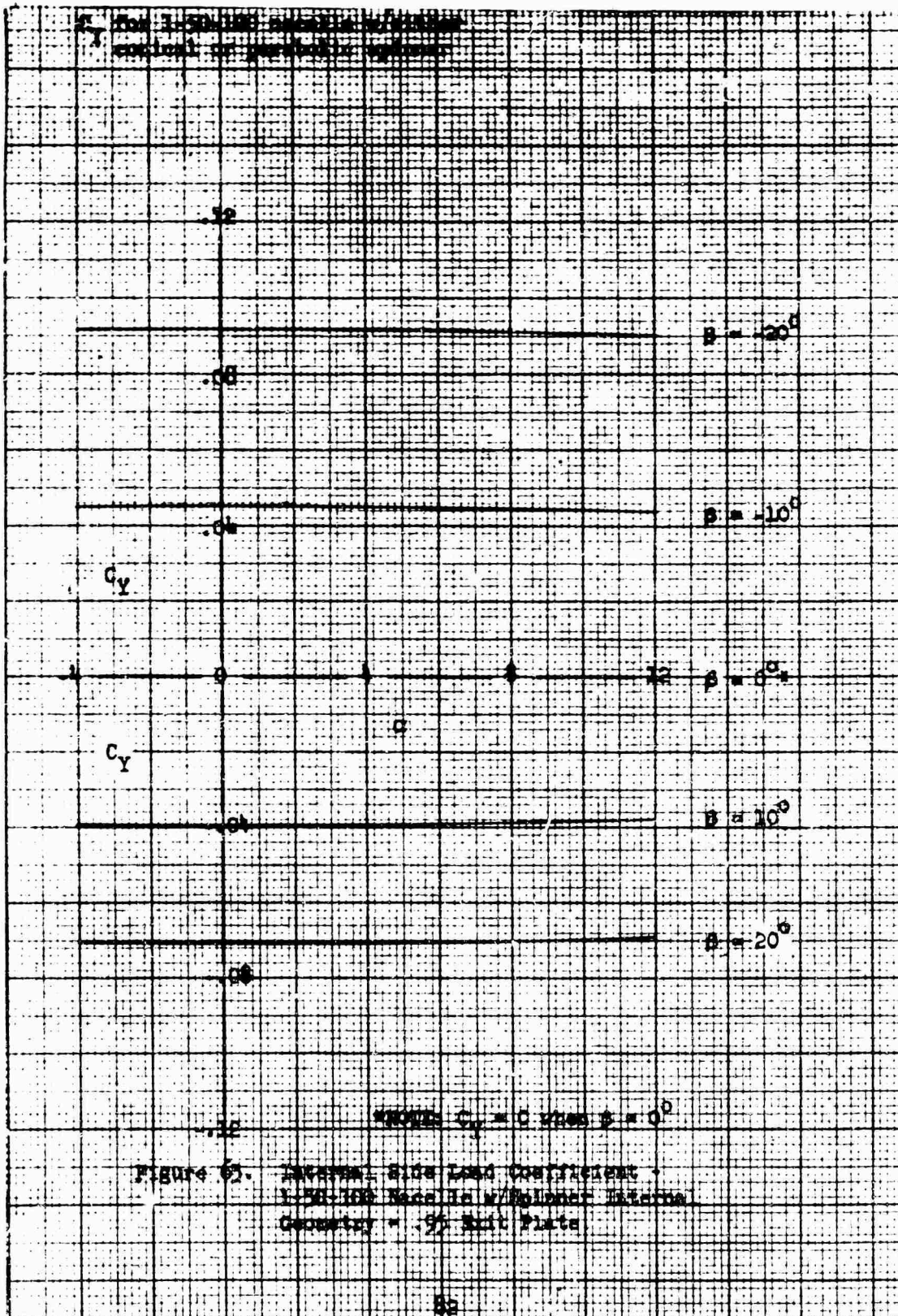
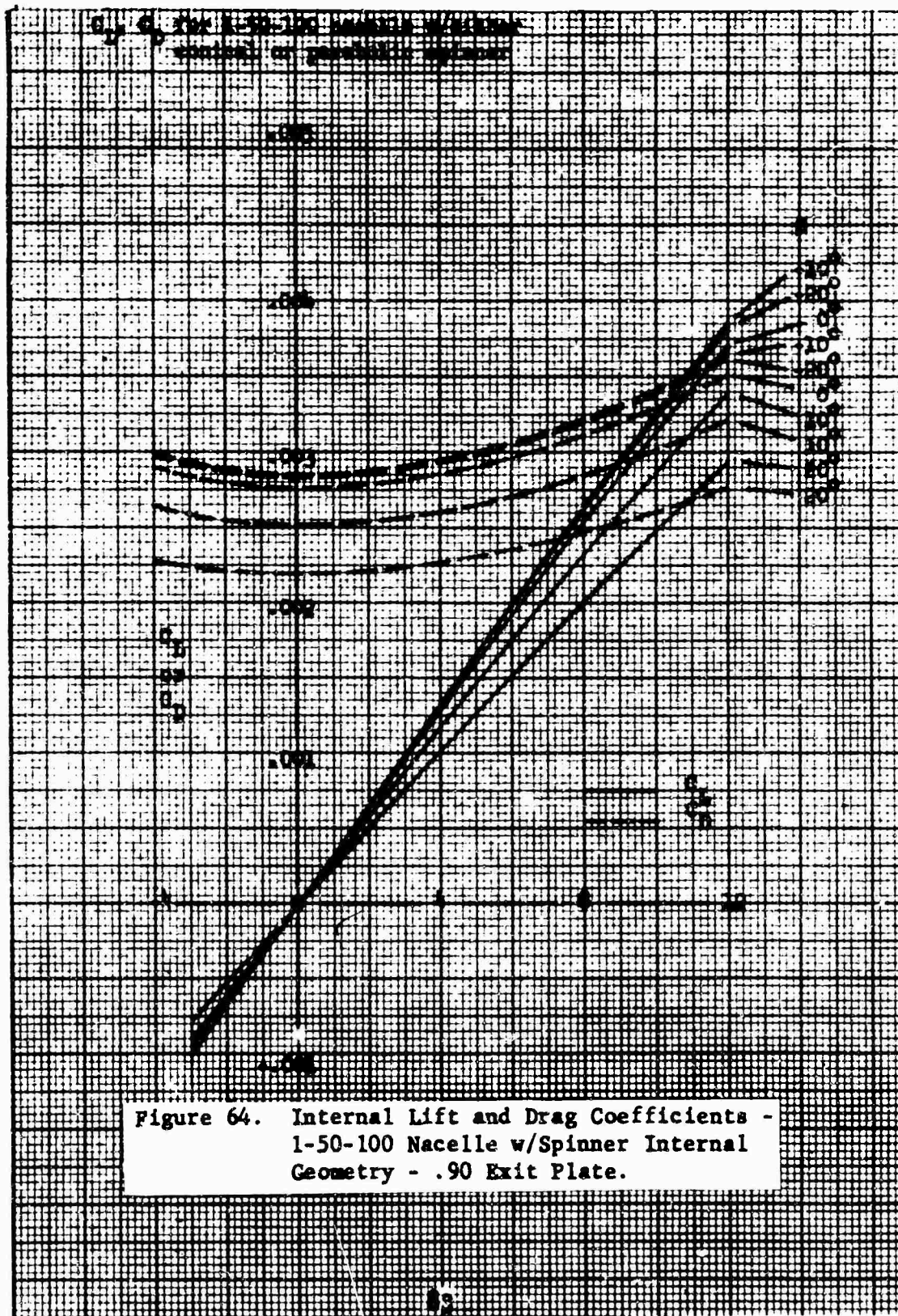
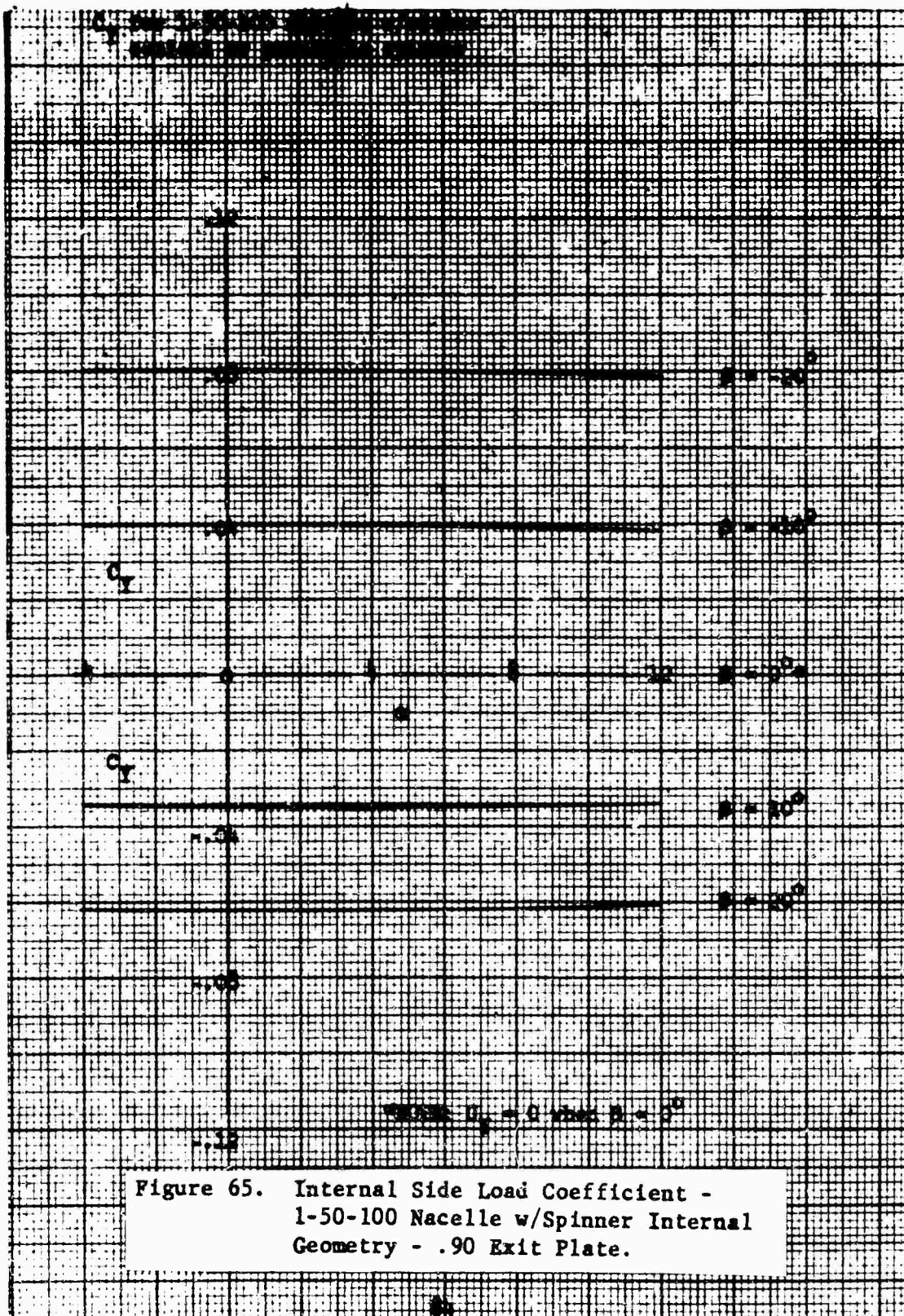


Figure 65. Internal Side Load Coefficient
1-50-100 Model with Internal
Control or Feedback System
Geometry - 50 Split Plate





C_L, C_D for E-50-100 Missile w/ External
control or parafoil: spinous

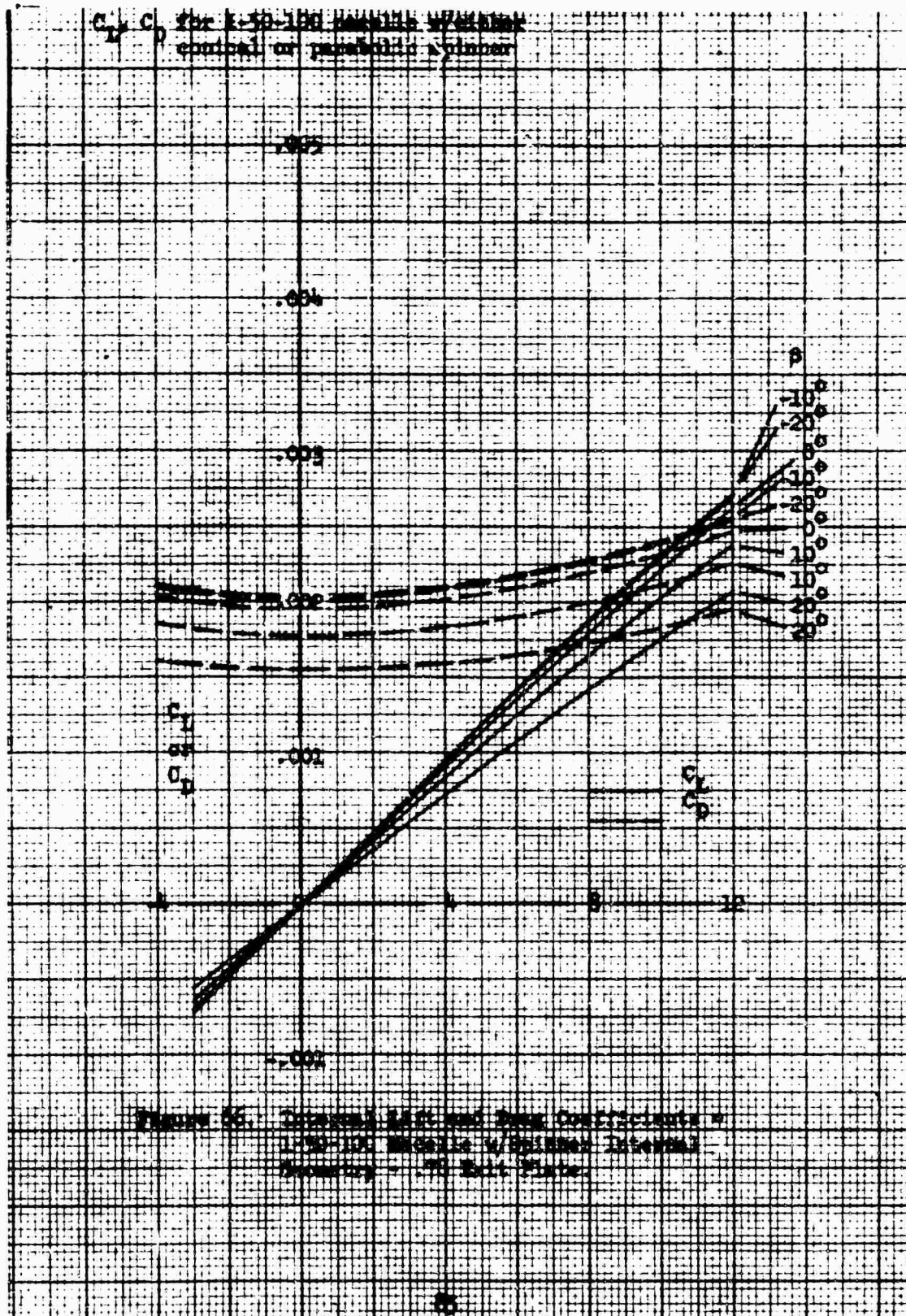
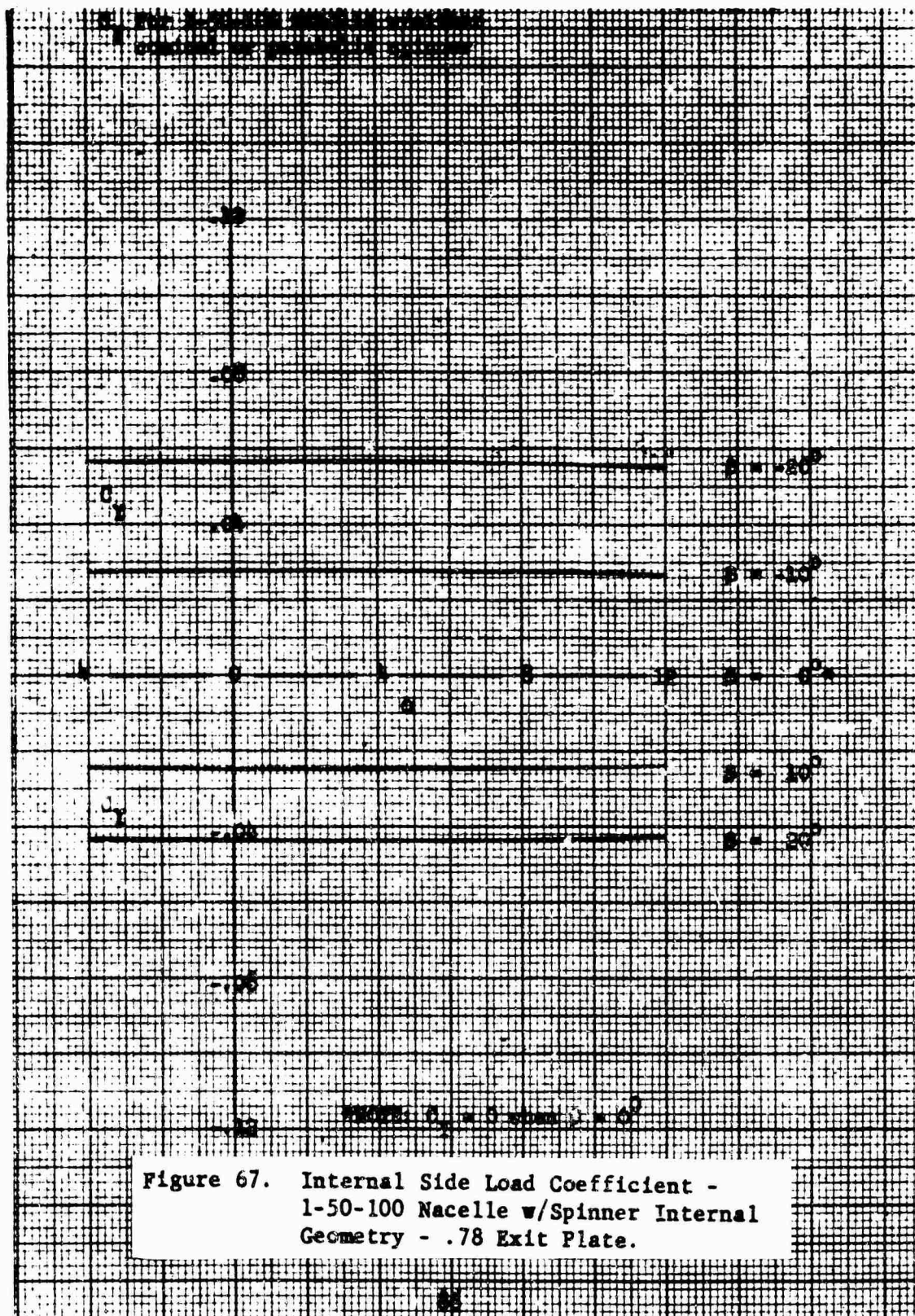


Figure 35. Lift and Drag Coefficients for
E-50-100 Missile w/ External Control
Boundary - 10 deg. Plane



4.0 REFERENCES

1. Baals, Donald D., Smith, Norman F., and Wright, John E., "The Development and Application of High Critical-Speed Nose Inlets," NACA Report 920, 1945.
2. Becker, John V., "Wind-Tunnel Investigation of Air Inlet and Outlet Openings on a Streamline Body," NACA TR 1038, 1951.
3. Pope, Alan, Wind-Tunnel Testing, 2nd Edition, John Wiley and Sons, Inc., New York, 1954.
4. "Design Handbook for Submerged Engine Cooling Systems and Duct Systems," BuAer, Washington, D. C. by Vertol Aircraft Corp, Morton, Penna., Contract NOas 56-880-f.
5. "Parametric Design Study," Heavy-Lift Tip Turbojet Rotor System, Volume II, Hiller Engineering Report No. 64-42, U. S. Army Transportation Research Command,* Fort Eustis, Virginia, October 1965.
6. Hoerner, S. F., Fluid-Dynamic Drag, Published by the author, Midland Park, New Jersey, 1958.

*Changed to U. S. Army Aviation Materiel Laboratories in March 1965.

5.0 DATA

5.1 Run Schedule

Run Schedule

Run	F 1 8	Blade Pitch Angle $\sim \alpha^\circ$						Blade Yaw Angle $\sim \beta^\circ$			Nacelle Exit Fwd. Nacelle Config.		Config. α_i°			Config.	Tunnel q ~ psi	Remarks
		3	0	3	6	9	12	30	10	0	10	20	0	78	90	95	100	
1		✓	✓	✓	✓	✓	✓	✓	✓	✓	✓	✓	✓	✓	✓	✓	48	BLADE STUB ONLY
2		✓	✓	✓	✓	✓	✓	✓	✓	✓	✓	✓	✓	✓	✓	✓		
3		✓	✓	✓	✓	✓	✓	✓	✓	✓	✓	✓	✓	✓	✓	✓		
4		✓	✓	✓	✓	✓	✓	✓	✓	✓	✓	✓	✓	✓	✓	✓		
5		✓	✓	✓	✓	✓	✓	✓	✓	✓	✓	✓	✓	✓	✓	✓	48	
6		✓	✓	✓	✓	✓	✓	✓	✓	✓	✓	✓	✓	✓	✓	✓	3	EXAMPLES
7		✓	✓	✓	✓	✓	✓	✓	✓	✓	✓	✓	✓	✓	✓	✓	6	NUMBER RUNS
8		✓	✓	✓	✓	✓	✓	✓	✓	✓	✓	✓	✓	✓	✓	✓	12	
9		✓	✓	✓	✓	✓	✓	✓	✓	✓	✓	✓	✓	✓	✓	✓	18	
10		✓	✓	✓	✓	✓	✓	✓	✓	✓	✓	✓	✓	✓	✓	✓	27	
11		✓	✓	✓	✓	✓	✓	✓	✓	✓	✓	✓	✓	✓	✓	✓	36	
12		✓	✓	✓	✓	✓	✓	✓	✓	✓	✓	✓	✓	✓	✓	✓	48	
13		✓	✓	✓	✓	✓	✓	✓	✓	✓	✓	✓	✓	✓	✓	✓		NO FAIRINGS
14		✓	✓	✓	✓	✓	✓	✓	✓	✓	✓	✓	✓	✓	✓	✓		
15		✓	✓	✓	✓	✓	✓	✓	✓	✓	✓	✓	✓	✓	✓	✓		
16		✓	✓	✓	✓	✓	✓	✓	✓	✓	✓	✓	✓	✓	✓	✓		
17		✓	✓	✓	✓	✓	✓	✓	✓	✓	✓	✓	✓	✓	✓	✓		
18		✓	✓	✓	✓	✓	✓	✓	✓	✓	✓	✓	✓	✓	✓	✓		
19		✓	✓	✓	✓	✓	✓	✓	✓	✓	✓	✓	✓	✓	✓	✓		
20		✓	✓	✓	✓	✓	✓	✓	✓	✓	✓	✓	✓	✓	✓	✓		
21		✓	✓	✓	✓	✓	✓	✓	✓	✓	✓	✓	✓	✓	✓	✓		
22		✓	✓	✓	✓	✓	✓	✓	✓	✓	✓	✓	✓	✓	✓	✓		
23		✓	✓	✓	✓	✓	✓	✓	✓	✓	✓	✓	✓	✓	✓	✓		
24		✓	✓	✓	✓	✓	✓	✓	✓	✓	✓	✓	✓	✓	✓	✓		
25		✓	✓	✓	✓	✓	✓	✓	✓	✓	✓	✓	✓	✓	✓	✓		
26		✓	✓	✓	✓	✓	✓	✓	✓	✓	✓	✓	✓	✓	✓	✓		
27		✓	✓	✓	✓	✓	✓	✓	✓	✓	✓	✓	✓	✓	✓	✓		

Run Schedule

Run	Blade Pitch Angle $\sim \alpha^\circ$						Blade Yaw Angle $\sim \beta^\circ$		Macelle Exit Config.		Fwd. Macelle Config. (Spinner Type)	Macelle α_i°			Config.	Tunnel $q \sim \text{psi}$	Remarks
	3	0	3	6	9	12	30	100	10	20		0	73	90			
28	✓	✓	✓	✓	✓	✓	✓	✓	✓	✓	1-42-100	✓	✓	✓	48	NO PAIRING	
29	✓	✓	✓	✓	✓	✓	✓	✓	✓	✓	(NONE)	✓	✓	✓			
30	✓	✓	✓	✓	✓	✓	✓	✓	✓	✓		✓	✓	✓			
31	✓	✓	✓	✓	✓	✓	✓	✓	✓	✓		✓	✓	✓			
32	✓	✓	✓	✓	✓	✓	✓	✓	✓	✓		✓	✓	✓			
33	✓	✓	✓	✓	✓	✓	✓	✓	✓	✓		✓	✓	✓			
34	✓	✓	✓	✓	✓	✓	✓	✓	✓	✓		✓	✓	✓			
35	✓	✓	✓	✓	✓	✓	✓	✓	✓	✓		✓	✓	✓			
36	✓	✓	✓	✓	✓	✓	✓	✓	✓	✓		✓	✓	✓			
37	✓	✓	✓	✓	✓	✓	✓	✓	✓	✓		✓	✓	✓			
38	✓	✓	✓	✓	✓	✓	✓	✓	✓	✓		✓	✓	✓			
39	✓	✓	✓	✓	✓	✓	✓	✓	✓	✓		✓	✓	✓			
40	✓	✓	✓	✓	✓	✓	✓	✓	✓	✓		✓	✓	✓			
41	✓	✓	✓	✓	✓	✓	✓	✓	✓	✓		✓	✓	✓			
42	✓	✓	✓	✓	✓	✓	✓	✓	✓	✓		✓	✓	✓			
43	✓	✓	✓	✓	✓	✓	✓	✓	✓	✓		✓	✓	✓			
44	✓	✓	✓	✓	✓	✓	✓	✓	✓	✓		✓	✓	✓			
45	✓	✓	✓	✓	✓	✓	✓	✓	✓	✓		✓	✓	✓			
46	✓	✓	✓	✓	✓	✓	✓	✓	✓	✓		✓	✓	✓			
47	✓	✓	✓	✓	✓	✓	✓	✓	✓	✓		✓	✓	✓			
48	✓	✓	✓	✓	✓	✓	✓	✓	✓	✓		✓	✓	✓			
49	✓	✓	✓	✓	✓	✓	✓	✓	✓	✓		✓	✓	✓			
50	✓	✓	✓	✓	✓	✓	✓	✓	✓	✓		✓	✓	✓			
51	✓	✓	✓	✓	✓	✓	✓	✓	✓	✓		✓	✓	✓			
52	✓	✓	✓	✓	✓	✓	✓	✓	✓	✓		✓	✓	✓			
53	✓	✓	✓	✓	✓	✓	✓	✓	✓	✓		✓	✓	✓			

Run Schedule

Run	Blade Pitch Angle ~ α°												Blade Yaw Angle ~ β°				Nacelle Exit Config.				Fwd. Nacelle Config. (Spinner Type)	Angle α_i°	Config.	Tunnel q ~ psi	Remarks																																																																																																																																																																																																																																																																																																																																																																																																																																																																																																																																																																																																																																																																																																																																																																																																																																																																																																																																																																																																																																																																																																																																																																																																																																																				
	30				36				9				12				20									10				20				0				78				90				95				100																																																																																																																																																																																																																																																																																																																																																																																																																																																																																																																																																																																																																																																																																																																																																																																																																																																																																																																																																																																																																																																																																																																																																																																																																											
	✓	✓	✓	✓	✓	✓	✓	✓	✓	✓	✓	✓	✓	✓	✓	✓	✓	✓	✓	✓	✓	✓	✓	✓	✓	✓	✓	✓	✓	✓	✓	✓	✓	✓	✓	✓	✓	✓	✓	✓	✓	✓	✓	✓	✓	✓	✓	✓	✓	✓	✓	✓	✓	✓	✓	✓	✓	✓	✓	✓	✓	✓	✓	✓	✓	✓	✓	✓	✓	✓	✓	✓	✓	✓	✓	✓	✓	✓	✓	✓	✓	✓	✓	✓	✓	✓	✓	✓	✓	✓	✓	✓	✓	✓	✓	✓	✓	✓	✓	✓	✓	✓	✓	✓	✓	✓	✓	✓	✓	✓	✓	✓	✓	✓	✓	✓	✓	✓	✓	✓	✓	✓	✓	✓	✓	✓	✓	✓	✓	✓	✓	✓	✓	✓	✓	✓	✓	✓	✓	✓	✓	✓	✓	✓	✓	✓	✓	✓	✓	✓	✓	✓	✓	✓	✓	✓	✓	✓	✓	✓	✓	✓	✓	✓	✓	✓	✓	✓	✓	✓	✓	✓	✓	✓	✓	✓	✓	✓	✓	✓	✓	✓	✓	✓	✓	✓	✓	✓	✓	✓	✓	✓	✓	✓	✓	✓	✓	✓	✓	✓	✓	✓	✓	✓	✓	✓	✓	✓	✓	✓	✓	✓	✓	✓	✓	✓	✓	✓	✓	✓	✓	✓	✓	✓	✓	✓	✓	✓	✓	✓	✓	✓	✓	✓	✓	✓	✓	✓	✓	✓	✓	✓	✓	✓	✓	✓	✓	✓	✓	✓	✓	✓	✓	✓	✓	✓	✓	✓	✓	✓	✓	✓	✓	✓	✓	✓	✓	✓	✓	✓	✓	✓	✓	✓	✓	✓	✓	✓	✓	✓	✓	✓	✓	✓	✓	✓	✓	✓	✓	✓	✓	✓	✓	✓	✓	✓	✓	✓	✓	✓	✓	✓	✓	✓	✓	✓	✓	✓	✓	✓	✓	✓	✓	✓	✓	✓	✓	✓	✓	✓	✓	✓	✓	✓	✓	✓	✓	✓	✓	✓	✓	✓	✓	✓	✓	✓	✓	✓	✓	✓	✓	✓	✓	✓	✓	✓	✓	✓	✓	✓	✓	✓	✓	✓	✓	✓	✓	✓	✓	✓	✓	✓	✓	✓	✓	✓	✓	✓	✓	✓	✓	✓	✓	✓	✓	✓	✓	✓	✓	✓	✓	✓	✓	✓	✓	✓	✓	✓	✓	✓	✓	✓	✓	✓	✓	✓	✓	✓	✓	✓	✓	✓	✓	✓	✓	✓	✓	✓	✓	✓	✓	✓	✓	✓	✓	✓	✓	✓	✓	✓	✓	✓	✓	✓	✓	✓	✓	✓	✓	✓	✓	✓	✓	✓	✓	✓	✓	✓	✓	✓	✓	✓	✓	✓	✓	✓	✓	✓	✓	✓	✓	✓	✓	✓	✓	✓	✓	✓	✓	✓	✓	✓	✓	✓	✓	✓	✓	✓	✓	✓	✓	✓	✓	✓	✓	✓	✓	✓	✓	✓	✓	✓	✓	✓	✓	✓	✓	✓	✓	✓	✓	✓	✓	✓	✓	✓	✓	✓	✓	✓	✓	✓	✓	✓	✓	✓	✓	✓	✓	✓	✓	✓	✓	✓	✓	✓	✓	✓	✓	✓	✓	✓	✓	✓	✓	✓	✓	✓	✓	✓	✓	✓	✓	✓	✓	✓	✓	✓	✓	✓	✓	✓	✓	✓	✓	✓	✓	✓	✓	✓	✓	✓	✓	✓	✓	✓	✓	✓	✓	✓	✓	✓	✓	✓	✓	✓	✓	✓	✓	✓	✓	✓	✓	✓	✓	✓	✓	✓	✓	✓	✓	✓	✓	✓	✓	✓	✓	✓	✓	✓	✓	✓	✓	✓	✓	✓	✓	✓	✓	✓	✓	✓	✓	✓	✓	✓	✓	✓	✓	✓	✓	✓	✓	✓	✓	✓	✓	✓	✓	✓	✓	✓	✓	✓	✓	✓	✓	✓	✓	✓	✓	✓	✓	✓	✓	✓	✓	✓	✓	✓	✓	✓	✓	✓	✓	✓	✓	✓	✓	✓	✓	✓	✓	✓	✓	✓	✓	✓	✓	✓	✓	✓	✓	✓	✓	✓	✓	✓	✓	✓	✓	✓	✓	✓	✓	✓	✓	✓	✓	✓	✓	✓	✓	✓	✓	✓	✓	✓	✓	✓	✓	✓	✓	✓	✓	✓	✓	✓	✓	✓	✓	✓	✓	✓	✓	✓	✓	✓	✓	✓	✓	✓	✓	✓	✓	✓	✓	✓	✓	✓	✓	✓	✓	✓	✓	✓	✓	✓	✓	✓	✓	✓	✓	✓	✓	✓	✓	✓	✓	✓	✓	✓	✓	✓	✓	✓	✓	✓	✓	✓	✓	✓	✓	✓	✓	✓	✓	✓	✓	✓	✓	✓	✓	✓	✓	✓	✓	✓	✓	✓	✓	✓	✓	✓	✓	✓	✓	✓	✓	✓	✓	✓	✓	✓	✓	✓	✓	✓	✓	✓	✓	✓	✓	✓	✓	✓	✓	✓	✓	✓	✓	✓	✓	✓	✓	✓	✓	✓	✓	✓	✓	✓	✓	✓	✓	✓	✓	✓	✓	✓	✓	✓	✓	✓	✓	✓	✓	✓	✓	✓	✓	✓	✓	✓	✓	✓	✓	✓	✓	✓	✓	✓	✓	✓	✓	✓	✓	✓	✓	✓	✓	✓	✓	✓	✓	✓	✓	✓	✓	✓	✓	✓	✓	✓	✓	✓	✓	✓	✓	✓	✓	✓	✓	✓	✓	✓	✓	✓	✓	✓	✓	✓	✓	✓	✓	✓	✓	✓	✓	✓	✓	✓	✓	✓	✓	✓	✓	✓	✓	✓	✓	✓	✓	✓	✓	✓	✓	✓	✓	✓	✓	✓	✓	✓	✓	✓	✓	✓	✓	✓	✓	✓	✓	✓	✓	✓	✓	✓	✓	✓	✓	✓	✓	✓	✓	✓	✓	✓	✓	✓	✓	✓	✓	✓	✓	✓	✓	✓	✓	✓	✓	✓	✓	✓	✓	✓	✓	✓	✓	✓	✓	✓	✓	✓	✓	✓	✓	✓	✓	✓	✓	✓	✓	✓	✓	✓	✓	✓	✓	✓	✓	✓	✓	✓	✓	✓	✓	✓	✓	✓	✓	✓	✓	✓	✓	✓	✓	✓	✓	✓	✓	✓	✓	✓	✓	✓	✓	✓	✓	✓	✓	✓	✓	✓	✓	✓	✓	✓	✓	✓	✓	✓	✓	✓	✓	✓	✓	✓	✓	✓	✓	✓	✓	✓	✓	✓	✓	✓	✓	✓	✓	✓	✓	✓	✓	✓	✓	✓	✓	✓	✓	✓	✓	✓	✓	✓	✓	✓	✓	✓	✓	✓	✓	✓	✓	✓	✓	✓	✓	✓	✓	✓	✓	✓	✓	✓	✓	✓	✓	✓	✓	✓	✓	✓	✓	✓	✓	✓	✓	✓	✓	✓	✓	✓	✓	✓	✓	✓	✓	✓	✓	✓	✓	✓	✓	✓	✓	✓	✓	✓	✓	✓	✓	✓	✓	✓	✓	✓	✓	✓	✓	✓	✓	✓	✓	✓	✓	✓	✓	✓	✓	✓	✓	✓	✓	✓	✓	✓	✓	✓	✓	✓	✓	✓	✓	✓	✓	✓	✓	✓	✓	✓	✓	✓	✓	✓	✓	✓	✓	✓	✓	✓	✓	✓	✓	✓	✓	✓	✓	✓	✓	✓	✓	✓	✓	✓	✓	✓	✓	✓	✓	✓	✓	✓	✓	✓	✓	✓	✓	✓	✓	✓	✓	✓	✓	✓	✓	✓	✓	✓	✓	✓	✓	✓	✓	✓	✓	✓	✓	✓	✓	✓	✓	✓	✓	✓	✓	✓	✓	✓	✓	✓	✓	✓	✓	✓	✓	✓	✓

Run Schedule

Run	Blade Pitch Angle $\sim \alpha^\circ$						Blade iaw Angle $\sim \beta^\circ$			Nacelle Exit Fwd. Nacelle Config. (Spinner Type)	Nacelle Exit Fwd. Nacelle Config. (Spinner Type)			Config.	Tunnel $q \sim \text{psi}$	Remarks
	-3	0	3	6	9	12	20-10	0	10	20	0	78	90	95	10	
82	✓	✓	✓	✓	✓	✓	✓	✓	✓	✓	✓	✓	✓	✓	✓	NO FAIRING
83	✓	✓	✓	✓	✓	✓	✓	✓	✓	✓	✓	✓	✓	✓	✓	
84	✓	✓	✓	✓	✓	✓	✓	✓	✓	✓	✓	✓	✓	✓	✓	
85	✓	✓	✓	✓	✓	✓	✓	✓	✓	✓	✓	✓	✓	✓	✓	
86	✓	✓	✓	✓	✓	✓	✓	✓	✓	✓	✓	✓	✓	✓	✓	
87	✓	✓	✓	✓	✓	✓	✓	✓	✓	✓	✓	✓	✓	✓	✓	
88	✓	✓	✓	✓	✓	✓	✓	✓	✓	✓	✓	✓	✓	✓	✓	
89	✓	✓	✓	✓	✓	✓	✓	✓	✓	✓	✓	✓	✓	✓	✓	
90	✓	✓	✓	✓	✓	✓	✓	✓	✓	✓	✓	✓	✓	✓	✓	
91	✓	✓	✓	✓	✓	✓	✓	✓	✓	✓	✓	✓	✓	✓	✓	
92	✓	✓	✓	✓	✓	✓	✓	✓	✓	✓	✓	✓	✓	✓	✓	
93	✓	✓	✓	✓	✓	✓	✓	✓	✓	✓	✓	✓	✓	✓	✓	
94	✓	✓	✓	✓	✓	✓	✓	✓	✓	✓	✓	✓	✓	✓	✓	
95	✓	✓	✓	✓	✓	✓	✓	✓	✓	✓	✓	✓	✓	✓	✓	
96	✓	✓	✓	✓	✓	✓	✓	✓	✓	✓	✓	✓	✓	✓	✓	
97	✓	✓	✓	✓	✓	✓	✓	✓	✓	✓	✓	✓	✓	✓	✓	
98	✓	✓	✓	✓	✓	✓	✓	✓	✓	✓	✓	✓	✓	✓	✓	
99	✓	✓	✓	✓	✓	✓	✓	✓	✓	✓	✓	✓	✓	✓	✓	
100	✓	✓	✓	✓	✓	✓	✓	✓	✓	✓	✓	✓	✓	✓	✓	
101	✓	✓	✓	✓	✓	✓	✓	✓	✓	✓	✓	✓	✓	✓	✓	
102	✓	✓	✓	✓	✓	✓	✓	✓	✓	✓	✓	✓	✓	✓	✓	
103	✓	✓	✓	✓	✓	✓	✓	✓	✓	✓	✓	✓	✓	✓	✓	
104	✓	✓	✓	✓	✓	✓	✓	✓	✓	✓	✓	✓	✓	✓	✓	
105	✓	✓	✓	✓	✓	✓	✓	✓	✓	✓	✓	✓	✓	✓	✓	
106	✓	✓	✓	✓	✓	✓	✓	✓	✓	✓	✓	✓	✓	✓	✓	
107	✓	✓	✓	✓	✓	✓	✓	✓	✓	✓	✓	✓	✓	✓	✓	
108	✓	✓	✓	✓	✓	✓	✓	✓	✓	✓	✓	✓	✓	✓	✓	

Run Schedule

R u n	Blade Pitch Angle ~ α°									Blade Yaw Angle ~ β°			Nacelle Exit Config.			Nacelle Config. (Spinner Type)	α_i°			Config.	Tunnel q ~ psi	Remarks			
	-3			0			3			6			9				12						15		
	0	3	6	9	12	15	0	3	6	9	12	15	0	3	6		0	3	6						
109	✓	✓	✓	✓	✓	✓	✓	✓	✓	✓	✓	✓	✓	✓	✓	1-50-100 (PARABOLIC)	✓	✓	✓	SINGLE ENGINE	48	NO FAIRING			
110	✓	✓	✓	✓	✓	✓	✓	✓	✓	✓	✓	✓	✓	✓	✓	✓	✓	✓	✓	✓	✓	✓	✓		
111	✓	✓	✓	✓	✓	✓	✓	✓	✓	✓	✓	✓	✓	✓	✓	✓	✓	✓	✓	✓	✓	✓	✓		
112	✓	✓	✓	✓	✓	✓	✓	✓	✓	✓	✓	✓	✓	✓	✓	✓	✓	✓	✓	✓	✓	✓	✓		
113	✓	✓	✓	✓	✓	✓	✓	✓	✓	✓	✓	✓	✓	✓	✓	✓	✓	✓	✓	✓	✓	✓	✓		
114	✓	✓	✓	✓	✓	✓	✓	✓	✓	✓	✓	✓	✓	✓	✓	✓	✓	✓	✓	✓	✓	✓	✓		
115	✓	✓	✓	✓	✓	✓	✓	✓	✓	✓	✓	✓	✓	✓	✓	✓	✓	✓	✓	✓	✓	✓	✓		
116	✓	✓	✓	✓	✓	✓	✓	✓	✓	✓	✓	✓	✓	✓	✓	✓	✓	✓	✓	✓	✓	✓	✓		
117	✓	✓	✓	✓	✓	✓	✓	✓	✓	✓	✓	✓	✓	✓	✓	✓	✓	✓	✓	✓	✓	✓	✓		
118	✓	✓	✓	✓	✓	✓	✓	✓	✓	✓	✓	✓	✓	✓	✓	✓	✓	✓	✓	✓	✓	✓	✓		
119	✓	✓	✓	✓	✓	✓	✓	✓	✓	✓	✓	✓	✓	✓	✓	✓	✓	✓	✓	✓	✓	✓	✓		
120	✓	✓	✓	✓	✓	✓	✓	✓	✓	✓	✓	✓	✓	✓	✓	✓	✓	✓	✓	✓	✓	✓	✓		
121	✓	✓	✓	✓	✓	✓	✓	✓	✓	✓	✓	✓	✓	✓	✓	✓	✓	✓	✓	✓	✓	✓	✓		
122	✓	✓	✓	✓	✓	✓	✓	✓	✓	✓	✓	✓	✓	✓	✓	✓	✓	✓	✓	✓	✓	✓	✓		
123	✓	✓	✓	✓	✓	✓	✓	✓	✓	✓	✓	✓	✓	✓	✓	✓	✓	✓	✓	✓	✓	✓	✓		
124	✓	✓	✓	✓	✓	✓	✓	✓	✓	✓	✓	✓	✓	✓	✓	✓	✓	✓	✓	✓	✓	✓	✓		
125	✓	✓	✓	✓	✓	✓	✓	✓	✓	✓	✓	✓	✓	✓	✓	✓	✓	✓	✓	✓	✓	✓	✓		
126	✓	✓	✓	✓	✓	✓	✓	✓	✓	✓	✓	✓	✓	✓	✓	✓	✓	✓	✓	✓	✓	✓	✓		
127	✓	✓	✓	✓	✓	✓	✓	✓	✓	✓	✓	✓	✓	✓	✓	✓	✓	✓	✓	✓	✓	✓	✓		
128	✓	✓	✓	✓	✓	✓	✓	✓	✓	✓	✓	✓	✓	✓	✓	✓	✓	✓	✓	✓	✓	✓	✓		
129	✓	✓	✓	✓	✓	✓	✓	✓	✓	✓	✓	✓	✓	✓	✓	✓	✓	✓	✓	✓	✓	✓	✓		
130	✓	✓	✓	✓	✓	✓	✓	✓	✓	✓	✓	✓	✓	✓	✓	✓	✓	✓	✓	✓	✓	✓	✓		
131	✓	✓	✓	✓	✓	✓	✓	✓	✓	✓	✓	✓	✓	✓	✓	✓	✓	✓	✓	✓	✓	✓	✓		
132	✓	✓	✓	✓	✓	✓	✓	✓	✓	✓	✓	✓	✓	✓	✓	✓	✓	✓	✓	✓	✓	✓	✓		
133	✓	✓	✓	✓	✓	✓	✓	✓	✓	✓	✓	✓	✓	✓	✓	✓	✓	✓	✓	✓	✓	✓	✓		
134	✓	✓	✓	✓	✓	✓	✓	✓	✓	✓	✓	✓	✓	✓	✓	✓	✓	✓	✓	✓	✓	✓	✓		
135	✓	✓	✓	✓	✓	✓	✓	✓	✓	✓	✓	✓	✓	✓	✓	✓	✓	✓	✓	✓	✓	✓	✓		

△ WITH AND WITHOUT BASE FAIRING

Run Schedule

Run	Blade Pitch Angle $\sim \alpha$						Blade Yaw Angle $\sim \beta$			Nacelle Exit Config.			Fwd. Nacelle Config. (Spinner Type)			α_i			Config.	Tunnel $q \sim \text{psi}$	Remarks
	3	0	3	6	9	12	20	10	0	10	20	0	78	90	100	0	3	6			
136	✓	✓	✓	✓	✓	✓	✓	✓	✓	✓	✓	✓	✓	✓	✓	✓	✓	✓	TWIN ENGINES VERTICAL	88	WITH FAIRING
137	✓	✓	✓	✓	✓	✓	✓	✓	✓	✓	✓	✓	✓	✓	✓	✓	✓	✓			
138	✓	✓	✓	✓	✓	✓	✓	✓	✓	✓	✓	✓	✓	✓	✓	✓	✓	✓			
139	✓	✓	✓	✓	✓	✓	✓	✓	✓	✓	✓	✓	✓	✓	✓	✓	✓	✓			
140	✓	✓	✓	✓	✓	✓	✓	✓	✓	✓	✓	✓	✓	✓	✓	✓	✓	✓			
141	✓	✓	✓	✓	✓	✓	✓	✓	✓	✓	✓	✓	✓	✓	✓	✓	✓	✓			
142	✓	✓	✓	✓	✓	✓	✓	✓	✓	✓	✓	✓	✓	✓	✓	✓	✓	✓			
143	✓	✓	✓	✓	✓	✓	✓	✓	✓	✓	✓	✓	✓	✓	✓	✓	✓	✓			
144	✓	✓	✓	✓	✓	✓	✓	✓	✓	✓	✓	✓	✓	✓	✓	✓	✓	✓			
145	✓	✓	✓	✓	✓	✓	✓	✓	✓	✓	✓	✓	✓	✓	✓	✓	✓	✓			
146	✓	✓	✓	✓	✓	✓	✓	✓	✓	✓	✓	✓	✓	✓	✓	✓	✓	✓			
147	✓	✓	✓	✓	✓	✓	✓	✓	✓	✓	✓	✓	✓	✓	✓	✓	✓	✓			
148	✓	✓	✓	✓	✓	✓	✓	✓	✓	✓	✓	✓	✓	✓	✓	✓	✓	✓			
149	✓	✓	✓	✓	✓	✓	✓	✓	✓	✓	✓	✓	✓	✓	✓	✓	✓	✓			
150	✓	✓	✓	✓	✓	✓	✓	✓	✓	✓	✓	✓	✓	✓	✓	✓	✓	✓			
151	✓	✓	✓	✓	✓	✓	✓	✓	✓	✓	✓	✓	✓	✓	✓	✓	✓	✓			
152	✓	✓	✓	✓	✓	✓	✓	✓	✓	✓	✓	✓	✓	✓	✓	✓	✓	✓			
153	✓	✓	✓	✓	✓	✓	✓	✓	✓	✓	✓	✓	✓	✓	✓	✓	✓	✓			
154	✓	✓	✓	✓	✓	✓	✓	✓	✓	✓	✓	✓	✓	✓	✓	✓	✓	✓			
155	✓	✓	✓	✓	✓	✓	✓	✓	✓	✓	✓	✓	✓	✓	✓	✓	✓	✓			
156	✓	✓	✓	✓	✓	✓	✓	✓	✓	✓	✓	✓	✓	✓	✓	✓	✓	✓			
157	✓	✓	✓	✓	✓	✓	✓	✓	✓	✓	✓	✓	✓	✓	✓	✓	✓	✓			
158	✓	✓	✓	✓	✓	✓	✓	✓	✓	✓	✓	✓	✓	✓	✓	✓	✓	✓	TWIN ENGINES HORIZONTAL		NO FAIRING
159	✓	✓	✓	✓	✓	✓	✓	✓	✓	✓	✓	✓	✓	✓	✓	✓	✓	✓			
160	✓	✓	✓	✓	✓	✓	✓	✓	✓	✓	✓	✓	✓	✓	✓	✓	✓	✓			
161	✓	✓	✓	✓	✓	✓	✓	✓	✓	✓	✓	✓	✓	✓	✓	✓	✓	✓			
162	✓	✓	✓	✓	✓	✓	✓	✓	✓	✓	✓	✓	✓	✓	✓	✓	✓	✓			

Δ WITH AND WITHOUT Balsa FAIRING
 Δ WITH AND WITHOUT Balsa FAIRING

Run Schedule

Run	Blade Pitch Angle $\sim \alpha^\circ$												Blade Yaw Angle $\sim \beta^\circ$				Nacelle Exit Fwd. Nacelle Config.		Config.	Tunnel $q \sim \text{psi}$	Remarks																																																																																																																																																																																																																																																																																																																																																																																																																																																																																																																																																																																																																																																																																																																																																																																																																																																																																																																																																																																																																																																																																																																																																																																																																																																																																																																																																																																																																																																																																																																																
	-3 0 3 6 9 12 15 18 20 22 24 26 28 30												0 10 20 30				Config.	Spinner Type)				0 3 6																																																																																																																																																																																																																																																																																																																																																																																																																																																																																																																																																																																																																																																																																																																																																																																																																																																																																																																																																																																																																																																																																																																																																																																																																																																																																																																																																																																																																																																																																																																															
	✓	✓	✓	✓	✓	✓	✓	✓	✓	✓	✓	✓	✓	✓	✓	✓							✓	✓	✓	✓	✓	✓	✓	✓	✓	✓	✓	✓	✓	✓	✓	✓	✓	✓	✓	✓	✓	✓	✓	✓	✓	✓	✓	✓	✓	✓	✓	✓	✓	✓	✓	✓	✓	✓	✓	✓	✓	✓	✓	✓	✓	✓	✓	✓	✓	✓	✓	✓	✓	✓	✓	✓	✓	✓	✓	✓	✓	✓	✓	✓	✓	✓	✓	✓	✓	✓	✓	✓	✓	✓	✓	✓	✓	✓	✓	✓	✓	✓	✓	✓	✓	✓	✓	✓	✓	✓	✓	✓	✓	✓	✓	✓	✓	✓	✓	✓	✓	✓	✓	✓	✓	✓	✓	✓	✓	✓	✓	✓	✓	✓	✓	✓	✓	✓	✓	✓	✓	✓	✓	✓	✓	✓	✓	✓	✓	✓	✓	✓	✓	✓	✓	✓	✓	✓	✓	✓	✓	✓	✓	✓	✓	✓	✓	✓	✓	✓	✓	✓	✓	✓	✓	✓	✓	✓	✓	✓	✓	✓	✓	✓	✓	✓	✓	✓	✓	✓	✓	✓	✓	✓	✓	✓	✓	✓	✓	✓	✓	✓	✓	✓	✓	✓	✓	✓	✓	✓	✓	✓	✓	✓	✓	✓	✓	✓	✓	✓	✓	✓	✓	✓	✓	✓	✓	✓	✓	✓	✓	✓	✓	✓	✓	✓	✓	✓	✓	✓	✓	✓	✓	✓	✓	✓	✓	✓	✓	✓	✓	✓	✓	✓	✓	✓	✓	✓	✓	✓	✓	✓	✓	✓	✓	✓	✓	✓	✓	✓	✓	✓	✓	✓	✓	✓	✓	✓	✓	✓	✓	✓	✓	✓	✓	✓	✓	✓	✓	✓	✓	✓	✓	✓	✓	✓	✓	✓	✓	✓	✓	✓	✓	✓	✓	✓	✓	✓	✓	✓	✓	✓	✓	✓	✓	✓	✓	✓	✓	✓	✓	✓	✓	✓	✓	✓	✓	✓	✓	✓	✓	✓	✓	✓	✓	✓	✓	✓	✓	✓	✓	✓	✓	✓	✓	✓	✓	✓	✓	✓	✓	✓	✓	✓	✓	✓	✓	✓	✓	✓	✓	✓	✓	✓	✓	✓	✓	✓	✓	✓	✓	✓	✓	✓	✓	✓	✓	✓	✓	✓	✓	✓	✓	✓	✓	✓	✓	✓	✓	✓	✓	✓	✓	✓	✓	✓	✓	✓	✓	✓	✓	✓	✓	✓	✓	✓	✓	✓	✓	✓	✓	✓	✓	✓	✓	✓	✓	✓	✓	✓	✓	✓	✓	✓	✓	✓	✓	✓	✓	✓	✓	✓	✓	✓	✓	✓	✓	✓	✓	✓	✓	✓	✓	✓	✓	✓	✓	✓	✓	✓	✓	✓	✓	✓	✓	✓	✓	✓	✓	✓	✓	✓	✓	✓	✓	✓	✓	✓	✓	✓	✓	✓	✓	✓	✓	✓	✓	✓	✓	✓	✓	✓	✓	✓	✓	✓	✓	✓	✓	✓	✓	✓	✓	✓	✓	✓	✓	✓	✓	✓	✓	✓	✓	✓	✓	✓	✓	✓	✓	✓	✓	✓	✓	✓	✓	✓	✓	✓	✓	✓	✓	✓	✓	✓	✓	✓	✓	✓	✓	✓	✓	✓	✓	✓	✓	✓	✓	✓	✓	✓	✓	✓	✓	✓	✓	✓	✓	✓	✓	✓	✓	✓	✓	✓	✓	✓	✓	✓	✓	✓	✓	✓	✓	✓	✓	✓	✓	✓	✓	✓	✓	✓	✓	✓	✓	✓	✓	✓	✓	✓	✓	✓	✓	✓	✓	✓	✓	✓	✓	✓	✓	✓	✓	✓	✓	✓	✓	✓	✓	✓	✓	✓	✓	✓	✓	✓	✓	✓	✓	✓	✓	✓	✓	✓	✓	✓	✓	✓	✓	✓	✓	✓	✓	✓	✓	✓	✓	✓	✓	✓	✓	✓	✓	✓	✓	✓	✓	✓	✓	✓	✓	✓	✓	✓	✓	✓	✓	✓	✓	✓	✓	✓	✓	✓	✓	✓	✓	✓	✓	✓	✓	✓	✓	✓	✓	✓	✓	✓	✓	✓	✓	✓	✓	✓	✓	✓	✓	✓	✓	✓	✓	✓	✓	✓	✓	✓	✓	✓	✓	✓	✓	✓	✓	✓	✓	✓	✓	✓	✓	✓	✓	✓	✓	✓	✓	✓	✓	✓	✓	✓	✓	✓	✓	✓	✓	✓	✓	✓	✓	✓	✓	✓	✓	✓	✓	✓	✓	✓	✓	✓	✓	✓	✓	✓	✓	✓	✓	✓	✓	✓	✓	✓	✓	✓	✓	✓	✓	✓	✓	✓	✓	✓	✓	✓	✓	✓	✓	✓	✓	✓	✓	✓	✓	✓	✓	✓	✓	✓	✓	✓	✓	✓	✓	✓	✓	✓	✓	✓	✓	✓	✓	✓	✓	✓	✓	✓	✓	✓	✓	✓	✓	✓	✓	✓	✓	✓	✓	✓	✓	✓	✓	✓	✓	✓	✓	✓	✓	✓	✓	✓	✓	✓	✓	✓	✓	✓	✓	✓	✓	✓	✓	✓	✓	✓	✓	✓	✓	✓	✓	✓	✓	✓	✓	✓	✓	✓	✓	✓	✓	✓	✓	✓	✓	✓	✓	✓	✓	✓	✓	✓	✓	✓	✓	✓	✓	✓	✓	✓	✓	✓	✓	✓	✓	✓	✓	✓	✓	✓	✓	✓	✓	✓	✓	✓	✓	✓	✓	✓	✓	✓	✓	✓	✓	✓	✓	✓	✓	✓	✓	✓	✓	✓	✓	✓	✓	✓	✓	✓	✓	✓	✓	✓	✓	✓	✓	✓	✓	✓	✓	✓	✓	✓	✓	✓	✓	✓	✓	✓	✓	✓	✓	✓	✓	✓	✓	✓	✓	✓	✓	✓	✓	✓	✓	✓	✓	✓	✓	✓	✓	✓	✓	✓	✓	✓	✓	✓	✓	✓	✓	✓	✓	✓	✓	✓	✓	✓	✓	✓	✓	✓	✓	✓	✓	✓	✓	✓	✓	✓	✓	✓	✓	✓	✓	✓	✓	✓	✓	✓	✓	✓	✓	✓	✓	✓	✓	✓	✓	✓	✓	✓	✓	✓	✓	✓	✓	✓	✓	✓	✓	✓	✓	✓	✓	✓	✓	✓	✓	✓	✓	✓	✓	✓	✓	✓	✓	✓	✓	✓	✓	✓	✓	✓	✓	✓	✓	✓	✓	✓	✓	✓	✓	✓	✓	✓	✓	✓	✓	✓	✓	✓	✓	✓	✓	✓	✓	✓	✓	✓	✓	✓	✓	✓	✓	✓	✓	✓	✓	✓	✓	✓	✓	✓	✓	✓	✓	✓	✓	✓	✓	✓	✓	✓	✓	✓	✓	✓	✓	✓	✓	✓	✓	✓	✓	✓	✓	✓	✓	✓	✓	✓	✓	✓	✓	✓	✓	✓	✓	✓	✓	✓	✓	✓	✓	✓	✓	✓	✓	✓	✓	✓	✓	✓	✓	✓	✓	✓	✓	✓	✓	✓	✓	✓	✓	✓	✓	✓	✓	✓	✓	✓	✓	✓	✓	✓	✓	✓	✓	✓	✓	✓	✓	✓	✓	✓	✓	✓	✓	✓	✓	✓	✓	✓	✓	✓	✓	✓	✓	✓	✓	✓	✓	✓	✓	✓	✓	✓	✓	✓	✓	✓	✓	✓	✓	✓	✓	✓	✓	✓	✓	✓	✓	✓	✓	✓	✓	✓	✓	✓	✓	✓	✓	✓	✓	✓	✓	✓	✓	✓	✓	✓	✓	✓	✓	✓	✓	✓	✓	✓	✓	✓	✓	✓	✓	✓	✓	✓	✓	✓	✓	✓	✓	✓	✓	✓	✓	✓	✓	✓	✓	✓	✓	✓	✓	✓	✓	✓	✓	✓	✓	✓	✓	✓	✓	✓	✓	✓	✓	✓	✓	✓	✓	✓	✓	✓	✓	✓	✓	✓	✓	✓	✓	✓	✓	✓	✓	✓	✓	✓	✓	✓	✓	✓	✓	✓	✓	✓	✓	✓	✓	✓	✓	✓	✓	✓	✓	✓	✓	✓	✓	✓	✓	✓	✓	✓	✓	✓	✓	✓	✓	✓	✓	✓	✓	✓	✓	✓	✓	✓	✓	✓	✓	✓	✓	✓	✓	✓	✓	✓	✓	✓	✓	✓	✓	✓	✓	✓	✓	✓	✓	✓	✓	✓	✓	✓	✓	✓	✓	✓	✓	✓	✓	✓	✓	✓	✓	✓	✓	✓	✓	✓	✓	✓	✓	✓	✓	✓	✓	✓	✓	✓	✓	✓	✓	✓	✓	✓	✓	✓	✓	✓	✓	✓	✓	✓	✓	✓	✓	✓	✓	✓	✓	✓	✓	✓	✓	✓	✓	✓	✓	✓	✓	✓	✓	✓	✓	✓	✓	✓	✓	✓	✓	✓	✓	✓	✓	✓	✓	✓	✓	✓	✓	✓	✓	✓	✓	✓	✓	✓	✓	✓	✓	✓	✓	✓	✓	✓	✓	✓	✓	✓	✓	✓	✓	✓	✓	✓	✓	✓	✓	✓	✓	✓	✓	✓	✓	✓	✓	✓	✓	✓	✓	✓	✓	✓	✓	✓	✓	✓	✓	✓	✓	✓	✓	✓	✓	✓	✓	✓	✓	✓	✓	✓	✓	✓	✓	✓	✓	✓	✓	✓	✓	✓	✓	✓	✓	✓	✓	✓	✓	✓	✓

Run Schedule

Run	Blade Pitch Angle ~ α°				Blade Yaw Angle ~ β°				Nacelle Exit Config.		Fwd. Nacelle Config. (Spinner Type)		α_i°			Config.	Tunnel q ~ psi	Remarks	
	3	0	3	6	9	12	15	18	20	0	78	90	95	100	0				3
190	✓	✓	✓	✓	✓	✓	✓	✓	✓	✓	✓	✓	✓	✓	✓	✓	✓	48	WITH FAIRING
191	✓	✓	✓	✓	✓	✓	✓	✓	✓	✓	✓	✓	✓	✓	✓	✓	✓	✓	NO FAIRING
192	✓	✓	✓	✓	✓	✓	✓	✓	✓	✓	✓	✓	✓	✓	✓	✓	✓	✓	WITH FAIRING
193	✓	✓	✓	✓	✓	✓	✓	✓	✓	✓	✓	✓	✓	✓	✓	✓	✓	✓	
194	✓	✓	✓	✓	✓	✓	✓	✓	✓	✓	✓	✓	✓	✓	✓	✓	✓	✓	
195	✓	✓	✓	✓	✓	✓	✓	✓	✓	✓	✓	✓	✓	✓	✓	✓	✓	✓	
196	✓	✓	✓	✓	✓	✓	✓	✓	✓	✓	✓	✓	✓	✓	✓	✓	✓	✓	
197	✓	✓	✓	✓	✓	✓	✓	✓	✓	✓	✓	✓	✓	✓	✓	✓	✓	✓	
198	✓	✓	✓	✓	✓	✓	✓	✓	✓	✓	✓	✓	✓	✓	✓	✓	✓	✓	
199	✓	✓	✓	✓	✓	✓	✓	✓	✓	✓	✓	✓	✓	✓	✓	✓	✓	✓	
200	✓	✓	✓	✓	✓	✓	✓	✓	✓	✓	✓	✓	✓	✓	✓	✓	✓	✓	NO FAIRING
201	✓	✓	✓	✓	✓	✓	✓	✓	✓	✓	✓	✓	✓	✓	✓	✓	✓	✓	
202	✓	✓	✓	✓	✓	✓	✓	✓	✓	✓	✓	✓	✓	✓	✓	✓	✓	✓	
203	✓	✓	✓	✓	✓	✓	✓	✓	✓	✓	✓	✓	✓	✓	✓	✓	✓	✓	
204	✓	✓	✓	✓	✓	✓	✓	✓	✓	✓	✓	✓	✓	✓	✓	✓	✓	✓	
205	REPEAT OF RUN 135																		

5.2 Tuft Photos

Tuft photos for runs 188 through 197 are given in Figures 68 through 79. These photographs were taken from the top of the test section.



Figure 68a: Run 188, $\alpha = 0$.



Figure 68b: Run 188, $\alpha = 0$.



Figure 69a: Run 188, $\alpha = 6$.



Figure 69b: Run 188, $\alpha = 6$.



Figure 70a: Run 188, $\alpha = 12$.



Figure 70b: Run 188, $\alpha = 12$.

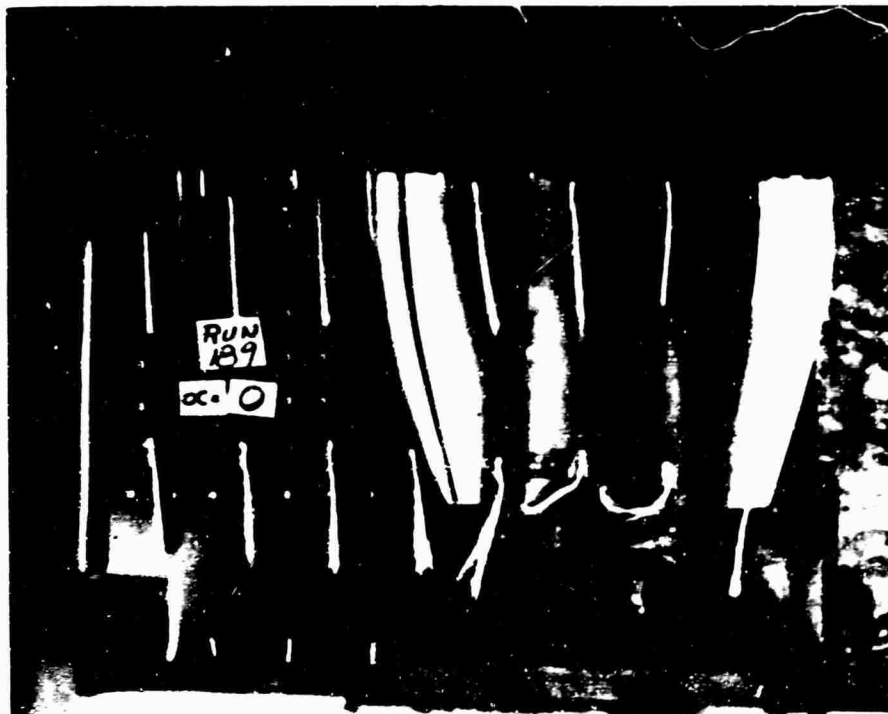


Figure 71a: Run 189, $\alpha = 0$.

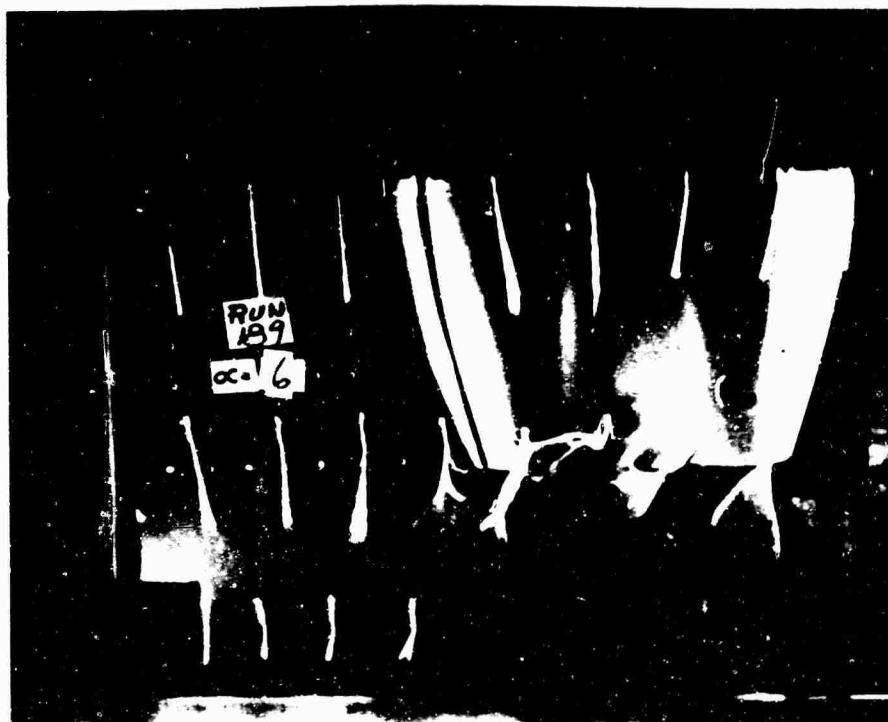


Figure 71b: Run 189, $\alpha = 6$.

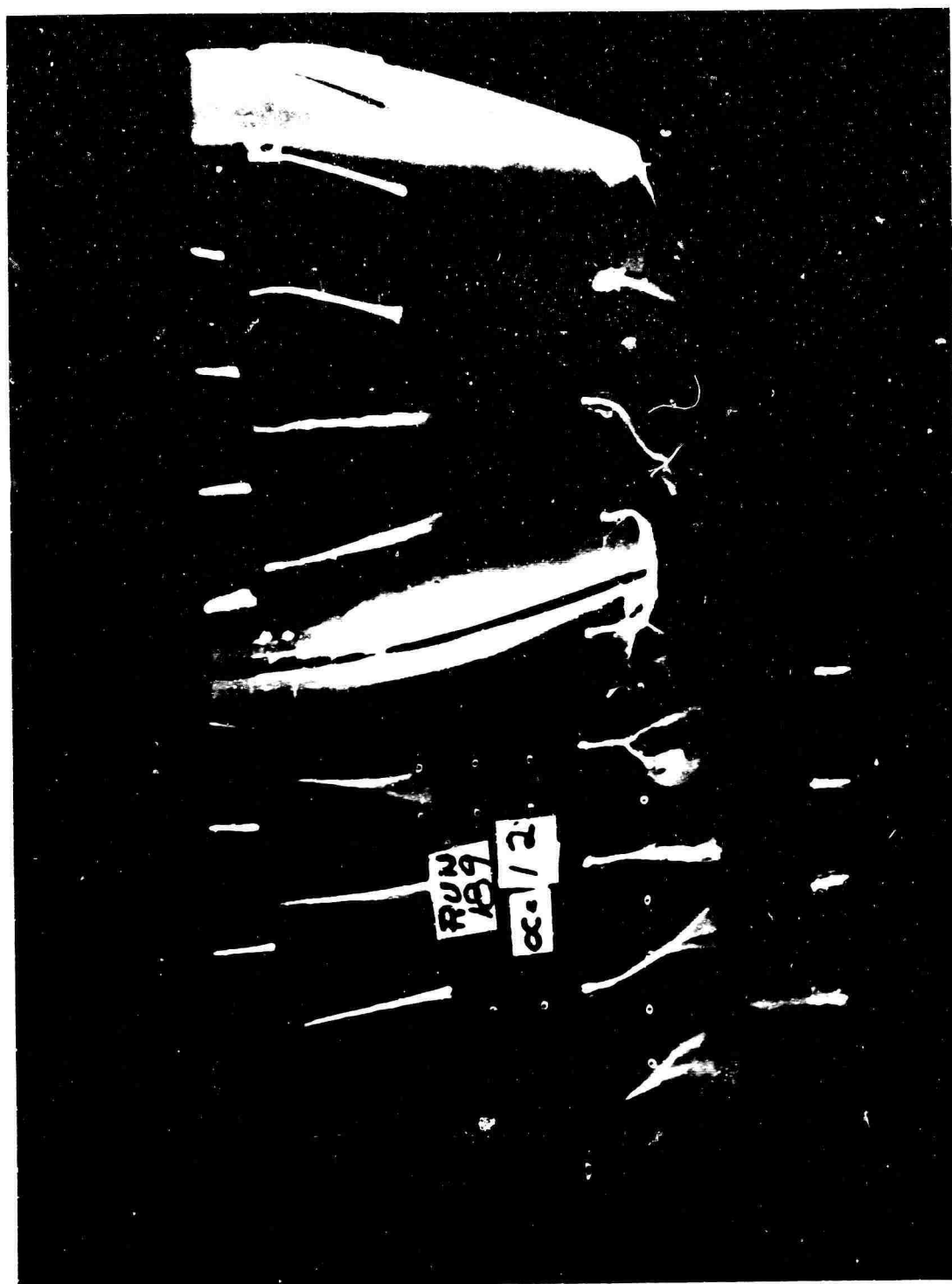


Figure 71c: Run 189, $\alpha = 12$.

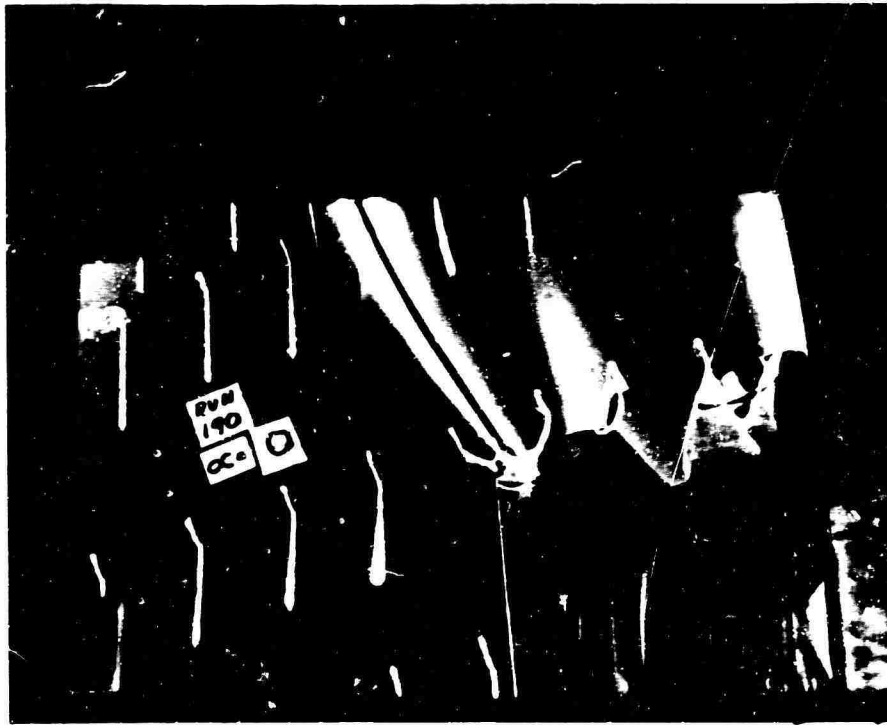


Figure 72a: Run 190, $\alpha = 0$.

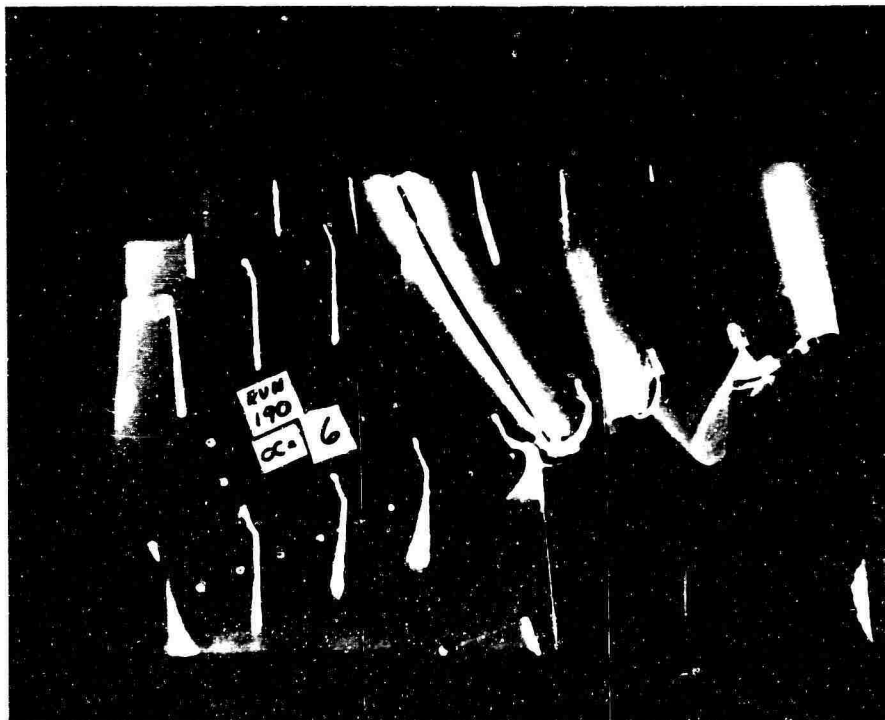


Figure 72b: Run 190, $\alpha = 6$.



Figure 72c: Run 190, $\alpha = 12$.

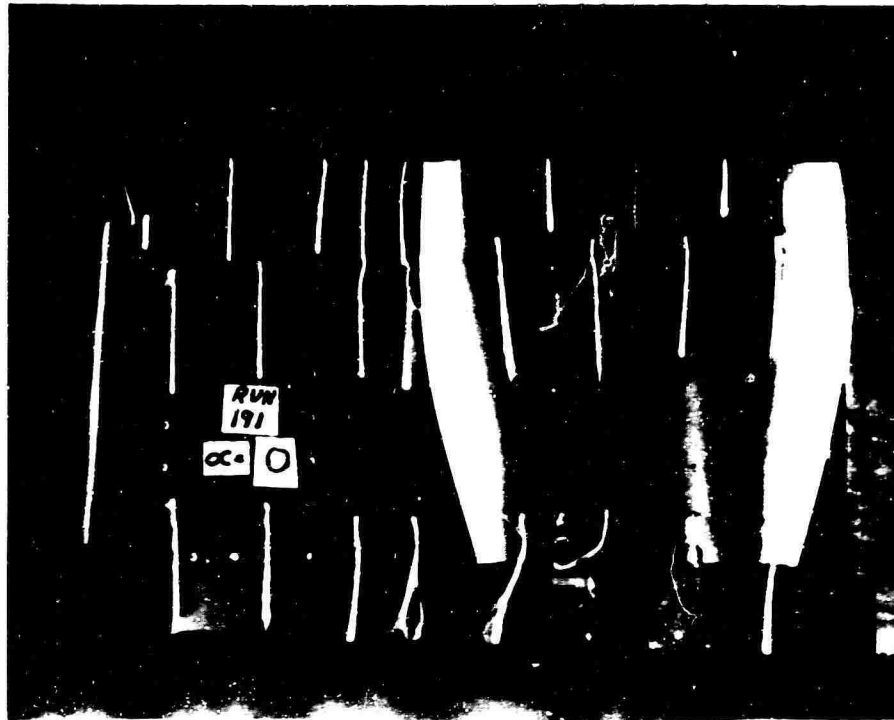


Figure 73a: Run 191, $\alpha = 0$.

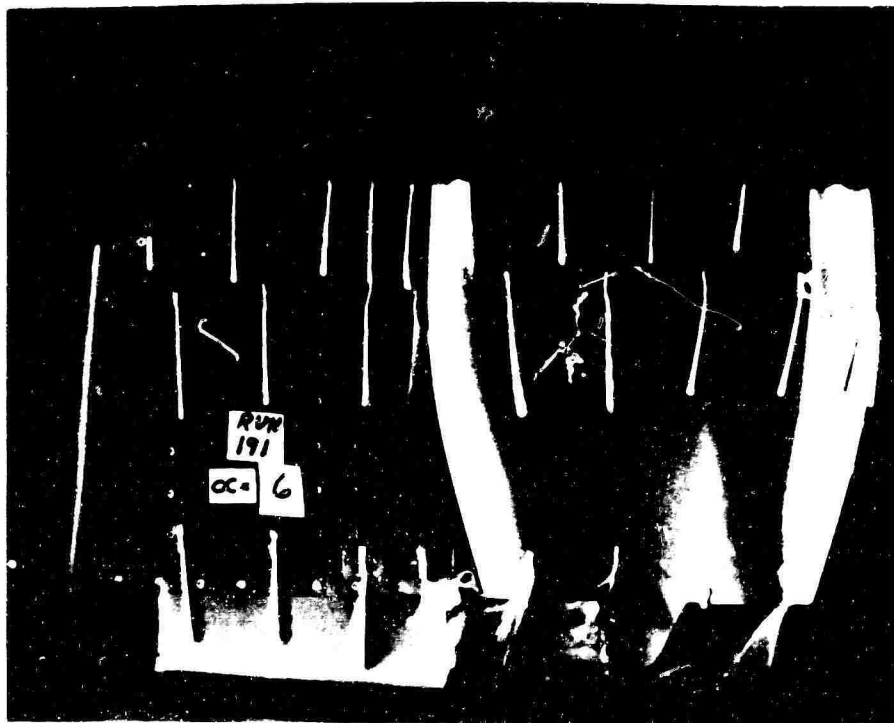


Figure 73b: Run 191, $\alpha = 6$.

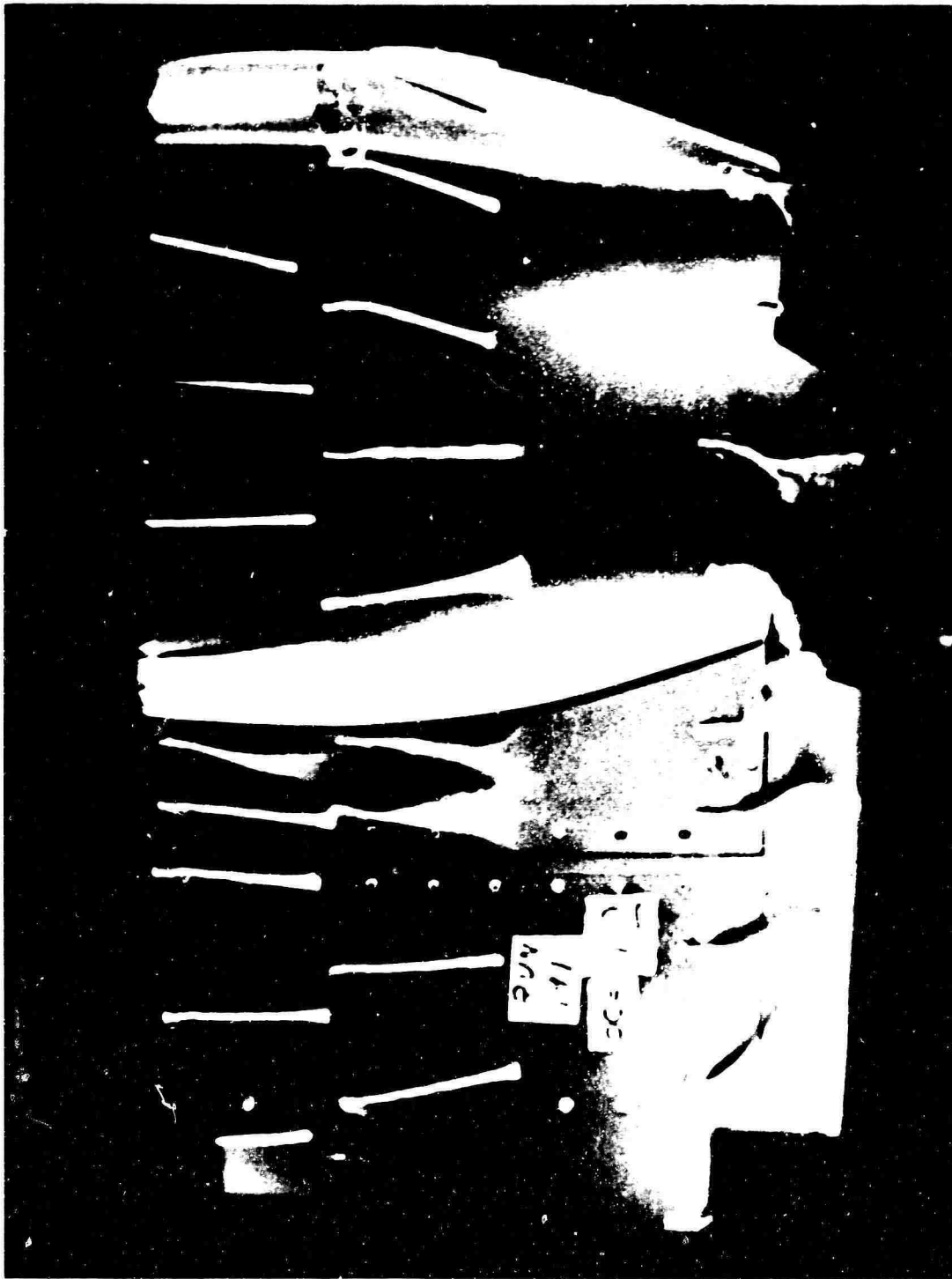


Figure 73c: Run 191, $\alpha = 12^\circ$.

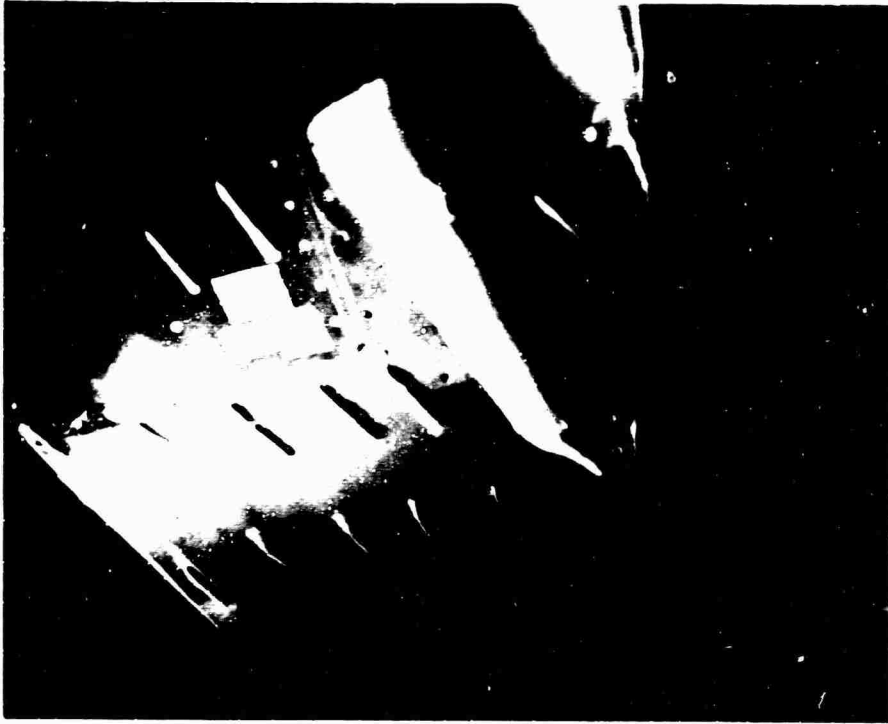


Figure 74a: Run 192, $\alpha = 0$.

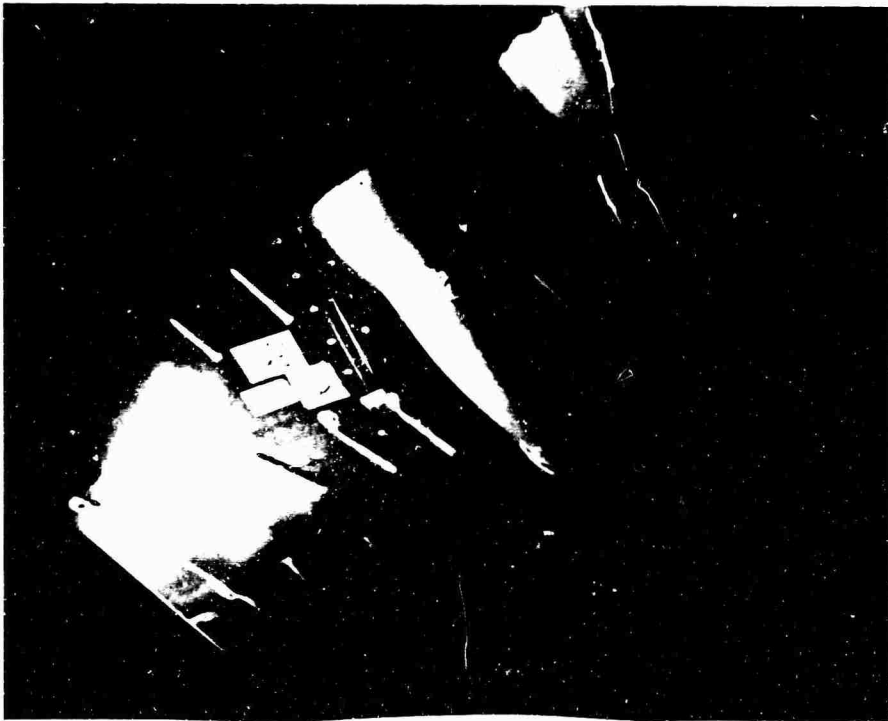


Figure 74b: Run 192, $\alpha = 6$.



Figure 74c: Run 192, $\alpha = 12^\circ$.

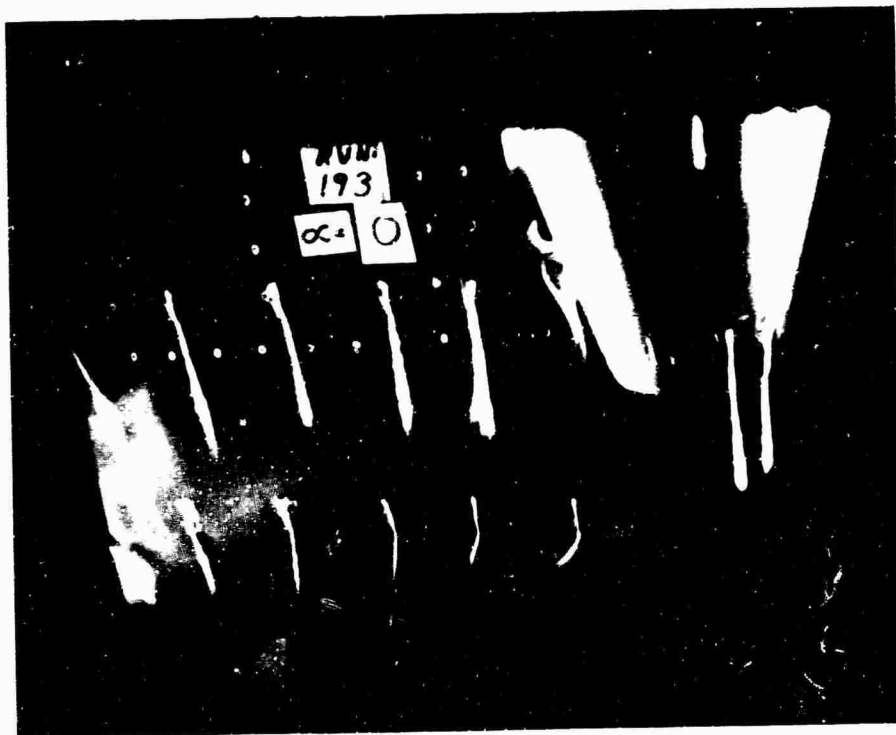


Figure 75a: Run 193, $\alpha = 0$.

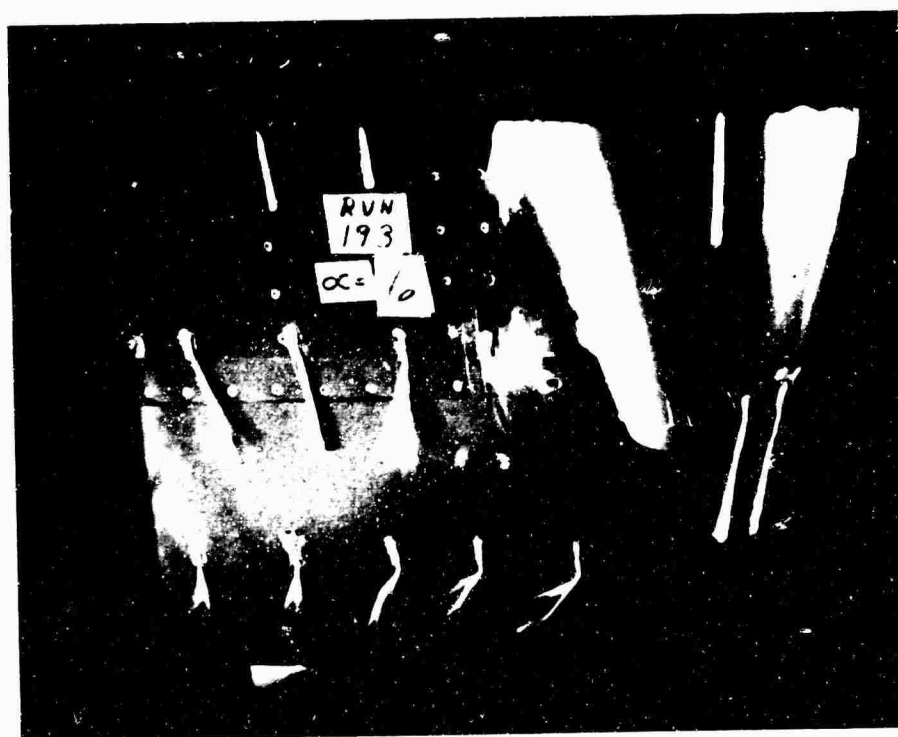


Figure 75b: Run 193, $\alpha = 6$.



Figure 75c: Run 193, $\alpha = 12$.

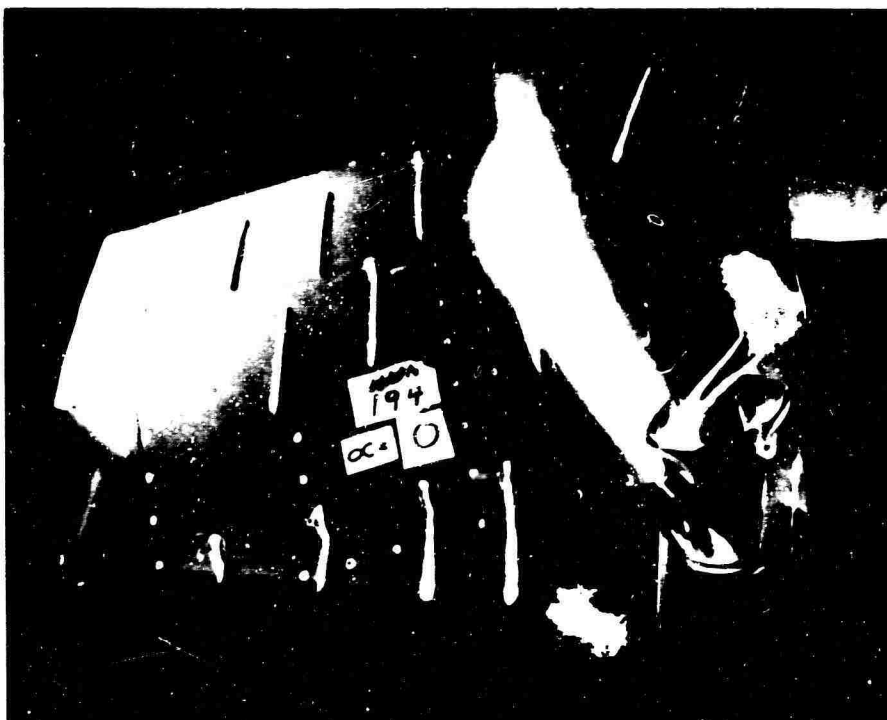


Figure 76a: Run 194, $\alpha = 0$.

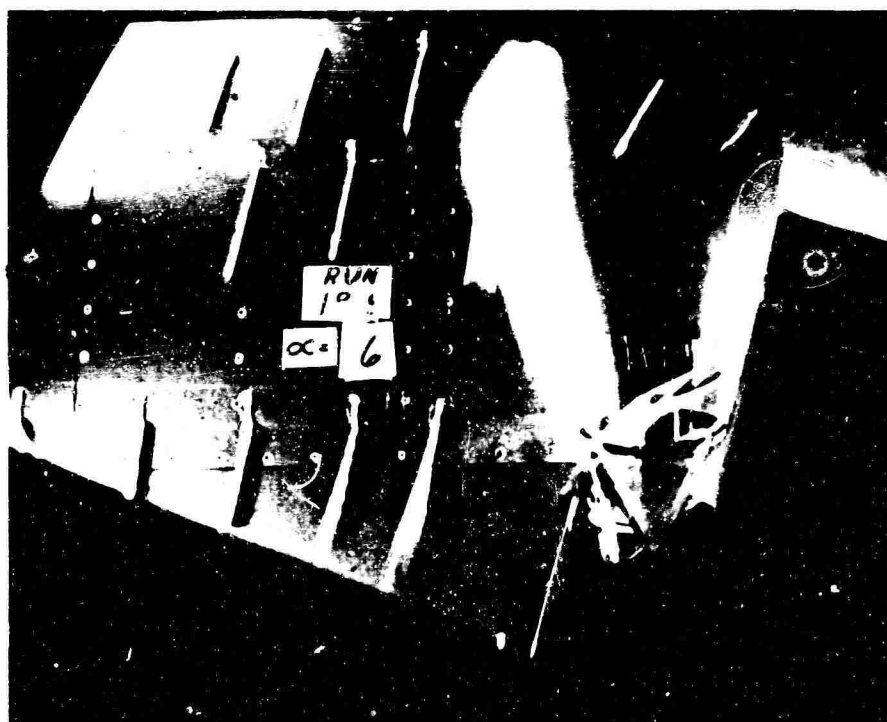


Figure 76b: Run 194, $\alpha = 6$.

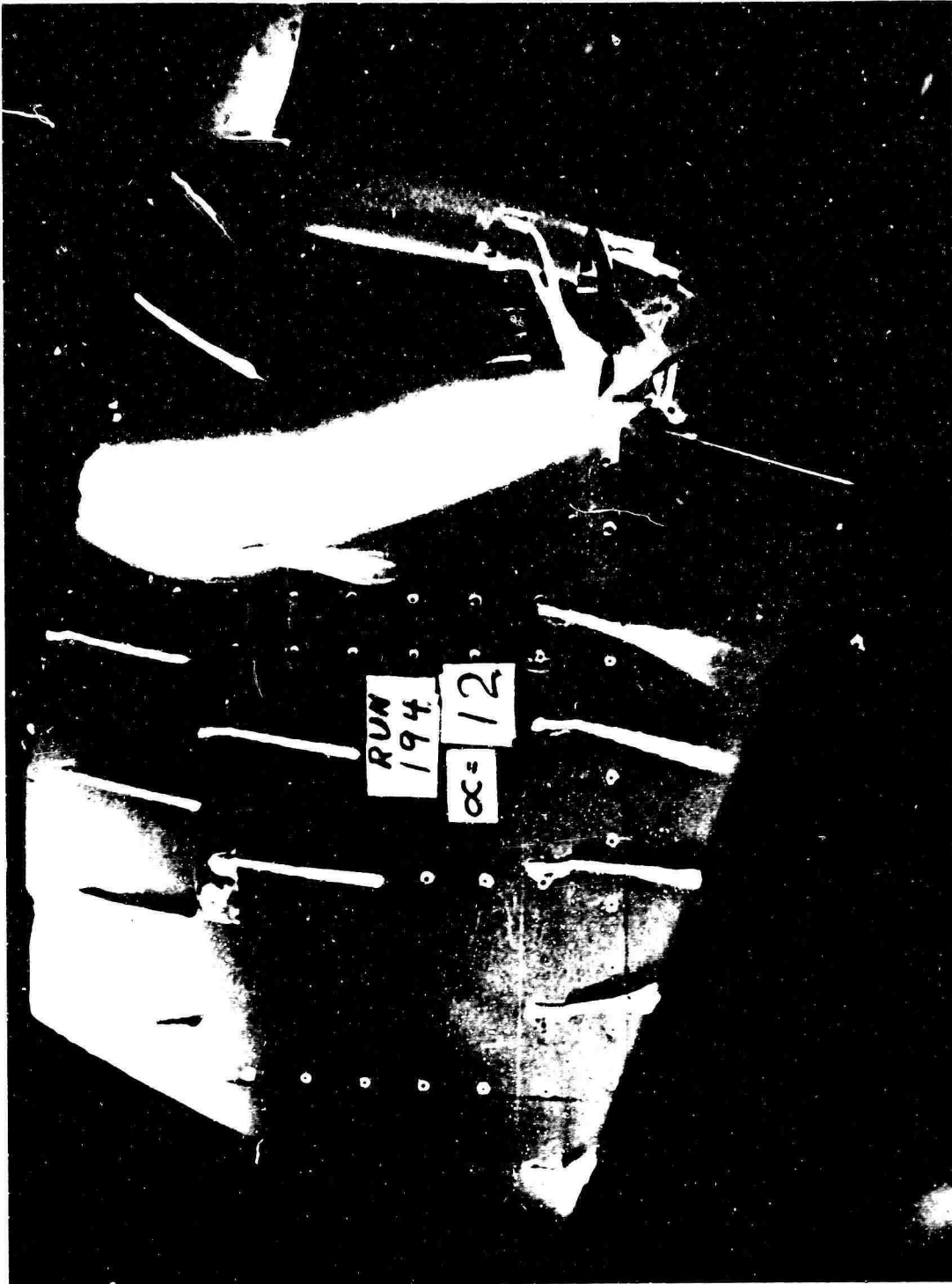


Figure 76c: Run 194, $\alpha = 12$.

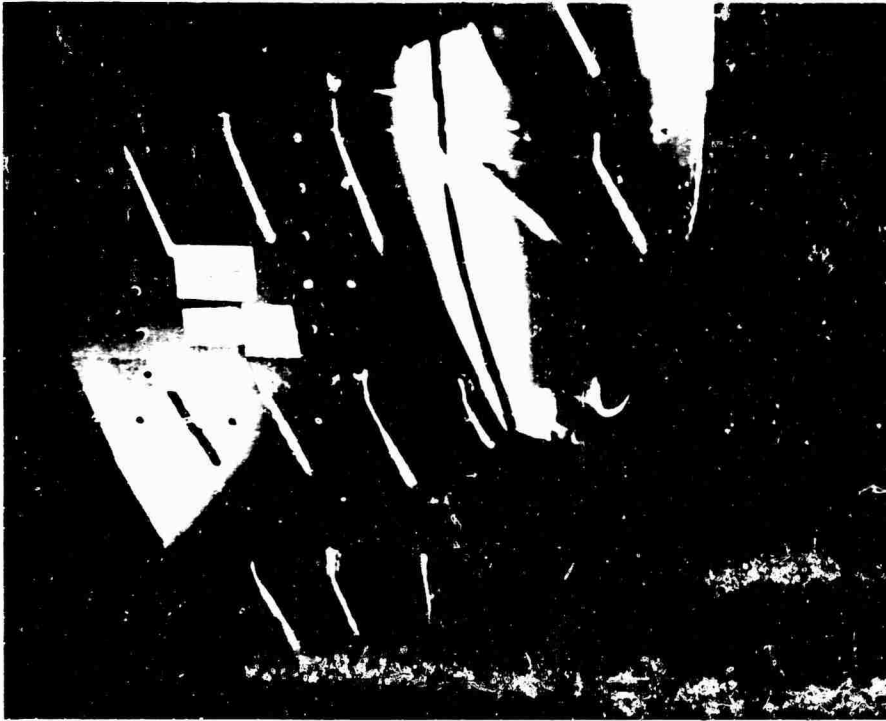


Figure 77a: Run 195, $\alpha = 0$.

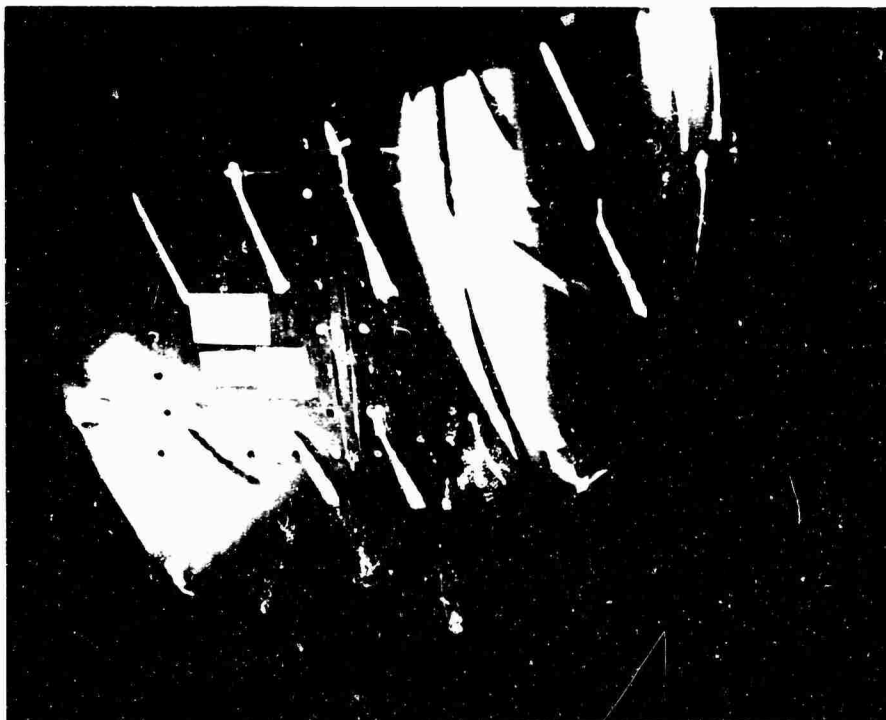


Figure 77b: Run 195, $\alpha = 6$.



Figure 77c: Run 195, $\alpha = 12$.

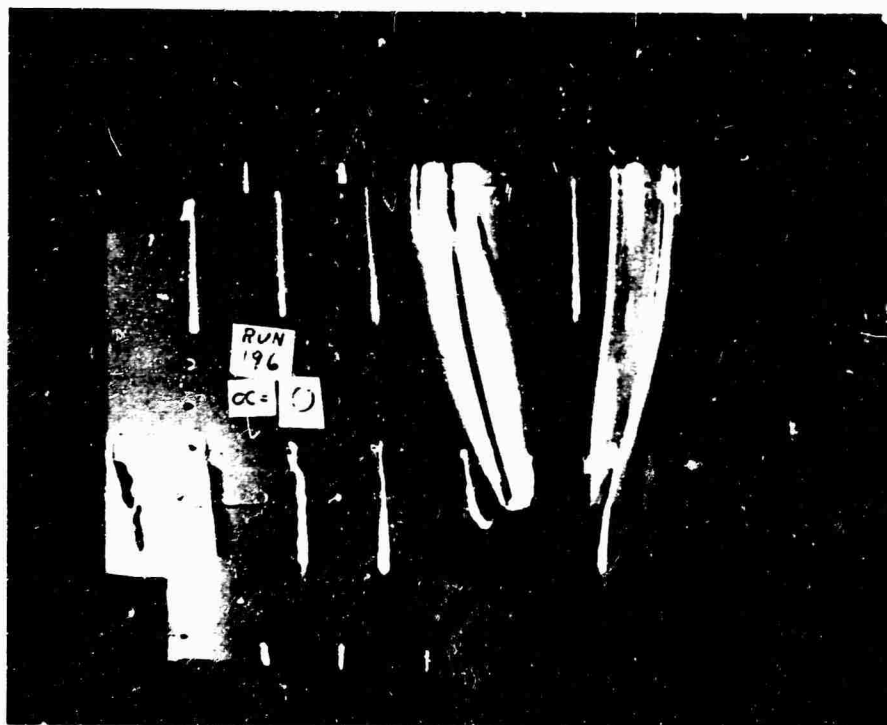


Figure 78a: Run 196, $\alpha = 0$.



Figure 78b: Run 196, $\alpha = 6$.



Figure 78c: Run 196, $\alpha = 12^\circ$.

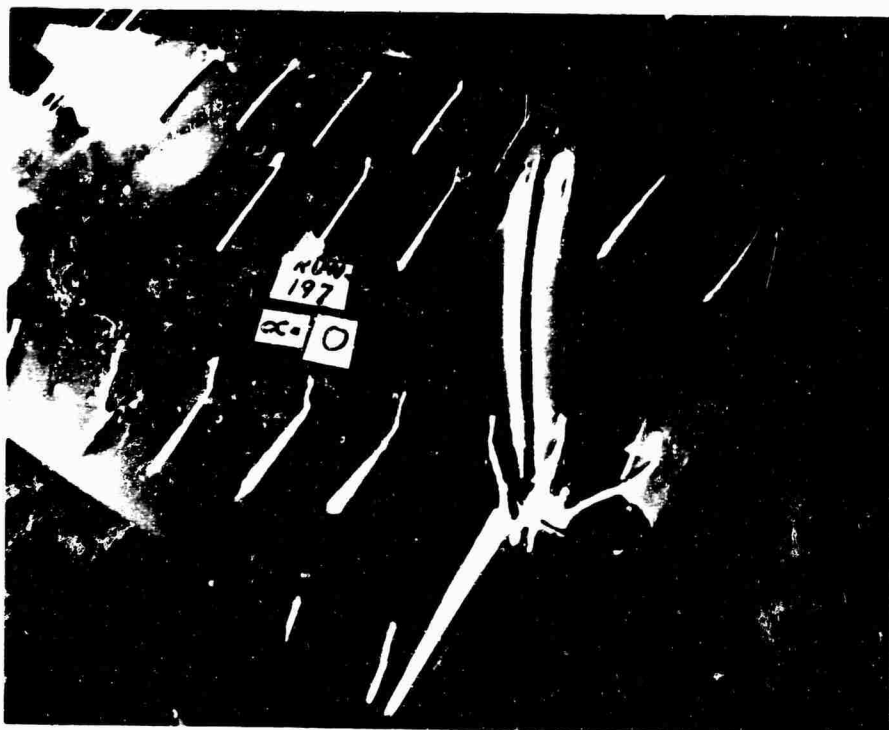


Figure 79a: Run 197, $\alpha = 0$.

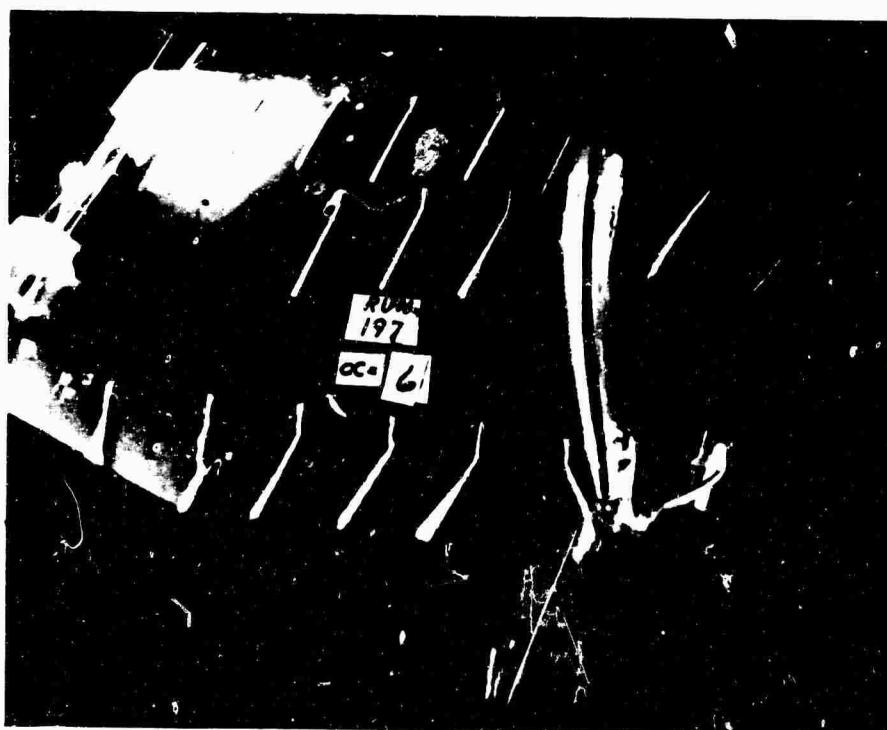
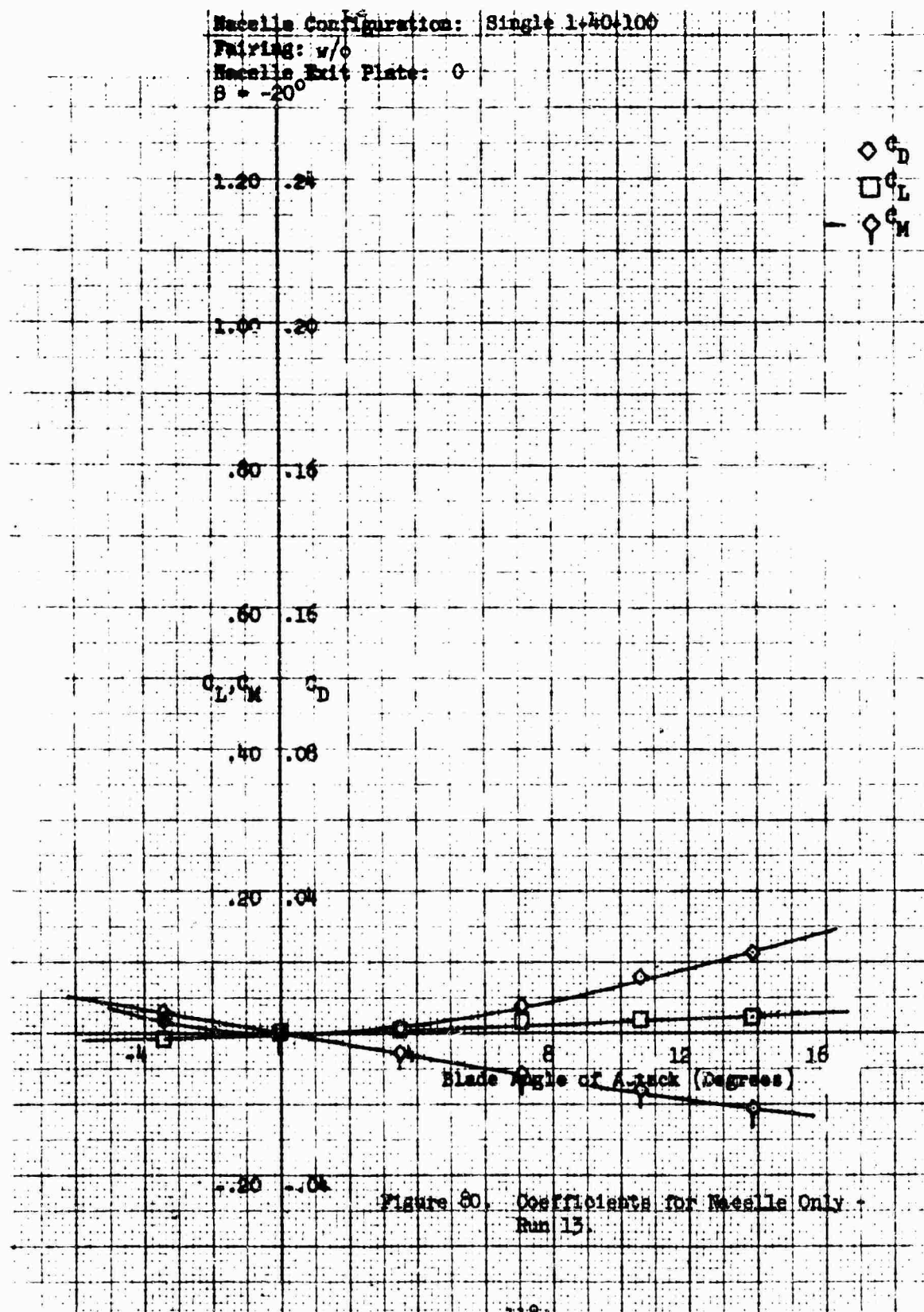


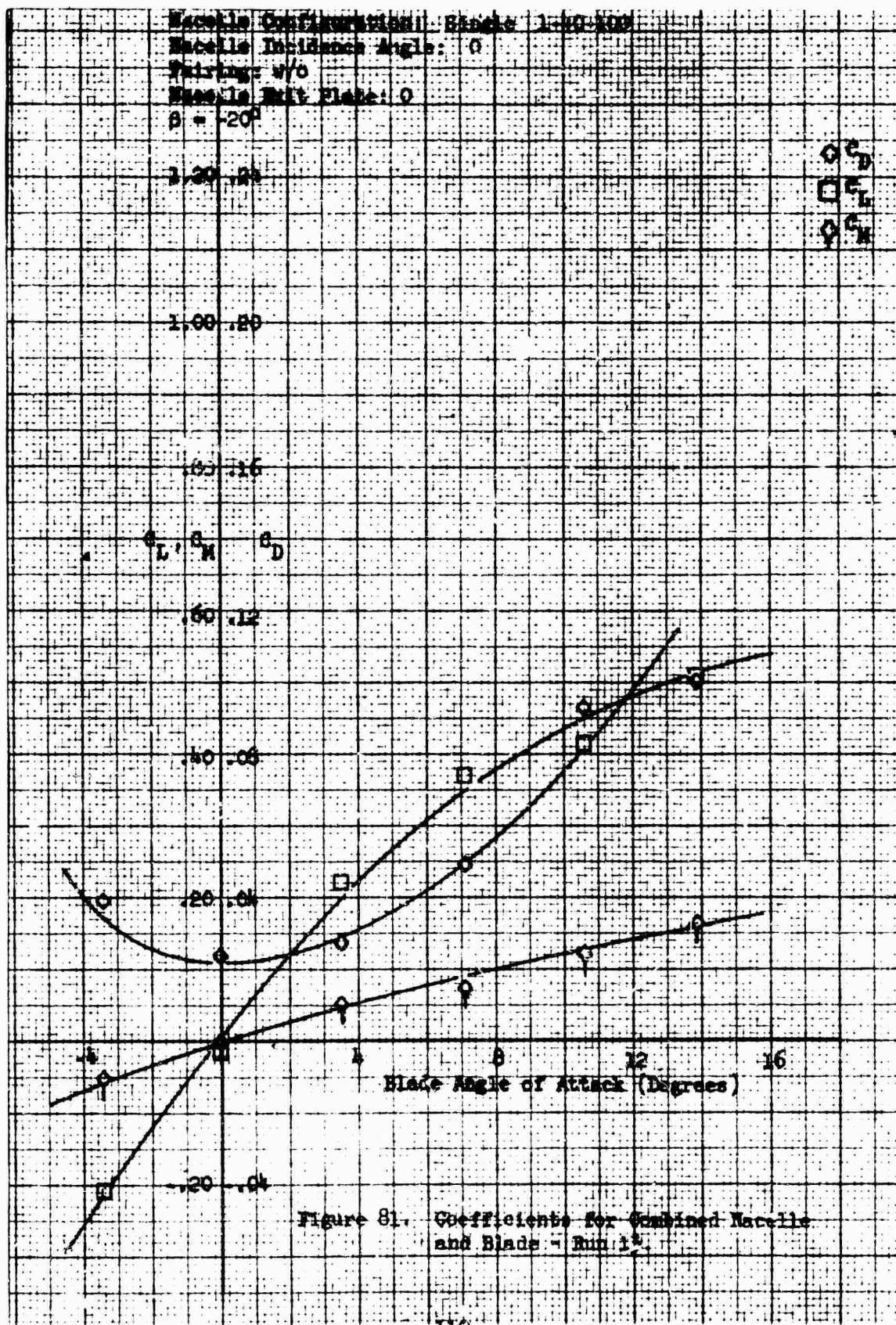
Figure 79b: Run 197, $\alpha = 6$.



Figure 79c: Run 197, $\alpha = 12$.

5.3 Data Plots



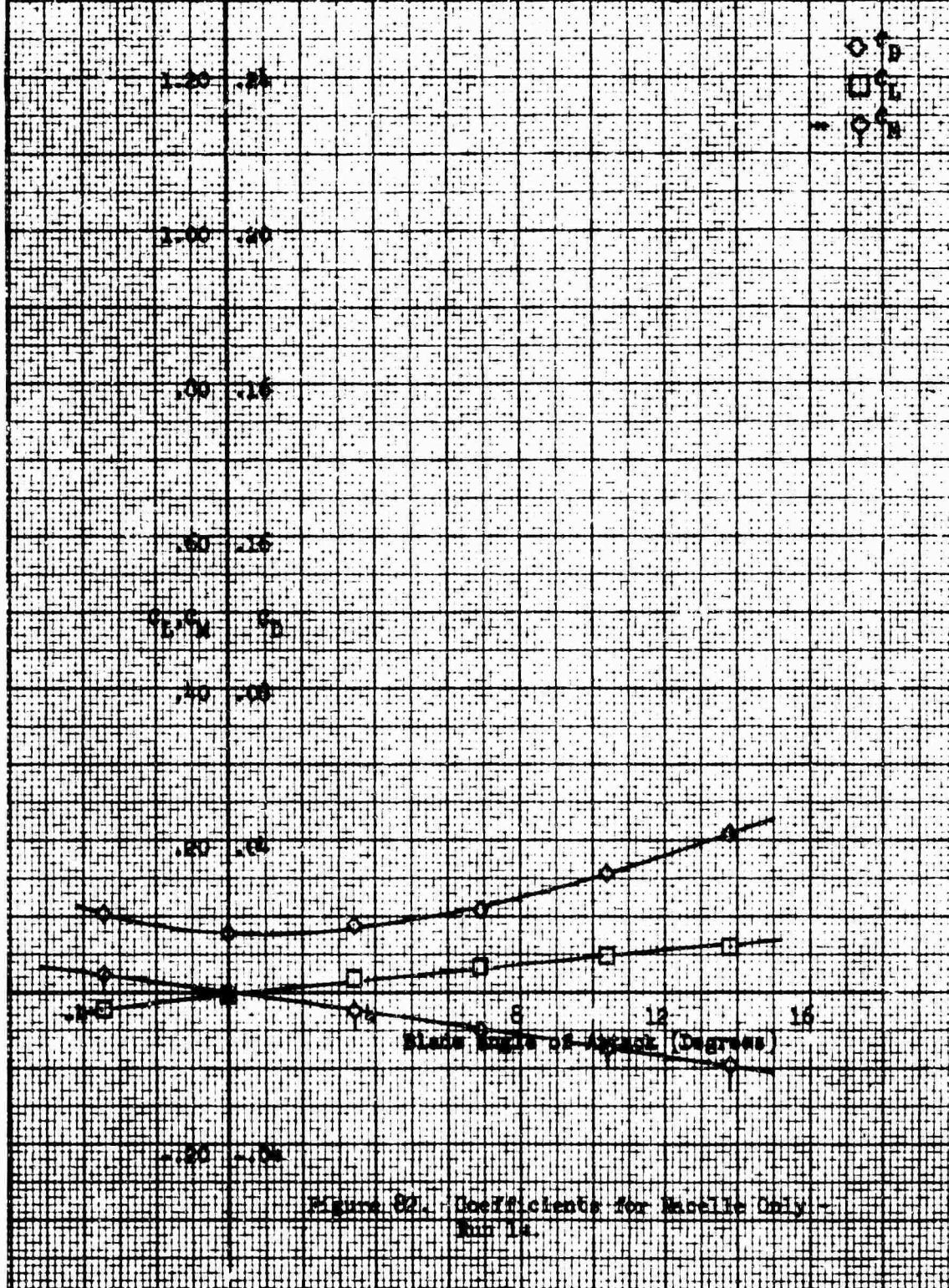


Blade Configuration: Single 1-40-100

Fairing: w/o

Blade Exit Plate: 0

$\beta = -10^\circ$



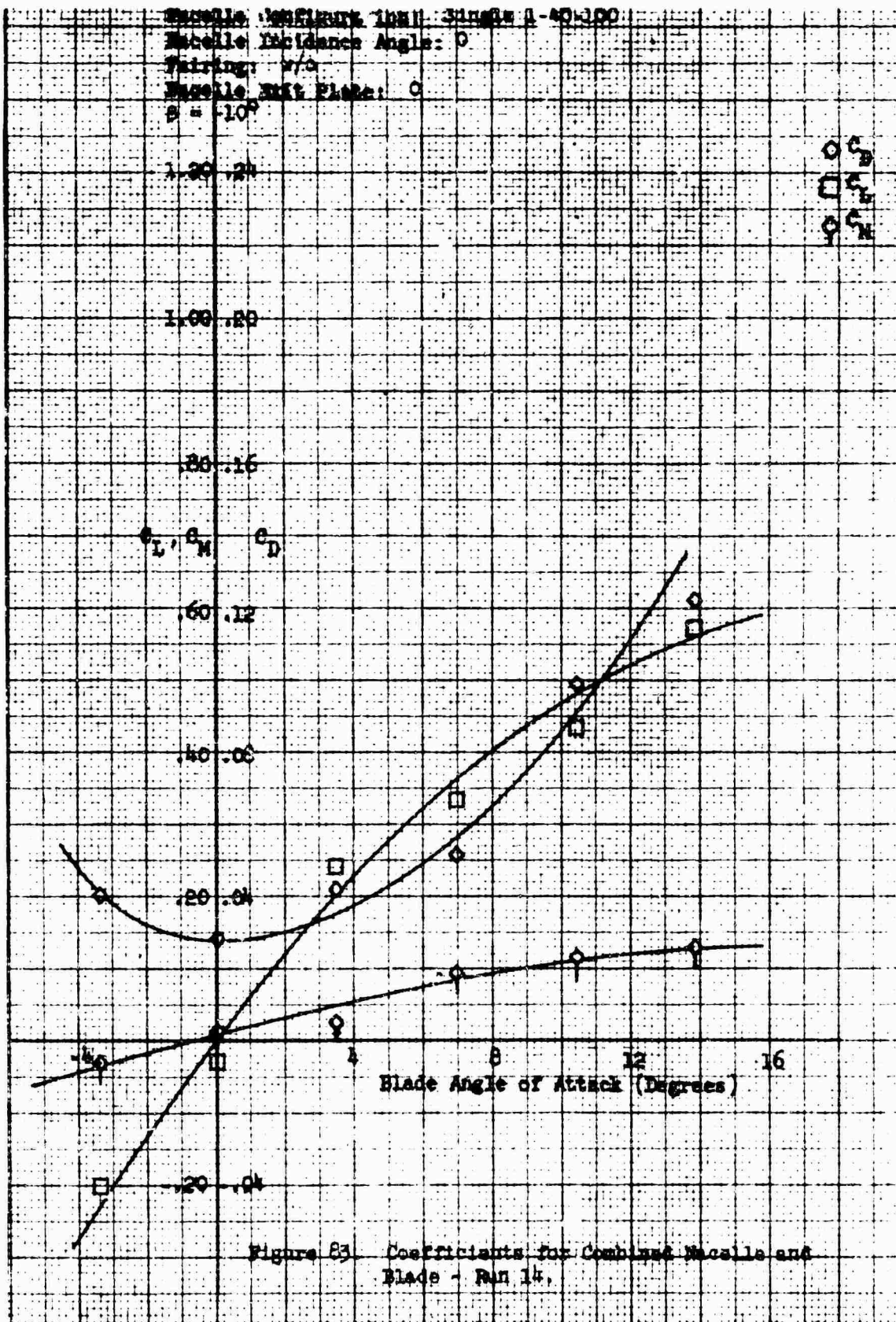
Wing Configuration: 100% Single 1-40-100

Wing Incidence Angle: 0

Fairing: w/o

Wing Root Plane: 0

$\beta = -10^\circ$

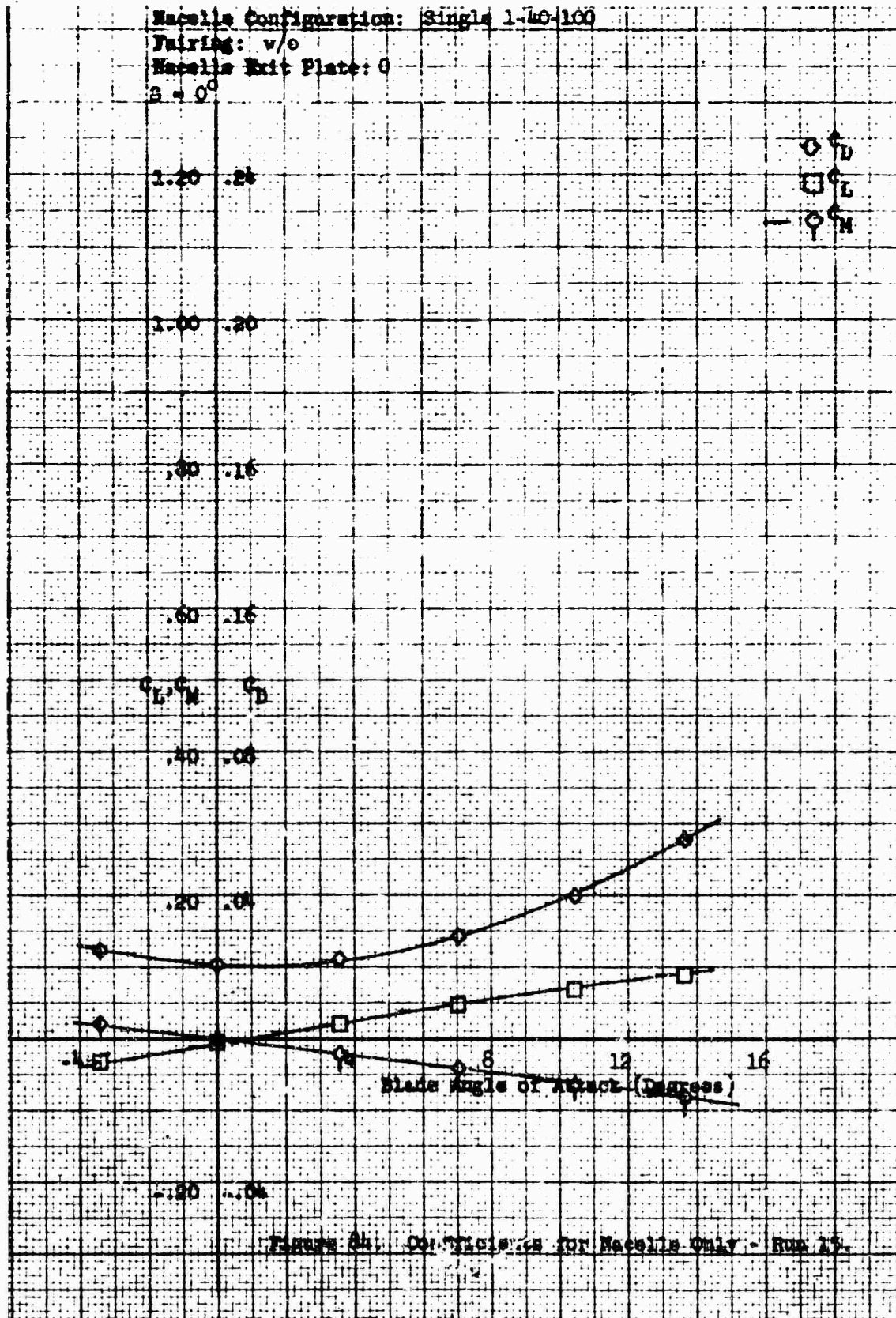


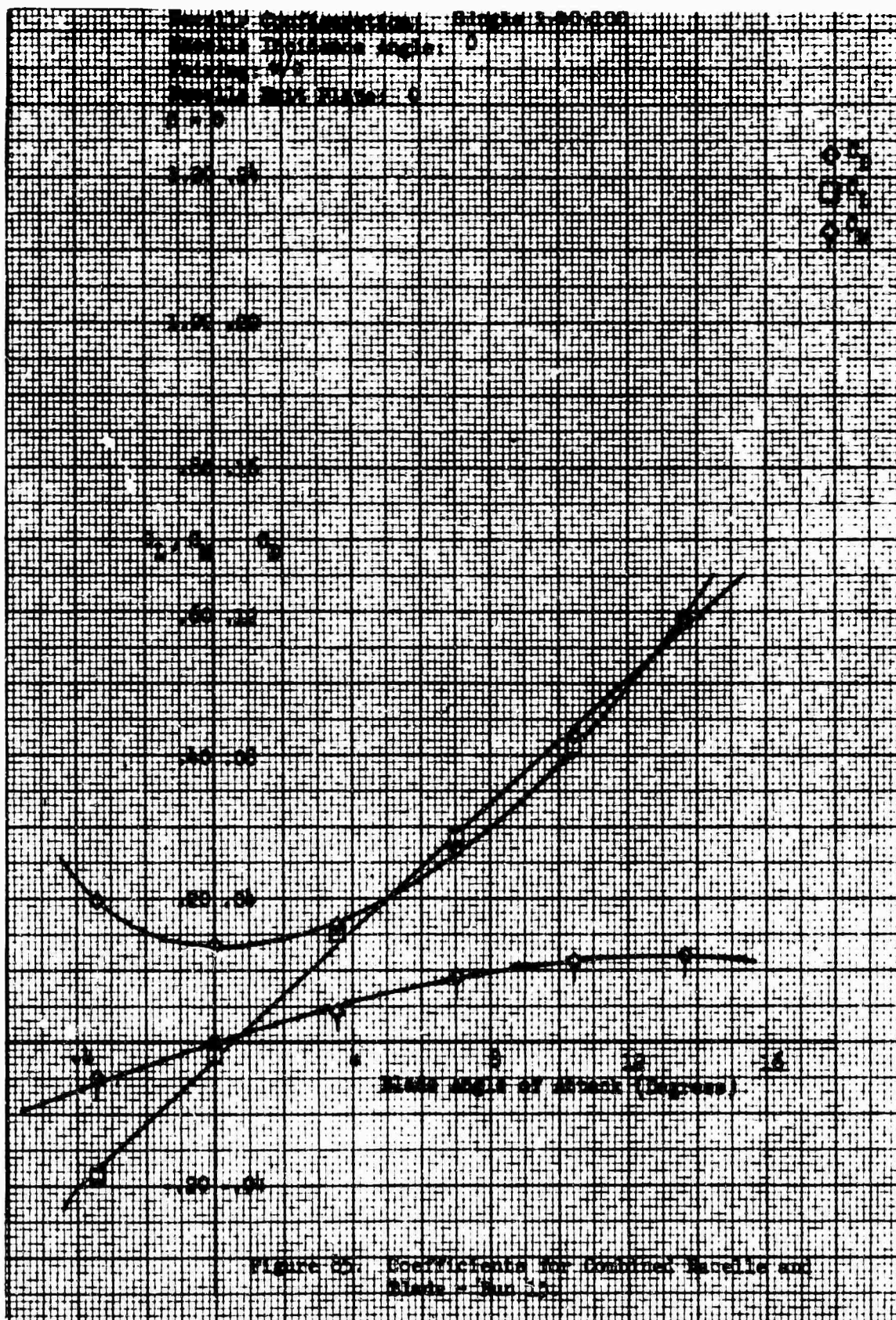
Nacelle Configuration: Single 1-40-100

Fairing: w/o

Nacelle Exit Plate: 0

$\alpha = 0^\circ$





Nacelle Configuration: Single 1-40-100

Fairing: v/o

Nacelle Exit Plate: 0

$\beta = 10^\circ$

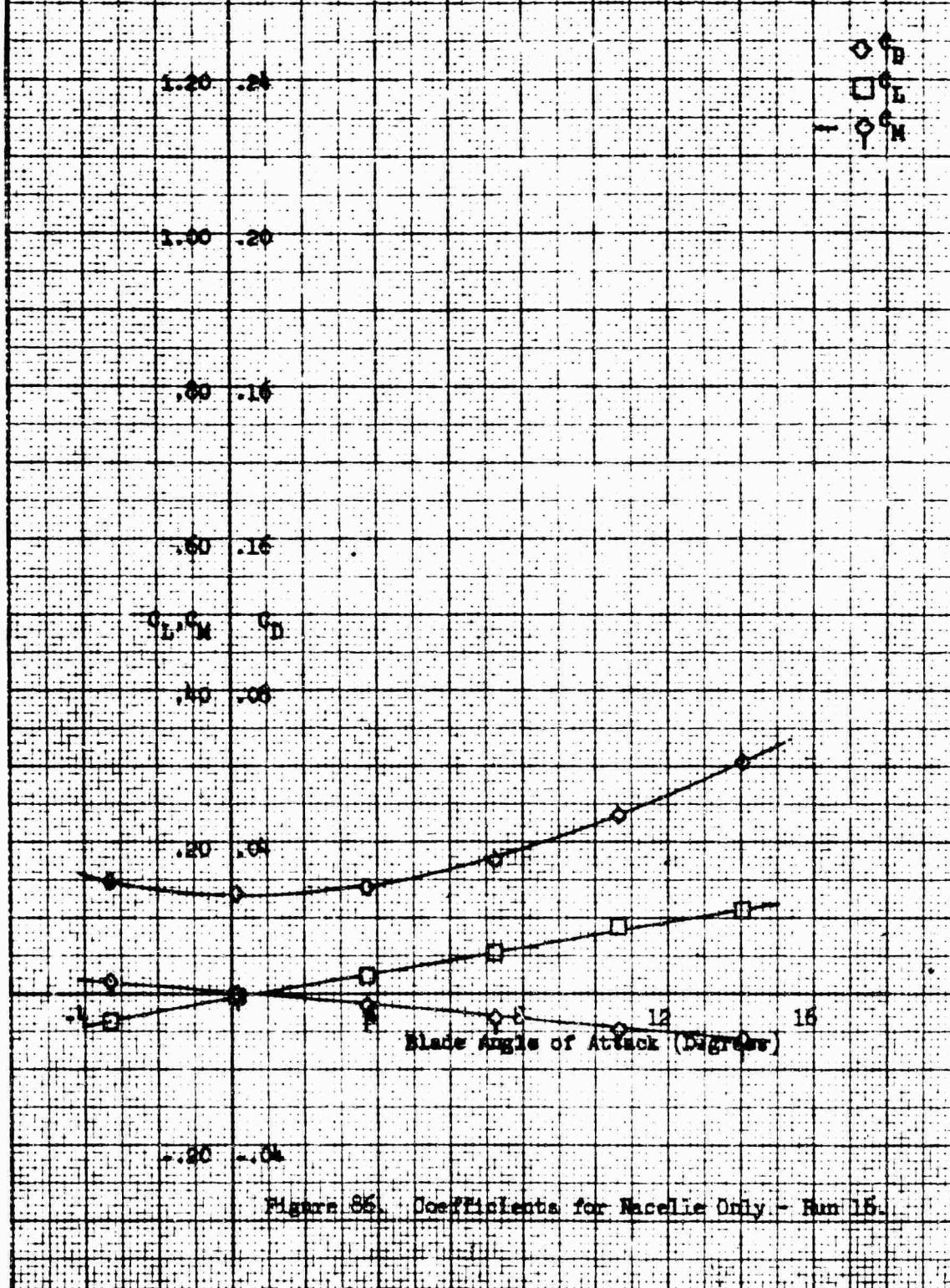
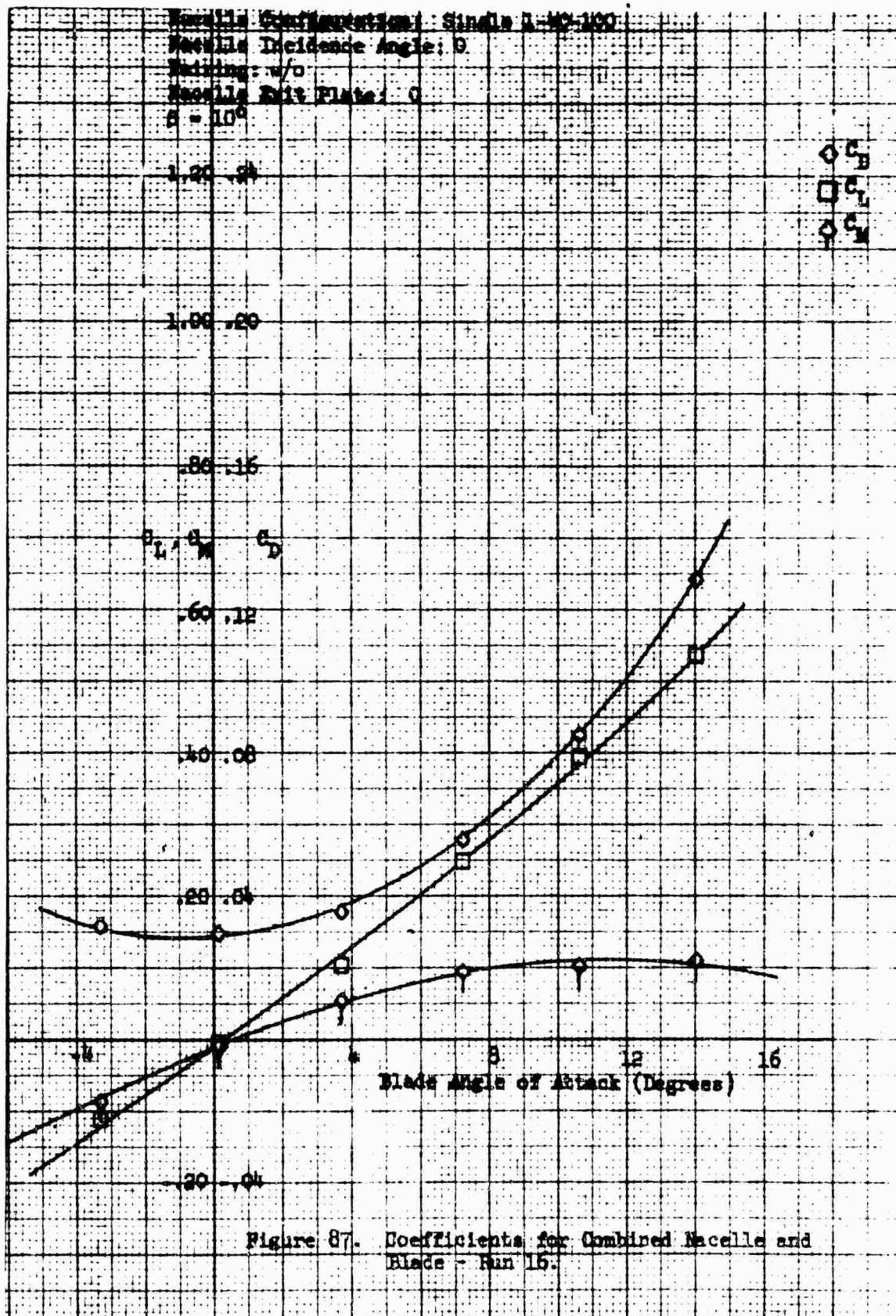


Figure 85. Coefficients for Nacelle Only - Run 15.



Nacelle Configuration: Single 1-40+100

Fairing: w/o

Nacelle Exit Plate: 0

$\delta = 20^\circ$

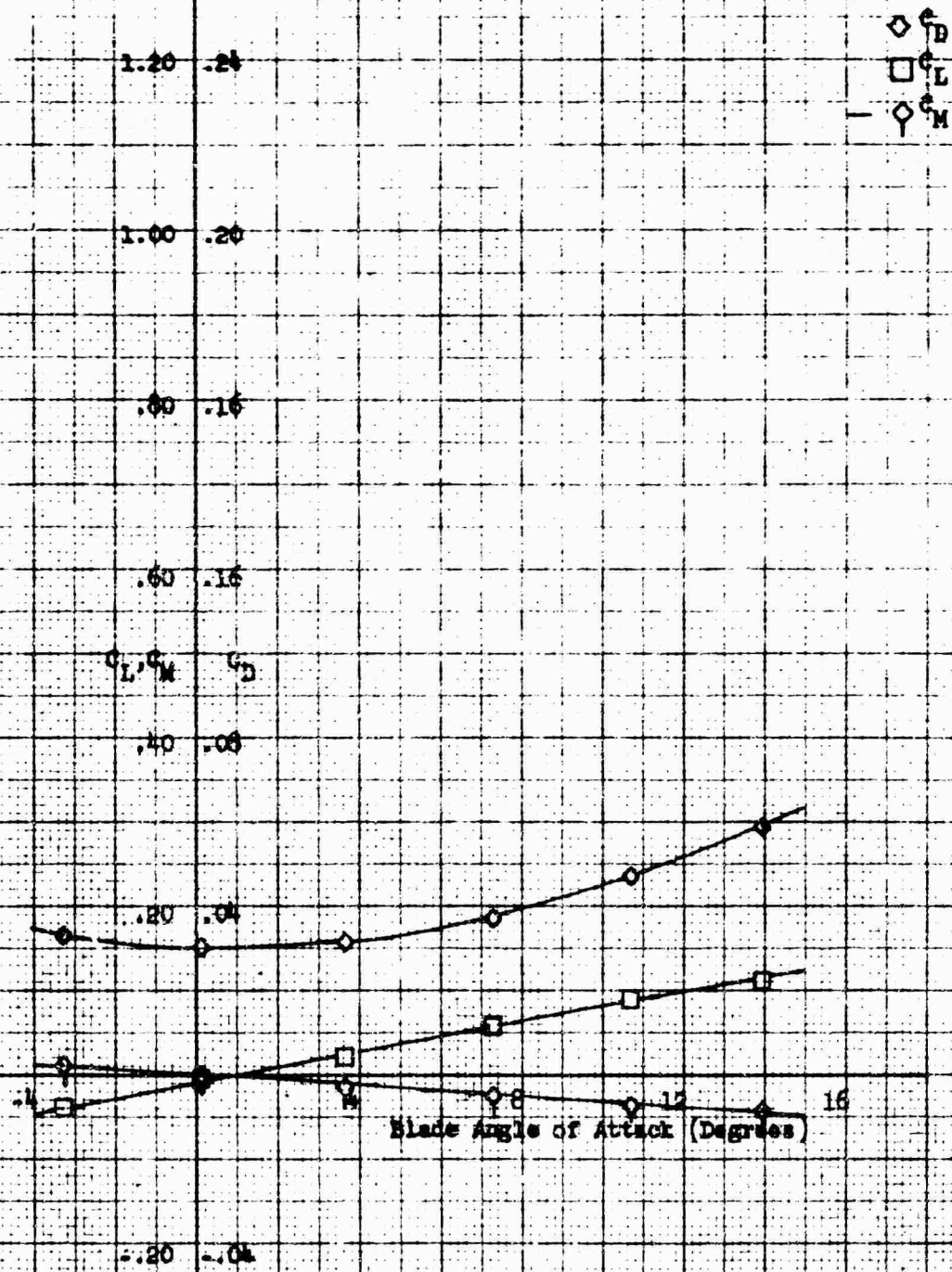
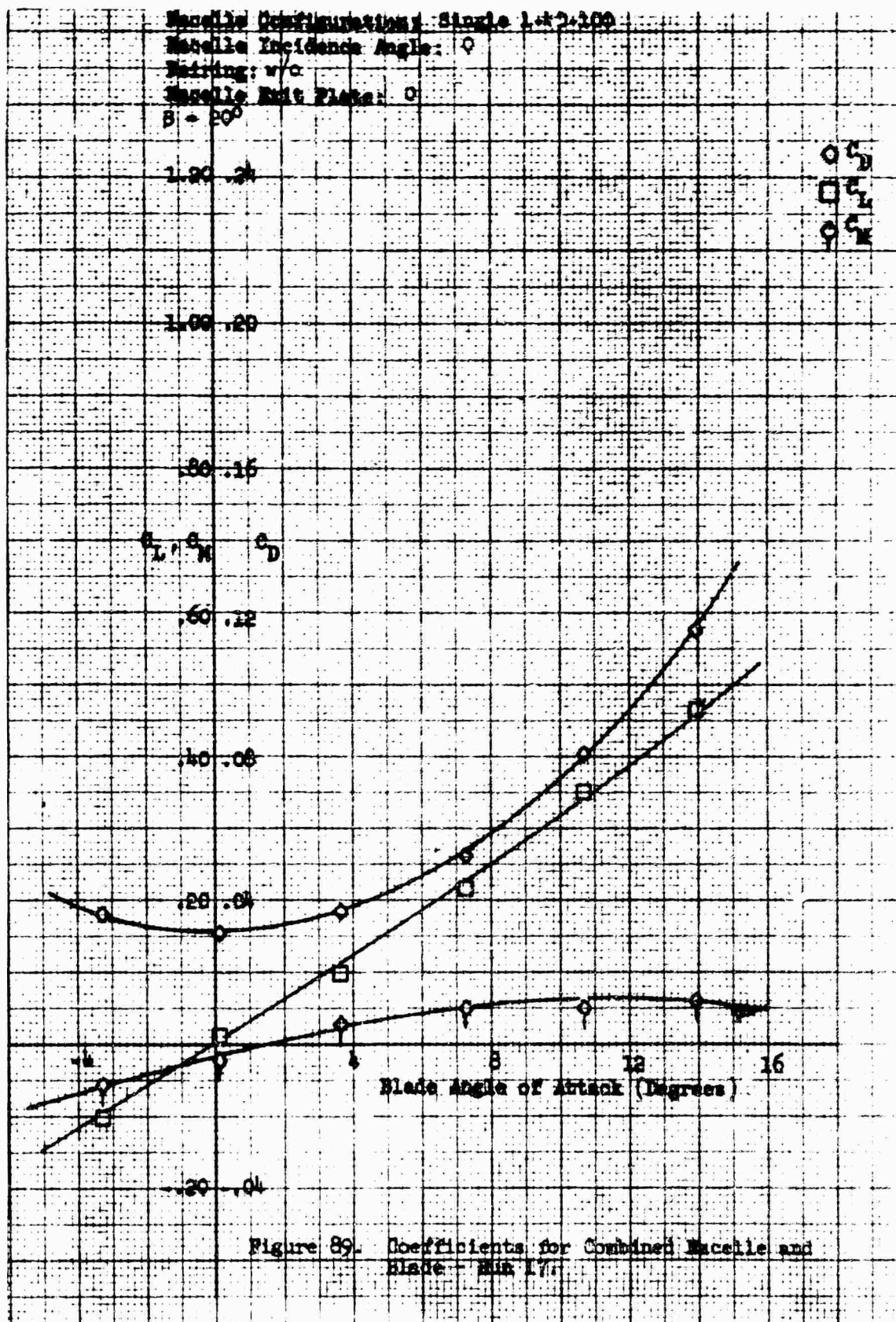


Figure 86. Coefficients for Nacelle Only - Run 17.



Nacelle Configuration: Single 1-40-100
 Fairing: w/o
 Nacelle Exit Plate: .78
 $\beta = 20^\circ$

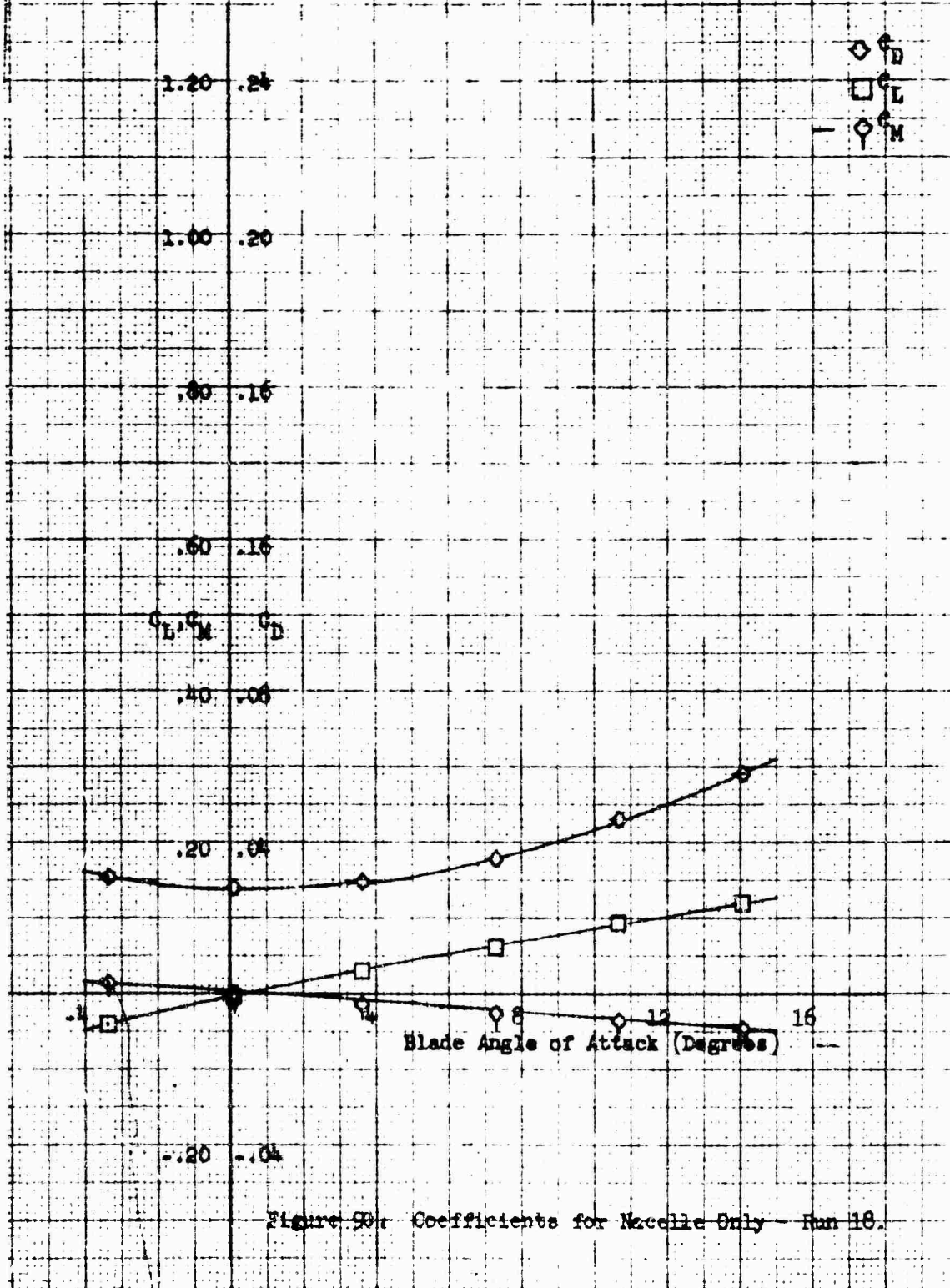


Figure 90. Coefficients for Nacelle Only - Run 18.

Blade Configuration: Blade 2-6-9-10-11
 Blade Incidence Angle: 0
 Fairing: w/o
 Blade Exit Plane: .78
 $\beta = 20^\circ$

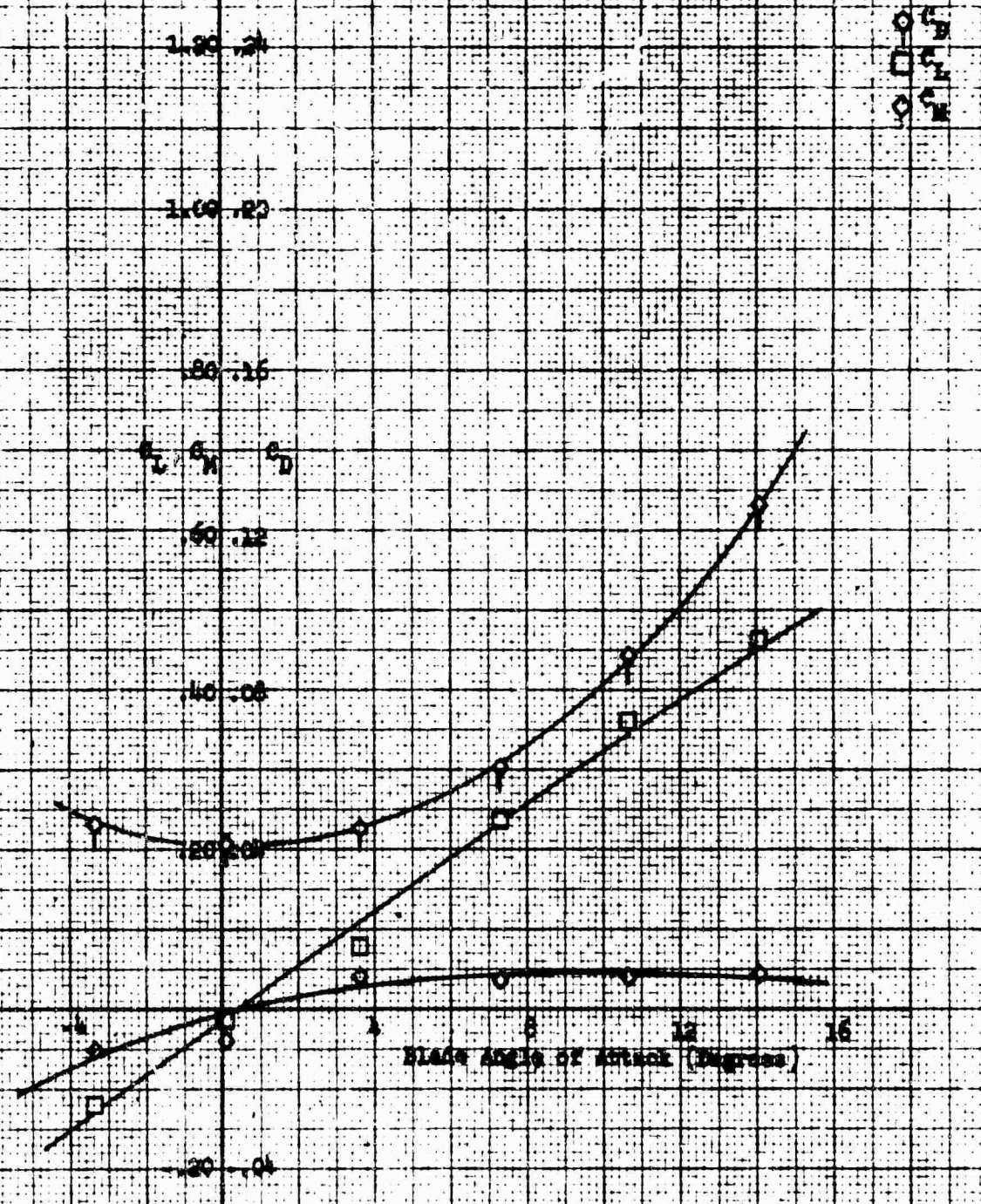


Figure 91. Coefficients for Combined Blade and Blade - Run 18.

Nozzle Configuration: Single 1.40-100
 Pairing: w/o
 Nozzle Exit Plate: .78
 $\beta = 10^\circ$

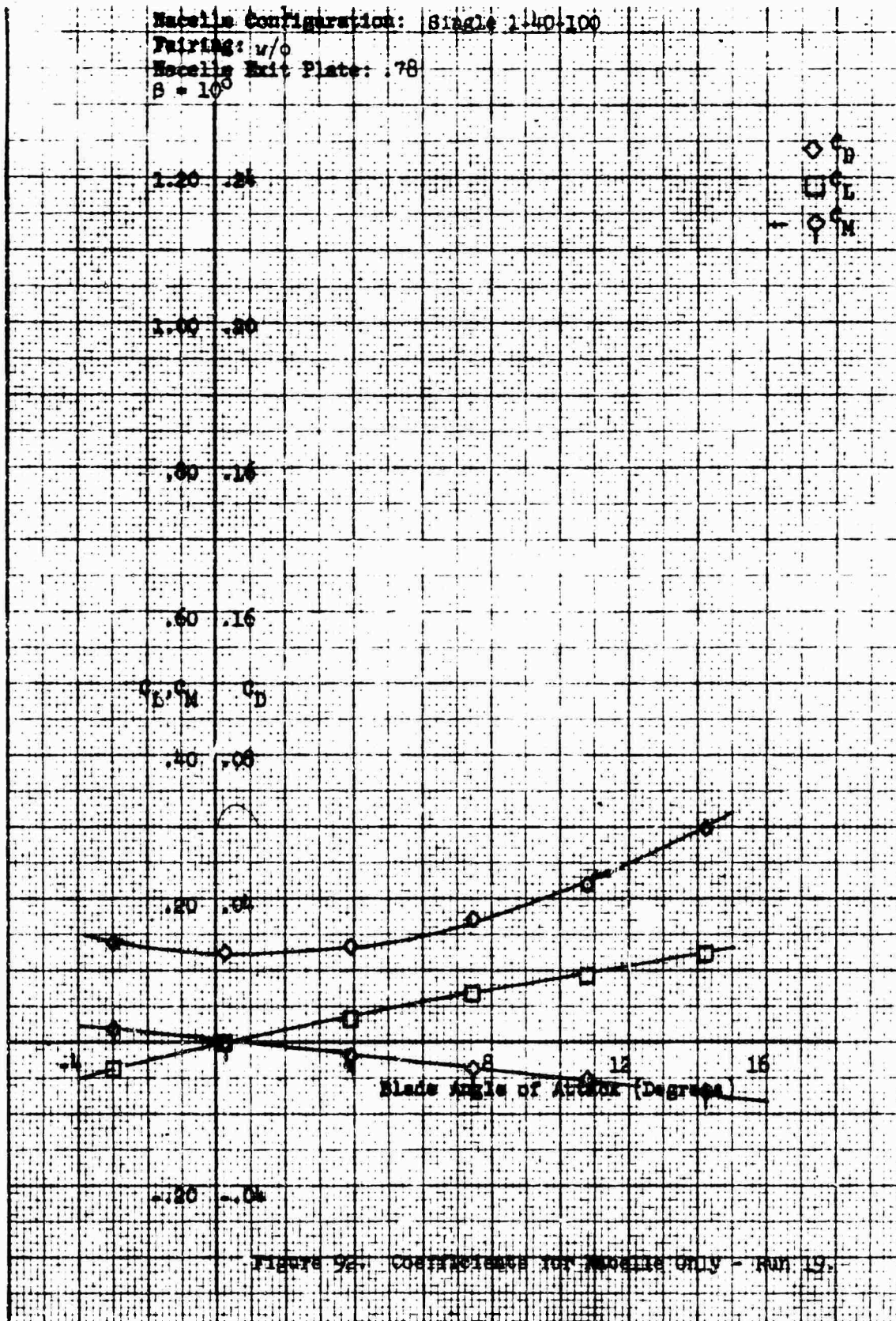


Figure 92. Coefficients for Nozzle Only - Run 19.

Macelle Configuration: Single 1-40-200
 Macelle Incidence Angle: 0
 Bathing: w/o
 Macelle Exit Plate: .78
 $\beta = 10^\circ$

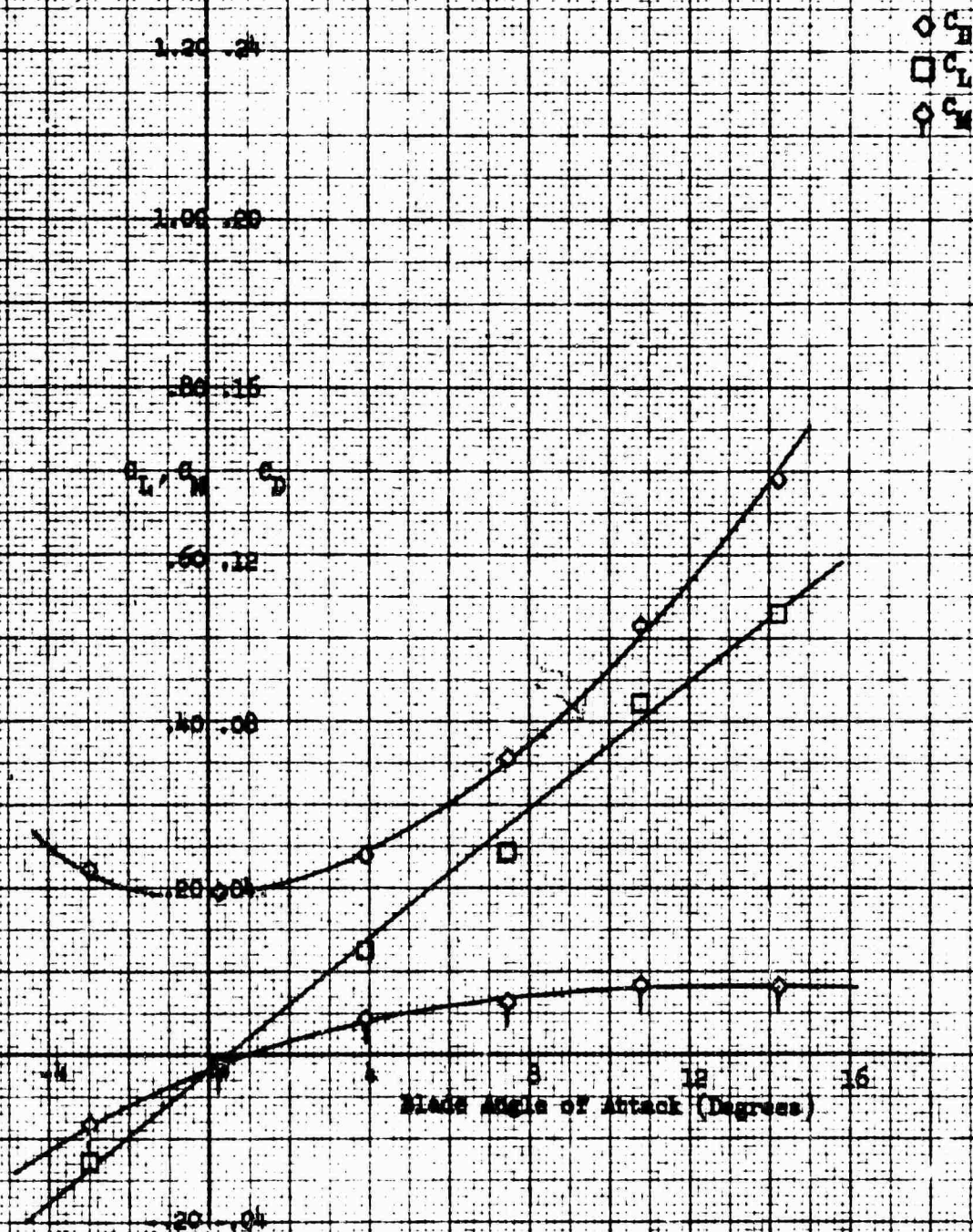
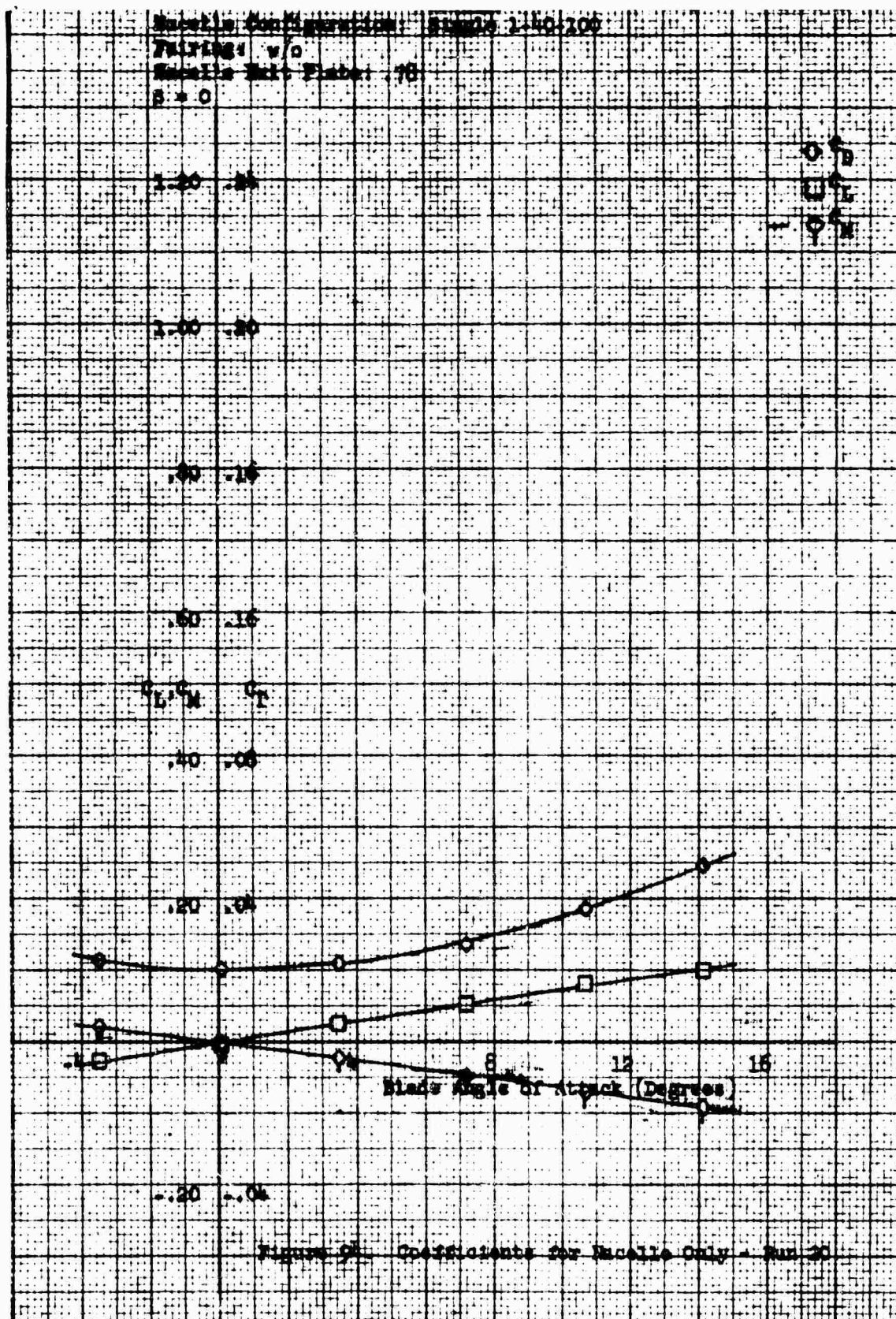
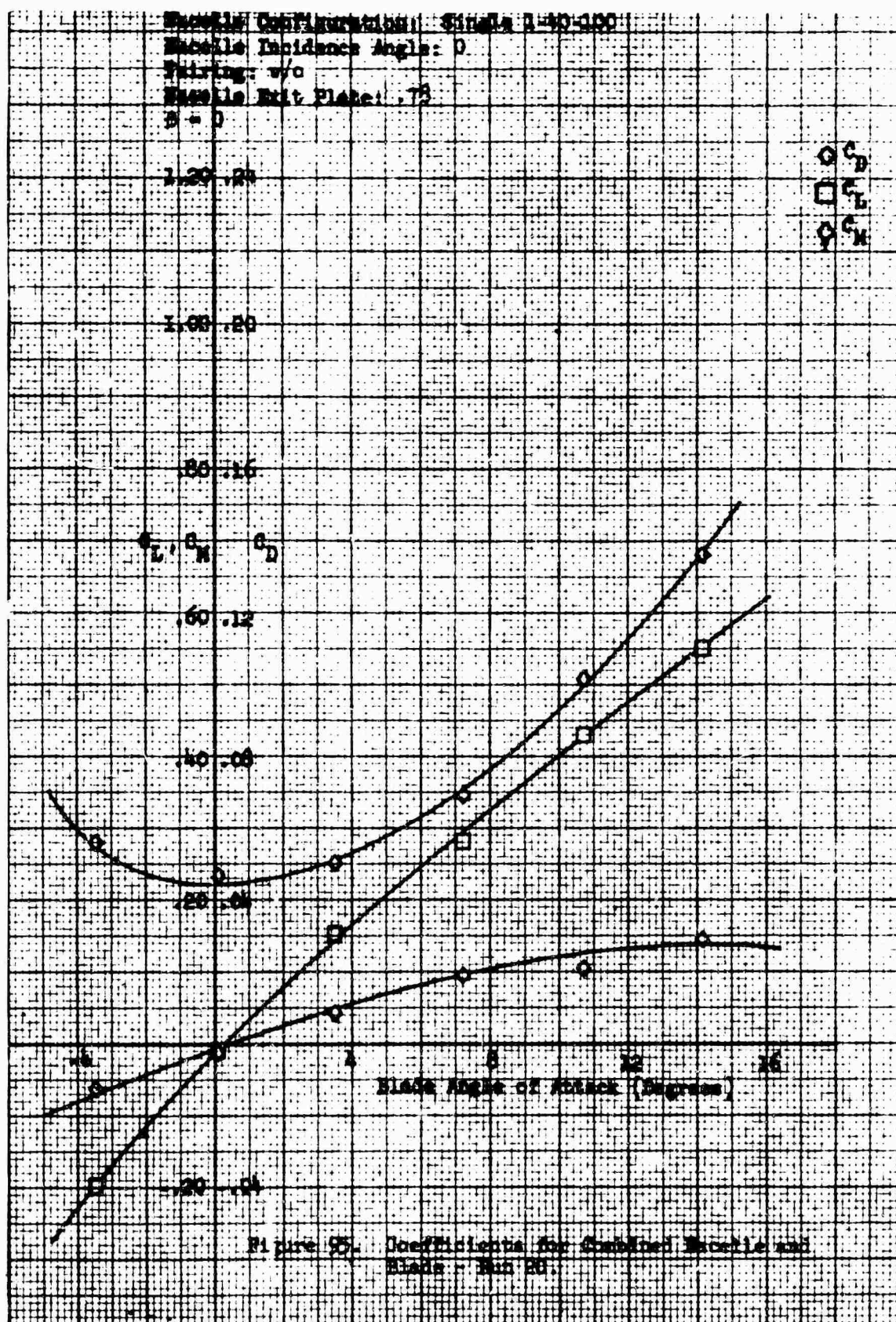


Figure 93. Coefficients for Combined Macelle and Blade - Run 19





Blade Configuration: Single 1-40-160

Pairing: w/o

Blade Exit Plate: .75

$\beta = -10^\circ$

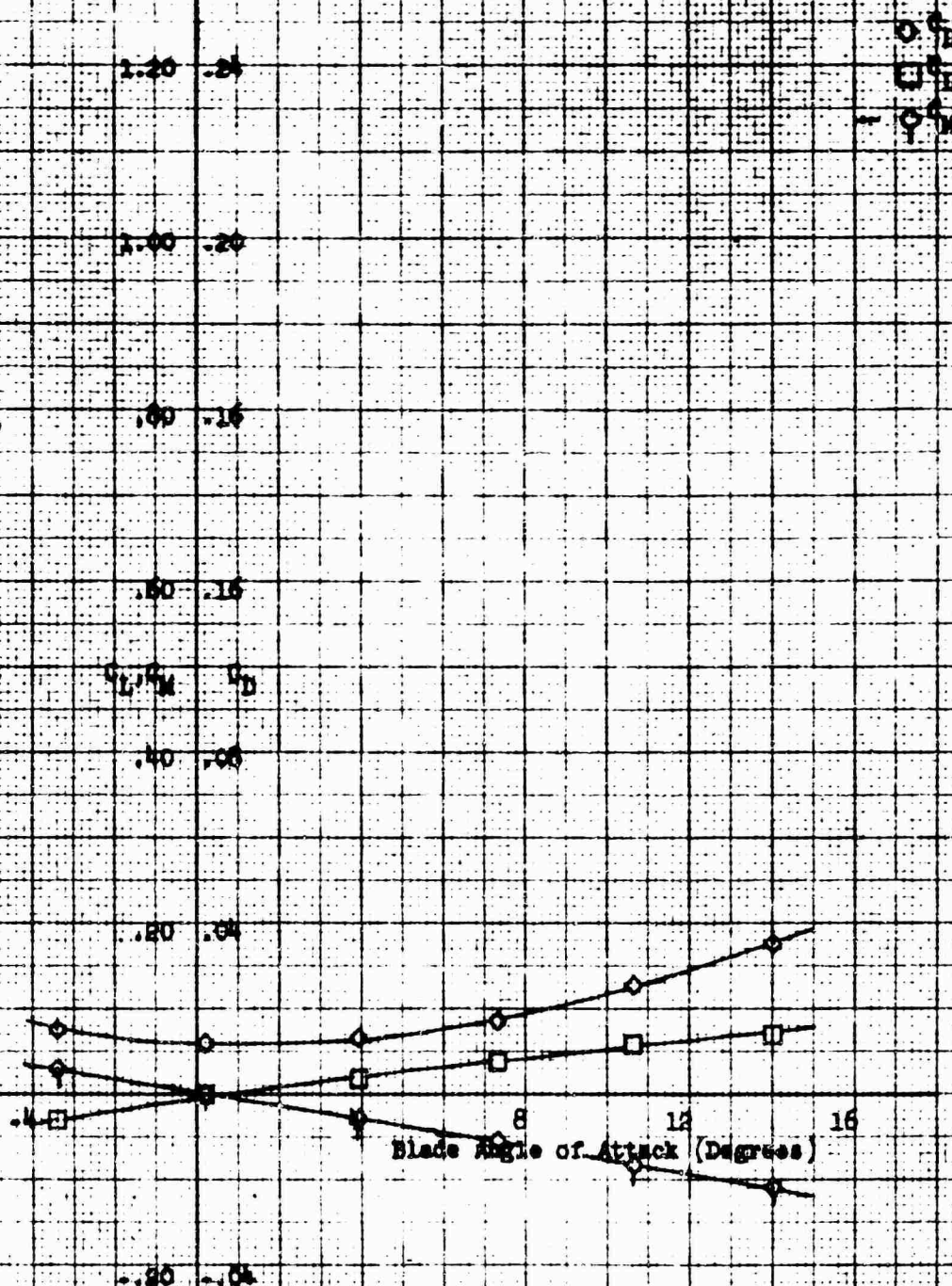


Figure 96. Coefficients for Blade Only - Run 21

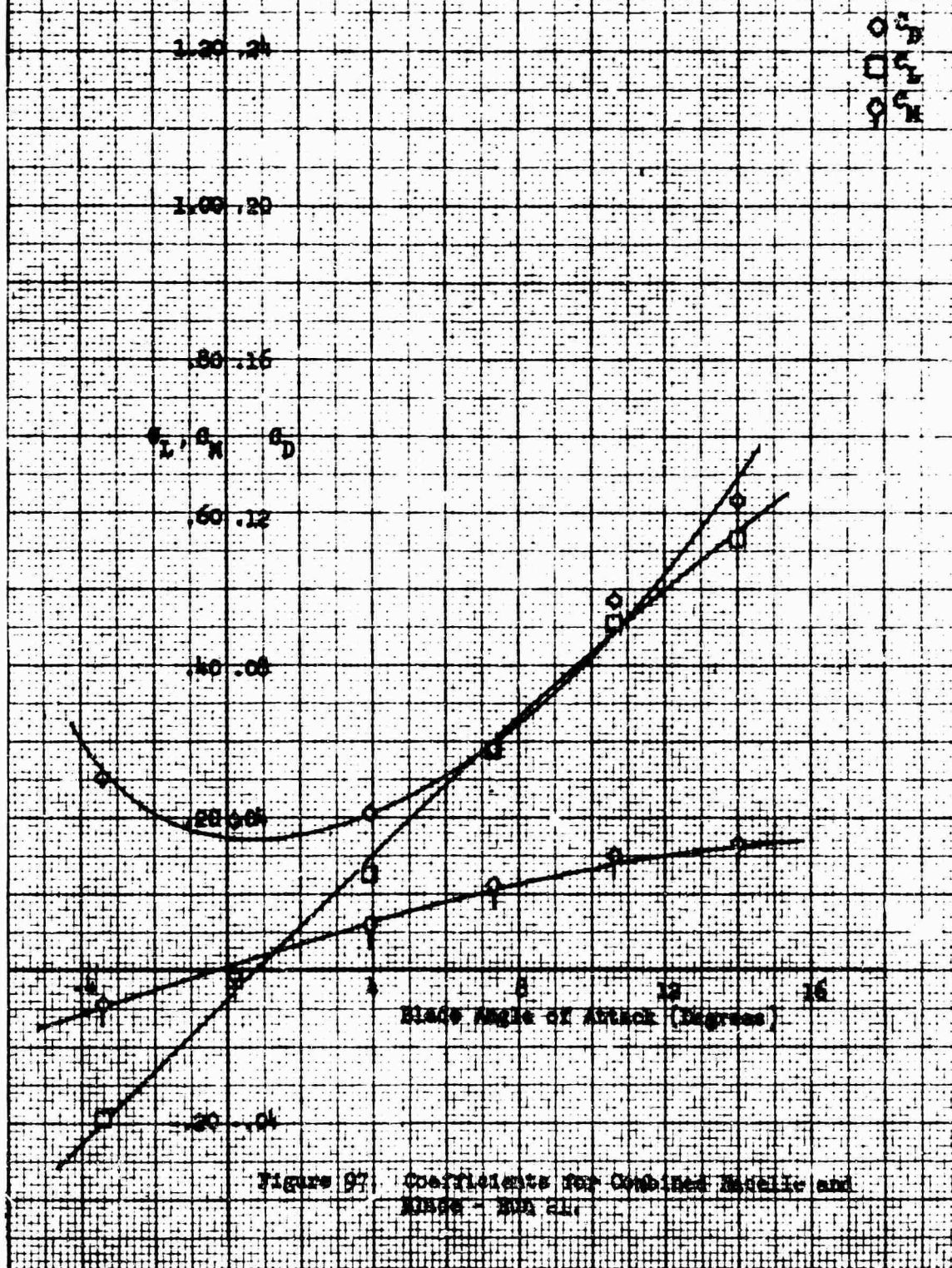
Wacelle Configuration: Single 1-40-100

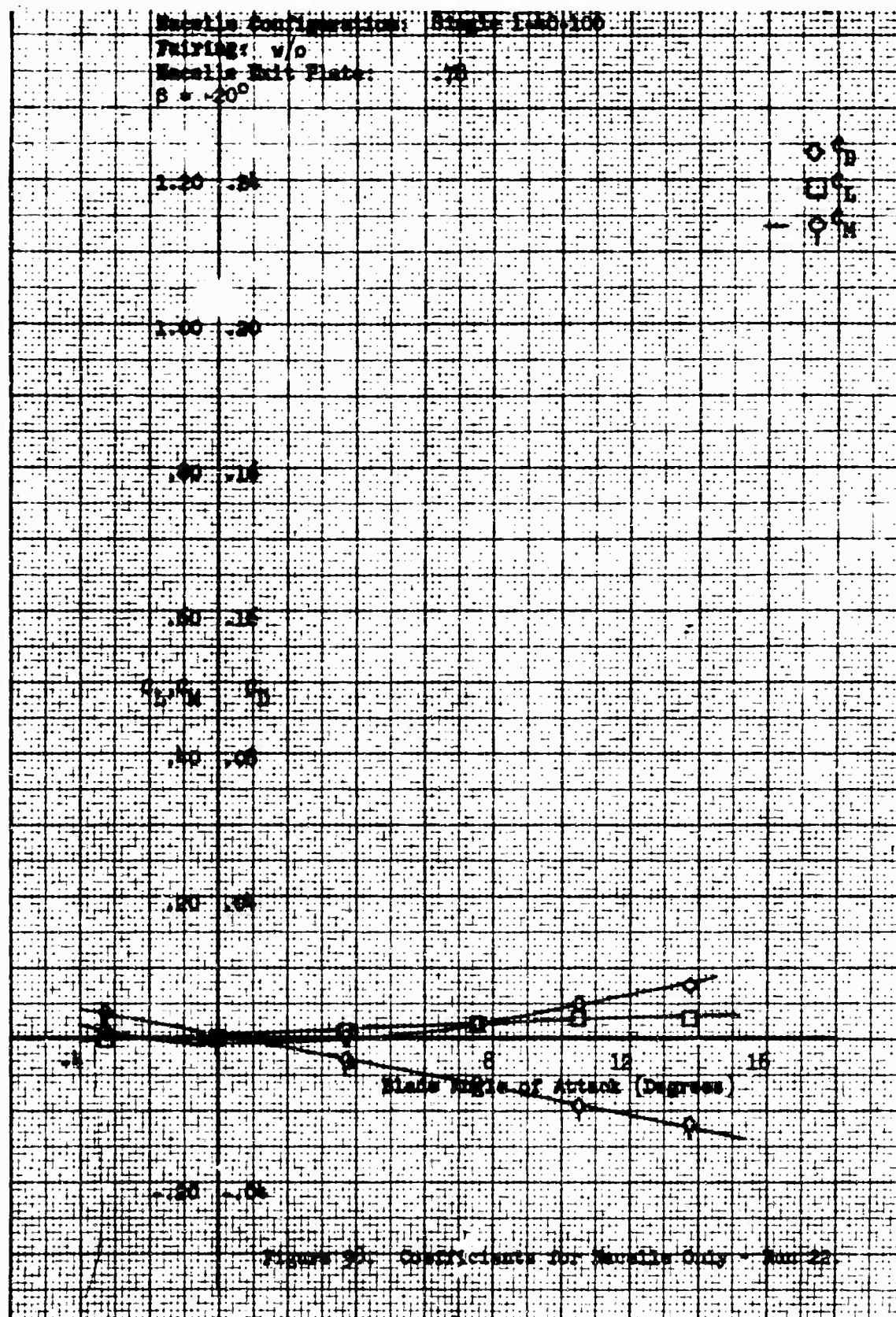
Wacelle Incidence Angle: 0

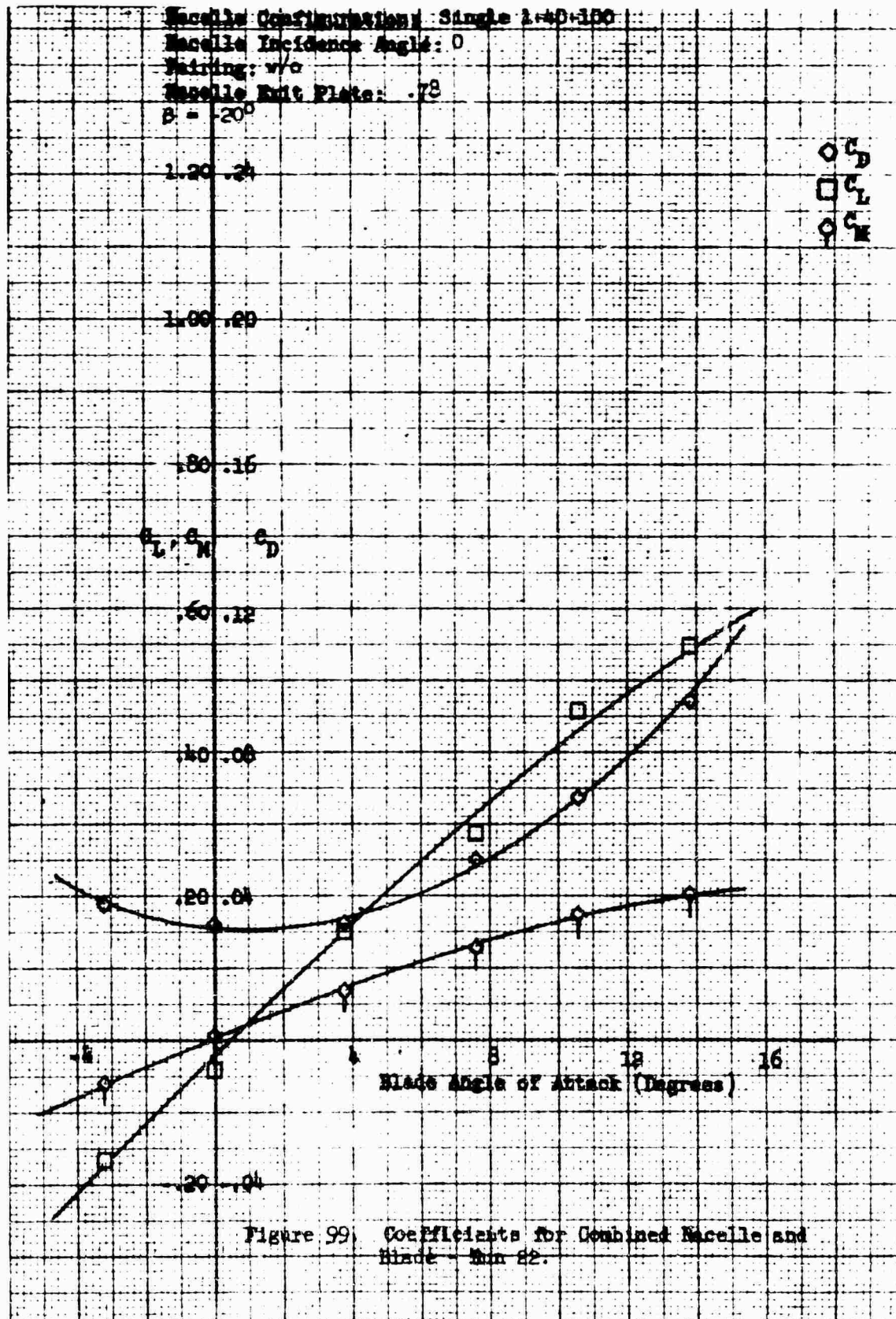
Pairing: w/o

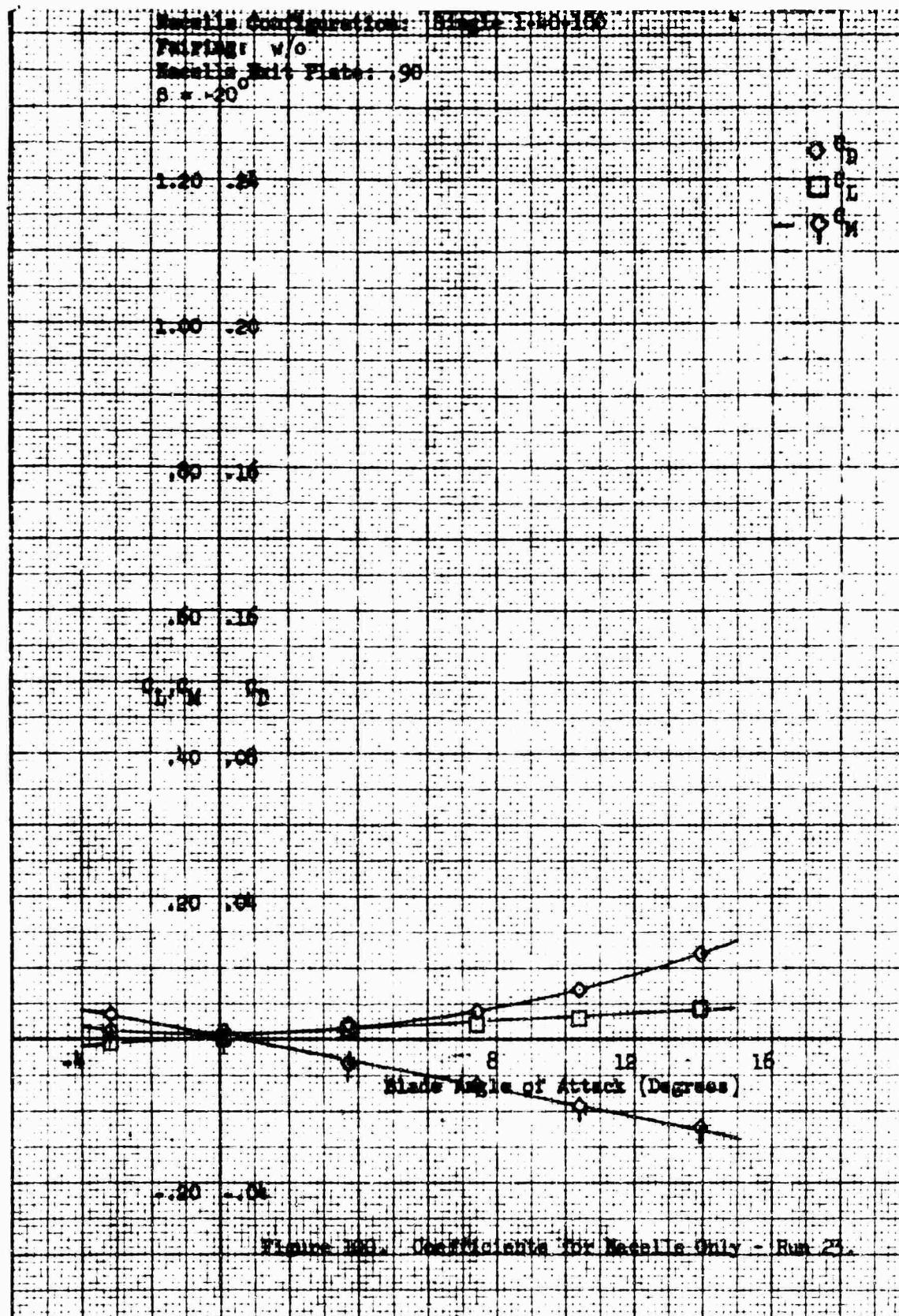
Wacelle Exit Plate: .78

$\theta = -10^\circ$









Nacelle Configuration: Single 1-40-100
 Nacelle Incidence Angle: 0°
 Pairing: w/o
 Nacelle Exit Plate: .90
 $\beta = -20^\circ$

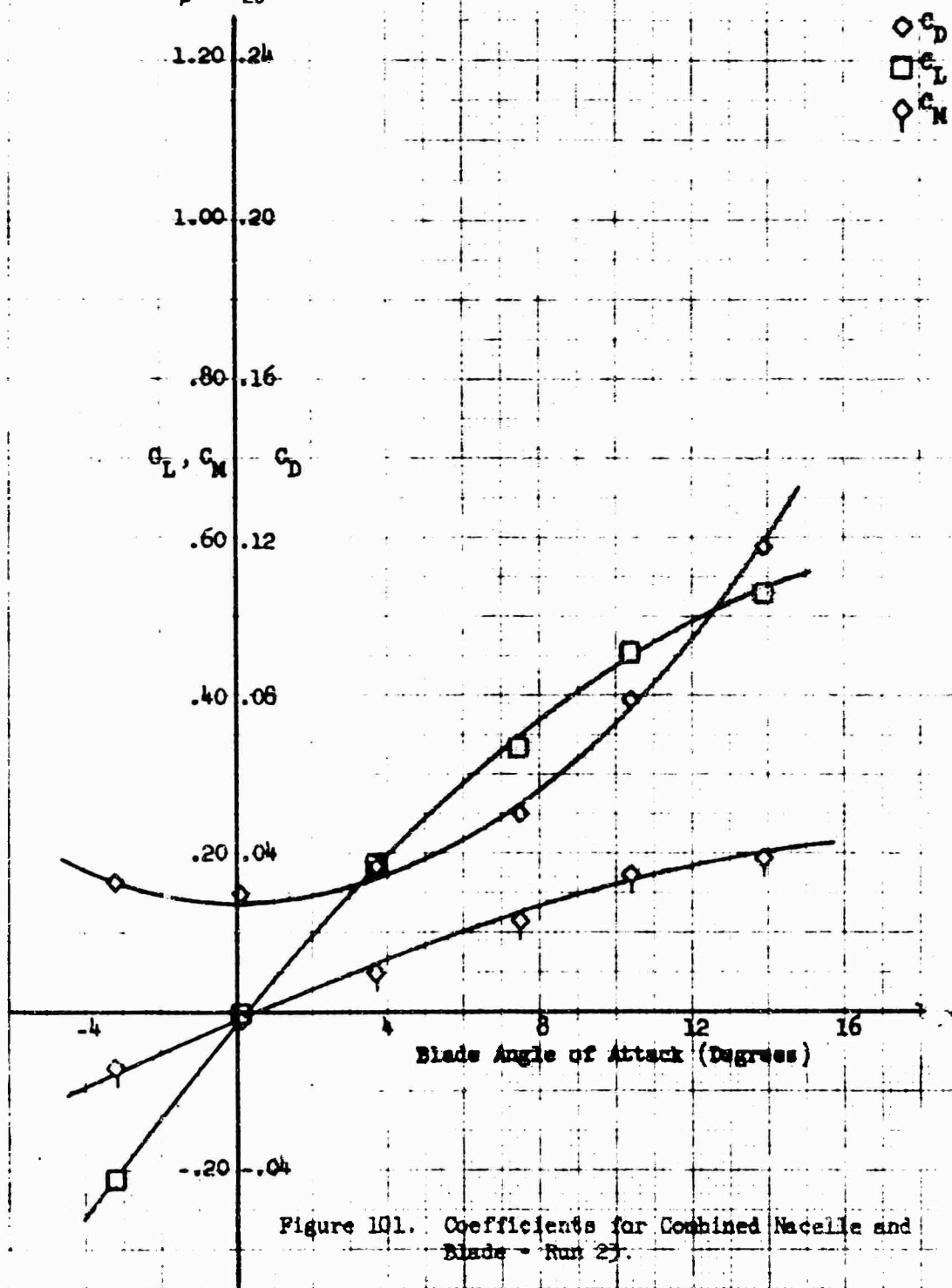
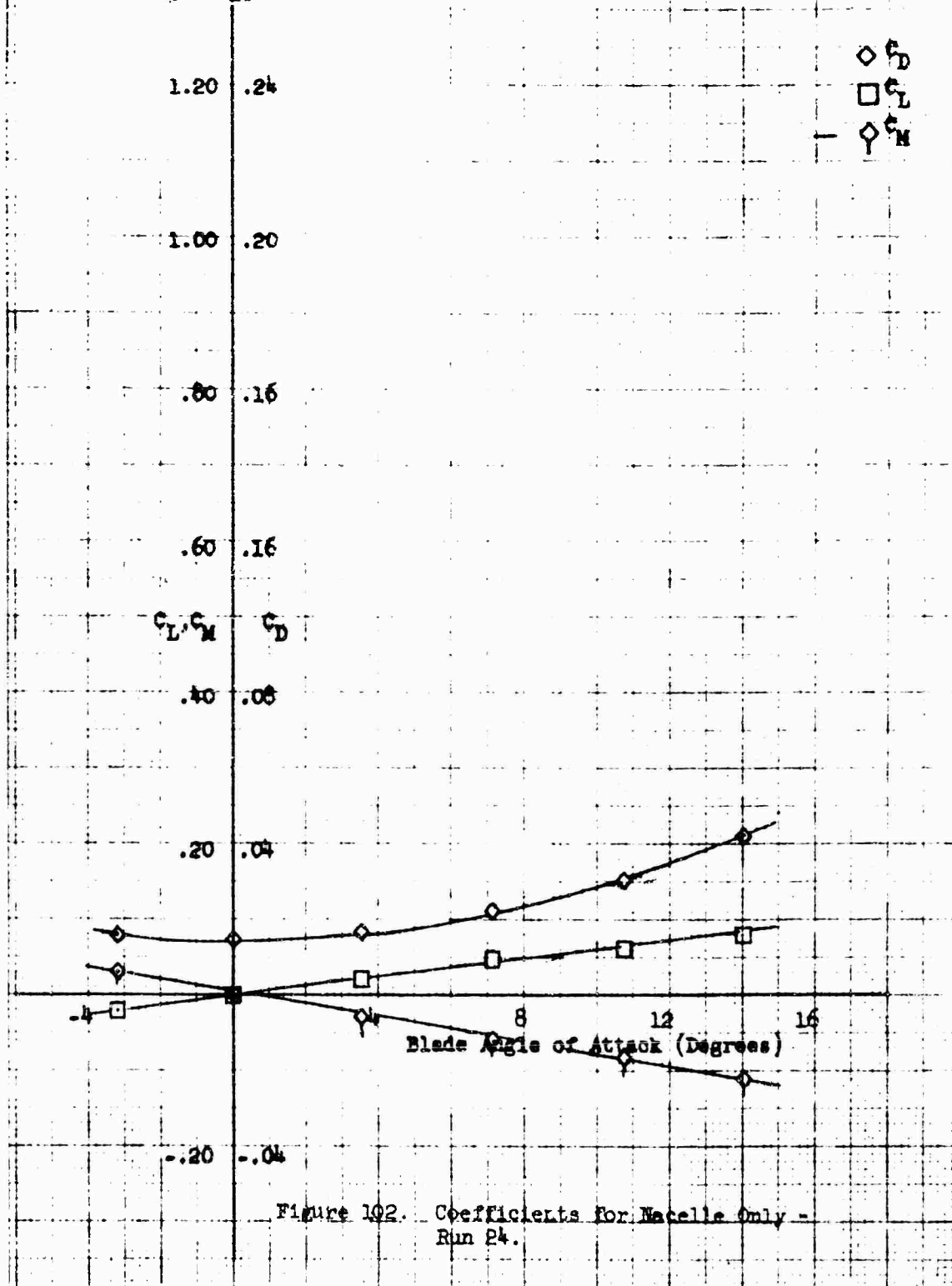


Figure 101. Coefficients for Combined Nacelle and Blade - Run 27.

Nacelle Configuration: Single 1-40+100
 Fairing: w/o
 Nacelle Exit Plate: .90
 $\beta = -10^\circ$



Nacelle Configuration: Single 1-40-100

Nacelle Incidence Angle: 0

Fairing: w/o

Nacelle Exit Plate: .80

$\theta = -10^\circ$

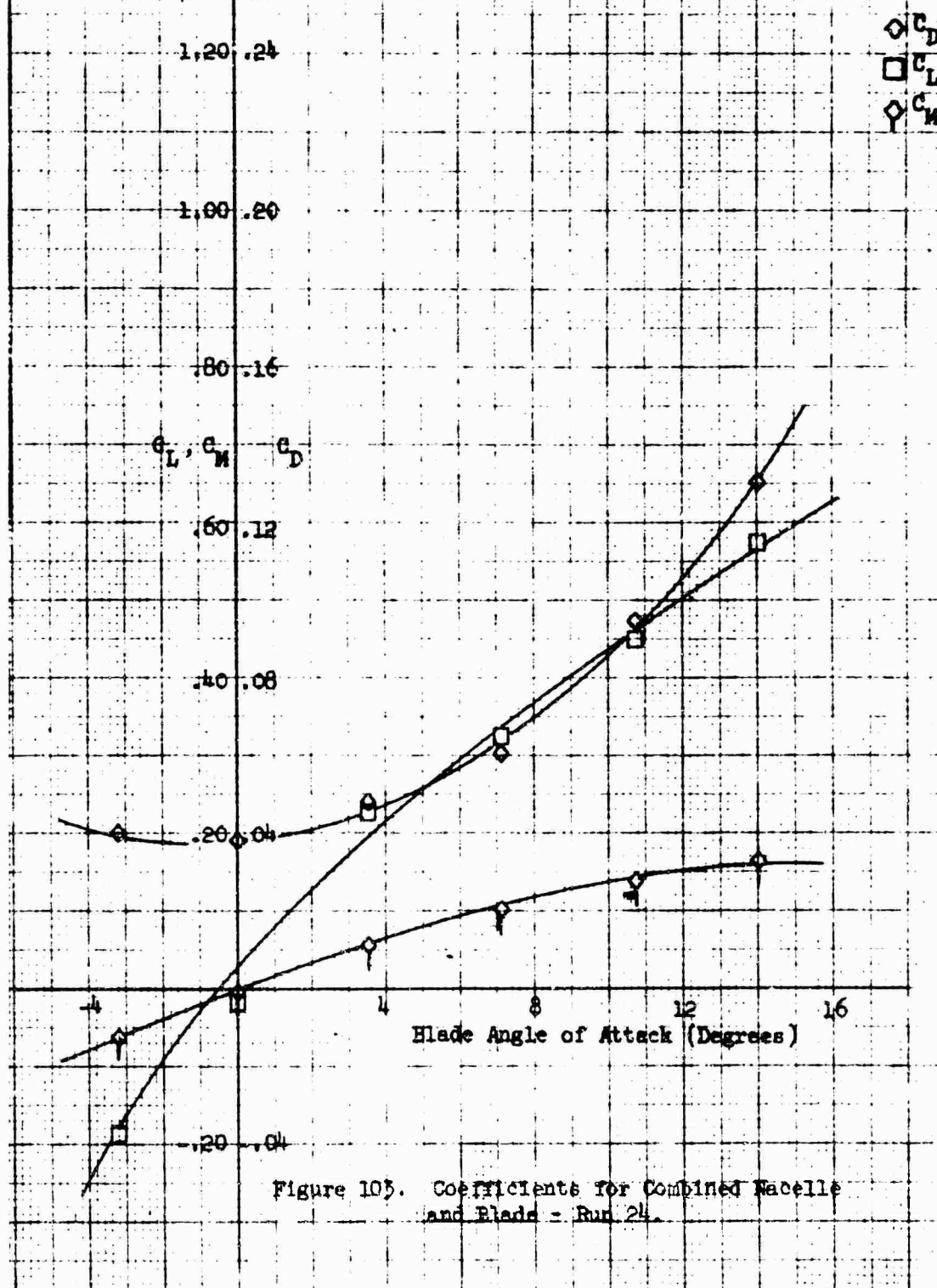
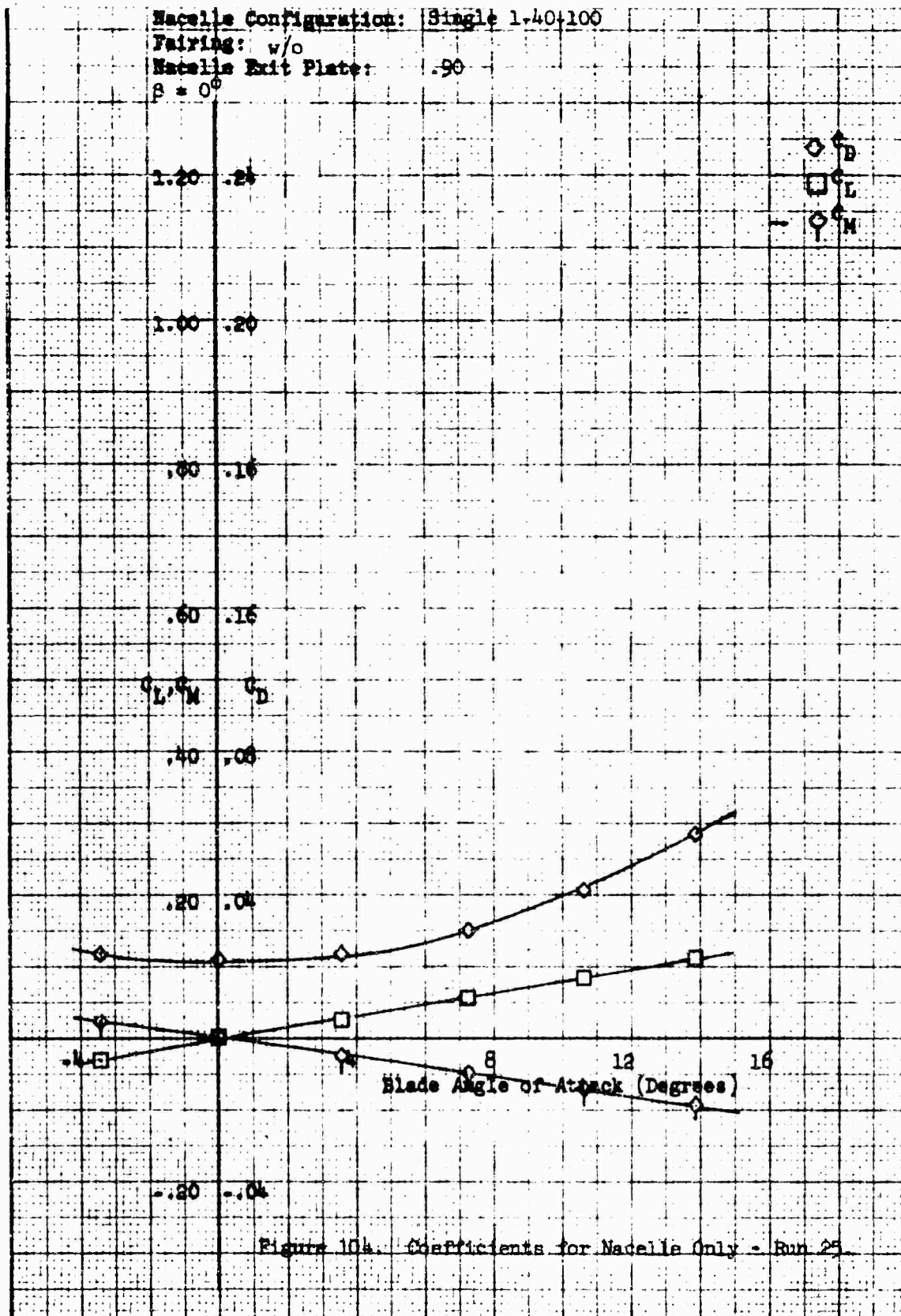


Figure 103. Coefficients for Combined Nacelle and Blade - Run 24.

Macelle Configuration: Single 1.40-100
 Fairing: w/o
 Macelle Exit Plate: .90
 $\beta = 0^\circ$



Macelle Configuration: Single 1-40-100

Macelle Incidence Angle: 0

Fairing: w/o

Macelle Exit Plate: 90

$\beta = 0$

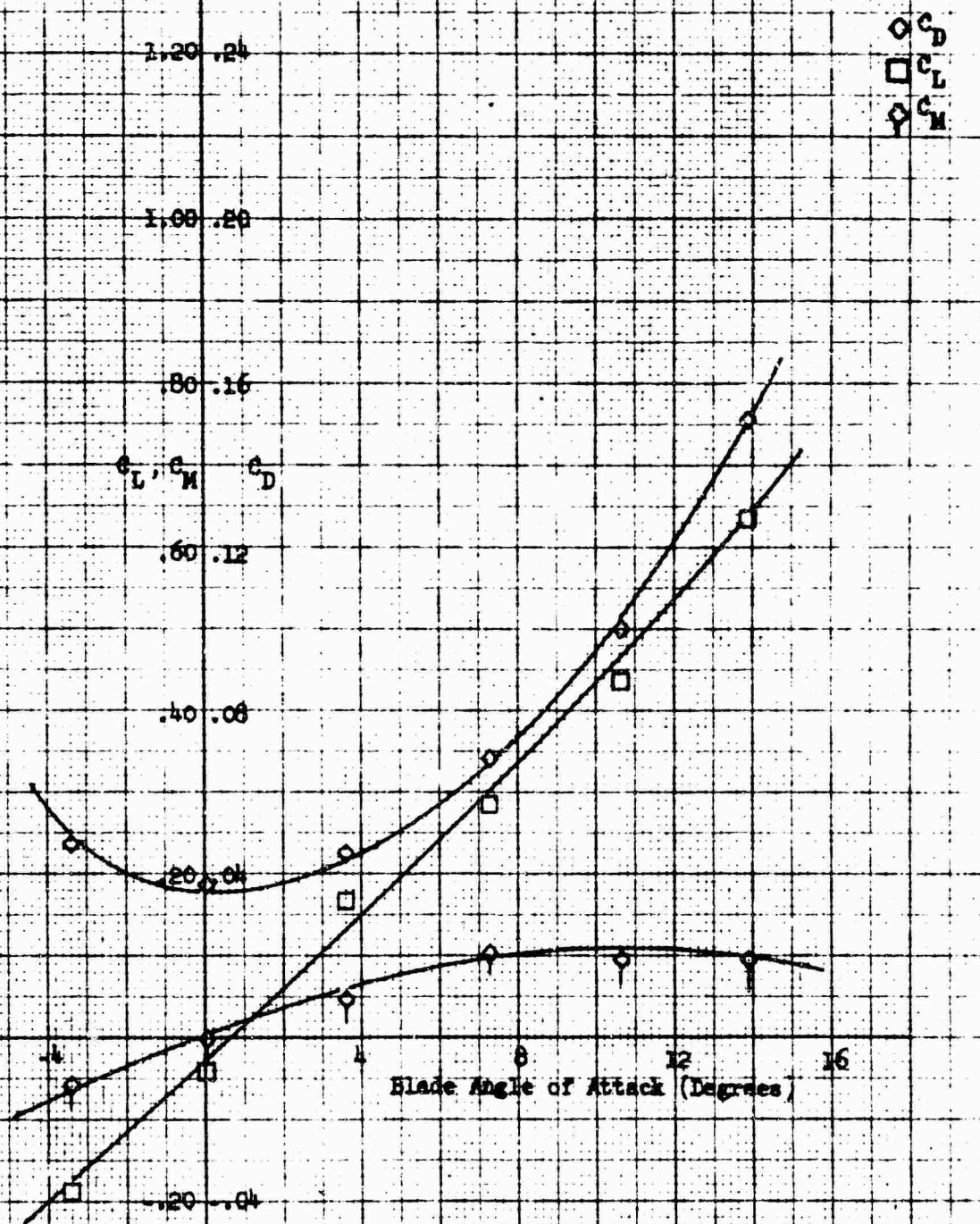


Figure 105. Coefficients for Combined Macelle and Blade - Run 25.

Blade Configuration: Single 1-20-100
 Pitch: 10°
 Blade Tip Plate: 10°
 $\delta = 10^\circ$

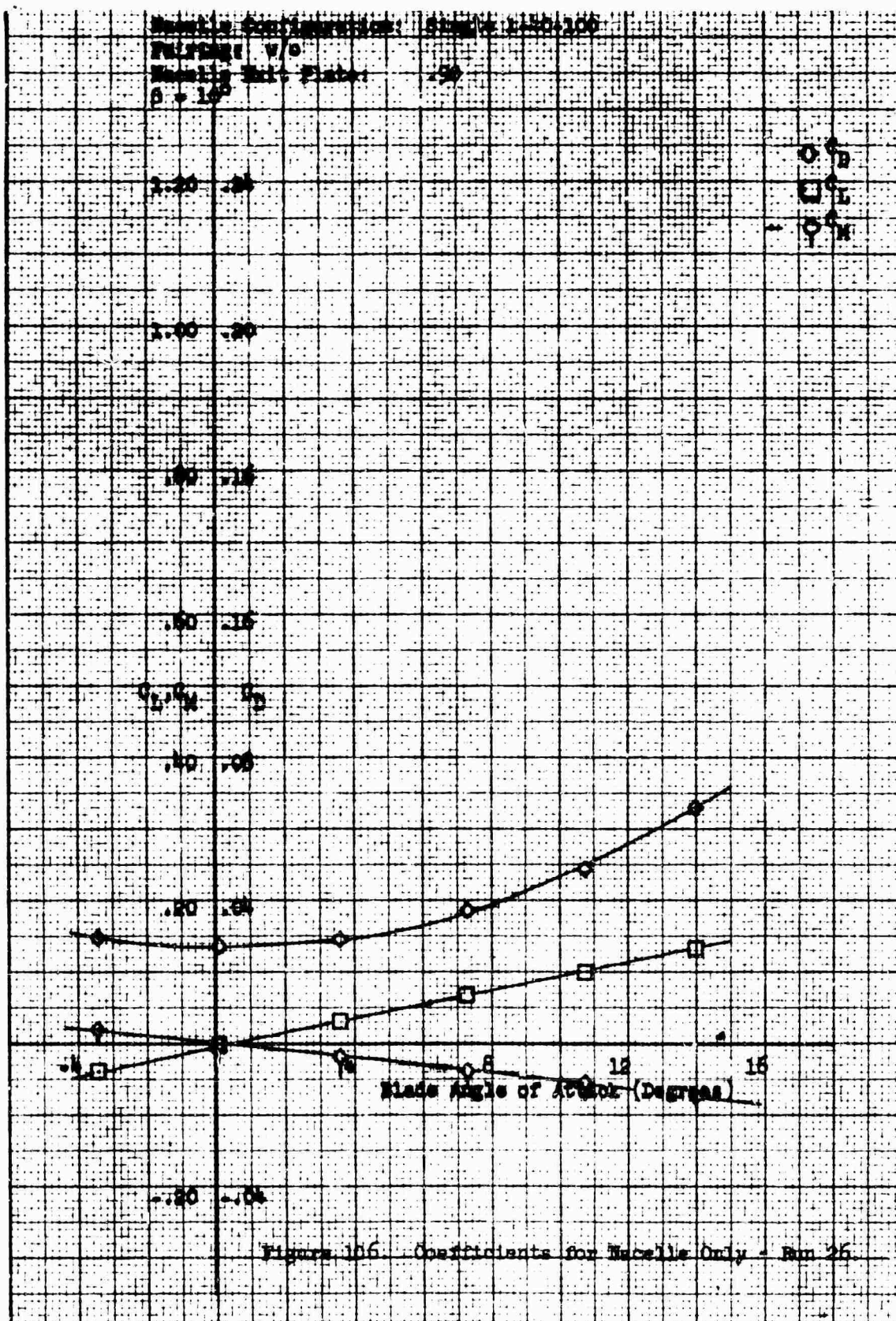


Figure 106. Coefficients for MacCull Only - Run 26

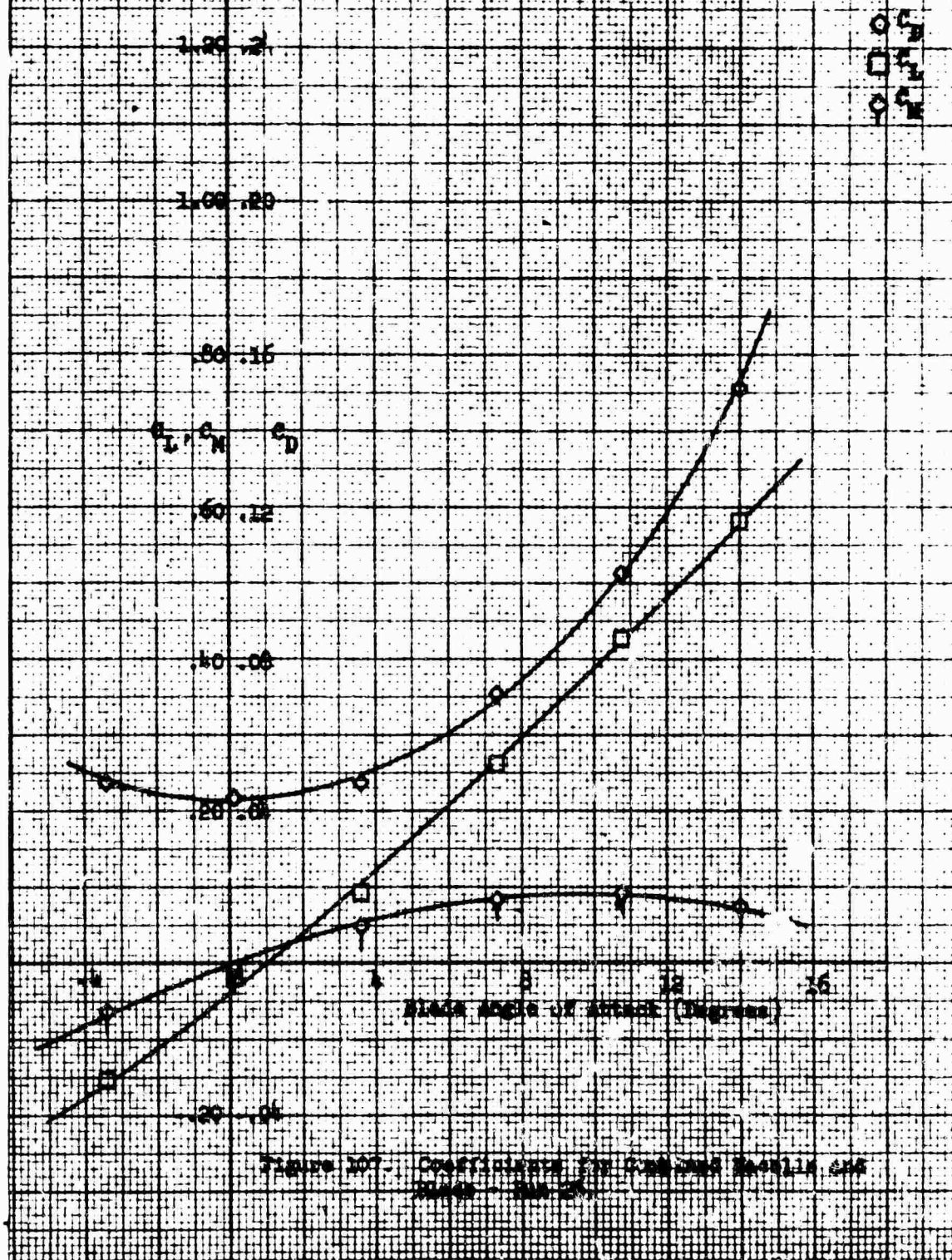
Nozzle Configuration: Single 1-40-100

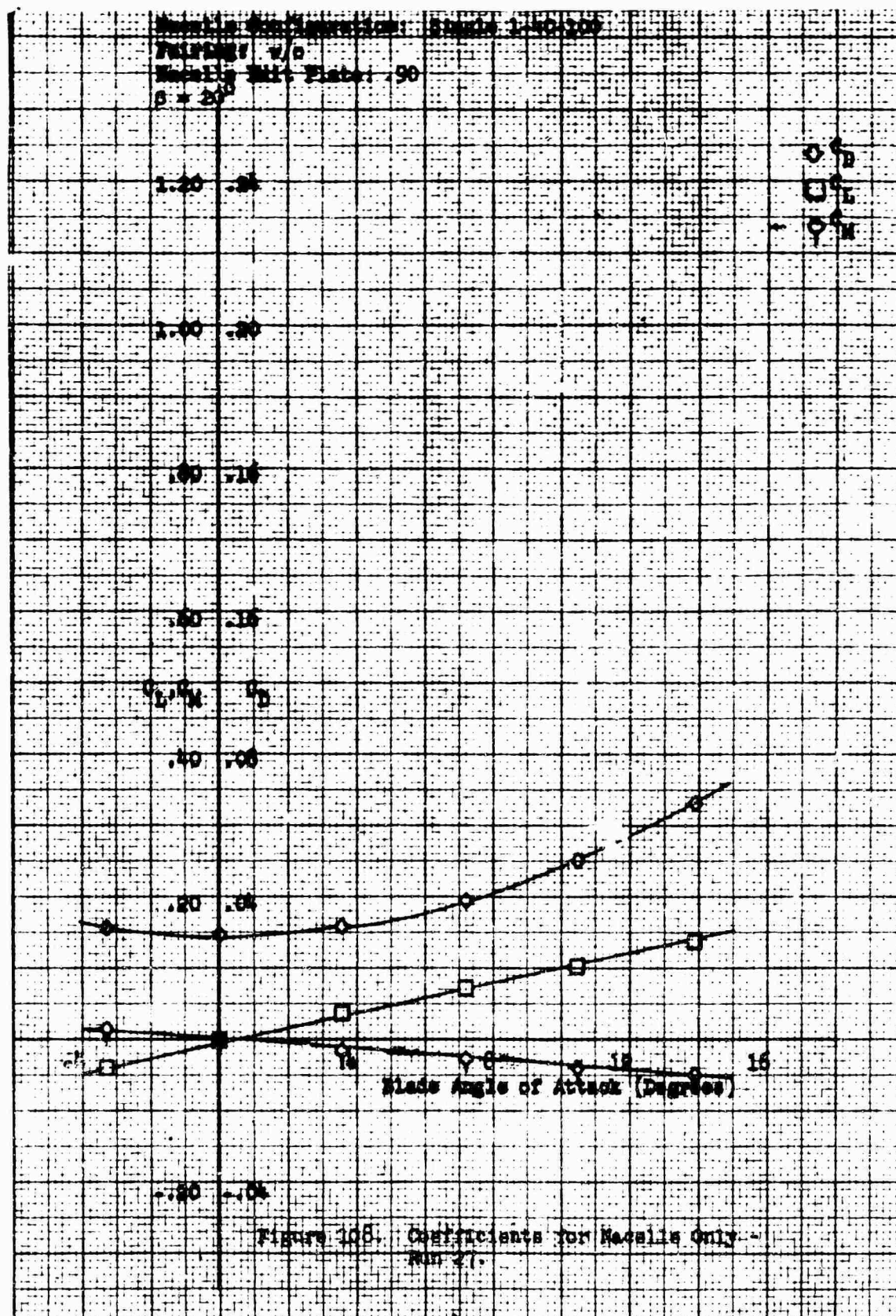
Nozzle Incidence Angle: 0

Feeding: w/o

Nozzle Exit Plane: .90

$\theta = 10^\circ$





Macelle Configuration: Single 1-40-100

Macelle Incidence Angle: 0

Fairing: w/o

Macelle Exit Plate: .90

$\beta = 20^\circ$

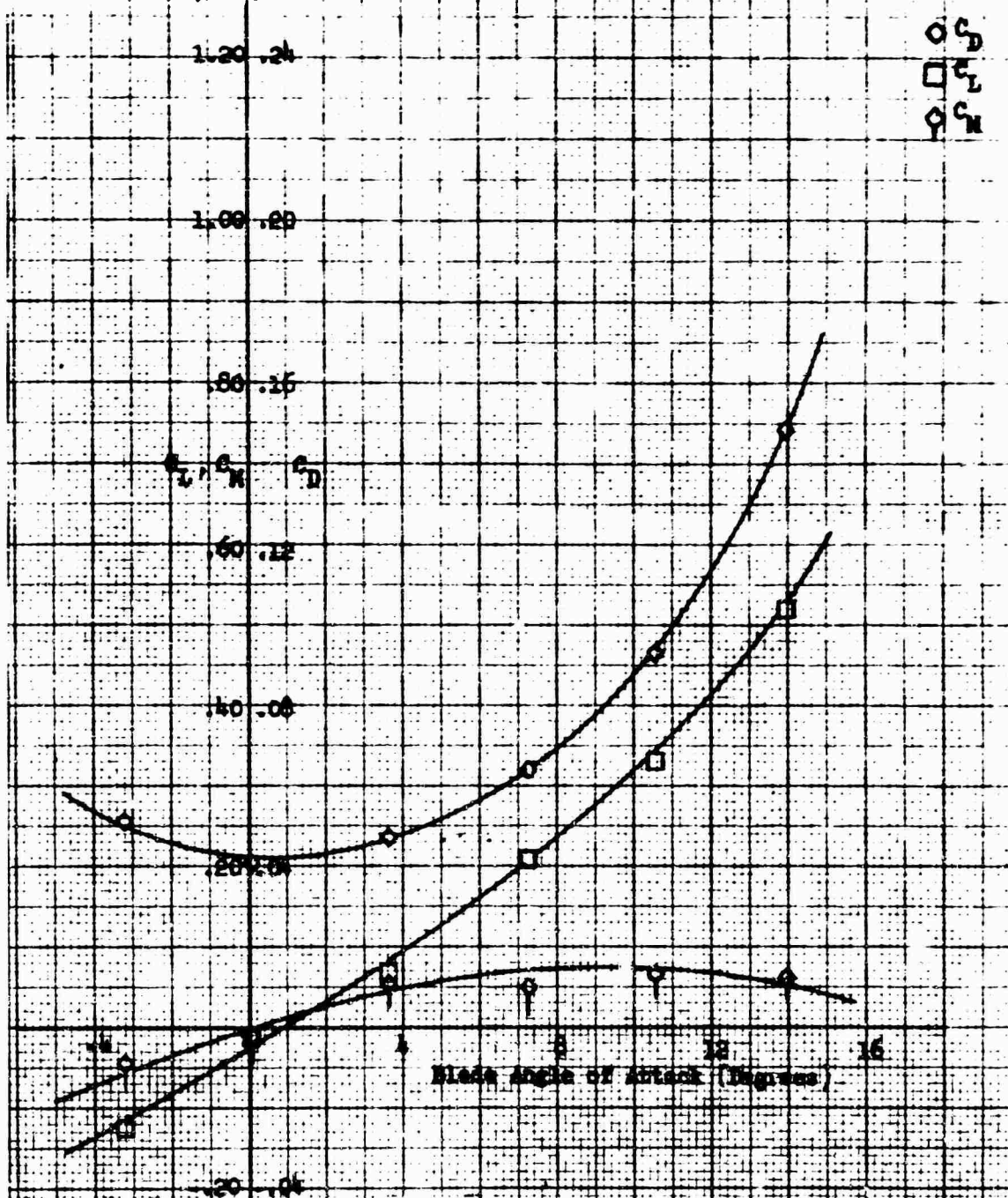
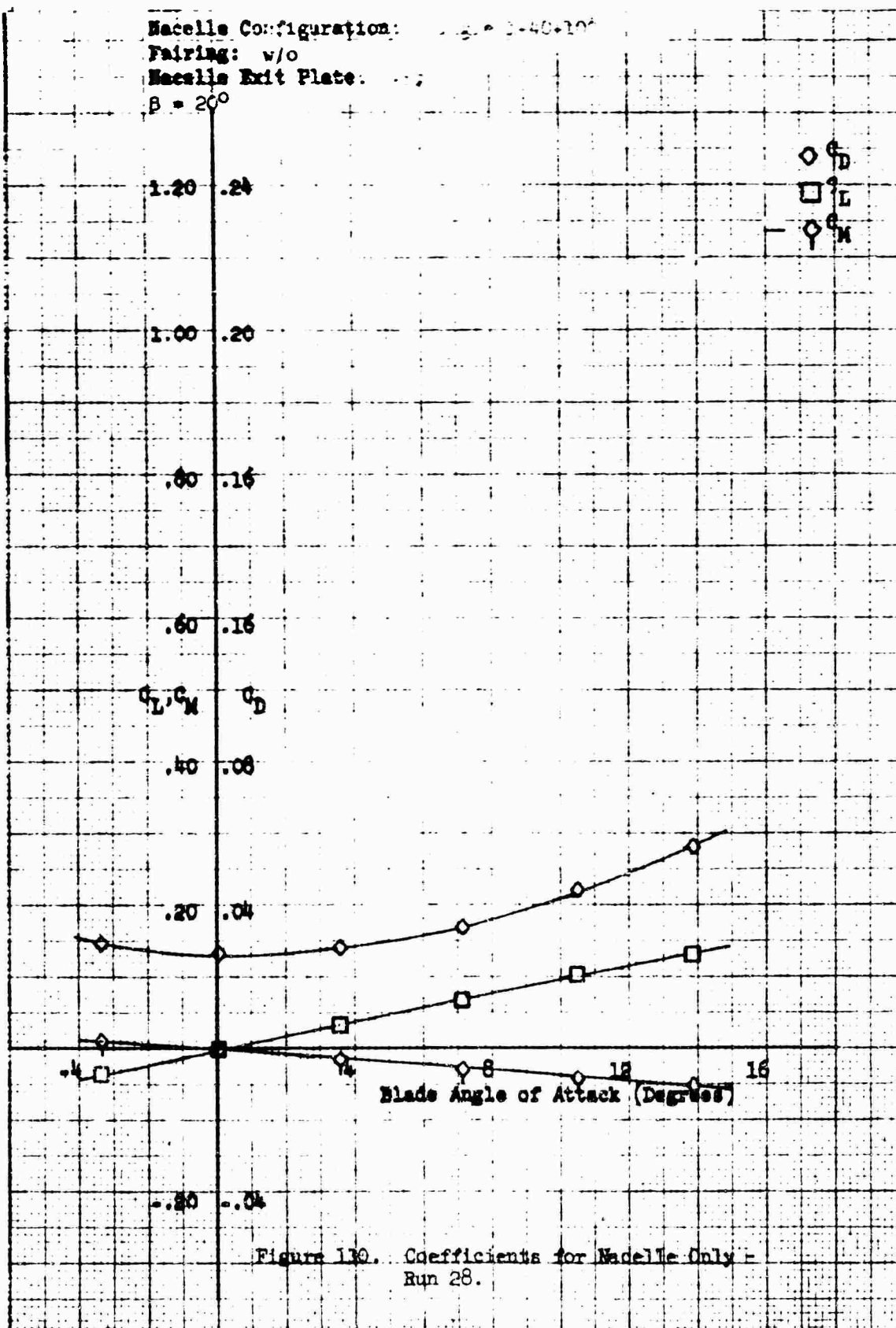


Figure 109. Coefficients for Combined Macelle and Blade Flow.

Macelle Configuration: 3-40-10°
 Pairing: w/o
 Macelle Exit Plate: ;
 $\beta = 20^\circ$



Macelle Configuration: Single 1-10-150

Macelle Incidence Angle: 0

Fairing: w/o

Macelle Exit Plate: .85

$\theta = 20^\circ$

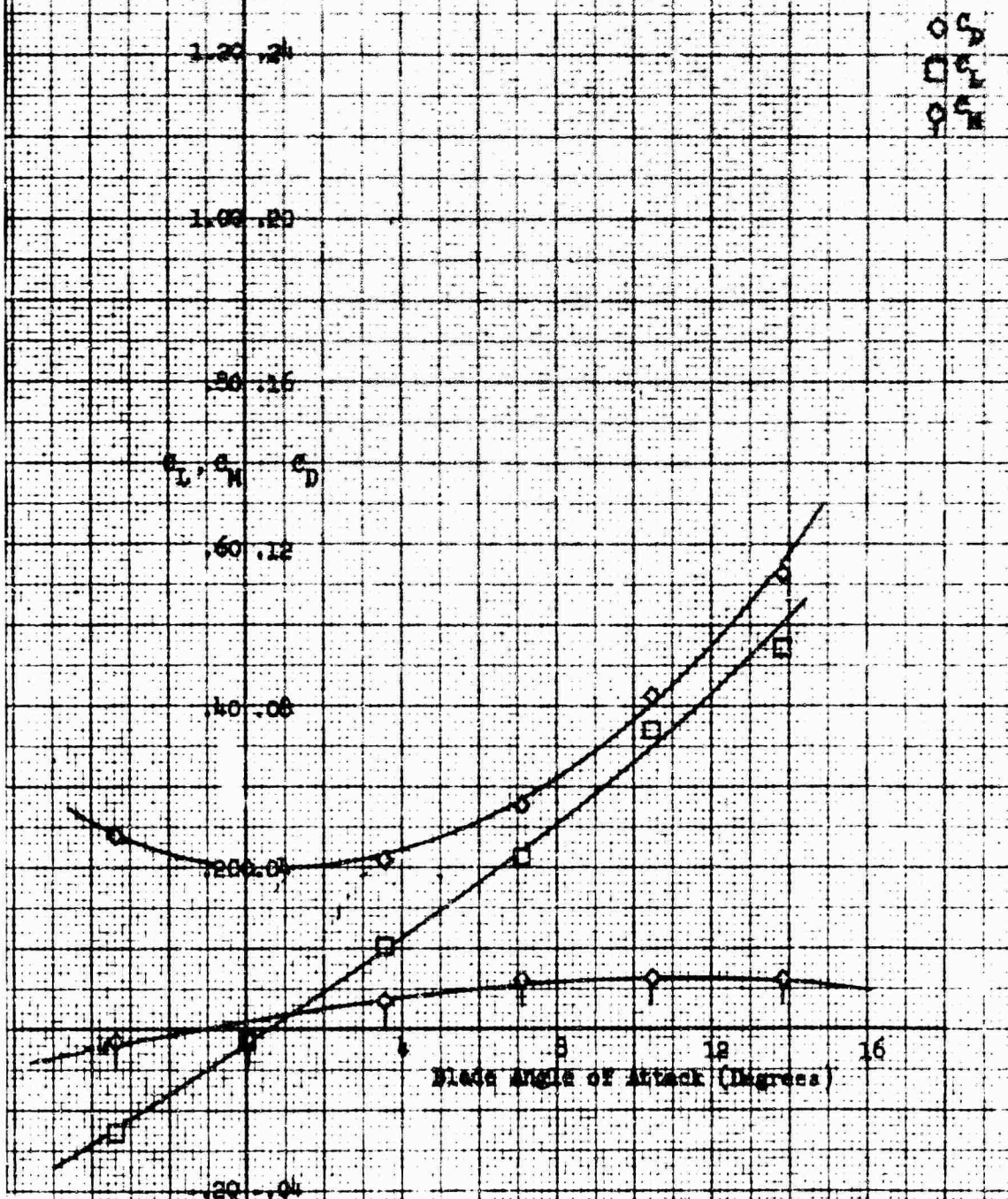


Figure 111. Coefficients for Combined Macelle and Blade - Run 101

Macelle Configuration: Single 1-40-100
 Pairing: w/o
 Macelle Exit Plate: .95
 $\beta = 10^\circ$

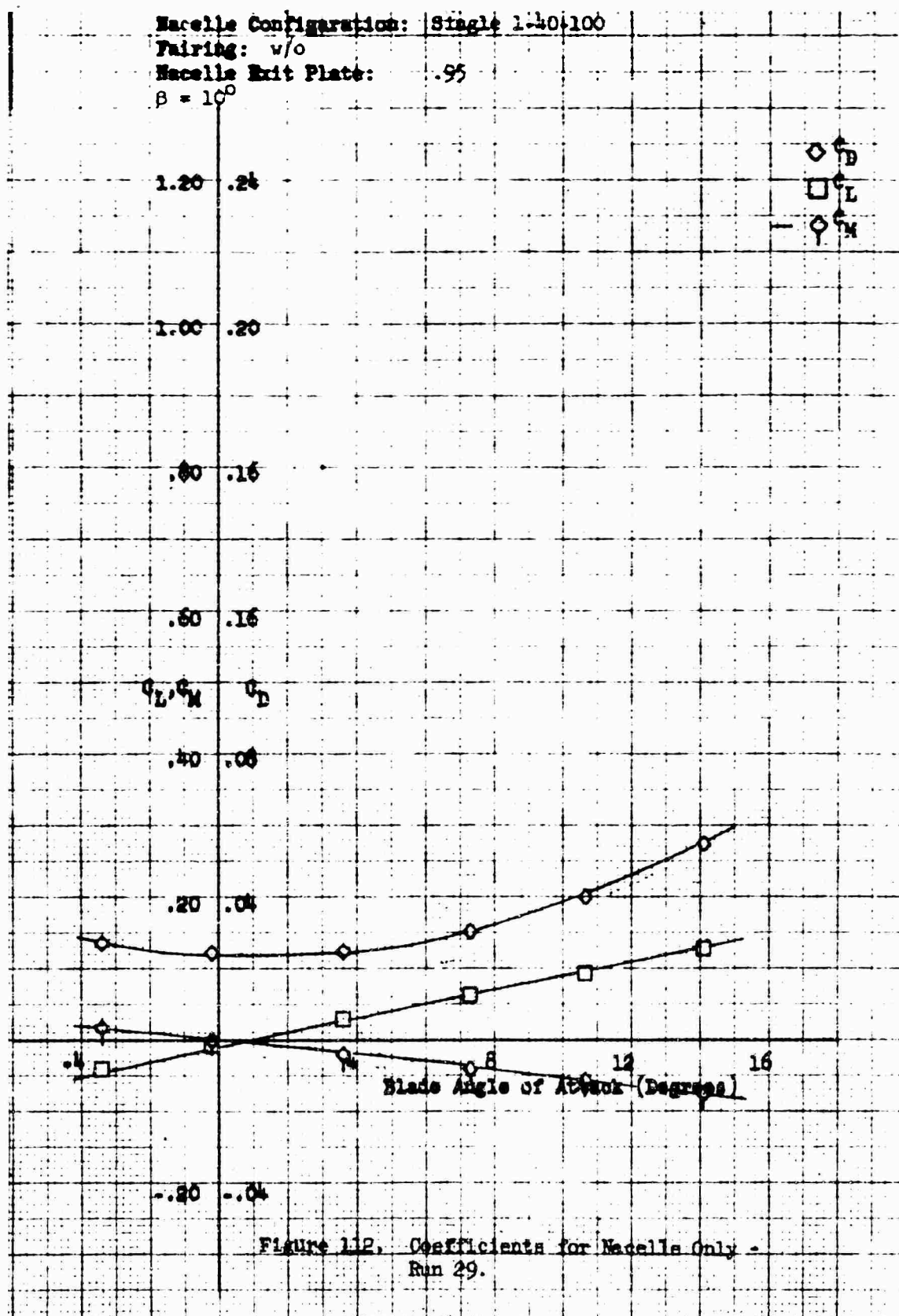
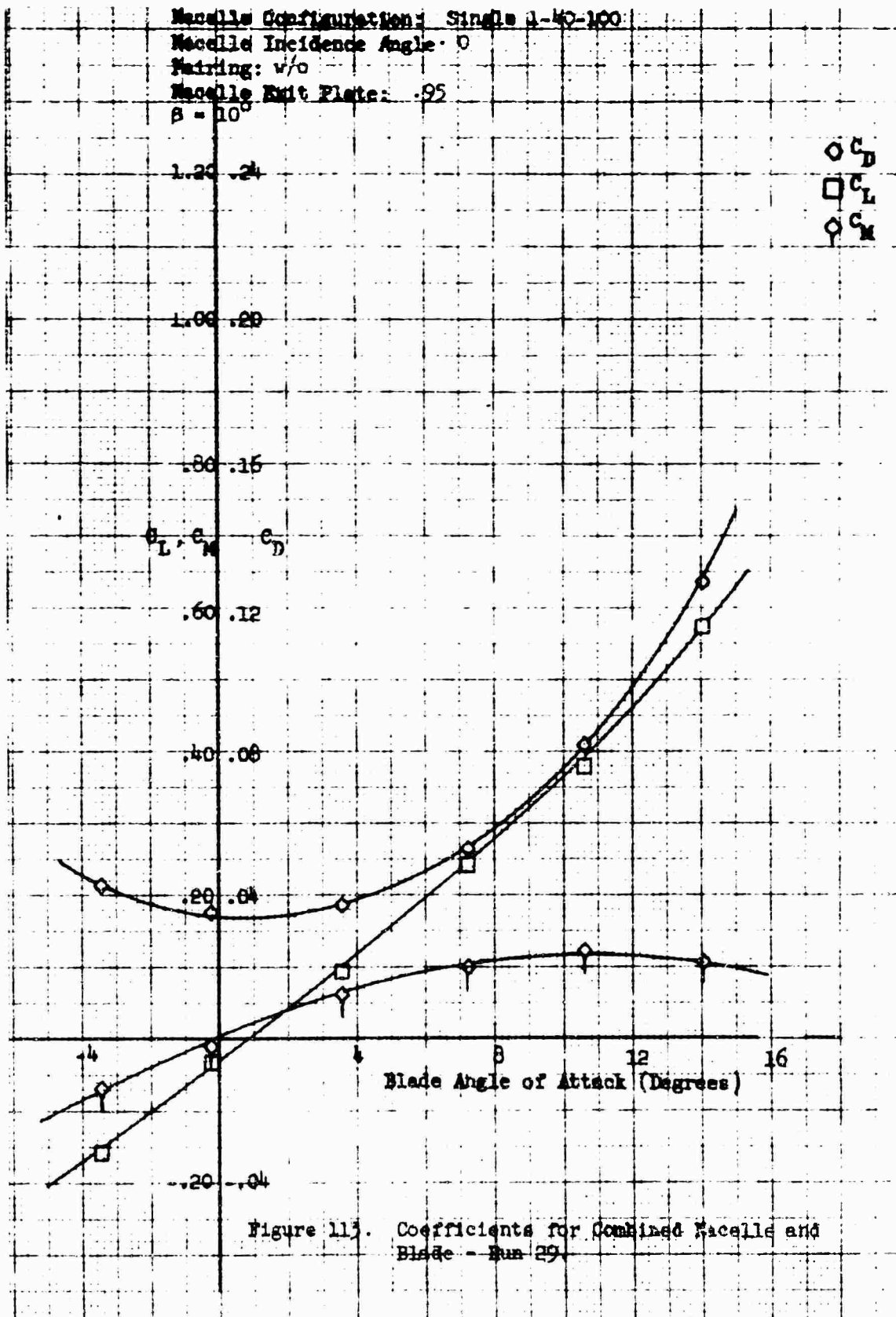


Figure 112. Coefficients for Macelle Only - Run 29.



Blade Configuration: Single 1.40-100

Pairing: w/o

Blade Exit Plate: .95

B = 0

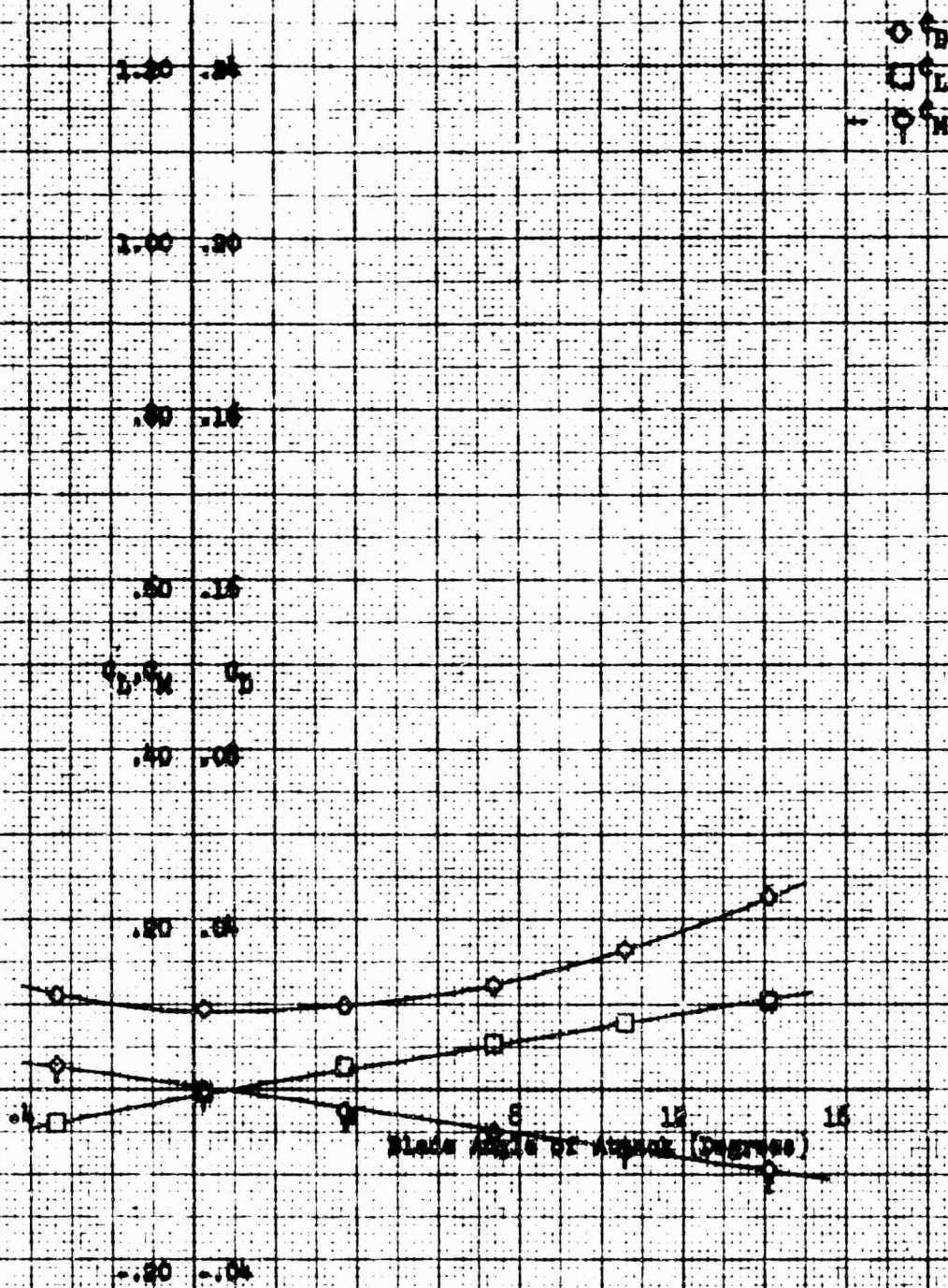
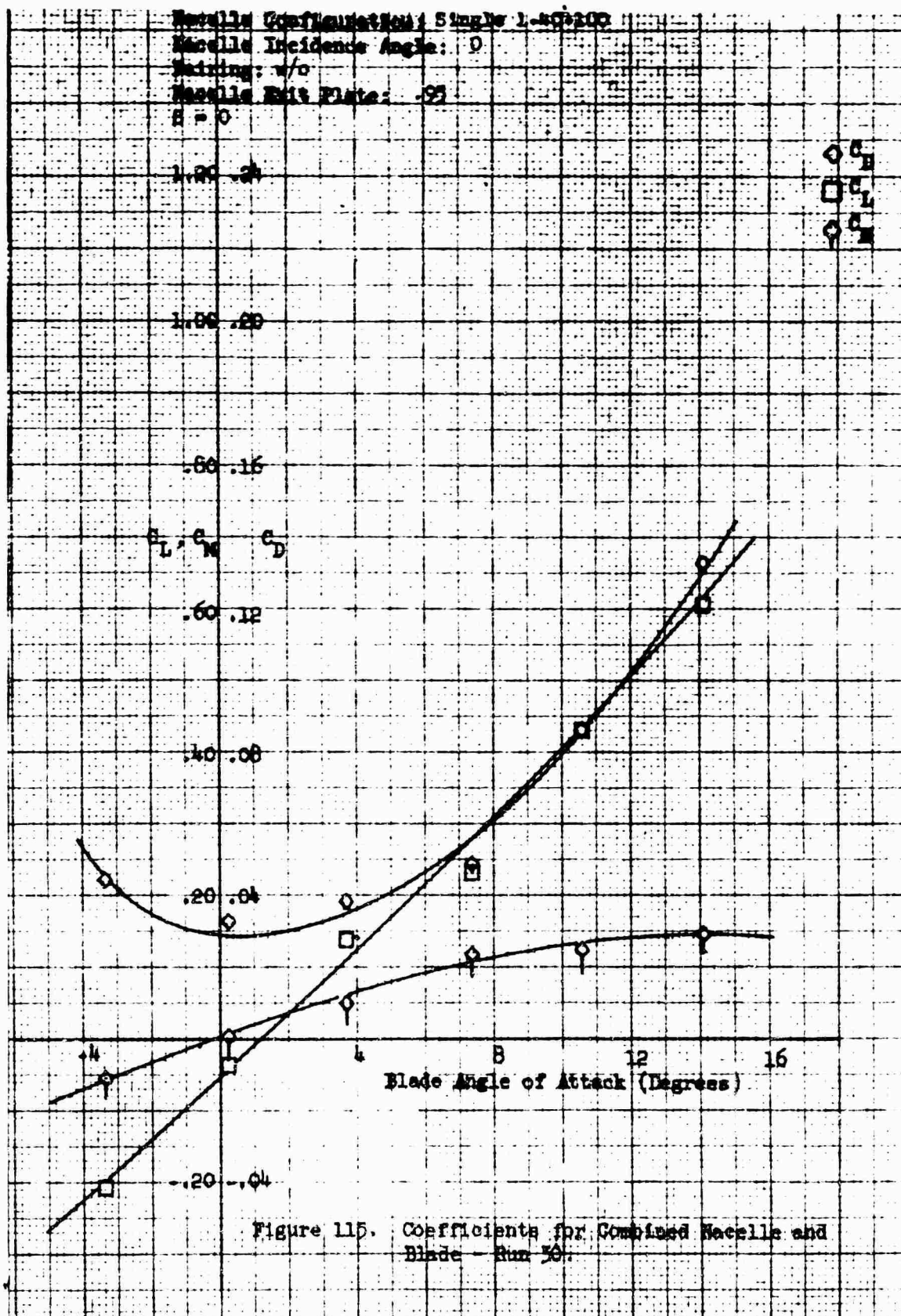
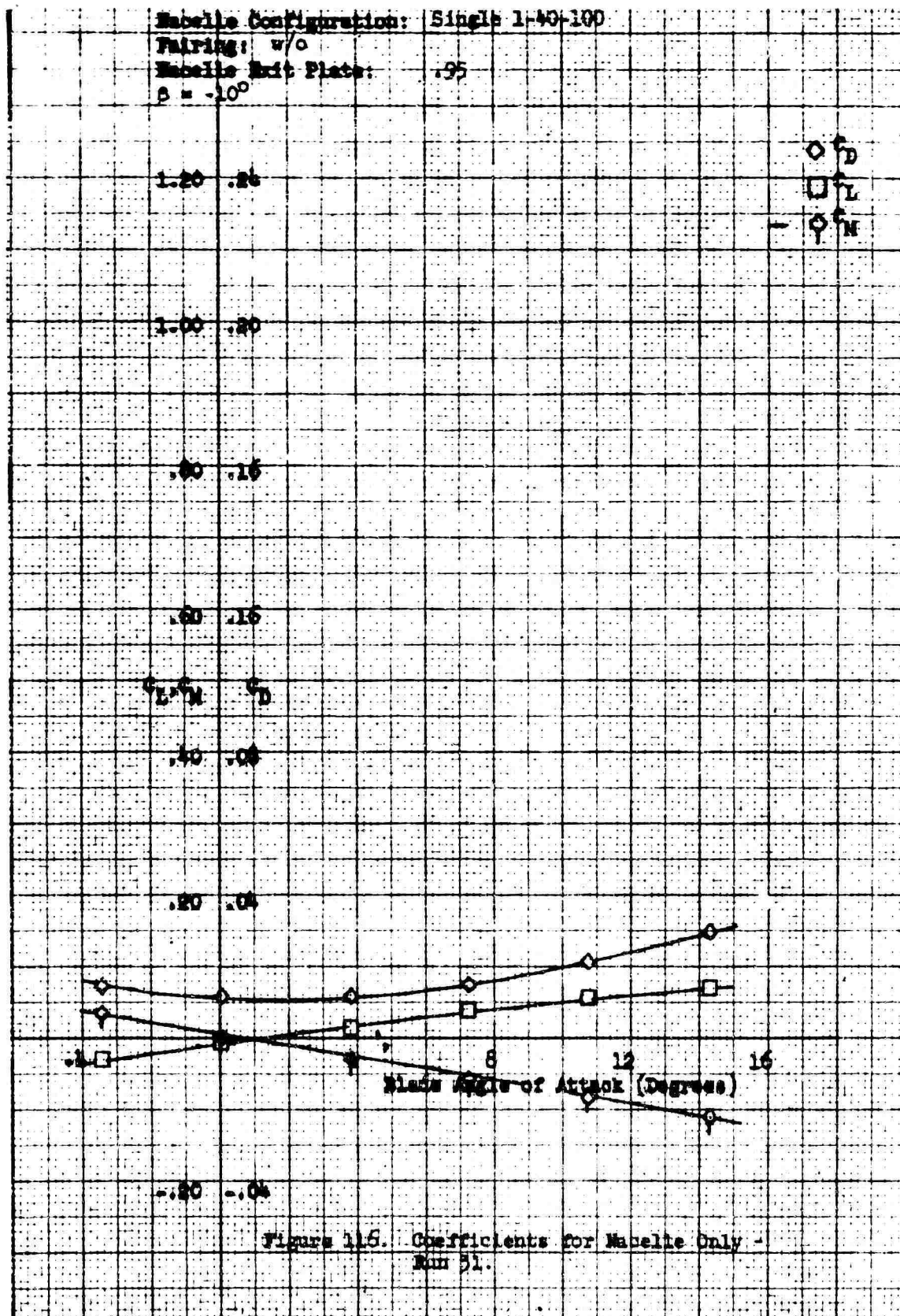


Figure 114. Coefficients for Blade Only - Run 30.





Macelle Configuration: Sample 1-40-100
 Macelle Incidence Angle: 0
 Twisting: w/o
 Macelle Exit Plate: .95
 $\beta = -10^\circ$

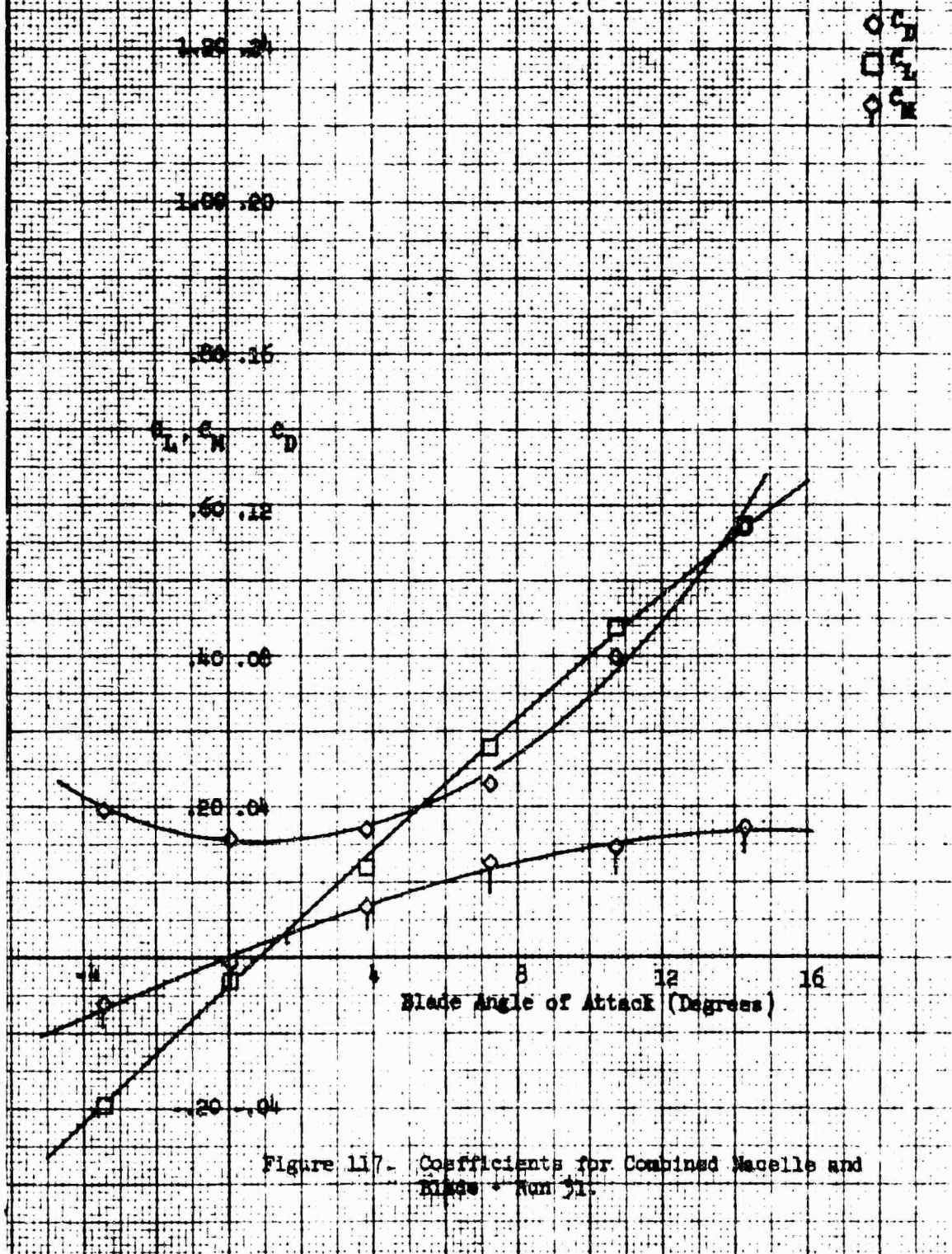


Figure 117- Coefficients for Combined Macelle and Blade - Run 51.

Wacelle Configuration: Single 1-40-100

Fairing: w/o

Wacelle Exit Plate: .95

$\beta = -20^\circ$

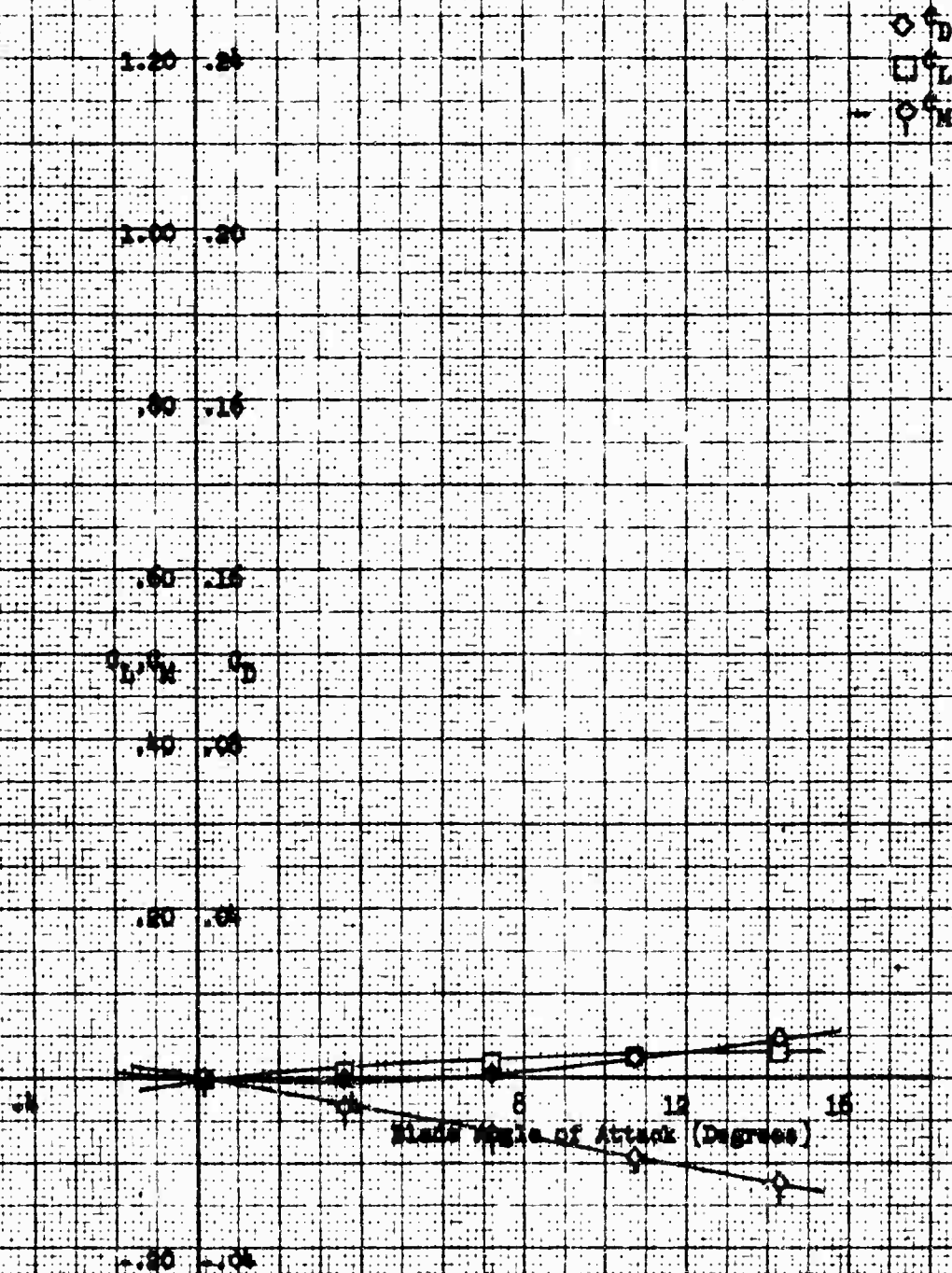


Figure 118. Coefficients for Wacelle Only - Run 52.

Nacelle Configuration: Single 1-40-100
 Nacelle Incidence Angle: 0
 Training: w/o
 Nacelle Exit Plate: -95
 $\beta = -20^\circ$

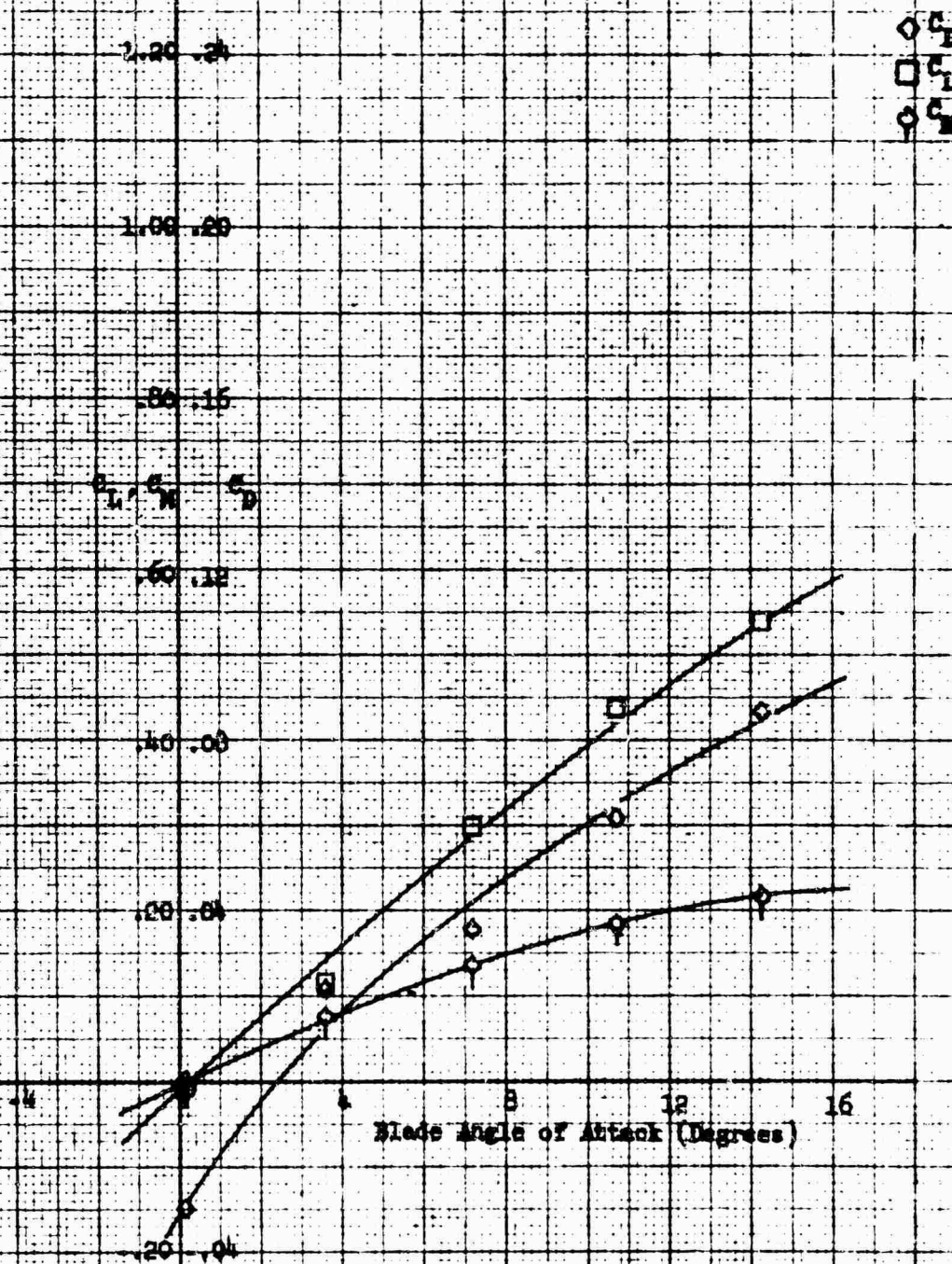


Figure 119. Coefficients for Combined Nacelle and
 Blade - Run 12.

Nozzle Configuration: Single 1-40-100

Pairing: w/o

Nozzle Exit Plane: 1-00

$\beta = -20^\circ$

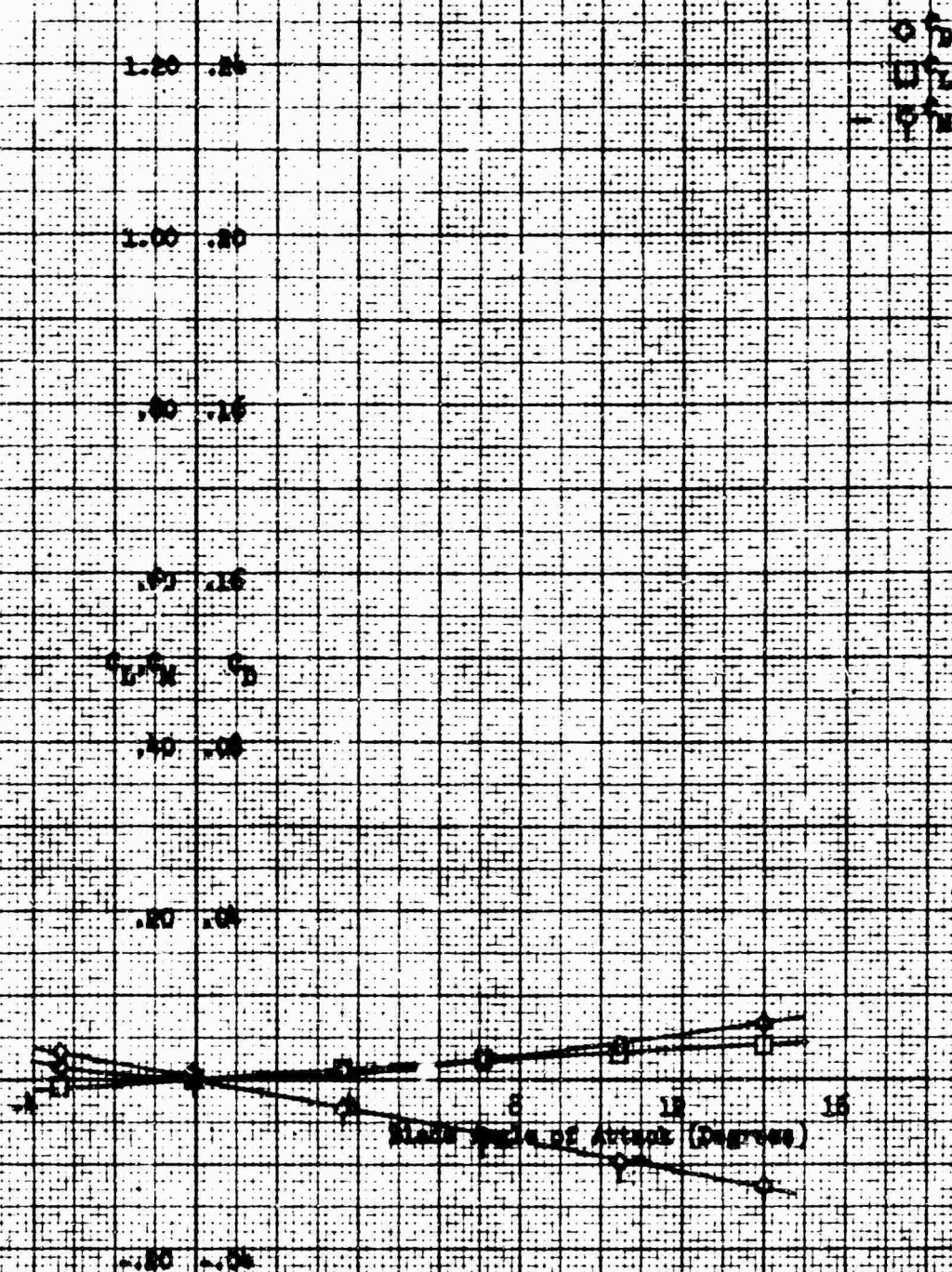
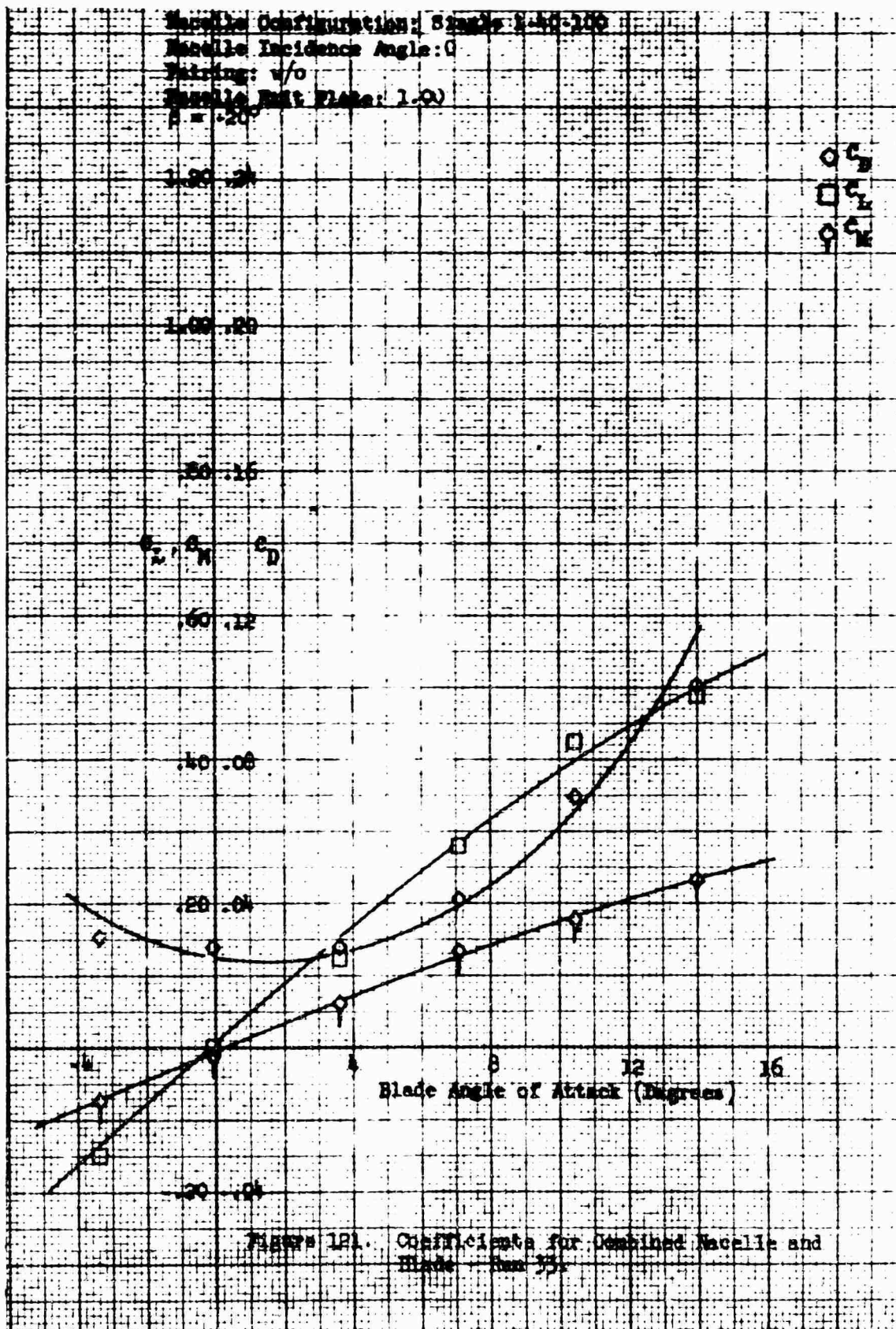


FIGURE 100. COEFFICIENTS FOR NOZZLE ONLY -
Run 55

Nozzle Configuration: Single 2-40-100
 Nozzle Incidence Angle: 0
 Pairing: w/o
 Nozzle Exit Plane: 1.0
 $\beta = 20^\circ$



Nacelle Configuration: Single 1:40-100

Pairing: w/o

Nacelle Exit Plate: 1.00

$\delta = -10^\circ$

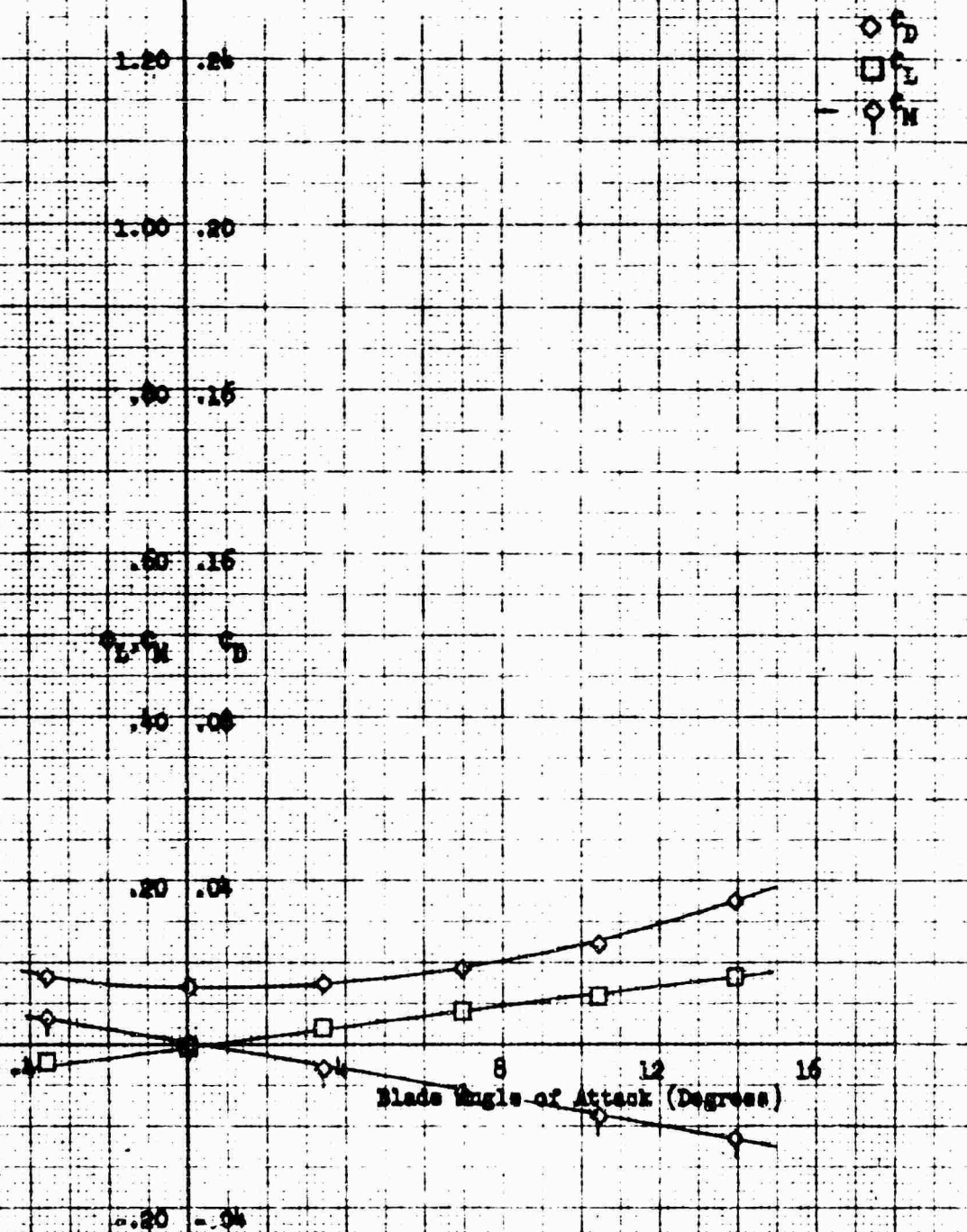


Figure 122. Coefficients for Nacelle Only -
Run 54.

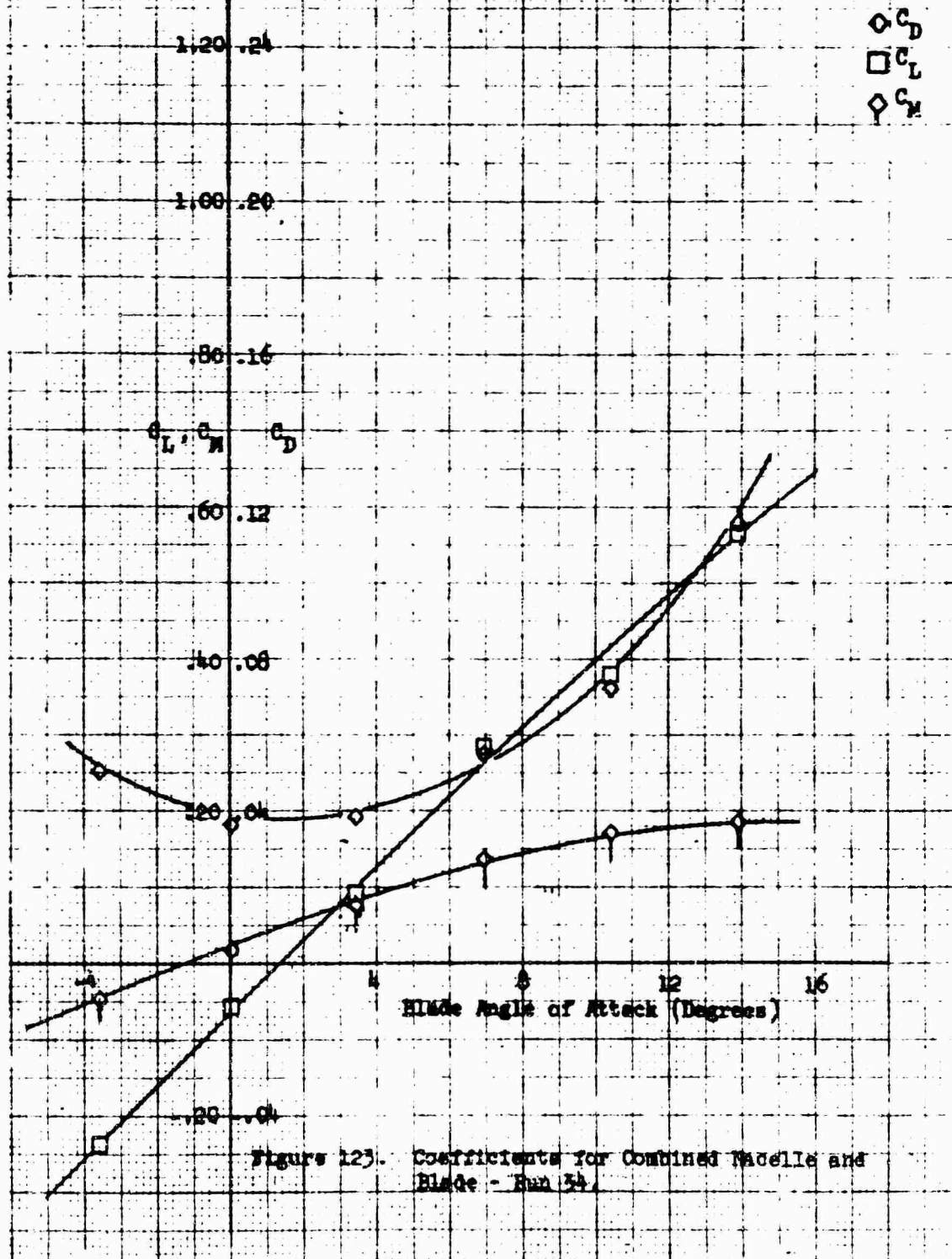
Wacelle Configuration: Single 1-40-100

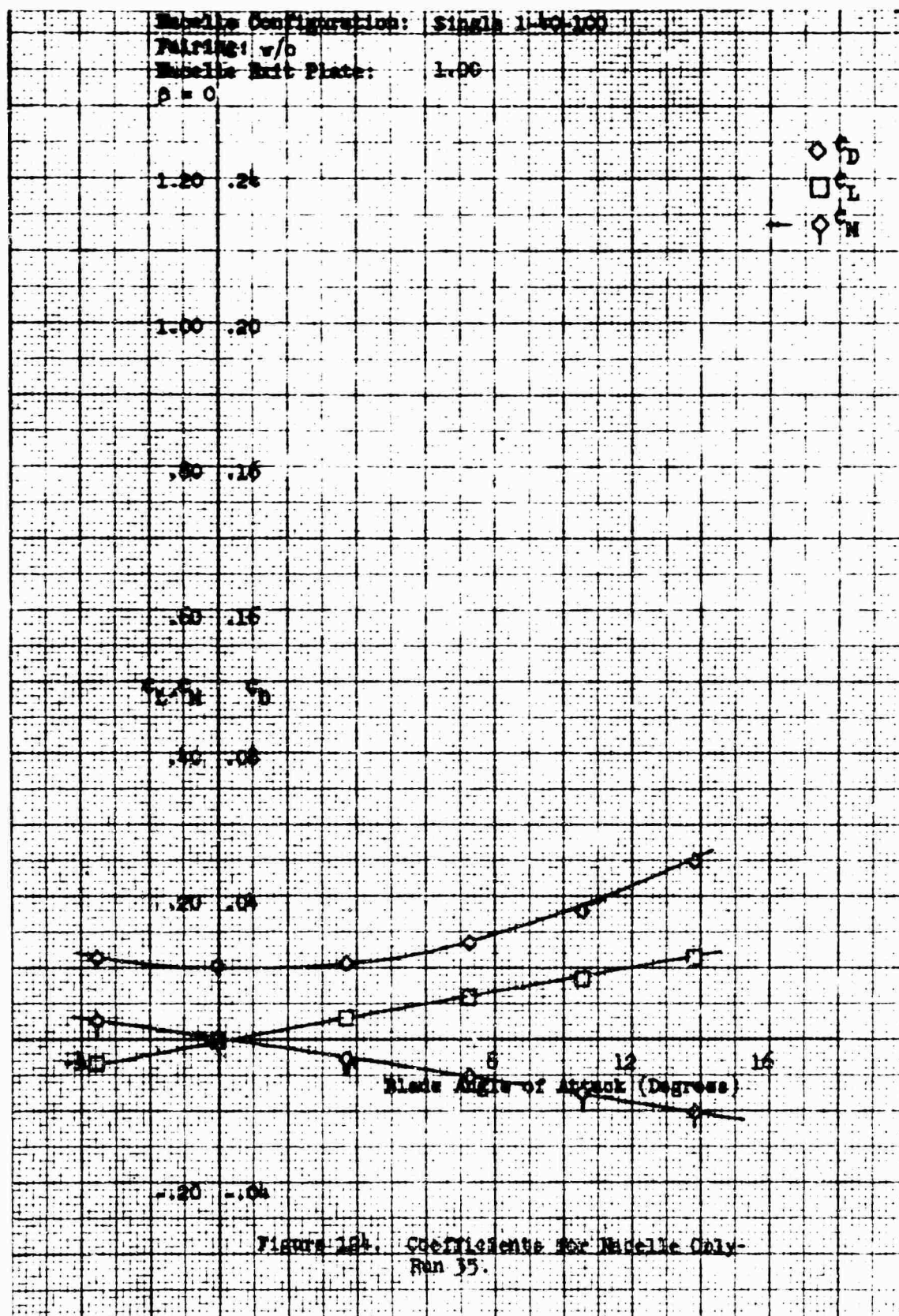
Wacelle Incidence Angle: 0

Pairing: v/b

Wacelle Exit Plate: 1.00

$\Delta = -10^\circ$





Macelle Configuration: Single 1-45-100

Macelle Incidence Angle: 0

Pairing: w/o

Macelle Exit Plate: 1.00

$\beta = 0$

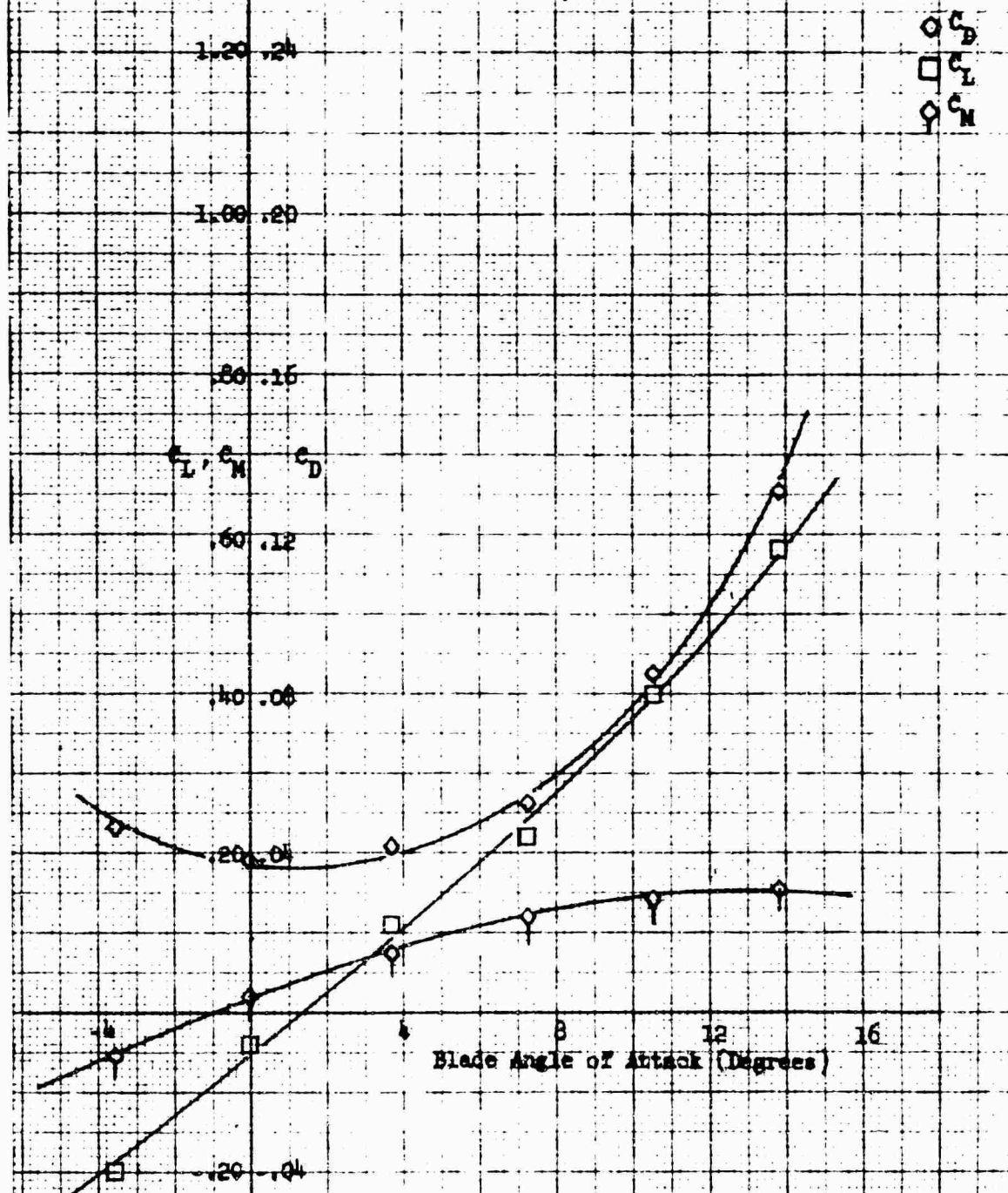
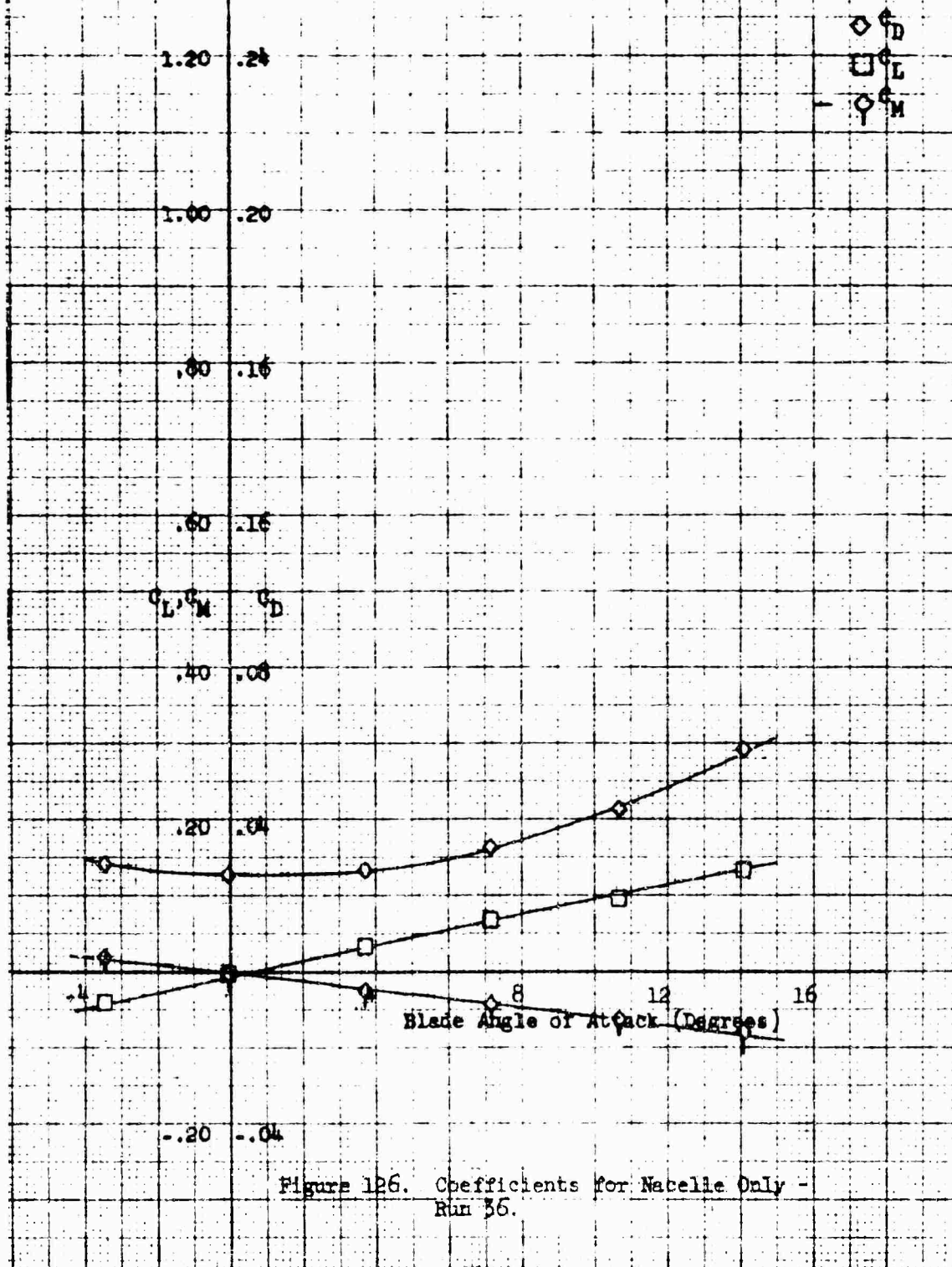


Figure 123. Coefficients for Combined Macelle and Blade - Run 35.

Macelle Configuration: Single 1-4C-100
 Fairing: w/o
 Macelle Exit Plate: 1.00
 $\beta = 10^\circ$



Nacelle Configuration: Single 1-40-100°

Nacelle Incidence Angle: 0

Fairing: w/o

Nacelle Exit Plate: 1.00

$\beta = 10^\circ$

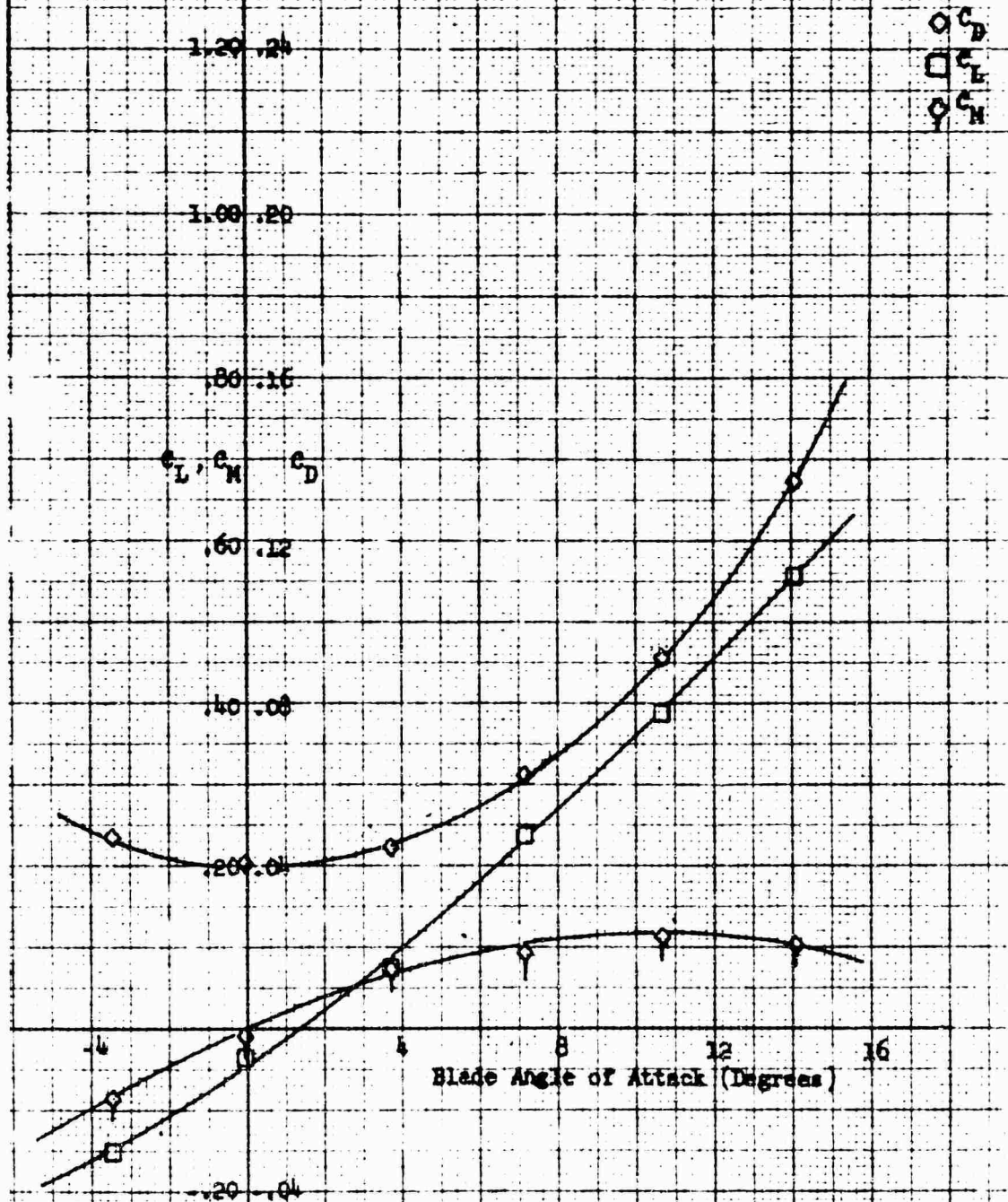


Figure 127. Coefficients for Combined Nacelle and Blade - Run 36.

Nacelle Configuration: Single 1-40-100
 Fairing: w/o
 Nacelle Exit Plate: 1.00
 $\beta = 20^\circ$

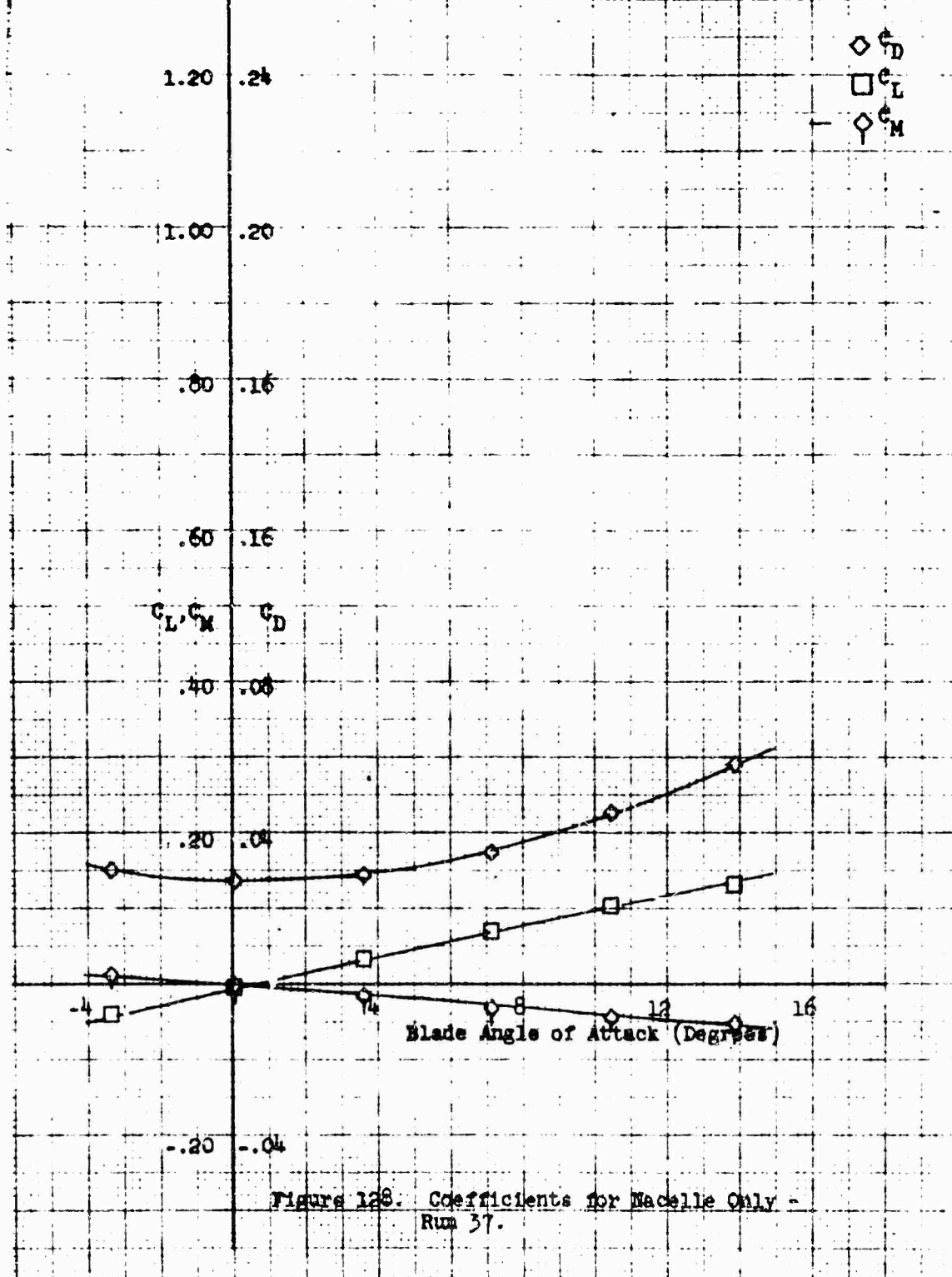
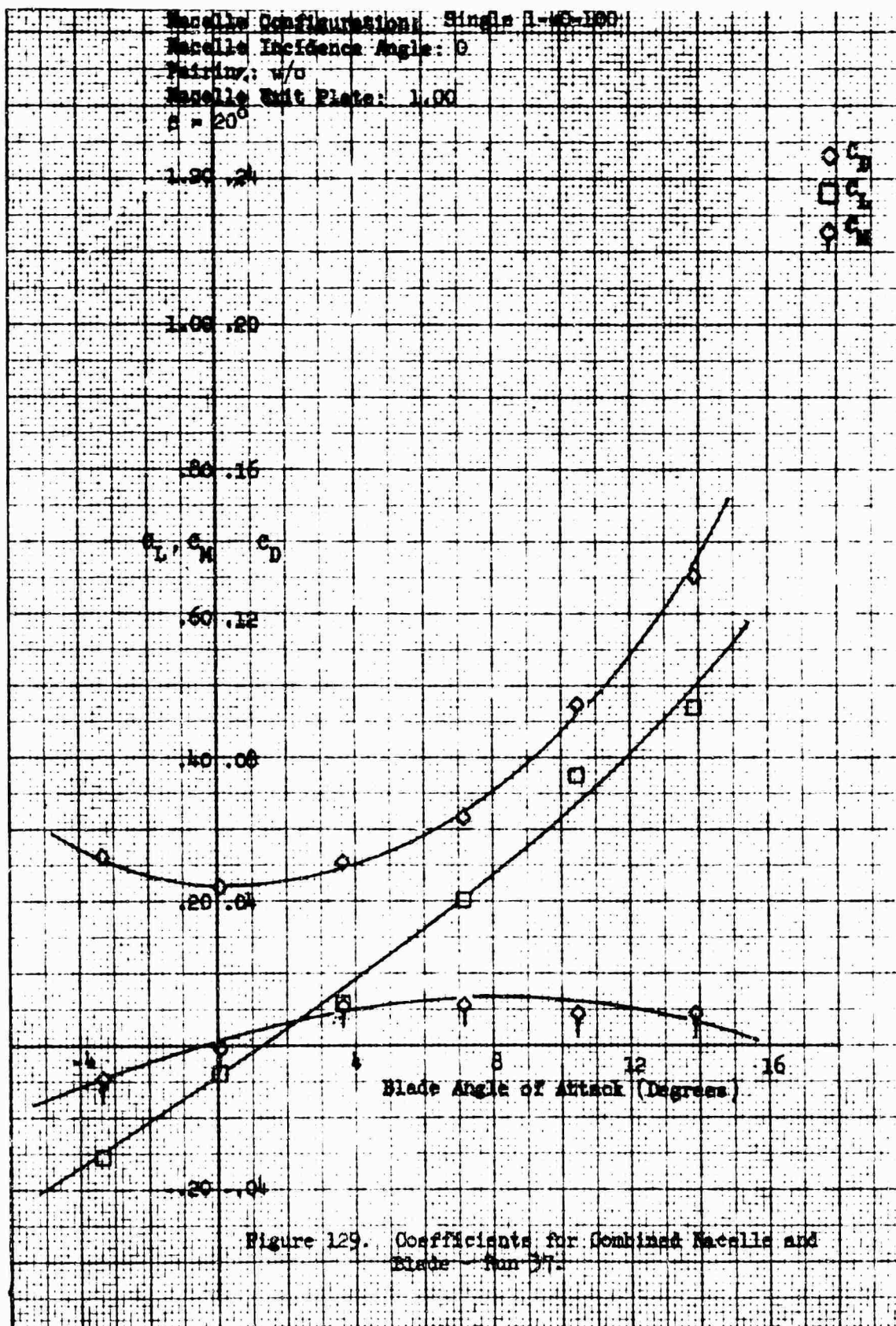
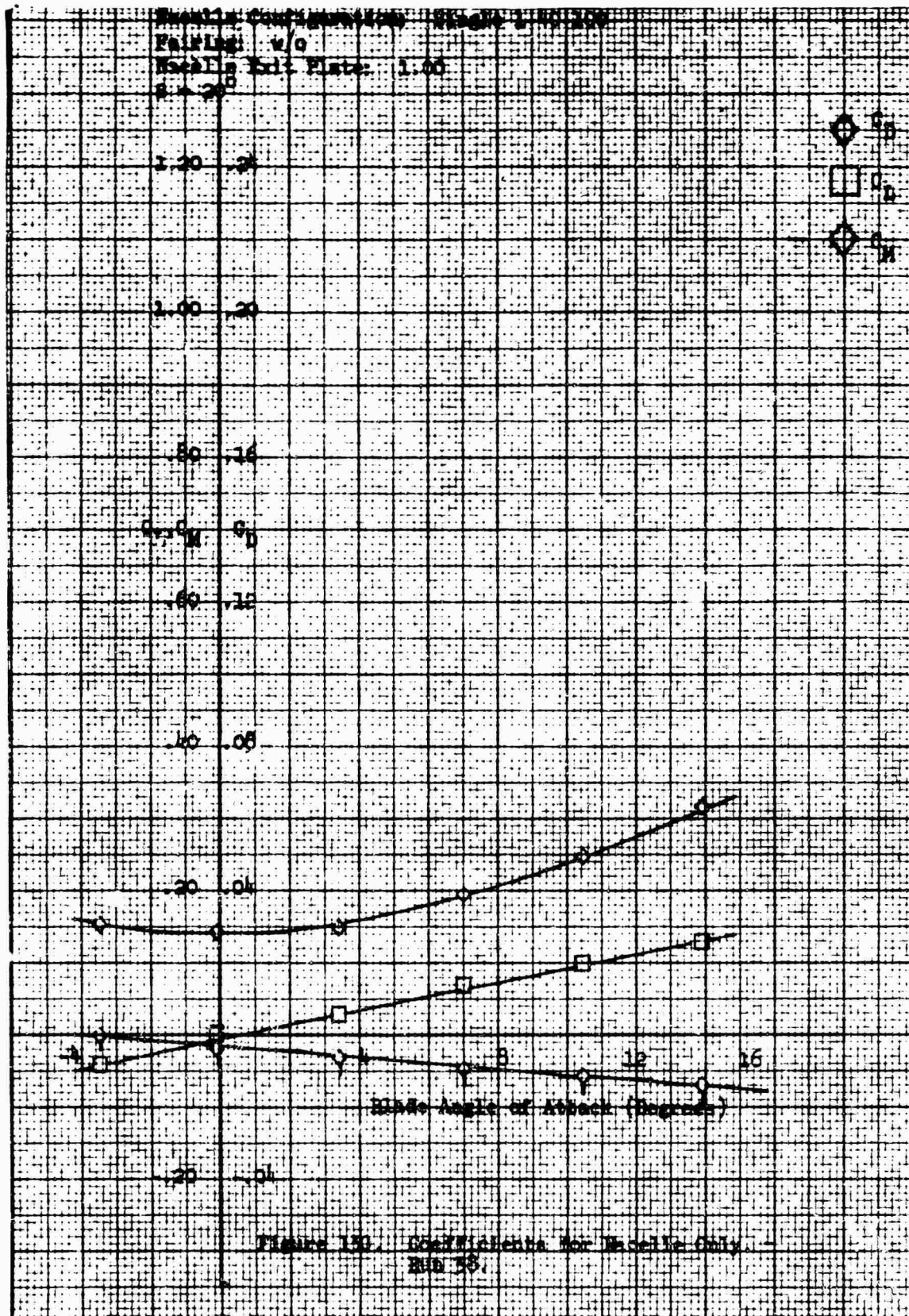
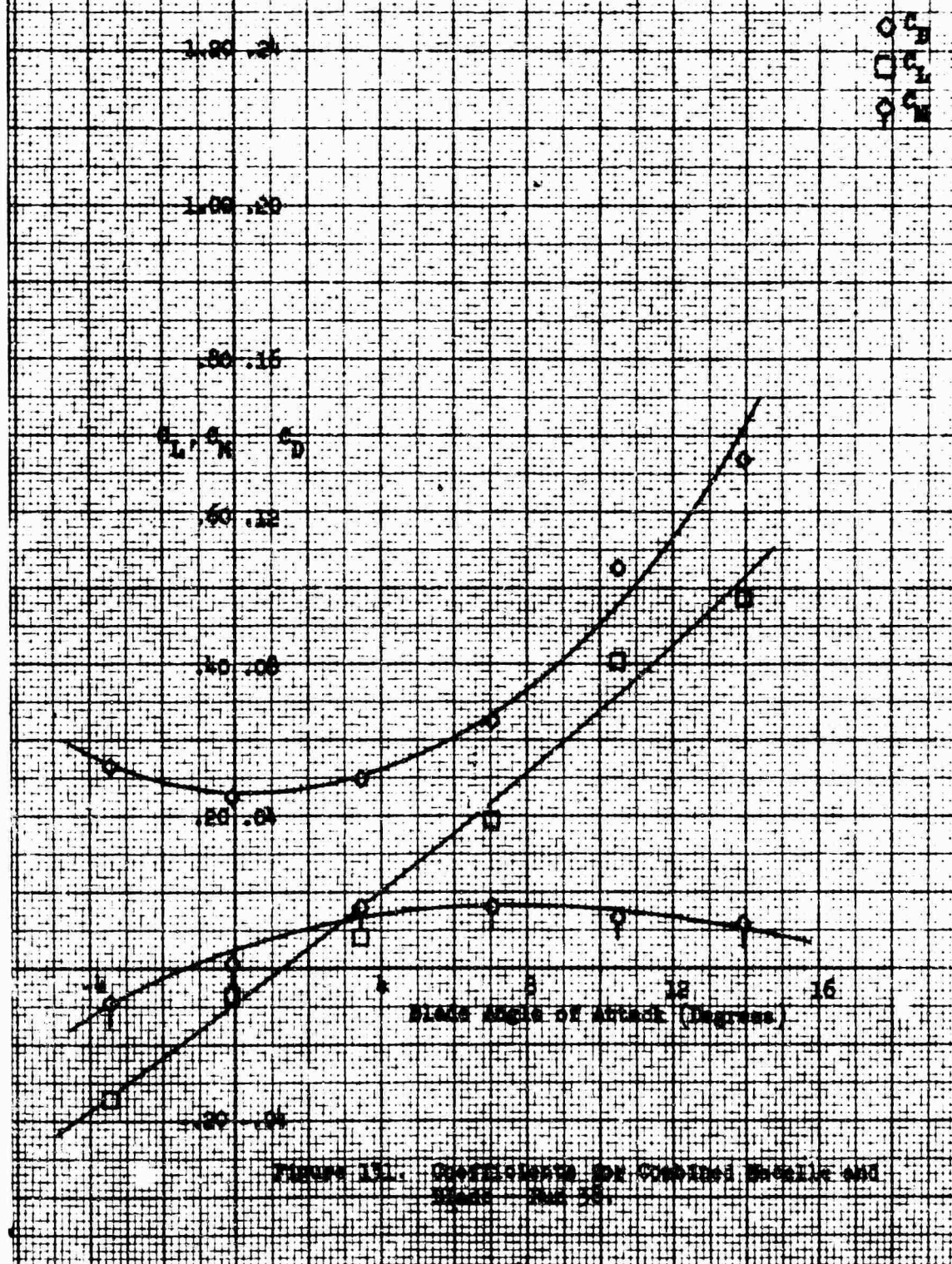


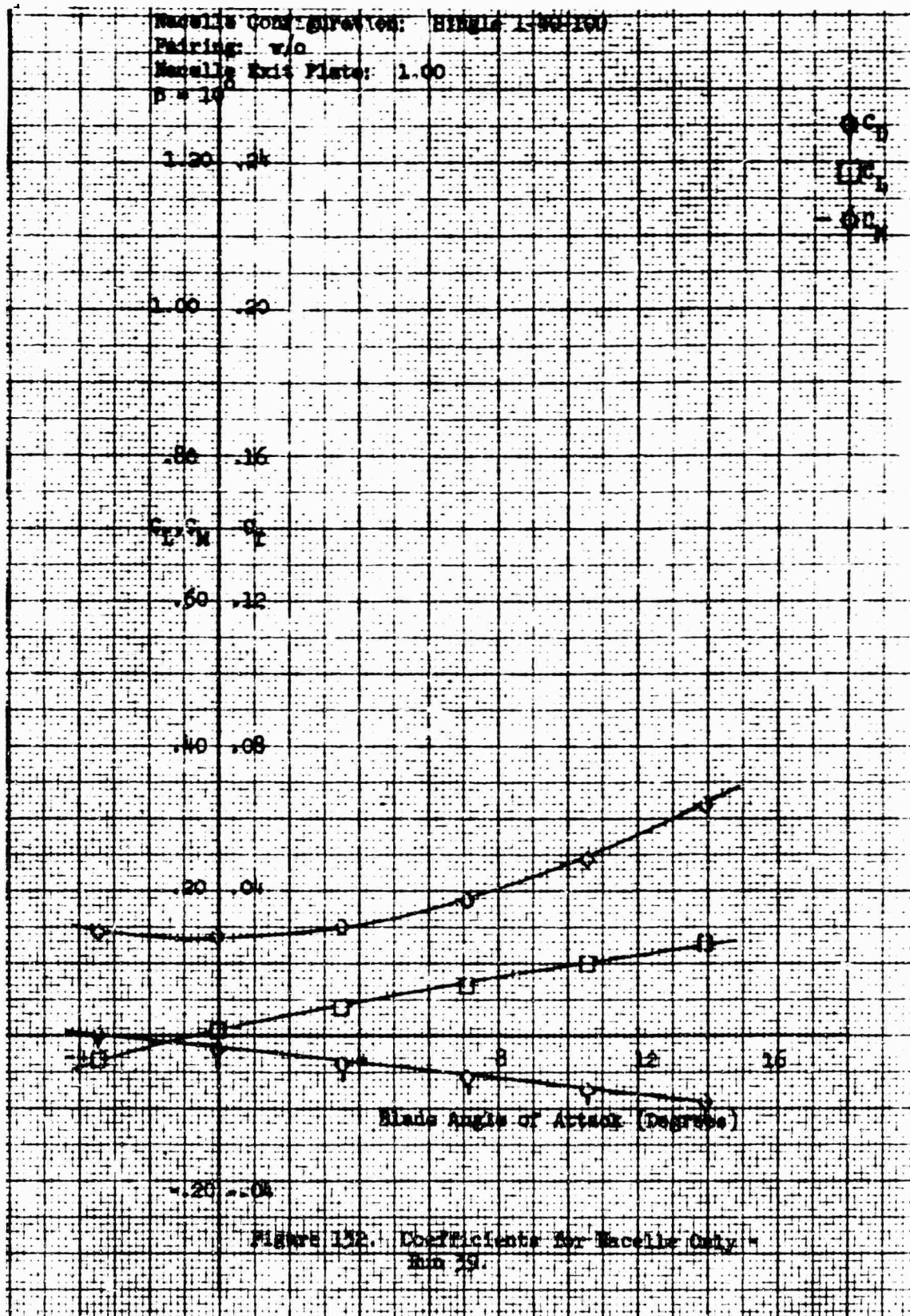
Figure 128. Coefficients for Nacelle Only -
 Run 37.





Nozzle Configuration: Single 1-40-100
 Nozzle Incidence Angle: 3°
 Nozzle Exit Plate: 1:00
 $\beta = 20^\circ$





Machine Configuration: Blade 1-40-100

Blade Incidence Angle: 30°

Pairing: 4/8

Blade Root Plate: 1.00

$\alpha = 15^\circ$

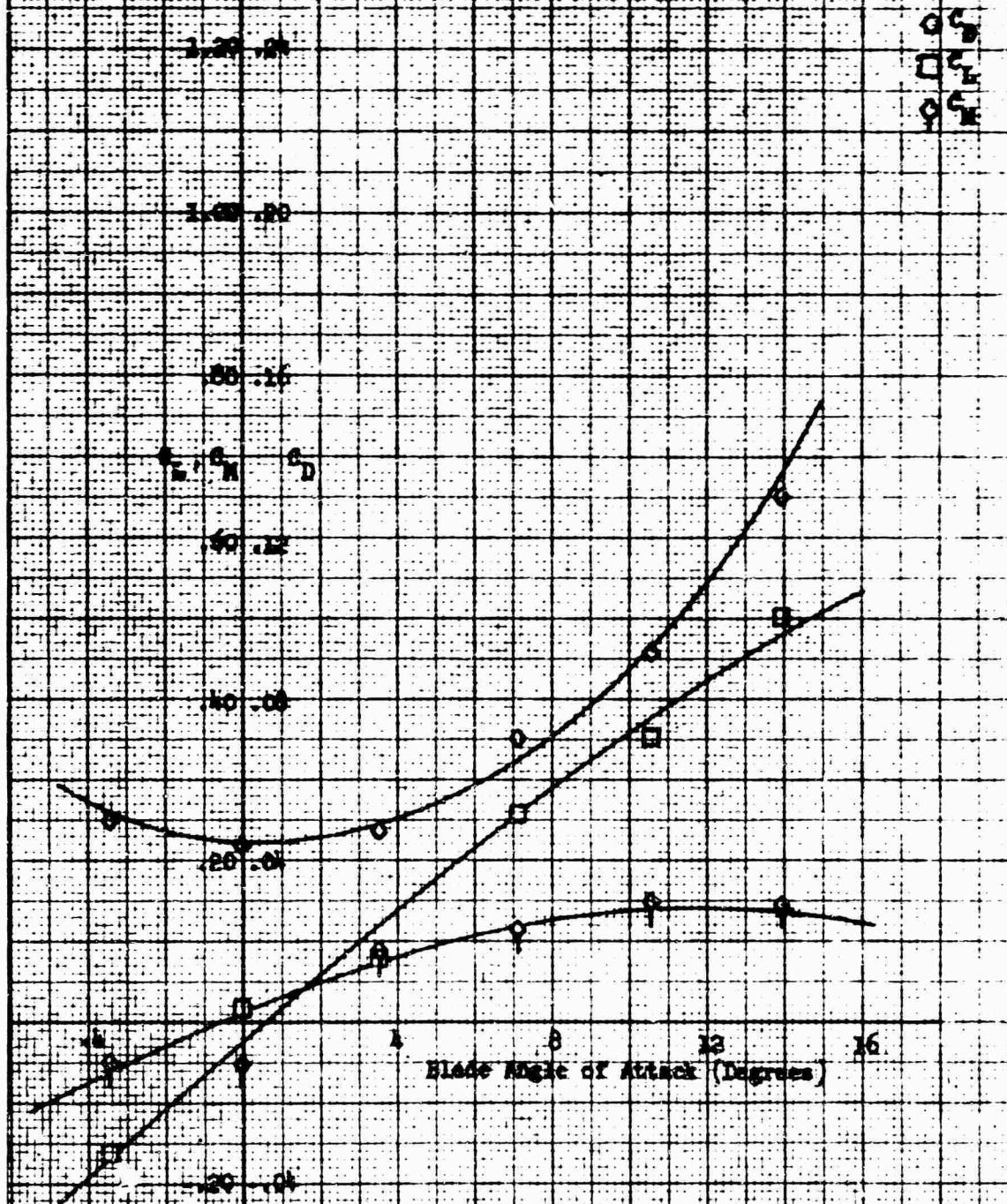
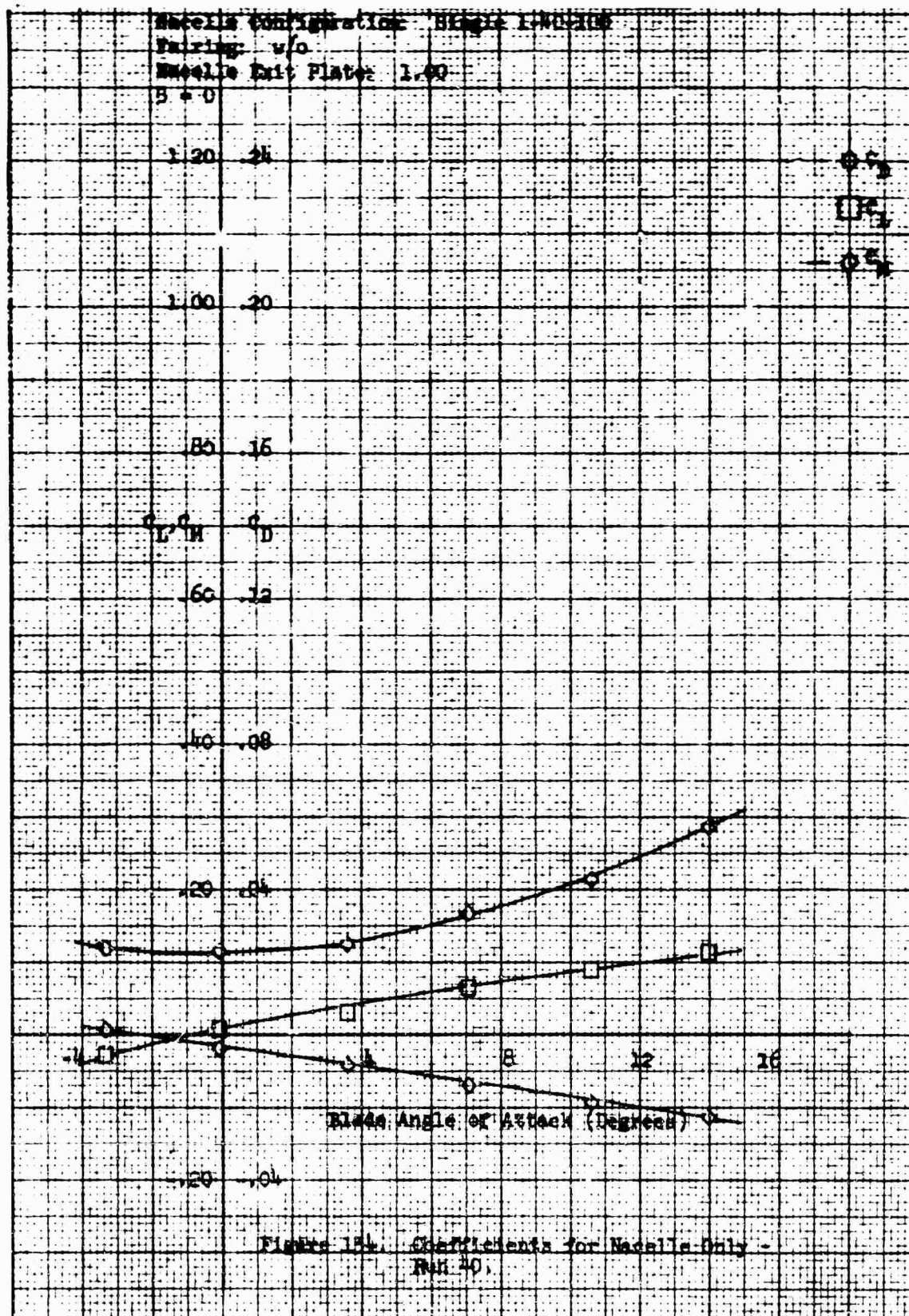


Figure 152. Coefficients for Combined Blade and Blade - Run 151



Nacelle Configuration: Single 1-40-10C
 Nacelle Incidence Angle: 3°
 Pairing: w/o
 Nacelle Exit Plate: 1.00
 $\beta = 0$

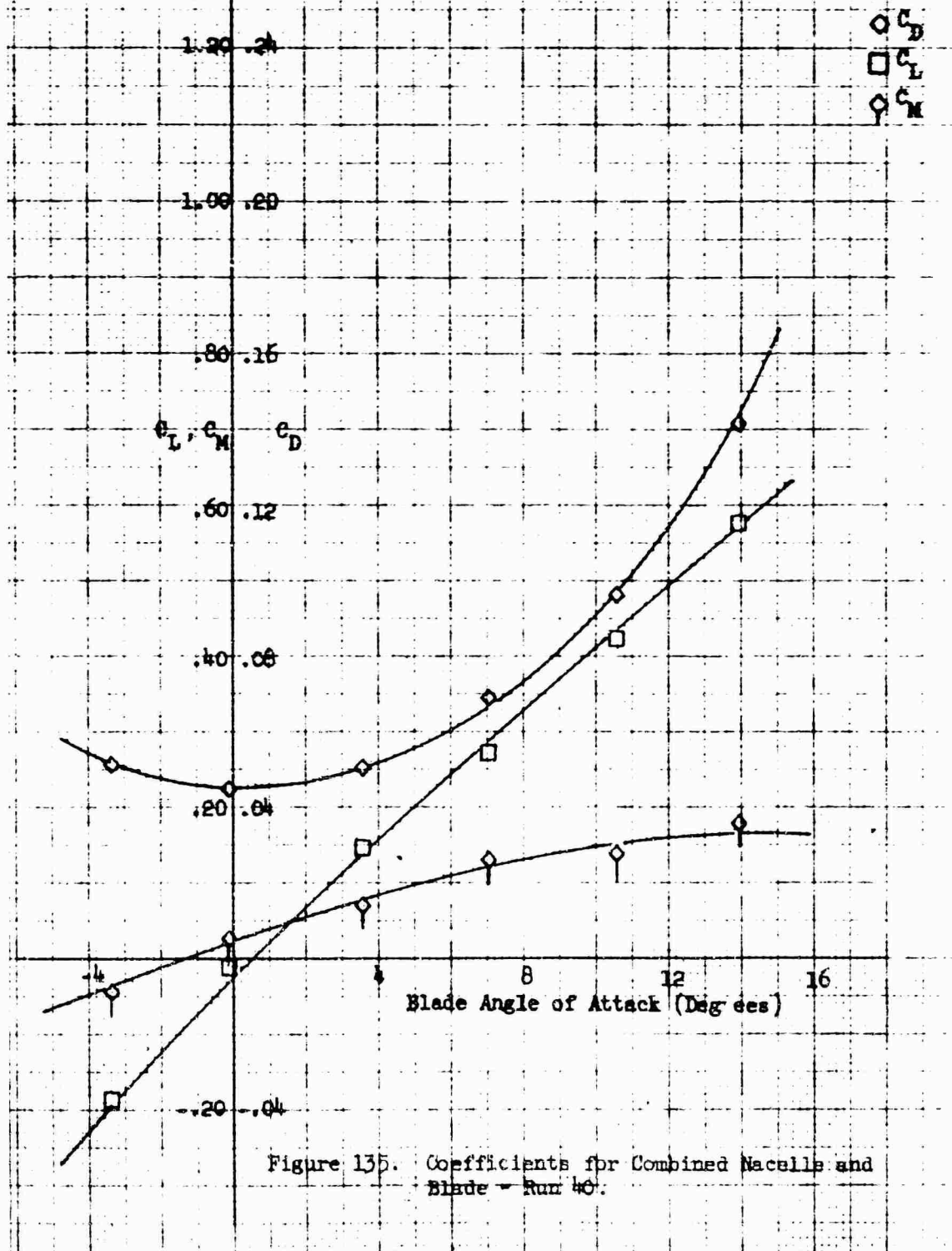
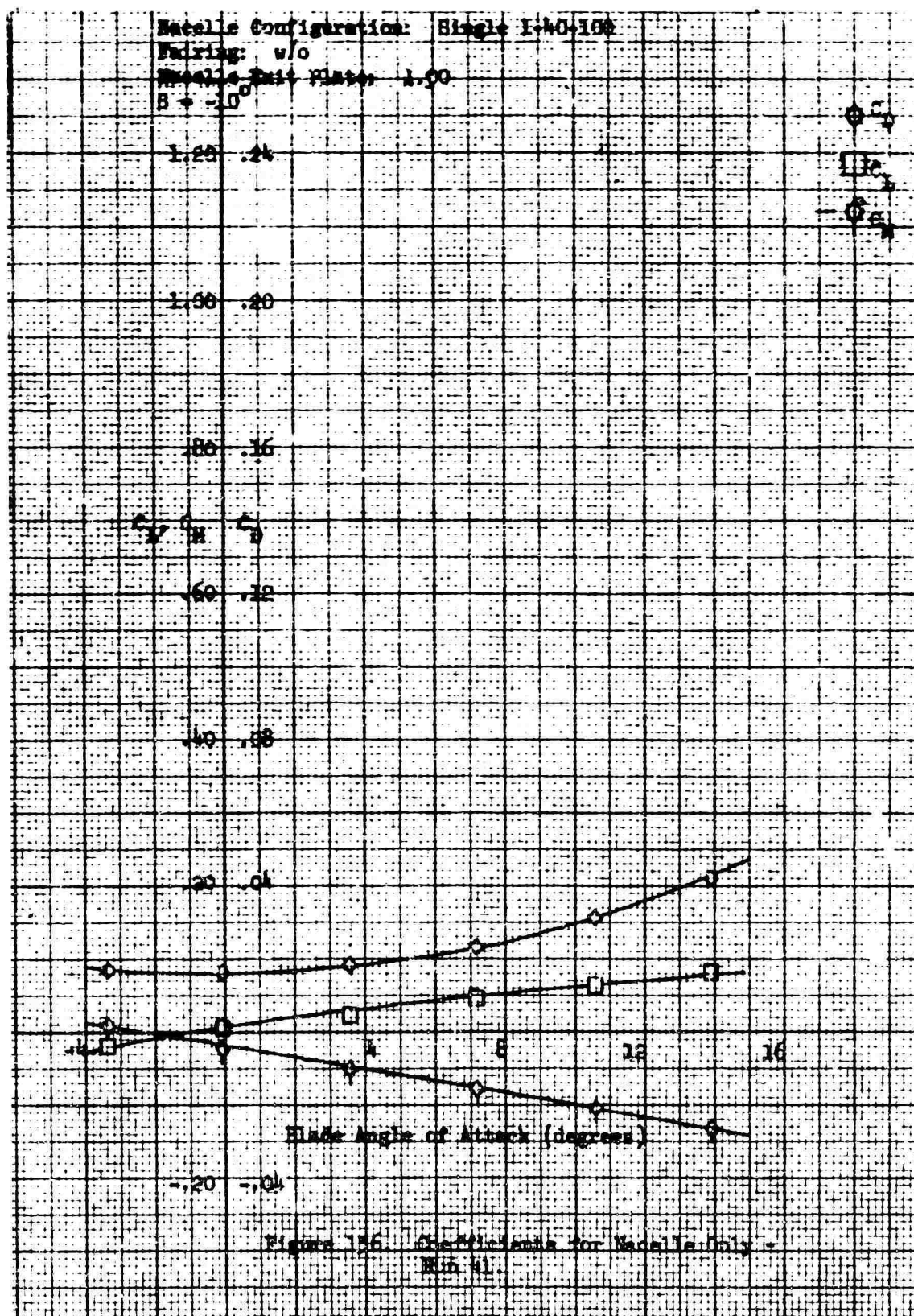
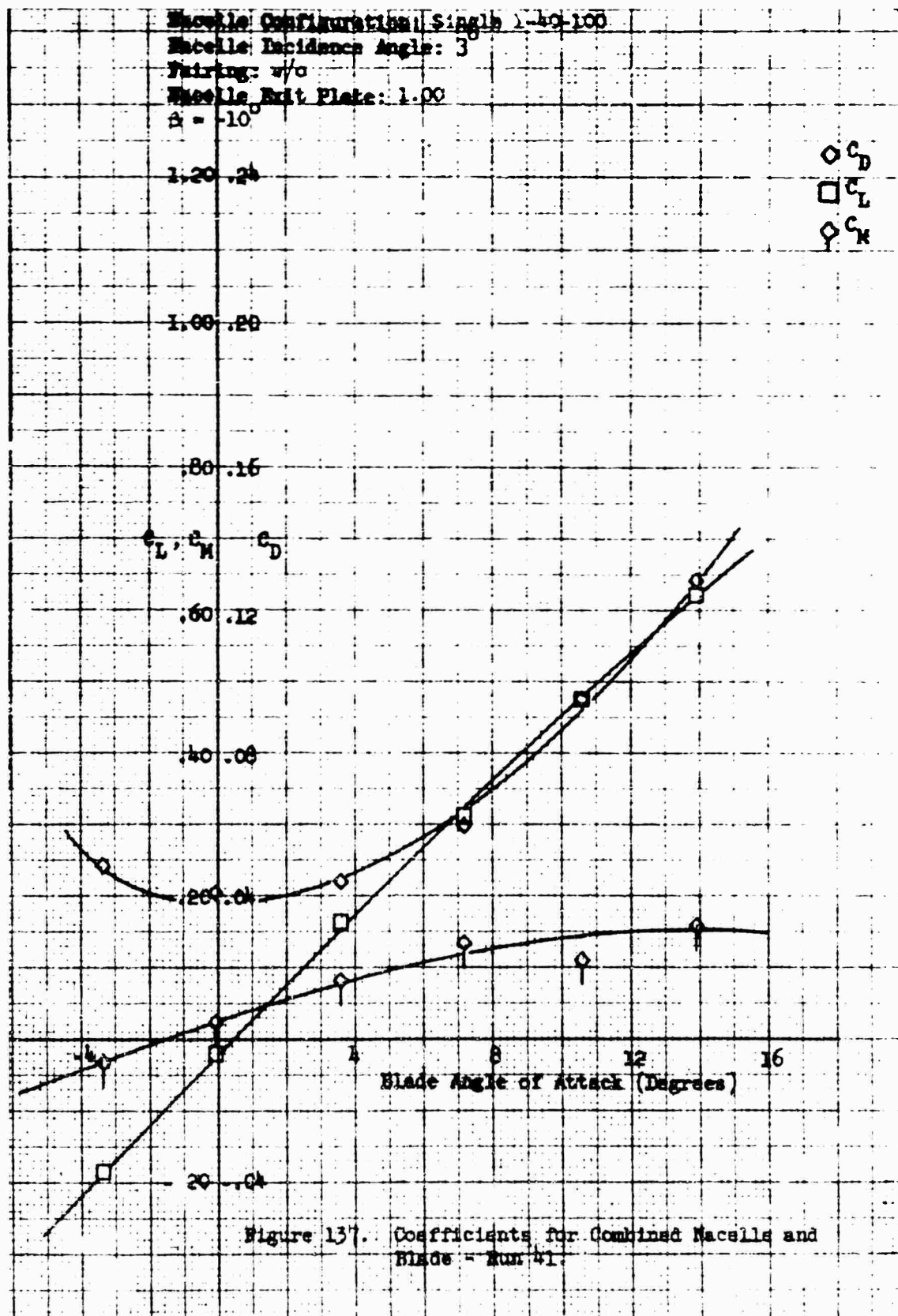
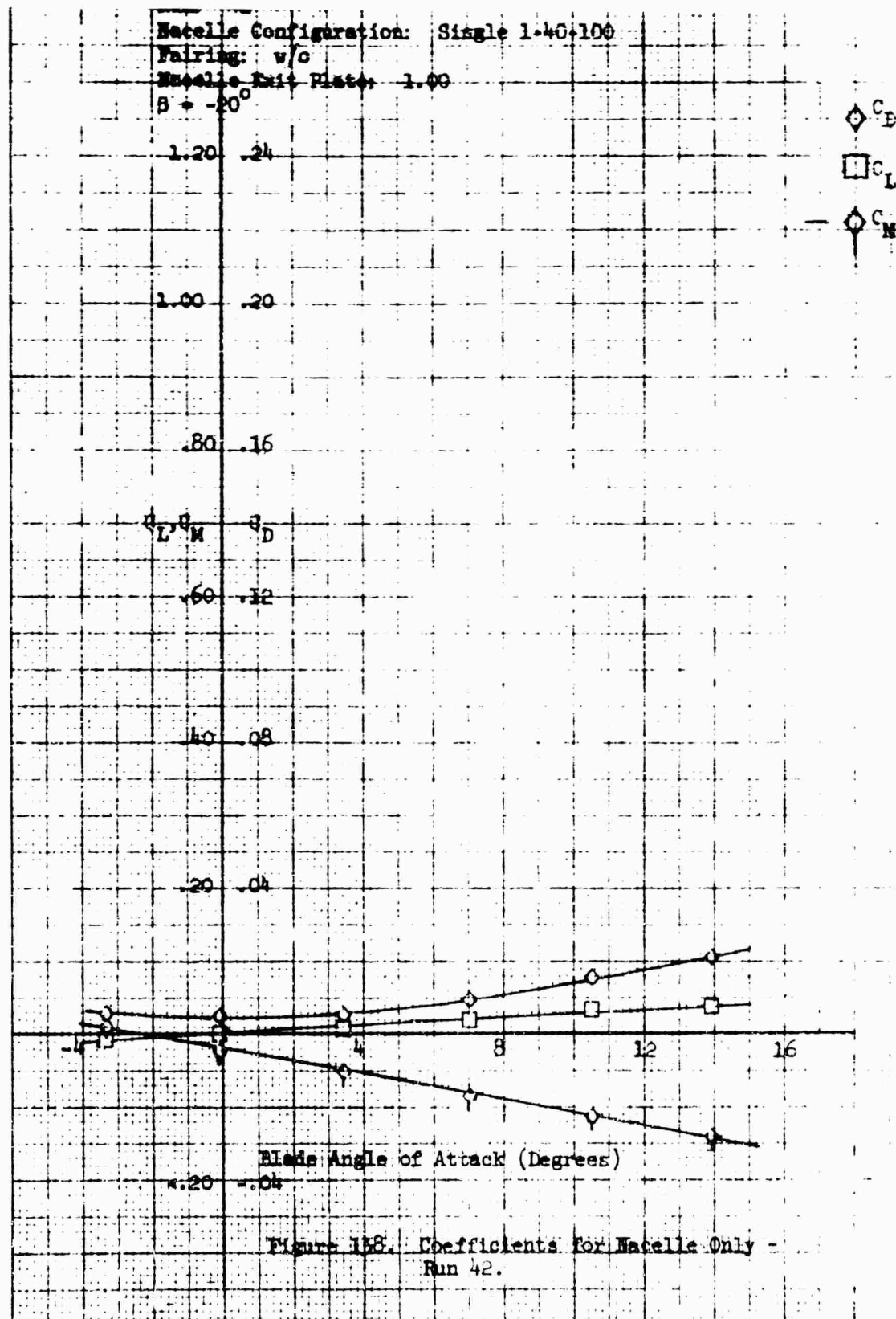
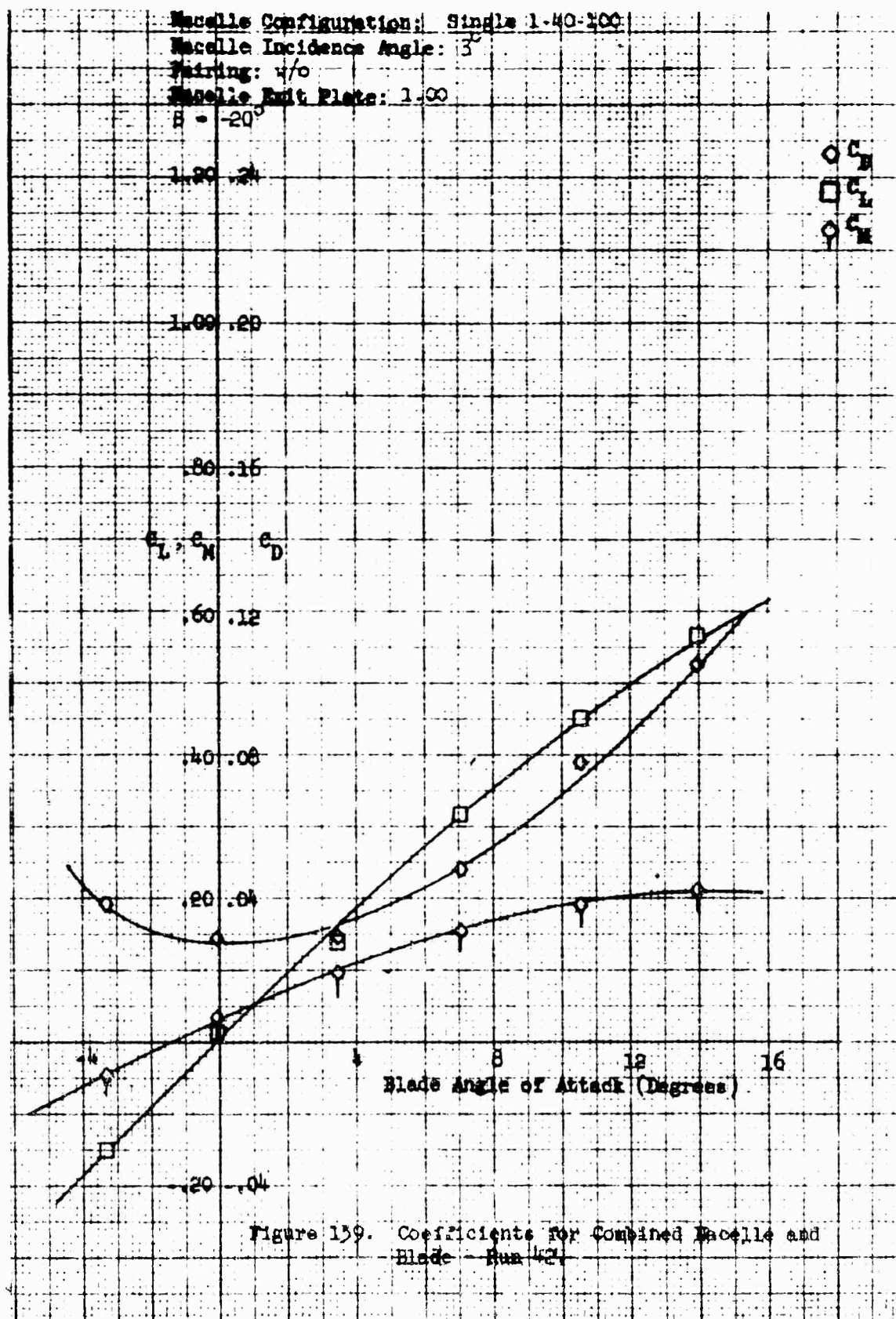


Figure 135. Coefficients for Combined Nacelle and
 Blade - Run 40.









Nacelle Configuration: Single 1-40-100

FAIRING: w/o

Nacelle Exit Plate: 0

$\beta = -20^\circ$

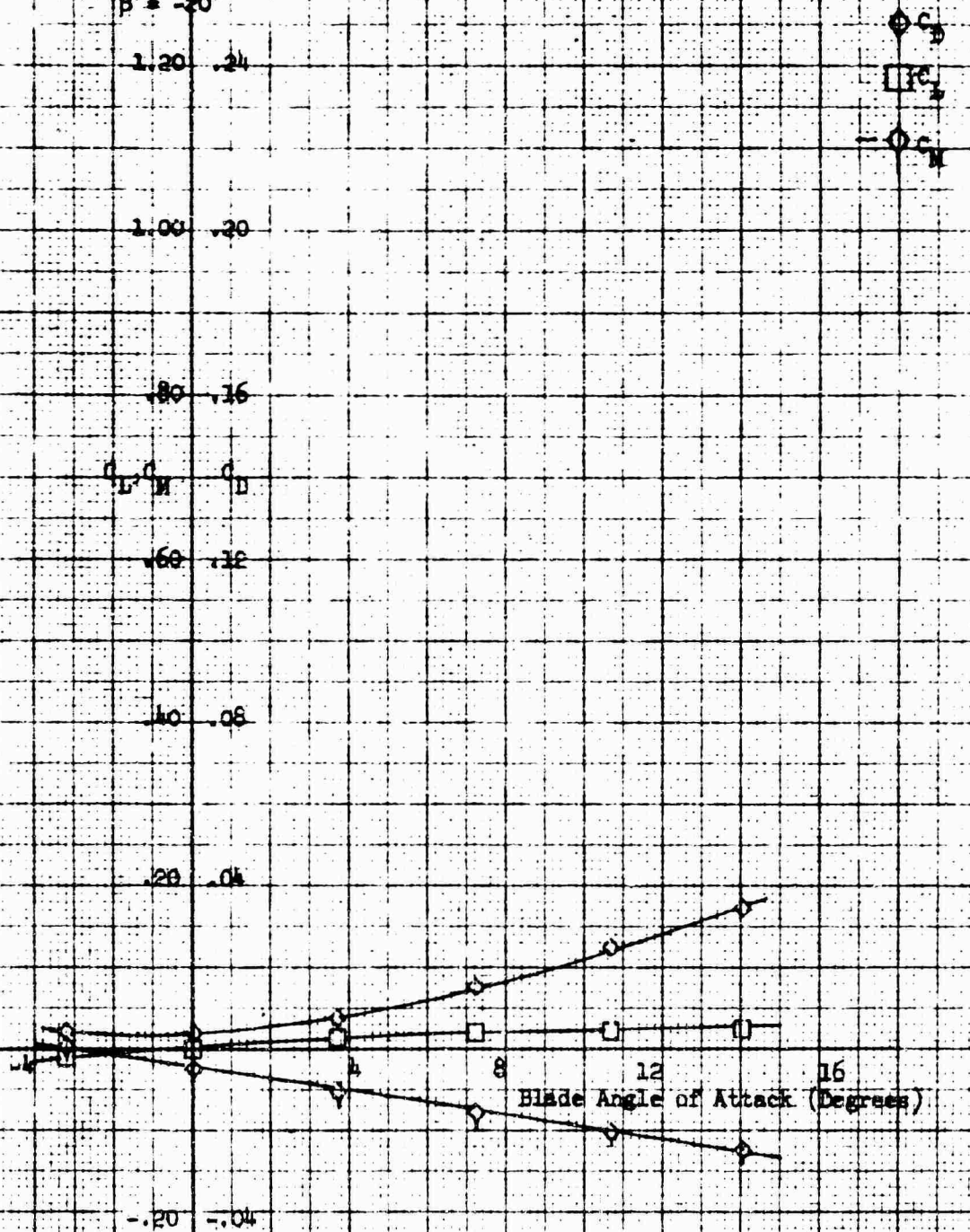


Figure 149. Coefficients for Nacelle Only - Run 43.

Blade Configuration: Single 1-40-100
 Blade Incidence Angle: 3°
 Pairing: w/o
 Blade Exit Plate: 0
 $\alpha = 120^\circ$

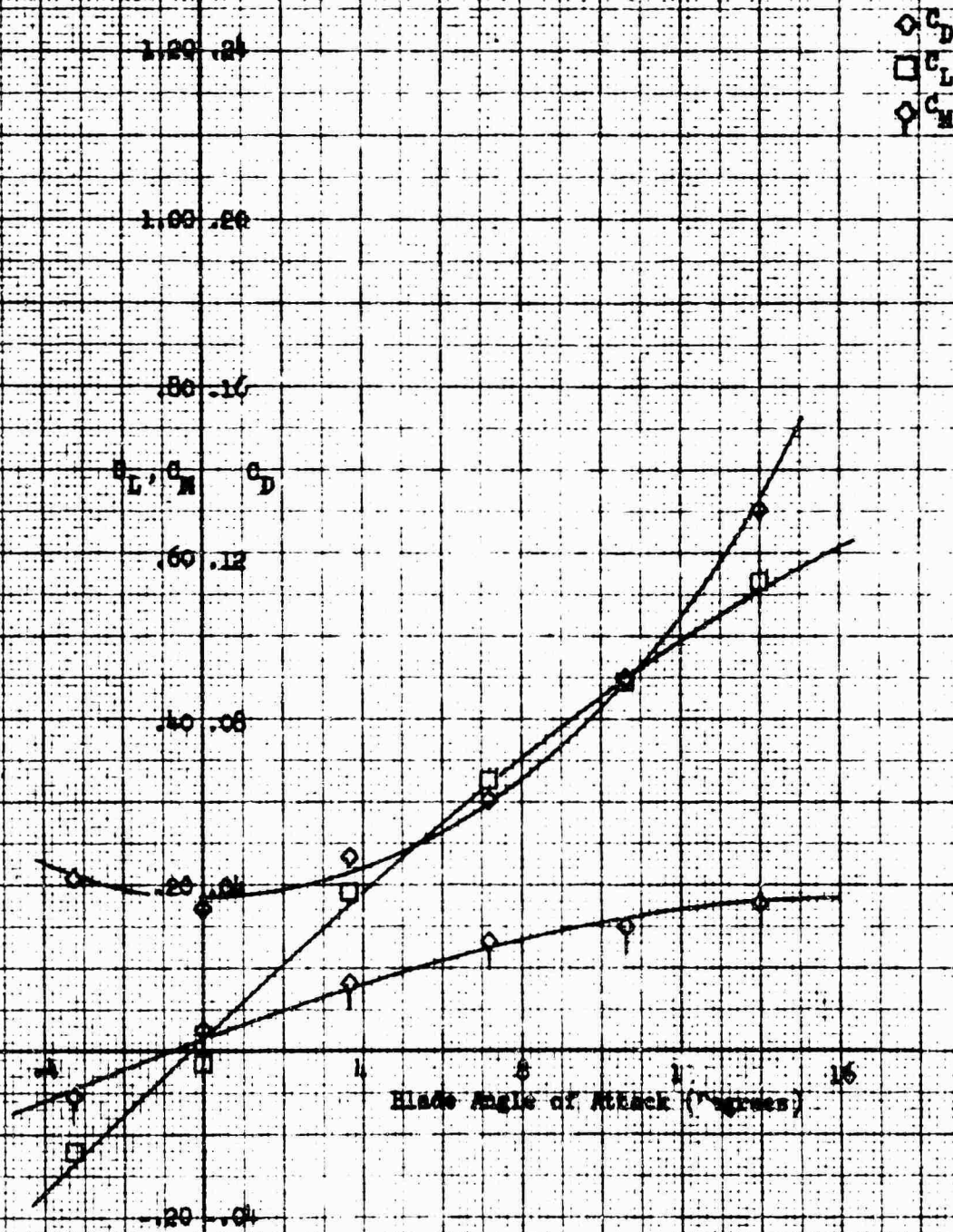
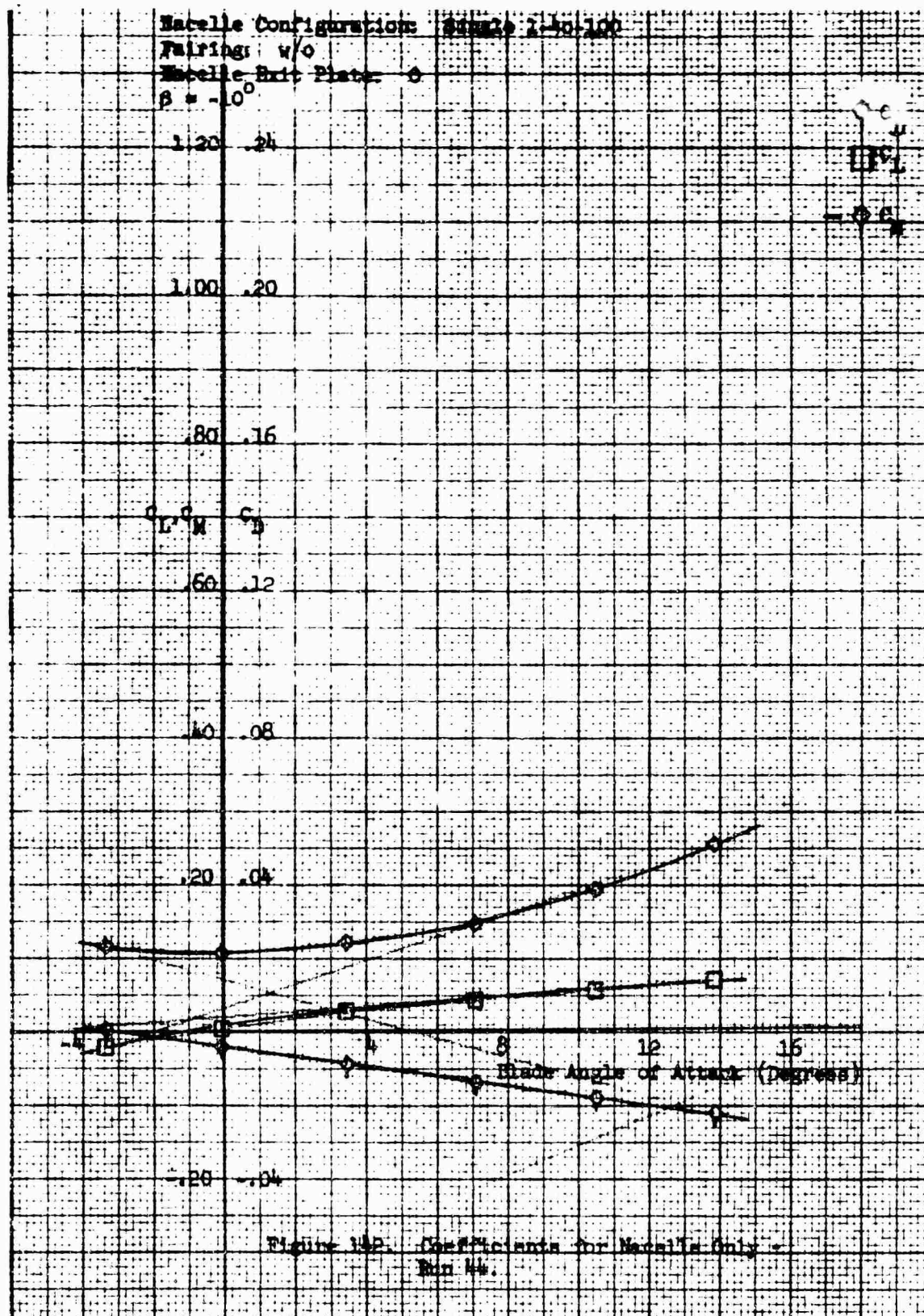
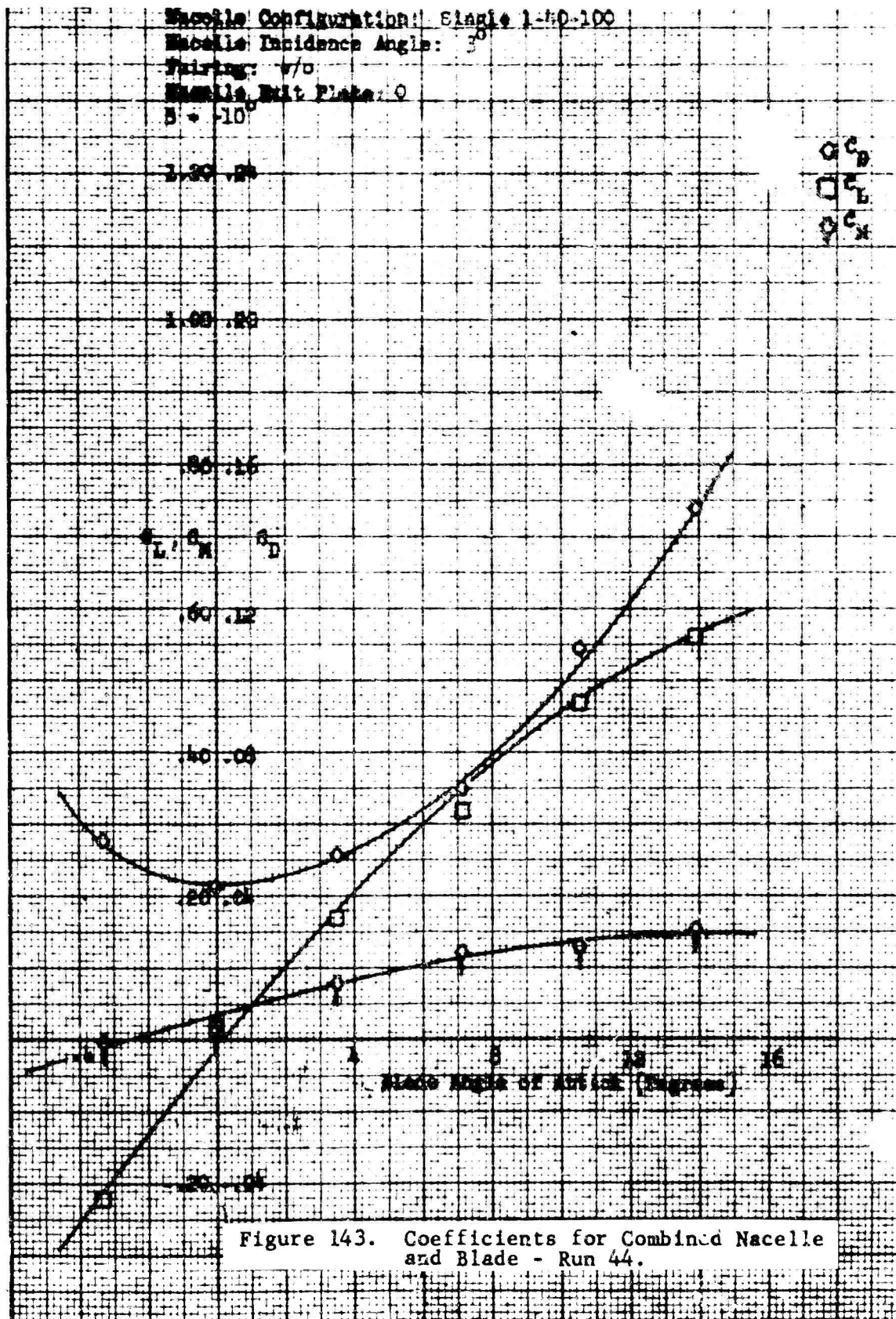
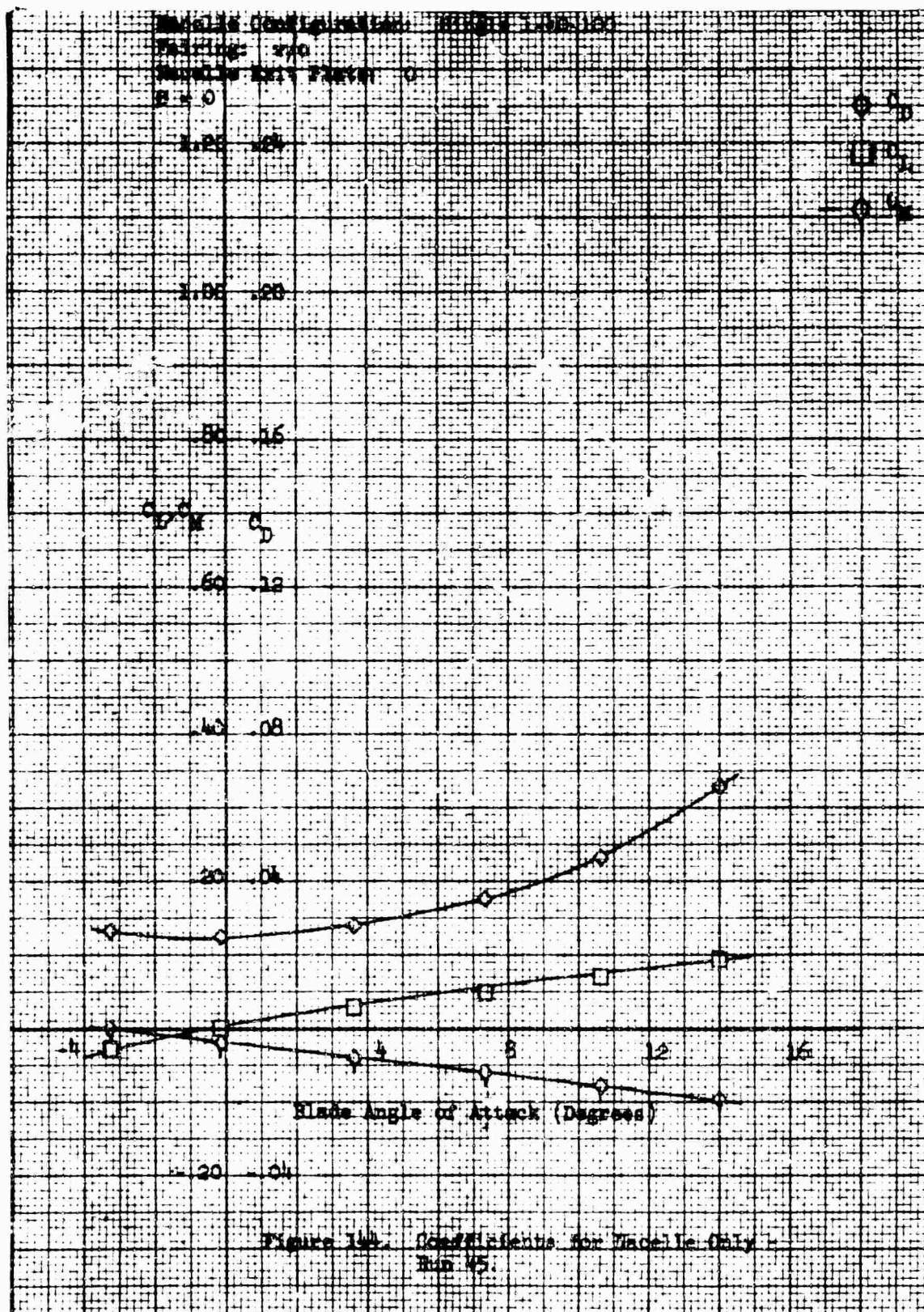


Figure 141. Coefficients for Combined Blade and Blade - Run 11.







Nacelle Configuration: Single L-40-100
 Nacelle Incidence Angle: 3
 Fairing: w/o
 Nacelle Exit Plate: 0
 $\beta = 0$

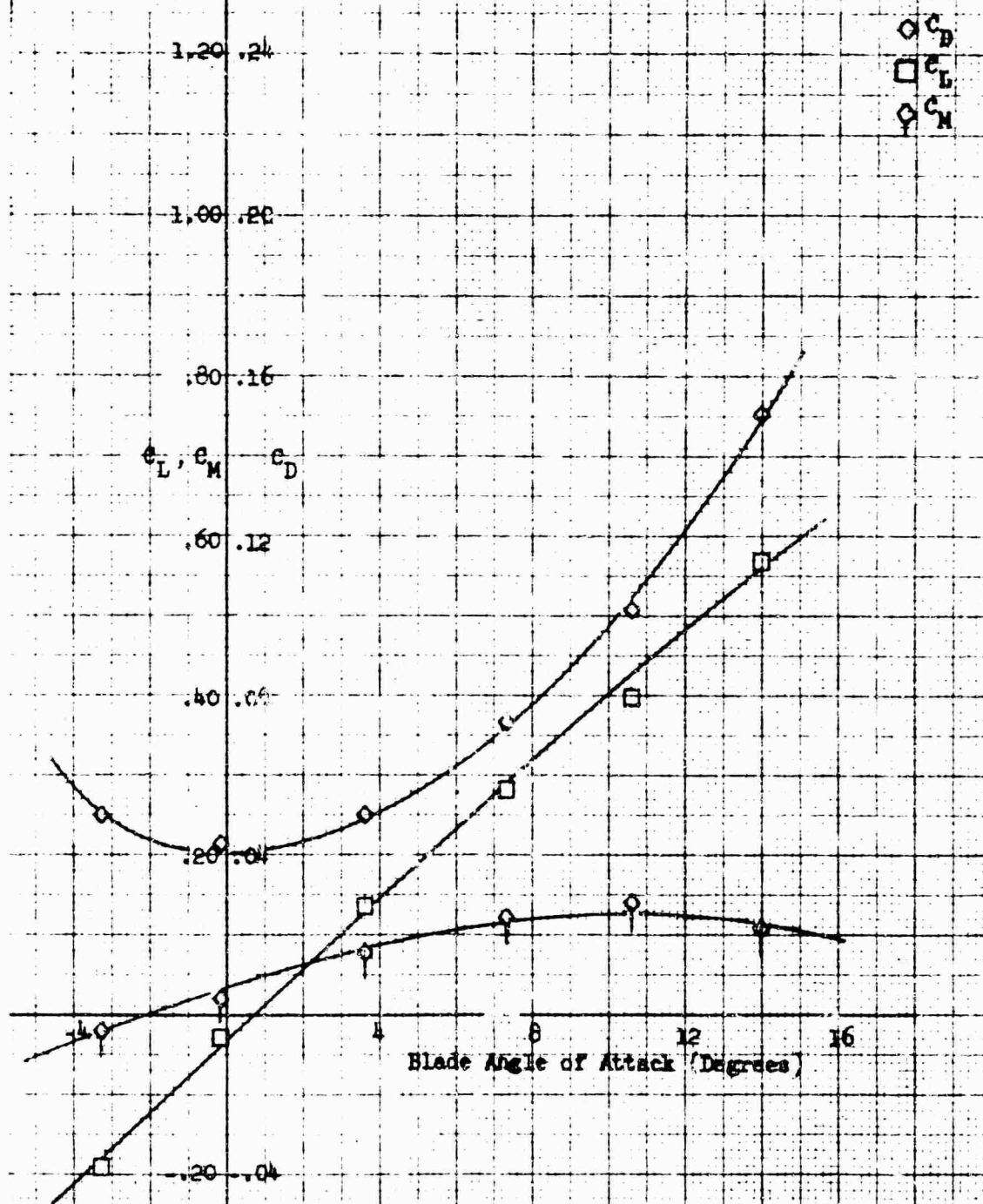
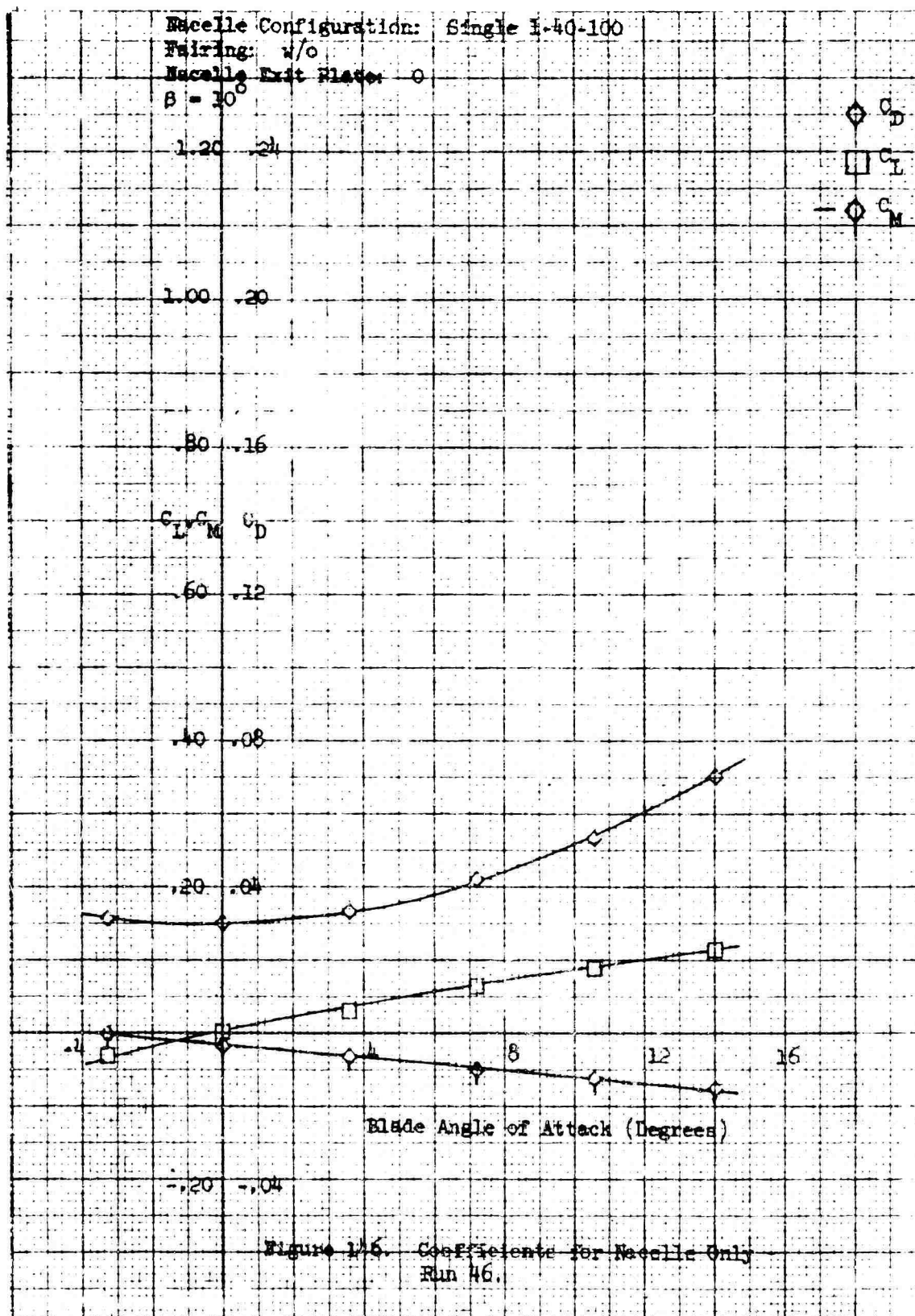


Figure 145. Coefficients for Combined Nacelle and Blade - Run 45.



Nacelle Configuration: Single 1-40-100
 Nacelle Incidence Angle: 3°
 Fairing: w/o
 Nacelle Exit Plate: 0
 $\beta = 10^\circ$

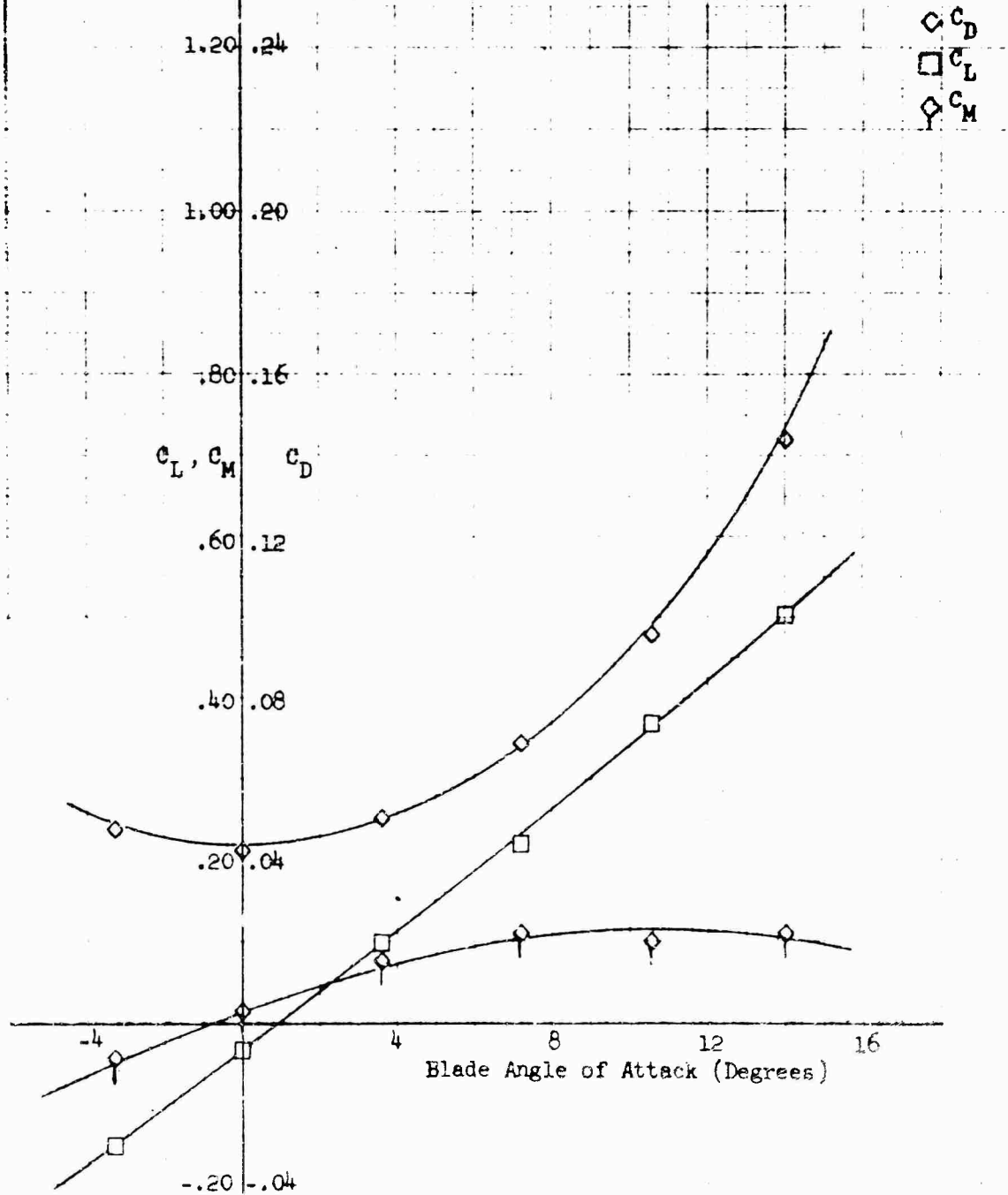


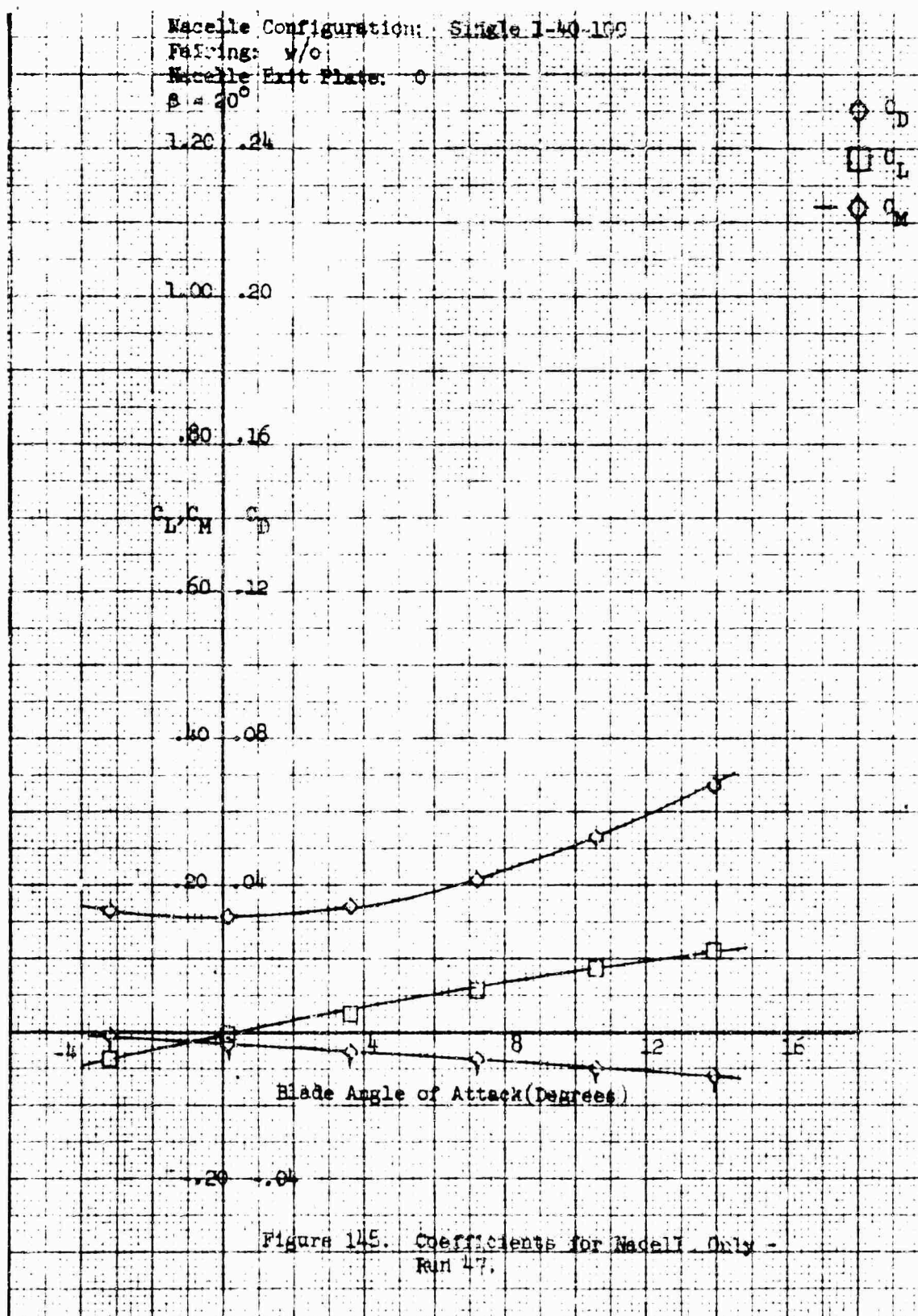
Figure 147. Coefficients for Combined Nacelle and Blade - Run 46.

Wacelle Configuration: Single 1-40-100

Fairing: w/o

Wacelle Exit Plate: 0

$\beta = 20^\circ$



Nacelle Configuration: Single 1-40-100
 Nacelle Incidence Angle: 3°
 Fairing: w/o
 Nacelle Exit Plate: 0
 $\beta = 20^\circ$

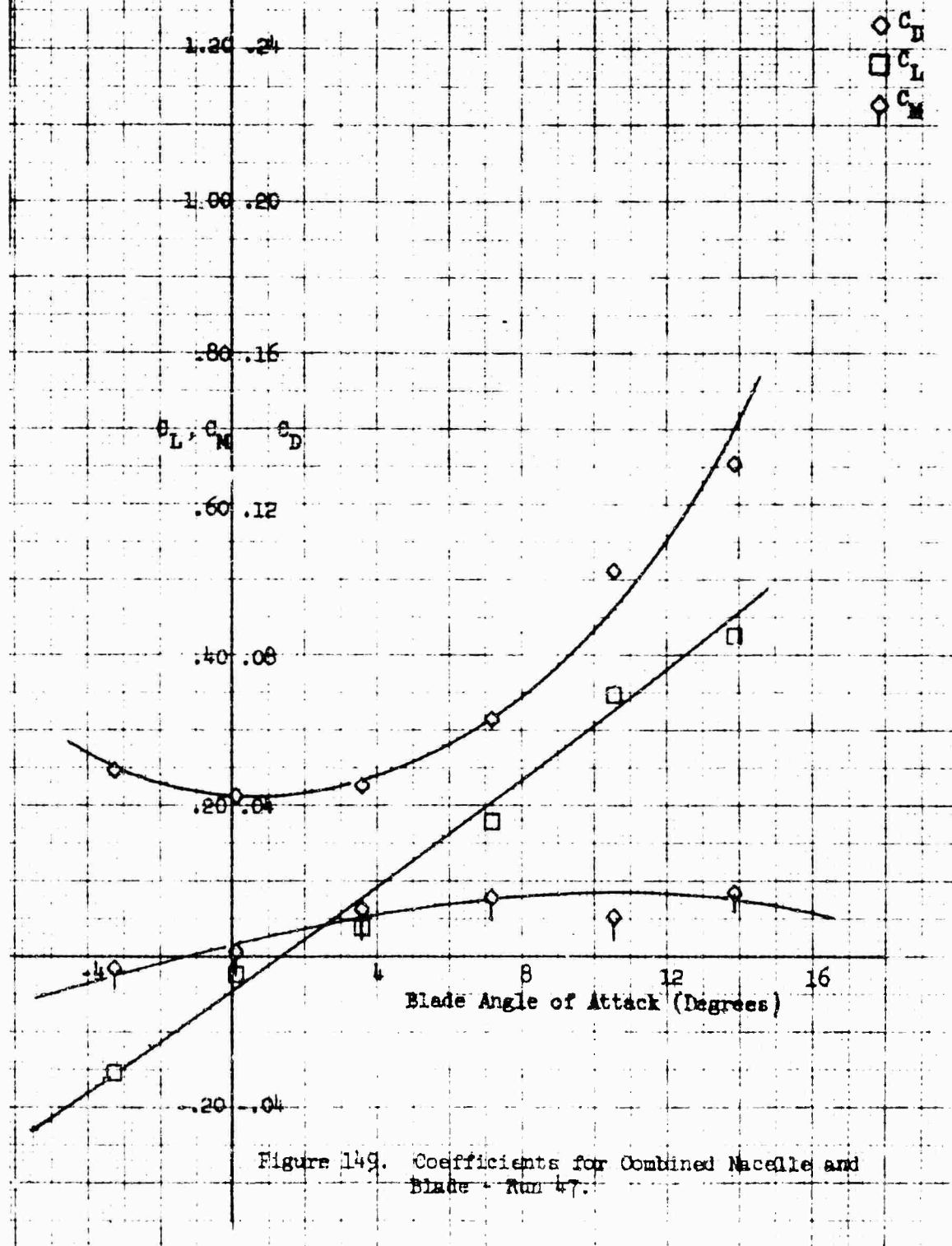


Figure 149. Coefficients for Combined Nacelle and Blade - Run 47.

Nacelle Configuration: Single 1-10-100
 Fairing: W/O
 Nacelle exit Plate: Q
 $\beta = 20^\circ$

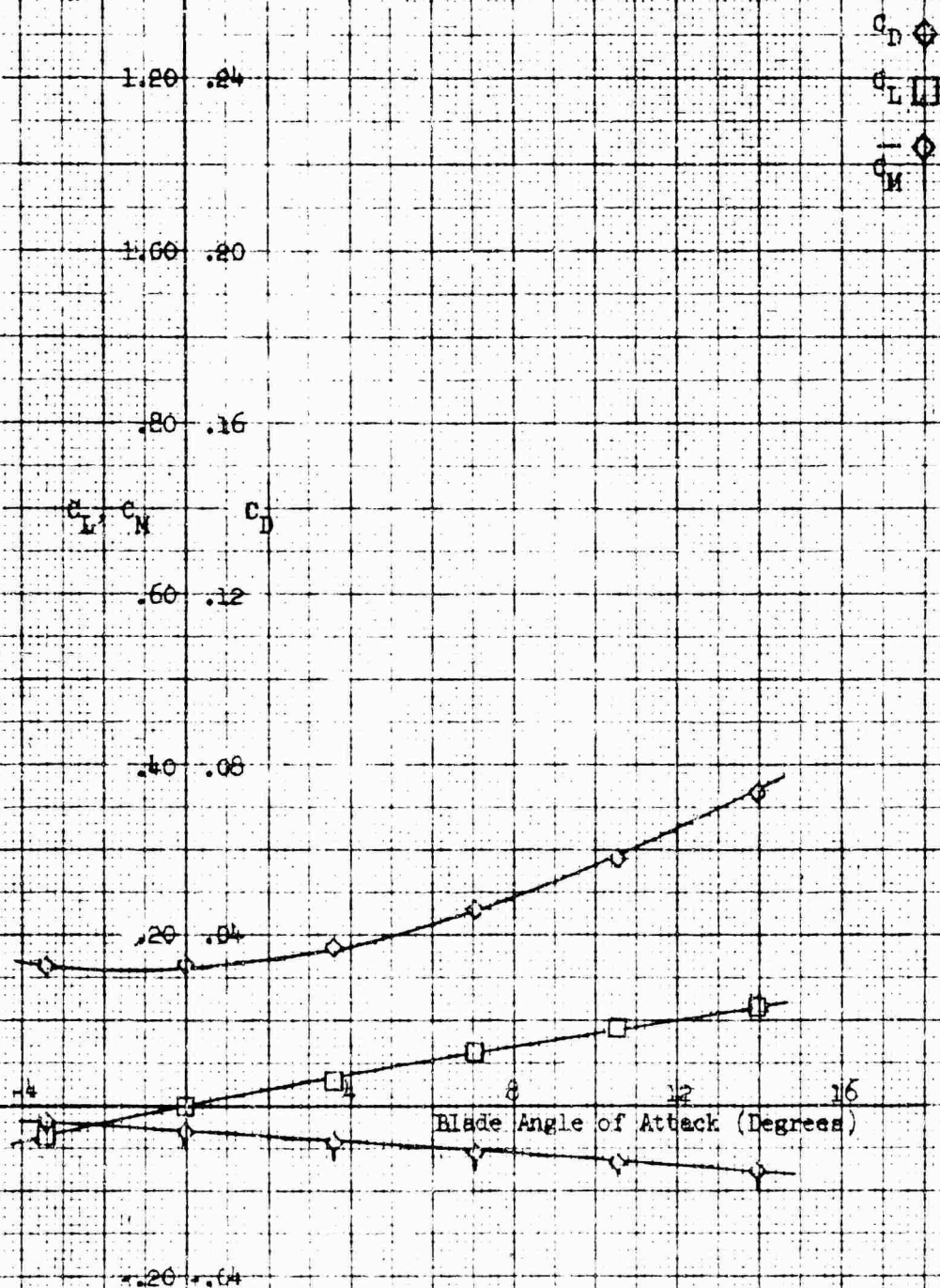


Figure 130. Coefficients for Nacelle Only -
 Run 48.

Nacelle Configuration: Single 1-40-100
 Nacelle Incidence Angle: 6°
 Fairing: w/o
 Nacelle Exit Plate: 0
 $\theta = 20^\circ$

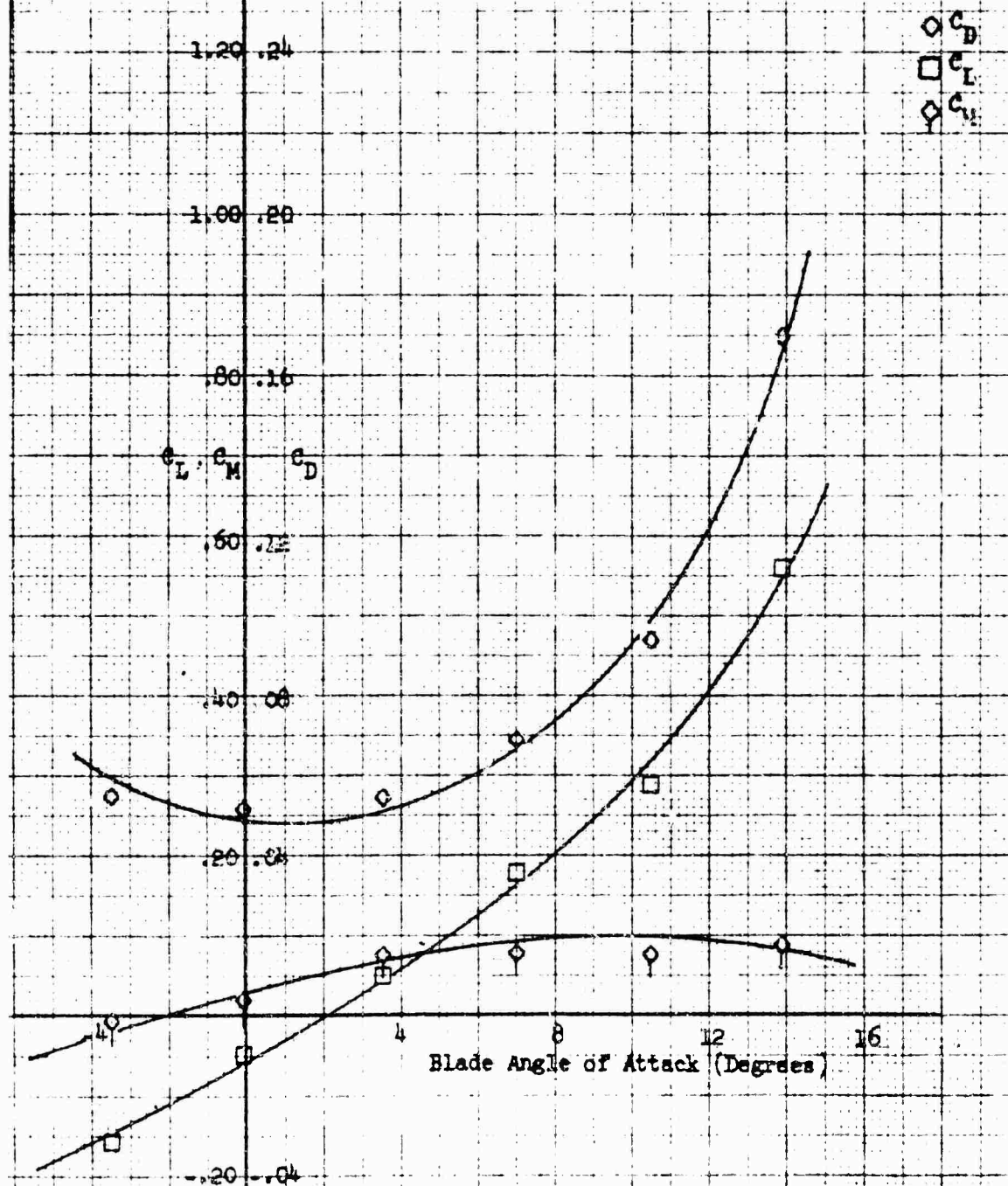


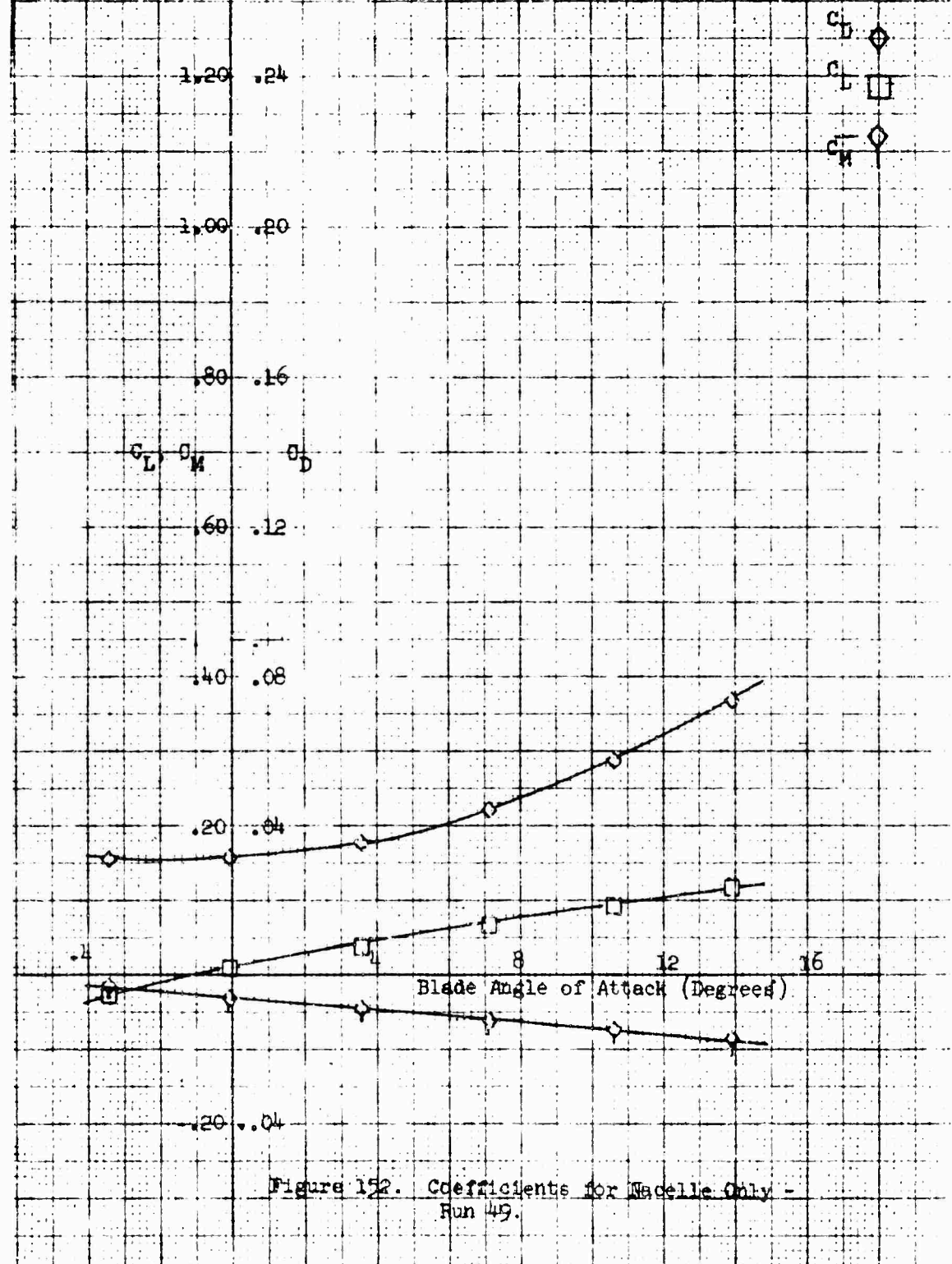
Figure 151. Coefficients for Combined Nacelle and Blade - Run #8.

Nacelle Configuration: Single 1-40-100

Fairing: W/O

Nacelle Exit Plate: 0

$\beta = 10^\circ$



Nacelle Configuration: Single 140-100

Nacelle Incidence Angle: 6°

Fairing: w/o

Nacelle Exit Plate: 0

$\beta = 10^\circ$

1.20 .24

C_D
 C_L
 C_M

1.00 .20

.80 .16

C_L, C_M, C_D

.60 .12

.40 .08

.20 .04

Blade Angle of Attack (Degrees)

-.20 .04

Figure 153. Coefficients for Combined Nacelle and Blade - Run 49.

Nacelle Configuration: Blade 1-40-100
 Pairing: W/O
 Nacelle Exit Plane: 0
 $\beta = 0^\circ$

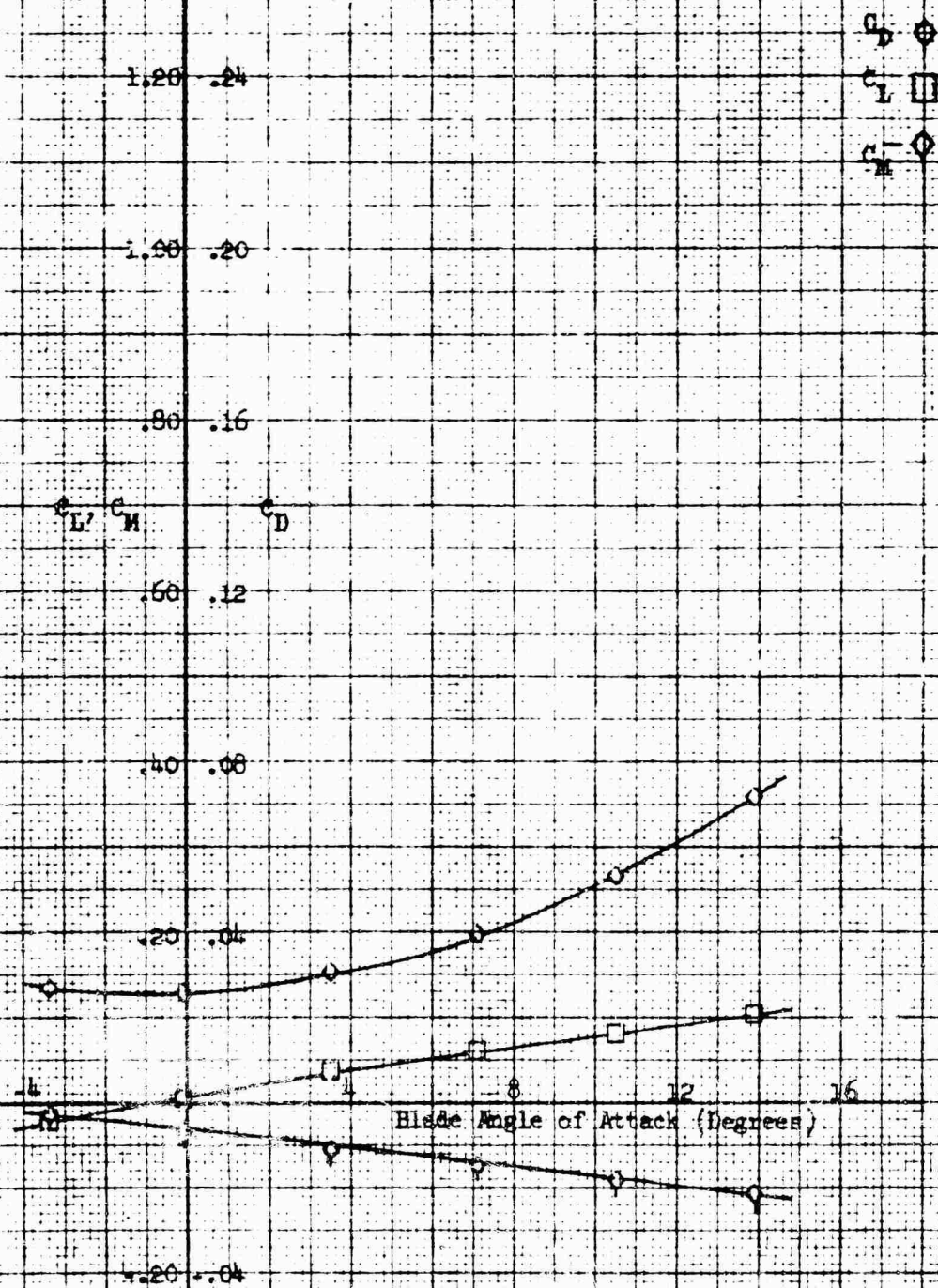


Figure 15. Coefficients for Nacelle Only -
 Run 30.

Macelle Configuration: Single 1-40-100

Macelle Incidence Angle: 6°

Fairing: w/o

Macelle Exit Plate: 0

$\beta = 0$

1.20 .24

1.00 .20

.80 .16

.60 .12

.40 .08

.20 .04

-.20 -.04

c_L, c_M, c_D

c_D
 c_L
 c_M

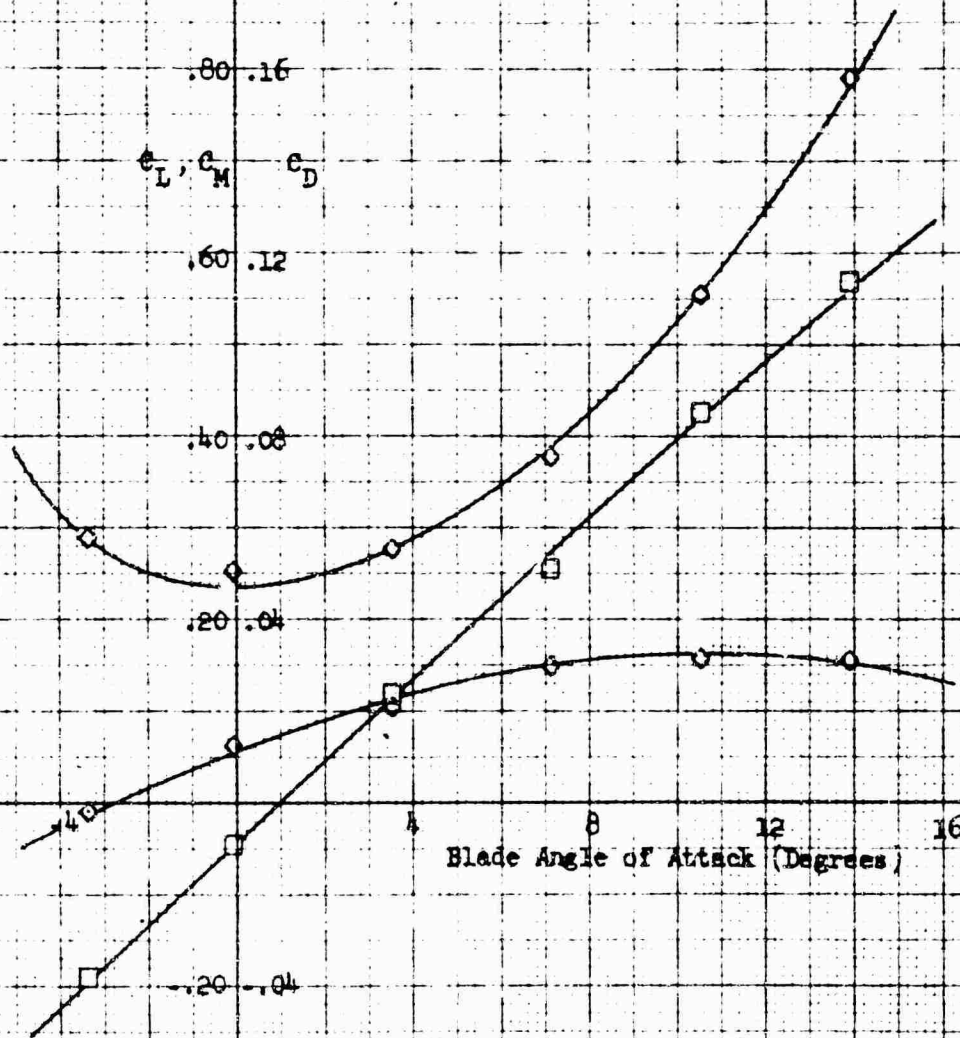


Figure 155. Coefficients for Combined Macelle and Blade - Run 30.

Nacelle Configuration: Single 1-10-100
 W/O Fairing
 Nacelle Exit Plate: 0
 $\beta = -10^\circ$

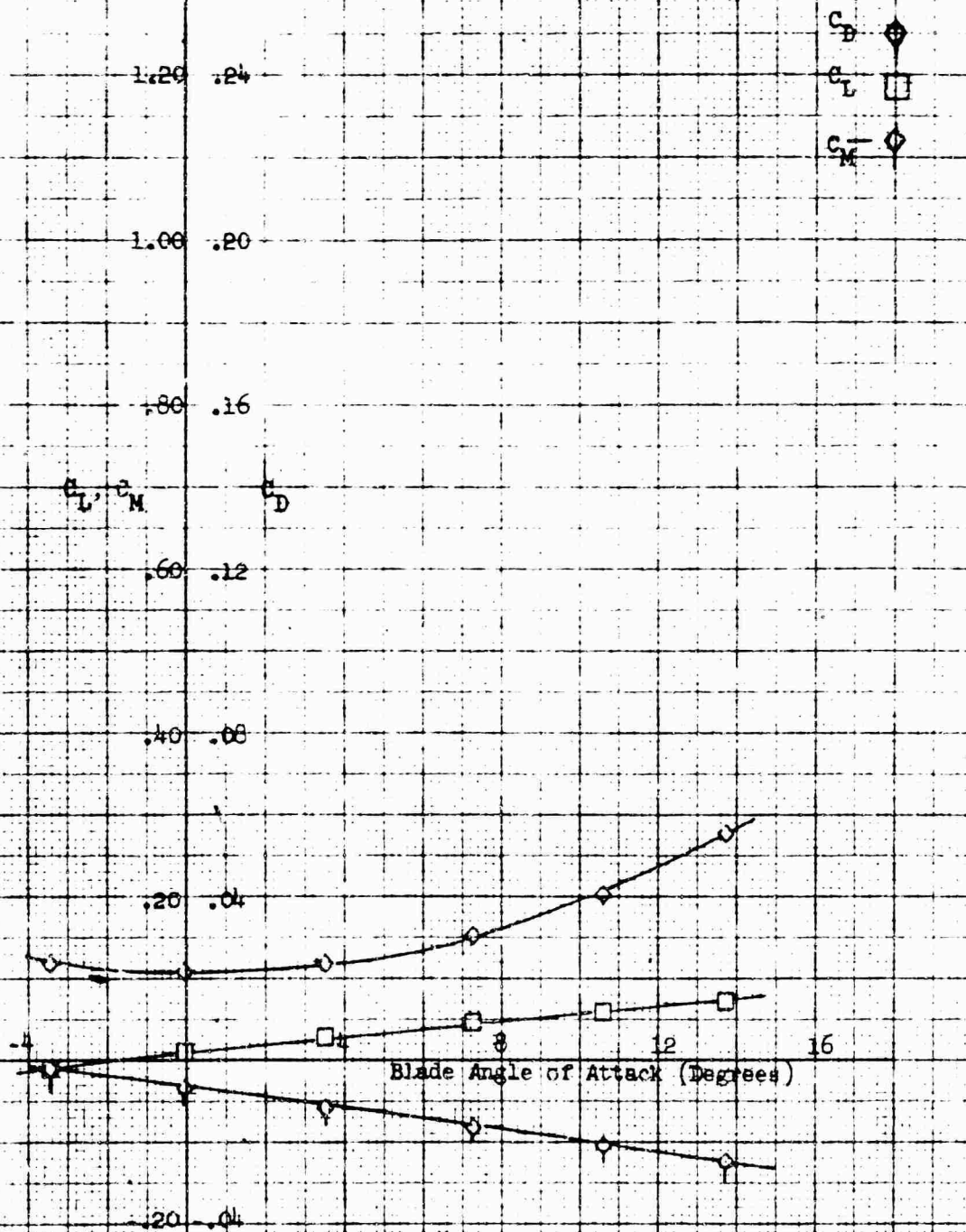
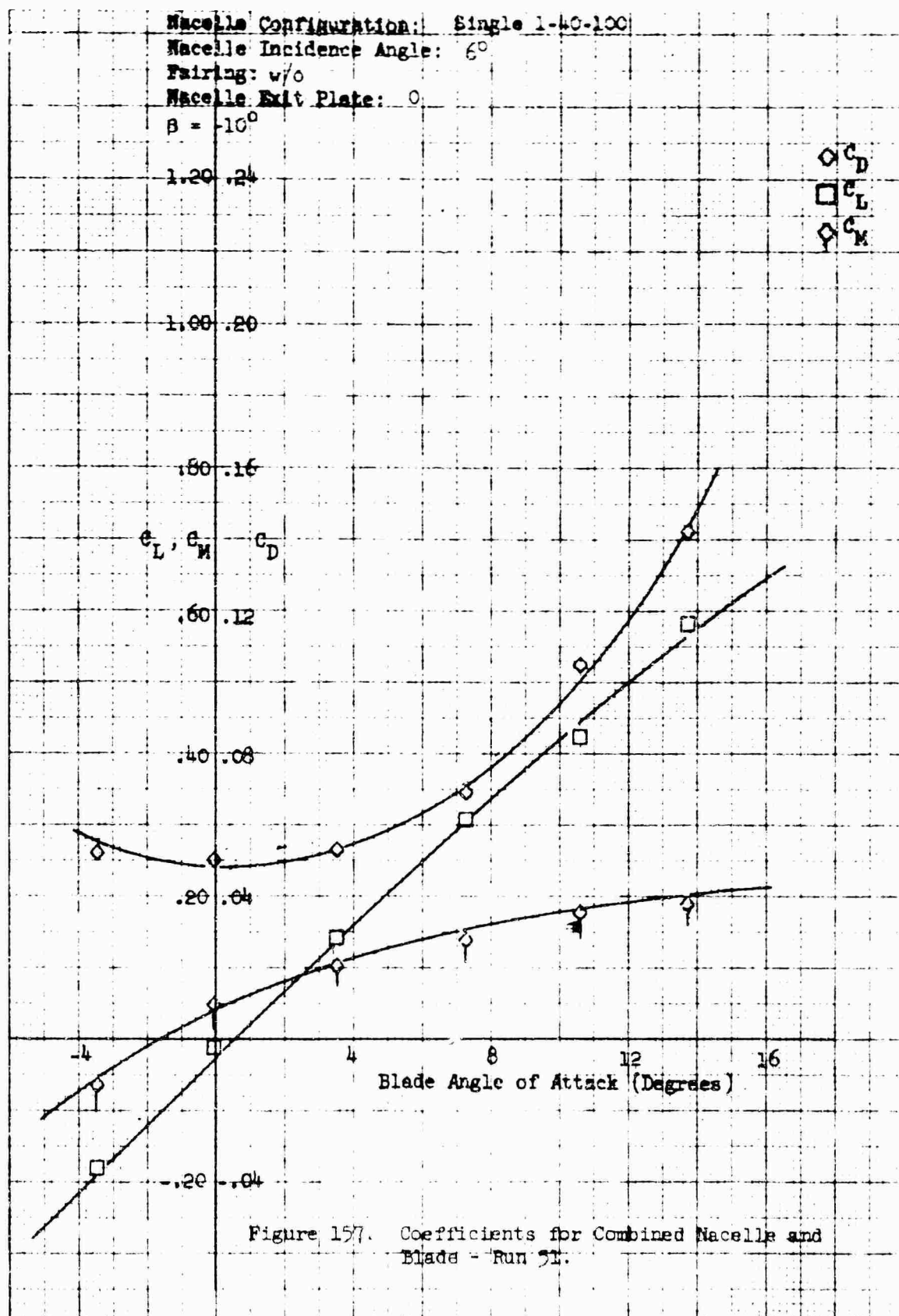


Figure 136. Coefficients for Nacelle Only -
 Run 51.



Nacelle Configuration: Single 1-4C-100
 Pairing: W/O
 Nacelle Exit Plate: 0
 $\beta = -20^\circ$

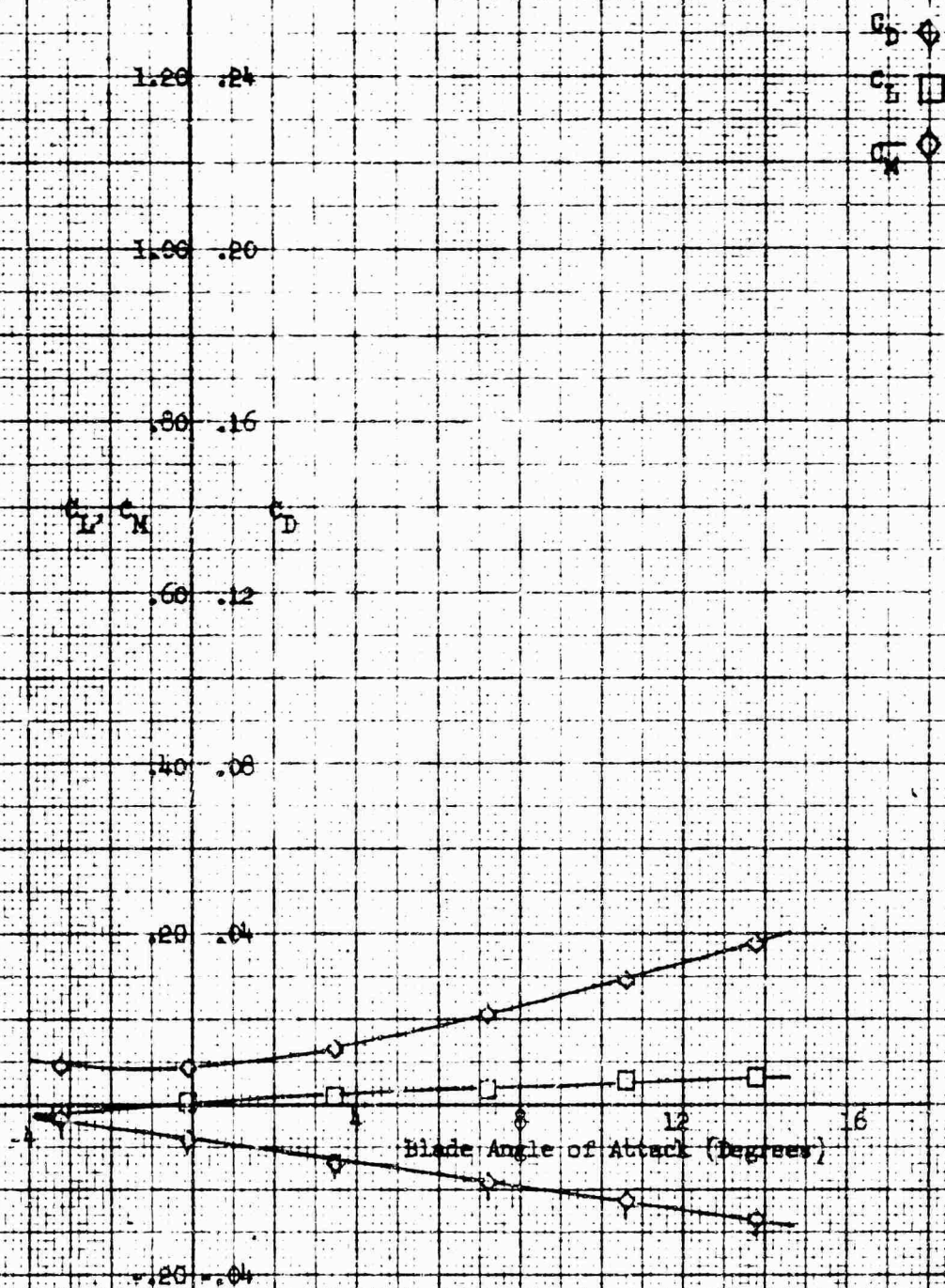
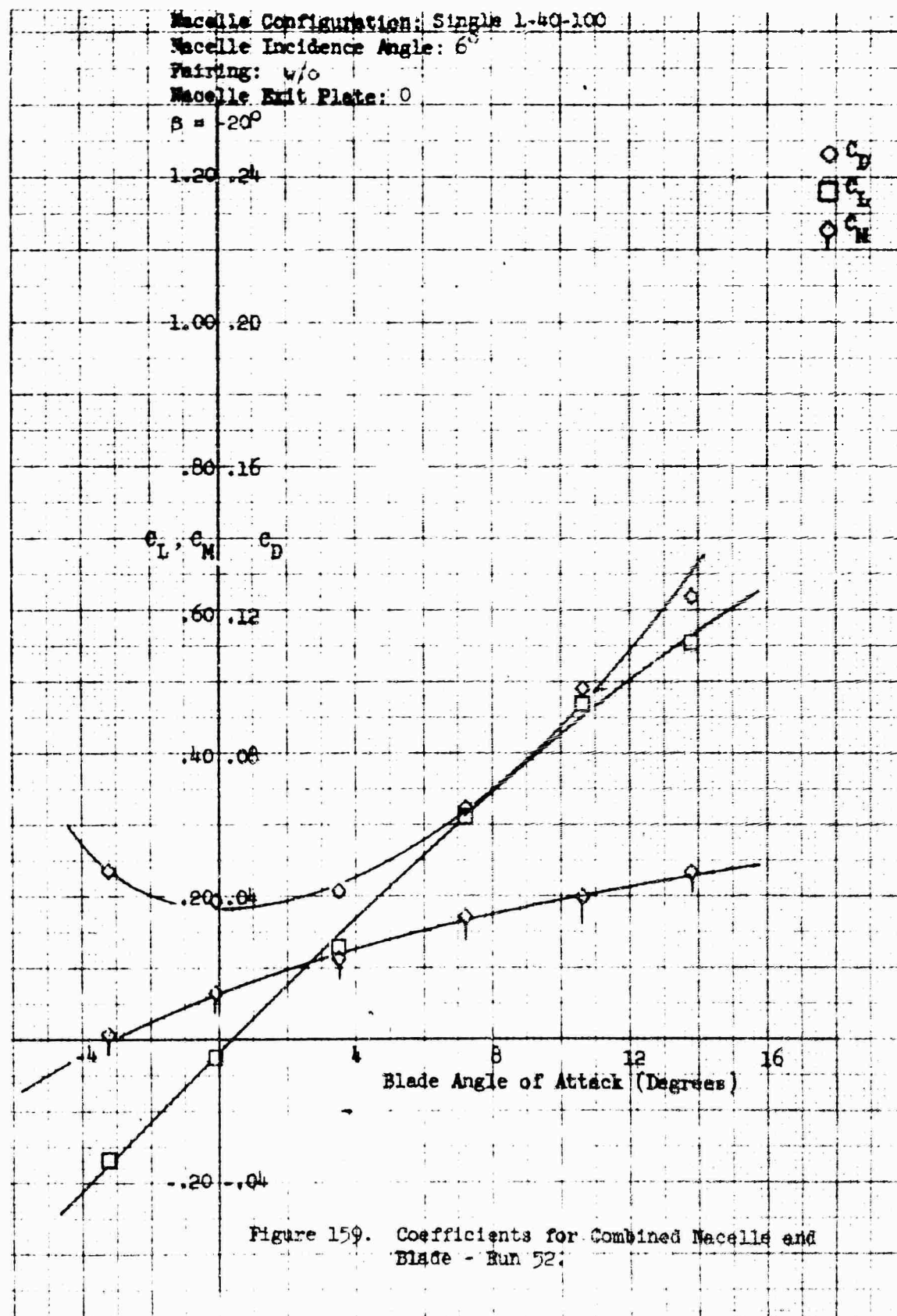


Figure 158. Coefficients for Nacelle Only -
 Run 52.



Nacelle Configuration: Single 1-40-100
 Pairing: W/O
 Nacelle Exit Plate: 1.00
 $\beta = -20^\circ$

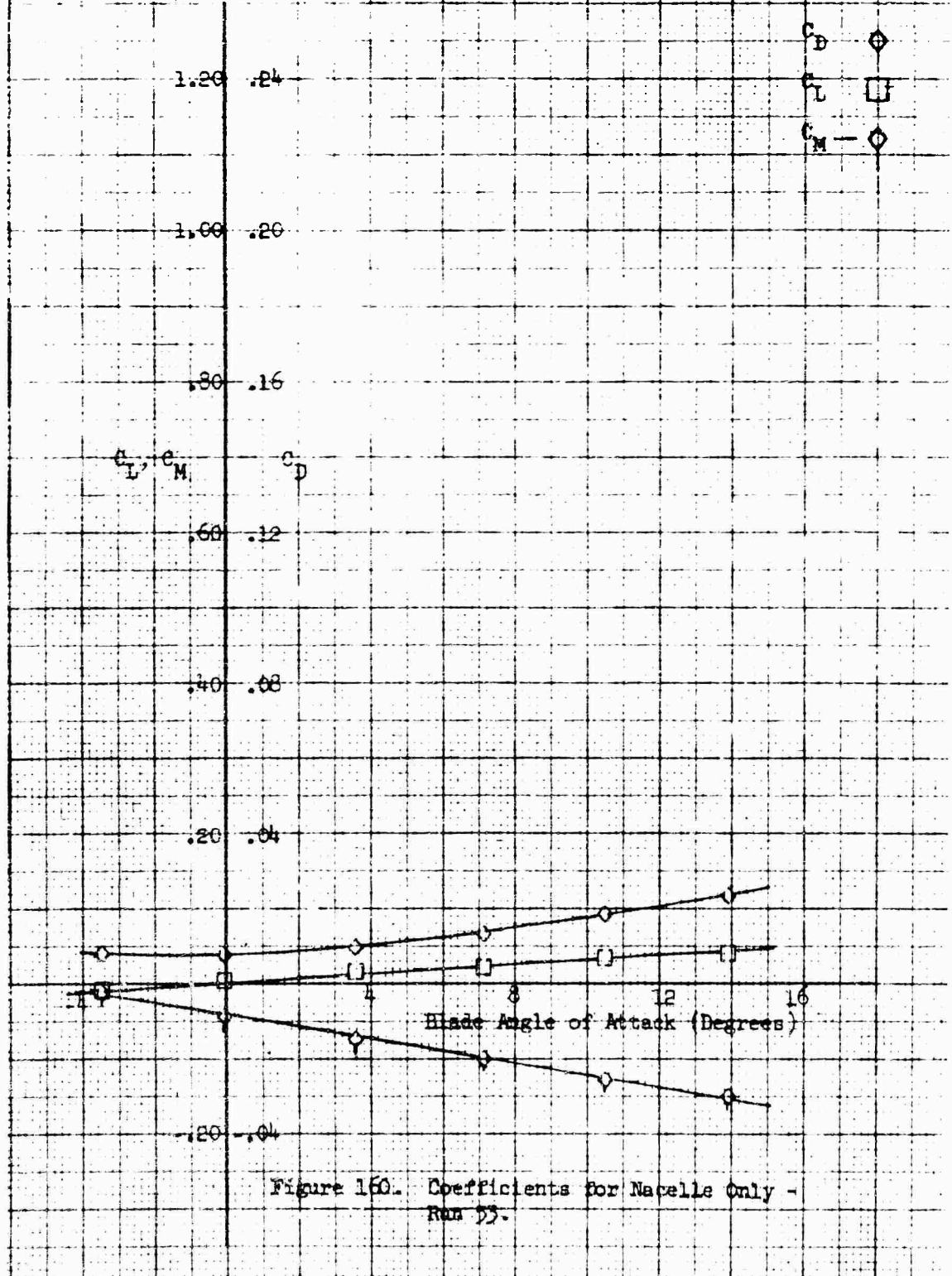


Figure 160. Coefficients for Nacelle Only - Run 23.

Macelle Configuration: Single 1-40-100

Macelle Incidence Angle: 5°

Pairing: w/o

Macelle Exit Plate: 1.00

$\beta = -20^\circ$

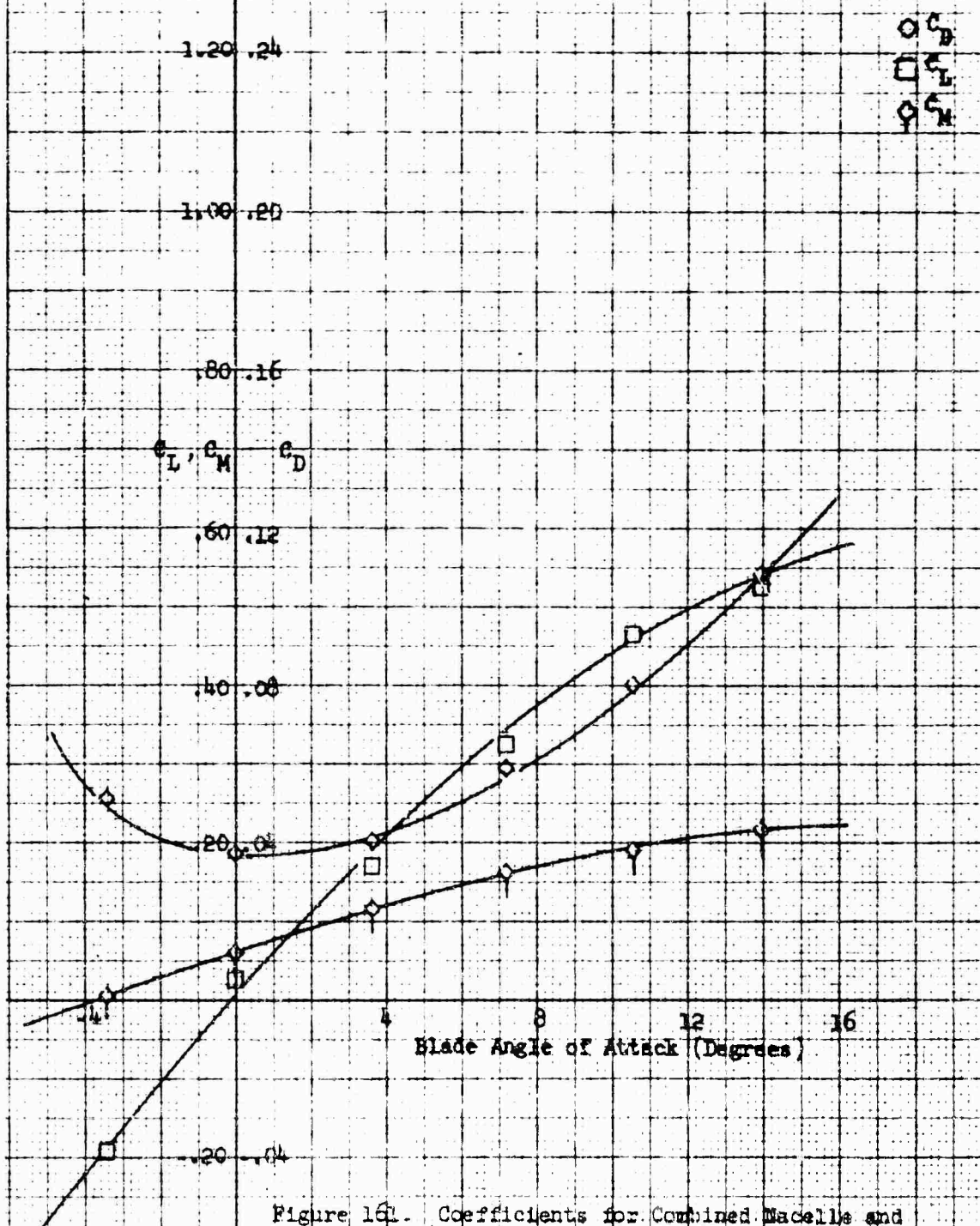


Figure 161. Coefficients for Combined Macelle and Blade - Run 33.

Blade Configuration: Single 1-10-100
 Setting: V/8
 Blade Exit Plane: 1.00
 $\beta = -10^\circ$

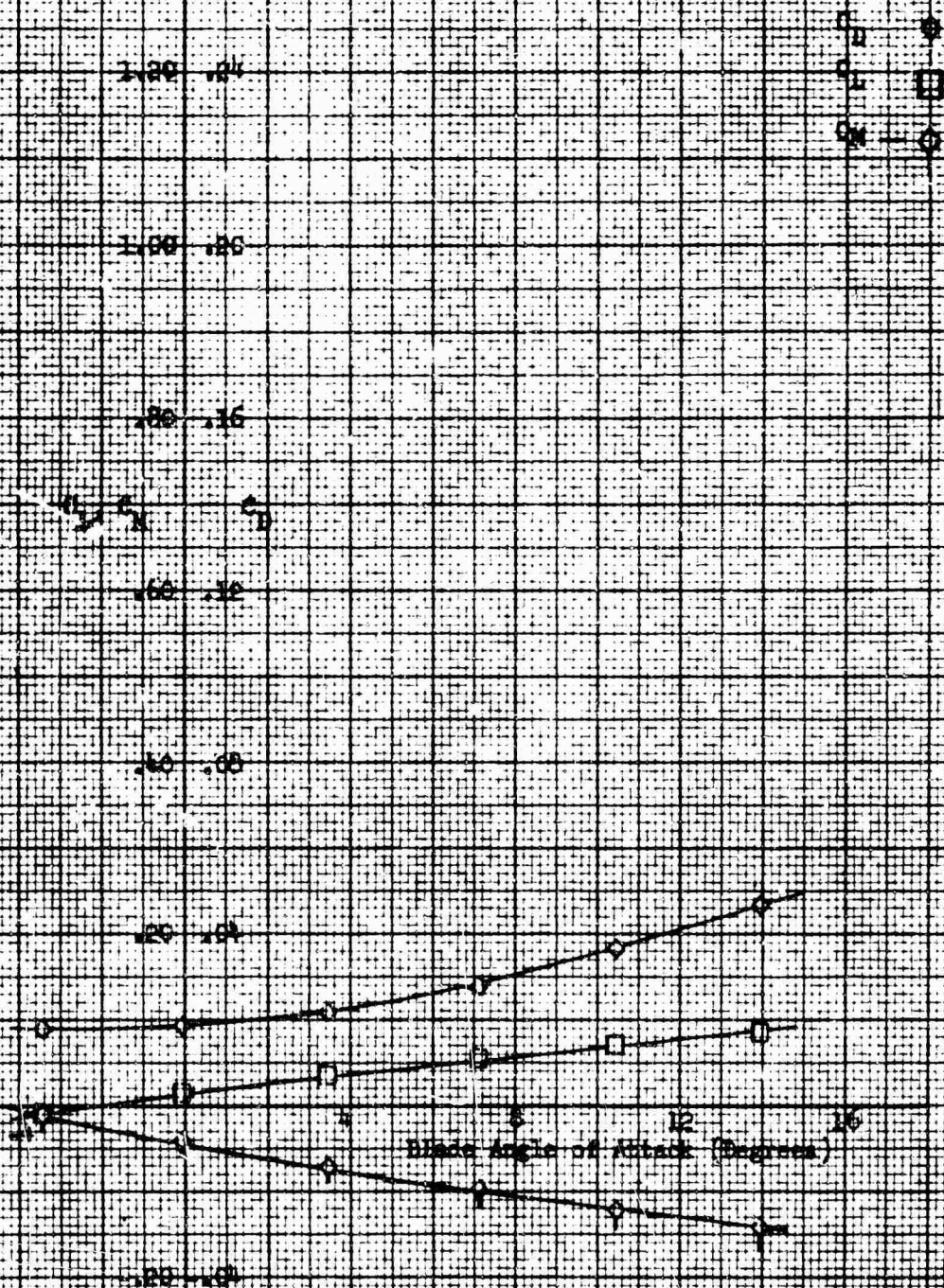


Figure 102: Coefficients for Blade Only -
 Part 51

Nacelle Configuration: Single 1-40-100
 Nacelle Incidence Angle: 5°
 Pairing: w/o
 Nacelle Exit Plate: 1.00
 $\beta = -10^\circ$

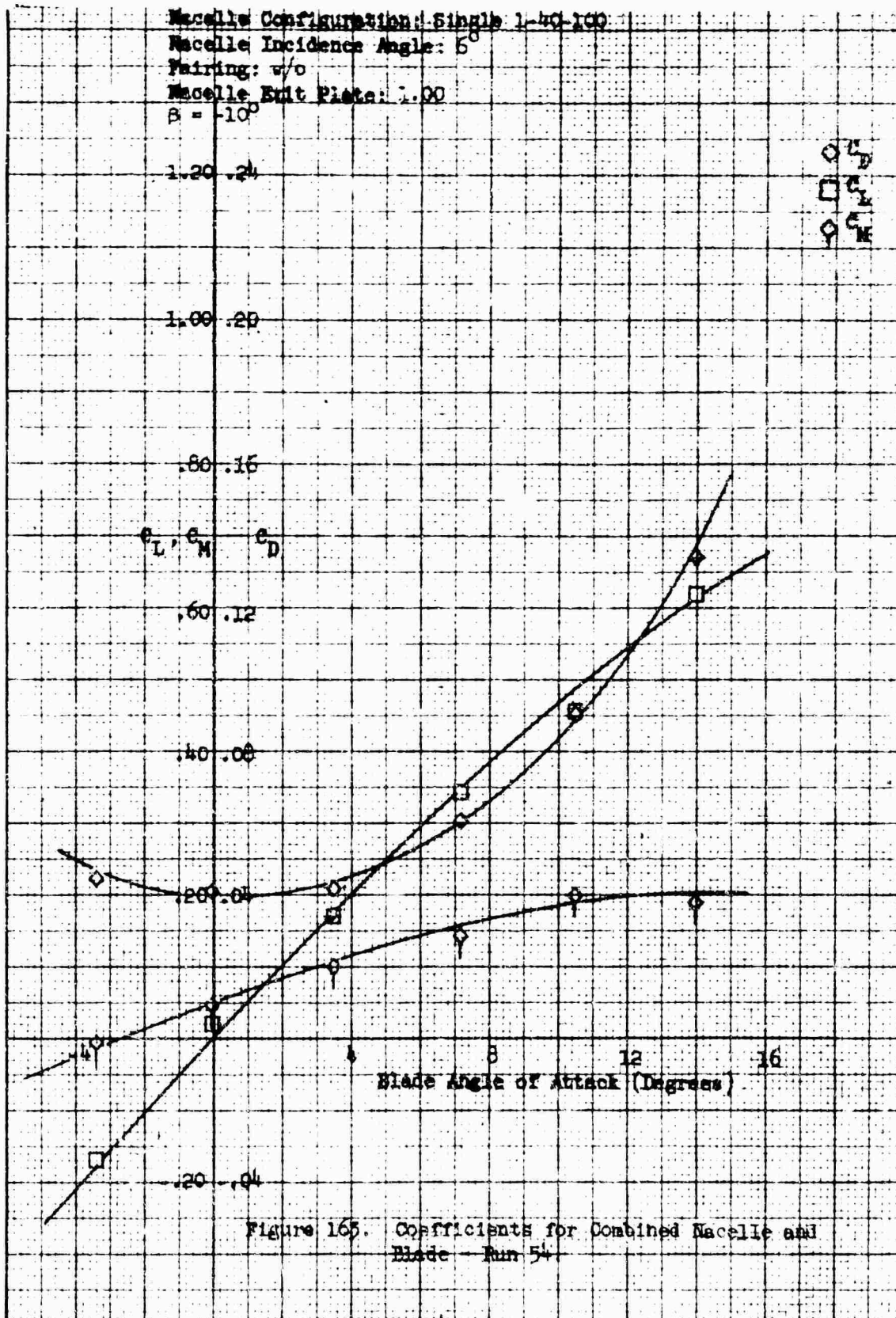


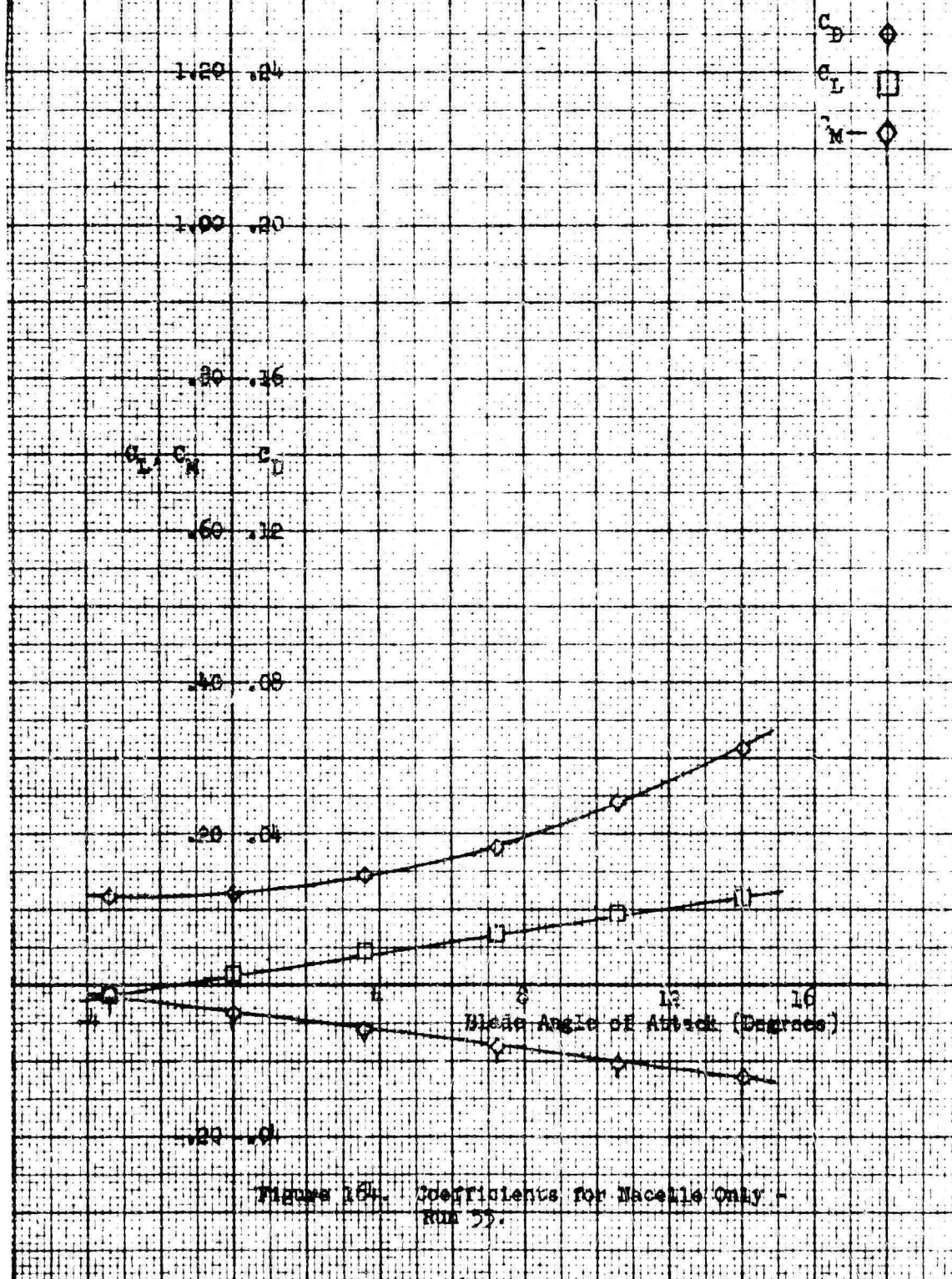
Figure 165. Coefficients for Combined Nacelle and Blade - Run 54

Nacelle Configuration: Single 1-40-100

Firing: W/O

Nacelle Exit Plate: 1.00

$\beta = 0^\circ$



Nozzle Configuration: Single 1-40-100
 Nozzle Incidence Angle: 6°
 Pairing: w/o
 Nozzle Exit Plane: 1.00
 $B = 0$

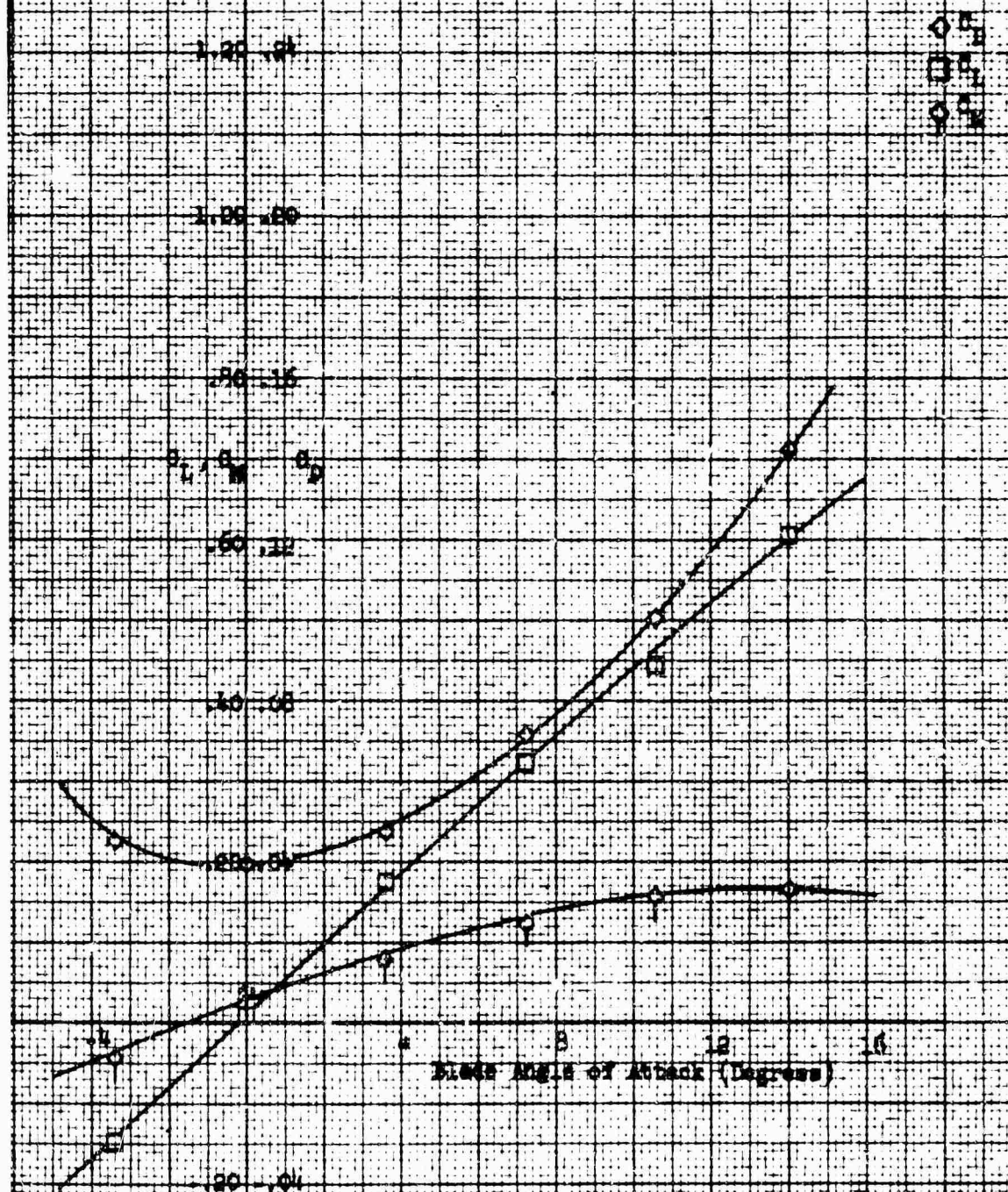
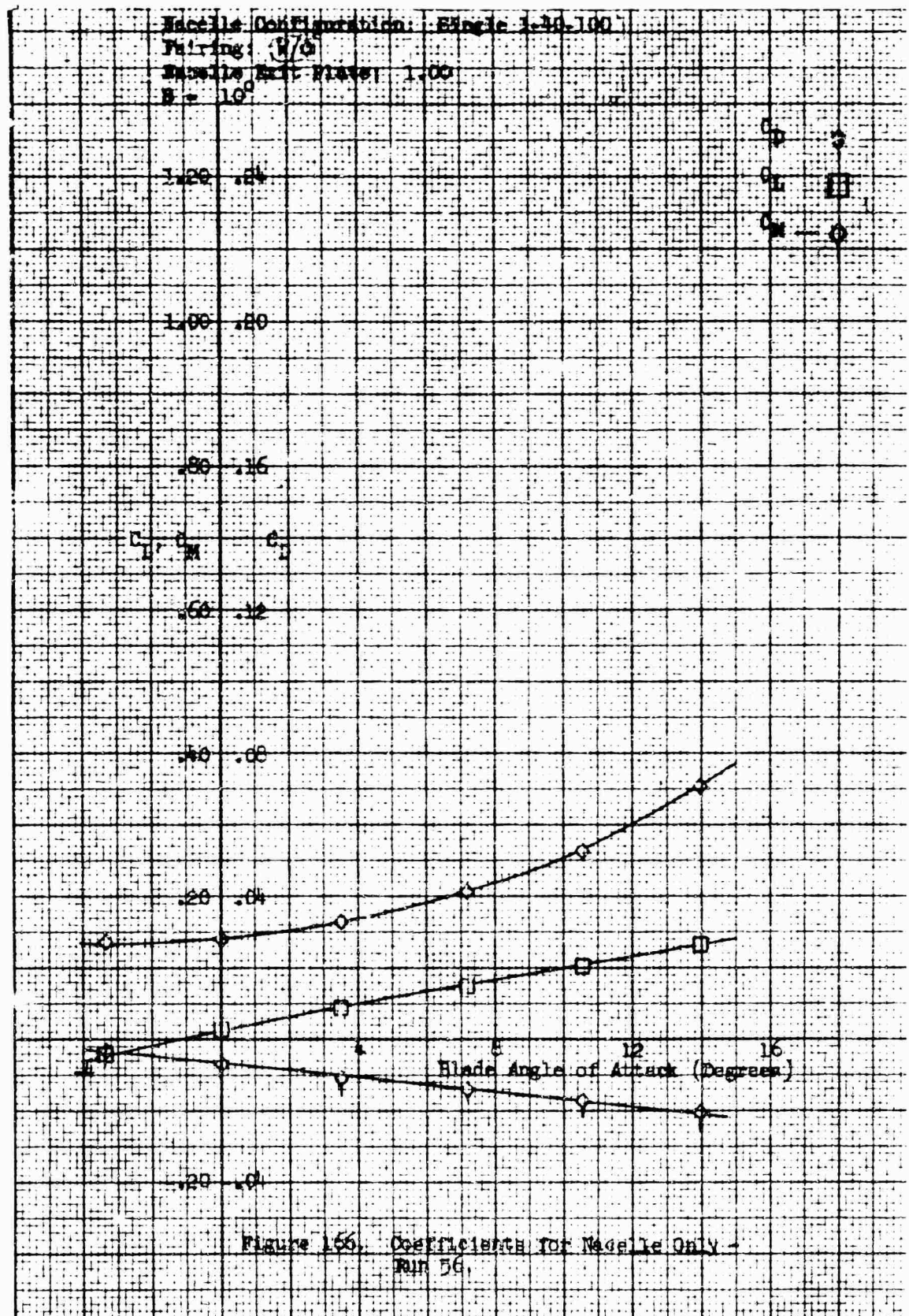


Figure 165. Coefficients for Combined Nozzle and Blade - Run 55.



Nacelle Configuration: Single 1-40-100

Nacelle Incidence Angle: 6°

Fairing: w/o

Nacelle Exit Plate: 1.00

$\beta = 10^\circ$

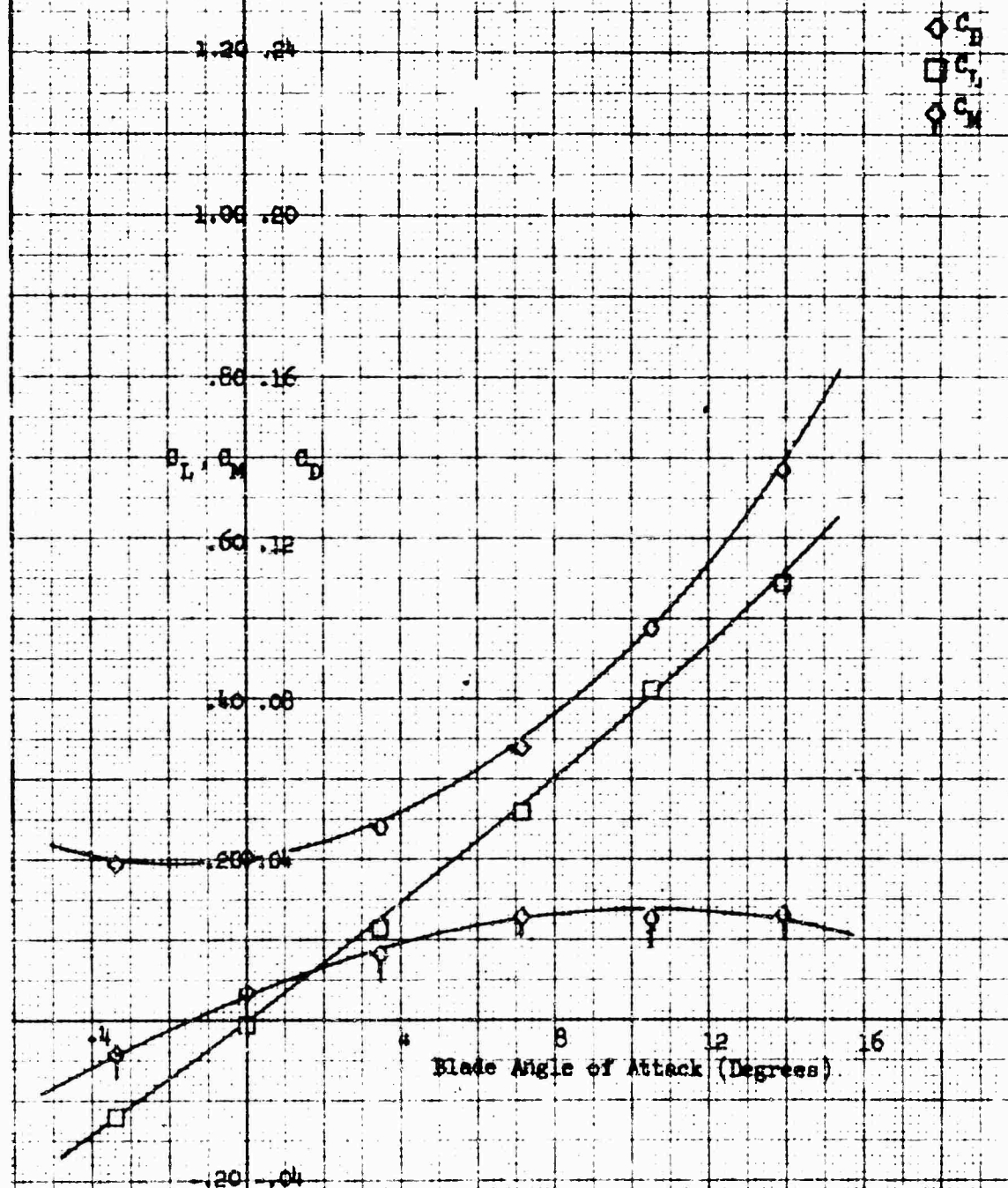


Figure 167. Coefficients for Combined Nacelle and Blade - Run 76.

Nozzle Configuration: Nozzle 1-10-106
 Pairing: 1/0
 Nozzle Exit Plane: 1.00
 $\theta = 20^\circ$

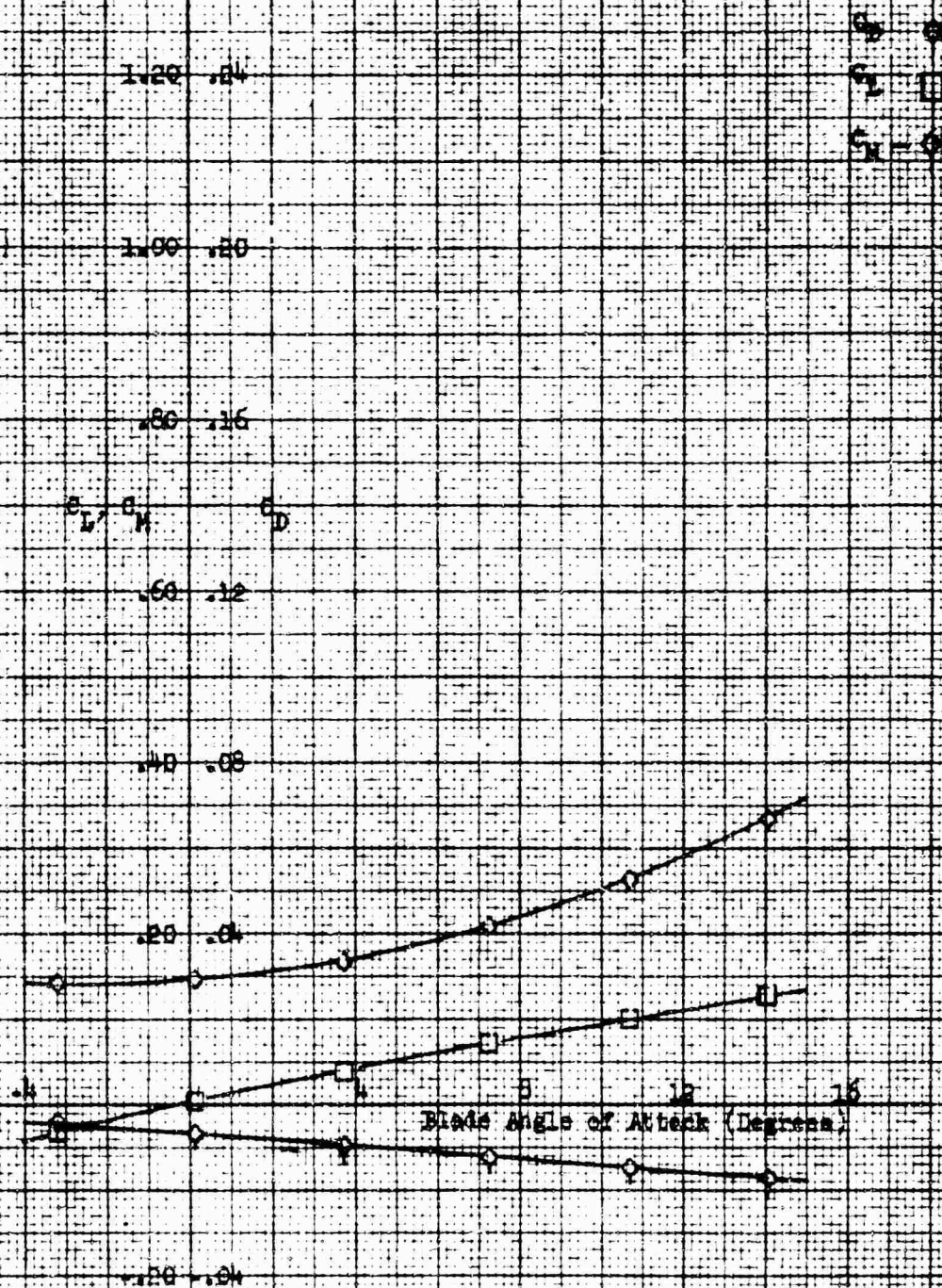


Figure 168. Coefficients for Nozzle Only -
 Run 57.

Nacelle Configuration: Single 1-40-100
 Nacelle Incidence Angle: 6°
 Fairing: w/o
 Nacelle Exit Plate: 1.00
 $\beta = 20^\circ$

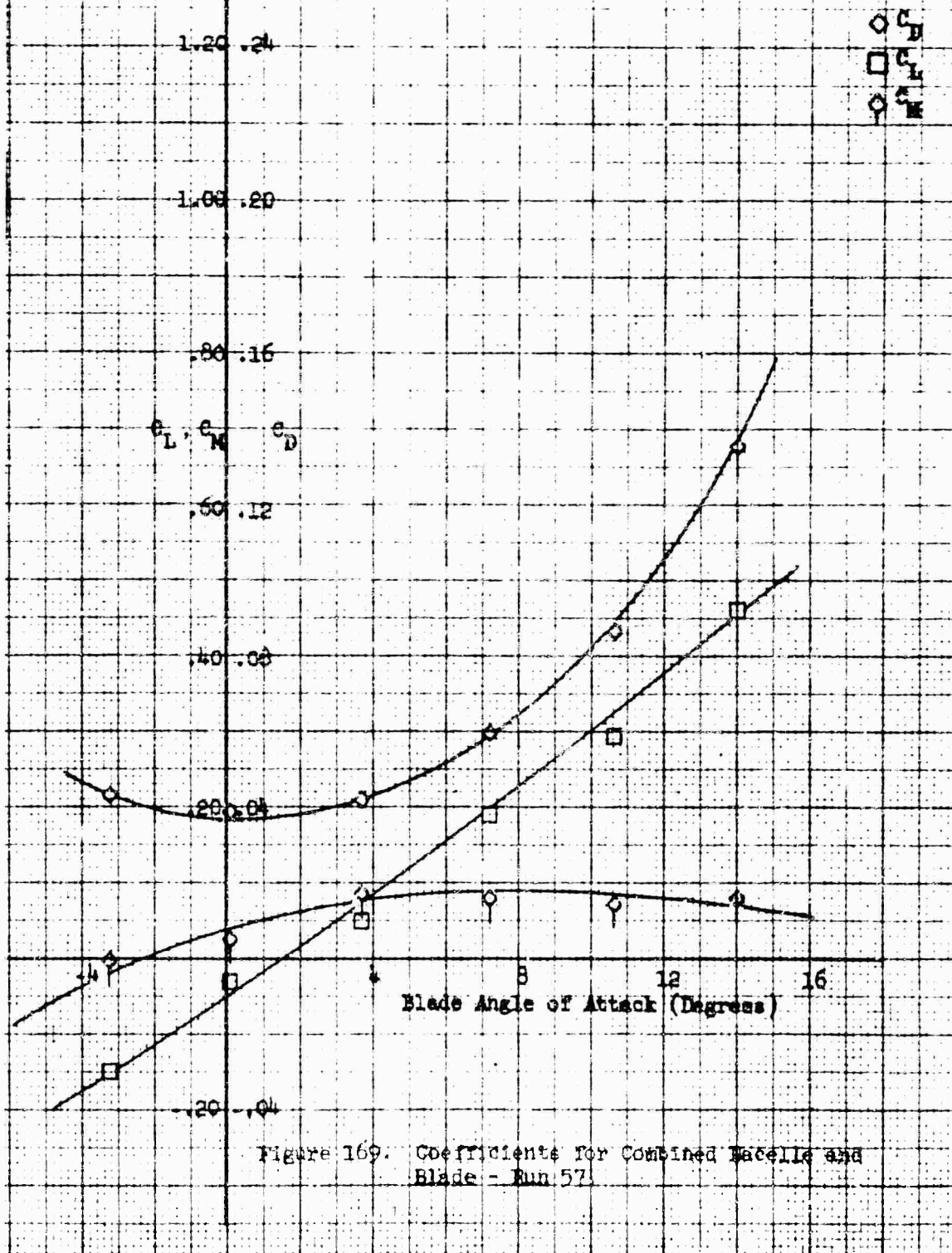
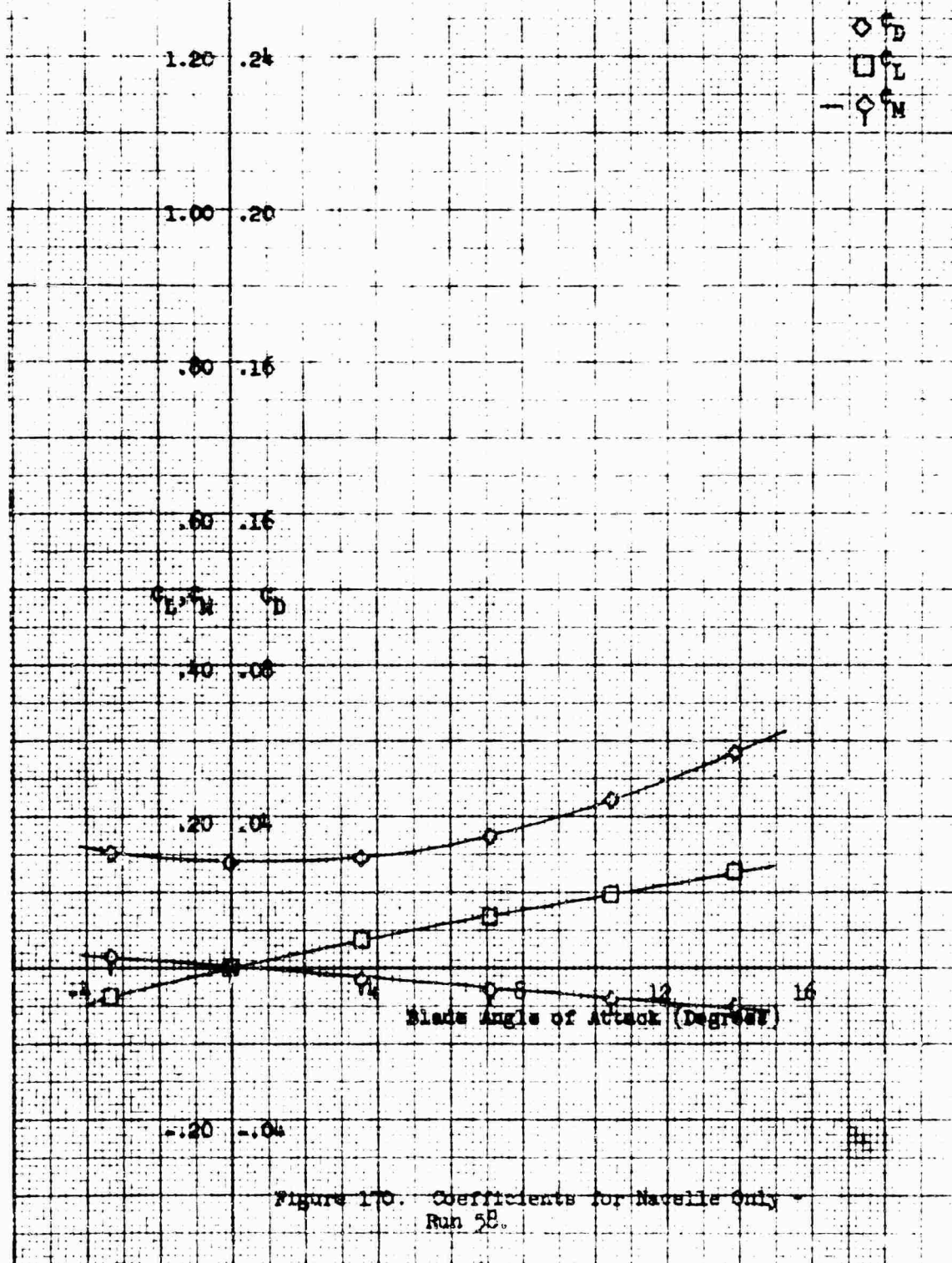


Figure 169. Coefficients for Combined Nacelle and Blade - Run 57

Macelle Configuration: Single 1-40-1.00
 Pairing: With
 Macelle Exit Plate: 1.00
 $\beta = 20^\circ$



Nacelle Configuration: Single 1-40-100
 Nacelle Incidence Angle: 0
 Fairing: with
 Nacelle Exit Plate: 1.09
 $\beta = 20^\circ$

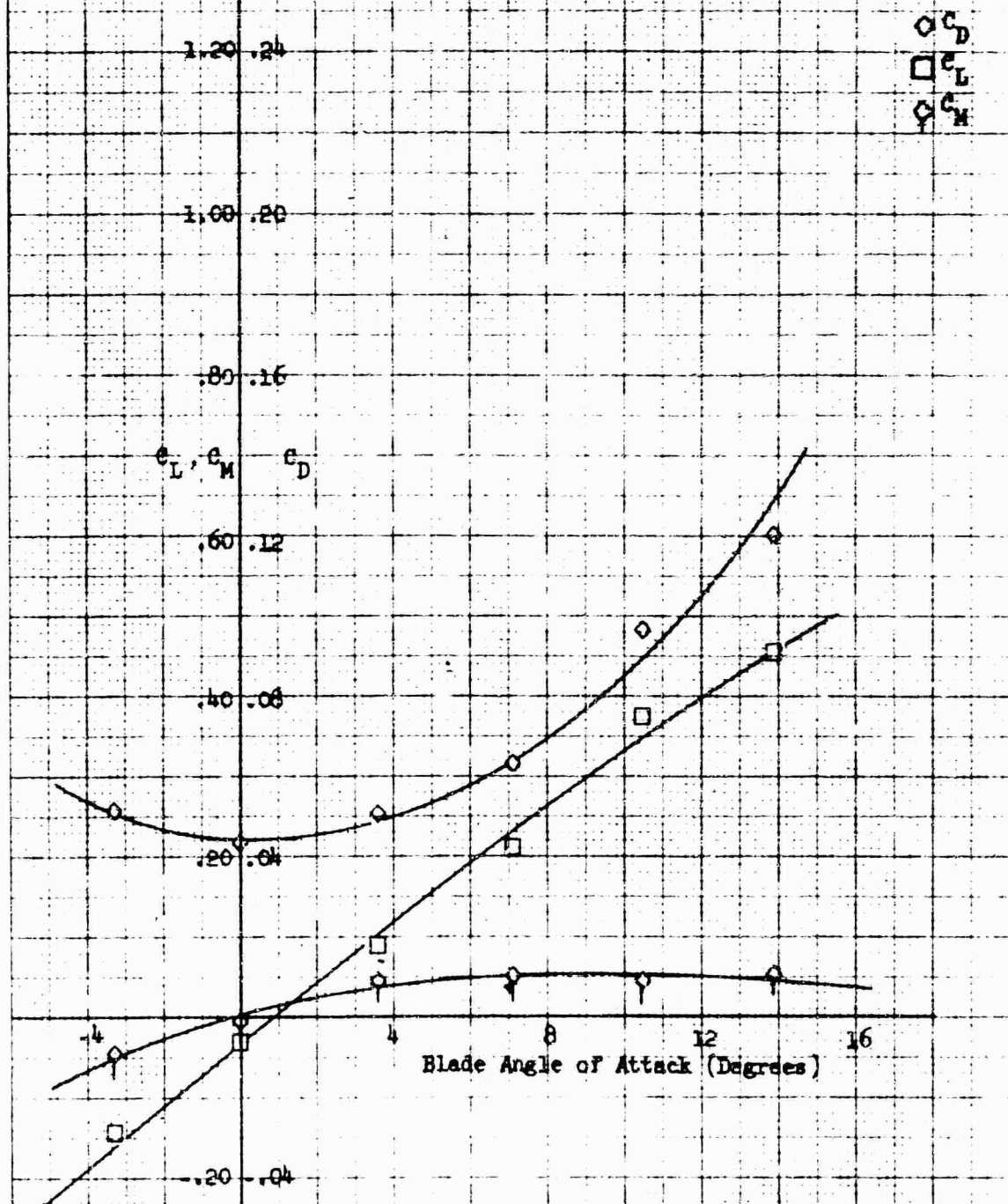
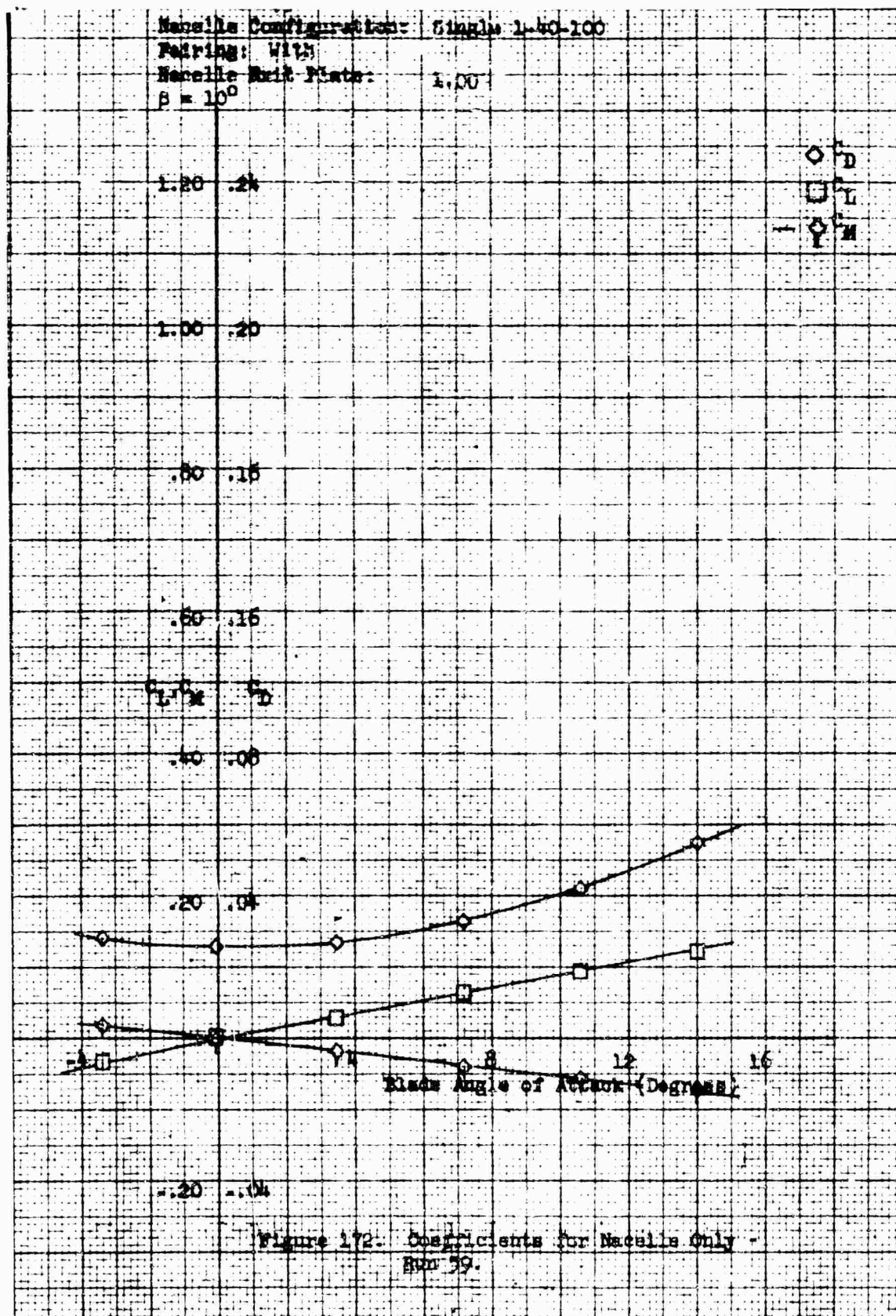


Figure 171. Coefficients for Combined Nacelle and Blade - Run 58.



Nacelle Configuration: Single 1-40-100

Nacelle Incidence Angle: 0

Fairing: With

Nacelle Exit Plate: 1.00

$\beta = 10^\circ$

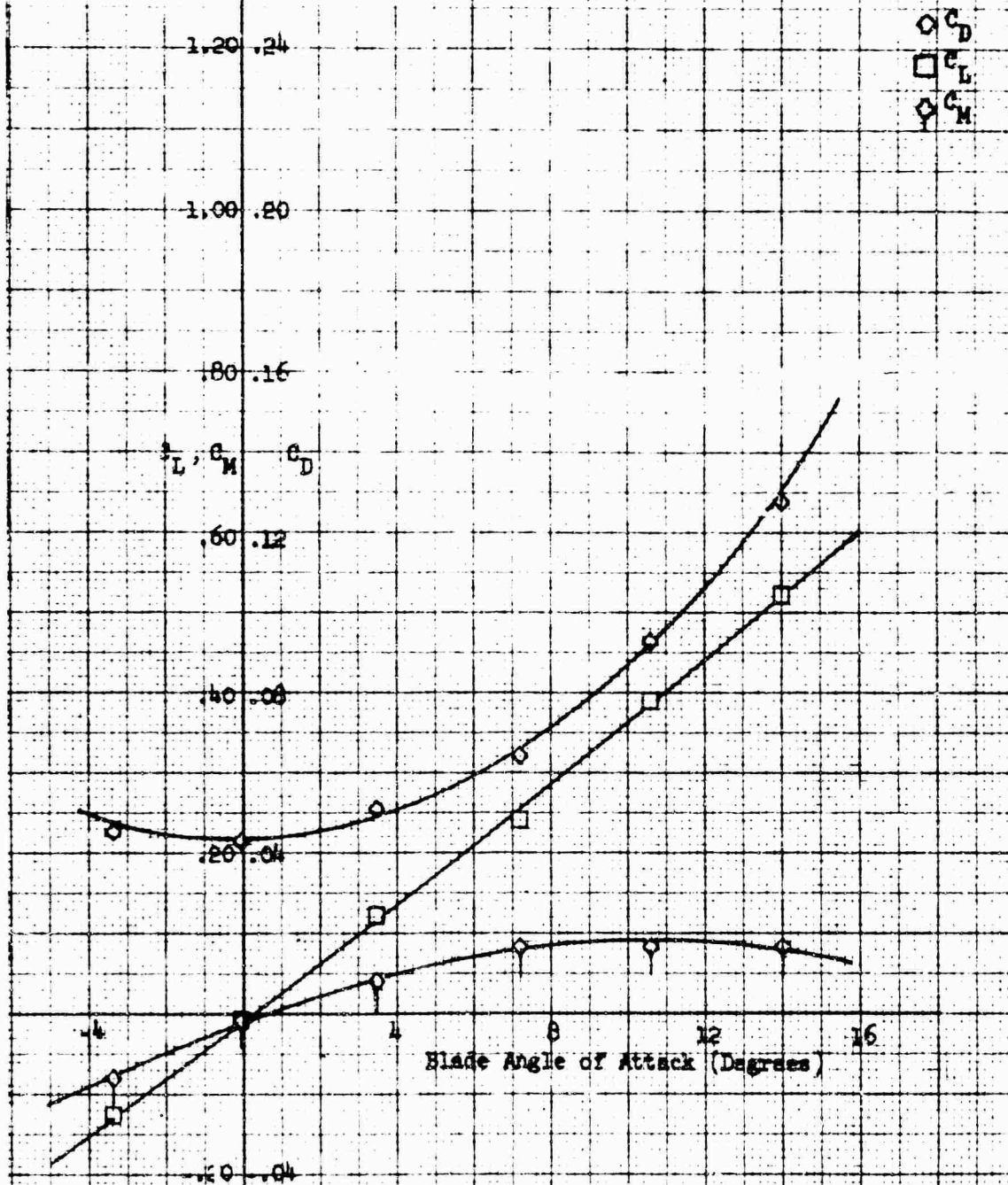


Figure 173. Coefficients for Combined Nacelle and Blade - Run 59.

Wacelle Configuration: 8Wacelle 1-40-100

Fairing: With

Wacelle Exit Plate: 1.00

$\beta = 0$

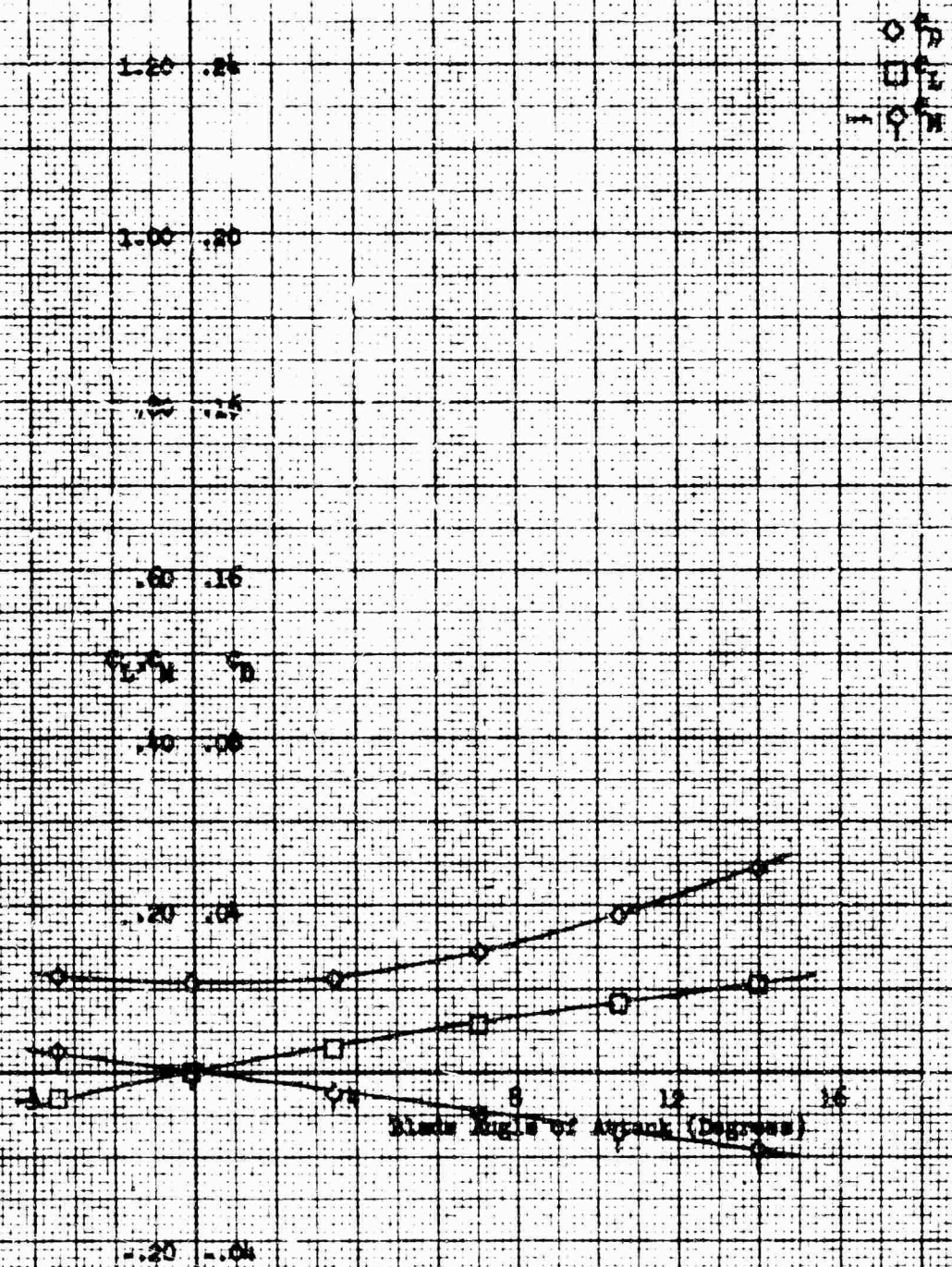
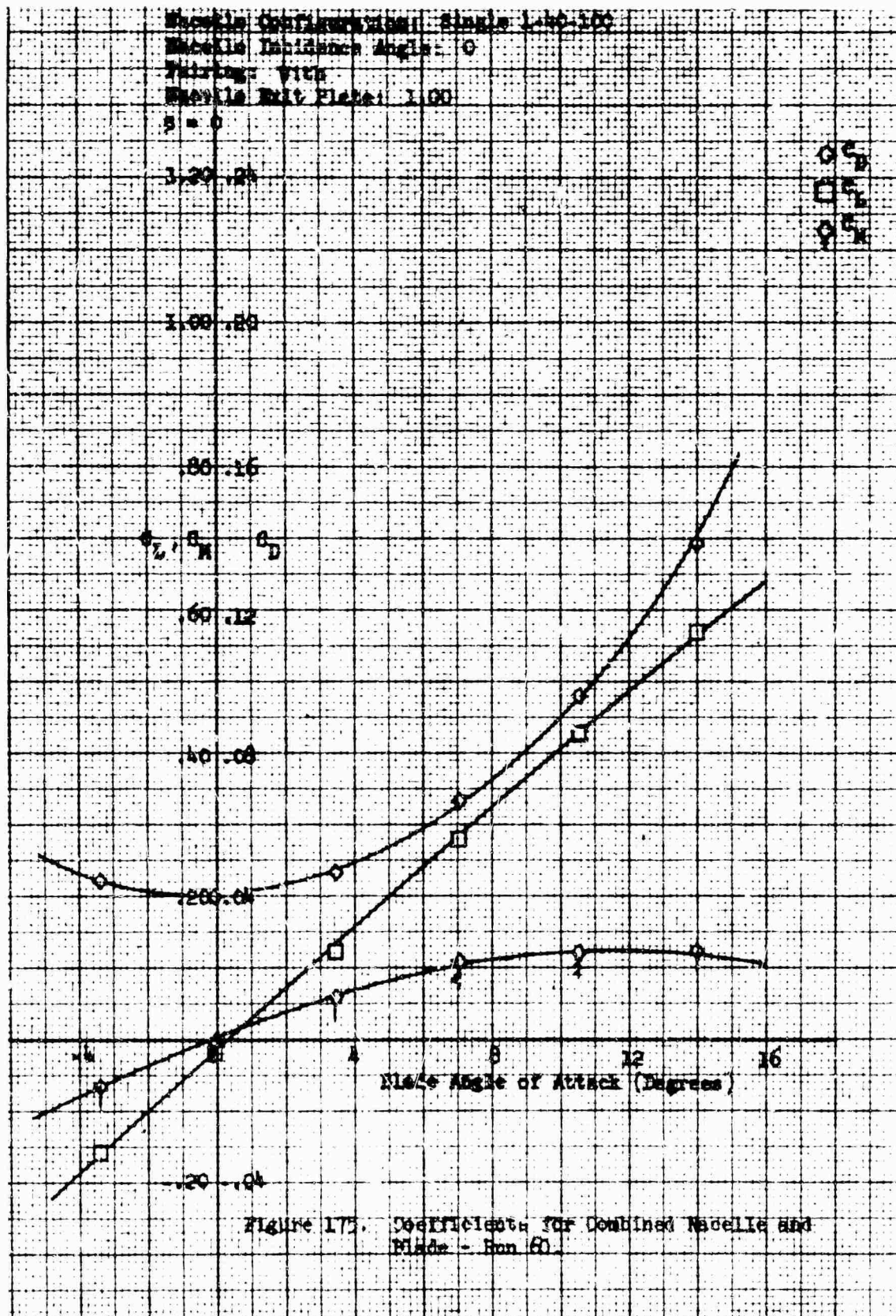
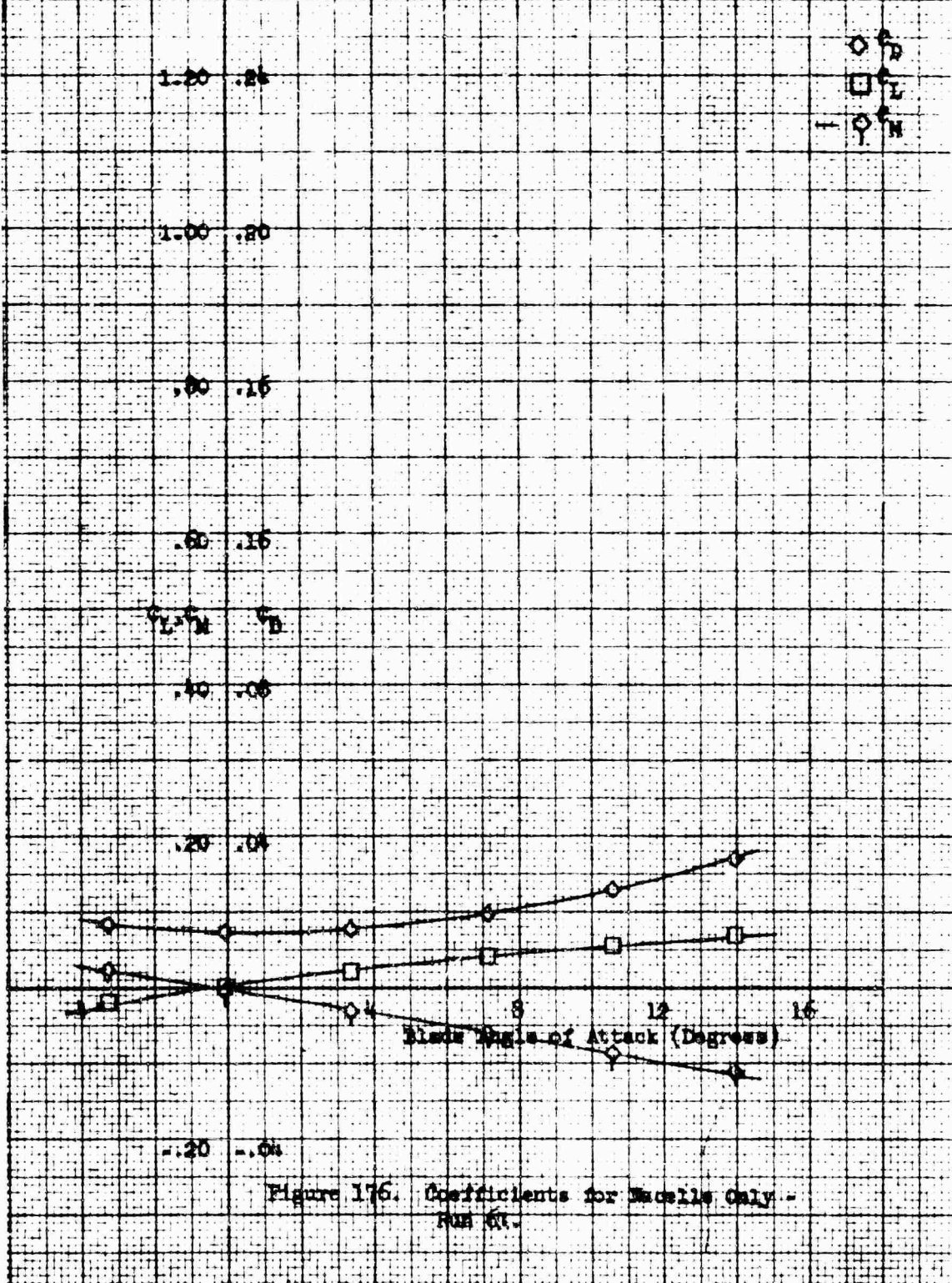


Figure 17a. Coefficients for Wacelle Only - Run 60.



Macelle Configuration: Stage 1-40-100
 Pairing: With
 Macelle Exit Plate: 1.00
 $\beta = .10^\circ$



Blade Configuration: Single 1-20-100

Blade Incidence Angle: 0

Pairing: With

Blade Exit Plane: 1.00

$\beta = 10^\circ$

1.20 .24

1.00 .20

.80 .16

C_L, C_M, C_D

.60 .12

.40 .08

.20 .04

Blade Angle of Attack (Degrees)

Figure 2.77. Coefficients for Combined Nozzle and Blade - Run 61.

Nacelle Configuration: Single 1.40-100

Fairing: With

Nacelle Exit Plate: 1.00

$\beta = -20^\circ$

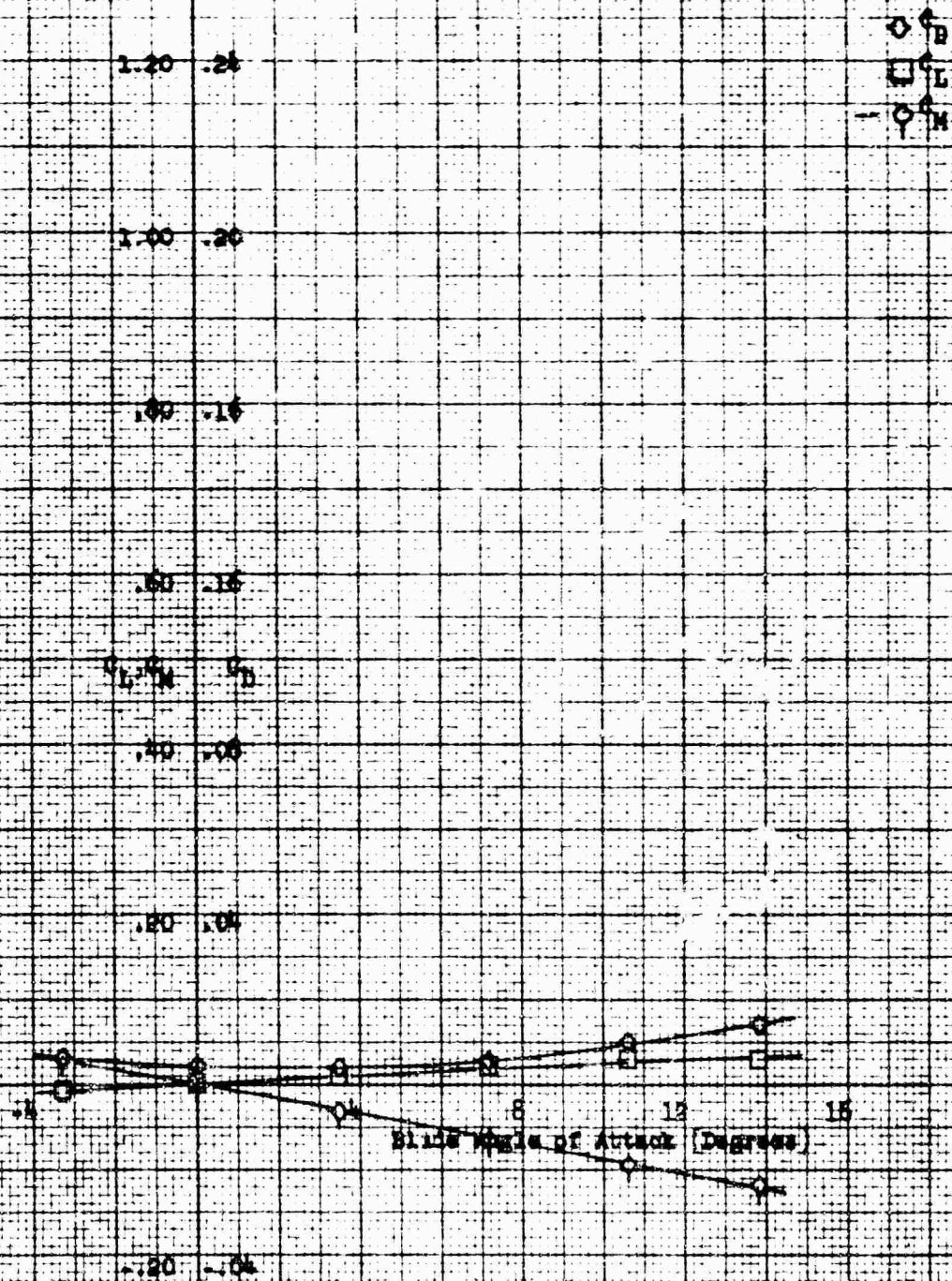


Figure 178. Coefficients for Nacelle Only -
Run 62.

Macelle Configuration: Single 1-40-100
 Macelle Incidence Angle: 0
 Fairing: With
 Macelle Exit Plate: 1.00
 $\beta = 20^\circ$

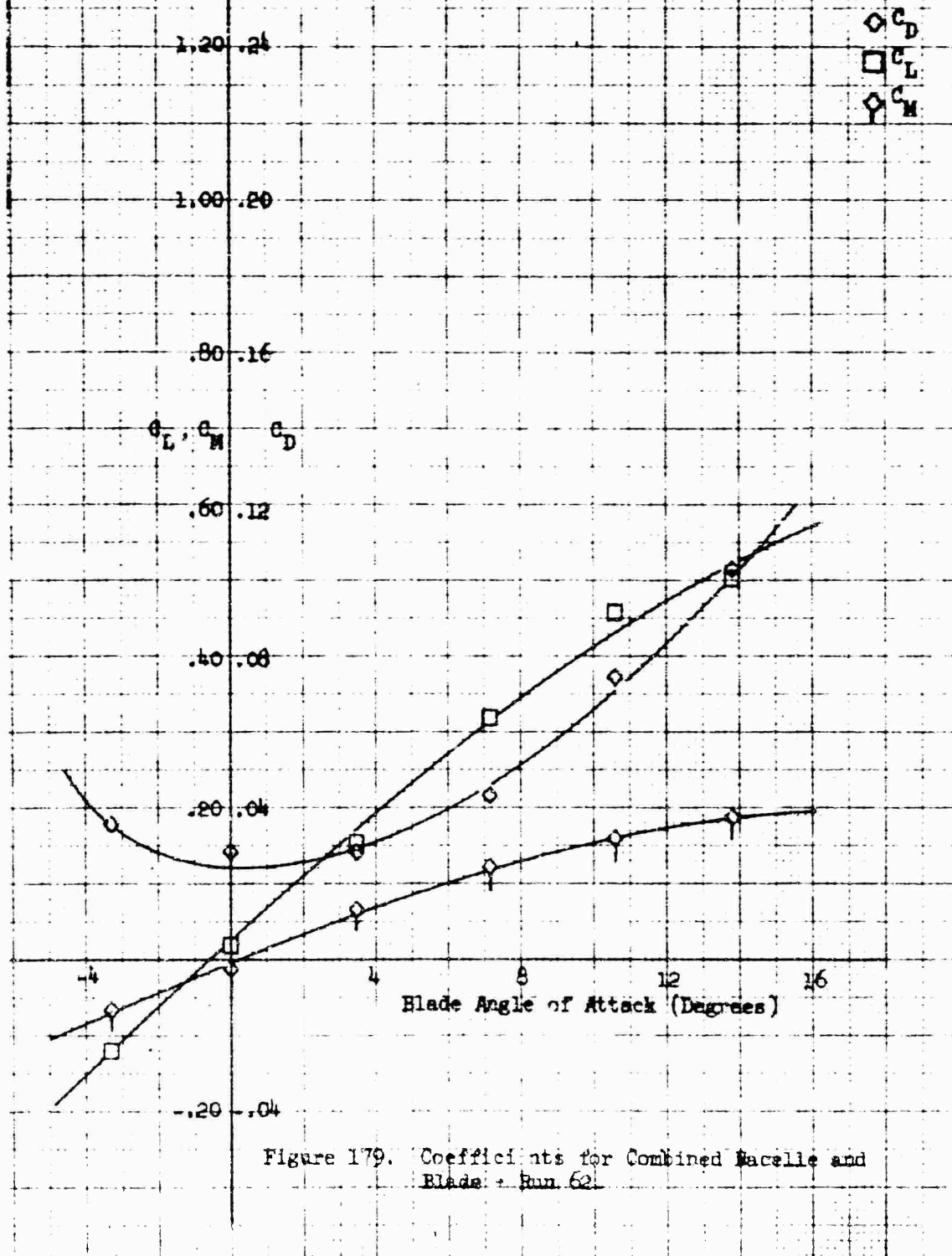
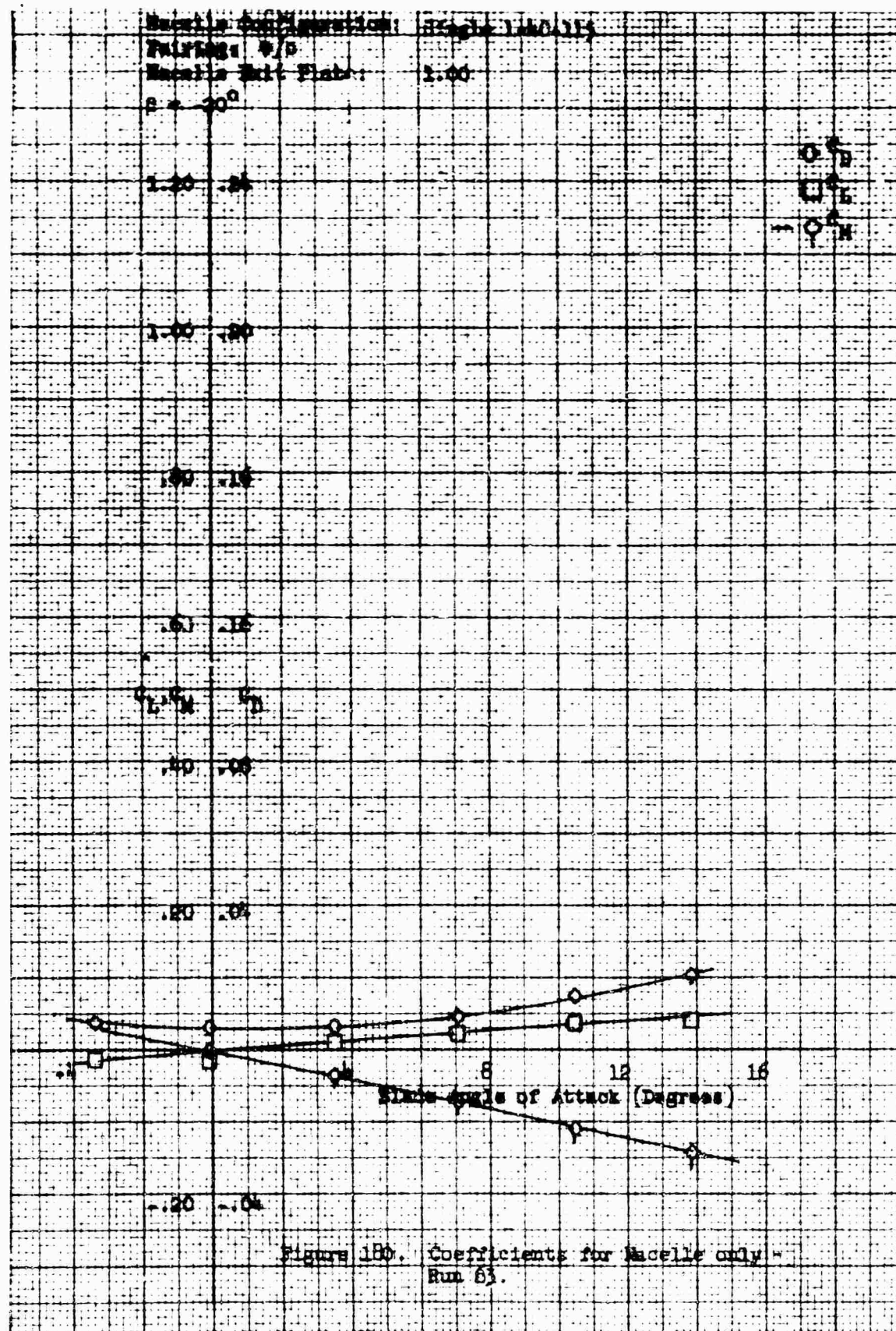


Figure 179. Coefficients for Combined Macelle and Blade: Run 62



Wacelle Configuration: Single 1-40-145

Wacelle Incidence Angle: 0

Pairing: w/o

Wacelle Exit Plate: 1.00

$\theta = -20^\circ$

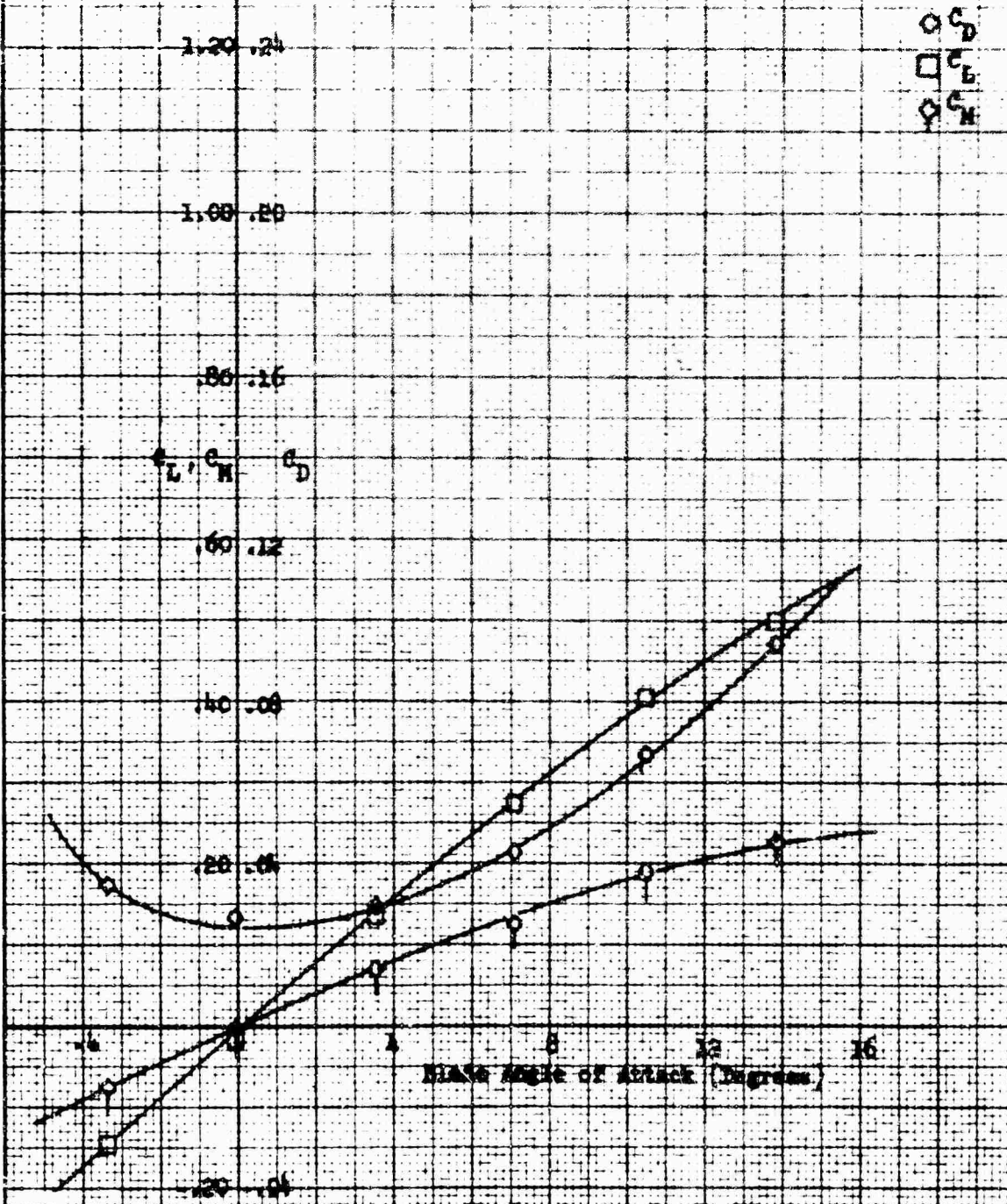
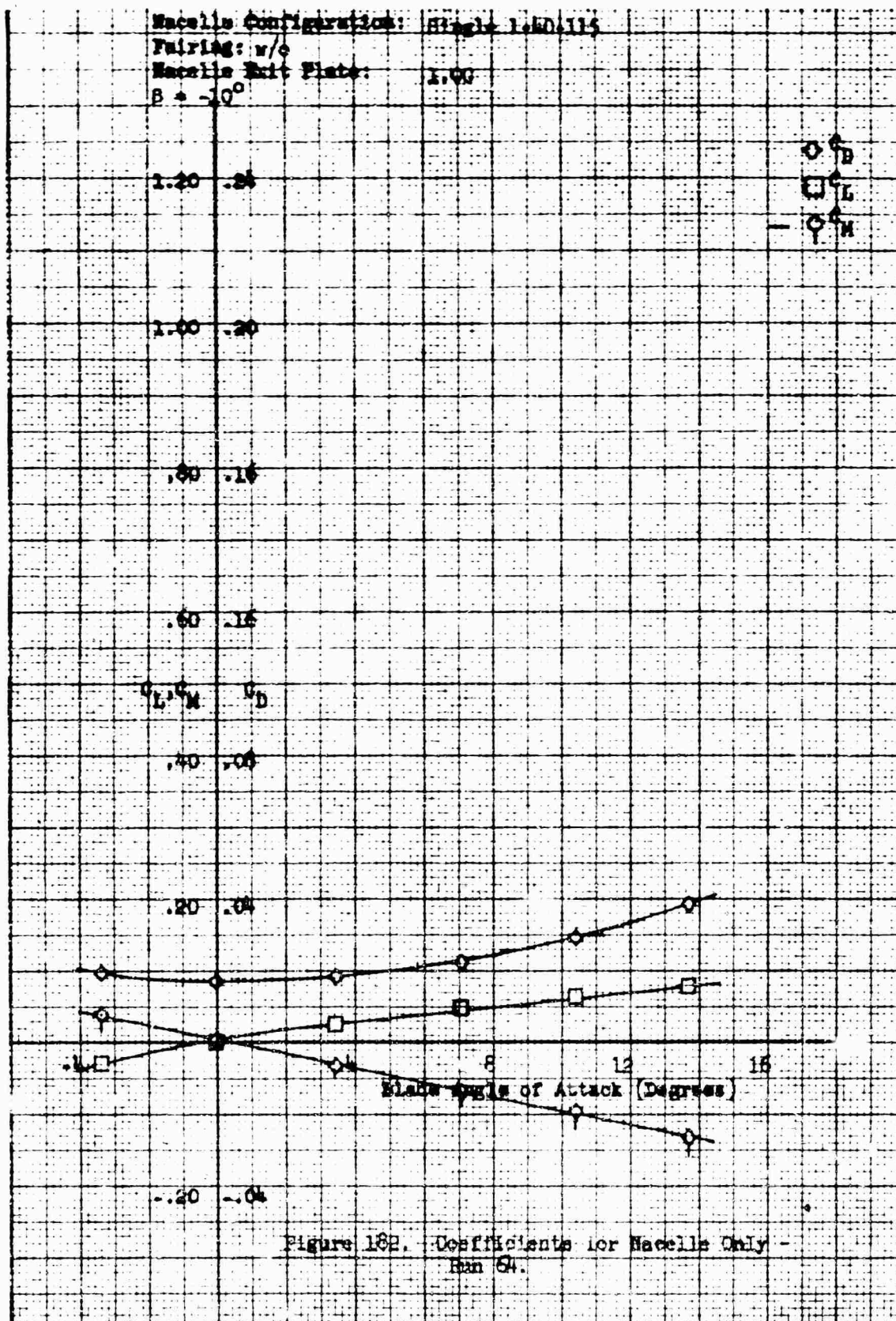


Figure 131. Coefficients for Unpaired Wacelle and Plate $\theta = -20^\circ$.



Wacelle Configuration: Single 1-40-115

Wacelle Incidence Angle: 0

Pairing: v/o

Wacelle Exit Plate: 1.00

$\beta = 10^\circ$

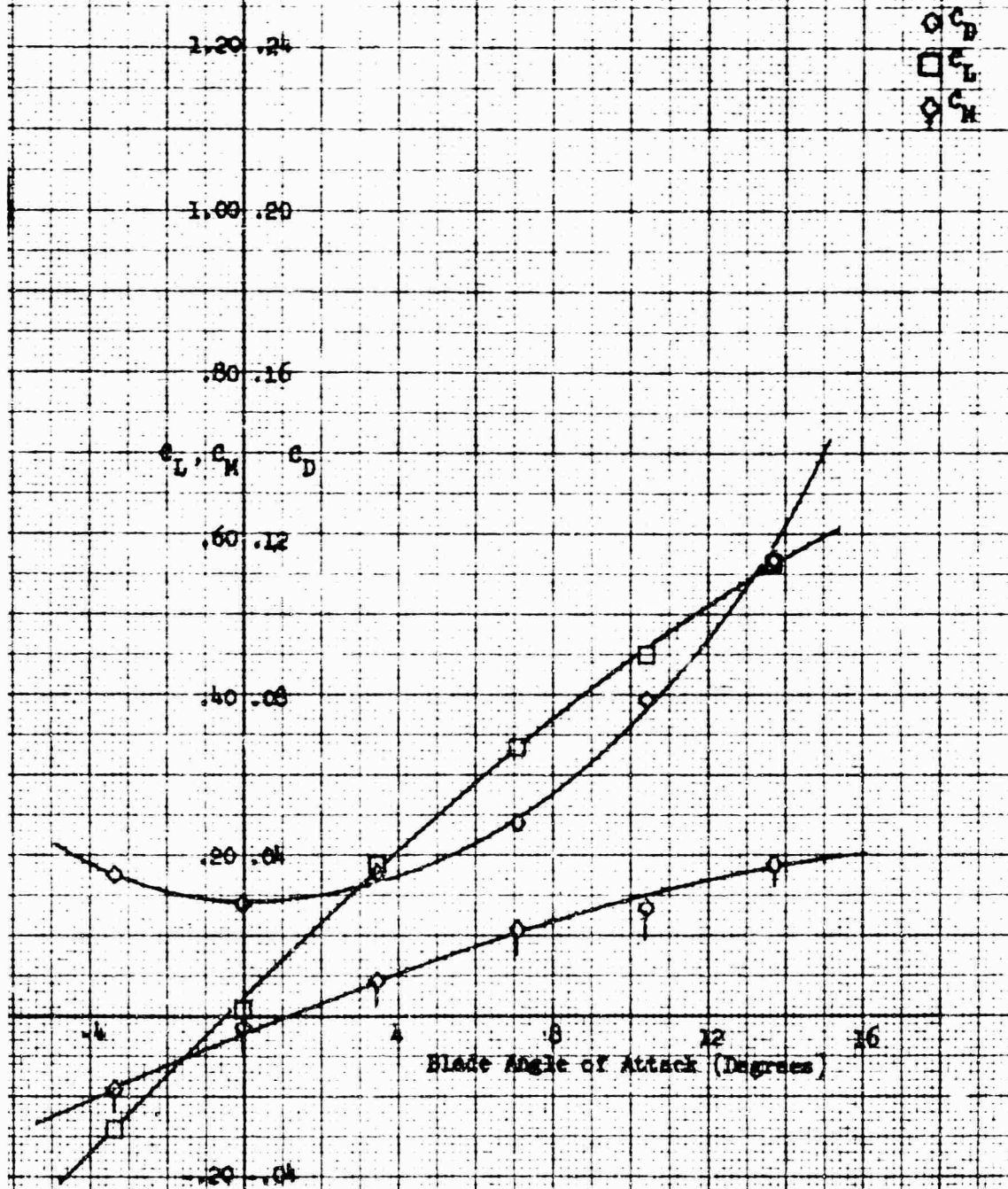


Figure 183. Coefficients for Combined Wacelle and Blade Run 5A.

Blade Configuration: Single 1-40-115
 Pairing: w/o
 Blade Exit Plane: 1.00
 $\beta = 0$

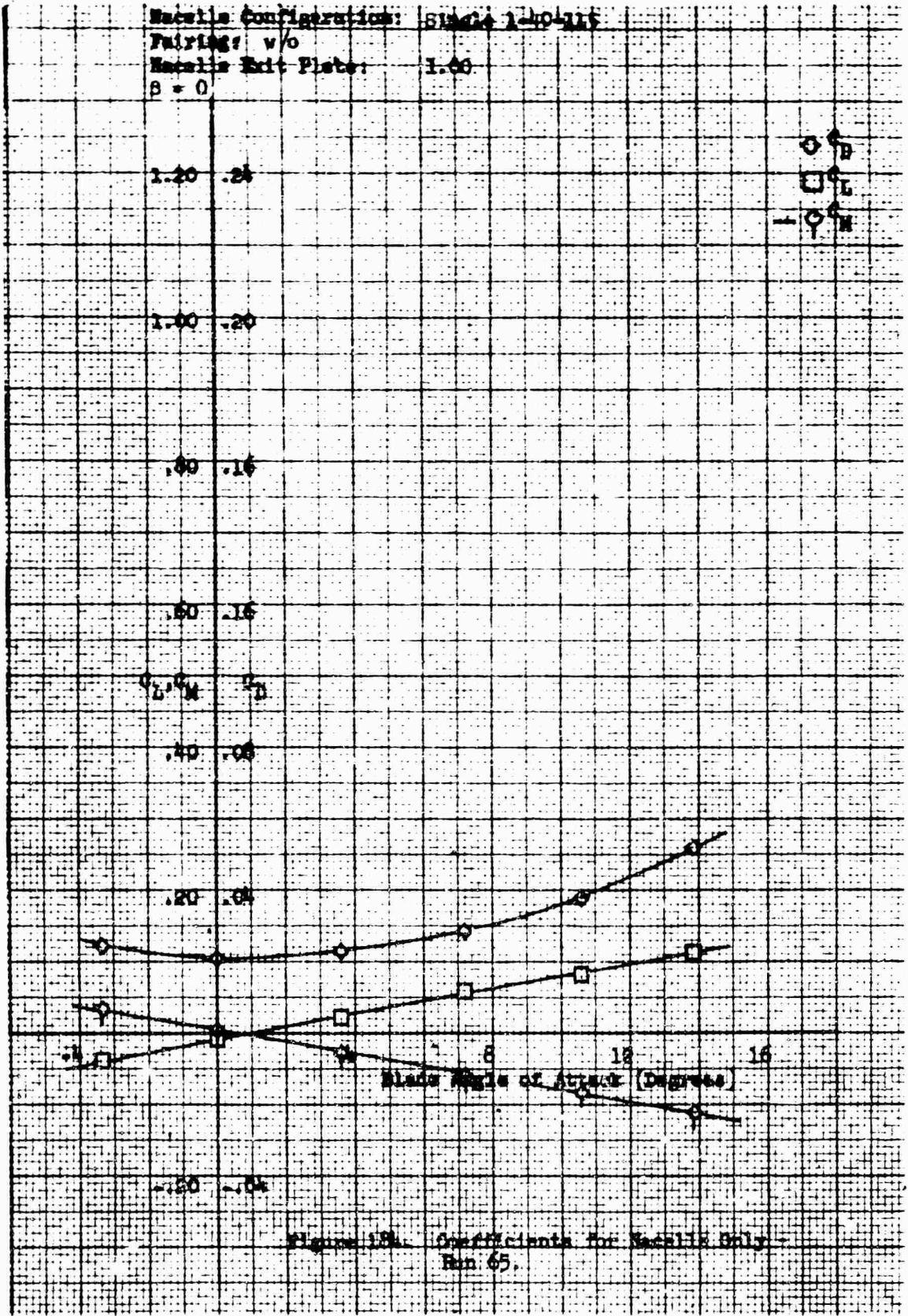


Figure 18. Coefficients for Blade Only -
 Run 65.

Macalle Configuration: Single 1-40-115

Needle Incidence Angle: 0

Feeding: w/o

Macalle Exit Plate: 1.00

$A = 0$

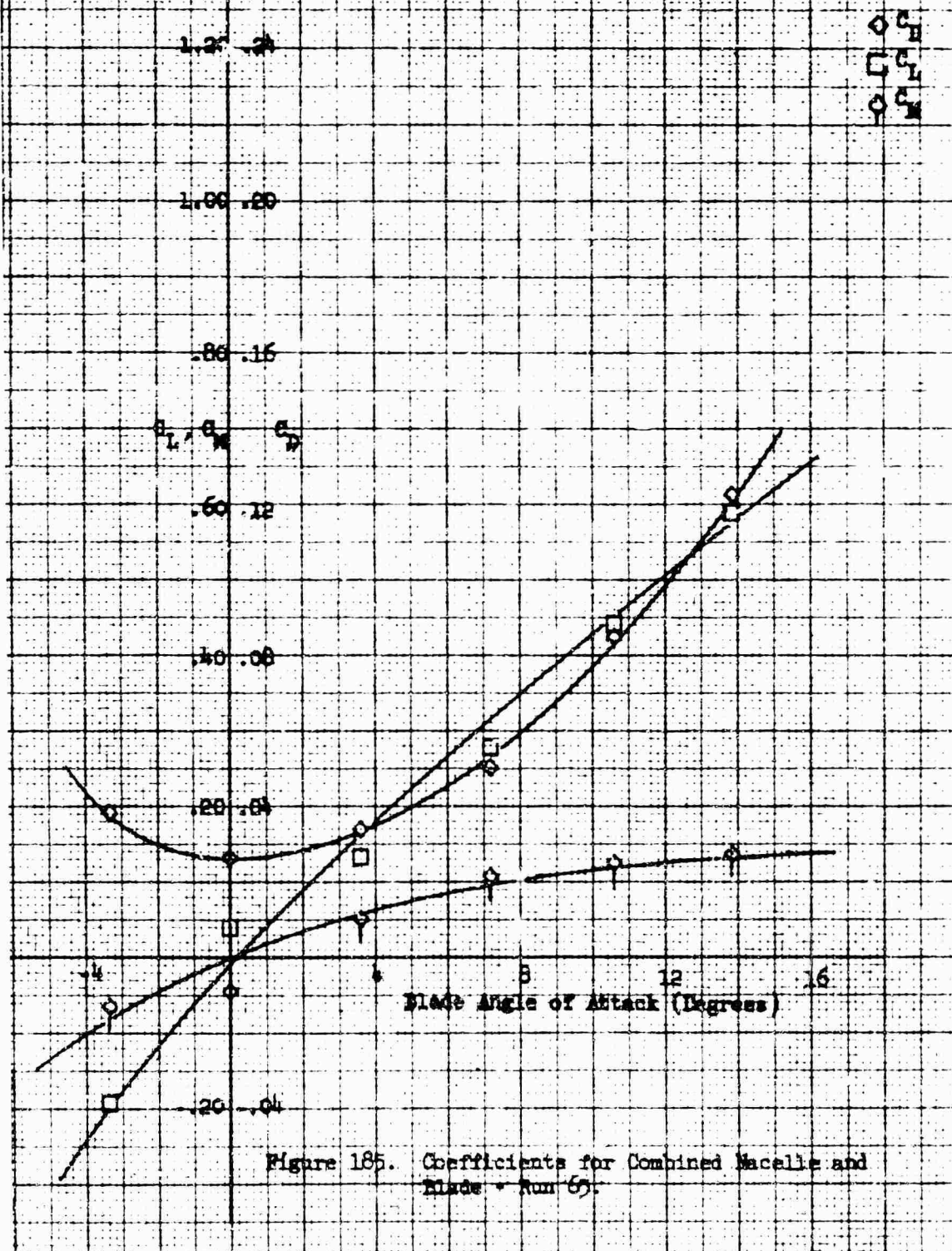


Figure 185. Coefficients for Combined Macalle and Blade - Run 67.

Macelle Configuration: Single 1-40-115
 Pairing: w/o
 Macelle Exit Plate: 1.00
 $B = 10^0$

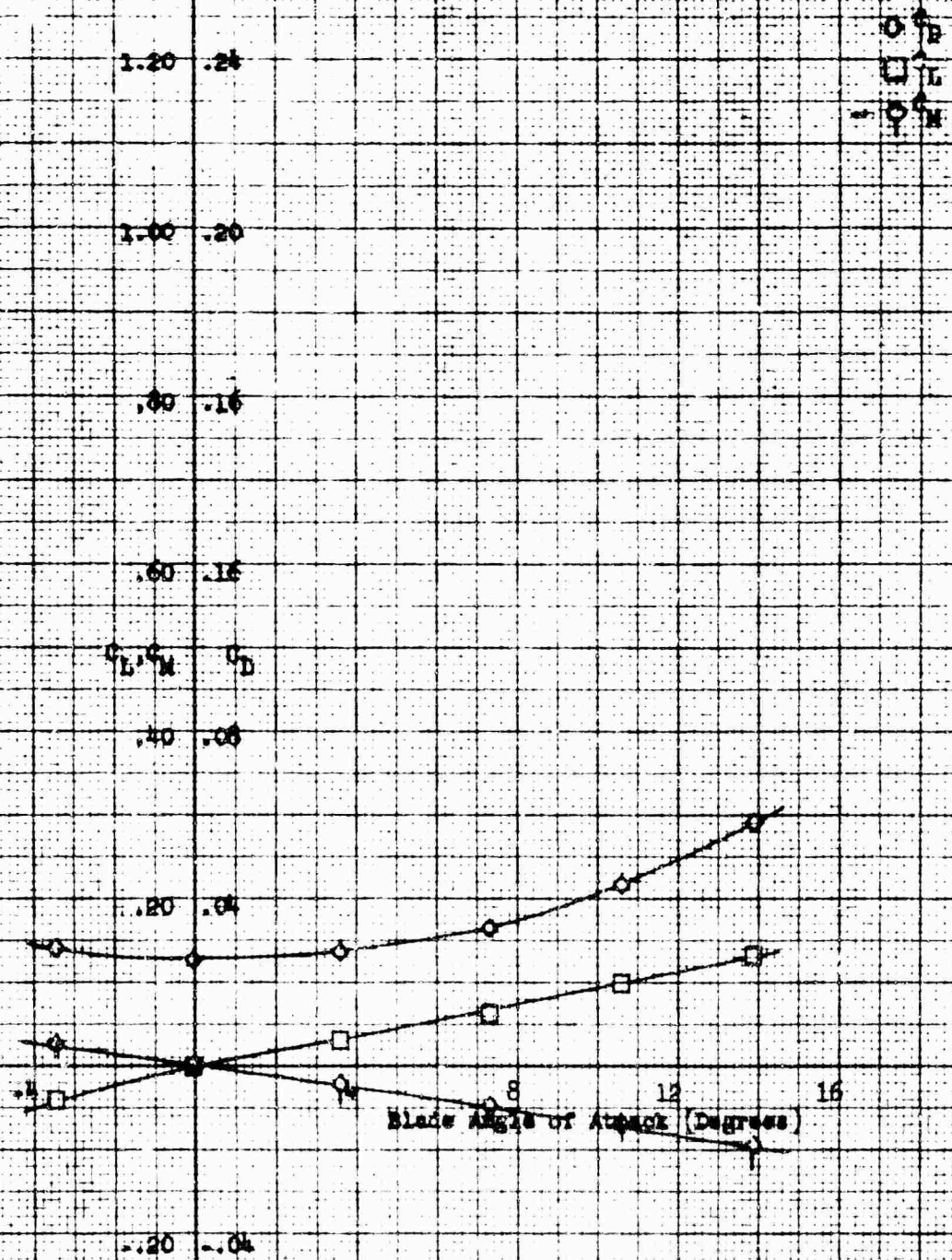


Figure 186. Coefficients for Macelle Only - Run 56.

Macelle Configuration: Single 1-10-217

Macelle Incidence Angle: 0

Fairing: w/o

Macelle Exit Plate: 1.00

$\beta = 10^\circ$

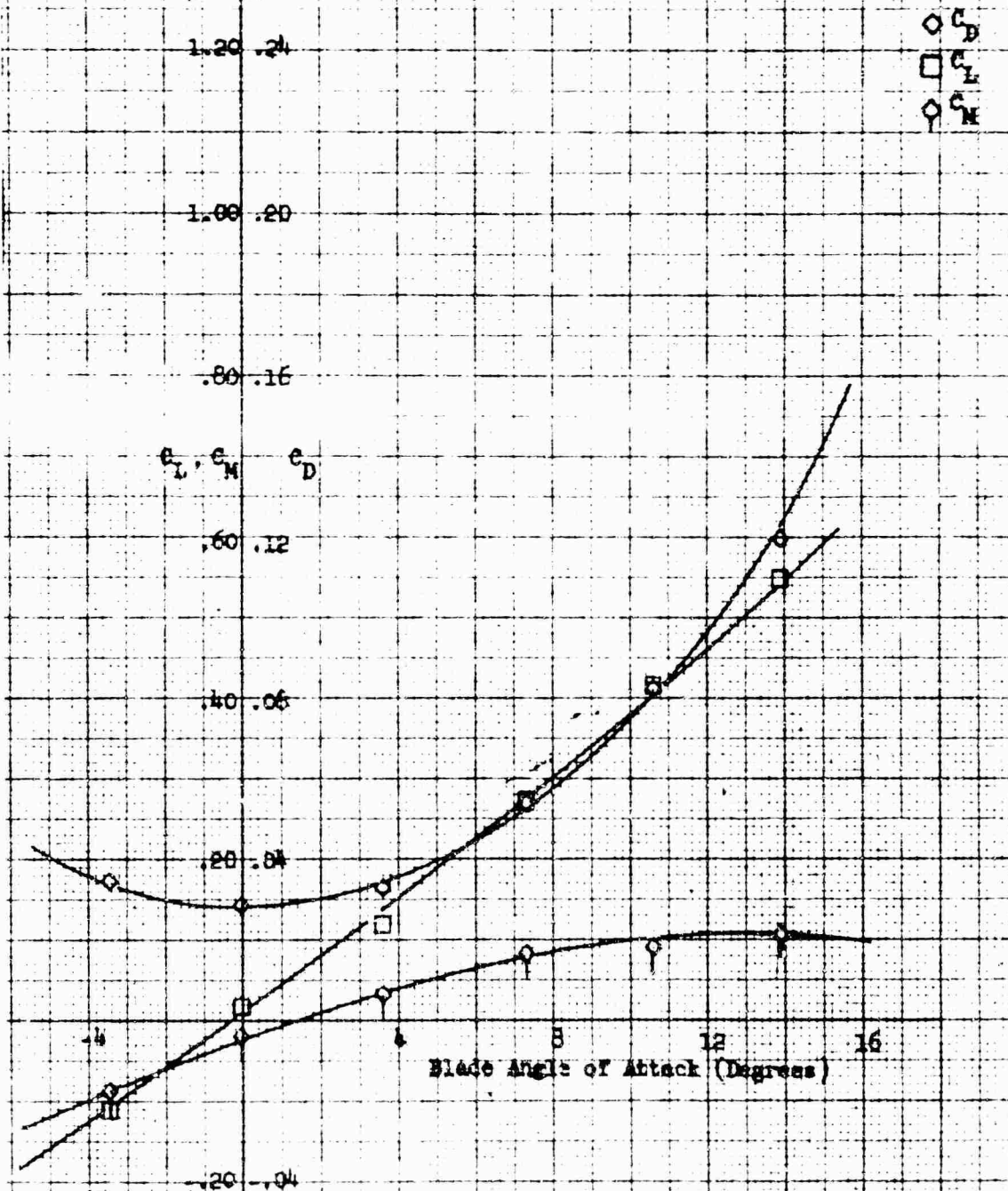
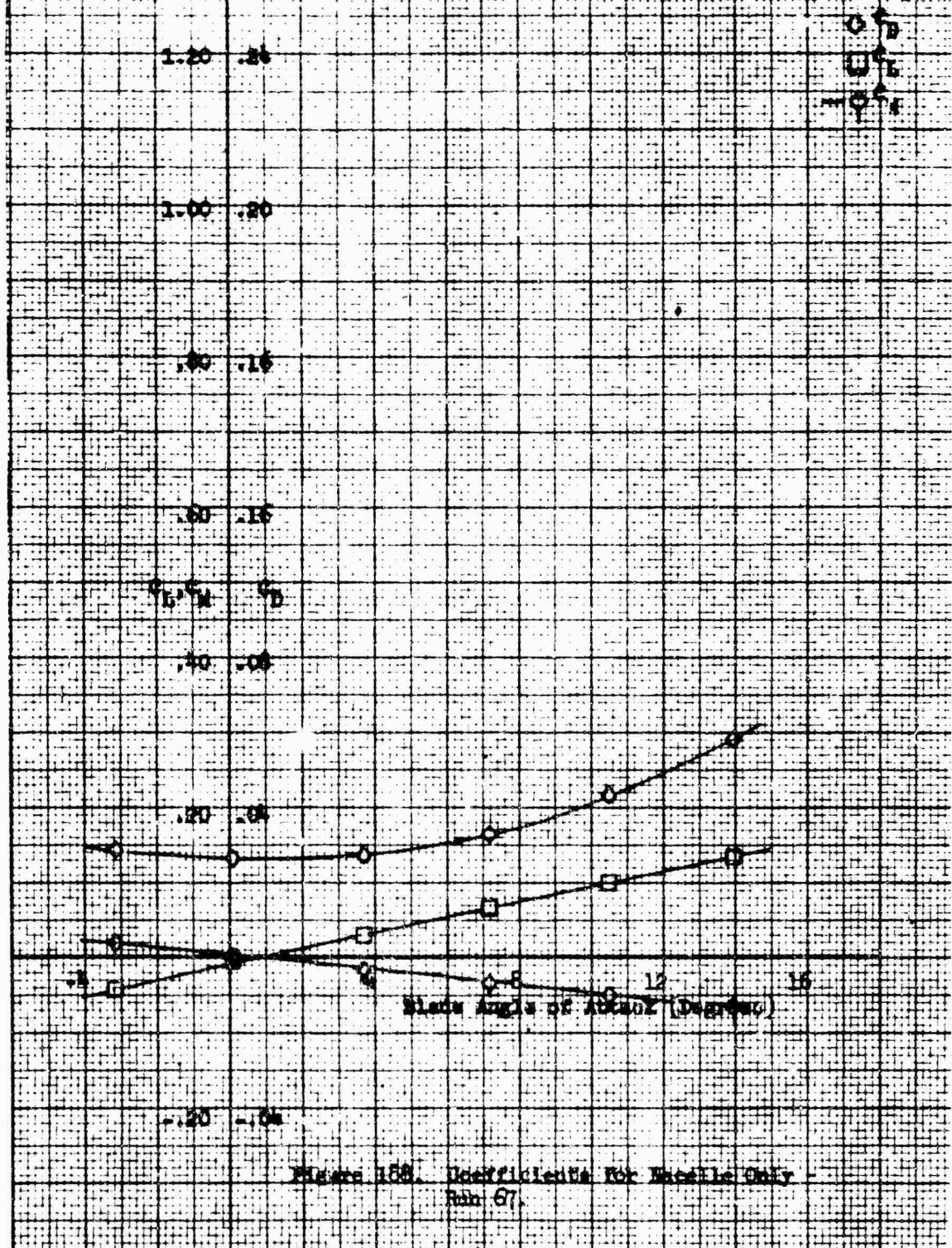


Figure 187. Coefficients for Combined Macelle and Blade - Run 66.

Nozzle Configuration: Single 2-40-135
 Fairing: w/o
 Nozzle Exit Plane: 1.00
 $\beta = 20^\circ$



Macelle Configuration: Single 1-60-119
 Macelle Incidence Angle: 0
 Fairing: w/o
 Macelle Exit Plate: 1.00
 $\beta = 20^\circ$

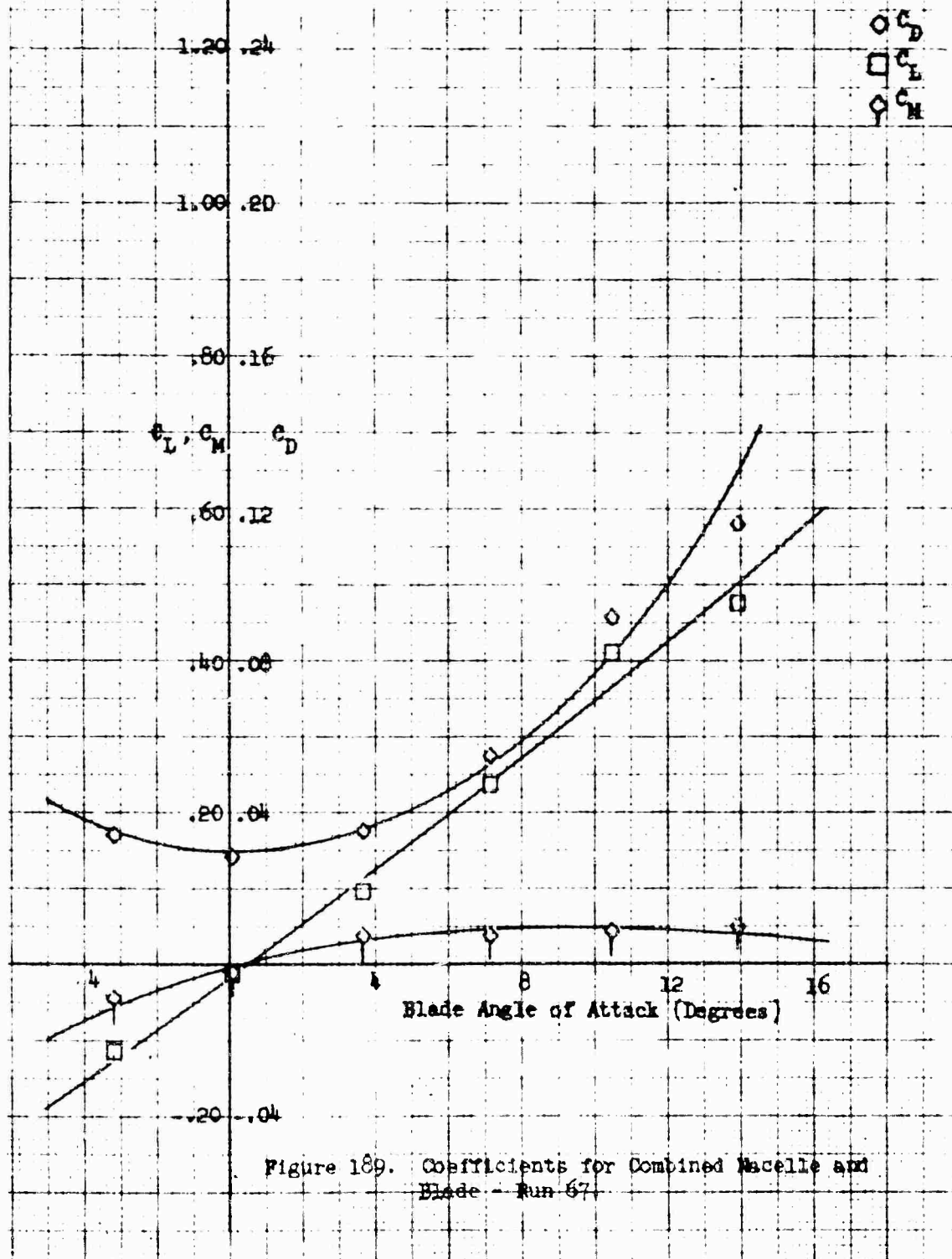
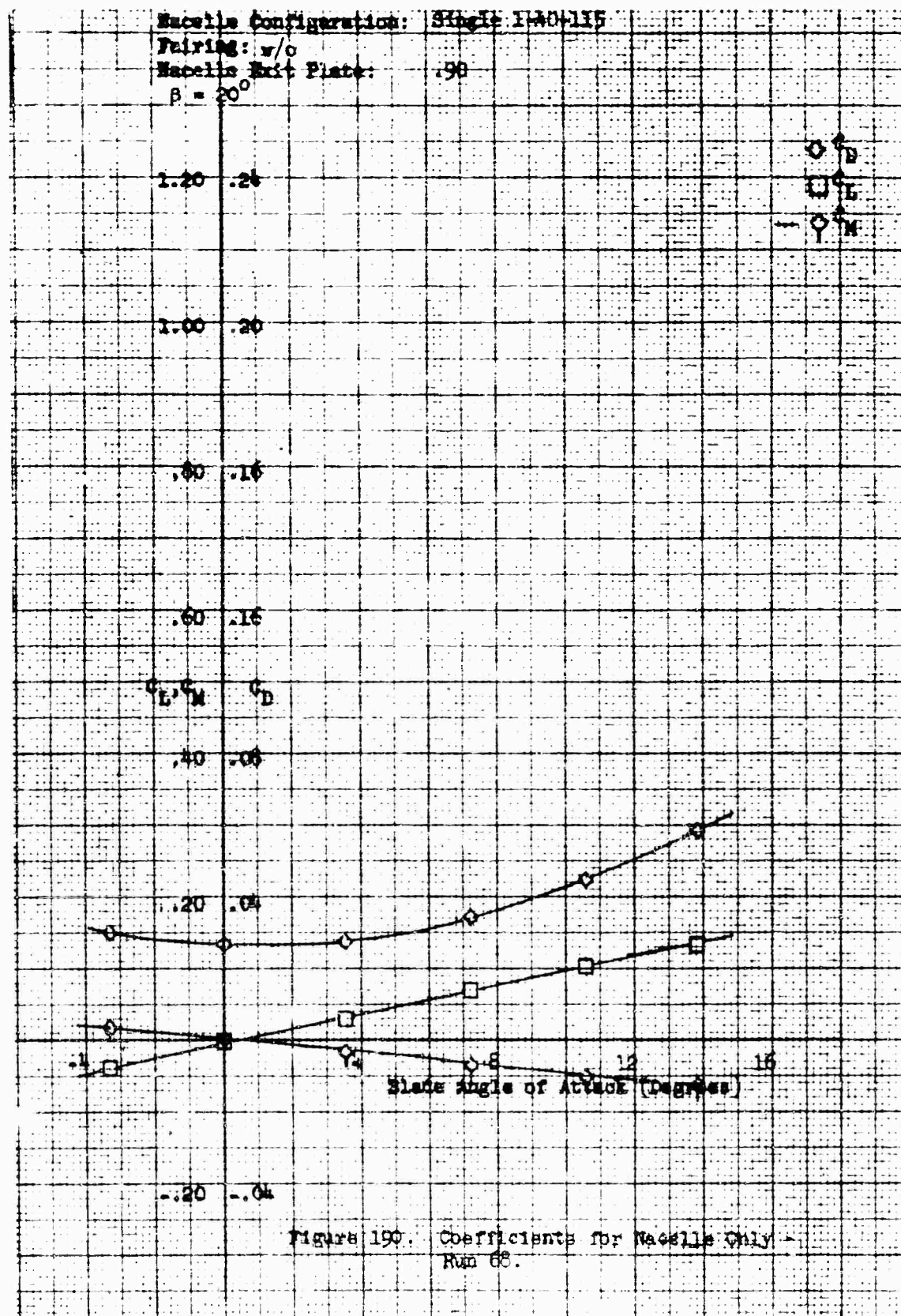


Figure 189. Coefficients for Combined Macelle and
 Blade - Run 67.



Nacelle Configuration: Single 1-40-115

Nacelle Incidence Angle: 0

Fairing: w/o

Nacelle Exit Plate: .90

$\beta = 20^\circ$

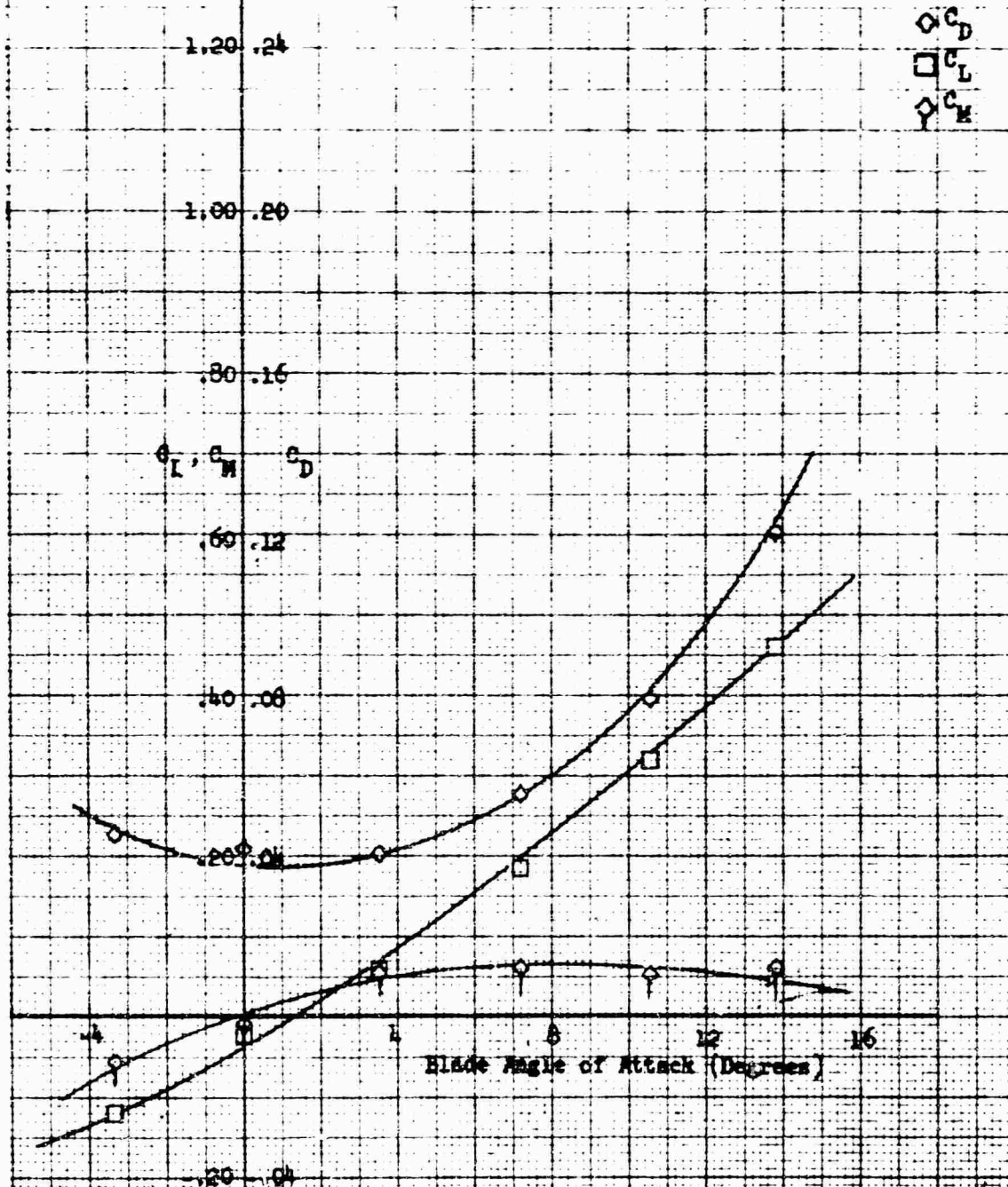


Figure 191. Coefficients for Combined Nacelle and Blade - Run 68

Nozzle Configuration: **Single 1-40-115**
 Pairing: **v/b**
 Nozzle Exit Plane: **.90**
 $\beta = 10^\circ$

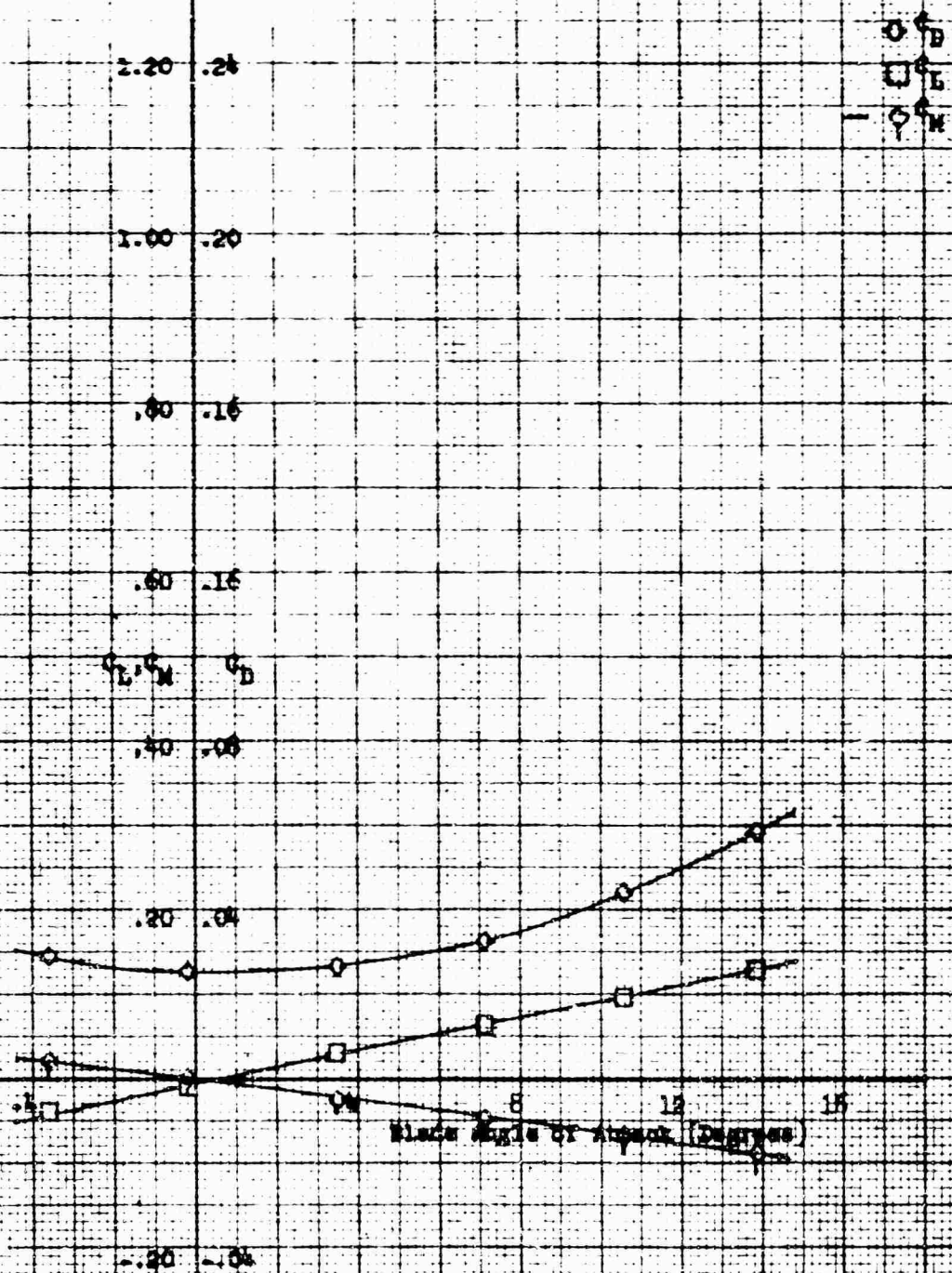


Figure 192. Coefficients for Nozzle Only -
 Run 69.

Nacelle Configuration: Single 1-40-115

Nacelle Incidence Angle: 0

Pairing: w/o

Nacelle Exit Plate: .90

$\beta = 10^\circ$

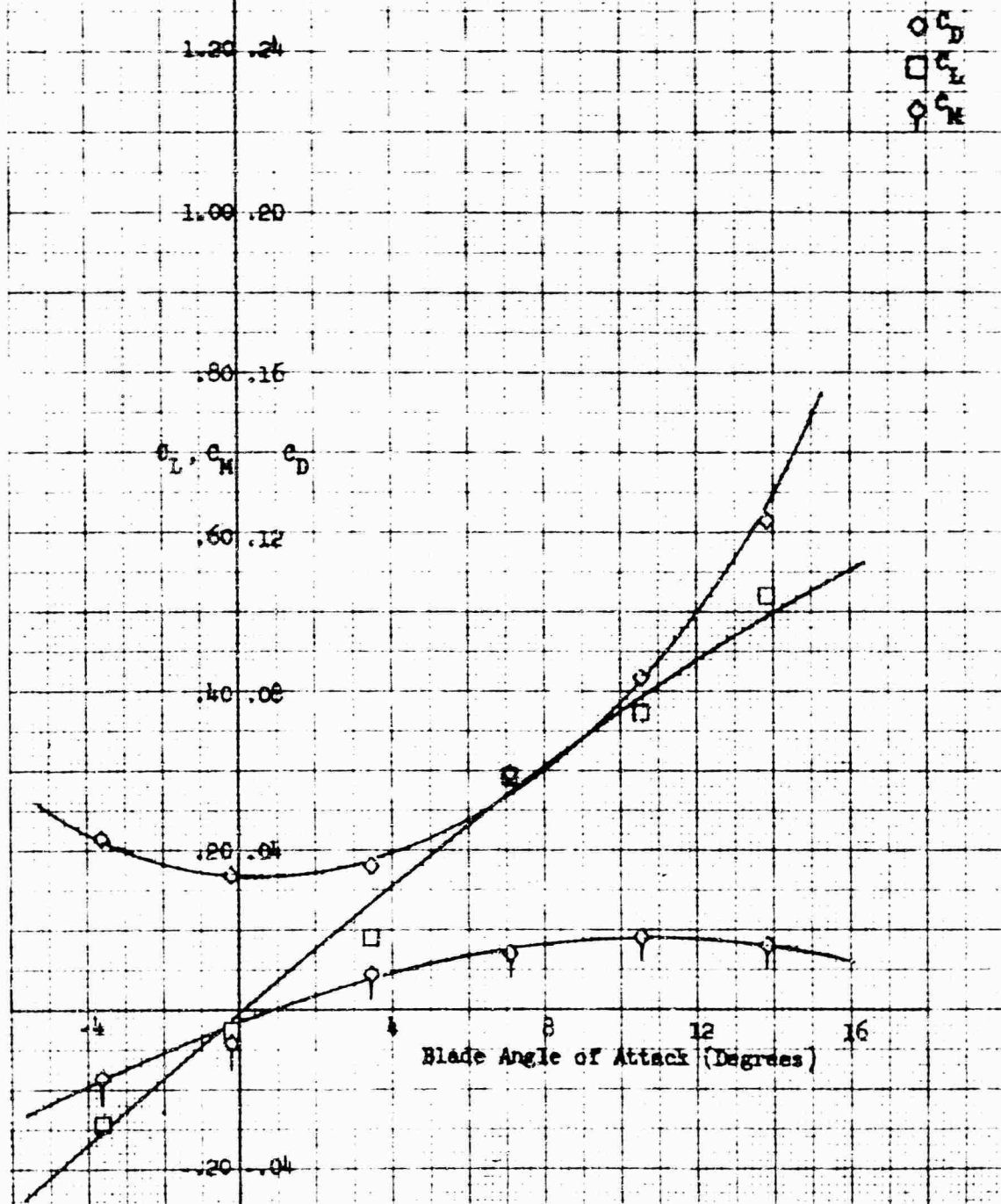


Figure 193. Coefficients for Combined Nacelle and Blade - Run 69.

Nacelle Configuration: Single 1-40-115
 Pairing: v/o
 Nacelle Exit Plate: .90
 B = 0

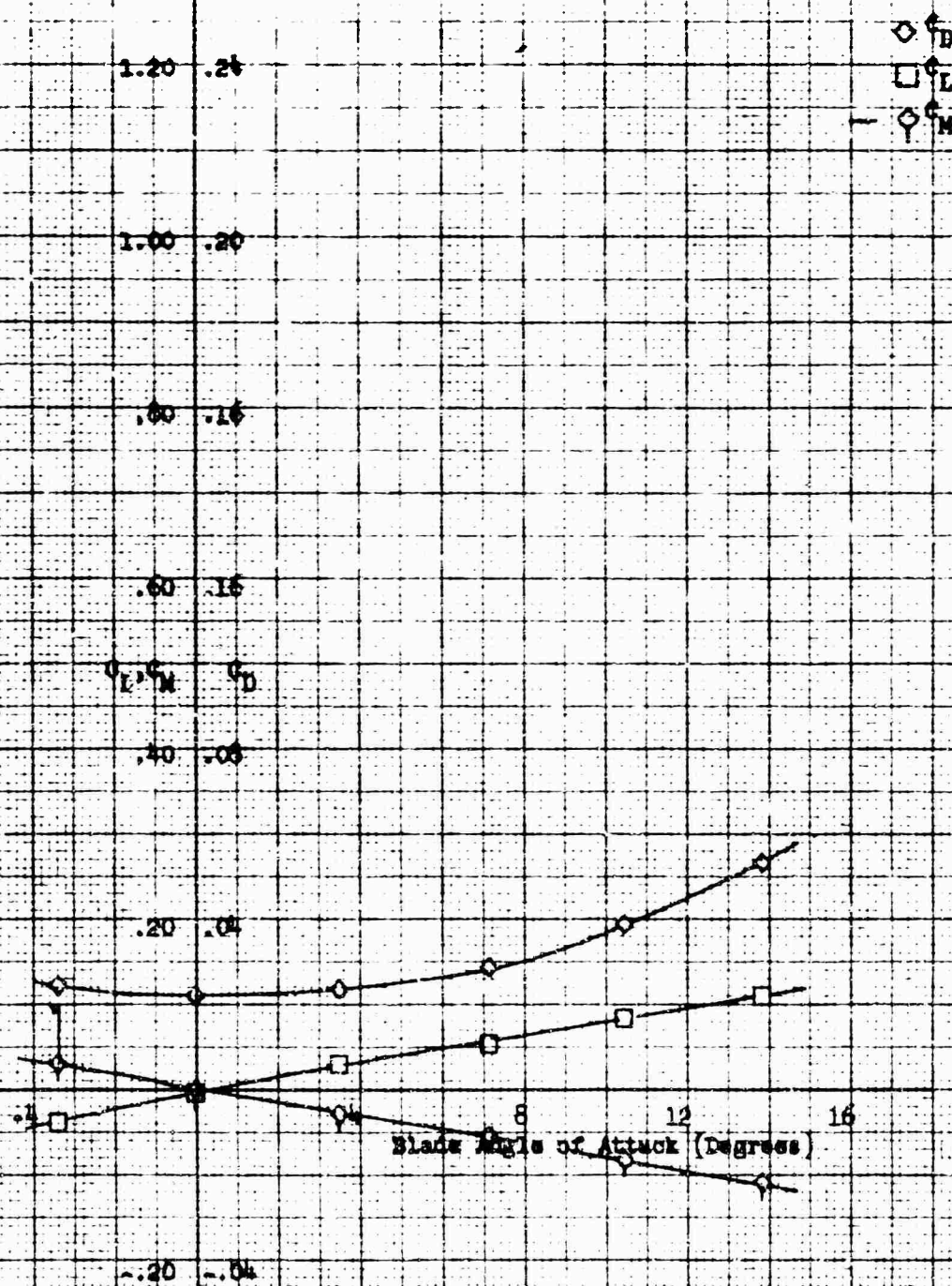


FIGURE 19. Coefficients for Nacelle Only -
 Run 70.

Nacelle Configuration: Single 1-40-215

Nacelle Incidence Angle: 0

Fairing: w/o

Nacelle Exit Plate: .90

B = 0

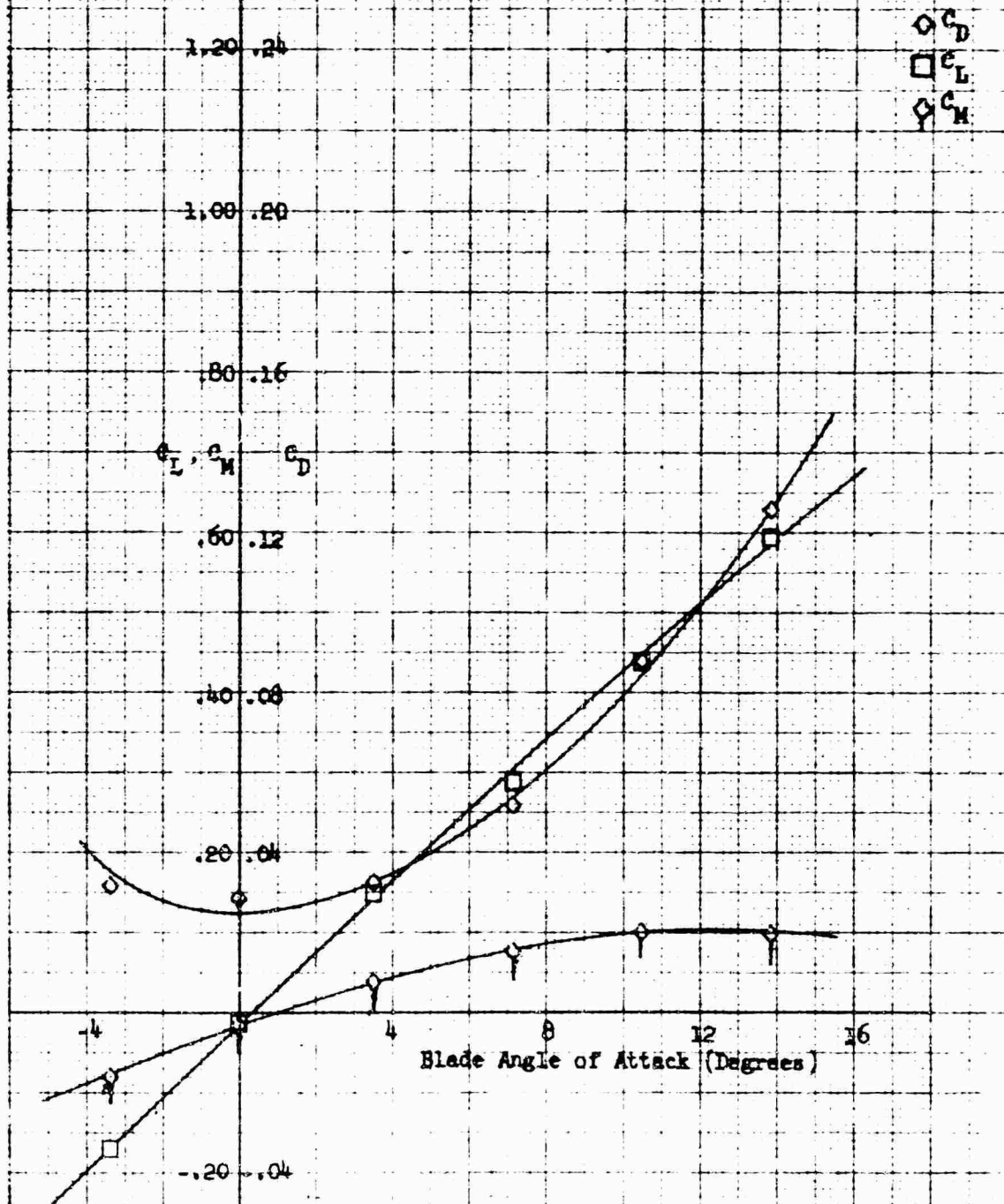
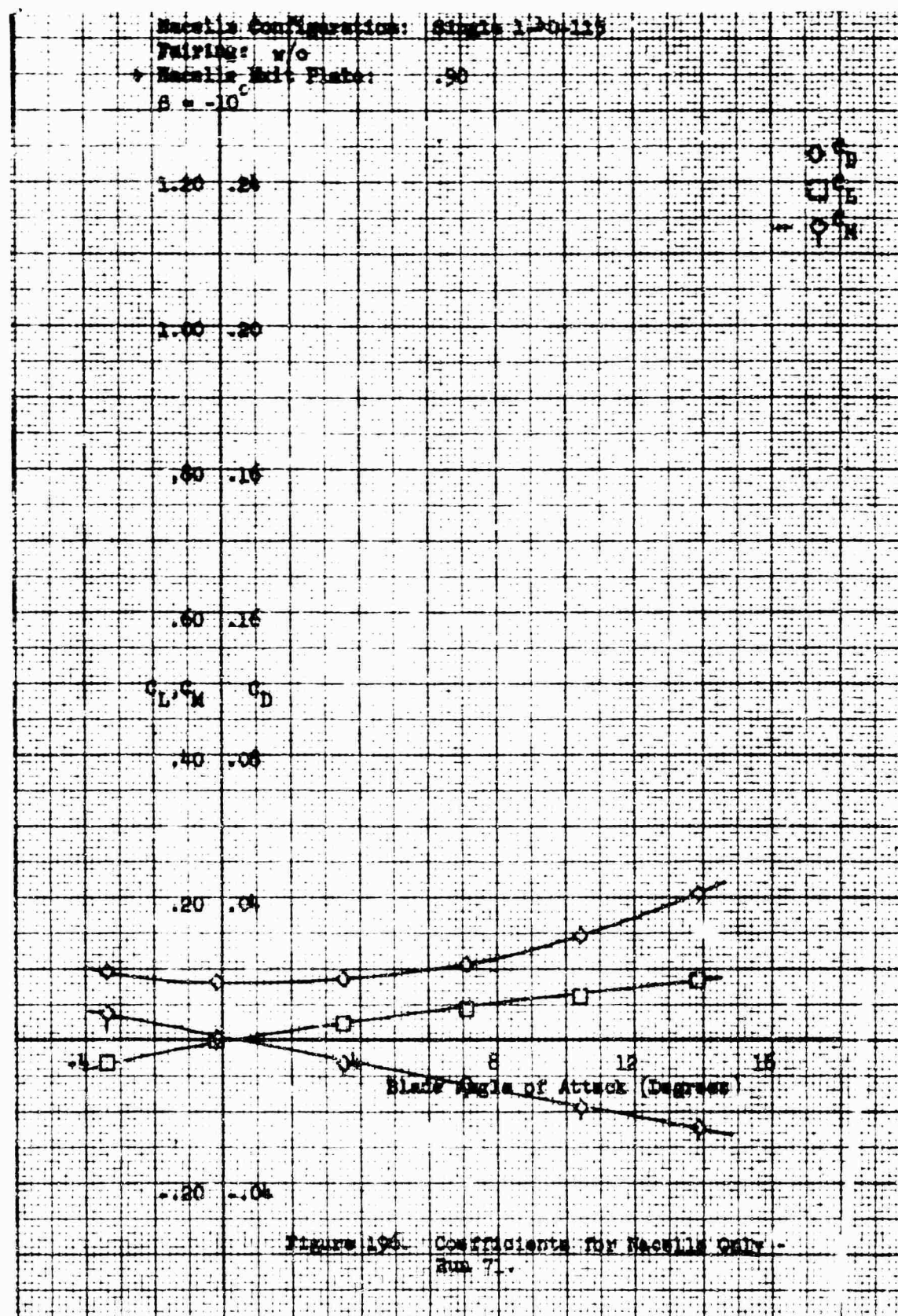


Figure 195. Coefficients for Combined Nacelle and Blade - Run 70.



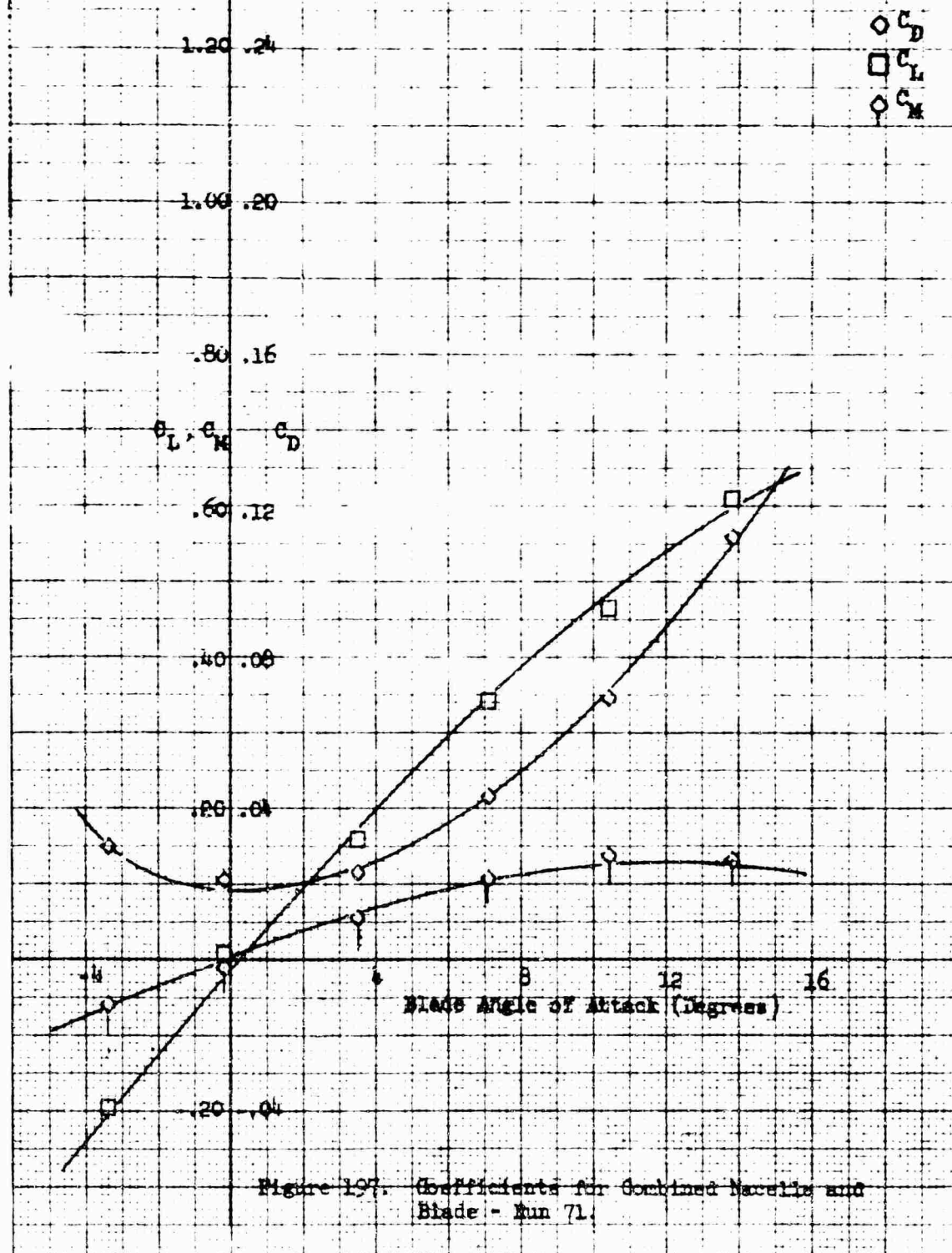
Nacelle Configuration: Single 1-40-115

Nacelle Incidence Angle: 0

Pairing: 4/6

Nacelle Exit Plane: 90

$\beta = -10^\circ$



Blade Configuration: Single 1-10-115

Twisting: π/c

Blade Exit Plate: .50

$\beta = -20^\circ$

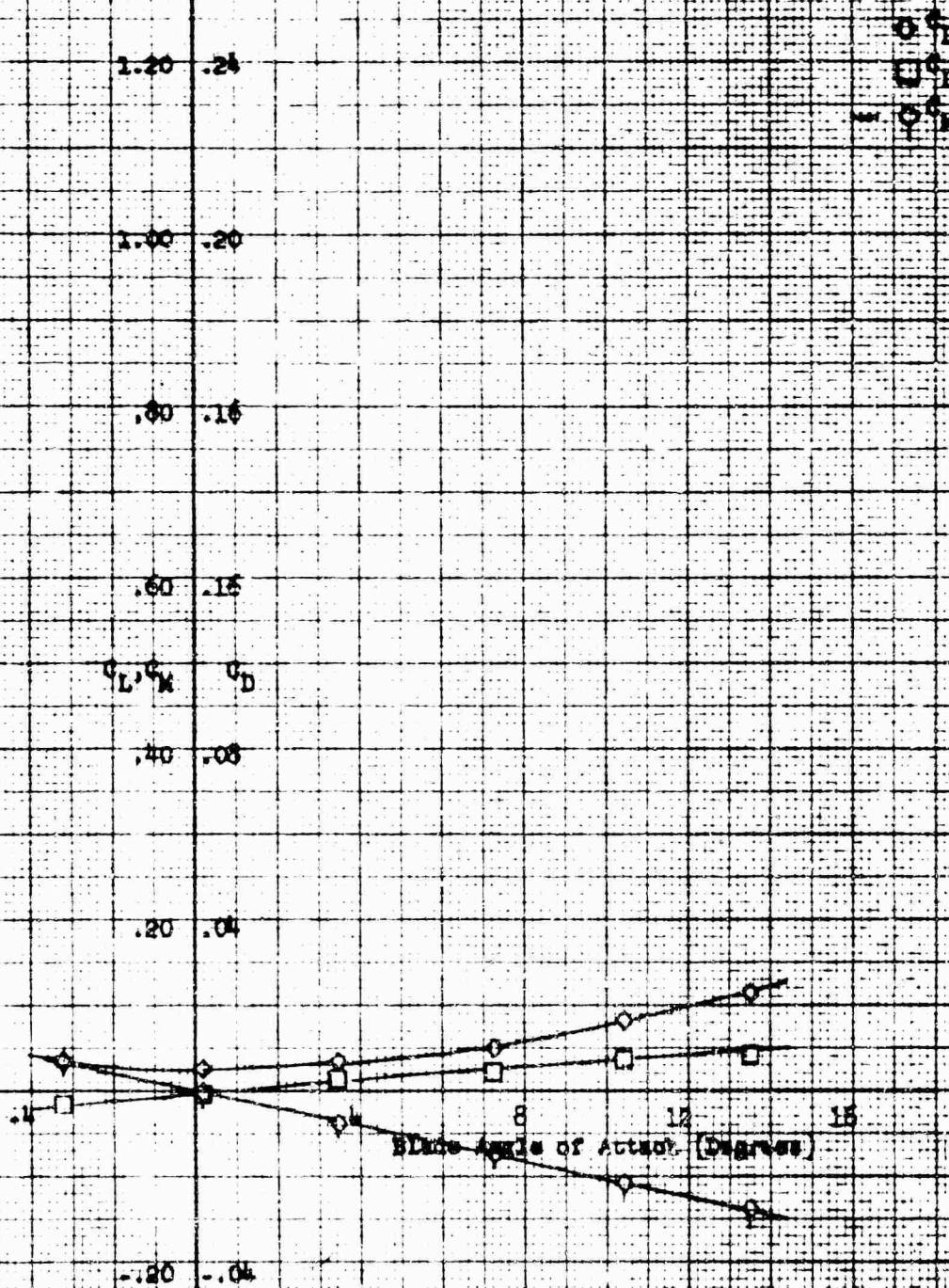


Figure 198. Coefficients for Blade Only.
Run 72.

Nacelle Configuration: Single 2-40-125

Nacelle Incidence Angle: 0

Fairing: w/c

Nacelle Exit Plate: .90

$\beta = -20^\circ$

1.20 .24

$\diamond C_D$
 $\square C_L$
 $\diamond C_M$

1.00 .20

.80 .16

C_L, C_M, C_D

.60 .12

.40 .08

.20 .04

Blade Angle of Attack (Degrees)

.20 .04

Figure 199. Coefficients for Combined Nacelle and Blade - Run 72.

Wacelle Configuration: Single 1-40-113

Pairing: w/o

Wacelle Exit Plate: 0

$\beta = 20^\circ$

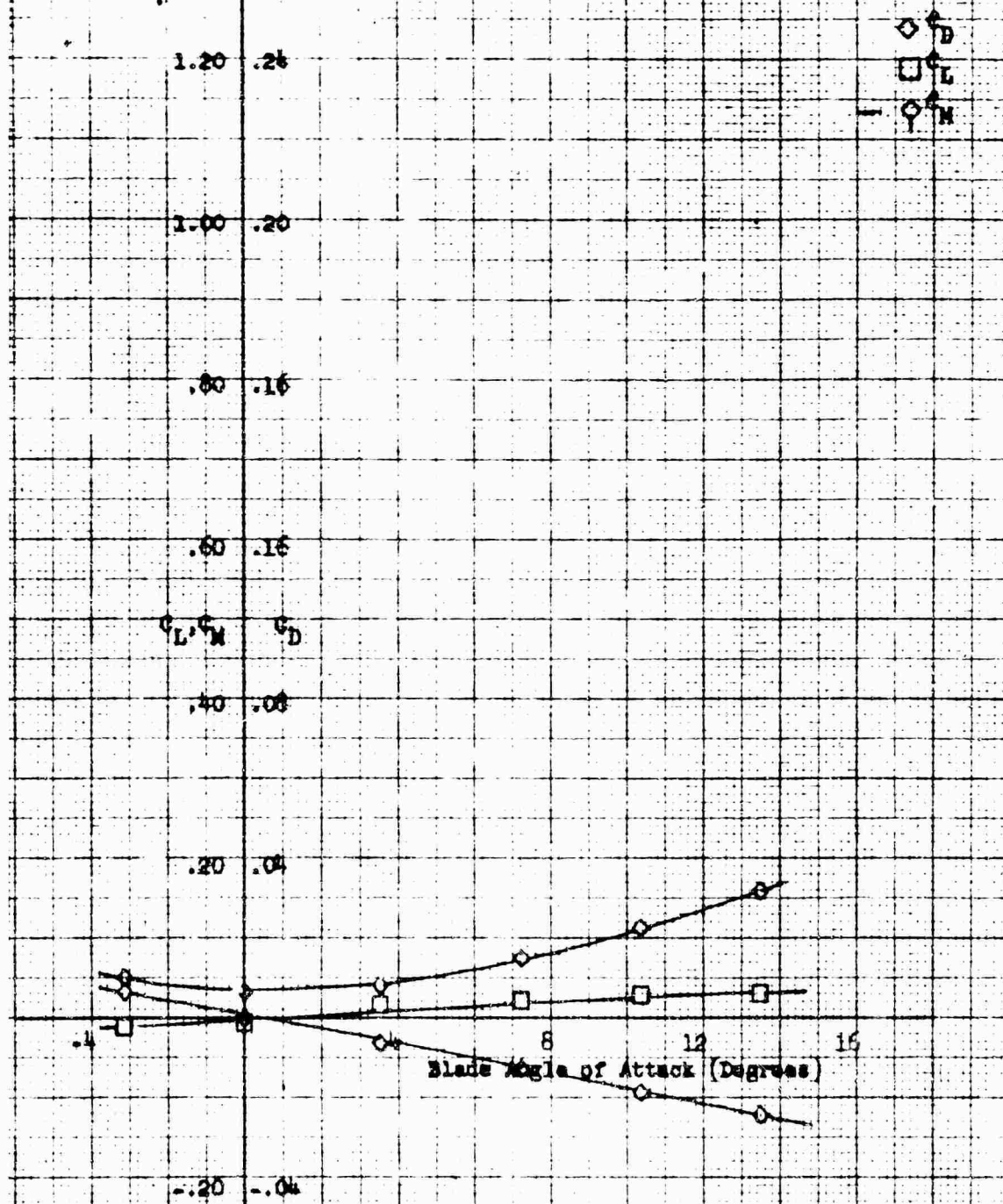


Figure 200. Coefficients for Wacelle Only - Run 73.

Nacelle Configuration: Single 1-40-115

Nacelle Incidence Angle: 0

Fairing: w/o

Nacelle Exit Plate: 0

$\beta = 20^\circ$

1.20 .24

C_D
 C_L
 C_M

1.00 .20

.80 .16

C_L, C_M, C_D

.60 .12

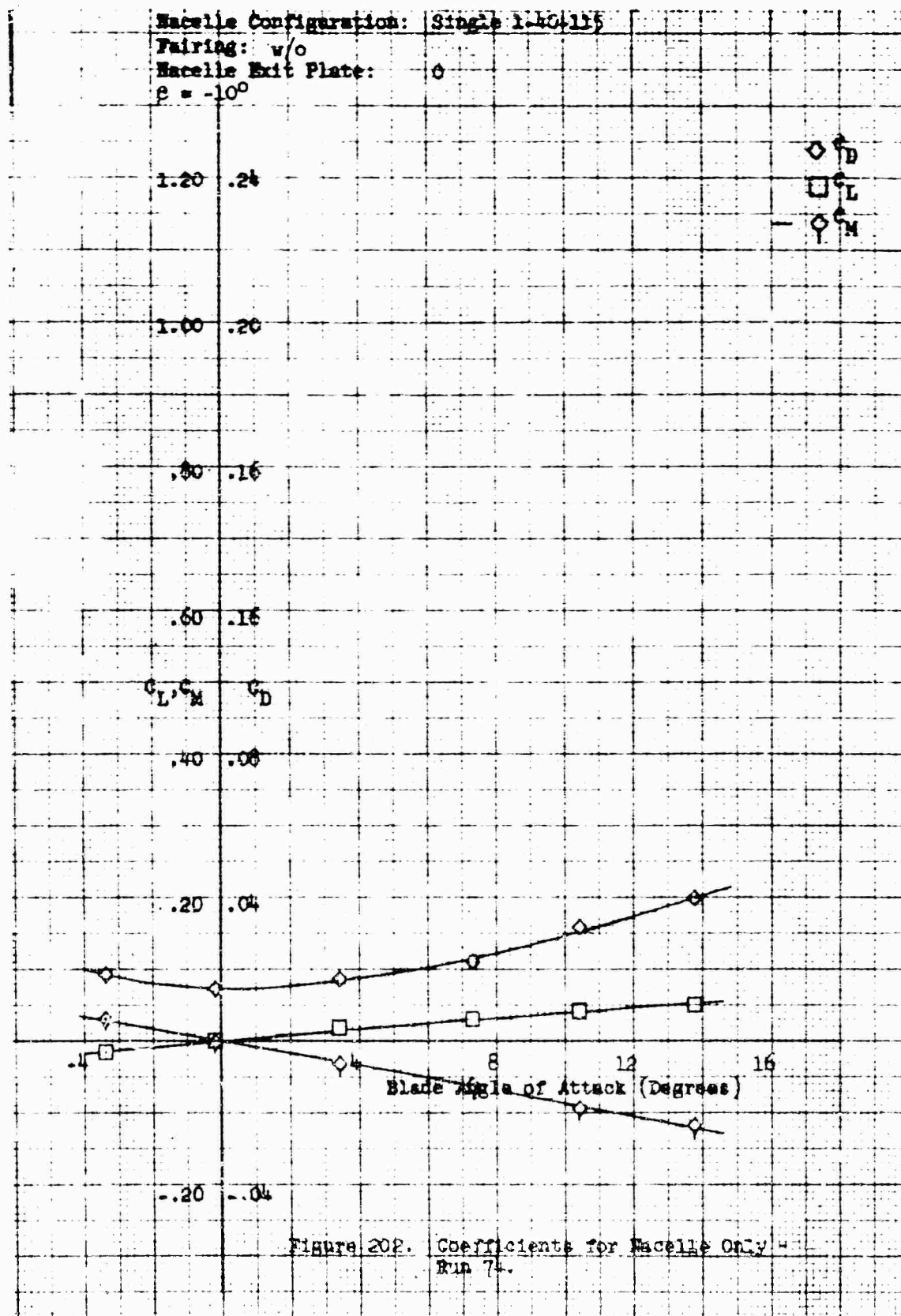
.40 .08

.20 .04

Blade Angle of Attack (Degrees)

-.20 .04

Figure 20. Coefficients for Combined Nacelle and Blade - Run 73.



Nacelle Configuration: Single 1-40-115

Nacelle Incidence Angle: 0

Pairing: w/o

Nacelle Exit Plate: C

$\beta = -10^\circ$

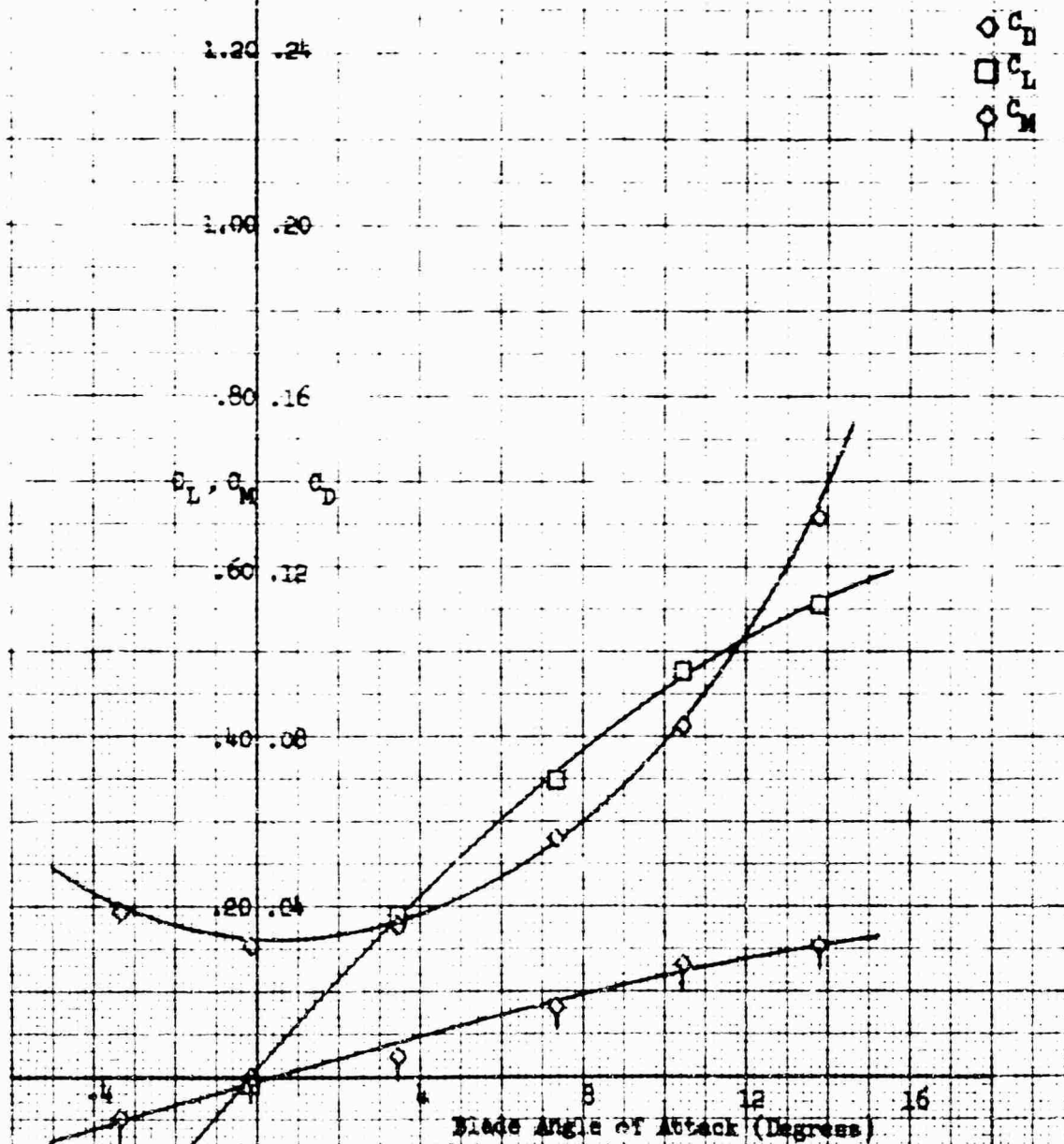


Figure 205. Coefficients for Combined Nacelle and Blade - Run 74.

Macelle Configuration: Series 1-40-115
 Fairing: w/o
 Macelle Exit Plate: 6
 $\beta = 0$

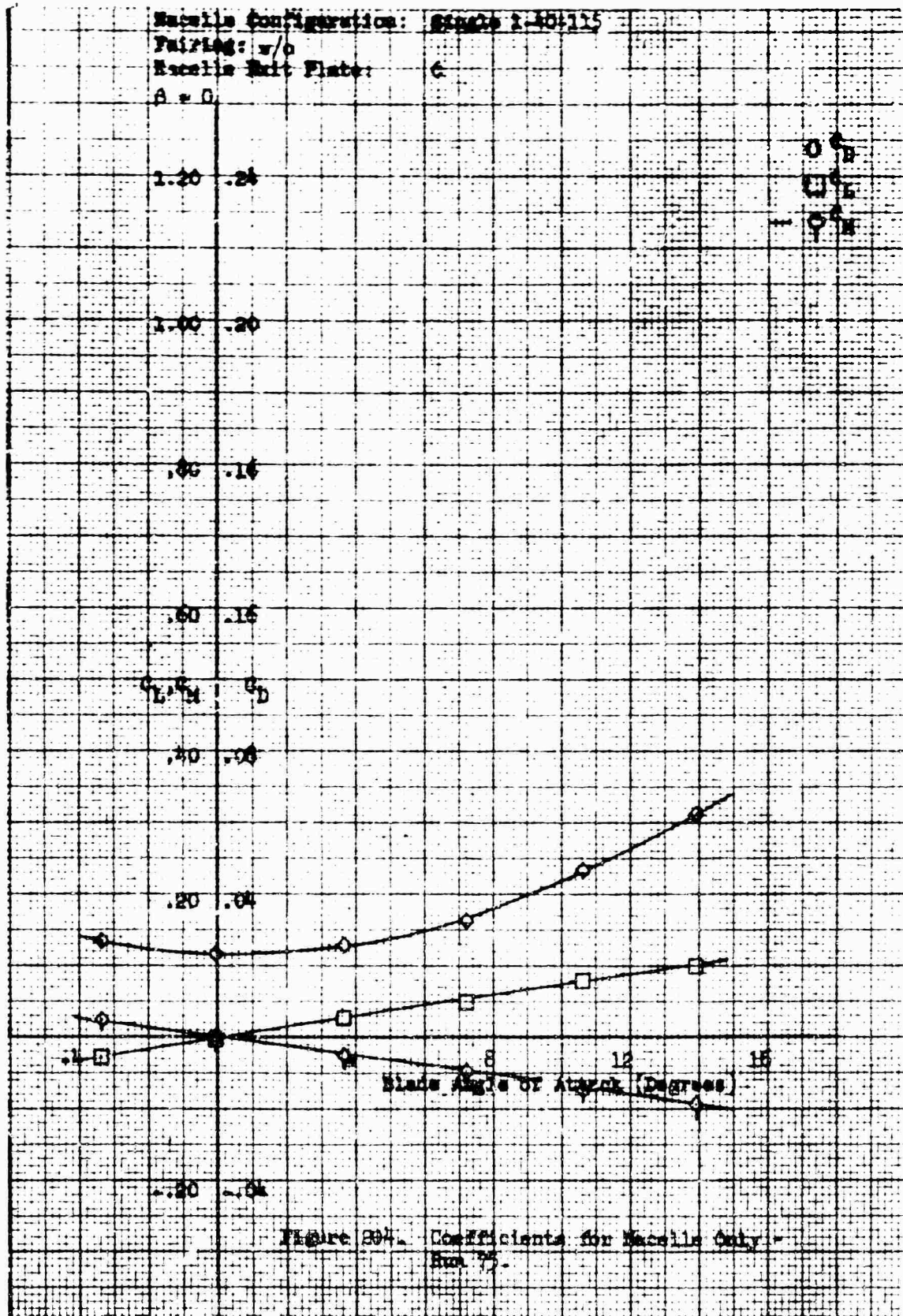


Figure 804. Coefficients for Macelle Only - Run 75.

Nacelle Configuration: Single 1-40-125

Nacelle Incidence Angle: 0

Fairing: w/o

Nacelle Exit Plane: 0

$\alpha = 0$

1.20 .28

1.00 .20

.80 .16

C_L, C_M, C_D

.60 .12

.40 .08

.20 .04

-.20 .04

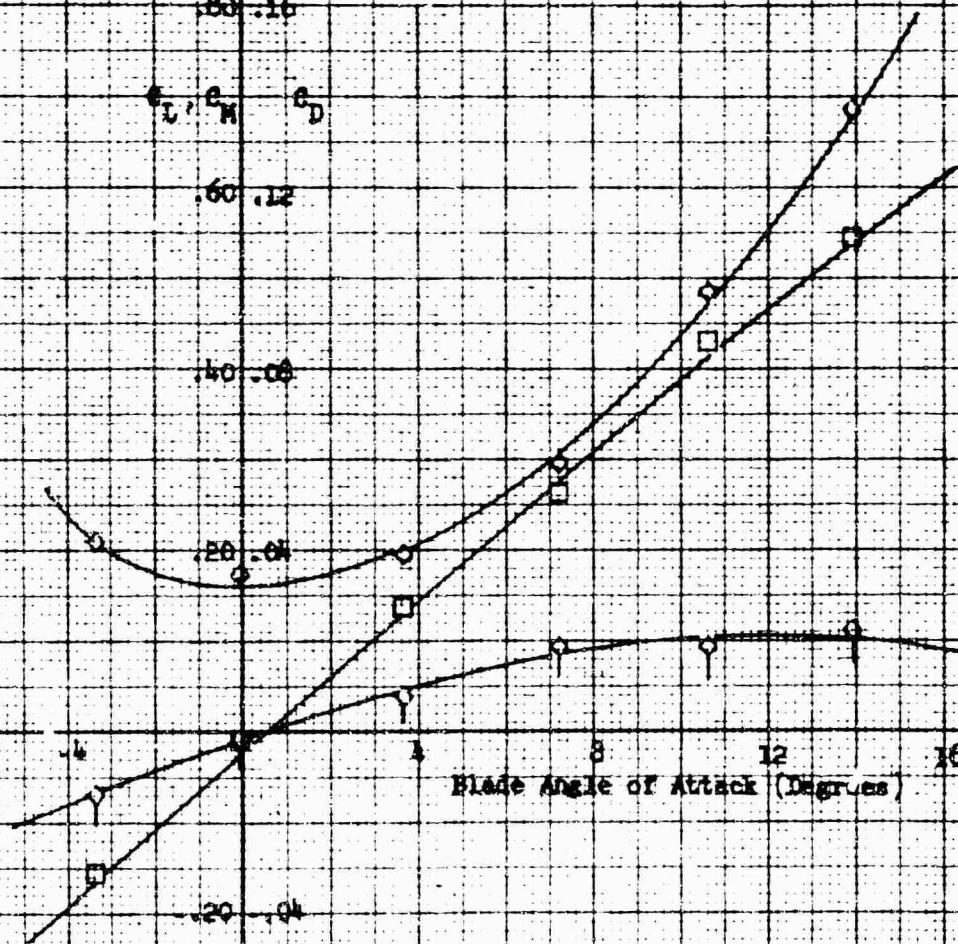
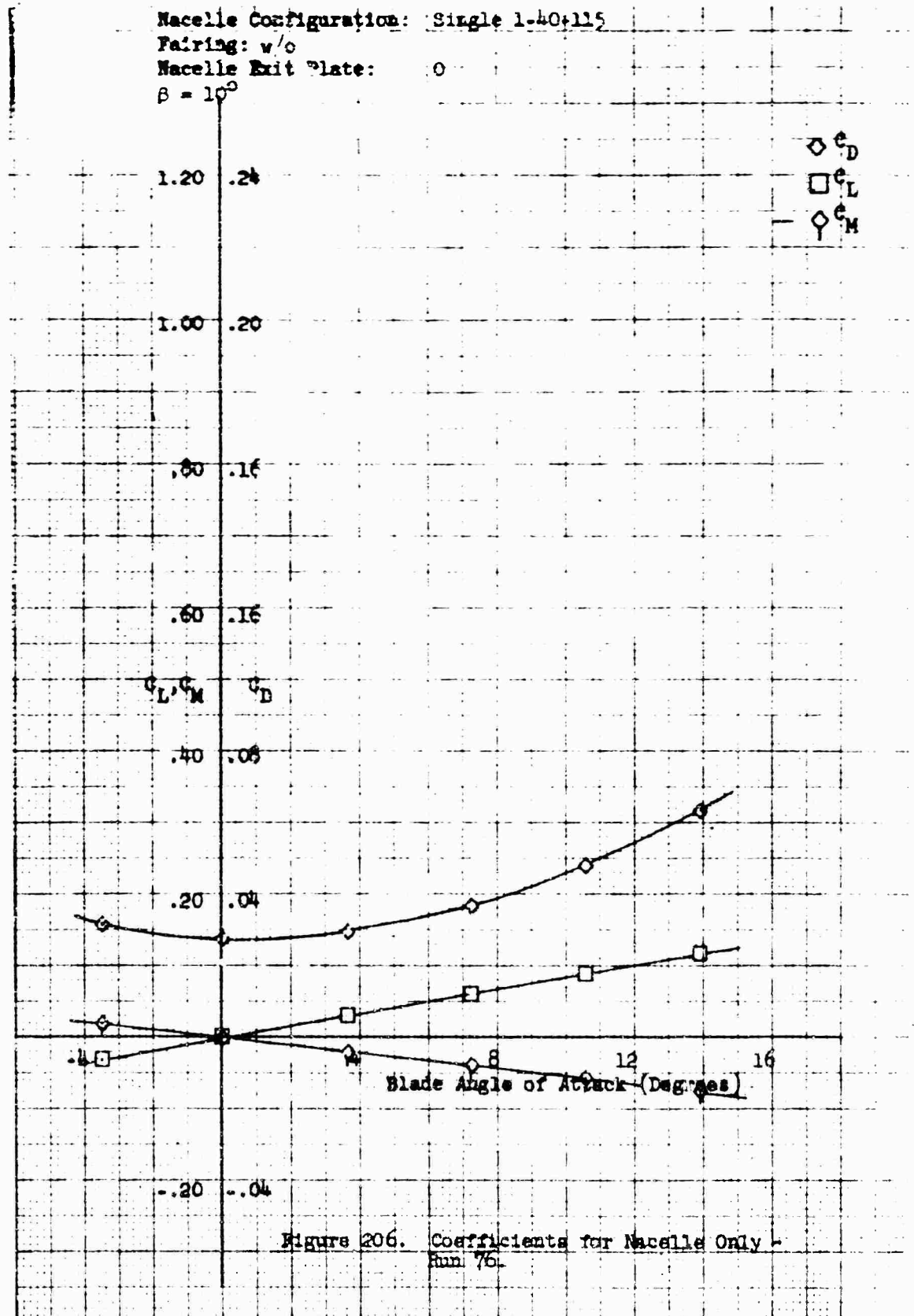


Figure 205. Coefficients for Combined Nacelle and Blade - Run 75.

Nacelle Configuration: Single 1-40+115
 Pairing: w/o
 Nacelle Exit Plate: 0
 $\beta = 10^\circ$



Wacelle Configuration: Single A-10-115

Wacelle Incidence Angle: 0

Pairing: w/o

Wacelle Exit Plane: 0

$\beta = 10^\circ$

1.20 .20

1.00 .20

.80 .15

C_L, C_M, C_D

.60 .12

.40 .08

.20 .04

.4

Blade Angle of Attack (Degrees)

.20 .04

Figure 207. Coefficients for Combined Wacelle and Blade - Run 76.

Macelle Configuration: $\beta = 20^\circ$
 Fairing: w/o
 Macelle Exit Plate: 0

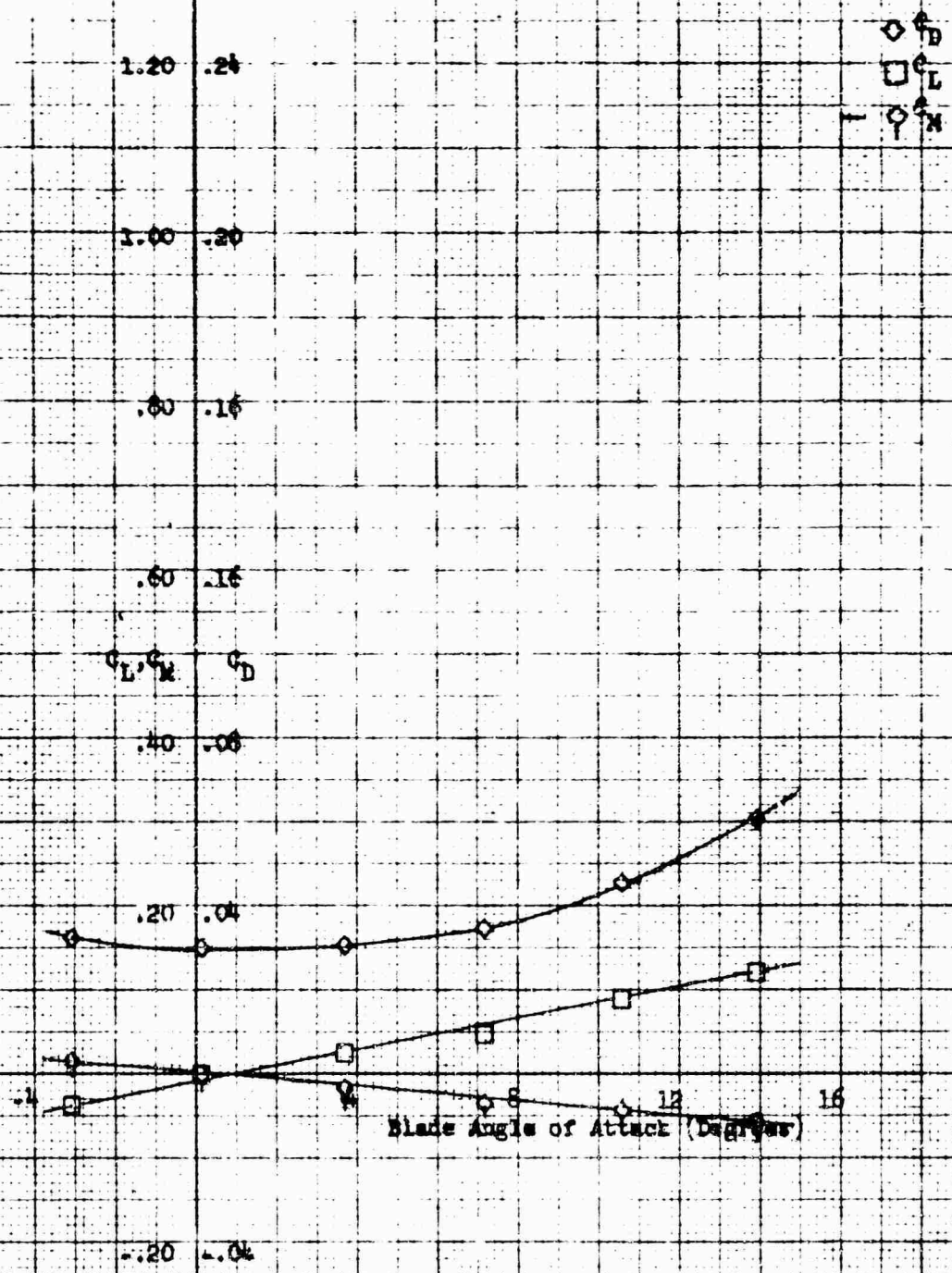


Figure 208. Coefficients for Macelle Only -
 Run 77.

Wacelle Configuration: Single 1-40-185

Wacelle Incidence Angle: 0

Pairing: w/o

Wacelle Exit Plane: 0

$\alpha = 20^\circ$

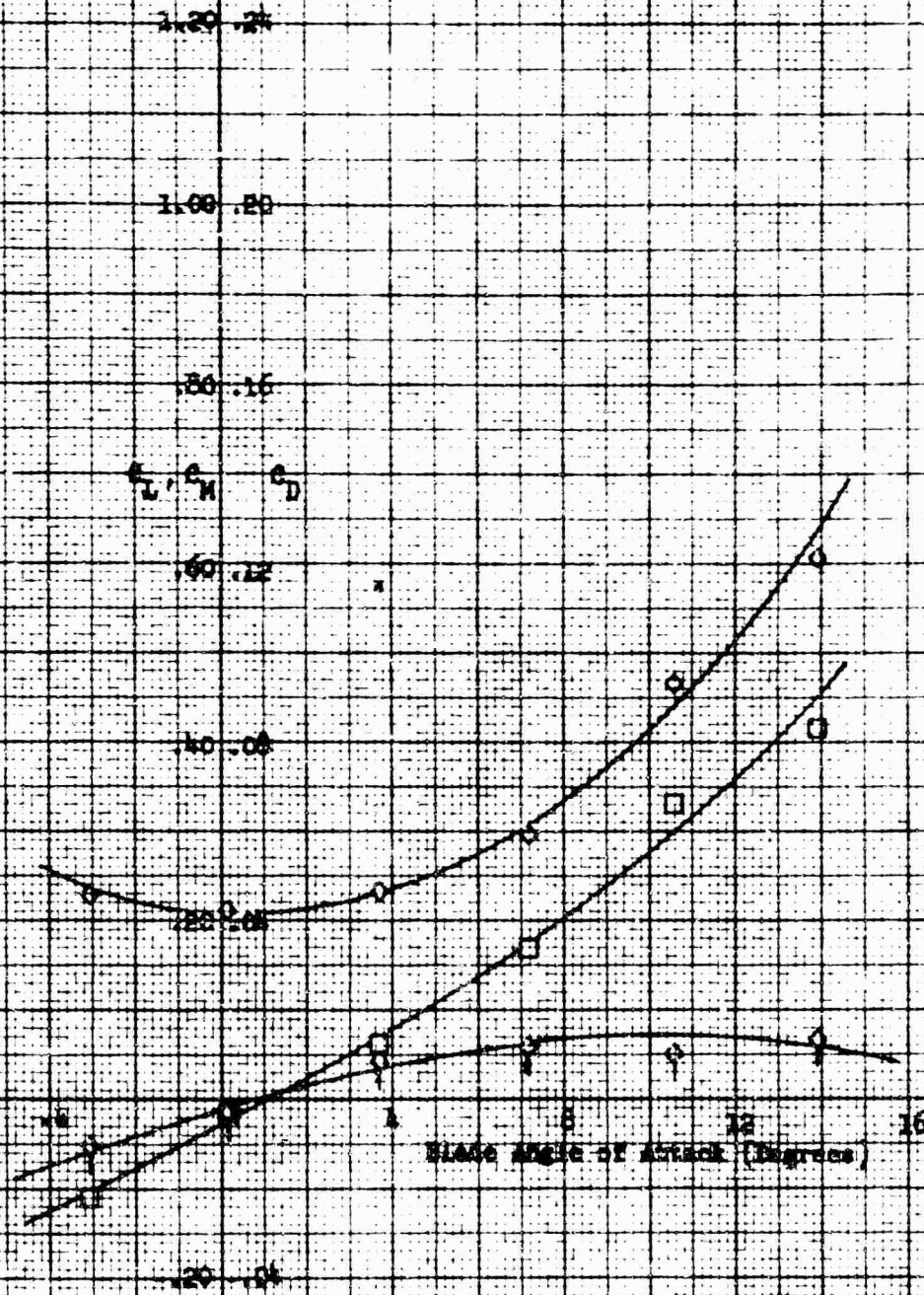


Figure 209. Coefficients for Combined Nacelle and Blade - Run 77

Racelle Configuration: 576416 1-43-130
 Fairing: w/o
 Racelle Exit Plate: 0
 $\delta = 20^\circ$

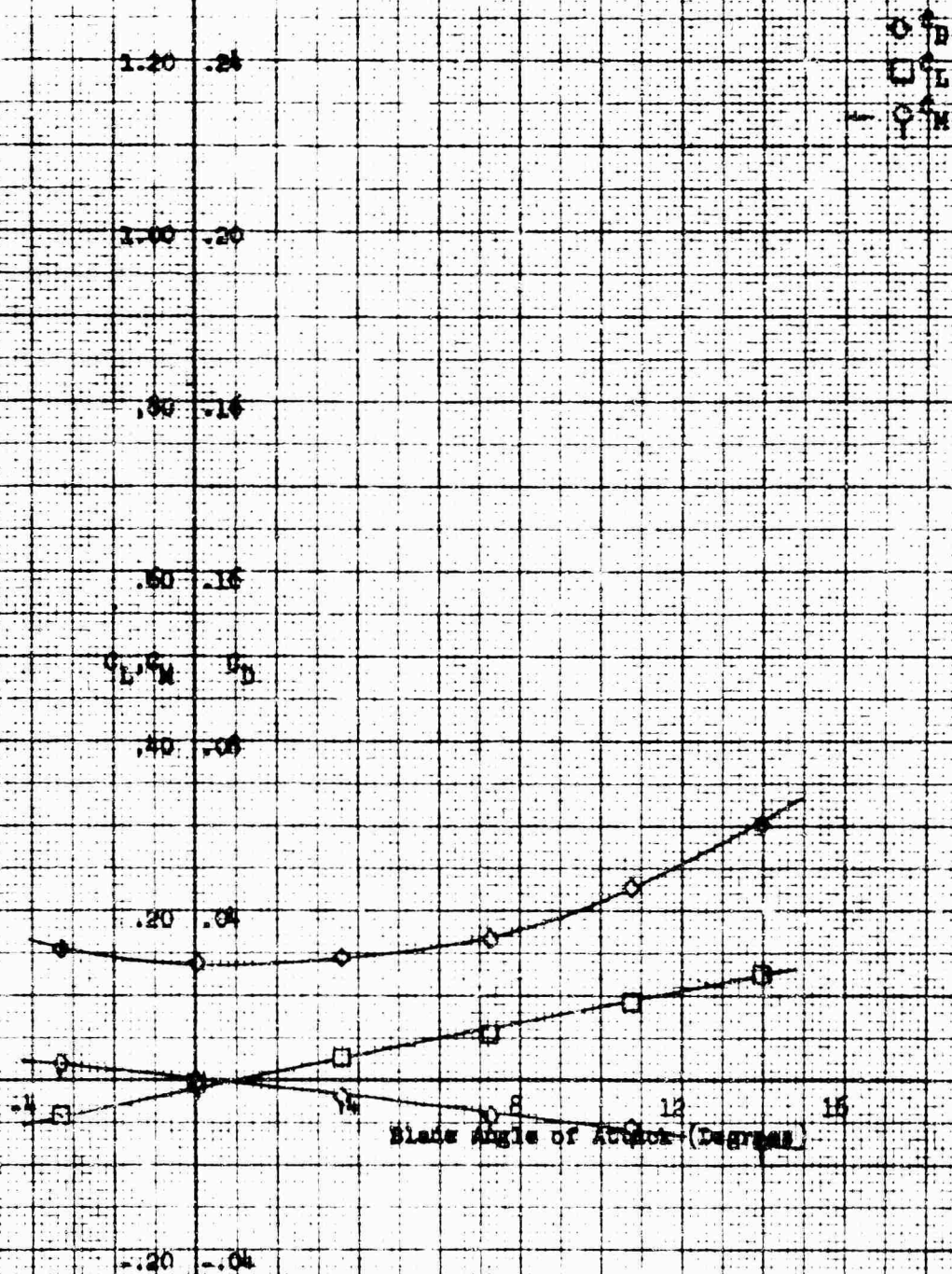


Figure 210. Coefficients for Racelle Only -
 Run 78.

Wacelle Configuration: Single 1-40-130

Wacelle Incidence Angle: 0

Wacelle: w/a

Wacelle Exit Plane: 0

$\beta = 20^\circ$

1.80 .24

1.00 .20

.80 .16

a_L, c_M, c_D

.60 .12

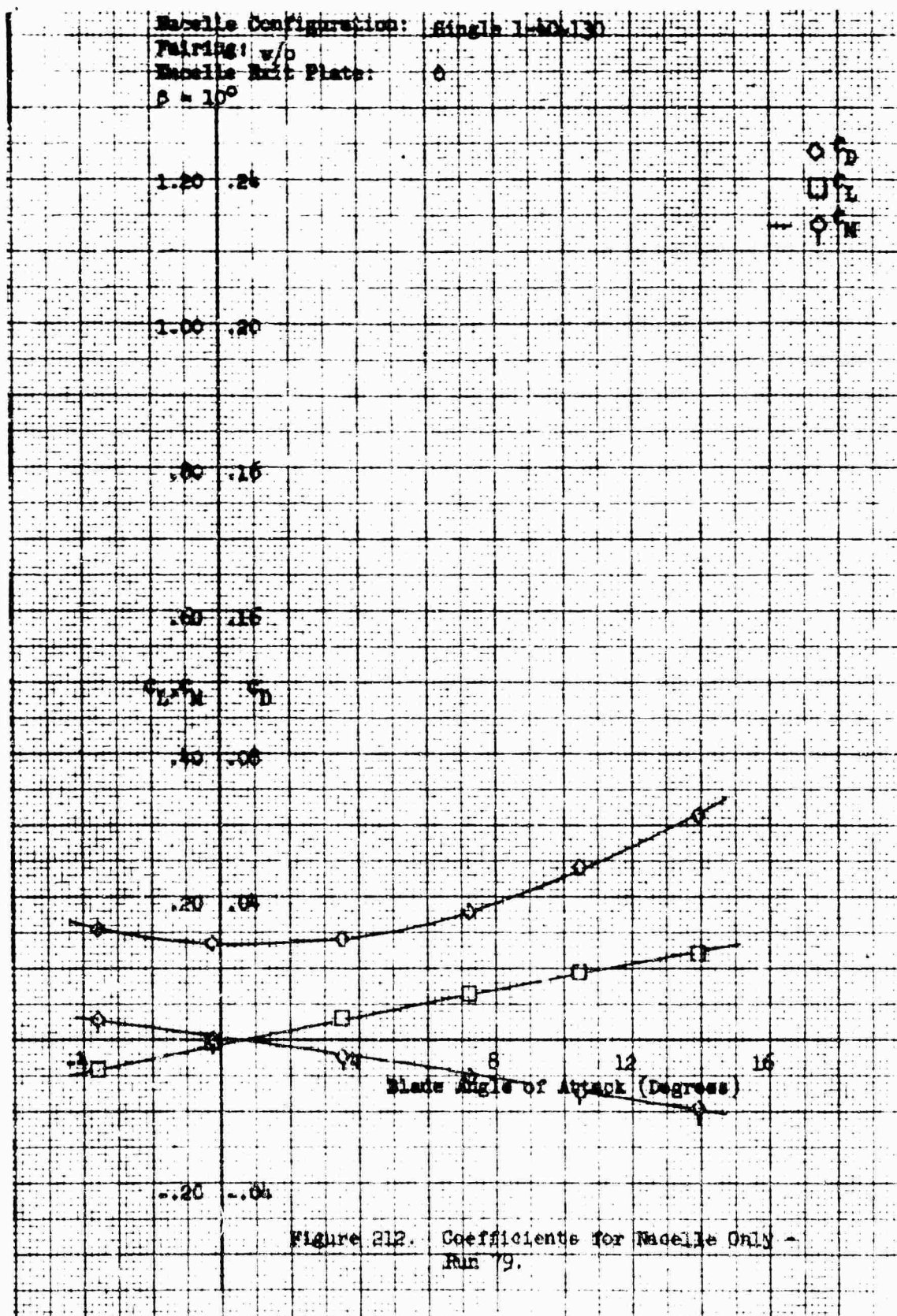
.40 .08

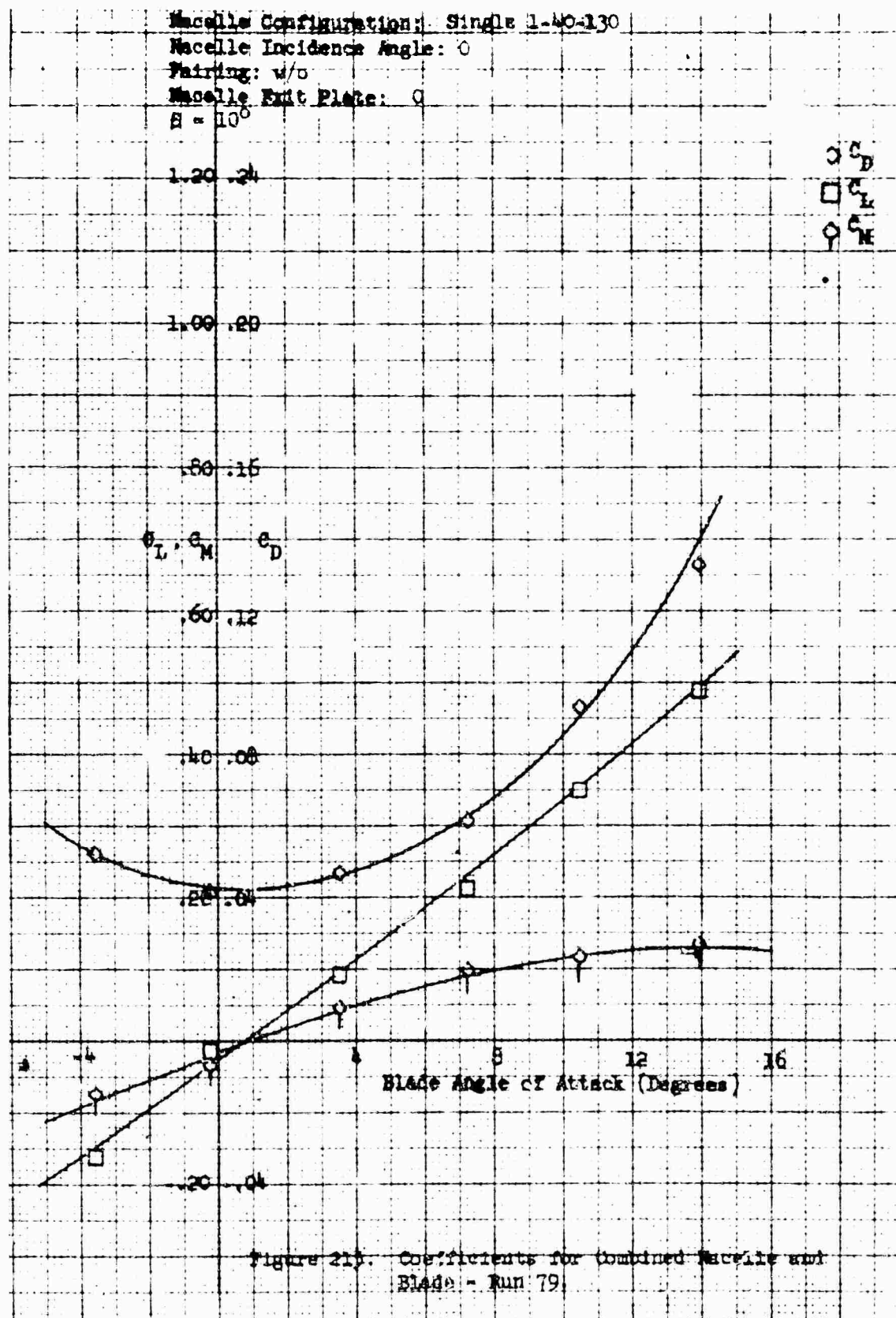
.20 .04

-.20 .04

Blade Angle of Attack (Degrees)

Figure 211. Coefficients for Combined Wacelle and Blade - Run 78.





Macelle Configuration: Single 1-40-130

Pairing: v/o

Macelle Exit Plate: 0

$\beta = 0$

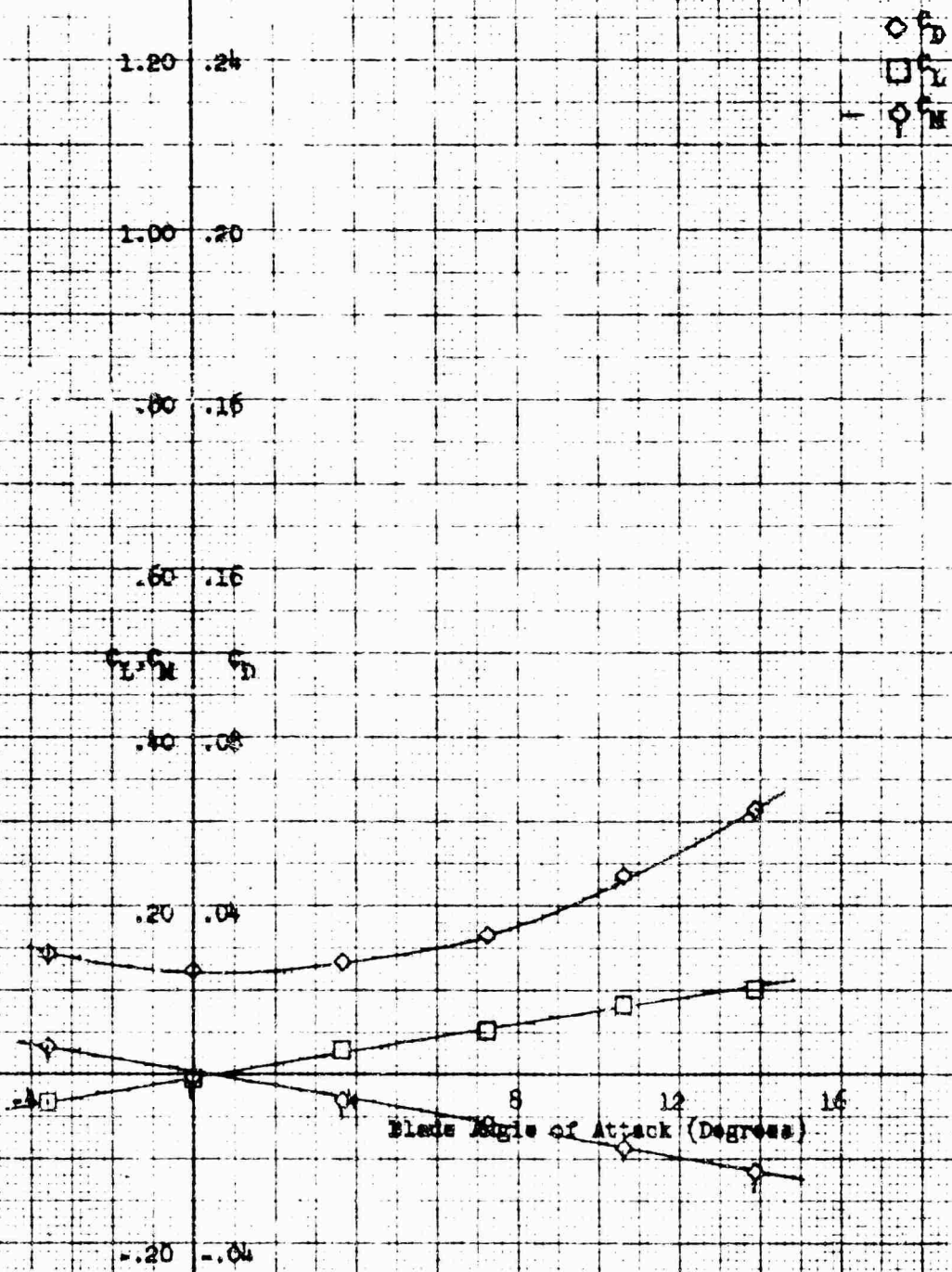
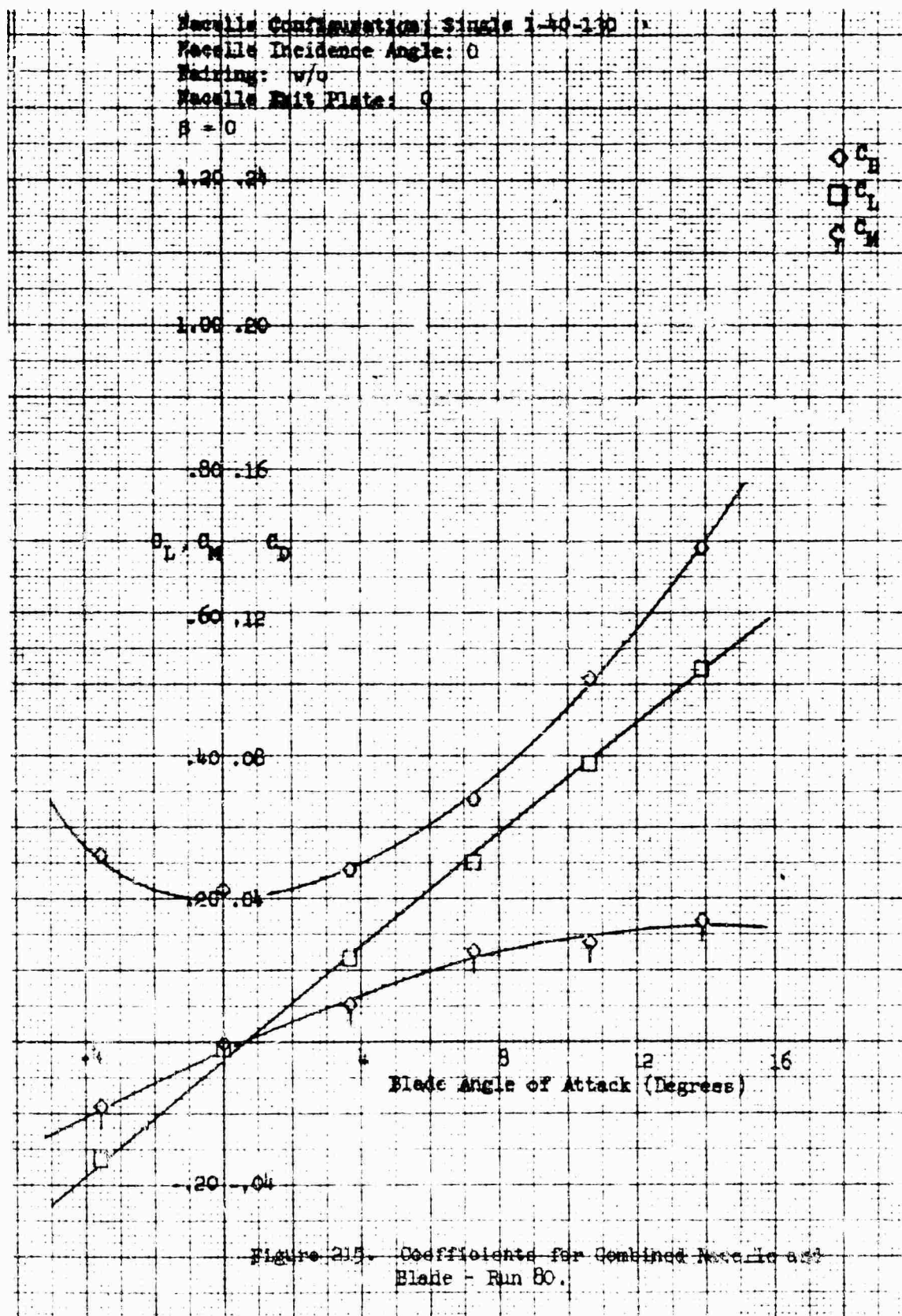
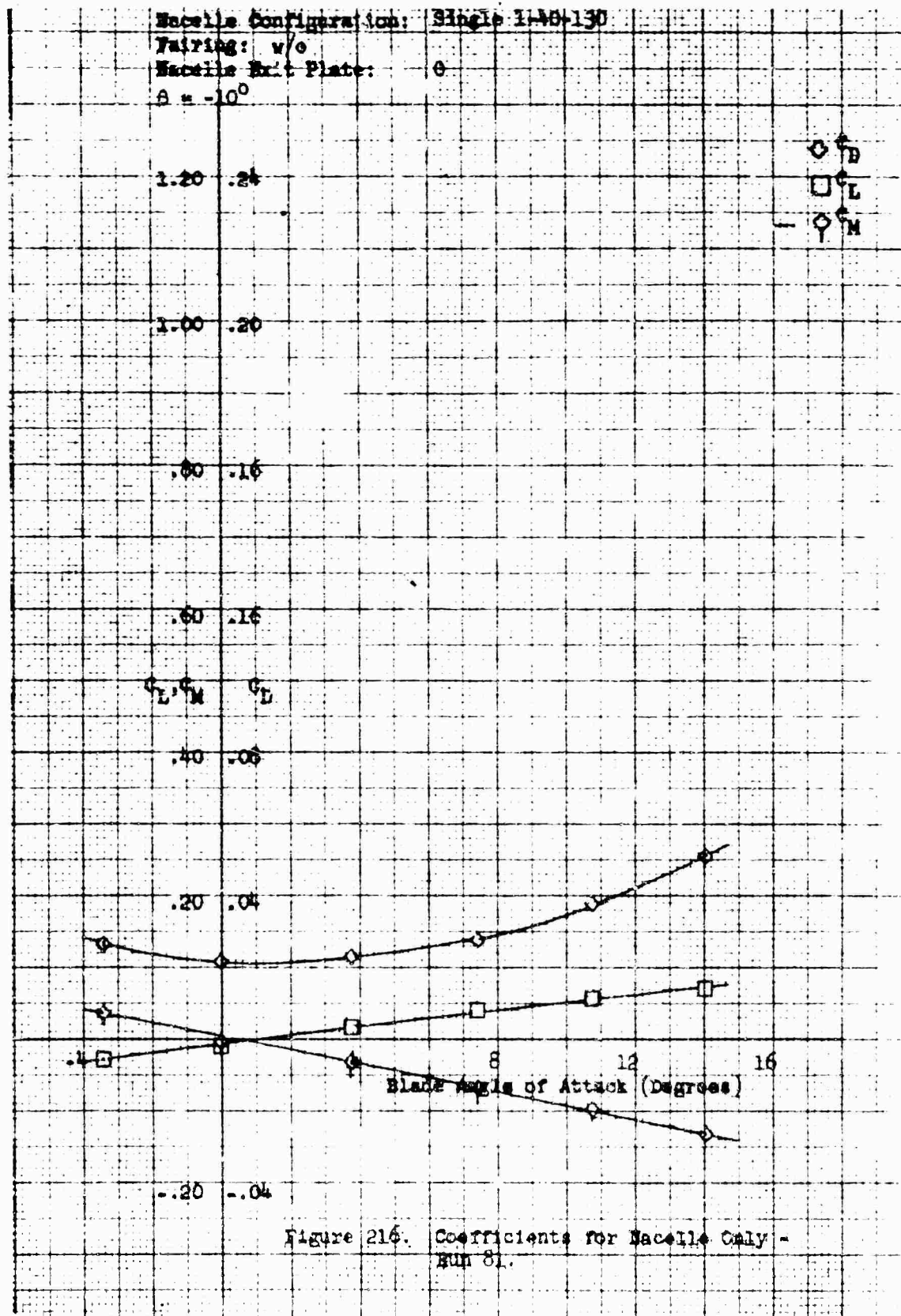


Figure 23. Coefficients for Macelle Only - Run 80.





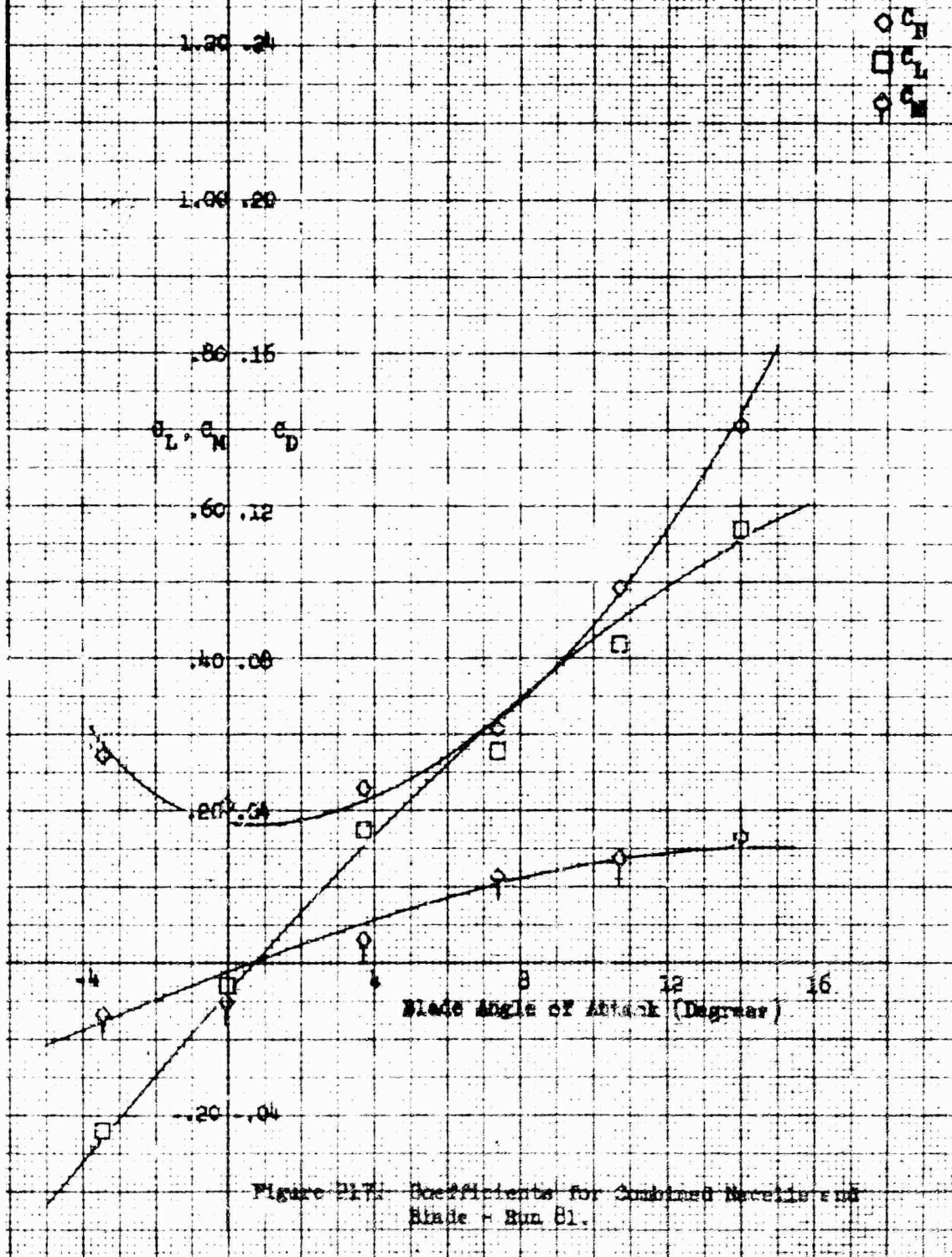
Macelle Configuration: Single 2-7-140

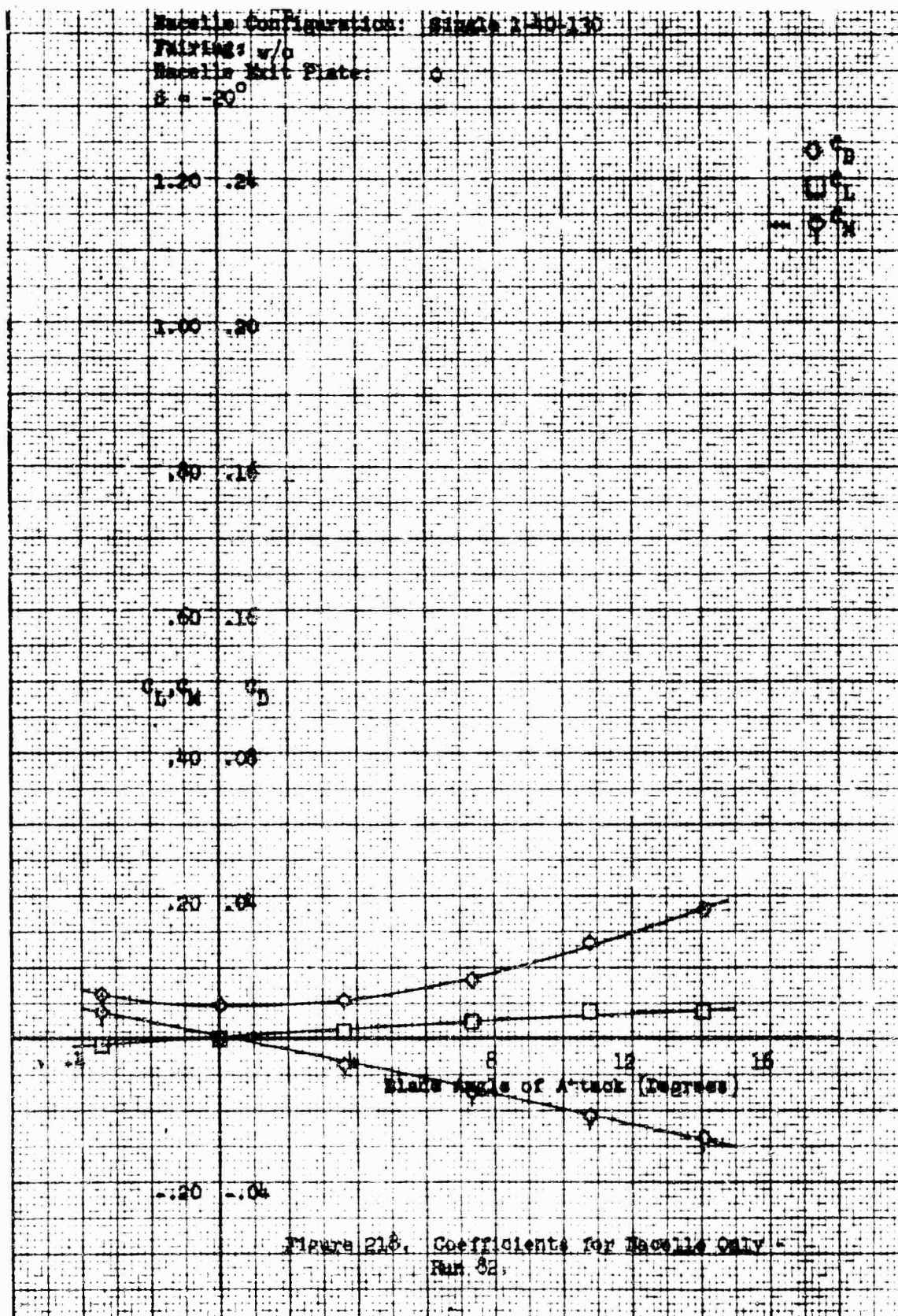
Macelle Incidence Angle: 0

Pairing: w/o

Macelle Exit Plane: 0

$\beta = -10^\circ$





Nozzle Configuration: Single 1-40-130

Nozzle Incidence Angle: 0

Pairing: w/c

Nozzle Exit Plane: 0

$\beta = -20^\circ$

1.20 .24

1.00 .20

.80 .16

C_L, C_M, C_D

.60 .12

.40 .08

.20 .04

.20 .04

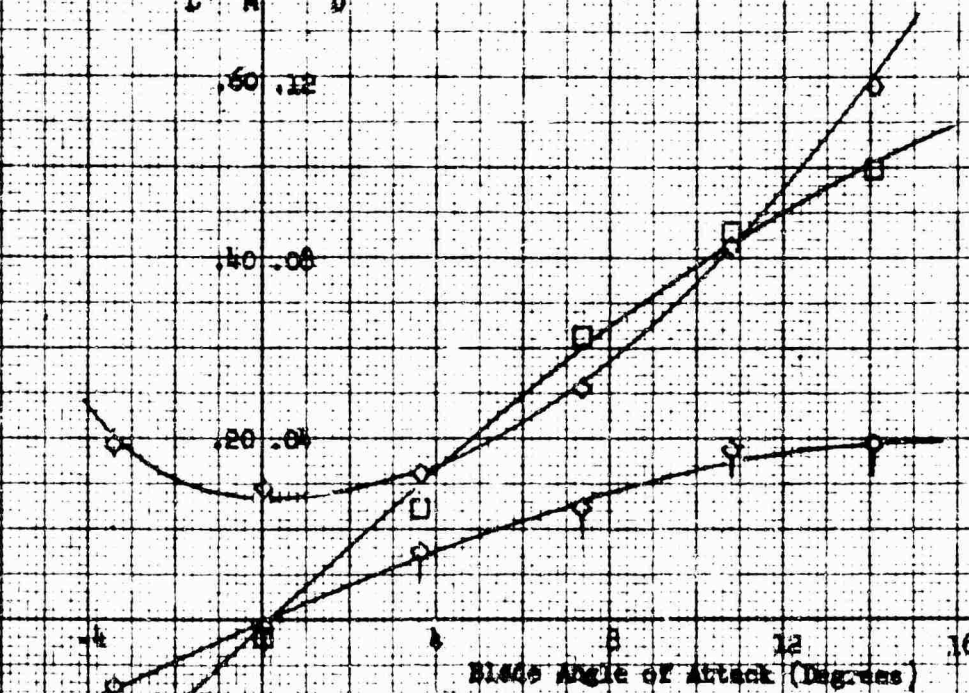
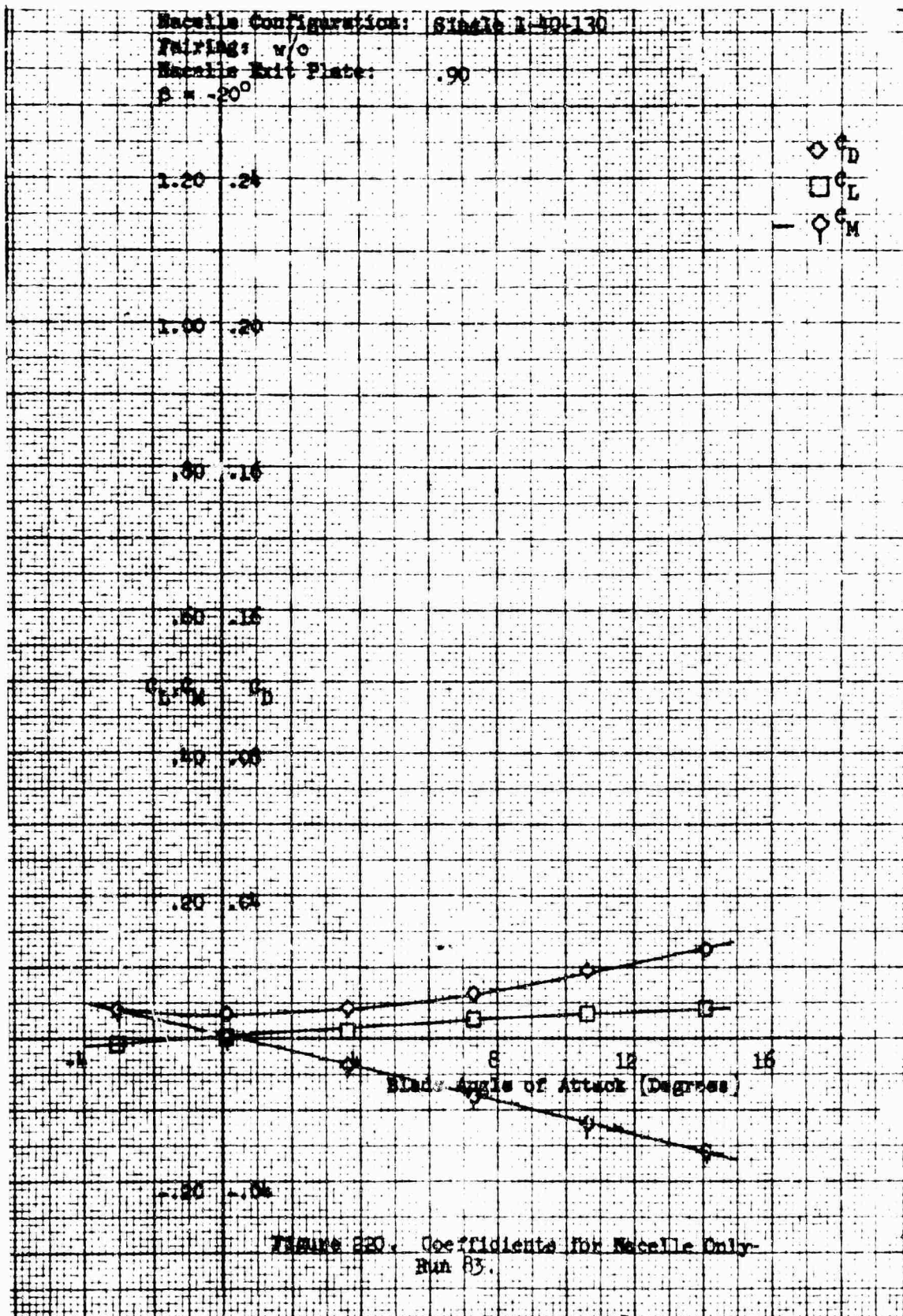


Figure 219. Coefficients for Combined Nozzle and Blade - Run 82.



Nacelle Configuration: Single 1-40-130

Nacelle Incidence Angle: 0

Fairing: w/o

Nacelle Exit Plate: .90

$\beta = -20^\circ$

1.20 .24

1.00 .20

.80 .16

C_L, C_M, C_D

.60 .12

.40 .08

.20 .04

-.20 -.04

C_D
 C_L
 C_M

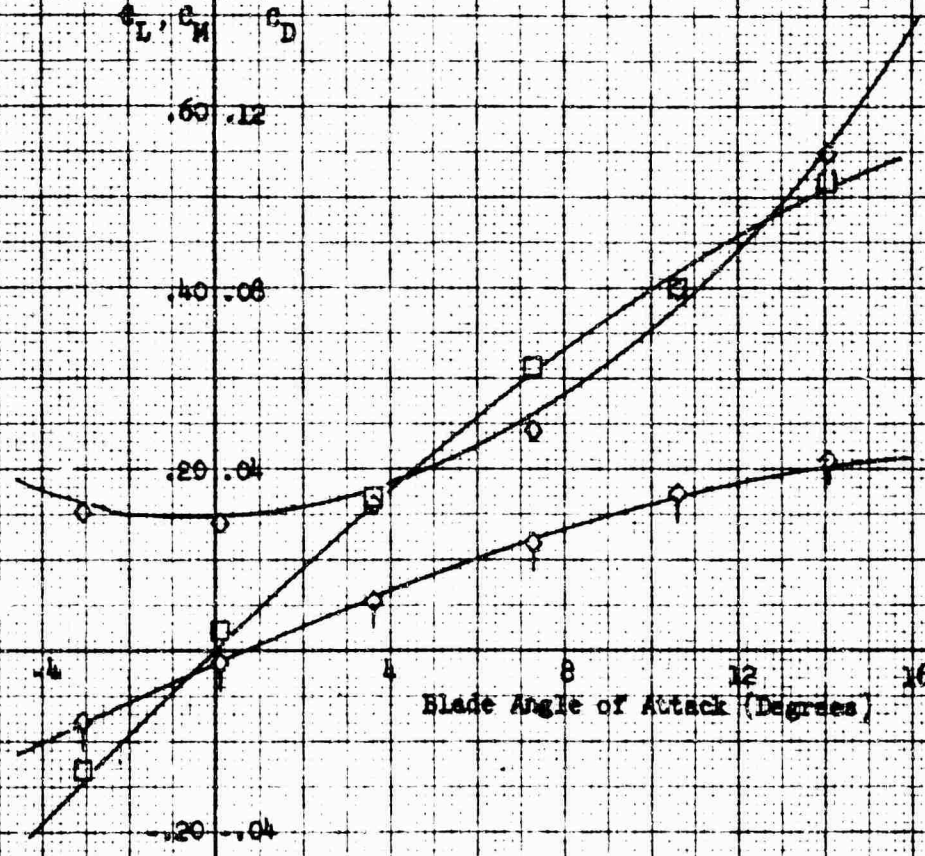
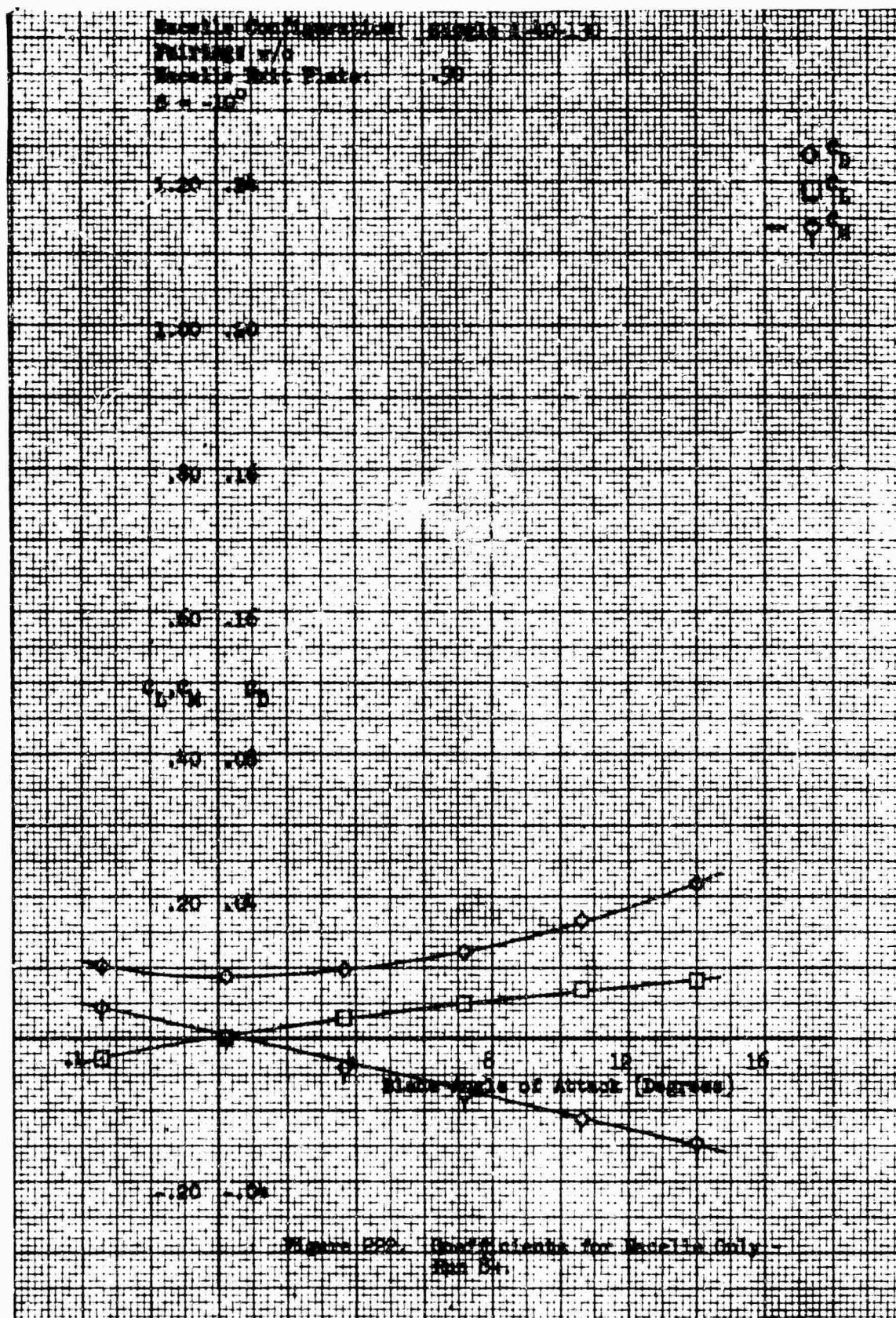


Figure 221. Coefficients for Combined Nacelle and Blade - Run 83



Macelle Configuration: Single 1-40-130
 Macelle Incidence Angle: 0
 Pairing: v/c
 Macelle Exit Plate: .90
 $\beta = 10^\circ$

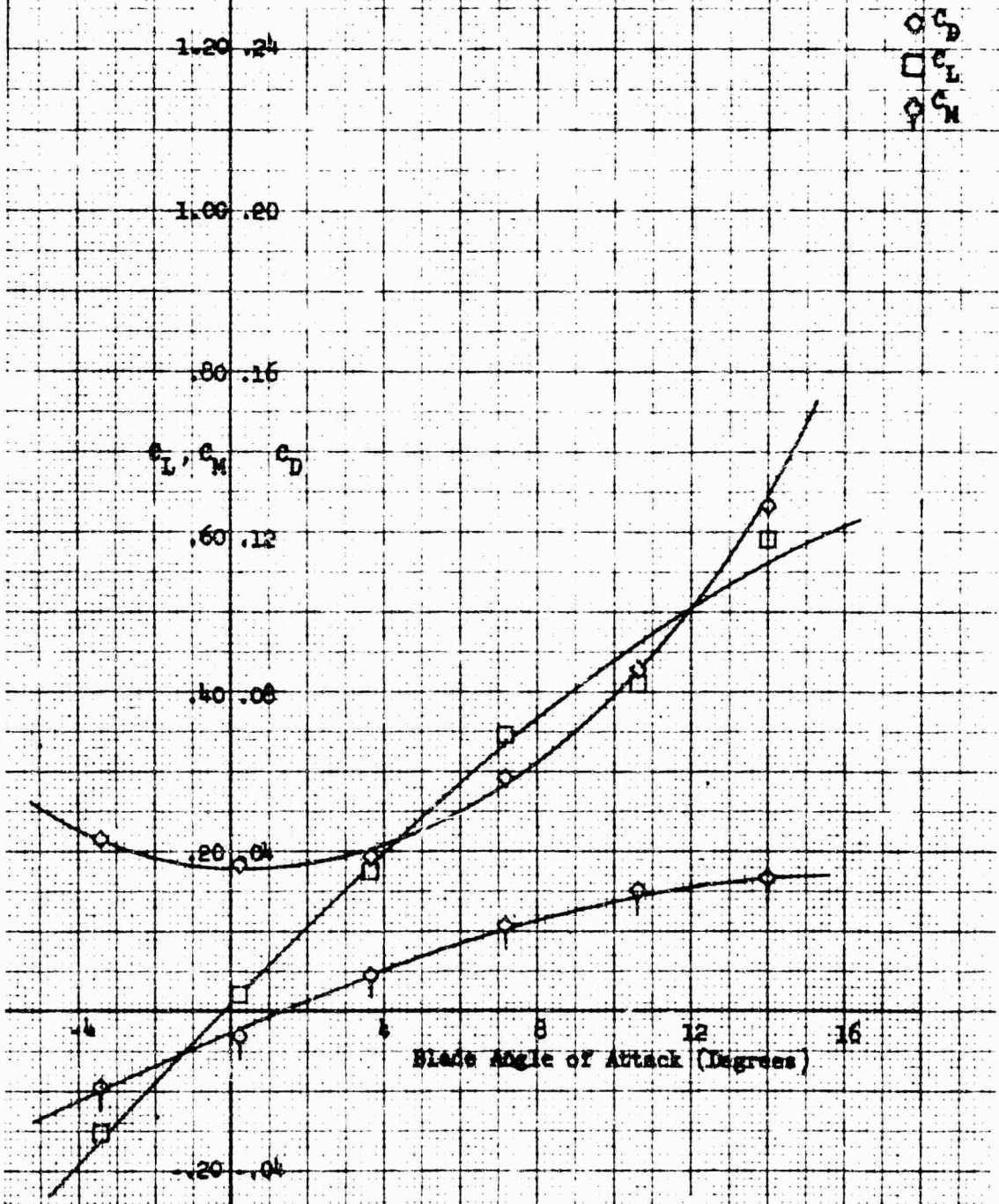


Figure 223. Coefficients for Combined Macelle and Blade - Run 84.

Nacelle Configuration: Single 1-40-130
 Fairing: w/o
 Nacelle Exit Plate: .90
 $\beta = 0$

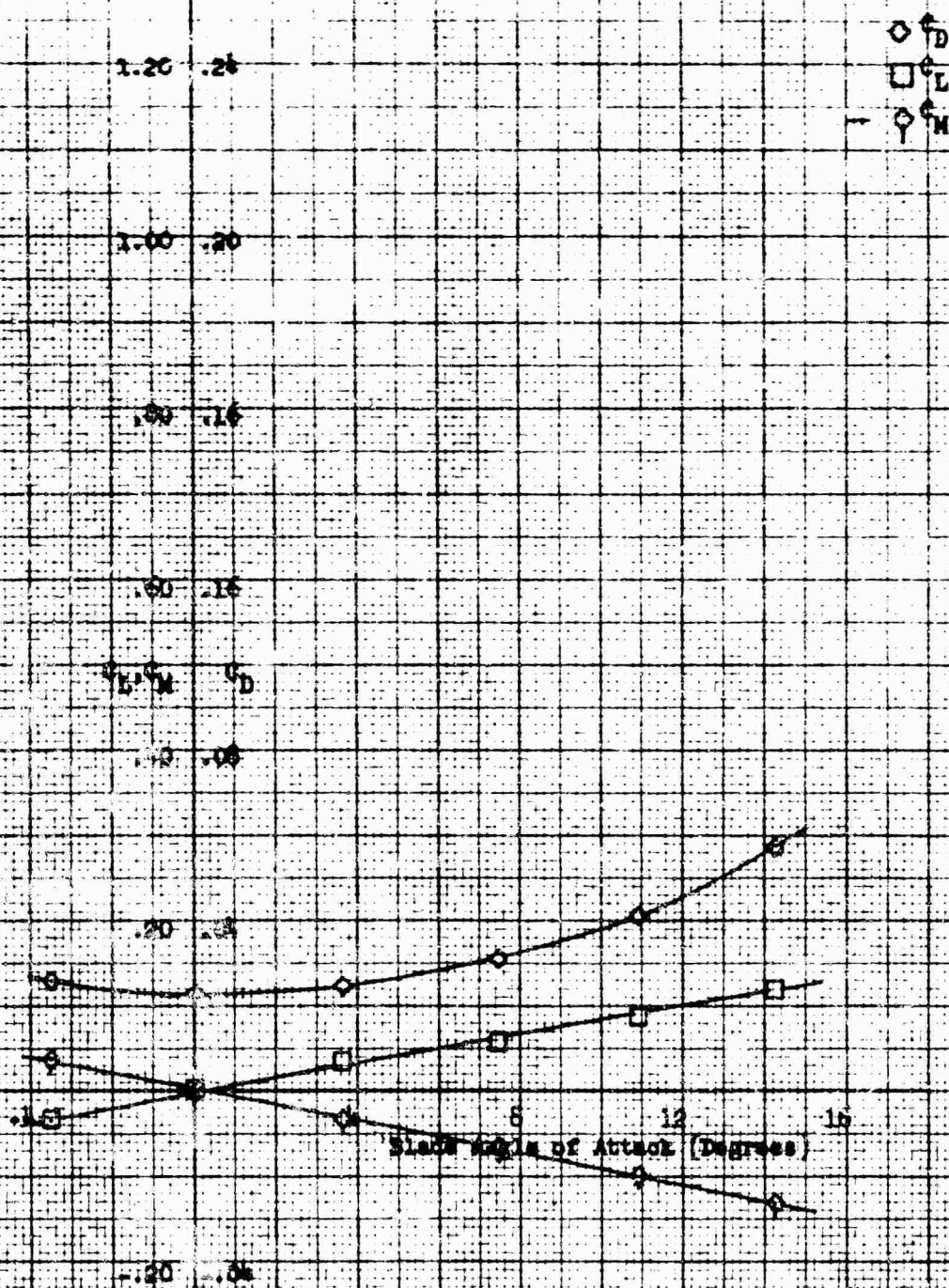


Figure 224. Coefficients for Nacelle Only -
 Run 85.

Macelle Configuration: Single 1-45-130

Macelle Incidence Angle: 0

Pairing: w/o

Macelle Exit Plate: .90

$\beta = 0$

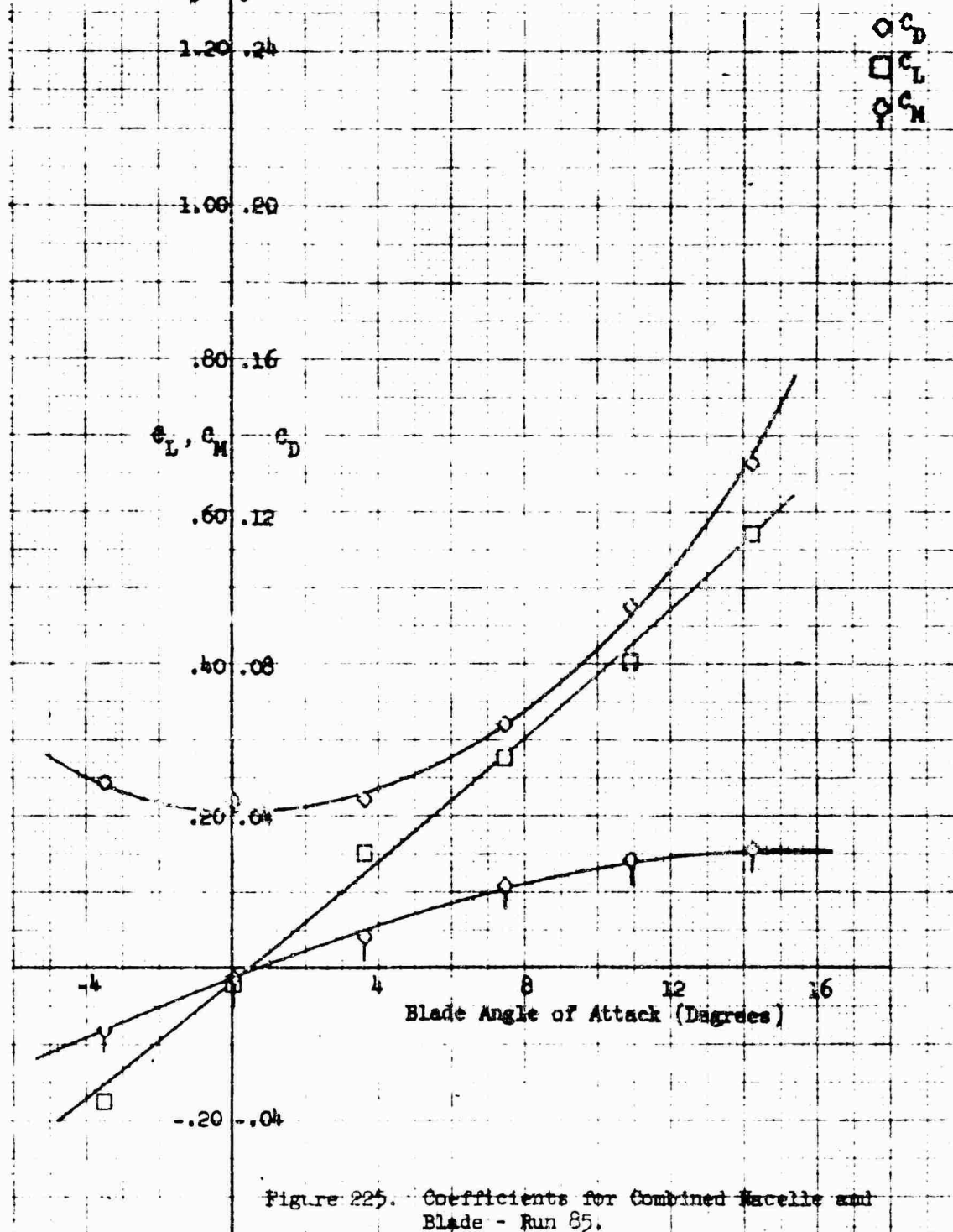


Figure 225. Coefficients for Combined Macelle and Blade - Run 85.

Blade Configuration: Single 1.40-1.30
 Pairing: w/o
 Blade Exit Plate: .90
 $\beta = 10^\circ$

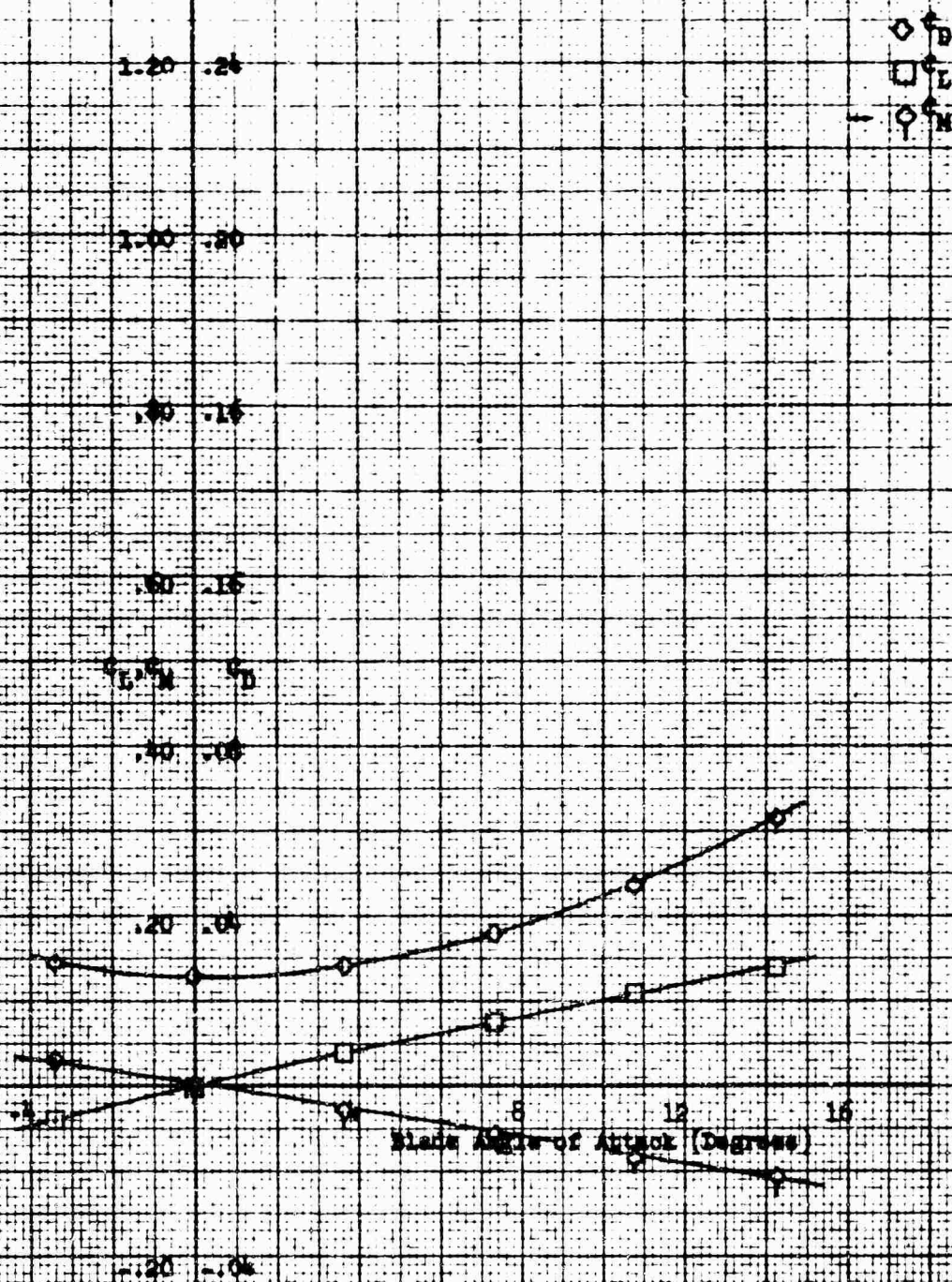


FIGURE 226. Coefficients for Blade Only -
 Run 86.

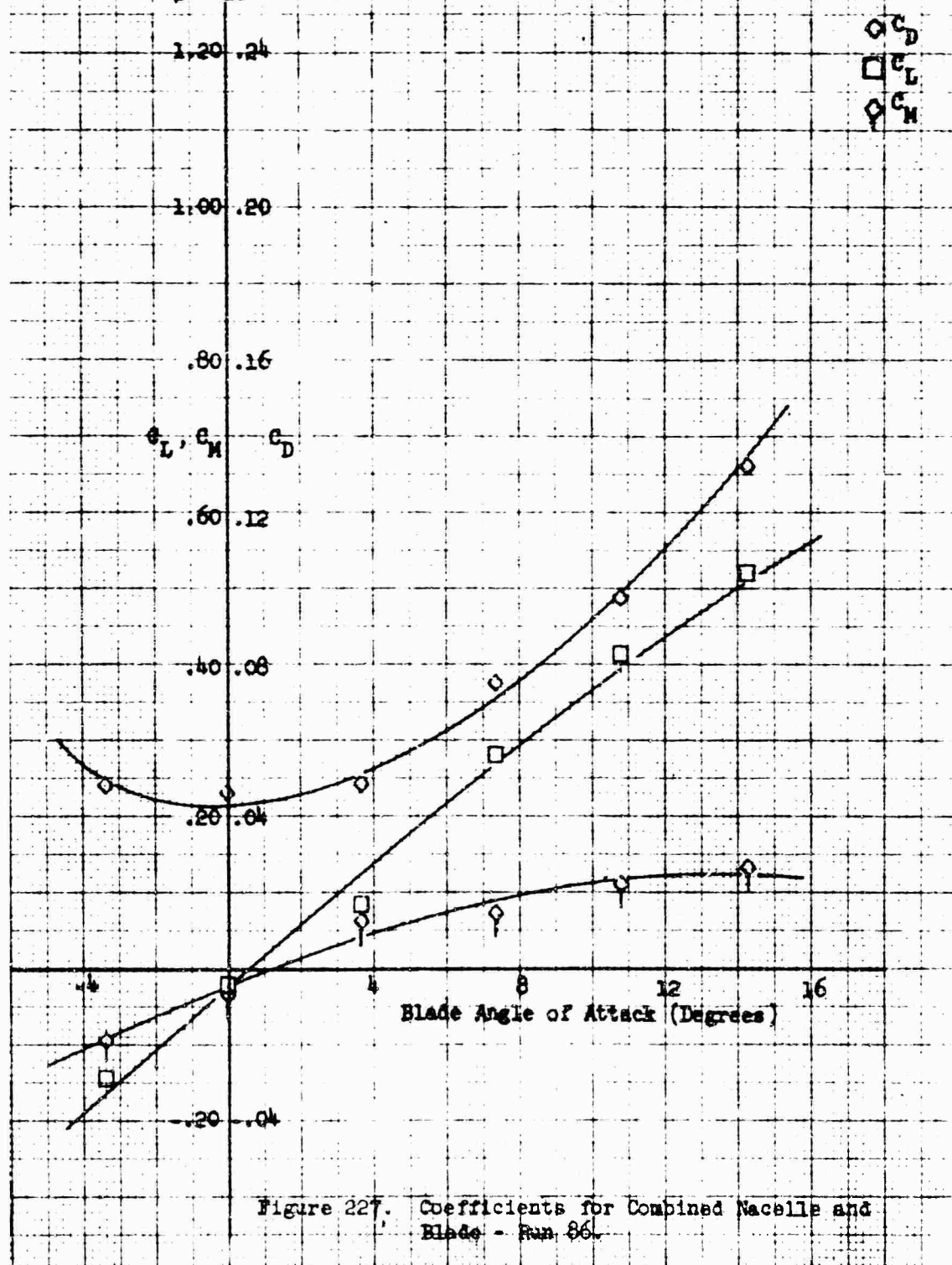
Nacelle Configuration: Single 1-40-130

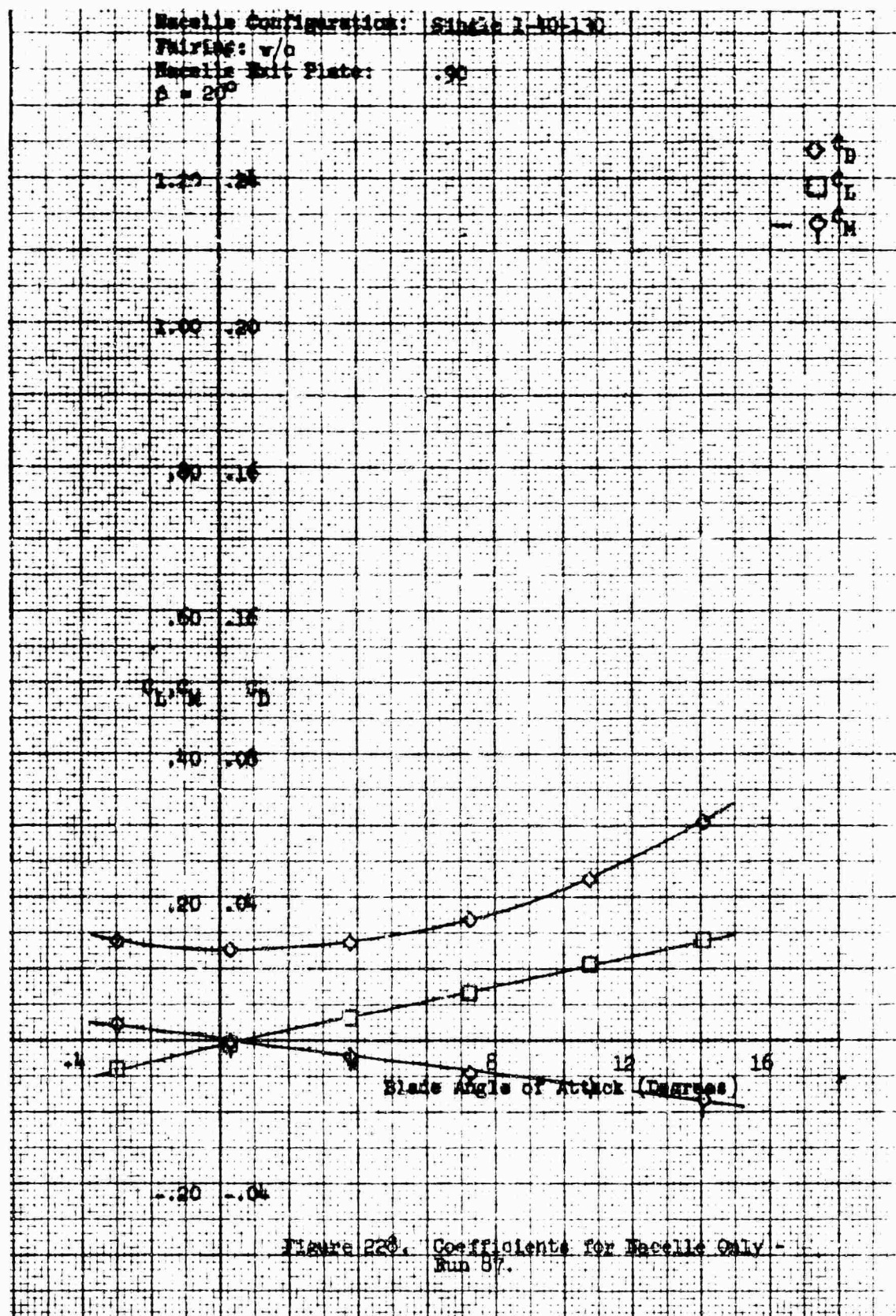
Nacelle Incidence Angle: 0

Fairing: w/o

Nacelle Exit Plate: .90

$\beta = 10^\circ$





Nacelle Incidence Angle: 0

Fairing: w/o

Nacelle Exit Plate: .90

$\beta = 20^\circ$

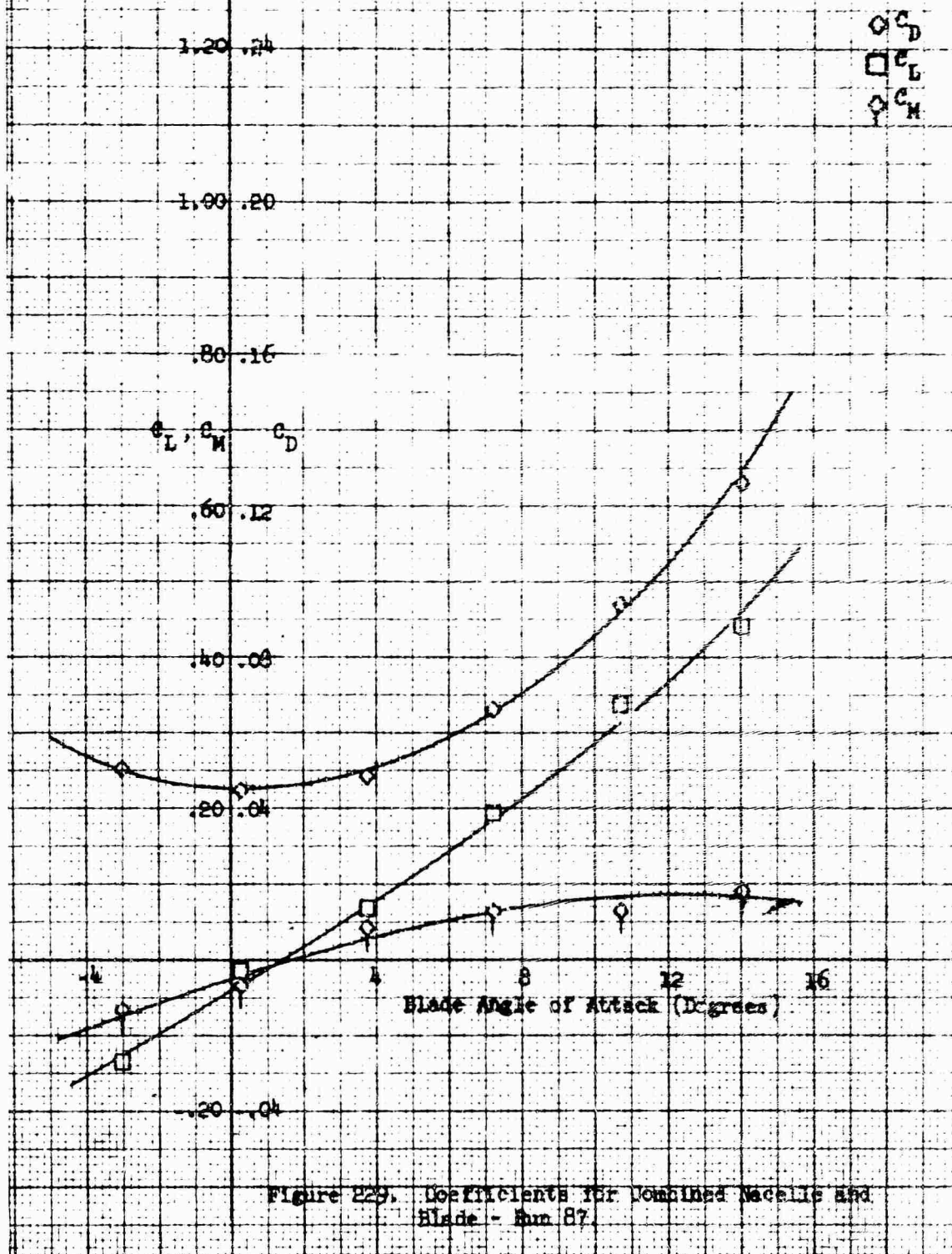


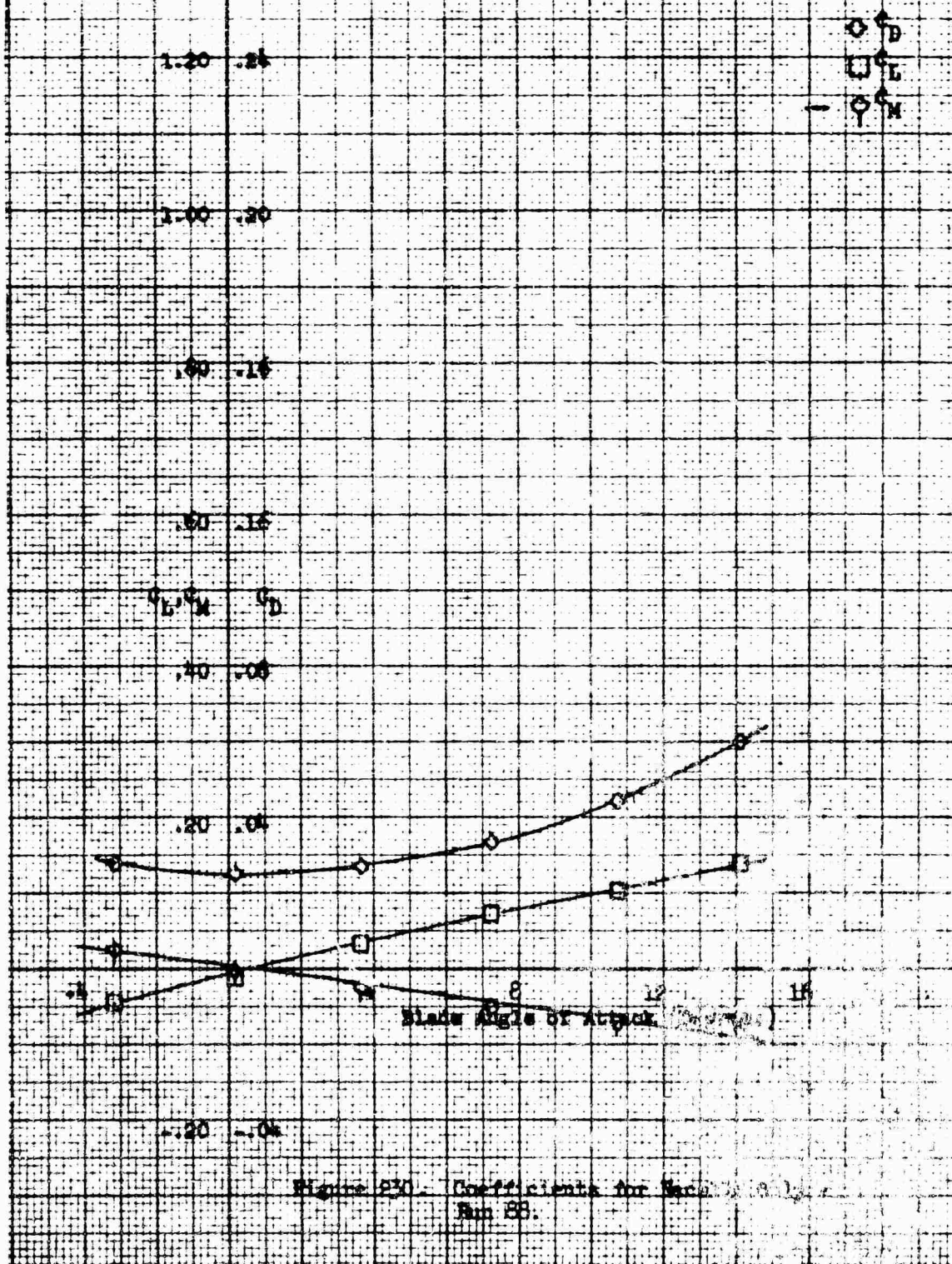
Figure 229. Coefficients for Dominant Nacelle and Blade - Run 87

Nacelle Configuration: Single 1-40-130

Fairing: w/o

Nacelle Exit Plate: 1-00

$\beta = 20^\circ$



Macelle Configuration: Blade 2-40-130
 Macelle Incidence Angle: 0
 Pairing: w/o
 Macelle Exit Plate: 1.00
 $\beta = 20^\circ$

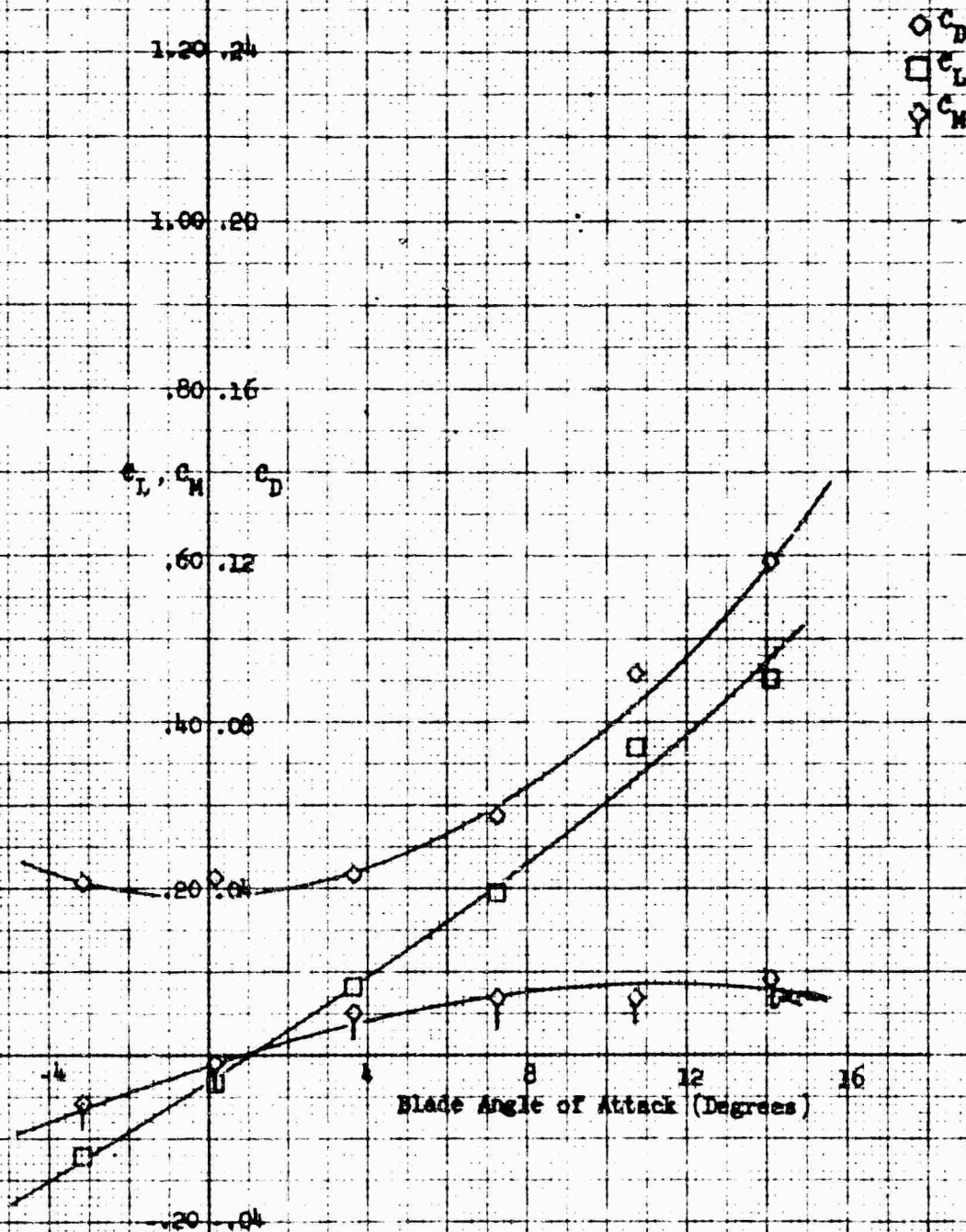
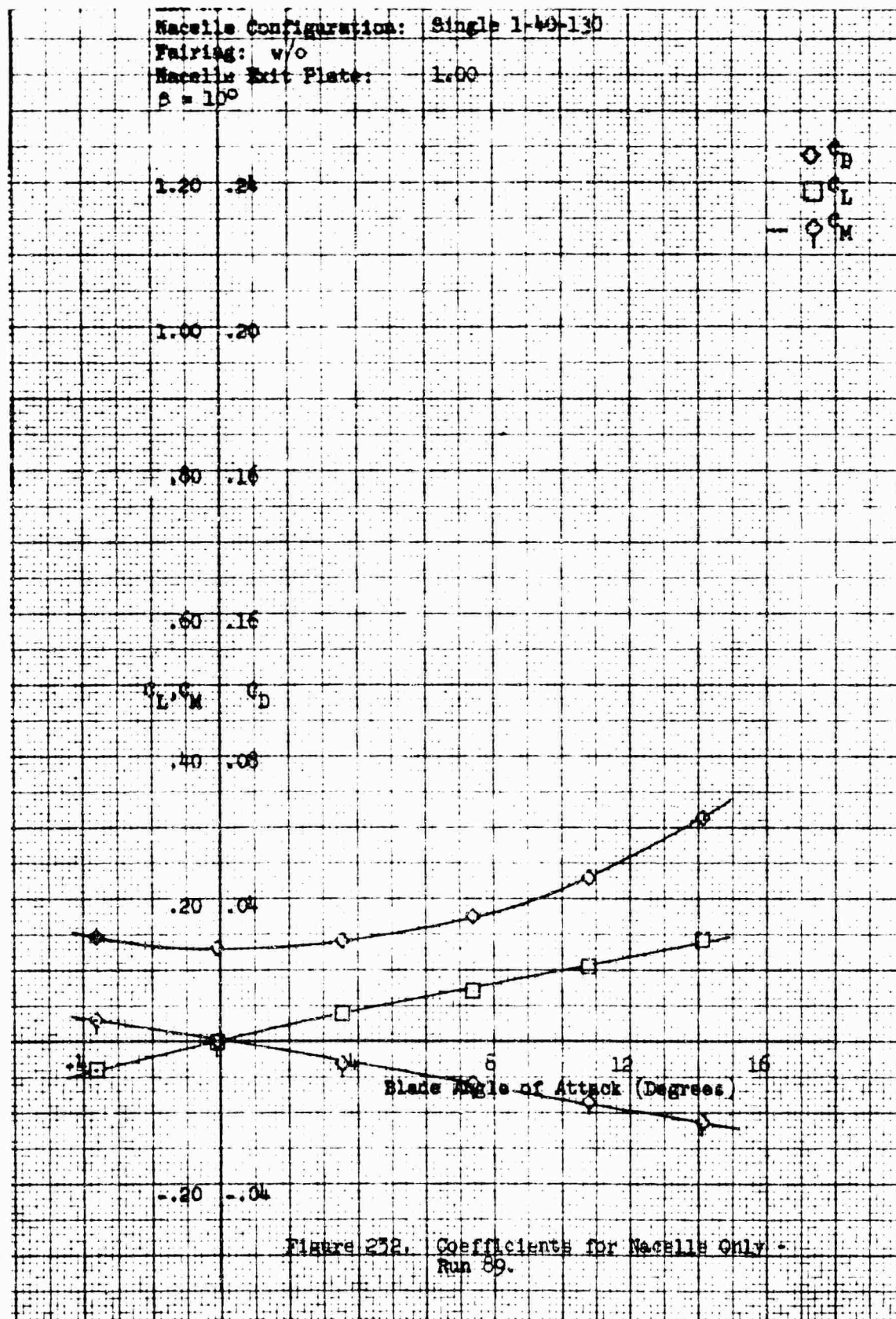


Figure 231. Coefficients for Combined Macelle and Blade - Run 88.



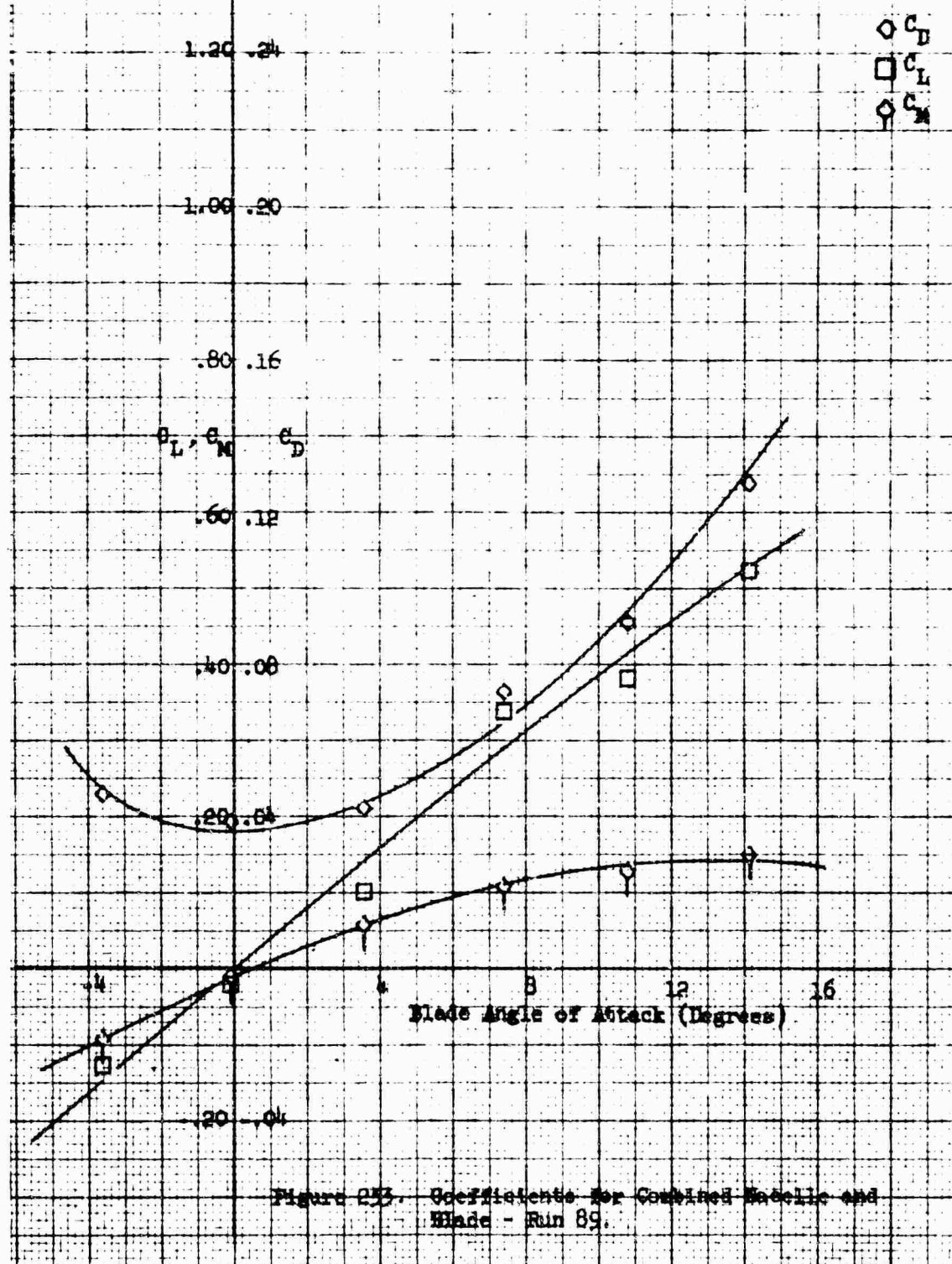
Nacelle Configuration: Single 1-40-130

Nacelle Incidence Angle: 0

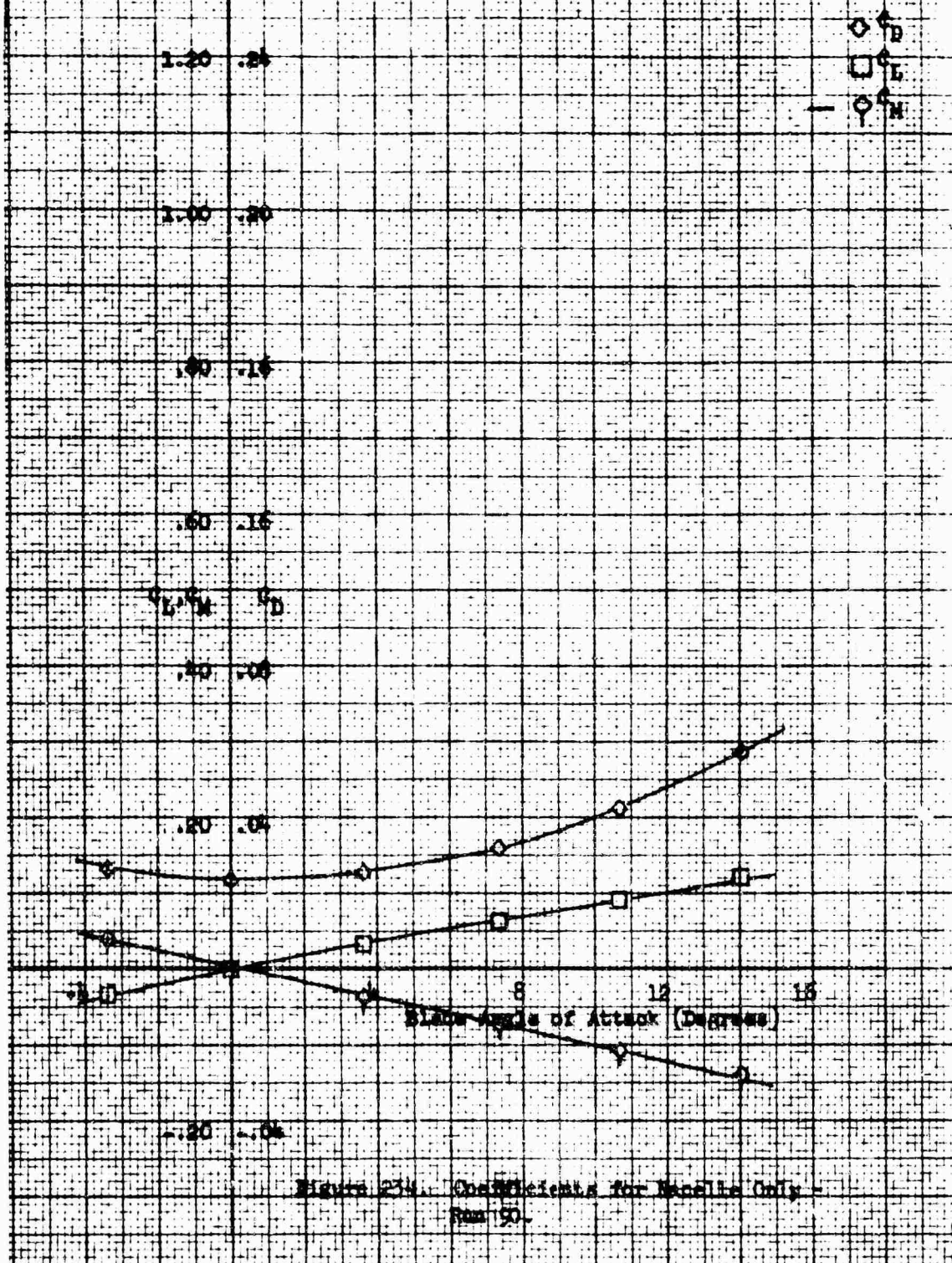
Pairing: w/o

Nacelle Exit Plate: 1.00

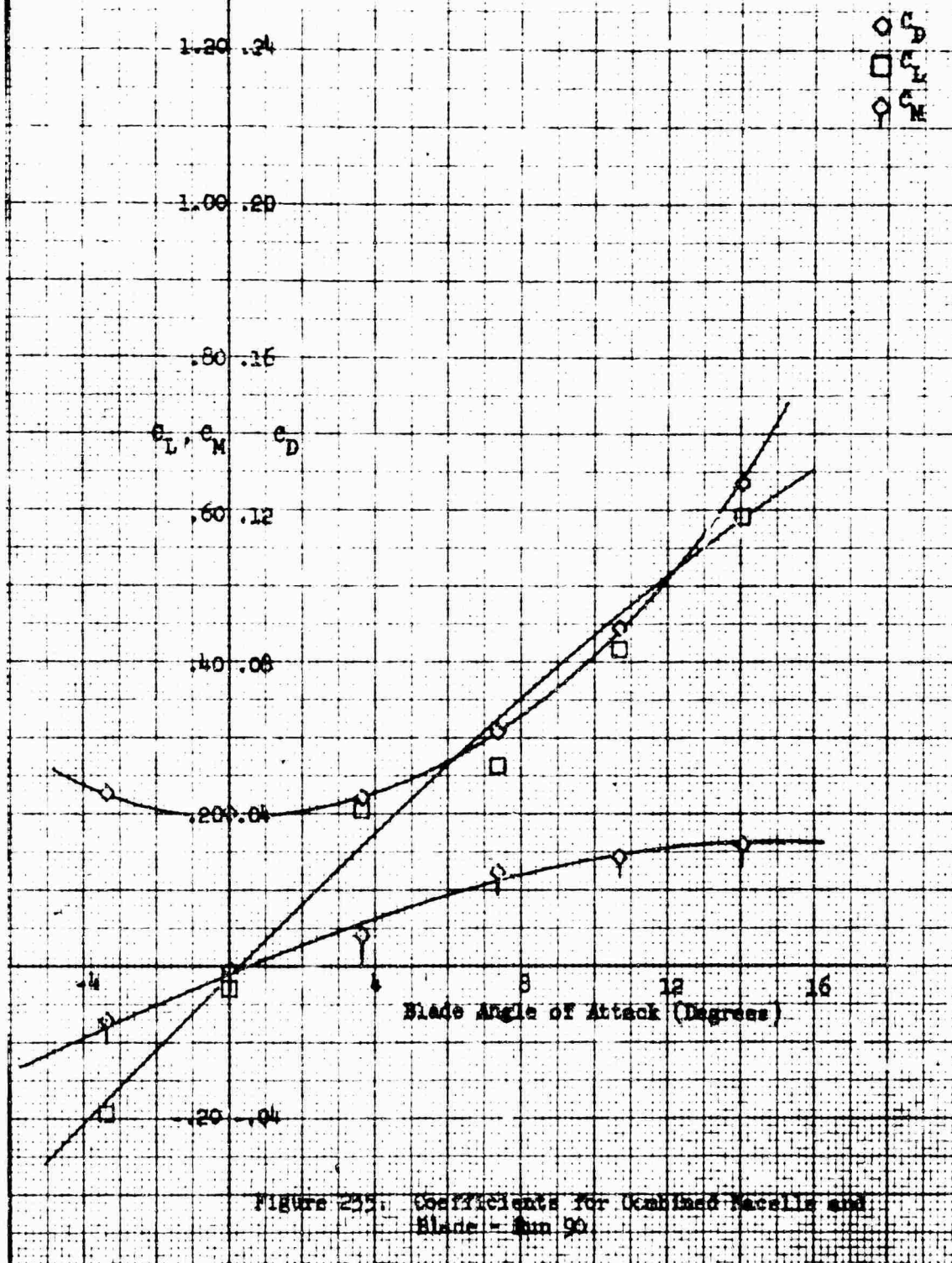
$\beta = 10^\circ$



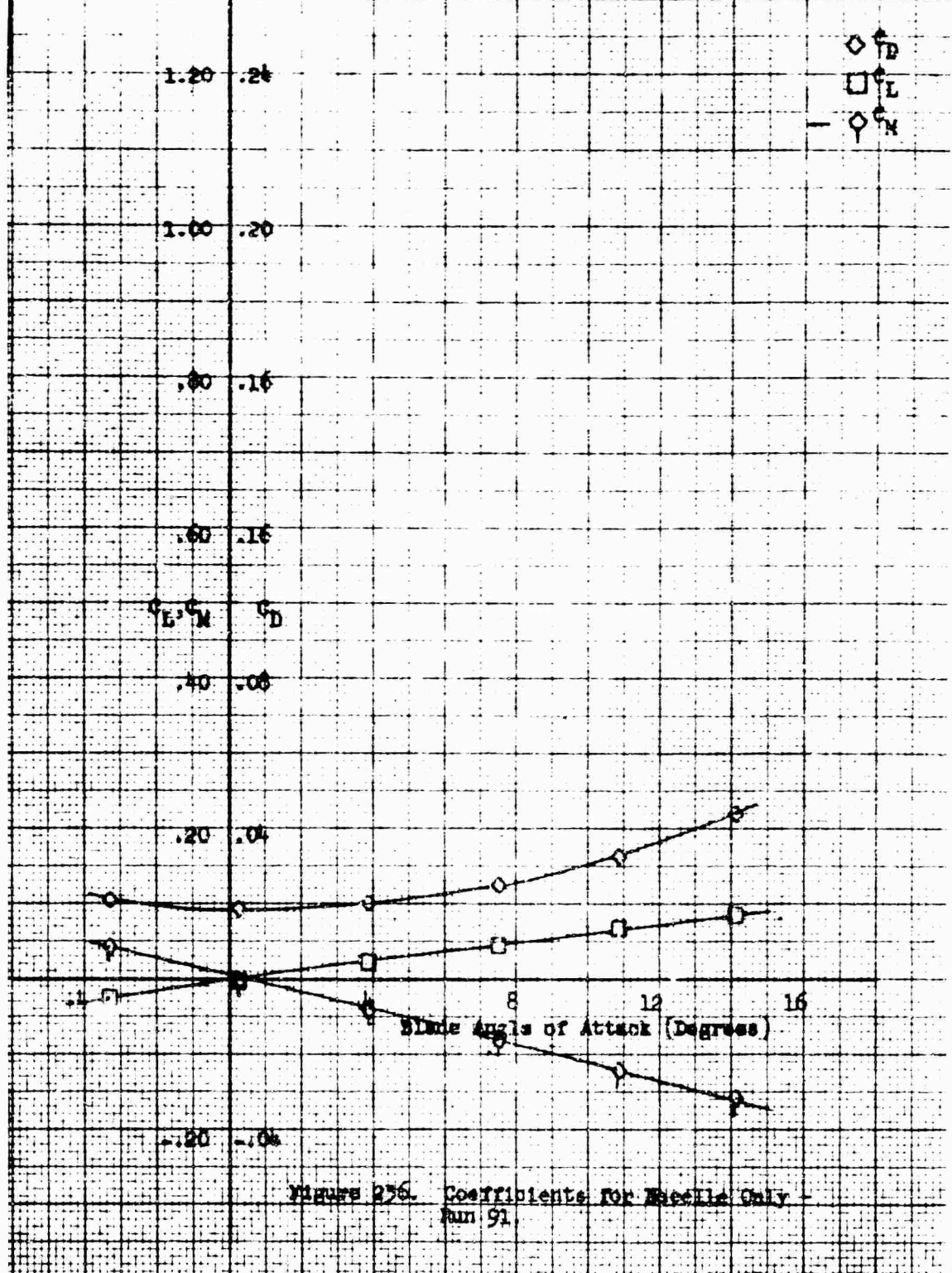
Nacelle Configuration: Single 1-40-100
 Fairing: w/o
 Nacelle Exit Plate: 1.00
 $\delta = 0$



Macelle Configuration: Single 1-40-130
 Macelle Incidence Angle: 0
 Pairing: w/o
 Macelle Exit Plate: 1.00
 $\beta = 0$



Nacelle Configuration: Single 1-40-130
 Fairing: w/o
 Nacelle Exit Plate: 1.00
 $\beta = -10^\circ$



Nacelle Configuration: Single 1-40-130
 Nacelle Incidence Angle: 0
 Pairing: w/o
 Nacelle Exit Plate: 1.00
 $\beta = -10^\circ$

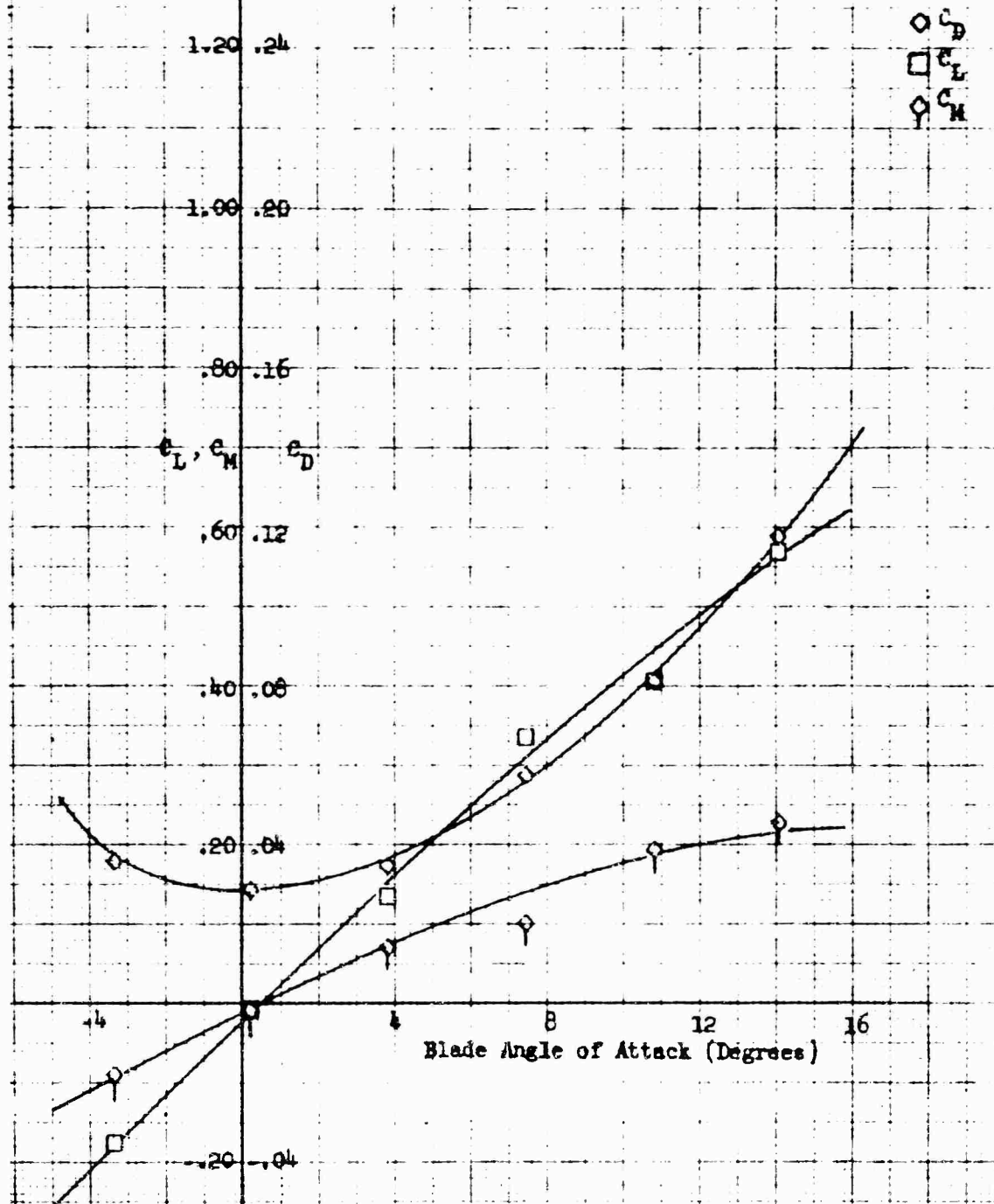
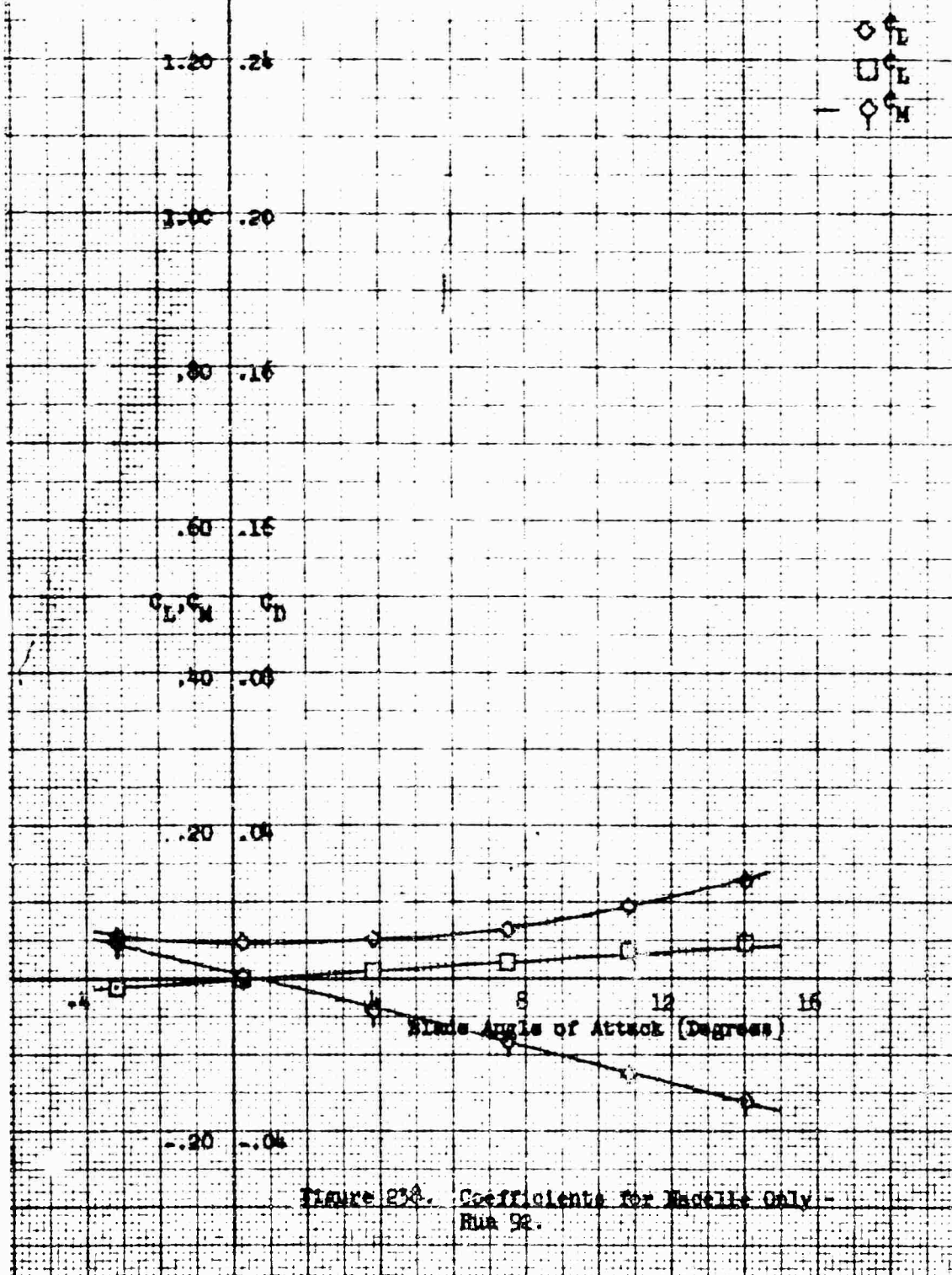


Figure 257. Coefficients for Combined Nacelle and Blade - Run 91.

Nacelle Configuration: S1b/Lt 1-40-130
 Fairing: $\gamma/0$
 Nacelle Exit Plate: 1.00
 $\beta = -20$



Macelle Configuration: Single 1-40-130
 Macelle Incidence Angle: 0
 Pairing: w/o
 Macelle Exit Plate: 1.00
 $\beta = -20^\circ$

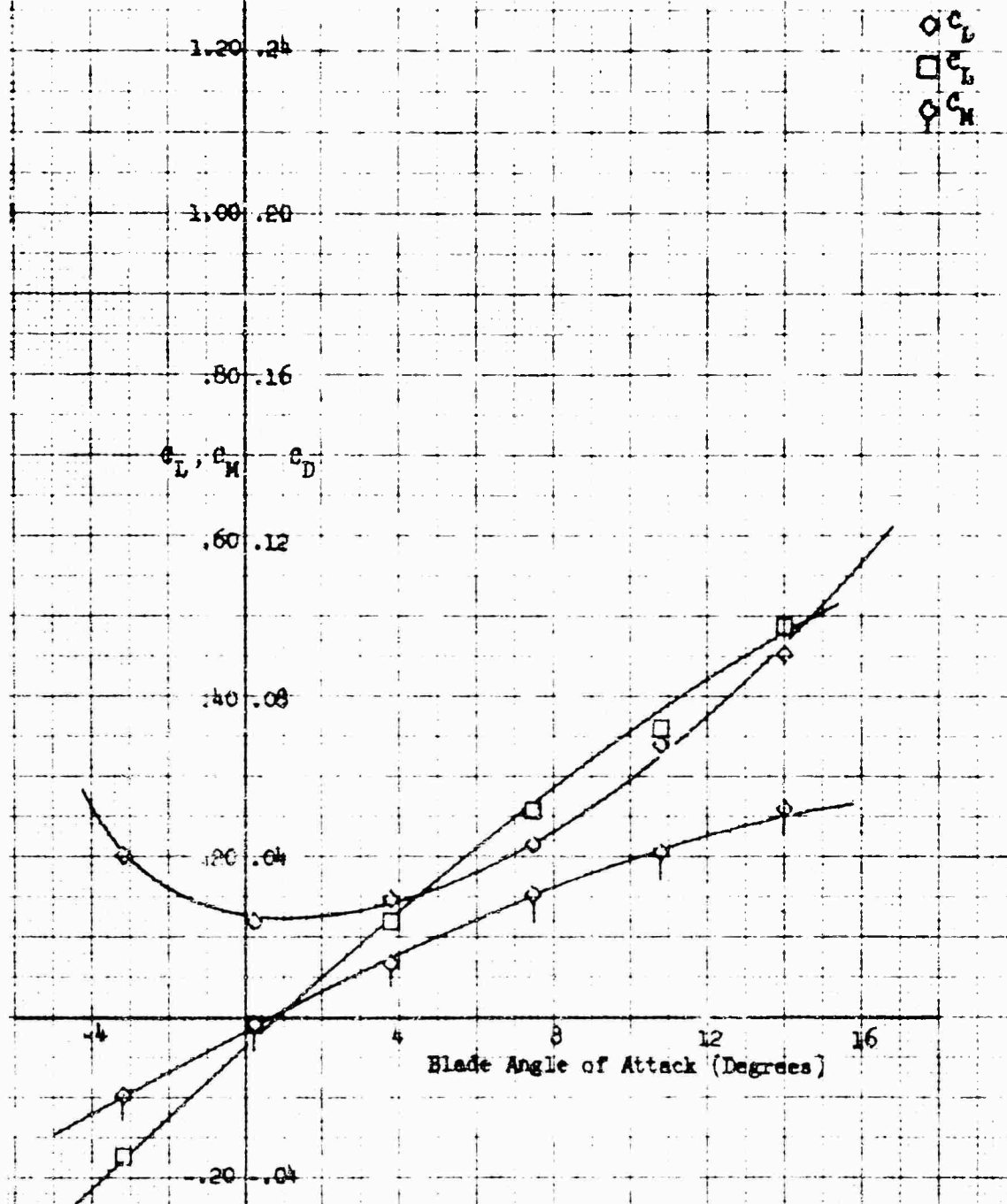
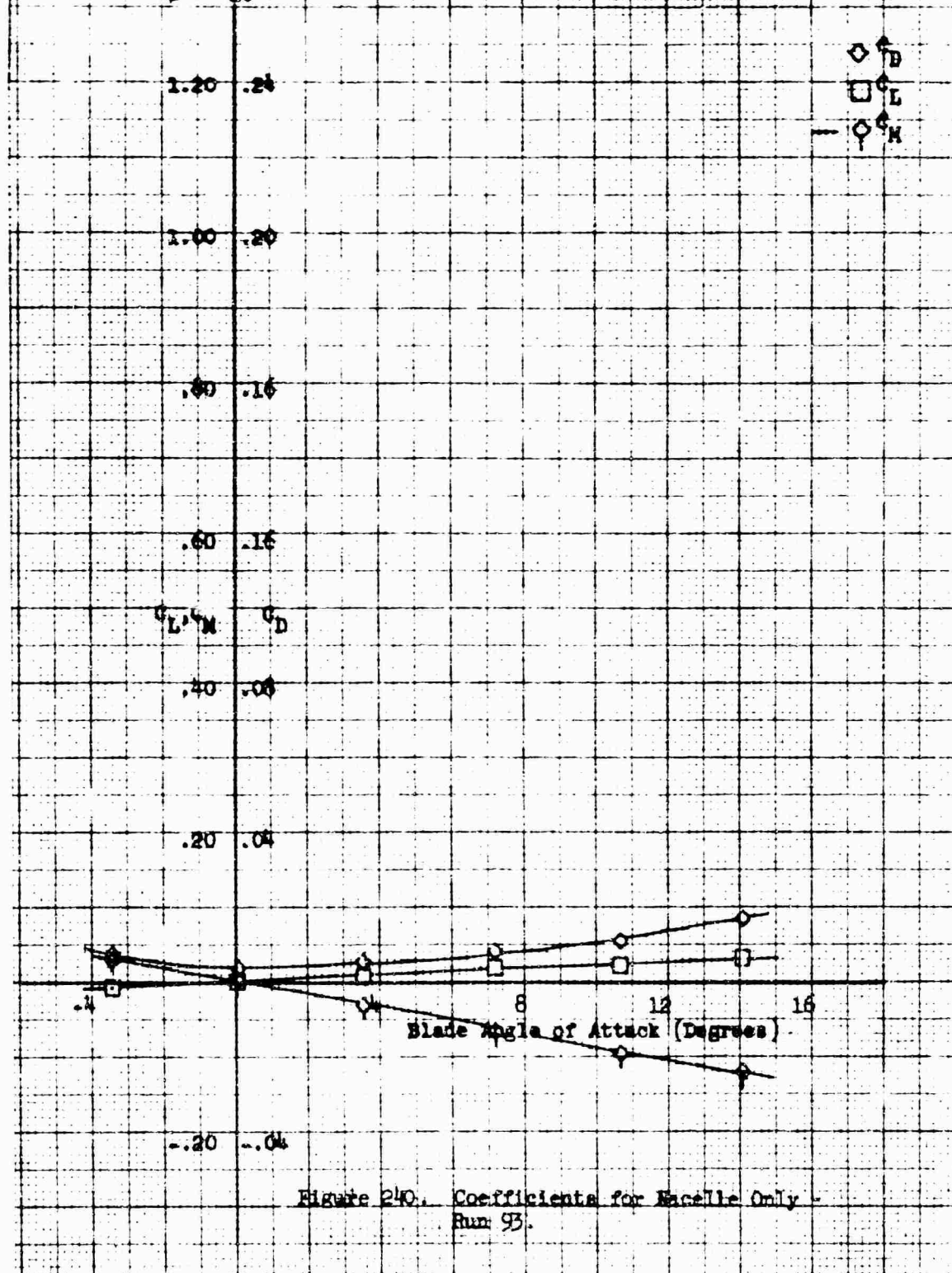


Figure 239. Coefficients for Combined Macelle and Blade - Run 92.

Nacelle Configuration: Single 1-50-100 Parabolic Spinner
 Pairing: w/o
 Nacelle Exit Plate: 1.00
 $\beta = -20^\circ$



Nacelle Configuration: Single 1-50-100 Parabolic Spinner
 Nacelle Incidence Angle: 0
 Fairing: w/o
 Nacelle Exit Plate: 1.00
 $\beta = -20^\circ$

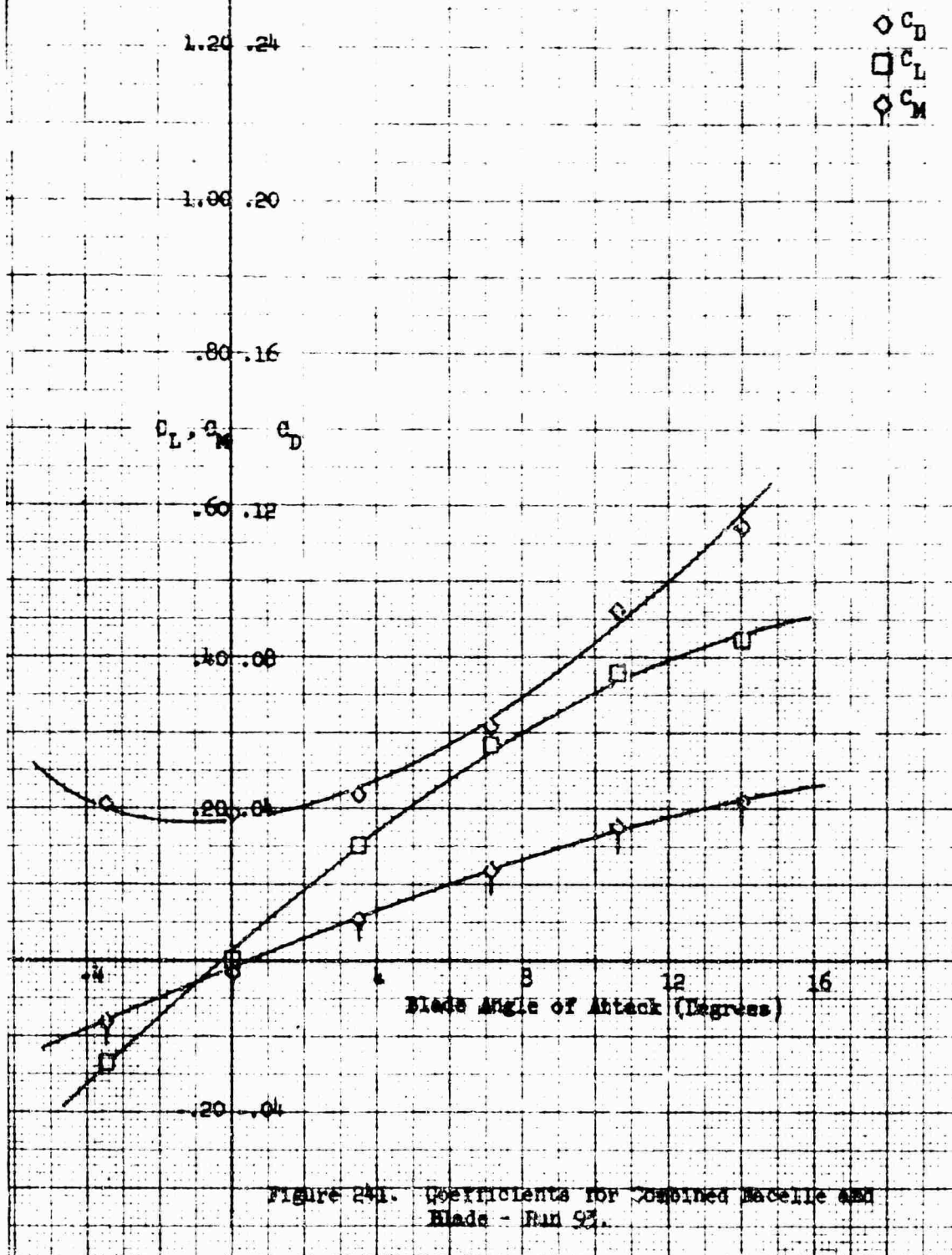


Figure 241. Coefficients for Combined Nacelle and Blade - Run 92.

Nacelle Configuration: Single 1-50-130 Parabolic Spinner
 Pairing: w/o
 Nacelle Exit Plate: 1.00
 $\beta = -10^\circ$

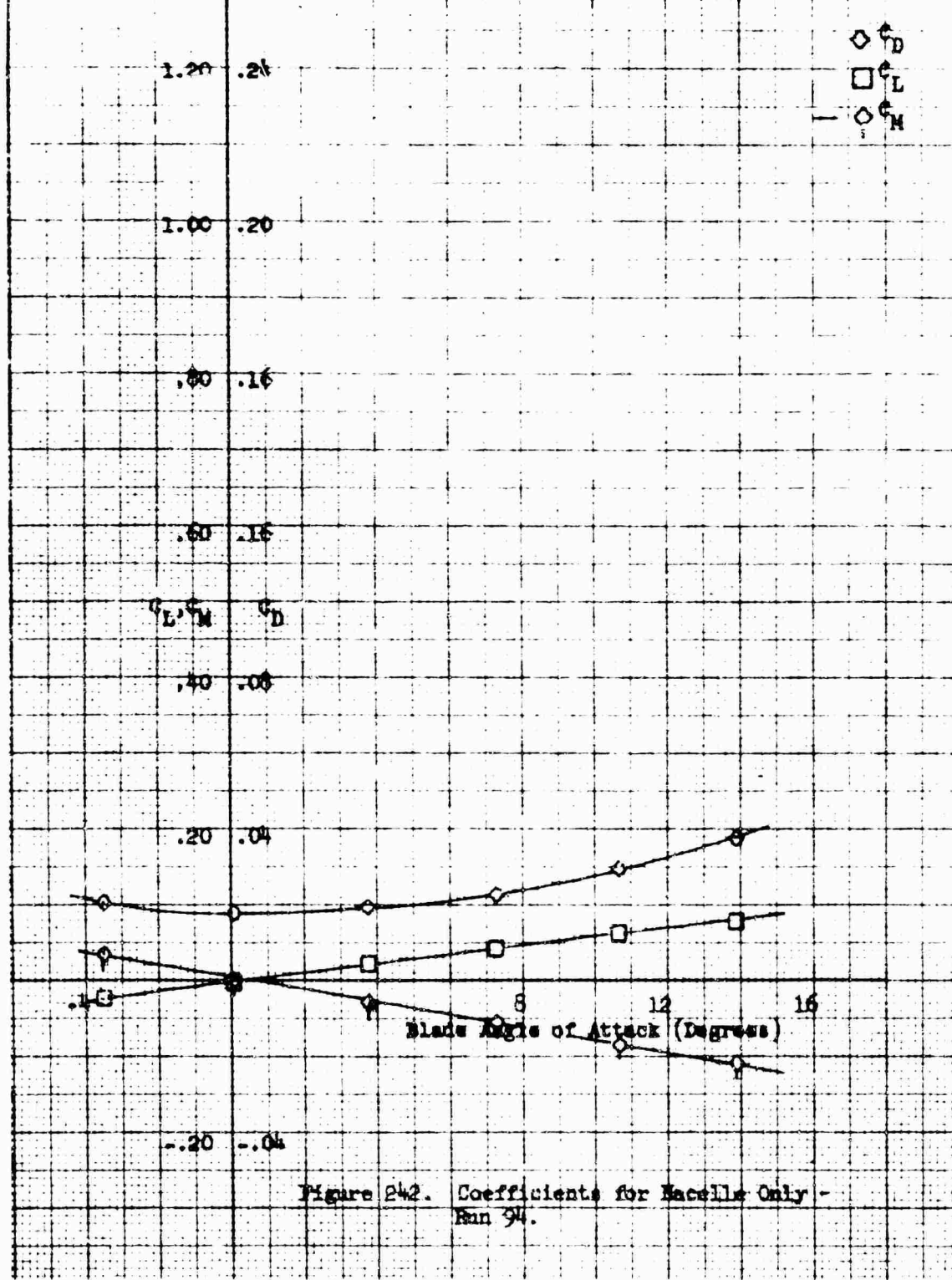


Figure 242. Coefficients for Nacelle Only - Run 94.

Nacelle Configuration: Single 1-90-100 Parabolic Spinner
 Nacelle Incidence Angle: 0
 Fairing: w/o
 Nacelle Exit Plate: 1.00
 $\beta = -10^\circ$

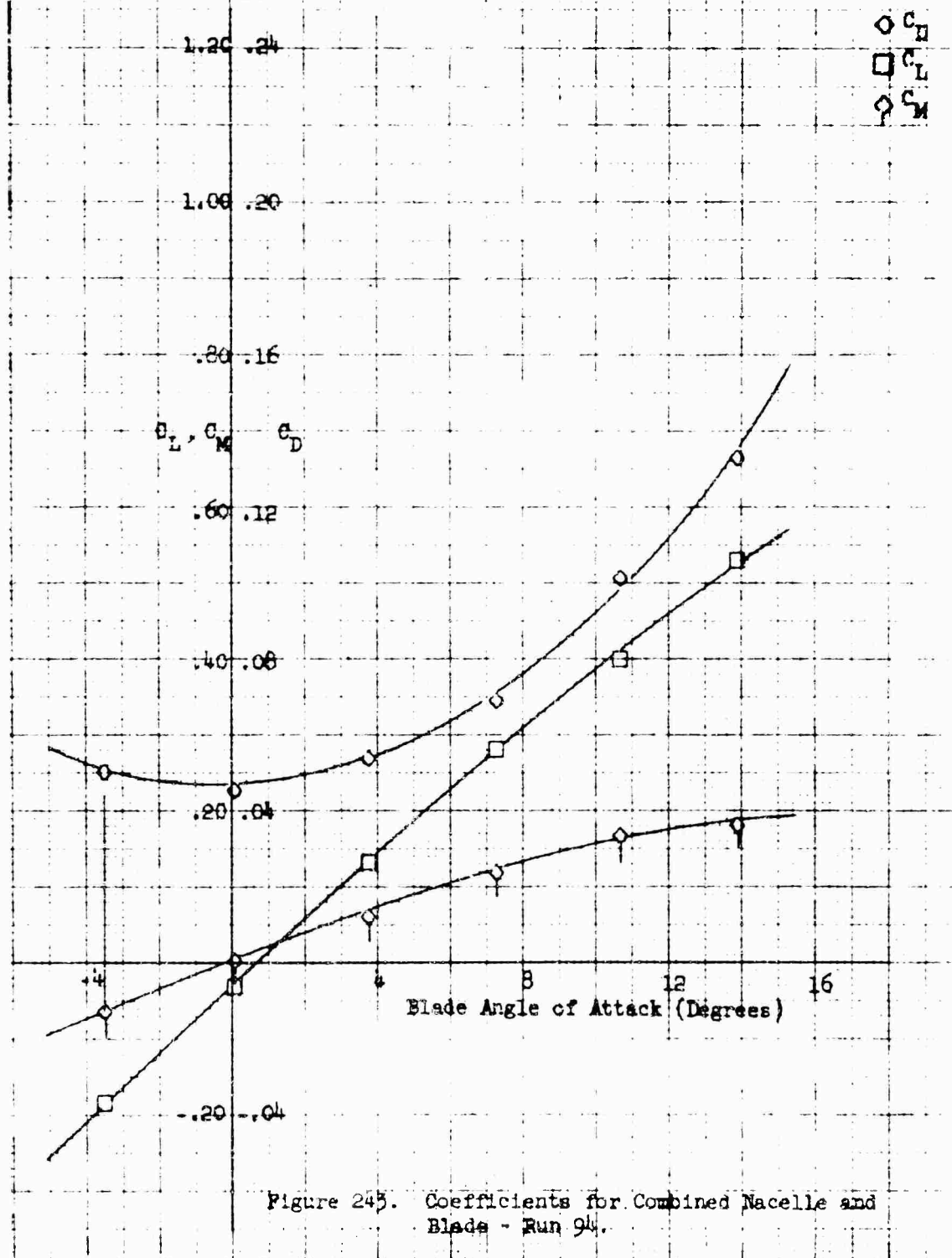


Figure 243. Coefficients for Combined Nacelle and Blade - Run 94.

Nacelle Configuration: Single 1-50-100 Parabolic Spinner
 Pairing: w/o
 Nacelle Exit Plate: 1.00
 $\beta = 0$

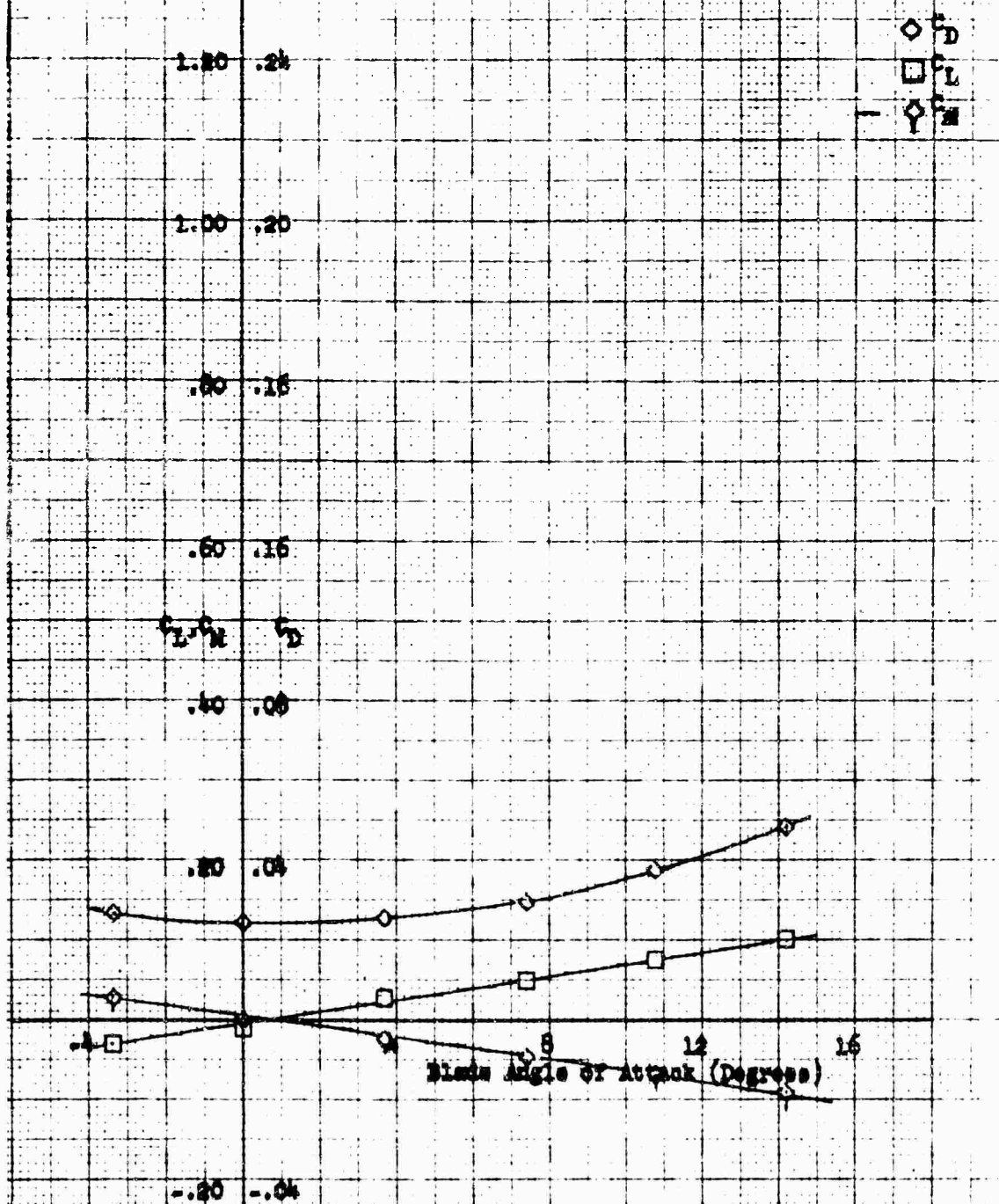


Figure 244. Coefficients for Nacelle Only -
 Run 95.

Nacelle Configuration: Single 1-50-100 Parabolic Spinner
 Nacelle Incidence Angle: 0
 Fairing: w/o
 Nacelle Exit Plate: 1.00
 $\beta = 0$

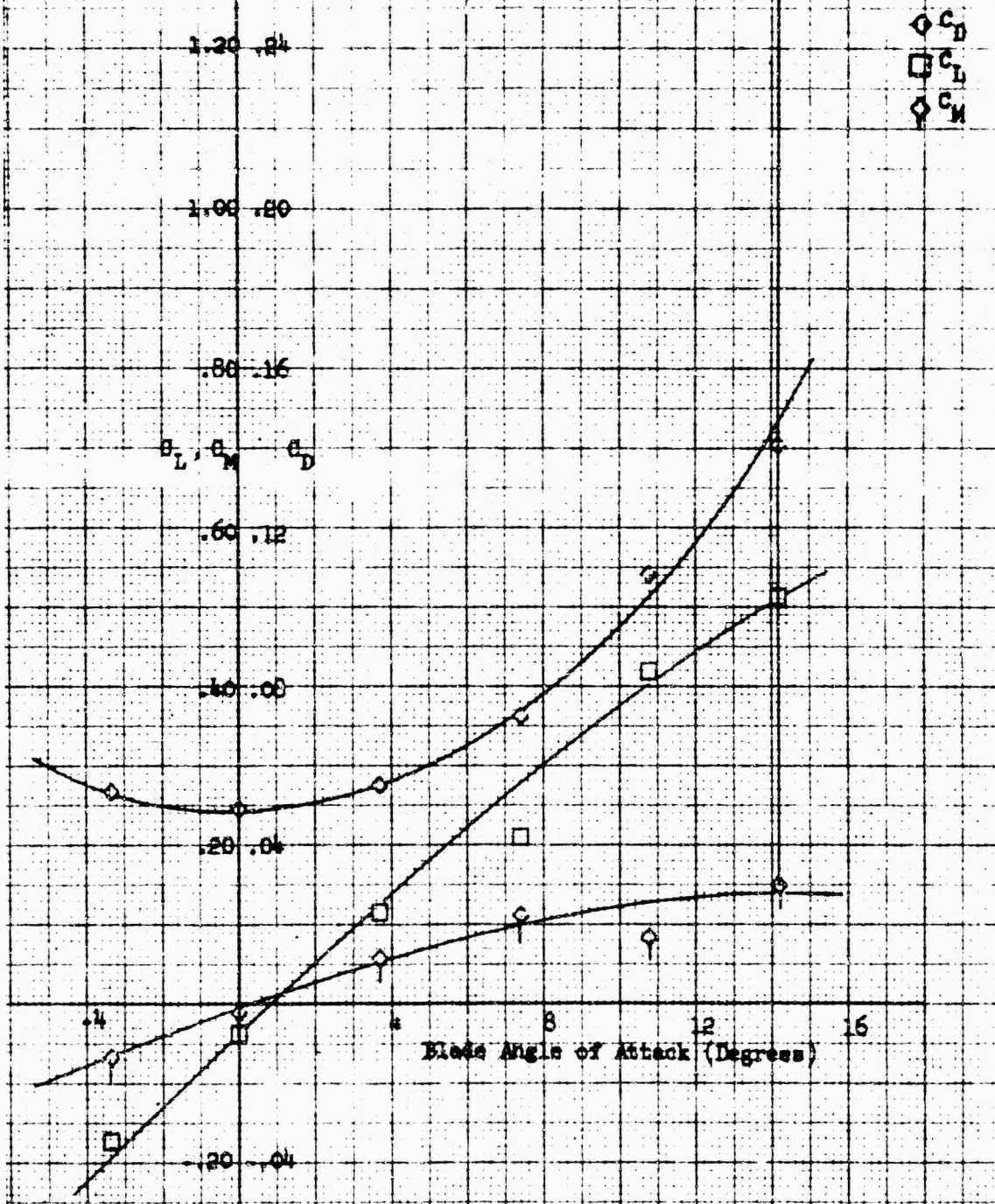


Figure 245. Coefficients for Combined Nacelle and Blade - Run 95.

Nozzle Configuration: Single 1-50-100 Parallel Spinner
 Pairing: v/o
 Nozzle Exit Plane: 1.00
 $\Delta = 10^\circ$

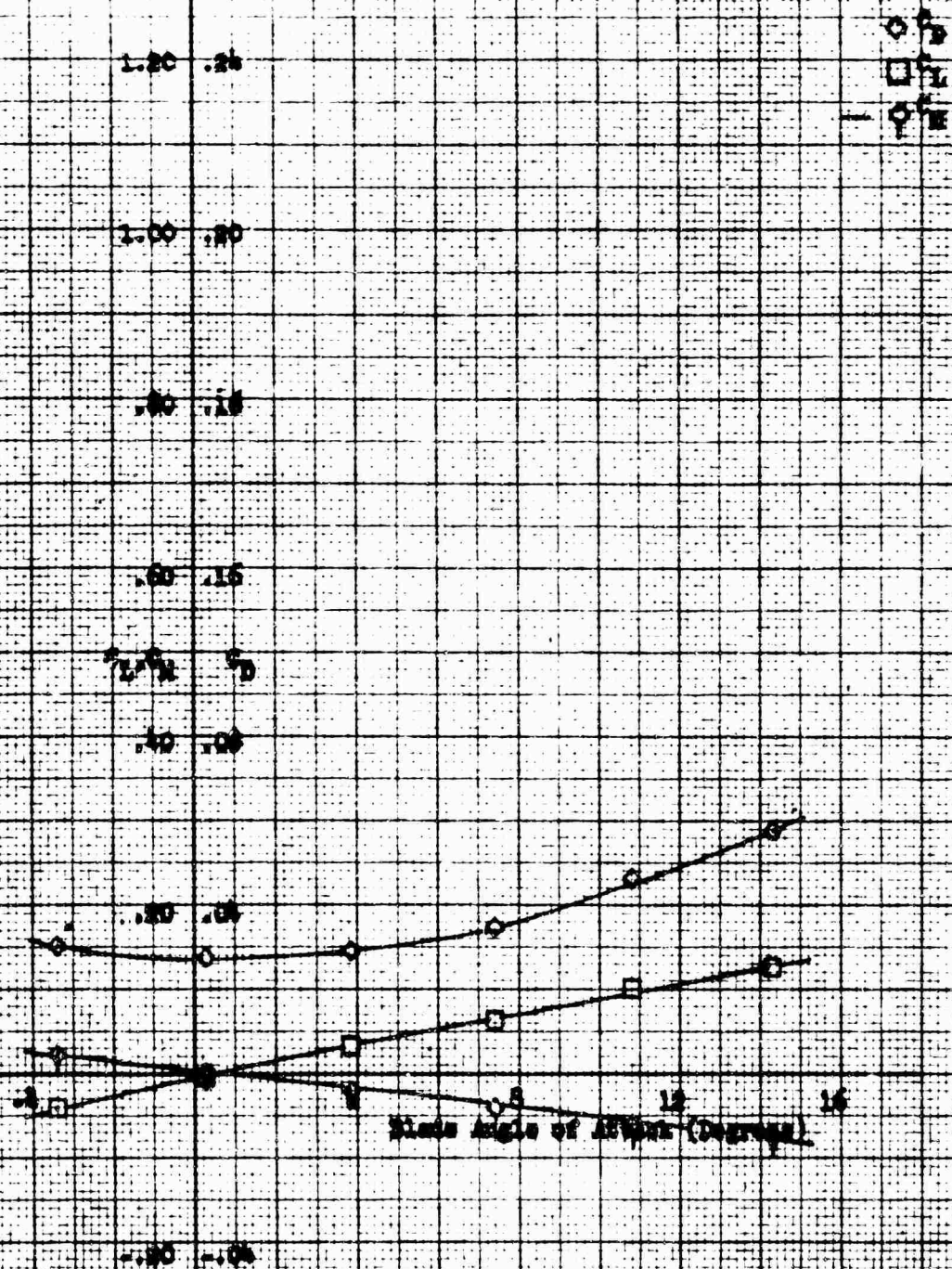


Figure 246. Coefficients for Nozzle Only - Run 96.

Nozzle Configuration: Single 1.50:1.00 Parabolic Symmer
 Nozzle Incidence Angle: 0
 Fairing: w/o
 Nozzle Exit Plate: 1.00
 $\beta = 10^\circ$

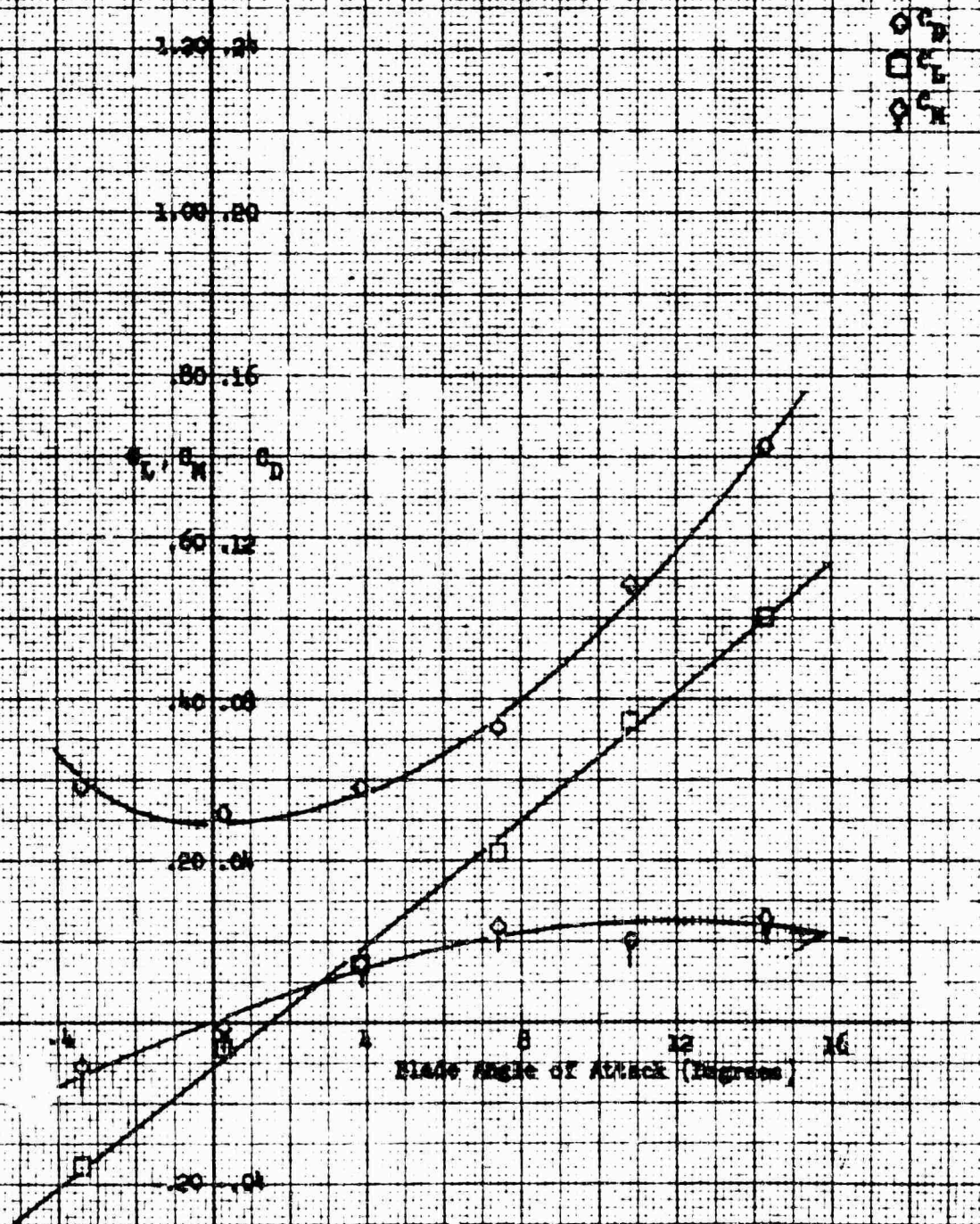


Figure 247. Coefficients for Combined Nozzle and
 Blade - Run 96.

Nozzle Configuration: Single 1-50-100 Parallel Spinner
 Fairing: w/o
 Nozzle Exit Plate: 1.00
 $\theta = 20^\circ$

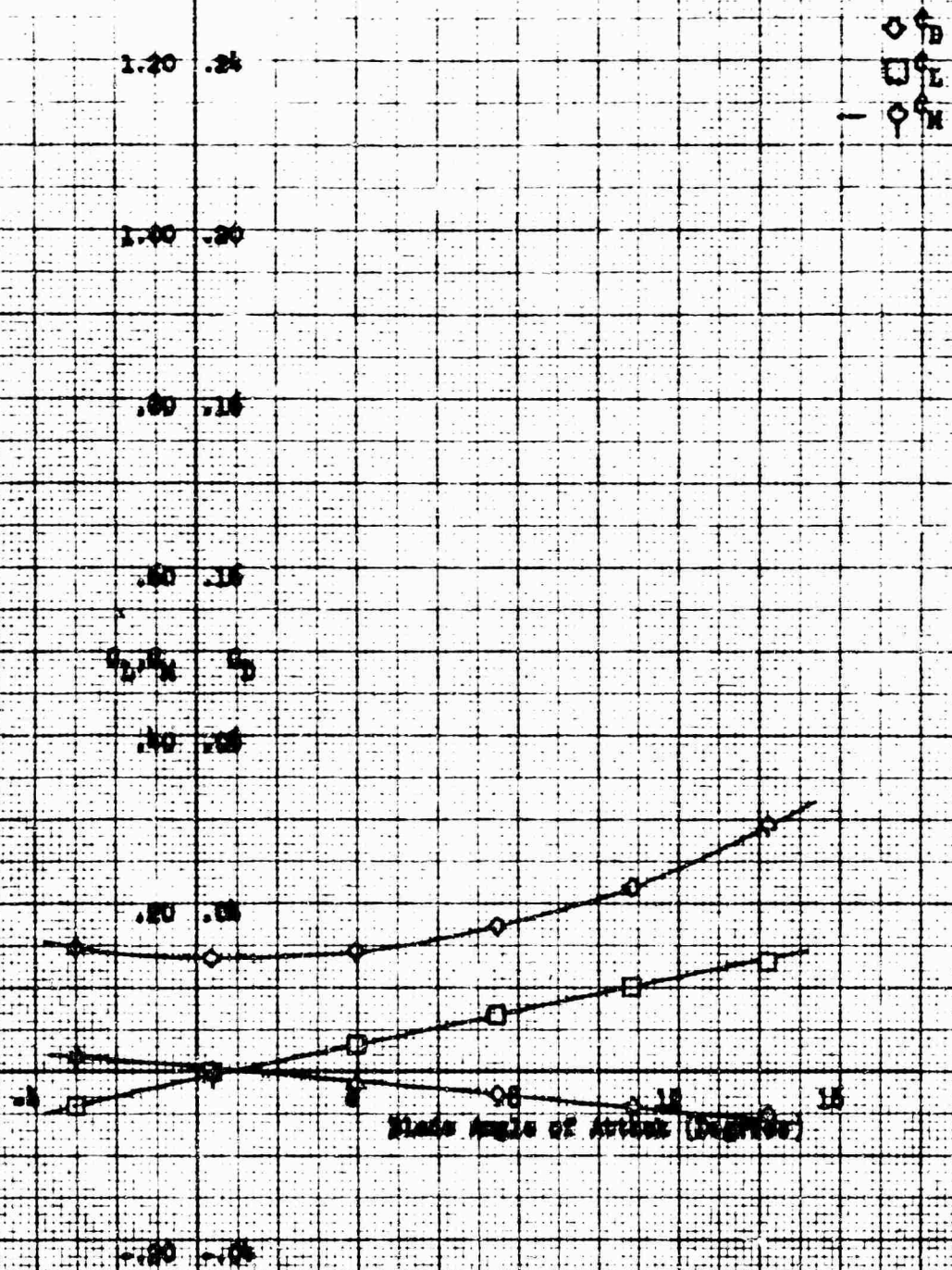
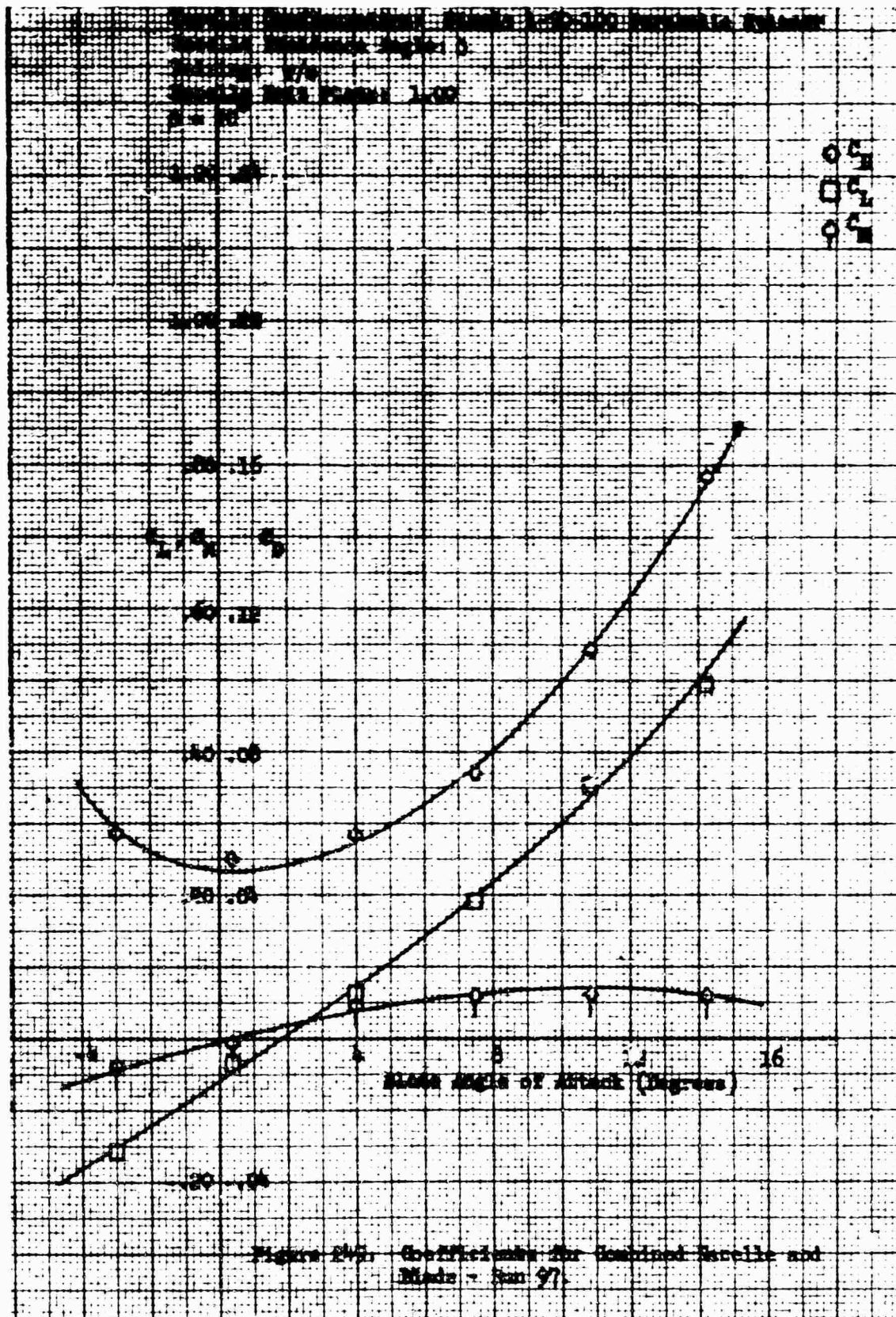
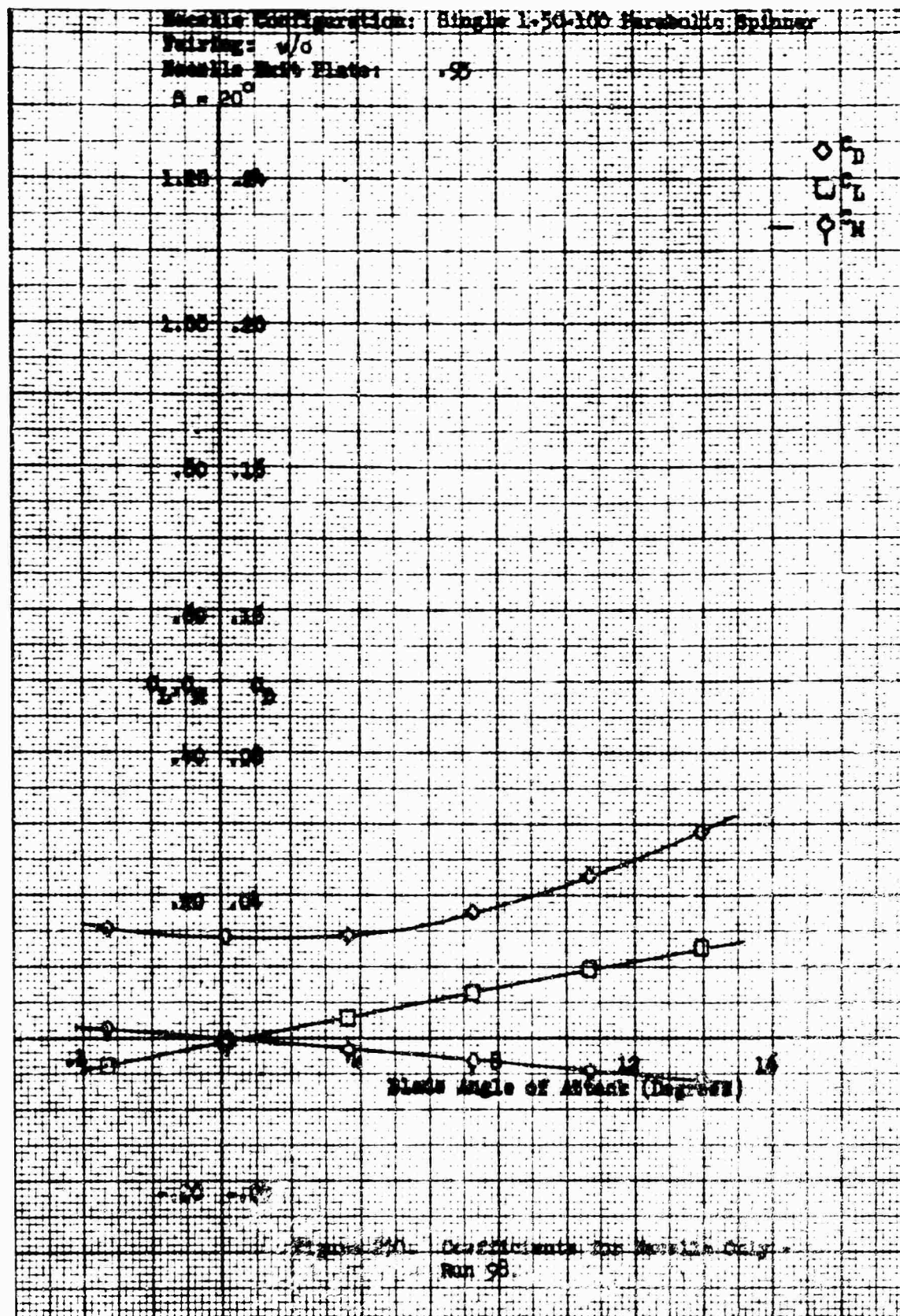


Figure 245. Coefficients for Nozzle Only - Run 97.





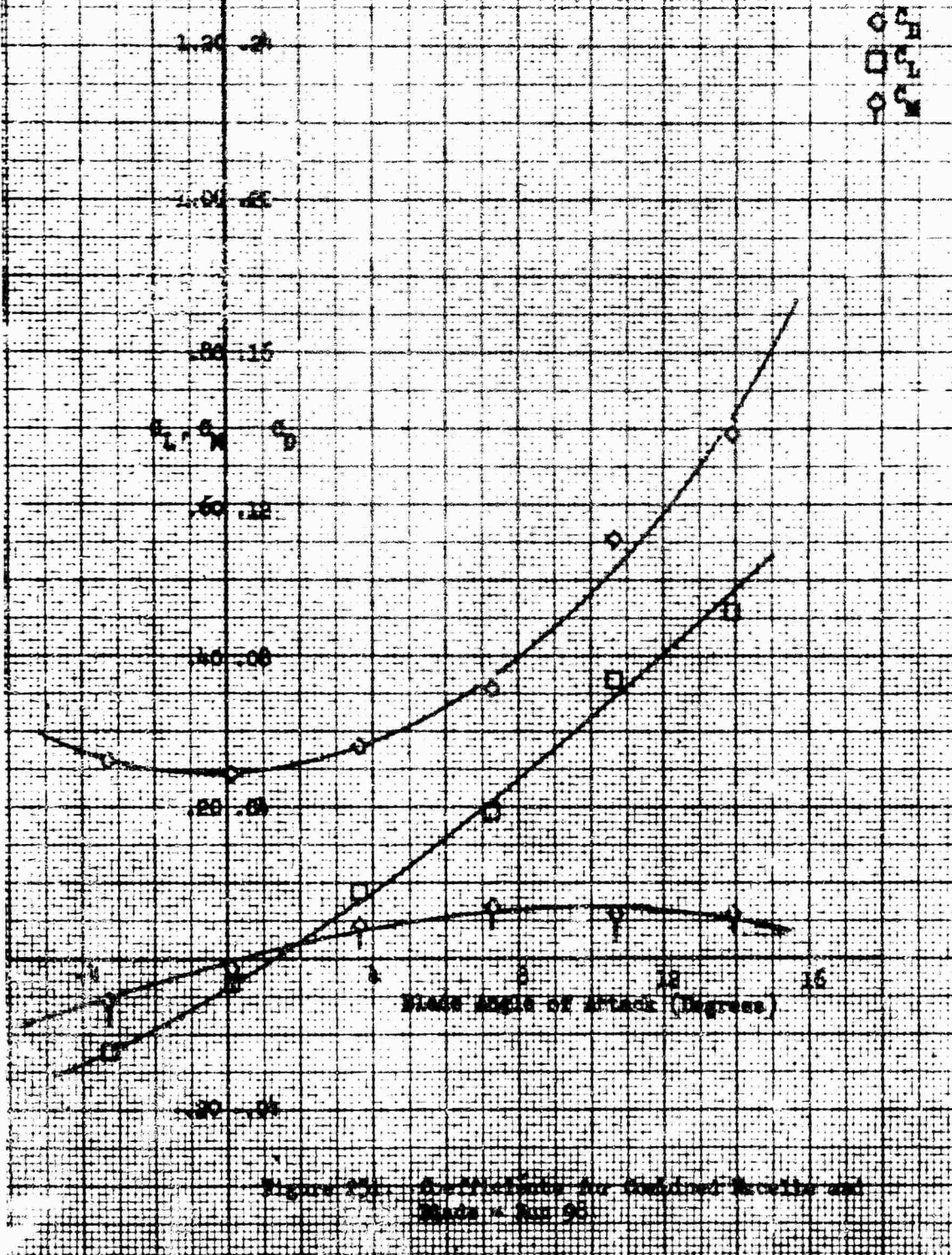
Nozzle Configuration: Blade 1-40-150 Parabolic Spinner

Nozzle Incidence Angle: 0

Pairing: +/0

Nozzle Exit Plane: .95

$\beta = 90^\circ$



Macelle Configuration: Single 1-90-100 Parabolic Spinner
 Pairing: w/o
 Macelle Exit Plate: .95
 $\beta = 16^\circ$

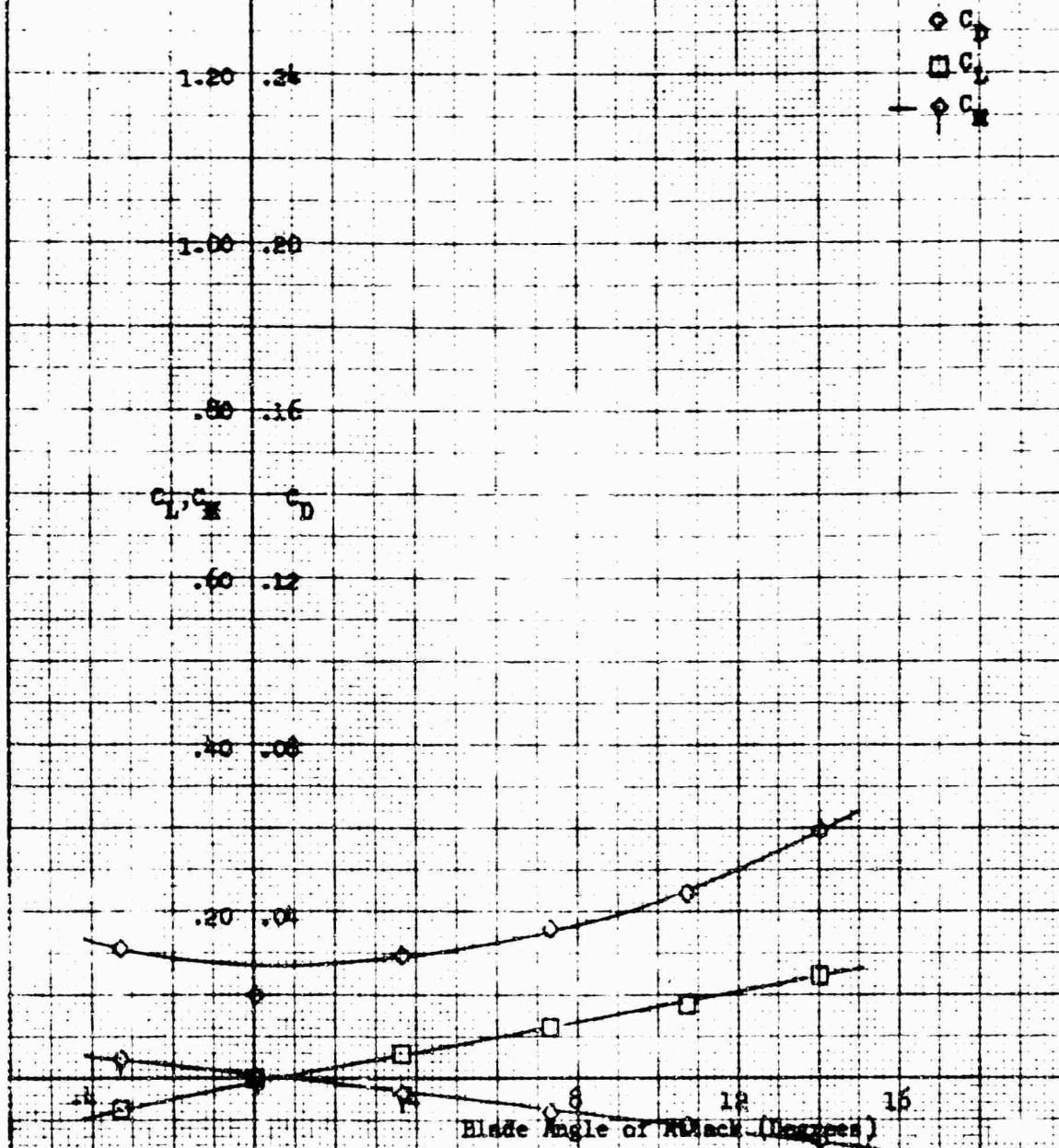


Figure 252. Coefficients for Macelle Only - Run 99.

Wacelle Configuration: Single 1-30-100 Parabolic Splaner

Wacelle Incidence Angle: 0

Pairing: w/o

Wacelle Exit Plate: .95

$\beta = 10^\circ$

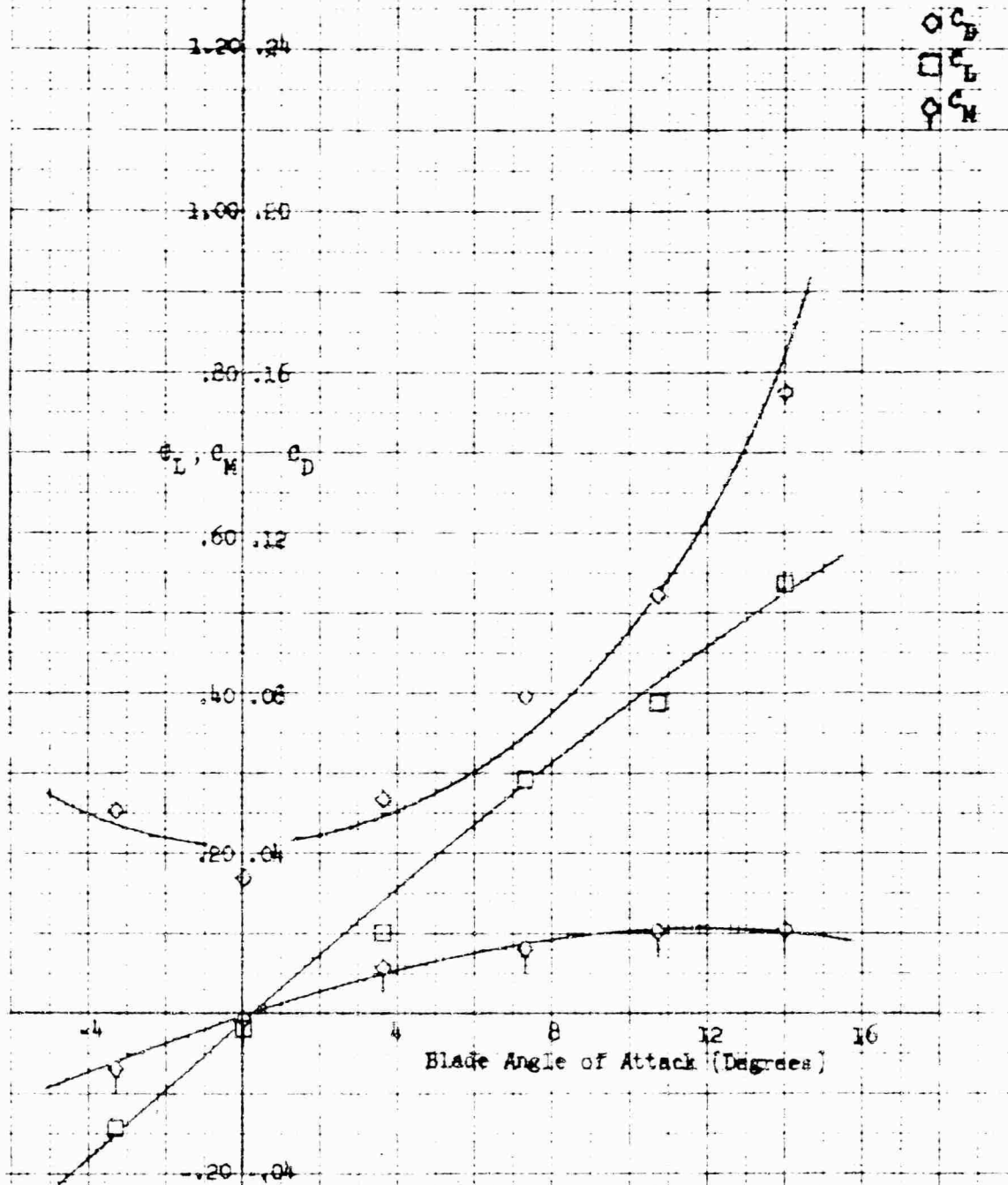


Figure 251. Coefficients for Combined Wacelle and Blade - Run 99

Nacelle Configuration: single 1-50:100 Parabolic Spinner
 Fairing: w/o
 Nacelle Exit Plate: .95
 $\beta = 0$

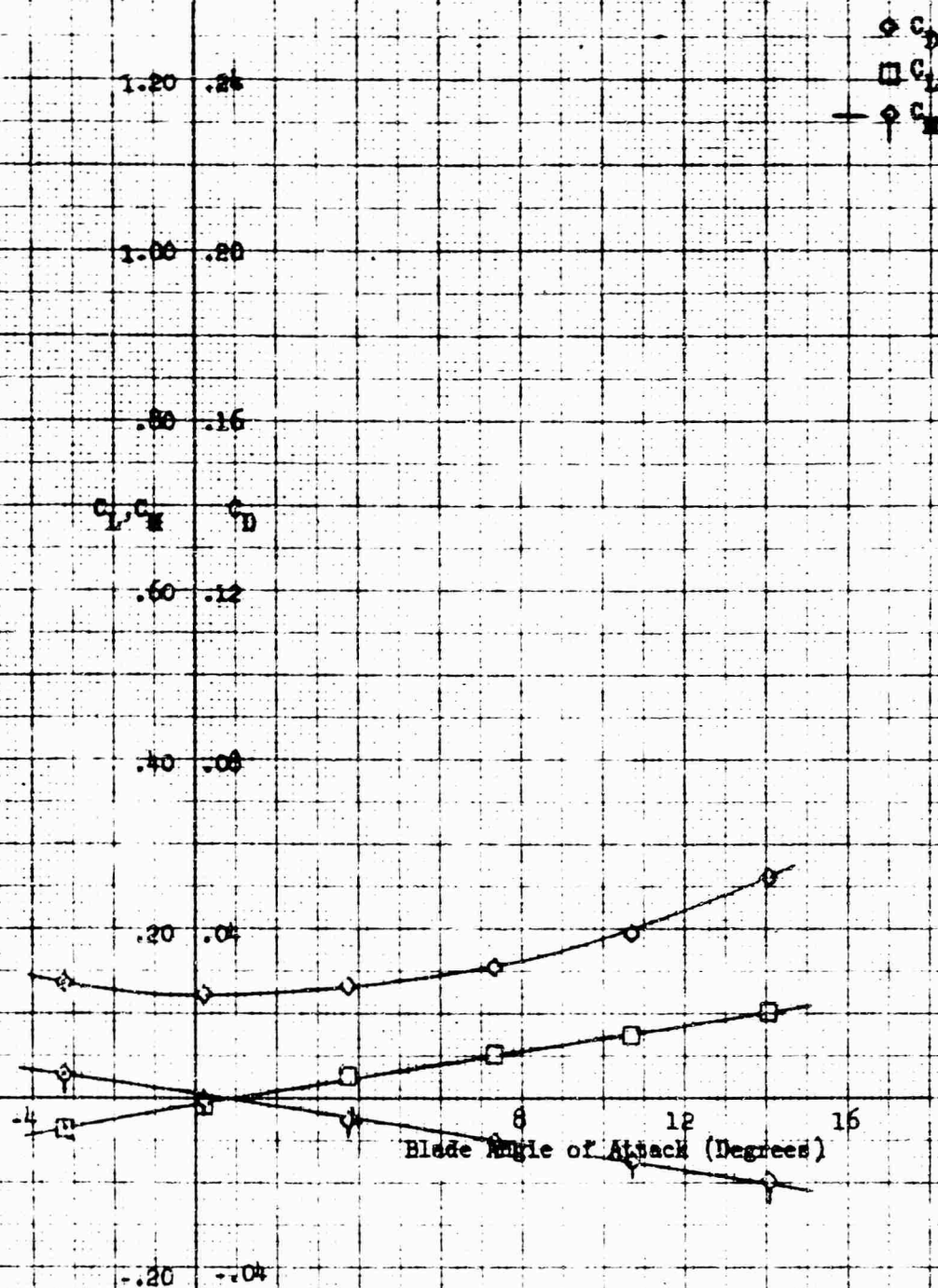
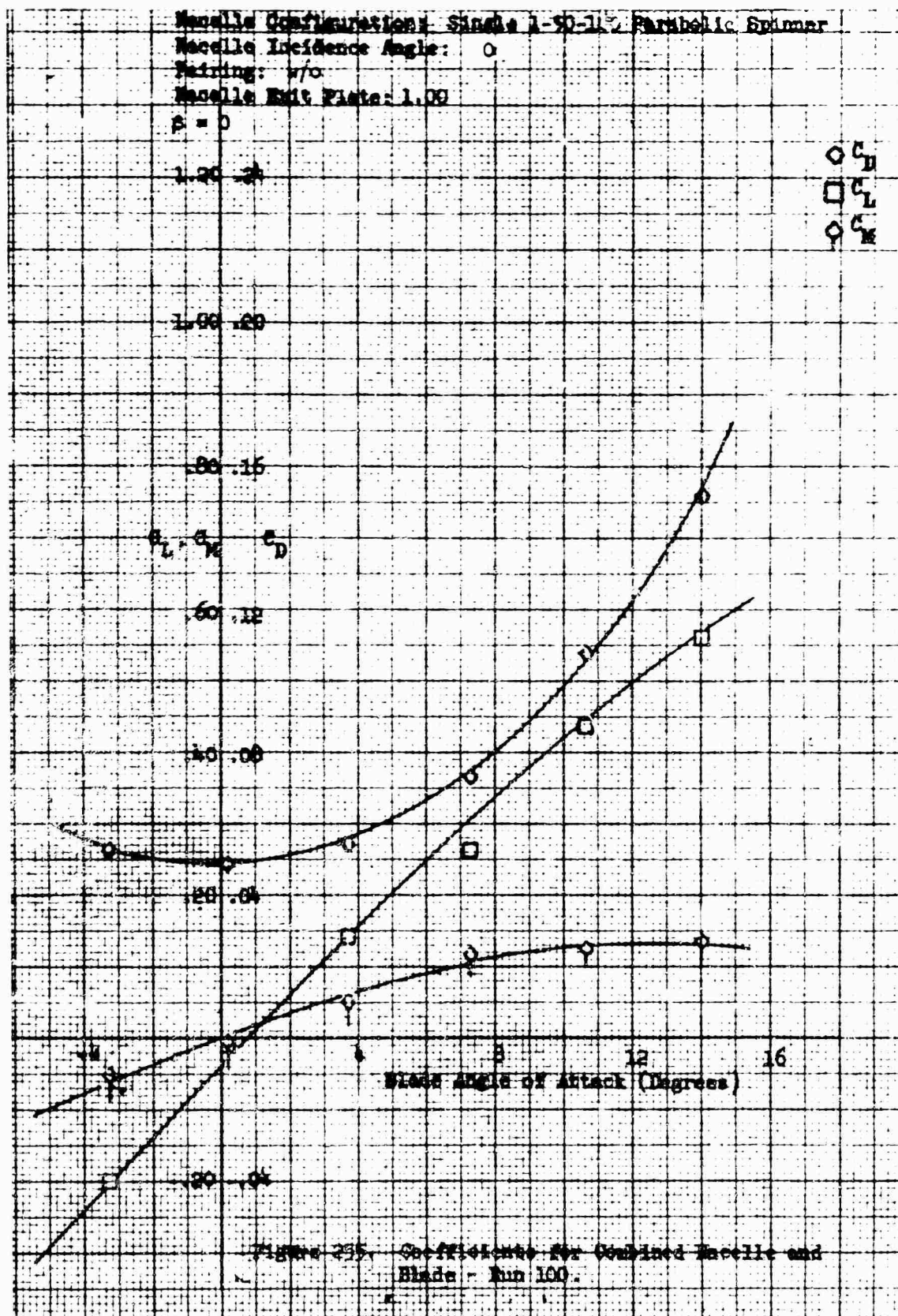
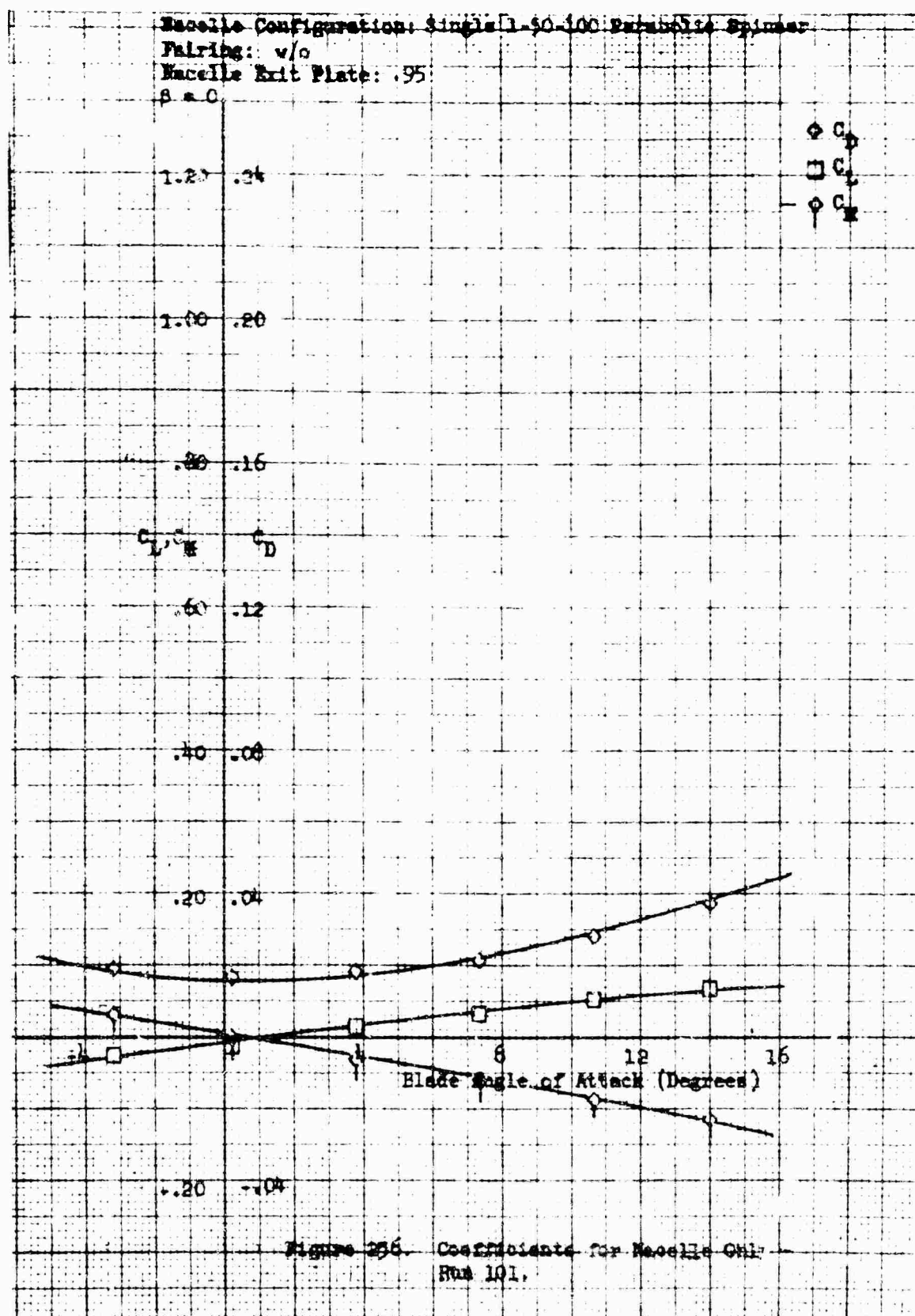


Figure 254. Coefficients for Nacelle Only -
 Run 100.





Macelle Configuration: Single 1-30-100 parabolic spinner
 Macelle Incidence Angle: 0°
 Fairing: W/O
 Macelle Exit Plate: .95
 $\beta = 0^\circ$

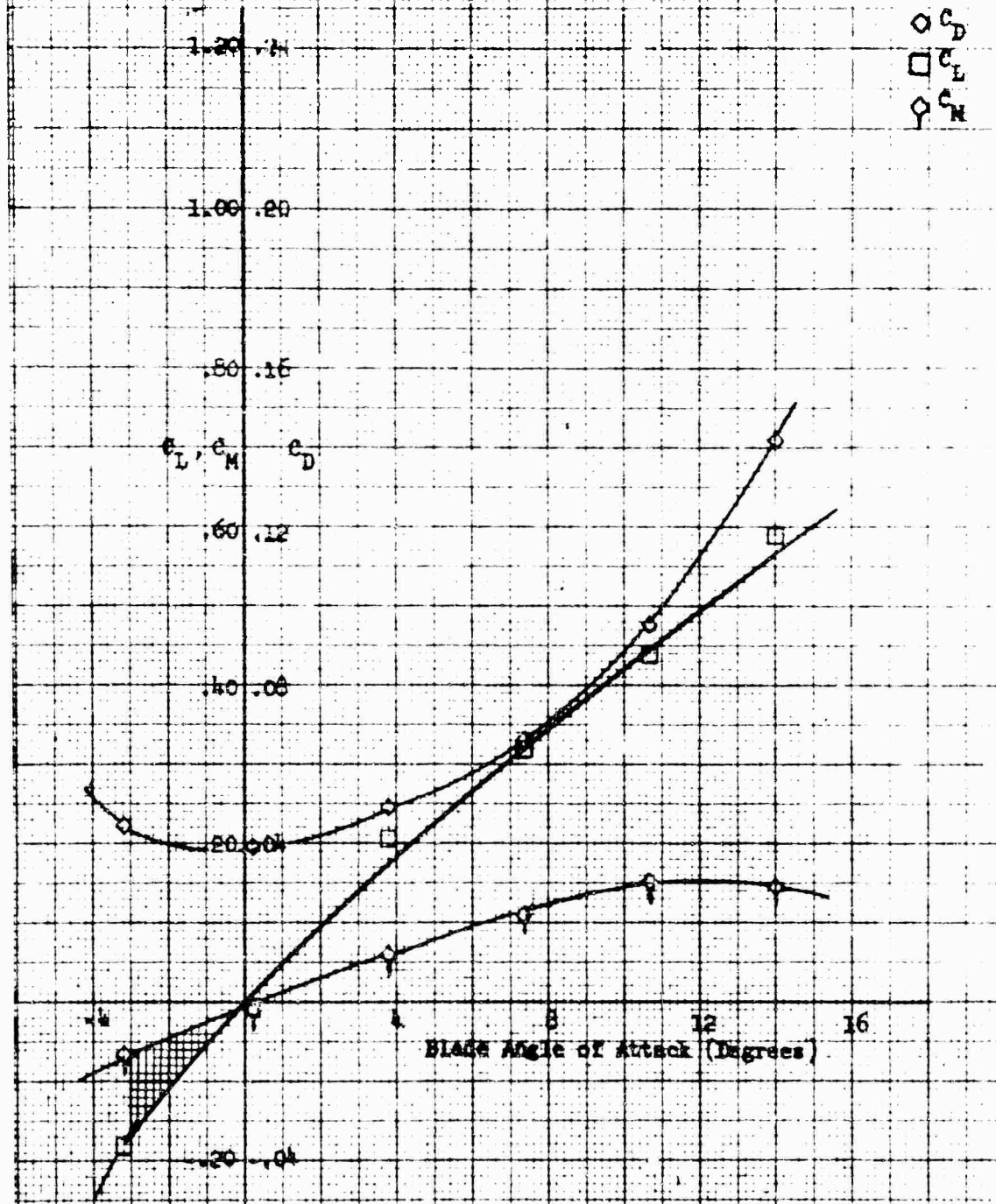


Figure 237. Coefficients for Combined Macelle and Blade - Run 201.

Nozzle Configuration: Single 1-50-100 Perforated Spinner
 Pairing: w/p
 Nozzle Exit Plane: .95
 $\alpha = -20^\circ$

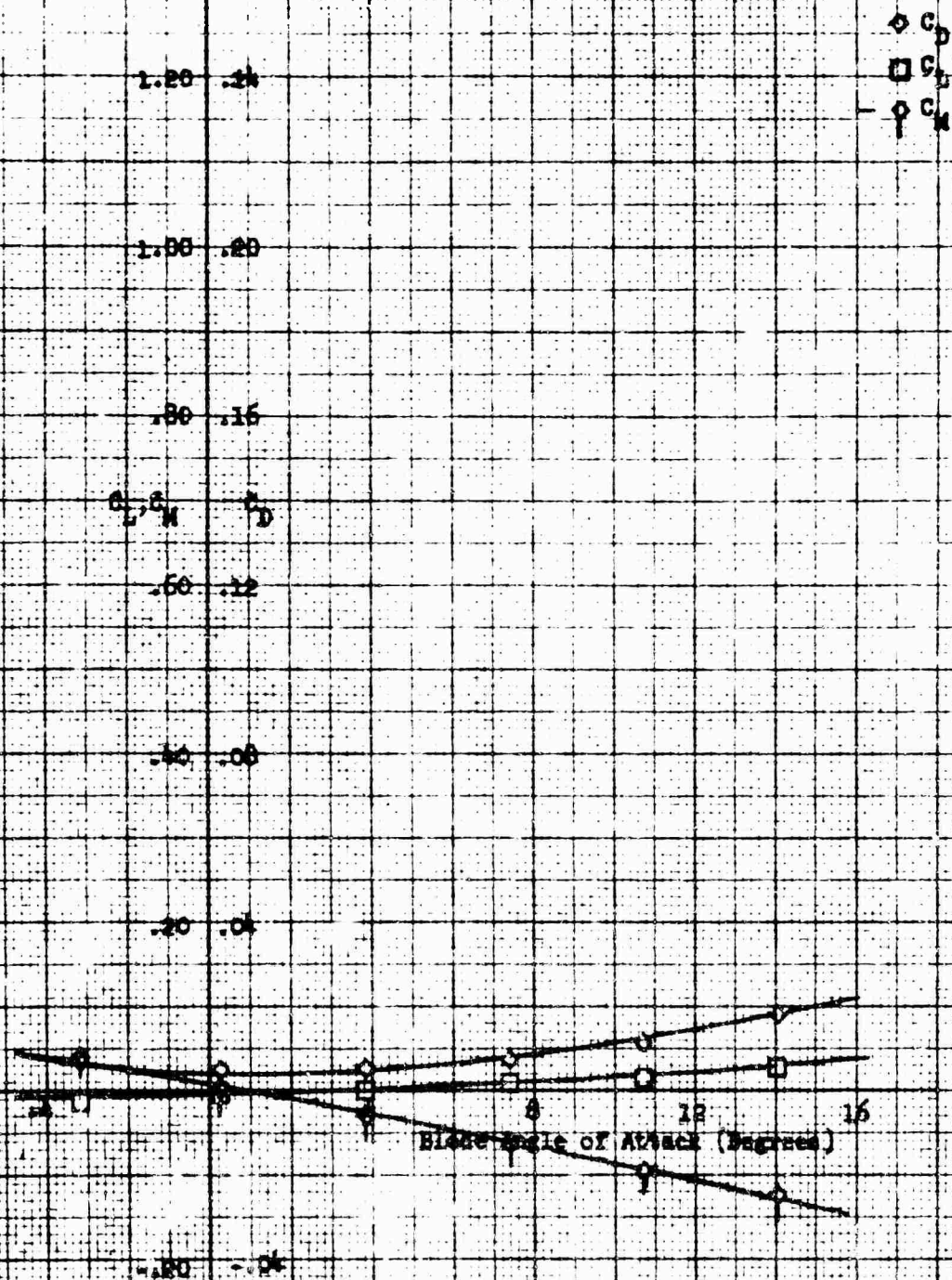
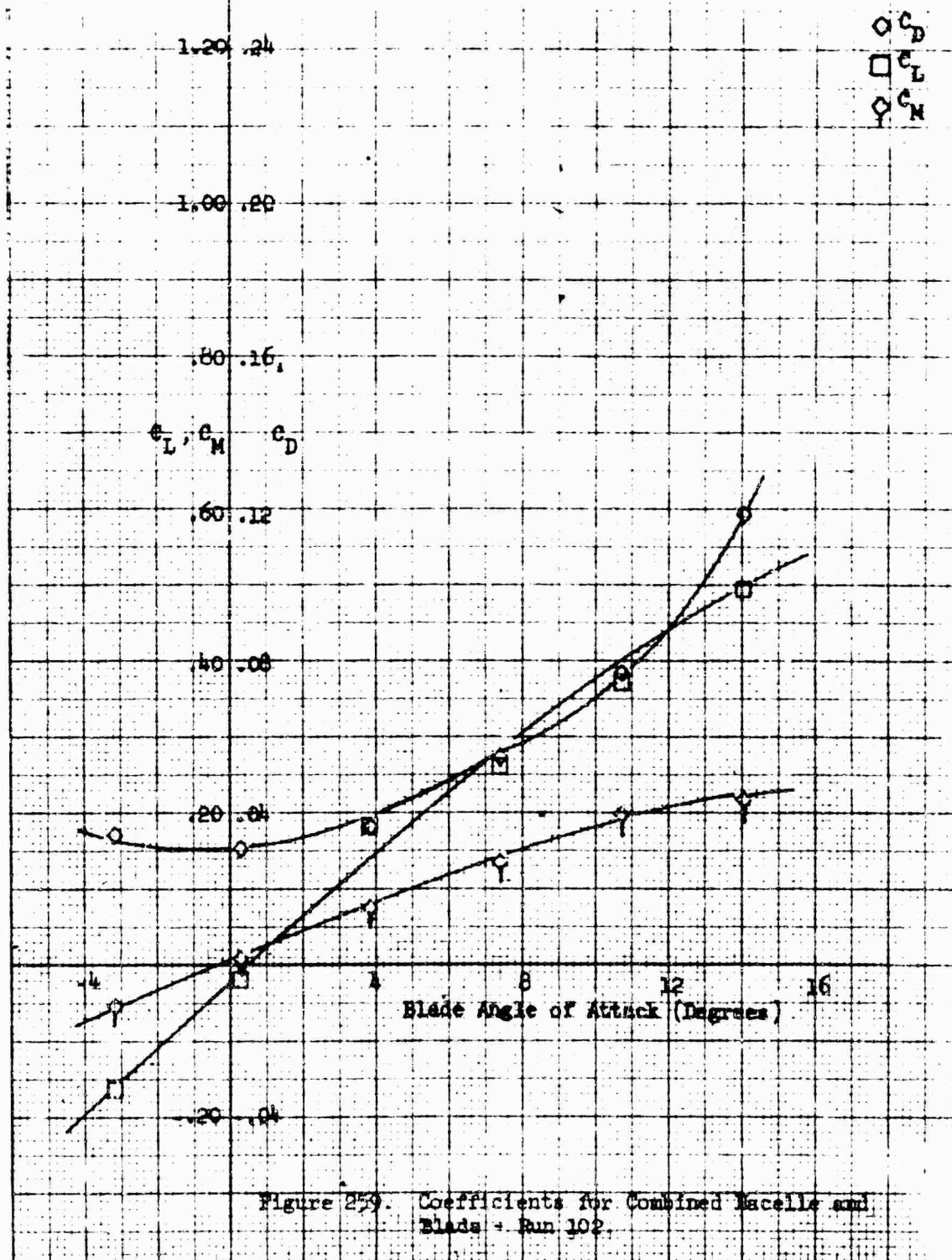
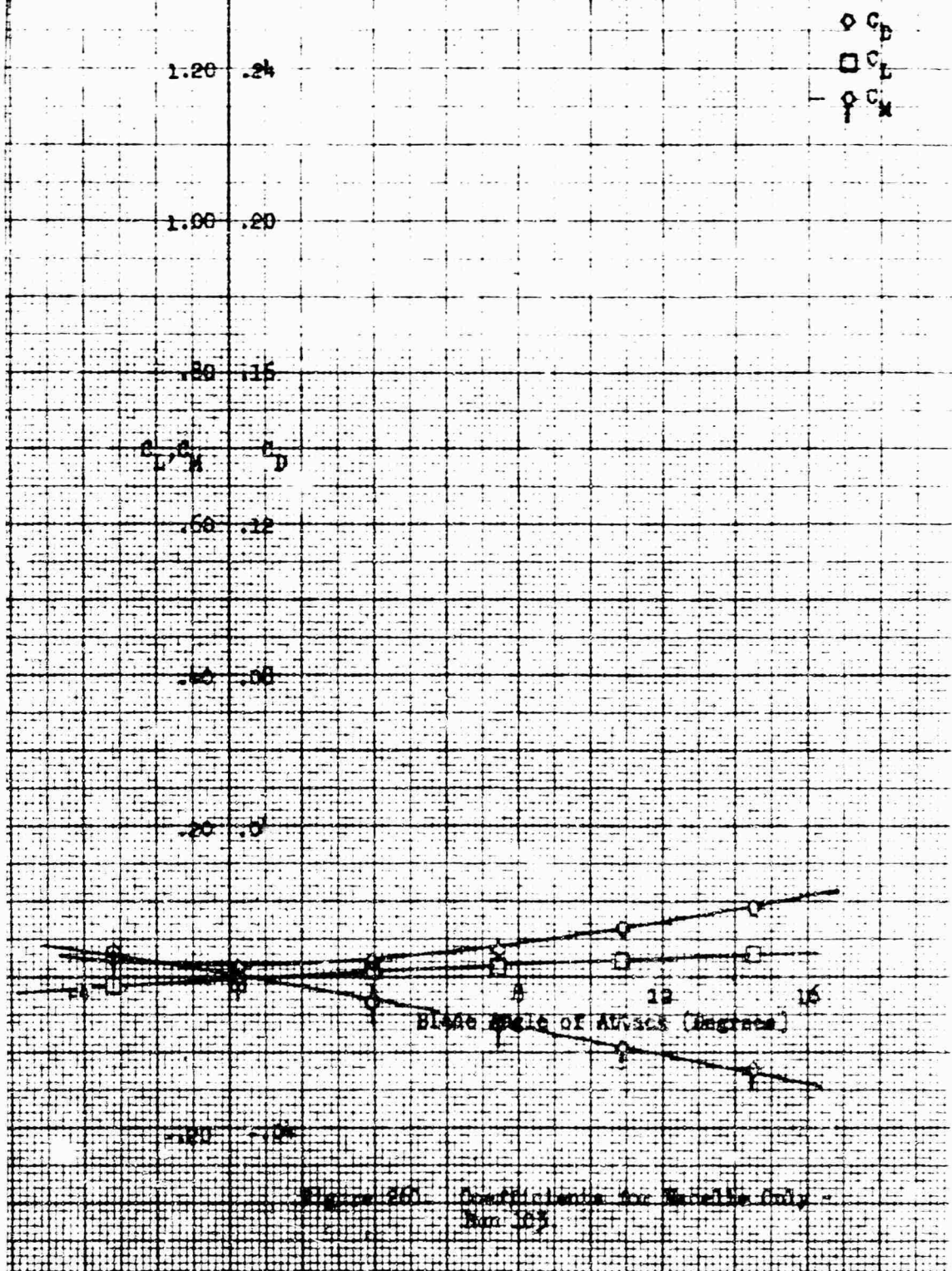


Figure 25A. Coefficients for Nozzle Only -
 Run 102.

Macelle Configuration: Single 1-5C-100 parabolic spinner
 Macelle Incidence Angle: 0°
 Pairing: W/O
 Macelle Exit Plate: 95°
 $\beta = 20^\circ$



Nacelle Configuration: Single .50:100 Parabolic Spinner
 Fairing: w/o
 Nacelle Exit Plate: .75
 $\alpha = -20^\circ$



Nacelle Configuration: Single 2-30-100 parabolic spinner
 Nacelle Incidence Angle: 0°
 Training: W/O
 Nacelle Exit Plate: .90
 $\beta = .20^\circ$

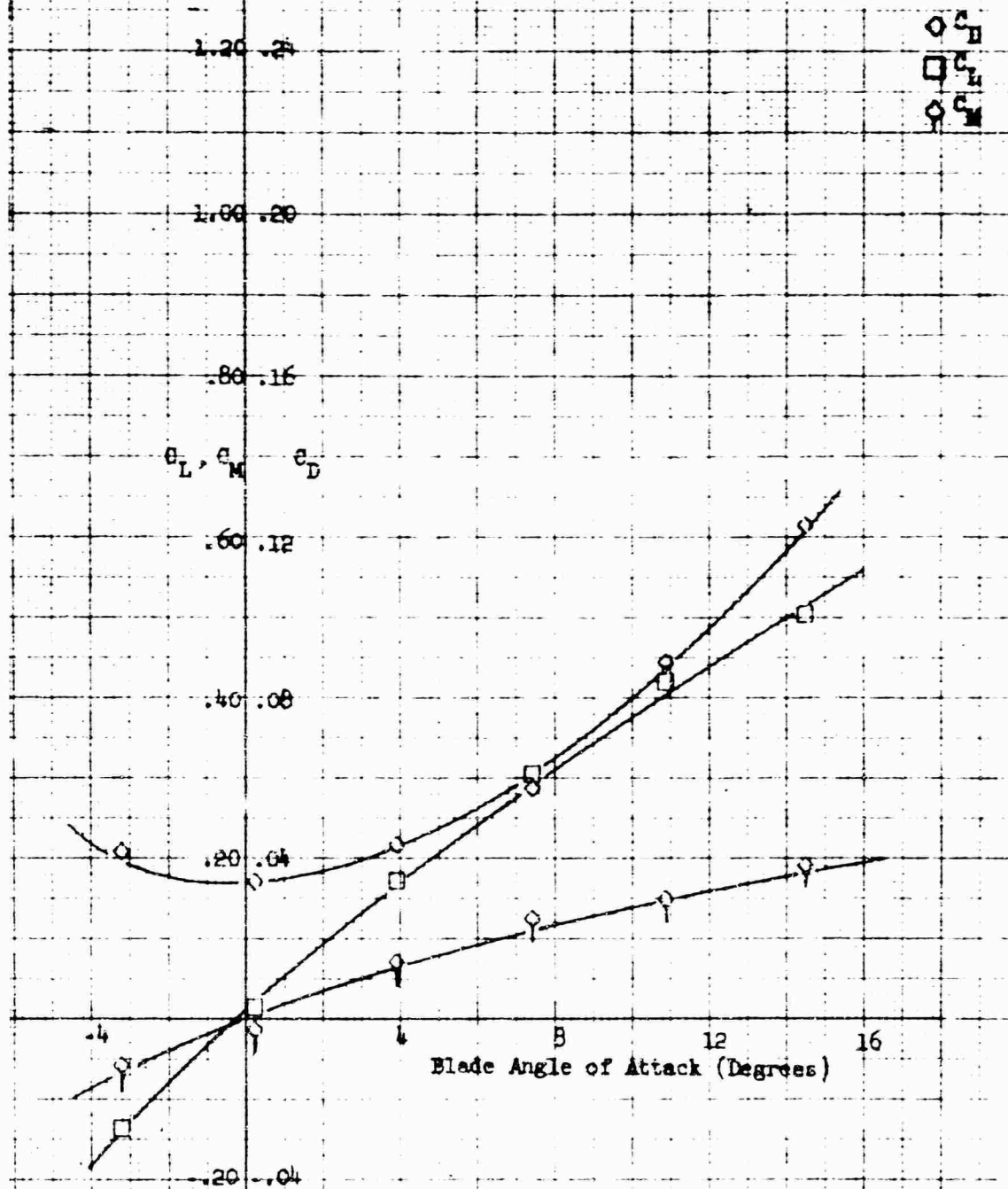


Figure 261. Coefficients for Combined Nacelle and Blade - Run 103.

Blade Configuration: Single Blade
 Fairing: v/o
 Blade Exit Plate: 2"
 $\alpha = 10^\circ$

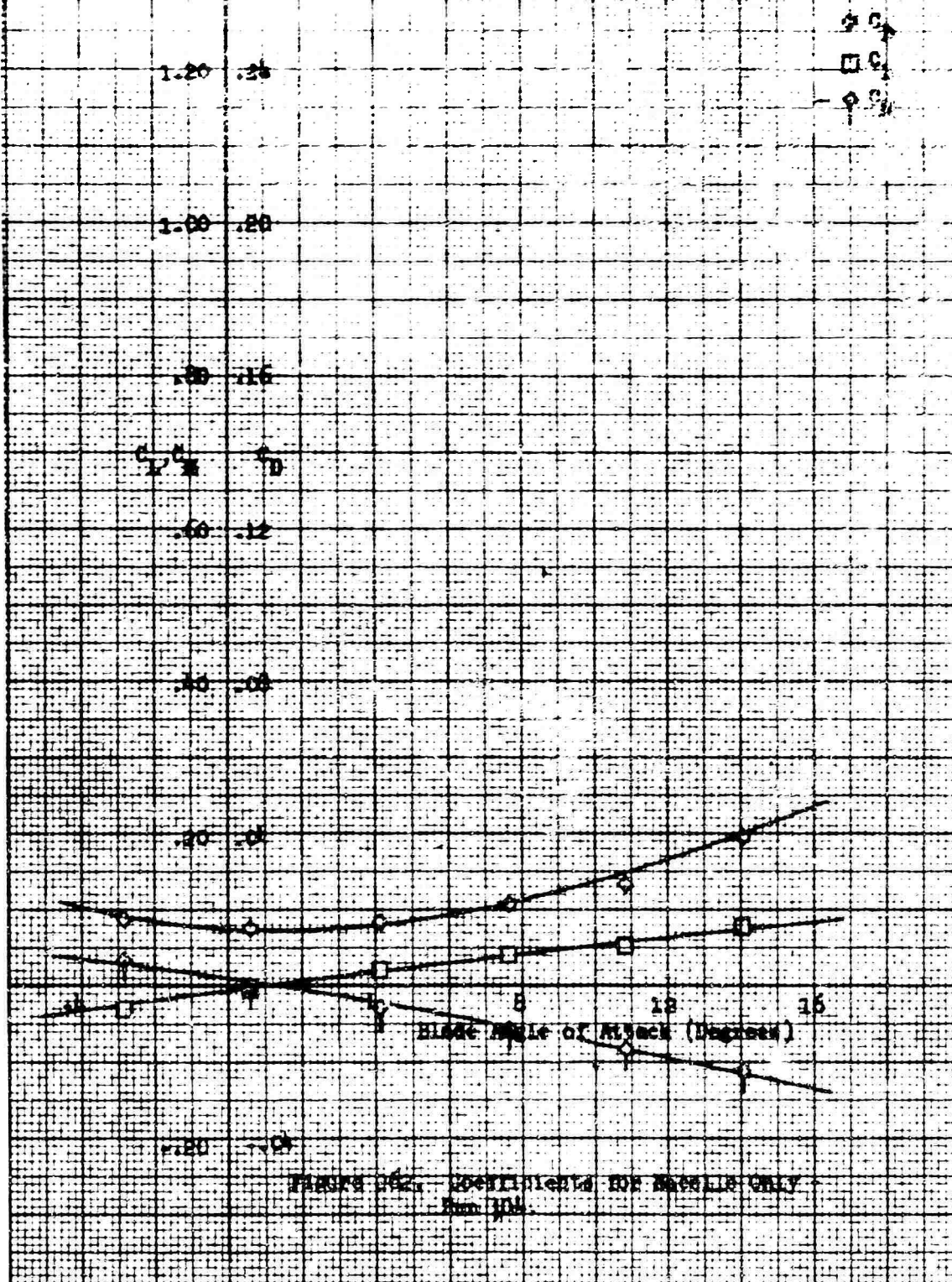


FIGURE 2-2. COEFFICIENTS FOR BLADE ONLY
 Run 104

Nacelle Configuration: Single 1-50-100 parabolic spinner
 Nacelle Incidence Angle: 0°
 Fairing: w/o
 Nacelle Exit Plane: 90°
 $\beta = 10^\circ$

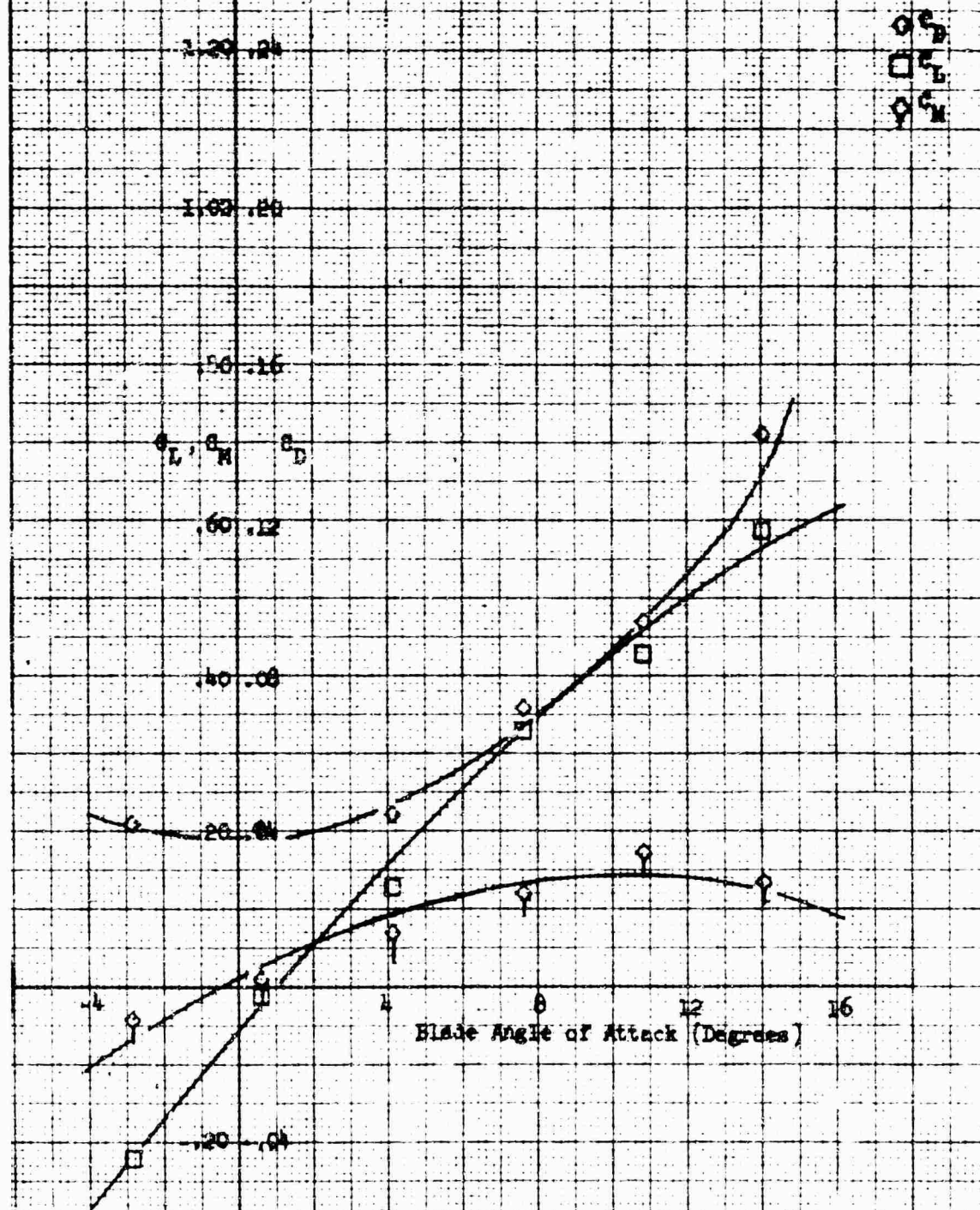


Figure 265. Coefficients for Combined Nacelle and Blade - Run 104.

Nacelle Configuration: Single 1-50-100 Parabolic Spinner
 Fairing: w/o
 Nacelle Exit Plate: .95
 $\delta = 0$

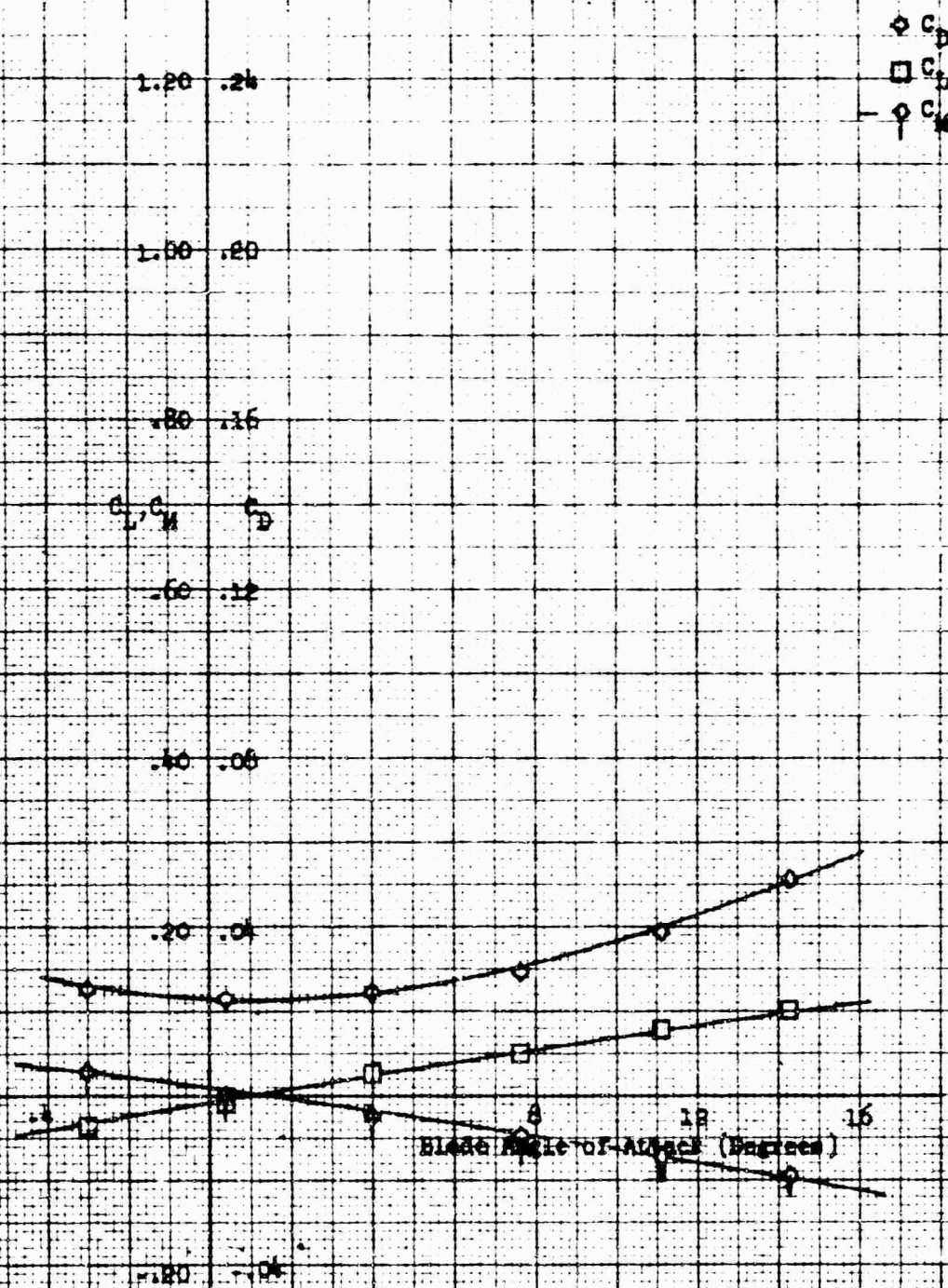
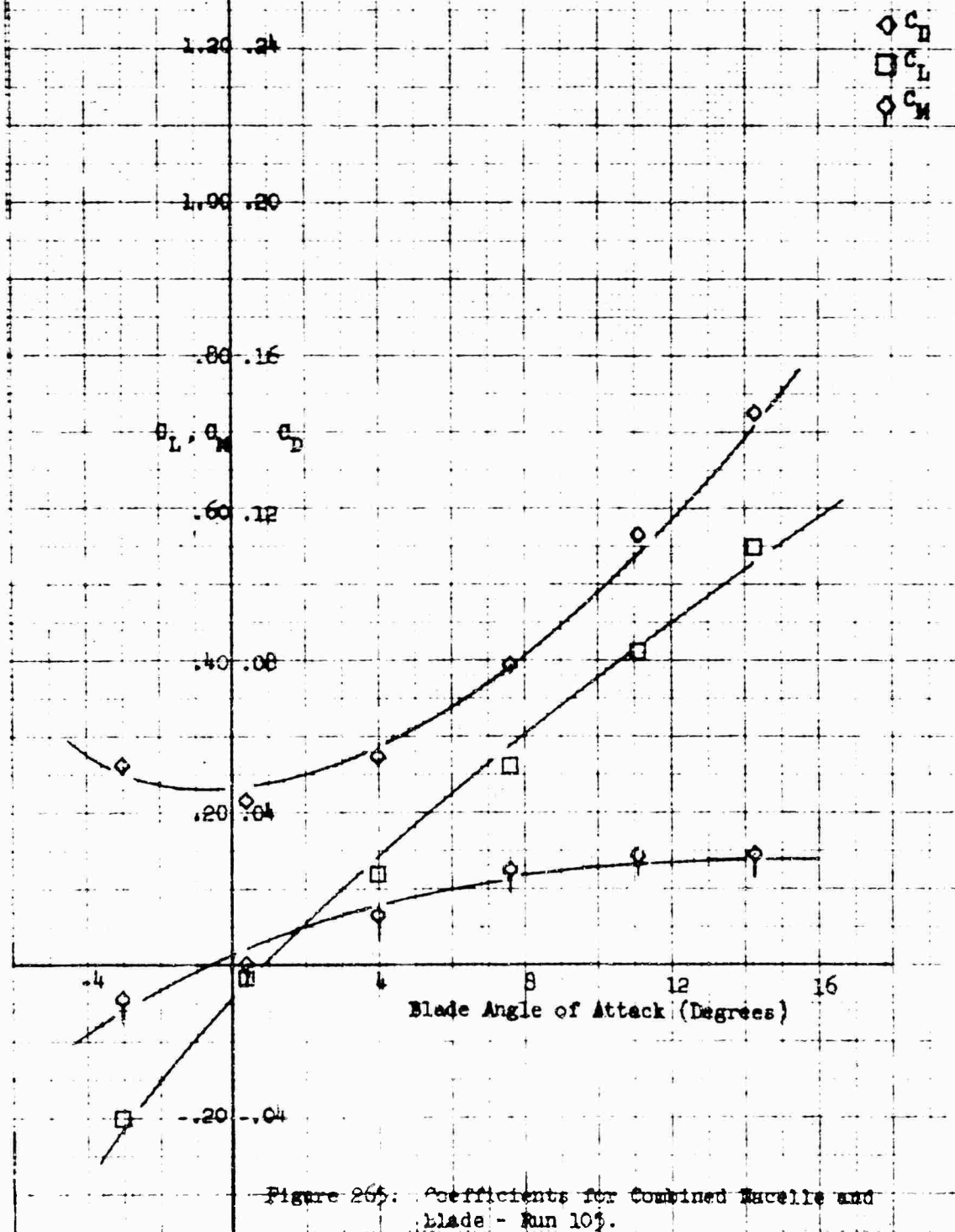


Figure 264. Coefficients for Nacelle Only -
 Run 105.

Macelle Configuration: Single 1-50-100 parabolic spinner
 Macelle Incidence Angle: 0°
 Fairing: 4/6
 Macelle Exit Flare: .95
 $\beta = 0$



Baseline Configuration: Single 1.50-100 Parabolic Primer

Pairing: N/O

Baseline Kri: Plate: .90

2.20

1.20 20

1.00 20

.80 20

.60 20

.40 20

.20 20

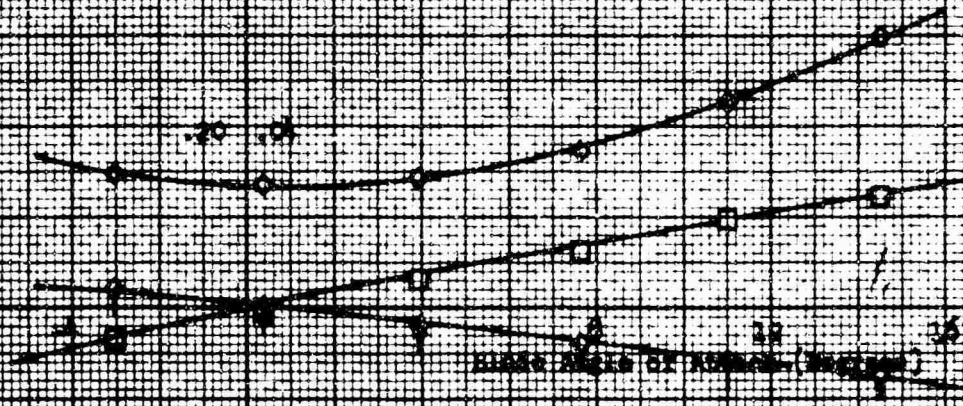
.00 20

1.20 20

0.0

0.1

0.2



Baseline Kri: Plate: .90

Baseline Configuration: Single 1.50-100 Parabolic Primer

Nacelle Configuration: Single 1-50-200 parabolic spinner
 Nacelle Incidence Angle: 0°
 Fairing: (W/O)
 Nacelle Exit Plate: .80
 $B = 10^\circ$

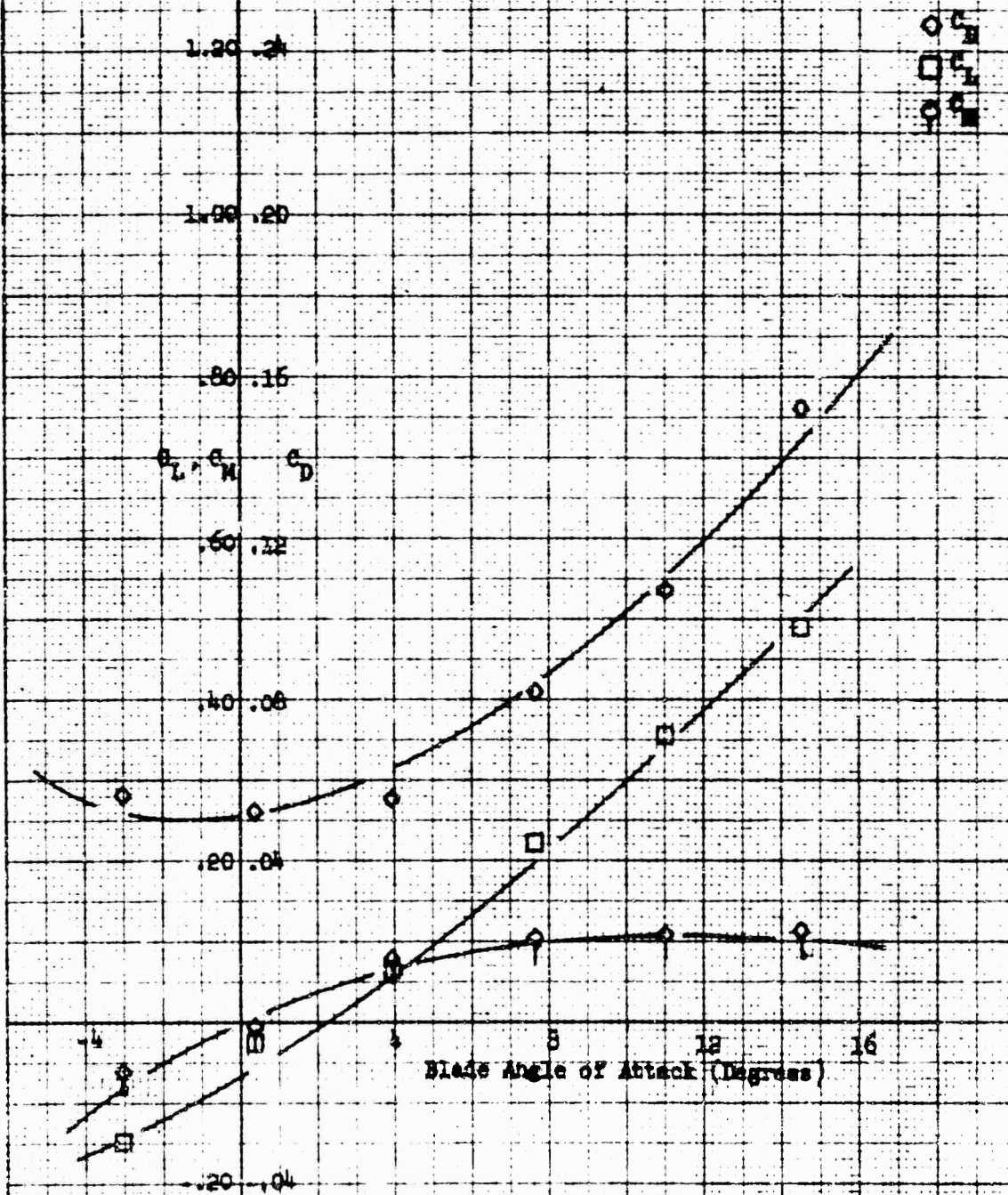
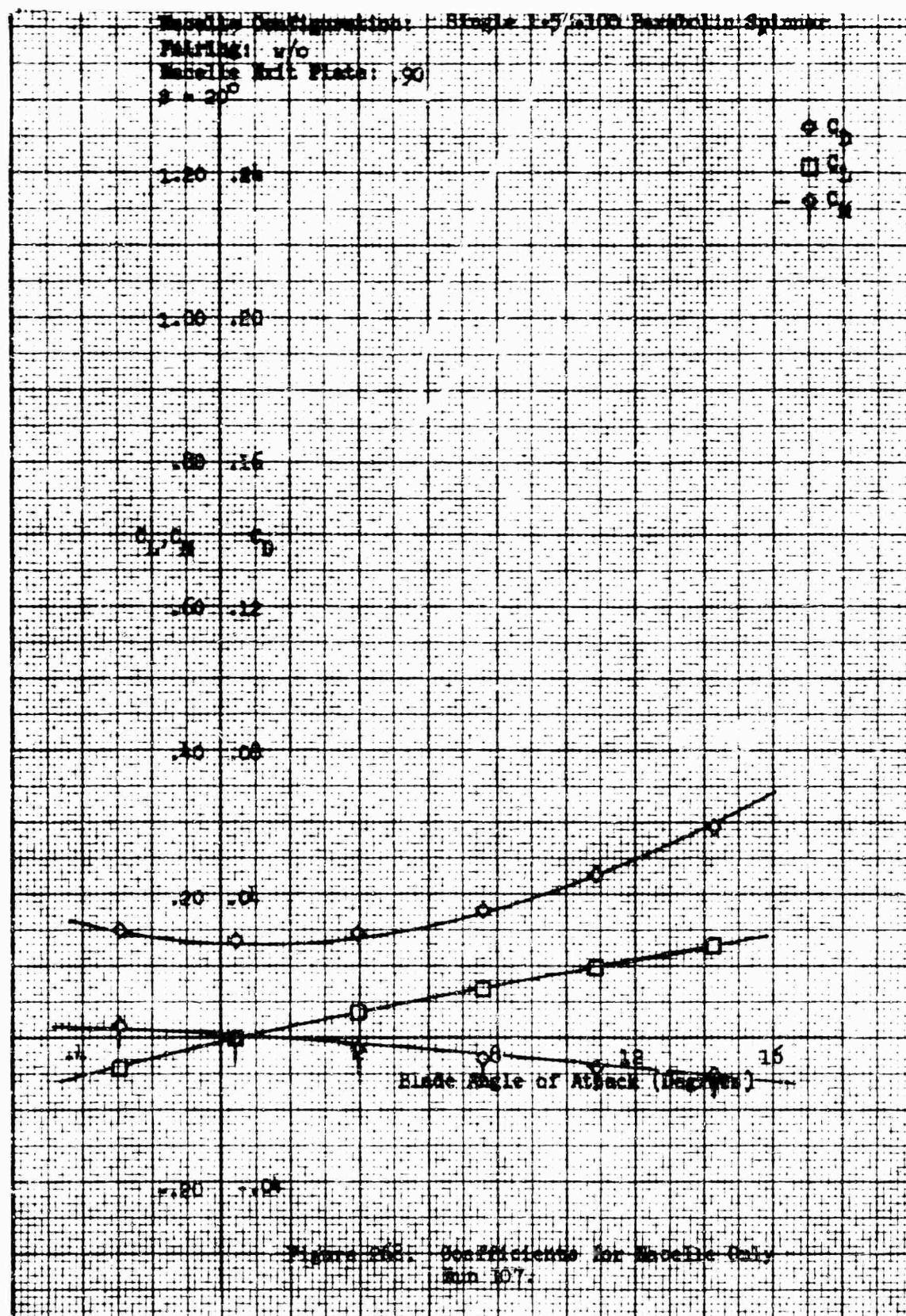
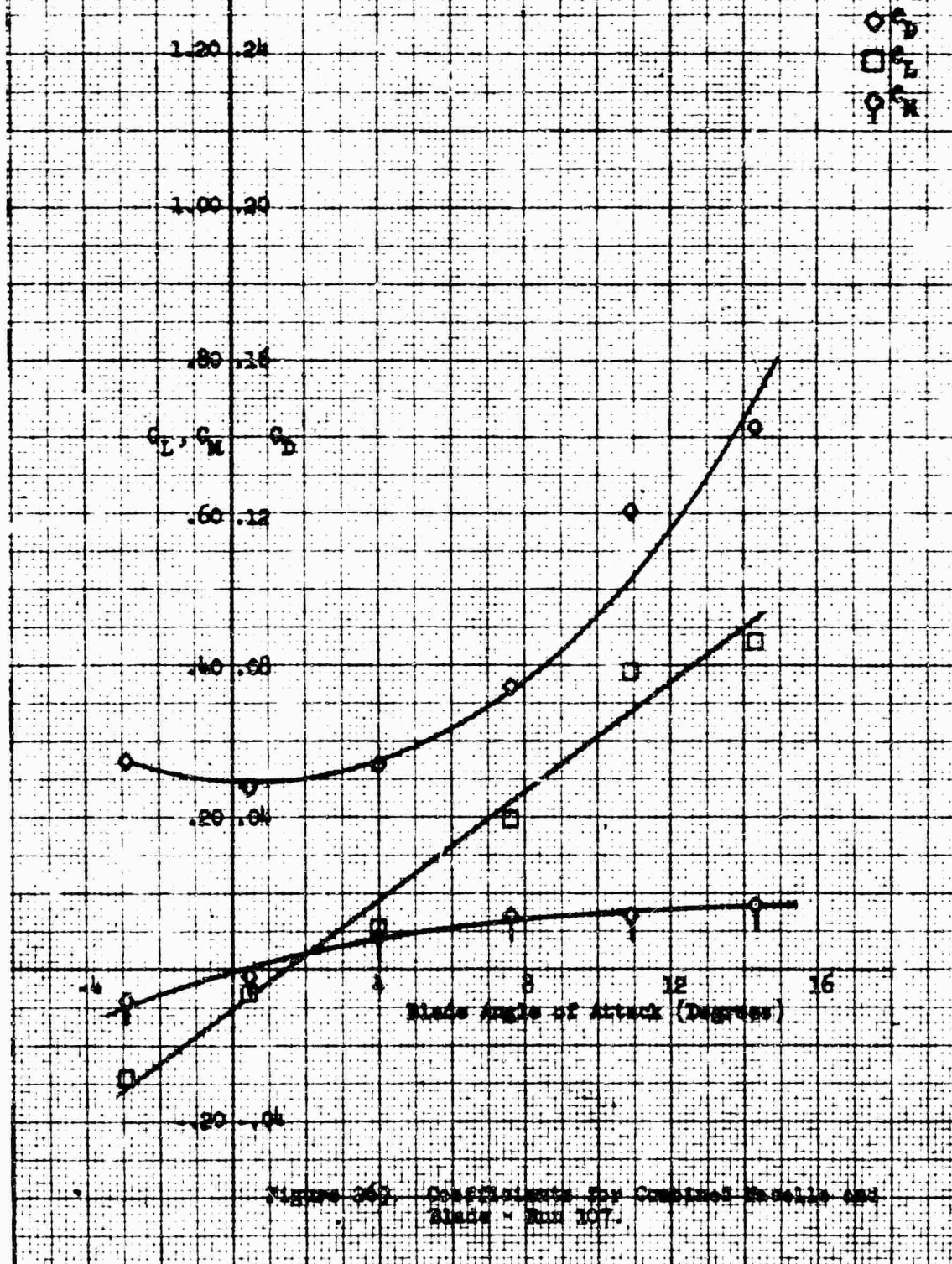


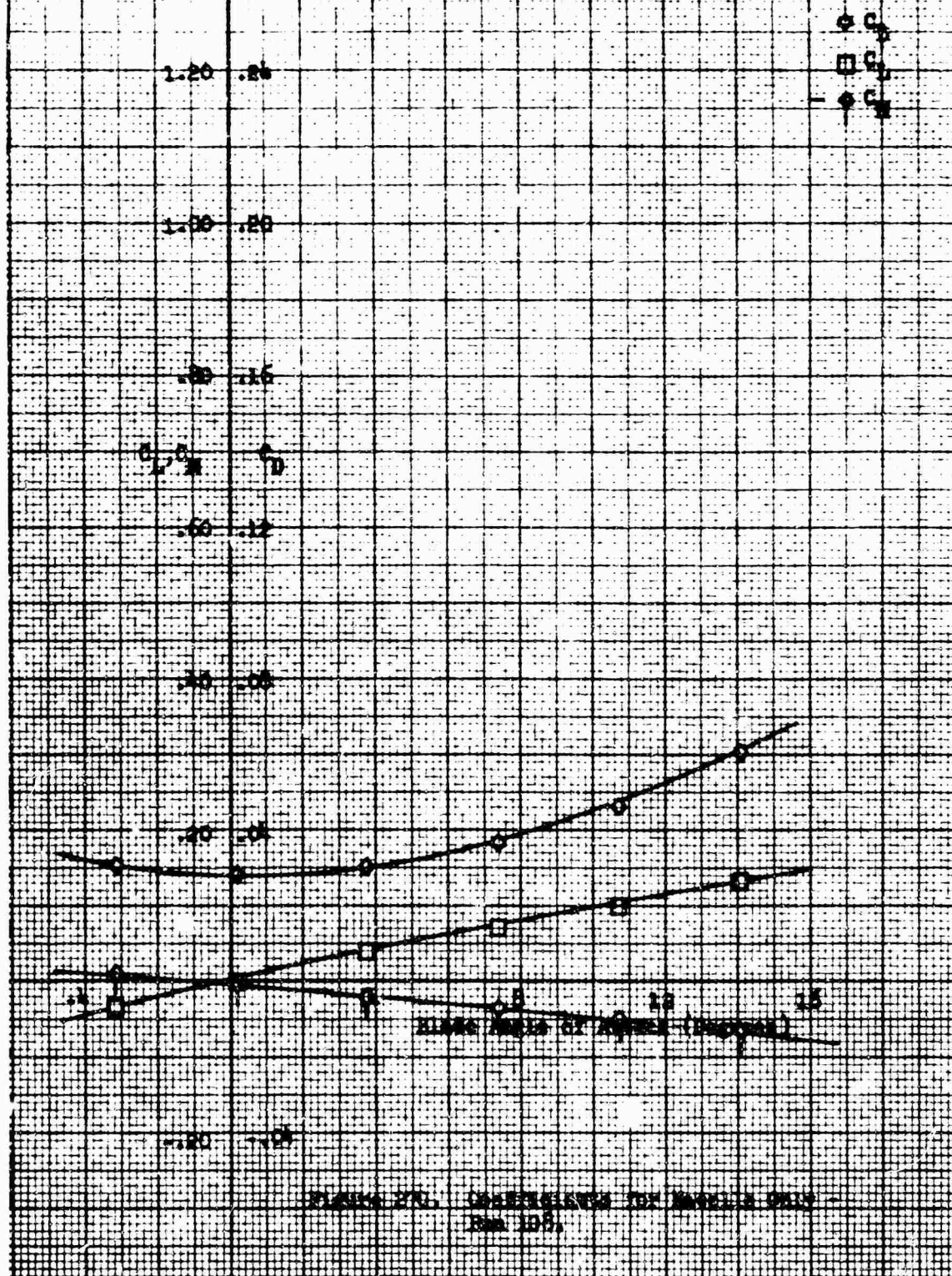
Figure 267. Coefficients for Combined Nacelle and Blade - Run 106.

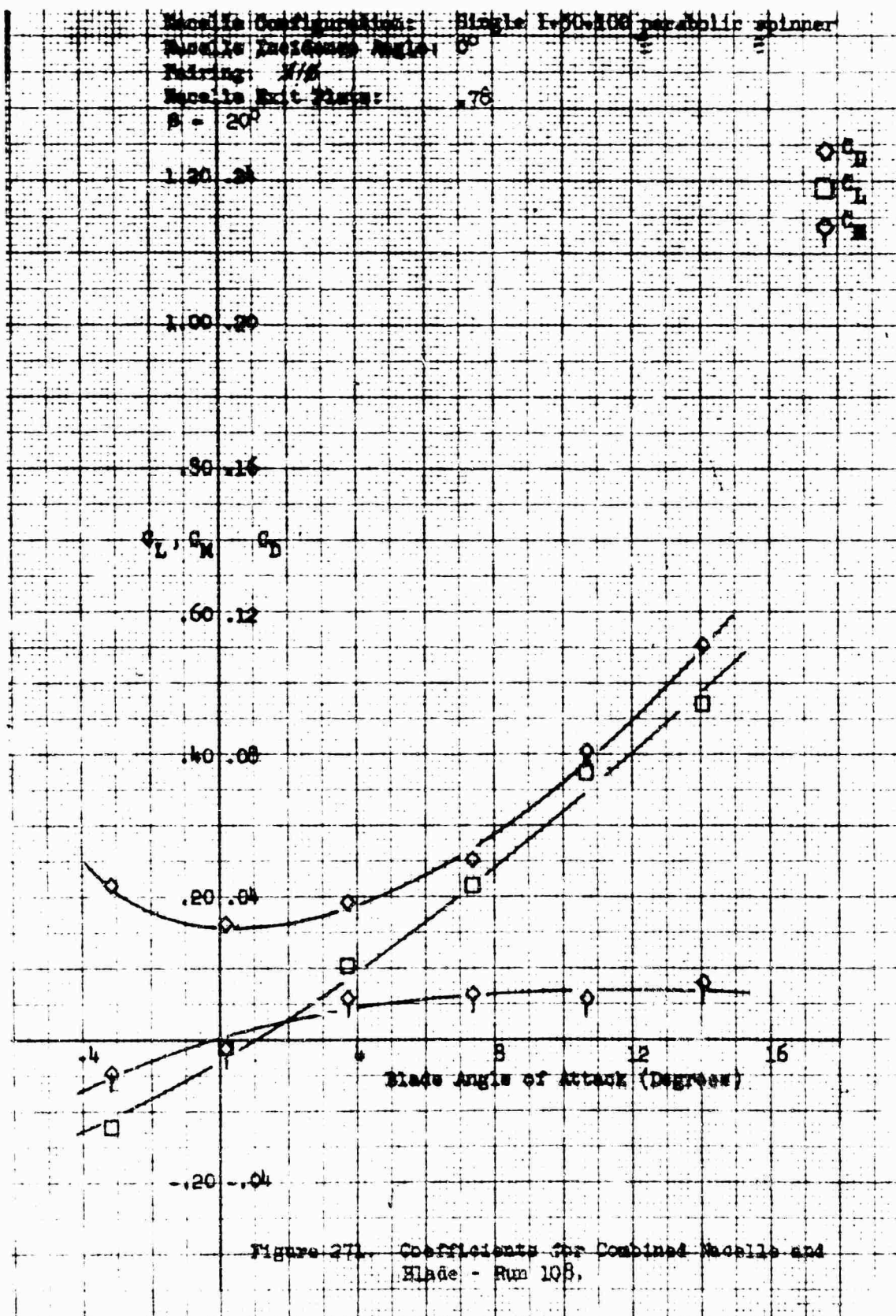


Nacelle Configuration: Single 1-50-100 parabolic spinner
 Nacelle Incidence Angle: 0°
 Fairing: W/O
 Nacelle Exit Plate: .90
 $\beta = 20^\circ$



Nozzle Configuration: Single 1-50-100 Parabolic Spinner
 Pairing: w/o
 Nozzle Exit Plane: .78
 $\alpha = 20^\circ$





Nacelle Configuration: Single 1:50:100 Parabolic Spinner
 Fairing: w/o
 Nacelle Exit Plate: .76
 $B = 10^\circ$

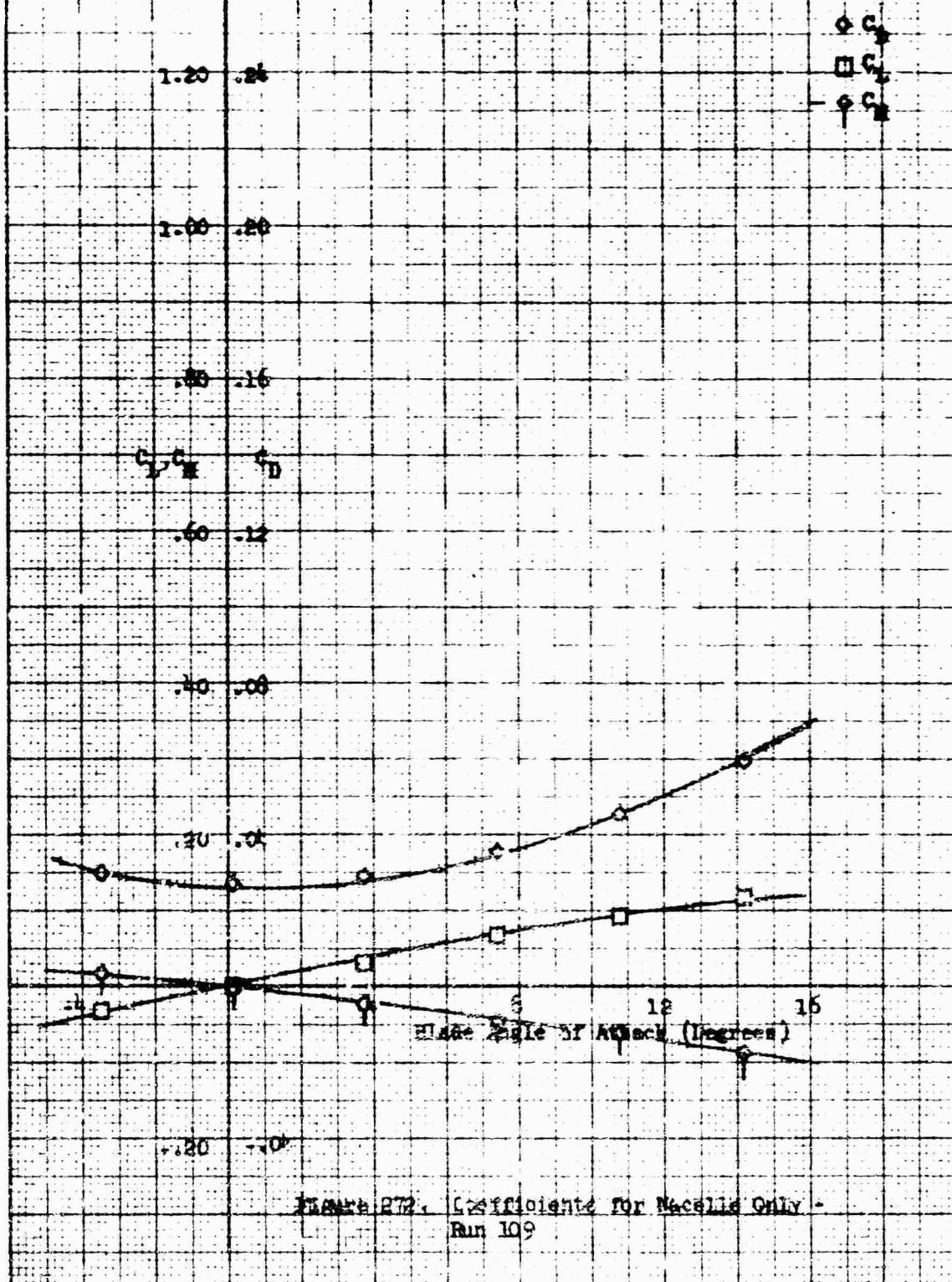
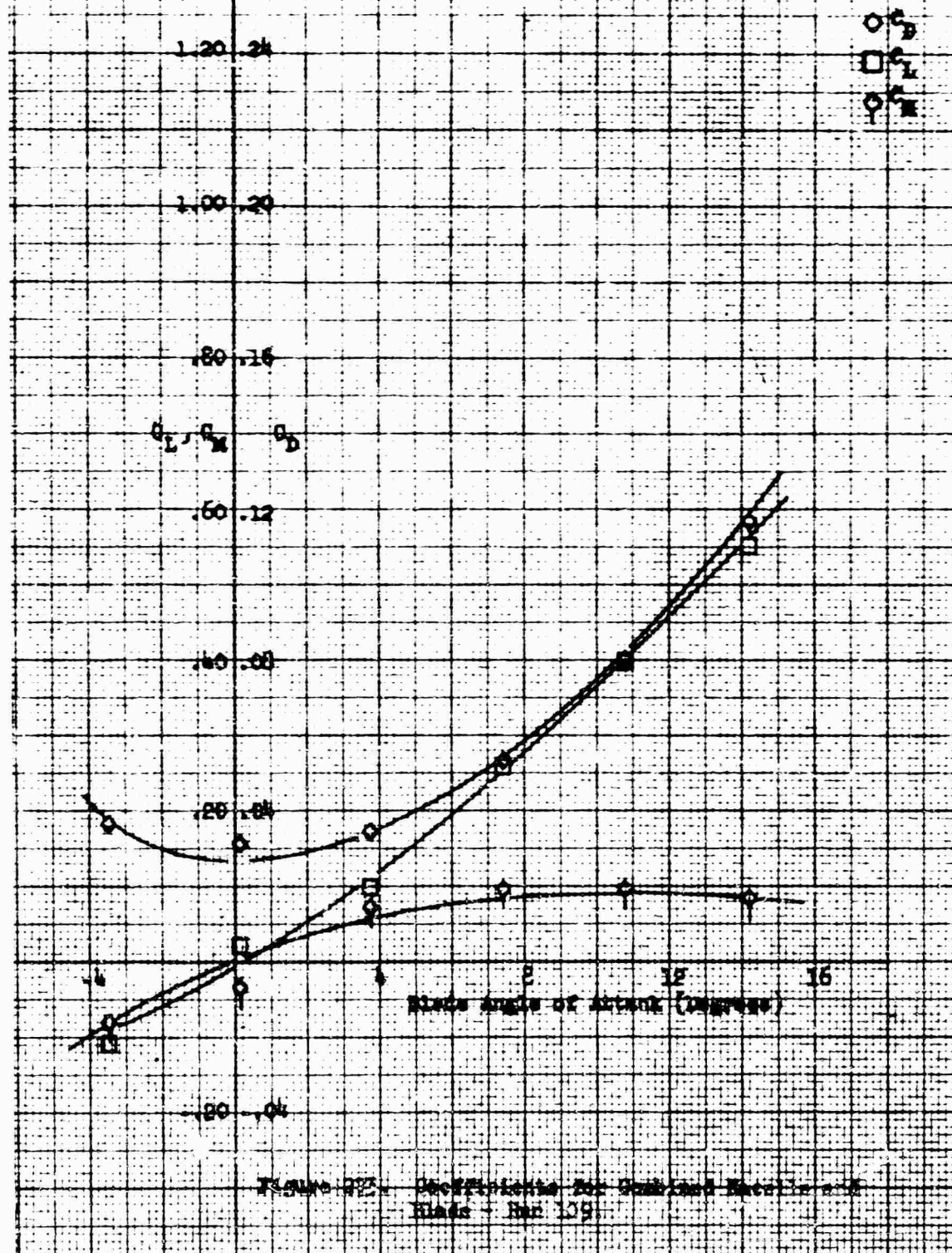
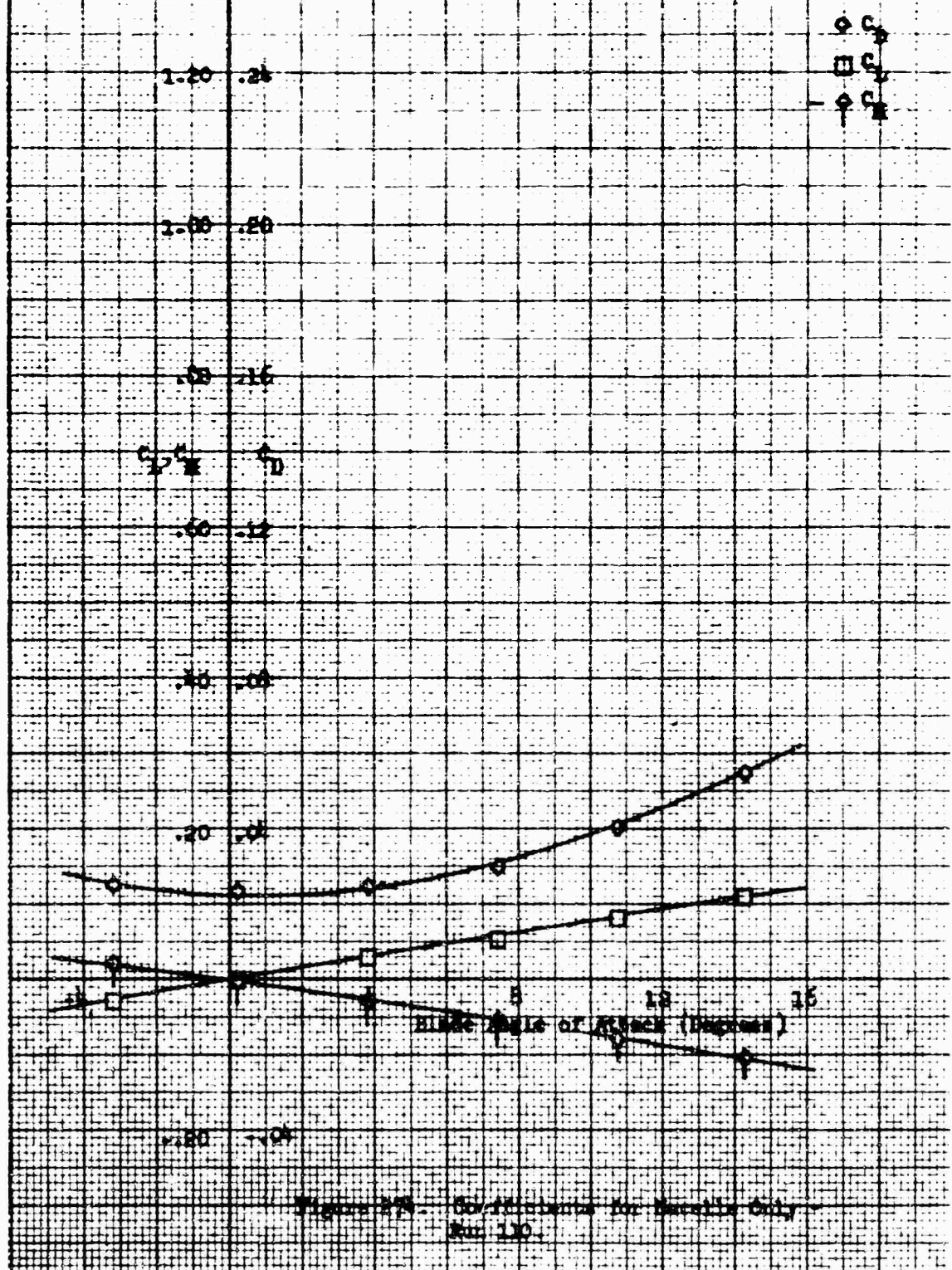


FIGURE B72. Coefficients for Nacelle Only -
 Run 109

Nozzle Configuration: Single 1-1/2-100 parabolic spinner
 Nozzle Incidence Angle: 0°
 Pairing: M/P
 Nozzle Exit Plane: .75
 $\beta = 10^\circ$



Nacelle Configuration: Single 1-50-100 Parabolic Spinner
 Fairing: w/o
 Nacelle Exit Plate: .78
 $\alpha = 0$



Blade Configuration: Single 1-50-100 Parabolic sp...
 Blade T. Idness Angle: 0°
 Pairing: N/B
 Blade First Plate: .78
 $\beta = 0$

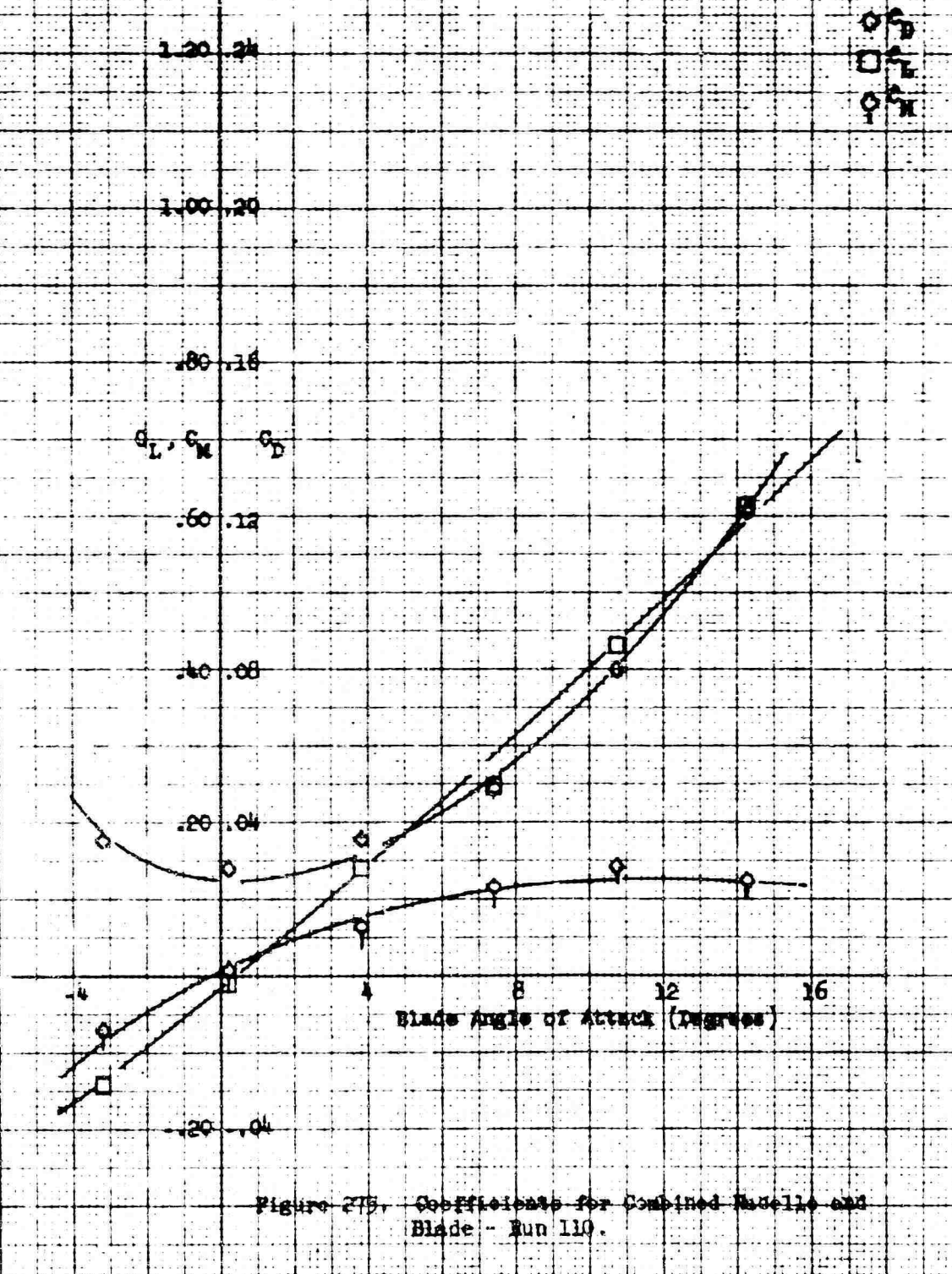


Figure 275. Coefficients for Combined Blade and Blade - Run 110.

Blade Configuration: Single 1-50-100 Parabolic Spinner
 Fairing: w/o
 Blade Exit Plate: .78
 $\alpha = -10^\circ$

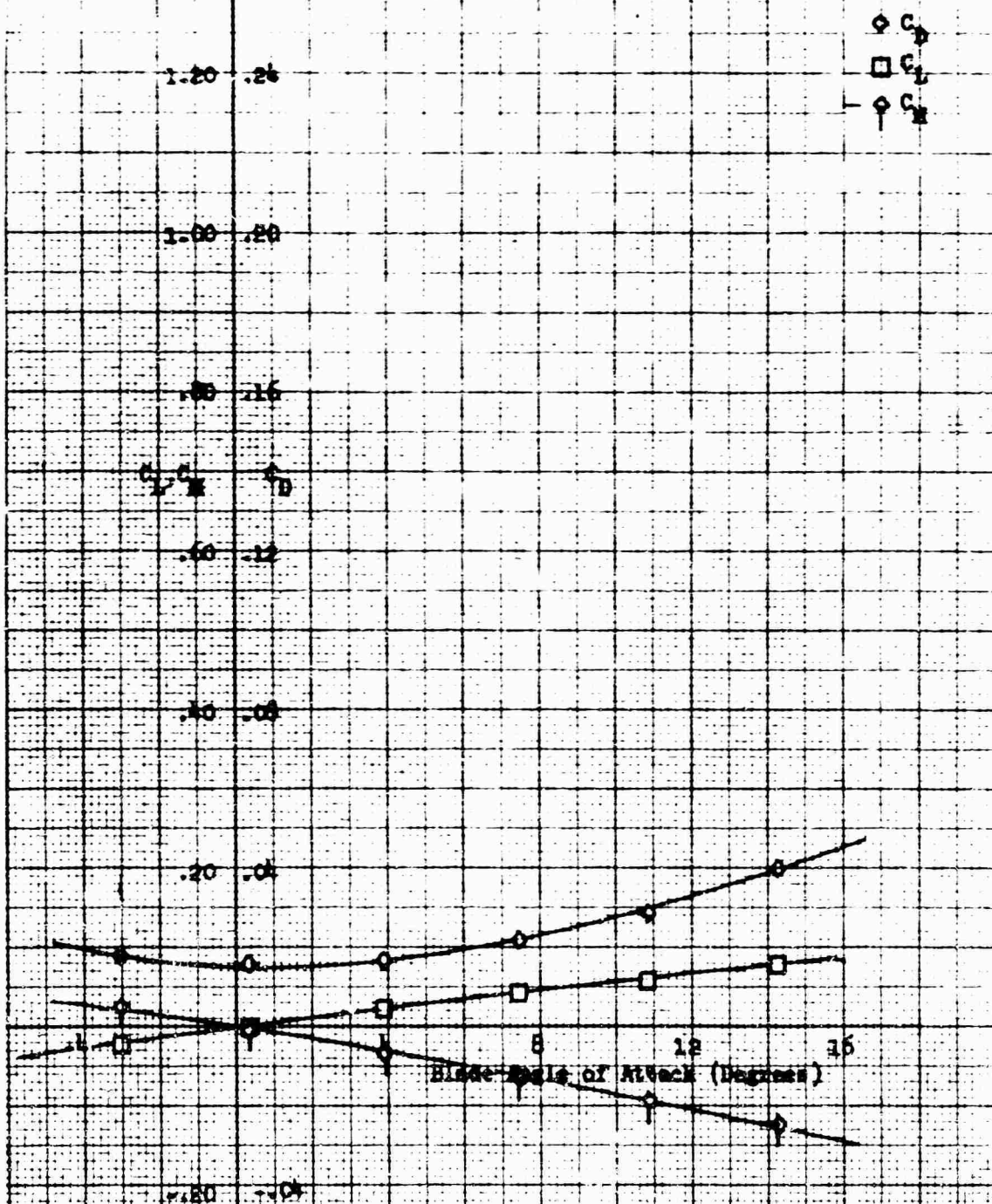
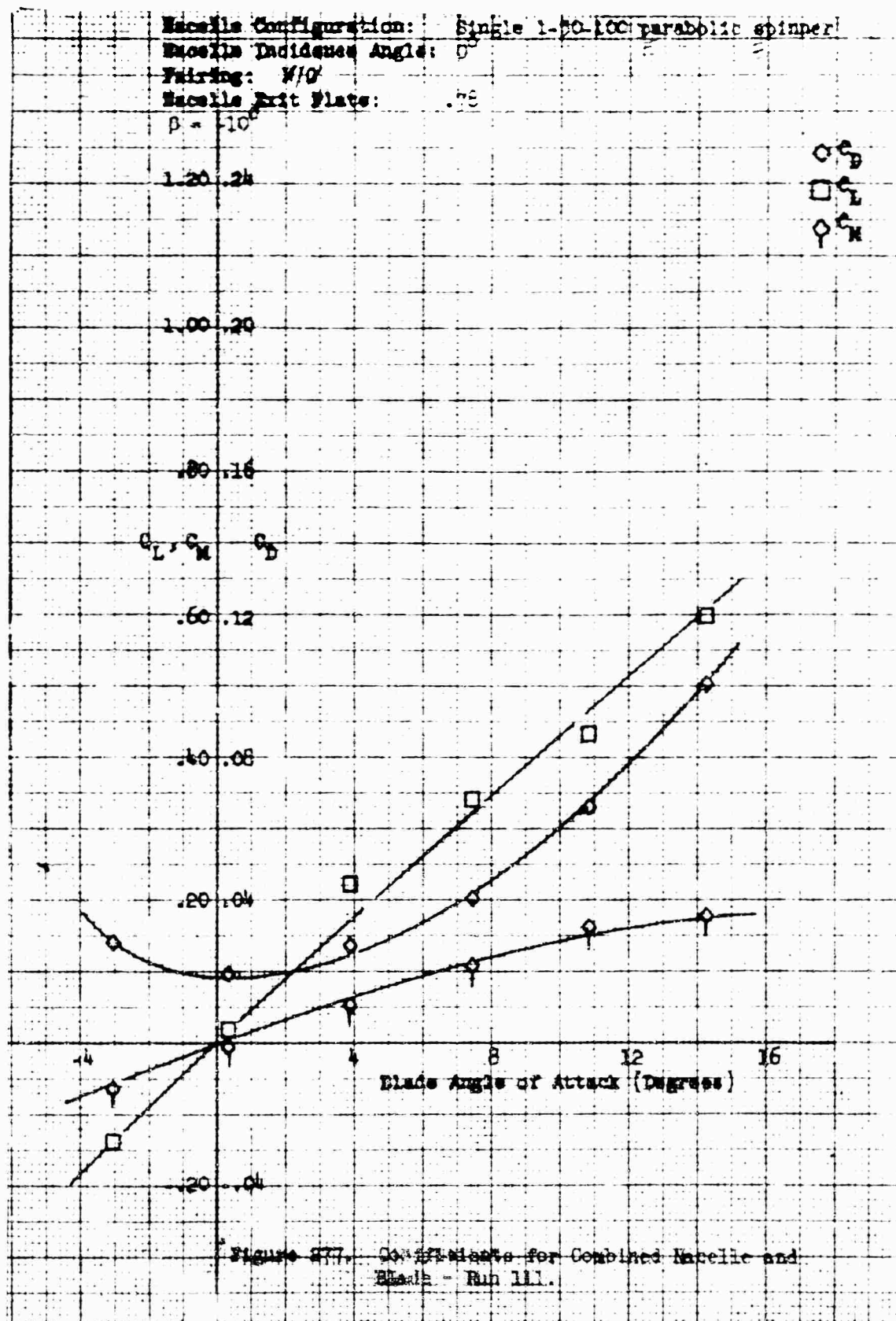


Figure B76. Coefficients for Blade Only -
 Run 111.



Nacelle Configuration: Single 1-50-100 Parabolic Spinner
 Pairing: w/o
 Nacelle Exit Plate: .78
 $\beta = -20^\circ$

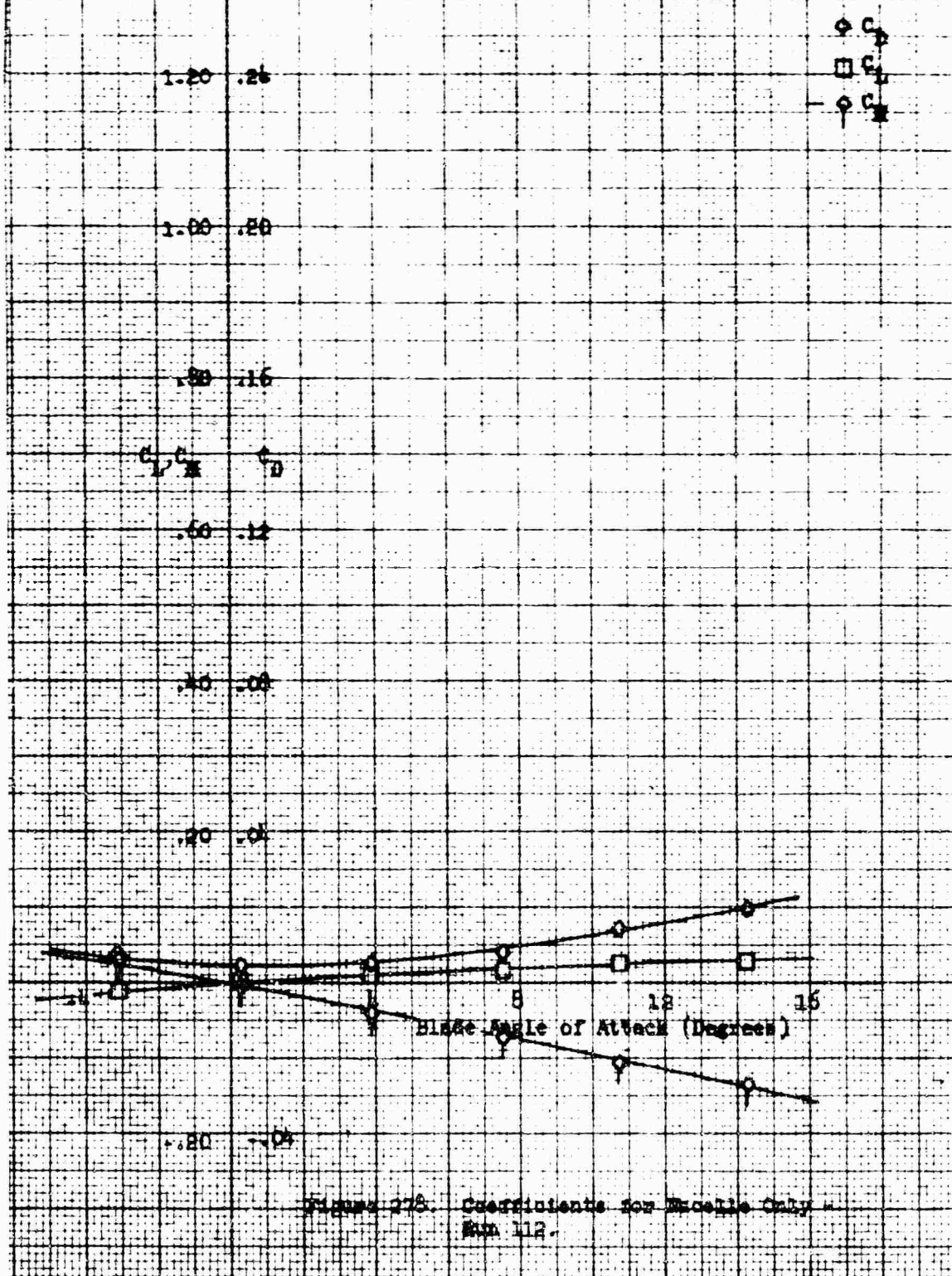
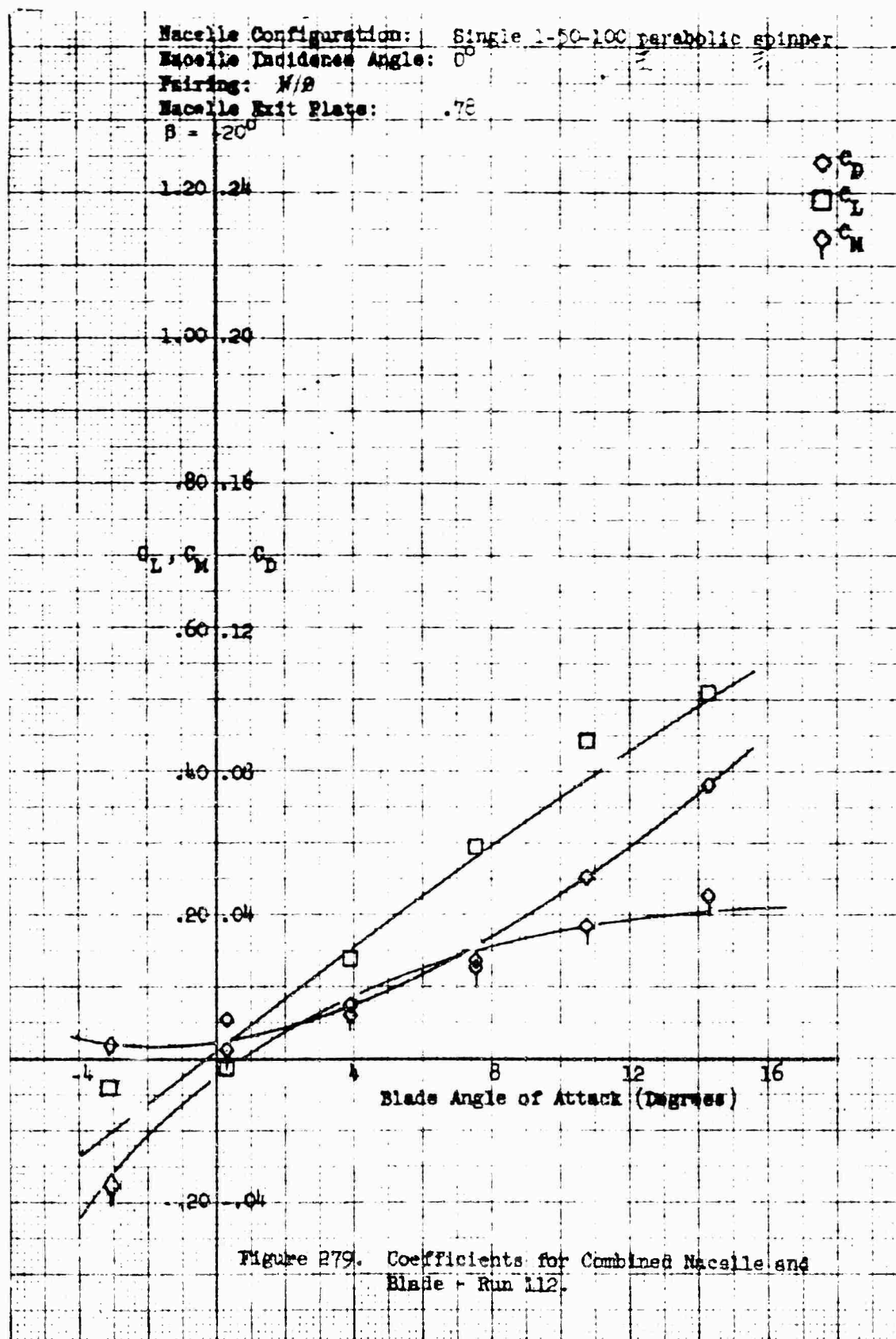


Figure 278. Coefficients for Nacelle Only
 Run 112.



Nacelle Configuration: Single 1-50-100 Parabolic System
 Fairing: w/o
 Nacelle Exit Plate: 0
 $\alpha = -20^\circ$

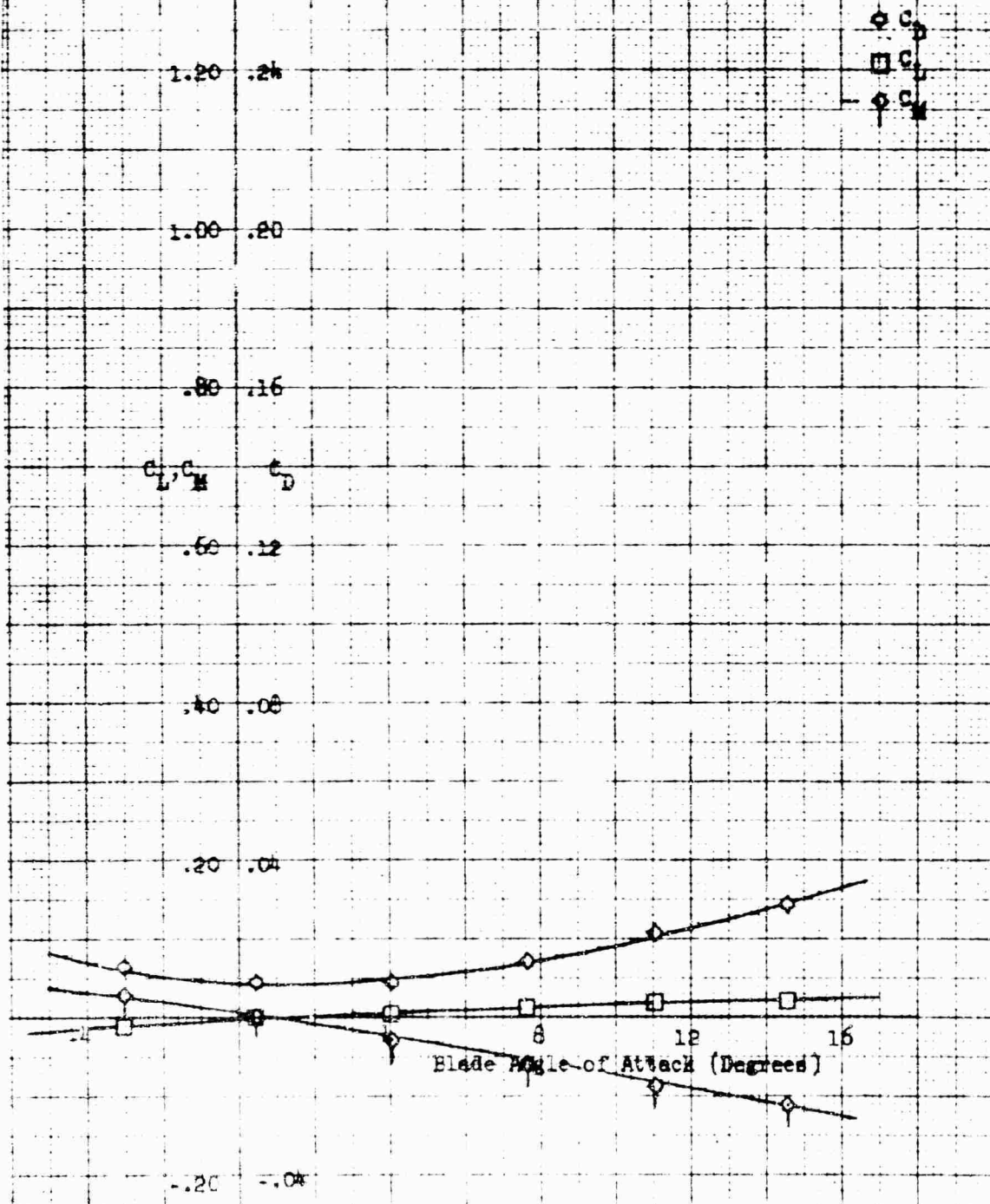


Figure 280. Coefficients for Nacelle Only - Run 115.

Nacelle Configuration: Single 1-50-100 parabolic spinner
 Nacelle Incidence Angle: 0°
 Fairing: N/B
 Nacelle Exit Plate: 0
 $\beta = 20^\circ$

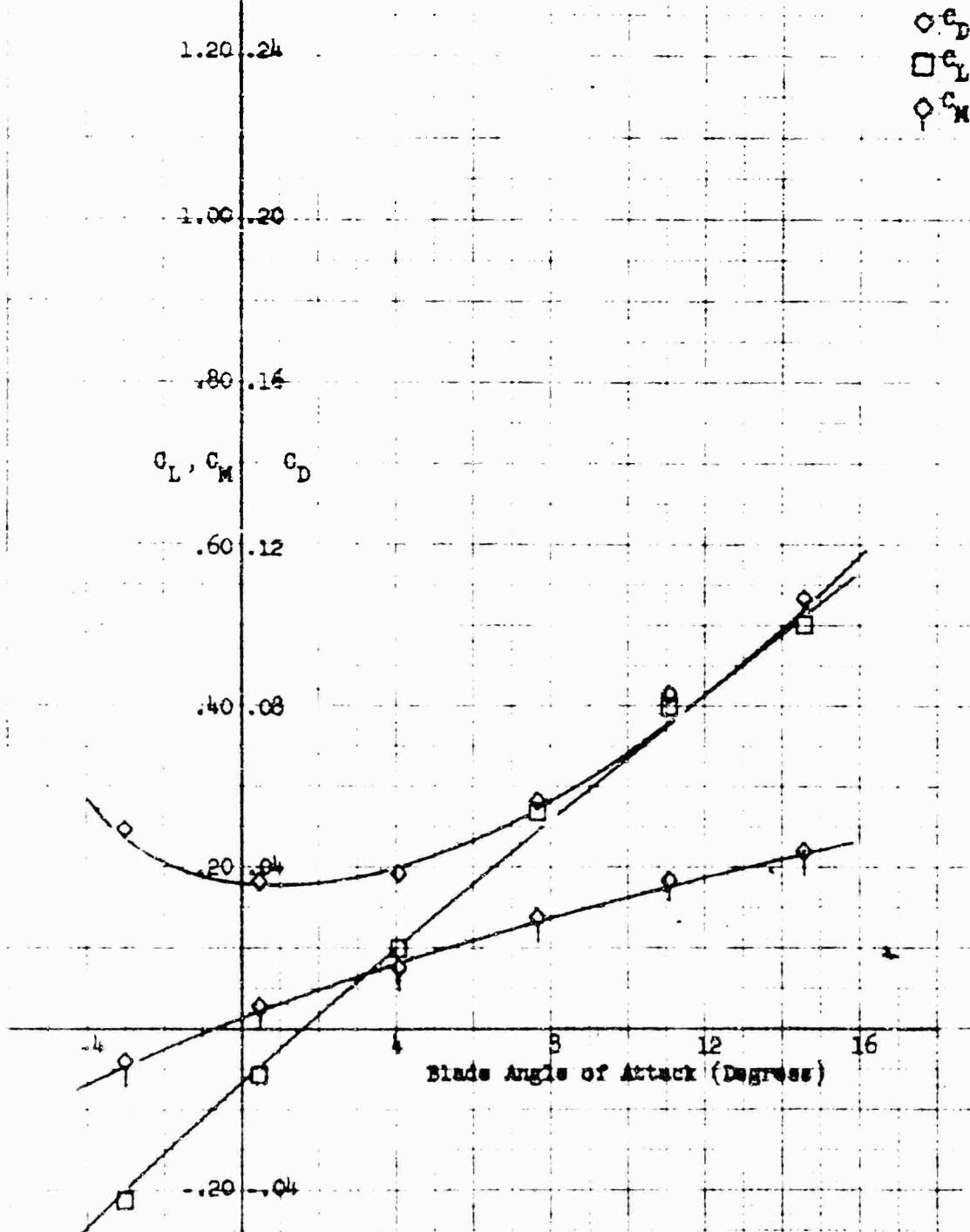


Figure 281. Coefficients for Combined Nacelle and Blade - Run 113.

Macelle Configuration: Single 1.50-1.00 Parabolic Spinner.
 Pairing: w/c
 Macelle Exit Plate: D
 $\delta = -10^\circ$

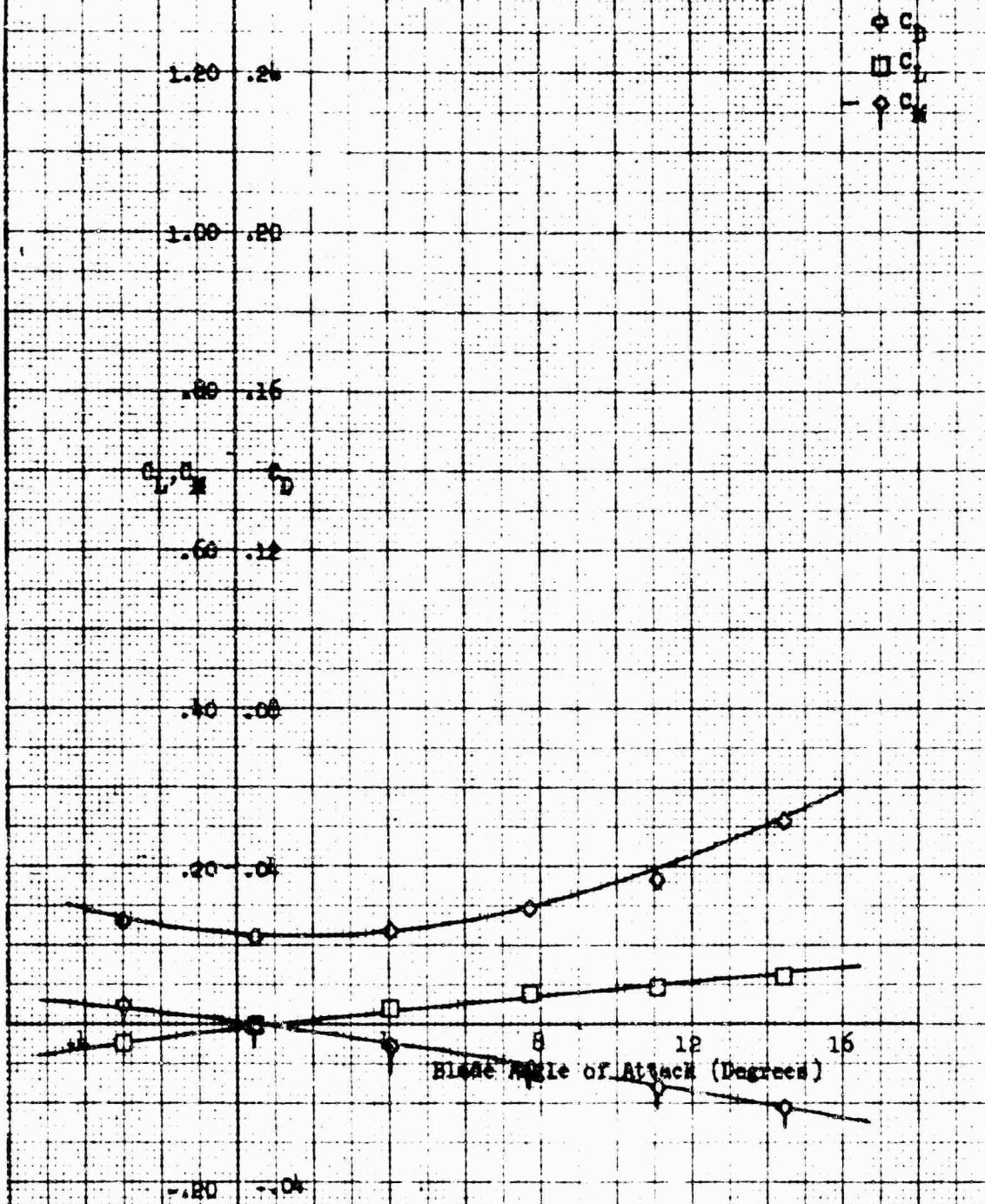


Figure 282. Coefficients for Macelle Only -
 Run 114.

Macelle Configuration: Single 1-50-100 parabolic spinner
 Macelle Incidence Angle: 0°
 Fairing: N/A
 Macelle Exit Plate: 0
 $\beta = -10^\circ$

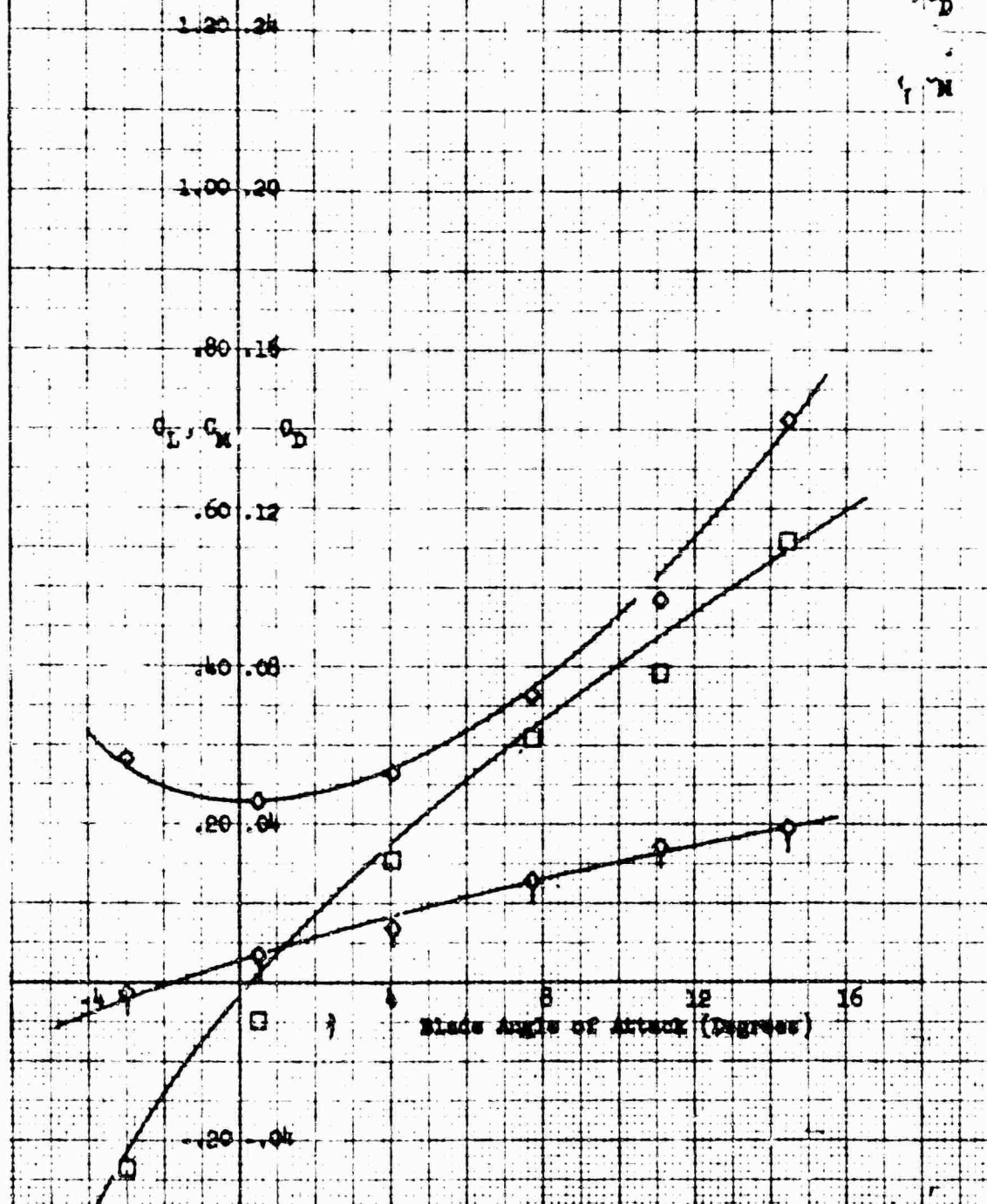
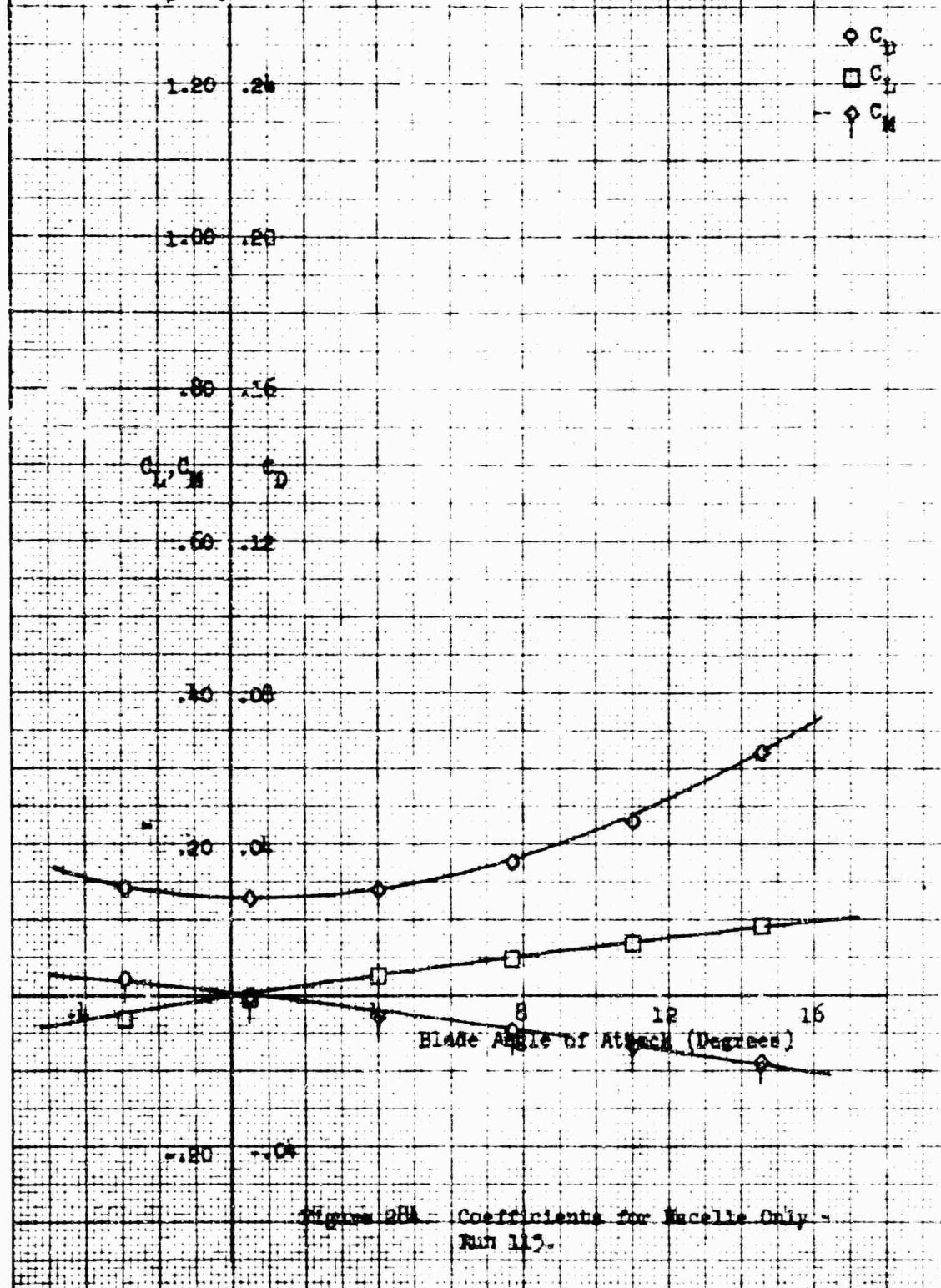
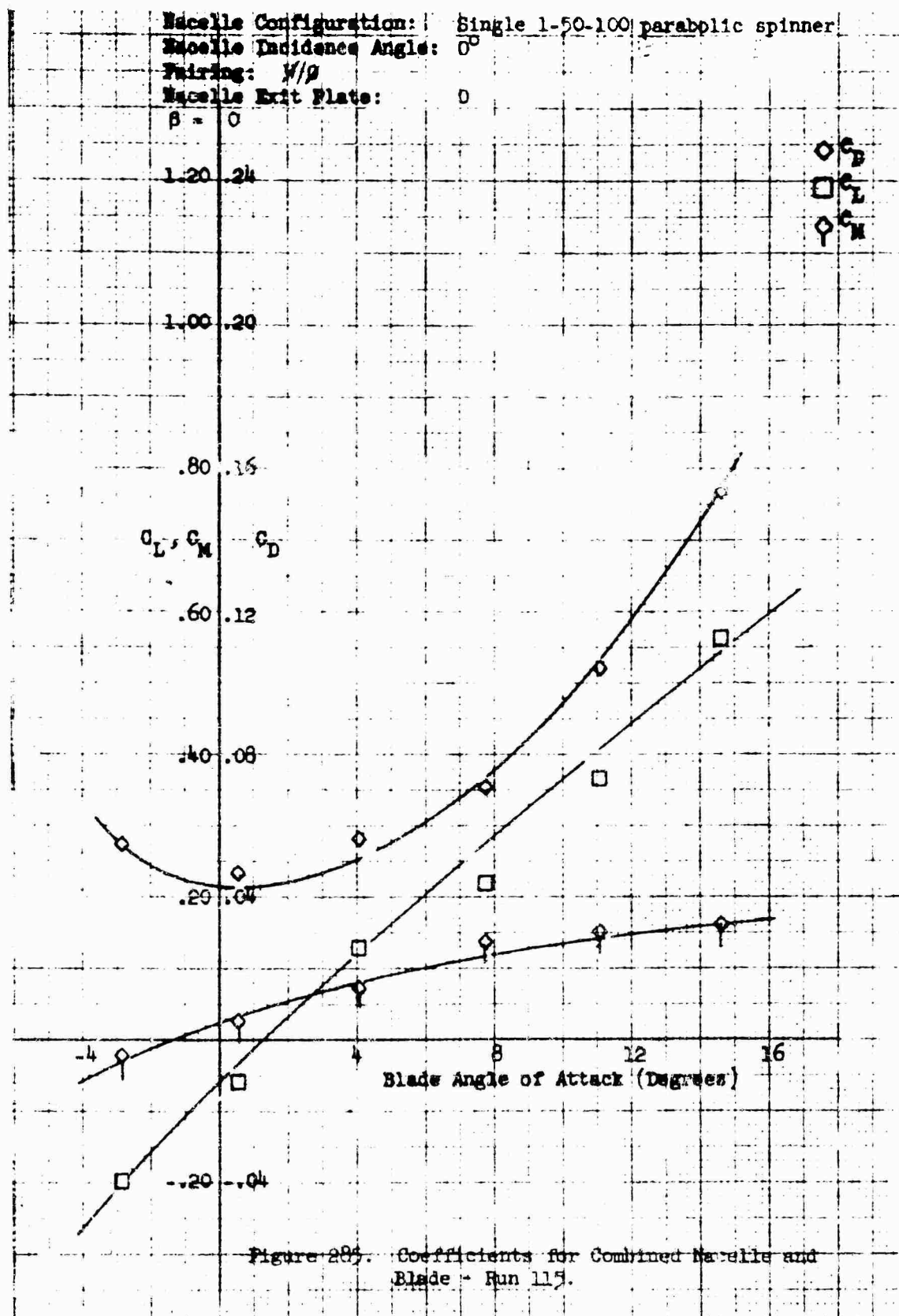
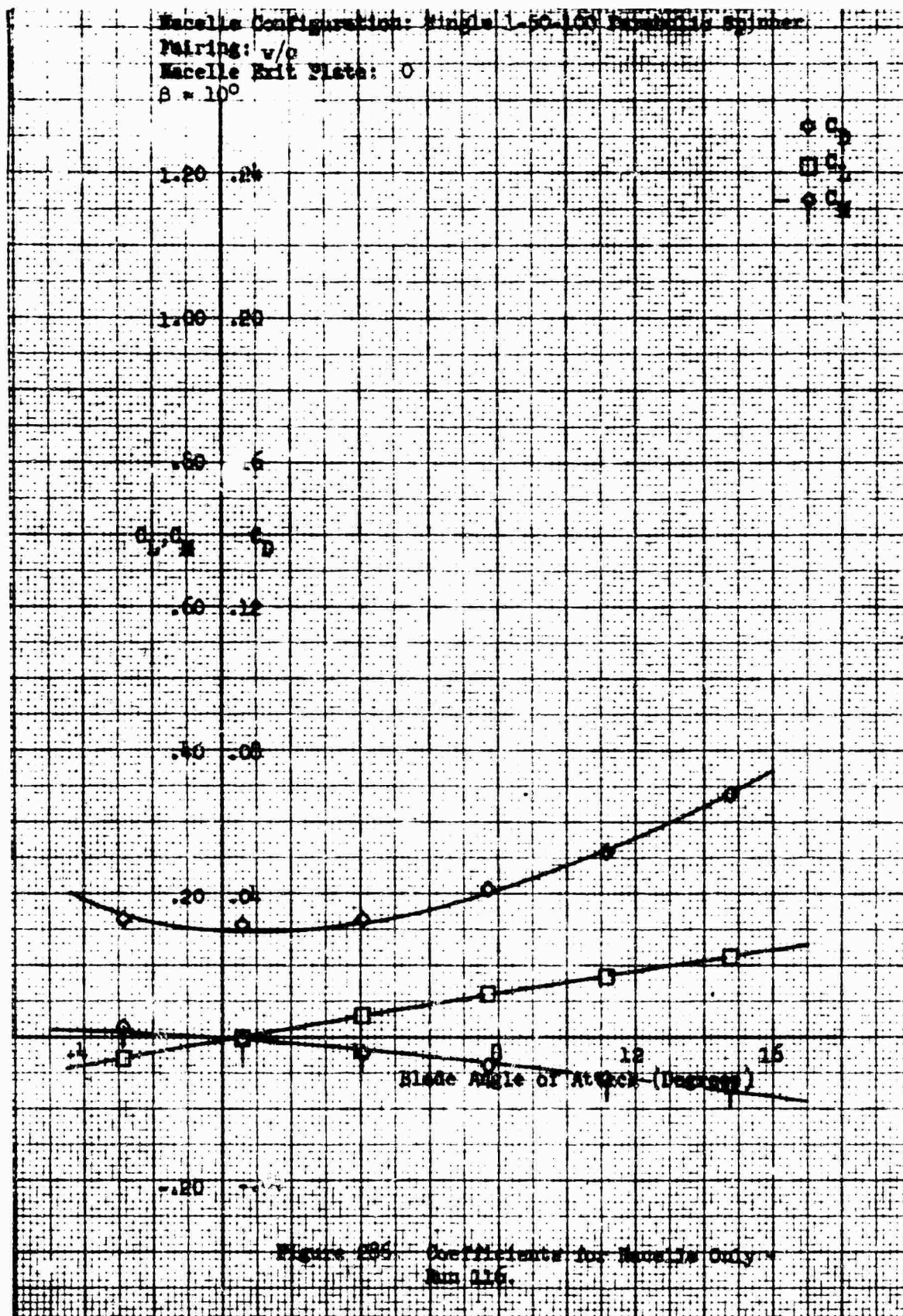


Figure 283. Coefficients for Combined Macelle and Blade - Run 11A.

Macelle Configuration: Single 1-50-100 Parabolic Spinner
 Fairing: w/o
 Macelle Brit Plate: 0
 $\beta = 0$







Nacelle Configuration: Single 1-50-100 parabolic spinner
 Nacelle Incidence Angle: 0°
 Fairing: ~~N/A~~
 Nacelle Exit Flare: 0
 $\beta = 10^\circ$

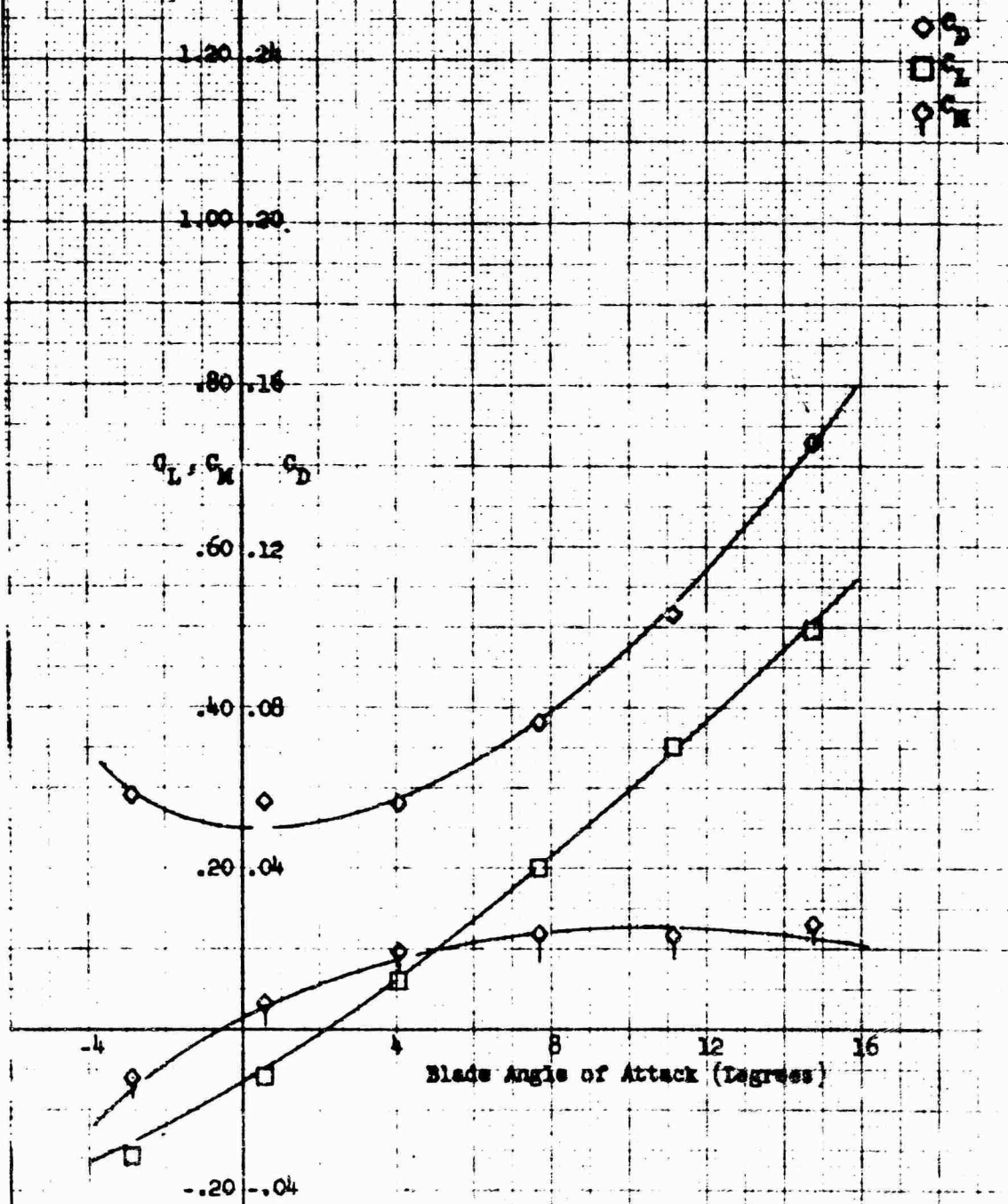


Figure 287. Coefficients for Combined Nacelle and Blade - Run 116.

Macelle Configuration: Single 1-50-100 Parabolic Spinner
 Fairing: w/o
 Macelle Exit Plate: D
 $\beta = 20^\circ$

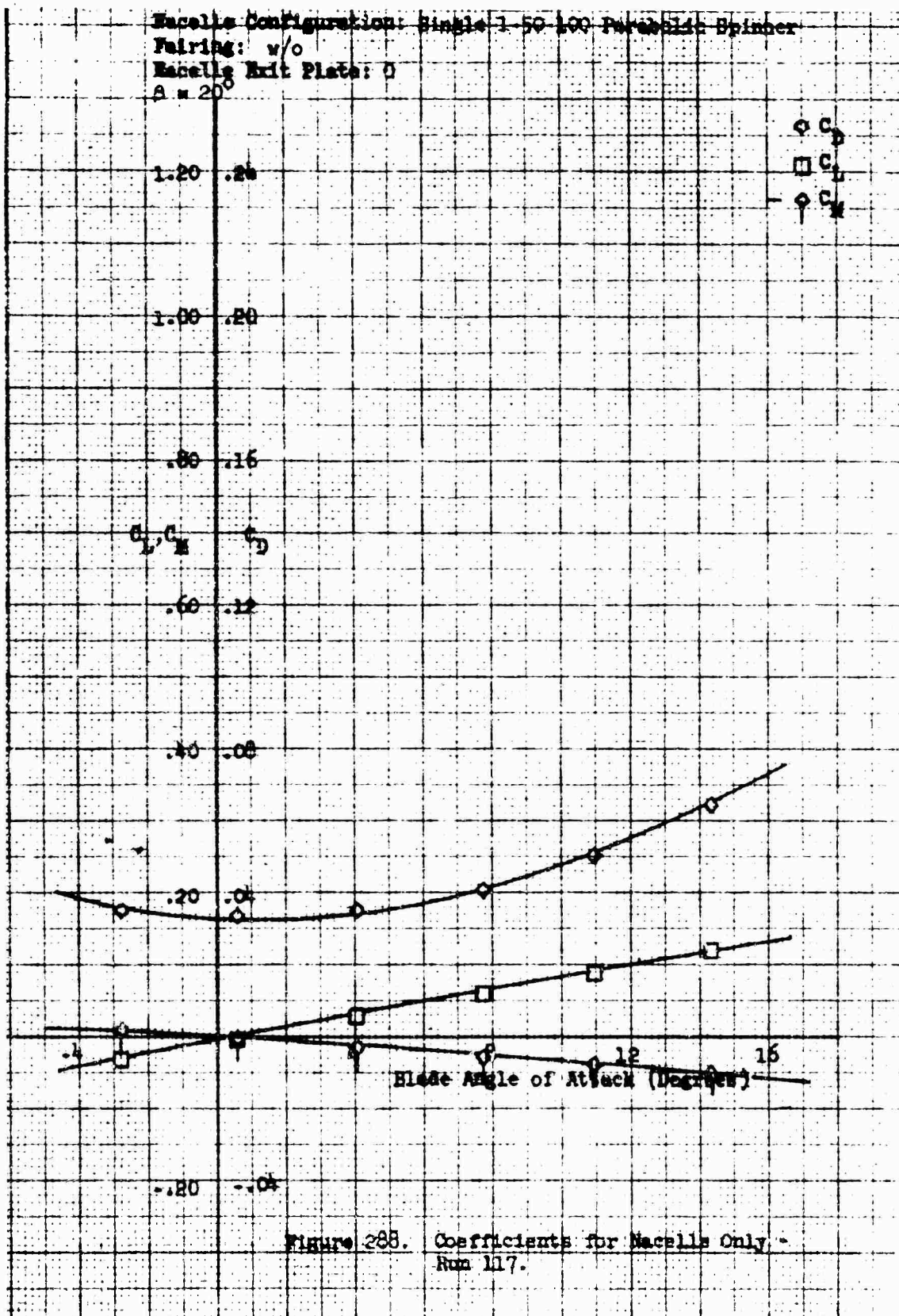


Figure 288. Coefficients for Macelle Only -
 Run 117.

Macelle Configuration: Single 1-50-100 parabolic spinner
 Macelle Incidence Angle: 0°
 Pairing: $\infty/0$
 Macelle Exit Plate: 0
 $\beta = 20^\circ$

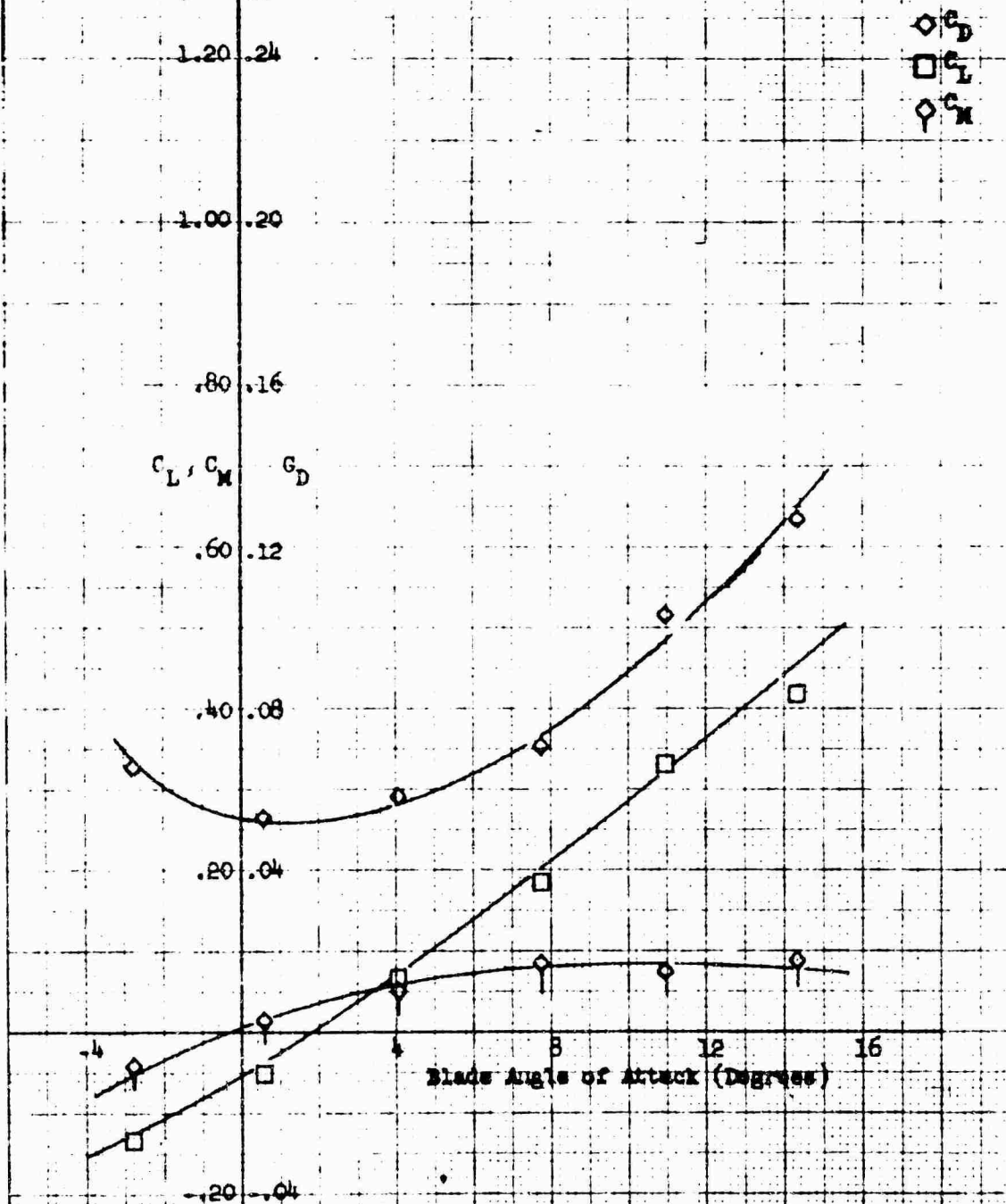
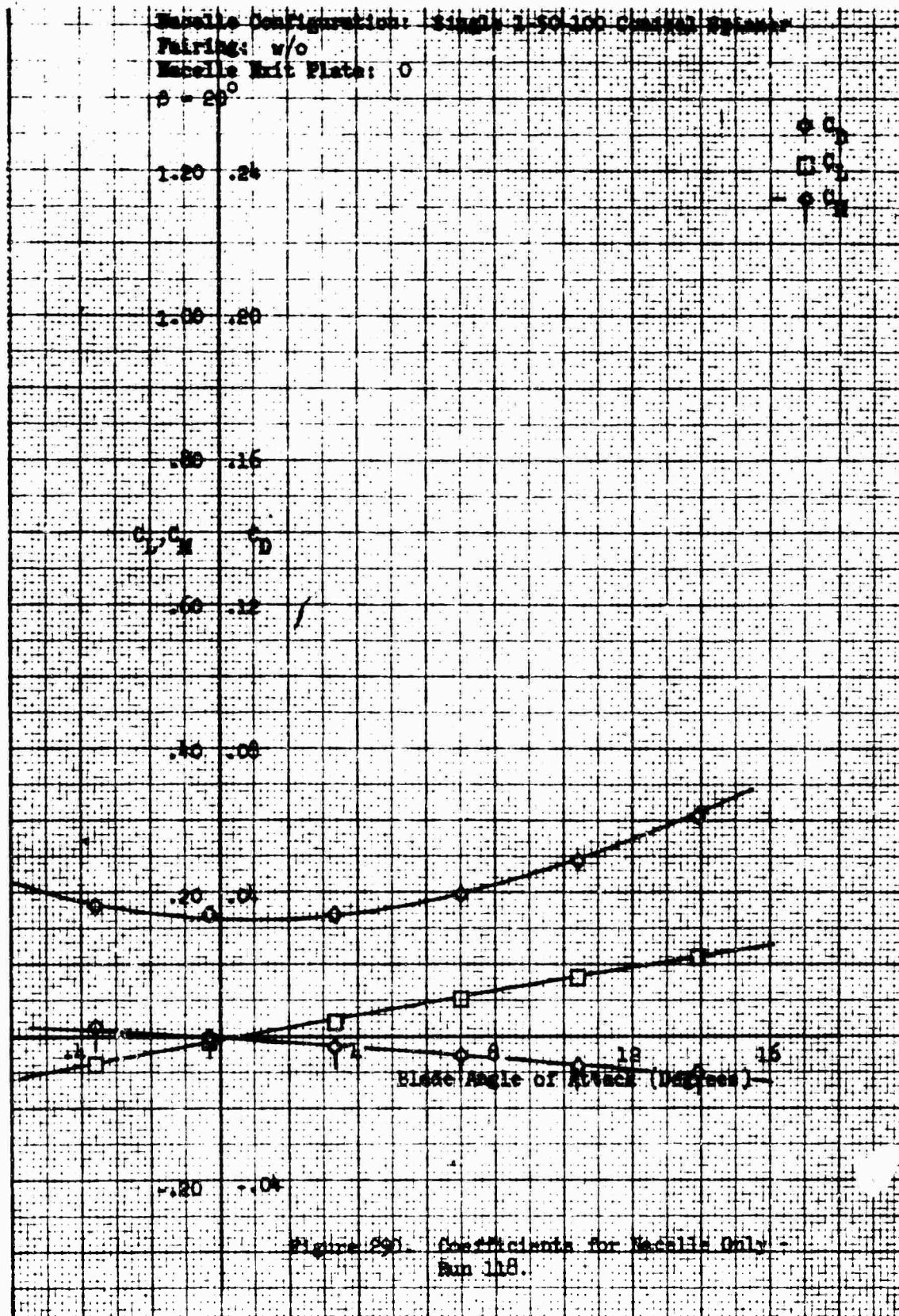


Figure 289. Coefficients for Combined Macelle and Blade - Run 117.



Nozzle Configuration: Single 1-50-100 conical spinner
 Nozzle Incidence Angle: 0°
 Pairing: N/S
 Nozzle Exit Plate: 0
 $\beta = 20^\circ$

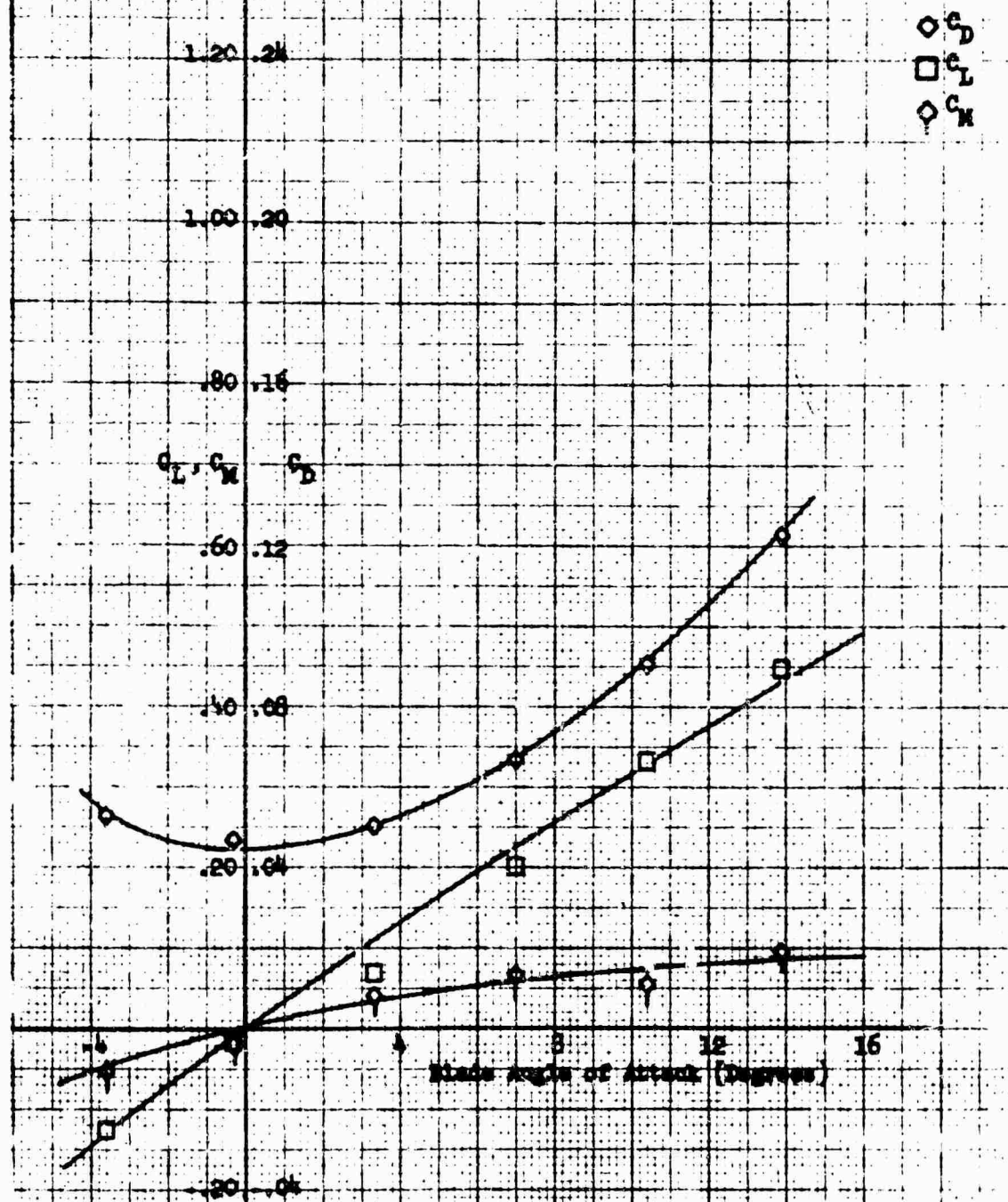
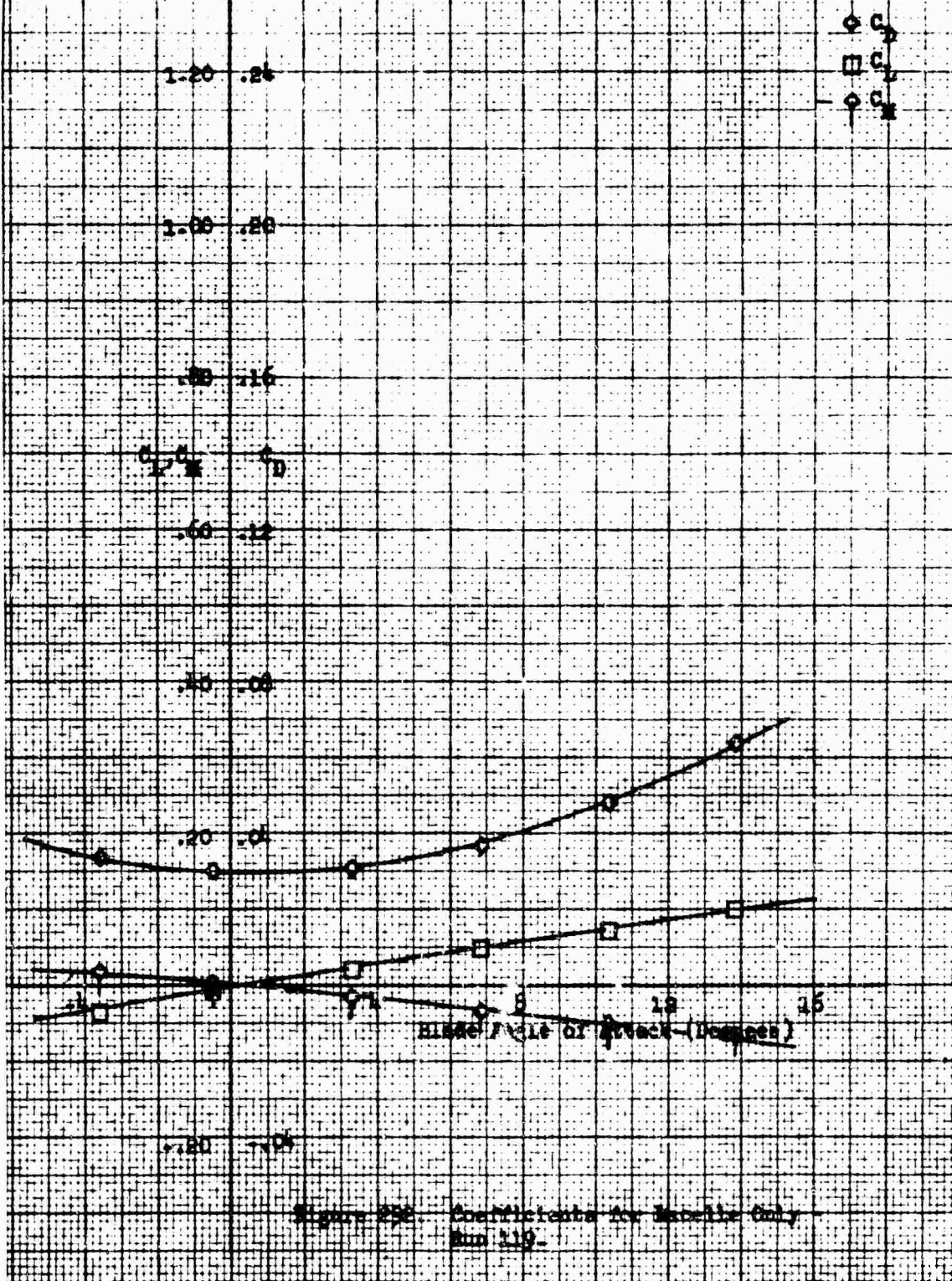


Figure P51. Coefficients for Conical Nozzle and
 Blade - Run 118.

Nozzle Configuration: Single 150-100 Conical Spinner
 Filling: w/o
 Nozzle Exit Plate: 0
 $\beta = 10^\circ$



Nacelle Configuration: Single 1-50-100 conical spinner
 Nacelle Incidence Angle: 0°
 Fairing: N/O
 Nacelle Exit Plate: 0
 $\beta = 10^\circ$

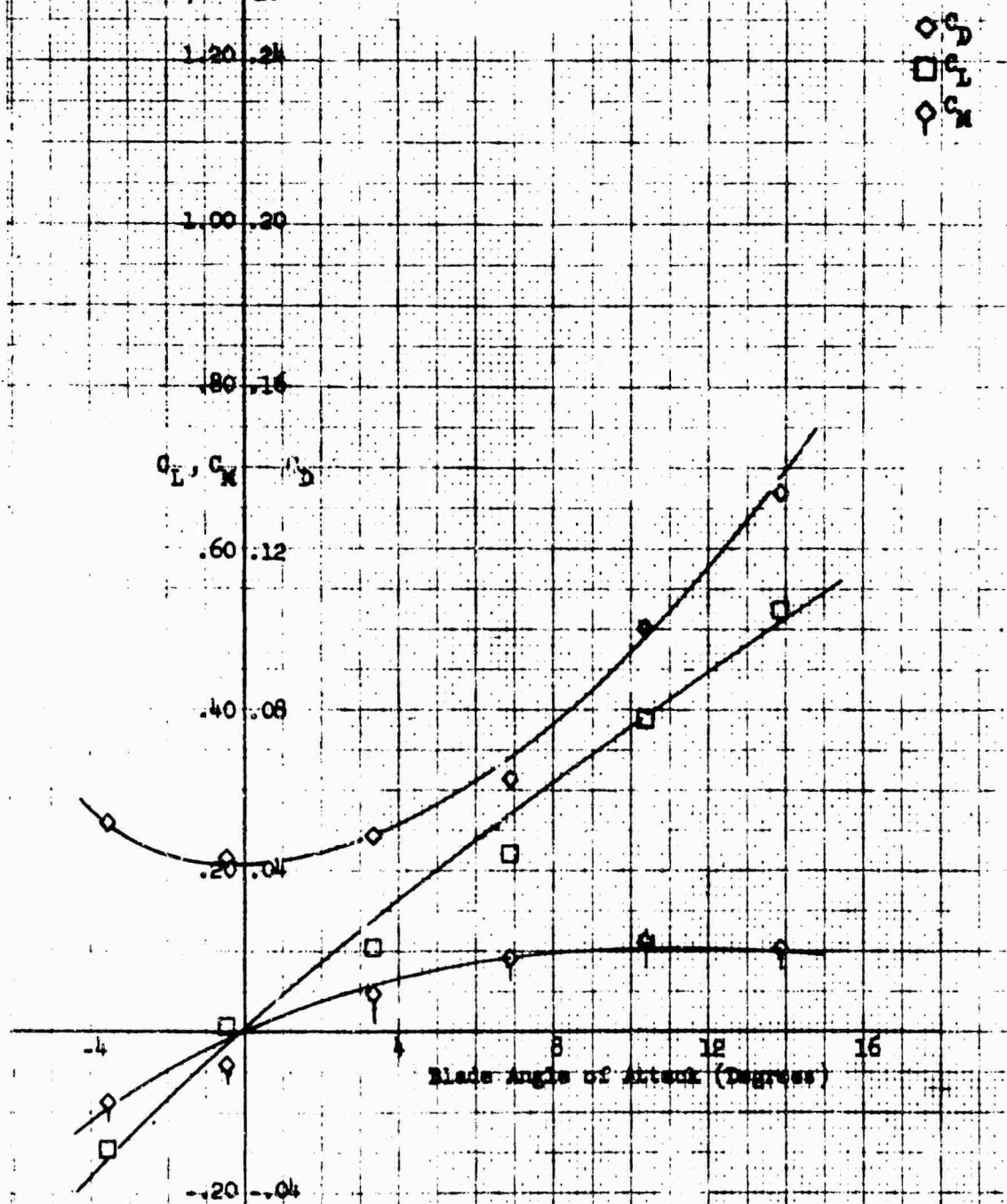


Figure 295. Coefficients for Combined Nacelle and Blade - Run 119.

Macelle Configuration: Single 1-50-100 Conical Spinner
 Pairing: v/b
 Macelle Exit Plate: 0
 $\beta = 0$

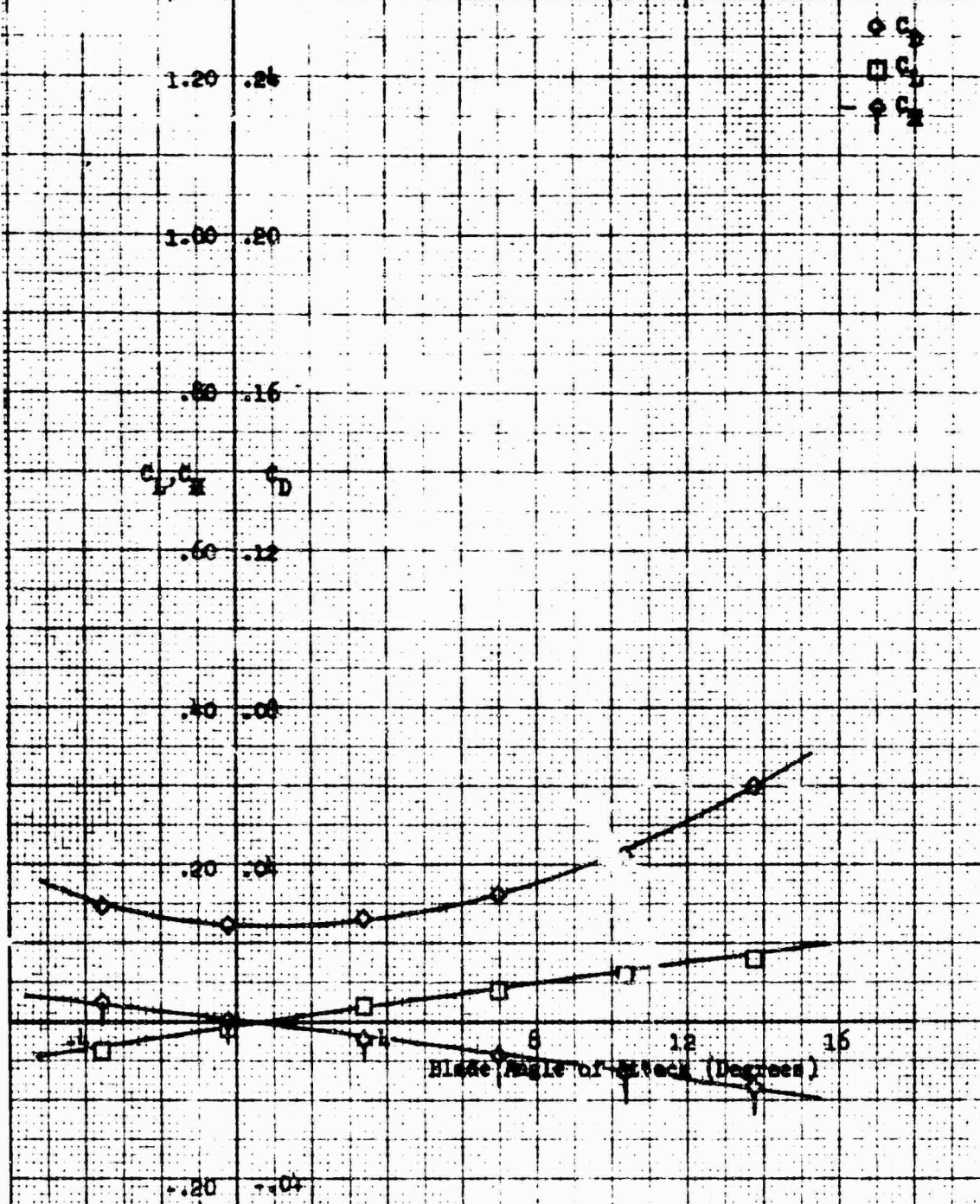


Figure 29. Coefficients for Macelle Only -
 Run 120.

Nacelle Configuration: Single 1-50-100 conical spinner

Nacelle Incidence Angle: 0°

Pairing: W/O

Nacelle Exit Plate: 0

$\beta = 0^\circ$

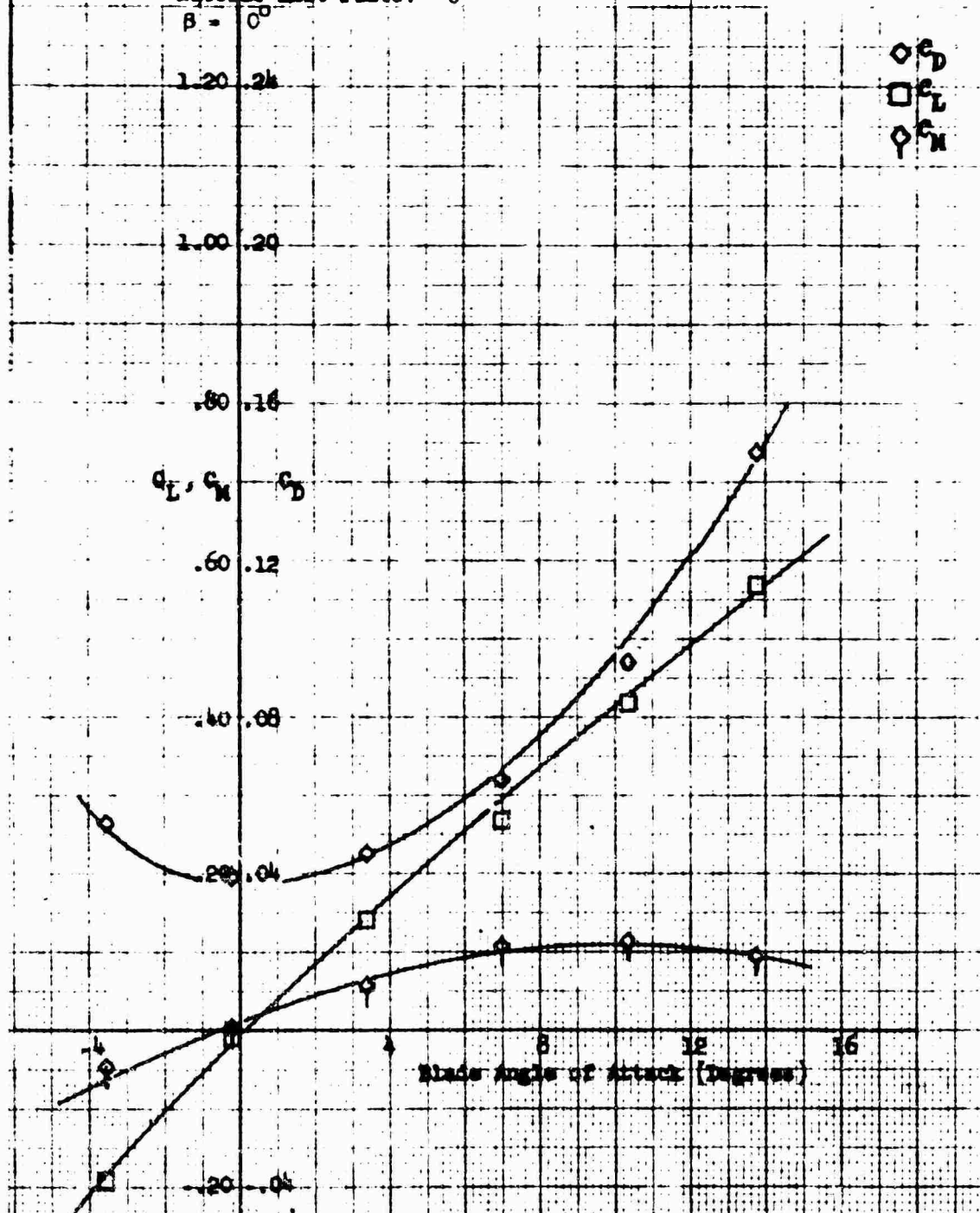
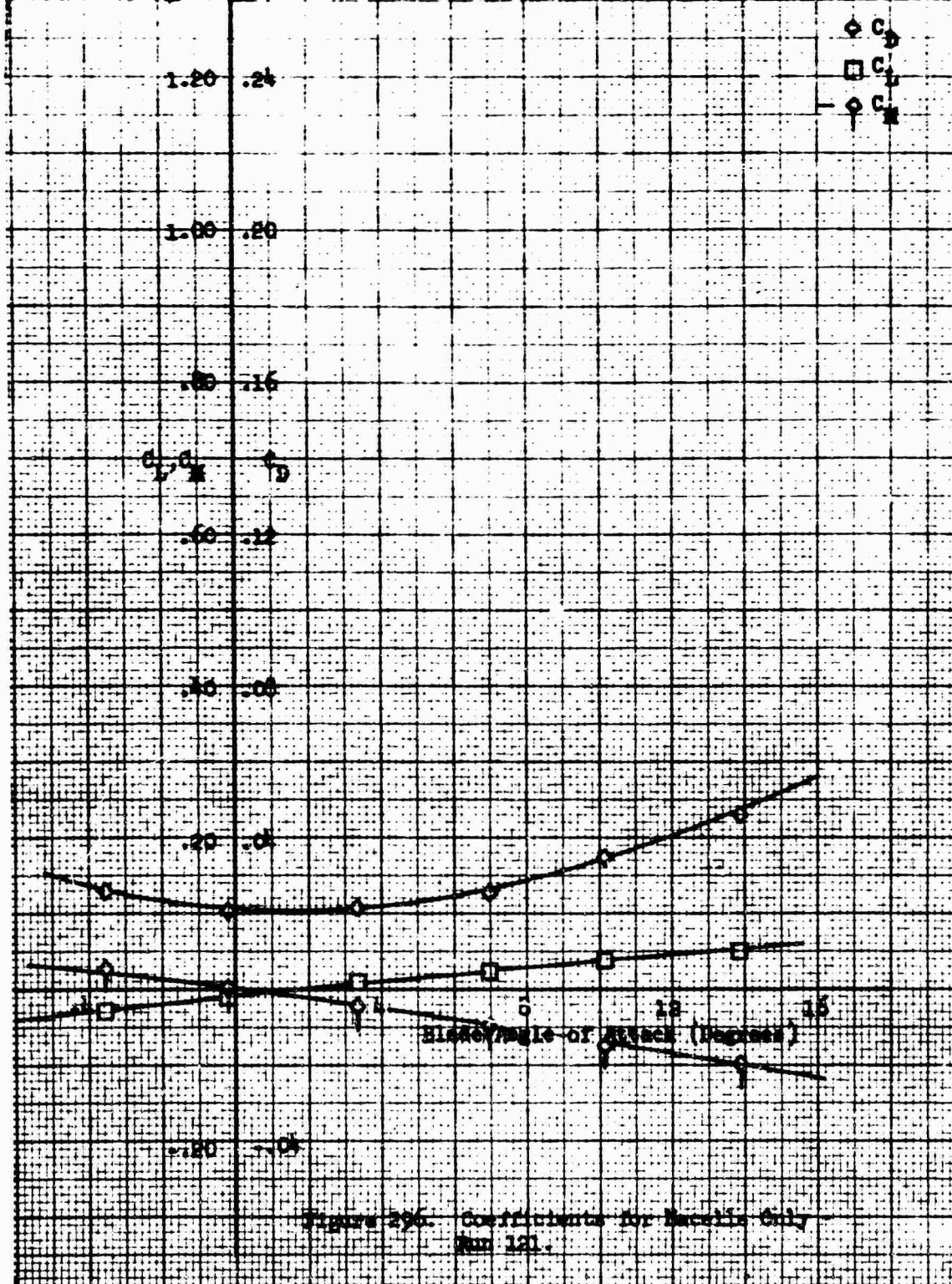
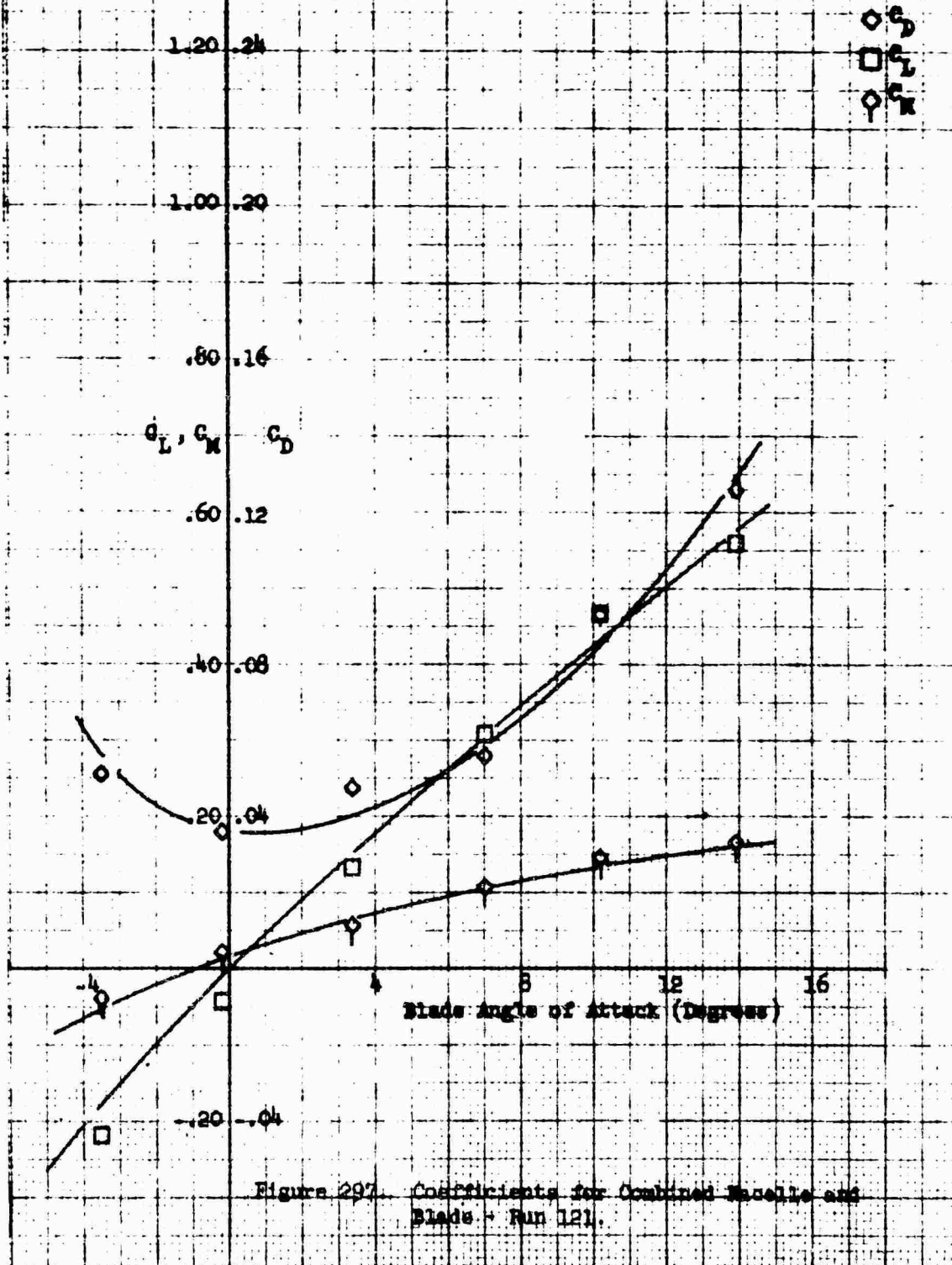


Figure 295 - Coefficients for Combined Nacelle and Blade - Run 121

Nacelle Configuration: Single 1-50-100 Conical Spinner
 Fairing: w/o
 Nacelle Exit Plate: 0
 $\beta = -10^\circ$



Macelle Configuration: Single 1-50-100 conical spinner
 Macelle Incidence Angle: 0°
 Pairing: W/d
 Macelle Exit Flaps: 0
 $\beta = 10^\circ$



Blade Configuration: NACA 1-20-100 Curved, Symmetrical
 Pairing: w/o
 Blade Writ Pitch: 0
 $\alpha = -20^\circ$

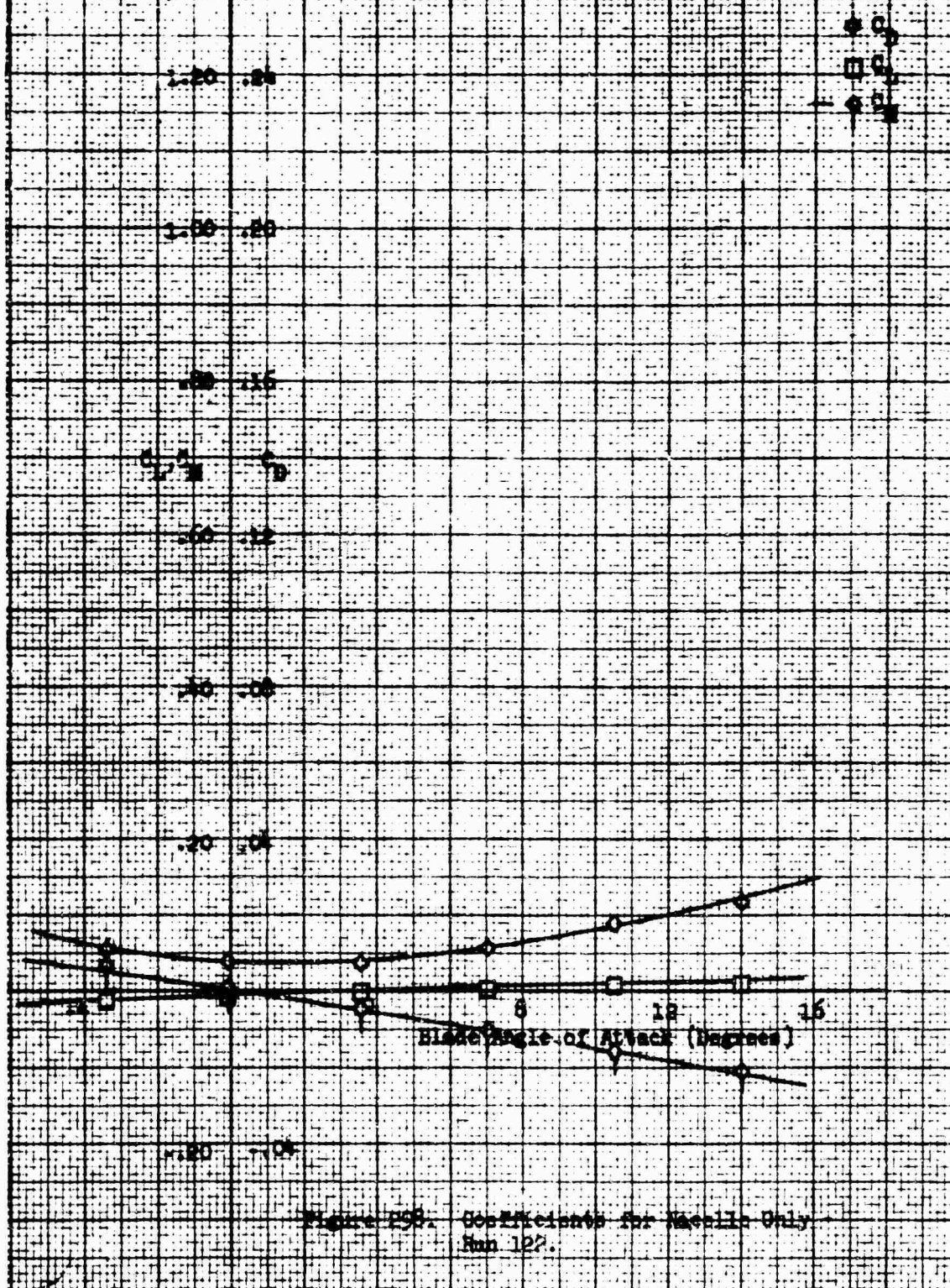
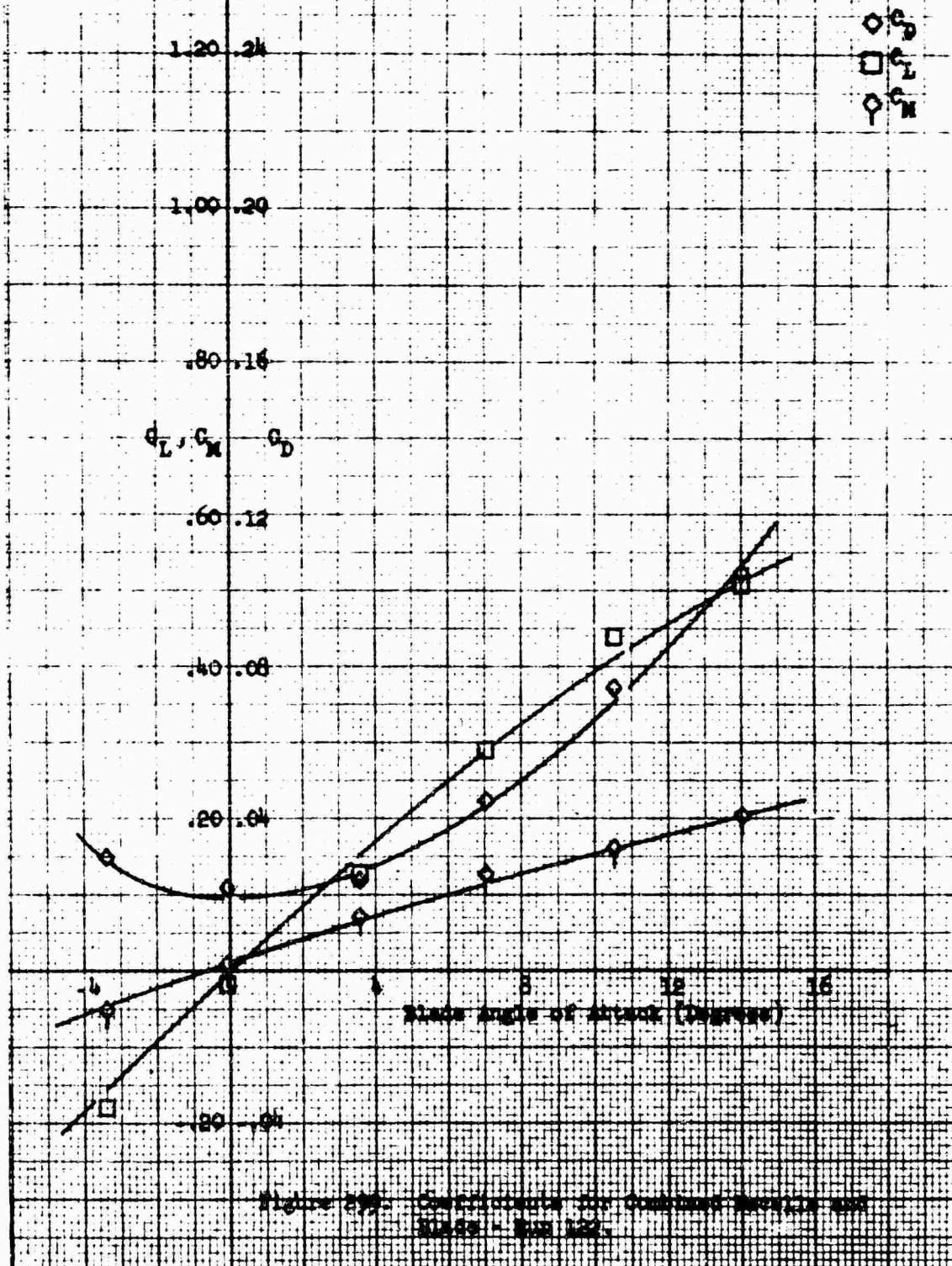
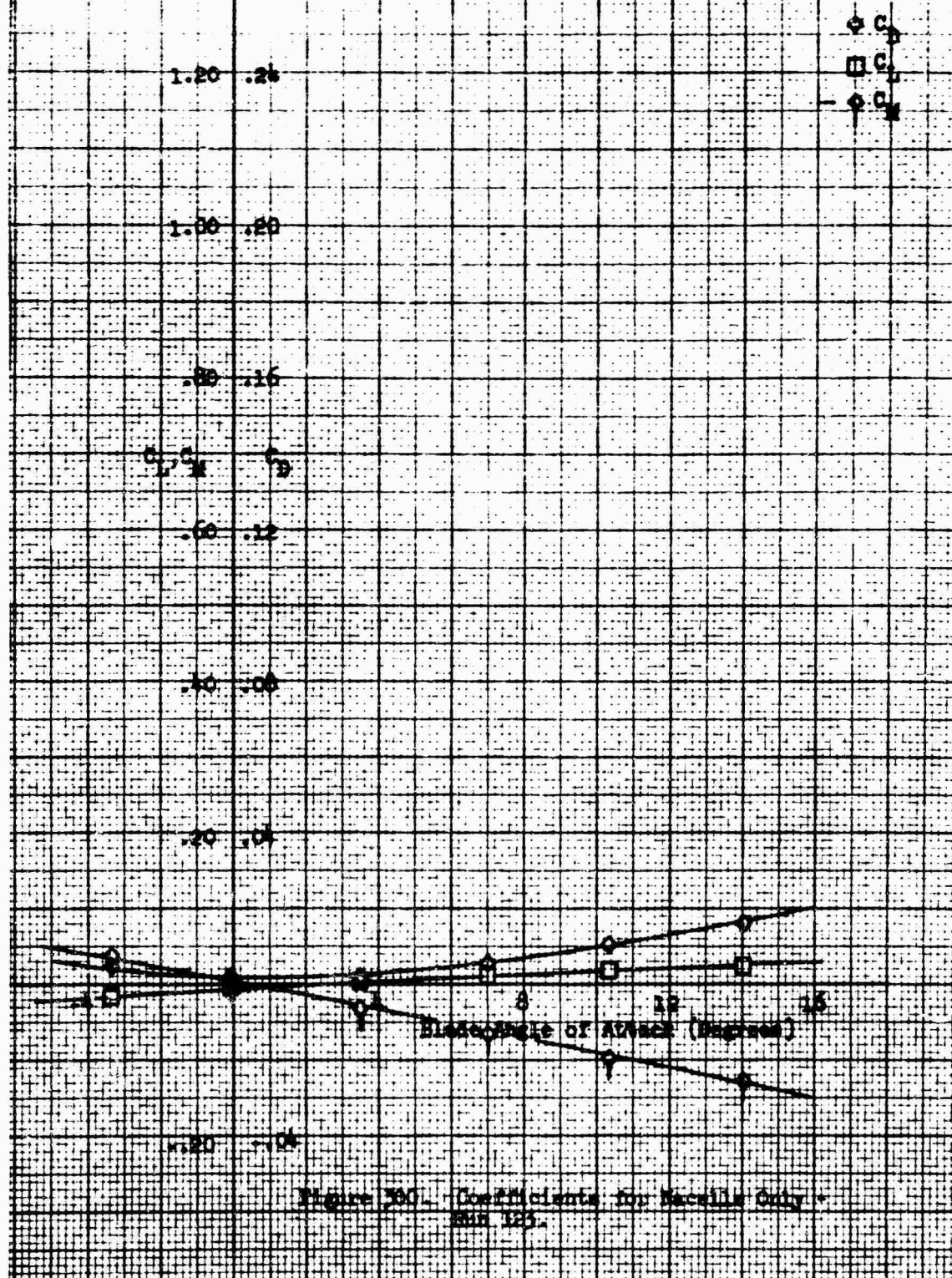


Figure 258. Coefficients for NACA 1-20-100 Curved, Symmetrical Blade Writ Pitch: 0 $\alpha = -20^\circ$.

Macelle Configuration: Single 1-50-100 conical spinner
 Macelle Incidence Angle: 0°
 Fairing: V/O
 Macelle Exit Plate: 0
 $\beta = 20^\circ$



Macelle Configuration: Single 1-50-100 Chemical Cylinder
 Pairing: v/o
 Macelle Exit Plate: .90
 $\theta = -20^\circ$



Macelle Configuration: Single 1-50-100 conical spinner
 Macelle Incidence Angle: 0°
 Pairing: W/B
 Macelle Exit Plate: .90
 $\beta = 20^\circ$

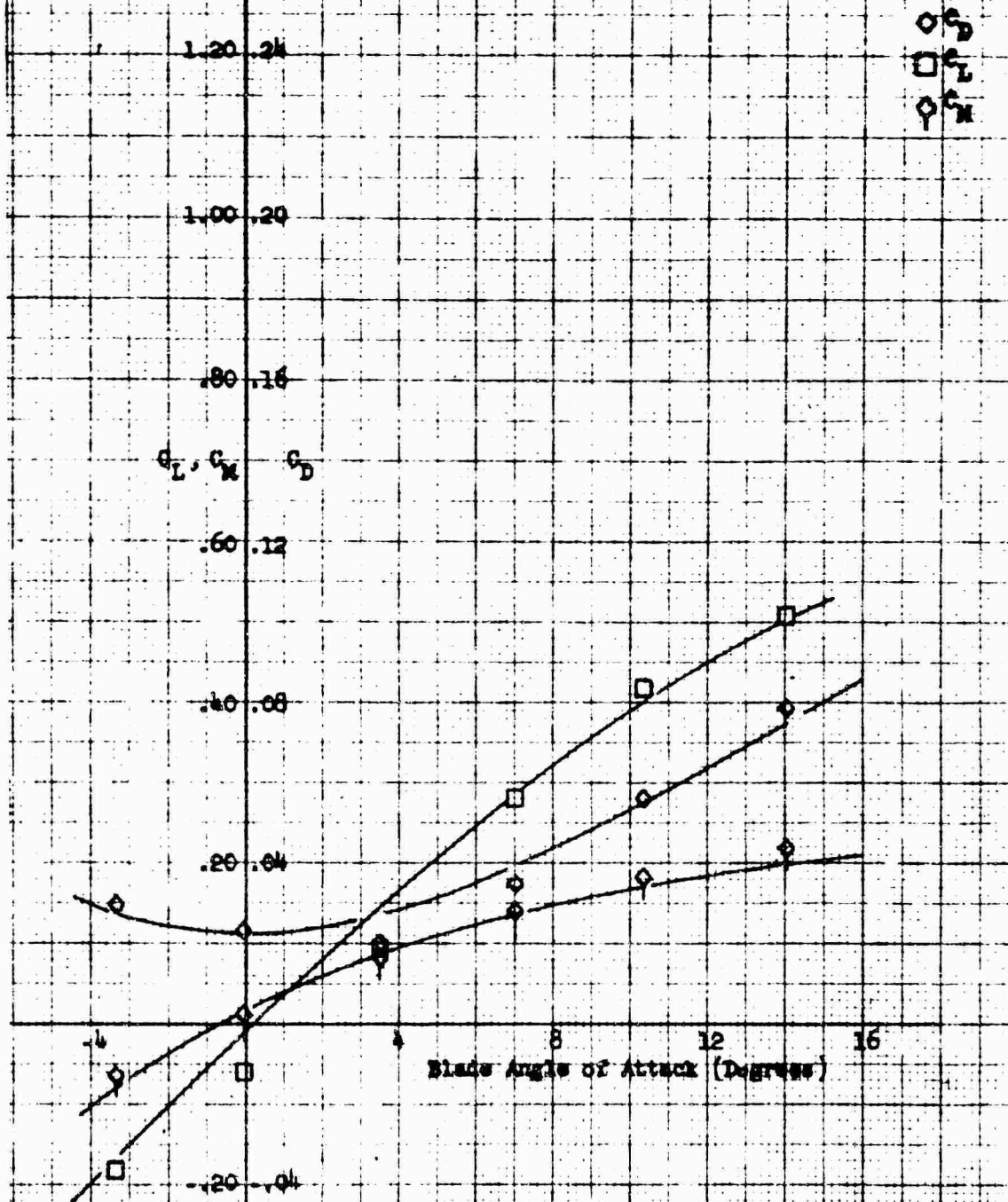


Figure 301. Coefficients for Combined Macelle and Blade - Run 123.

Nacelle Configuration: Single 1-50-100 Conical Spinner
 Fairing: w/o
 Nacelle Exit Plate: .90
 $\beta = -10^\circ$

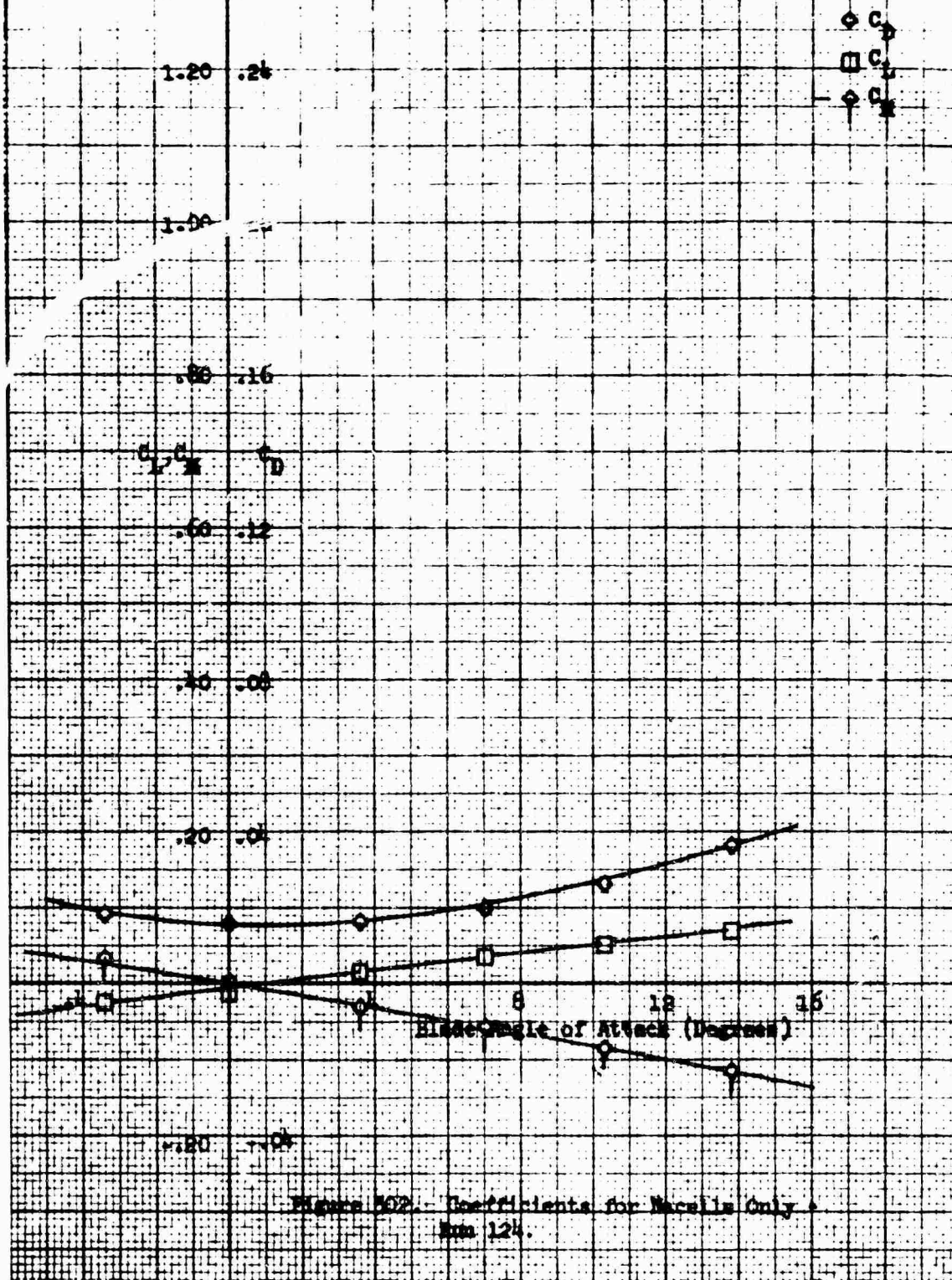


Figure 102. - Coefficients for Nacelle Only.
 Run 124.

Macelle Configuration: Single 1-50-100 conical spinner
 Macelle Incidence Angle: 0°
 Fairing: ~~1/8~~
 Macelle Exit Plate: .90
 $\beta = 10^\circ$

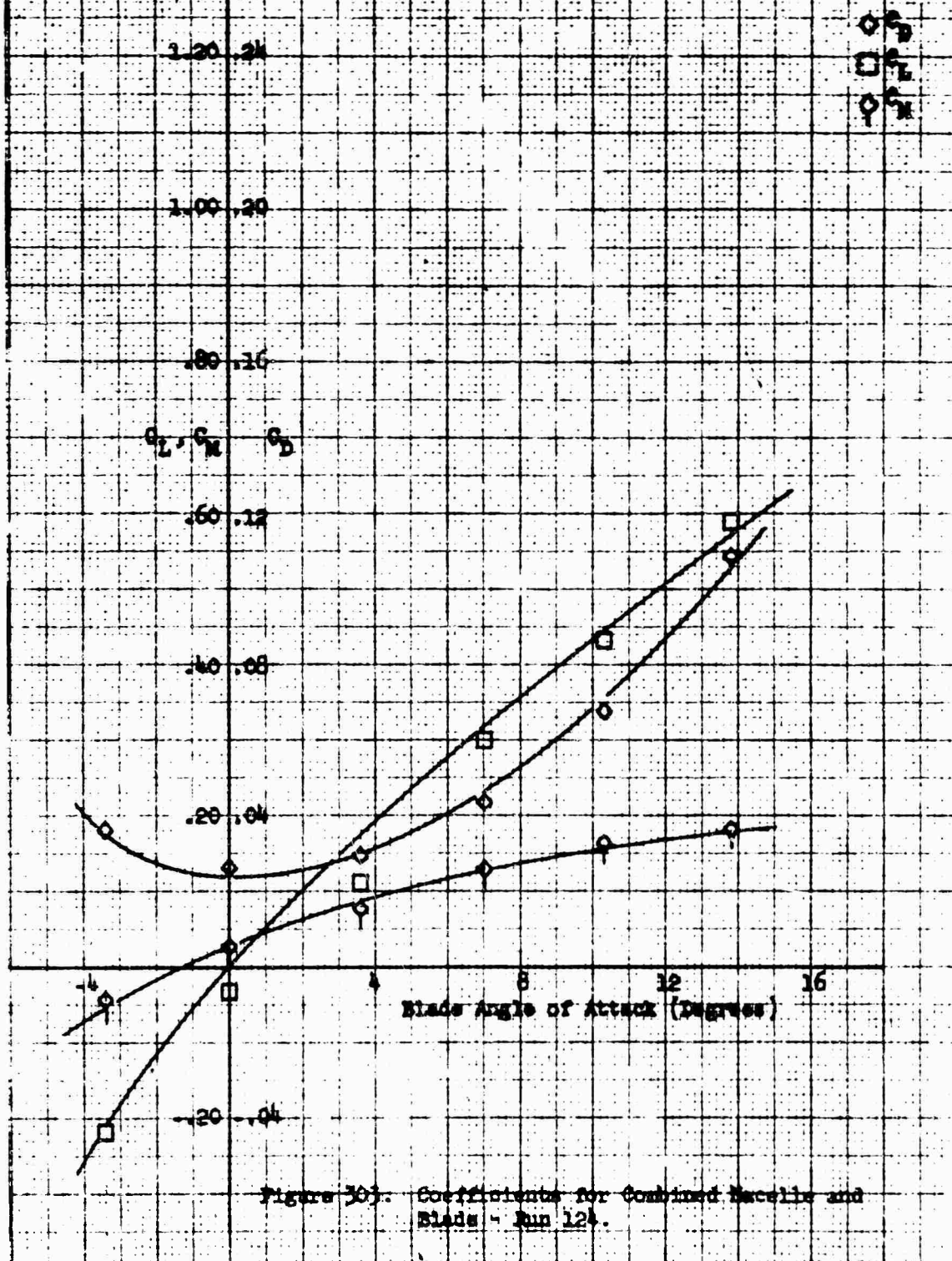
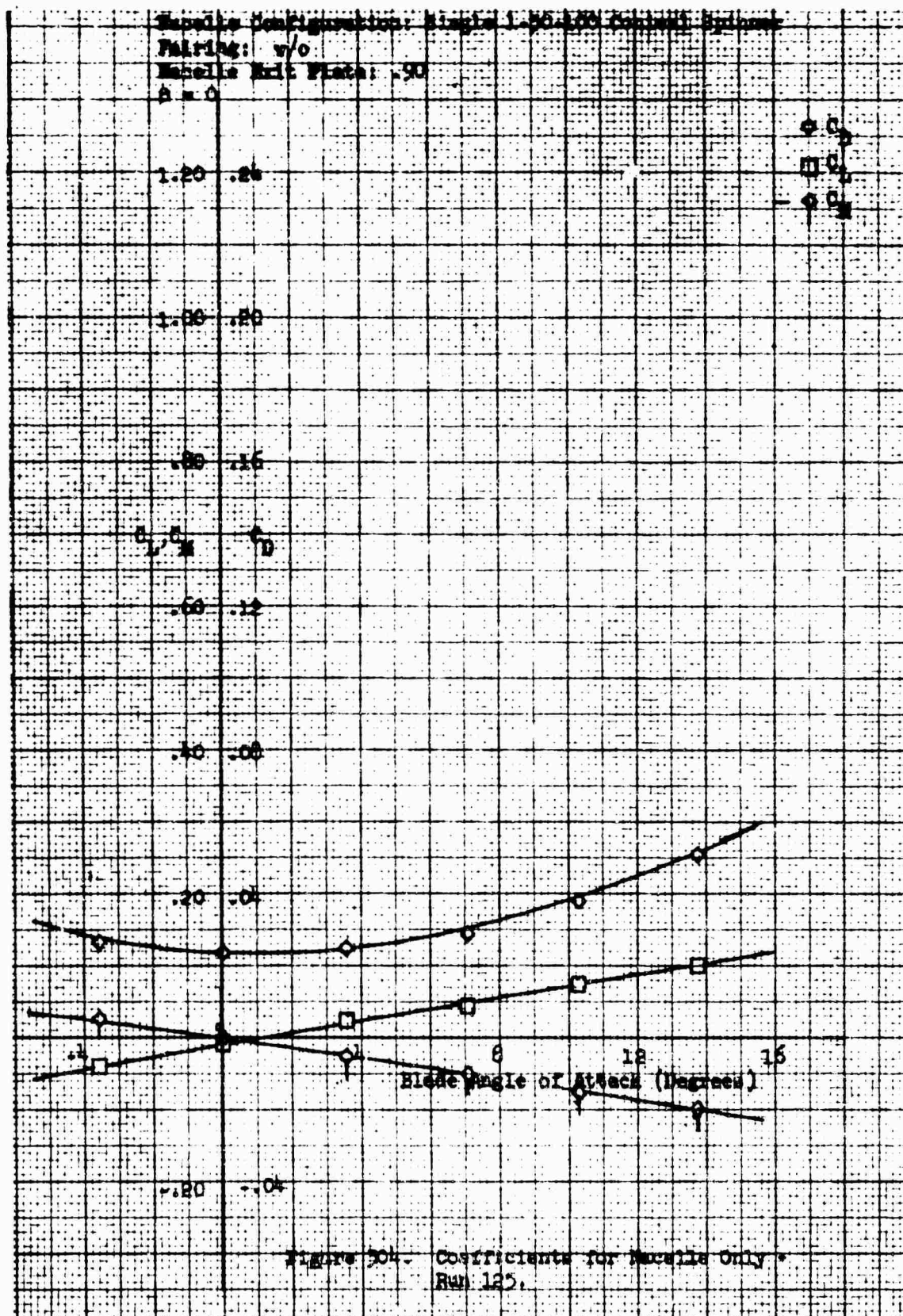


Figure 303. Coefficients for Combined Macelle and Blade - Run 124.



Wacelle Configuration: Single 1-50-100 conical spinner

Wacelle Incidence Angle: 0°

Pairing: V/θ

Wacelle Exit Plate: $.90$

$\beta = 0$

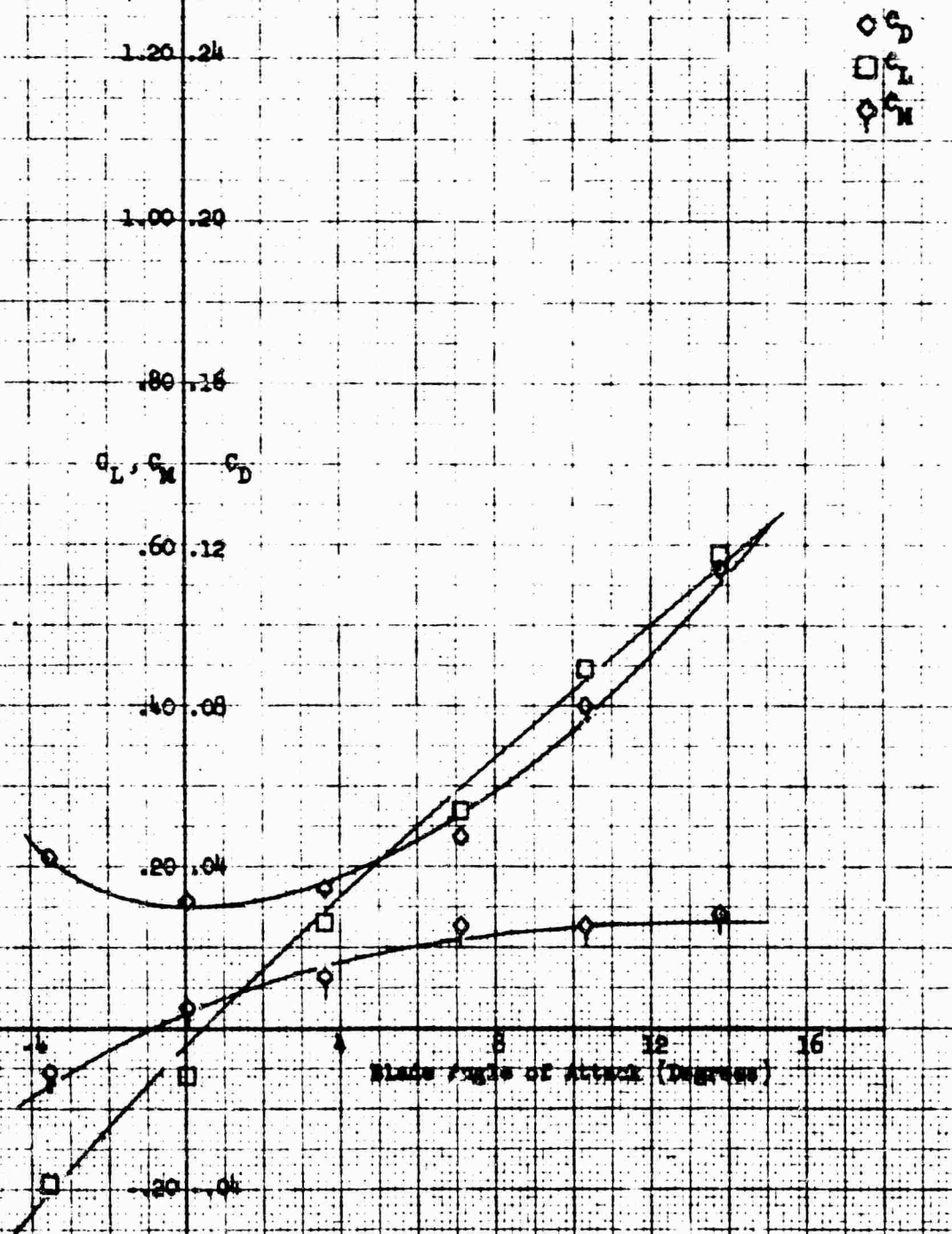
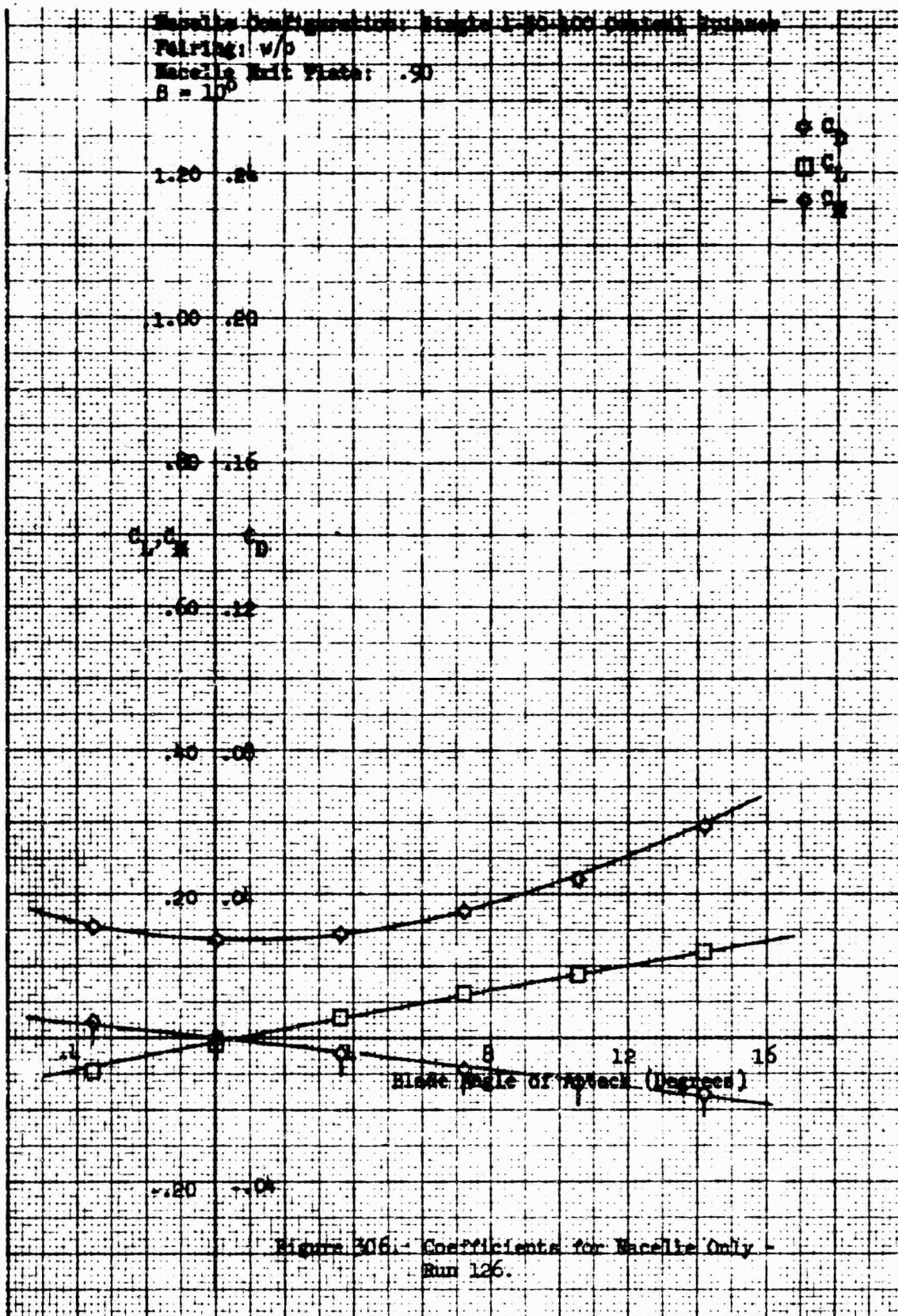


Figure 305. Coefficients for Combined Wacelle and Blade - Run 125.

Nozzle Configuration: Single 1-20-200 Conical Exhaust
 Pairing: w/o
 Nozzle Exit Plane: .90
 $\theta = 10^\circ$



Macelle Configuration: Single 1-50-100 conical spinner
 Macelle Incidence Angle: 0°
 Pairing: #/0
 Macelle Exit Plate: .90
 $\beta = 10^\circ$

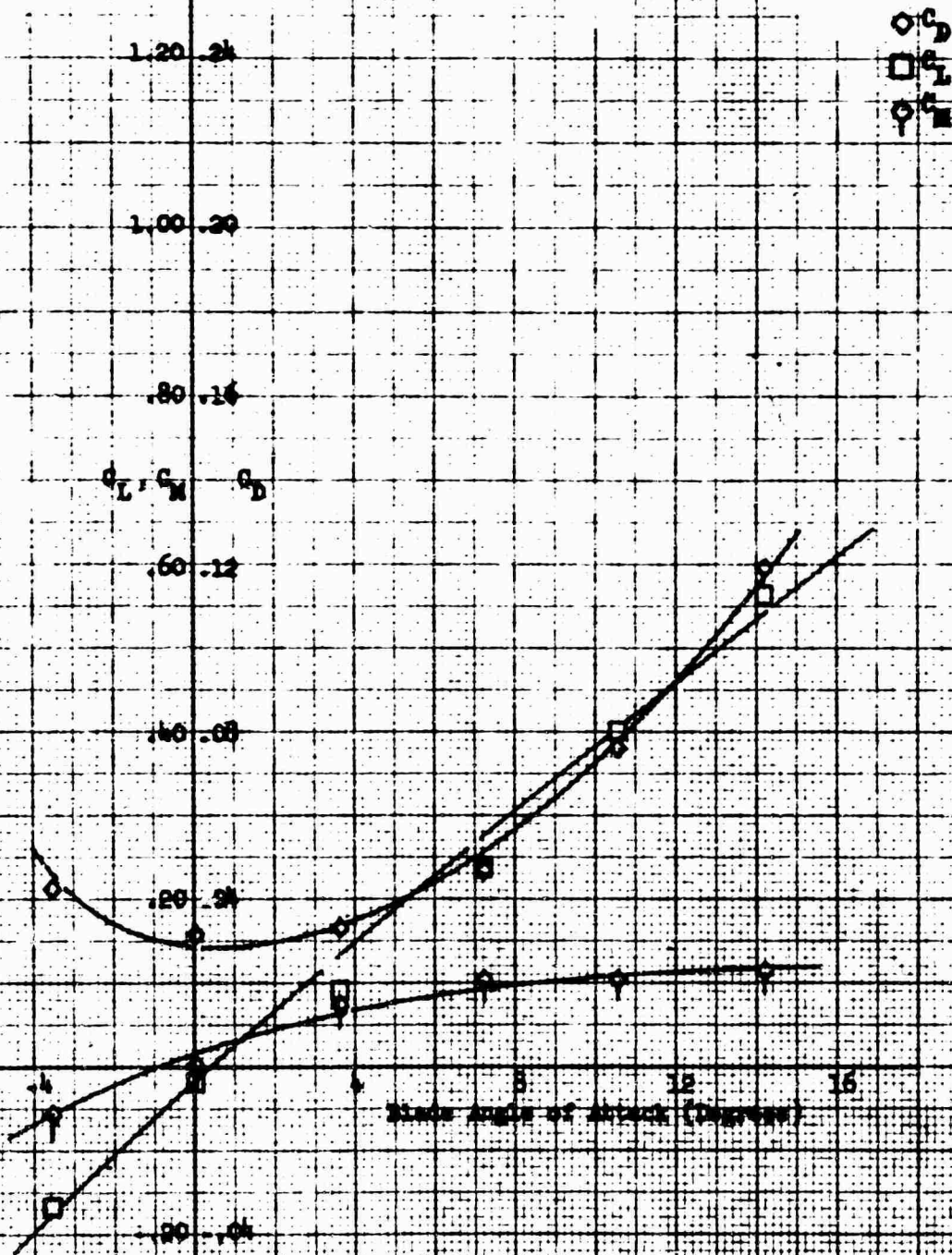
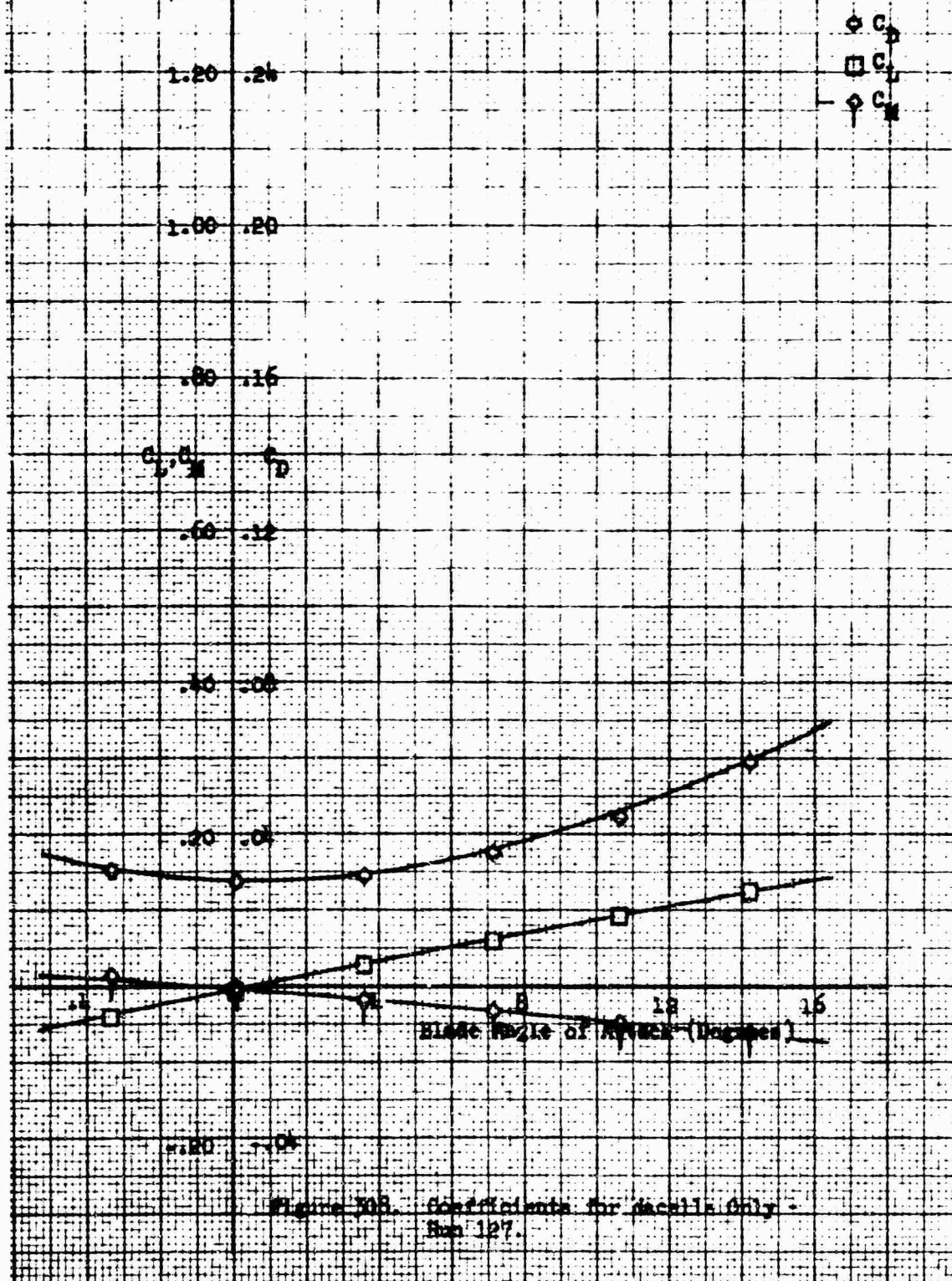


Figure 307. Coefficients for Conical Macelle and Plate - Run 124.

Blade Configuration: Single 1-50-100 Centical Spinner
 Pairing: w/o
 Macelle Exit Plate: .90
 $\beta = 20^\circ$



Blade Configuration: Single 1-50-100 conical spinner
 Blade Incidence Angle: 0°
 Pairing: N/A
 Blade Exit Plate: .90
 $\beta = 20^\circ$

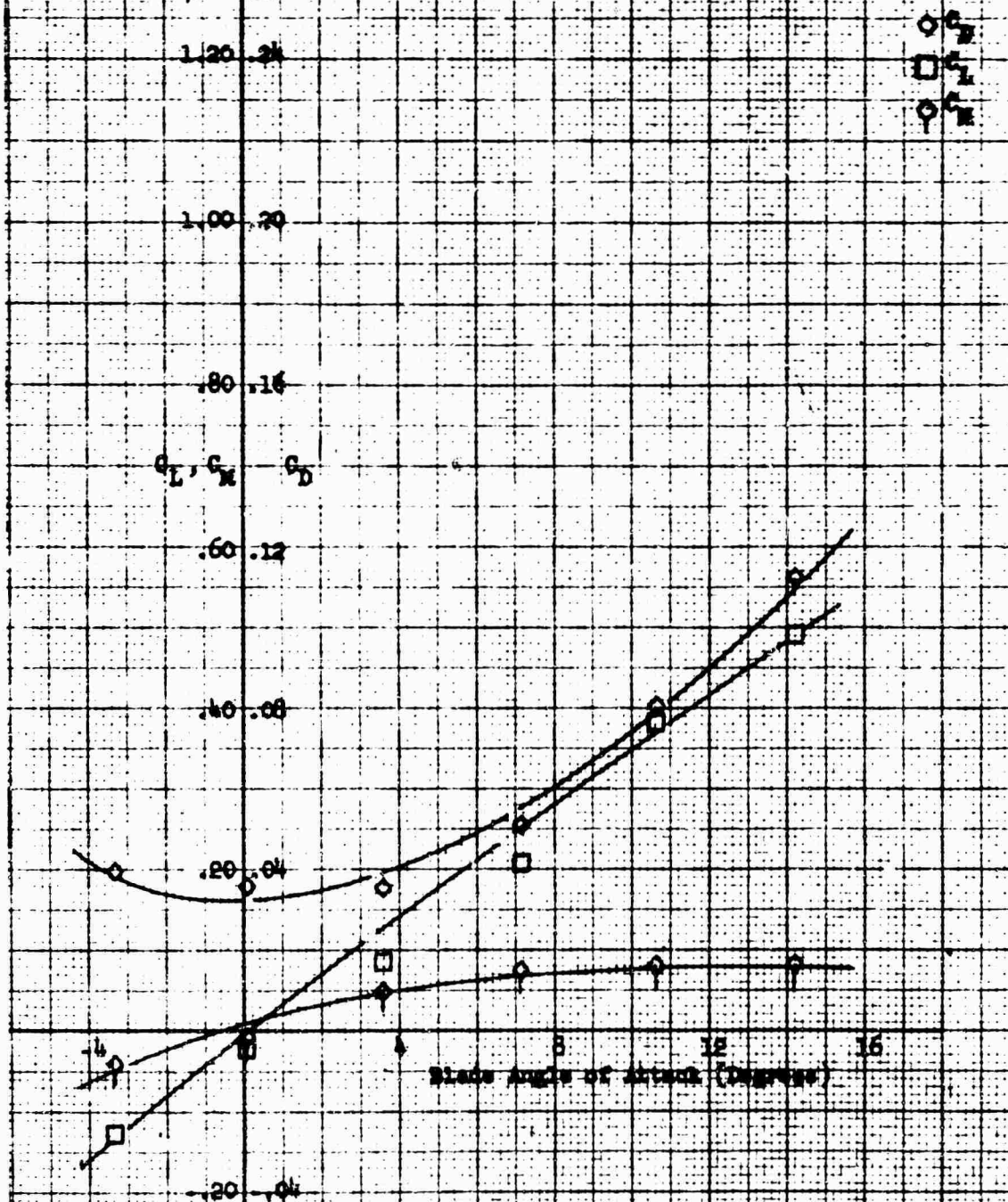
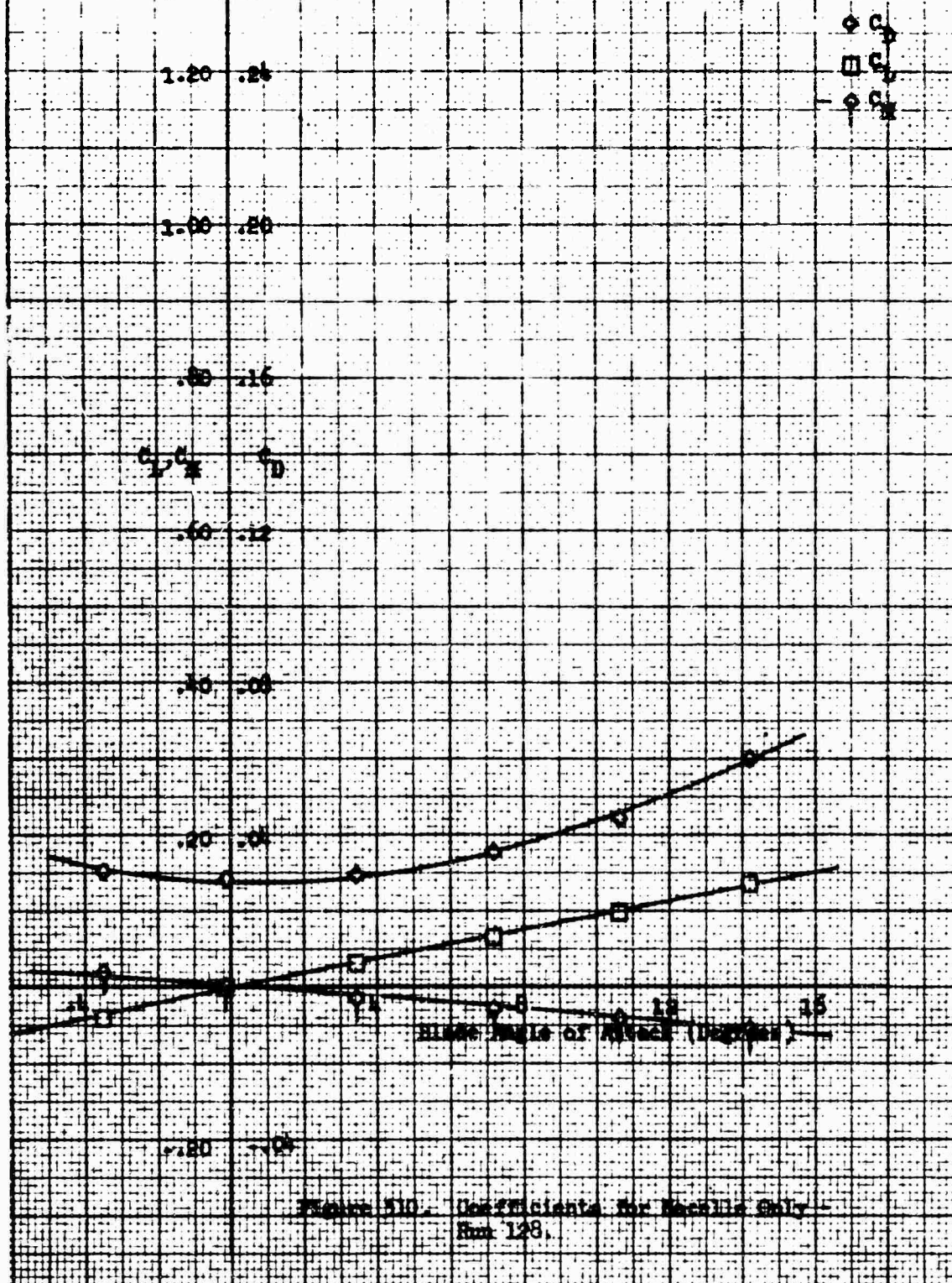
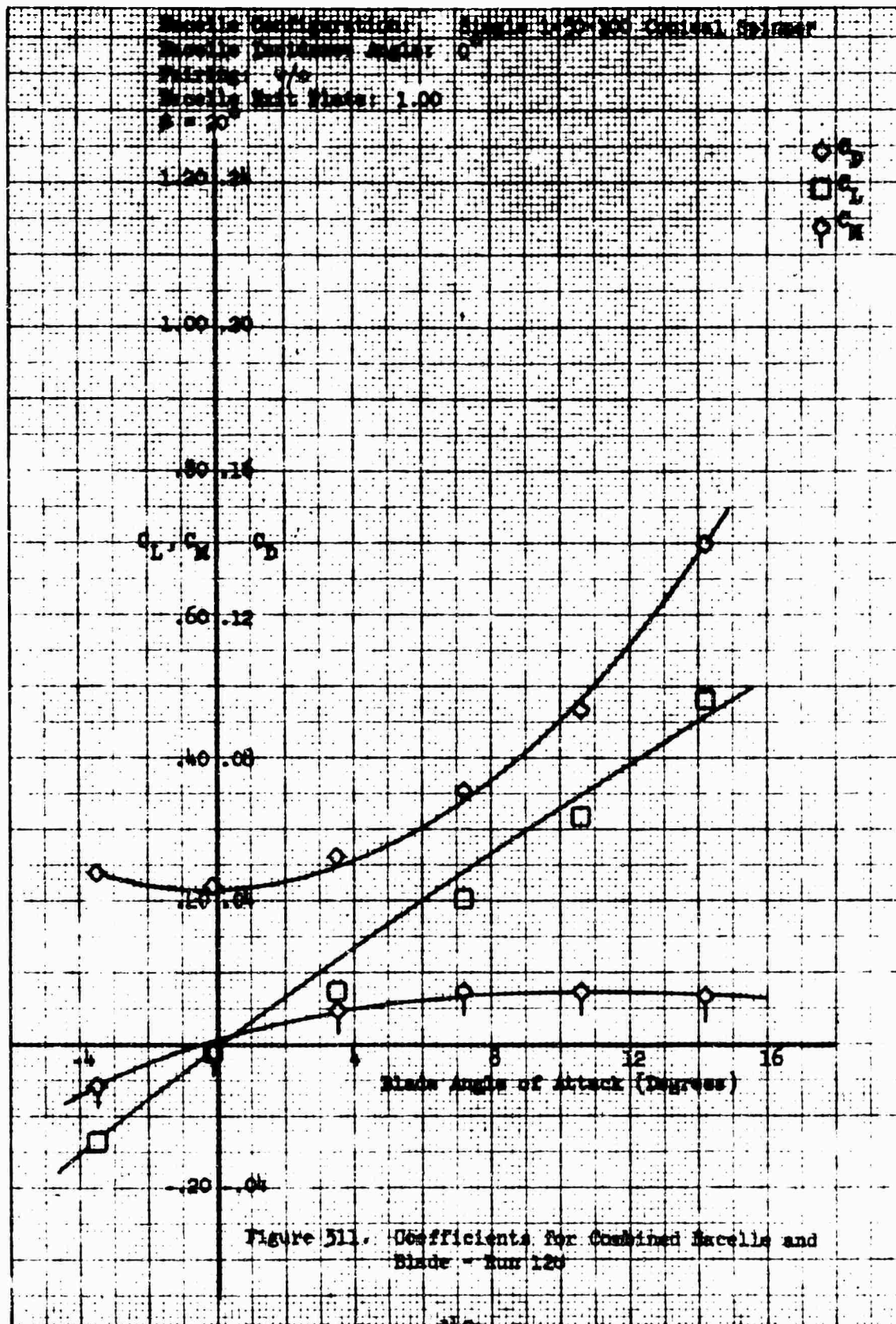


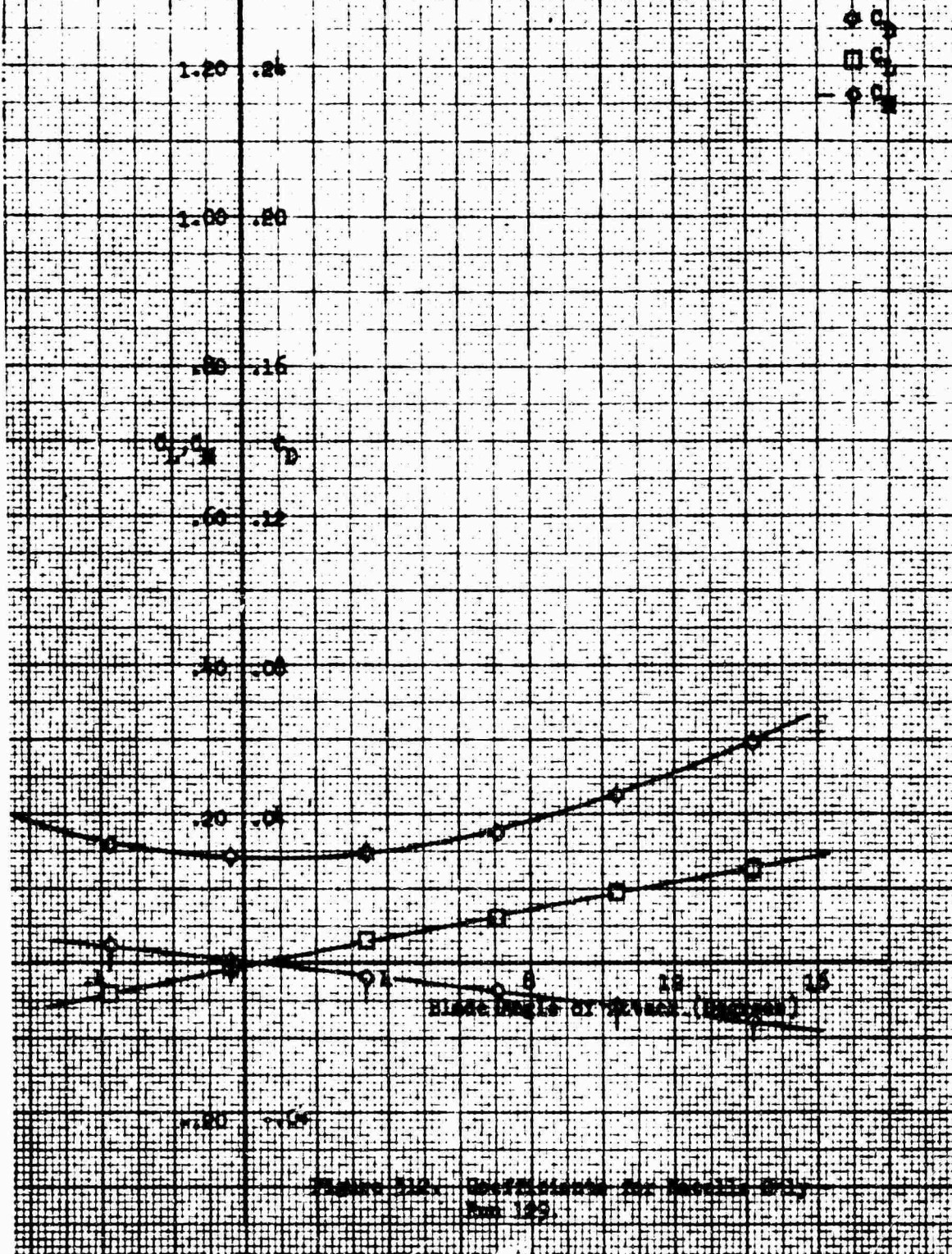
Figure 309. Coefficients for Combined Nacelle and Blade - Run 127.

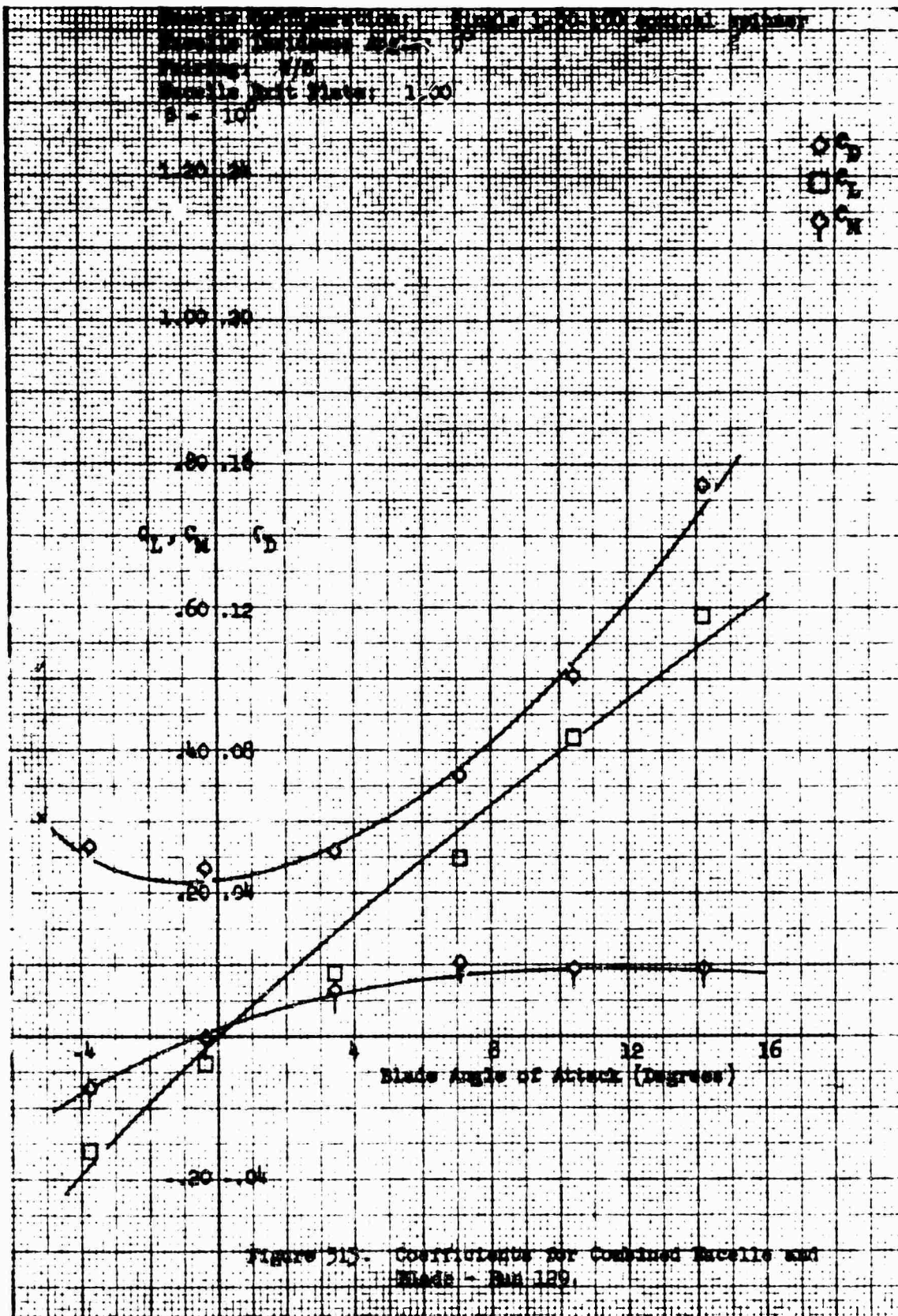
Nozzle Configuration: Single 1-50-100 contour sprayer
 Pairing: w/o
 Nozzle Exit Plate: 1.00
 $\theta = 20^\circ$



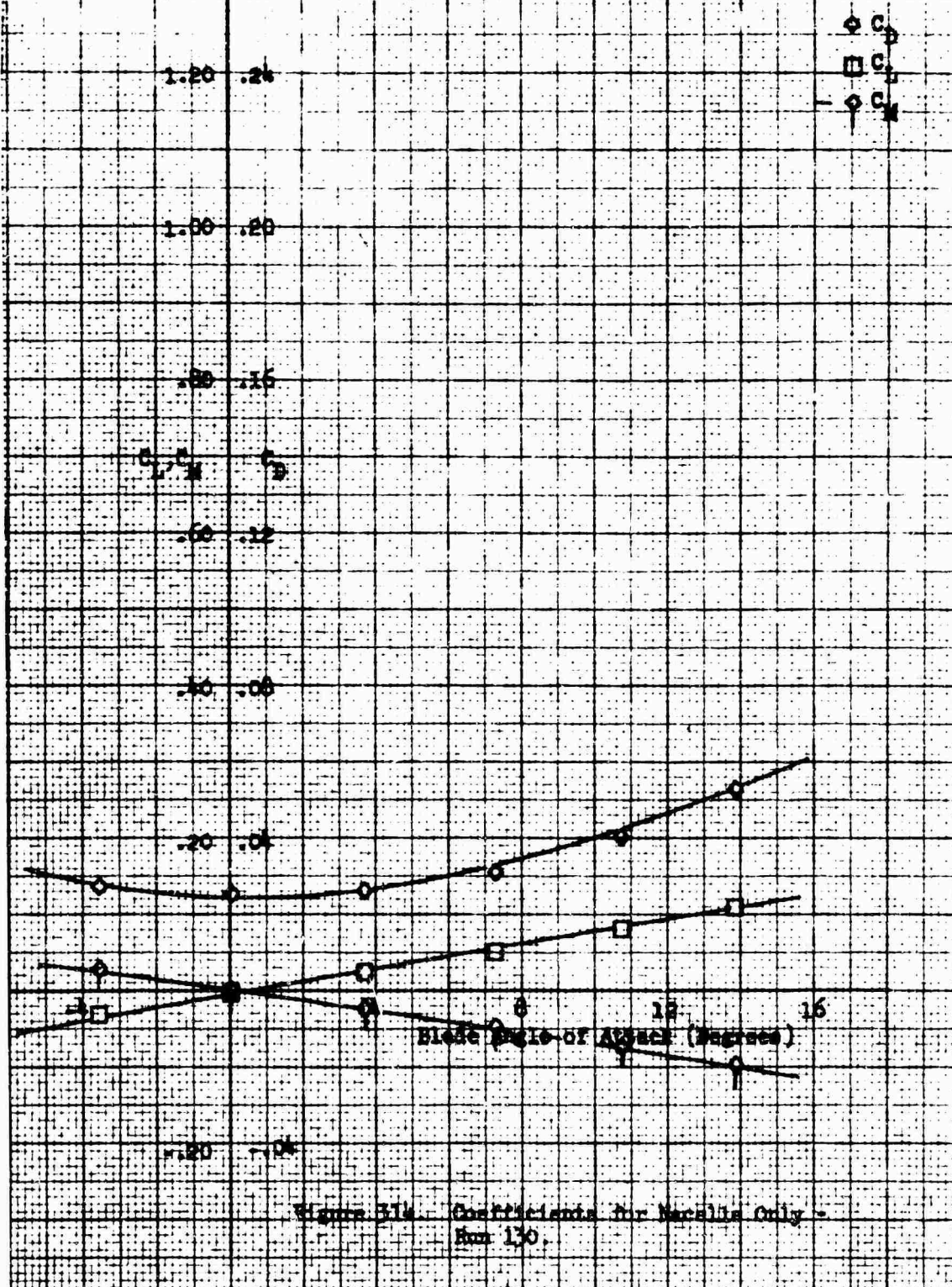


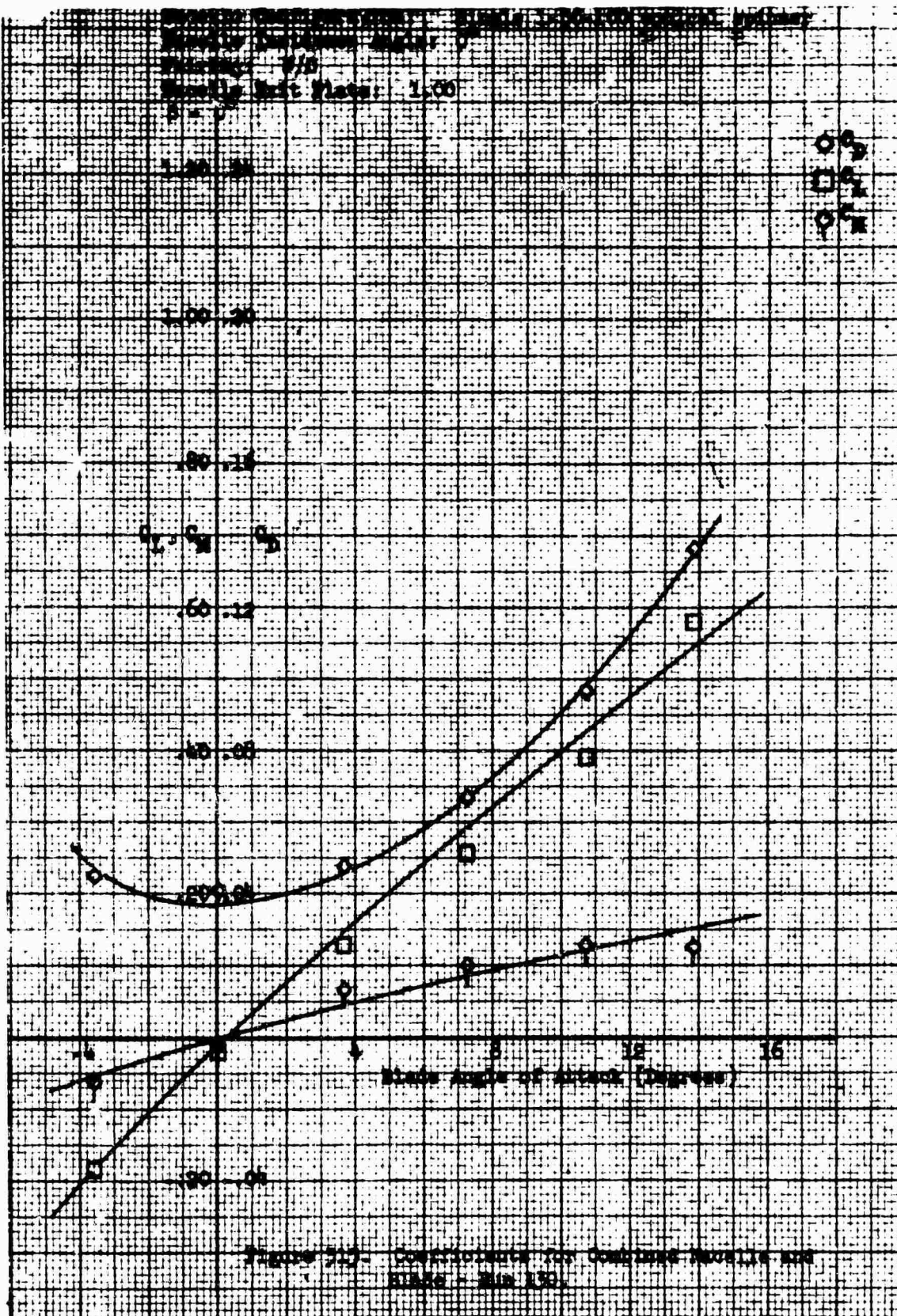
Macelle Configuration: Single 1-50-100 Control System
 Pairing: w/o
 Macelle Exit Plate: 1.05
 $\theta = 10^\circ$

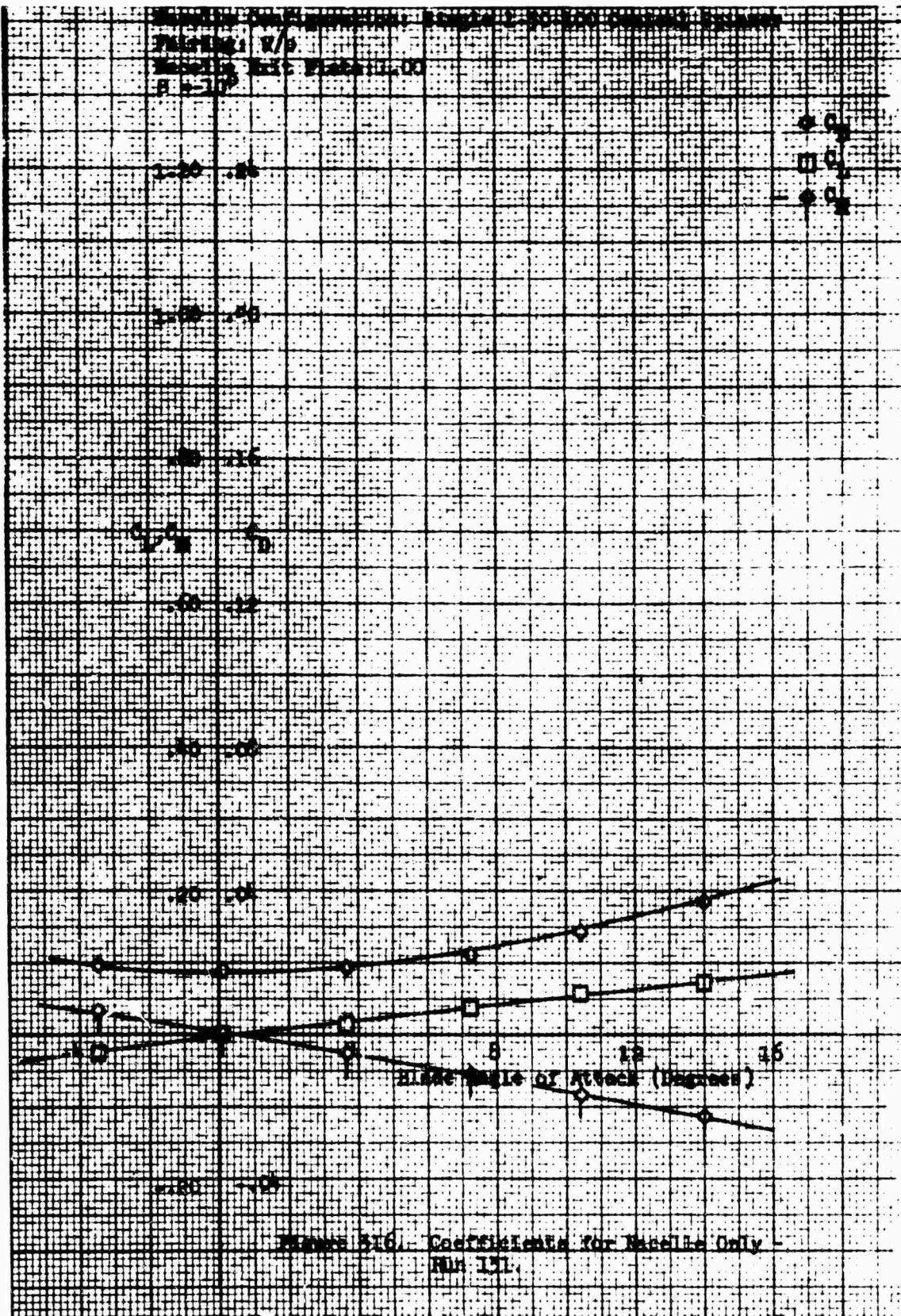




Blade Configuration: Single 1-50-100 Conical Spinner
 Pairing: v/p
 Macellie Exit Plate: 1.00
 $\theta = 0$







Macelle Configuration: Single 1-50-100 conical spinner
 Macelle Incidence Angle: 0°
 Pairing: W/S
 Macelle Exit Plate: 1.00
 $\beta = -10^\circ$

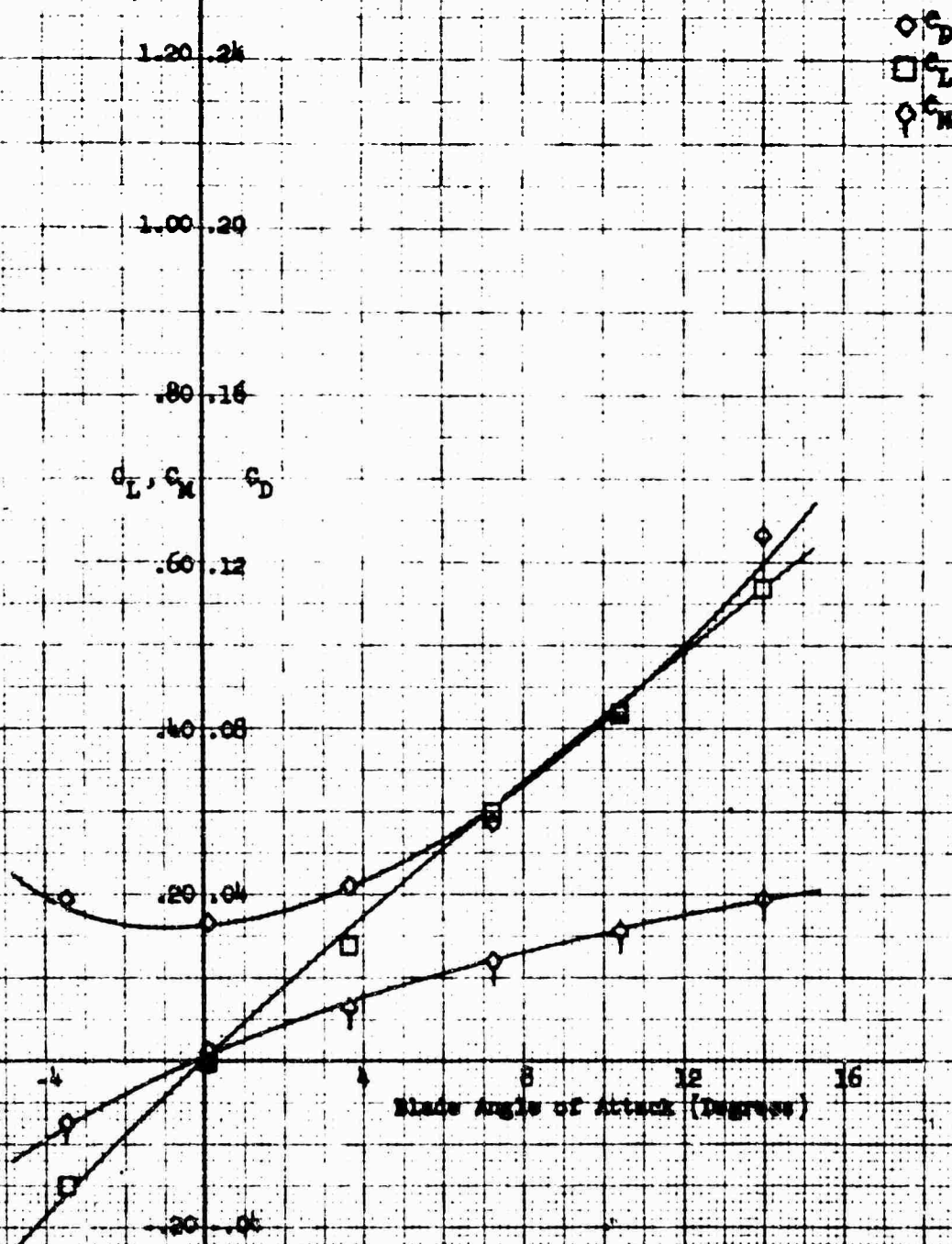
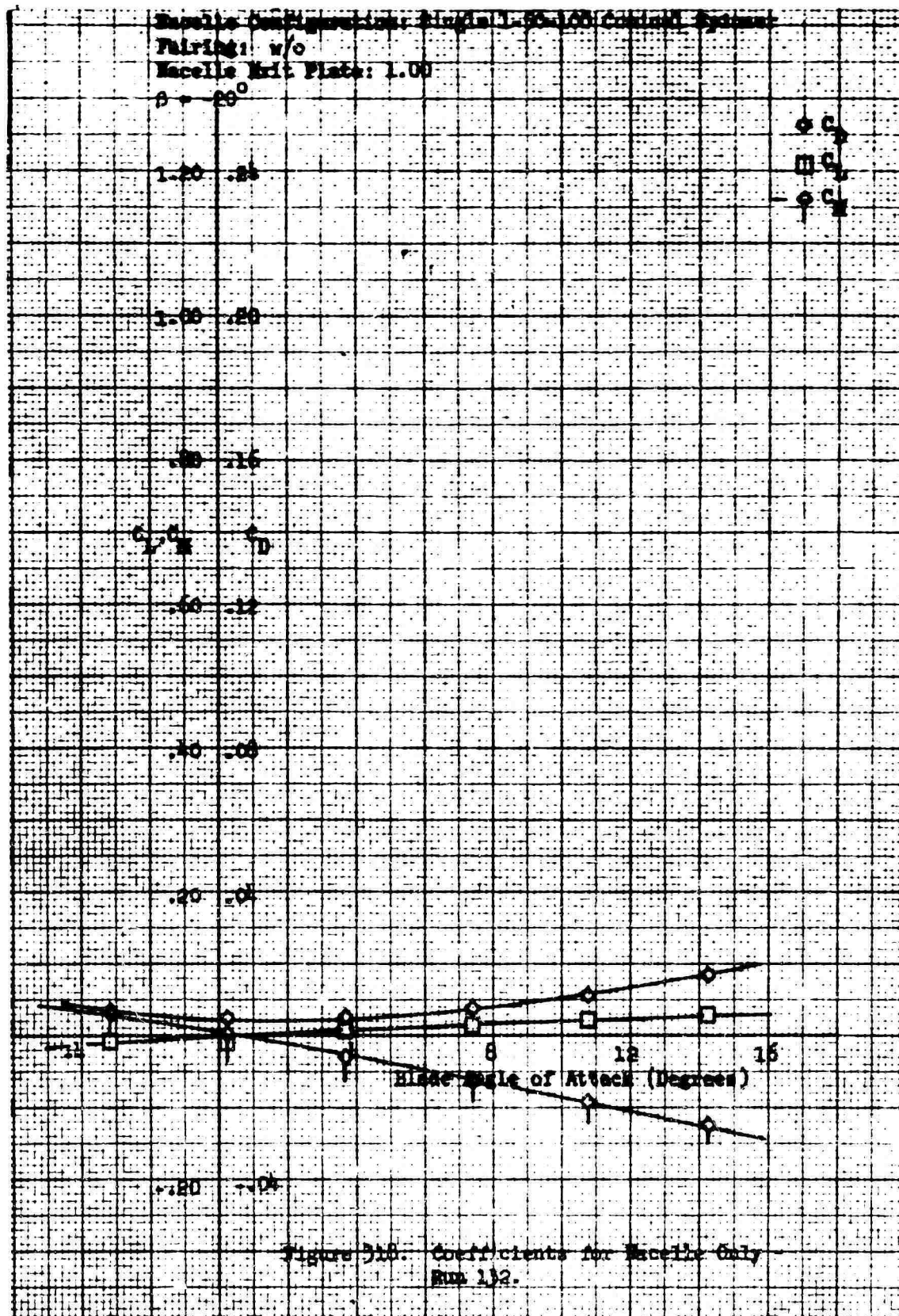


Figure 517. Coefficients for Combined Macelle and Blade - Run 132.



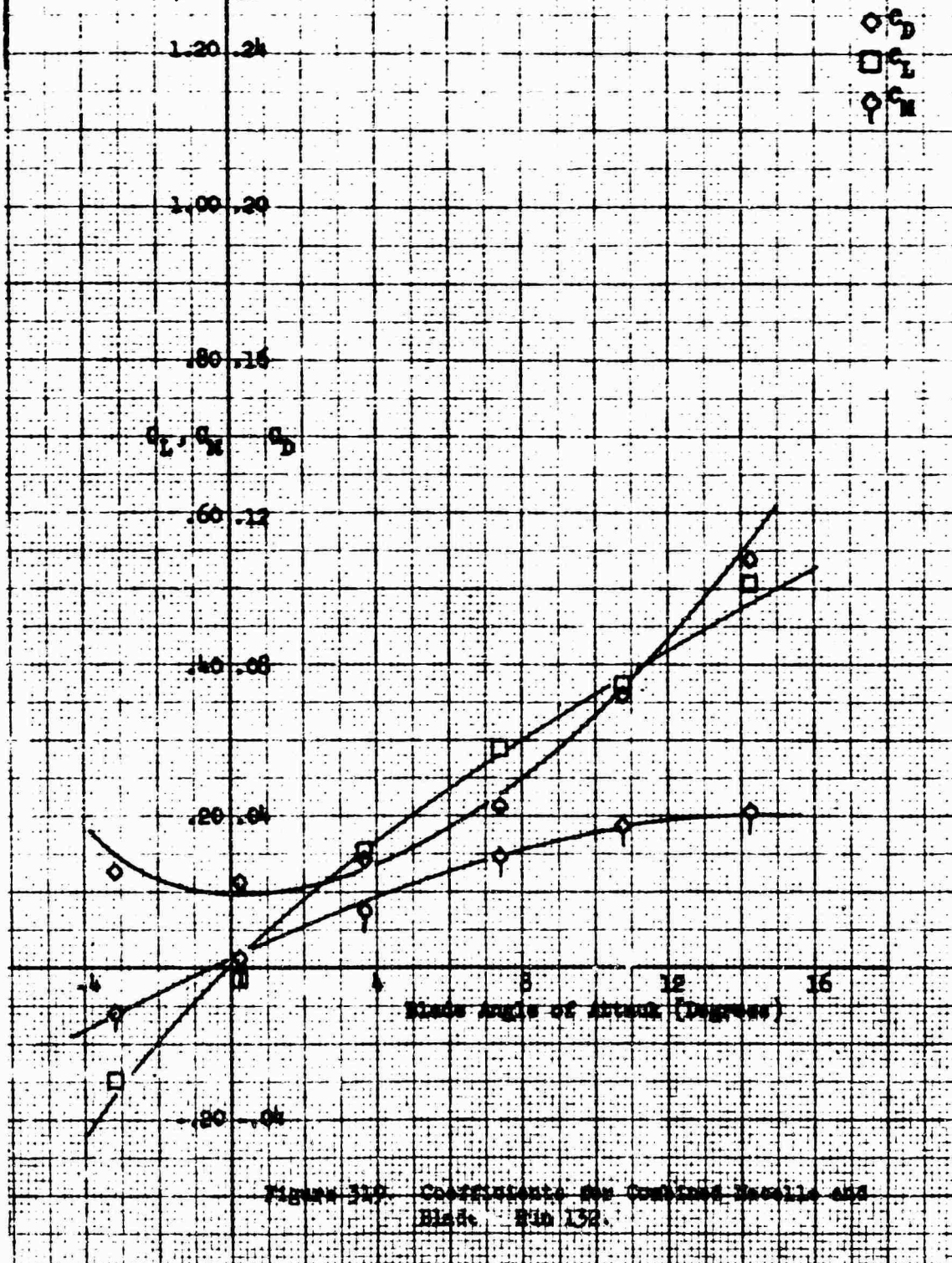
Macelle Configuration: Single 1-50-100 conical spinner

Macelle Incidence Angle: 0°

Fairing: W/C

Macelle Exit Plate: 1.00

$\beta = 20^\circ$



Sample Configuration: Twin Vertical 1-10-100
 Pairing: With
 Macelle Exit Plate: 1.00
 $\theta = -20^\circ$

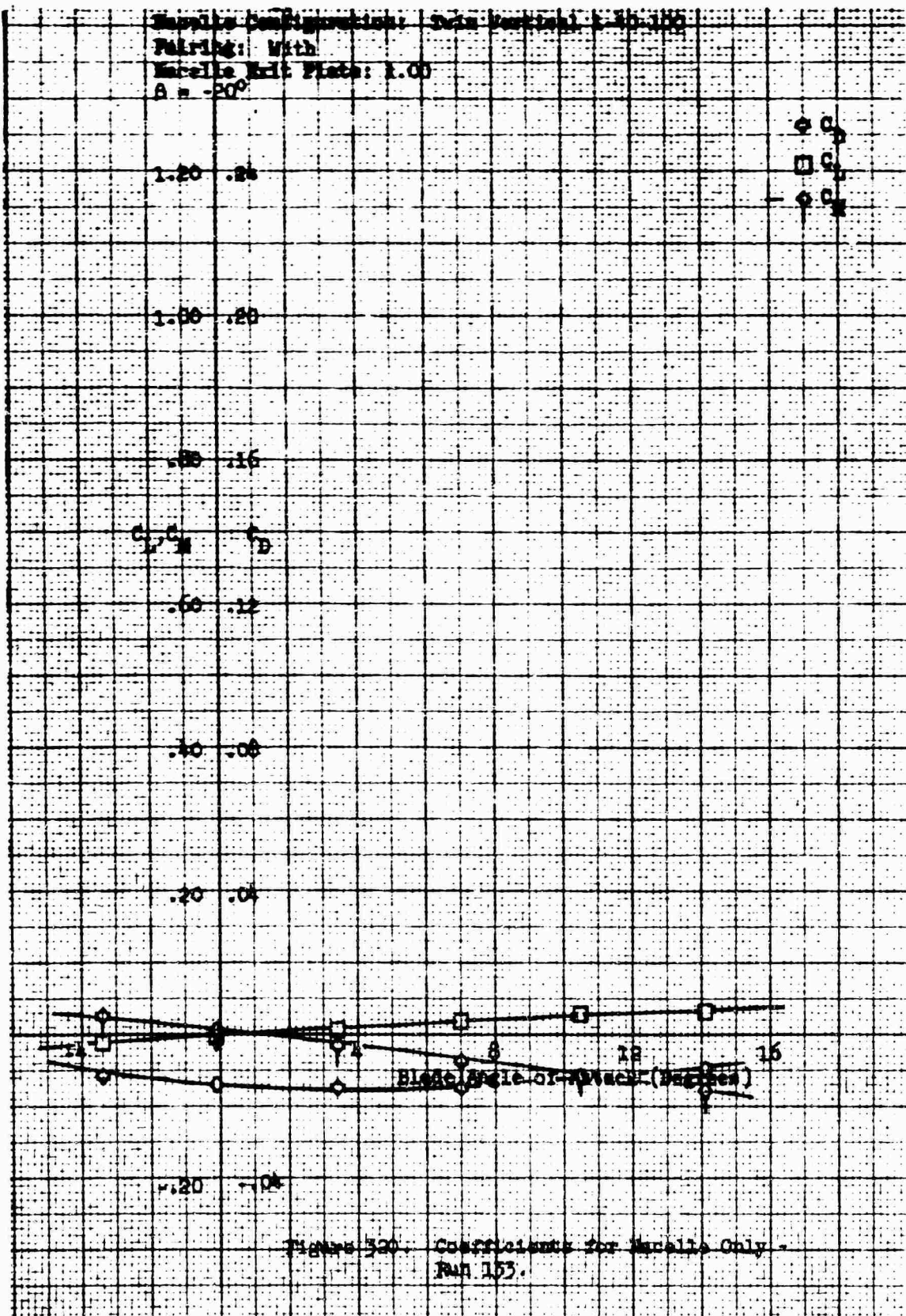
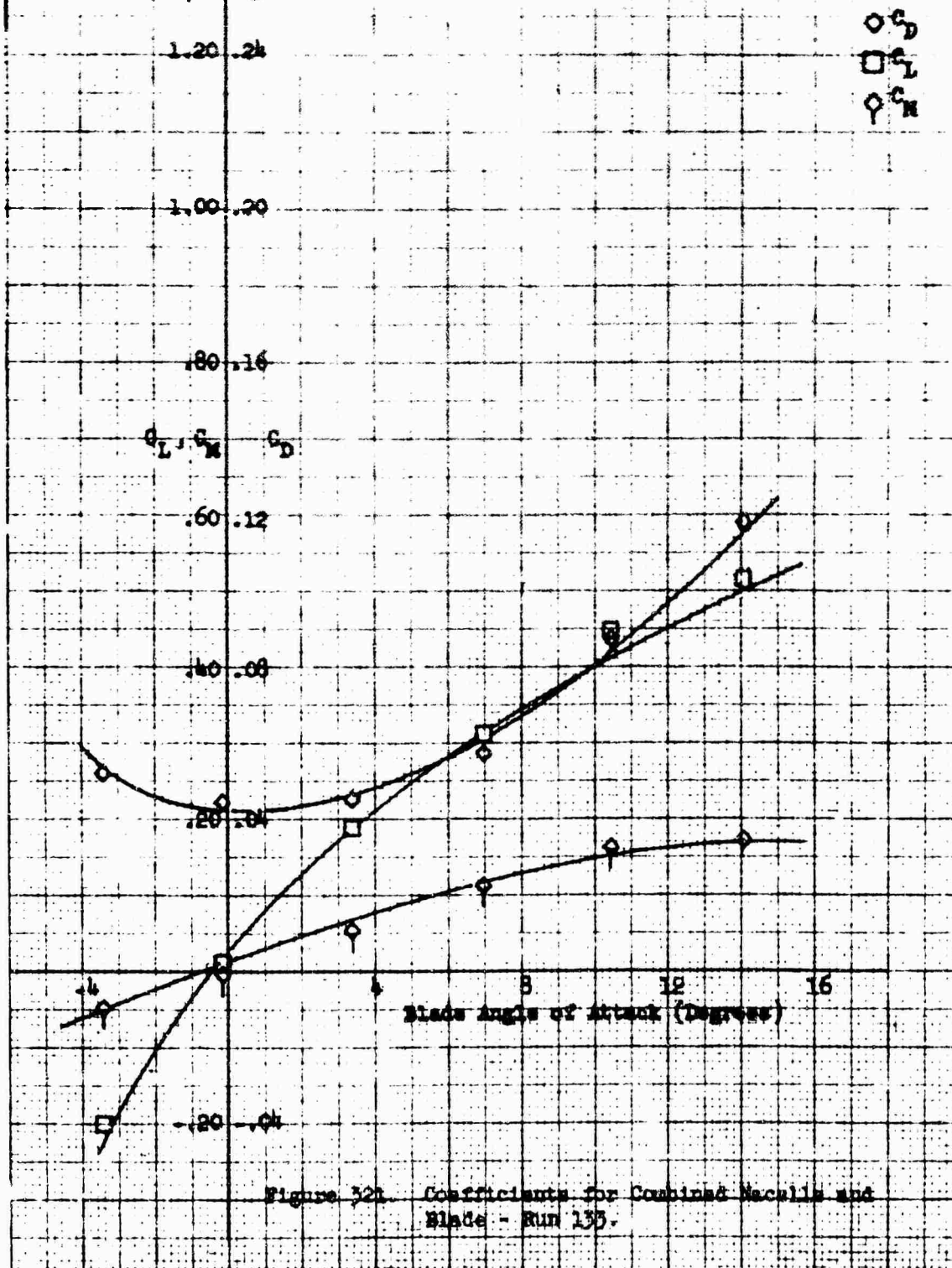


Figure 320: Coefficients for Macelle Only -
 Run 153.

Macelle Configuration: Twin vertical 1-40-100
 Macelle Incidence Angle: 0°
 Pairing: With
 Macelle Exit Plate: 1.00
 $\beta = -20^\circ$



Mapelle Configuration: Thin Vortex 1-10-100

Fairing: With

Mapelle Exit Plate: 1.00

$\alpha = 20^\circ$

With trailing edge fairing

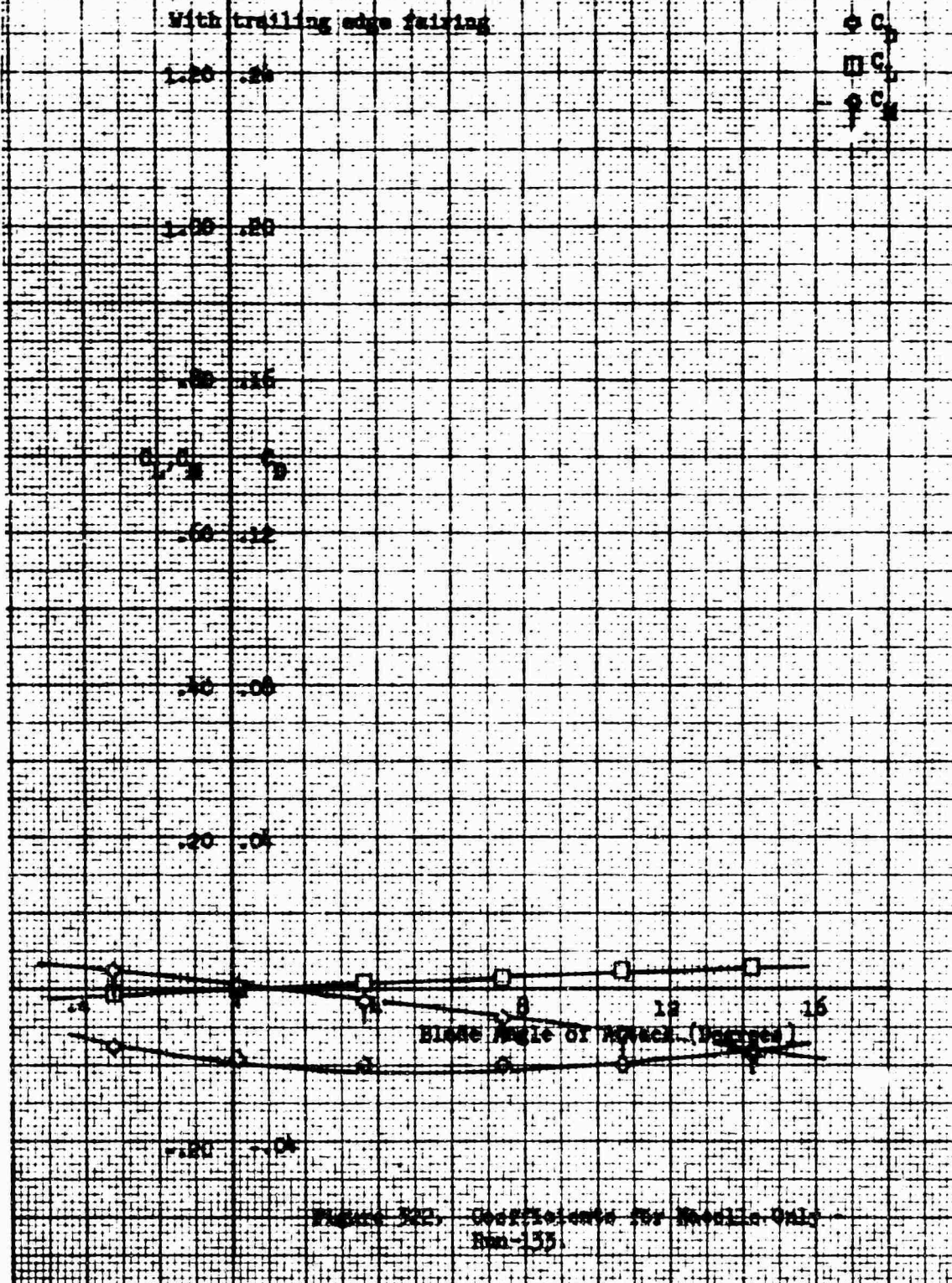


Figure 5-21. Coefficients for Mapelle Unit
Rm-155

Blade Configuration: Twin vertical 1-40-100

Blade Incidence Angle: 0°

Fairing: With

Blade Exit Slats: 1.00

With trailing edge fairing

$\beta = -25^\circ$

1.20 .24

1.00 .20

.80 .16

C_L, C_M, C_D

.60 .12

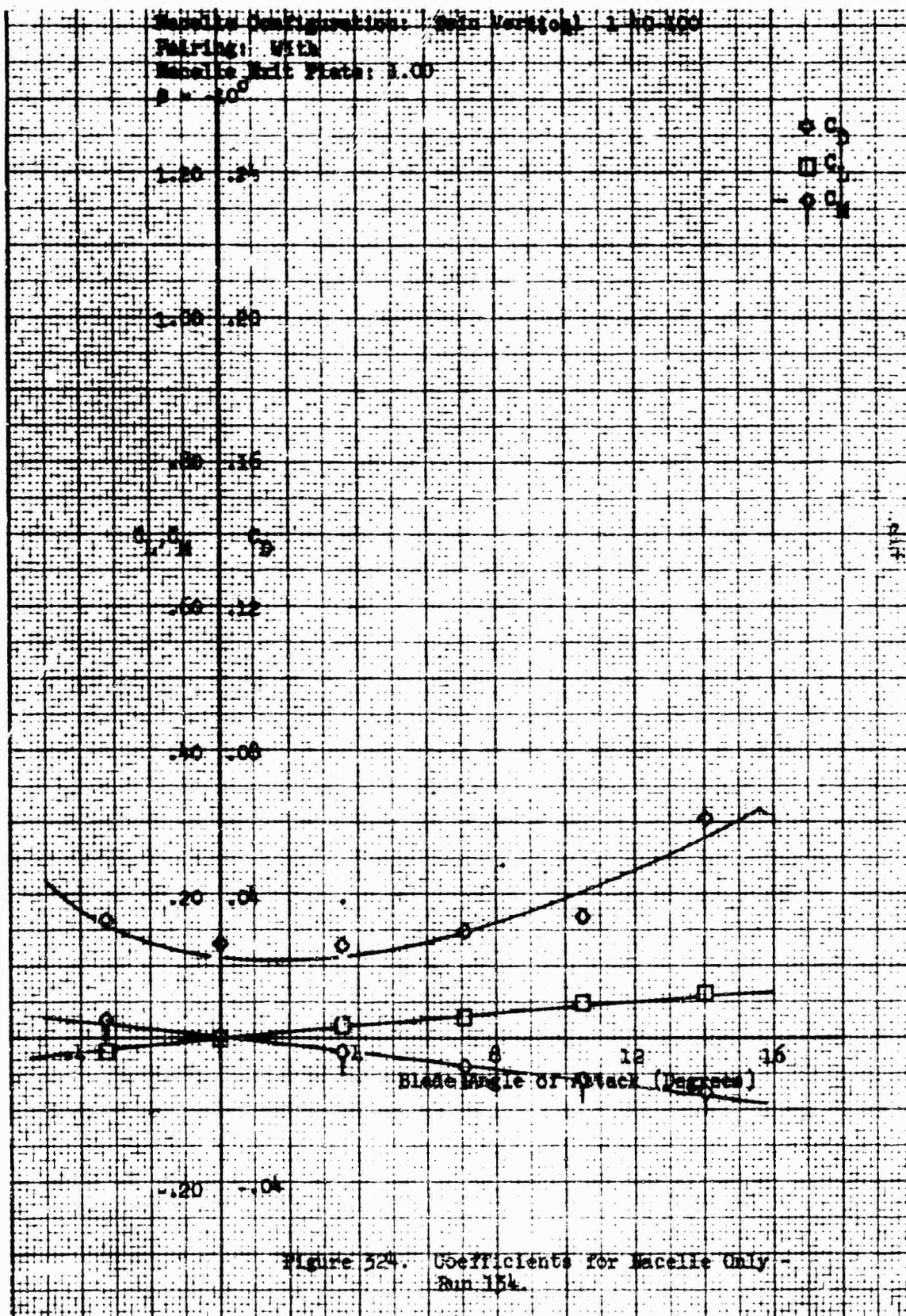
.40 .08

.20 .04

.20 .04

Blade Angle of Attack (Degrees)

Figure 323. Coefficients for Combined Blade and Blade - Run-131.



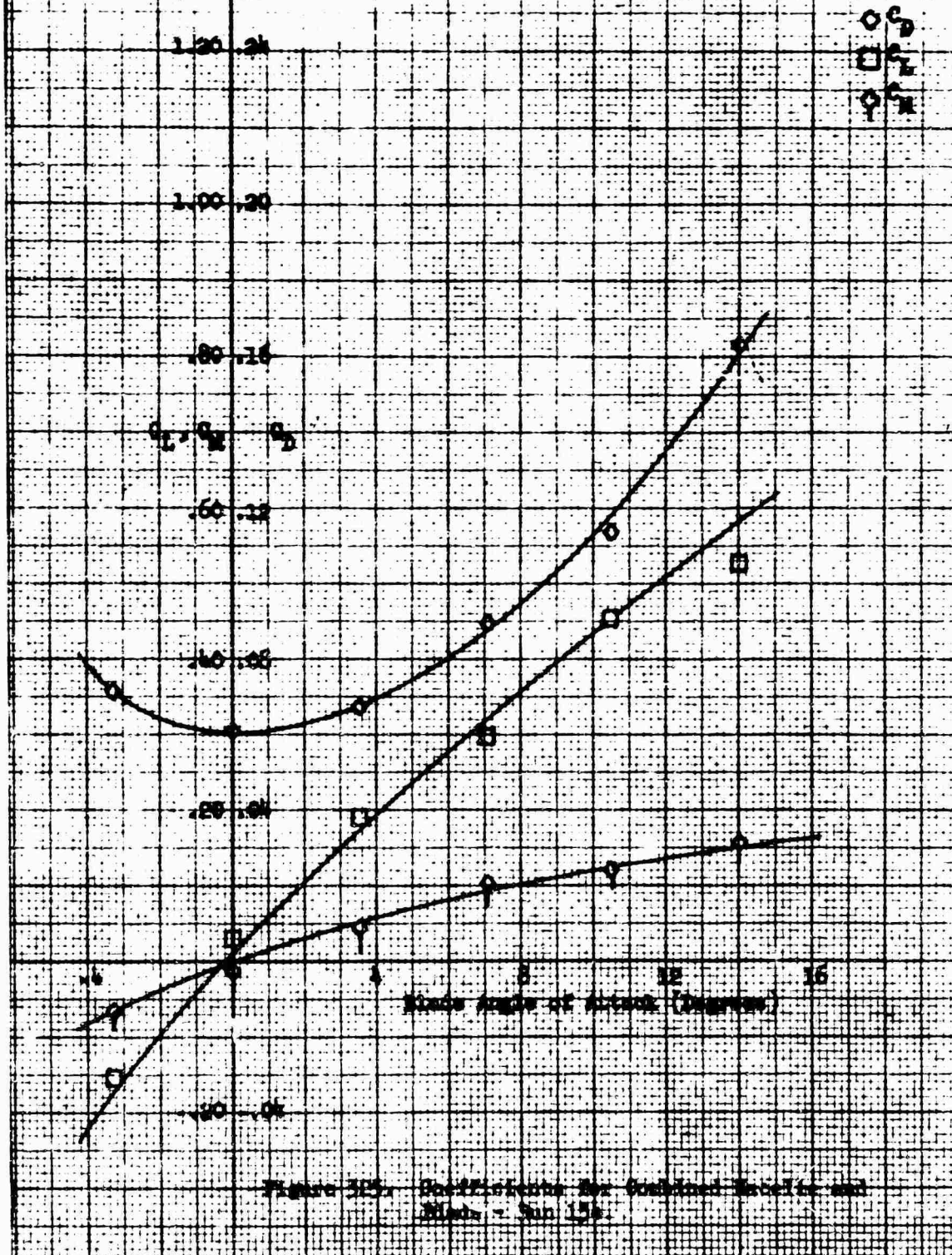
Nozzle Configuration: Twin vertical 1-40-100

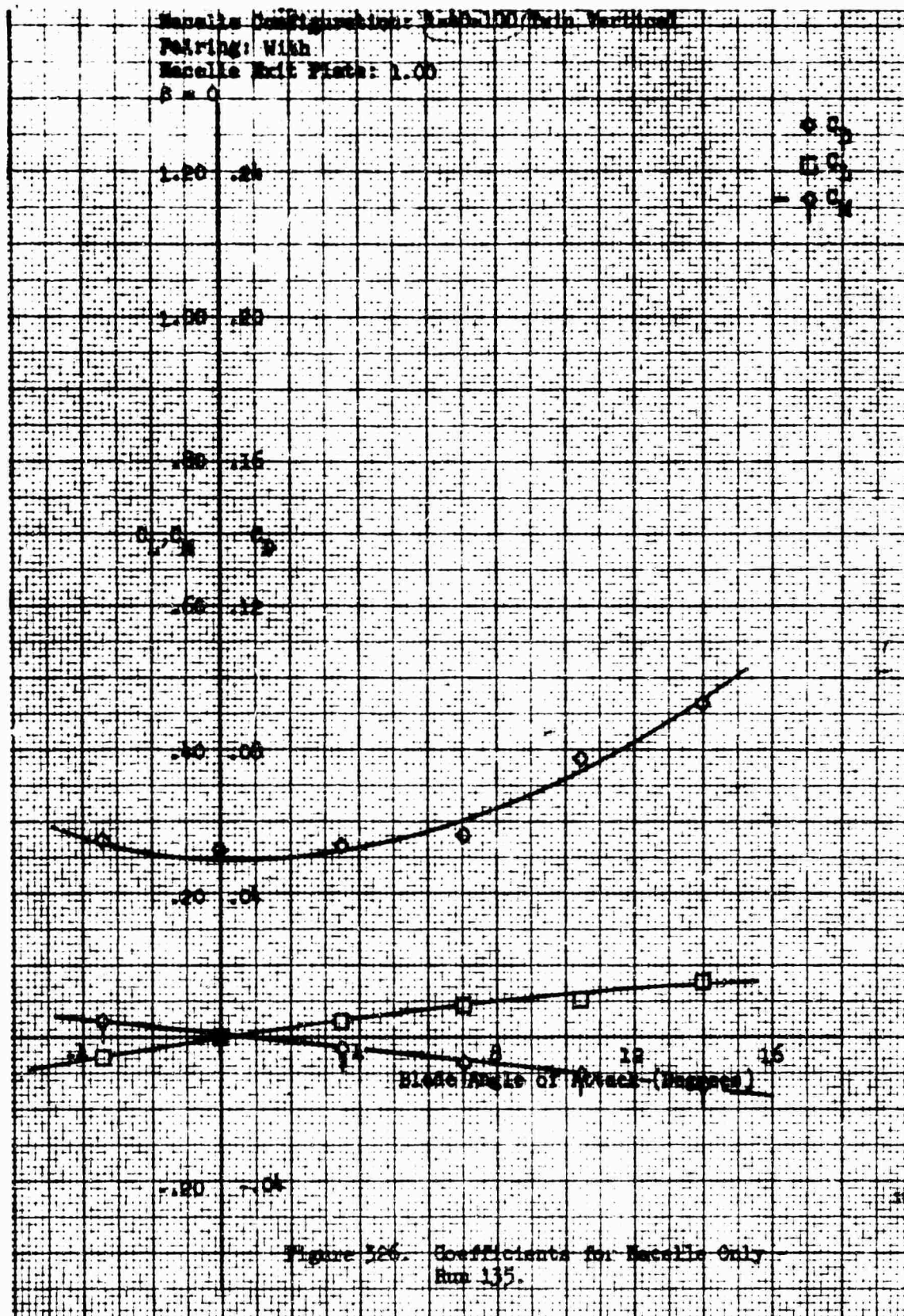
Nozzle Incidence Angle: 0°

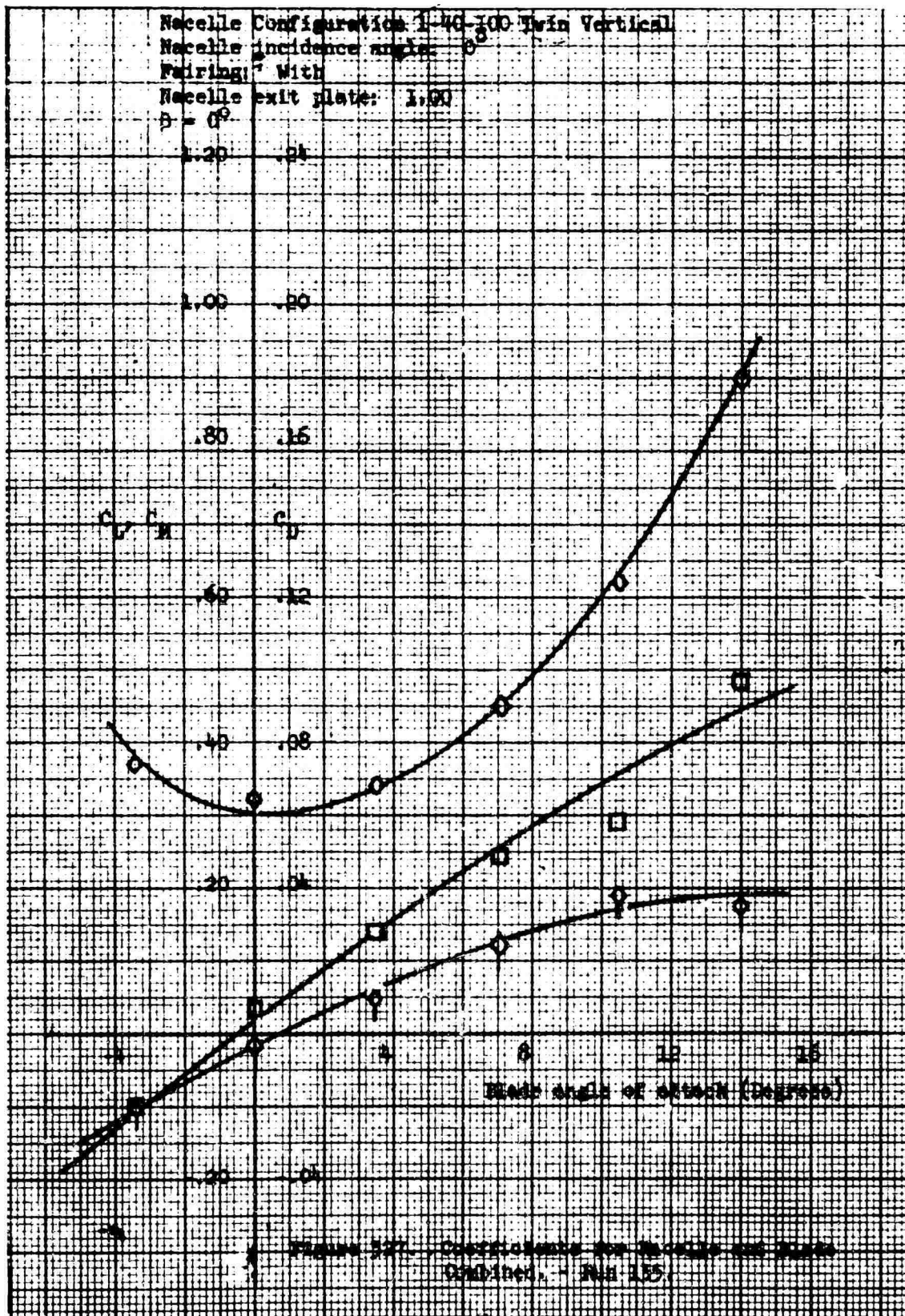
Fairing: With

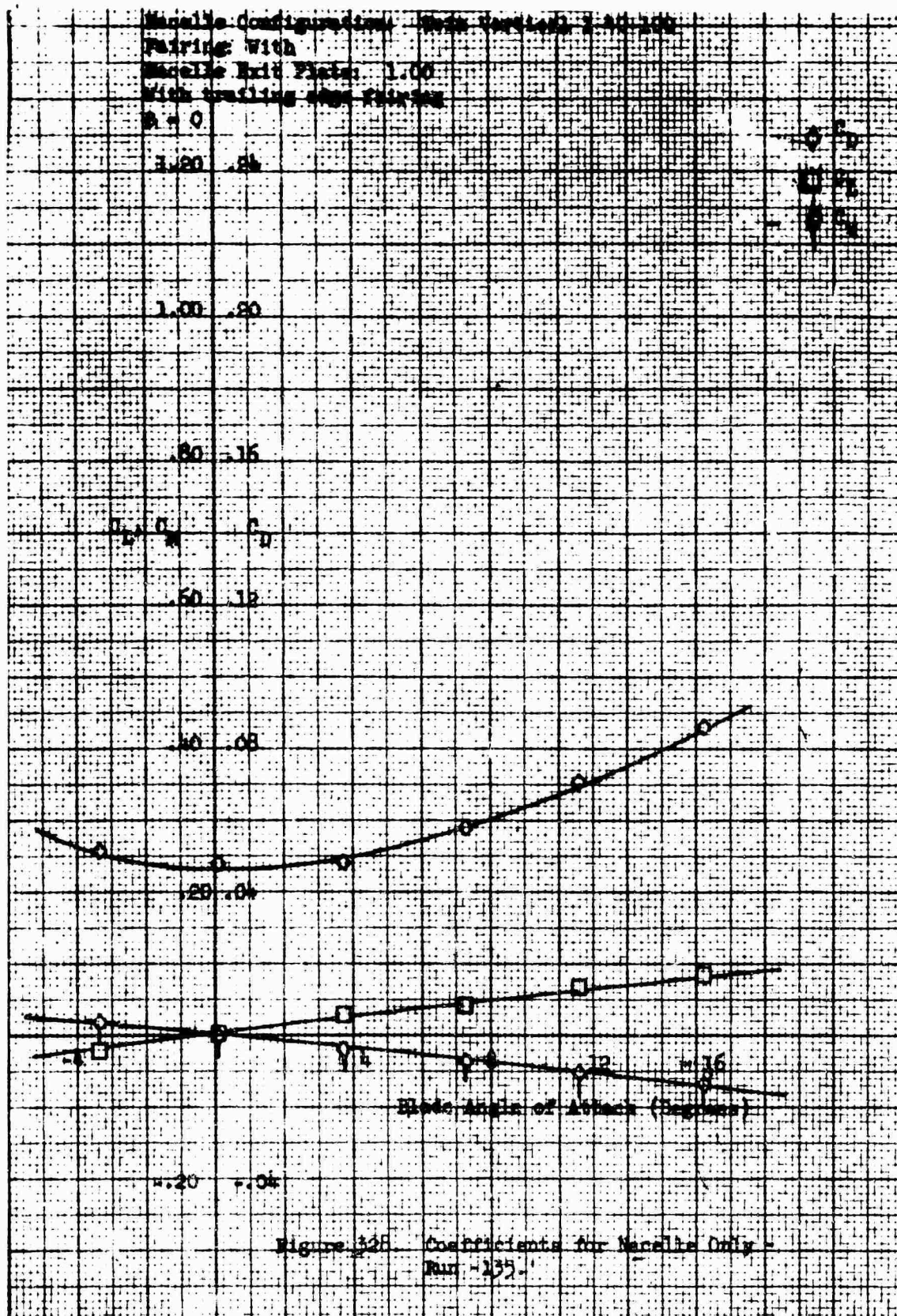
Nozzle Exit Plate: 1.00

$\beta = -10^\circ$









Macelle Configuration: With vertical 1-40-160
 Macelle Incidence Angle: 0°
 Fairing: With
 Macelle Exit Flare: 1.00
 With trailing edge Fairing
 $\beta = 0^\circ$
 1.20 - 24

C_L
 C_M
 C_D

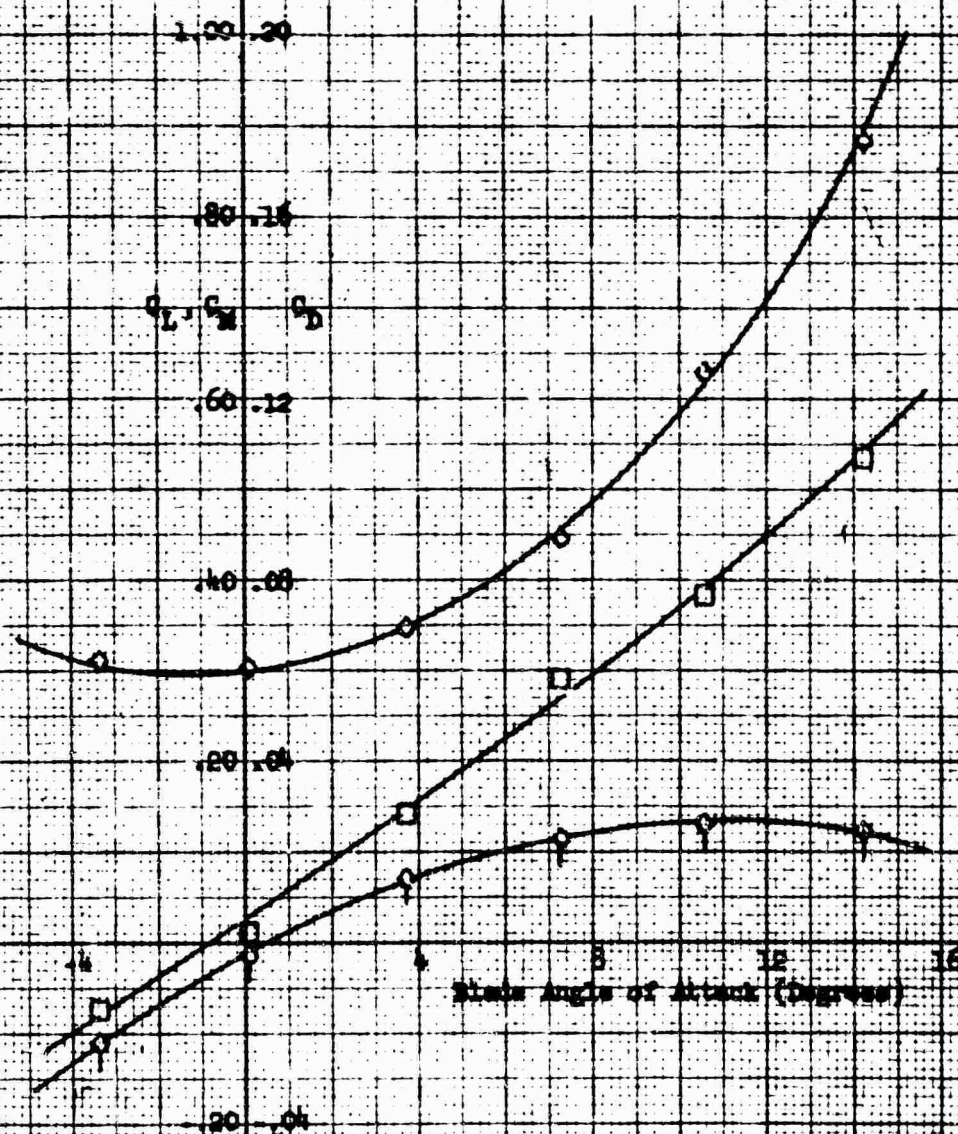


Figure 389. Coefficients for Combined Macelle and
 Blade - Run -135.

Exp. 1b Configuration: Body Vertical 1-40-300

Pairing: With

Maxella Exit Plate: 1.06

$\beta = 100$

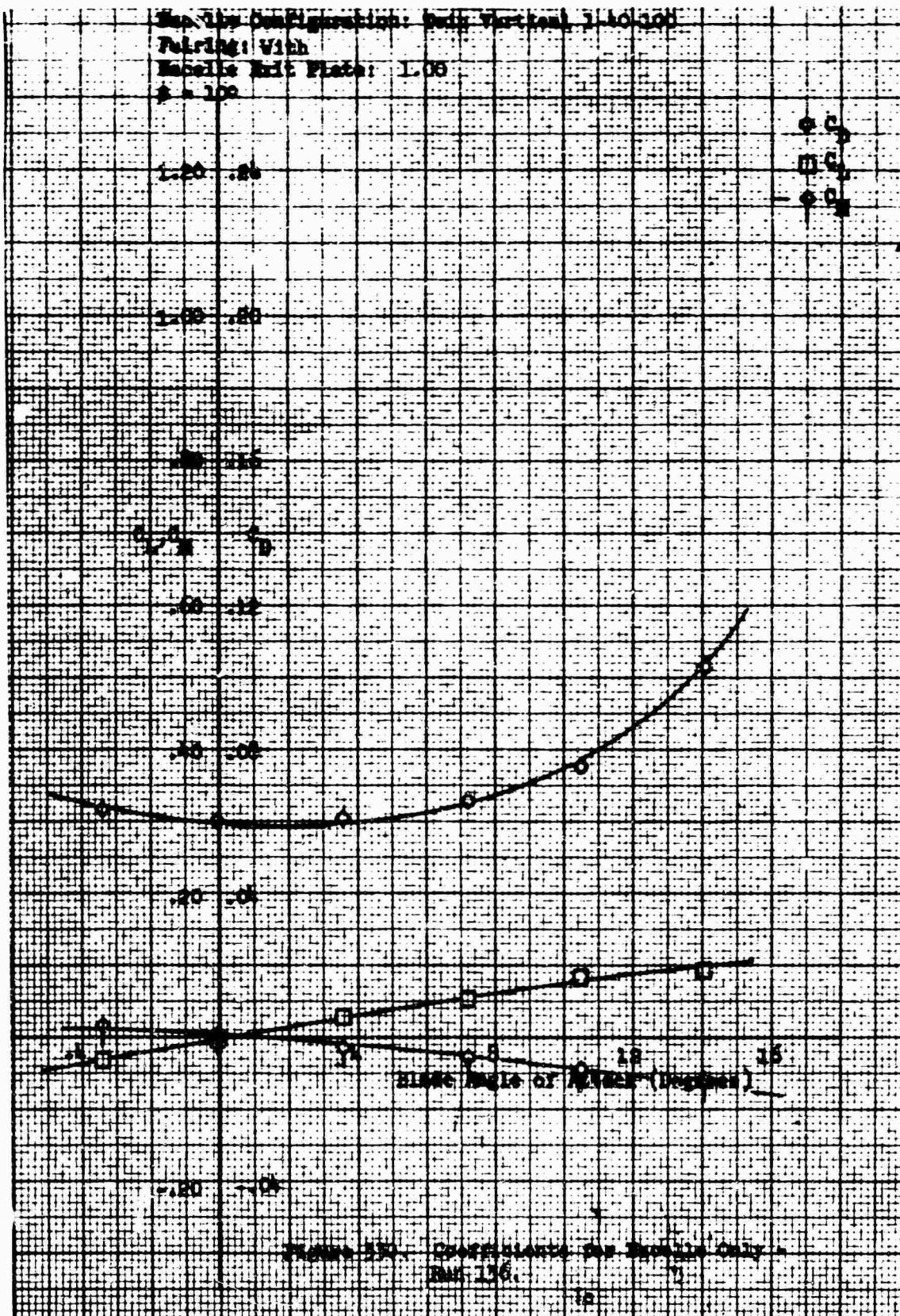


Figure 151. Coefficients for Body Vertical 1-40-300.

Blade Configuration: Semi-circular 1.00-1.00
 Blade Distance: Angle: 0°
 Fairing: With
 Blade Root Plate: 1.00
 $\beta = 10^\circ$

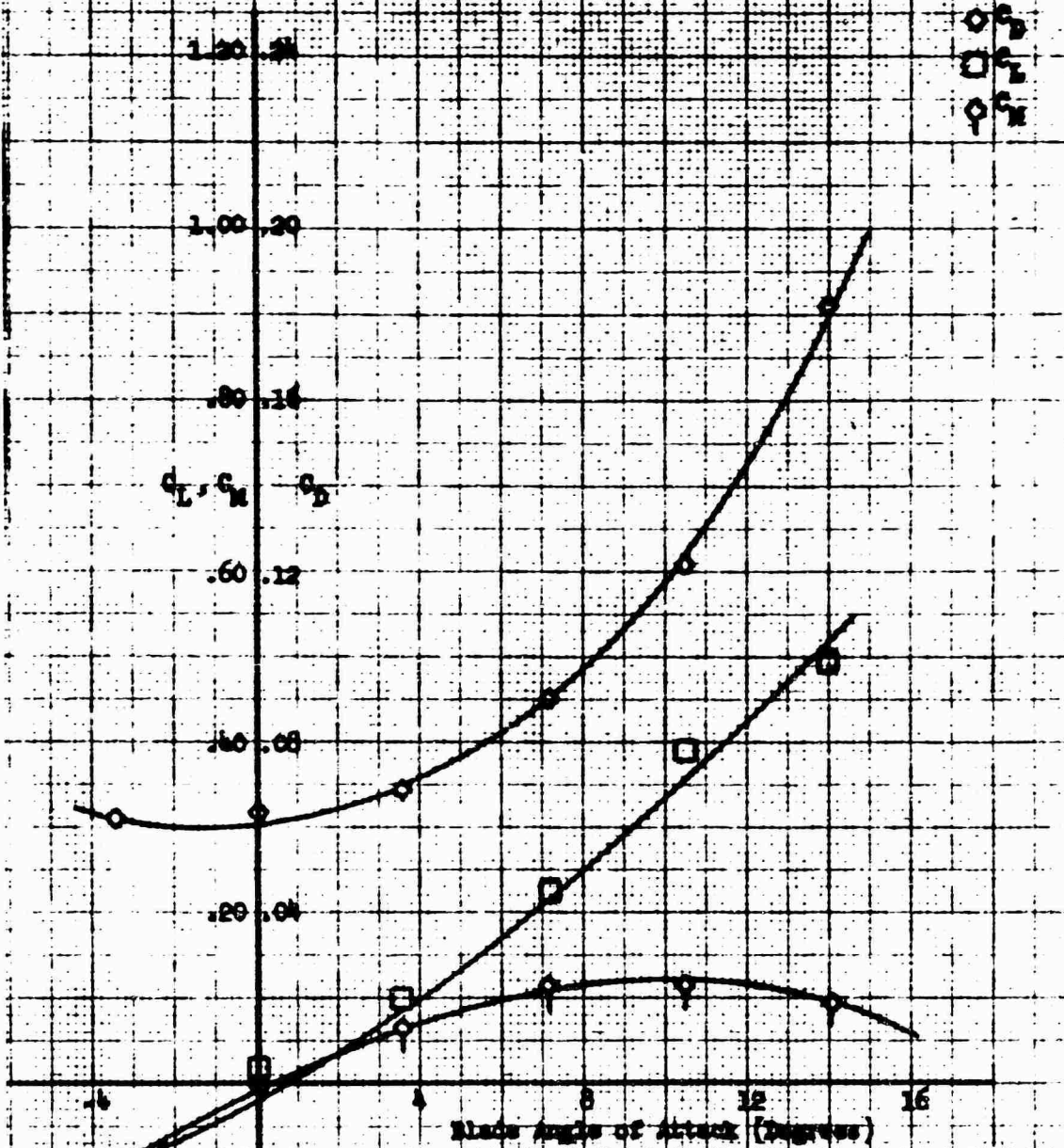


Figure 351. Coefficients for Combined Blade and
 Blade - Jan 1950

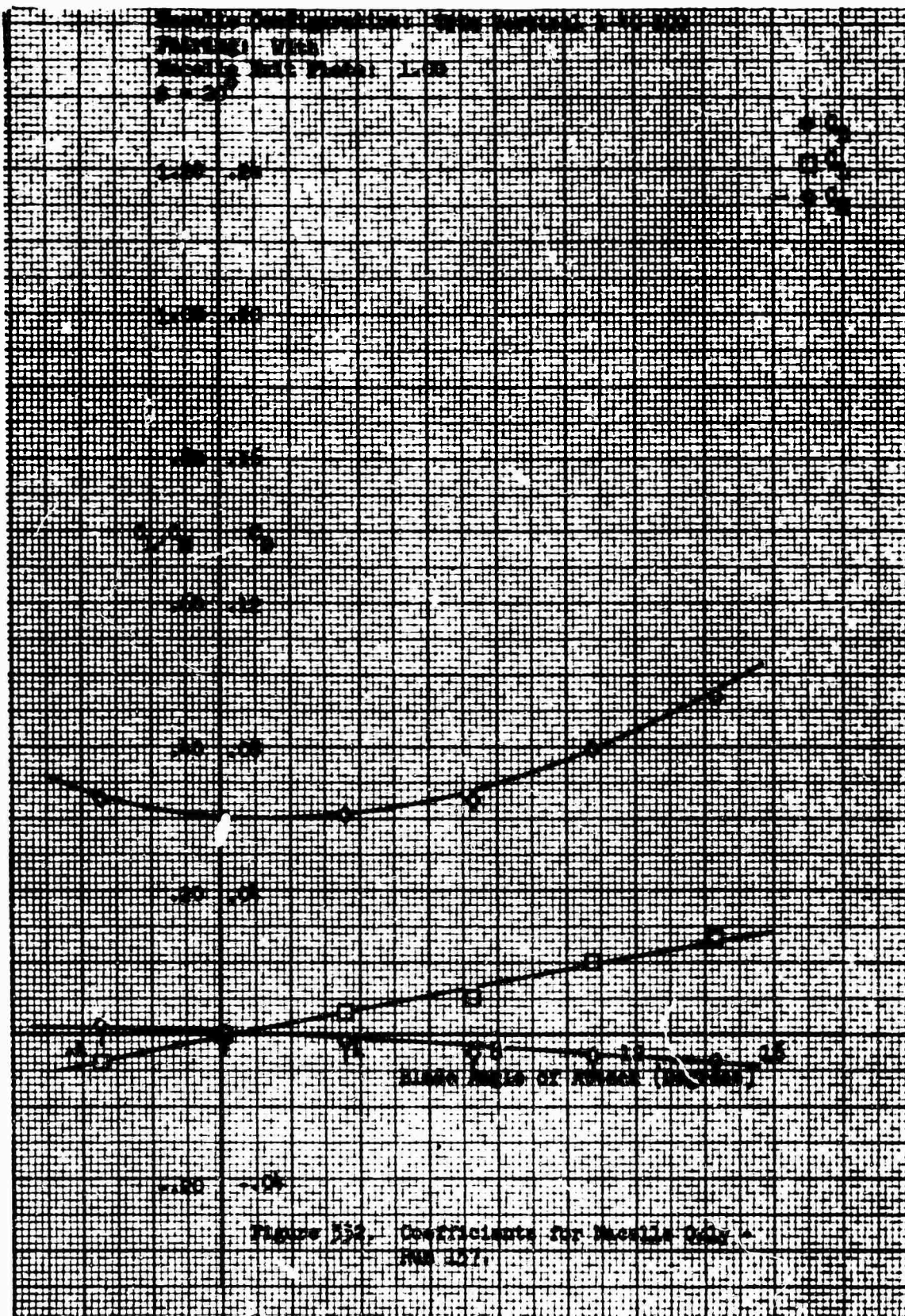
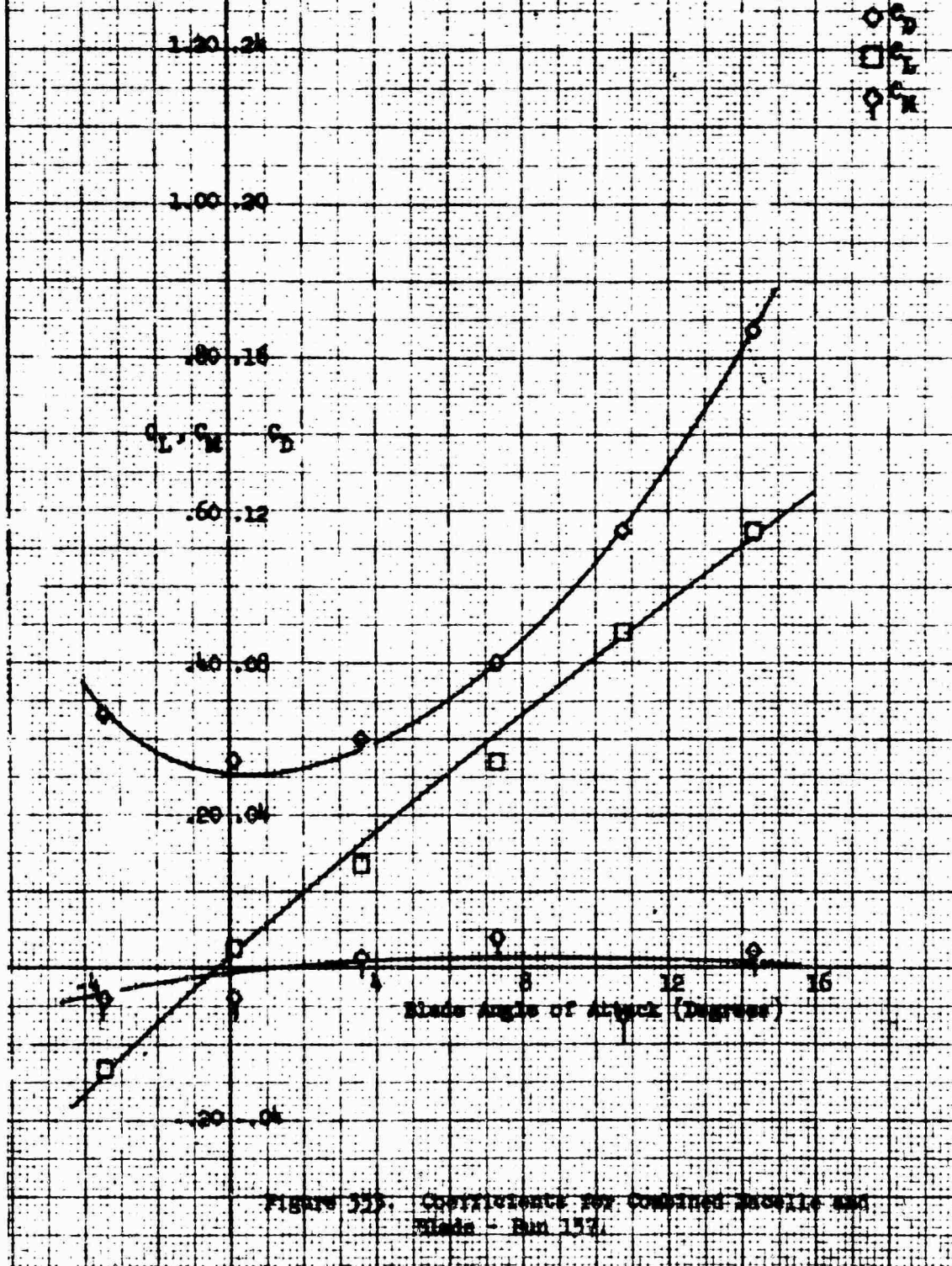
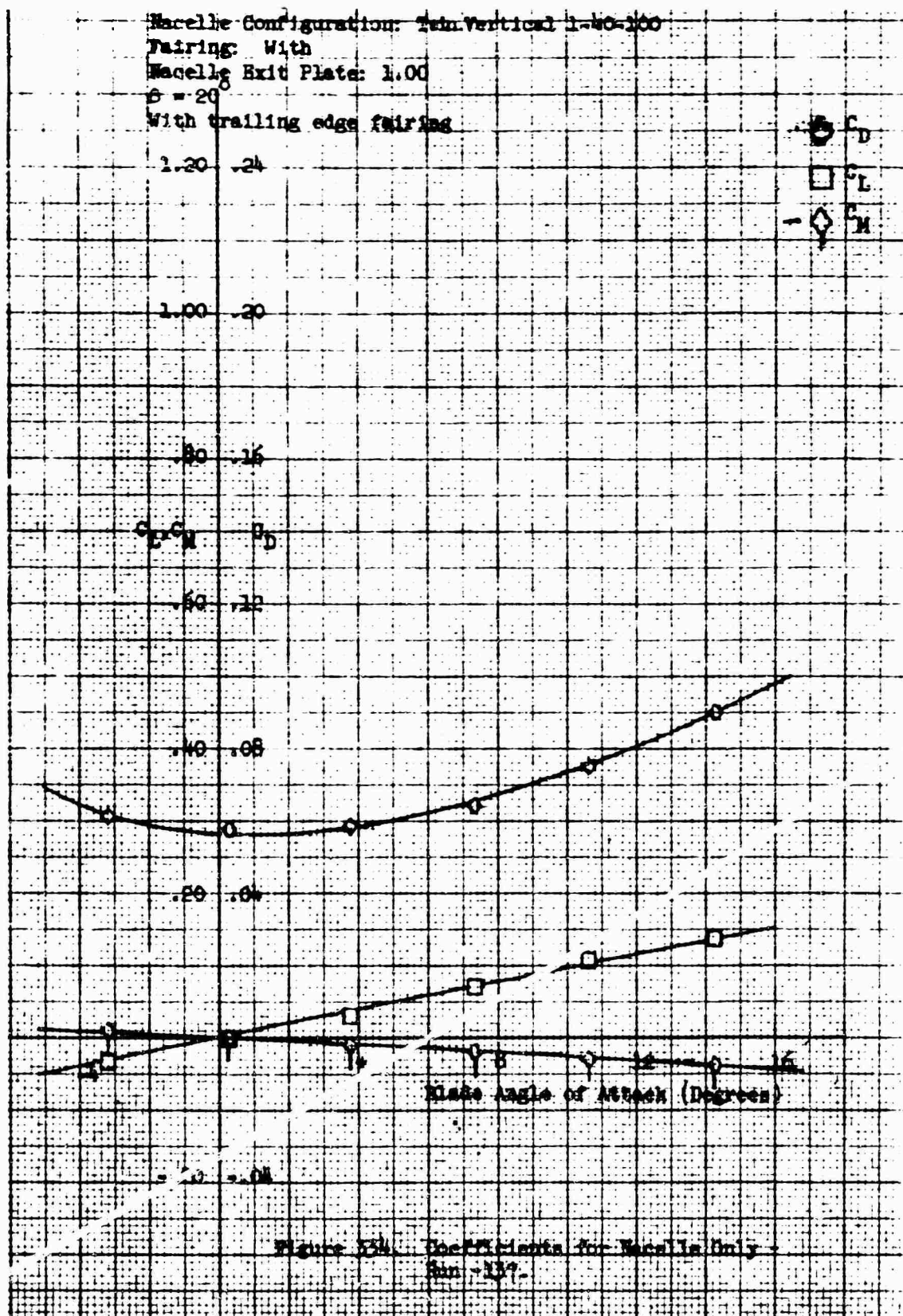


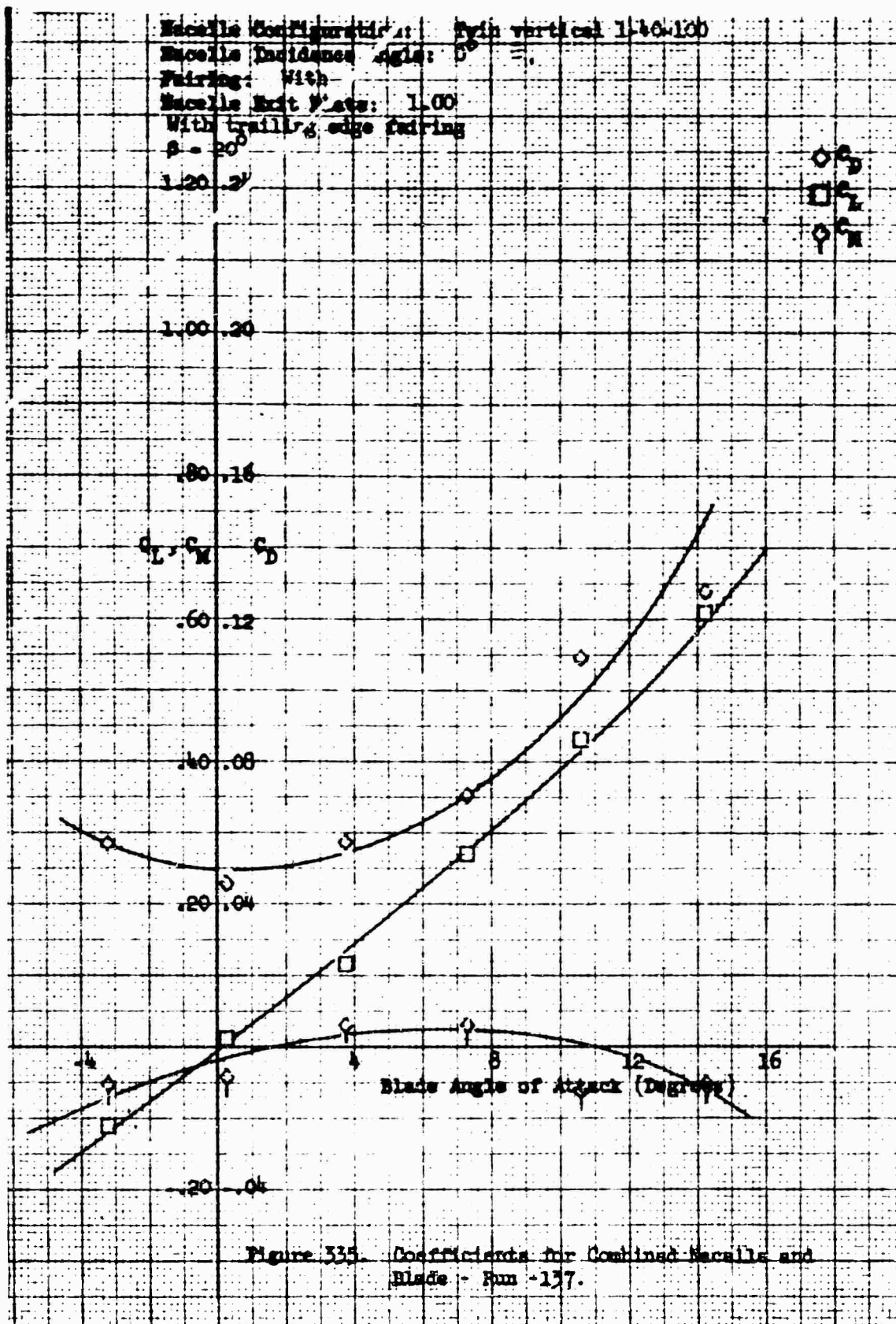
Figure 534. Coefficients for Nozzle 200.
 Run 157.

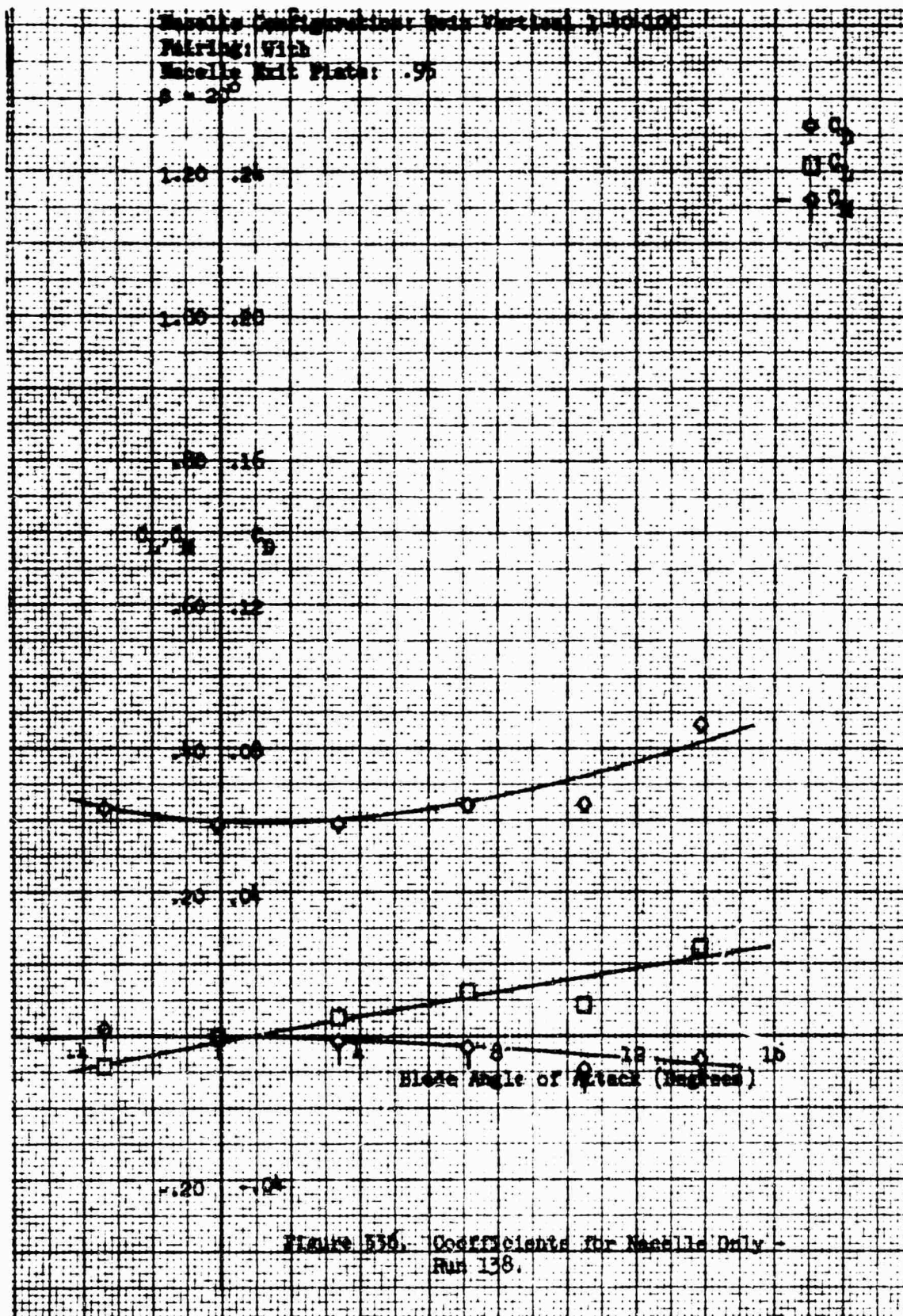
Macelle Configuration: Tyin vertical 1-40-100
 Macelle Incidence Angle: 0°
 Firing: With
 Macelle Exit Plate: 1.00
 $\beta = 20^\circ$



Macelle Configuration: Thin Vertical 1-40-200
 Fairing: With
 Macelle Exit Plate: 1.00
 $\phi = 20^\circ$
 With trailing edge fairing







Macelle Configuration: Twin vertical 1-40-100
 Macelle Incidence Angle: 0°
 Pairing: With
 Macelle Exit Plate: .95
 $\beta = 20^\circ$

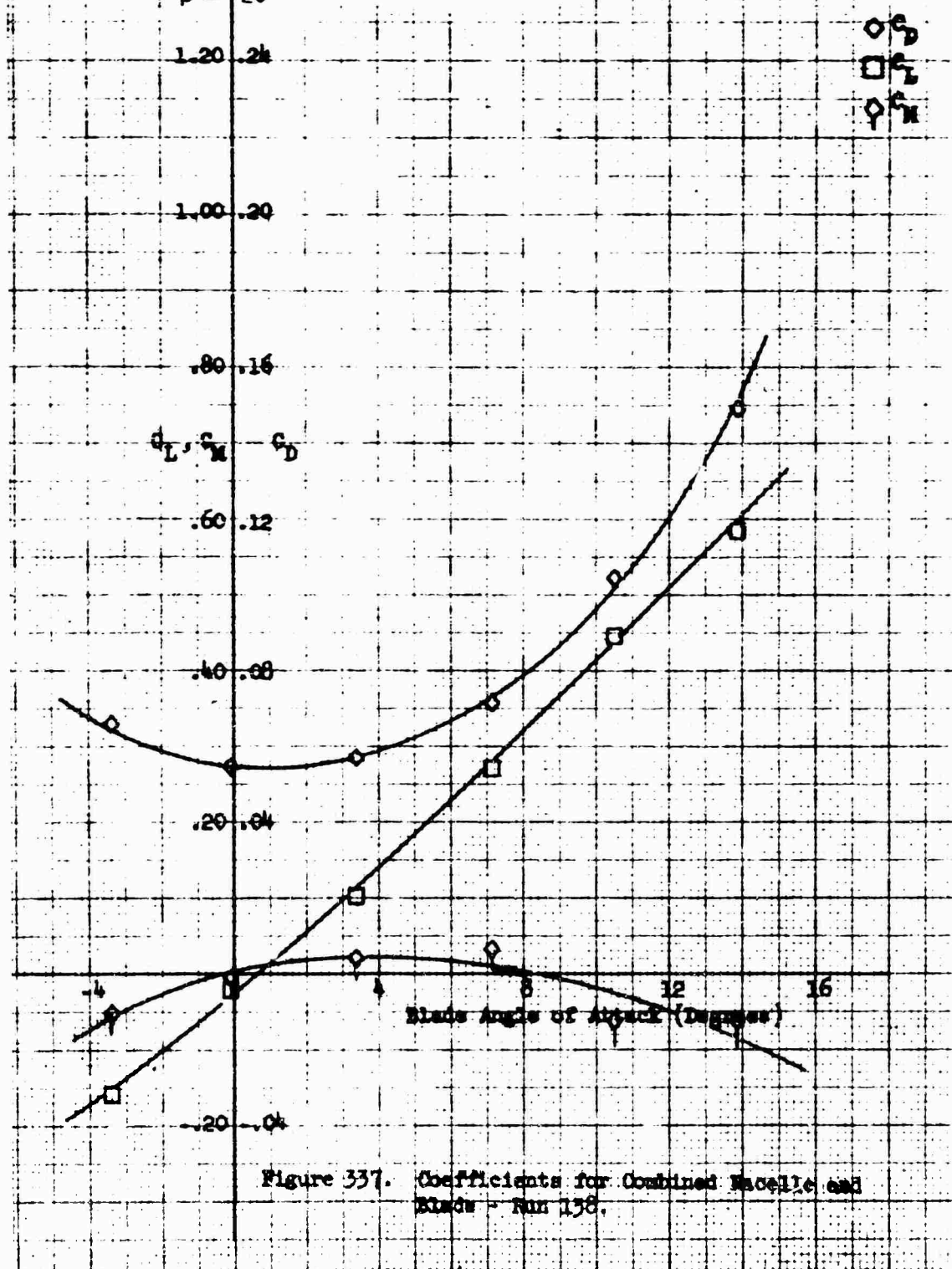


Figure 337. Coefficients for Combined Macelle and Blade - Run 138.

Nozzle Configuration: Twin Vertical 1-40-150
 Pairing: With
 Nozzle Exit Plate: .95
 $\alpha = 10^\circ$

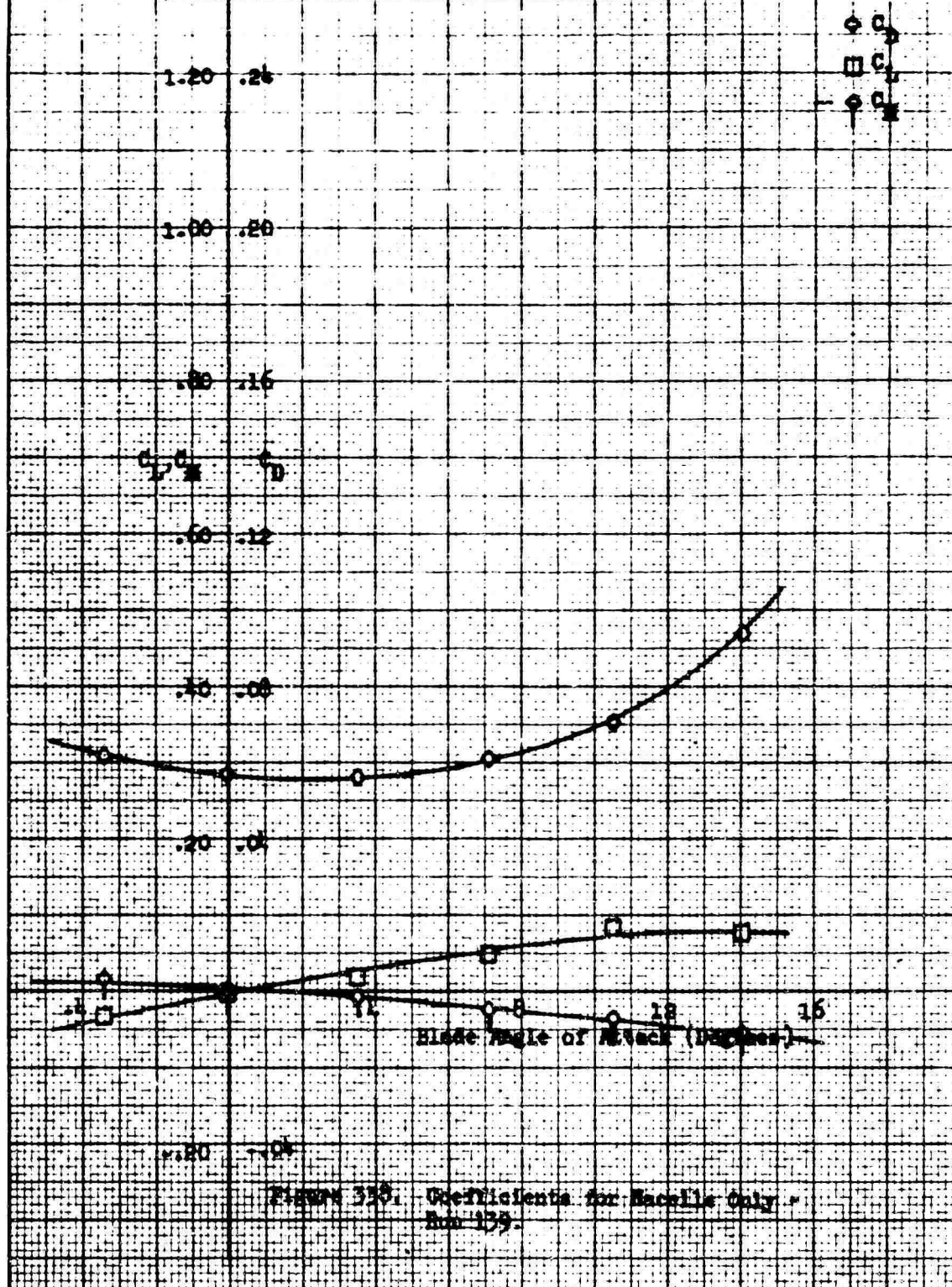


Figure 330. Coefficients for Nozzle Only -
 Run 139.

Macelle Configuration: Twin vertical 1-40-100
 Macelle Incidence Angle: 0°
 Pairing: With
 Macelle Exit Plate: .95
 $\beta = 10^\circ$

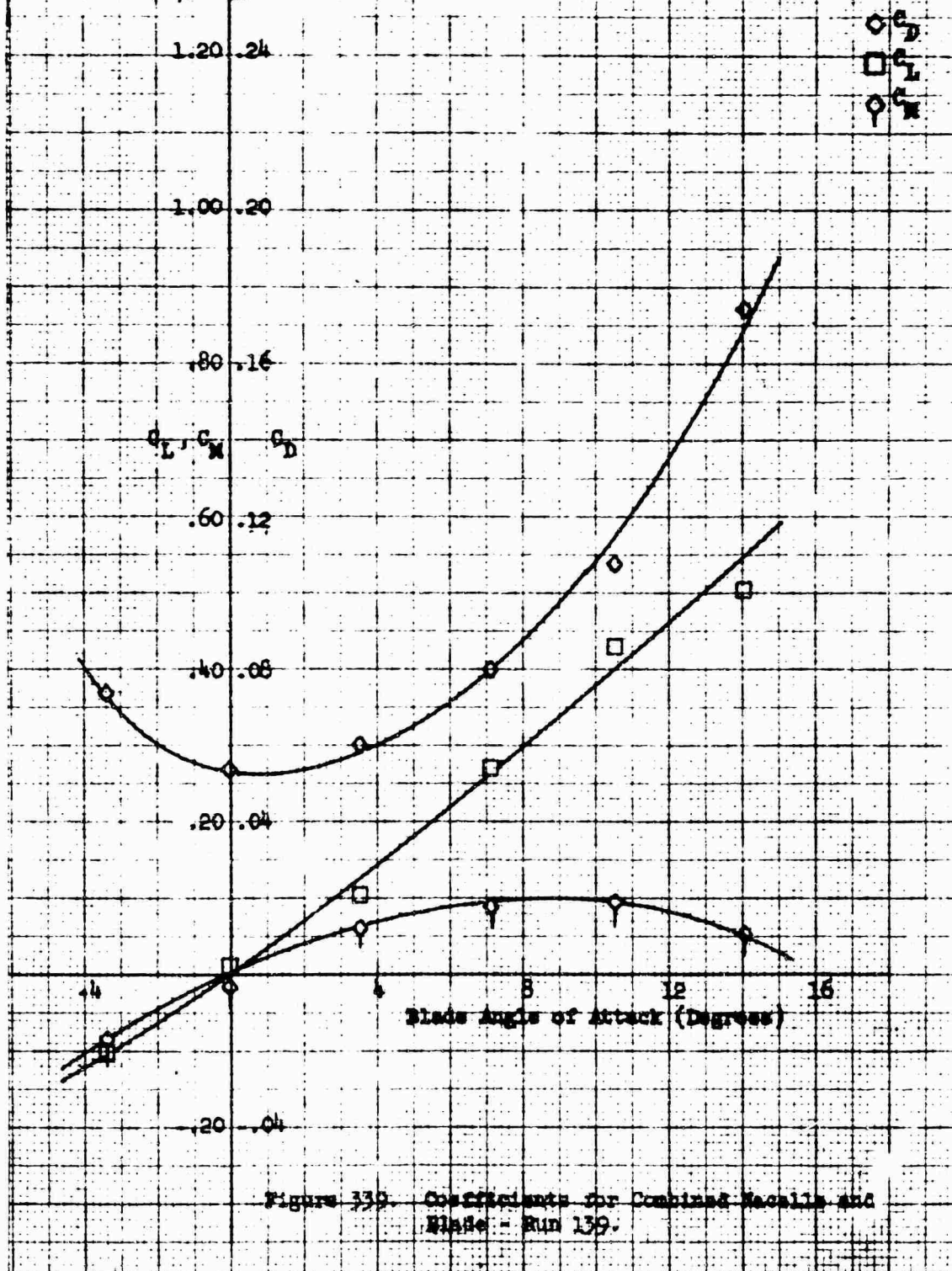
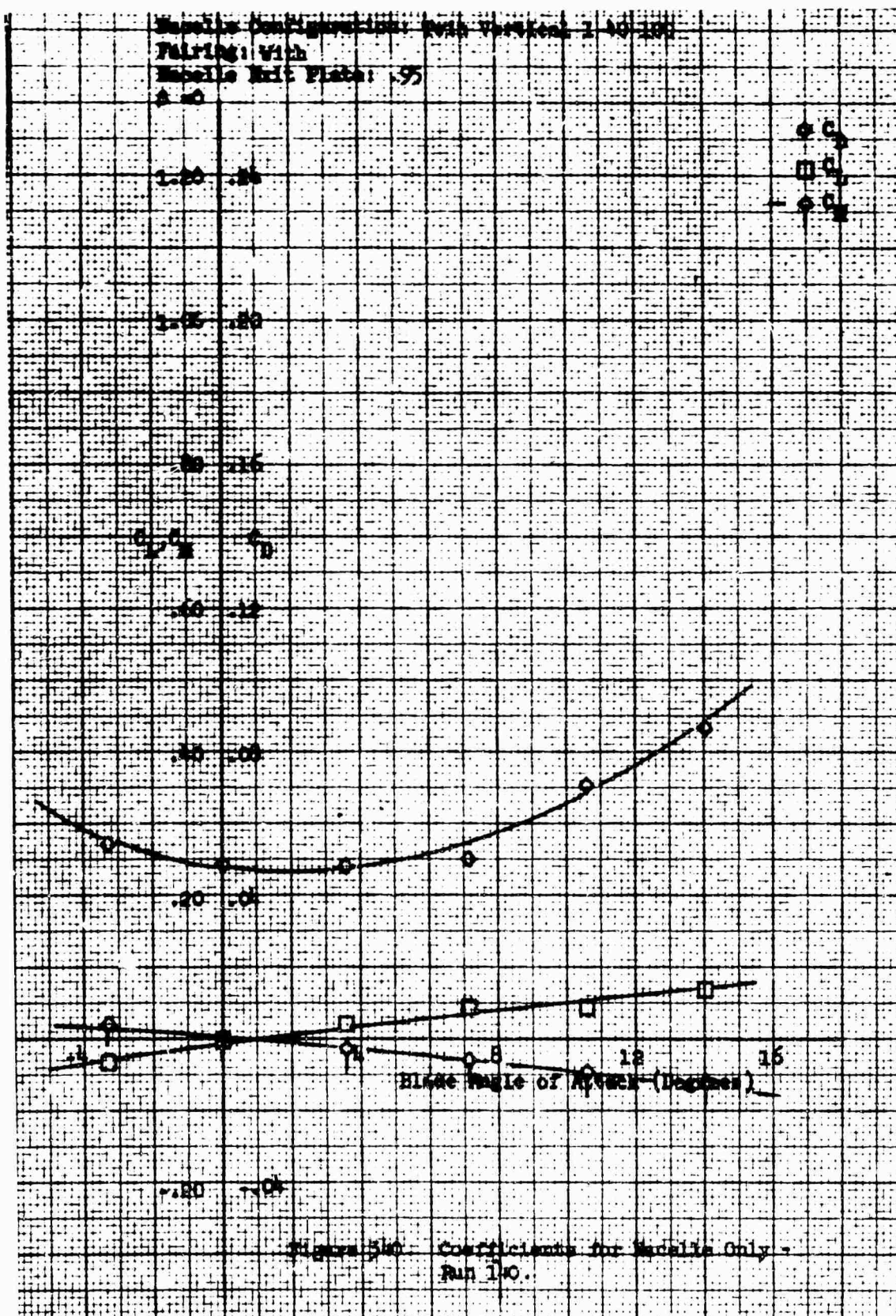


Figure 339. Coefficients for Combined Macelle and Blade - Run 139.



Macelle Configuration: Twin vertical 1-10-100

Macelle Incidence Angle: 0°

Firing: With

Macelle Exit Plate: .95

$\beta = 0$

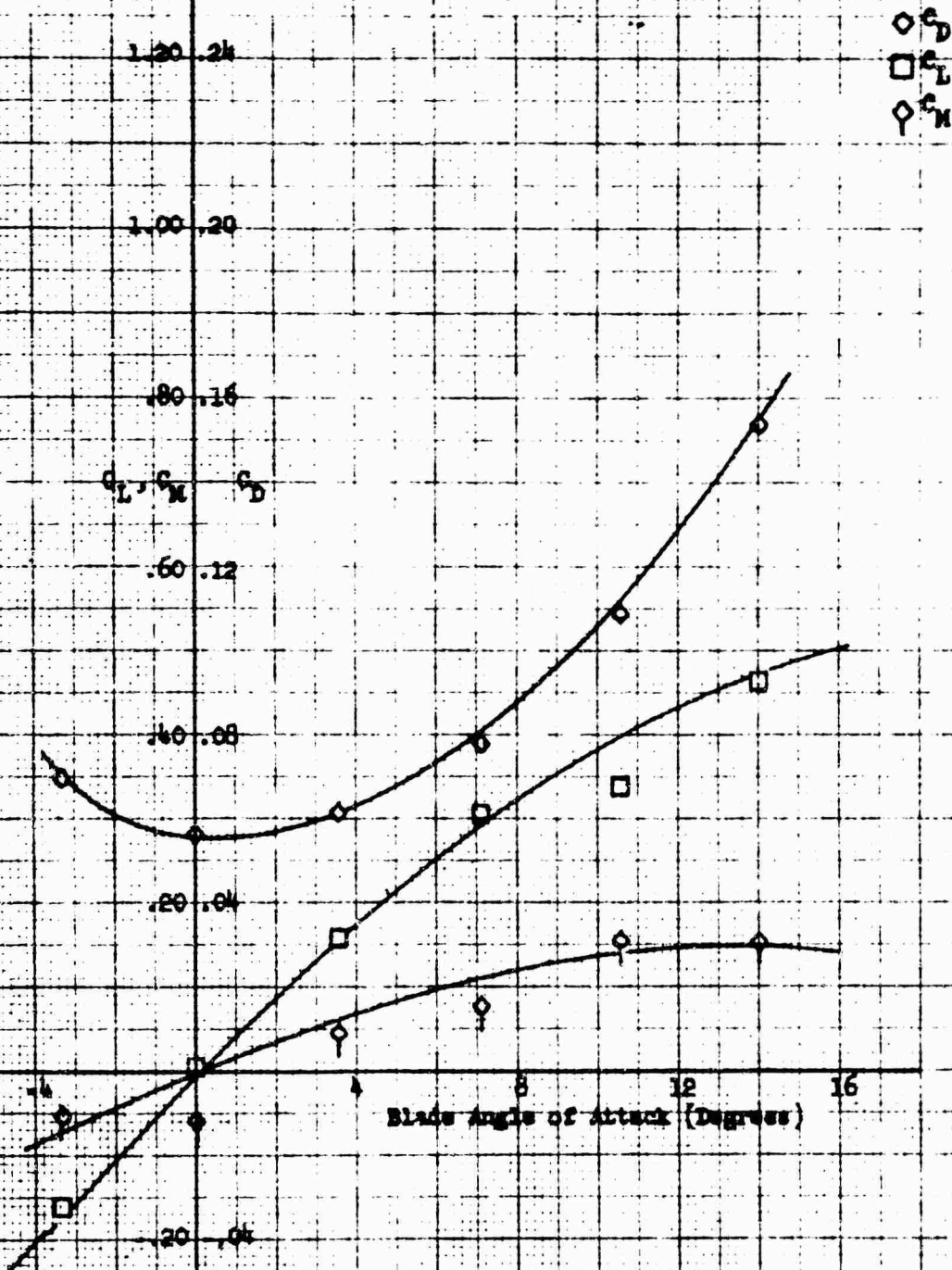


Figure 34. Coefficients for Combined Macelle and Blade - Run 140.

Nozzle Configuration: Twin Venturi Type 100
 Fueling: Visk
 Nozzle Exit Plane: .95
 $\theta = 10^\circ$

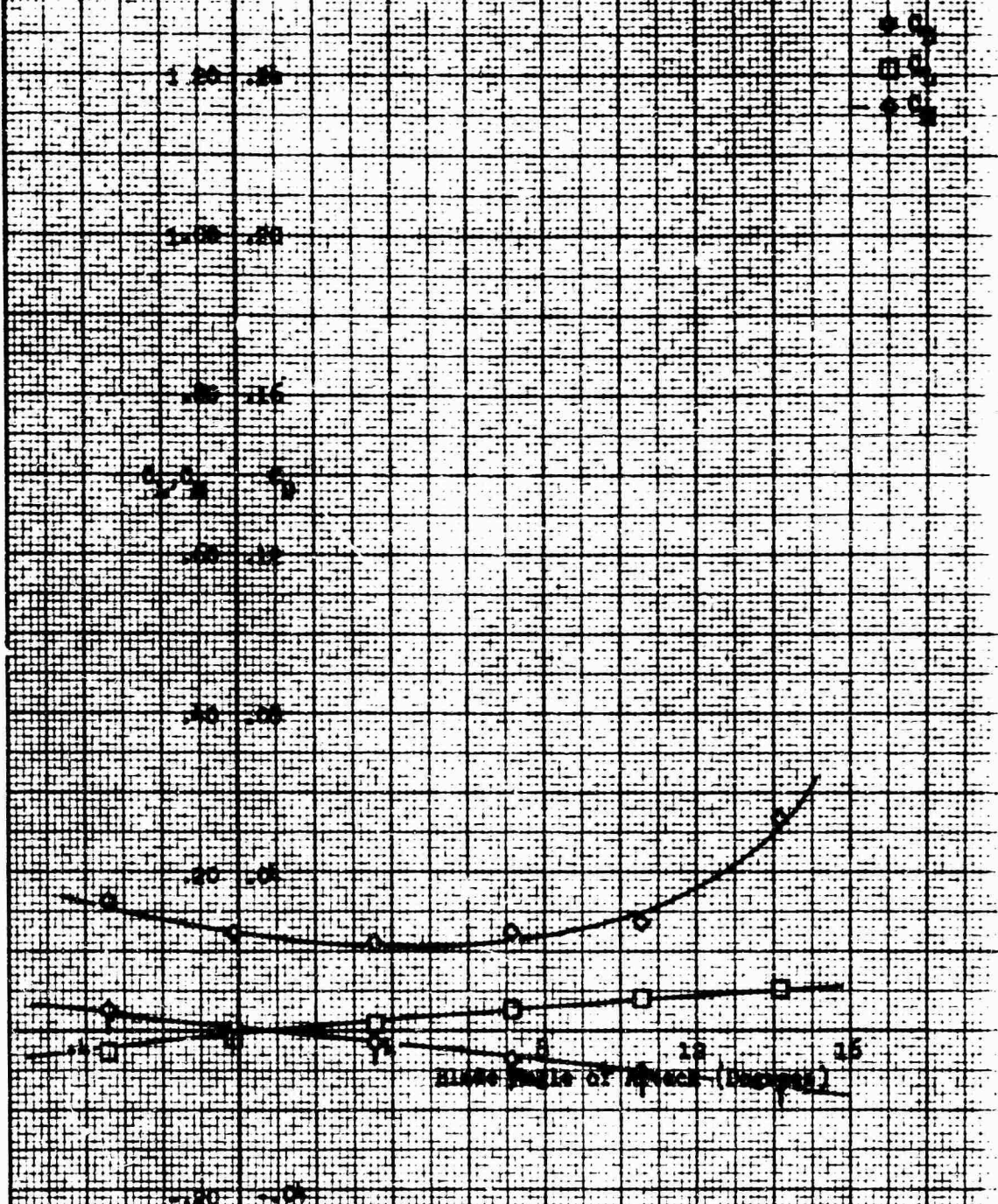


Figure 342- Coefficients for Nozzle Only -
 Run 141.

Nacelle Configuration: Twin vertical 1-40-100

Nacelle Incidence Angle: 0°

Pairing: With

Nacelle Exit Plate: .95

$\beta = 10^\circ$

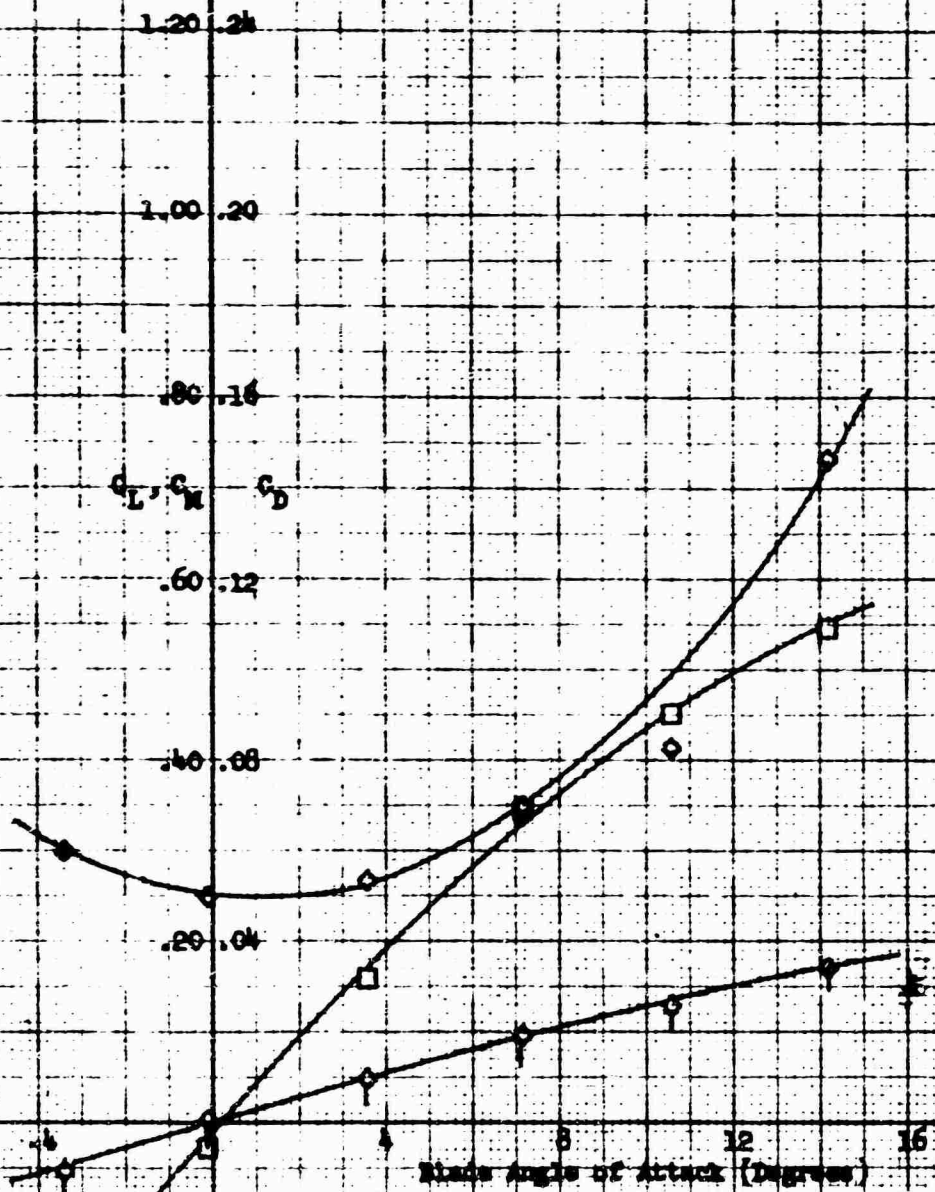
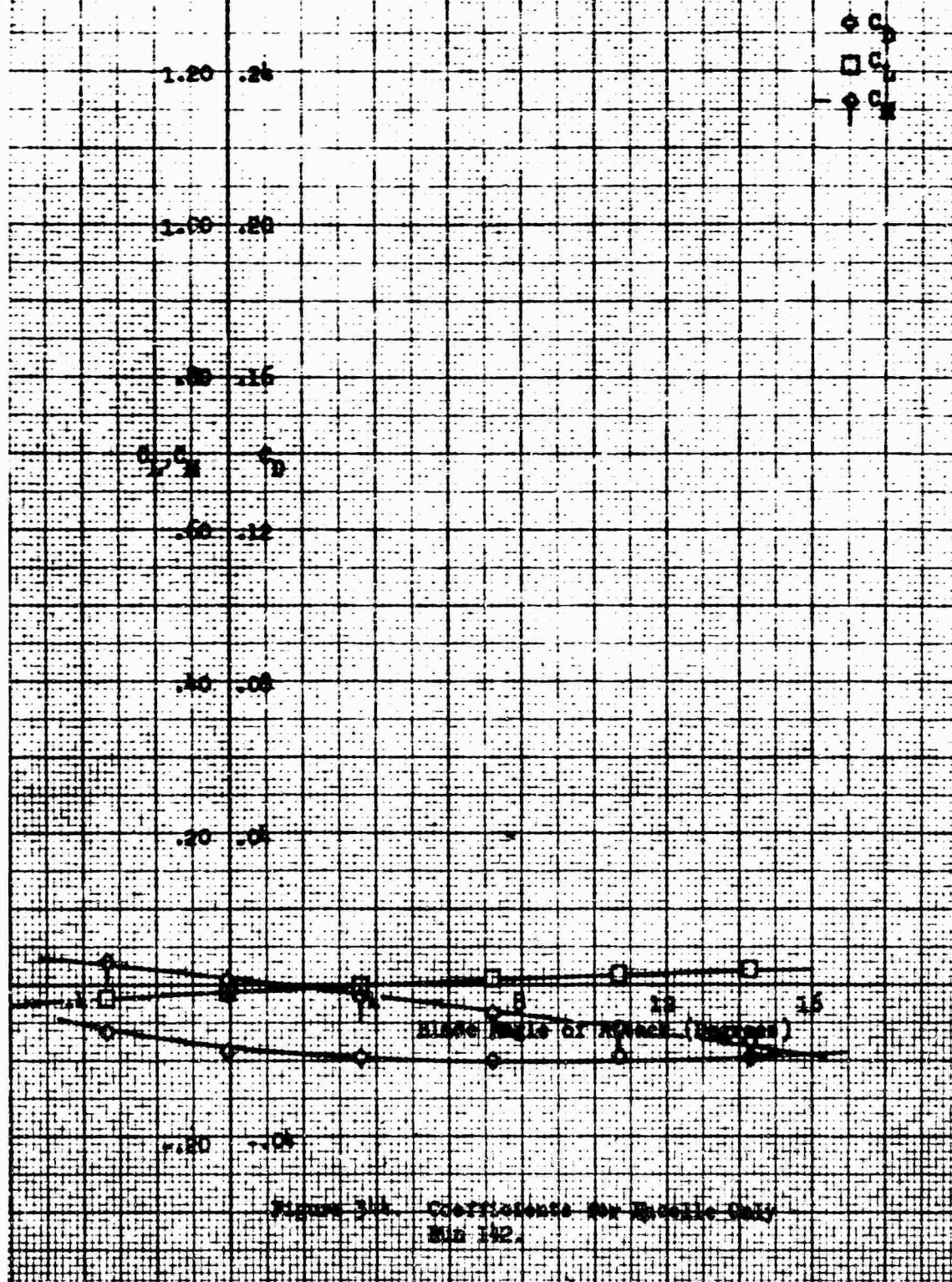


Figure 343. Coefficients for Combined Nacelle and Blade - Run 141.

Missile Configuration: Twin Vertical 1-40-100
 Pairing: With
 Missile Exit Plate: .95
 $\theta = -20^\circ$



Macelle Configuration: Twin vertical 1.40-100
 Macelle Incidence Angle: 0°
 Fairing: With
 Macelle Exit Plate: .95
 $\beta = 20^\circ$

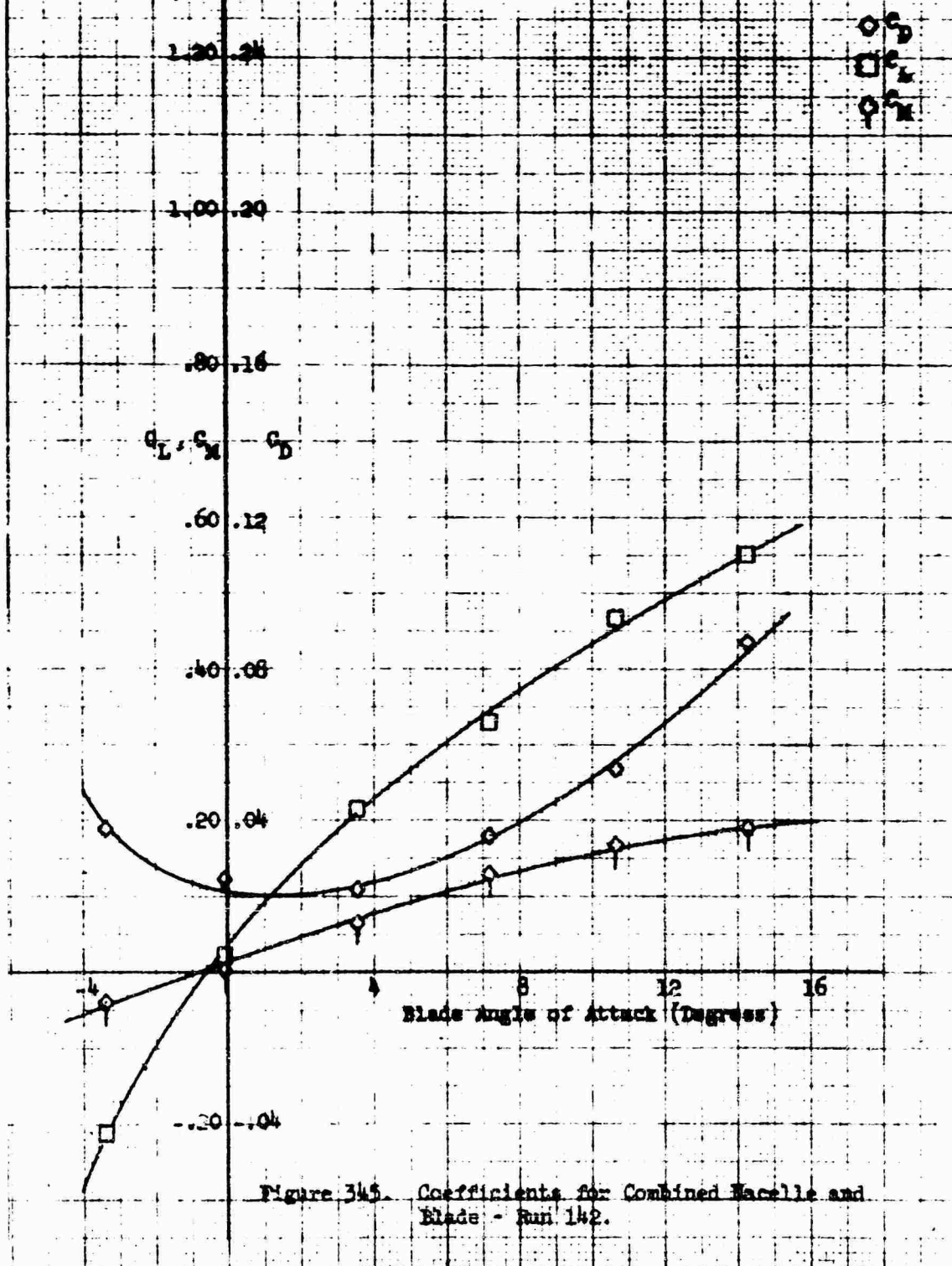
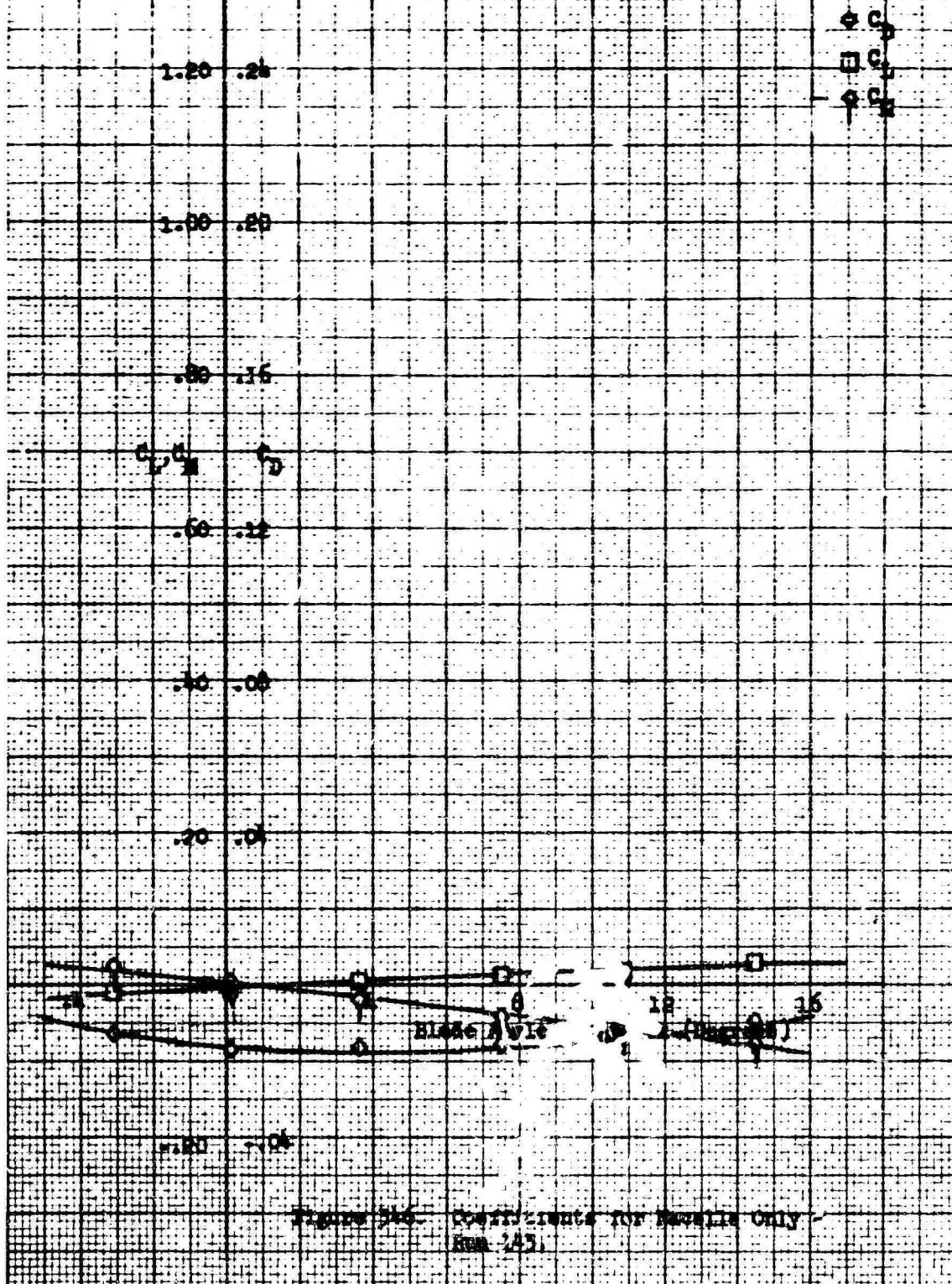


Figure 345. Coefficients for Combined Macelle and Blade - Run 142.

Run No.: 143
 Missile Configuration: Twin Vertical 1.480.300
 Fairing: With
 Missile Exit Plate: .95
 $\beta = -200$



Macelle Configuration: Twin vertical 1-40-100
 Macelle Incidence Angle: 0°
 Pairing: With
 Macelle Exit Plate: .95
 $\beta = -20^\circ$

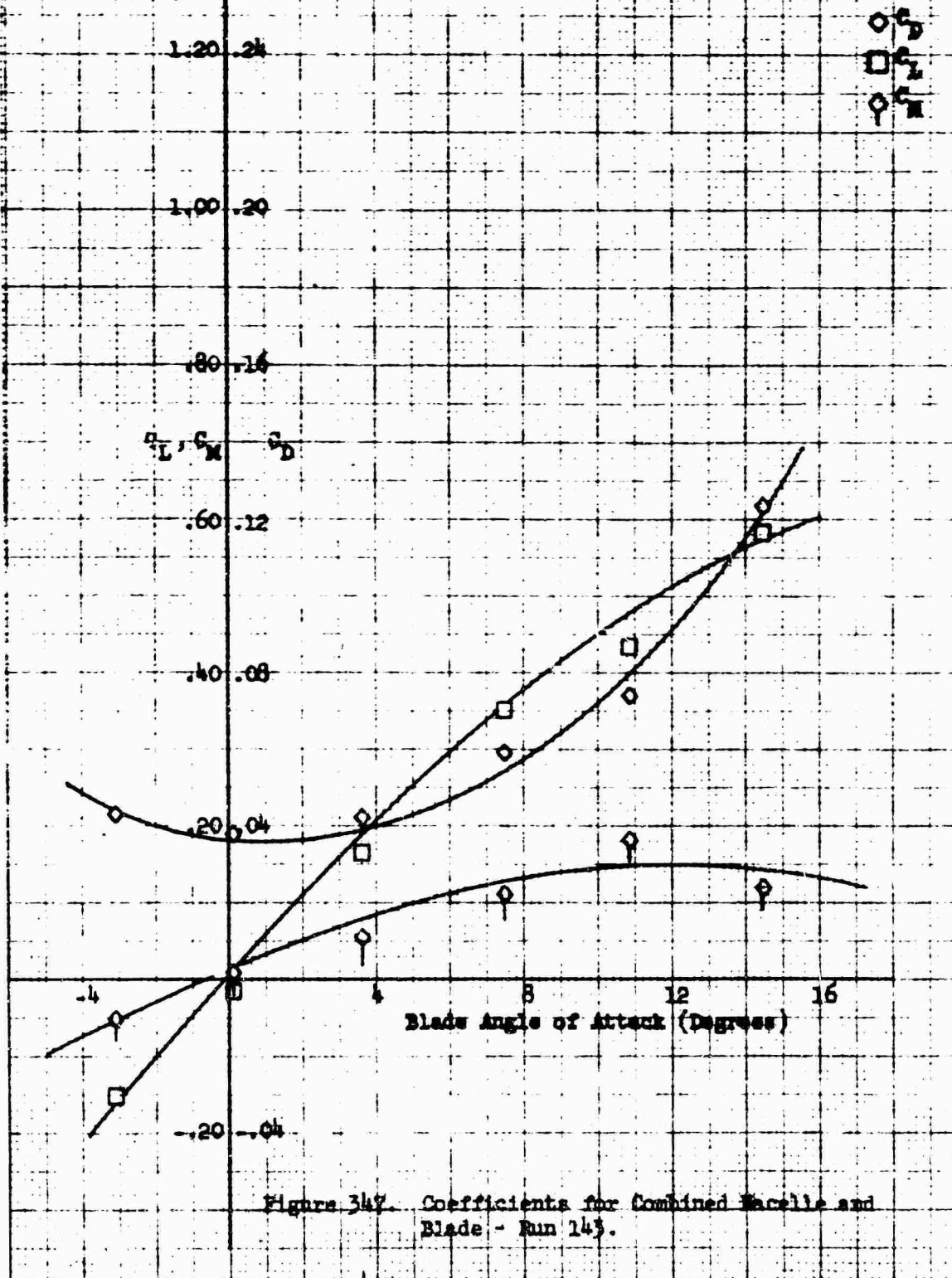
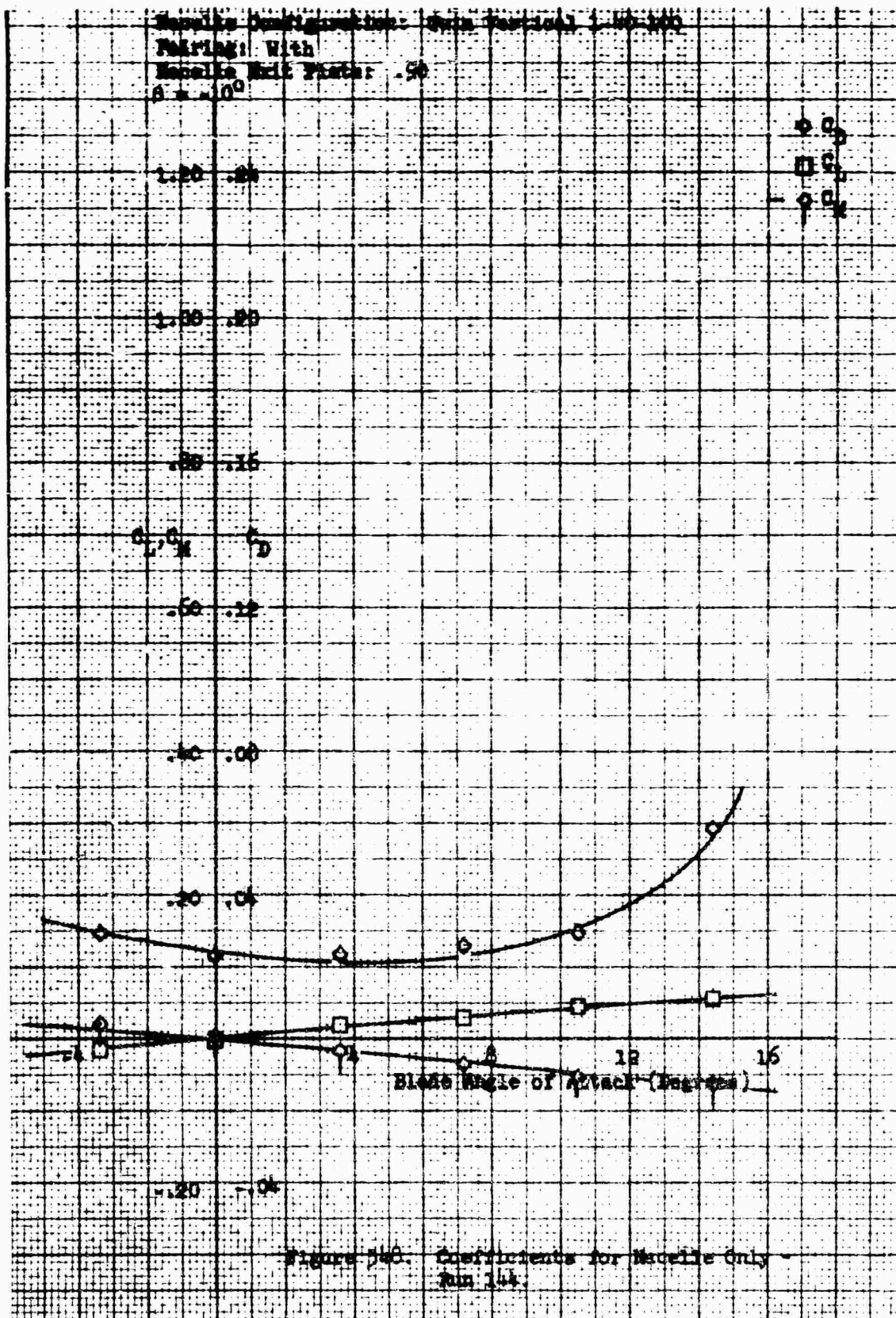


Figure 347. Coefficients for Combined Macelle and Blade - Run 143.



Wacelle Configuration: Twin vertical 1-40-100

Wacelle Incidence Angle: 0°

Fairing: With

Wacelle Exit Plate: .90

$\beta = -10^\circ$

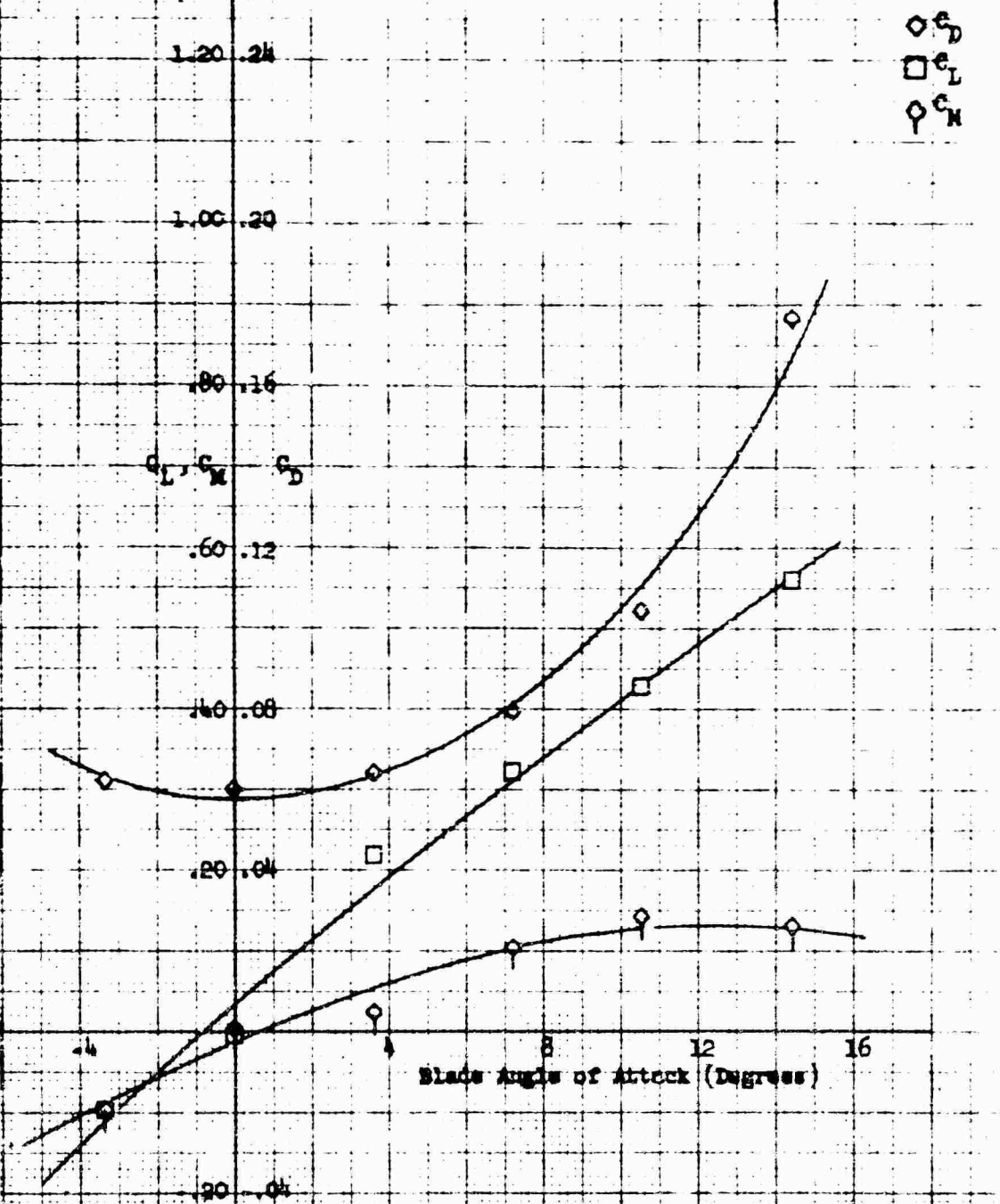


Figure 349 Coefficients for Combined Wacelle and Blade - Run 144.

Macelle Configuration: Twin Vertical 1-40-100

Fairing: With

Macelle Exit Plate: .90

$\beta = 0$

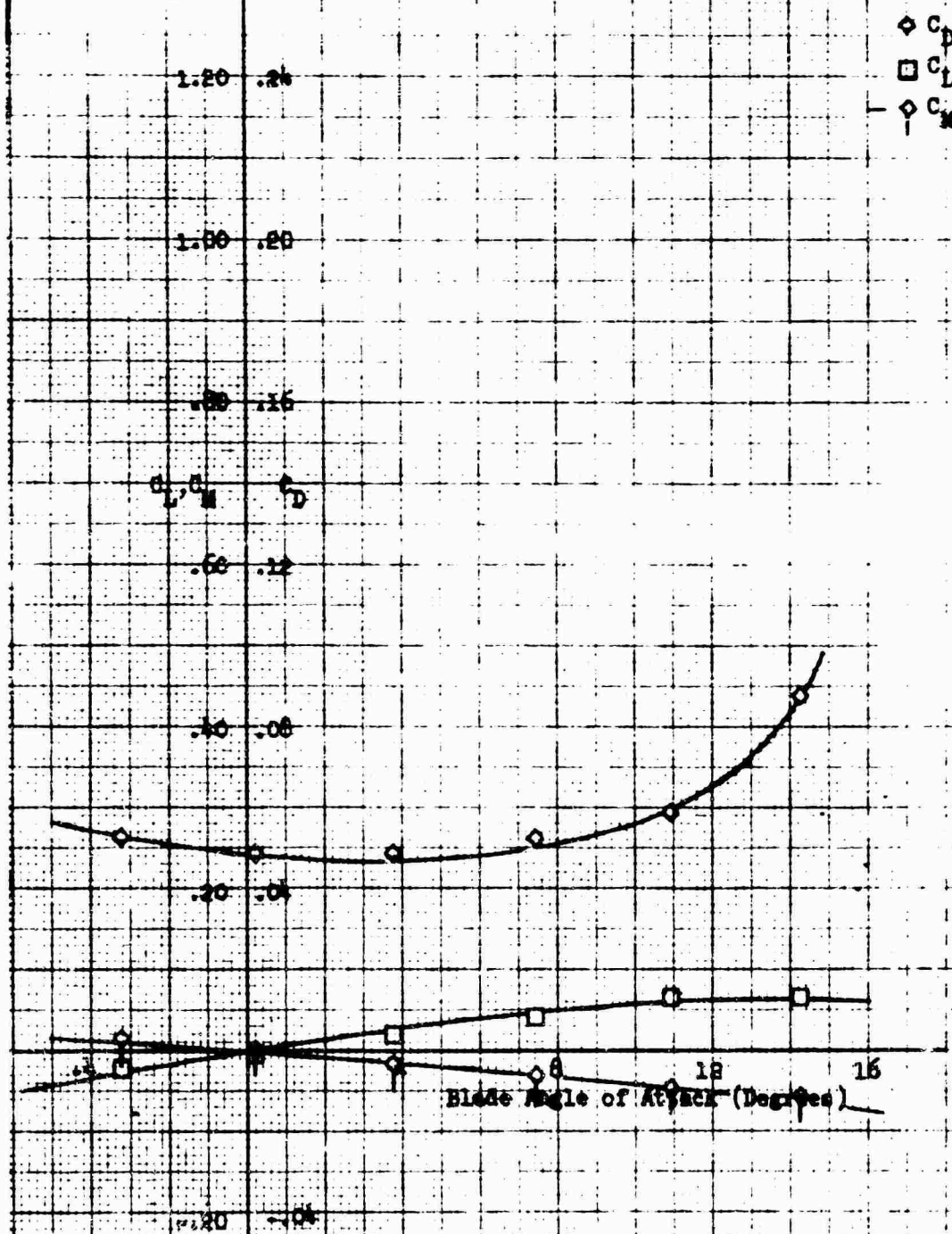


Figure 350. Coefficients for Macelle Only -
Run 145.

Macelle Configuration: Twin vertical 1-40-100
 Macelle Incidence Angle: 0°
 Fairing: With
 Macelle Exit Plate: .90
 $\beta = 0$

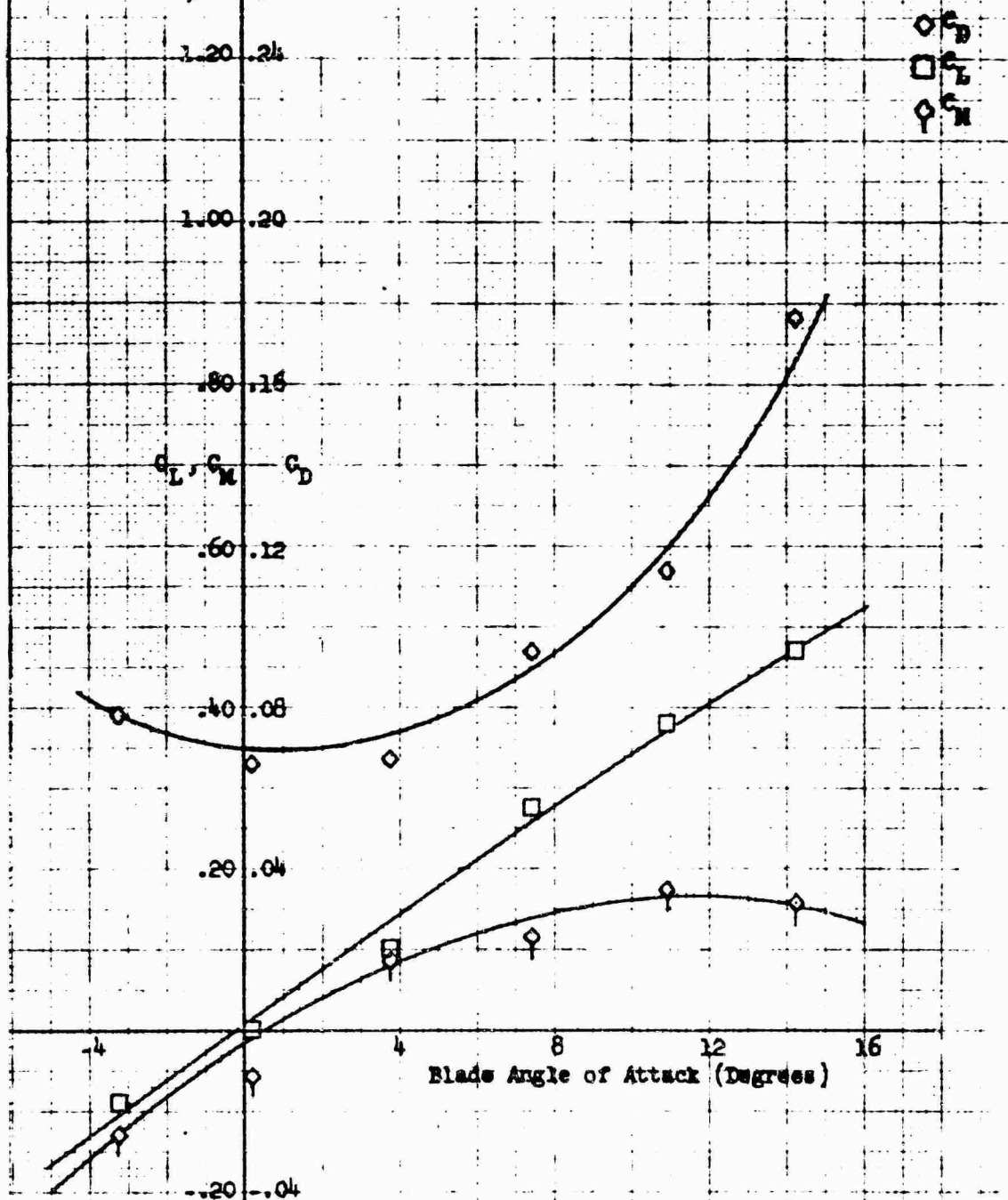


Figure 351. Coefficients for Combined Macelle and Blade - Run 145.

Missile Configuration: Spin Vertical 1.45-1.55
 Pairing: With
 Missile Exit Plate: .90
 S = 10

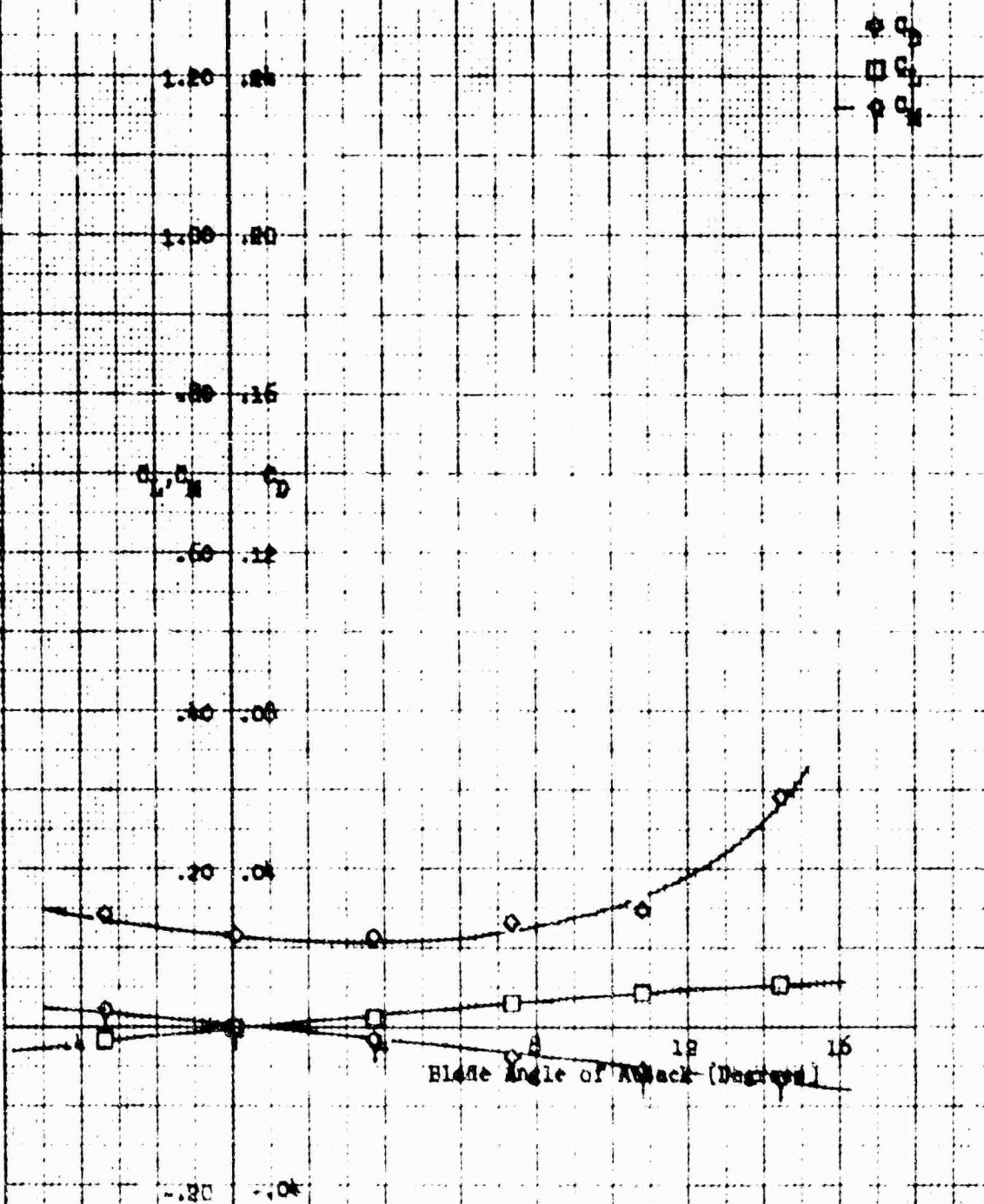


FIGURE 157. COEFFICIENTS FOR MISSILE ONLY -
 Run 146.

Nacelle Configuration: Twin vertical 1-40-100

Nacelle Incidence Angle: 0°

Fairing: With

Nacelle Exit Plate: .90

$\beta = 10^\circ$

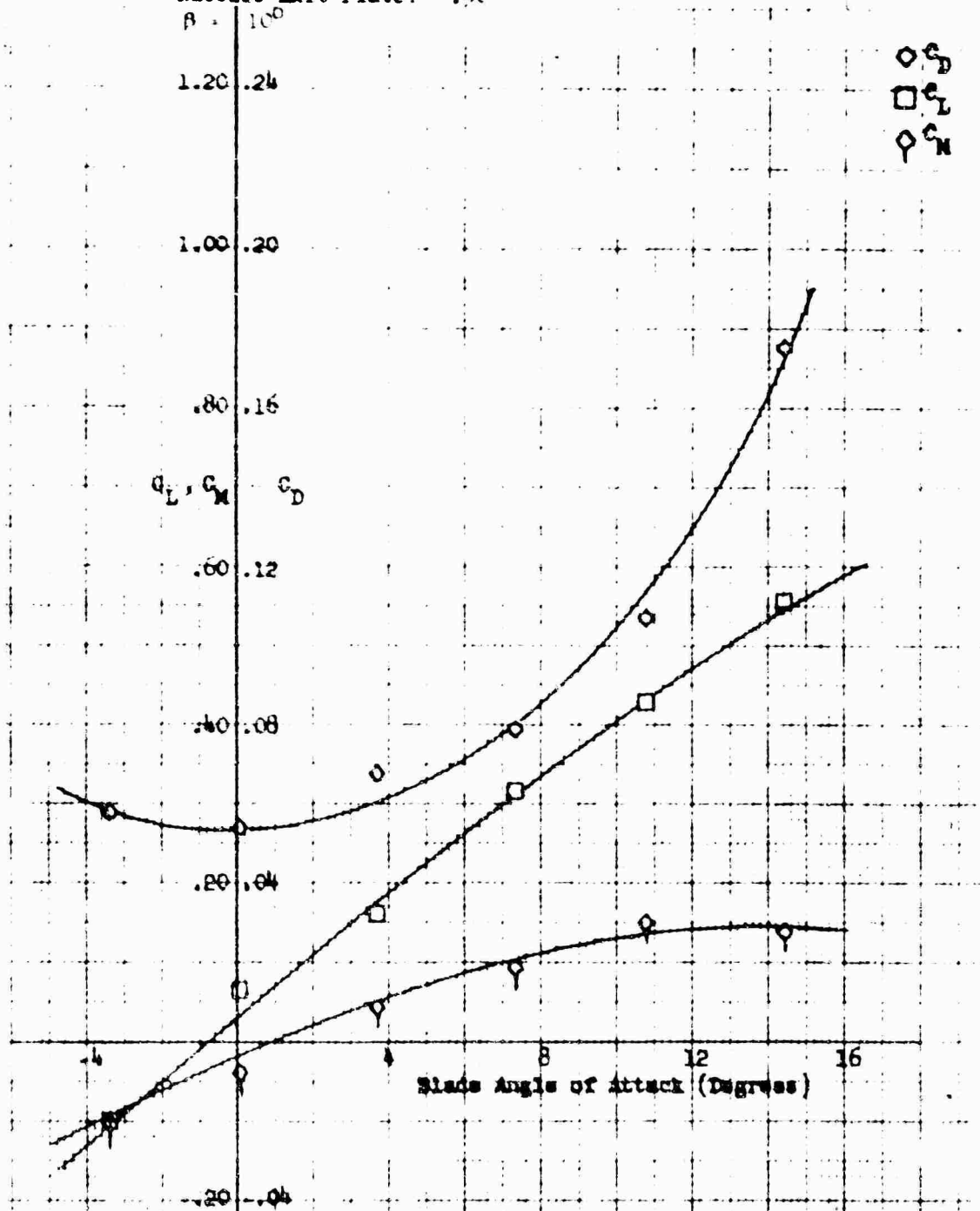


Figure 553. Coefficients for Combined Nacelle and Blade - Run 146.

Macelle Configuration: Twin Vertical 1.40-1.60
 Pairing: With
 Macelle Exit Plate: .90
 $\beta = 20^\circ$

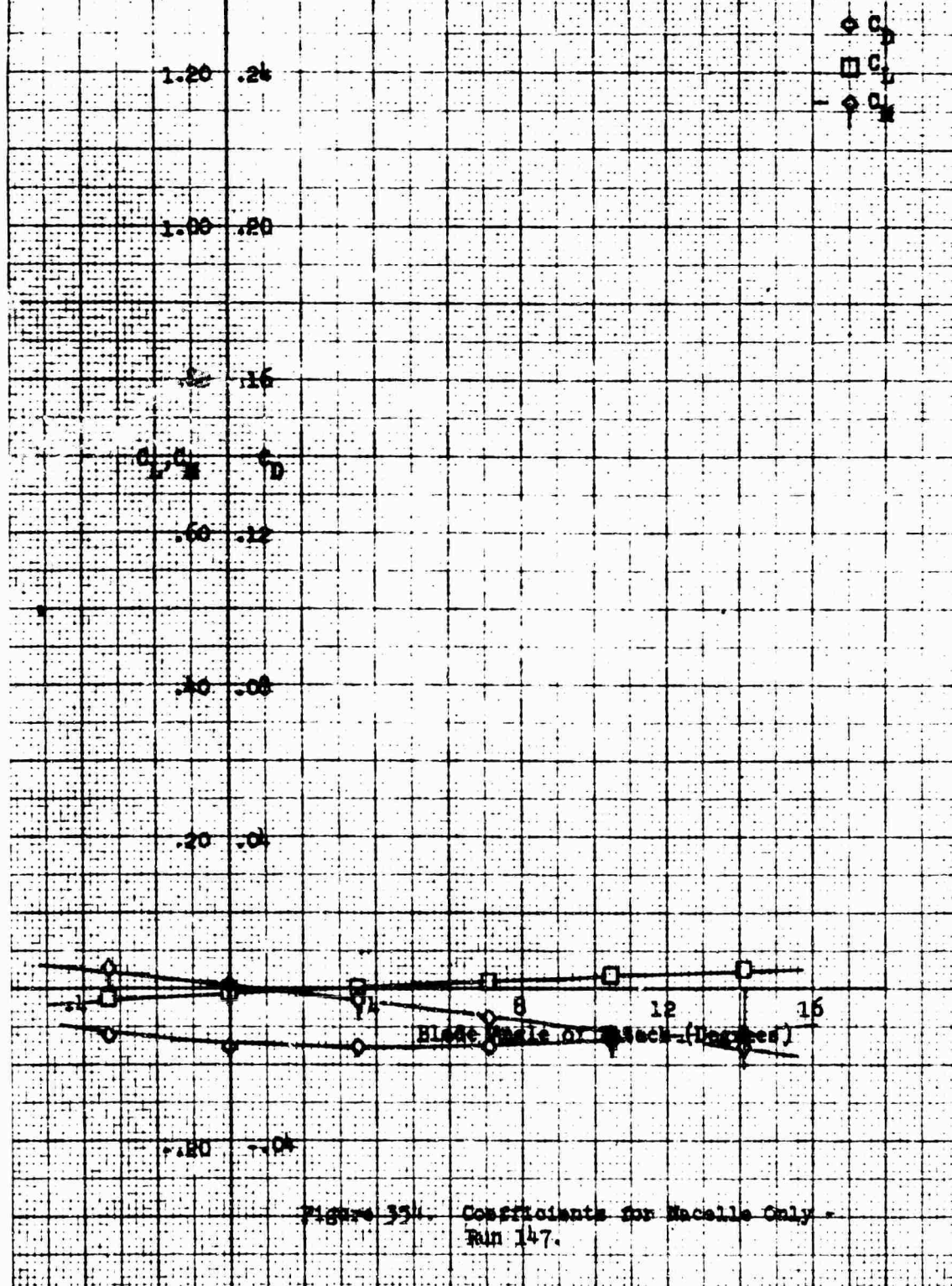


Figure 354. Coefficients for Macelle Only -
 Run 147.

Hecelle Configuration: Twin vertical 1-40-100
 Hecelle Incidence Angle: 0°
 Pairing: With
 Hecelle Exit Plate: .90
 $\beta = 20^\circ$

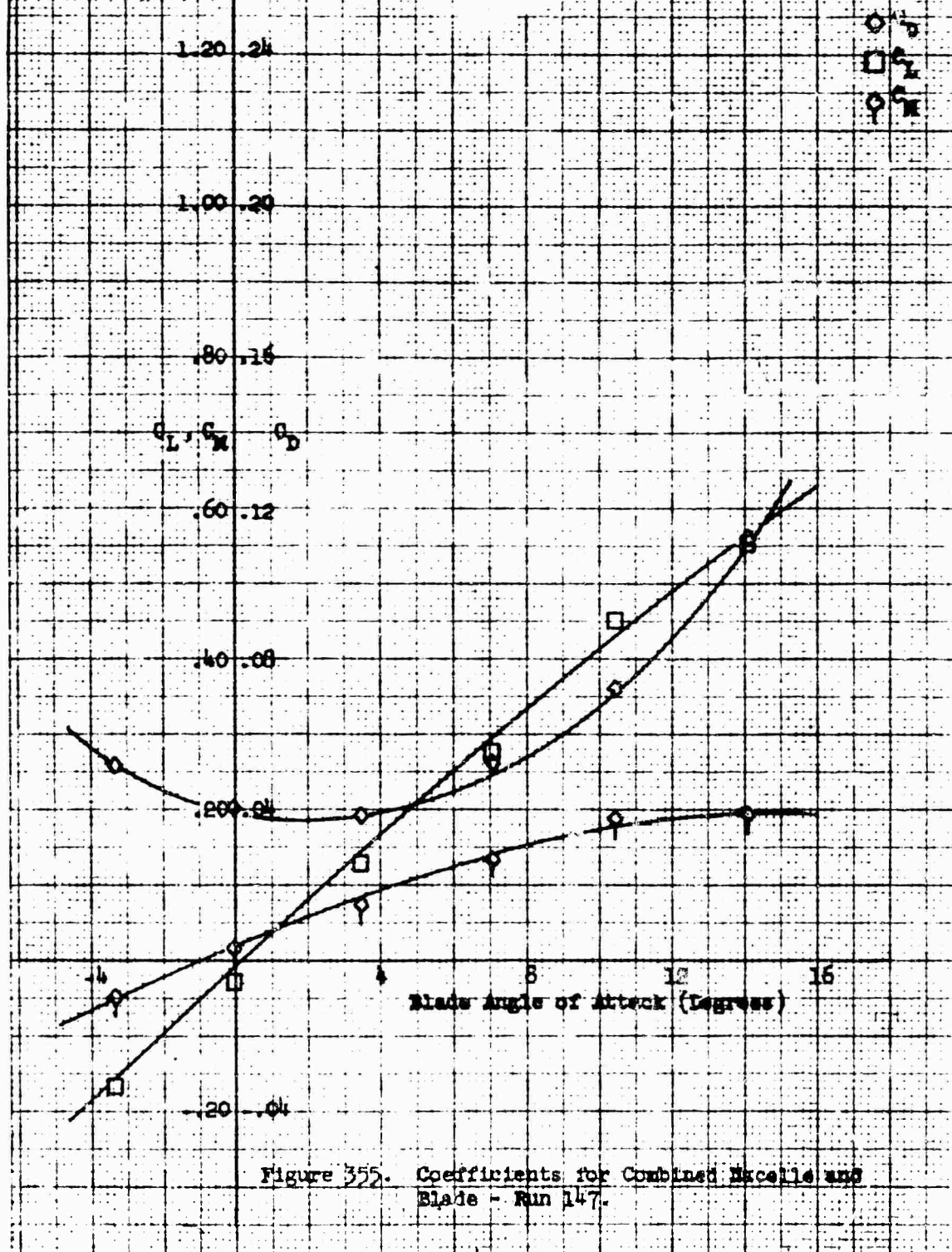
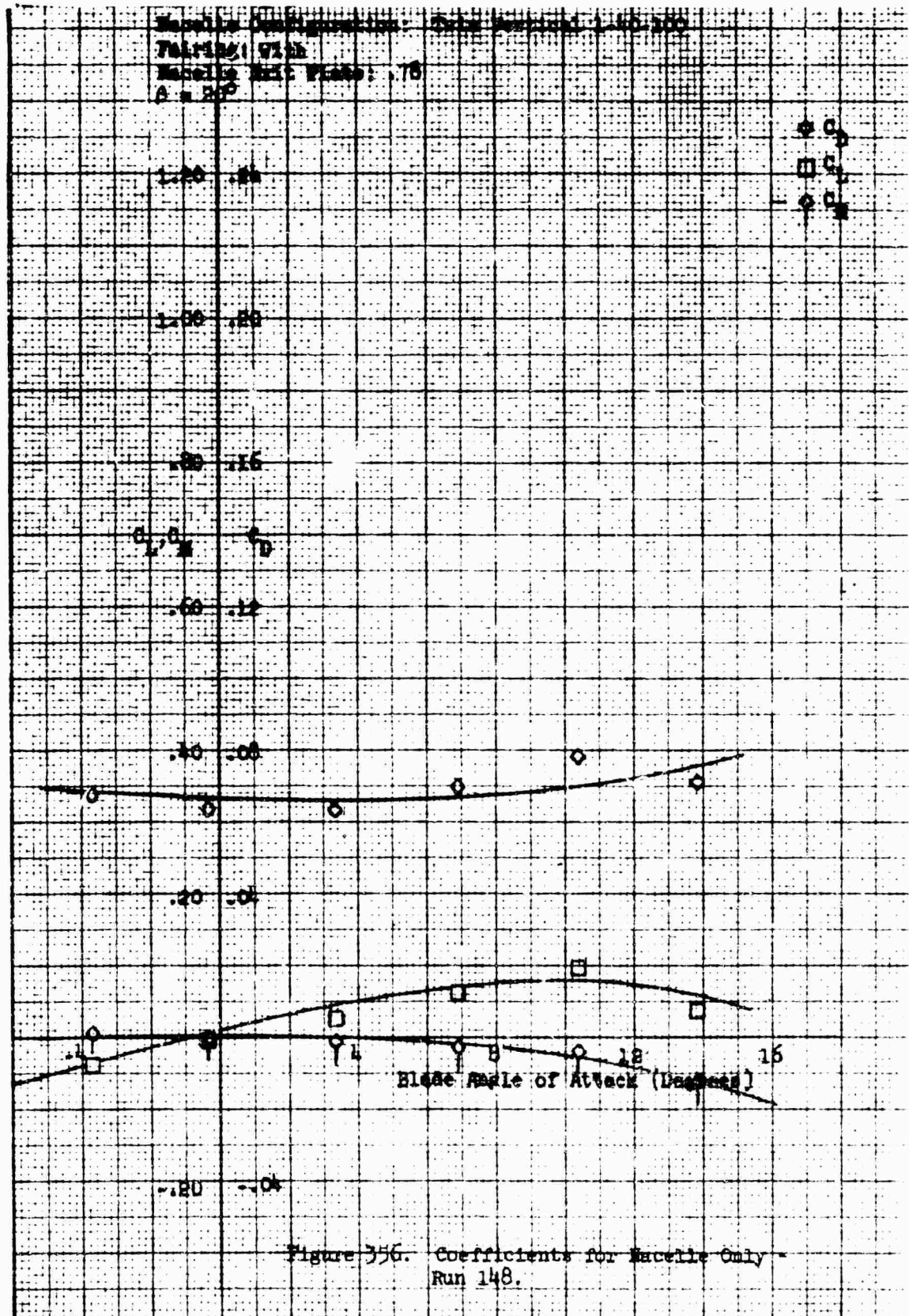


Figure 355. Coefficients for Combined Hecelle and
 Blade - Run 147.



Nacelle Configuration: Twin vertical 1-40-100
 Nacelle Incidence Angle: 0°
 Pairing: With
 Nacelle Exit Plate: .78
 $\beta = 20^\circ$

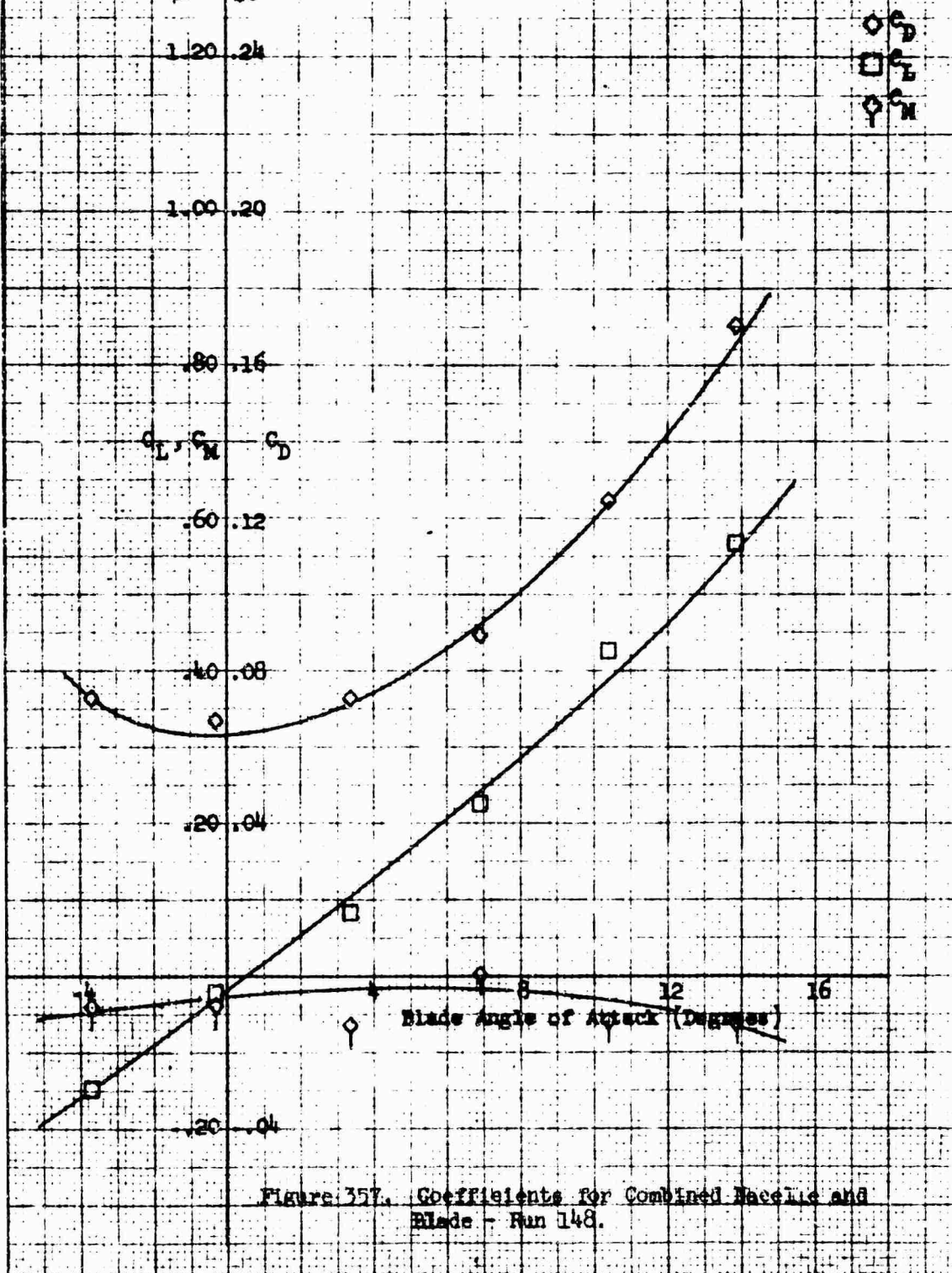
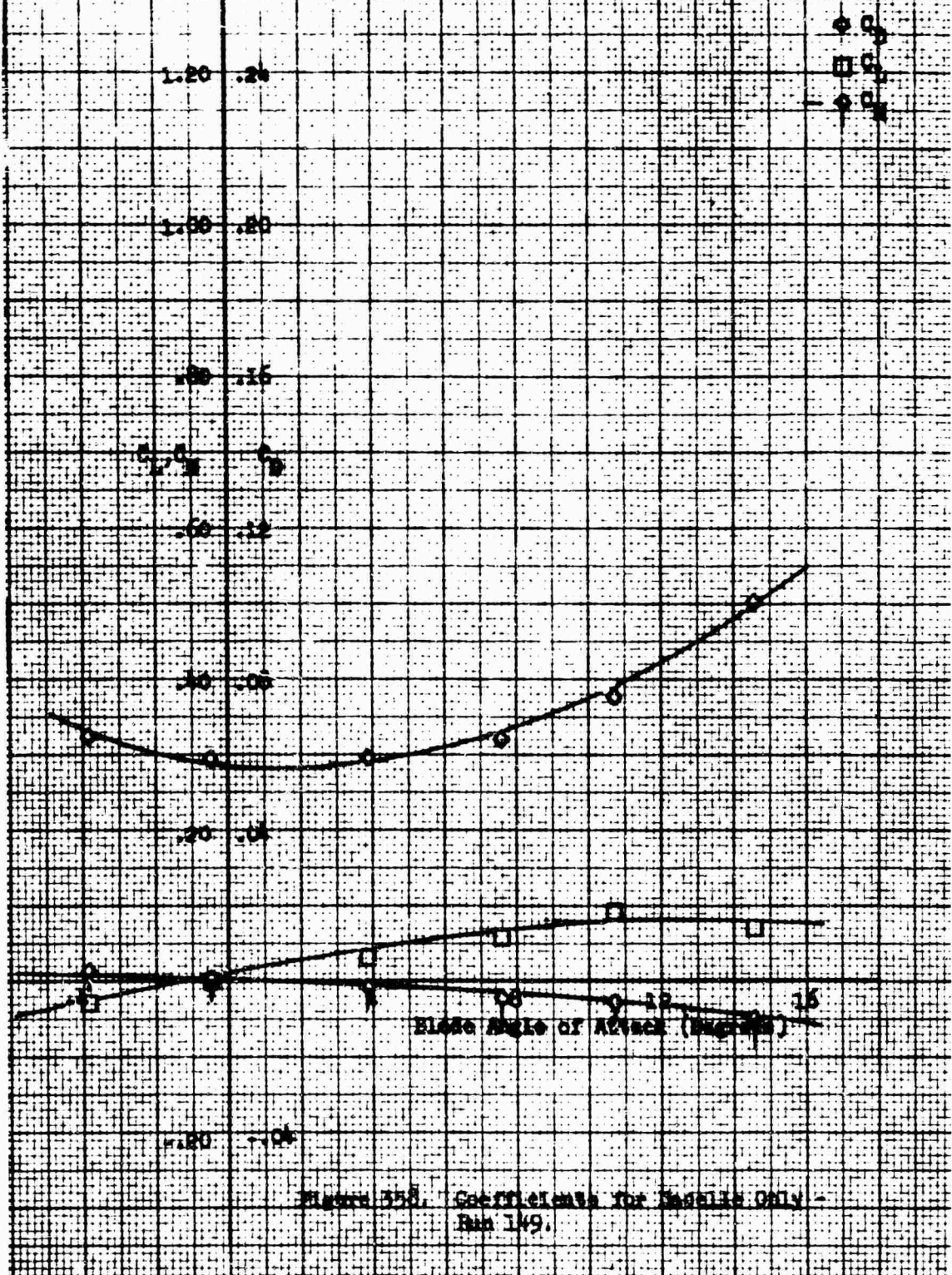
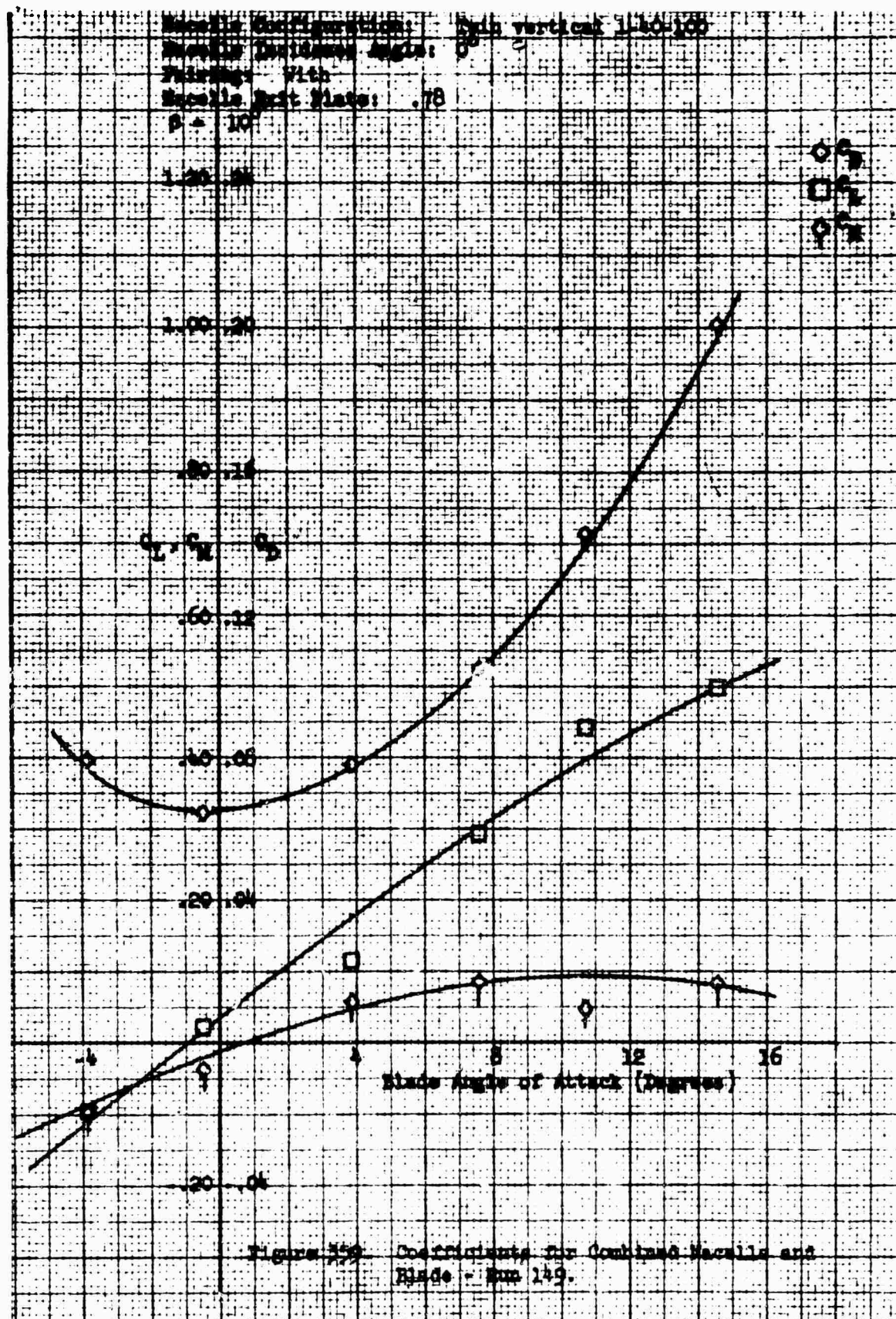


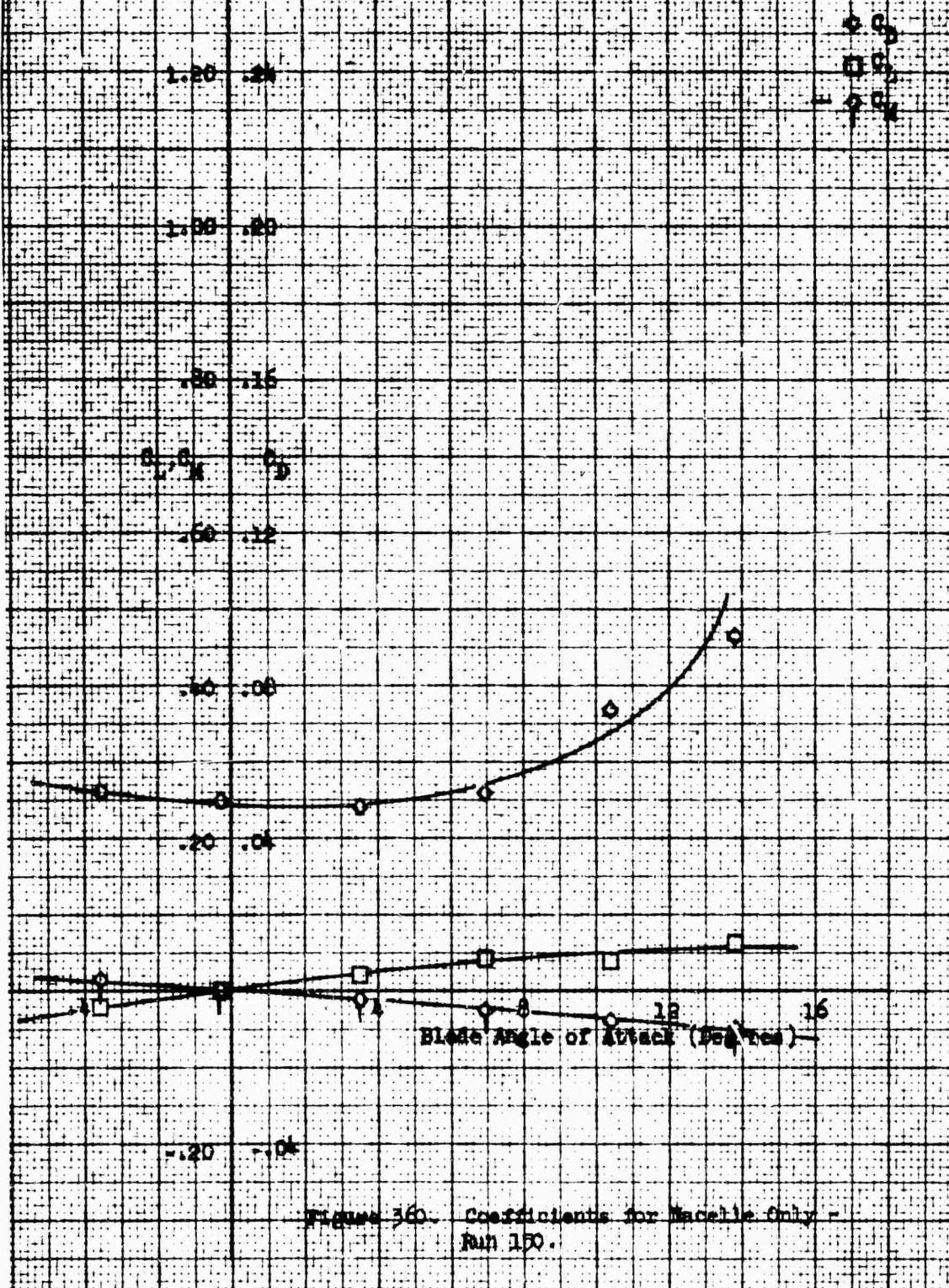
Figure 357. Coefficients for Combined Nacelle and Blade - Run 148.

Nozzle Configuration: Twin Vertical 1.50-100
 Feiring: With
 Nozzle Exit Plate: .78
 $B = 10^\circ$





Macelle Configuration: Data Part 141 1-10-100
 Pairing: With
 Macelle Exit Plane: 1.78
 $\alpha = 0$



Macelle Configuration: Twin vertical 1:40-100
 Macelle Incidence Angle: 0°
 Fairing: With
 Macelle Exit Plate: .78
 $\beta = 0$

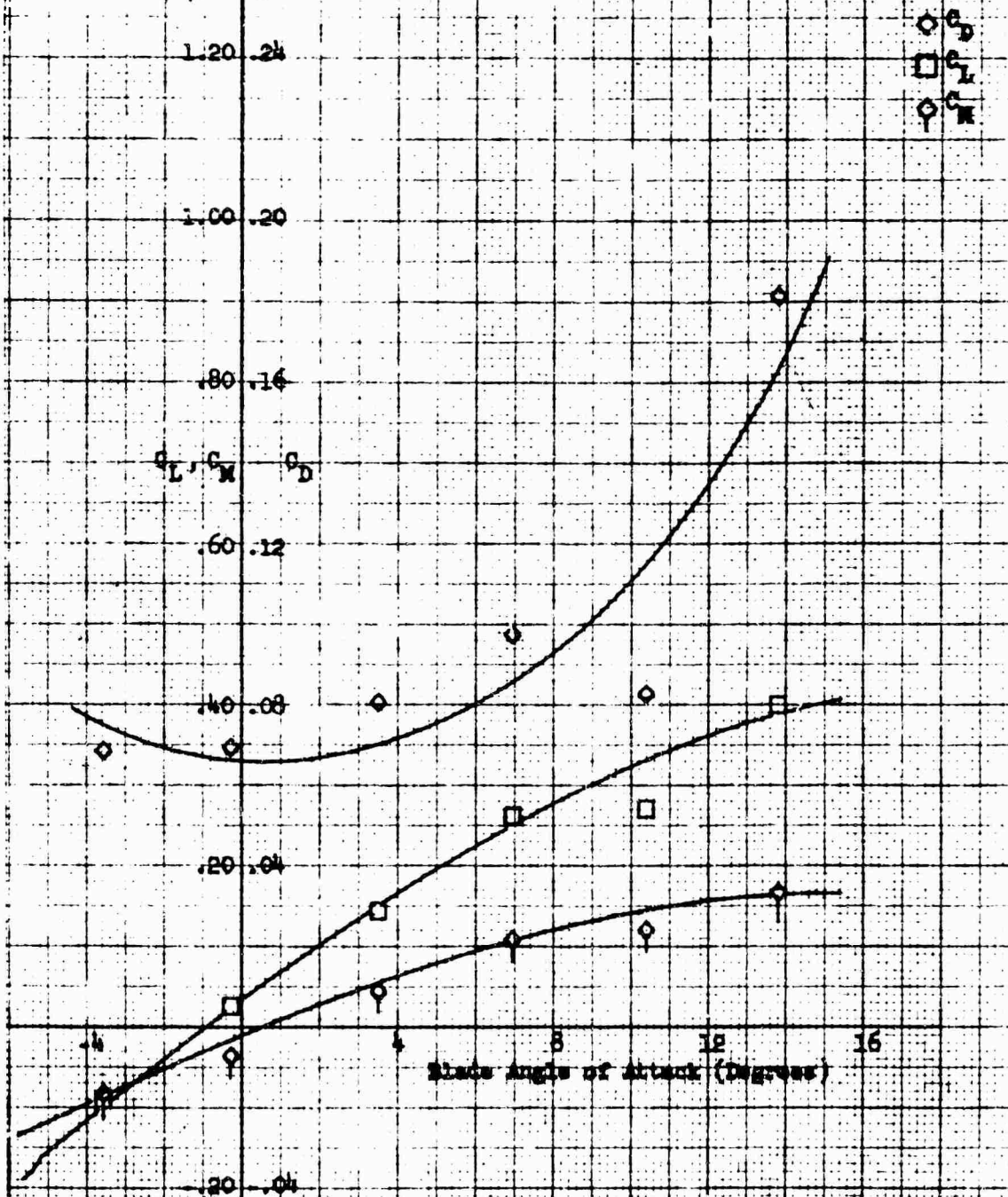


Figure 361. Coefficients for Combined Macelle and
 Plate - Run 150.

Macelle Configuration: Twin Vertical 1.40-100
 Pairing: With
 Macelle Kri Plate: .78
 $\alpha = 10^\circ$

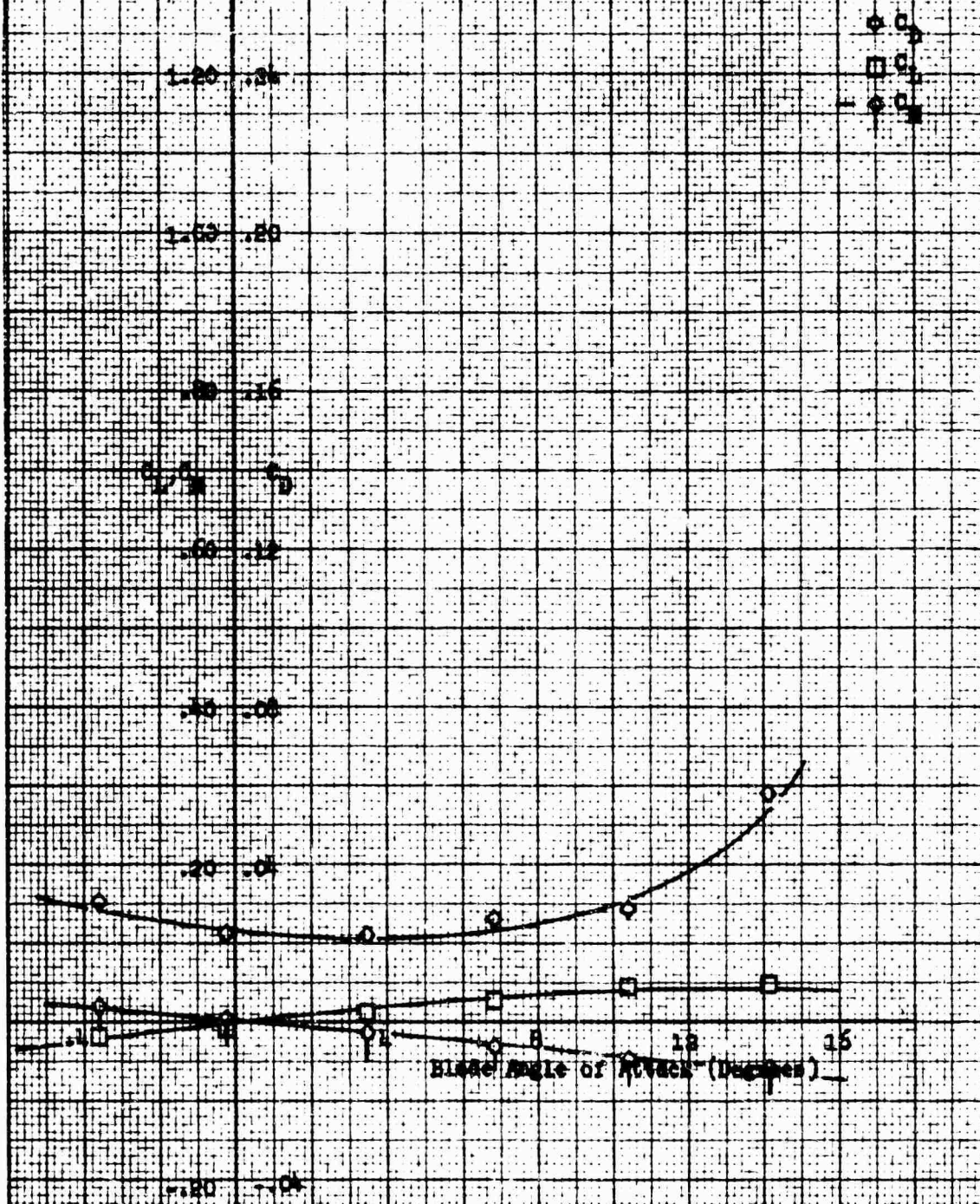
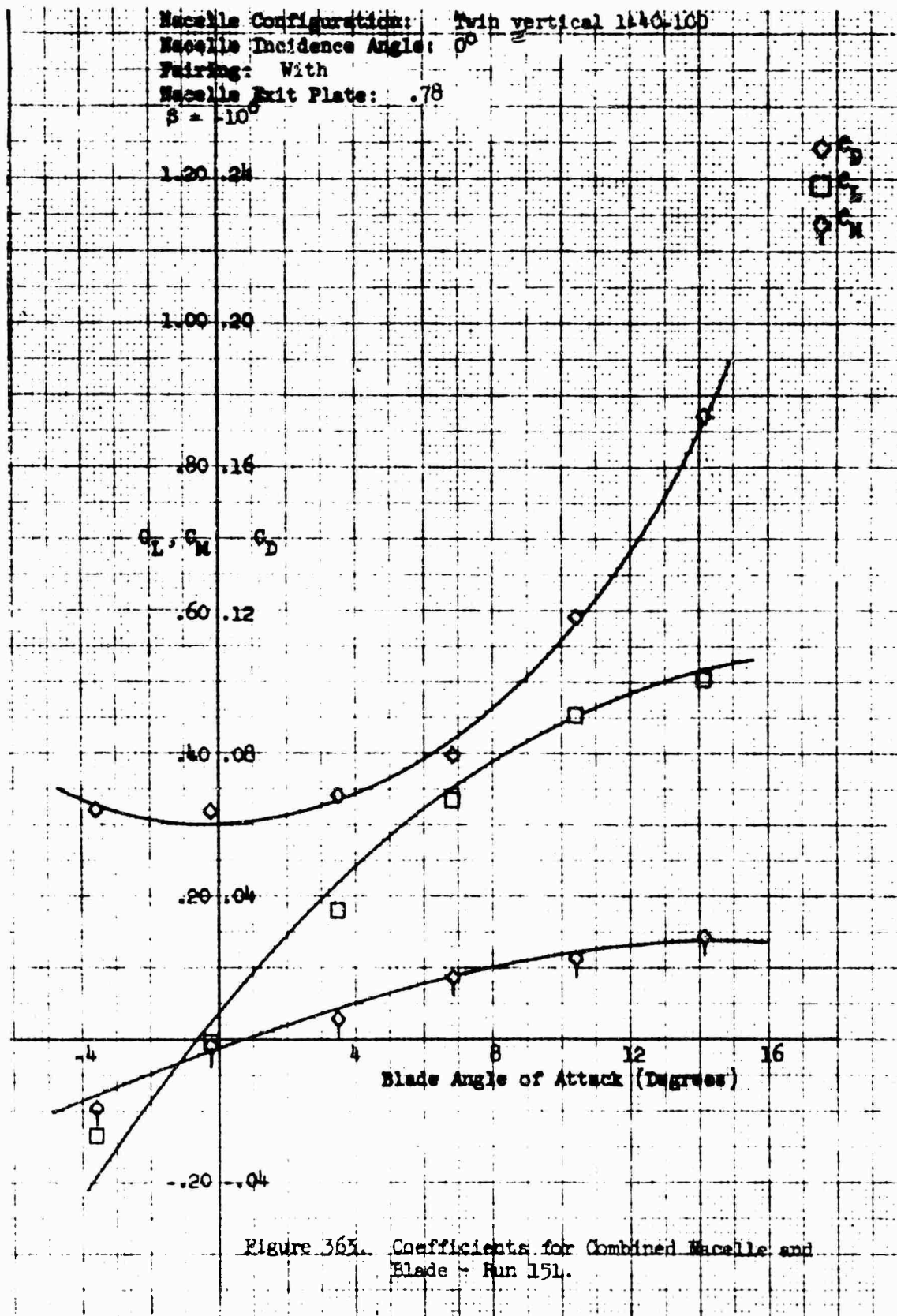
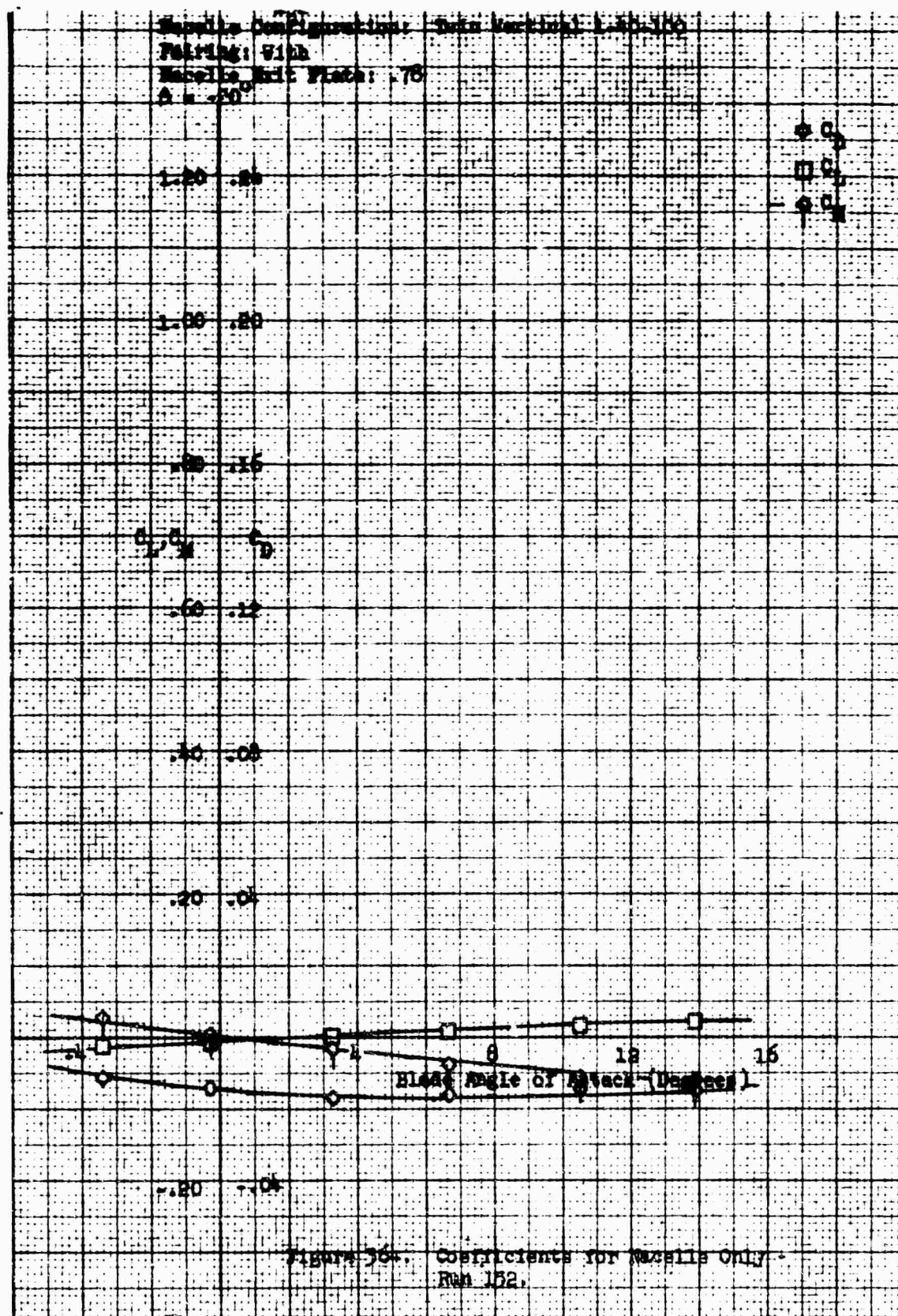


Figure 362. Coefficients for Macelle Only -
 Run 151.





Nacelle Configuration: Twin vertical 1-40-100
 Nacelle Incidence Angle: 0°
 Pairing: With
 Nacelle Exit Plate: .78
 $\beta = 20^\circ$

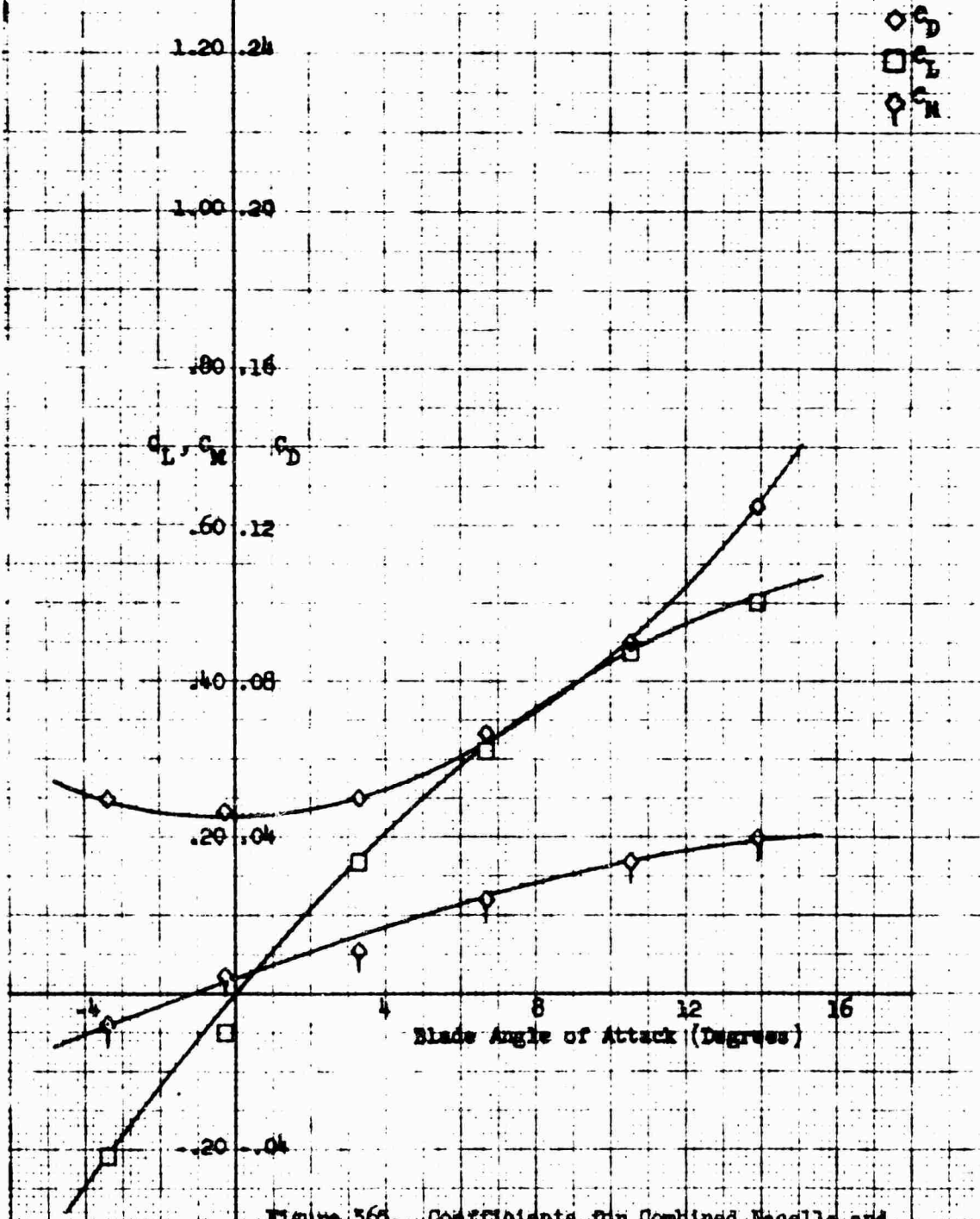


Figure 365. Coefficients for Combined Nacelle and Blade - Run 152.

Blade Configuration: Semi Vertical 1.50/100
 Pairing: With
 Blade Exit Plate: 0
 $\beta = -20^\circ$

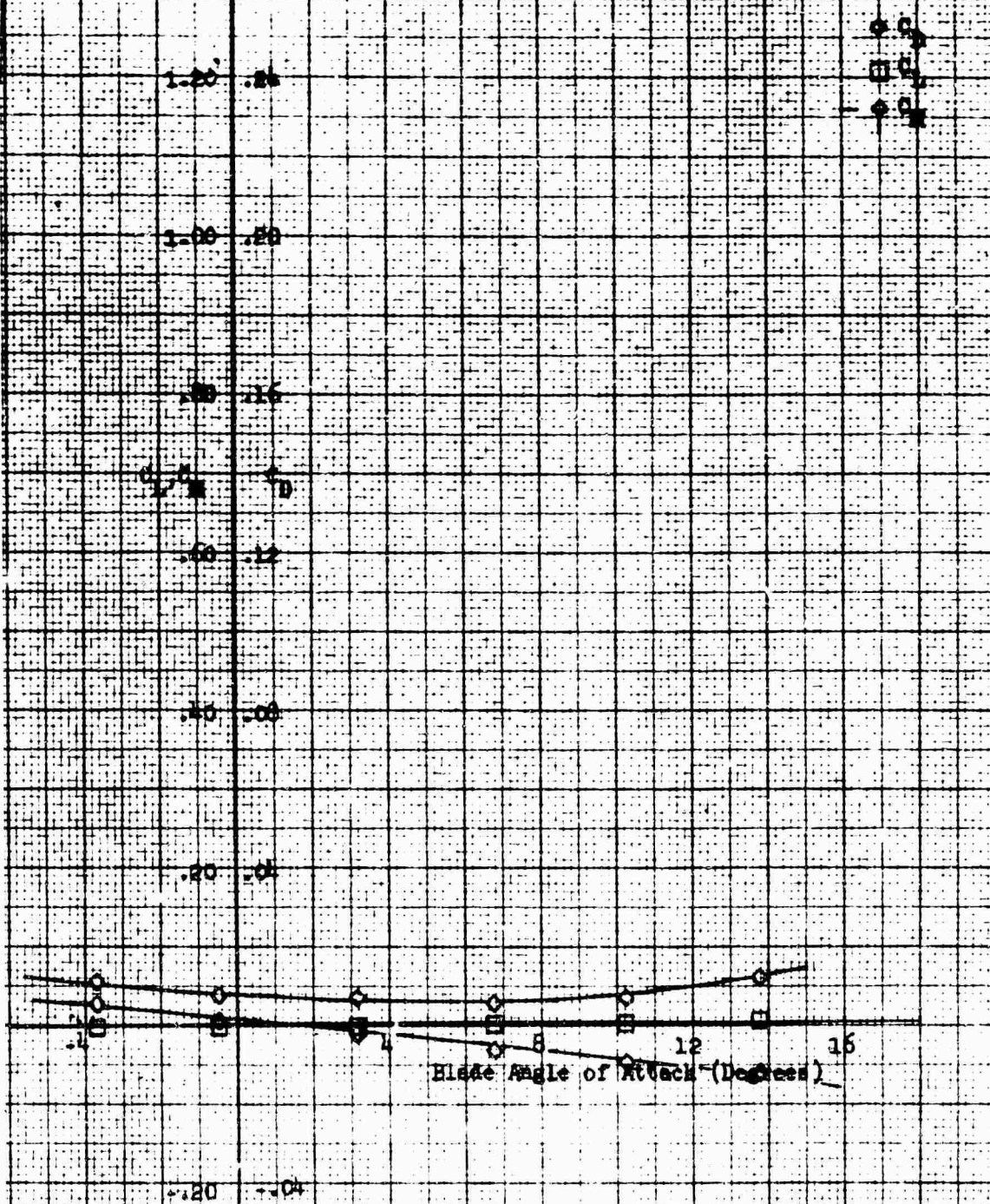
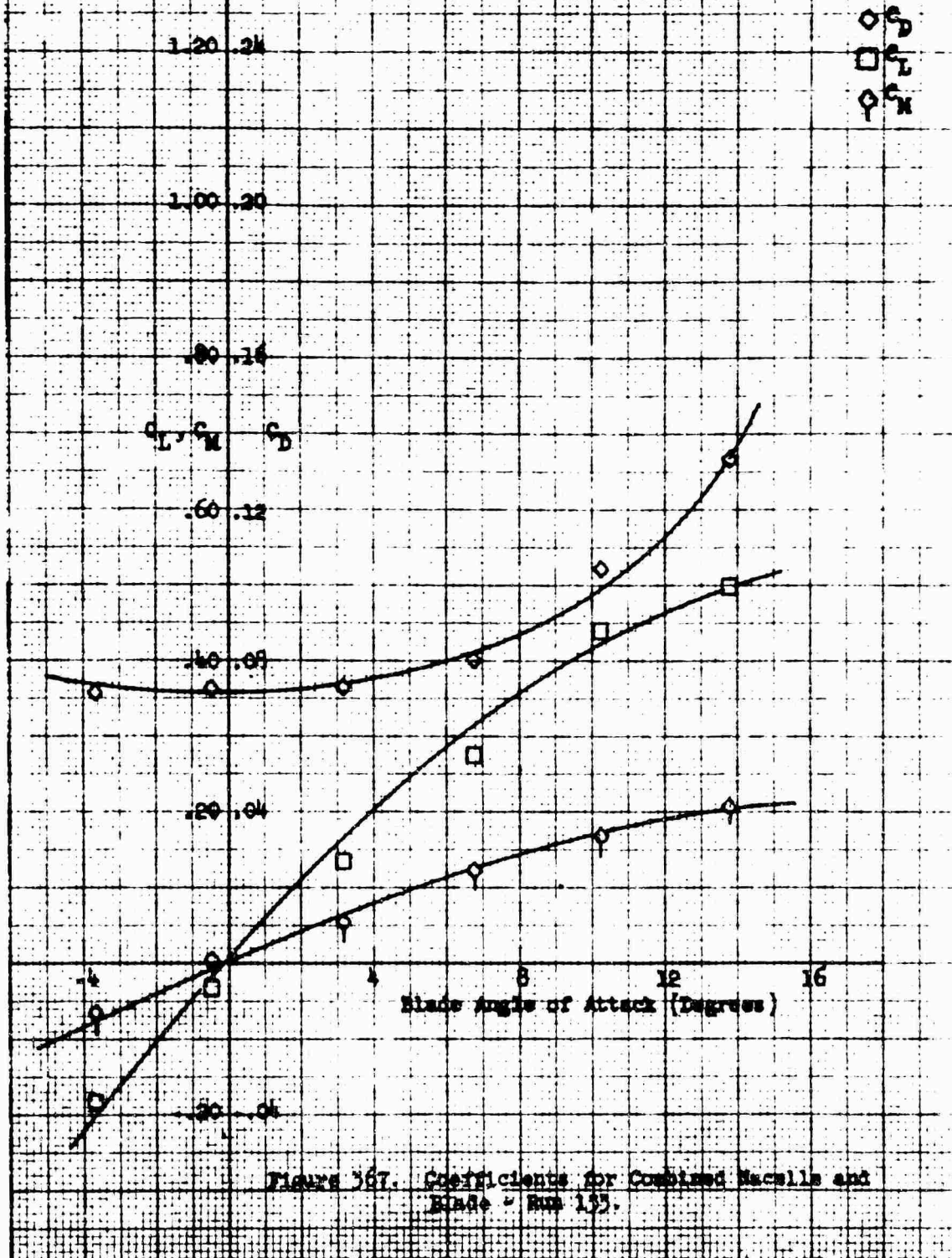
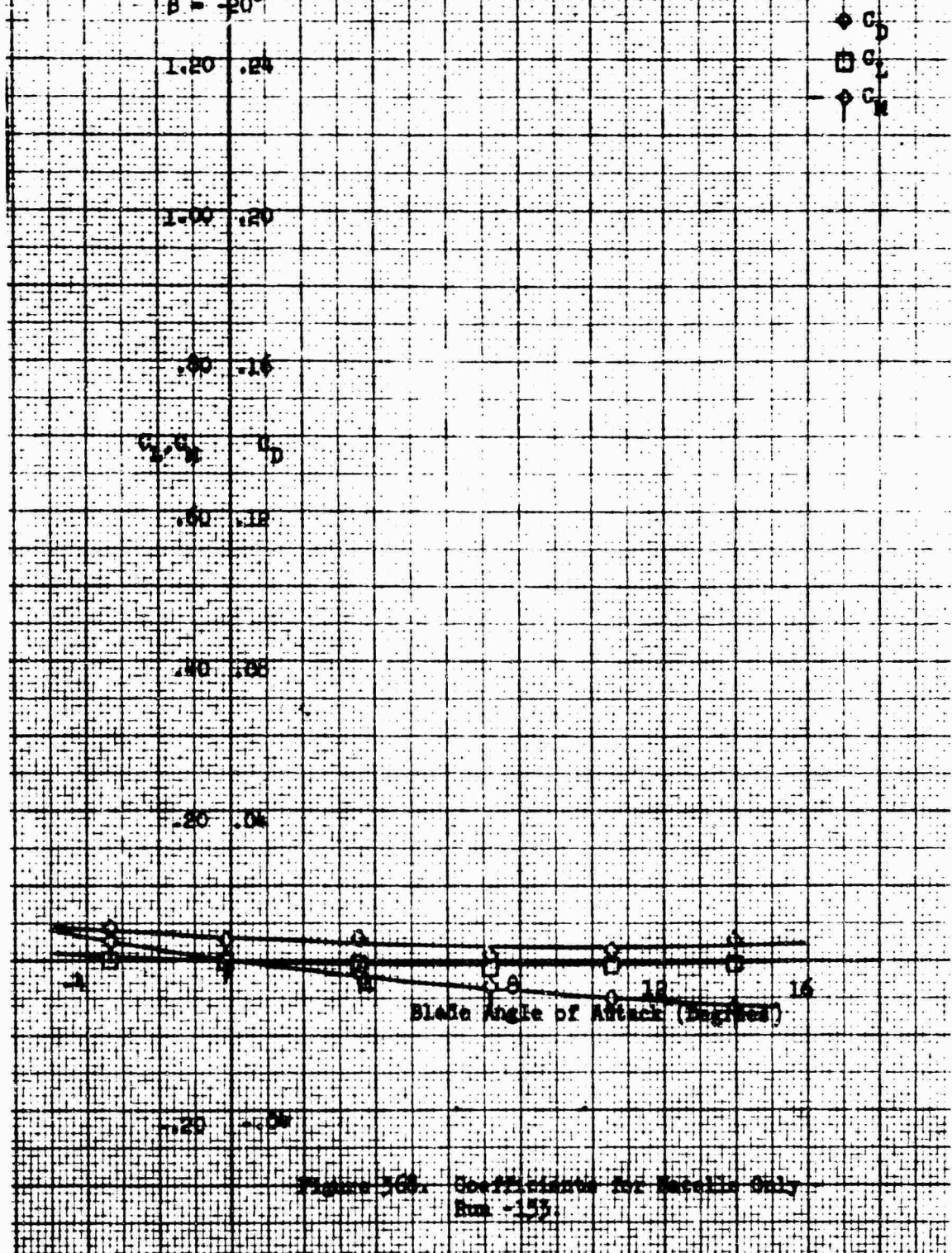


Figure 366. Coefficients for Blade Only -
 Run 153.

Macelle Configuration: Twin vertical 1-40-100
 Macelle Incidence Angle: 0°
 Fairing: With
 Macelle Exit Plate: 0
 $\beta = 20^\circ$



Nozzle Configuration: Twin Vertical 1-50-100
 Pairing: With
 Nozzle Exit Plate: 0
 With trailing edge fairing
 $\beta = -20^\circ$



Macelle Configuration: Twin vertical 1-10-100
 Macelle Incidence Angle: 0°
 Fairing: With
 Macelle Exit Plate: 0
 With trailing edge fairing
 $\beta = 20^\circ$
 1.20 .24

C_L
 C_M
 C_D

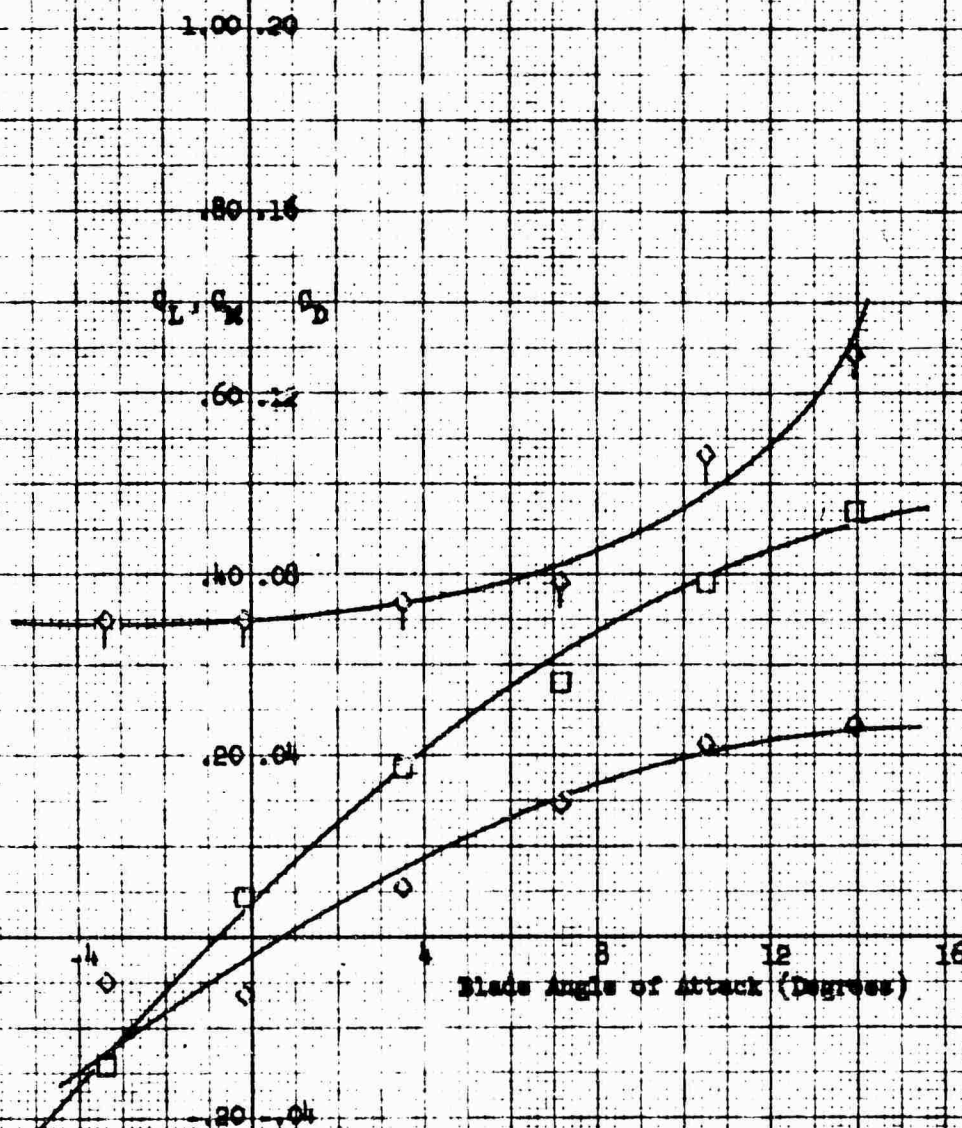
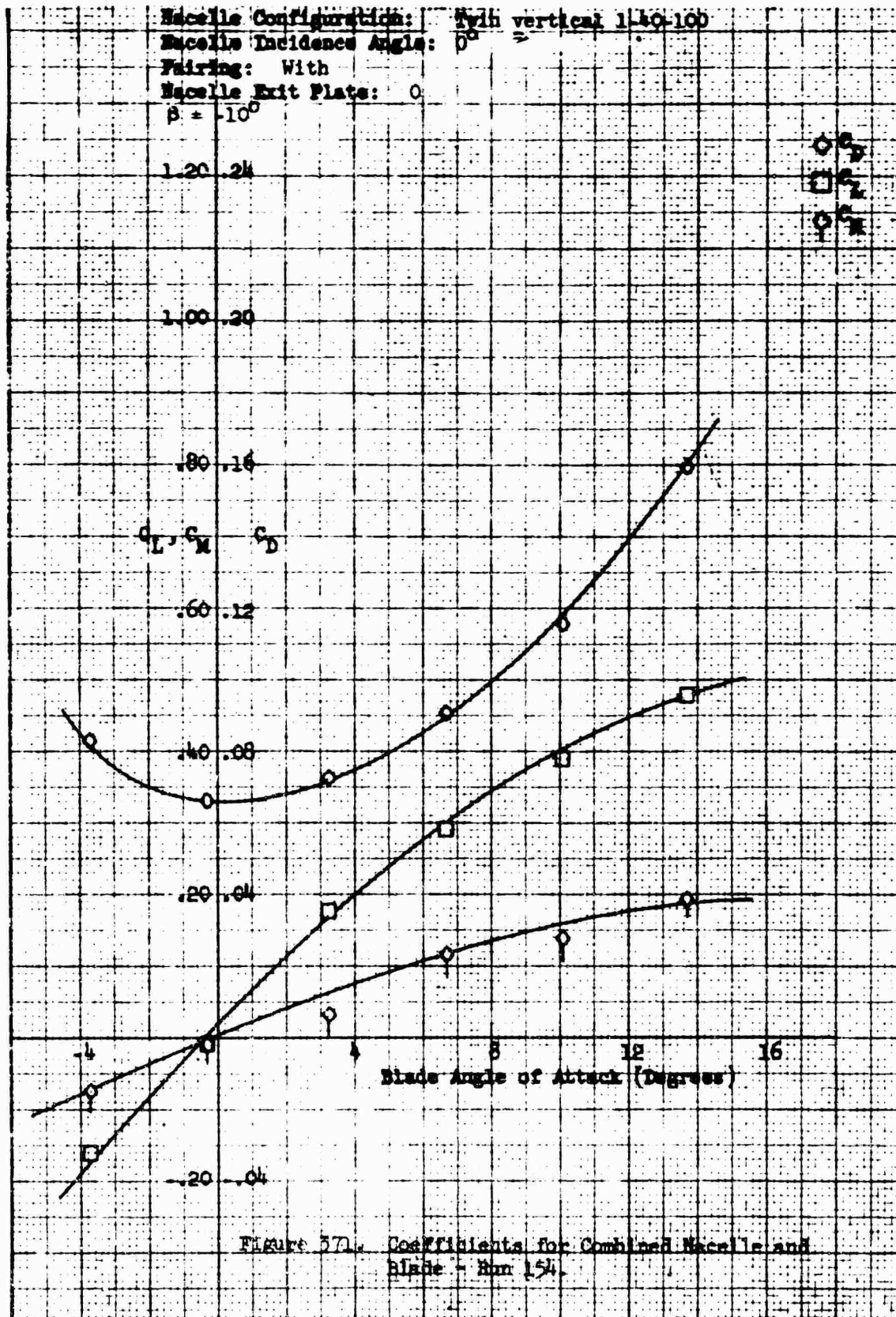
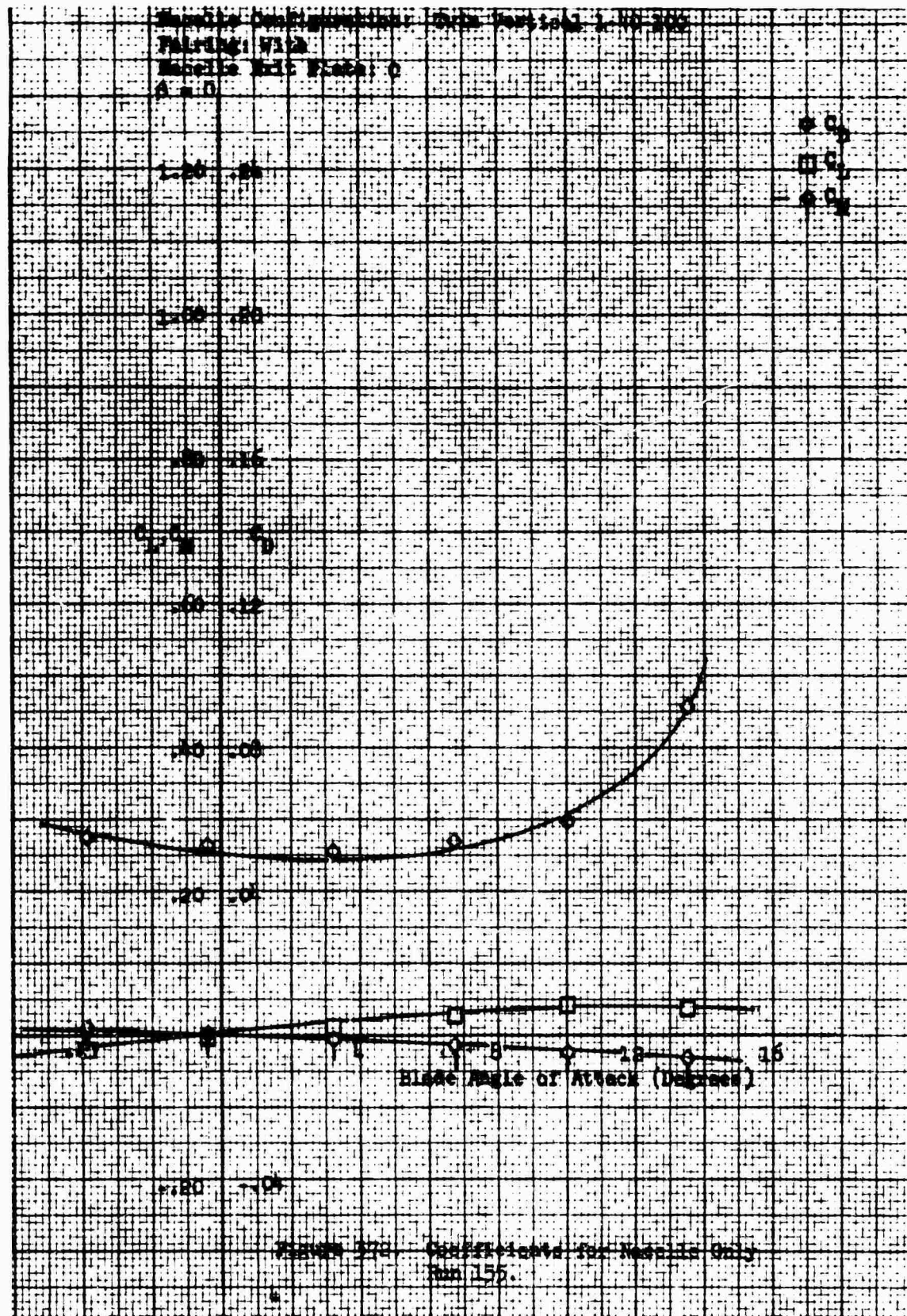
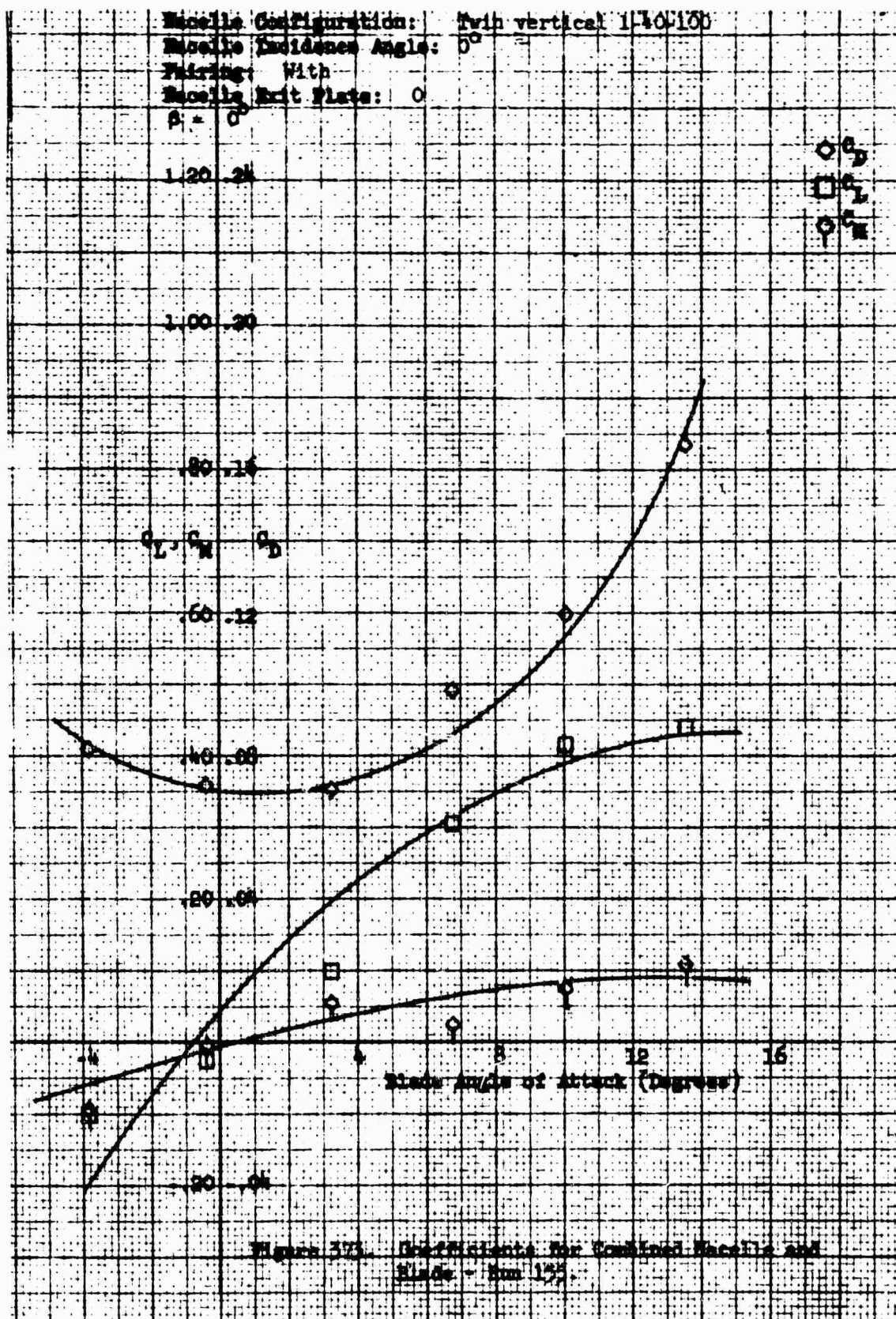


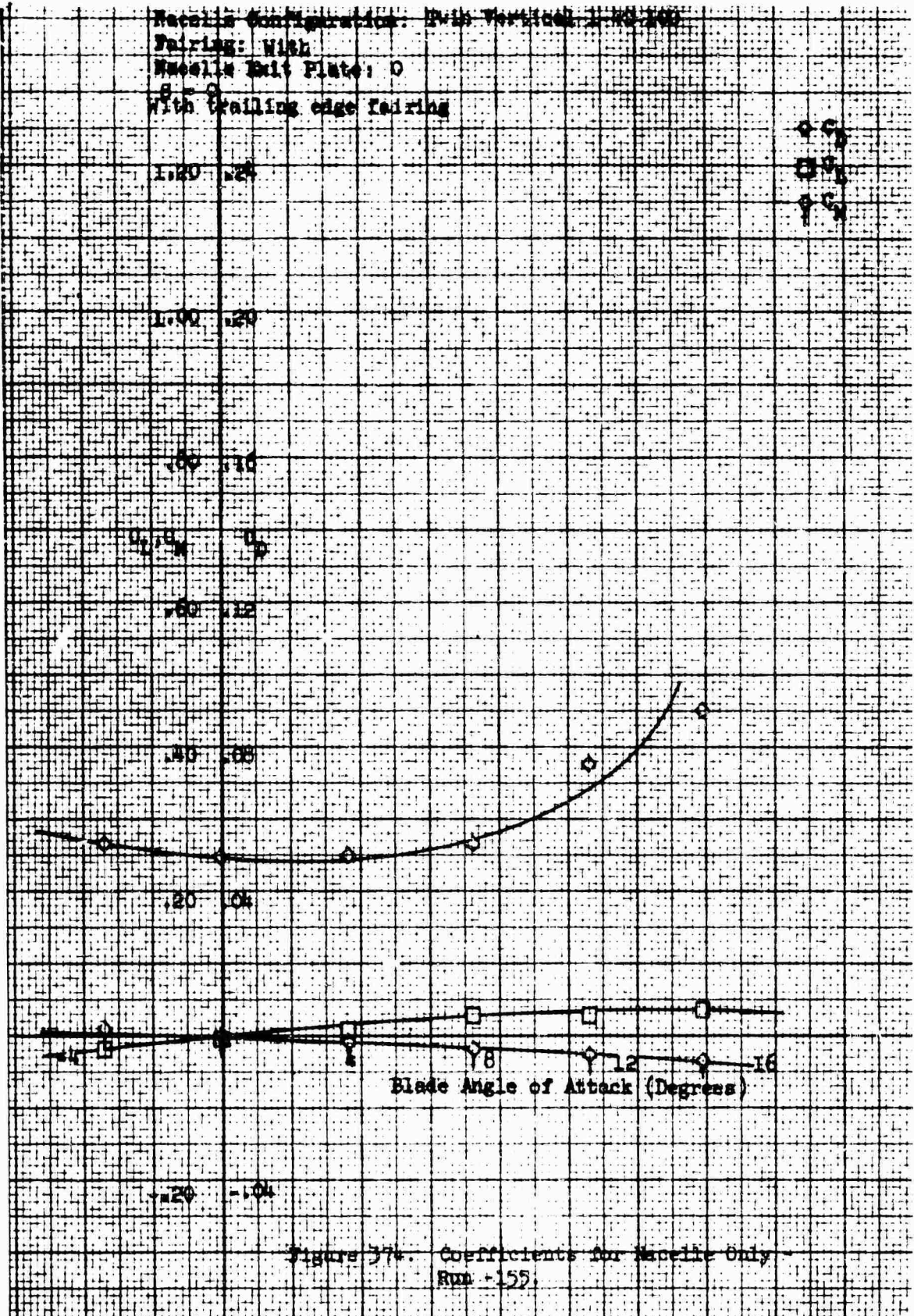
Figure 369. Coefficients for Combined Macelle and Blade - Run - 133.







Blade Configuration: Thin Vertical, L=1.00
 Fairing: With
 Blade Exit Plate: 0
 $\beta = 0$
 With trailing edge fairing



Nacelle Configuration: Twin vertical 1-40-100
 Nacelle Incidence Angle: 0°
 Fairing: With
 Nacelle Exit Plate: 0
 With trailing edge fairing
 $\beta = 0^\circ$
 1.20 .24

$\diamond C_D$
 $\square C_L$
 $\circ C_M$

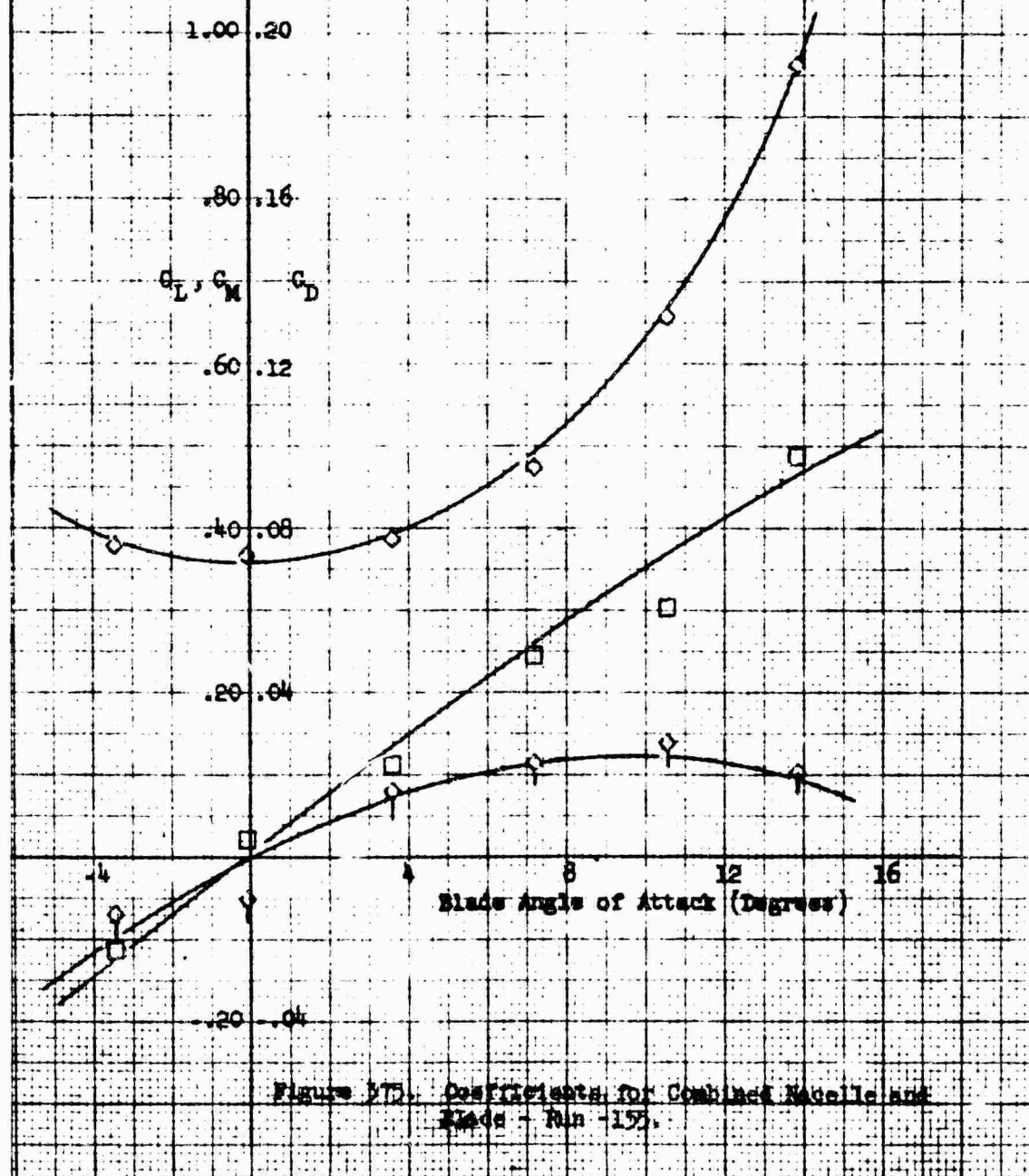
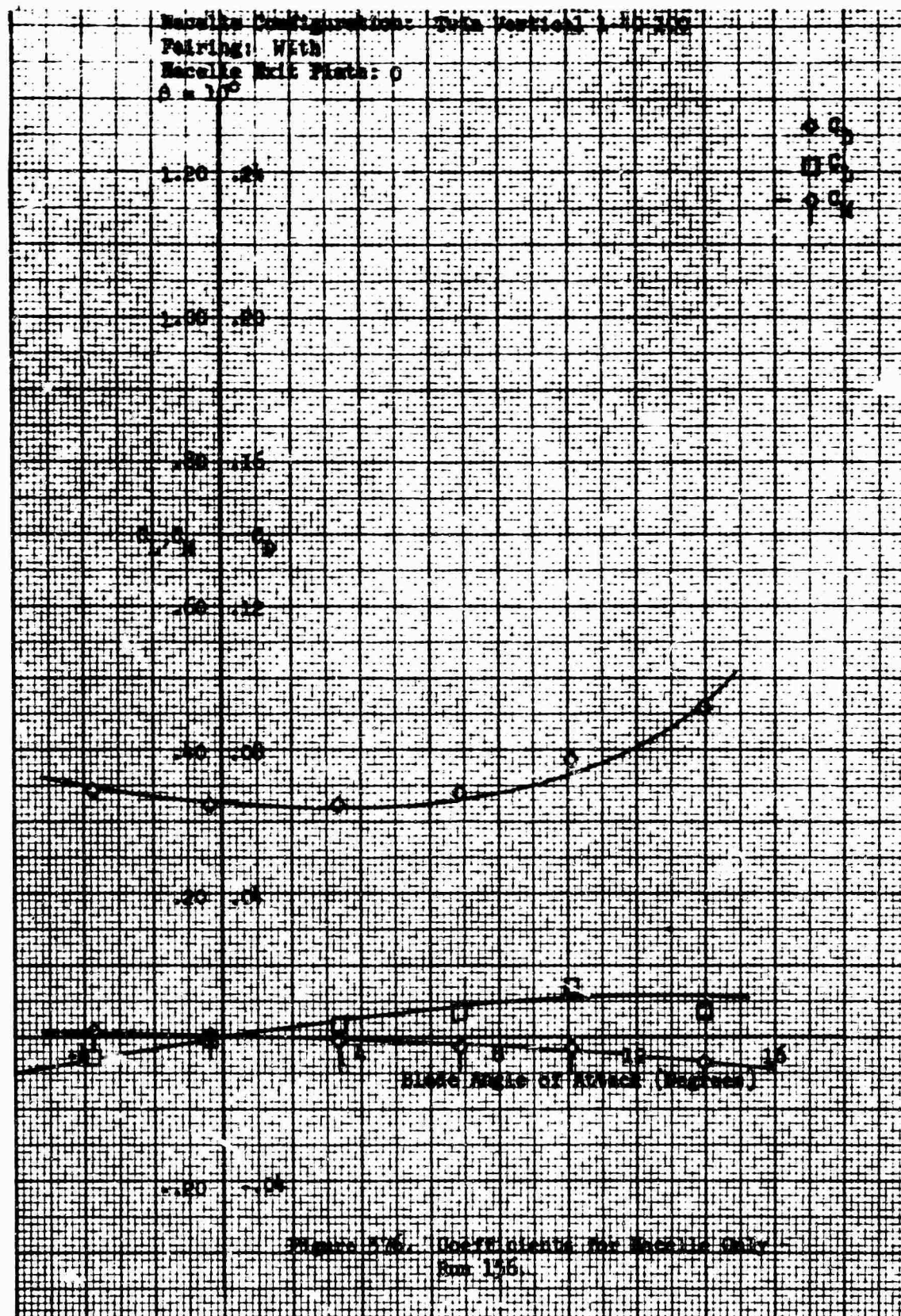


Figure 175. Coefficients for Combined Nacelle and
 Blade - Run - 155.



Nacelle Configuration: Twin vertical 1:10-100
 Nacelle Incidence Angle: 0°
 Fairing: With
 Nacelle Exit Plate: 0
 $\beta = 10^\circ$

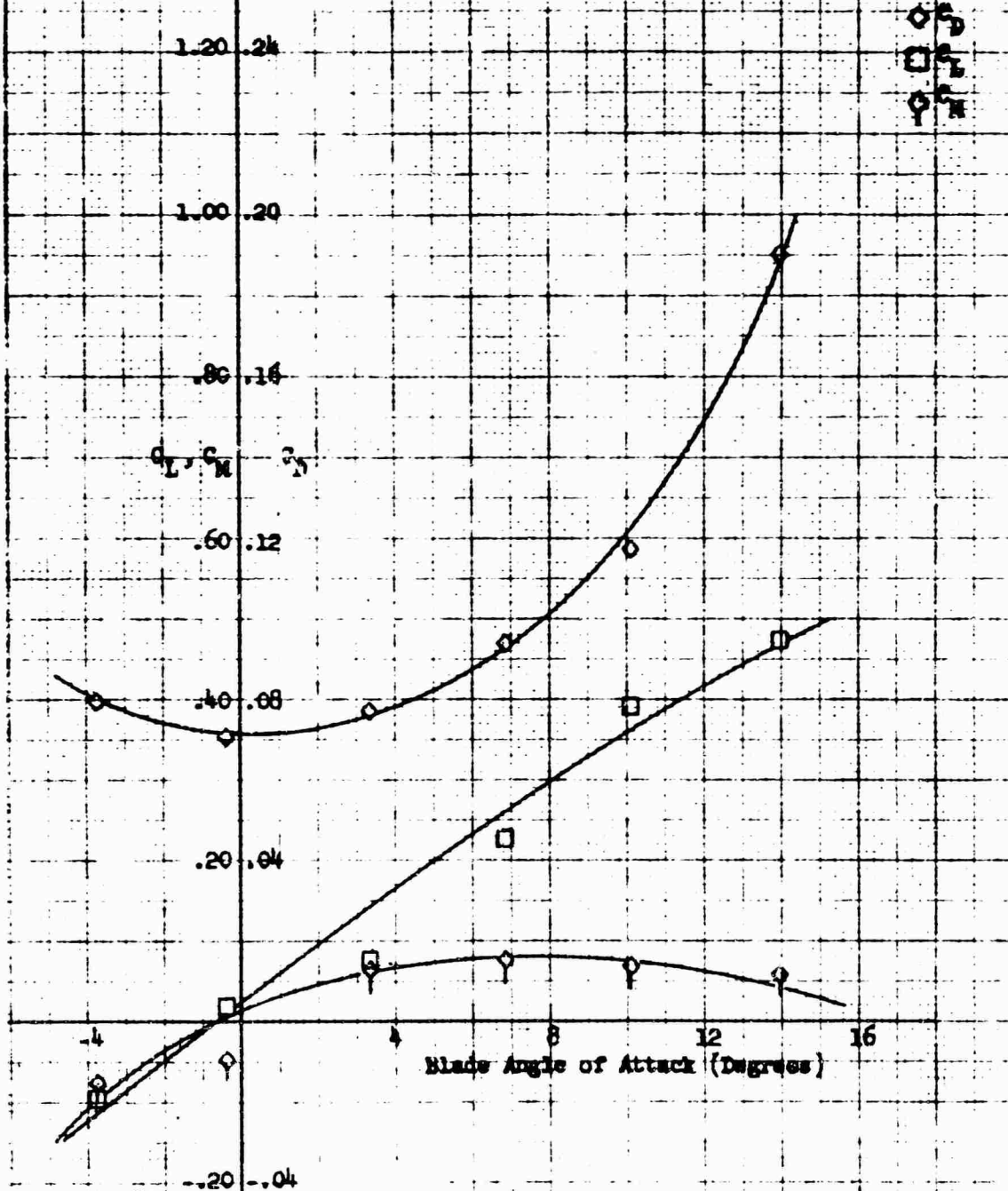
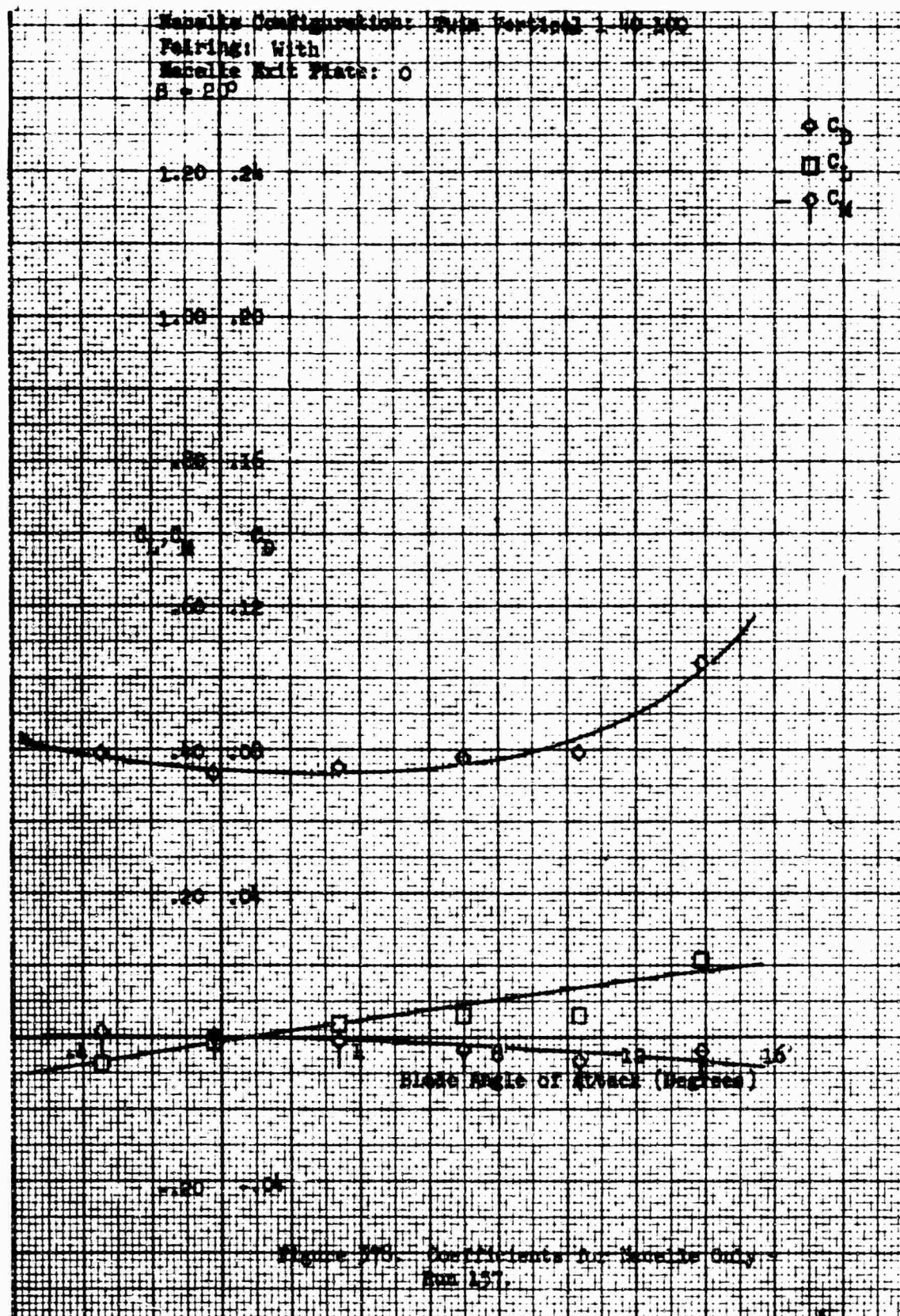


Figure 377. Coefficients for Combined Nacelle and Blade - Run 156.



Macelle Configuration: Twin vertical 1-4C-100
 Macelle Incidence Angle: 0°
 Pairing: With
 Macelle Exit Plate: 0
 $\beta = 20^\circ$

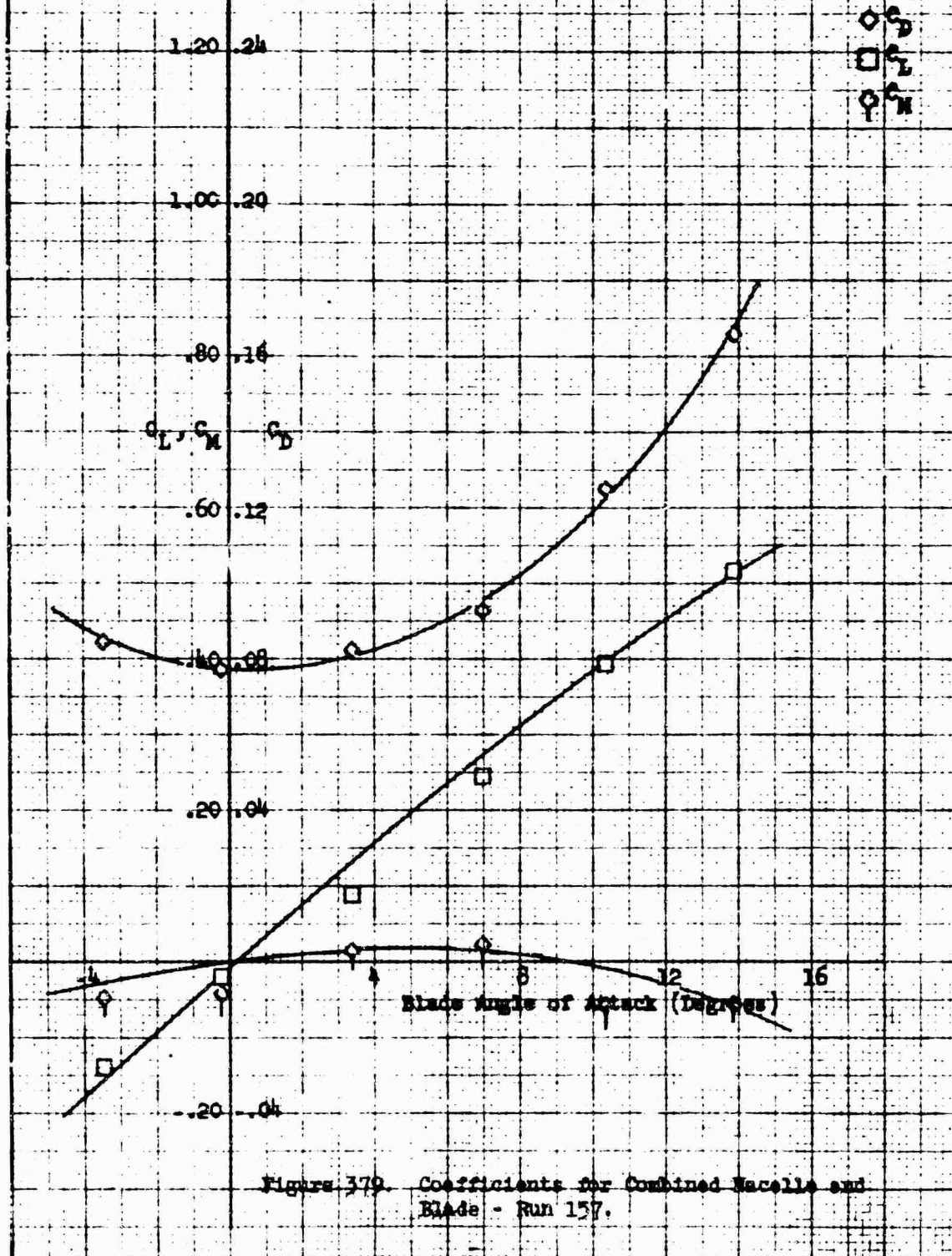
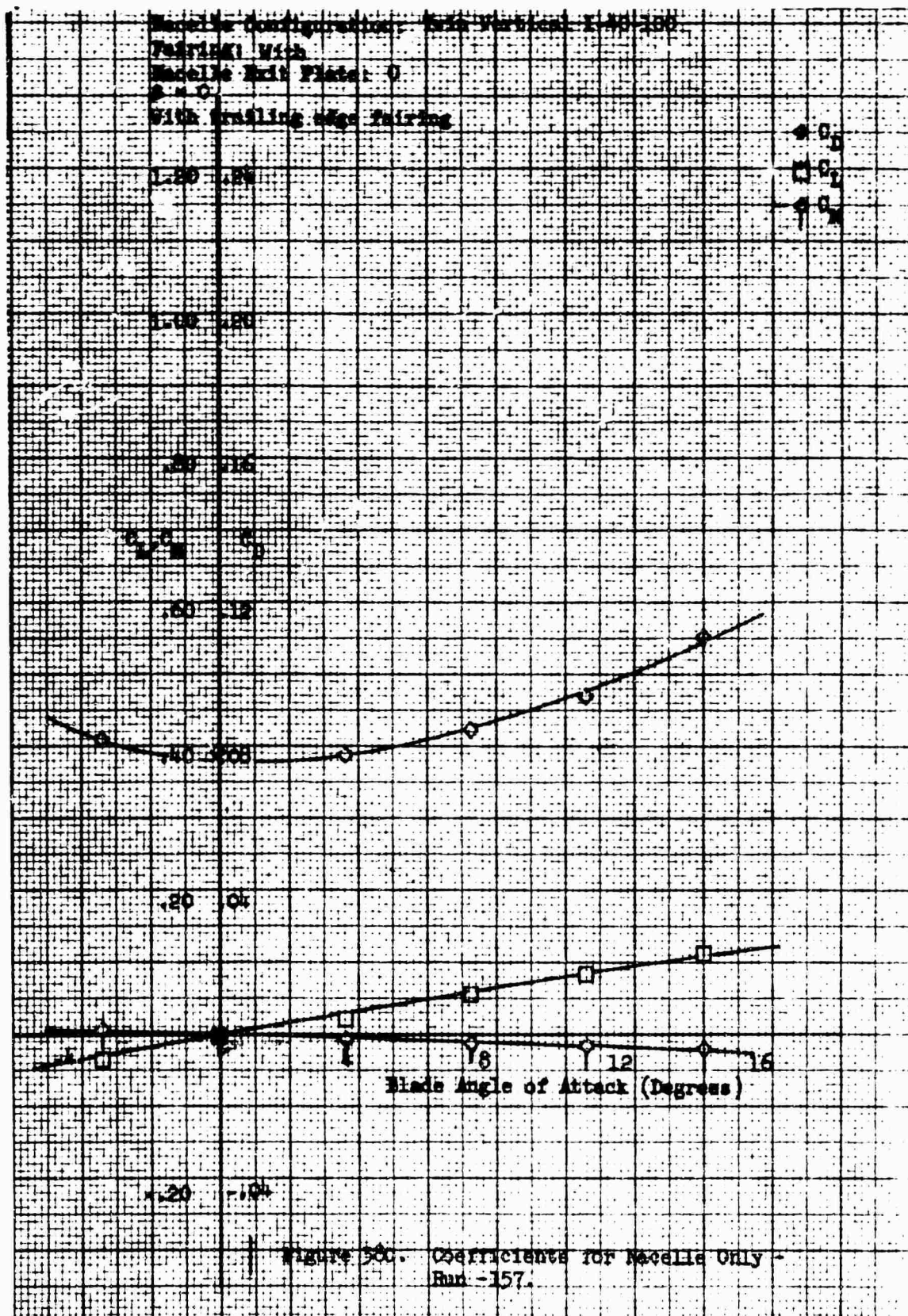


Figure 379. Coefficients for Combined Macelle and Blade - Run 157.



Nacelle Configuration: Twin vertical 1-40-100
 Nacelle Incidence Angle: 0°
 Fairing: With
 Nacelle Exit Plate: 0
 With trailing edge fairing
 $\beta = 20^\circ$
 1.20 .24

C_D
 C_L
 C_M

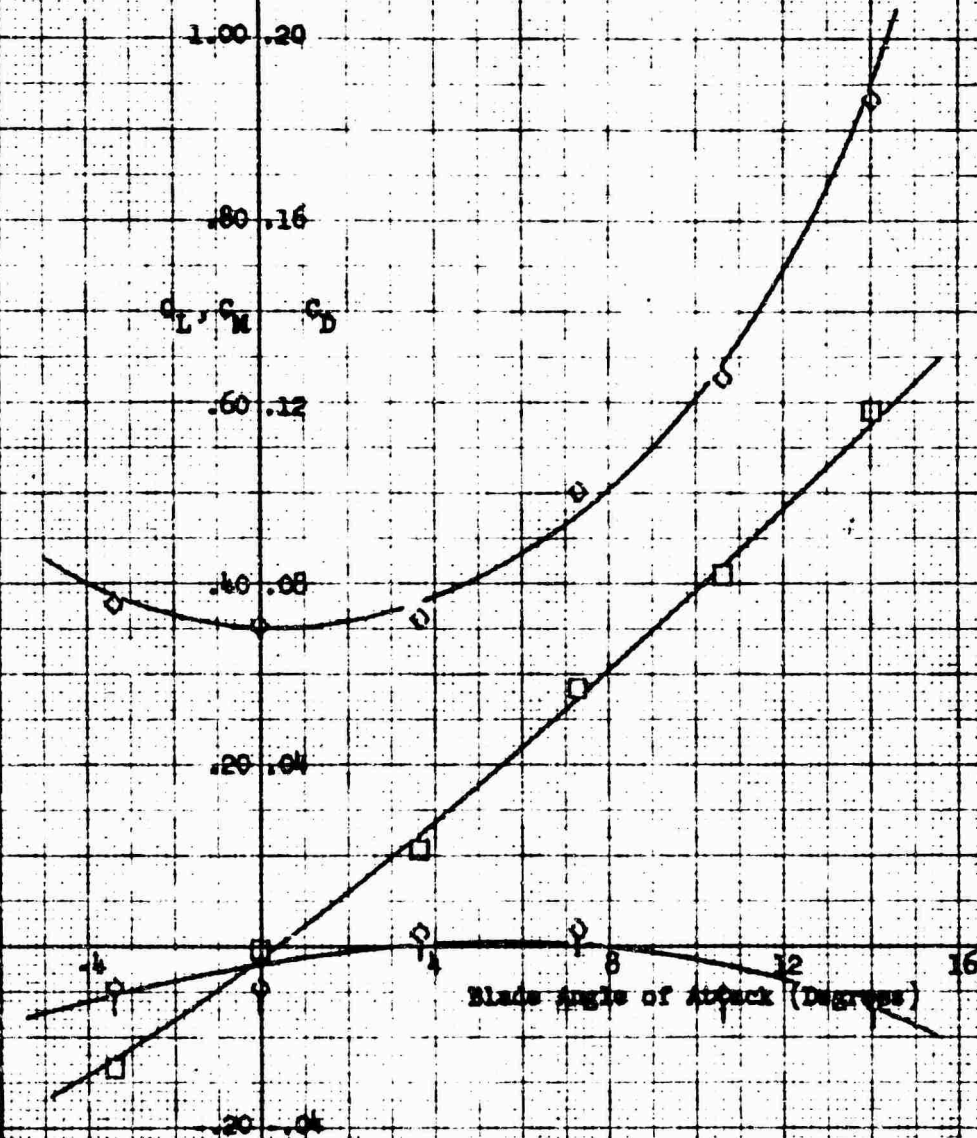
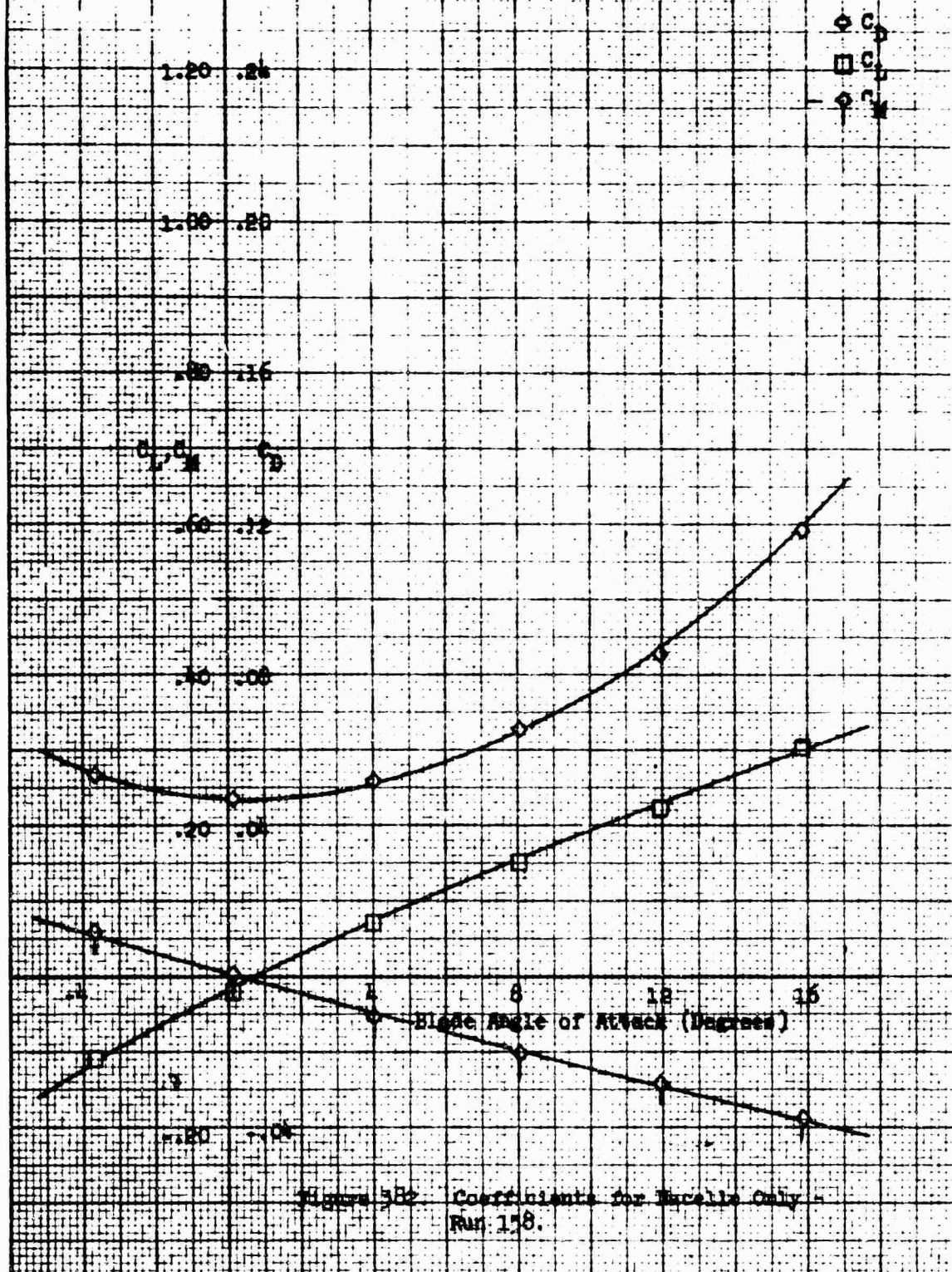
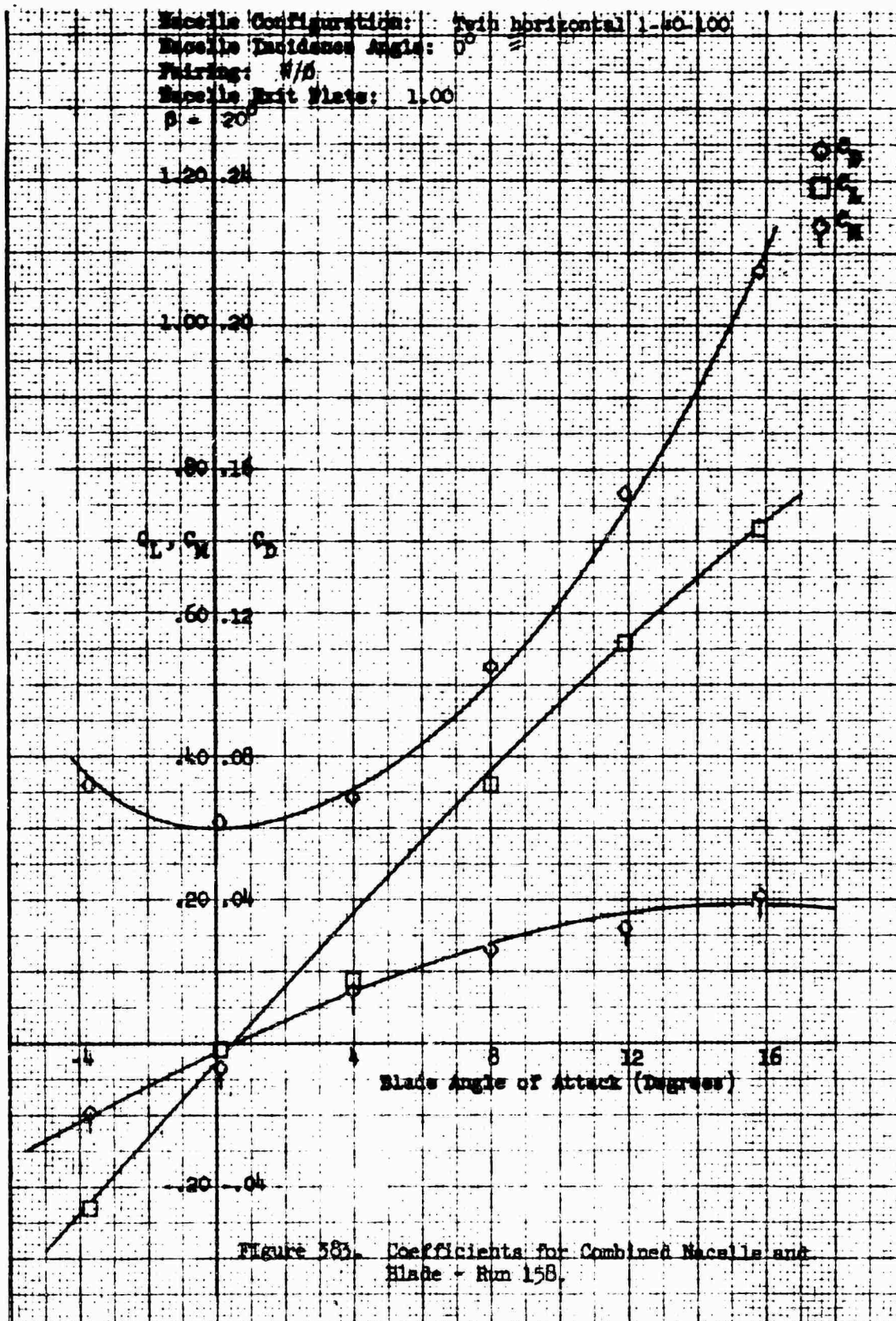
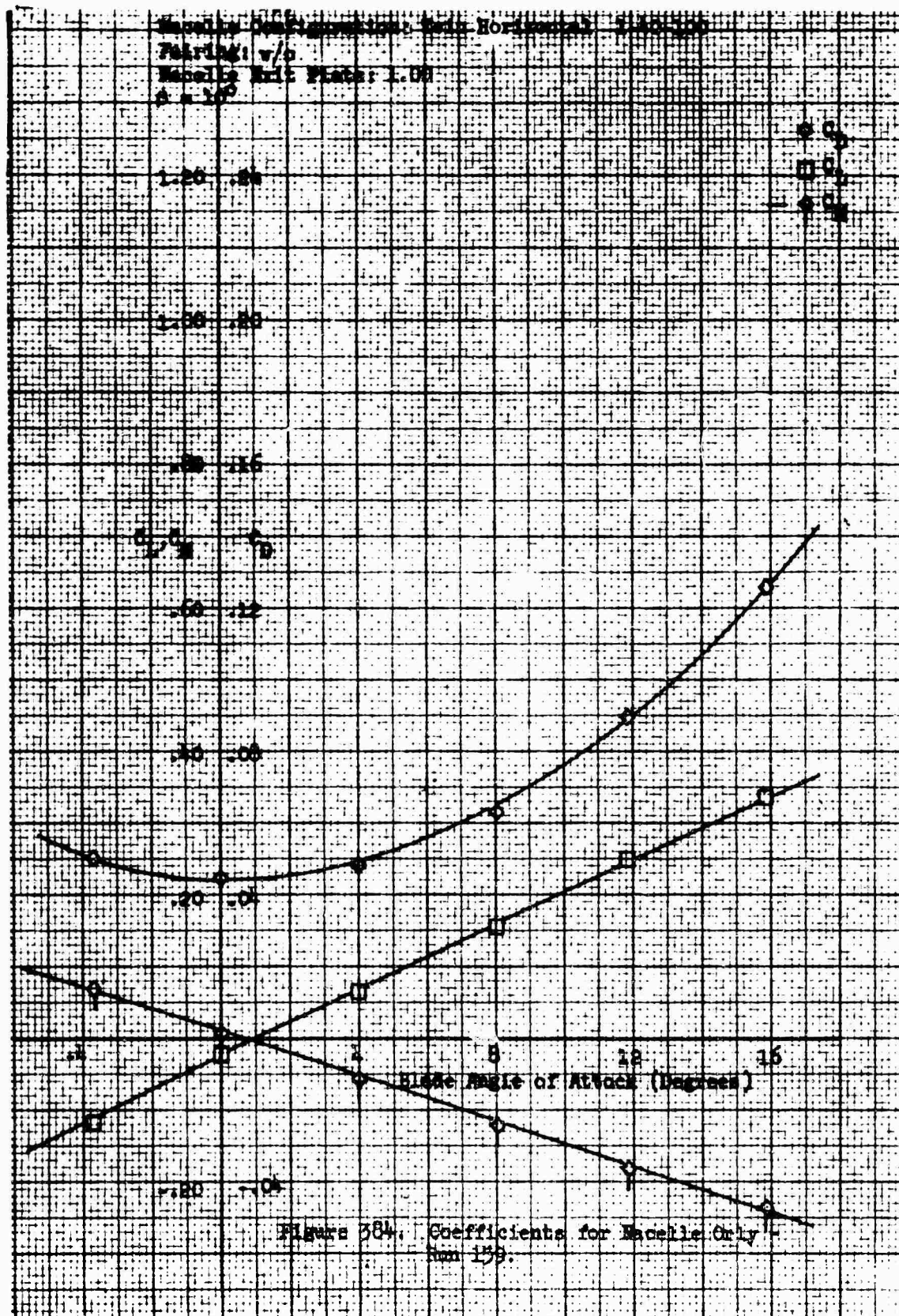


Figure 381. Coefficients for Combined Nacelle and Blade - Run -157.

Macelle Configuration: Twin Horizontal 1-40-100
 Pairing: w/o
 Macelle Exit Plate: 1.00
 $\beta = 20^\circ$







Macelle Configuration: Twin horizontal 1.40-1.00
 Macelle Incidence Angle: 0°
 Pairing: W/O
 Macelle Exit Plate: 1.00
 $\beta = 10^\circ$

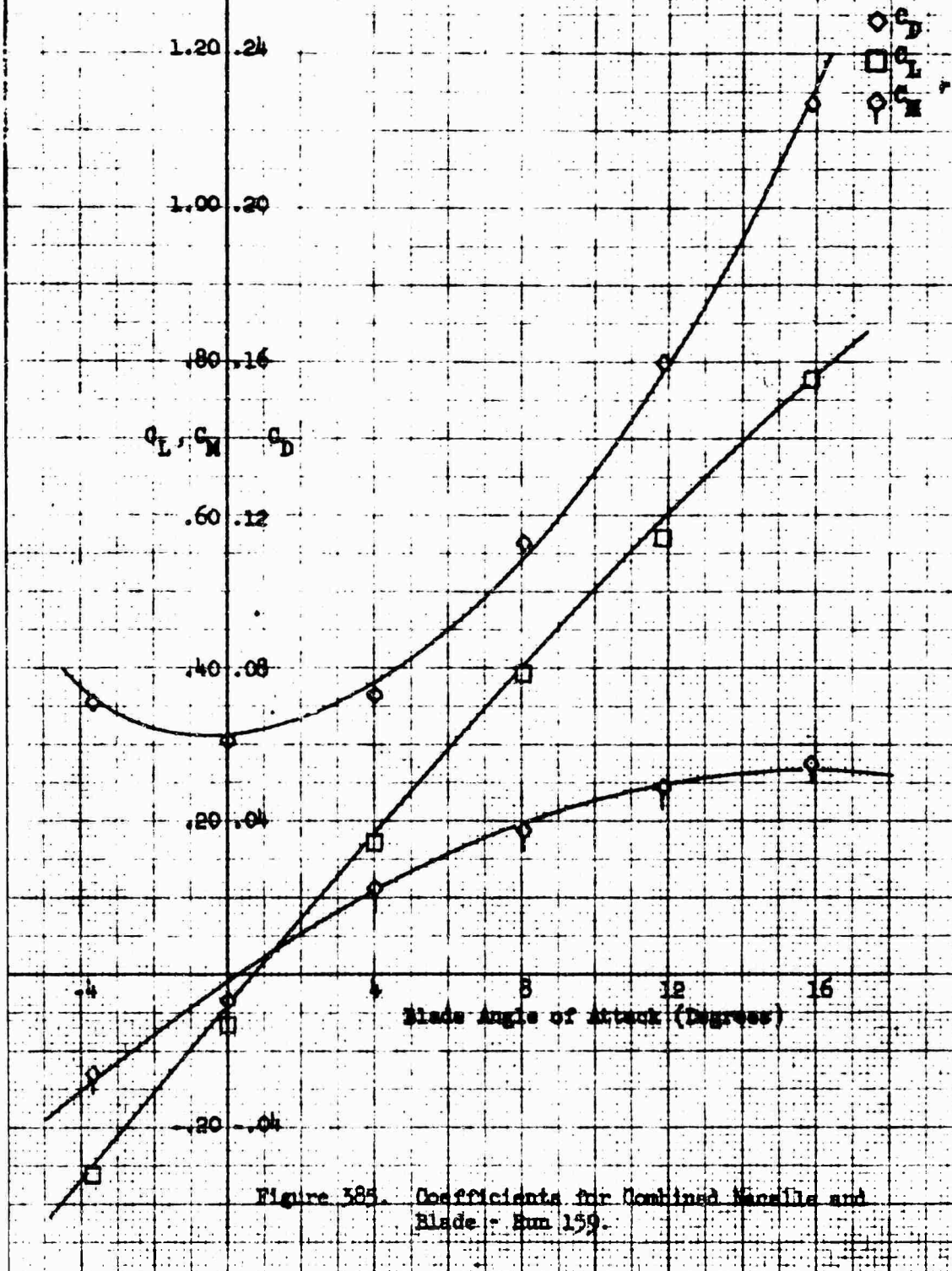


Figure 585. Coefficients for Combined Macelle and Blade - Run 159.

Nacelle Configuration: With Horizontal L-48-100
 Pairing: v/o
 Nacelle Exit Plate: 1.00
 $B = 0$

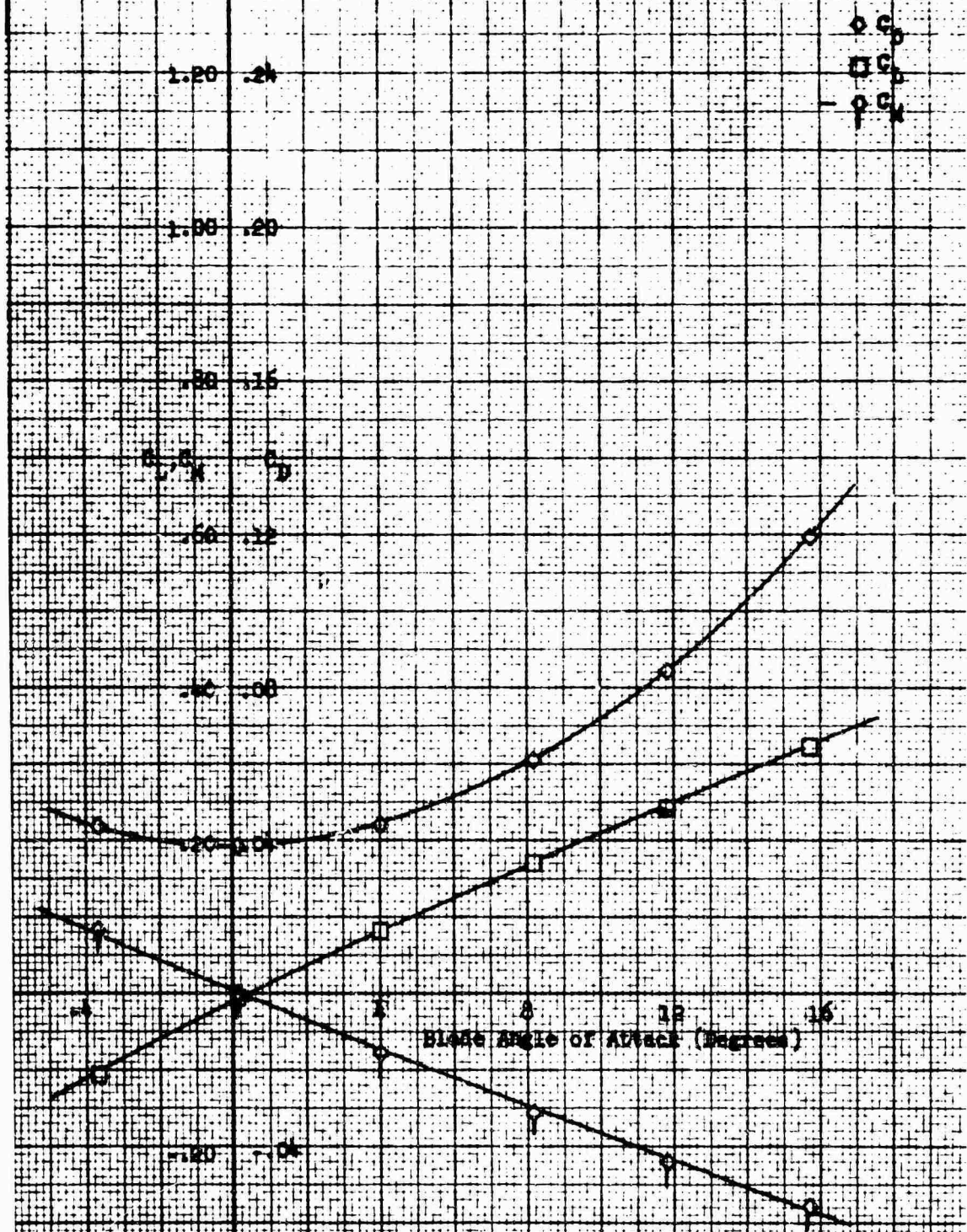


Figure 386. Coefficients for Nacelle Only - Run 100.

Macelle Configuration: Twin horizontal 1-40-100
 Macelle Incidence Angle: 0°
 Pairing: W/D
 Macelle Exit Ratio: 1.00
 $\beta = 0^\circ$

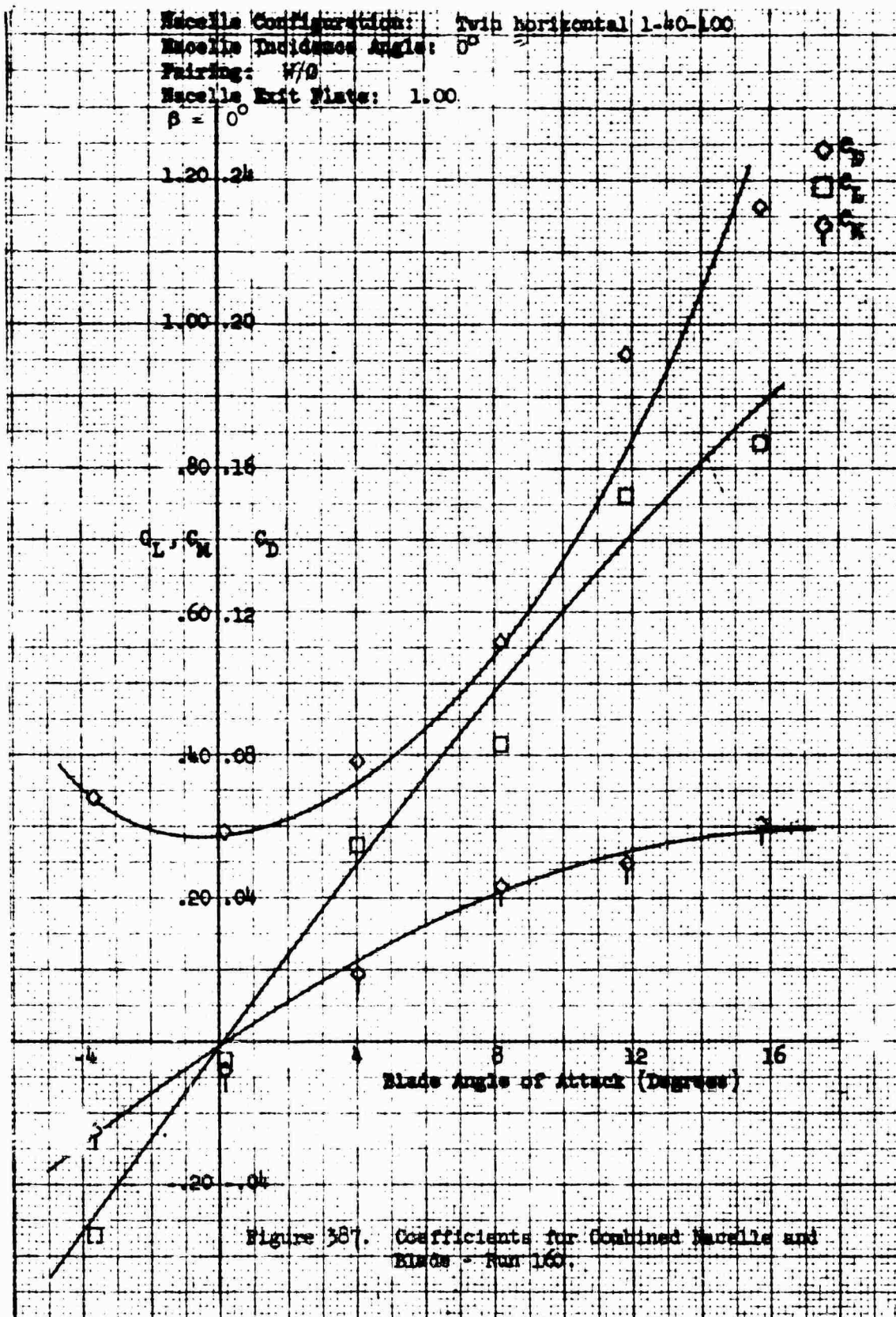
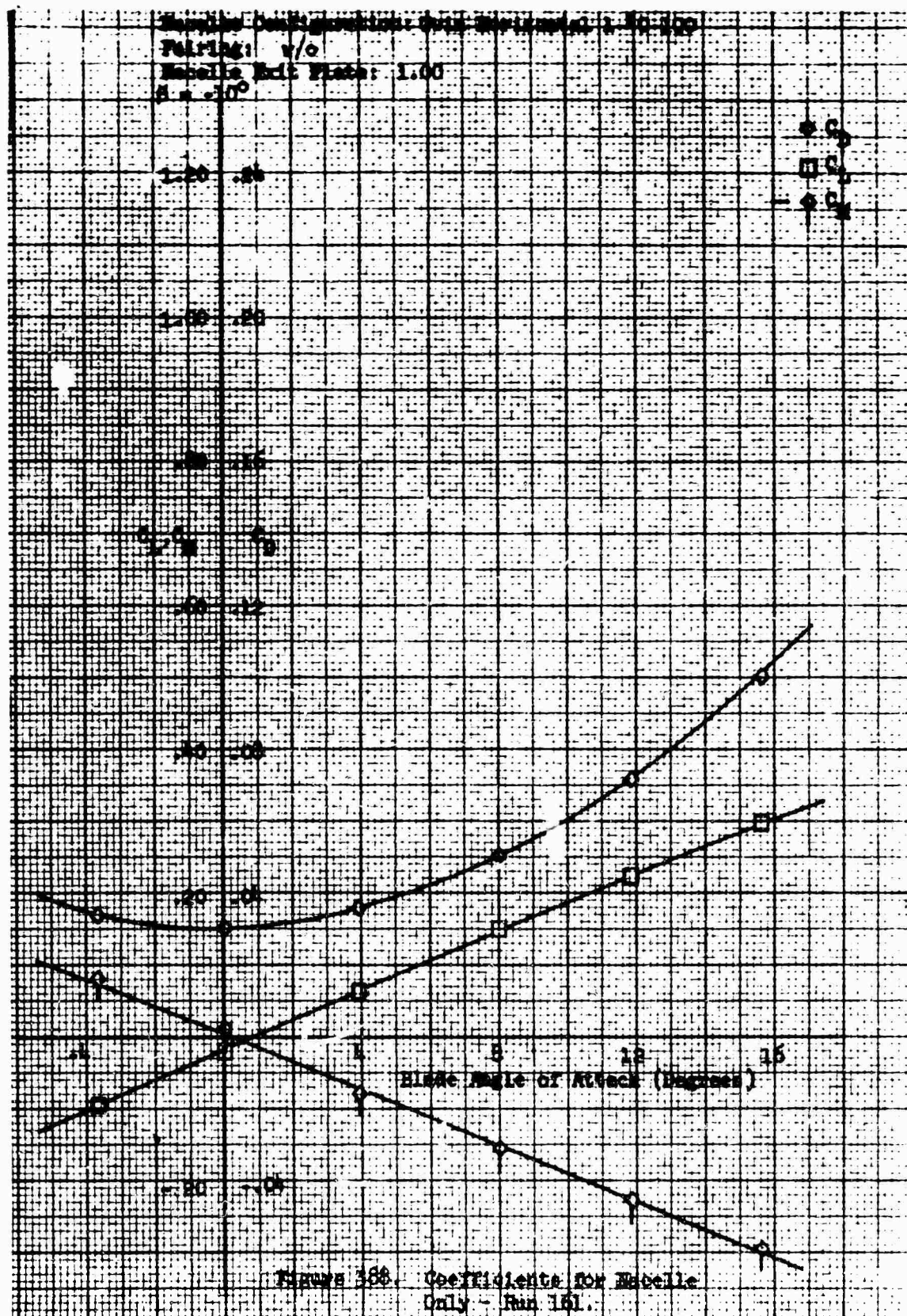


Figure 387. Coefficients for Combined Macelle and Blade - Run 160.



Macelle Configuration: Twin horizontal 1-40-100
 Macelle Incidence Angle: 0°
 Pairing: W/B
 Macelle Exit Plate: 1.00
 $\beta = -10^\circ$

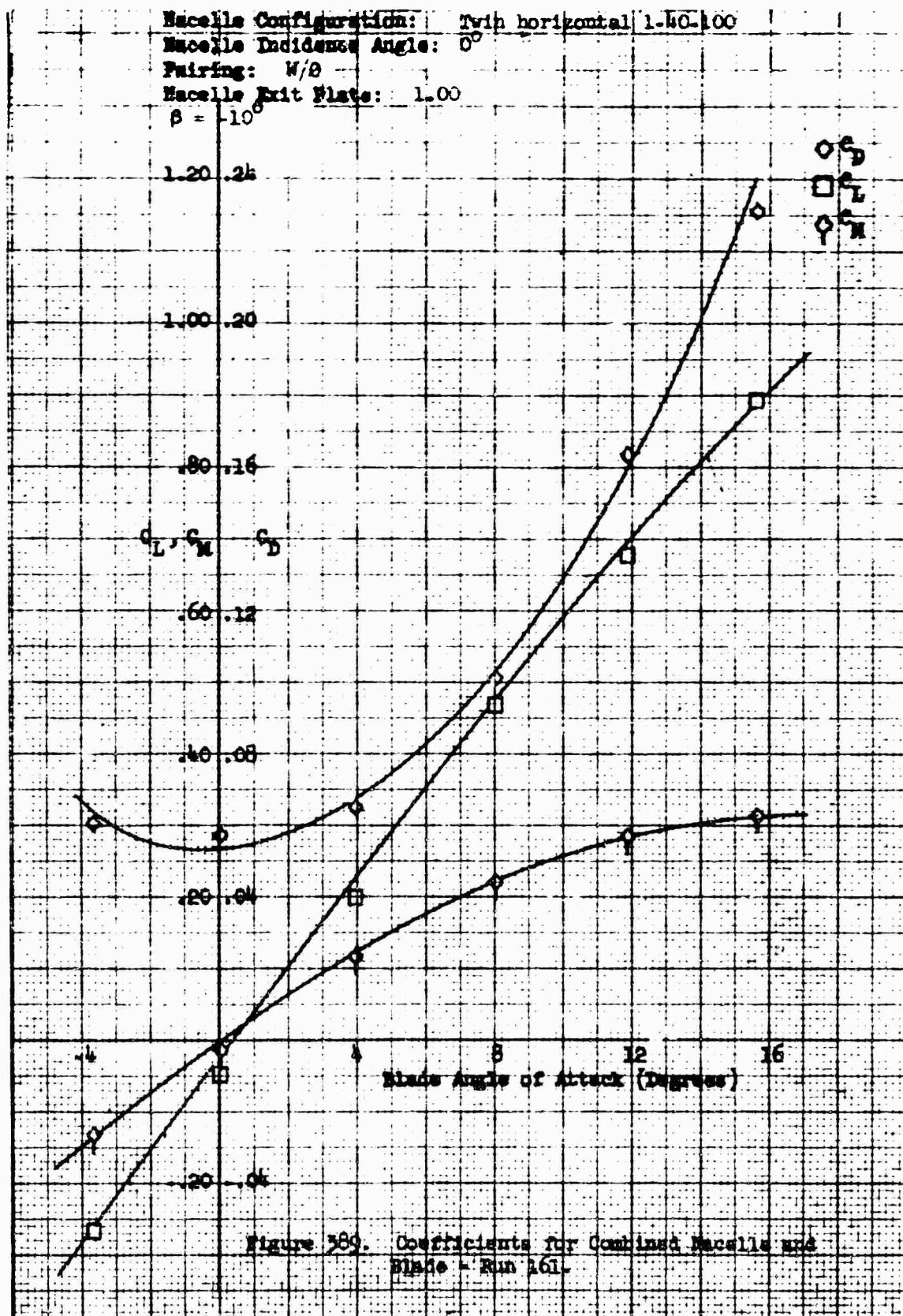


Figure 389. Coefficients for Combined Macelle and
 Blade - Run 161.

Nacelle Configuration: Twin Horizontal 14M1500
 Fairing: w/o
 Nacelle Exit Plate: 1.00
 $\beta = -20^\circ$

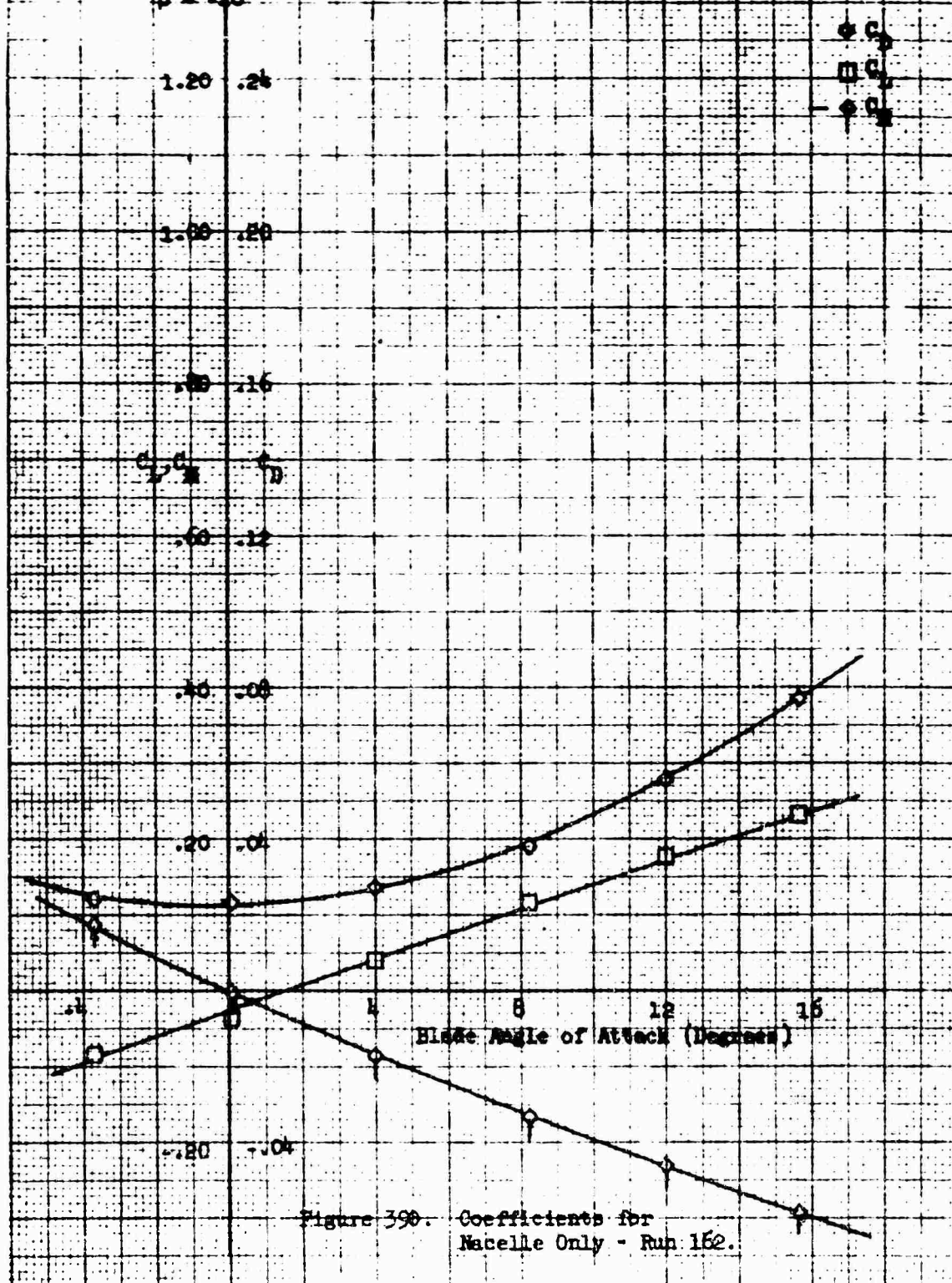
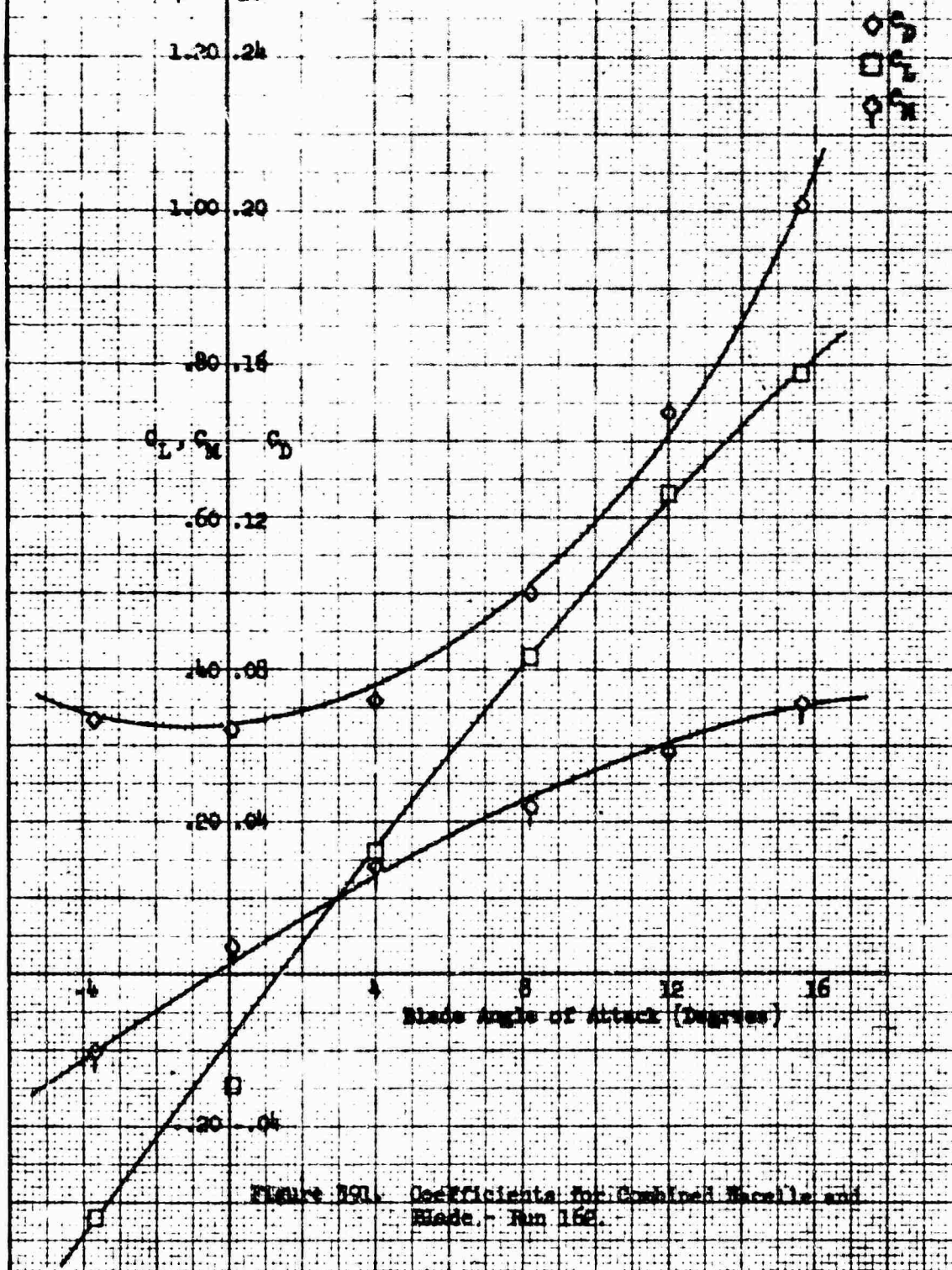
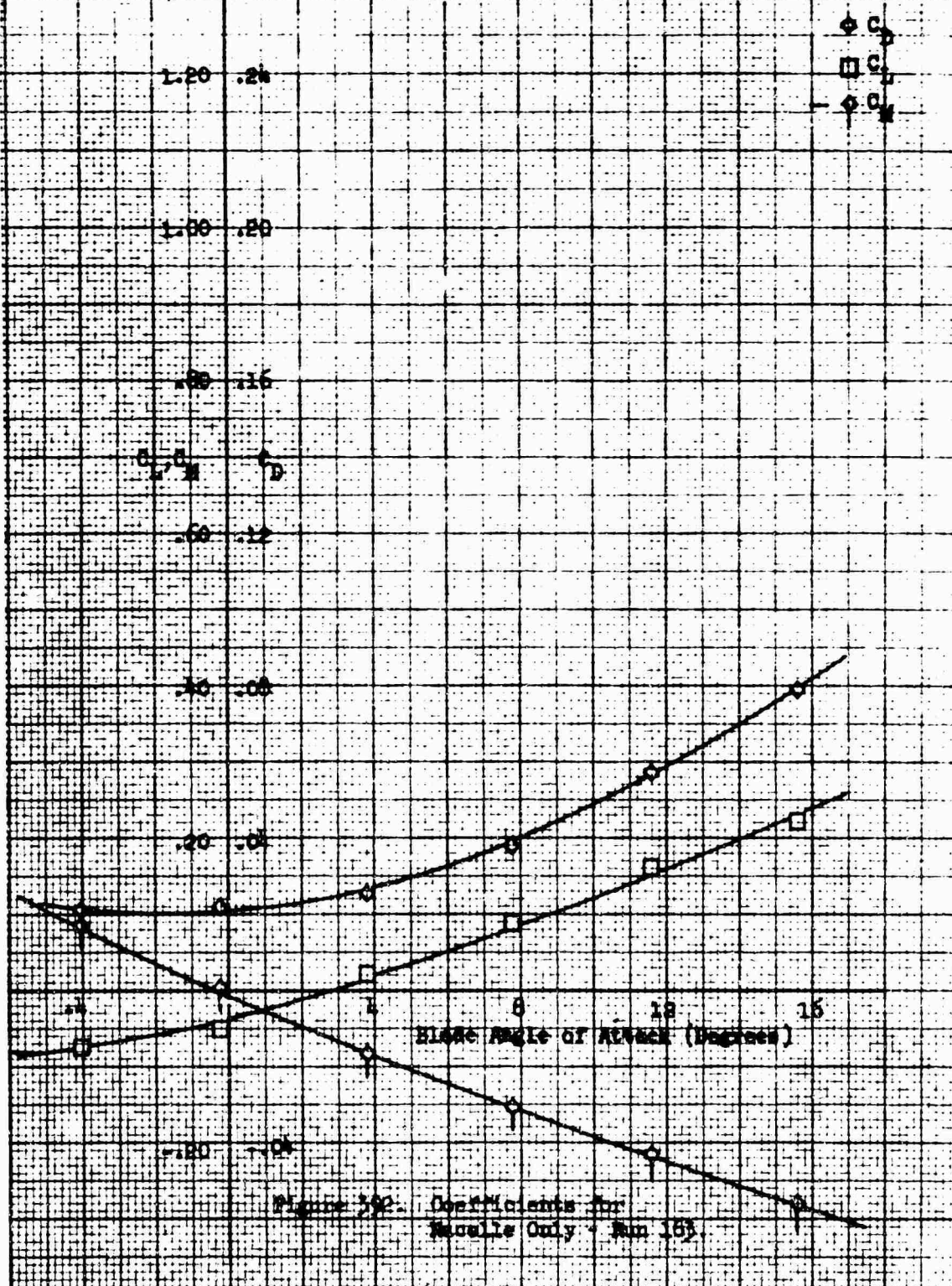


Figure 390. Coefficients for
 Nacelle Only - Run 152.

Macelle Configuration: Twin horizontal 1-40-100
 Macelle Incidence Angle: 0°
 Pairing: W/O
 Macelle Exit Plate: 1.00
 $\beta = -20^\circ$



Nacelle Configuration: Twin Horizontal 1.50-1.00
 Pairing: with
 Nacelle Exit Plate: 1.00
 $\beta = 20^\circ$



Macelle Configuration: Twin horizontal 1-40-100
 Macelle Incidence Angle: 0°
 Pairing: With
 Macelle Exit Plate: 1.00
 $\beta = 20^\circ$

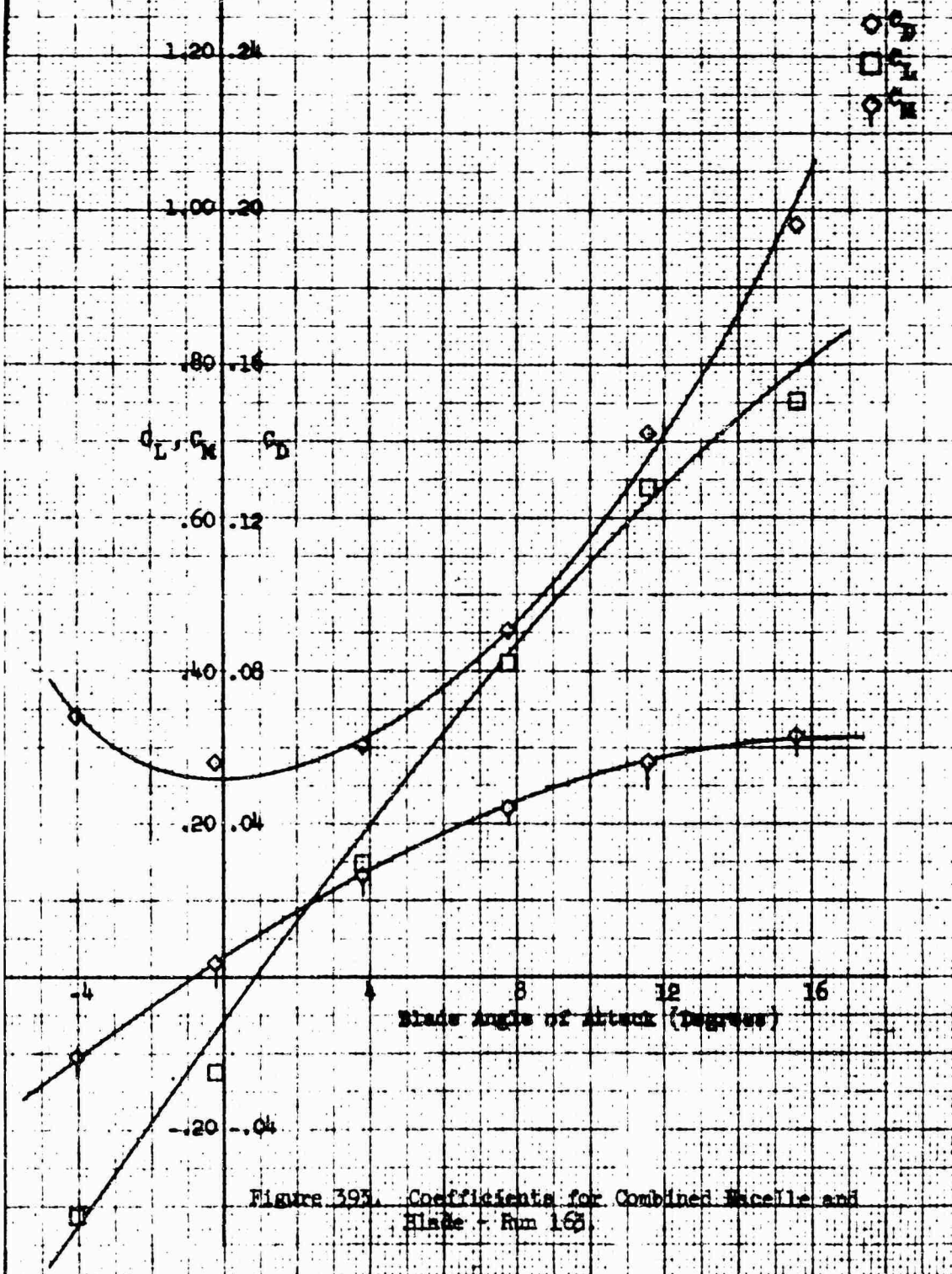


Figure 393. Coefficients for Combined Macelle and Blade - Run 163.

Nozzle Configuration: Semi Horizontal 1-20-100
 No. 124: Pith
 Nozzle Exit Plate: 1.00
 $\beta = 10^\circ$

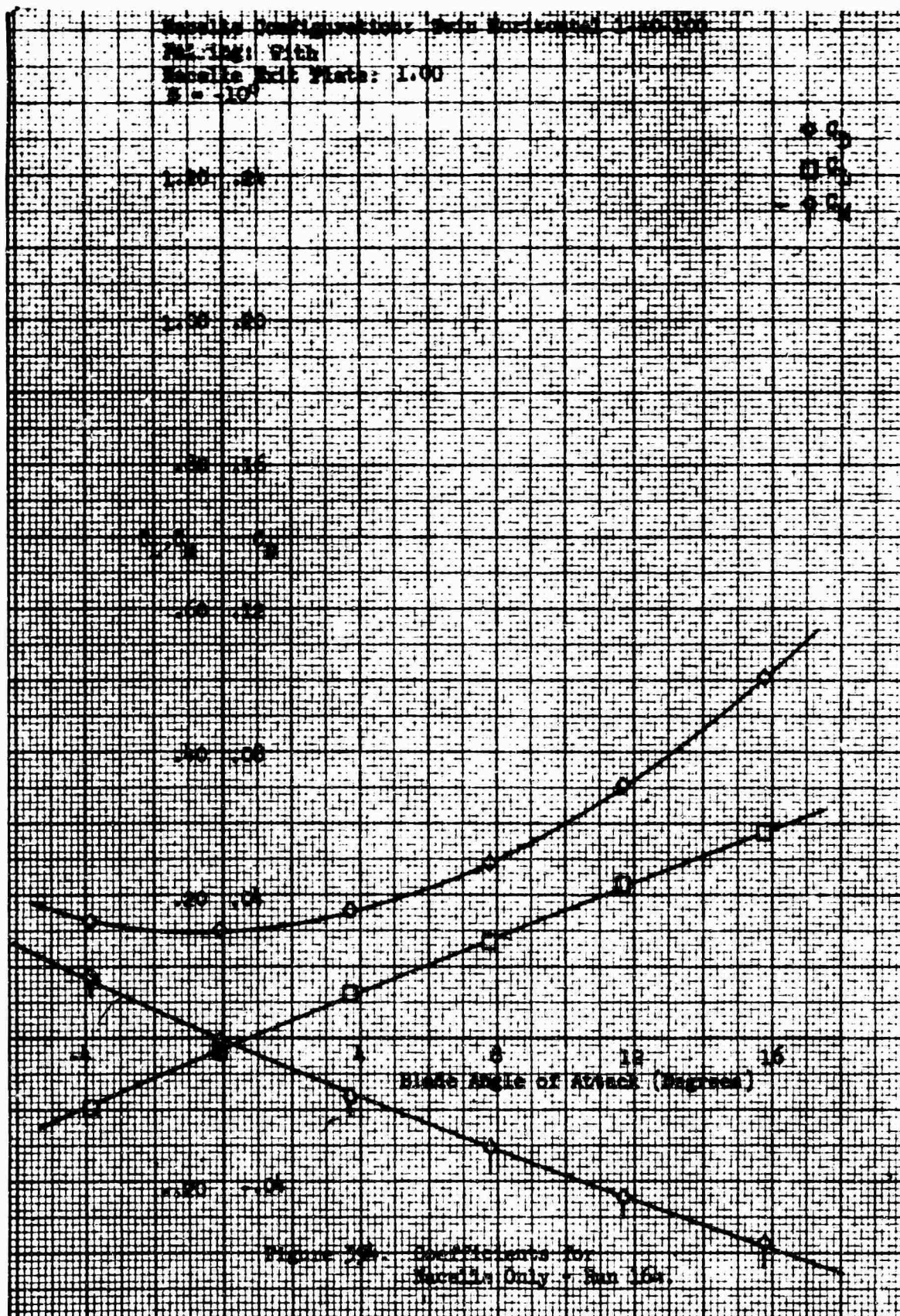
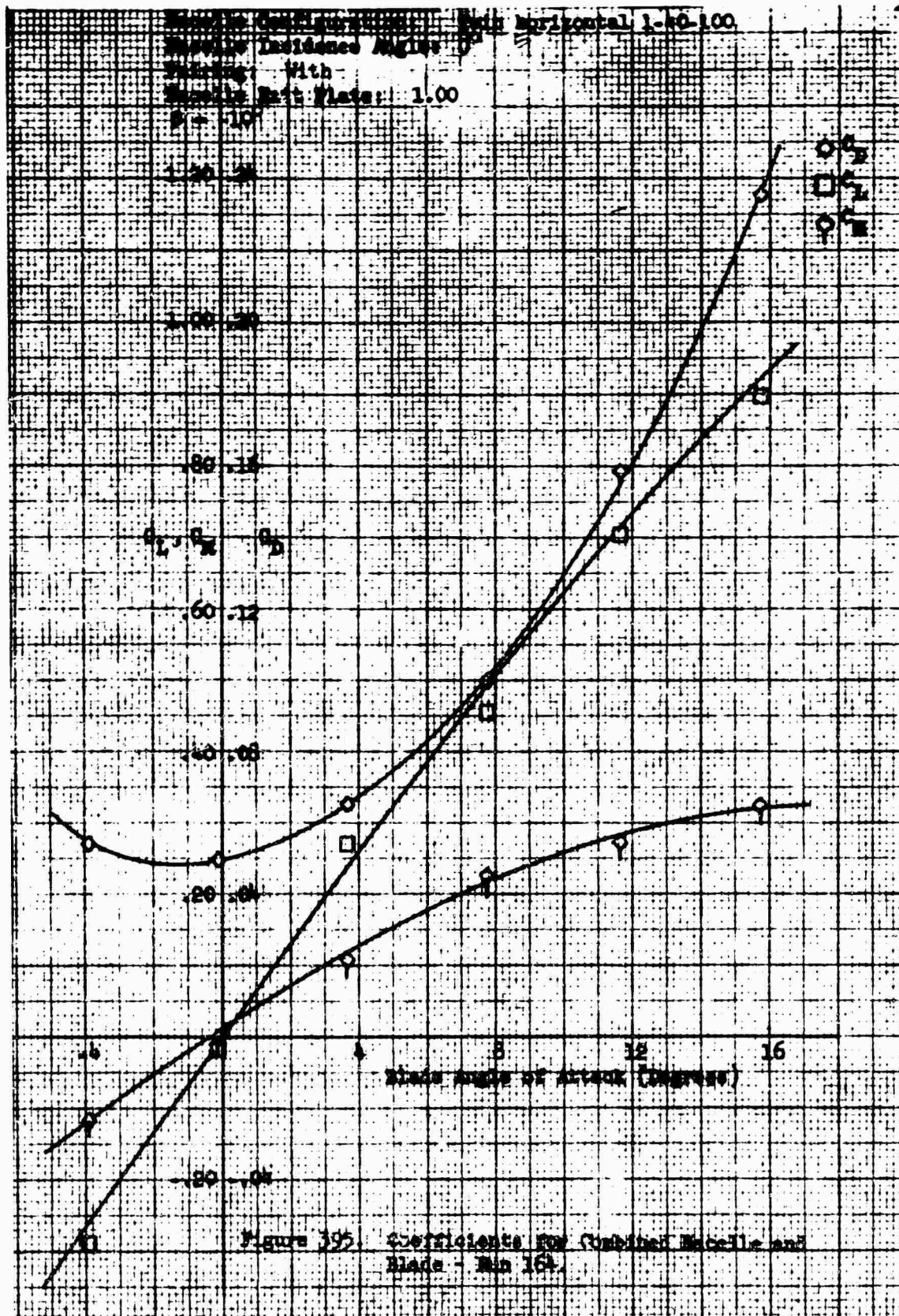


Figure 30 - Coefficients for
 Nozzle Only - Run 164



Blade Configuration: Twin Horizontal Pitch 90°
 Pairing: With
 Macellie Exit Plate: 1.00
 Run 0

Blade Angle of Attack (Degrees)	C_L (Circles)	C_D (Squares)	C_M (Diamonds)	C_T (Triangles)
0	0.00	0.00	0.00	0.00
2	0.05	0.02	-0.05	-0.02
4	0.10	0.04	-0.10	-0.04
6	0.15	0.06	-0.15	-0.06
8	0.20	0.08	-0.20	-0.08
10	0.25	0.10	-0.25	-0.10
12	0.30	0.12	-0.30	-0.12
14	0.35	0.14	-0.35	-0.14
16	0.40	0.16	-0.40	-0.16

Figure 32A. Coefficients for Macellie Only - Run 135.

Macelle Configuration: Twin horizontal 1-40-100
 Macelle Incidence Angle: 0°
 Fairing: With
 Macelle Exit Plate: 1.00
 $z = 0$

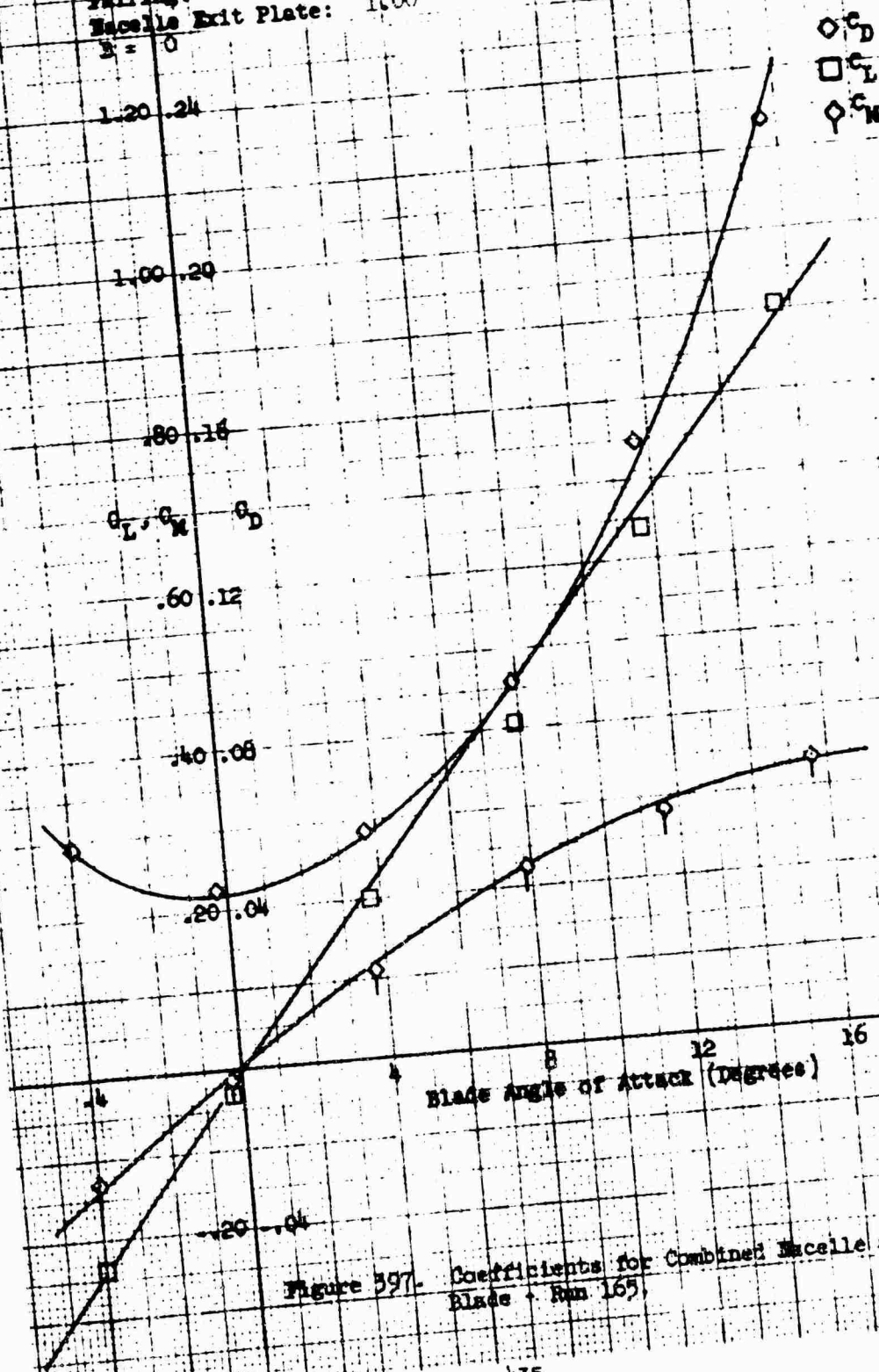
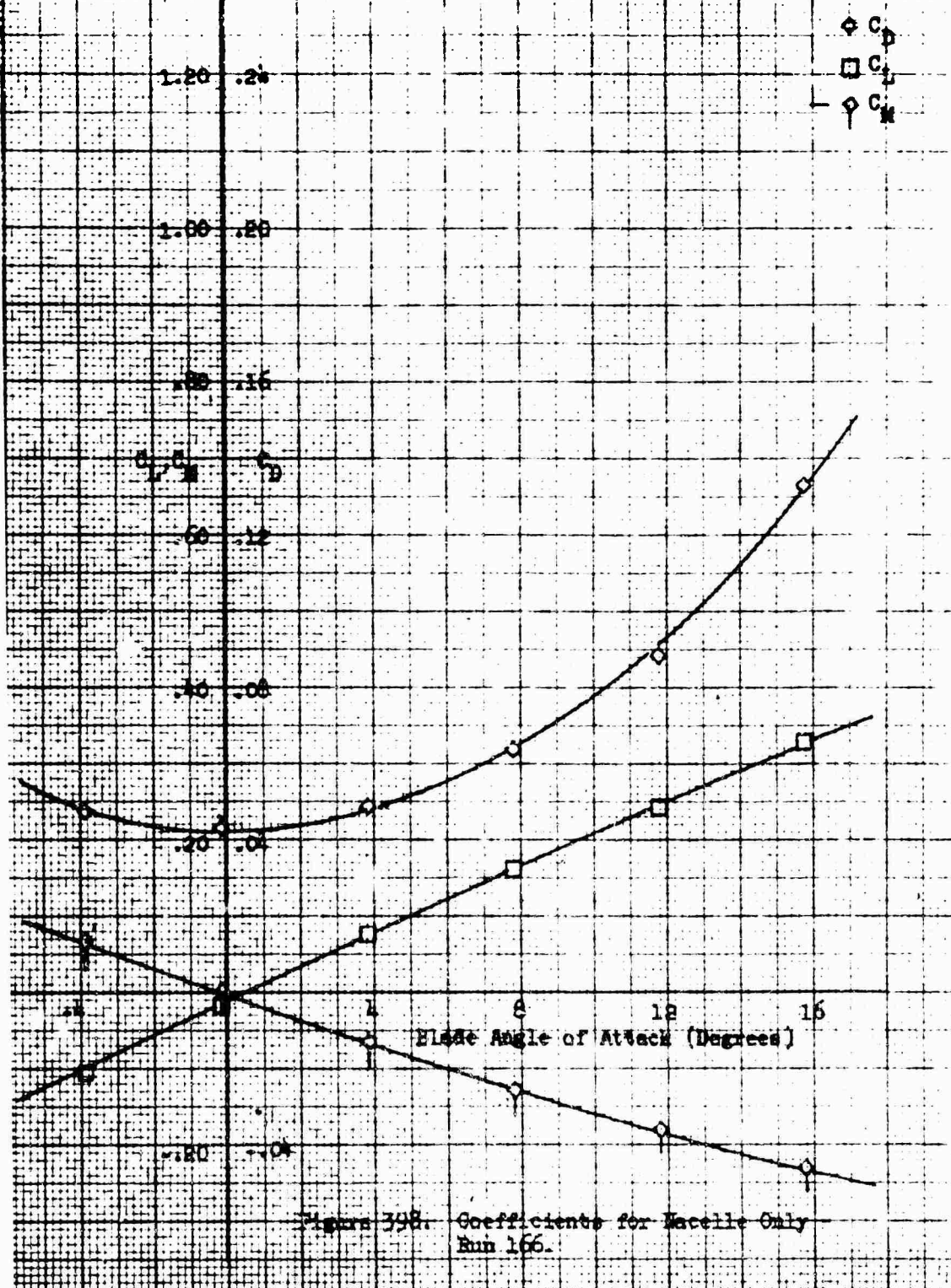


Figure 397. Coefficients for Combined Macelle and
 Blade - Run 165.

Macelle Configuration: Twin Horizontal 1-40-100
 Pairing: With
 Macelle Exit Plate: 1.00
 $\beta = 10^\circ$



Macelle Configuration: Twin horizontal 1-40-100
 Macelle Incidence Angle: 0°
 Pairing: With
 Macelle Exit Plate: 1.00
 $\beta = 10^\circ$

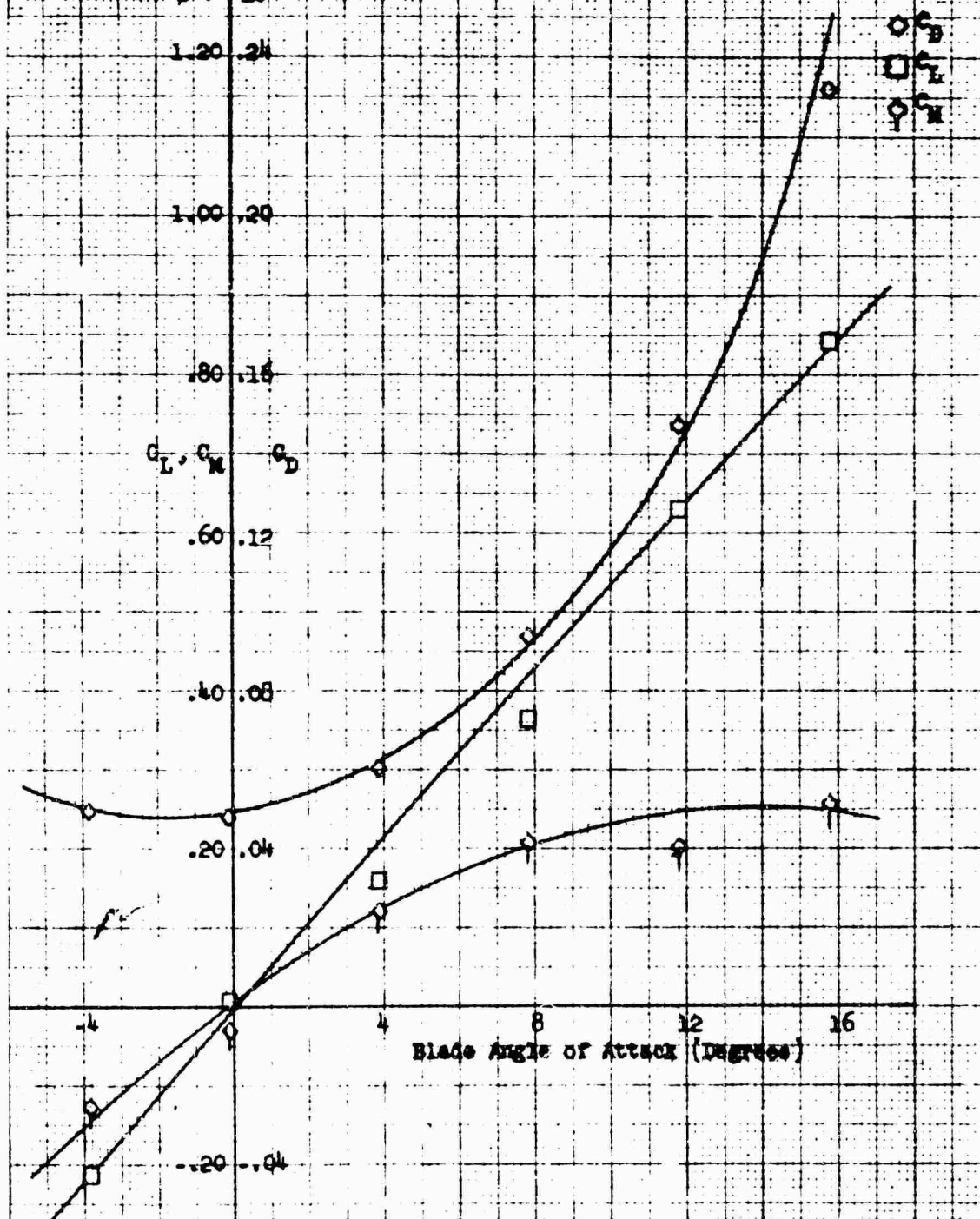


Figure 399. Coefficients for Combined Macelle and Blade - Run 166.

Nacelle Configuration: Twin Horizontal 1-40-100
 Pairing: With
 Nacelle Exit Plate: 1.00
 $\delta = 20^\circ$

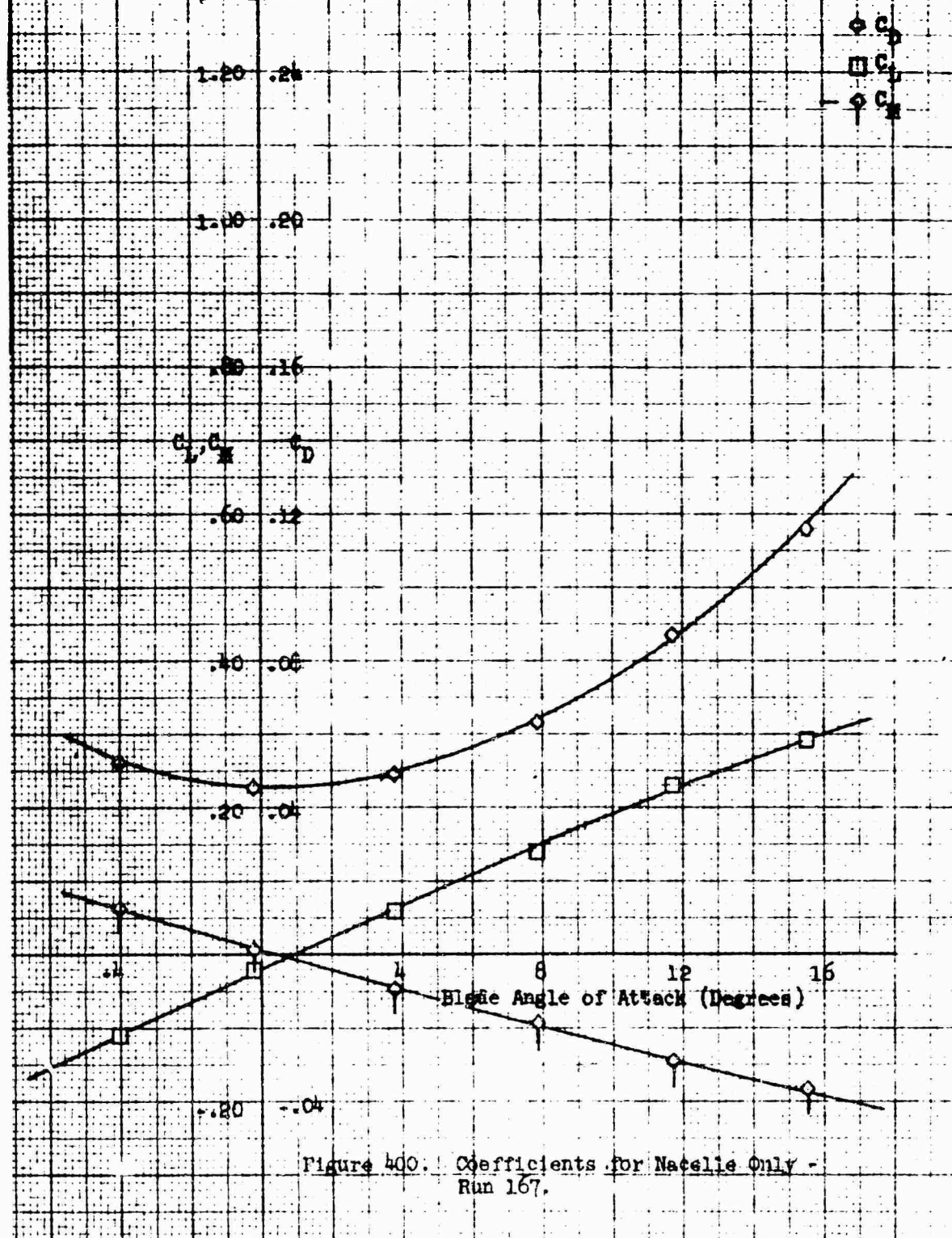


Figure 400. Coefficients for Nacelle Only -
 Run 167.

Macelle Configuration: Twin horizontal 1-40-100
 Macelle Incidence Angle: 0°
 Pairing: With
 Macelle Exit Plate: 1.00
 $\beta = 20^\circ$

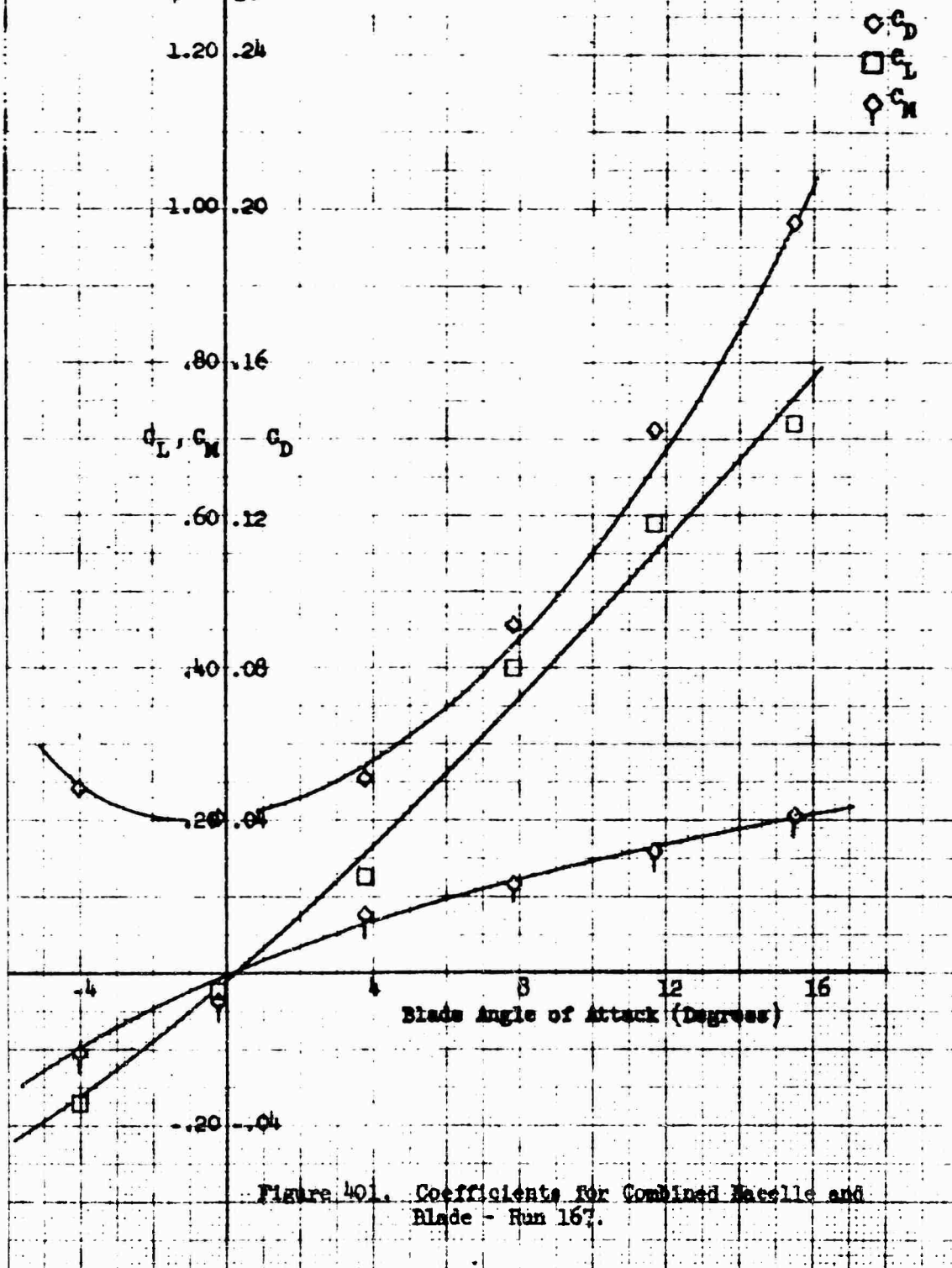


Figure 401. Coefficients for Combined Macelle and Blade - Run 167.

Macelle Configuration: Twin Horizontal 1.40-1.00

Fairings: With

Macelle Exit Plate: .95

$\beta = 20^\circ$

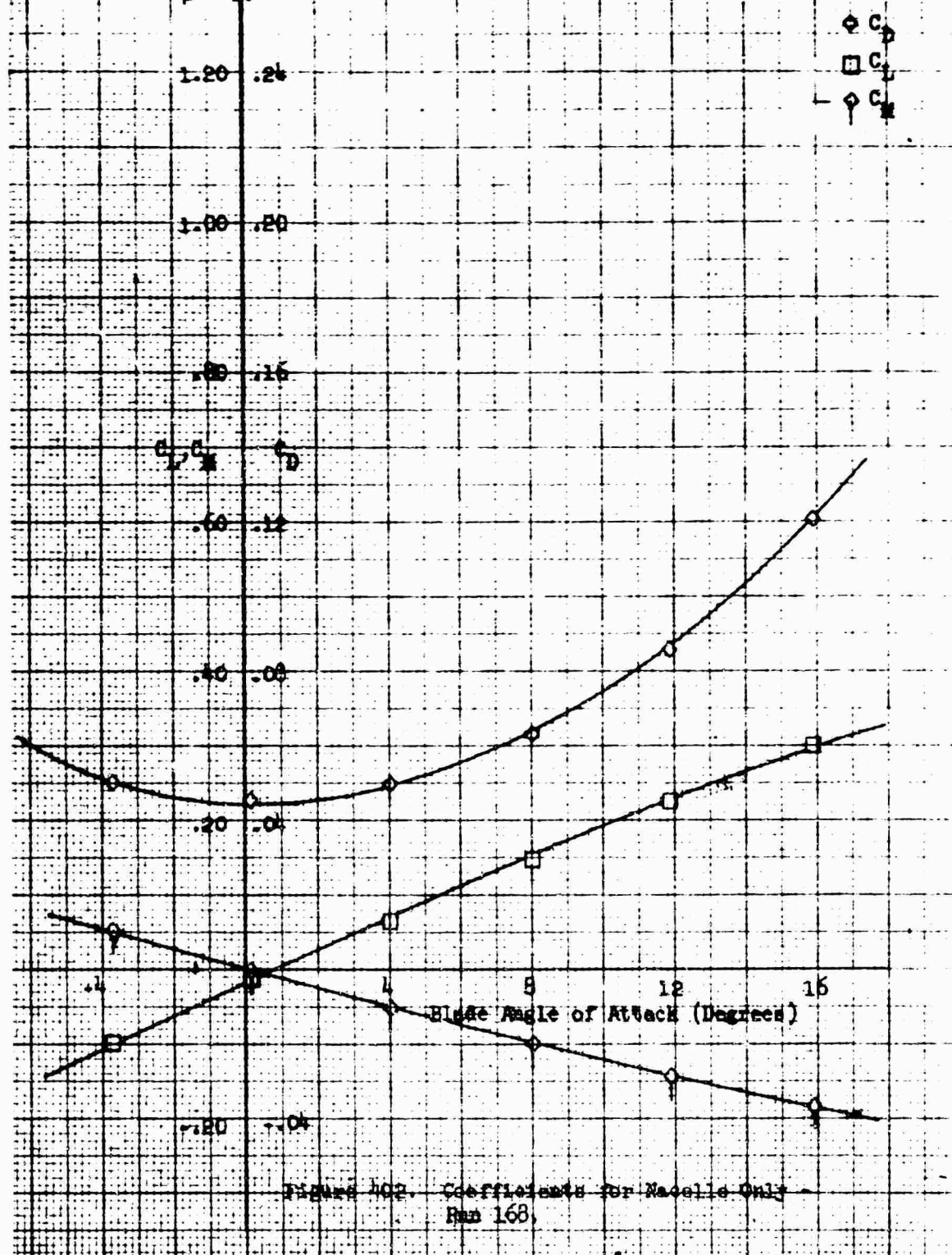


Figure 402. Coefficients for Macelle Only -
Run 168.

Racelle Configuration: Twin horizontal 1-40-100
 Racelle Incidence Angle: 0°
 Pairing: With
 Racelle Exit Flare: .95
 $\beta = 20^\circ$

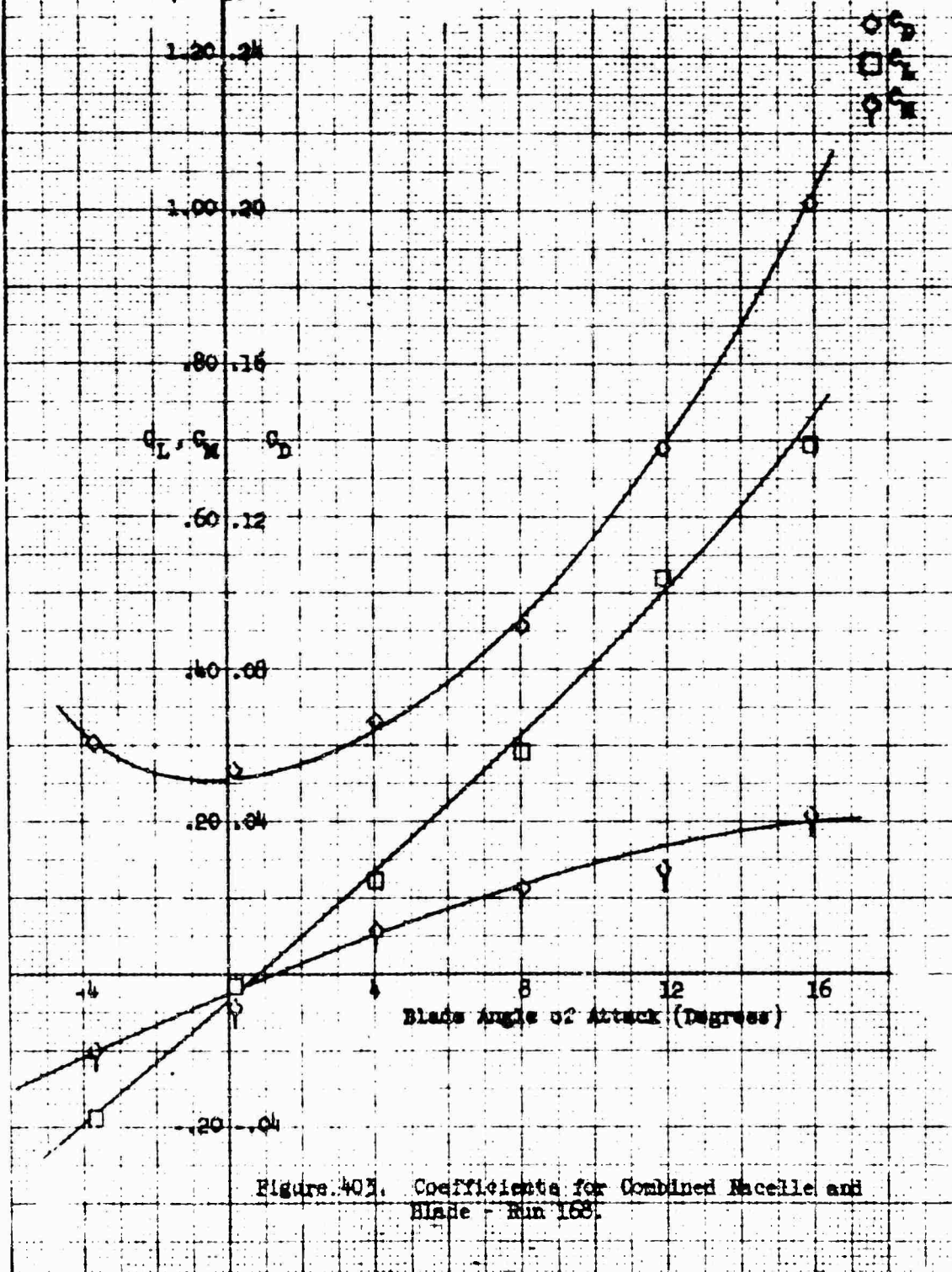


Figure 402. Coefficients for Combined Racelle and
 Blade - Run 168.

Nacelle Configuration: Twin Horizontal 1-10-100
 Fairing: With
 Nacelle Exit Plate: .95
 $\beta = 10^\circ$

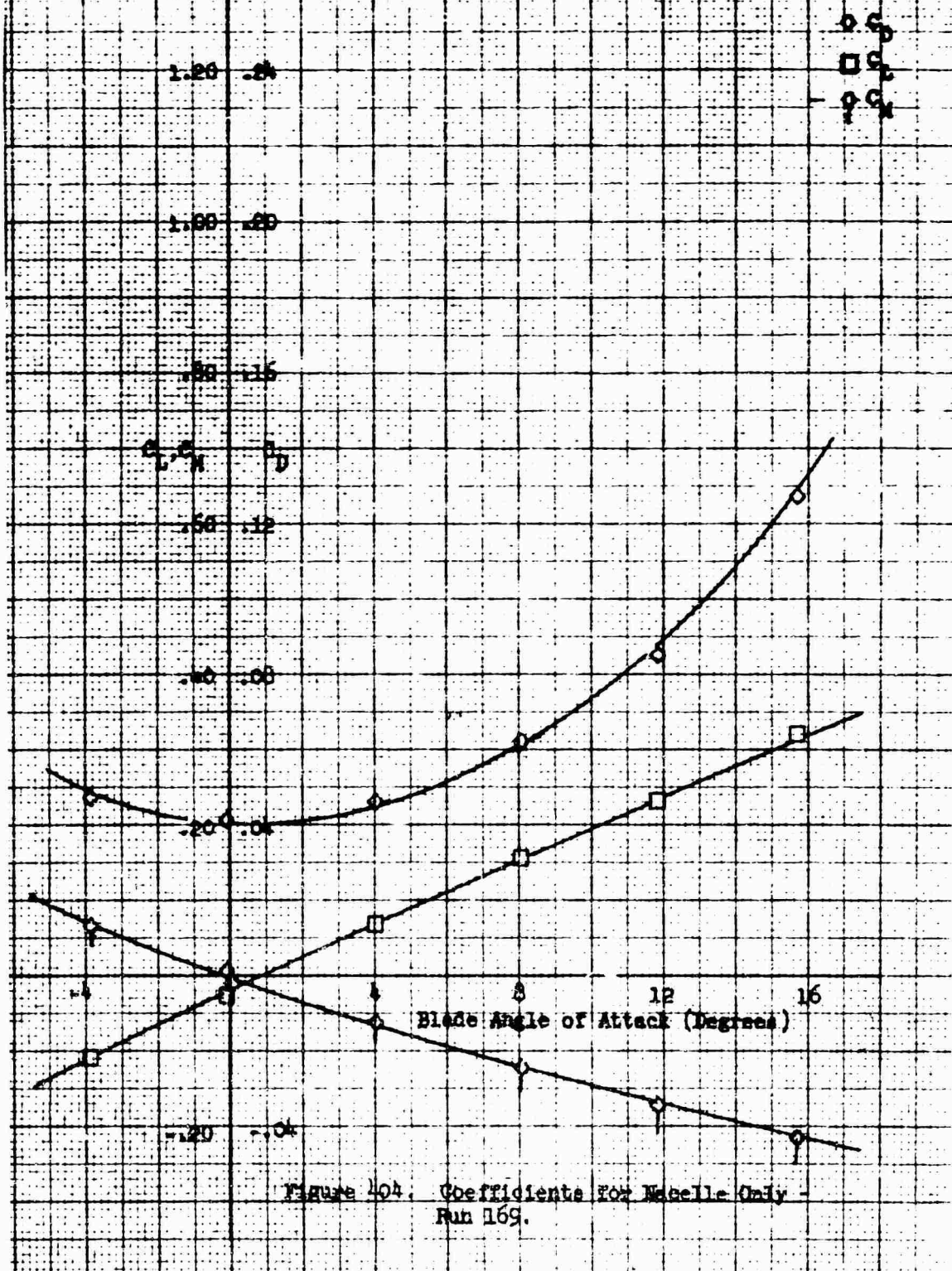
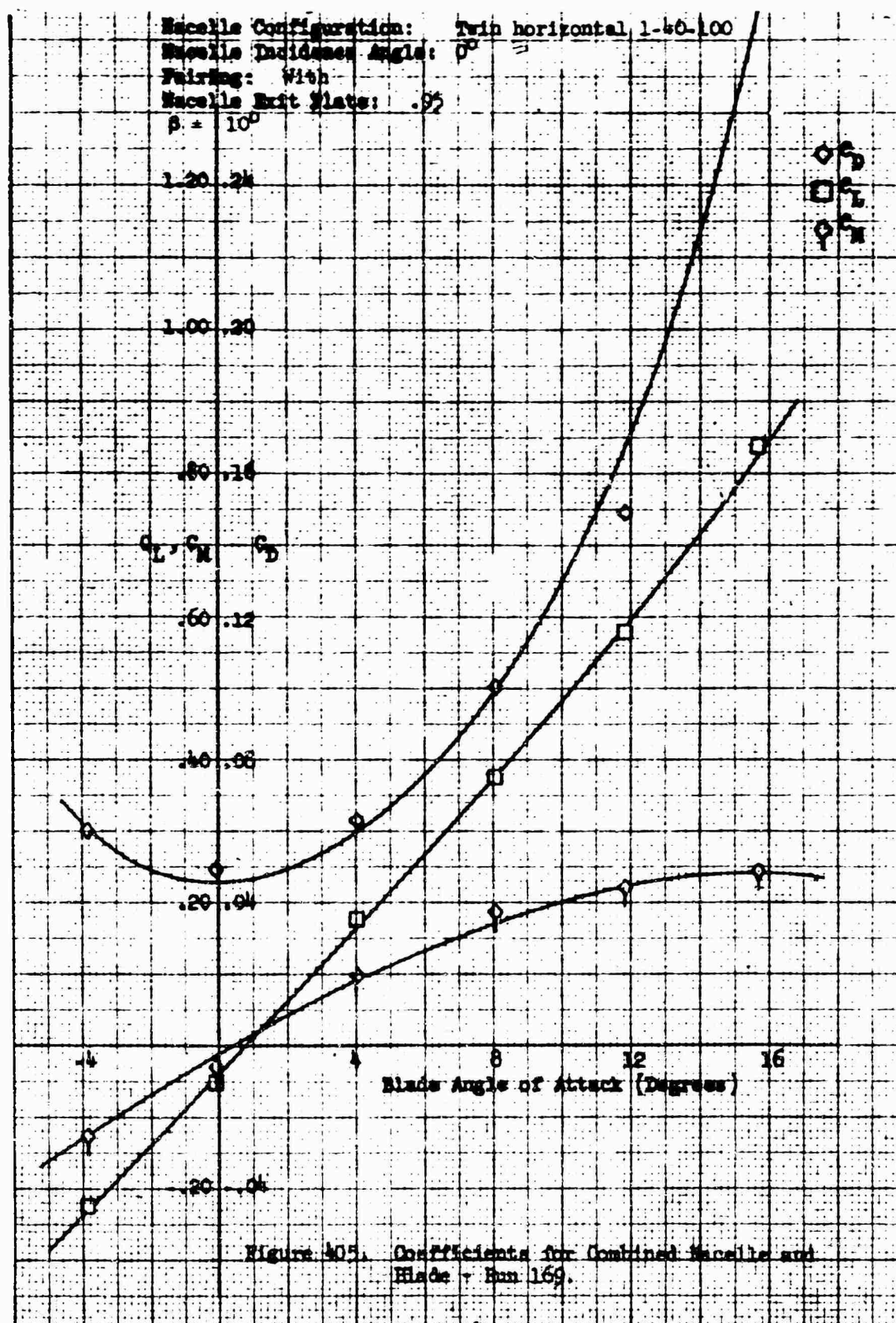


Figure 404. Coefficients for Nacelle Only -
 Run 169.



Nozzle Configuration: Type Horizontal 1-42-100
 Pairing: With
 Nozzle Exit Plate: .95
 $\beta = 0$

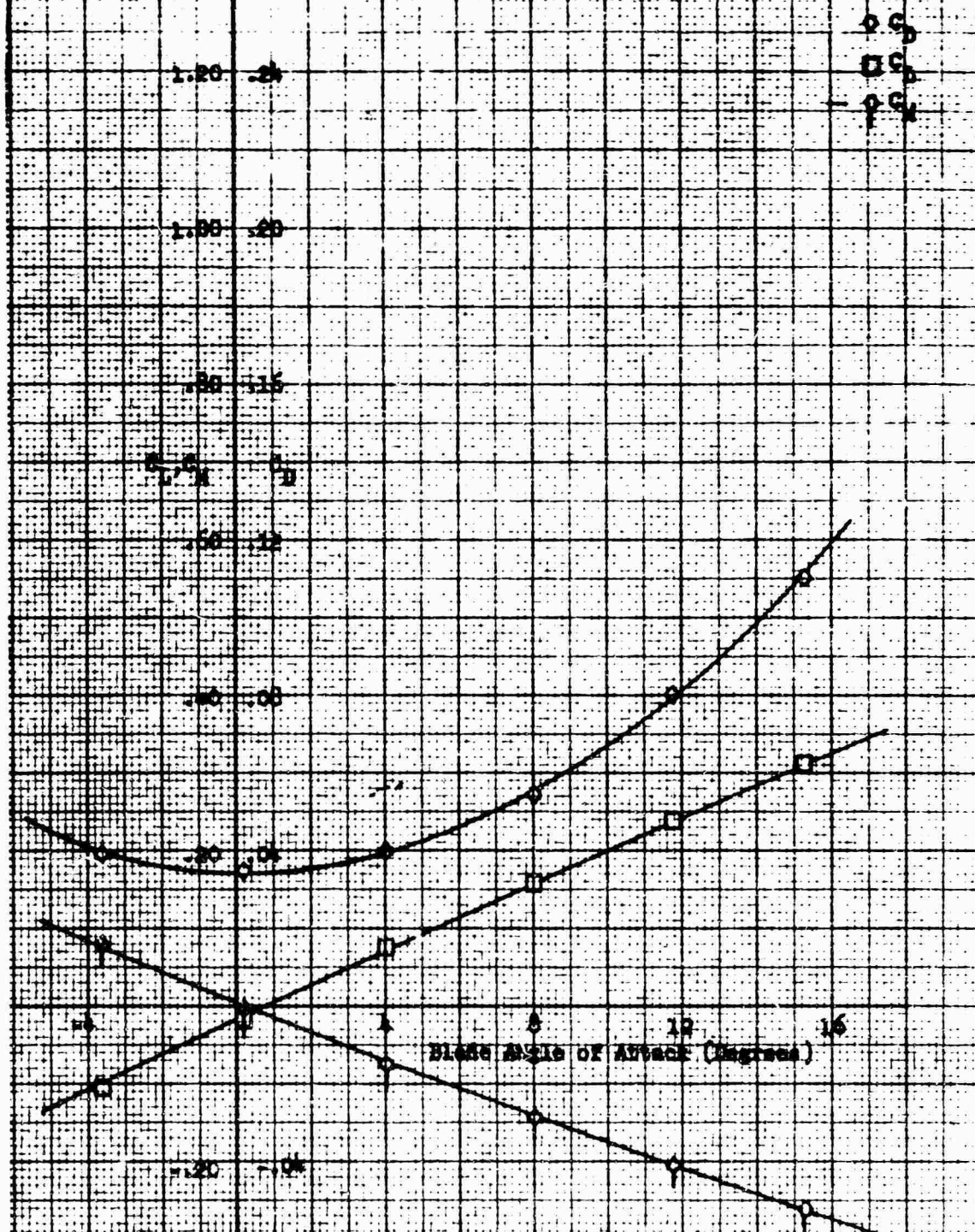


Figure 406. Coefficients for Nozzle Only -
 Run 10.

Racelle Configuration: Twin horizontal 1, 0.100
 Racelle Incidence Angle: 0°
 Firing: With
 Racelle Exit Plate: .92
 $\beta = 0$

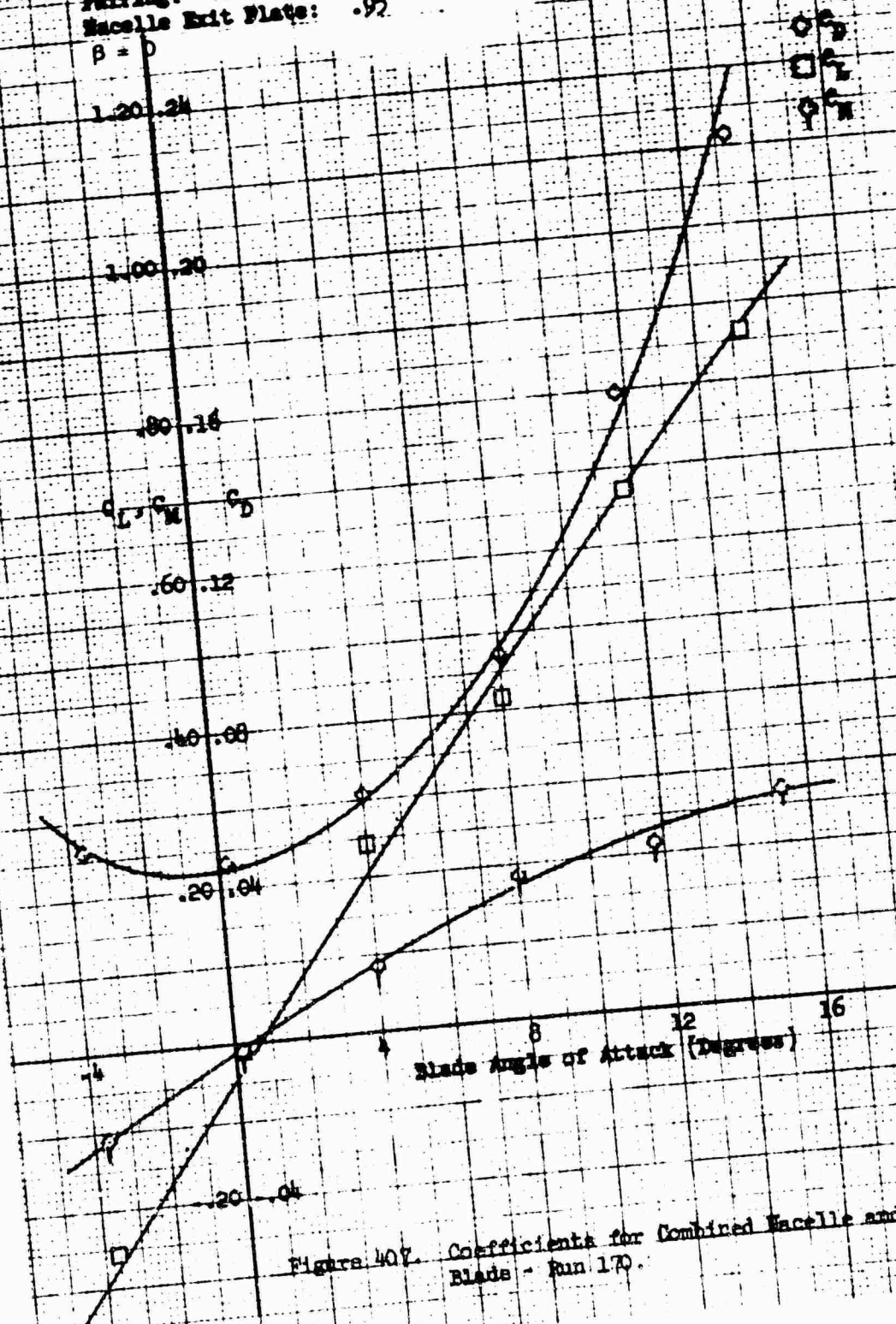
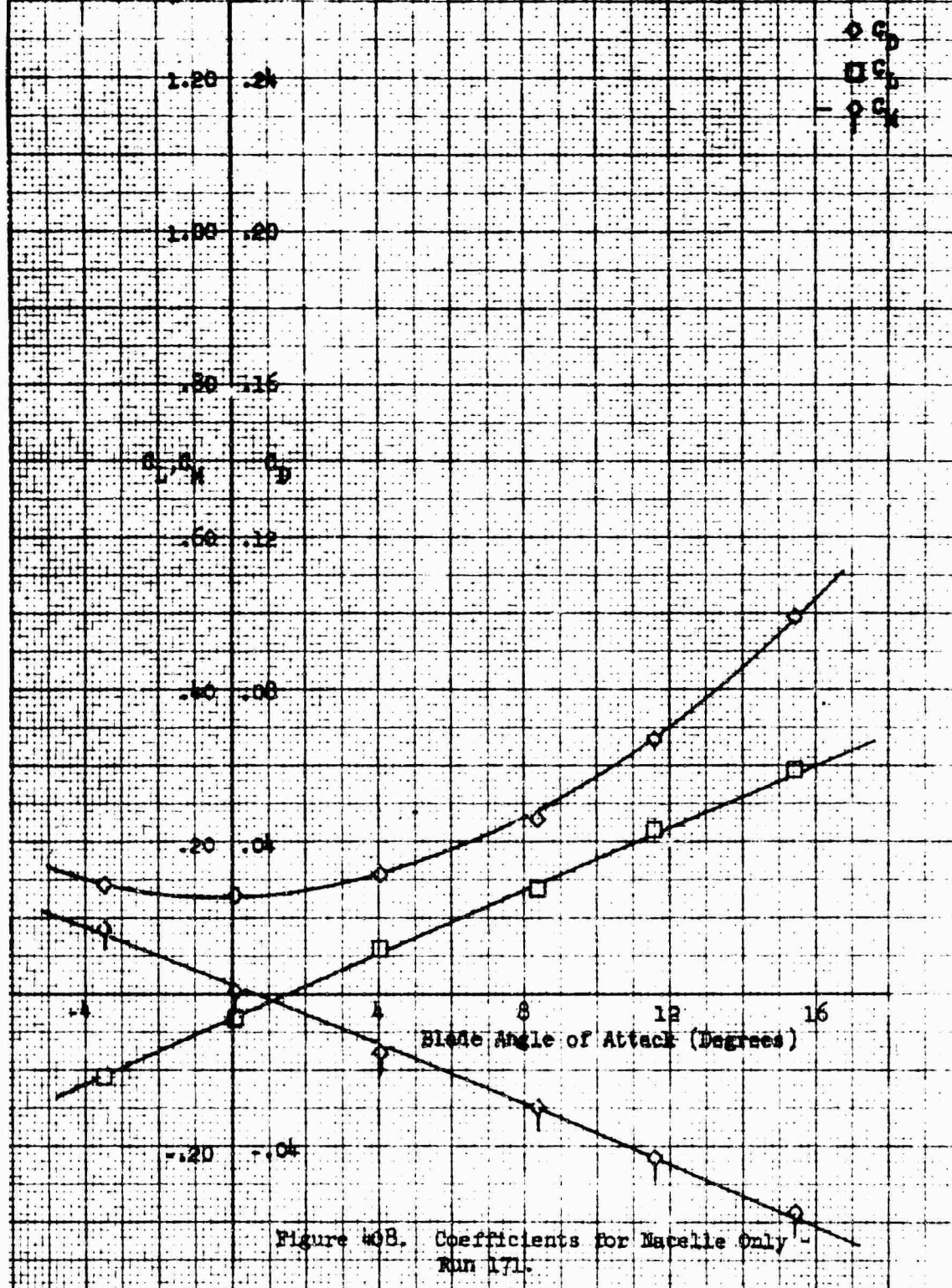


Figure 407. Coefficients for Combined Racelle and Blade - Run 170.

Nacelle Configuration: Twin Horizontal 144B-150
 Feeding: With
 Nacelle Exit Plate: .95
 $\alpha = -10^\circ$



Macelle Configuration: Twin Horizontal 1-50-100
 Macelle Incidence Angle: 0°
 Pairing: With
 Macelle Exit Plate: .92
 $\beta = -10^\circ$

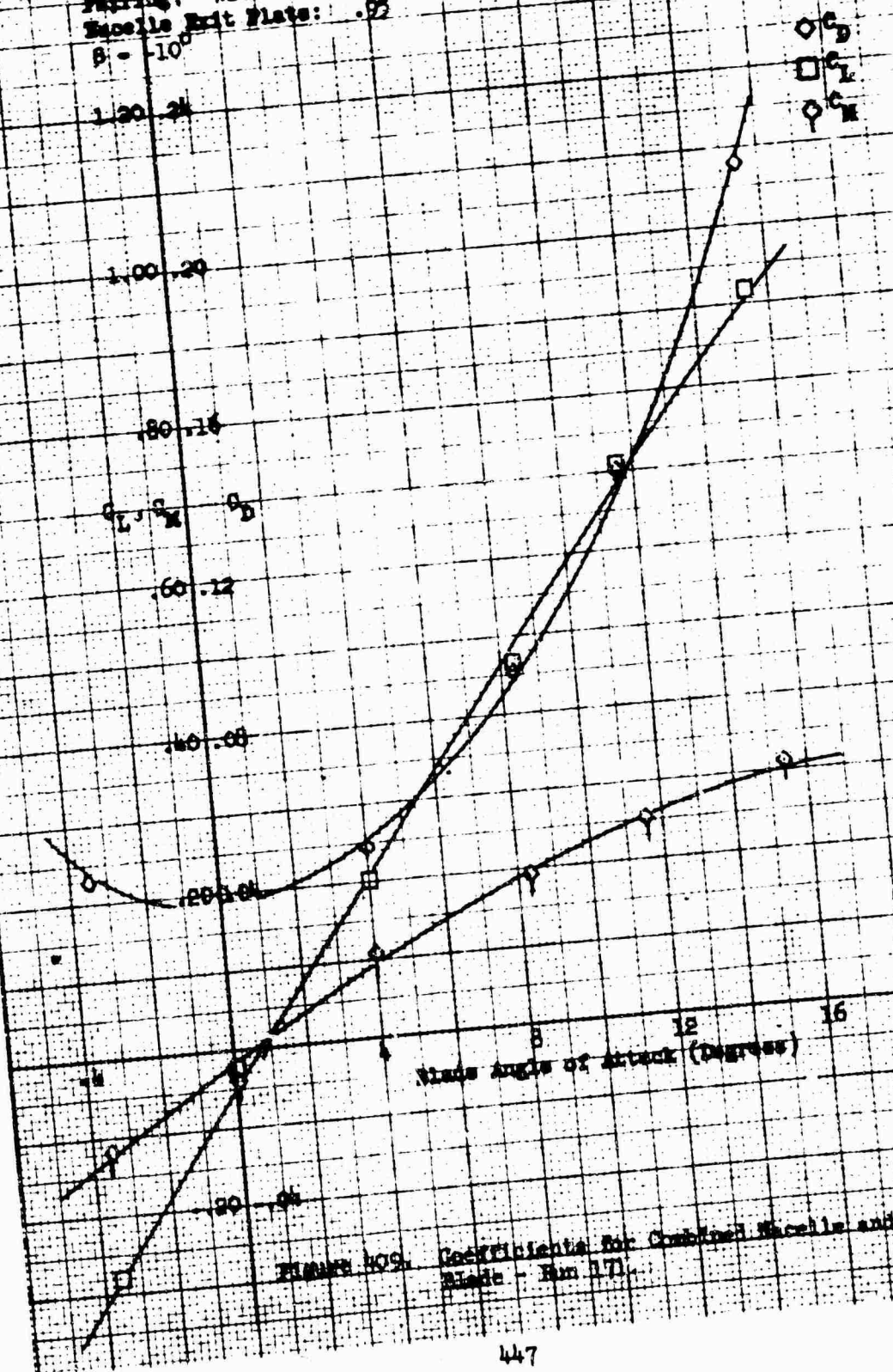
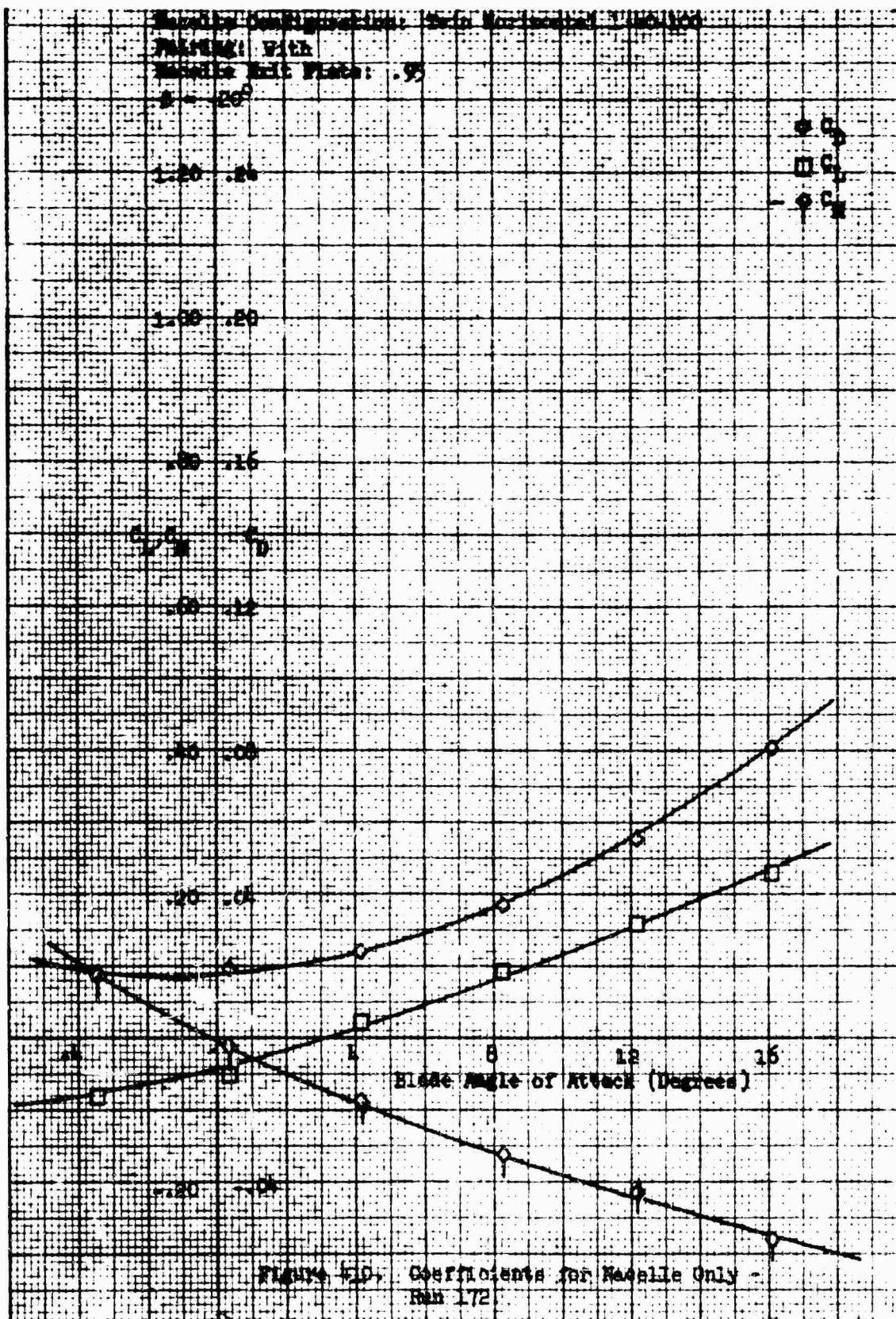
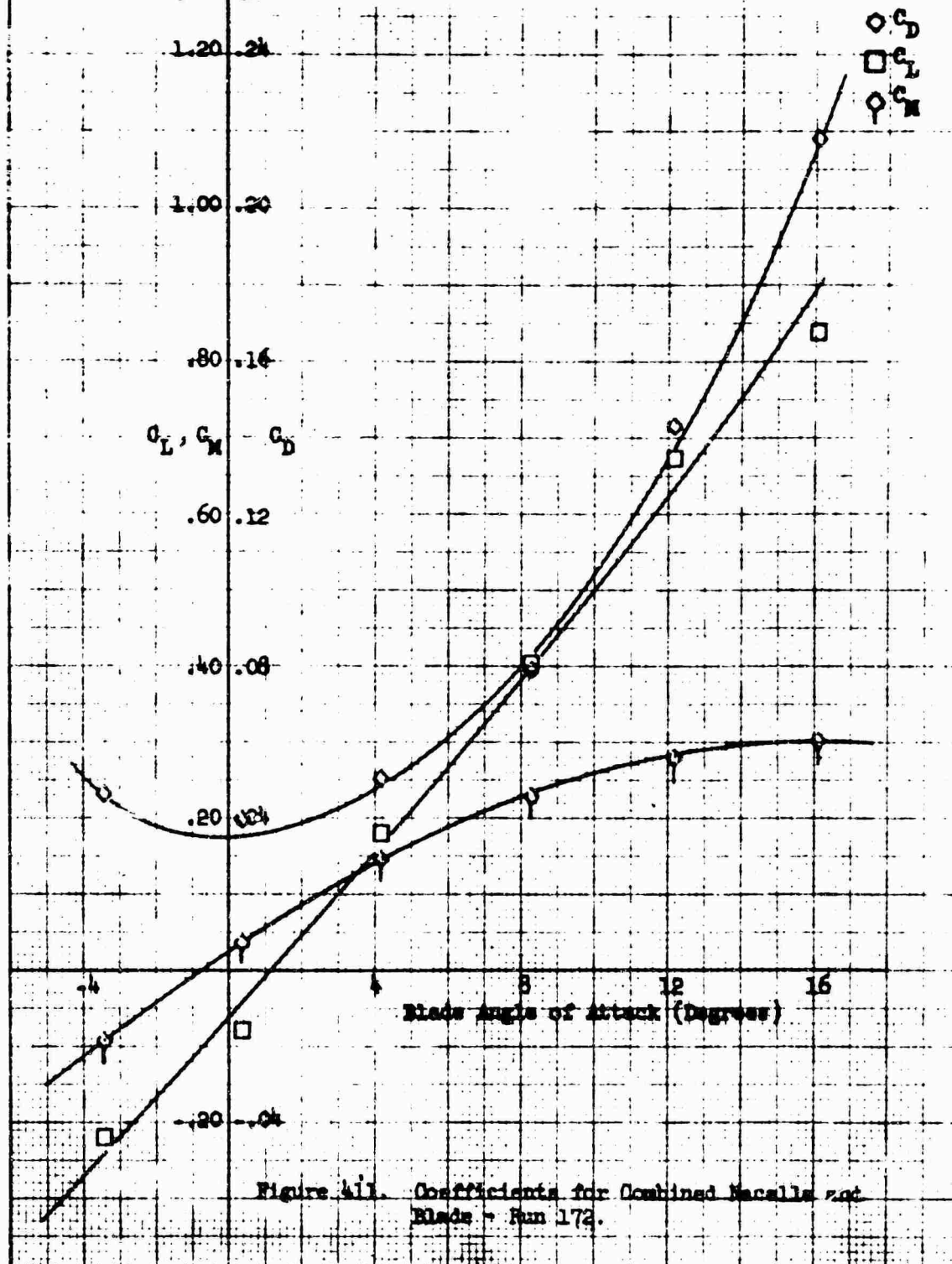


FIGURE 409. Coefficients for Combined Macelle and
 Blade - Run 171.



Macelle Configuration: Twin horizontal 1-40-100
 Macelle Incidence Angle: 0°
 Pairing: With
 Macelle Exit Plate: .95
 $\beta = -20^\circ$

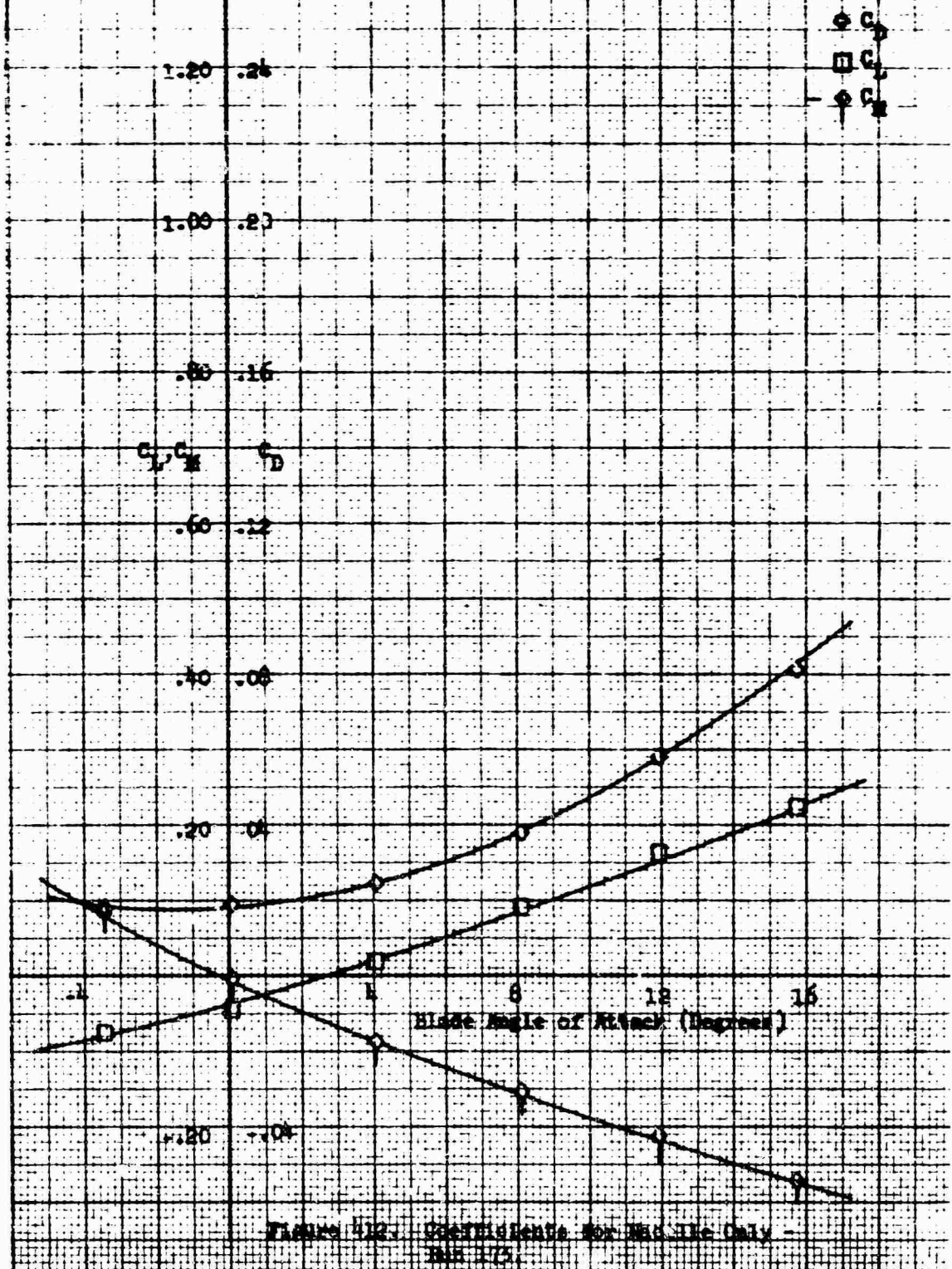


Blade Configuration: Twin Horizontal 1-40-100

Pairing: With

Macelle Exit Plate: .90

$\beta = 20^\circ$



Nozzle Configuration: Twin horizontal 1-40-100
 Nozzle Incidence Angle: 0°
 Pairing: With
 Nozzle Exit Plane: $.90$
 $\beta = 1.20^\circ$

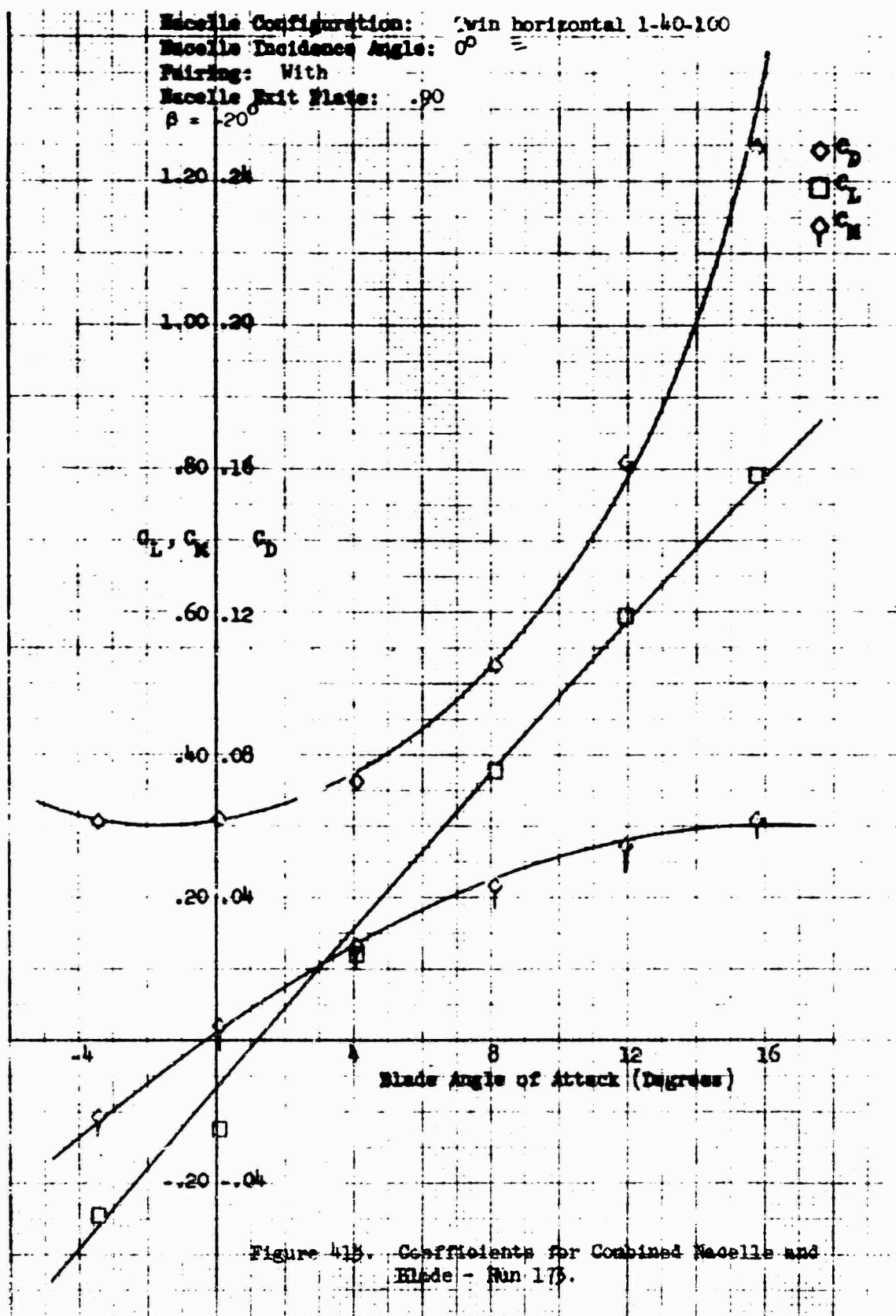
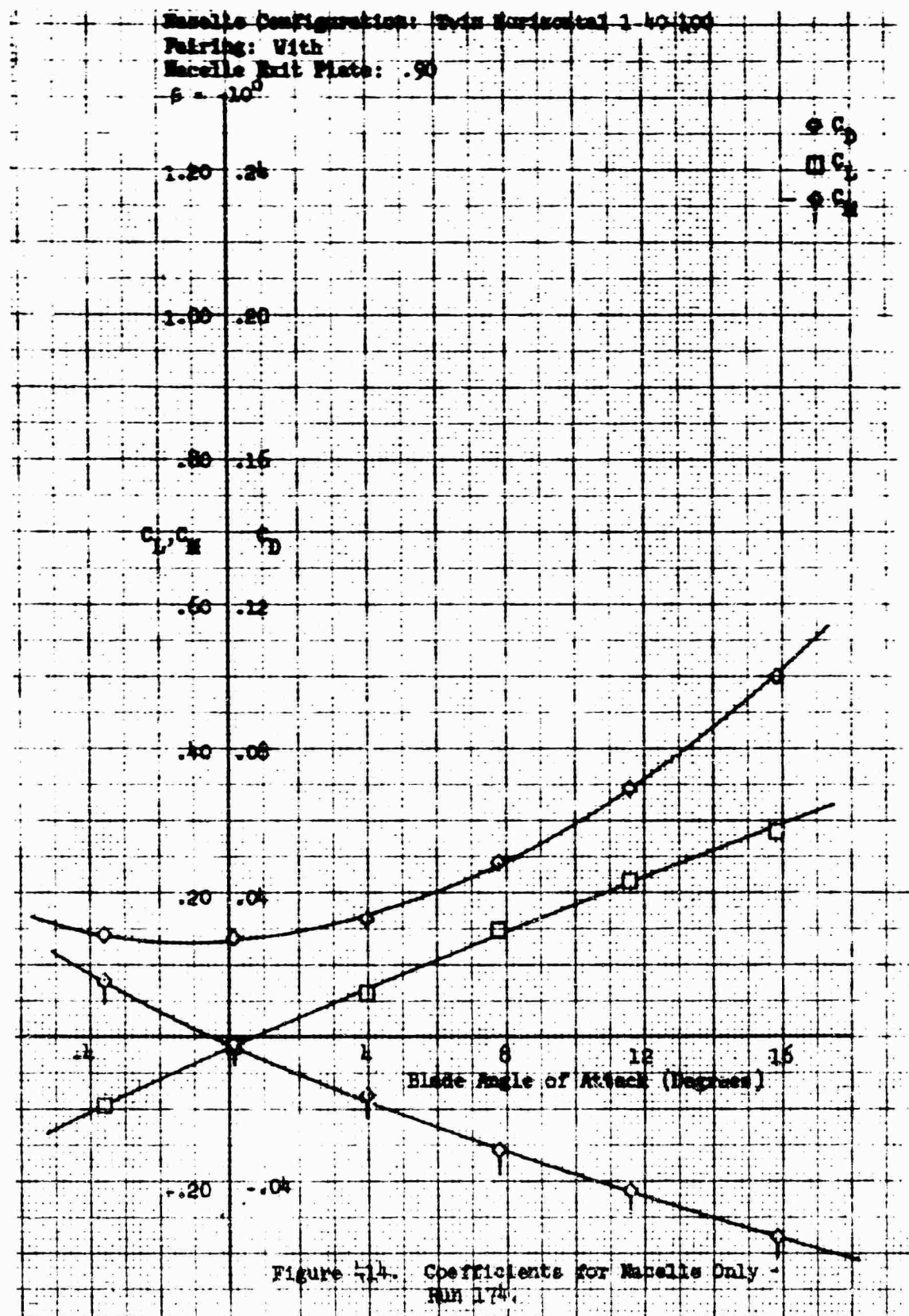


Figure 415. Coefficients for Combined Nozzle and Blade - Run 175.



Nozzle Configuration: Twin horizontal 1-40-100
 Nozzle Incidence Angle: 0°
 Pairing: With
 Nozzle Exit Plate: .90
 $\beta = -10^\circ$

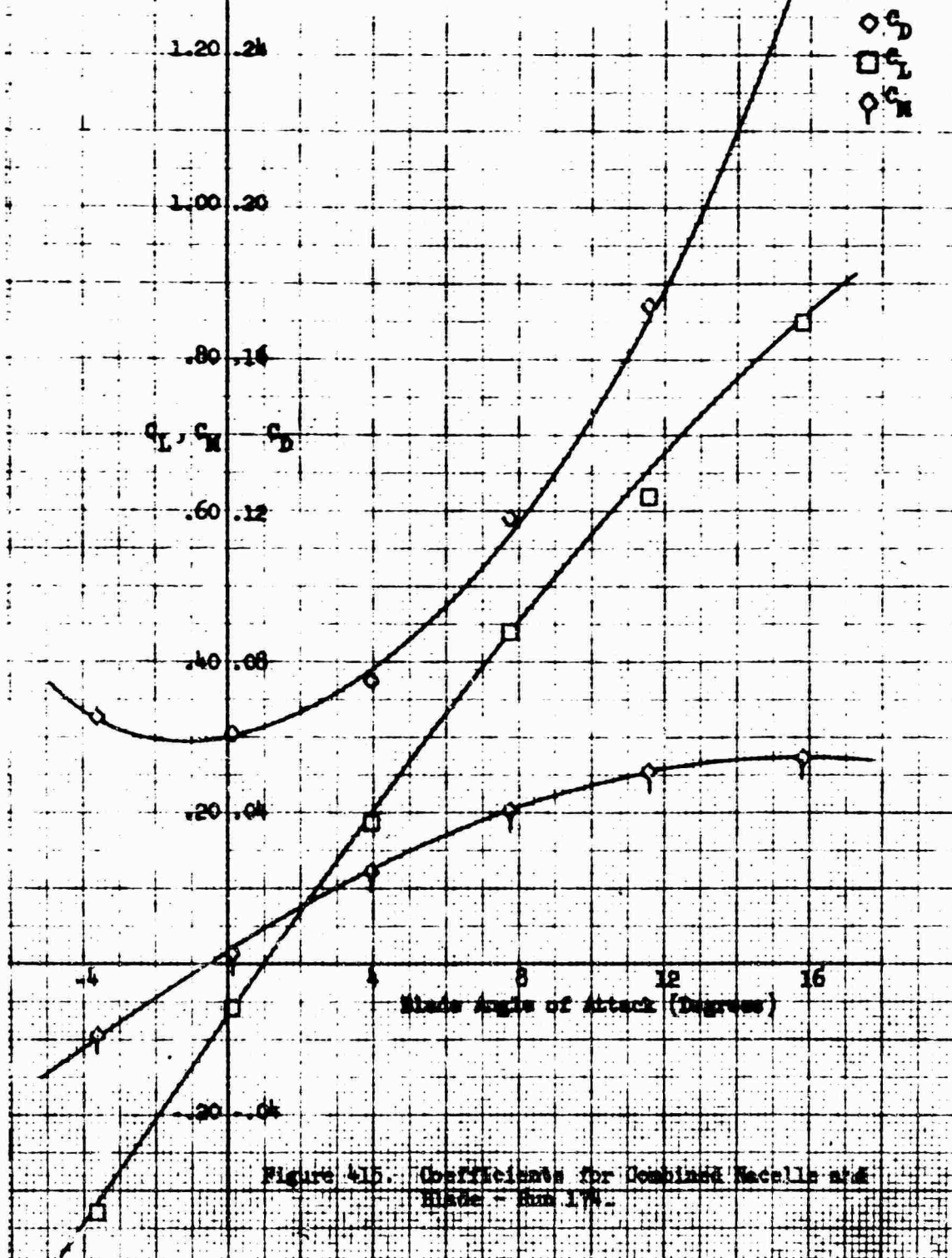
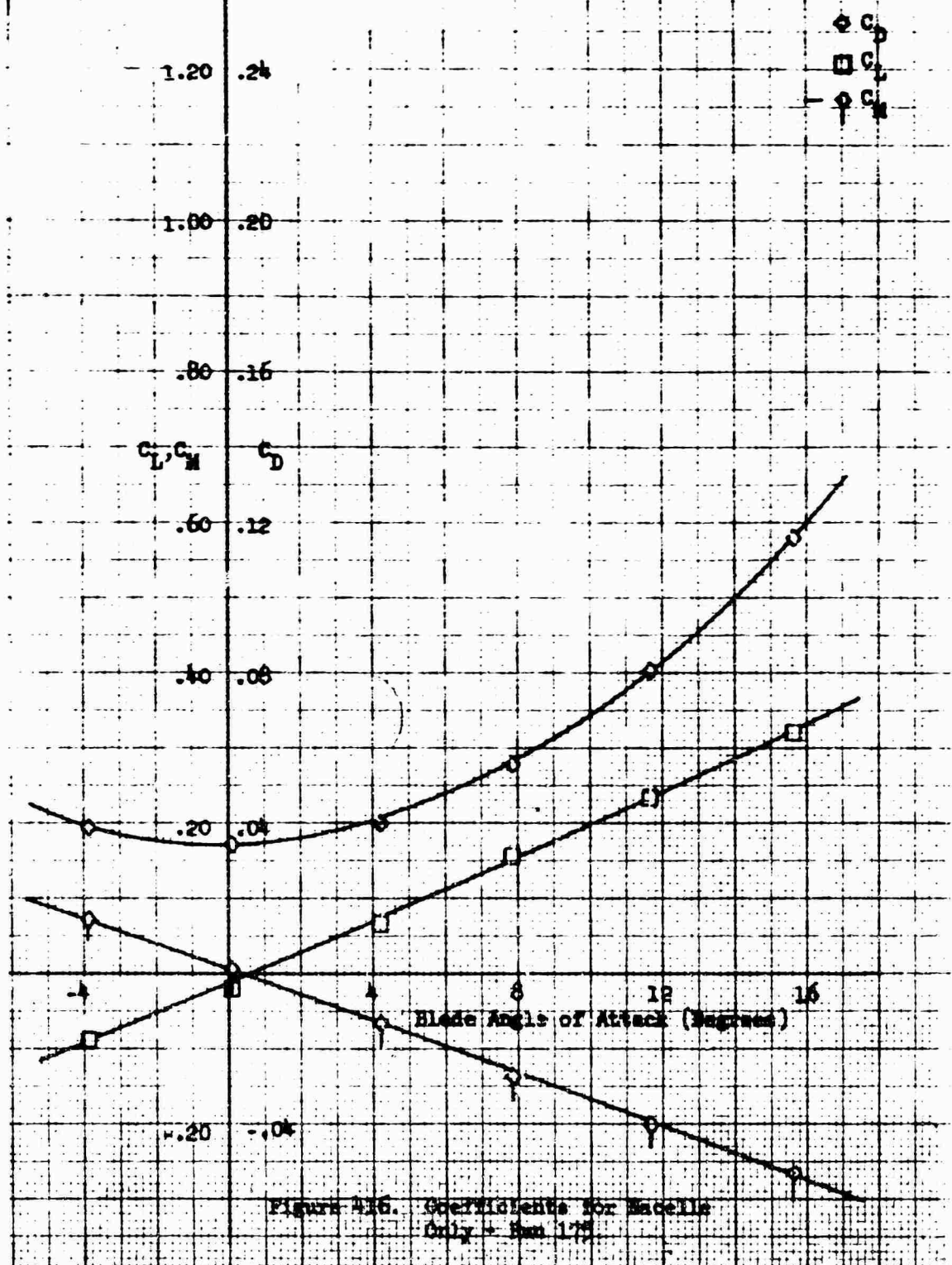
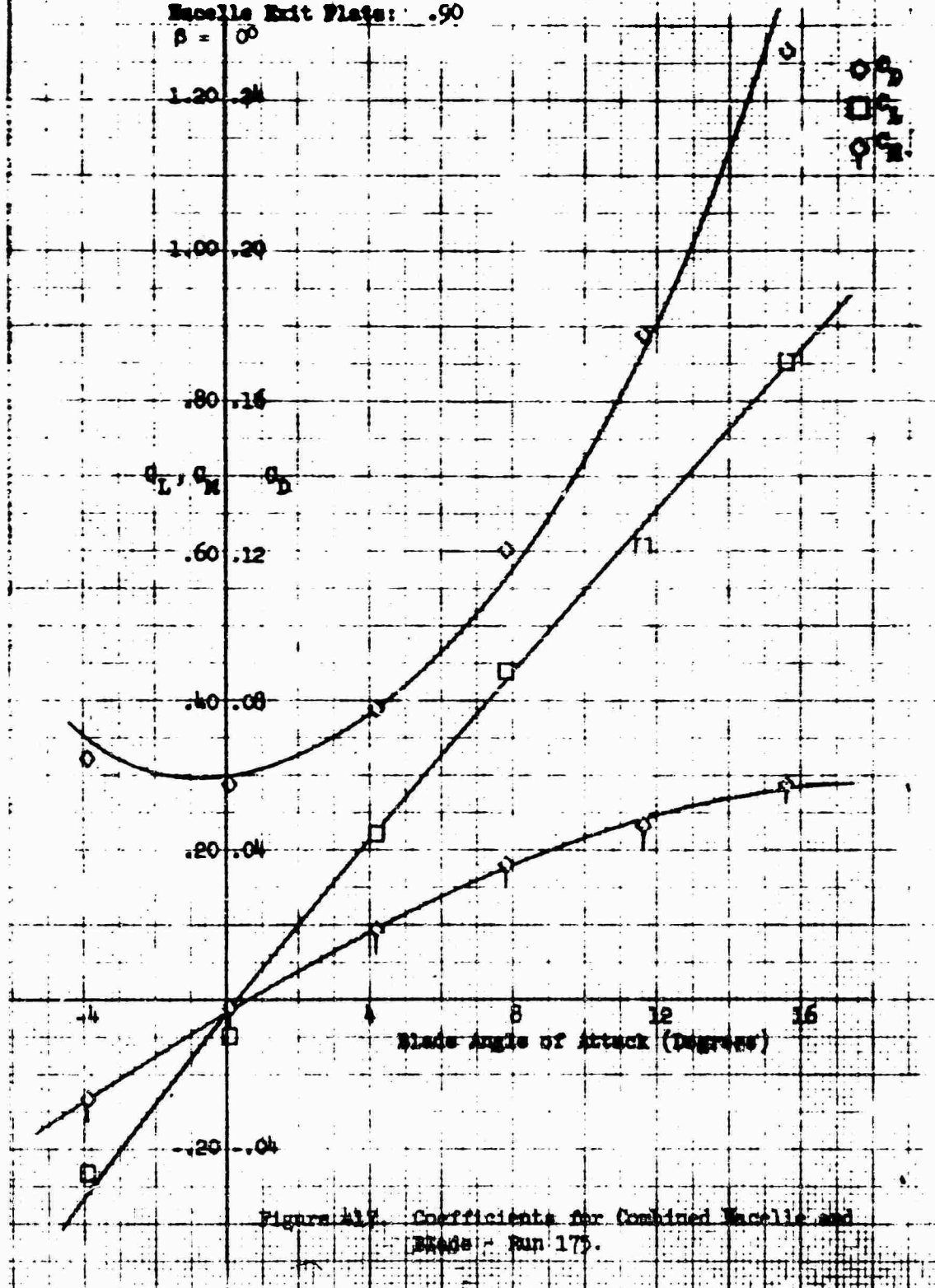


Figure 415. Coefficients for Combined Nozzle and Blade - Run 174.

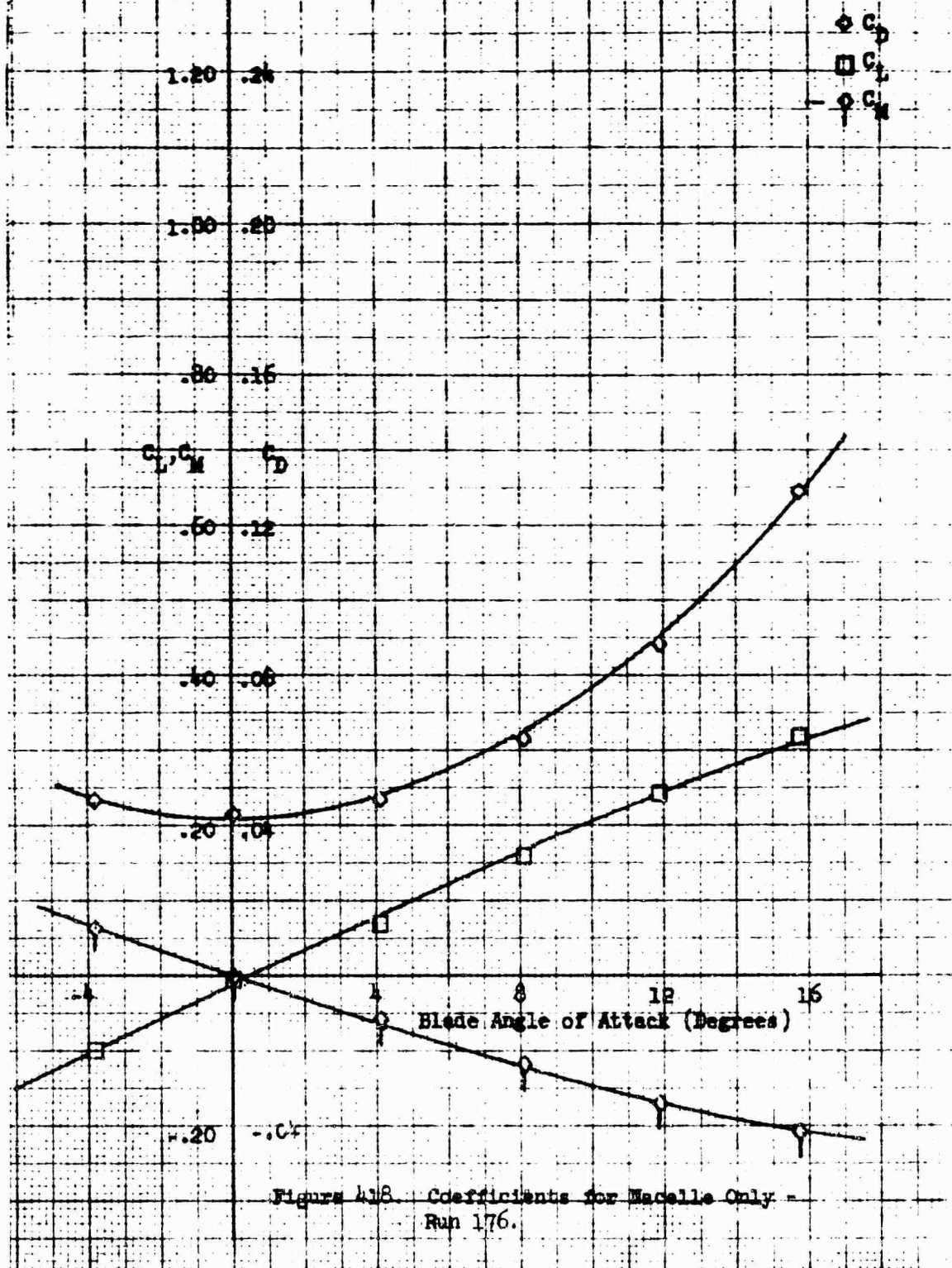
Macelle Configuration: Twin Horizontal 1-40-100
 Pairing: With
 Macelle Exit Plate: .90
 $\beta = 0$

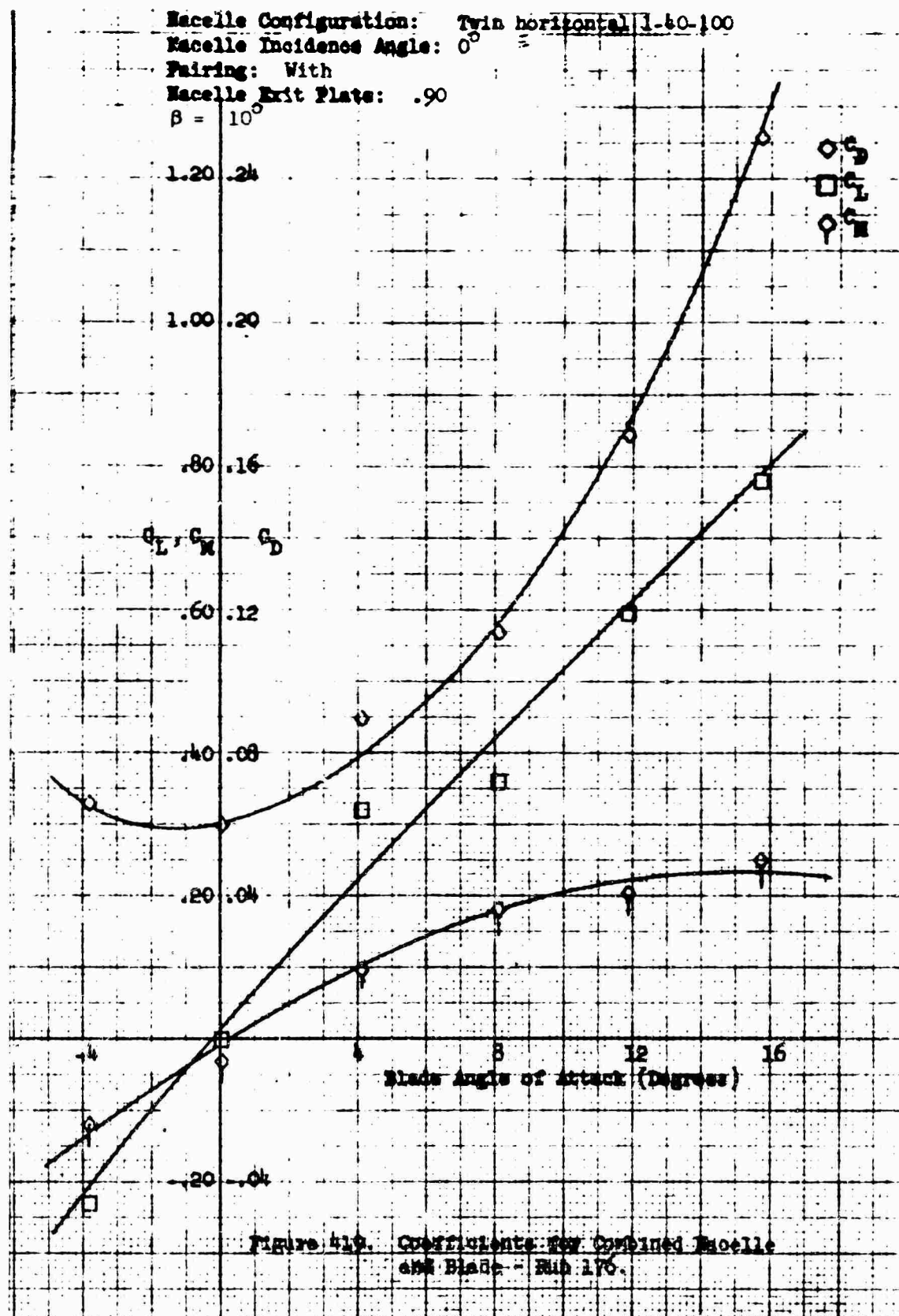


Macelle Configuration: Twin horizontal 1-40-100
 Macelle Incidence Angle: 0°
 Pairing: With
 Macelle Exit Plate: .90
 $\beta = 0^\circ$

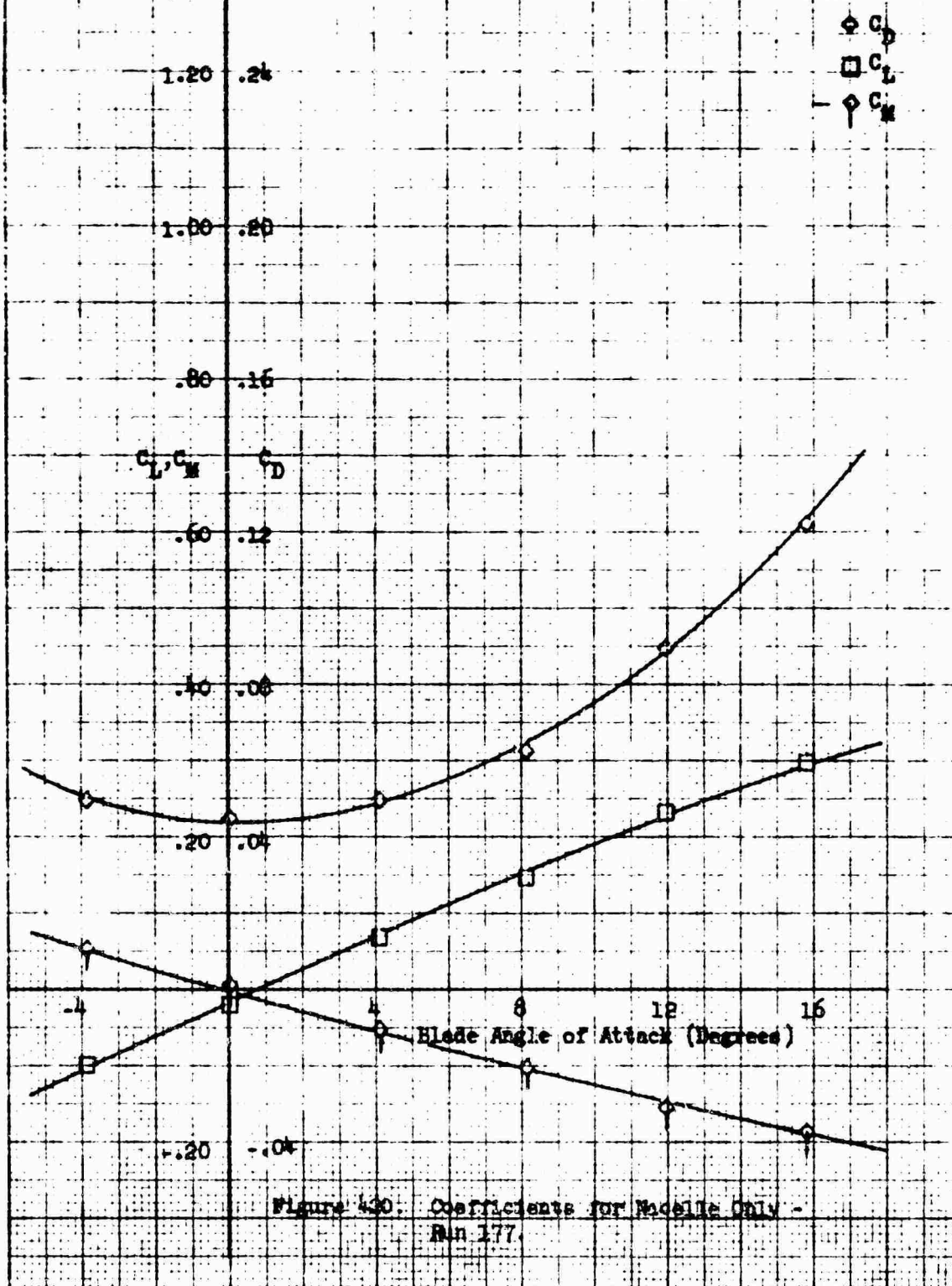


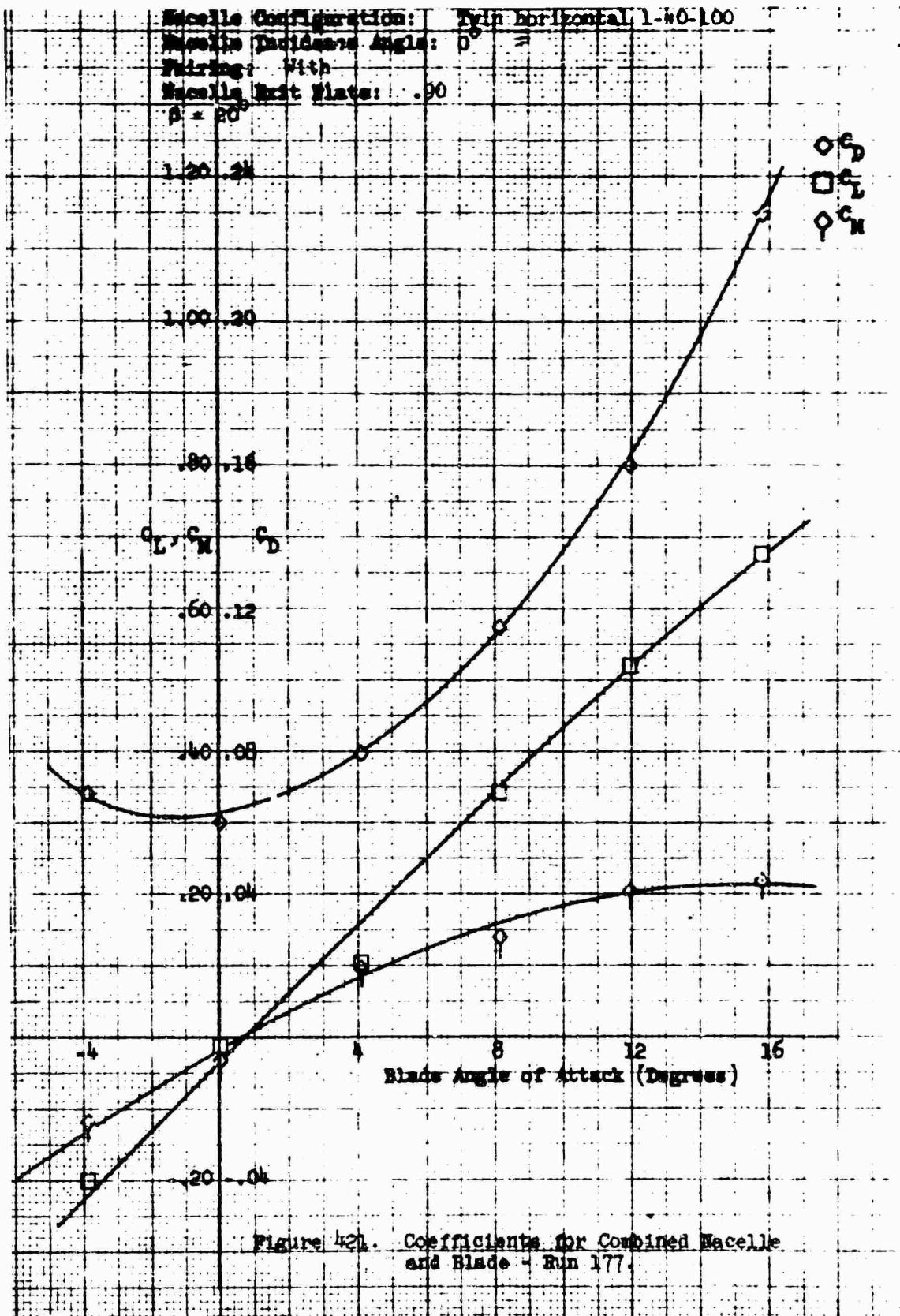
Macelle Configuration: Twin Horizontal 1-40-100
 Pairing: With
 Macelle Exit Plate: .90
 $\theta = 10^\circ$





Macelle Configuration: Twin Horizontal 1-40-100
 Pairing: With
 Macelle Exit Plate: .90
 $\beta = 20^\circ$





Missile Configuration: Twin Horizontal 1-40-100
 Fairing: With
 Missile Exit Plate: .75
 $\beta = 30^\circ$

$\diamond C_D$
 $\square C_L$
 ∇C_M

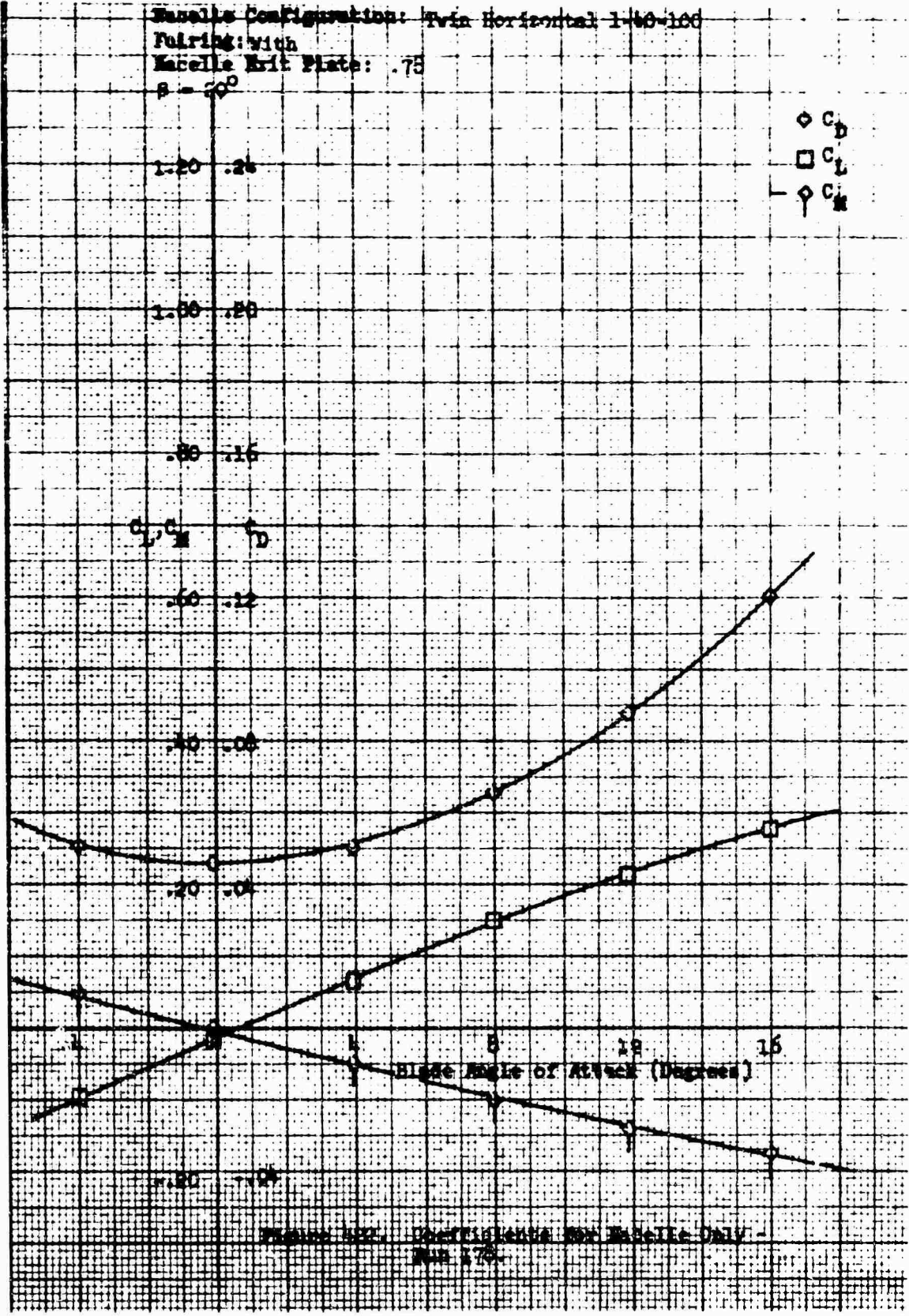
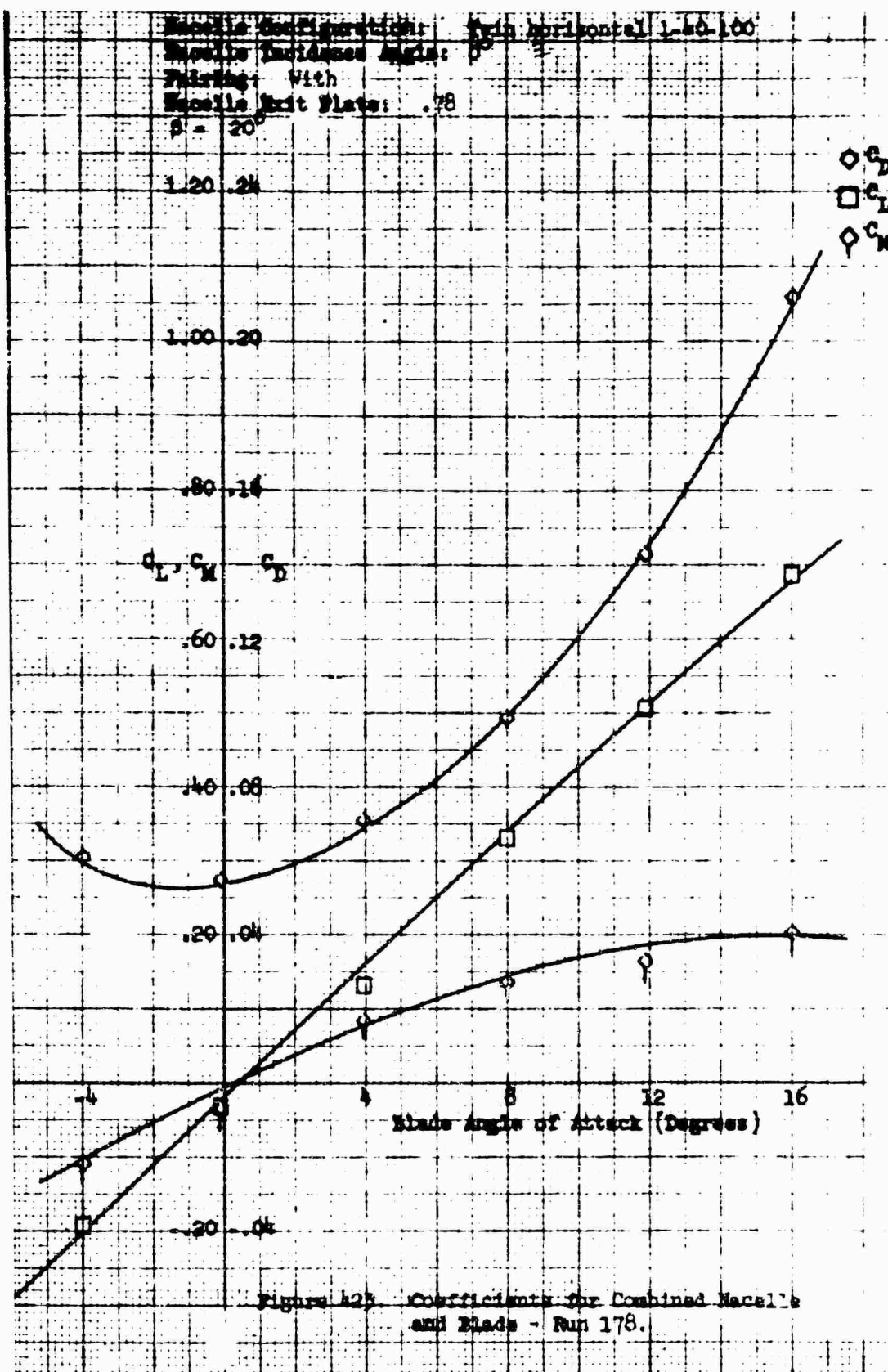
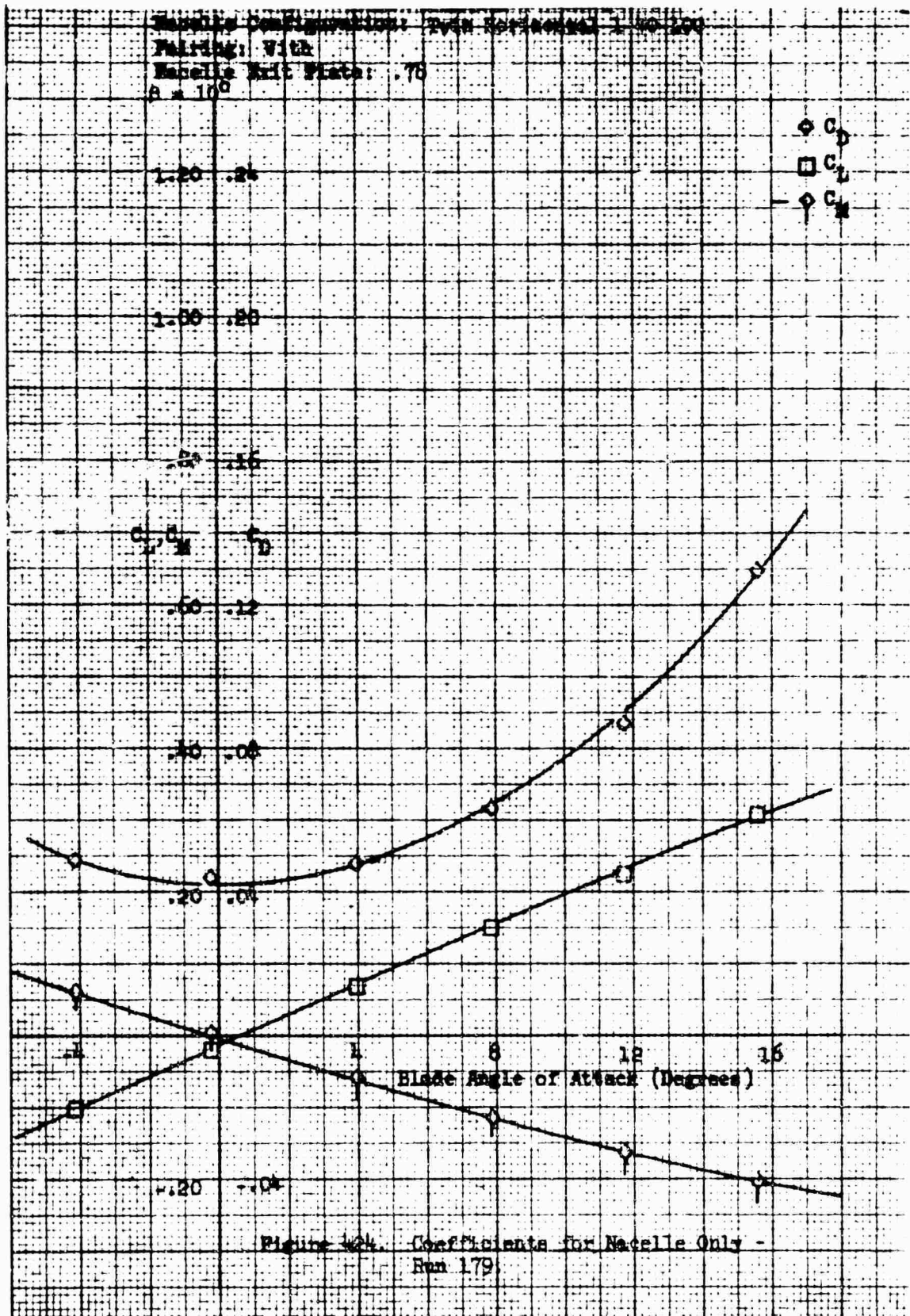


Figure 402. Coefficients for Missile Only -
 Sub 175





Macelle Configuration: Twin horizontal 1-40-100
 Macelle Incidence Angle: 0°
 Pairing: With
 Macelle Exit Plate: .78
 $\beta = 10^\circ$

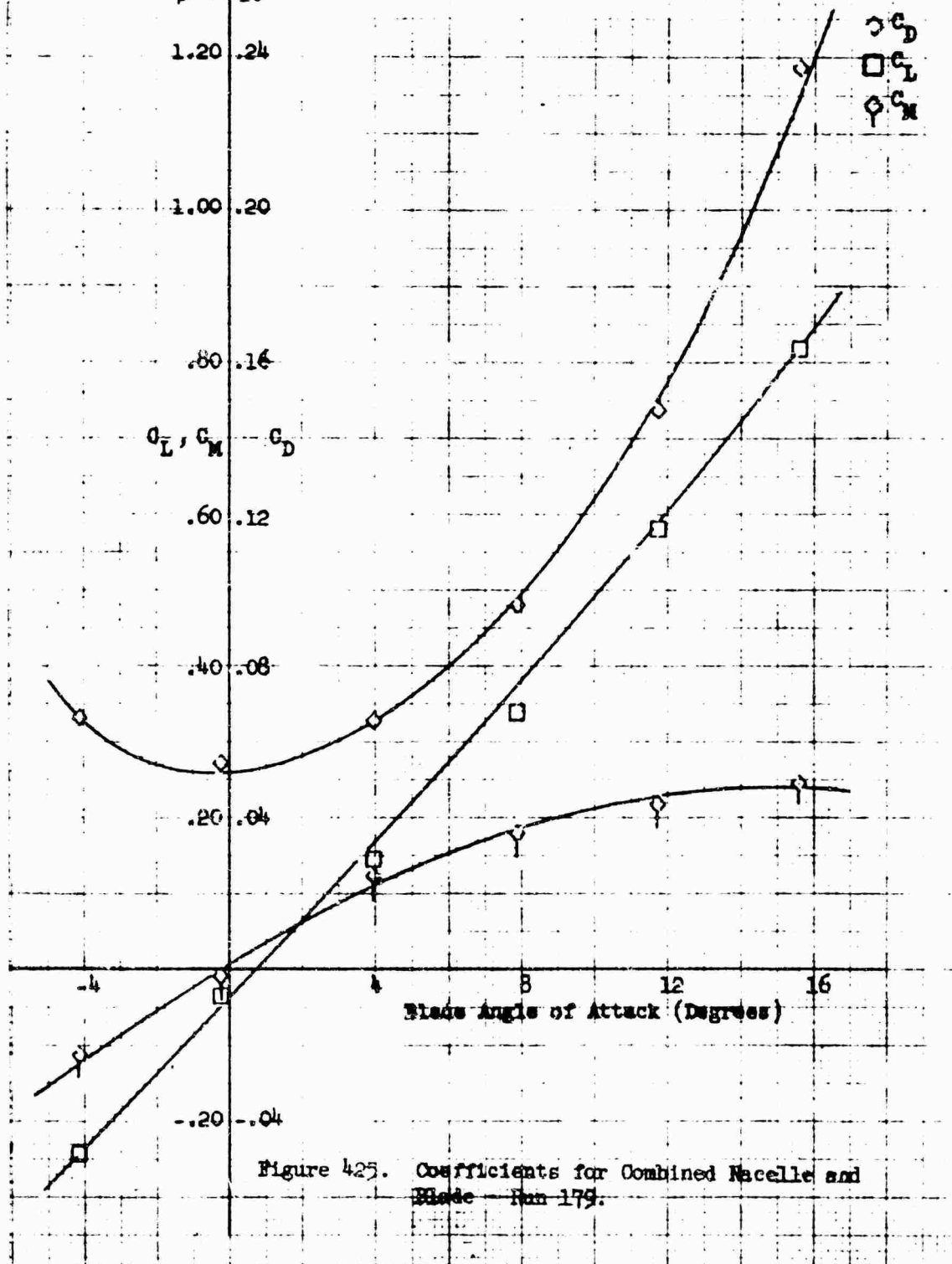


Figure 425. Coefficients for Combined Macelle and Blade - Run 179.

Nacelle Configuration: Twin Horizontal 1-40-101

Fairing: With

Nacelle Exit Plate: .78

$\beta = 0$

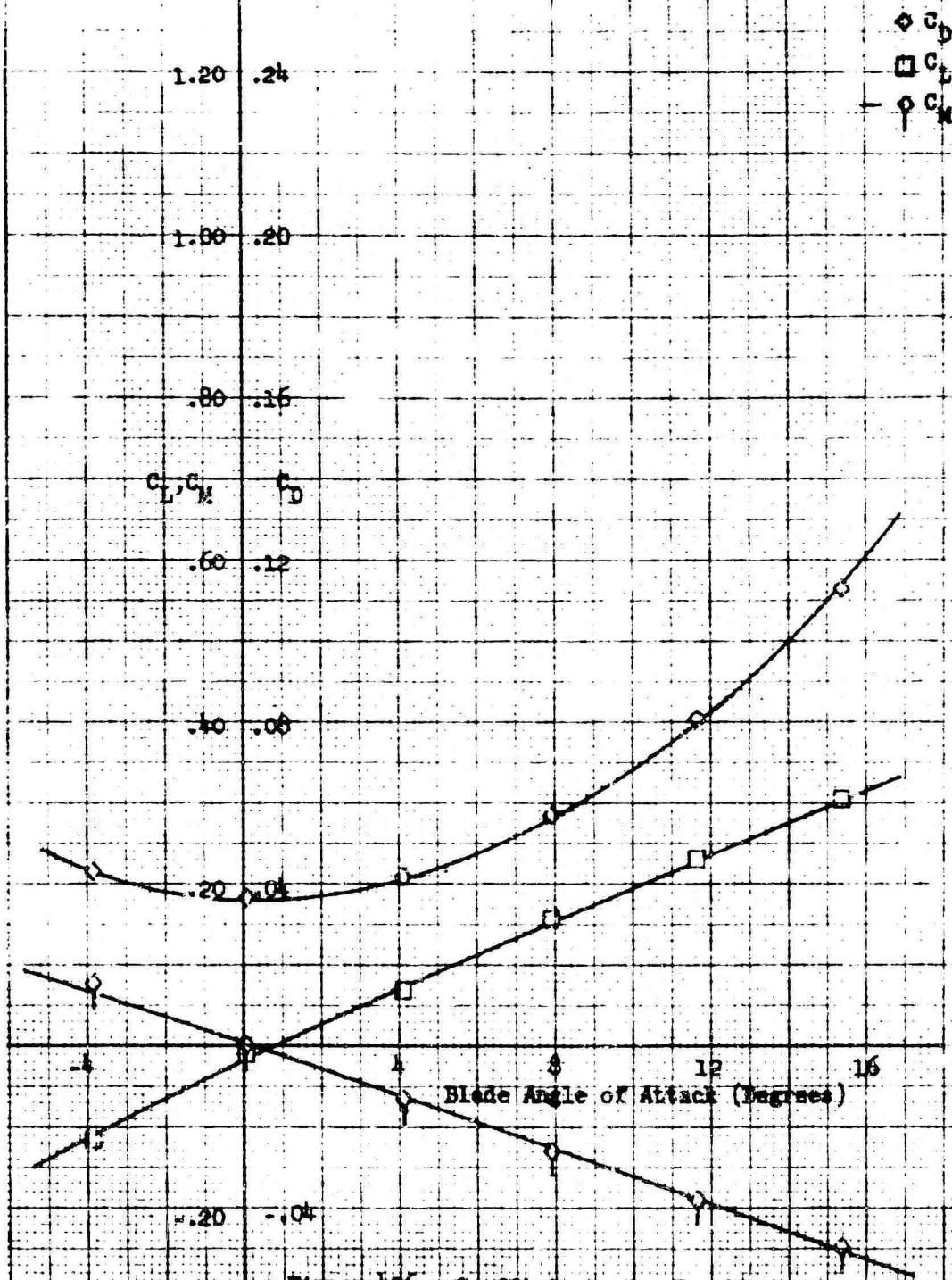
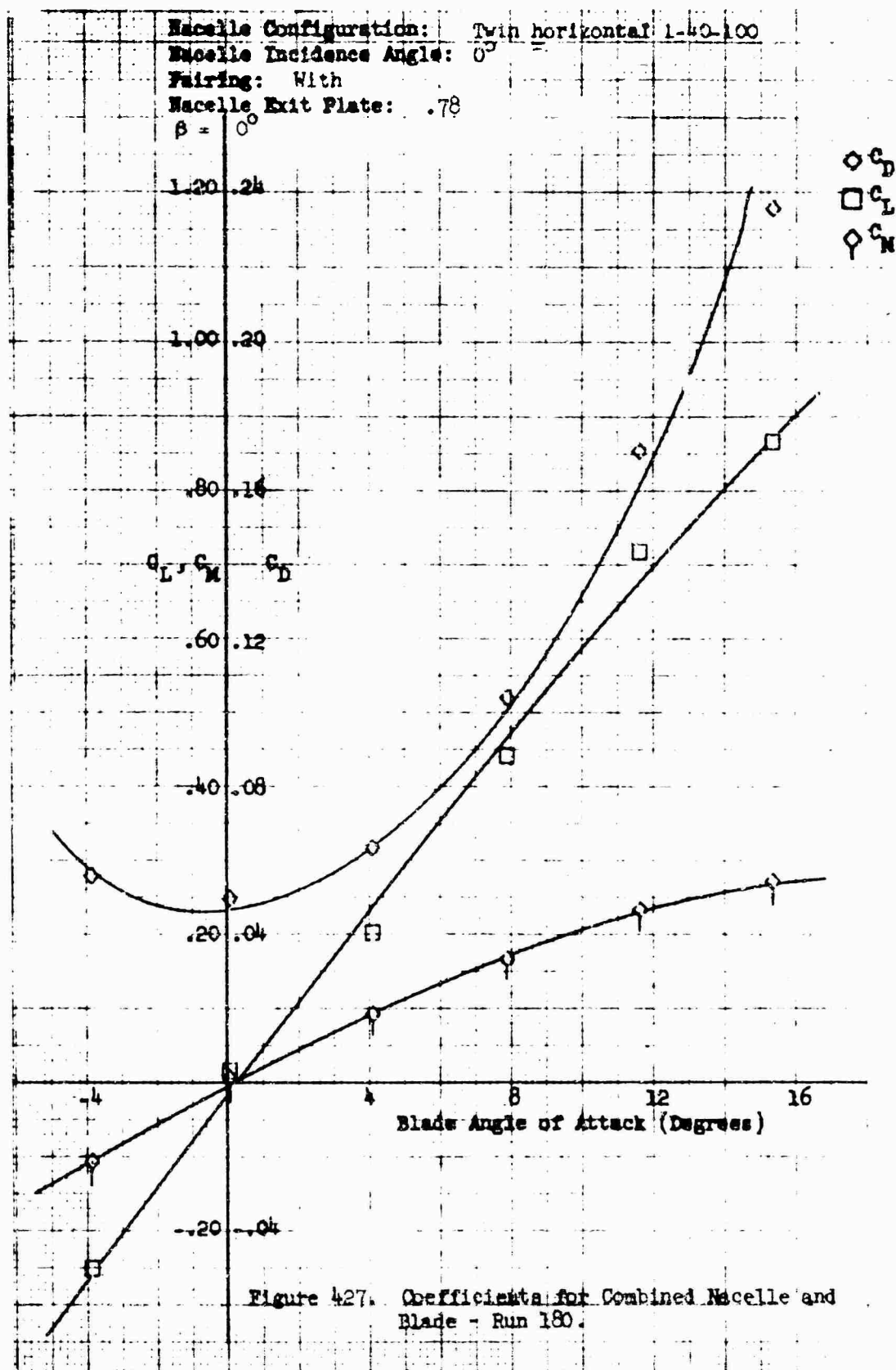


Figure 436. Coefficients for Nacelle Only
Run 180.



Macelle Configuration: Twin Horizontal 1-10-100
 Pairing: With
 Macelle Exit Plate: .78
 $\alpha = -10^\circ$

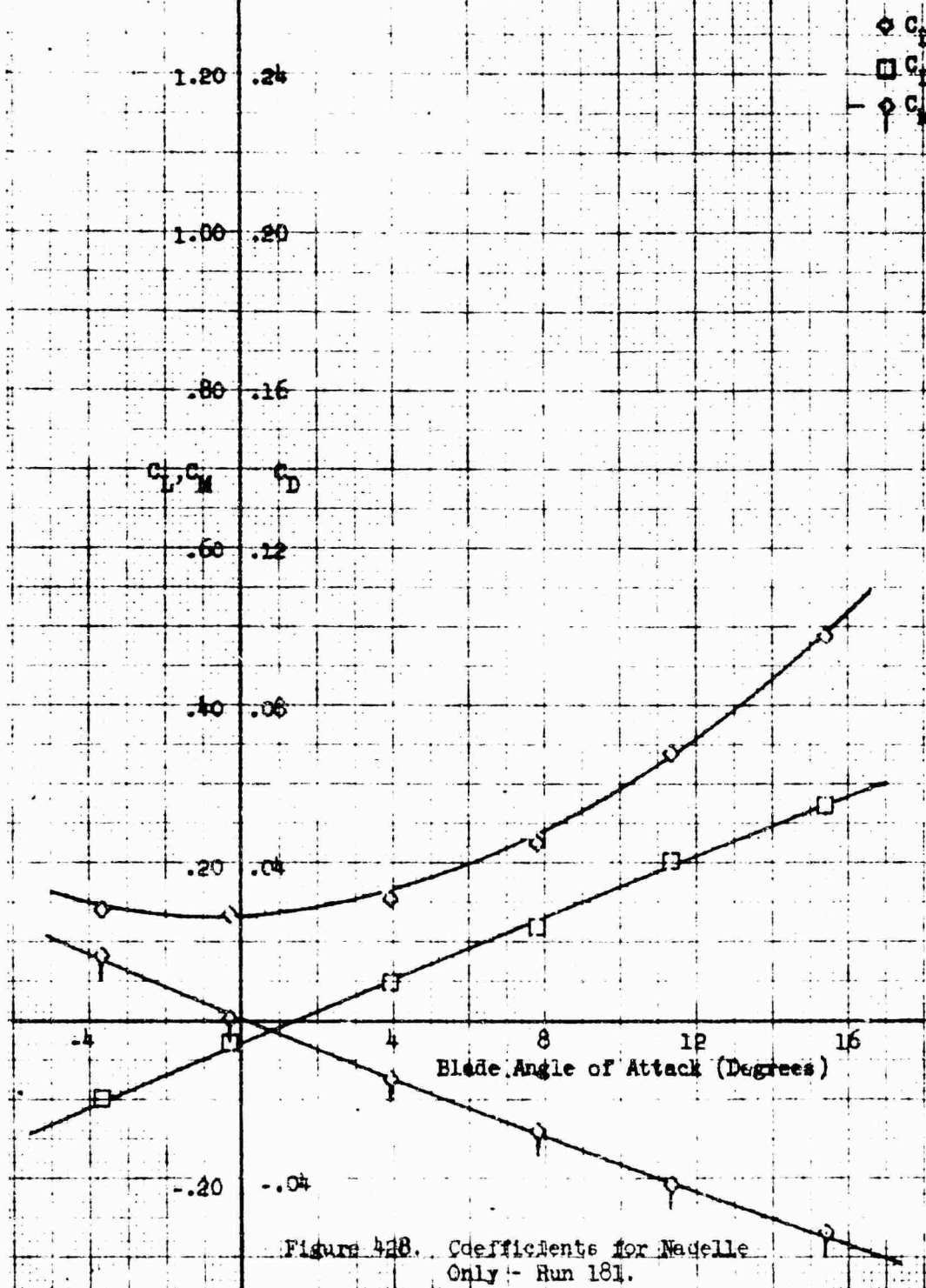


Figure 428. Coefficients for Macelle
 Only - Run 181.

Macelle Configuration: Twin horizontal 1-40-100
 Macelle Incidence Angle: 0°
 Fairing: With
 Macelle Exit Plate: .78
 $\beta = -10^\circ$

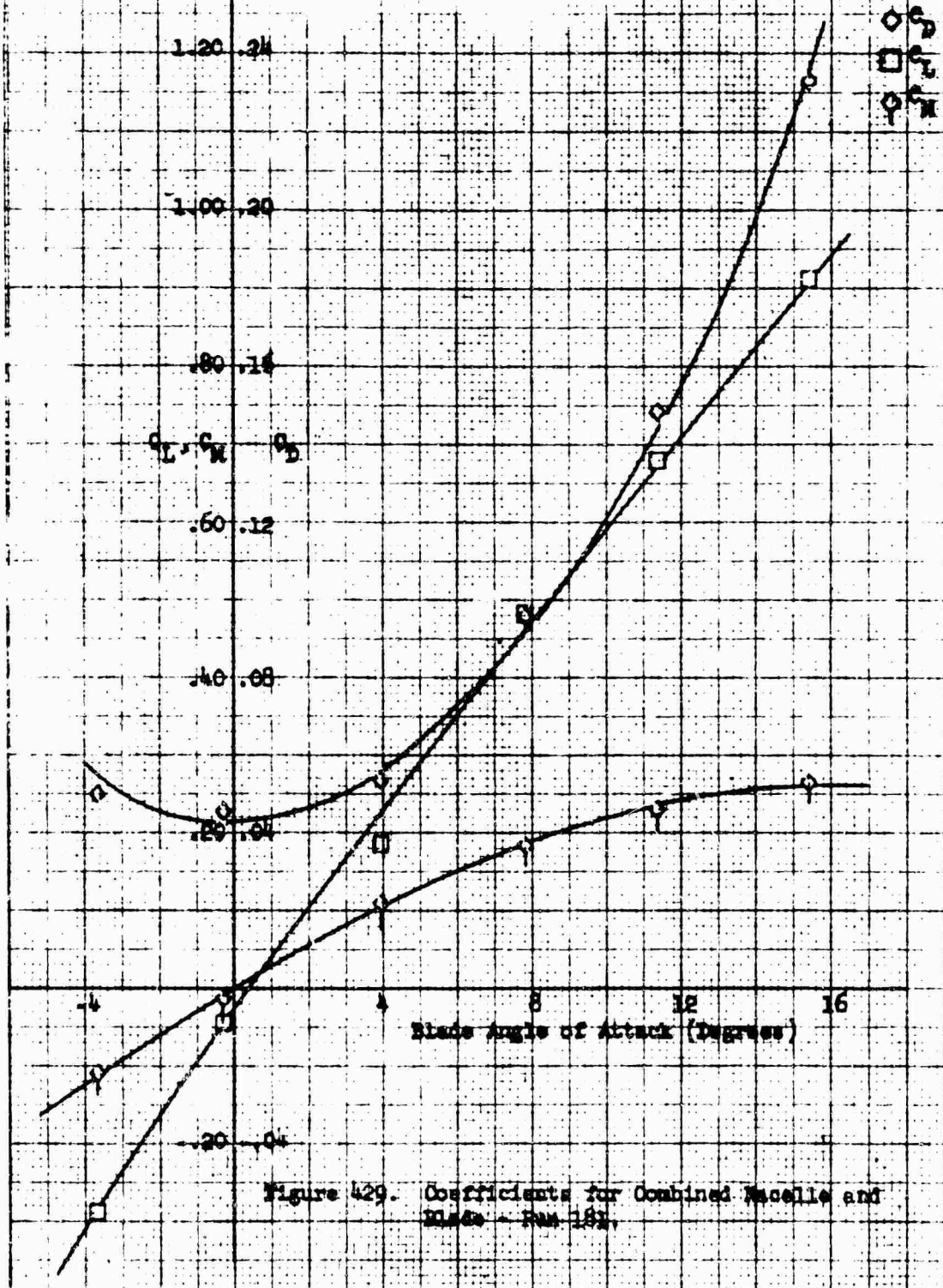


Figure 429. Coefficients for Combined Macelle and Blade - Run 181.

Blade Configuration: Twin Horizontal 1-4/100
 Pairing: With
 Blade Exit Plate: .78
 $\beta = 20^\circ$

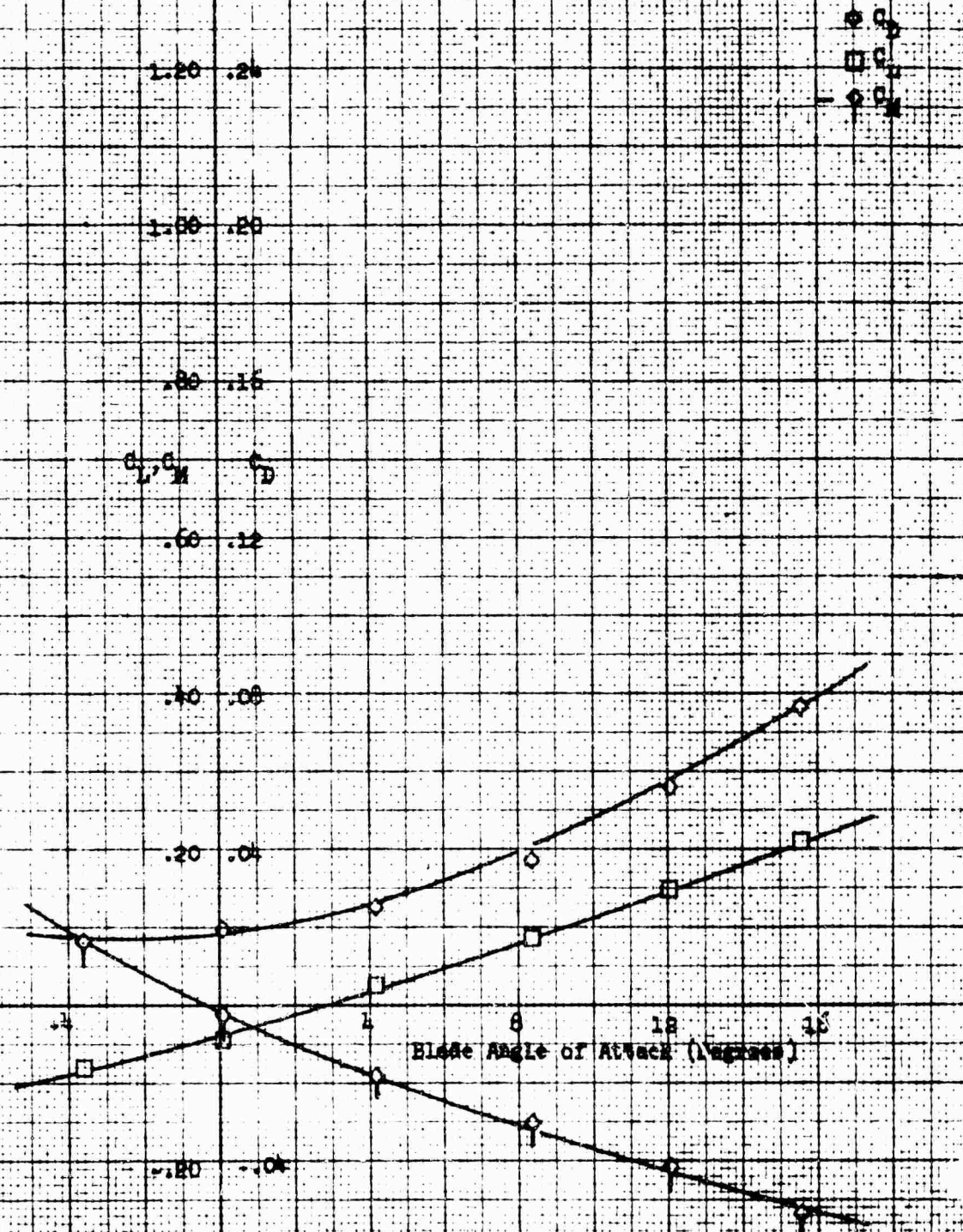


Figure 450. Coefficients for Blade Only -
Run 152.

Nacelle Configuration: Twin horizontal 1-40-100

Nacelle Incidence Angle: 0°

Pairing: With

Nacelle Exit Plate: .78

$\beta = 20^\circ$

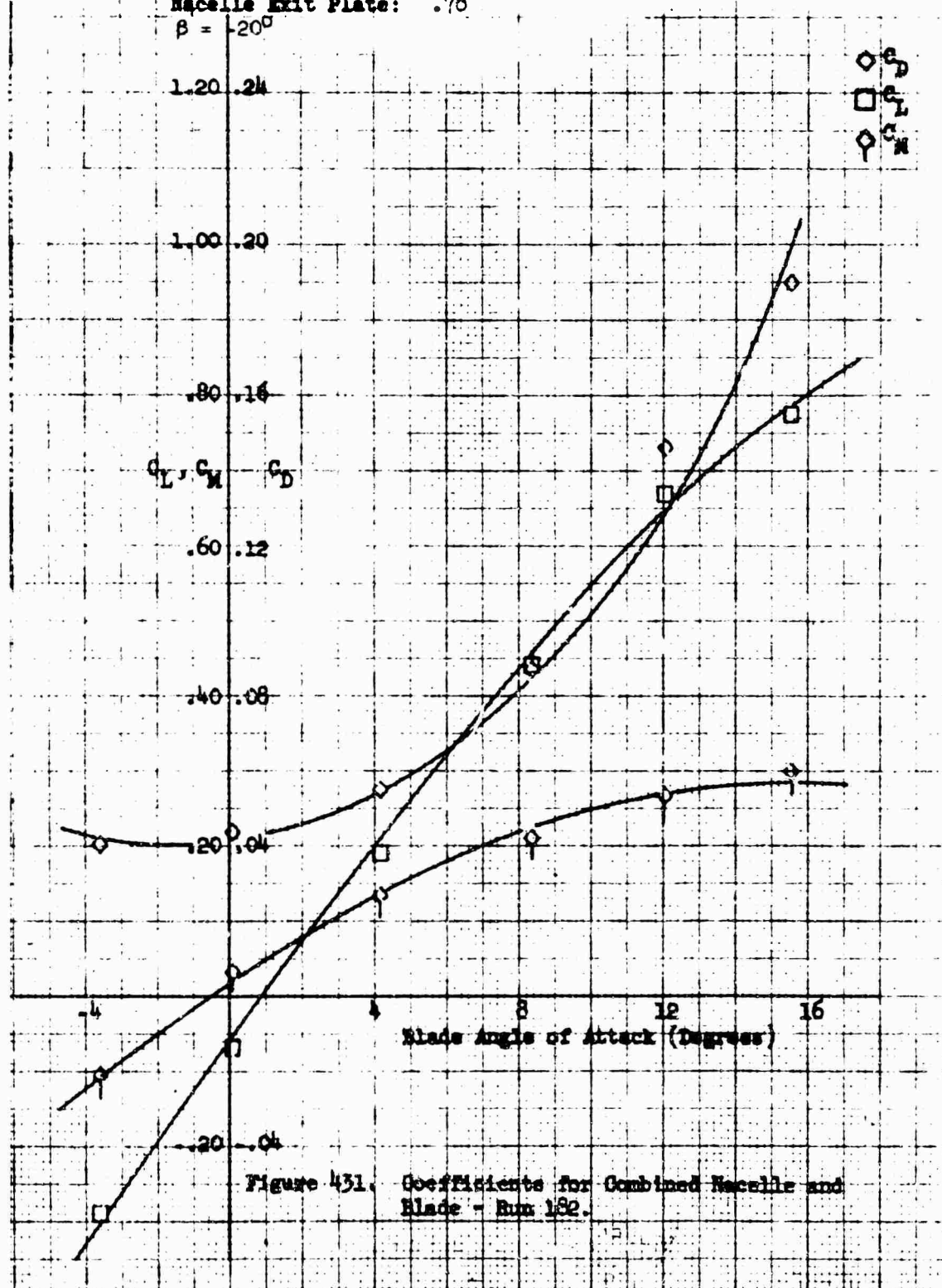
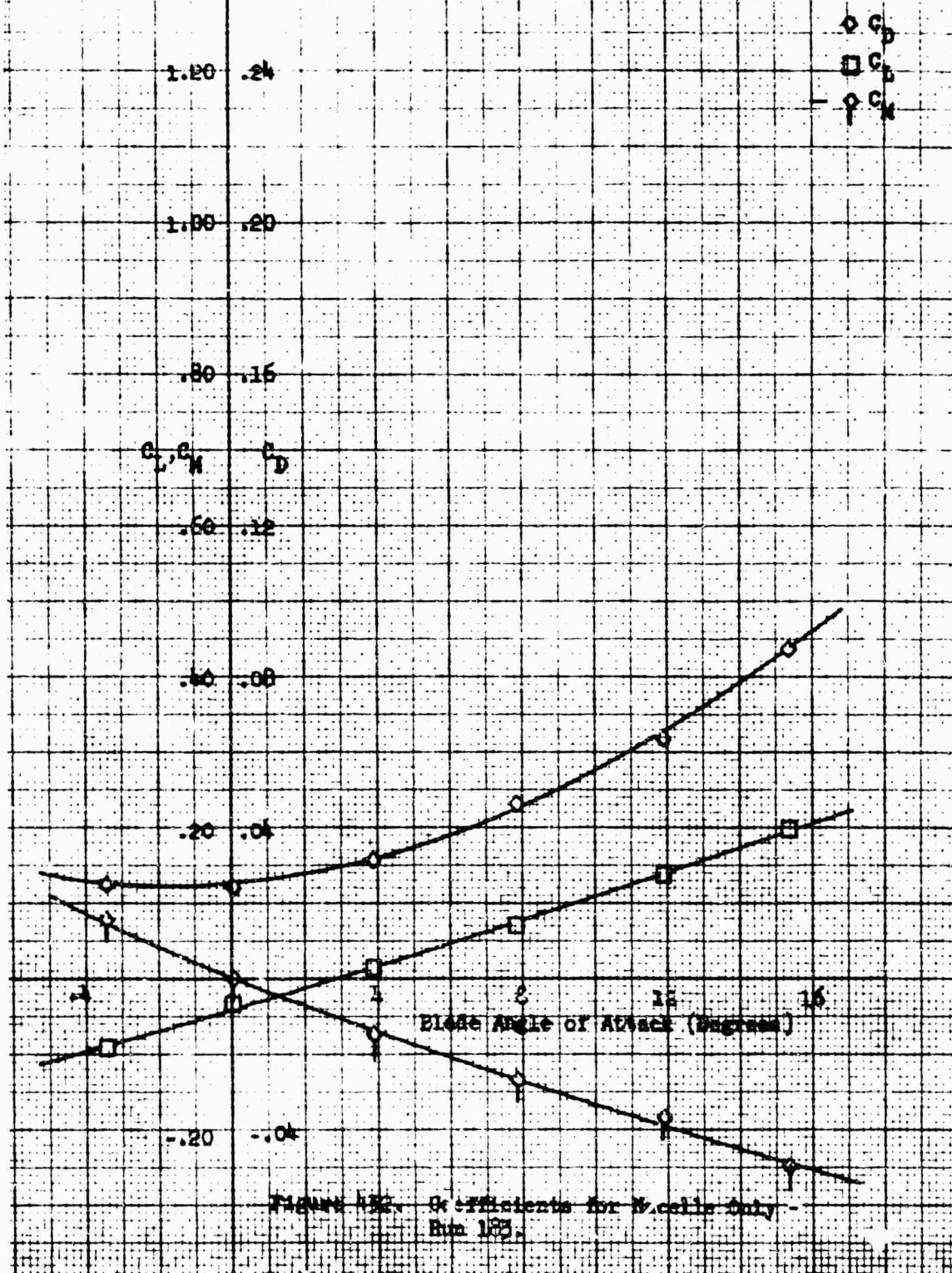
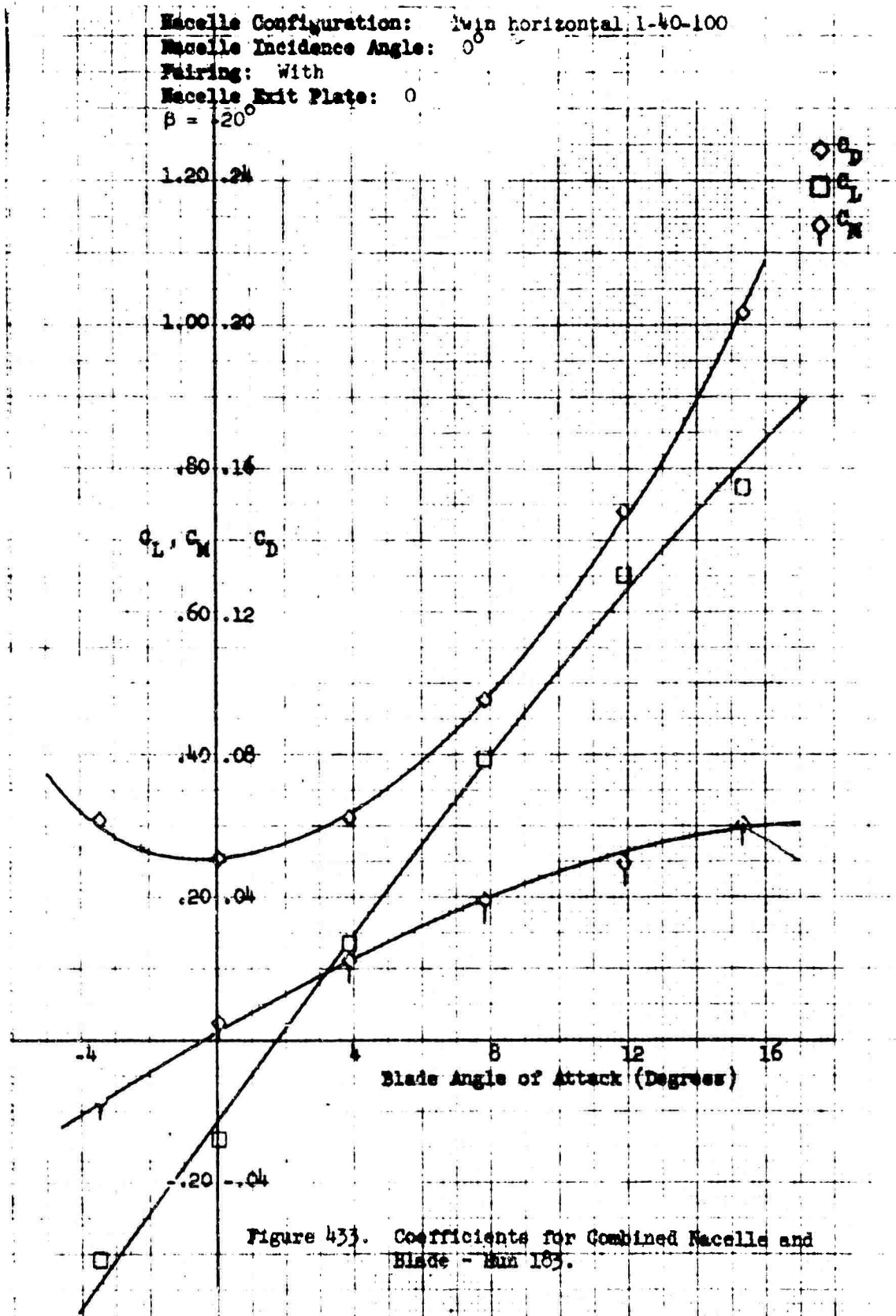


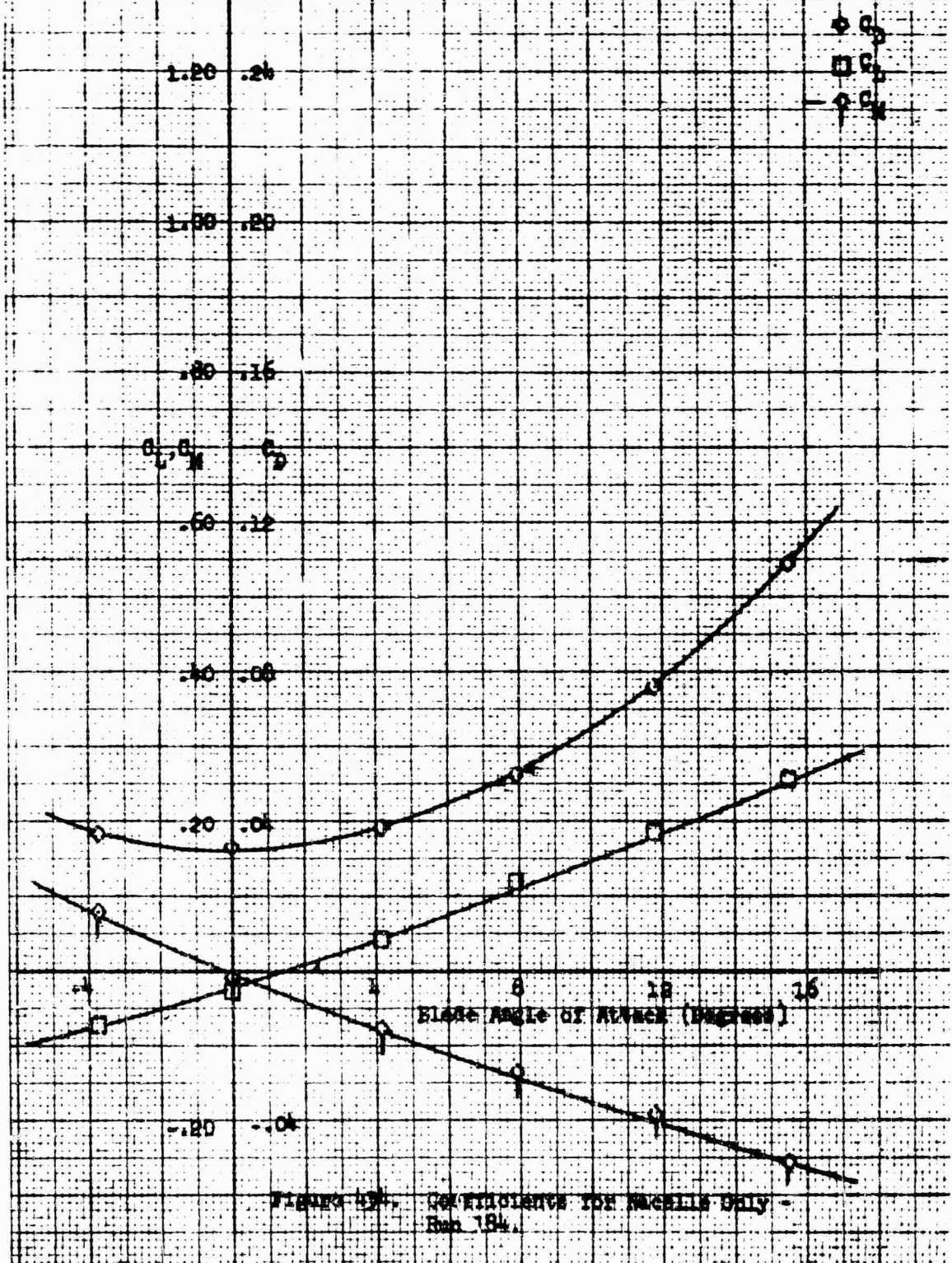
Figure 431. Coefficients for Combined Nacelle and Blade - Run 182.

Nacelle Configuration: Twin Horizontal 1-40-100
 Fairing: With
 Nacelle Exit Plate: 0°
 $\alpha = -20^\circ$





Nozzle Configuration: Total Nozzle Angle 150-155
 Pairing: With
 Nozzle Exit Plate: 0
 $\delta = -10^\circ$



Nacelle Configuration: Twin Horizontal 1-40-100
 Nacelle Incidence Angle: 0°
 Pairing: With
 Nacelle Exit Plate: 0
 $\beta = 10^\circ$

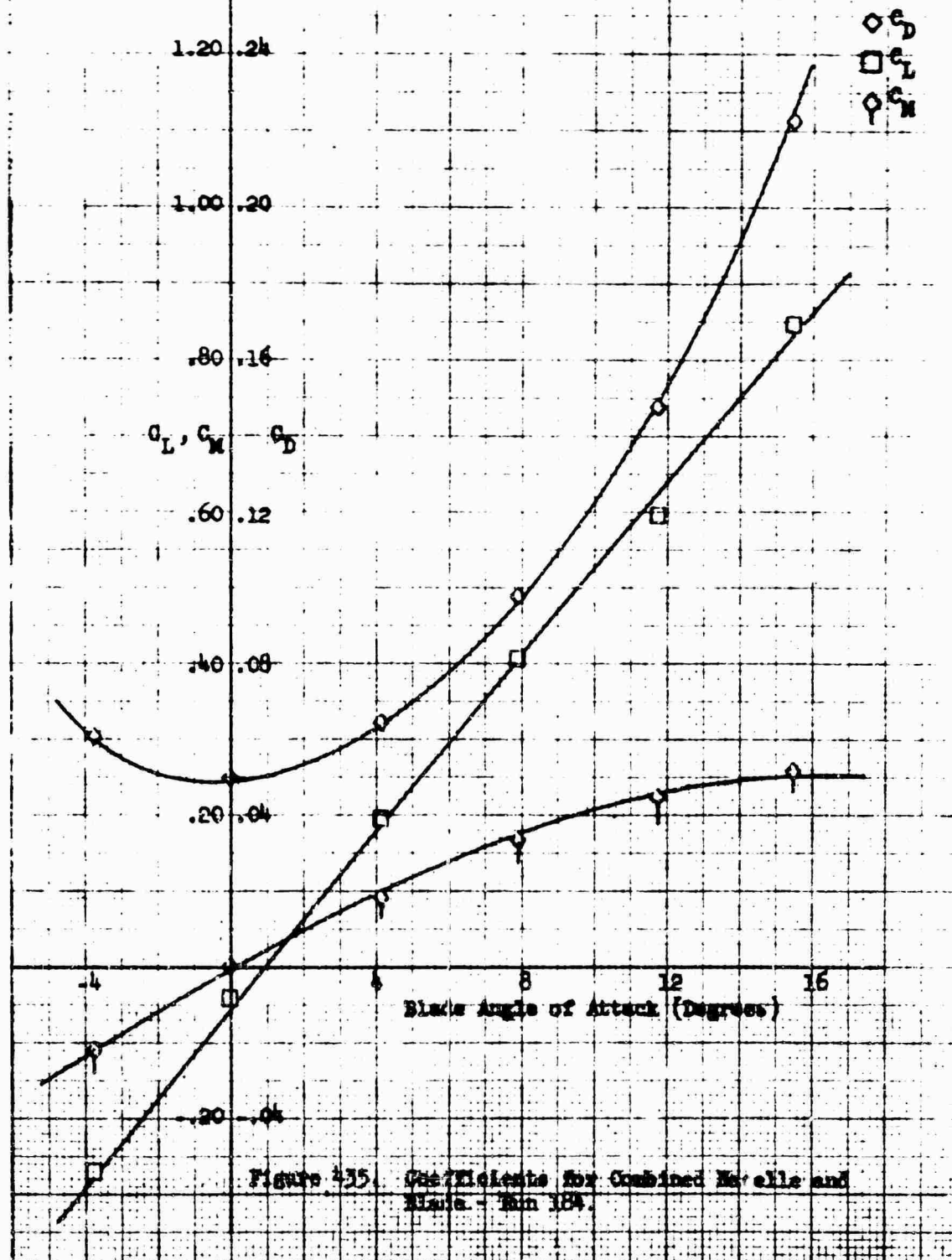


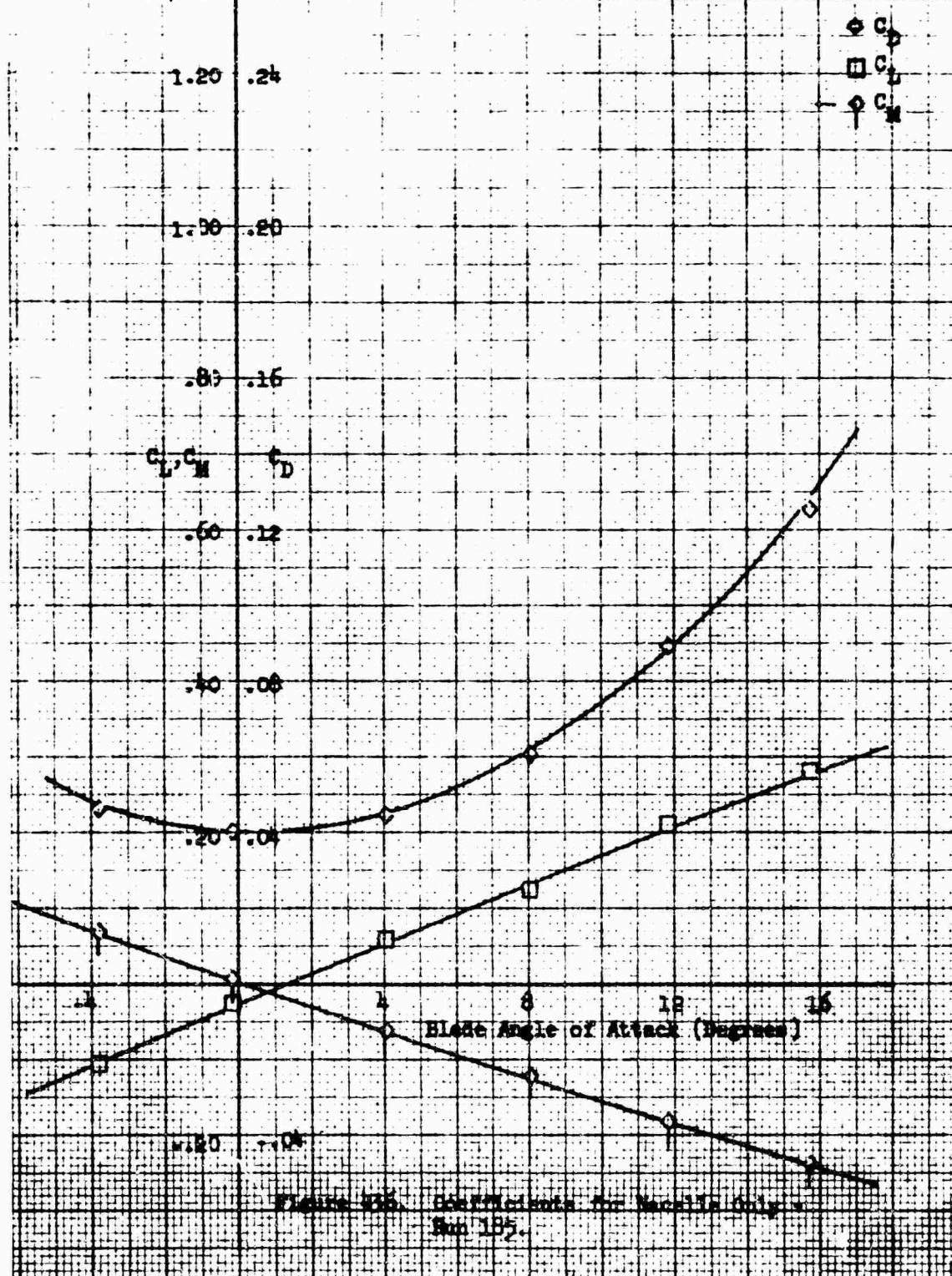
Figure 435. Coefficients for Combined Nacelle and Blade - Run 184.

Wacelle Configuration: Twin Horizontal 1-40-100

Fairing: With

Wacelle Exit Plate: 0

$\beta = 0$



Nacelle Configuration: Twin horizontal 1-40-100
 Nacelle Incidence Angle: 0°

Fairing: With
 Nacelle Exit Plate: 0

$\beta = 0$

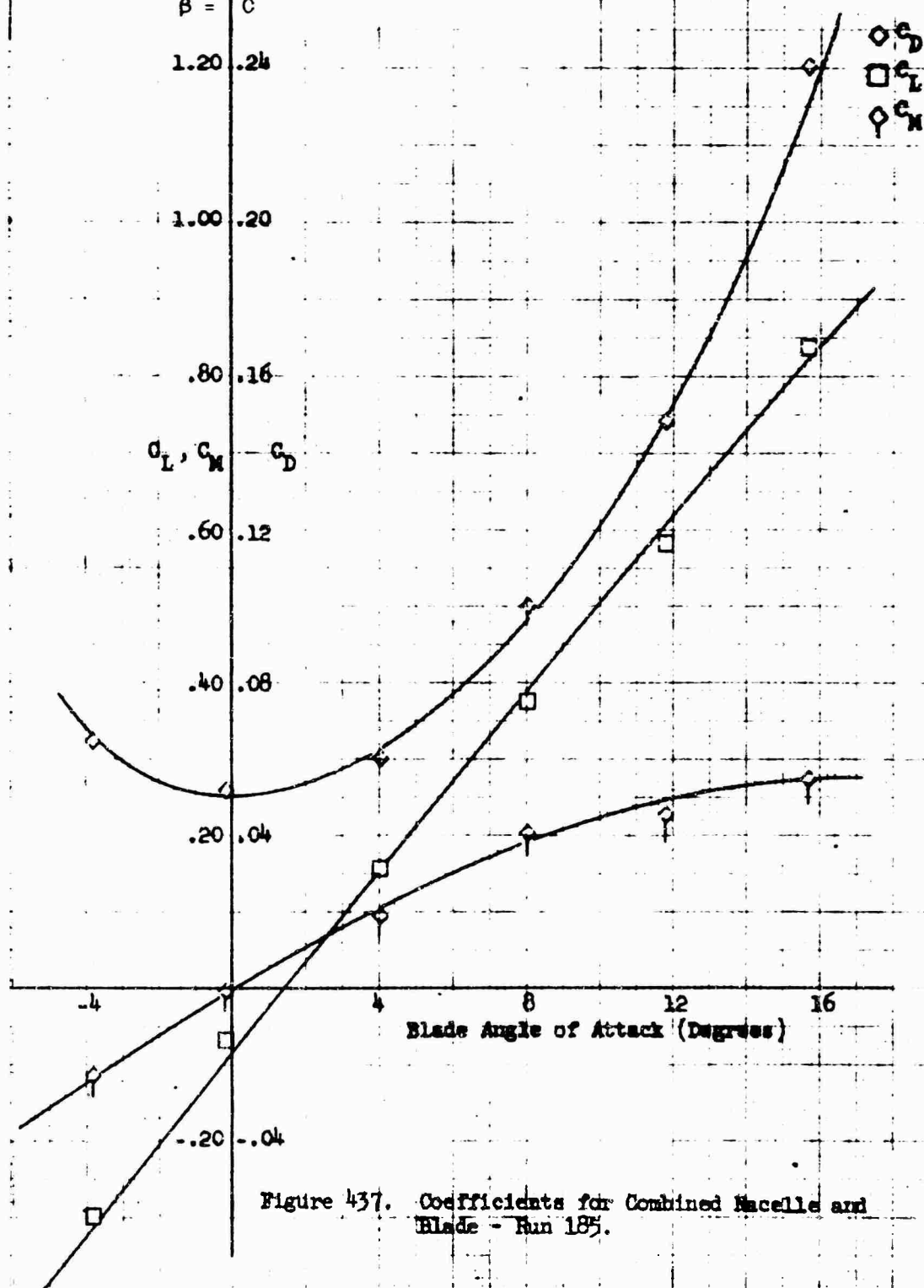
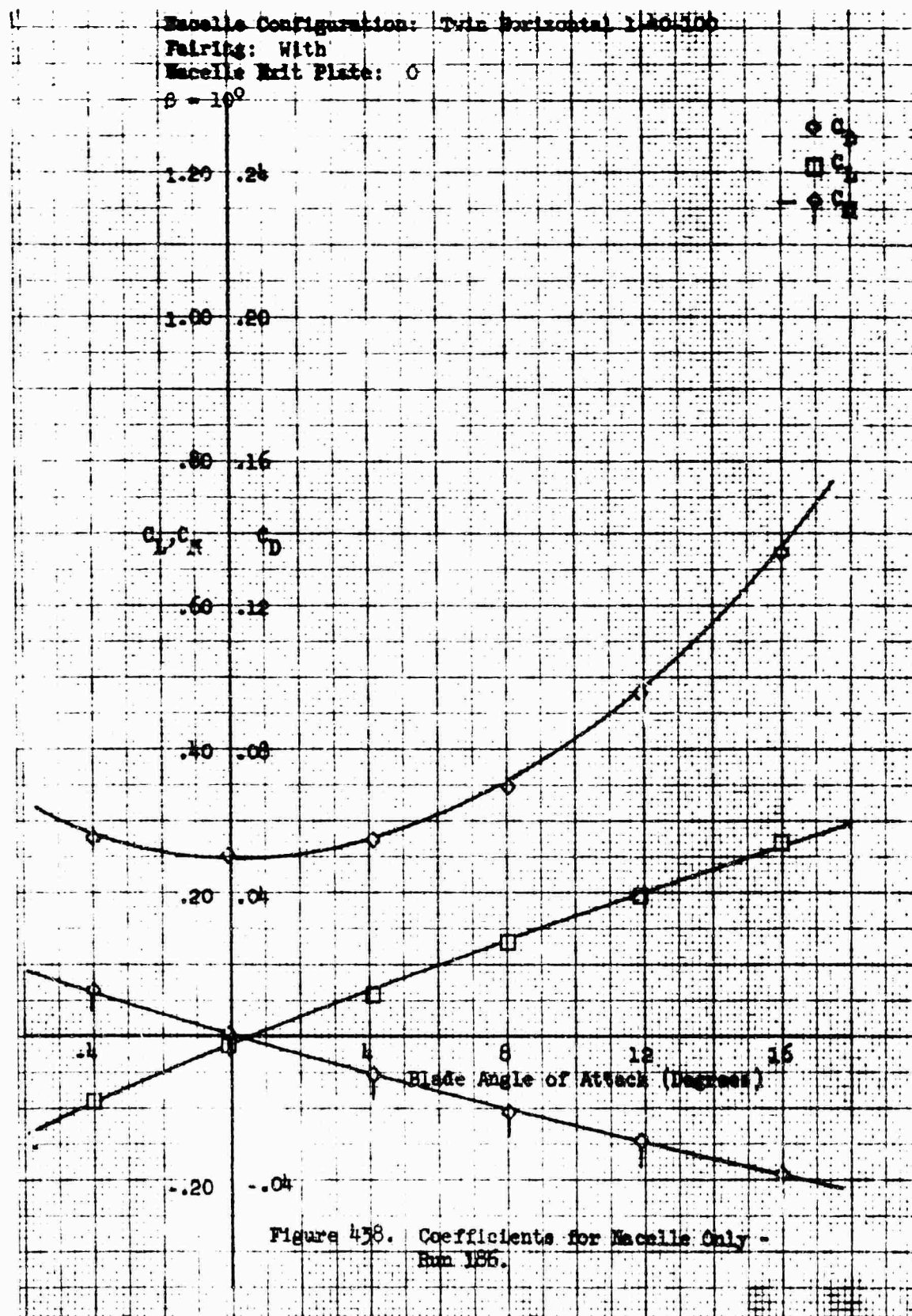


Figure 437. Coefficients for Combined Nacelle and Blade - Run 185.



Nacelle Configuration: Twin horizontal 1-40-100
 Nacelle Incidence Angle: 0°
 Pairing: With
 Nacelle Exit Plate: 0
 $\beta = 10^\circ$

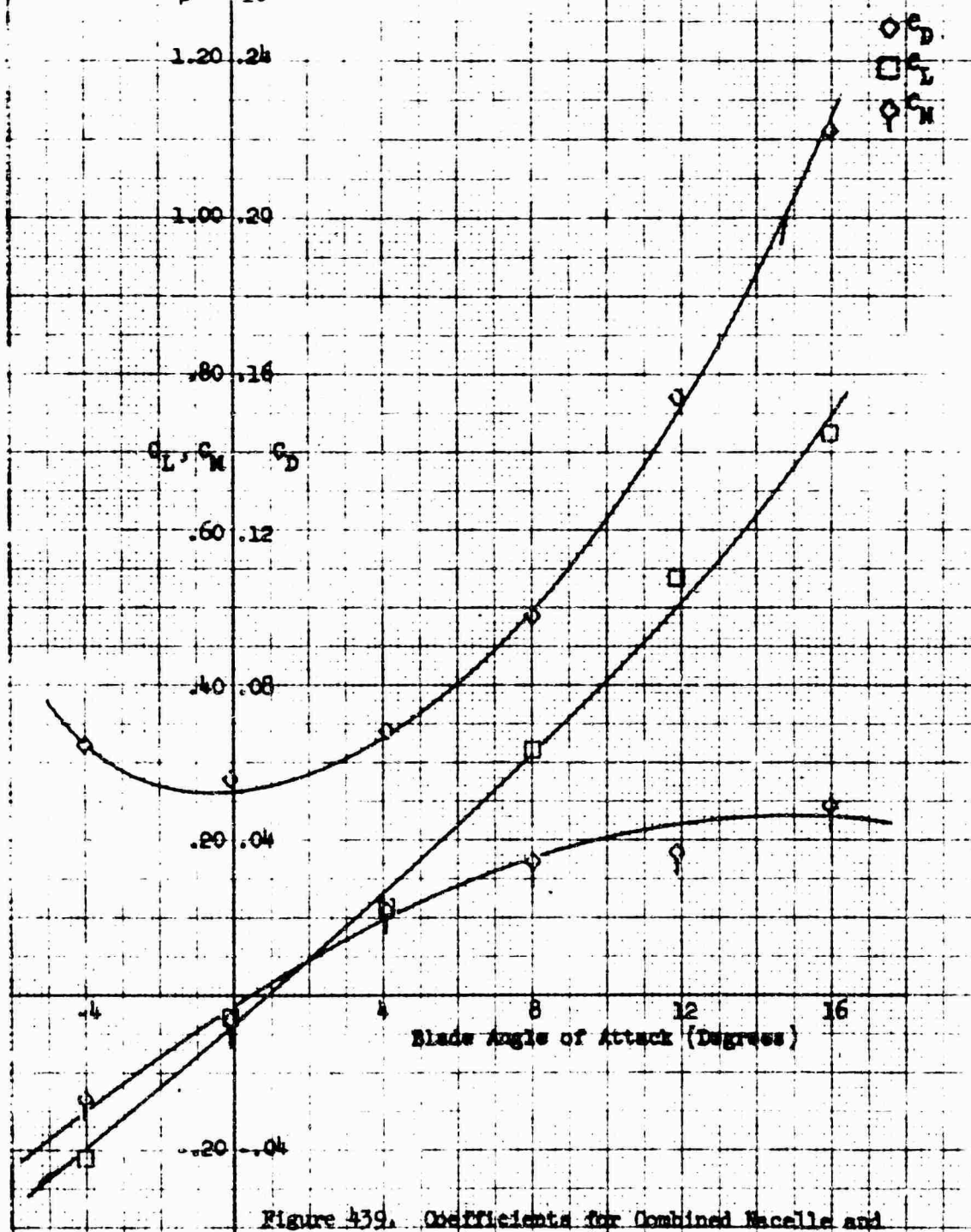


Figure 439. Coefficients for Combined Nacelle and Blade - Run 186.

Macelle Configuration: Twin Horizontal 1-40-100
 Fairing: With
 Macelle Exit Plate: 0
 $\beta = 20^\circ$

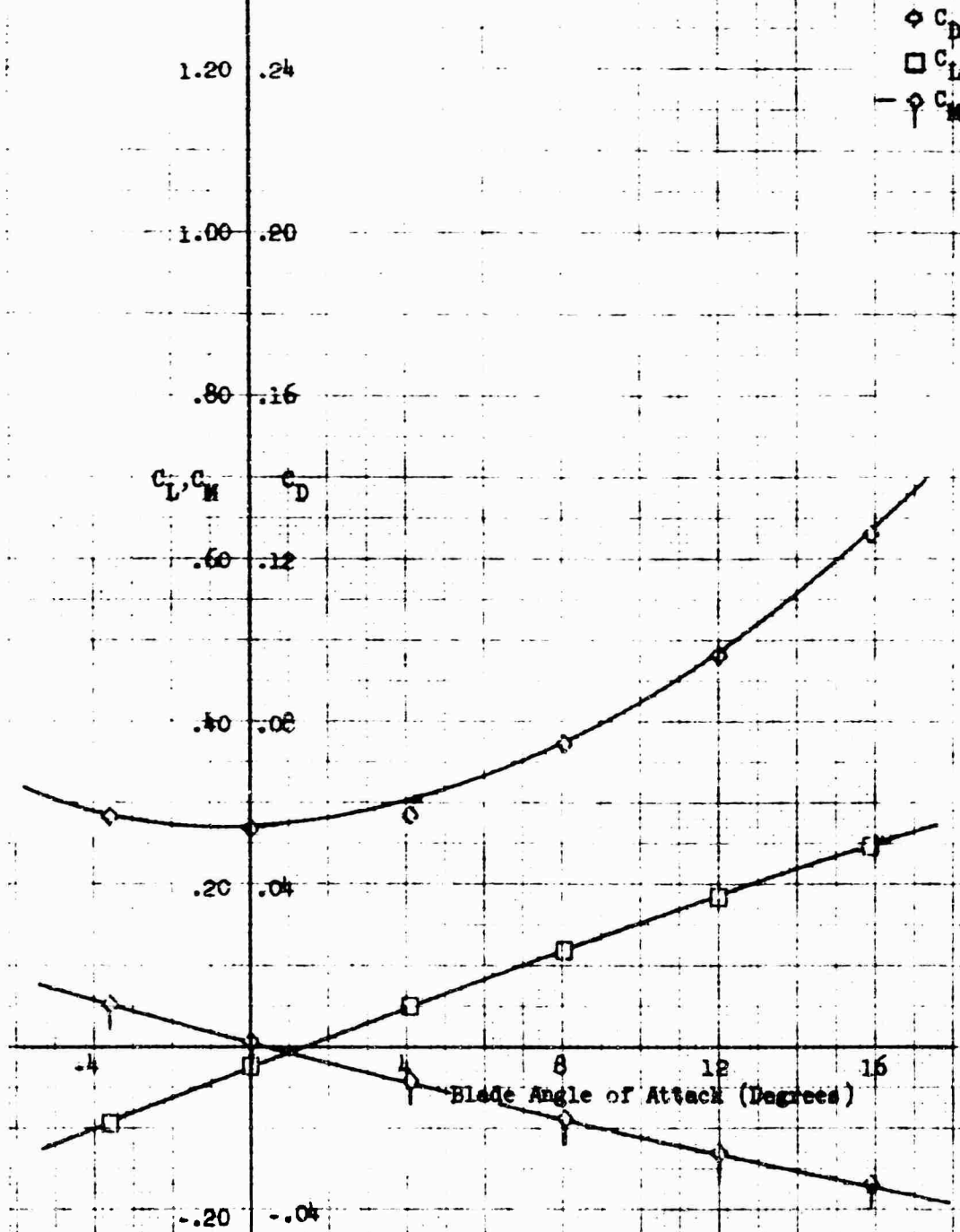


Figure 440. Coefficients for Macelle Only -
 Run 187.

Macelle Configuration: Twin horizontal 1-40-100
 Macelle Incidence Angle: 0°
 Pairing: With
 Macelle Exit Plate: 0
 $\beta = 20^\circ$

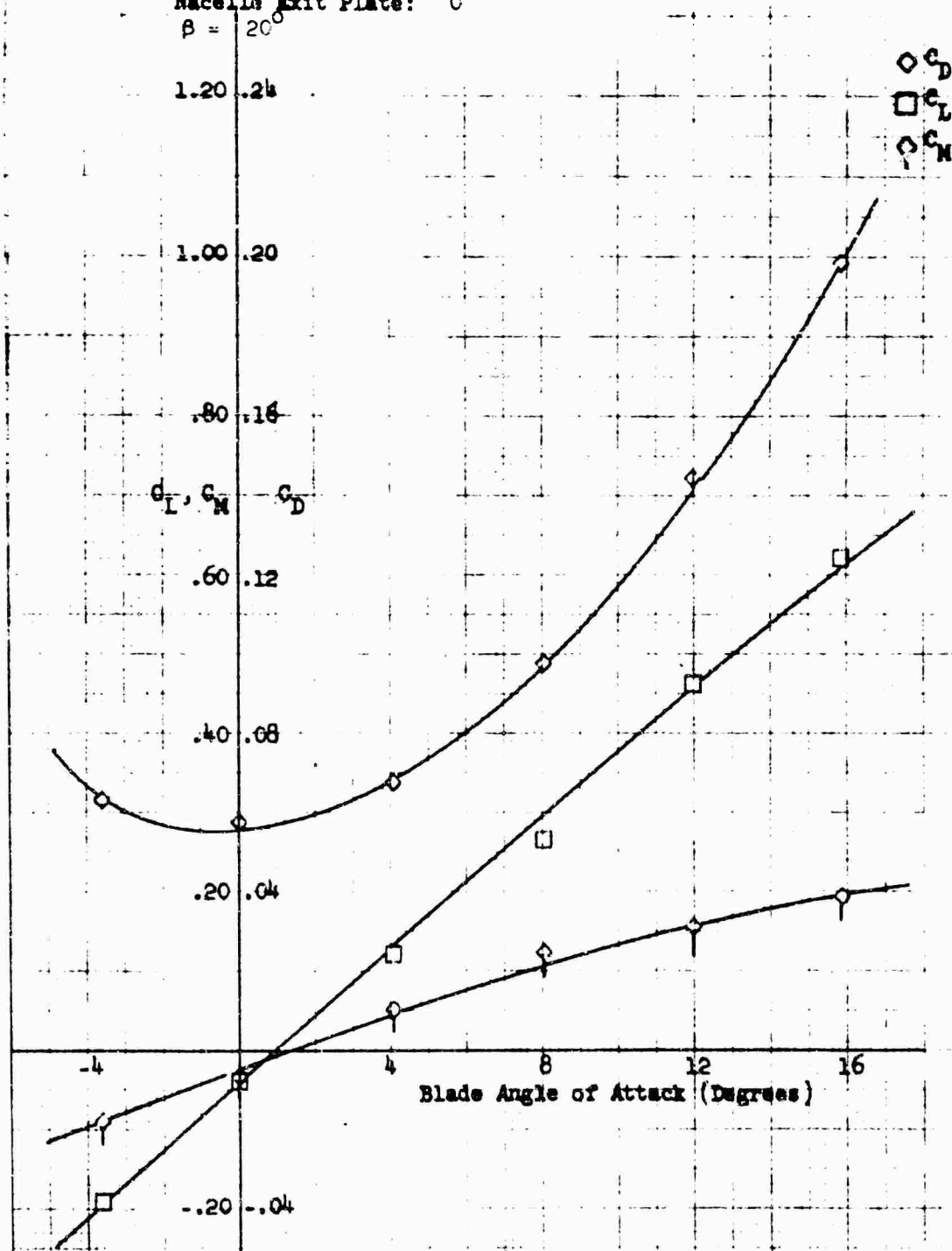
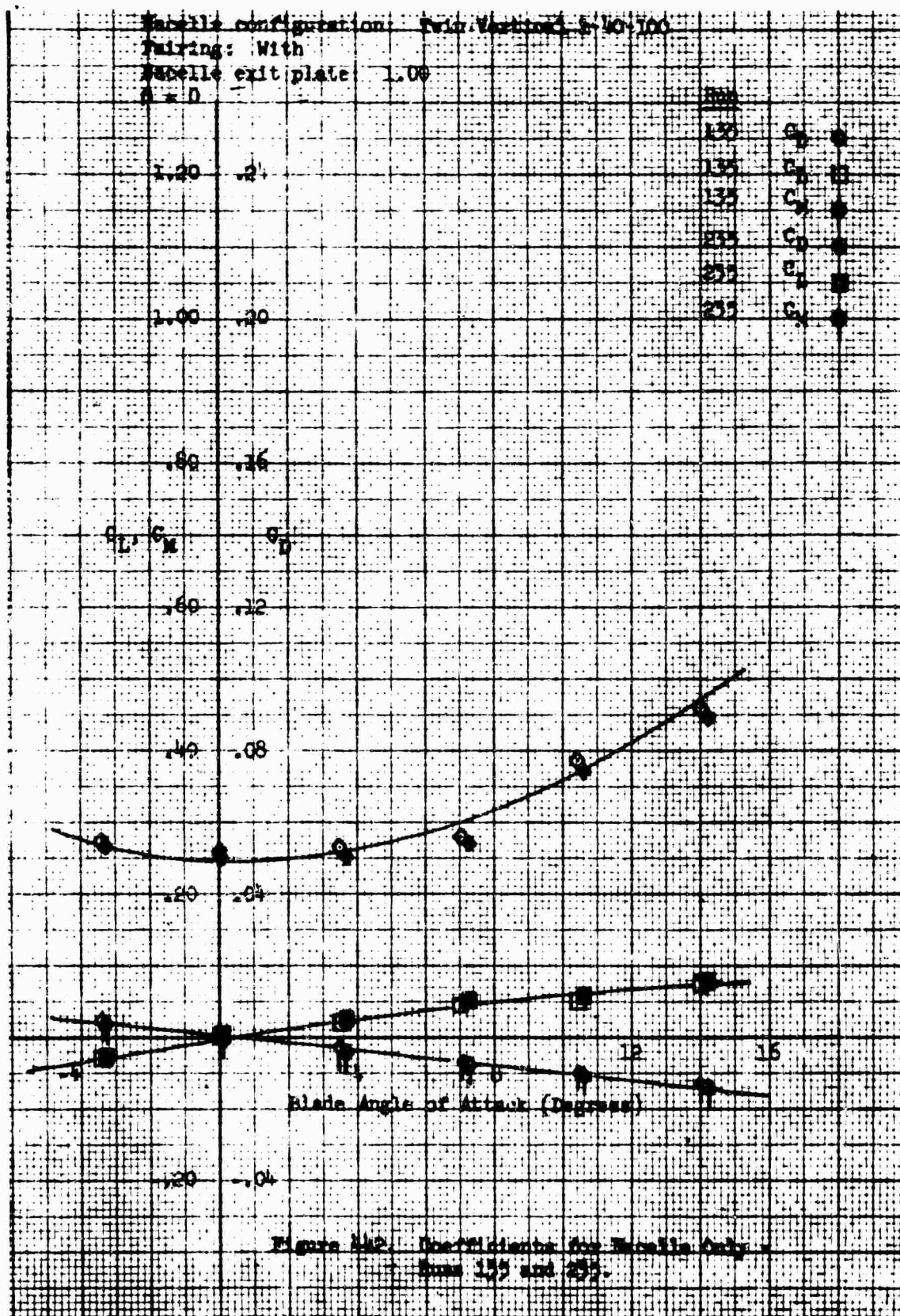


Figure 441. Coefficients for Combined Macelle and Blade - Run 187.



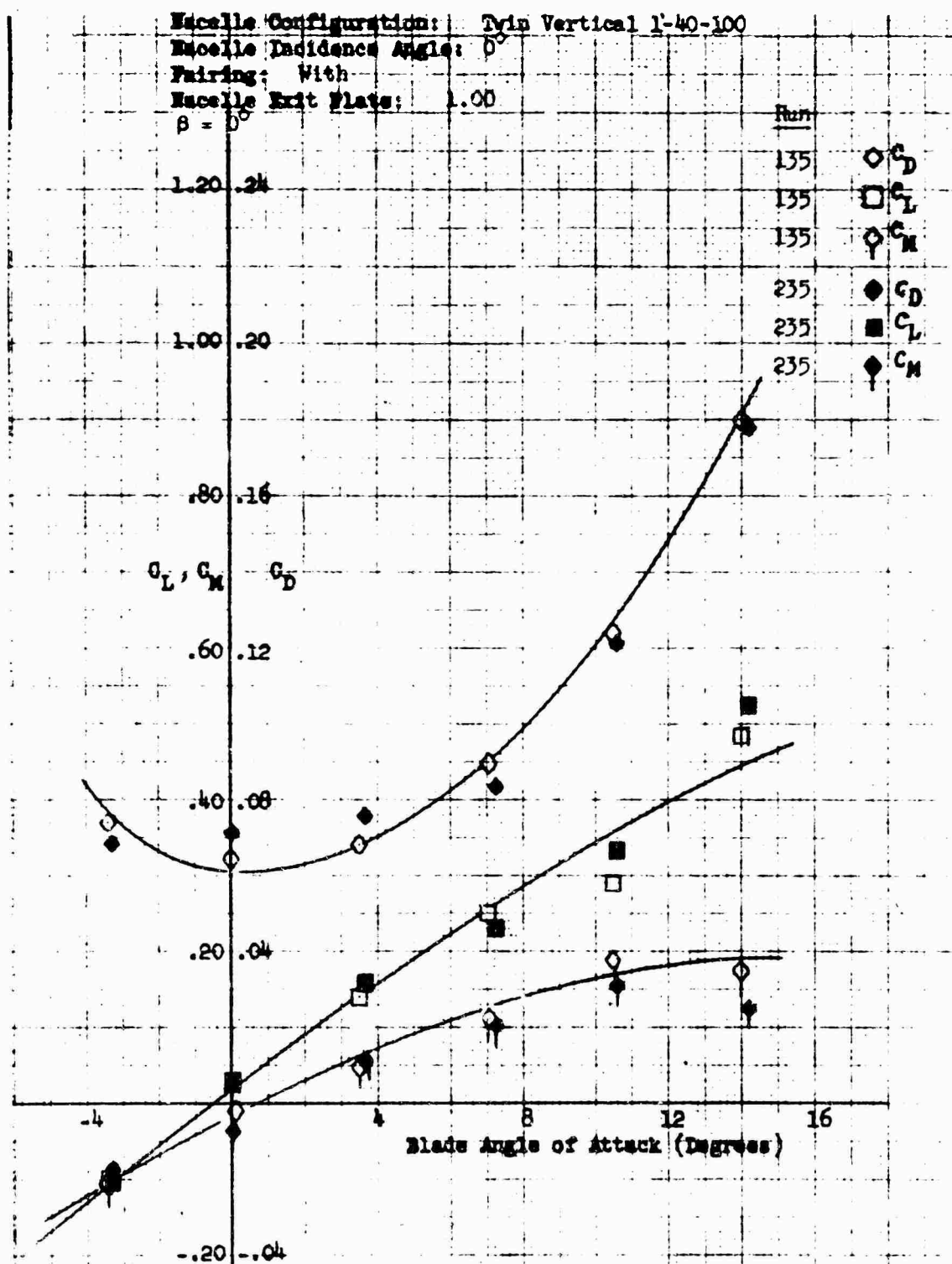


Figure 443. Coefficients for Combined Nacelle and Blade - Runs 135 and 235.

Nozzle configuration: Single 1-15-180

Pairing: N/A

Nozzle exit plate: 0

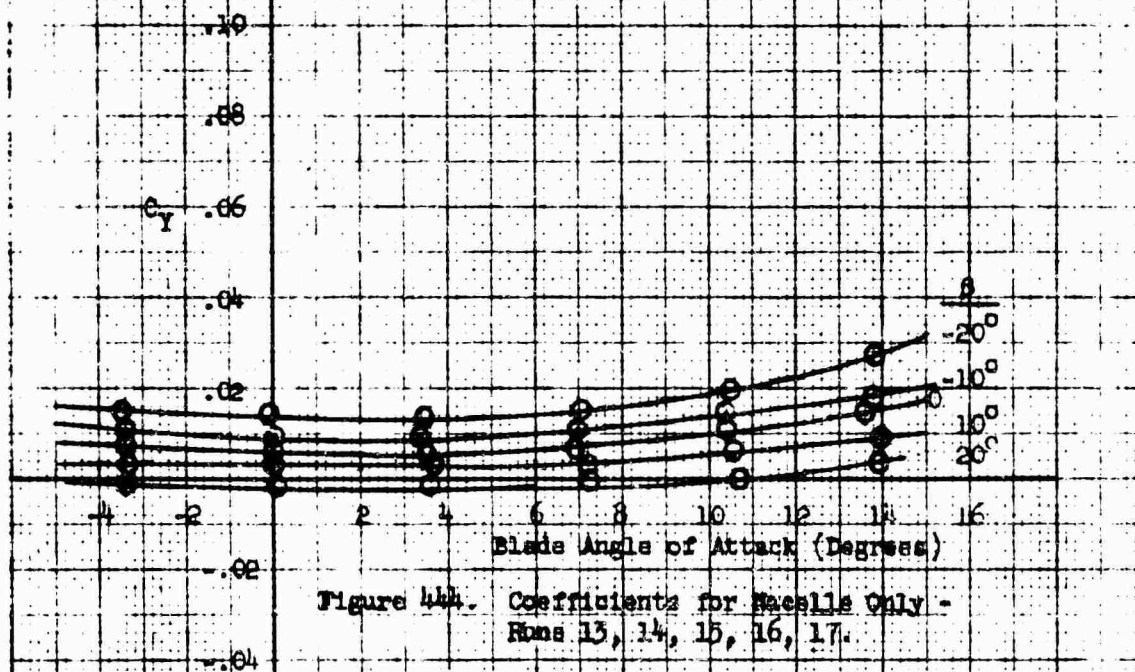


Figure 444. Coefficients for Nozzle Only -
Runs 13, 14, 15, 16, 17.

Nacelle configuration: Single 1-40-100
 Pairing: W/O
 Nacelle Exit Plate: 1.00

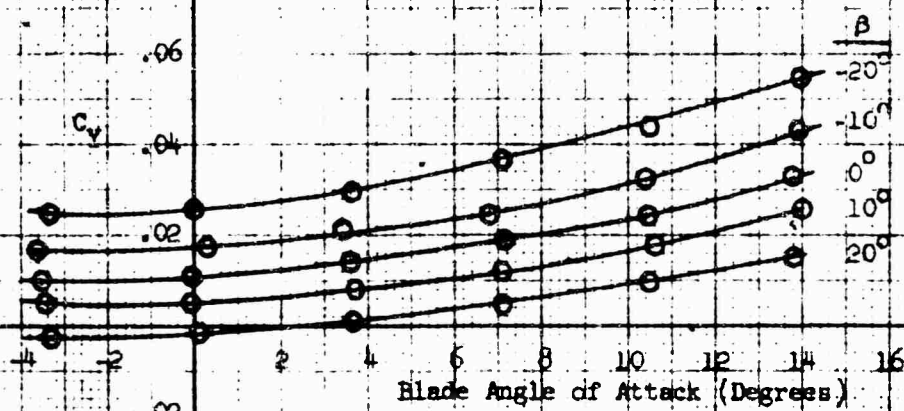


Figure 445. Coefficients for Nacelle Only -
 Runs 33, 34, 35, 36, 37.

Nacelle configuration: Twin vertical 1-16-100
 Pairing: With
 Nacelle exit plate: 1.00

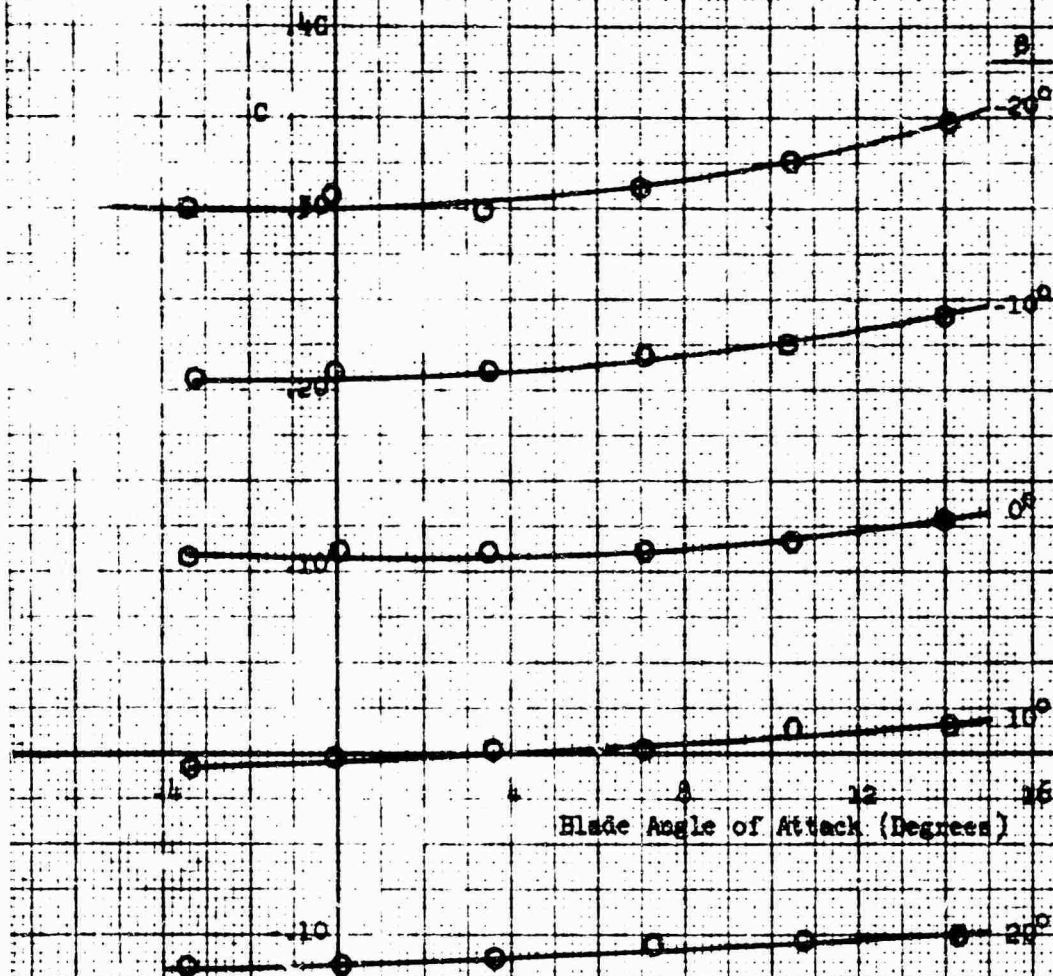


Figure 446. Coefficients for Nacelle Only
 Runs 153, 154, 155, 156, 157.

Macelle configuration: Twin vertical 1.40-100
 Pairing: With
 Macelle exit plate: 0

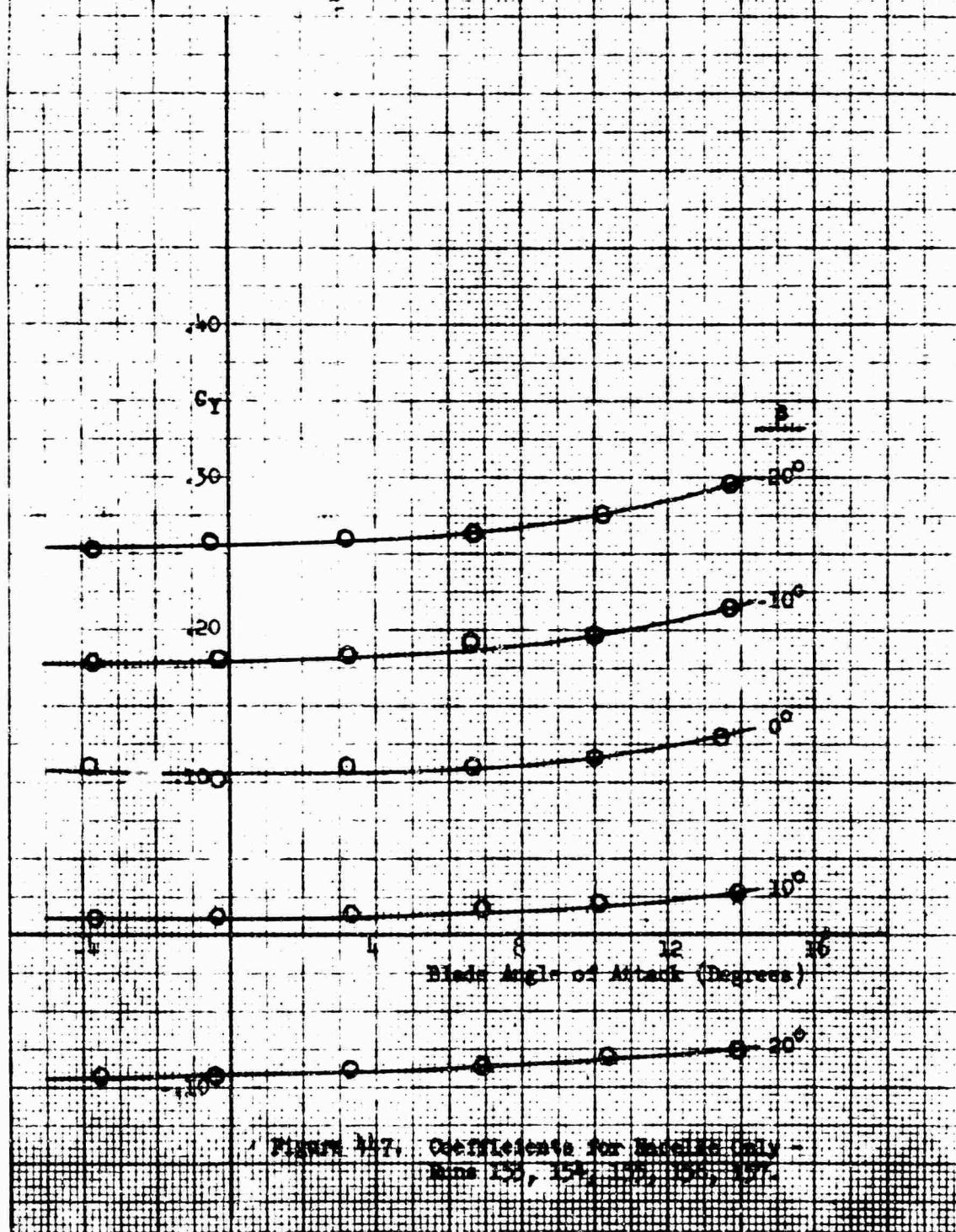


Figure 147. Coefficients for Macelle Only -
 Runs 150, 154, 158, 162, 167.

Nacelle configuration: Twin horizontal 1-40-100
 Fairing: With
 Nacelle exit plate: 1.00

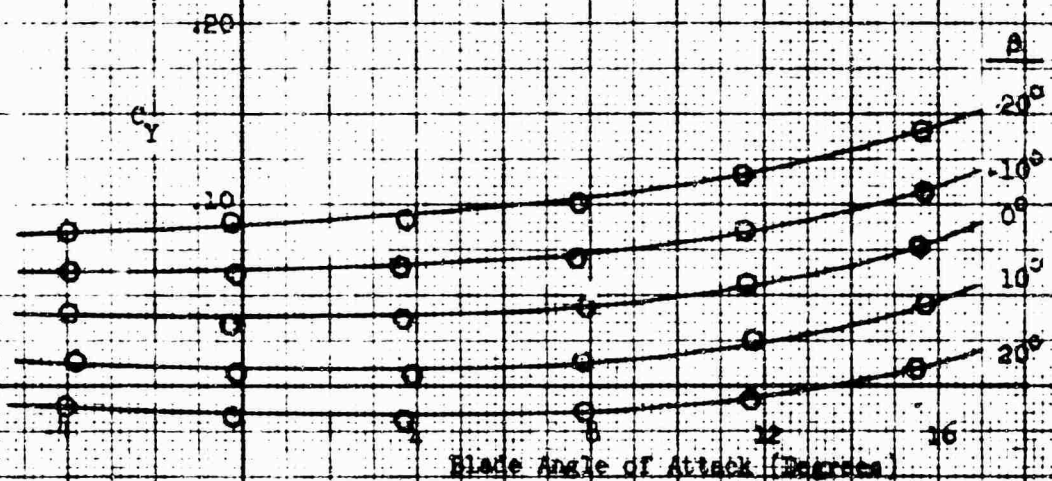


Figure 44B. Coefficients for Nacelle Only -
 Runs 163, 164, 165, 166, 167.

Nacelle configuration: Twin Horizontal 1-40-100
 Fairing: With
 Nacelle exit plate: 0

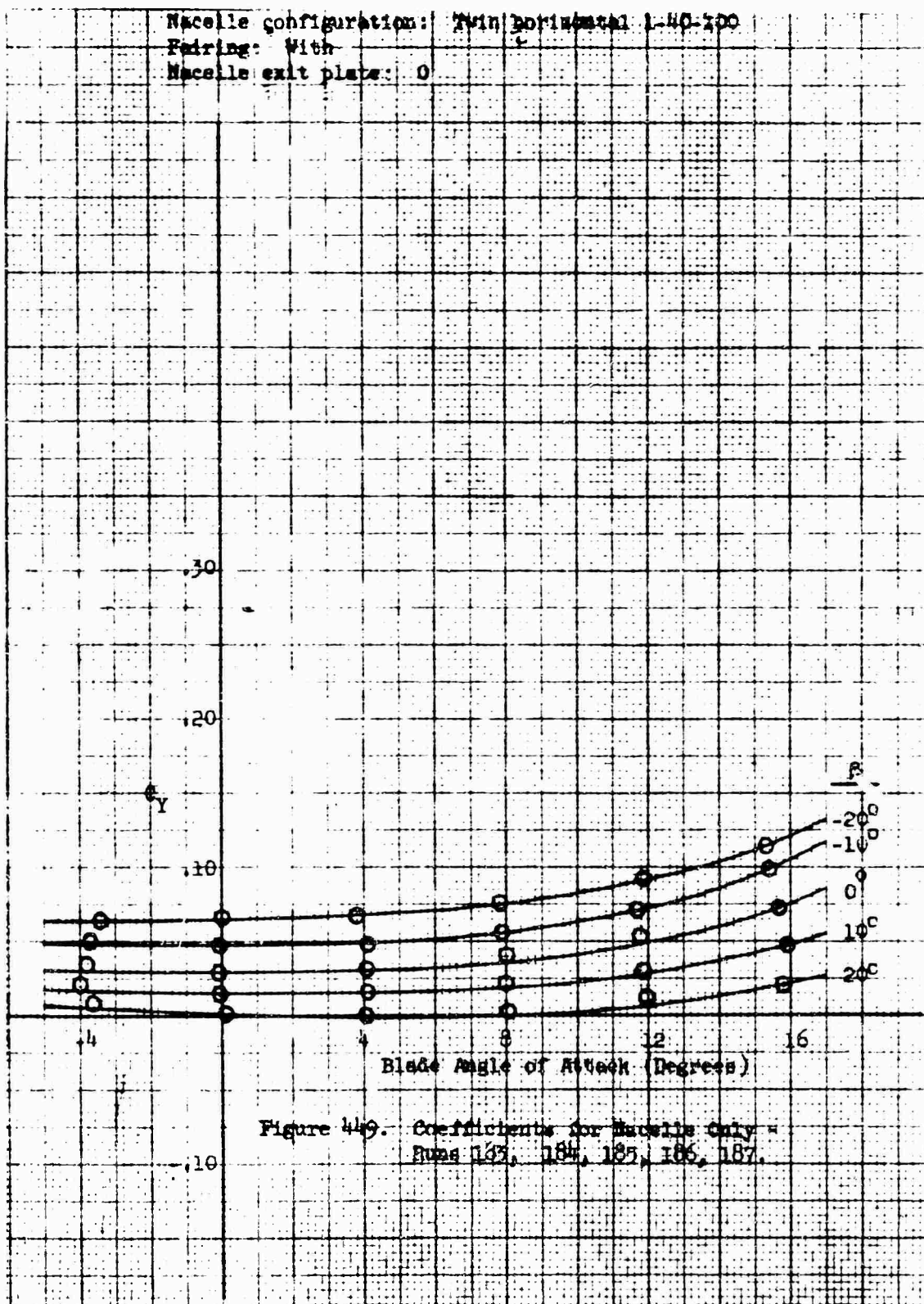


Figure 449. Coefficients for Nacelles Only -
 Runs 183, 184, 185, 186, 187.

6.0 APPENDIX

6.1 Strain-Gage Balance Reduction Method

6.1.1 Introduction

A strain-gage wind-tunnel balance is a force transducer that is designed to measure the aerodynamic forces on a wind-tunnel model. All forces and moments produced by the air flow or weight of the model are transferred to the supporting structure through the balance.

Figure 450 indicates the sign convention and typical balance calibration loading stations with the correct output signs for various positive loads.

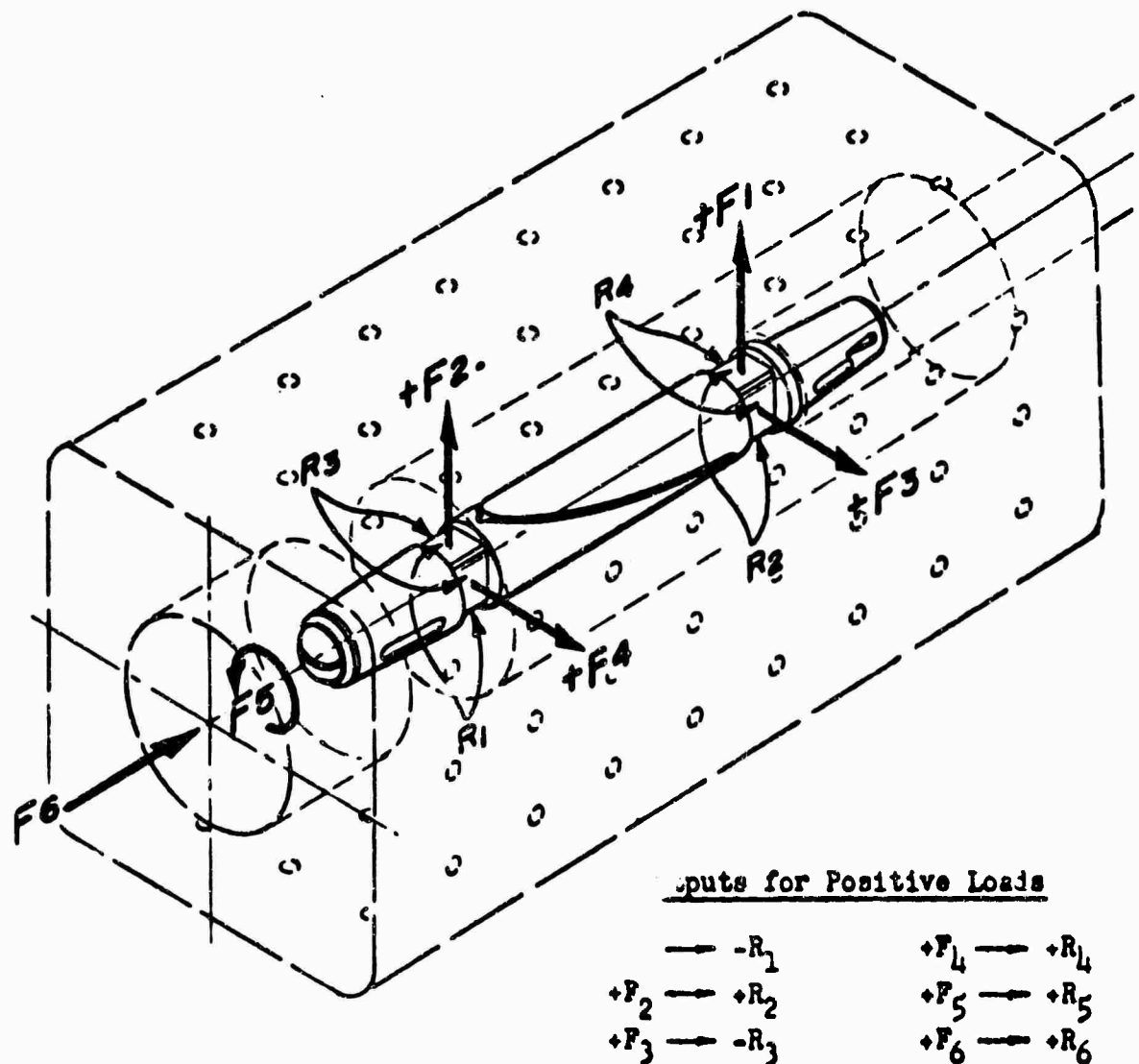


Figure 450. Typical Balance Calibration Setup and Designations.

6.1.2 Theory

The strain-gage balance consists of six temperature-compensated, full-bridge, strain-gage circuits mounted to and housed in a suitable structure. The balance under discussion is of the "two-moment" type, where the outputs of two strain-gage bridges provide bending moments at two points, separated by a known distance. A given pair of parallel co-planar bending moment vectors can be caused by one - and only one - force located at a fixed position relative to the moment vectors.

When the balance bridges are excited by a constant voltage, a pair of strain-gage bridges produce outputs (R_1 and R_2) which are proportional to the pitching moment at the electrical centers of bridges R_1 and R_2 , respectively. If the distance between the electrical centers of these bridges is known, the lift force and its location with respect to these electrical centers can be calculated. From this may be obtained the force and moment about any point. The side load and yawing moment are handled in the same way using the outputs of R_3 and R_4 . The rolling moment and drag are directly proportional to the R_5 and R_6 outputs, respectively.

6.1.3 Calibration

The equipment necessary to calibrate a strain-gage balance must include:

- (1) A regulated D.C. voltage power source.
- (2) A suitable millivolt measuring system to register the output of the bridges.
- (3) A suitable balance support which provides accurate adjustments in the balance attitude.
- (4) A calibration shell which provides accurate loading points.
- (5) An accurate level.
- (6) Weights and weight holders which allow loads to be applied without inducing unwanted moments.

The balance is leveled in pitch and roll with the calibration equipment installed. After power is applied and a steady-state temperature is reached, all bridge outputs are recorded or balanced to zero. Each bridge is loaded in sequence with several weights between negative and positive full load. After each load is applied, the balance is leveled to compensate for deflection and the output of all bridges is recorded.

Note that in loading the pitch and roll bridges, the weights would be applied over fore and aft bridge stations with the balance roll position adjusted to provide F_1 , F_2 , F_3 , or F_4 loading, but never combining loads

(i.e., F_2 and F_4). It is also evident that to load in positive and negative directions the balance should be rotated 180 degrees and the electrical output balanced. In this way the loads are simple weights with no mechanical losses due to pulleys or linkages.

The balance calibration is completed when the slopes (output millivolts per unit load) are tabulated for all bridge outputs with each primary load application (Tables 8 and 9).

TABLE 8 NACELLE BALANCE CALIBRATION CONSTANTS 5-VOLT EXCITATION (mv/lb.)						
	F_1	F_2	F_3	F_4	F_5	F_6
R_1	$-.69664 \times 10^{-1}$	$-.16023 \times 10^{-4}$	$+.66954 \times 10^{-3}$.00000	$-.48012 \times 10^{-3}$	$+.13734 \times 10^{-4}$
R_2	$+.82905 \times 10^{-2}$	$+.69010 \times 10^{-1}$	$-.15946 \times 10^{-3}$	$-.43710 \times 10^{-3}$	$+.16061 \times 10^{-4}$	$-.44743 \times 10^{-4}$
R_3	$-.64274 \times 10^{-3}$	$-.32853 \times 10^{-3}$	$-.70152 \times 10^{-1}$.00000	$-.12499 \times 10^{-3}$	$+.44836 \times 10^{-3}$
R_4	$+.17387 \times 10^{-3}$	$+.26396 \times 10^{-4}$	$+.78866 \times 10^{-2}$	$+.66409 \times 10^{-1}$	$-.27514 \times 10^{-3}$	$+.71269 \times 10^{-3}$
R_5	$-.74859 \times 10^{-3}$	$-.67207 \times 10^{-4}$	$-.32646 \times 10^{-2}$	$+.58315 \times 10^{-3}$	$+.64947 \times 10^{-1}$	$+.15409 \times 10^{-3}$
R_6	$+.87380 \times 10^{-3}$	$+.27144 \times 10^{-4}$	$+.42621 \times 10^{-3}$	$-.11089 \times 10^{-4}$	$+.11753 \times 10^{-3}$	$+.23039 \times 10^0$

TABLE 9 QUARTER CHORD BLADE BALANCE CALIBRATION CONSTANTS 5-VOLT EXCITATION (mv/lb.)					
	F_1	F_2	F_3	F_4	F_5
R_1'	$-.40161 \times 10^{-1}$.00000	$+.41732 \times 10^{-3}$	$-.18166 \times 10^{-3}$	$+.88034 \times 10^{-3}$
R_2'	$+.33588 \times 10^{-2}$	$+.49586 \times 10^{-1}$	$+.23075 \times 10^{-3}$	$+.22093 \times 10^{-3}$	$-.23273 \times 10^{-3}$
R_3'	$-.43467 \times 10^{-3}$	$-.85600 \times 10^{-4}$	$-.57390 \times 10^{-1}$	$+.49097 \times 10^{-4}$	$-.21250 \times 10^{-3}$
R_4'	$+.15147 \times 10^{-3}$	$+.56970 \times 10^{-3}$	$+.25923 \times 10^{-2}$	$+.49279 \times 10^{-1}$	$+.16190 \times 10^{-3}$
R_5'	$-.72440 \times 10^{-4}$	$-.13100 \times 10^{-4}$	$-.78556 \times 10^{-4}$	$-.29458 \times 10^{-4}$	$+.22201 \times 10^{-1}$

6.1.4 Weight Tares

The weight of the model will produce an output from one or more bridges. These outputs can be electrically balanced ("zeroed") or subtracted from the wind-on outputs.

The procedure used for the tip turbojet wind-tunnel tests was to periodically (and after each model change) record the balance weight tare outputs for three angles of attack covering the angle range. These weight tares were used to provide an equation of bridge output versus angle and the bridge weight tare was subtracted from all following outputs. The resulting change in bridge output was that resulting from aerodynamic forces. The bridge output due to aerodynamic loads and the calibration data provide the necessary data to calculate model axis coefficients.

6.1.5 Interactions

The primary load application produces secondary outputs from bridges which are not loaded (by design); these secondary outputs are termed interactions. In Table 8 each primary load produces one primary output and five secondary outputs. To determine the load from the six bridge outputs, the output on one bridge due to the load on another bridge must be removed before the primary output is a true representation of the primary load. The calibration data (Tables 8 and 9) provide the numerical values for the interactions, and it is a simple matter to remove them mathematically. The interactions are in essence higher order terms and removal of the largest or largest two interactions are normally sufficient to produce balance accuracy within the overall accuracy of each of the other variables; i.e., angle of attack, model detail reproduction, etc. The equations required to remove the interactions from the balance output will be obtained.

When an aerodynamic load is applied to the model, the balance produces output voltages R_1 through R_6 . If interactions are neglected, the R values are substituted into Equations (28) through (34). However, if interactions are to be considered, the corrected R_c values must be used.

Let δ represent any interaction coefficient and let the superscript represent the influenced output while the subscript denotes the influencing component. Thus, δ_3^1 is the R_3 influence coefficient to be applied to the R_1 output.

The influence coefficient is the ratio of the secondary output to the primary output produced by a unit load on a bridge. The δ values are independent of loading and are determined from the calibration data. The product of an influence coefficient and the corresponding strain-gage output voltage results in a correction that is applied to an output designated by the superscript.

Therefore: $\delta_3^1 R_3 = \frac{R_1 \text{ mv./unit } F_2}{R_3 \text{ mv./unit } F_2} \times R_3 \text{ output voltage}$

and $\delta_3^1 R_3 = -R_1 \text{ (mv.) due to the } R_3 \text{ loading}$

It is normally sufficiently accurate to consider only the two largest interactions; however, the complete expression for the corrected outputs are as follows:

$$R_{1C} = R_1 - \delta_2^1 R_2 - \delta_3^1 R_3 - \delta_4^1 R_4 - \delta_5^1 R_5 - \delta_6^1 R_6 \quad (19)$$

$$R_{2C} = R_2 - \delta_1^2 R_1 - \delta_3^2 R_3 - \delta_4^2 R_4 - \delta_5^2 R_5 - \delta_6^2 R_6 \quad (20)$$

$$R_{3C} = R_3 - \delta_1^3 R_1 - \delta_2^3 R_2 - \delta_4^3 R_4 - \delta_5^3 R_5 - \delta_6^3 R_6 \quad (21)$$

$$R_{4C} = R_4 - \delta_1^4 R_1 - \delta_2^4 R_2 - \delta_3^4 R_3 - \delta_5^4 R_5 - \delta_6^4 R_6 \quad (22)$$

$$R_{5C} = R_5 - \delta_1^5 R_1 - \delta_2^5 R_2 - \delta_3^5 R_3 - \delta_4^5 R_4 - \delta_6^5 R_6 \quad (23)$$

$$R_{6C} = R_6 - \delta_1^6 R_1 - \delta_2^6 R_2 - \delta_3^6 R_3 - \delta_4^6 R_4 - \delta_5^6 R_5 \quad (24)$$

6.1.6 Nacelle Balance; Balance Axis Forces and Moments

Figure 451 represents a cross section through the strain-gage balance and shows schematically the forward R_1 and aft R_2 bending bridges. With the force F applied at x , the bending moment at R_1 and R_2 can be calculated.

$$M_1 = -Fx \quad (25)$$

$$M_2 = -Fx + Fa_1 \quad (26)$$

$$M_1 = M_2 - Fa_1$$

$$Fa_1 = M_2 - M_1$$

Let $M = KR$

Then $Fa_1 = K_2 R_2 - K_1 R_1 \quad (27)$

and $K_2 = \frac{dM_2}{dR_2}, K_1 = \frac{dM_1}{dR_1}$

By using two calibration loading stations which are a known distance apart, the change in moment per change in output, or sensitivity coefficient (K), can be obtained.

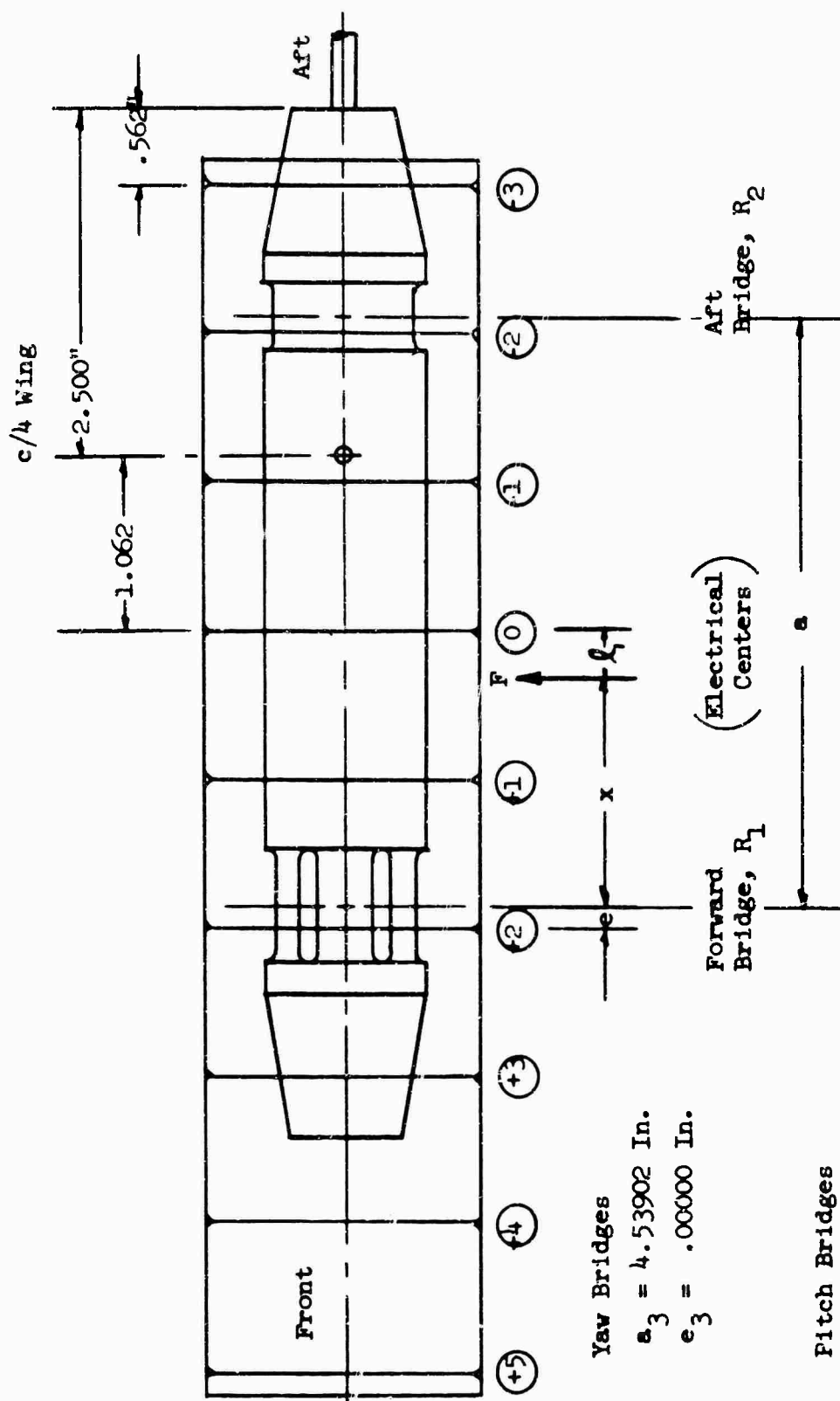


Figure 451. Nacelle Balance.

Loading Condition	"A"	"B"
F	1.0	1.0
F applied at station	-2.00 (F_1)	+2.00 (F_2)
R_1 (output)	-.069664	-.000016
R_2 (output)	+.0082905	+.069010
$\Delta M = (M_B - M_A)$	+4.00	+4.00
$\Delta R = (R_B - R_A)$	+.069648 = ΔR_1	+.0607195 = R_2
$K = \frac{\Delta M}{\Delta R}$	+57.43166 = K_1	+65.87669 = K_2

Therefore, from equation (27) and loading condition "A":

$$a_1 = \frac{K_2 R_2 - K_1 R_1}{F} \quad \text{and} \quad F = \text{unit load}$$

$$a_1 = 65.87669(.0082905) - 57.43166(-.069664) = 4.54707 \text{ in.}$$

The position of the electrical centers of the bridge can be found with respect to the balance calibration stations. From Equation (25):

$$x = -\frac{M_1}{F} = -\frac{K_1 R_1}{F} = -57.43166 R_1 / F$$

For F applied at station 2.0, loading condition "B": $x = e_1$.

$$e_1 = -57.43166 \left(\frac{-.000016}{1.00} \right)$$

$$e_1 = +.00092 \text{ in.}$$

The electrical center of the forward pitch bridge (R_1) is located at balance station, $2 - e_1 = 1.99908$.

The pitching moment about balance calibration shell station 0.00 is:

$$M_0 = F l_1 \quad \text{and} \quad l_1 = 1.99908 - x$$

$$\therefore M_0 = 1.99908 F + R_1 K_1 F / F = 1.99908 F + R_1 K_1$$

But $F = \frac{R_2 K_2 - R_1 K_1}{a_1}$ (28)

$$\text{and} \quad M_0 = \frac{1.99908}{a} (R_2 K_2 - R_1 K_1) + R_1 K_1$$

This equation can be written in general terms for the moment about any balance equation.

$$M_{\text{sta.}} = \left(\frac{1.99908 - \text{sta.}}{a_1} \right) (R_2 K_2 - R_1 K_1) + R_1 K_1 \quad (29)$$

The model axis moments are resolved about the quarter-chord axis of the blade. The blade quarter chord is located at station -1.062 of the nacelle balance. The equation for the moment about the blade quarter chord is then,

$$M_{1/4 \text{ chord}} = \left[\frac{1.99908 - (1.062)}{a_1} \right] (R_2 K_2 - R_1 K_1) + R_1 K_1$$

$$M_{1/4 \text{ chord}} = \frac{3.06108}{a_1} (R_2 K_2 - R_1 K_1) + R_1 K_1 \quad (30)$$

To determine side load and yawing moment, the process is repeated using the R_3 and R_4 outputs instead of the R_1 and R_2 outputs. This results in the following equations:

$$K_3 = 57.01904$$

$$K_4 = 68.34920$$

$$a_3 = 4.53902 \text{ in.}$$

$$y = \frac{K_4 R_4 - K_3 R_3}{a_3} \quad (31)$$

The yawing moment equation is derived in the same manner as was the pitching moment.

$$e_3 = - \frac{K_3 R_3}{F} = \frac{-57.01904(+.00000)}{1.000} = 0.0000$$

The R_3 electrical center is at balance calibration shell station:

$$2.0 - e = 2.00000$$

and the yawing moment is:

$$N_o = F l_3 \quad l_3 = 2 - x$$

$$N_o = \frac{2}{a_3} (R_4 K_4 - R_3 K_3) + R_3 K_3$$

In general terms about any balance calibration station (sta.):

$$N_{\text{sta.}} = \left(\frac{2.00000 - \text{sta.}}{a_3} \right) (R_4 K_4 - R_3 K_3) + R_3 K_3 \quad (32)$$

The drag and rolling moment are directly proportional to the R_6 and R_5 outputs.

$$D = R_6 K_6 \quad (33)$$

$$K_6 = \frac{1}{.23039} = 4.34047 \text{ lb/mv.}$$

$$R = R_5 K_5 \quad (34)$$

$$K_5 = \frac{1}{.064947} = 15.39717 \text{ in-lb/mv.}$$

The influence coefficients which influence the R_1 output are calculated from the calibration data (Table 8), as an example.

$$\delta'_2 = \frac{-.16023 \times 10^{-4}}{+.69010 \times 10^{-1}} = -.00023$$

$$\delta'_3 = \frac{+.66954 \times 10^{-3}}{-.70152 \times 10^{-1}} = -.00954$$

$$\delta'_4 = \frac{.00000}{+.66409 \times 10^{-1}} = 0.00000$$

$$\delta'_5 = \frac{-.48012 \times 10^{-3}}{+.64947 \times 10^{-1}} = -.00739$$

$$\delta'_6 = \frac{+.13734 \times 10^{-4}}{+.23039 \times 10^0} = +.00006$$

The forces (Equations 28, 31, and 33) and the moments (Equations 29, 32, and 34) can be transferred to any desired axis or point. The general practice is to transfer from model axis to wind axis.

Note that if the balance is supported on the forward end and loaded on the aft end, as was the case for the nacelle balance, the balance outputs must all be changed in sign.

6.1.7 Blade Quarter-Chord Balance; Balance Axis Forces and Moments

Figure 452 represents a cross section through the blade quarter-chord strain-gage balance and shows schematically the forward R_1 and aft R_2 bending bridges. With the force F applied at x , the bending moment at R_1 and R_2 can be calculated as was done for the nacelle balance.

$$M_1 = -F_x \quad (35)$$

$$M_2 = -Fx + Fa \quad (36)$$

$$M_1 = M_2 - Fa$$

$$Fa = M_2 - M_1$$

Let $M = K'R'$

Then $Fa = K'_2 R'_2 - K'_1 R'_1$

and $K'_2 = \frac{dM_2}{dR_2}$, $K'_1 = \frac{dM_1}{dR_1}$

By using two calibration loading stations which are a known distance apart, the change in moment per change in output, or sensitivity coefficient (K), can be obtained.

Loading condition	"A"	"B"
F	1.0 lb.	1.0 lb.
F applied at station	-2.00 (F_1)	+2.00 (F_2)
R'_1 (output)	-.040161 mv.	0.00000 mv.
R'_2 (output)	+.0033588 mv.	.049586 mv.
$\Delta M = (M_B - M_A)$	+4.00	+4.00
$\Delta R' = (R'_B - R'_A)$	+.040161 = ΔR_1 mv.	+.046227 = ΔR_2 mv.
$K = \frac{\Delta M}{\Delta R}$	$K'_1 = +99.59911$ mv/in.-lb.	$K'_2 = 86.52952$ mv/in.-lb.

From Equation (37) and loading condition "A":

$$a'_1 = \frac{K'_2 R'_2 - K'_1 R'_1}{F} \text{ and } F = \text{unit load.}$$

$$a'_1 = .049586 \times 86.52914 = 4.29063 \text{ in.}$$

$$e'_1 = -R'_1 K'_1 / F = -99.59911 \times .00000 = .00000$$

The electrical center of the forward pitch bridge (R'_1) is located at balance station 2 - 'e' = 2.00.

The pitching moment about any balance station is:

$$M'_{\text{sta.}} = \left(\frac{2.0 - \text{sta.}}{a'_1} \right) (R'_2 K'_2 - R'_1 K'_1) + R'_1 K'_1 \quad (38)$$

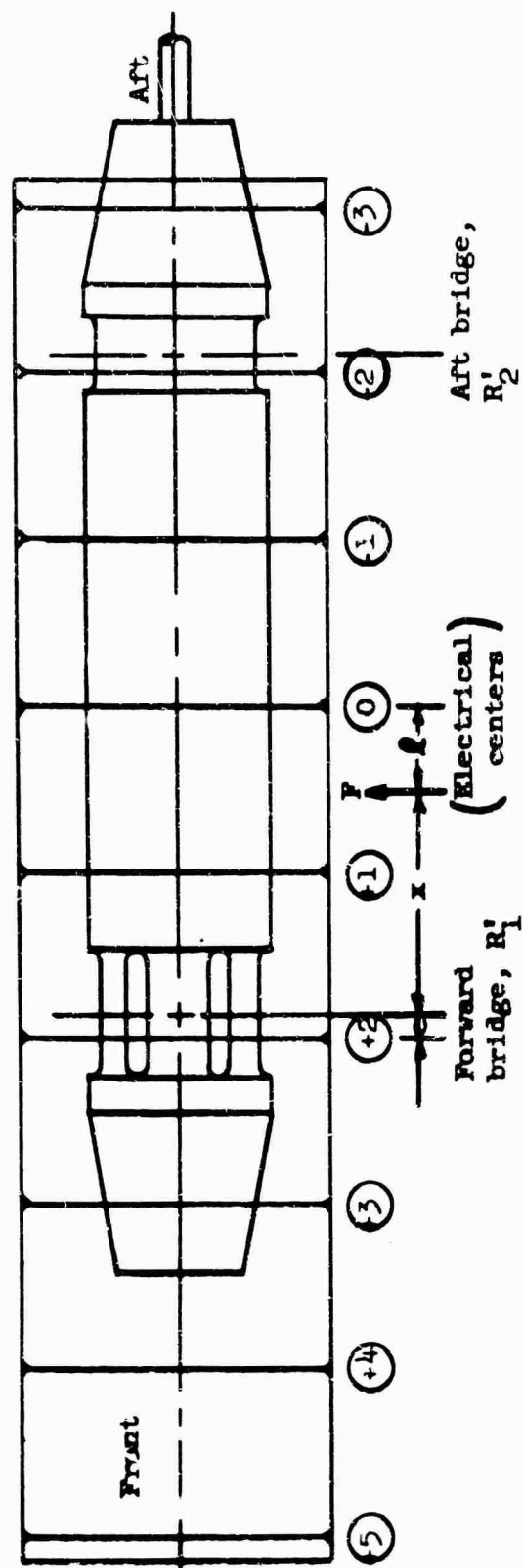


Figure 452. Blade Quarter-Chord Balance.

$$\text{and } L = \frac{K_2' R_2' - K_1' R_1'}{a_1'} \quad (39)$$

Repeating the calculations for the side load and yawing moment:

$$K_3' = 69.63897 \text{ mv/in-lb.}$$

$$K_4' = 85.67750 \text{ mv/in-lb.}$$

$$a_3' = 4.21868 \text{ in.}$$

$$e_3' = -.00342 \text{ in.}$$

$$N_{3 \text{ sta}}' = \frac{2.00342 - \text{sta.}}{a_3'} (R_4' K_4' - R_3' K_3') + R_3' K_3' \quad (40)$$

$$Y = \frac{R_4' K_4' - R_3' K_3'}{a_3'} \quad (41)$$

The rolling moment is directly proportional to the R_5' output.

$$\text{Rolling moment} = R_5' K_5'$$

$$K_5' = \frac{1}{.22201 \times 10^{-1}} = 45.04302 \text{ in-lb/mv.} \quad (42)$$

Blade quarter-chord balance is installed in the model with the balance axis along the blade quarter-chord line. The balance lift represents total aerodynamic lift on the model, and the balance side load (Y) is the total model drag. The pitching moment and yawing moment could be used to find the center of lift and drag, respectively; however, this information is not used. The balance rolling moment is the total model pitching moment about the quarter-chord line.

After removing the interactions, Equation (39) gives total model lift, and Equations (41) and (42) give the total drag and pitching moment.

6.2 Nacelle Airloads at Typical Forward Flight Condition

The following discussion is presented for the purpose of illustrating the method used to determine nacelle airloads as they vary with blade azimuth position during forward flight. The configuration used is a single engine nacelle with a conical spinner and no nacelle exit restriction. Any other nacelle configuration could be used as well since this is only intended to be a sample calculation.

Figure 453 shows a plan view of the rotor disk with a blade located in a general azimuth position, ψ , where ψ is measured in the direction of rotor rotation from the aft position of the rotor disk.

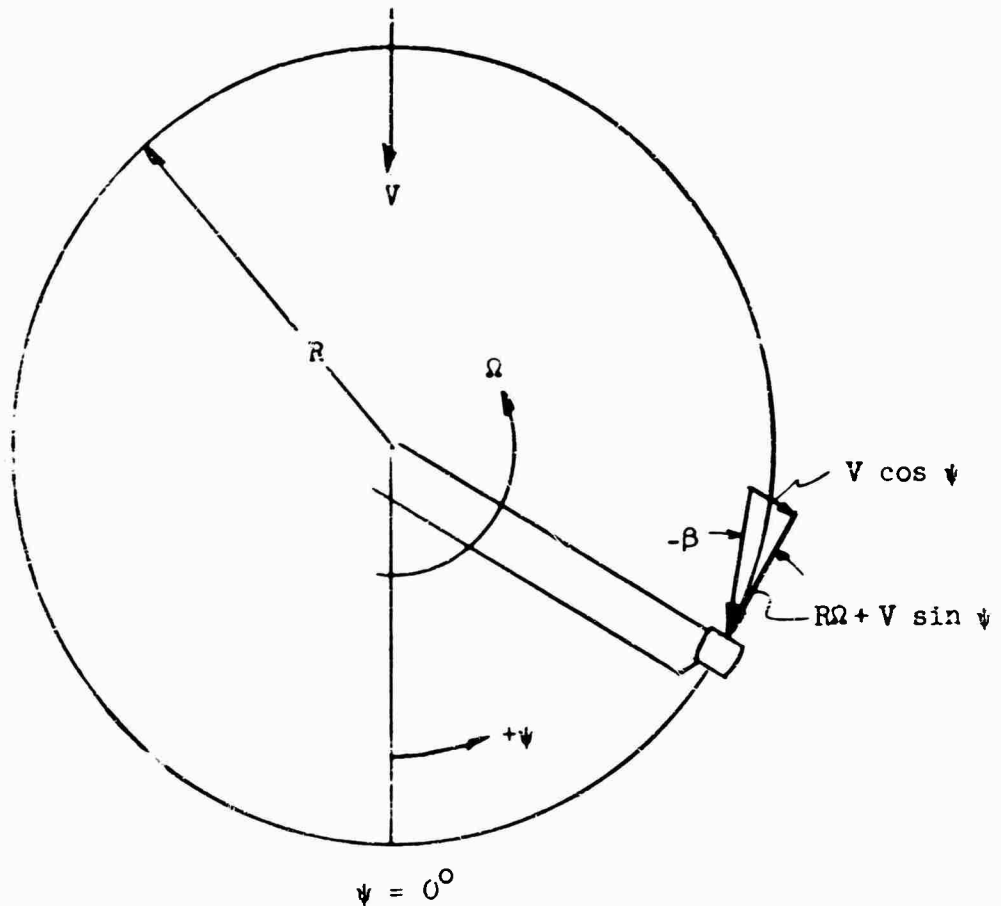


Figure 453. Plan View of Rotor Disk in Forward Flight.

It can be seen from Figure 453 that the relative yaw angle of the nacelle at any azimuth angle is given by the following expression:

$$\beta = -\arctan \frac{V \cos \psi}{R\Omega + V \sin \psi} \quad (43)$$

where: V = forward flight speed, f.p.s.

$R\Omega$ = rotor tip speed, V_T , f.p.s.

Equation (43) shows that β is positive for ψ between 90 degrees and 270 degrees and negative for ψ between 270 degrees and 90 degrees as the blade traverses the azimuth.

So that interpolation of wind-tunnel data is not necessary, two values of advance ratio, μ , are calculated for which β varies between +10 degrees and -10 degrees at μ_1 and for which β varies between +20 degrees and -20 degrees at μ_2 . Equation (43) states the maximum positive β occurs at $\psi = 180^\circ$ and so μ_1 and μ_2 can be calculated as follows:

$$V = - \frac{V_T + V \sin 180^\circ}{\cos 180^\circ} \tan \beta = +V_T \tan \beta$$

or $\mu = \tan \beta$

$$\mu_1 = \tan 10^\circ = 0.176$$

$$\mu_2 = \tan 20^\circ = 0.364$$

The resultant velocity vector at the nacelle shown in Figure 453 corresponds to the velocity vector in the wind-tunnel, and so the dynamic pressure at any azimuth position is given by the following expression:

$$\begin{aligned} q_o &= \frac{1}{2} \rho (V_T^2 + 2V_T V \sin \psi + V^2 \sin^2 \psi + V^2 \cos^2 \psi) \\ &= \frac{1}{2} \rho (V_T^2 + 2V_T V \sin \psi + V^2) \\ &= \frac{1}{2} \rho V_T^2 (1 + 2\mu \sin \psi + \mu^2) \end{aligned} \quad (44)$$

where: ρ = air density, .002378 slugs/ft³

μ = advance ratio, V/V_T

In order to complete the description of the aerodynamic environment of the nacelle, some assumption must be made which defines the pitching angle of attack of the nacelle with the resultant velocity vector. No attempt will be made to define any of the parameters needed to determine the nacelle angle of attack as a function of azimuth (i.e., collective pitch settings, cyclic pitch settings, blade twist, blade flapping angles, etc.), but instead a rational variation of pitch angle with azimuth is assumed. Nacelle pitching angles of attack, α , are assumed to be 6° , 0° , 6° , and 12° for blade azimuth positions of 0° , 90° , 180° , and 270° , respectively.

The force measurements in the wind-tunnel resolved the nacelle lift, drag and side forces into vectors in either of two axis systems, a model axis system and a stability axis system. This analysis is intended to show the nacelle airloads as they are oriented with respect to the rotor disk axes and so the wind-tunnel stability axis system coefficients are used. The nacelle pitching, rolling, and yawing moments are not calculated in this example since they are of less interest than the forces.

Before proceeding with the force calculations, it is well to summarize the formulas and reference areas which will be used. The wind-tunnel force coefficients were derived using the following formulas:

$$\text{Lift force: } L_s = C_L q A_R \quad (2)$$

$$\text{Drag force: } D_s = C_D q A_R \quad (1)$$

$$\text{Side force: } Y_s = C_Y q A_R \quad (4)$$

where A_R was the area of blade (supporting the nacelle) which projected into the tunnel. This area changed with yaw angle as described in Section 3.4.2 of this report.

Equations (2), (1), and (4) define the total forces including those which result from air flow through the nacelle. These forces due to air flow through the nacelle were also determined so that they could be subtracted from the total forces to give only the lift, drag and side forces due to external air flow. The nacelle internal force coefficients were derived using the following formulas:

$$\text{Lift force: } L' = C_L' q A_R \quad (45)$$

$$\text{Drag force: } D' = C_D' q A_R \quad (46)$$

$$\text{Side force: } Y' = C_Y' q A_R \quad (47)$$

The force coefficients defined by Equations (1), (2), (4), (45), (46), and (47) are based upon an area and dynamic pressure which change with blade azimuth position. In this form the coefficients for the four azimuth positions cannot be directly added or algebraically manipulated. If, however, all of the coefficients are revised so that they are based upon an area and "reference" dynamic pressure which are common to both the model and full size nacelle, direct comparisons can be made. The reference area is chosen to be the compressor inlet area, designated A_I , and the reference dynamic pressure is chosen to be $\rho V_T^2/2$, designated q_T .

Subtracting Equation (45) from Equation (2) and rearranging gives:

$$C_L - C_L' = \frac{L - L'}{q A_R} = \frac{L - L'}{\frac{1}{2} \rho V_T^2 (1 + 2\mu \sin \psi + \mu^2) A_R}$$

$$\text{or } C_L - C_L' = \frac{L - L'}{q_T A_R (1 + 2\mu \sin \psi + \mu^2)}$$

$$\text{Since it is desired to define } C_L'' = \frac{L - L'}{q_T A_R}$$

it is obvious that

$$C_L'' = (C_L - C_L') (1 + 2\mu \sin \psi + \mu^2) \frac{A_R}{A_I} \quad (48)$$

Equation (48), then, is the nacelle lift coefficient due to external air flow and is based upon compressor inlet area, A_I , and dynamic pressure $\rho V_T^2/2$. A similar modification of the drag and side force coefficients yields the following formulas:

$$C_D'' = (C_D - C_D')(1 + 2\mu \sin \psi + \mu^2) \frac{A_R}{A_I} \quad (49)$$

$$C_Y'' = (C_Y - C_Y')(1 + 2\mu \sin \psi + \mu^2) \frac{A_R}{A_I} \quad (50)$$

Table 10 summarizes the nacelle aerodynamic environment at the four azimuth positions chosen for this example and presents the lift, drag, and side force coefficients defined by Equations (1), (2), (4), and (45) through (50). The run numbers refer to the wind-tunnel runs which pertain to the nacelle configuration and β values which have been assumed.

TABLE 10 NACELLE LIFT, DRAG AND SIDE FORCE COEFFICIENTS								
Advance Ratio	$\mu_1 = 0.176$				$\mu_2 = 0.364$			
Run No.	131	130	129	130	132	130	128	130
ψ	0°	90°	180°	270°	0°	90°	180°	270°
α	6°	0°	6°	12°	6°	0°	6°	12°
β	-10°	0°	+10°	0°	-20°	0°	+20°	0°
A_R (ft ²)	2.307	2.470	2.617	2.470	2.119	2.470	2.760	2.470
A_I (ft ²)	.0620							
C_L	.0280	-.0055	.0520	.0910	.0110	-.0055	.0530	.0910
C_D	.0205	.0250	.0325	.0445	.0065	.0250	.0325	.0445
C_Y	.0370	.0110	.0030	.0400	.0645	.0110	-.0125	.0400
C_L'	.0026	0	.0023	.0048	.0026	0	.0020	.0048
C_D'	.0040	.0036	.0035	.0046	.0040	.0036	.0031	.0046
C_Y'	.0051	0	-.0045	0	.0104	0	-.0080	0
C_L''	.97	-.30	2.16	2.33	.33	-.41	2.57	1.39
C_D''	.63	1.18	1.26	1.08	.10	1.59	1.48	.64
C_Y''	1.22	.61	.33	1.08	2.09	.82	-.23	.64

The drag and side force coefficients, C_D and C_Y , in Table 10 are plotted as vectors in Figure 454 for advance ratios of 0.176 and 0.364. It is immediately obvious that the nacelle side forces contribute a net in-plane drag force for the rotor blade locations shown. If similar calculations to those of Table 10 were done for the blades in intermediate positions (i.e., $\psi = 45^\circ, 135^\circ, 225^\circ$, and 315°), a plot of the fore and aft components of side load versus azimuth would reveal a 4-cycle-per-revolution varying load which could be integrated to give an average in-plane drag force during forward flight.

Figures 455 through 459 are graphs of axial pressure distribution along the nacelle surface for two single-engine configurations: 1-40-100 and 1-50-100 (conical spinner).

The pressure distributions shown are representative of four blade azimuthal positions: $\psi = 0^\circ, 90^\circ, 180^\circ$, and 270° . At each azimuth the blade angle of attack is representative of that encountered in forward flight: $\alpha = 6^\circ$ at $\psi = 0^\circ$ and 180° ; $\alpha = 0^\circ$ at $\psi = 90^\circ$; and $\alpha = 12^\circ$ at $\psi = 270^\circ$.

Since the sideslip angle on the nacelle is characteristic of the vector combination of the forward flight velocity V and blade tip speed V_T in any azimuth except $\psi = 90^\circ$ or $\psi = 270^\circ$, pressure distributions at the 180° and 0° azimuth positions are shown for two different advance ratios, $\mu = .176$ and $\mu = .364$, on the 1-50-100 nacelle.

Figures 461 through 464 show representative plots of the inlet total pressure recovery and the mean variation of these recoveries about the average. Plots are presented for four selected inlets at two advance ratios. The inlet total pressure recovery is an area weighted compressor inlet station total pressure to freestream total pressure ratio, and has a value of 1.0 for reversible flow. The mean variation in total pressure recovery about the average is obtained by numerically summing the individual deviations from the average area weighted total pressure and dividing by the average value; this has a value of zero for uniform total pressure. The superiority of the inlet with the centerbody (Figure 462), particularly at high advance ratios, is clearly evident.

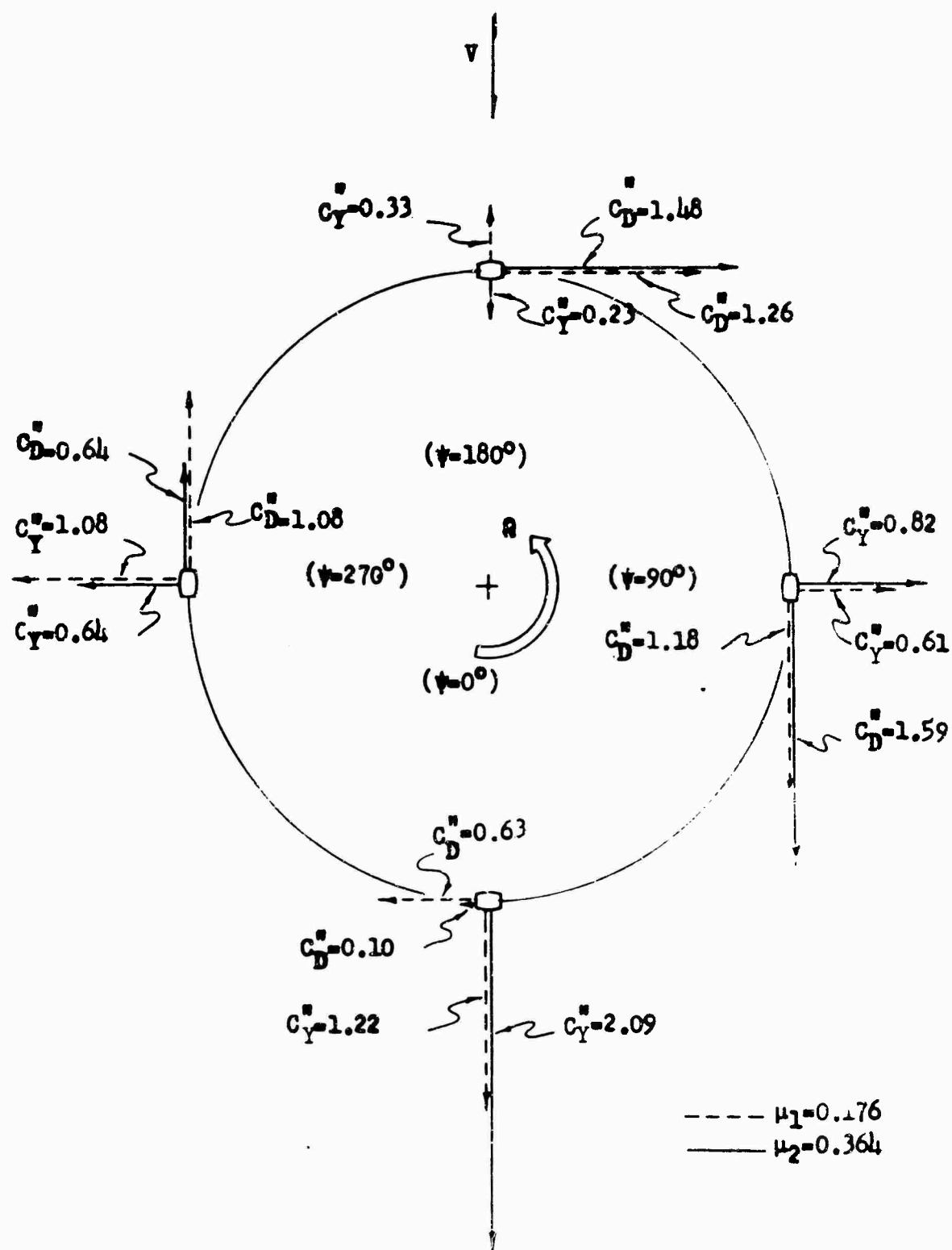


Figure 454. Nacelle Drag and Side Force Coefficients for $\mu_1 = 0.176$ and $\mu_2 = 0.364$.

Configuration: 1-50-100 Conical Spinner

Pairing: None

Nacelle Exit Plane: None

——— Nacelle Top θ
 - - - Nacelle Outboard θ
 ——— Nacelle Bottom θ

$\theta = 0^\circ$
 $\alpha = 0^\circ$
 $\mu = .354$

Run 122

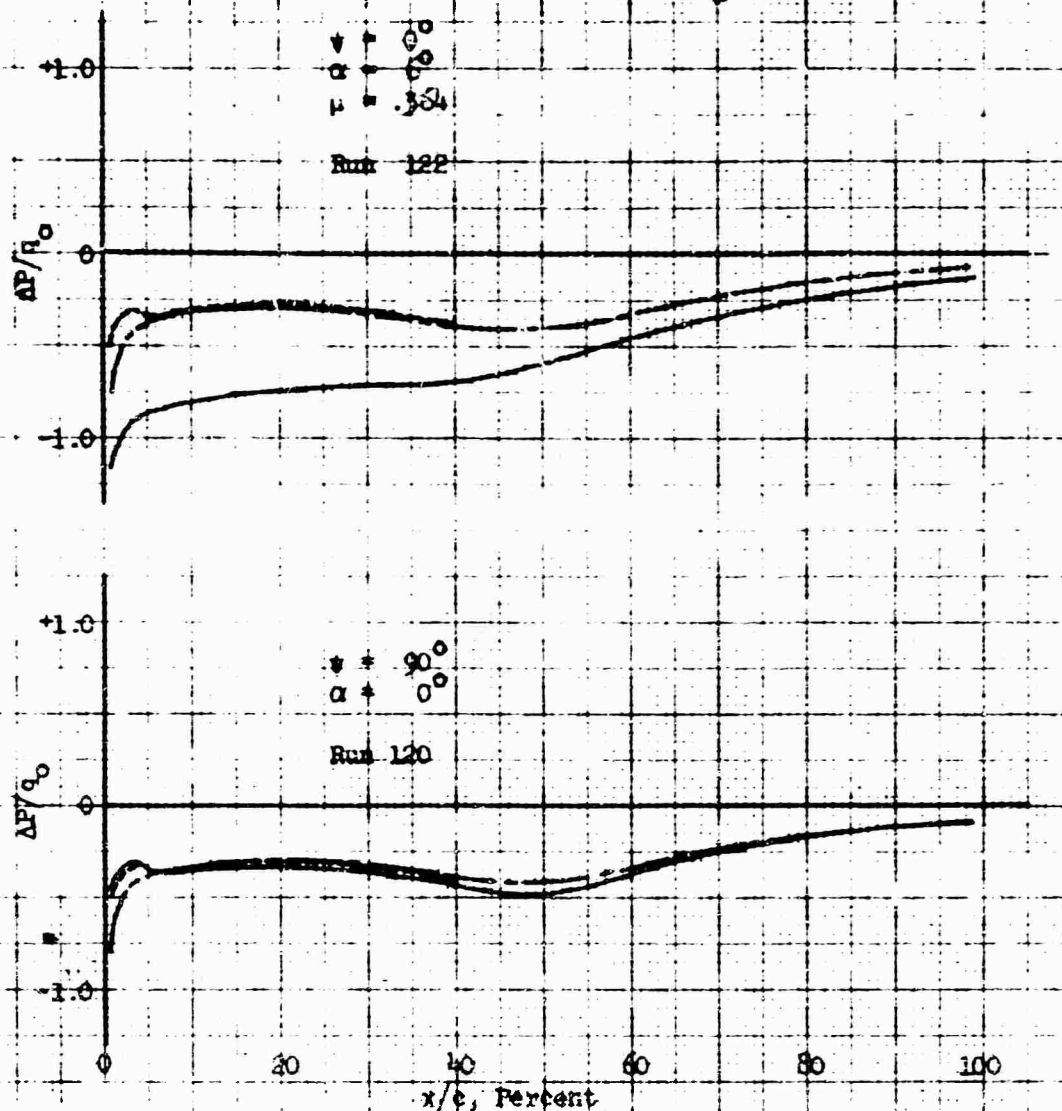


Figure 455. Nacelle Surface Static Pressure
 $P - P_0/q_0$ Versus Percent Nacelle Chord.

Configuration: 1-50-100 Conical Spinner
 Fairing: None
 Nacelle Exit Plate: None

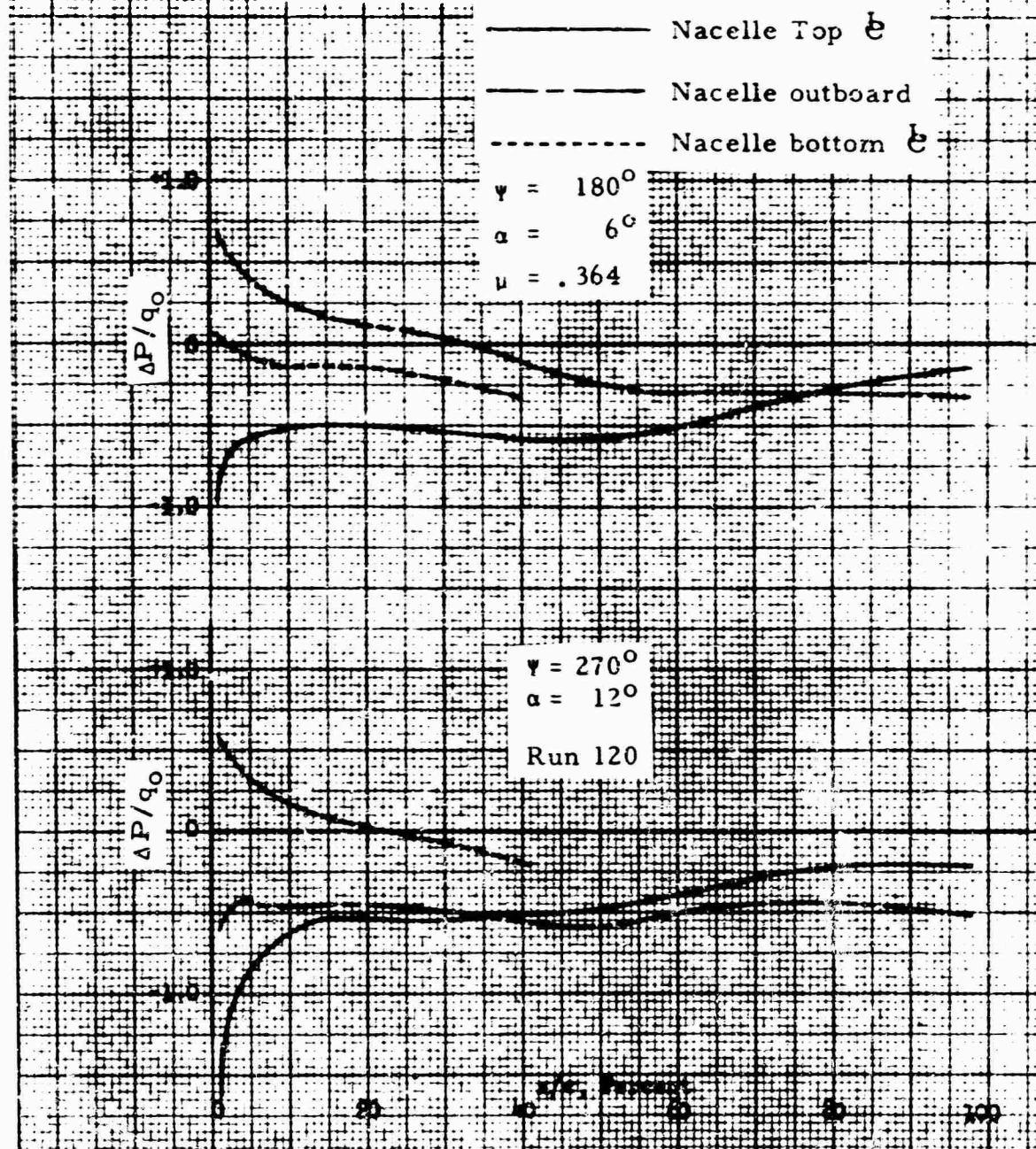
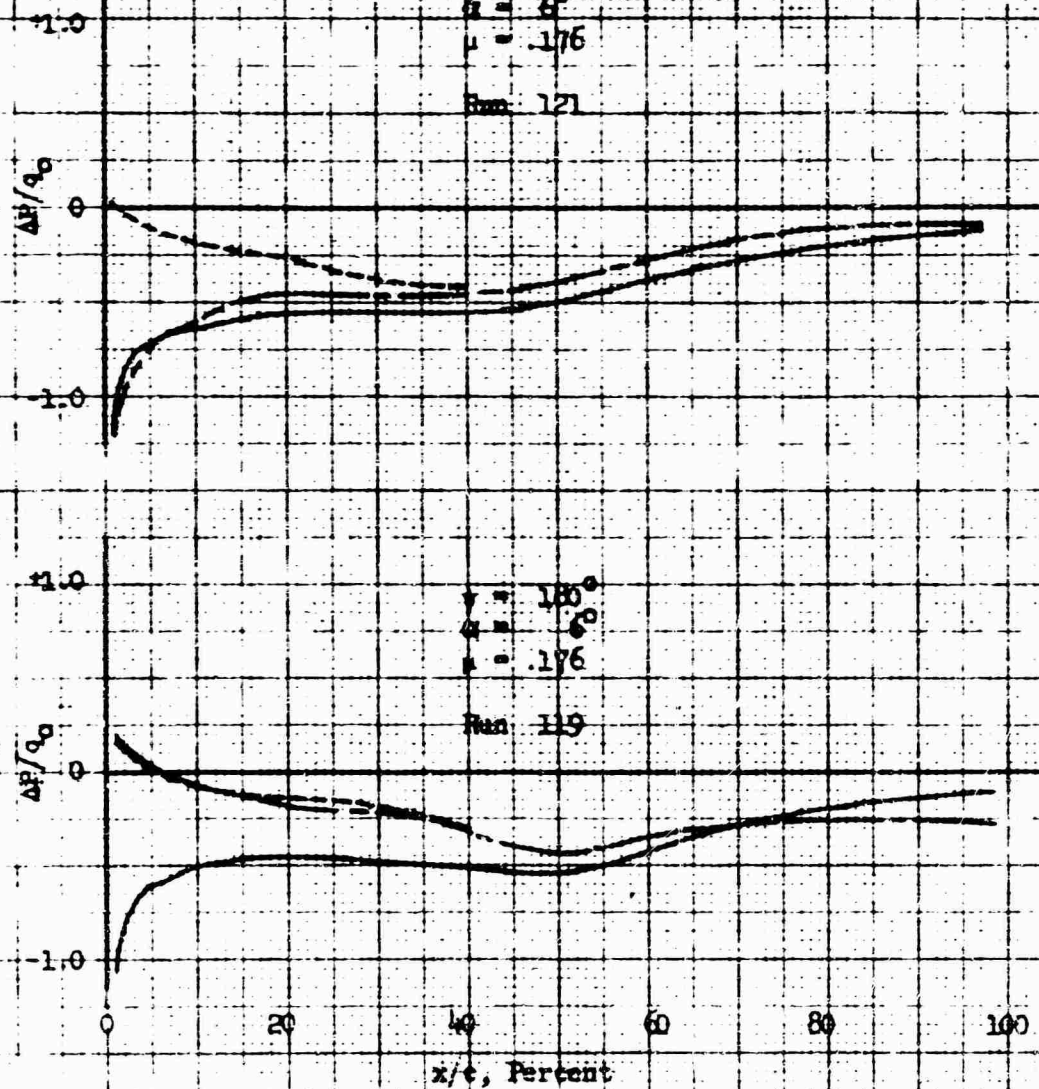


Figure 456. Nacelle Surface Static Pressure -
 $P - P_0/q_0$ Versus Percent Nacelle Chord.

Configuration: 1-72-109 Conical Spinner
 Sizing: 1/2 in.
 Nacelle End Fixer: None

Nacelle top θ
 Nacelle outboard θ
 Nacelle bottom θ

$\alpha = 0^\circ$
 $\beta = 0^\circ$
 $M = 1.76$
 Run 121



$\alpha = 180^\circ$
 $\beta = 0^\circ$
 $M = 1.76$
 Run 119

Figure 457. Nacelle Surface Static Pressure *
 $P - P_0/a_0$ Versus Percent Nacelle Chord.

Configuration: 1-40-100 No Spinner

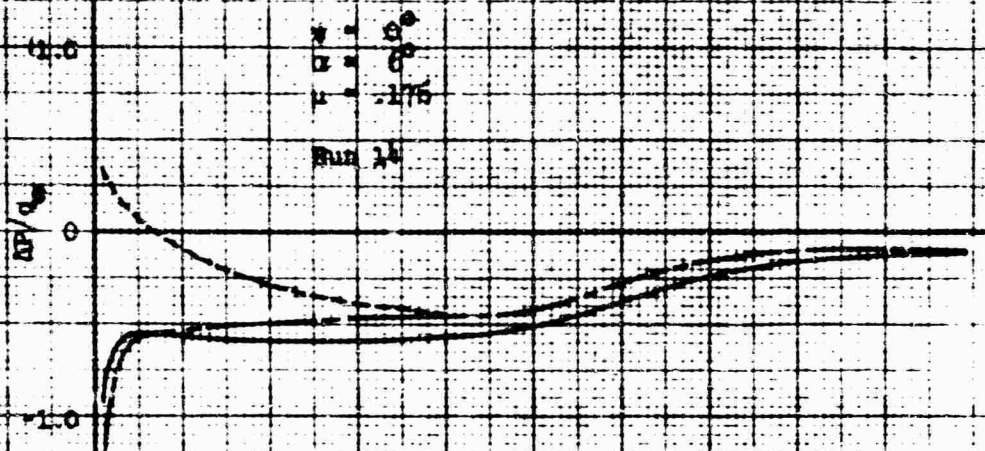
Fairing: None

Nacelle Exit Plate: None

— Nacelle top $\frac{P}{P_0}$
 - - - Nacelle outboard $\frac{P}{P_0}$
 — Nacelle bottom $\frac{P}{P_0}$

$\alpha = 0^\circ$
 $\beta = 0^\circ$
 $\gamma = -175^\circ$

Run 14



$\alpha = 90^\circ$
 $\beta = 0^\circ$

Run 15

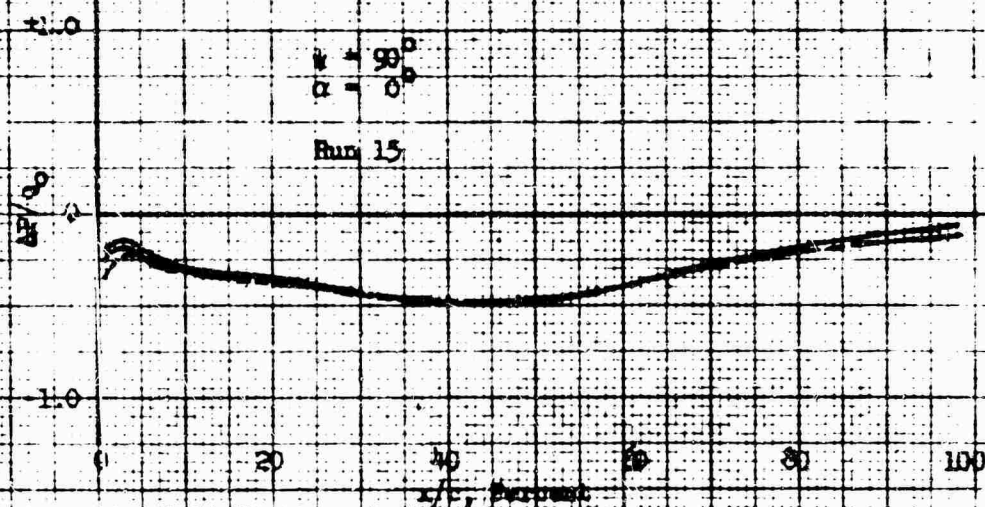


Figure 45a Nacelle Surface Static Pressure -
 $P - P_0/P_0$ Versus Percent Nacelle Chord.

Configuration: 1-40-100 No Spinner
 Pairing: None
 Nacelle Exit Plate: None

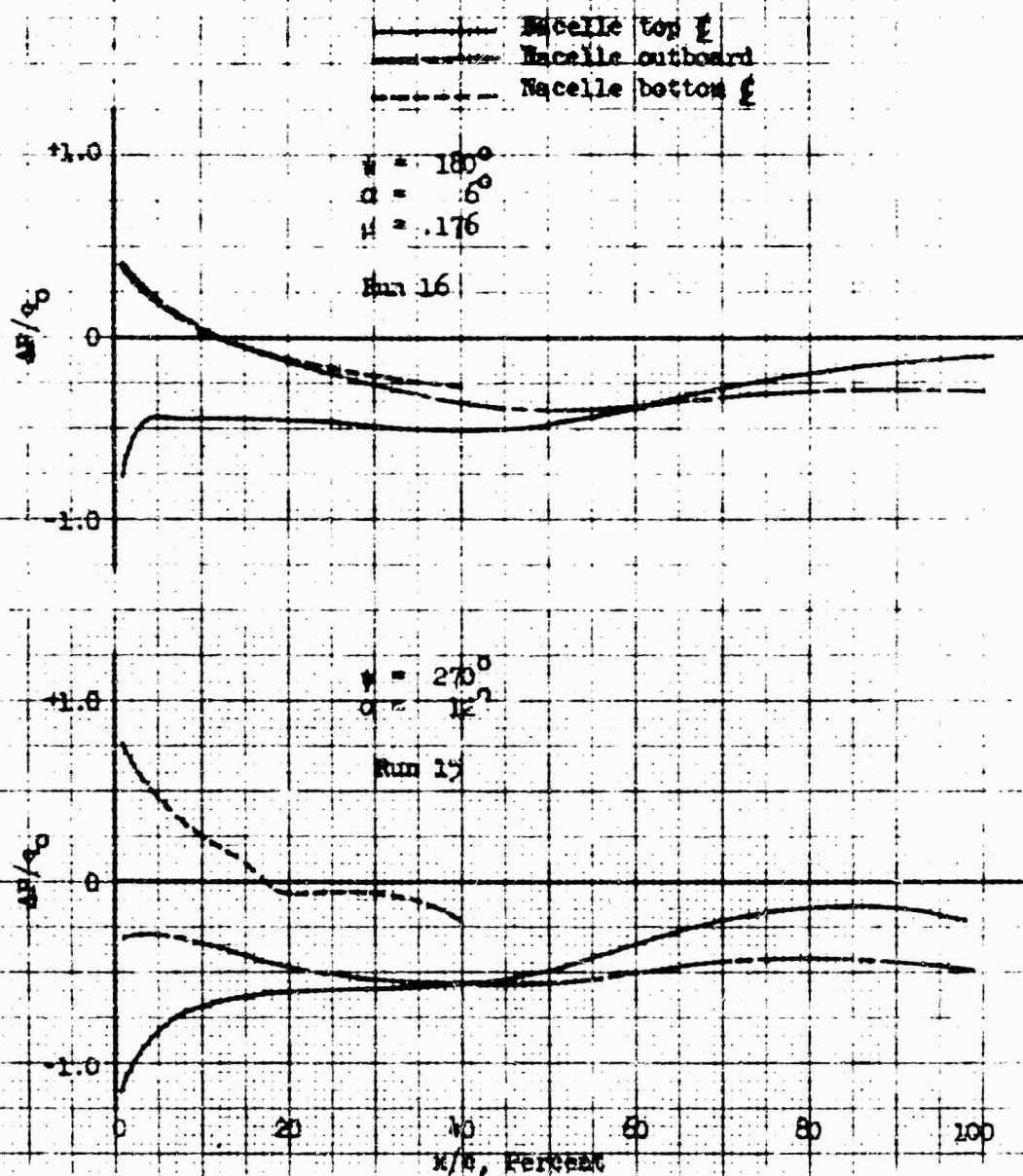


Figure 439. Nacelle Surface Static Pressure -
 $P - P_0/q_0$ Versus Percent Nacelle Chord.

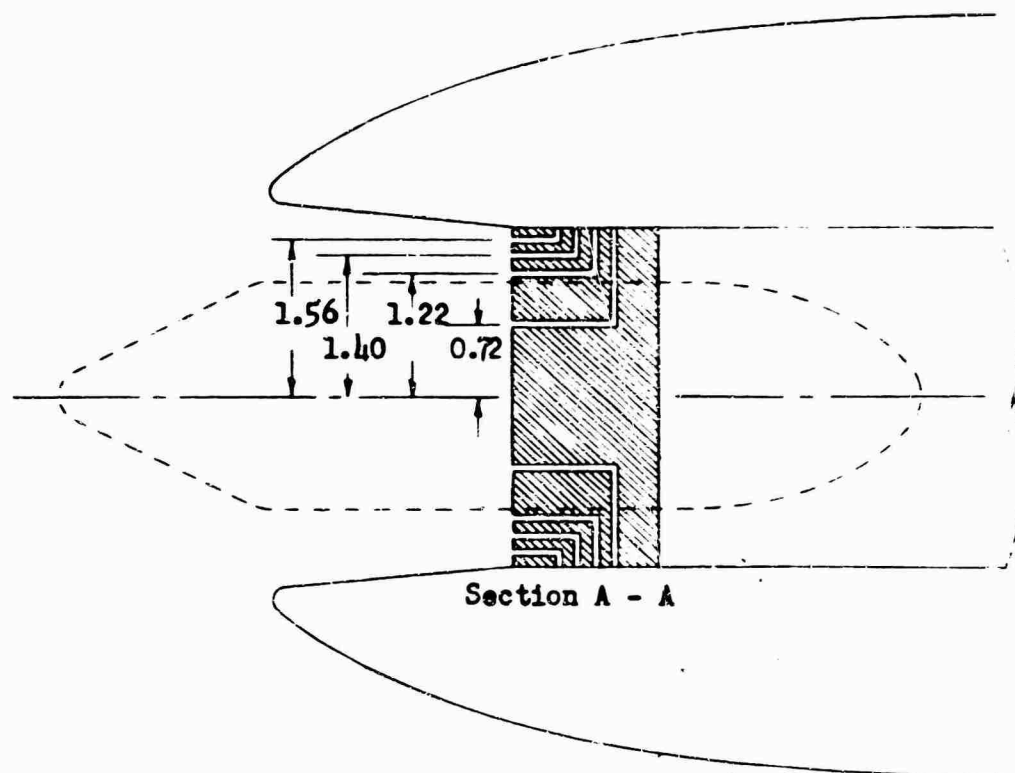
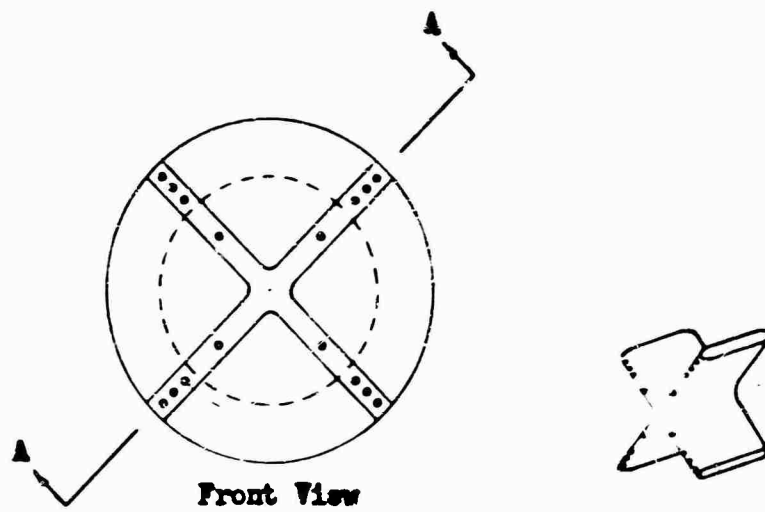


Figure 460. Internal Pressure Rake Configuration.

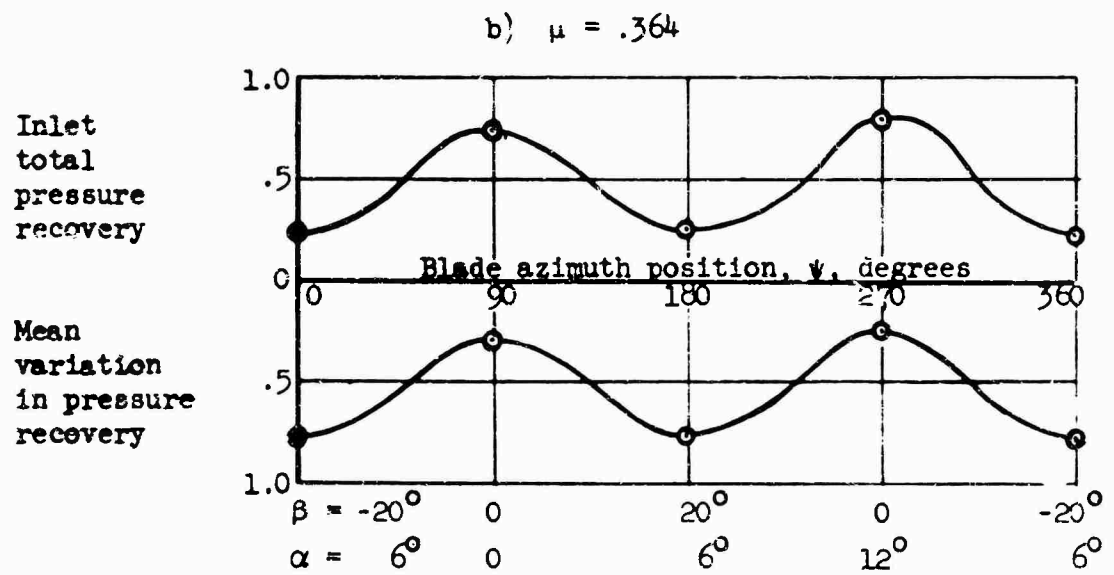
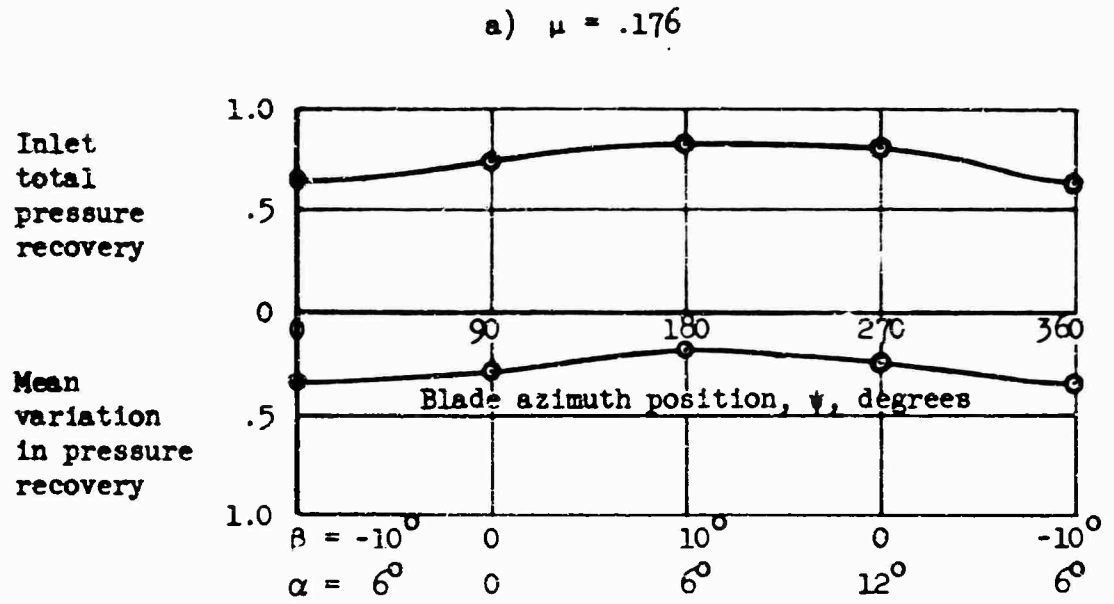


Figure 461. Pressure Recovery at Compressor Face for Inlet 1-40-100.

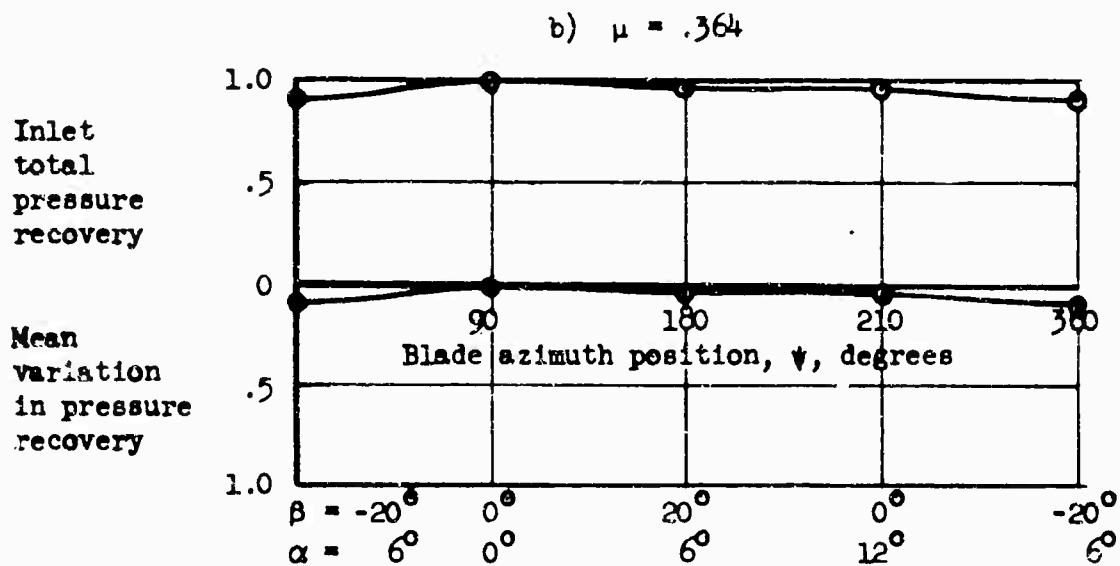
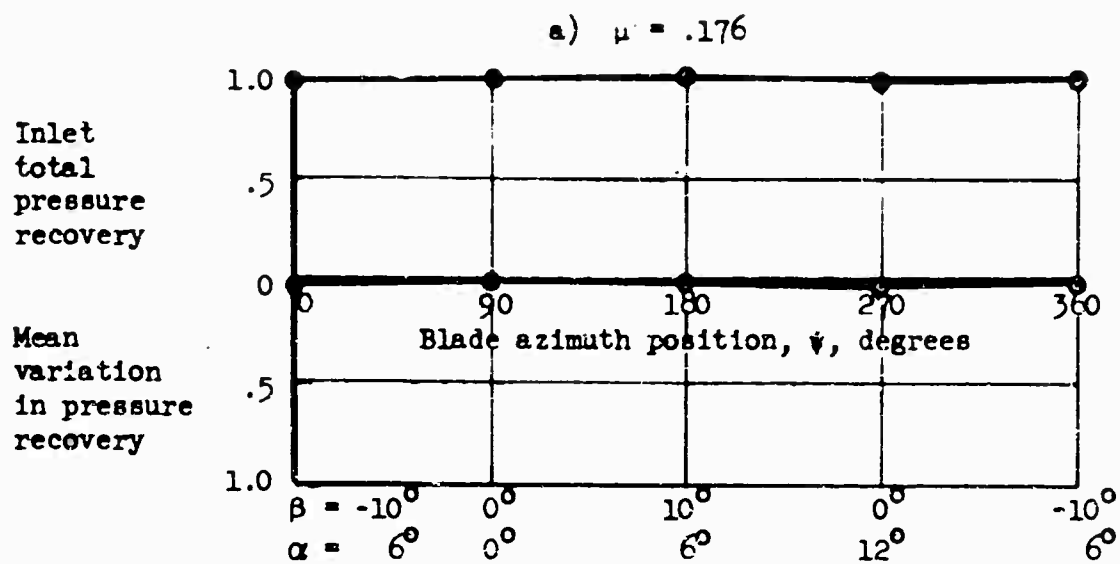


Figure 462. Pressure Recovery at Compressor Face for Inlet 1-50-100 with Conical Center.

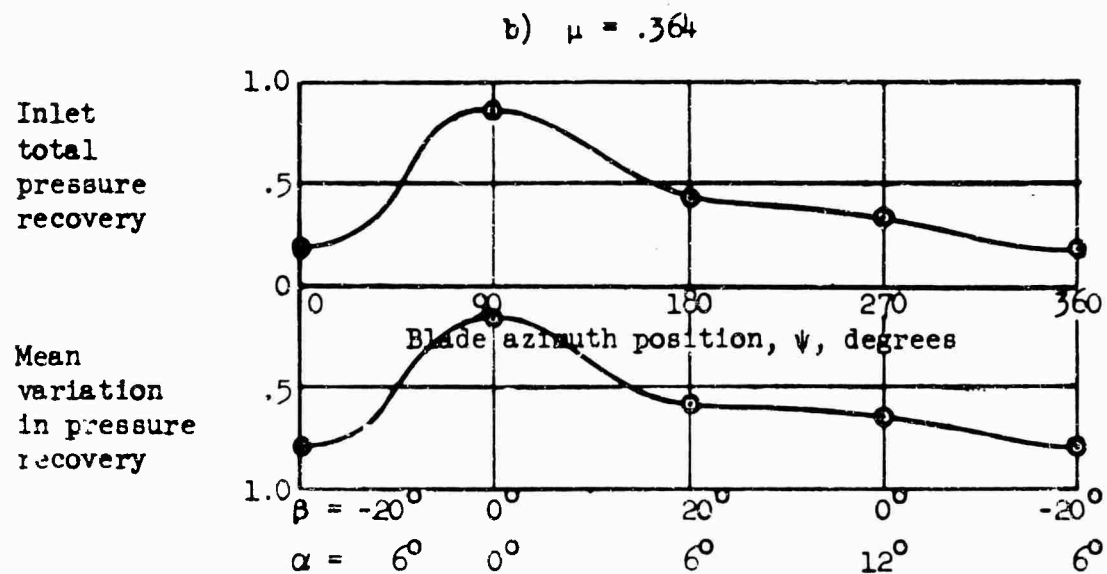
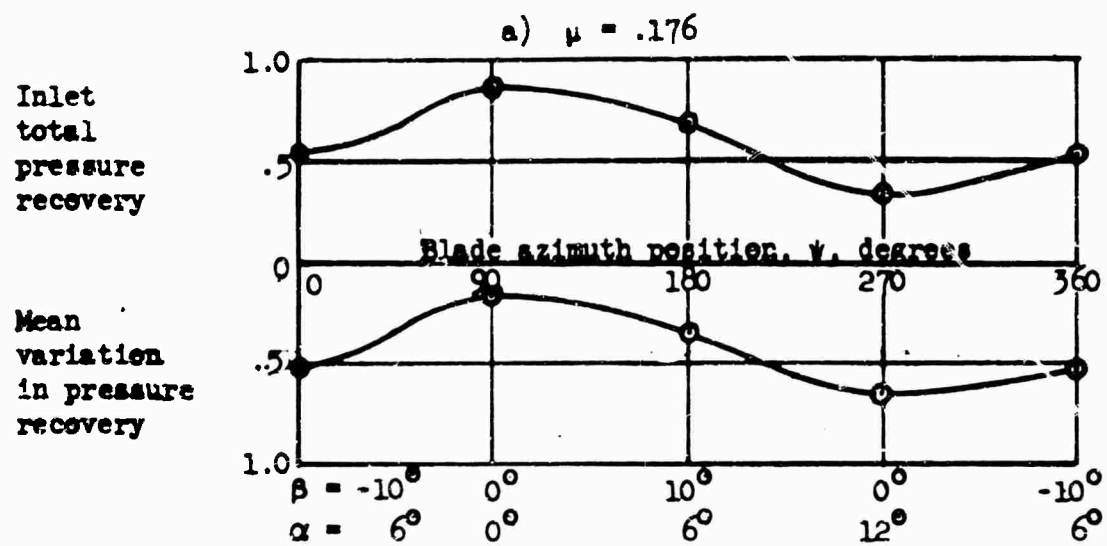
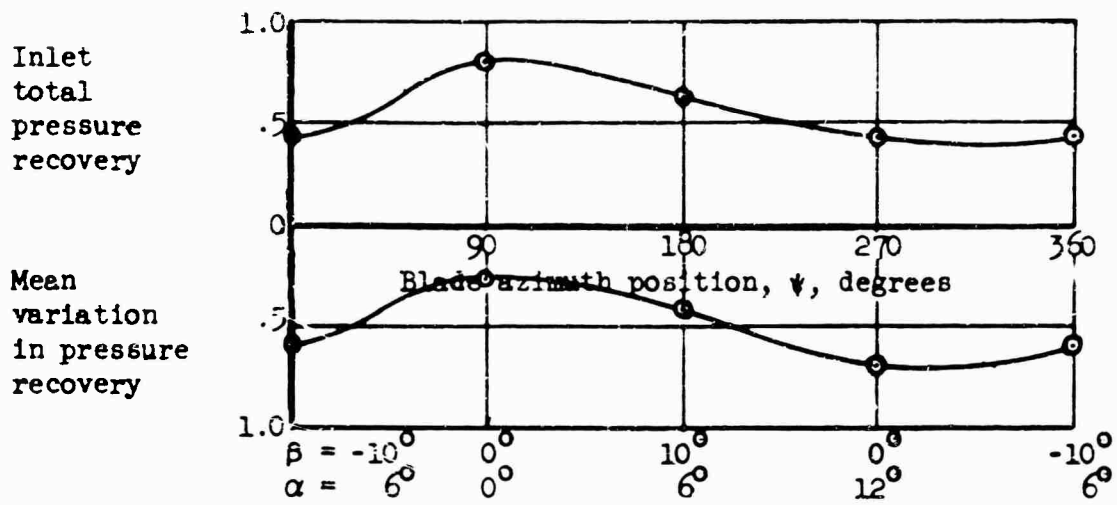


Figure 463. Pressure Recovery at Compressor Face for Side-by-Side 1-40-100 Inlets.

a) $\mu = .176$



b) $\mu = .364$

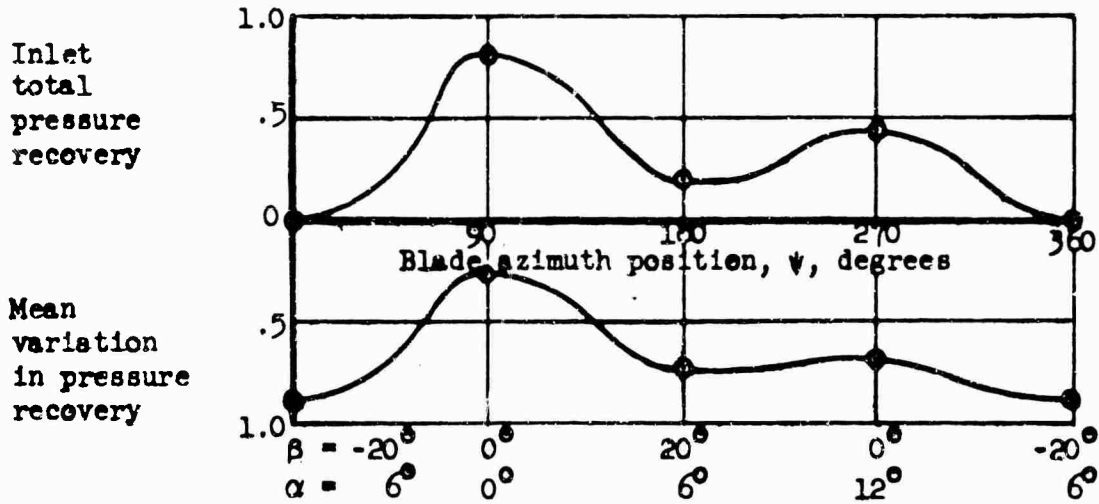


Figure 464. Pressure recovery at Compressor Face for Twin Over-Under 1-40-100 Inlets.

6.2.1 Comparison of Wind-Tunnel Nacelle Drag to Parametric Study Values

It is advantageous to compare wind-tunnel drag coefficients for various nacelle configurations with the values used in Reference 5 for the parametric study so that (1) the applicability of the assumptions in Reference 5 can be evaluated and (2) improvements of nacelle designs from those used in the wind tunnel can be made.

The drag data derived from the wind-tunnel tests have been revised so that the reference area for drag calculations is the nacelle frontal area, designated A_F . The reason for this is that a direct comparison can be made with published literature, such as Reference 6, which normally use frontal area of streamlined bodies as a reference. The parametric study of Reference 5 uses compressor inlet area as a reference, and so the nacelle drag equation will have to be altered as follows:

From paragraph 6.1, Reference 5, the nacelle drag is assumed to be

$$D = \frac{1}{2} \rho V^2 (\delta_{0I} + \delta_{2I} C_{L_T}^2 + \delta_{2I}' \beta^2) A_I \quad (51)$$

where: C_{L_T} = blade lift coefficient, 5.73α
 α = nacelle pitch angle of attack, rad.
 β = nacelle yaw angle of attack, rad.
 A_I = compressor inlet area, ft^2

The parametric study uses an $A_I = 1.04 \text{ feet}^2$ (per engine) and an $A_F = 4.91 \text{ feet}^2$ (per engine). Since the ratio A_I/A_F remains about the same for both a single nacelle or a double nacelle, Equation (51) can be rewritten as follows:

$$D = \frac{1}{2} \rho V^2 \left[\left(\frac{A_I}{A_F} \right) \delta_{0I} + \left(\frac{A_I}{A_F} \right) (5.73)^2 \delta_{2I} \alpha^2 + \left(\frac{A_I}{A_F} \right) \delta_{2I}' \beta^2 \right] A_F \quad (52)$$

Evaluating the drag coefficient of Equation (52) using the δ_{0I} , δ_{2I} , and δ_{2I}' values listed in Table 1, Reference 5, for a four-bladed rotor gives the following formulas based on nacelle frontal area:

$$C_D = .060 + .695\alpha^2 + 1.059\beta^2 \quad (\text{twin over-under nacelle}) \quad (53)$$

$$C_D = .059 + 1.043\alpha^2 + .68\beta^2 \quad (\text{twin side-by-side nacelle}) \quad (54)$$

$$C_D = .056 + .835\alpha^2 + .815\beta^2 \quad (\text{single nacelle}) \quad (55)$$

It is convenient to compare nacelle drag coefficients from wind-tunnel data to those of Equations (53), (54), and (55) by holding first one angle constant while varying the other and then reversing the process.

This has been done and the results are shown in Figures 465, 466, and 467 for two single-nacelle configurations, a twin over-under nacelle, and a twin side-by-side nacelle, respectively.

The results of this comparison show two things. It is immediately obvious that the drag of the wind-tunnel models is approximately double that used in the parametric study for the engine α range and the positive β range. The second observation of importance is that the drag curve for varying yaw angle is not symmetrical about $\beta = 0^\circ$ as is assumed in Reference 5. This lack of symmetry, of course, is due to the presence of the rotor blade on the inboard side of the nacelle.

Although achieved drag of the nacelle is in excess of that assumed in Reference 5, it is felt that the assumed values can be achieved. Tuft studies showed that the flow over the aft portion of the blade tip and the aft inboard part of the nacelle was separated and therefore producing excessive drag. Figure 469 shows that considerable reduction in drag can be expected before reaching levels of drag of streamlined nacelles of similar wetted area. Wind-tunnel tests would be necessary to insure that improved nacelles meet assumed levels of drag.

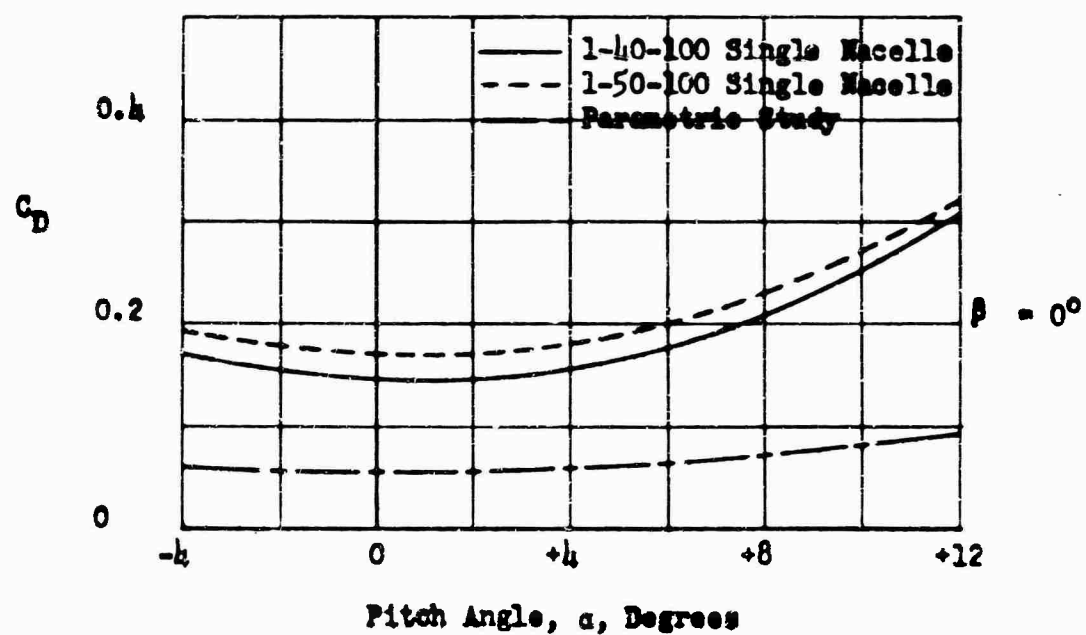
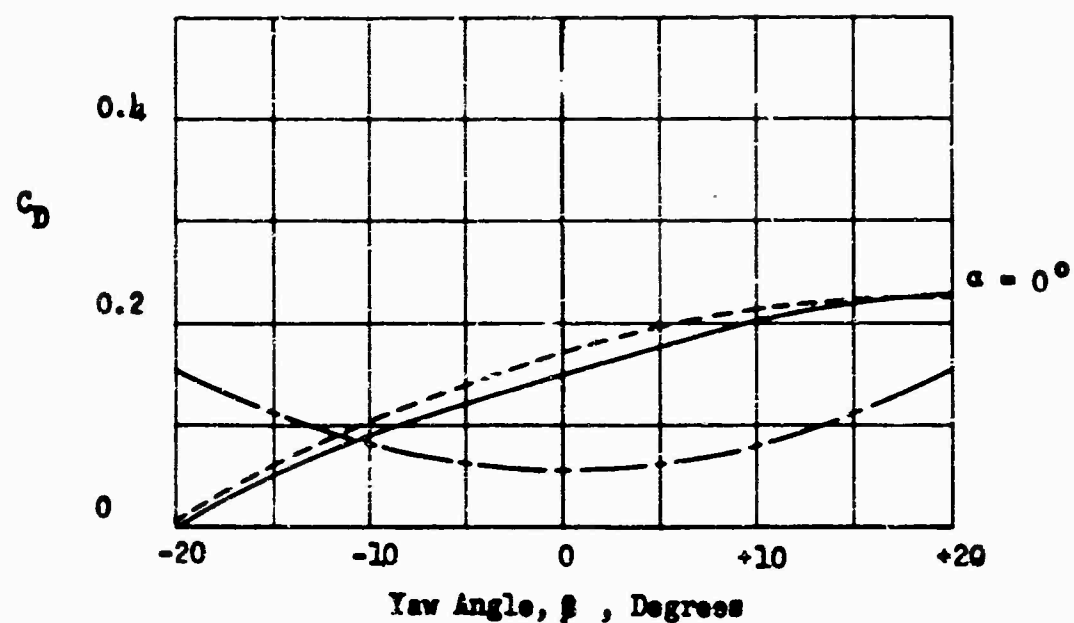


Figure 465. Drag Coefficient Versus Angle of Attack - 1-40-100 and 1-50-100 Single Nacelles.

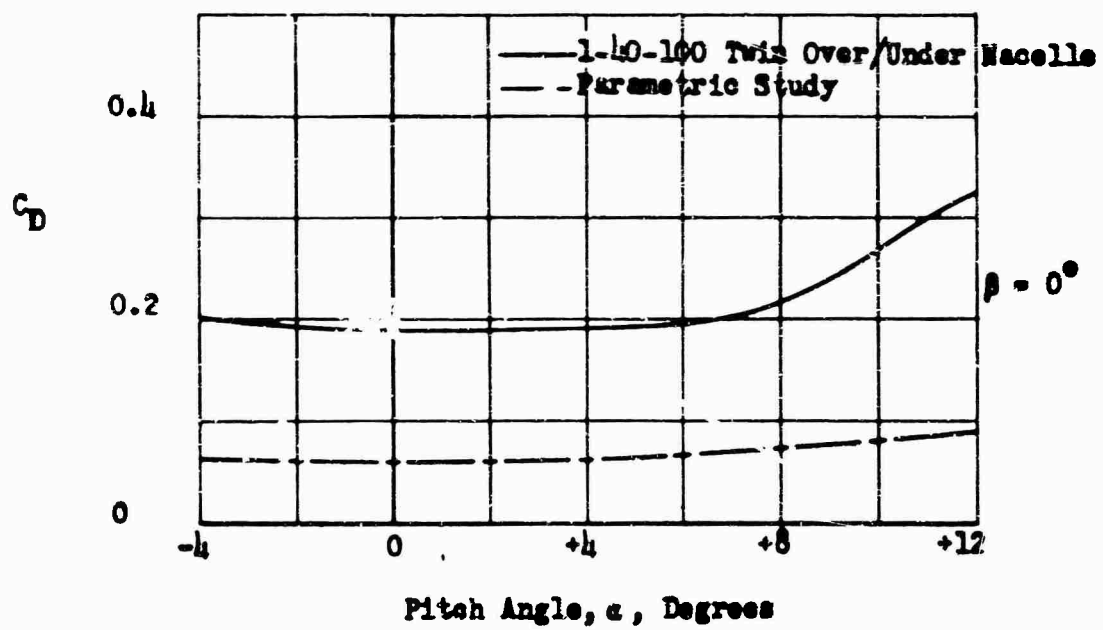
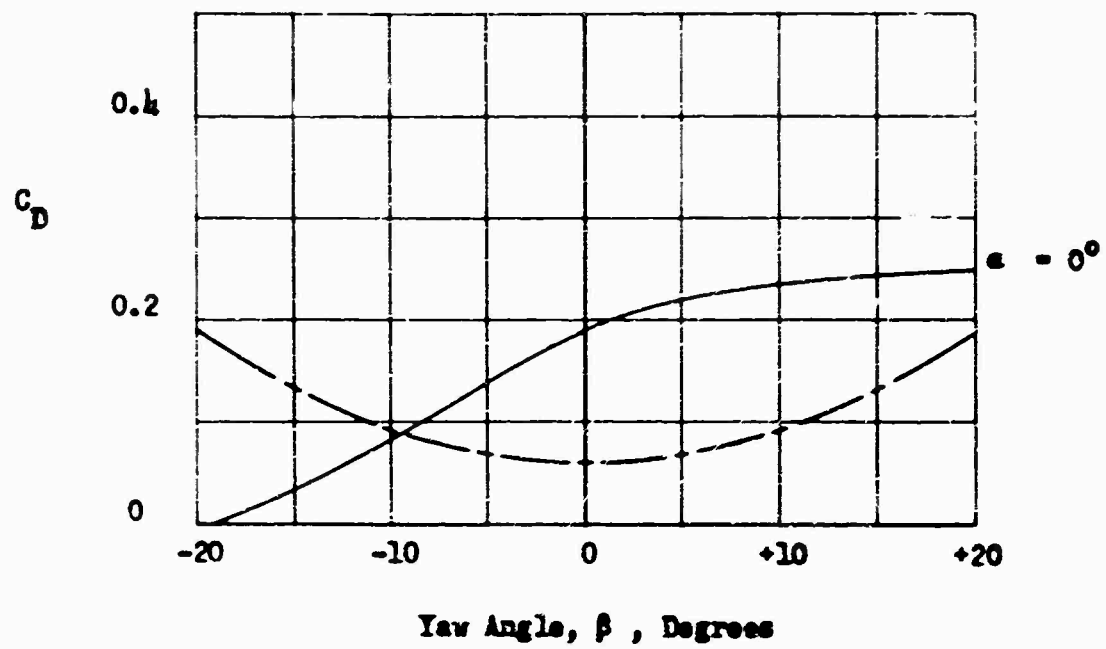


Figure 466 Drag Coefficient Versus Angle of Attack - 1-40-100 Twin Over/Under Nacelle .

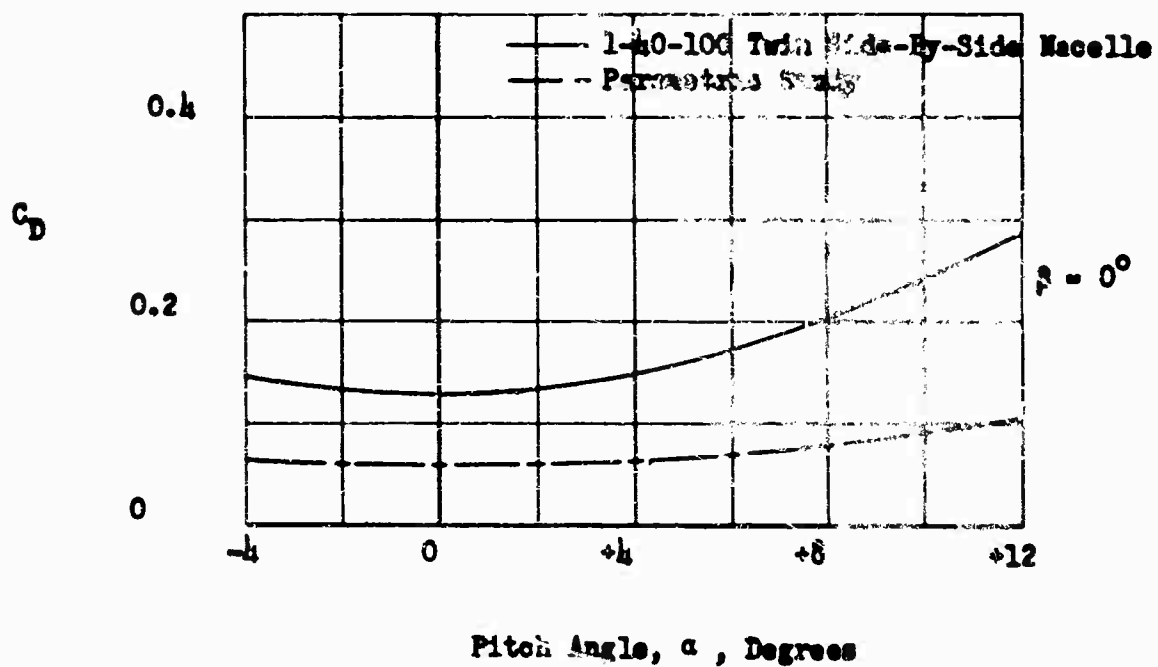
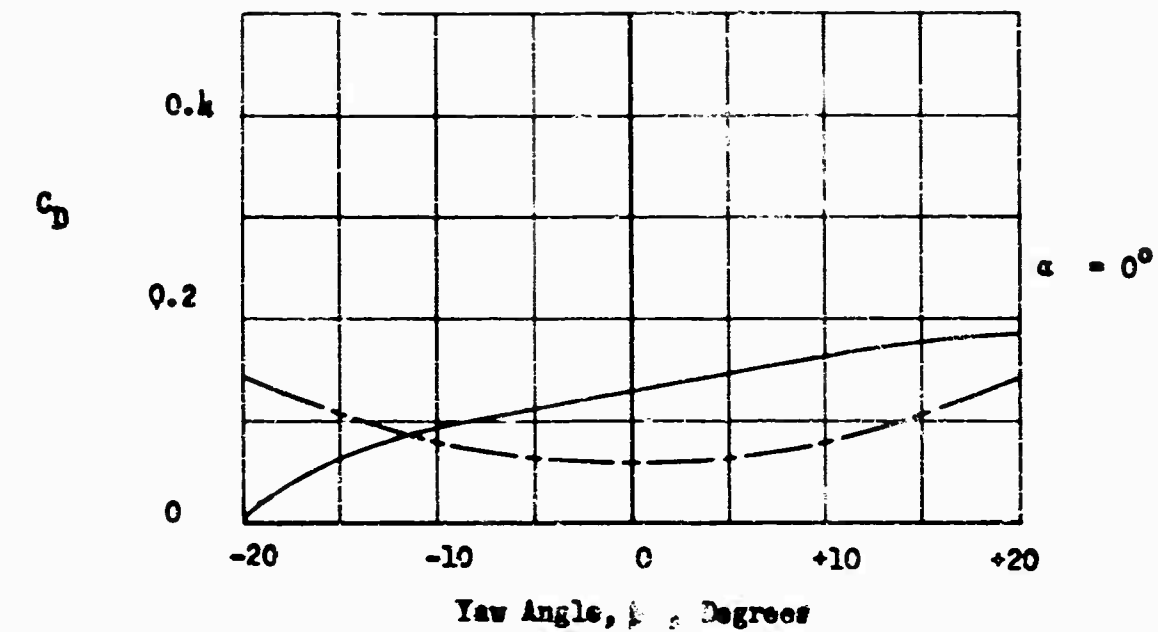


Figure 467. Drag Coefficient Versus Angle of Attack -
1-40-100 Twin Side-By-Side Nacelle.

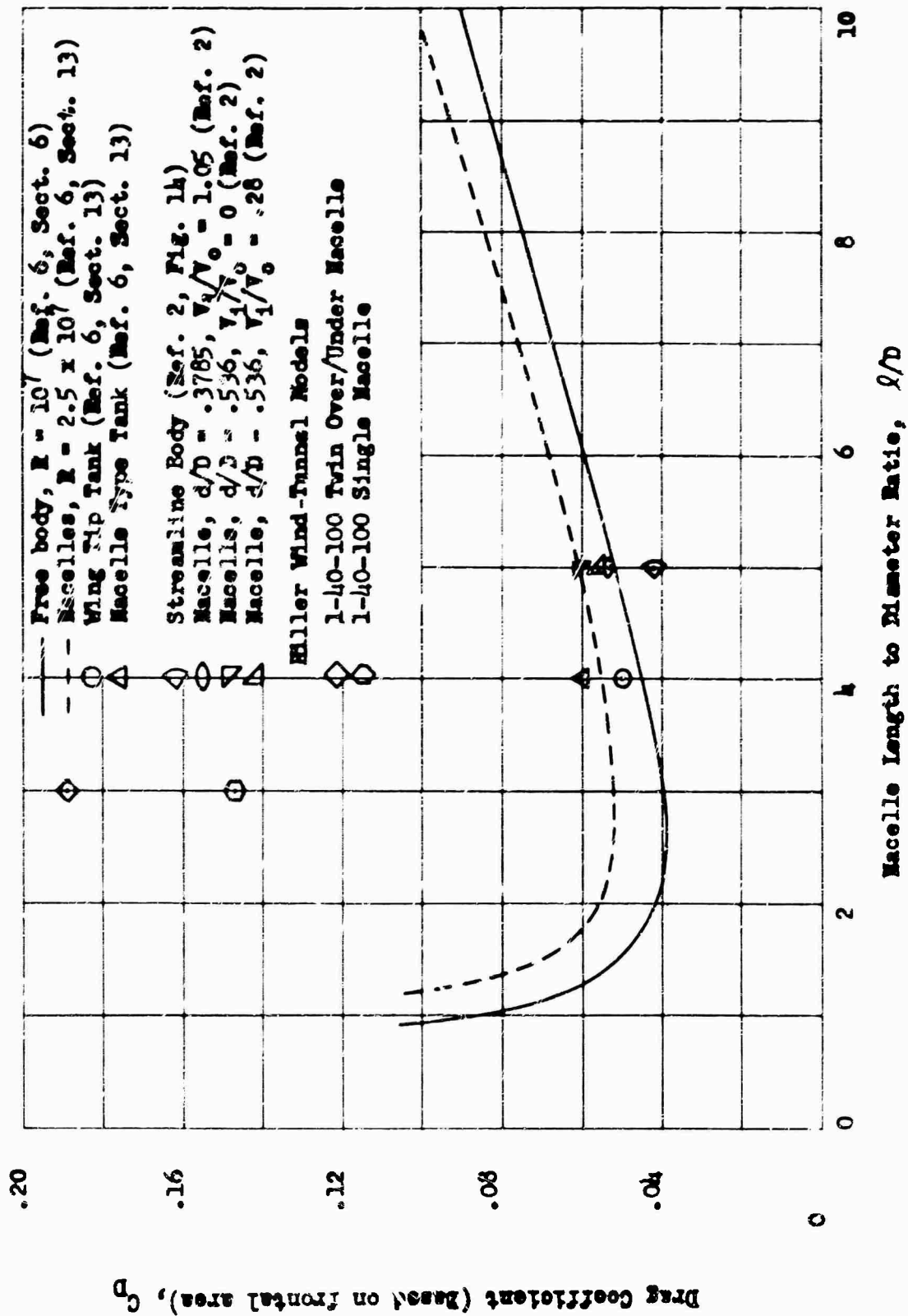


Figure 468. Drag Coefficient Versus Length/Diameter Ratio.

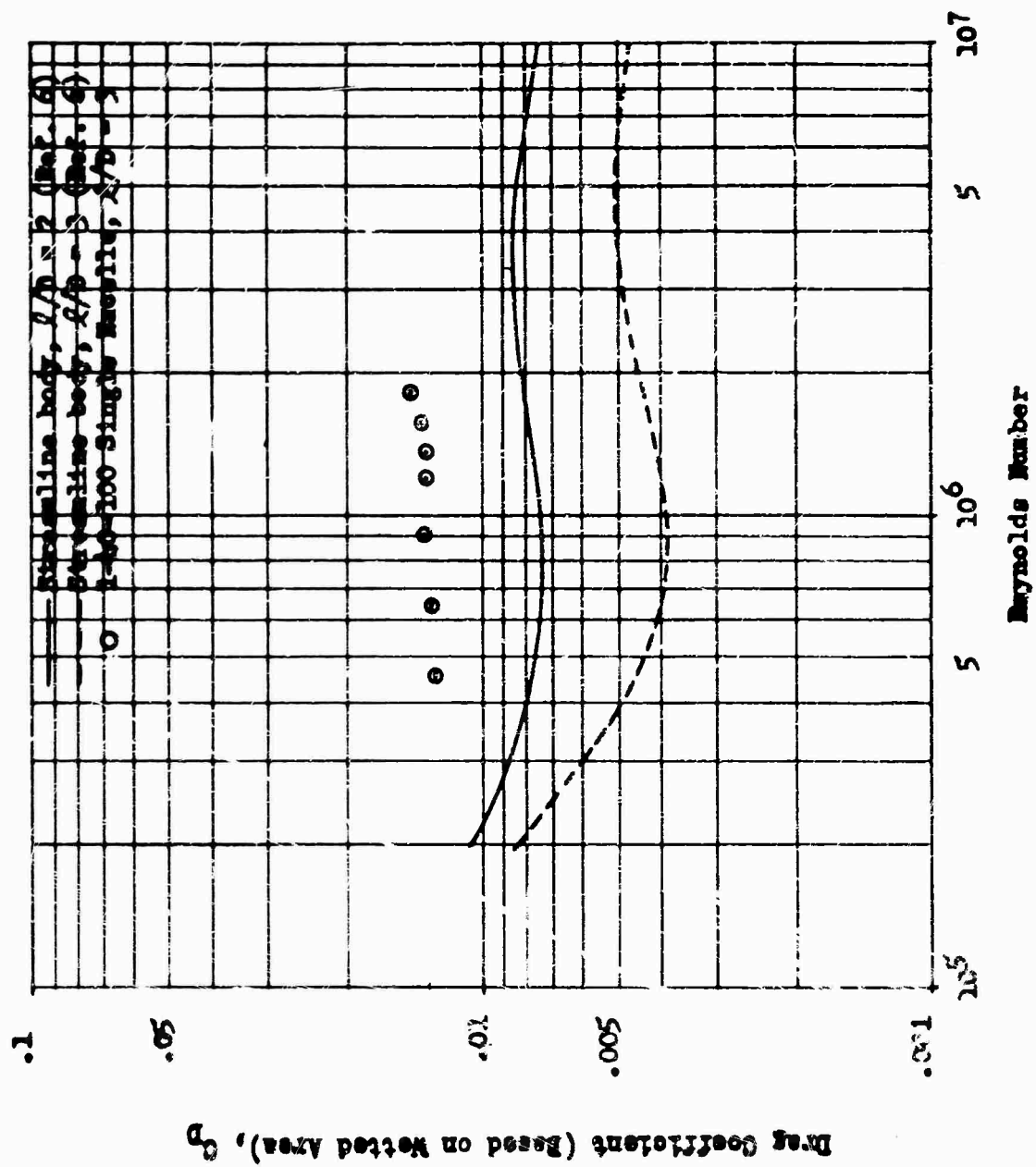


Figure 469. Drag Coefficient versus Reynolds Number.

Unclassified

Security Classification

DOCUMENT CONTROL DATA - R&D		
(Security classification of title, body of abstract and indexing annotation must be entered when the report is classified)		
1. ORIGINATING ACTIVITY (Corporate author)		2a. REPORT SECURITY CLASSIFICATION
Hiller Aircraft Company, Inc. Palo Alto, California		Unclassified
		2b. GROUP
3. REPORT TITLE		
Heavy-Lift Tip Turbojet Rotor System, (Wind-Tunnel Studies), Volume VIII		
4. DESCRIPTIVE NOTES (Type of report and inclusive dates)		
5. AUTHOR(S) (Last name, first name, initial)		
6. REPORT DATE		
October 1965		
7a. TOTAL NO. OF PAGES		7b. NO. OF REFS
525		6
8a. CONTRACT OR GRANT NO.		9a. ORIGINATOR'S REPORT NUMBER(S)
DA 44-177-AMC-25(T)		USAAV LABS Technical Report 64-68H
8. PROJECT NO.		9b. OTHER REPORT NO(S) (Any other numbers that may be assigned this report)
Task 111121401D14412		Hiller Engineering Report No. 64-48
10. AVAILABILITY LIMITATION NOTICES		
Qualified requesters may obtain copies of this report from DDC. This report has been furnished to the Department of Commerce for sale to the public.		
11. SUPPLEMENTARY NOTES		12. SPONSORING MILITARY ACTIVITY
		US Army Aviation Materiel Laboratories Fort Eustis, Virginia
13. ABSTRACT		
Volume VIII of <u>Heavy-Lift Tip Turbojet Rotor System</u> discusses the results of wind-tunnel force and pressure distribution measurements for a group of nacelle rotor blade tip combinations. Configurations tested included single nacelles with different centerbodies and without centerbody, dual nacelles disposed vertically and horizontally, and with fairings. Variables included nacelle mass flow, angle of attack, angle of sideslip, nacelle-blade incidence, Reynolds number, and forebody length.		

DD FORM 1473
1 JAN 64

Unclassified

Security Classification

Unclassified

Security Classification

KEY WORDS	LINK A		LINK B		LINK C	
	ROLE	WT	ROLE	WT	ROLE	WT
Tip Turbojet Rotor System Wind Tunnel Studies						

INSTRUCTIONS

1. ORIGINATING ACTIVITY: Enter the name and address of the contractor, subcontractor, grantee, Department of Defense activity or other organization (corporate author) issuing the report.

2a. REPORT SECURITY CLASSIFICATION: Enter the overall security classification of the report. Indicate whether "Restricted Data" is included. Marking is to be in accordance with appropriate security regulations.

2b. GROUP: Automatic downgrading is specified in DoD Directive 5200.10 and Armed Forces Industrial Manual. Enter the group number. Also, when applicable, show that optional markings have been used for Group 3 and Group 4 as authorized.

3. REPORT TITLE: Enter the complete report title in all capital letters. Titles in all cases should be unclassified. If a meaningful title cannot be selected without classification, show title classification in all capitals in parenthesis immediately following the title.

4. DESCRIPTIVE NOTES: If appropriate, enter the type of report, e.g., interim, progress, summary, annual, or final. Give the inclusive dates when a specific reporting period is covered.

5. AUTHOR(S): Enter the name(s) of author(s) as shown on or in the report. Enter last name, first name, middle initial. If military, show rank and branch of service. The name of the principal author is an absolute minimum requirement.

6. REPORT DATE: Enter the date of the report as day, month, year. If more than one date appears on the report, use date of publication.

7a. TOTAL NUMBER OF PAGES: The total page count should follow normal pagination procedures, i.e., enter the number of pages containing information.

7b. NUMBER OF REFERENCES: Enter the total number of references cited in the report.

8a. CONTRACT OR GRANT NUMBER: If appropriate, enter the applicable number of the contract or grant under which the report was written.

8b, 8c, & 8d. PROJECT NUMBER: Enter the appropriate military department identification, such as project number, subproject number, system numbers, task number, etc.

9a. ORIGINATOR'S REPORT NUMBER(S): Enter the official report number by which the document will be identified and controlled by the originating activity. This number must be unique to this report.

9b. OTHER REPORT NUMBER(S): If the report has been assigned any other report numbers (either by the originator or by the sponsor), also enter this number(s).

10. AVAILABILITY LIMITATION NOTICES: Enter any limitations on further dissemination of the report, other than those imposed by security classification, using standard statements such as:

- (1) "Qualified requesters may obtain copies of this report from DDC."
- (2) "Foreign announcement and dissemination of this report by DDC is not authorized."
- (3) "U. S. Government agencies may obtain copies of this report directly from DDC. Other qualified DDC users shall request through _____."
- (4) "U. S. military agencies may obtain copies of this report directly from DDC. Other qualified users shall request through _____."
- (5) "All distribution of this report is controlled. Qualified DDC users shall request through _____."

If the report has been furnished to the Office of Technical Services, Department of Commerce, for sale to the public, indicate this fact and enter the price, if known.

11. SUPPLEMENTARY NOTES: Use for additional explanatory notes.

12. SPONSORING MILITARY ACTIVITY: Enter the name of the departmental project office or laboratory sponsoring (paying for) the research and development. Include address.

13. ABSTRACT: Enter an abstract giving a brief and factual summary of the document indicative of the report, even though it may also appear elsewhere in the body of the technical report. If additional space is required, a continuation sheet shall be attached.

It is highly desirable that the abstract of classified reports be unclassified. Each paragraph of the abstract shall end with an indication of the military security classification of the information in the paragraph, represented as (TS), (S), (C), or (U).

There is no limitation on the length of the abstract. However, the suggested length is from 150 to 225 words.

14. KEY WORDS: Key words are technically meaningful terms or short phrases that characterize a report and may be used as index entries for cataloging the report. Key words must be selected so that no security classification is required. Identifiers, such as equipment model designation, trade name, military project code name, geographic location, may be used as key words but will be followed by an indication of technical context. The assignment of links, rules, and weights is optional.

Unclassified

Security Classification

6533-65